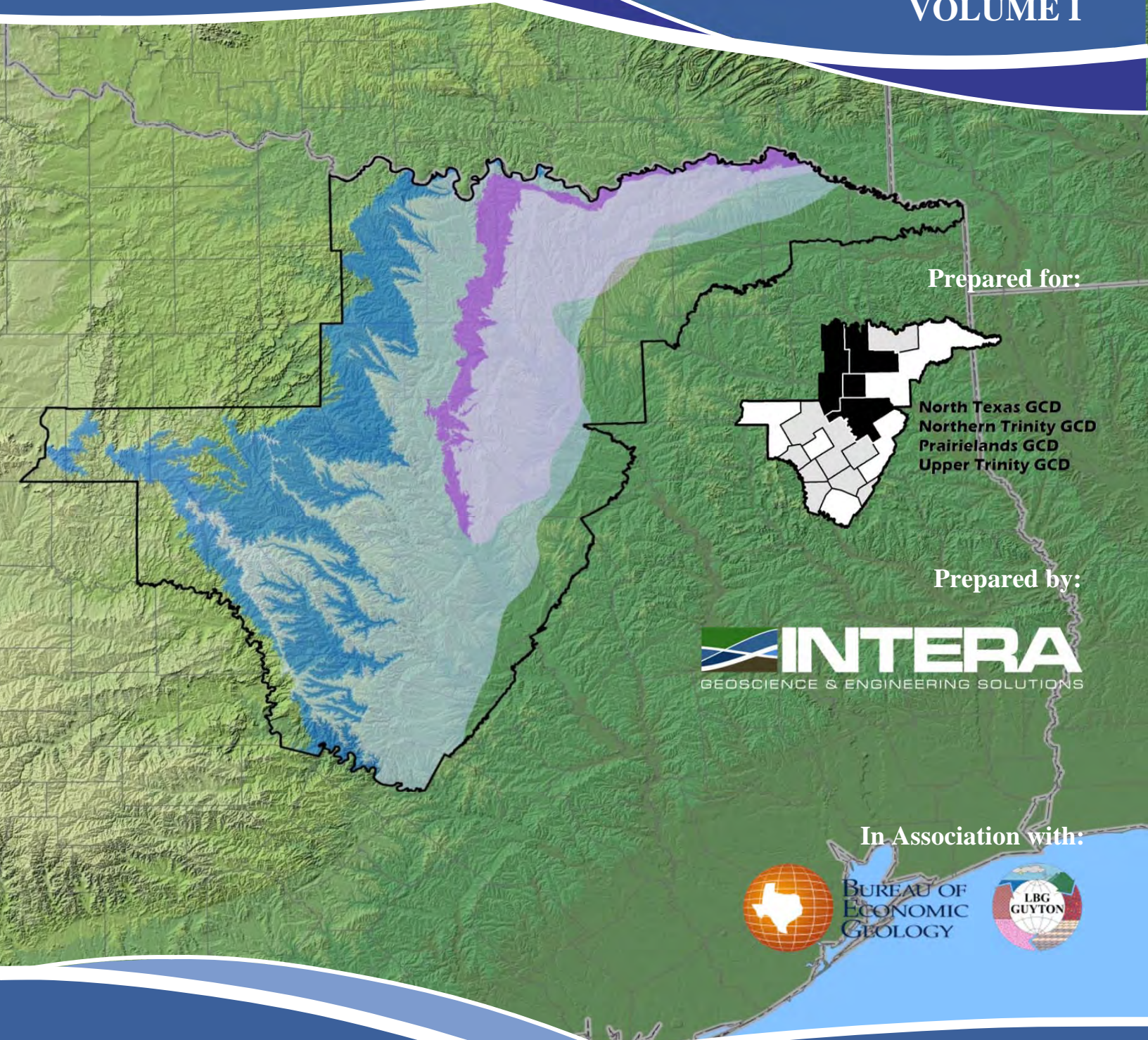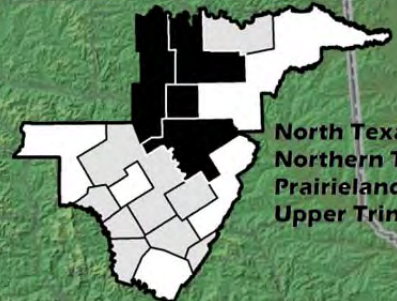# Updated Groundwater Availability Model of the Northern Trinity and Woodbine Aquifers

FINAL MODEL REPORT

VOLUME I

Prepared for:

North Texas GCD
Northern Trinity GCD
Prairielands GCD
Upper Trinity GCD

Prepared by:

INTERA
GEOSCIENCE & ENGINEERING SOLUTIONS

In Association with:

BUREAU OF ECONOMIC GEOLOGY

LBG GUYTON

AUGUST 2014

FINAL REPORT
Updated Groundwater Availability Model of the Northern Trinity and Woodbine Aquifers

Editors

Van A. Kelley, P.G.
John Ewing, P.E.
Toya L. Jones, P.G.
Steven C. Young, Ph.D., P.E.
Neil Deeds, Ph.D., P.E.
INTERA Incorporated

Scott Hamlin, Ph.D.
Bureau of Economic Geology
The University of Texas at Austin

Contributors

Marius Jigmond, Jevon Harding, James Pinkard, Ting Ting Yan
INTERA Incorporated

Bridget Scanlon, Ph.D., P.G; Bob Reedy, P.G.
Bureau of Economic Geology
The University of Texas at Austin

James Beach, P.G.; Tyler Davidson, P.E.; Kristie Laughlin, P.G.
LBG-Guyton Associates

August 2014

This page is intentionally blank.
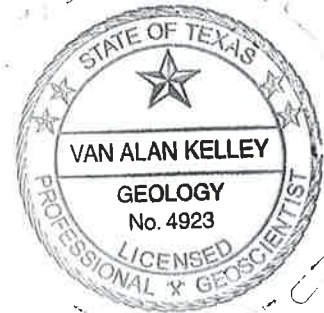
Geoscientist and Engineering Seal

This report documents the work of the following Licensed Texas Geoscientists and Licensed Texas Professional Engineers:

Van A. Kelley, P.G.,

> Mr. Kelley was the Project Manager for this work and was responsible for oversight on the project.

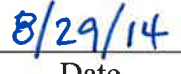_____   8/29/14
Signature   Date

John Ewing, P.E.,

> Mr. Ewing was the lead modeler for the project.

_____   8/29/14
Signature   Date

Toya L. Jones [Dale], P.G.,

> Ms. Jones assisted with development of the conceptual model for the Northern Trinity and Woodbine aquifers. Her contributions also focused on the analysis of hydraulic heads and groundwater flow, natural aquifer discharge, and finalizing groundwater pumping.

_____   8/29/14
Signature   Date
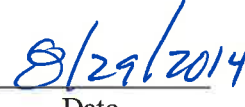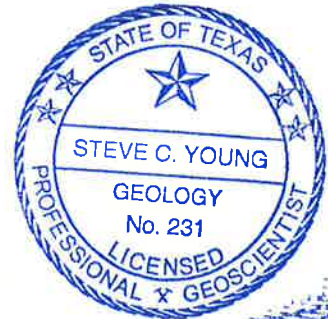
Steven C. Young., Ph.D., P.E., P.G.,

> Dr. Young assisted with development of the conceptual model for the Northern Trinity and Woodbine aquifers. His contributions also focused on the analysis and development of hydraulic properties and groundwater quality analyses. He also supported Mr. Ewing and Dr. Deeds in model development.

_____   8/29/2014
Signature   Date

iii

Neil Deeds, Ph.D., P.E.,

> Dr. Deeds supported Mr. Ewing and Dr. Young in model development.

_____   _____
         Signature   2014/8/29
                                                   Date

Scott Hamlin, Ph.D., P.G.,

> Dr. Hamlin was responsible for the development of the hydrogeologic
> framework for the Northern Trinity and Woodbine aquifers.

_____   _____
         Signature   8/29/2014
                                                   Date

Dr. Bridget Scanlon, Ph.D., P.G.

> Dr. Scanlon led efforts with respect to a review of recharge estimates
> and studies for the project. Dr. Scanlon reviewed the recharge
> implementation approach for the model.

_____   _____
         Signature   8/29/2014
                                                   Date

iv

Table of Contents

Table of Contents, continued

Table of Contents, continued

Table of Contents, continued

Table of Contents, continued

Table of Contents, continued

List of Figures

List of Figures, continued

List of Figures, continued

List of Figures, continued

List of Figures, continued

List of Figures, continued

List of Figures, continued

List of Figures, continued

List of Figures, continued

List of Figures, continued

List of Figures, continued

List of Figures, continued

List of Figures, continued

List of Figures, continued

List of Figures, continued

List of Figures, continued

List of Figures, continued

List of Figures, continued

List of Figures, continued

List of Figures, continued

List of Figures, continued

List of Figures, continued

List of Figures, continued

List of Figures, continued

List of Figures, continued

This page intentionally left blank.

List of Tables

List of Tables, continued

List of Tables, continued

List of Tables, continued

List of Tables, continued

List of Tables, continued

Acronyms

AFY   acre-feet per year

amsl   above mean sea level

BFZ   Balcones Fault Zone

CMB   chloride mass balance

ET   evapotranspiration

GAM   groundwater availability model

GCD   Groundwater Conservation District

GHS   geohydrostratigraphic

GIS   geographic information system

GMA   Groundwater Management Area

PWS   Public Water Supply

RWPG   Regional Water Planning Group

TAC   Technical Advisory Committee

TCEQ   Texas Commission on Environmental Quality

TDS   total dissolved solids

TWDB   Texas Water Development Board

U.S.   United States

USGS   United States Geological Survey

This page intentionally left blank.

Executive Summary

This report documents the development of a three-dimensional groundwater model for the northern Trinity and Woodbine aquifers. The model also includes the Washita/Fredericksburg groups as a confining layer separating the northern Trinity Aquifer from the overlying Woodbine Aquifer. The Trinity Aquifer is a major aquifer in Texas [George and others, 2011; Texas Water Development Board (TWDB), 2012] and the northern portion is a major water resource for a large portion of north-central Texas and growing population centers along the Interstate 35 corridor from the Dallas-Fort Worth Metropolitan Area to Austin. The northern Trinity Aquifer generally coincides with the portion of the Trinity Group located north of the Colorado River. The northern Trinity Aquifer outcrops in a broad area in Texas along its western extent from Montague County in the north, as far west as Eastland and Callahan counties, and south to Travis County. North of the Brazos River, the northern Trinity Aquifer is overlain by the Woodbine Aquifer, designated as a minor aquifer in Texas by the TWDB (George and others, 2011; TWDB, 2012). The Woodbine Aquifer is named for the Cretaceous-age Woodbine Group. In Texas, this aquifer generally outcrops in a band parallel to and east of the northern Trinity Aquifer outcrop and is an aquifer from the Texas-Oklahoma border south to northern McLennan County. The eastern extent of the northern Trinity and Woodbine aquifers is defined by the TWDB to be an arc extending from middle of Red River County in northeast Texas through western Kaufman County south to northwestern Bastrop County.

Both the northern Trinity and Woodbine aquifers were deposited in a variety of terrestrial and marine depositional environments. This variety in depositional environments resulted in a complex system of aquifers that can be mapped in the subsurface but have wide variation in lithology from sand and gravel dominated systems to shale and limestone. This large degree of variability has led to a very complex geologic nomenclature. However, persistent stratigraphic layers are physically continuous across the study area while their thickness and dominant lithology may change. This study defines five distinct aquifers/formations within the northern Trinity Aquifer from oldest to youngest; the Hosston Aquifer, the Pearsall Formation, the Hensell Aquifer, the Glen Rose Formation, and the Paluxy Aquifer. The aquifers are comprised of interbedded sands and shales and potable water quality can be found over most of the study

area with the exception of the Paluxy Aquifer. The Paluxy Aquifer only extends as far south as northern McLennan County.

The Washita/Fredericksburg groups are situated between the northern Trinity Aquifer and the Woodbine Aquifer and constitute what is generally considered a confining unit but can produce potable groundwater. The Edwards Balcones Fault Zone (BFZ) Aquifer, designated as a major aquifer (George and others, 2011; TWDB, 2012), is situated within the Washita/Fredericksburg groups in Travis, Williamson, and Bell counties. The Woodbine Aquifer is the youngest aquifer included in this model and is predominantly a sandstone with interbedded shale. The Woodbine Group is an aquifer from the Texas-Oklahoma state line in the north to northernmost McLennan County in the south where it thins and becomes predominantly shale. Potable water quality is found in the Woodbine Aquifer outcrop and in some areas the subcrop. Water quality is variable in the confined portions of the aquifer downdip of the outcrop.

This report documents the updated northern Trinity and Woodbine aquifers groundwater availability model (GAM) which is a redevelopment of the original northern Trinity and Woodbine aquifers GAM developed by Bené and others (2004). This updated northern Trinity and Woodbine aquifers GAM was developed using the groundwater simulation code MODFLOW-NWT. MODFLOW is a three-dimensional finite-difference groundwater flow code that is supported by enhanced boundary condition packages to handle recharge, evapotranspiration (ET), streams, springs, and reservoirs. The updated northern Trinity and Woodbine aquifers GAM is divided into eight model layers. Model Layer 1 represents the shallow surficial flow system in the outcrop areas of the northern Trinity Aquifer, Washita/Fredericksburg groups, and Woodbine Aquifer as well as the younger formations overlying the Woodbine and Washita/Fredericksburg groups east of the Woodbine Aquifer and Washita/Fredericksburg groups outcrops. Model Layers 2 through 8 represent the Woodbine Aquifer, Washita/Fredericksburg groups, Paluxy Aquifer, Glen Rose Formation, Hensell Aquifer, Pearsall Formation, and Hosston Aquifer, respectively. The model grid cells are quarter-mile by quarter-mile squares throughout the model domain, which has 1,412 columns and 1,124 rows for a total of 12,696,704 grid cells for the eight model layers. The model grid origin (lower left-hand corner) is located at GAM coordinates 19,067,743 feet north and

6,169,014 feet east. The model is oriented with the x-axis 65 degrees counter-clockwise of east-west to directly overly the grid for the 2004 northern Trinity and Woodbine aquifers GAM.

The first phase of work in the model development was the development of the conceptual model for the northern Trinity and Woodbine aquifers. A conceptual model is a description of the physical processes governing groundwater flow in an aquifer system. During development of the conceptual model, data was collected and interpreted for all the important hydrogeological features that govern groundwater flow in the aquifers including hydrostratigraphy, hydraulic properties, hydraulic heads, recharge, mechanisms of natural discharge, and pumping and information regarding flowing wells. The data collected, the interpretation of that data, and how the data were used to define the conceptual understanding of the northern Trinity and Woodbine aquifers is discussed in detail in this report. The data are also publically available so that future investigators can build on the data and the interpretation of that data.

The more significant contributions of the analyses performed in support of the aquifers conceptual model are hydrostratigraphy, properties, water quality, and pumping. The northern Trinity and Woodbine aquifers are a complex aquifer system with significant variability in aquifer and formation properties in the study area.

The study used 1,302 geophysical logs to correlate stratigraphic boundaries and interpret lithologies. Stratigraphic unit boundaries were defined in outcrop and traced into the subsurface using advanced modern well log correlation techniques. Lithology was interpreted at the scale of 2 to 3 feet creating a high resolution three-dimensional lithologic data set of the aquifers. Net sand and percent sand maps were developed as well as maps of the dominant depositional environments for each aquifer/formation. This stratigraphic framework provided the basis for developing initial model hydraulic properties.

This study collected, analyzed, and/or reviewed over 1,000 long-term (24 hours or longer) aquifer pumping tests collected from the Texas Commission on Environmental Quality (TCEQ) Public Water Supply well records and literature and over 29,000 specific capacity tests obtained from TCEQ well driller's reports. An assessment of the quality of the hydraulic tests resulted in 450 good aquifer pumping tests and 16,000 good specific capacity tests. Hydraulic conductivity values were estimated using multiple datasets including values available from the literature.

A conceptual geohydrostratigraphic (GHS) model was used for estimating hydraulic properties for the aquifers and formations in the northern Trinity and Woodbine aquifers. The GHS model combined depositional and lithological information interpreted in this study with aquifer pumping test data collected and analyzed to provide a framework for estimating hydraulic properties for each aquifer/formation in the model. The GHS model was used to provide an initial, regional set of aquifer parameters for model calibration and to guide the adjustment of aquifer parameters during model calibration. This approach enabled the use of the larger lithologic dataset to estimate aquifer properties across the model domain.

Several methods were used to estimate recharge including water balance methods, the chloride mass balance method, and stream hydrograph separation analyses. Stream hydrograph separation analysis (sometimes referred to as base flow analysis) was conducted on 36 stream gages and associated watersheds intersecting outcrops of the northern Trinity Aquifer, Washita/Fredericksburg groups, and Woodbine Aquifer. These data were used to develop a recharge model for the northern Trinity and Woodbine aquifers. The recharge rate estimated for the outcrop areas of the northern Trinity and Woodbine aquifers in the study area averaged 1.6 inches per year and ranged from a high of 7.2 inches per year in southwestern Arkansas to a low of 0.25 inches per year in Taylor County, Texas. Because the recharge model is fundamentally based upon precipitation, recharge varies spatially and temporally as a function of climate (precipitation). The recharge model also takes into account the effects of urbanization through the historical period.

This study reviewed the relevant literature discussing water quality of the northern Trinity and Woodbine aquifers and developed maps of total dissolved solids (TDS), chloride, and hydrogeochemical facies to better describe and understand the hydrodynamics of the aquifers. The hydrogeochemical facies analysis suggested that the outcrop areas of the northern Trinity and Woodbine aquifers are an active recharge zone with a strong similarity in groundwater chemistry (calcium-magnesium facies) across aquifers and formations suggesting a well-connected shallow groundwater system. The extent of TDS concentration less than or equal to 1,000 mg/L was mapped for each of the aquifers. It is important to note that the model includes significant portions of the northern Trinity and Woodbine aquifers that would be classified as brackish groundwater (greater than 1,000 mg/L and less than 10,000 mg/L).

Pumping was estimated for the northern Trinity and Woodbine aquifers in Texas from 1890 through 2012. A variety of sources and methods were used to estimate pumping in the period prior to 1980. Because flowing wells were an important source of aquifer discharge prior to the 1930s, a literature review was performed to locate flowing wells and obtain estimates of flow rates where available. After 1980, pumping was estimated using water use survey data from the TWDB and metered data made available by Groundwater Conservation Districts (GCDs) in the study area. Groundwater production increased significantly from the late 1930s through 1980 and is still increasing to date but at a slower rate than that prior to 1980. It is estimated that approximately 260,000 acre-feet of groundwater was pumped from the aquifers/formations in the study area in 2012 (this includes the Edwards BFZ Aquifer).

This updated northern Trinity and Woodbine aquifers GAM was developed using a modeling protocol that is standard to the groundwater modeling industry and has been adopted by the TWDB in their GAM Program. This protocol is based upon industry standards and American Society for Testing and Materials standard guides. The GAM protocol includes: (1) the development of a conceptual model for groundwater flow in the aquifers, including defining physical limits and properties, (2) model design, (3) model calibration, (4) sensitivity analysis, and (5) reporting. The conceptual model is a description of the physical processes governing groundwater flow in the aquifer system. Model design is the process used to translate the conceptual model into a physical model, which in this case is a numerical model of groundwater flow. This involves organizing and distributing model parameters, developing a model grid and model boundary conditions, and determining the model integration time scale. Model calibration is the process of modifying model parameters so that observed field measurements (e.g., water levels in wells) can be reproduced.

The updated GAM for the northern Trinity and Woodbine aquifers was calibrated to predevelopment conditions representing, as closely as possible, conditions in the aquifers prior to significant development and to transient aquifer conditions from predevelopment through 2012. The steady-state model and transient model are combined into the same model to ensure consistent model parameterization between the models and to allow the steady-state hydraulic heads to set the initial transient hydraulic heads. The generally accepted practice for groundwater calibration includes performance of a sensitivity analysis, which was performed as

part of model calibration. Sensitivity analyses were performed on both the steady-state and transient portions of the model to offer insight into the uniqueness of the model and the impact of uncertainty in model parameter estimates.

The steady-state model represents a period of long-term equilibrium between aquifer recharge and aquifer discharge. Simulating steady-state conditions is important in overall model calibration because it ensures that the model of the aquifers is physically plausible in ways a transient model cannot. The transient model calibration period extends predevelopment from 1890 through 2012. An effort was made to include as many water-level observations as possible and to simulate, to the degree possible, the significant regional water-level declines that resulted from initial development and the practice of allowing wells to freely flow and the historical onset of significant groundwater development in the 1940s and 1950s. Relative to the 2004 northern Trinity and Woodbine aquifers GAM, this updated GAM extends the calibration period 90 years prior to 1980 and 12 years past 2000.

Both the steady-state and transient calibrations adequately reproduce aquifer hydraulic heads within their bounds of uncertainty and within engineering best practices and consistent with the standards required in previous TWDB GAMs (TWDB, 2014). Steady-state targets included water-level measurements from 96 well locations in the northern Trinity and Woodbine aquifers. By comparison to the transient model (27,490 water-level targets) there is a distinct lack of water-level data for the steady-state model. To help better constrain the steady-state model, several other metrics were used to guide calibration. These included a comparison to the number and location of flowing wells and the location and extent of the artesian zone as reported in the literature. Particle tracking was performed to qualitatively evaluate whether groundwater age dates were within reason given the observed water quality within the aquifers.

The adjusted mean absolute error (i.e., mean absolute error divided by the range in observed hydraulic heads) is 9.1 percent for the steady-state model, which is within the acceptable GAM standard of 10 percent for the adjusted mean absolute error. The mean error for the steady-state model is 12.0 feet, indicating that the model simulates hydraulic heads slightly higher than the hydraulic head targets. This is considered acceptable because the hydraulic head targets were

expected to be biased low due to reductions in hydraulic heads prior to early water-level measurements.

Out of a total of 420 flowing well locations included in the model, 304 exhibit artesian conditions within the Hensell Aquifer and an additional 47 wells exhibit flowing conditions in the Hosston Aquifer. This qualitative check indicates that the steady-state model is consistent with regard to the artesian conditions observed at the turn of the 20th century. Groundwater age contours were calculated based on particle tracking for 30,000 and 100,000 years in the Hensell and Hosston aquifers and both were qualitatively consistent with the extent of freshwater.

The calibrated average recharge to the northern Trinity and Woodbine aquifers (including the Fredericksburg and Washita groups) totals 1,766,567 acre-feet per year (AFY) which is approximately 4.4 percent of precipitation model wide. Water discharges from the northern Trinity and Woodbine aquifers through ephemeral streams (54.1 percent of net inflow), perennial streams (41.7 percent of net inflow), riparian ET (3.0 percent of net inflow), net upward cross-formational flow to the overlying younger formations (0.8 percent of net inflow), and to springs (0.1 percent of net inflow). It is important to note that only 0.8 percent of the entire water budget gets to the confined downdip aquifers and discharges through diffuse discharge to the overlying younger formations or through the Mexia-Talco Fault Zone. This is a low percent of the predevelopment water balance. However, particle tracking shows that the groundwater velocities downdip are reasonable. Under predevelopment conditions, the northern Trinity and Woodbine aquifers were full and almost all recharge was rejected back to the surface through discharge to surface processes. Development altered this condition as can be seen in the transient model results.

The northern Trinity and Woodbine aquifers transient model simulates the period from 1890 through 2012. Calibration targets included water-level measurements, long-term hydrographs of water levels, which document transient water-level trends over time, and streamflow measurements. There were 27,490 individual water-level measurements used in the calibration period. Wells selected for hydrograph comparisons were chosen from the entire historical period from 1890 to 2012. The many hydrographs that show evidence of drawdown indicate that drawdown began occurring long before 1980, after which the most reliable pumping estimates

are available from the TWDB water use survey data. These early water-level declines motivated the inclusion of pre-1980 water-level measurements in the transient calibration. Transient water-level data with at least five measurements over a period of years were selected as long-tern hydrographs for comparison to model results. This yielded 706 hydrographs. The model streamflows were compared to available base flow estimates.

The transient model performs well at reproducing transient hydraulic heads across the historical calibration period. The model hydraulic head residuals (defined as the simulated hydraulic head minus the observed hydraulic head) show no systematic bias, with a relatively even distribution around zero. The calibration statistics for all layers meet the GAM requirement of a model simulated mean absolute error divided by the range in observed hydraulic heads of less than 10 percent. Typically, GAMs look at calibration statistics for the period from 1980 through the latest date of pumping estimates from the TWDB water use survey data because those data are considered to have the least pumping uncertainty. The mean absolute error from 1980 to 2012 ranges from 38.3 to 56.2 feet across all model layers. The mean absolute error divided by the range in observed hydraulic heads ranges from 1.8 to 5.2 percent for all model layers.

Calibration statistics for the transient period from 1890 through 1949 and from 1950 through 1979 were also calculated. Much fewer calibration targets exist for the pre-1950 time period. The mean absolute error ranges from 28.3 to 74.1 feet for the pre-1950 period and from 34.2 to 64.2 feet for the period between 1950 and 1980. The mean absolute error divided by the range is less than 10 percent in all units, with the exception of the Washita/Fredericksburg groups prior to 1950, when it is 14.5 percent.

Analysis of the transient water budget provides insight into the current conditions within the deep confined portions of the northern Trinity Aquifer. As pumping rapidly increases from 1940 through 1980 in the deeper confined portions of the aquifer downdip of the outcrop, the amount of groundwater flowing to the deep aquifer increases by a factor of four. Early on, a large fraction of deep pumping is supplied by aquifer storage. However, by 1980, capture from the updip portions of the northern Trinity aquifer supplies greater than 60 percent of the groundwater pumped at depth. By 2010, it is estimated that storage contributes less than 15 percent to the groundwater pumped at depth.

The results from this study suggest that this aquifer behavior is the result of the very low vertical conductivities of the northern Trinity and Woodbine aquifers and the low aquifer storage coefficients. The result is that deep pumping quickly depletes available storage with very large water-level declines. At this point, the groundwater must be supplied by capture of water that would normally discharge at ground surface in the outcrop. This is a very inefficient process because it would likely take tens, if not hundreds, of years for the deepest wells to benefit from the discharge capture of the shallower groundwater. The net result is that water levels keep declining even as the rate of groundwater use stabilizes.

The purpose of this model update was to make improvements to the original 2004 GAM by Bené and others (2004), including incorporation of data collected after the 2004 GAM was developed and results from recent studies in the region, and implementation of the model at a scale that better bridges the gap between regional models and a model that can be used at the scale of a typical GCD for pursuit of their groundwater management objectives. This study provides a model that has been calibrated across the entire period of record through 2012, which is a benefit to GCDs, Groundwater Management Area (GMA) 8, and stakeholders. This study provides significant advancement in the hydrogeological framework and understanding of these aquifers. The updated GAM and the information collected and interpreted to support the study provide GCDs with the best available science to inform final rule making, groundwater management within GCD boundaries, and joint planning. The data collected and made public from this study provides a wealth of knowledge to support GCDs in local-scale hydraulic calculations with analytic tool to address such issues as well spacing.

Development of this updated GAM was unique in Texas in that the entire effort was organized and funded by four GCDs in GMA 8. Desiring to make improvements and updates to the 2004 northern Trinity and Woodbine aquifers GAM and to enhance understanding of the aquifers, the North Texas, Northern Trinity, Prairielands, and Upper Trinity GCDs entered into an inter-local agreement in 2012 to support and fund this updated GAM for the northern Trinity and Woodbine aquifers in GMA 8. This work was performed in a public process similar to that used by the TWDB in their GAM Program. A Technical Advisory Committee made up of technical representatives from the GCDs within GMA 8, the TWDB, and the United States Geological

Survey were appointed and utilized throughout development of this updated GAM to ensure, for one, that local hydrological conditions were accurately incorporated into the model.

Through consultation with the Contract Management Committee and the Contract Manager, INTERA was requested to perform three predictive simulations with the updated GAM to support the GMA 8 joint planning process. Those runs are documented in Kelley and Ewing (2014).

1.0   Introduction

The Texas Water Development Board (TWDB) has identified the major and minor aquifers in Texas on the basis of regional extent and amount of water produced. The major and minor aquifers are shown in Figures 1.0.1 and 1.0.2, respectively. Major aquifers are those that supply large quantities of water over large areas of the state and minor aquifers are those that supply relatively small quantities of water over large areas of the state or supply large quantities of water over small areas of the state. A general discussion of the major and minor aquifers in Texas is found in George and others (2011).

The Trinity Aquifer is a major aquifer in Texas (see Figure 1.0.1) and the northern portion is a major water resource for a large portion of north-central Texas and growing population centers along the Interstate 35 corridor from the Dallas-Fort Worth Metroplex to Austin. The northern Trinity Aquifer generally coincides with the portion of the Trinity Group north of the Colorado River. The northern Trinity Aquifer outcrops in Texas along its western extent. North of the Brazos River, the northern Trinity Aquifer is overlain by the Woodbine Aquifer, defined as a minor aquifer in Texas by the TWDB (see Figure 1.0.2). The Woodbine Aquifer is named for the Cretaceous-age Woodbine Group (George and others, 2011). In Texas, this aquifer generally outcrops in a band parallel to and east of the northern Trinity Aquifer outcrop and is an aquifer from the Texas-Oklahoma border to northern McLennan County. South of northern McLennan County, the Woodbine Group is composed predominantly of shale and is not an aquifer.

The primary objective of this study was to develop an updated groundwater availability model (GAM) for the northern Trinity and Woodbine aquifers. This updated northern Trinity and Woodbine aquifers GAM was developed using a modeling protocol that is standard to the groundwater modeling industry and has been adopted by the TWDB in their GAM Program. This protocol is based upon industry standards and American Society for Testing and Materials (ASTM) standard guides D5447-04, D5609-94, D5610-94, D5981-96, D5490-93, D5611-94 and D5718-95 (ASTM International, 2004, 2008a, 2008b, 2008c, 2008d, 2008e, 2006, respectively). The GAM protocol includes: (1) the development of a conceptual model for groundwater flow in the aquifers, including defining physical limits and properties, (2) model design, (3) model calibration, (4) sensitivity analysis, and (5) reporting. The conceptual model is a description of

the physical processes governing groundwater flow in the aquifer system. Model design is the process used to translate the conceptual model into a physical model, which in this case is a numerical model of groundwater flow. This involves organizing and distributing model parameters, developing a model grid and model boundary conditions, and determining the model integration time scale. Model calibration is the process of modifying model parameters so that observed field measurements (e.g., water levels in wells) are reproduced. The updated GAM for the northern Trinity and Woodbine aquifers was calibrated to predevelopment conditions representing, as closely as possible, conditions in the aquifers prior to significant development and to transient aquifer conditions from predevelopment through 2012. Sensitivity analyses were performed on both the steady-state and transient portions of the model to offer insight to the uniqueness of the model and the impact of uncertainty in model parameter estimates.

This report documents the development of the updated GAM for the northern Trinity and Woodbine aquifers in a format consistent with the TWDB standards for GAMs (TWDB, 2014) and in an order consistent with accepted modeling protocols. Sections 1 through 5 document development of the conceptual model. All aspects of the numerical model development and calibration are discussed in Sections 6 through 9. Section 10 discusses limitations of the model, Section 11 provides suggestions for future improvements to the model, and Section 12 presents conclusions. In addition, numerous appendices are included with this report and are described in Table 1.0.1. The entire report is provided in three volumes with the first volume containing the body of the report text, the second volume containing appendices A through L and electronic data, and the third volume containing Appendix M.

Significant groundwater use in the northern Trinity and Woodbine aquifers started in the late 1800s with the construction of deep (termed artesian in the literature because they flowed at surface) flowing wells in the Waco and Fort Worth areas. Hill (1901) documented many flowing wells in both the northern Trinity and Woodbine aquifers in north-central Texas. While some of these wells or "springs" continue to flow today, most ceased flowing by about 1950 in Waco and by about 1914 in Fort Worth (Leggat, 1957). With the advent of modern pumping technology and significant population growth in the late 1940s and 1950s, groundwater use within the region increased dramatically. As a result, water levels declined significantly (TWDB, 2007a; George and others, 2011) in the northern Trinity and Woodbine aquifers. In some areas, water levels

have declined as much as 850 feet locally in the northern Trinity Aquifer and as much as 400 feet locally in the Woodbine Aquifer. While there has been a conscious effort to move to surface water as the region's population has increased, expanded growth in near-urban areas continue to put pressure on the area's aquifers with trends of increasing groundwater pumping in many counties.

As a result of the recognized need to protect groundwater resources in the northern Trinity and Woodbine aquifers, the Texas Commission on Environmental Quality (TCEQ) designated the Central Texas - Trinity Aquifer Priority Groundwater Management Area (PGMA) in 2008 and the North-Central Texas - Trinity and Woodbine Aquifers PGMA in 2009 (Figure 1.0.3). A PGMA is an area designated and delineated by the TCEQ that is experiencing, or is expected to experience within 50 years, critical groundwater problems including shortages of surface water or groundwater, land subsidence resulting from groundwater withdrawal, and contamination of groundwater supplies. The purpose of a PGMA is to ensure the management of groundwater in areas of the state with critical groundwater problems. After designation of a PGMA, the TCEQ makes specific recommendations on Groundwater Conservation District (GCD) creation within the counties comprising the PGMA. State law allows citizens in the PGMA 2 years to establish GCDs, at which point the TCEQ has the authority to establish a GCD or multiple GCDs. With the designation by the TCEQ of the Central Texas – Trinity Aquifer PGMA and the North-Central Texas - Trinity and Woodbine Aquifers PGMA, several new GCDs were formed in the northern Trinity and Woodbine aquifers region. The 2012 State Water Plan (TWDB, 2012) projects that the population in many of the counties within the northern Trinity and Woodbine aquifers region within the designated PGMAs will experience greater than 100 percent growth over the next 50 years.

Groundwater models provide a unique planning tool for groundwater resources. Specifically, they are uniquely suited for studies of groundwater availability and for assessing the cumulative effects of water management strategies and increased water use during times of drought. A groundwater model is a numerical representation of the aquifer system capable of simulating historical conditions and predicting future conditions.

Since 1999, the Texas Legislature has approved funding for the GAM Program by the TWDB.
This program incorporates substantial stakeholder involvement; the development of
standardized, thoroughly documented, and publicly available numerical groundwater flow
models and supporting data; and other information and tools for managing the groundwater
resources of Texas. Due to the early success of the GAM program, Senate Bill 2 (77th
Legislature in 2001) mandated that the TWDB obtain or develop GAMs for all major and minor
aquifers in Texas in coordination with GCDs and Regional Water Planning Groups (RWPGs).

The northern Trinity and Woodbine aquifers were considered for GAM creation during the first
round of GAM funding based upon their importance and priority as groundwater resources in the
State. The GAM was completed and submitted to the TWDB in 2004 (Bené and others, 2004).
The GAM Program was conceived with the idea that GAMs would be reviewed for revision
every 5 years. This paradigm recognized that models will need to be revised as new studies and
data come available and lessons are learned from applying the GAMs to real world problems.

With passage of House Bill 1763 in 2005 by the 79th Legislature and Senate Bill 737 in 2011 by
the 82nd Legislature, the importance of the state GAMs and their role in regional groundwater
planning has increased. This legislation established a methodology for GCDs within
Groundwater Management Areas (GMAs) to define groundwater availability in their GMA
through the definition of the Desired Future Conditions (DFCs) of the aquifers within their
GMA. Once the DFC has been adopted, the TWDB uses the state adopted GAM to determine
the Modeled Available Groundwater (MAG). The MAG is the amount of groundwater that can
be produced on an average annual basis to achieve a DFC established by the GCDs within a
GMA.

The northern portion of the Trinity Aquifer and the Woodbine Aquifer are located in GMA 8
(Figure 1.0.4). The first round of joint planning within GMA 8 employed the 2004 northern
Trinity and Woodbine aquifers GAM developed by Bené and others (2004) to determine the
MAG (then termed Managed Available Groundwater) based upon GMA 8 developed DFCs.
Many of the new GCDs formed after the designation by TCEQ of the Central Texas – Trinity
Aquifer PGMA and the North-Central Texas – Trinity and Woodbine Aquifers PGMA were
created during or after the first GMA 8 joint-planning cycle, which ended in September of 2010.

In preparation for the second round of GMA 8 joint planning, the GCDs within GMA 8 recognized the benefits of an improved modeling tool to support joint planning as well as the management of groundwater resources within many of the new GCDs. By 2011, it was apparent that state funding would not be available for a revision to the northern Trinity and Woodbine aquifers GAM. The Texas Water Code §36.1086 states that "Districts within the same management areas or in adjacent management areas may contract to jointly conduct studies or research, or to construct projects, under terms and conditions that the districts consider beneficial. These joint efforts may include studies of groundwater availability and quality, aquifer modeling, and the interaction of groundwater and surface water; educational programs; the purchase and sharing of equipment; and the implementation of projects to make groundwater available, including aquifer recharge, brush control, weather modification, desalination, regionalization, and treatment or conveyance facilities."

Desiring to make improvements to the 2004 GAM and to enhance understanding of the northern Trinity and Woodbine aquifers, four GCDs within GMA 8 entered an inter-local agreement in 2012 to support and fund a new GAM for the northern Trinity and Woodbine aquifers in GMA 8. These districts are the North Texas, Northern Trinity, Prairielands, and Upper Trinity GCDs. These funding districts hired an independent Contract Manager ("owners representative") who reports to a Contract Management Committee representing a member from each funding districts.

The four GCDs that entered into the inter-local agreement provided the opportunity for all other GCDs within GMA 8 to join their efforts. While no other GCDs funded the project, the active GCDs within GMA 8 supported the study and provided in-kind services through their participation in the Technical Advisory Committee (TAC) and through submittal of GCD data and reports to the study team. The TWDB also supported the study and had two members sitting on the TAC.

The TAC is an advisory committee made up of technical representatives from the active GCDs within GMA 8, the TWDB, and the United States Geological Survey (USGS). The TAC members were periodically updated throughout the project and also provided technical review of

deliverables. The members of the TAC at the time of this report (August 2014) are provided in Table 1.0.2 along with their affiliation. The project team is indebted to their commitment.

The updated GAM for the northern Trinity and Woodbine aquifers offers improvements to the 2004 GAM, including incorporation of newly collected data and results from recent studies in the region and implementation of the model at a scale that provides a bridge between the scale needed by individual GCDs and that needed by regional joint planning.   In addition to the benefits to the GCDs and stakeholders in GMA 8, this study provides significant advancement in the hydrogeological framework and understanding of these aquifers. The updated GAM and the information collected and interpreted to support the study provide the newly formed GCDs with the best available science to inform final rule making, groundwater management within GCD boundaries, and joint planning.

While this study has advanced the knowledge base for management of the northern Trinity and Woodbine aquifers, models are inherently uncertain. As data, understanding, and modeling technology improves, it is incumbent on groundwater managers in the region to revise the GAM in the future. The updated GAM was developed at a grid-scale that is currently technologically challenging. However, this improvement in model grid scale provides a tool that is better representative at the scale of a typical GCD and can be further refined by a GCD within the model region. The GAM is applicable for regional joint-planning use and for GCD use at the scale of miles. The GAM is not applicable to individual well hydraulics predictions typical of an assessment of well-spacing calculations. However, the model provides needed data to make these types of calculations with analytical tools more amenable to close borehole predictions. Hydraulic analyses should always augment data associated with this report with new data collected or other local data when available.

Table 1.0.1   **Summary of report appendices.**

Appendix	Description
A	a database of the data obtained from GCDs in support of development of this updated GAM
B	a bibliography of historical reports relevant to development of this updated GAM
C	dip and strike cross sections across the active model area with digital logs shown; the non-proprietary image and digital logs used in development of the hydrostratigraphy discussed in Section 4.1 of this report
D	the plots used to display and analyze the aquifer pumping test data discussed in Section 4.2 of this report
E	a summary of the developmental history of the northern Trinity and Woodbine aquifers
F	additional data supporting the study of natural aquifer discharge discussed in Section 4.6 of this report
G	additional information supporting the historical pumping estimates discussed in Section 4.7 of this report
H	three-dimensional geologic models for the North Texas, Northern Trinity, Prairielands, and Upper Trinity GCDs
I	hydrographs of observed hydraulic head data and the hydraulic head data simulated with the calibrated transient portion of this updated GAM
J	the electronic data included with this report, including the geodatabase and files associated with Appendices A through D, H, and K through M
K	comments on the draft conceptual model report and responses to those comments
L	comments on the draft final model report and responses to those comments
M	a discussion of hydrograph plots created to display transient hydraulic head data and hydrograph plots

Table 1.0.2   Members of the TAC for the updated northern Trinity and Woodbine aquifers GAM.

Member[a]	Affiliation
Bill Mullican	NTWO Project Contract Manager and TAC Chairman
Dirk Aaron[b]	Clearwater GCD
Bobby Bazan[b]	Post Oak Savannah GCD
Al Blair[b]	Southern Trinity GCD
Dan Caudle	Upper Trinity GCD
Hughbert Collier	Collier Consulting representing the North Texas GCD
Joe B. Cooper[b]	Middle Trinity GCD
Dennis Erinakes	Prairielands GCD
David Gattis	Red River GCD
Joshua Grimes	Prairielands GCD
Robert Joseph	USGS representing the Northern Trinity GCD
Robert Mace	TWDB (Larry French designated alternate)
Bob Patterson	Upper Trinity GCD
Drew Satterwhite[b]	North Texas GCD
Richard Sawey	Northern Trinity GCD
Jerry Shi	TWDB
Mitchell Sodek	Central Texas GCD

[a] in August 2014
[b] denotes new member
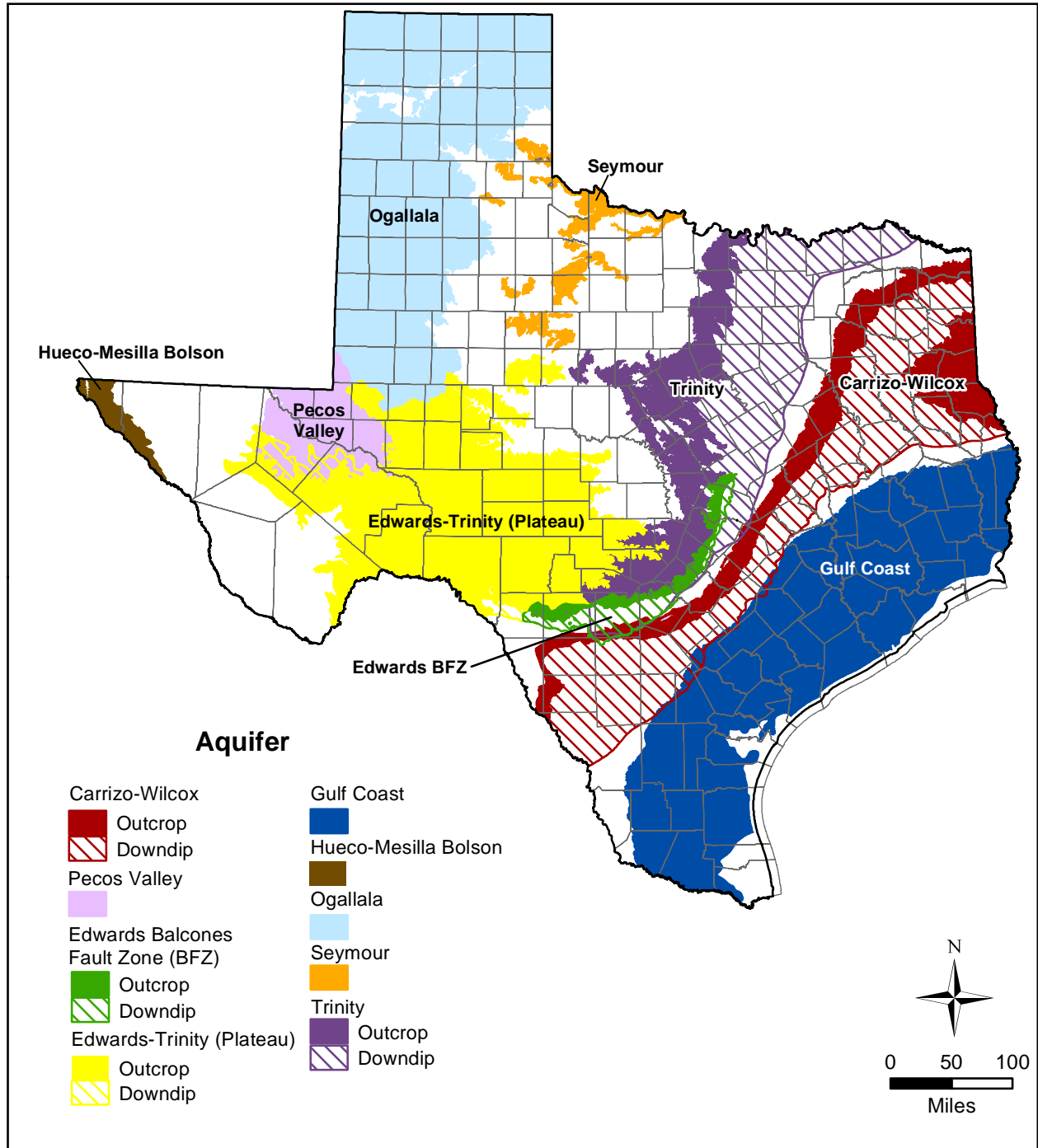
Figure 1.0.1   Locations of major aquifers in Texas (TWDB, 2006a, 2012).
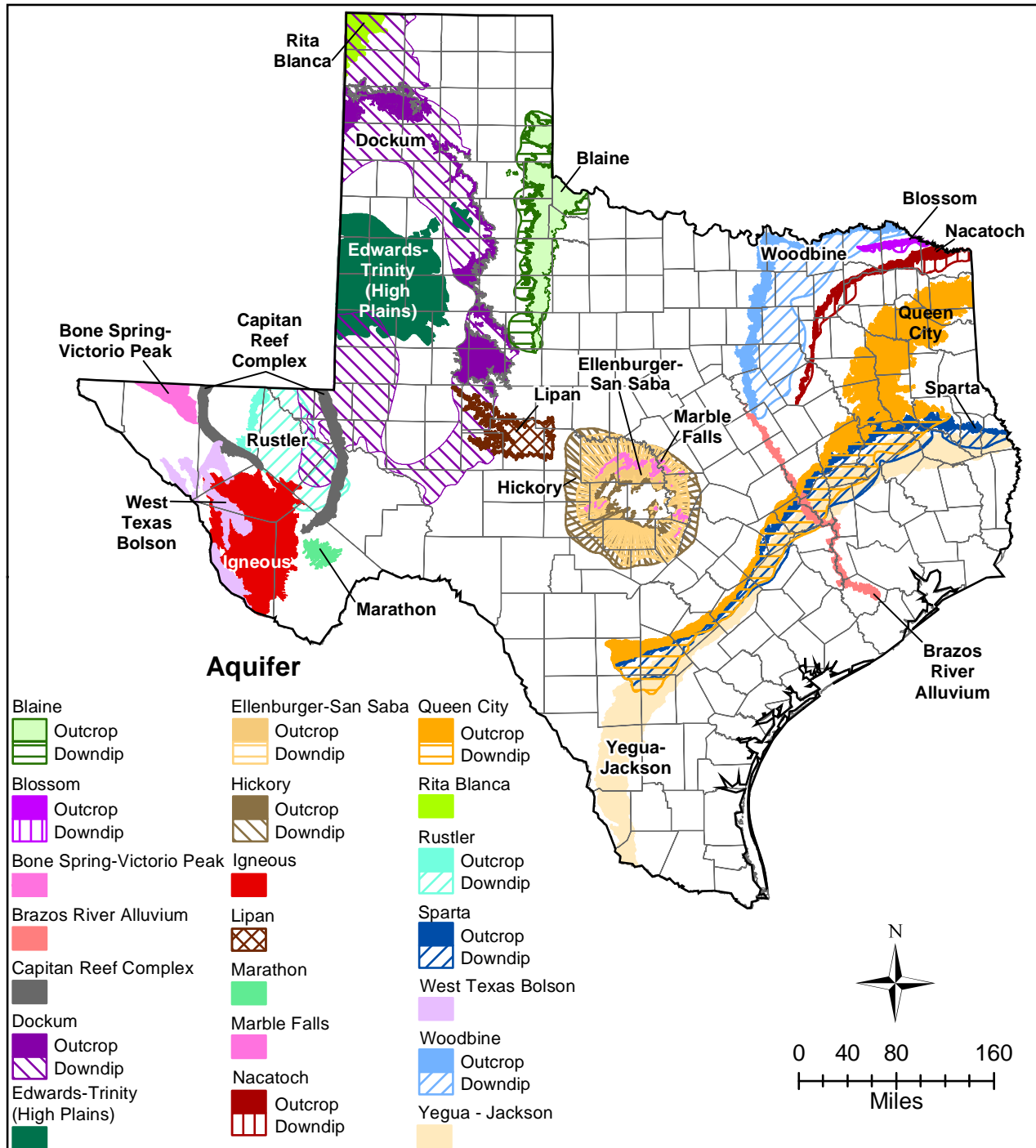
Figure 1.0.2   Locations of minor aquifers in Texas (TWDB, 2006b, 2012).
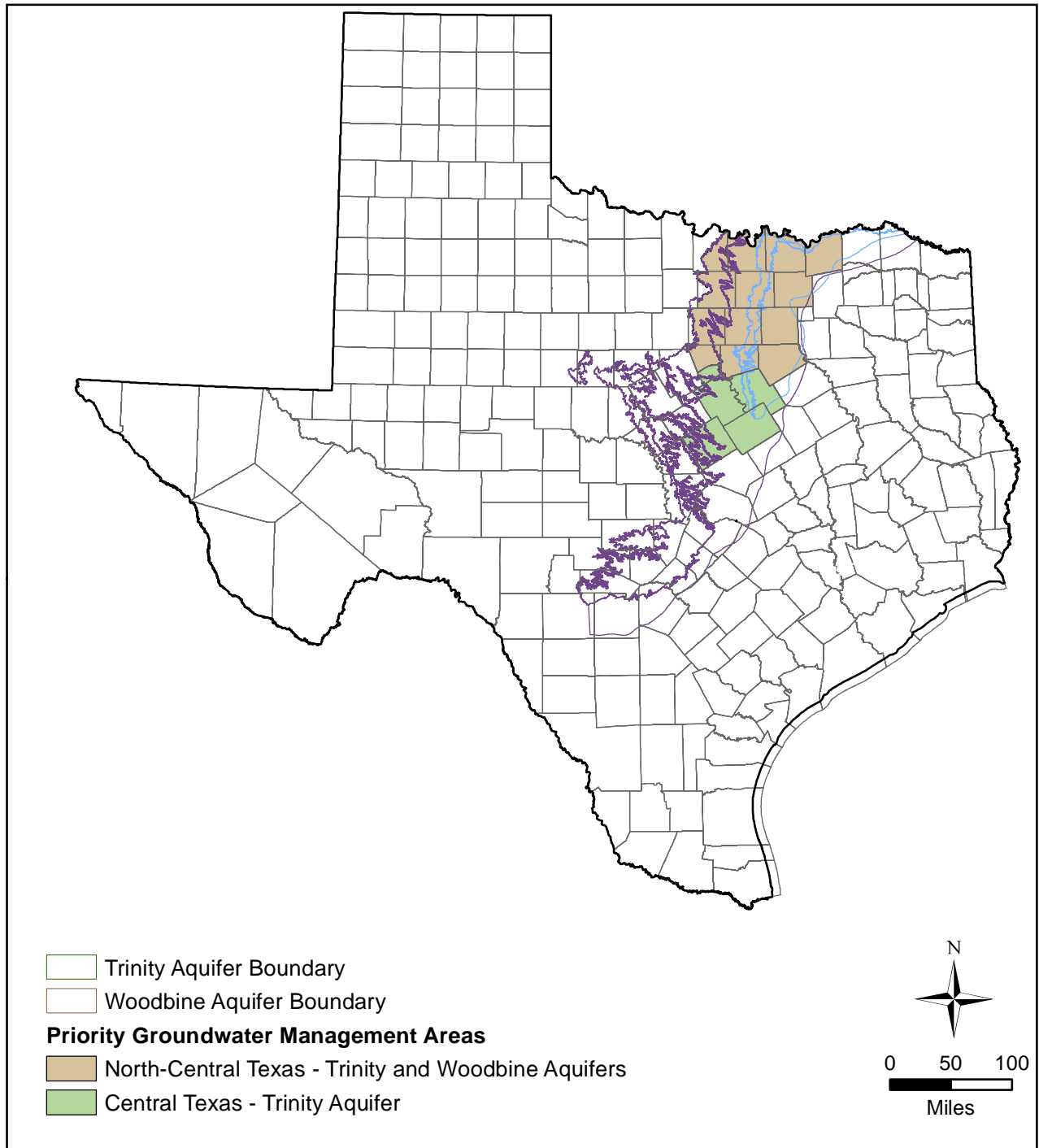
Figure 1.0.3 **Location of the Central Texas - Trinity Aquifer PGMA and the North-Central Texas - Trinity and Woodbine Aquifers PGMA.**

GMA 8
Trinity Aquifer Outcrop
Trinity Aquifer Downdip
Woodbine Aquifer Outcrop
Woodbine Aquifer Downdip
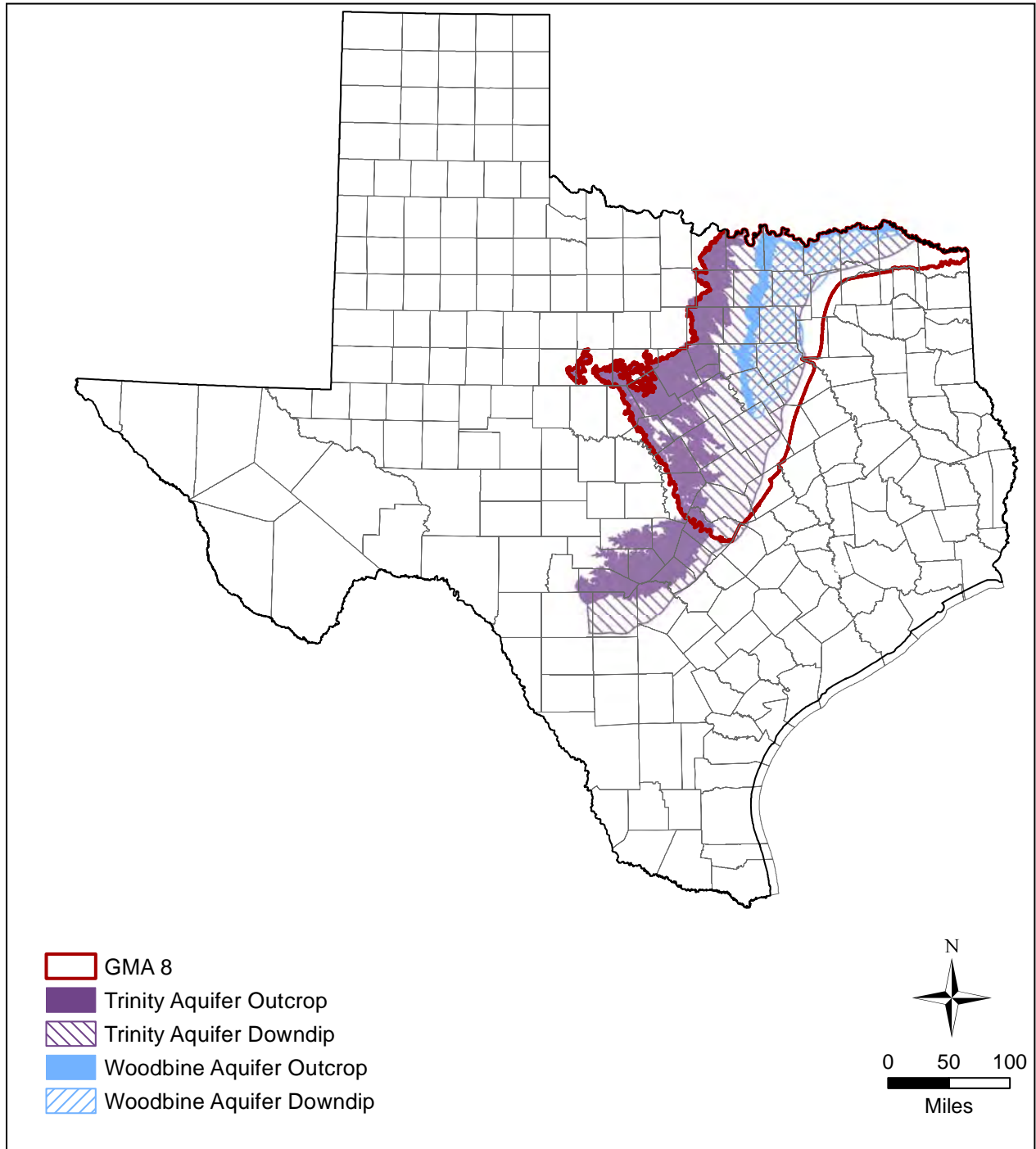
Figure 1.0.4   Location of GMA 8.

2.0   Study Area

The location of the study area, as defined by the active model boundary, for the update of the northern Trinity and Woodbine aquifers GAM is shown in Figure 2.0.1. This area includes a large portion of central and north-central Texas, a narrow band in southeastern Oklahoma, and a small portion of southwestern Arkansas. The outcrop and downdip boundaries of the northern Trinity and Woodbine aquifers in the study area are shown in Figure 2.0.2. In Texas, these boundaries are defined by the Texas Water Development Board (TWDB) (George and others, 2011; TWDB, 2012). The spatial extent of the aquifers has been extended beyond the official TWDB boundaries into Oklahoma and Arkansas based on surface geology and estimated downdip extents. The active model boundary is defined on the west and north as the contact between northern Trinity Group formations and the underlying Paleozoic-age strata, on the south by the Colorado River, and on the east by the approximate center line of the Mexia-Talco Fault Zone. The eastern boundary in Arkansas connects the eastern extent of the northern Trinity Group with the center line of the Mexia-Talco Fault Zone.

In Texas, the northern Trinity Aquifer extends across much of the central and north-central portions of the state (see Figure 2.0.2). The outcrop consists of a north-south trending band from Montague County in the north to Travis County in the south. The outcrop width varies across this band, which exists in parts of 26 counties in Texas, and is widest in the area of Callahan, Eastland, Comanche, Erath, and Somervell counties. The outcrop extends into Oklahoma and Arkansas as a relatively narrow band trending east-west. The downdip portion of the northern Trinity Aquifer lies to the east and south of the outcrop area and exists in 39 counties.

In Texas, the Woodbine Aquifer is located in the north-central portion of the State (Figure 2.0.2). The aquifer outcrops in a north-south trending band from Cooke and Grayson counties in the north to McLennan County in the south and as a narrow, east-west trending band from Grayson County in the west to Red River County in the east. The aquifer outcrops in parts of 11 Texas counties. The downdip portion of the Woodbine Aquifer lies to the east and south of the outcrop area and exists in 13 Texas counties.

Roadways, cities, and towns located in the study area are shown in Figure 2.0.3. The largest urban area in the study area is the Dallas-Fort Worth Metroplex. In general, urban areas lie along the Interstate 35 corridor in Texas from Austin to the Dallas-Fort Worth Metroplex and along U.S. 82 in the northern part of Texas and U.S. 75 from Dallas north to Sherman and Denison, Texas. Figure 2.0.4 shows the locations of rivers and lakes/reservoirs in the study area. Numerous small streams and rivers are located in the study area as well as five major rivers, which, from north to south, are the Red, Sabine, Trinity, Brazos, and Colorado rivers. Numerous large and small lakes/reservoirs are also located in the study area.

Figures 2.0.5 and 2.0.6 show the surface outcrop and downdip subcrop of the Texas major and minor aquifers, respectively, that are present in the study area. In addition to the northern Trinity Aquifer, major aquifers are the northern segment of the Edwards Balcones Fault Zone (BFZ) Aquifer and small portions of the Carrizo Aquifer outcrop and subcrop. In addition to the Woodbine Aquifer, minor aquifers include the entire Blossom Aquifer, the majority of the Nacotoch Aquifer, portions of the Brazos River Alluvium Aquifer, an insignificant portion of the Queen City Aquifer outcrop and subcrop, and small portions of the Marble Falls Aquifer outcrop, Hickory Aquifer subcrop, and Ellenburger-San Saba Aquifer outcrop and subcrop.

Portions of six RWPGs are located in the study area as shown on Figure 2.0.7. They are Region D (North East Texas), Region B, Region C, Brazos G, Region F, and Region K (Lower Colorado). Six GCDs and portions of nine other GCDs are located in the study area. Figure 2.0.8 and Table 2.0.1 provide the locations of and list, respectively, these GCDs. The study area includes most of GMA 8 and small portions of GMAs 6, 11, and 12 (Figure 2.0.9). River authorities in the study area include the Red River Authority, Sulphur River Basin Authority, Sabine River Authority, Trinity River Authority, Brazos River Authority, and Lower Colorado River Authority (Figure 2.0.10). The study area includes portions of six river basins (Figure 2.0.11). These are the Red, Sulphur, Sabine, Trinity, Brazos, and Colorado river basins.

Table 2.0.1   Texas GCDs in the study Area.

GCDs Located in the Study Area	GCDs Located Partially in the Study Area
Clearwater UWCD	Brazos Valley GCD
North Texas GCD	Central Texas GCD
Northern Trinity GCD	Fox Crossing WD
Prairielands GCD	Lost Pines GCD
Red River GCD	Middle Trinity GCD
Southern Trinity GCD	Neches & Trinity Valleys GCD
	Post Oak Savannah GCD
	Saratoga UWCD
	Upper Trinity GCD

UWCD – Underground Water Conservation District

Table 2.0.2   River basins and approximate river length and river basin area in the study area.

River Basin	Approximate River Length (miles)	Approximate River Basin Area (square miles)
Brazos	259	13,860
Colorado	145	1,879
Red	1,010	9,634
Sabine	23	542
Sulphur	56	2,267
Trinity	199	9,455
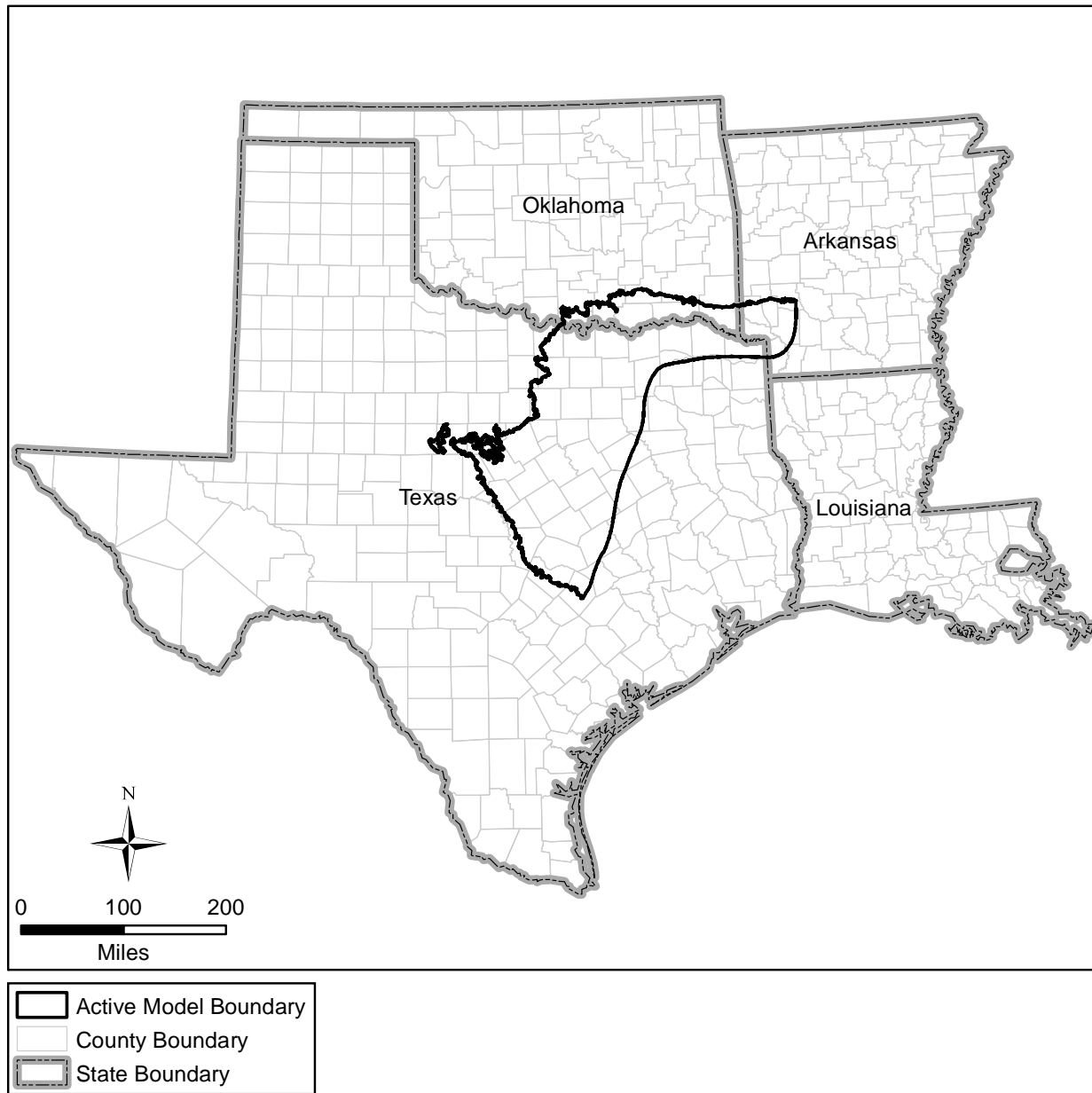
Figure 2.0.1   Study area for the updated northern Trinity and Woodbine aquifers GAM.
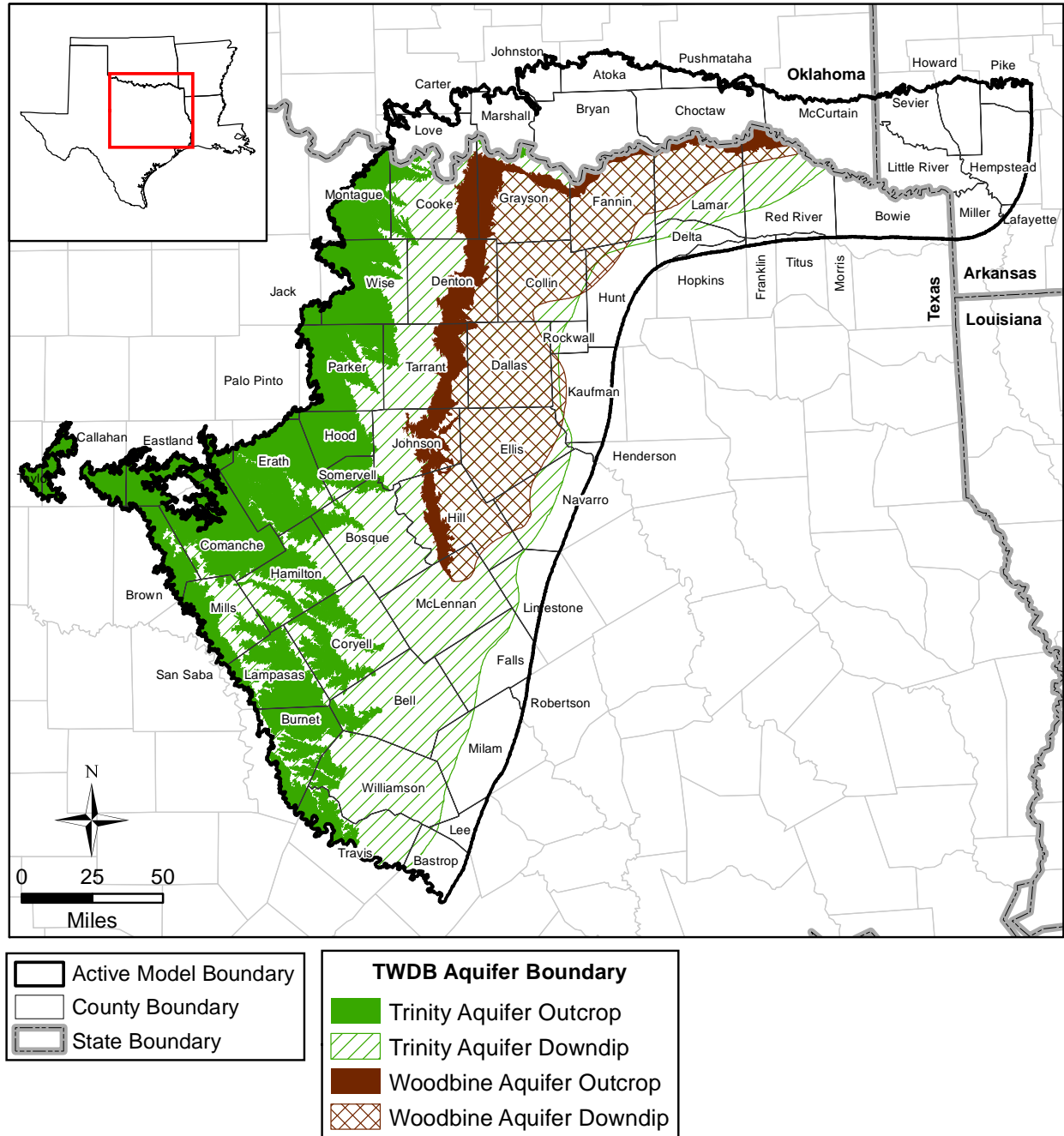
Figure 2.0.2 **Boundaries for the northern Trinity and Woodbine aquifers in the study area as determined by the TWDB in Texas (TWDB, 2006a, b, 2012) and extrapolated into Oklahoma and Arkansas.**
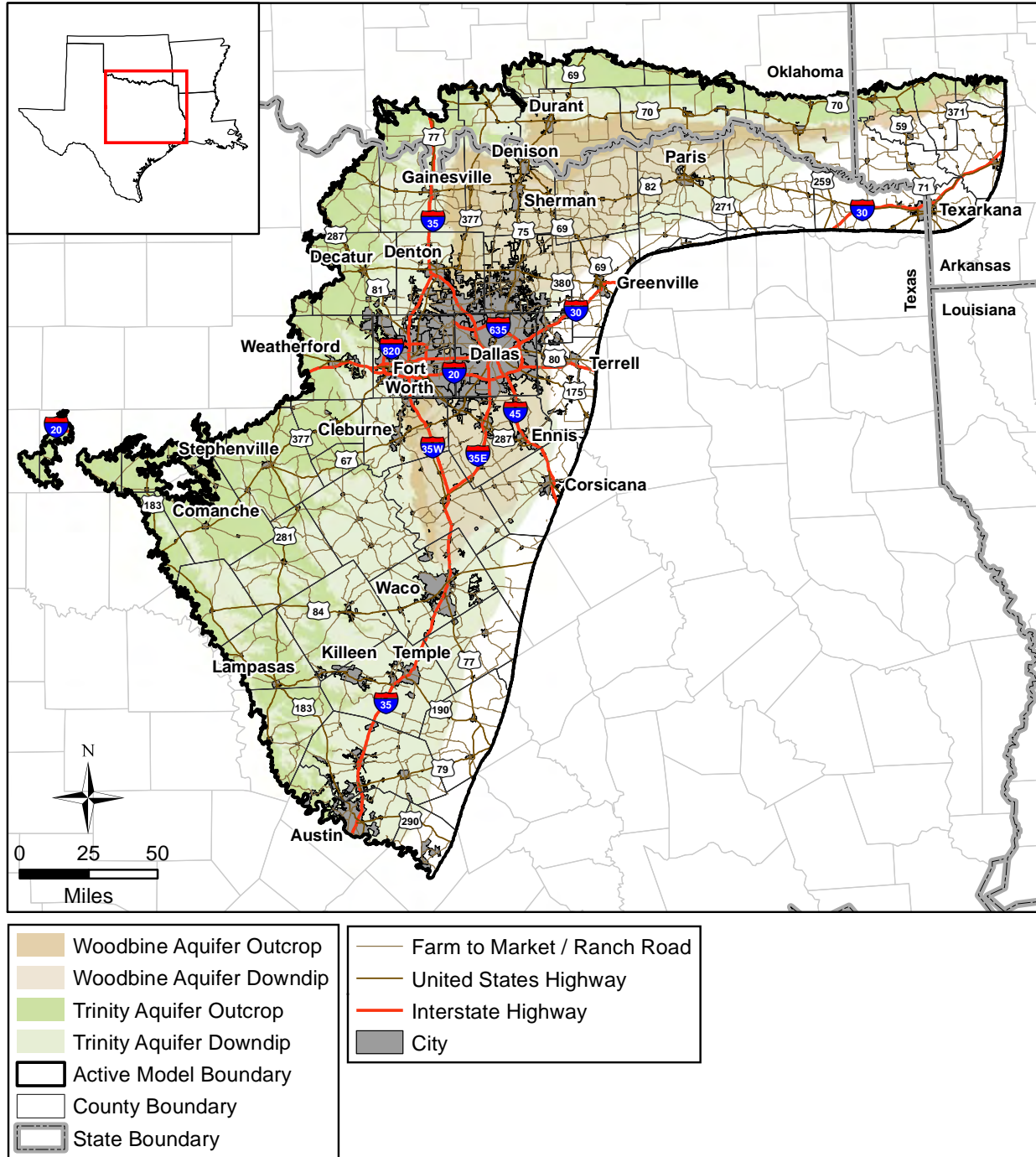
Figure 2.0.3   Cities and major roadways in the study area.
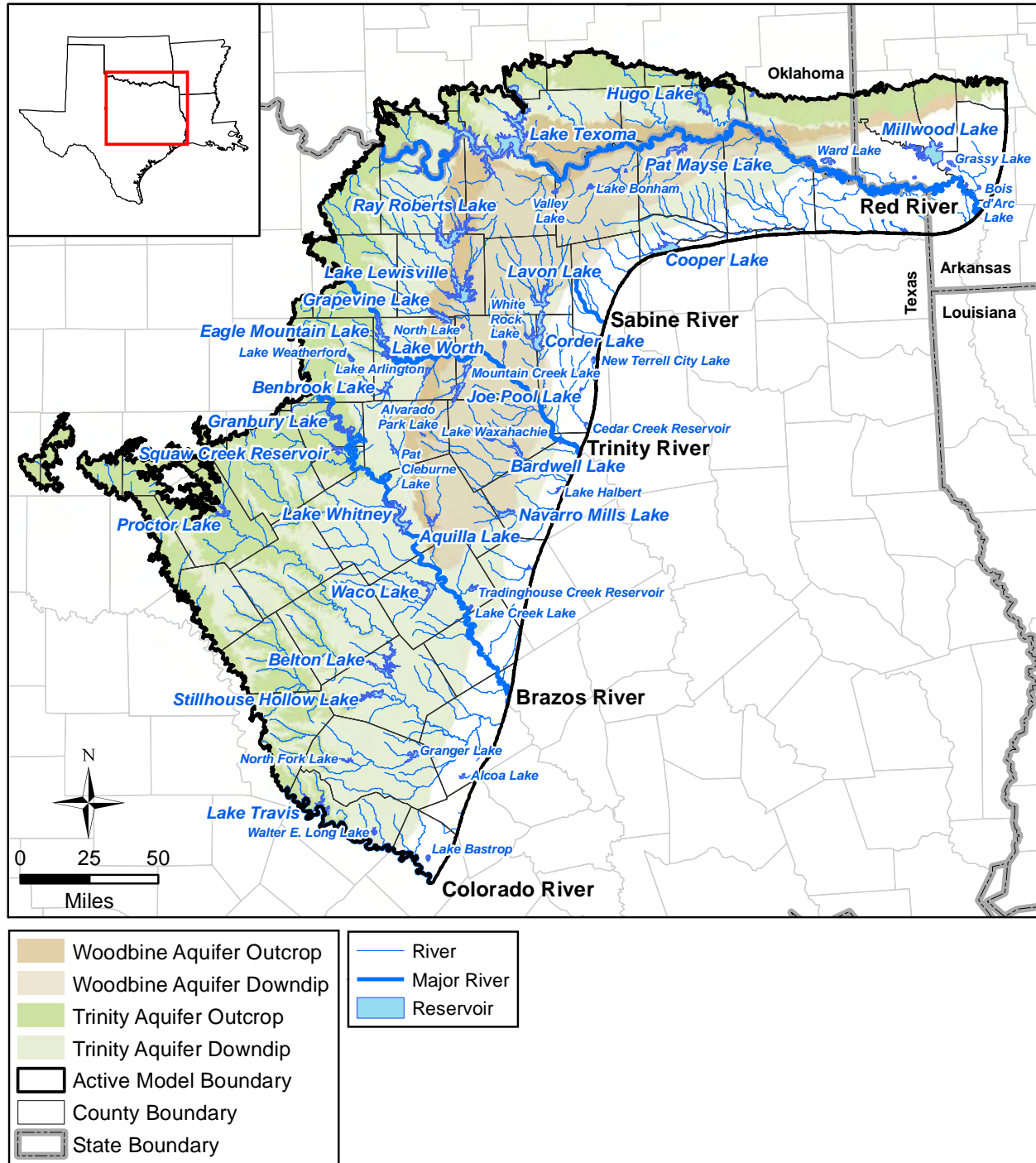
Figure 2.0.4   Rivers, streams, lakes, and reservoirs in the study area.
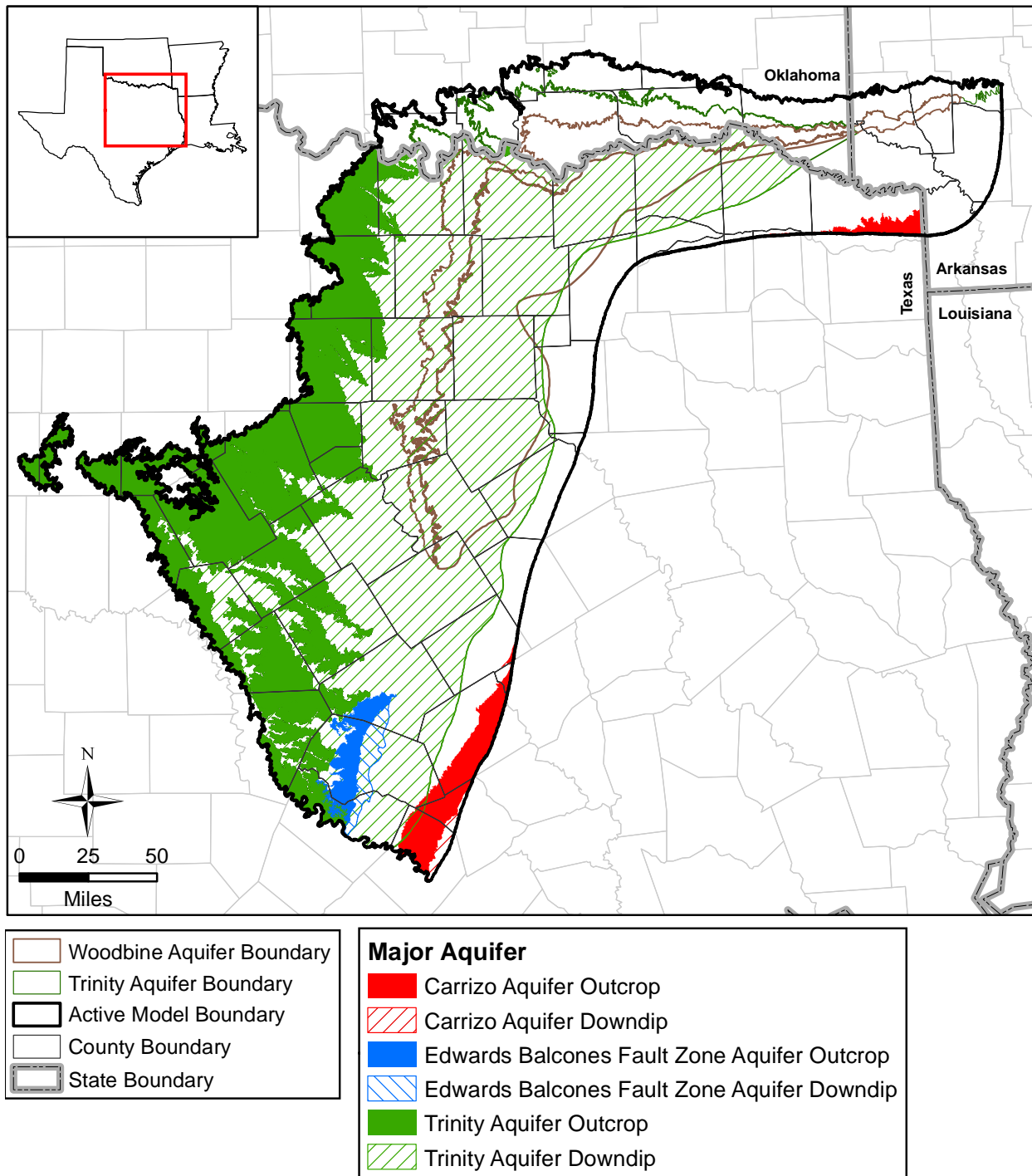
Figure 2.0.5   Major Texas aquifers in the study area (TWDB, 2006a, 2012).
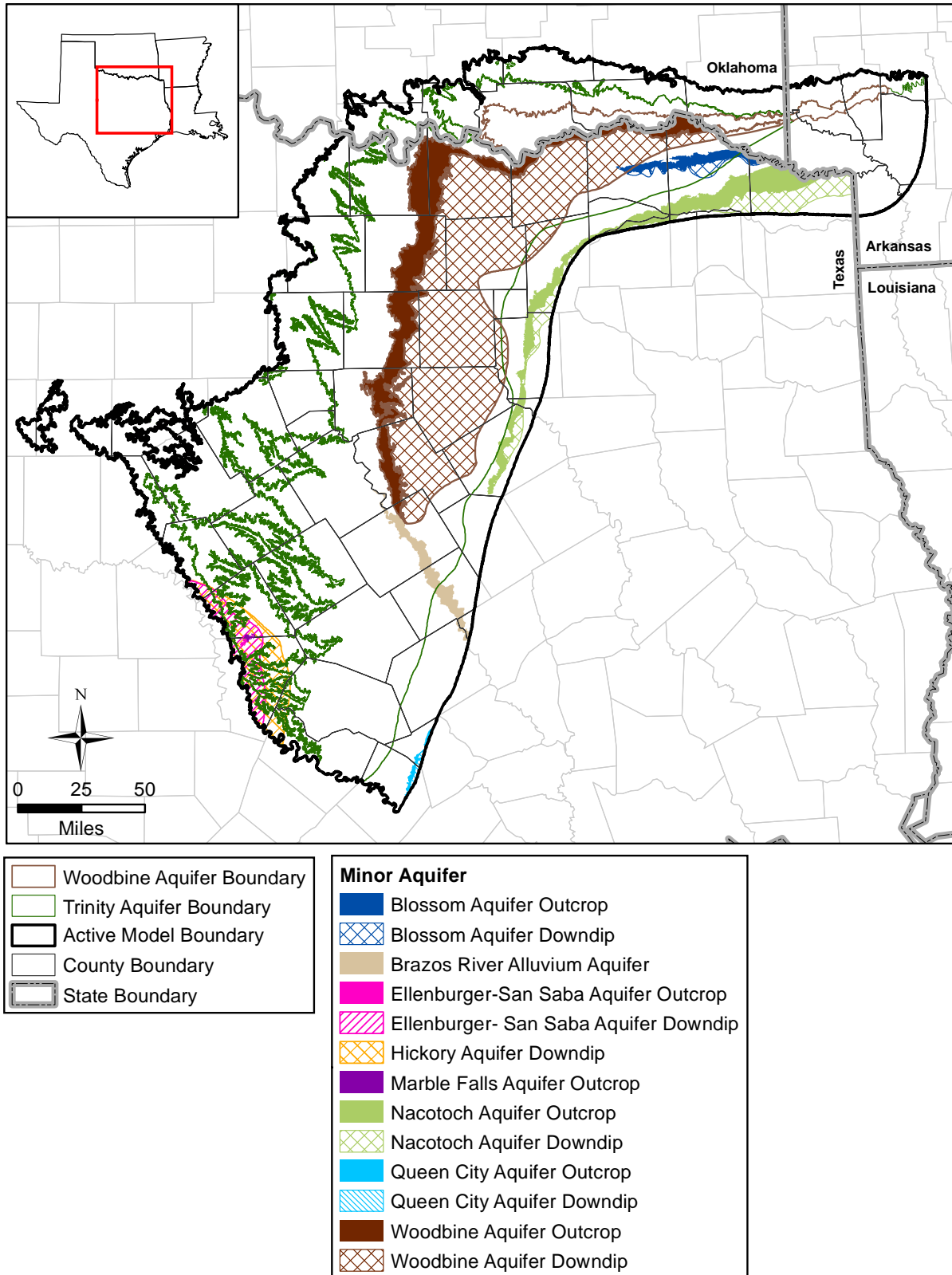
Figure 2.0.6   Minor Texas aquifers in the study area (TWDB, 2006b, 2012).
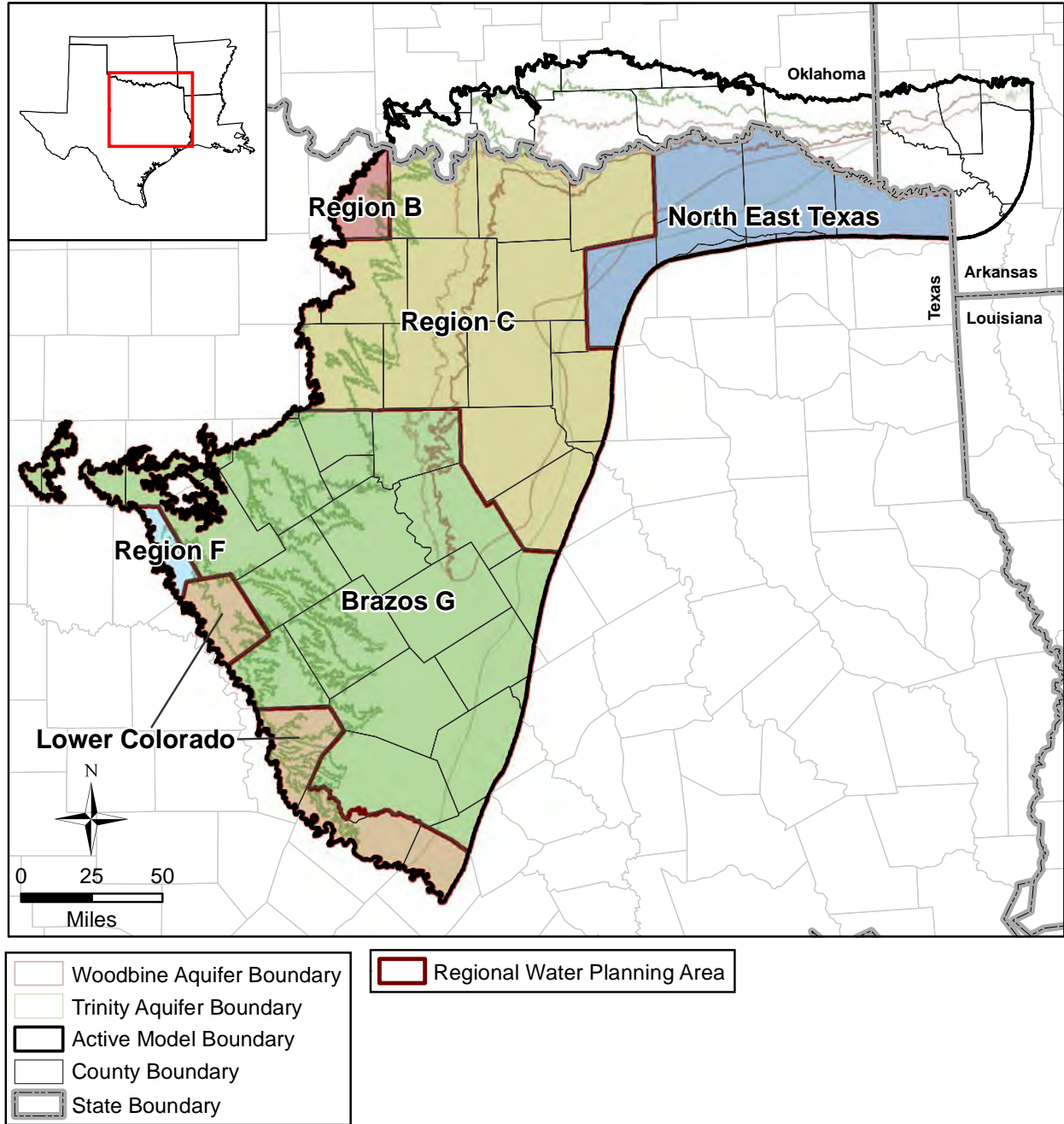
Figure 2.0.7   Texas RWPGs in the study area (TWDB, 2008).
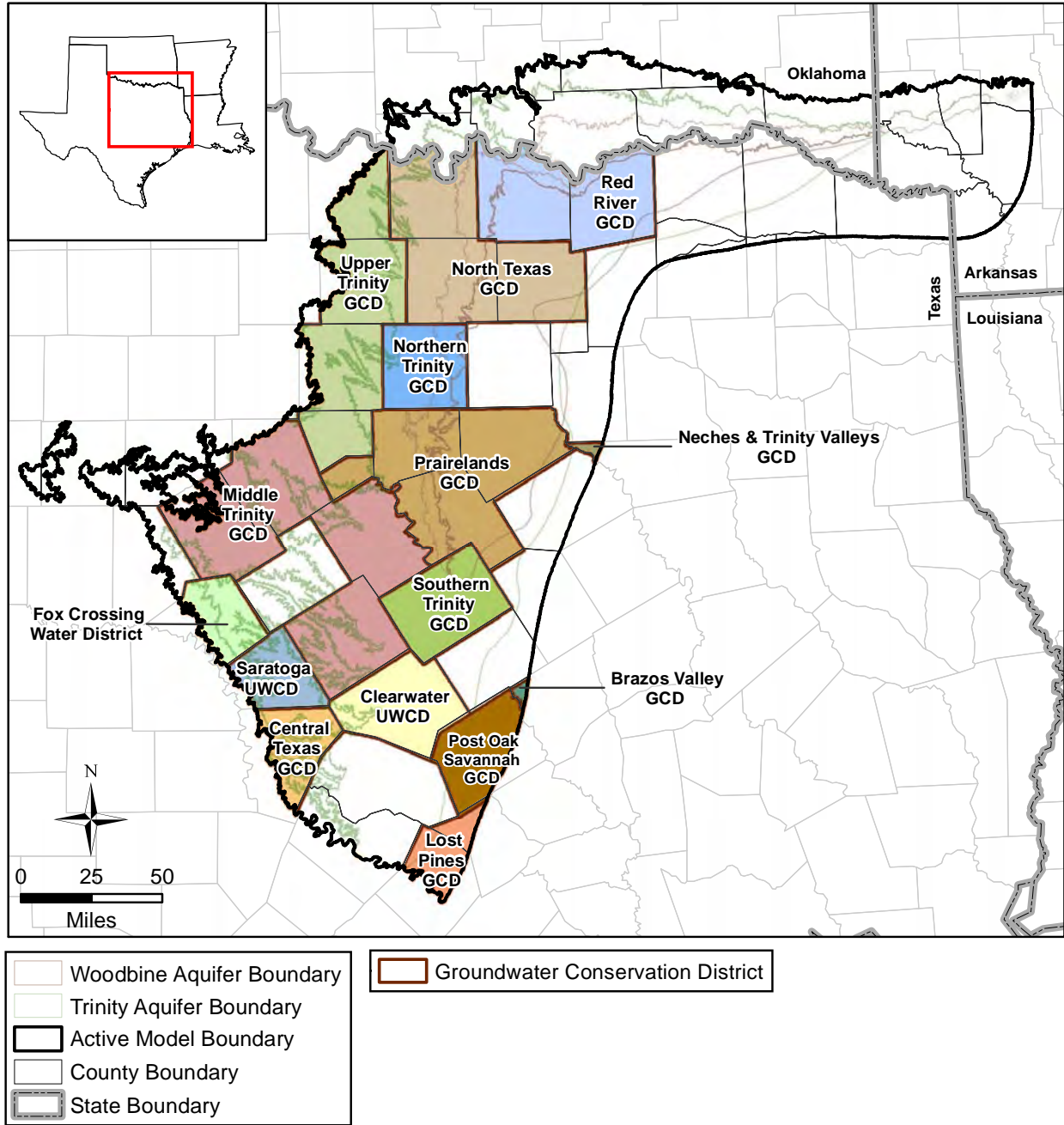
Figure 2.0.8   Texas GCDs in the study area (TWDB, 2010a).
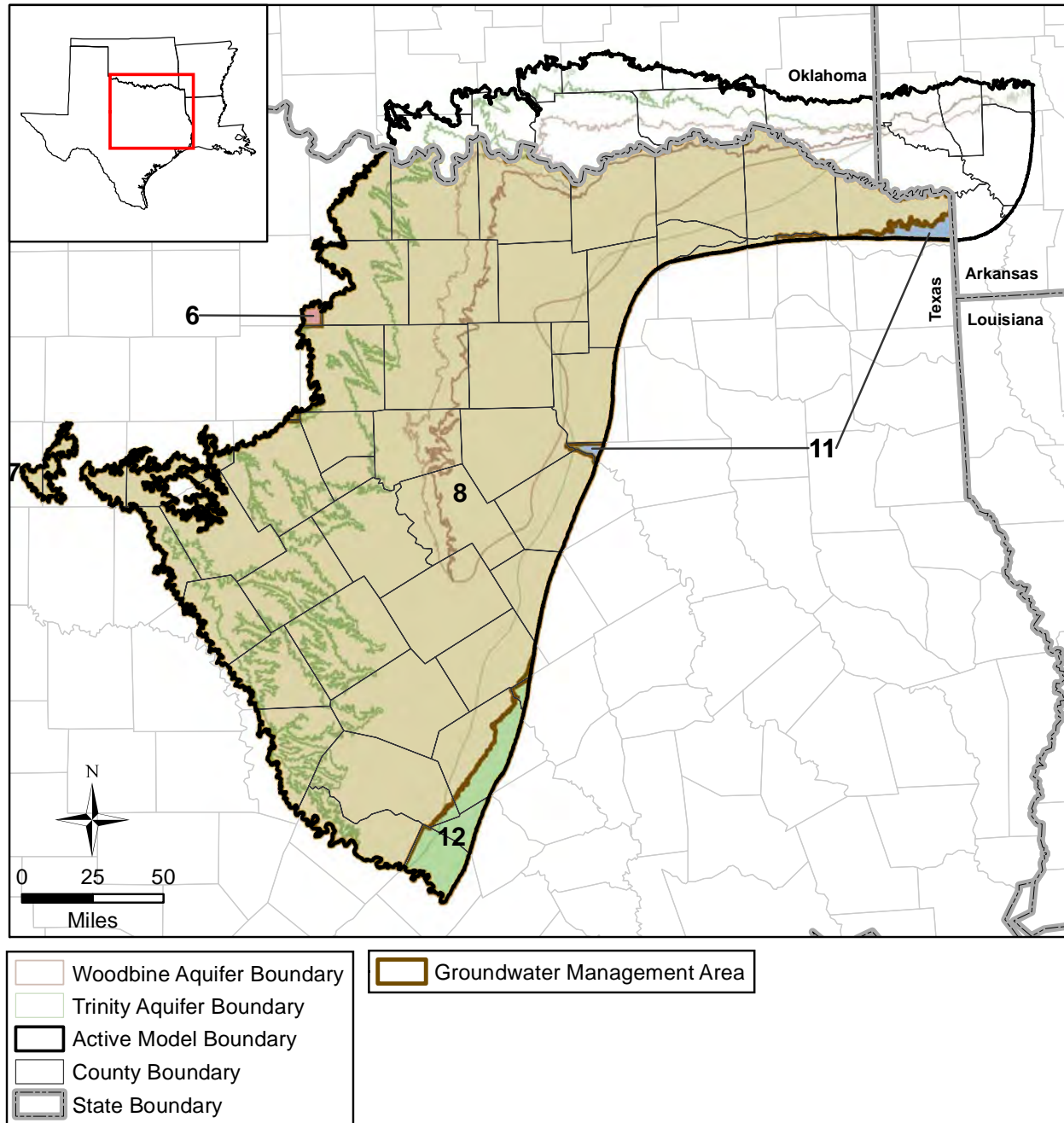
Figure 2.0.9   Texas GMAs in the study area (TWDB, 2007b).
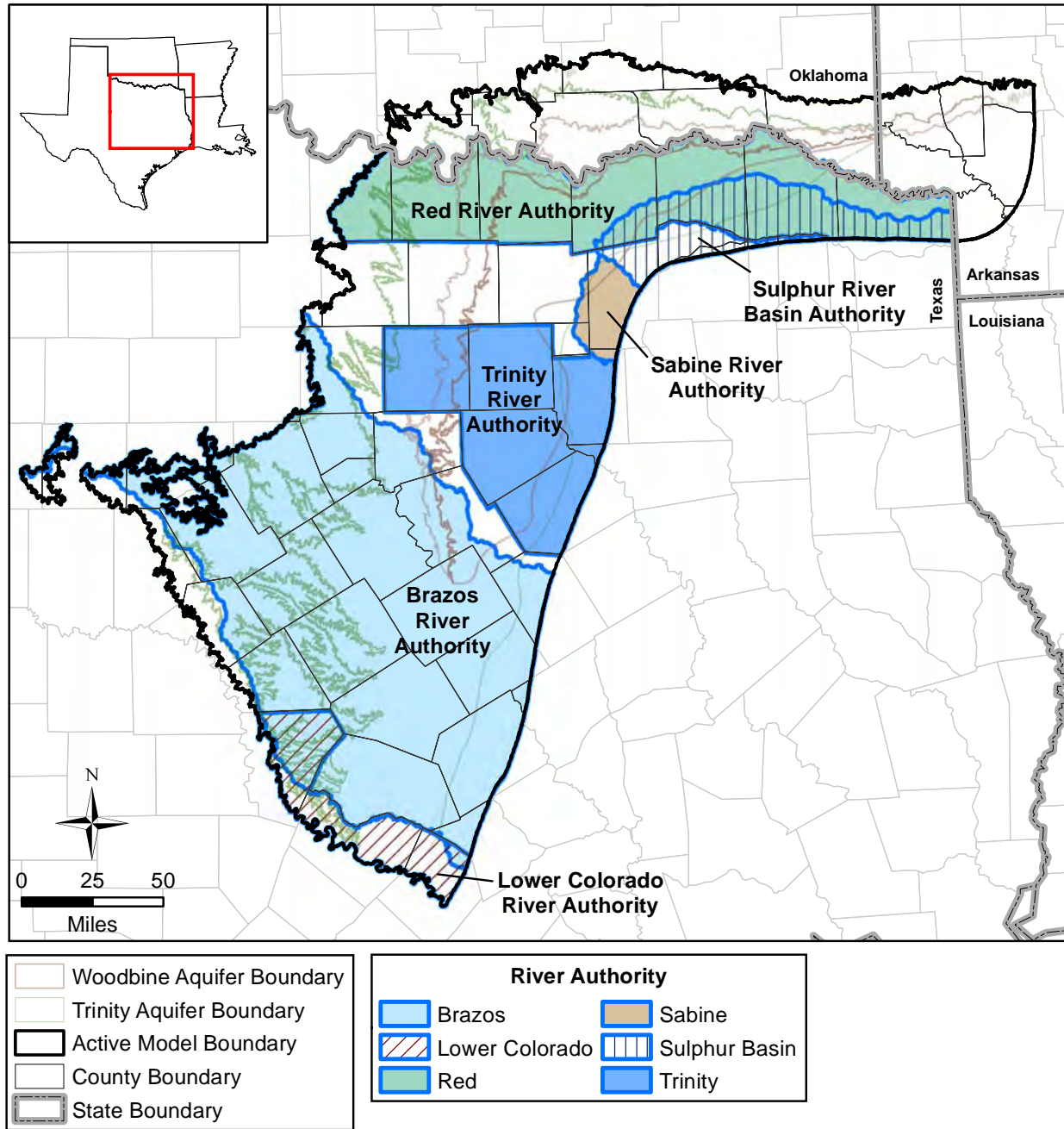
Figure 2.0.10   Texas river authorities in the study area (TWDB, 1999).
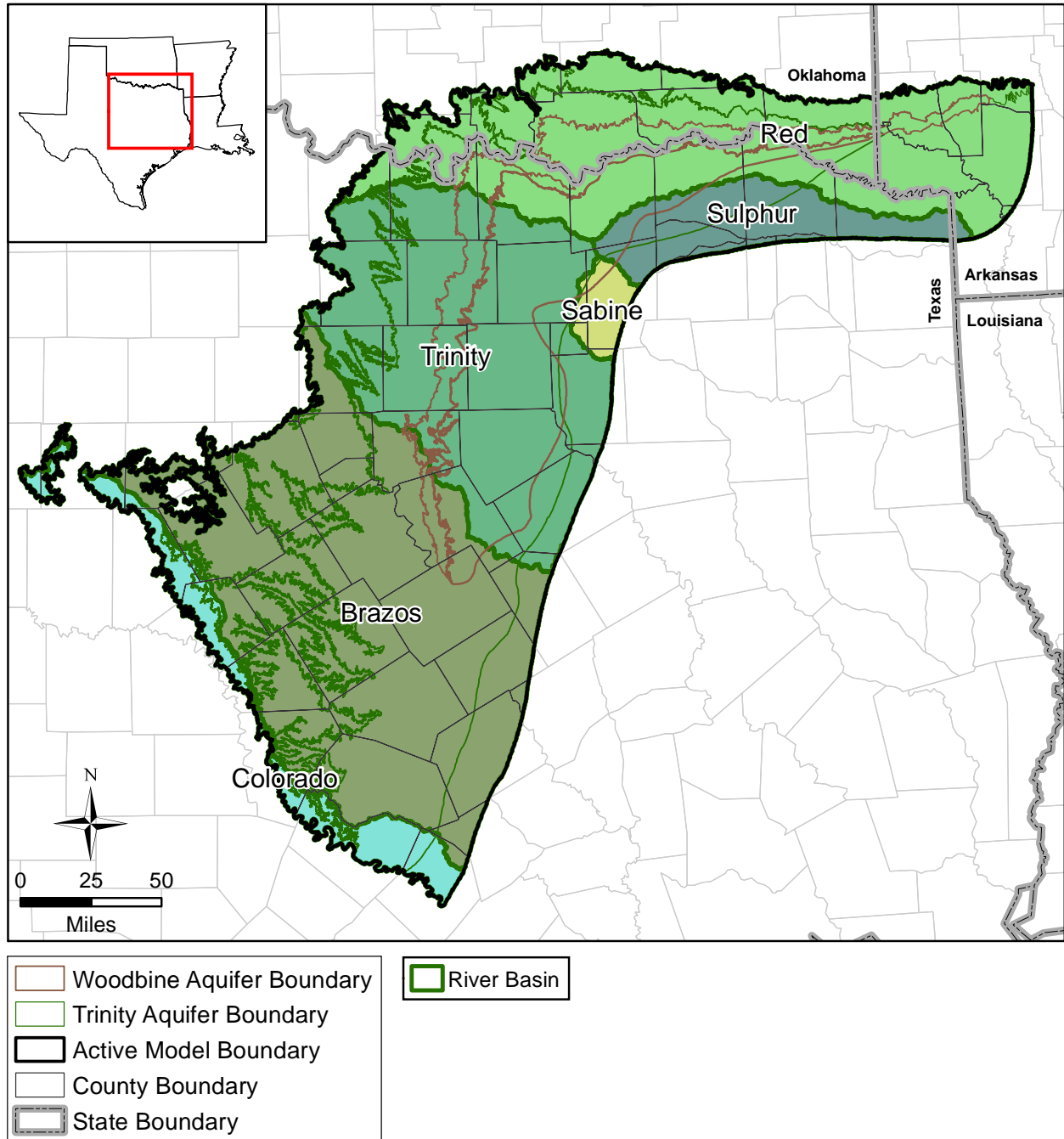
Figure 2.0.11   Major river basins in the study area (TWDB, 2010b; Oklahoma Water Resources Board, 2013; U.S. Department of Agriculture, 2013).

2.1   Physiography and Climate

The study area is located in the Coastal Plain, Central Lowland, and Great Plains physiographic provinces [United States Geological Survey (USGS), 2002] (Figure 2.1.1). In addition to these physiographic regions defined at the national level, in an earlier study, Wermund (1996) defined the Texas Physiographic Provinces. He divides the study area in Texas into the Blackland Prairies, Grand Prairie, and Edwards Plateau. Wermund (1996) describes the Blackland Prairies as a gently rolling surface with deep, fertile soil; the Grand Prairie as a well exposed plateau-like surface dissected by numerous streams and having rocky soil; and the Edwards Plateau as a limestone plateau entrenched with local streams.

Figure 2.1.2 plots the Level III Ecological Regions in the study area. The regions in Texas are based on a study funded by the TCEQ (Griffith and others, 2007). Ecological regions (also referred to as ecoregions) denote areas of general similarity in ecosystems and in the type, quality, and quantity of environmental resources. The definition of an ecological framework is a valuable tool for environmental research, assessment, management, and monitoring of ecosystems and ecosystem components. There are six ecological regions within the study area: the South Central Plains, East Central Texas Plains, Texas Black-Land Prairies, Cross Timber, Edwards Plateau, and Central Great Plains.

The following descriptions of the ecological regions are taken from Griffith and others (2007). The Southern Central Plains ecological region is locally termed the Piney Woods and represents the western edge of the southern coniferous forest belt. Two thirds of the region in Texas can be characterized by forests and woodlands and soils are predominantly acidic sands and sandy loams. The East Central Texas Plains ecological region is also known as the Post Oak Savannah because it was originally covered by post oak savannah type vegetation. Most of this region is currently pasture land. The soils in this region are dominantly acidic sandy loam along ridges and clay loams in the lowlands. Many areas have an underlying hard pan which inhibits moisture infiltration and, for this reason, the East Central Texas Plains ecological region has also been called the hardpan.

The Texas Black Land Prairie is the dominant ecological region east of the Woodbine Aquifer outcrop. This region is typified by fine-textured, clayey soils and tends to include a higher percentage of cropland than surrounding ecological regions. The Cross Timbers ecological region is a transitional region of forest, prairie, woodland and savannah. This ecological region overlies both the northern Trinity and Woodbine aquifer outcrops, which are recharge areas for the aquifers. The Edwards Plateau ecological region is typified by a hilly, dissected limestone plateau with ground cover consisting mostly of juniper-oak savannah and mesquite-oak savannah. Soils in this region can be very thin or reasonably thick and developed over clayey or marl geologic units. The Central Great Plains ecological region was once grassland but is now transitional prairie. Soils in this region are deep except on highlands.

Figure 2.1.3 shows the topography in the study area. In general, the ground surface elevation decreases from west to east. The maximum elevation of about 2,500 feet is observed in Taylor and Callahan counties and the lowest elevations are observed along the stream valleys in southwest Arkansas and northeast Texas. The drainage features of the major rivers can clearly be seen in the topographic gradients in much of the study area, although the drainage patterns are somewhat muted as the terrain flattens to the east.

The climate in the study area is classified as Subtropical, or Modified Marine climate, as defined in Larkin and Bomar (1983) (Figure 2.1.4). Onshore flow of air from the Gulf of Mexico causes the marine climate. Distinctions in the climate occur based on the moisture content of the maritime air. Air from the Gulf of Mexico decreases in moisture content from east to west as it travels across the State. Intrusion of continental air into the maritime air occurs seasonally and also affects the moisture content of the air. In the study area, the Subtropical classification is subdivided based on this moisture content into Humid and Subhumid regions. The Woodbine Aquifer outcrop essentially falls on the transition zone between the Humid and Subhumid classification so that the eastern part of the study area is Humid and the western part is Subhumid. Subtropical Humid climate is most noted for warm summers and Subtropical Subhumid climate is characterized by hot summers and dry winters.

Parameter-elevation Regressions on Independent Slopes Model (PRISM) datasets developed and presented online by Oregon State University provide distributions of average annual temperature

and precipitation across the conterminous United States (U.S.) for the 30-year period 1981 to 2010 (PRISM Climate Group, 2014). Based on these data, the average annual temperature in the study area ranges from a low of 61 degrees Fahrenheit in the north to a high of 69 degrees Fahrenheit in the south (Figure 2.1.5). The average annual precipitation decreases across the study area from the northeast to the southwest and from a high of 57 inches at the northeastern boundary to a low of 26 inches in the southwest.

Precipitation data are available at over 131 Texas stations within the study area (Figure 2.1.7) from as early as 1931 through the present. Measurement of precipitation at most gages began in the 1940s or 1950s. In general, measurements are not continuous on a month-by-month or year-by-year basis for the gages. Examples of the historical variation in annual precipitation at a few selected gages are shown in Figure 2.1.8. The long-term monthly variation in precipitation for these same selected gages is shown in Figure 2.1.9. For each selected gage, the time period for the monthly average precipitations shown in Figure 2.1.9 is the same as the time period for the annual precipitation shown in Figure 2.1.8 The monthly average data indicate that precipitation peaks in late spring to early summer, and again in early fall.

Average annual lake evaporation in the study area ranges from a high of 63 inches per year in the west to a low of 40 inches per year in the east (TWDB, 2009), as shown in Figure 2.1.10. The evaporation rates in the western portion of the study area significantly exceed the average annual rainfall, with deficits (evaporation exceeds precipitation) of over 30 inches per year. Most of the study area has a precipitation deficit, with the exception of the northeast portion, where evaporation rates are approximately similar or slightly less than average annual rainfall rates. Monthly variations in lake surface evaporation are shown in Figure 2.1.11 for five locations in the study area. These values represent the average of the monthly lake surface evaporation data from January 1954 through December 2011. Figure 2.1.11 shows that average lake evaporation peaks in July.
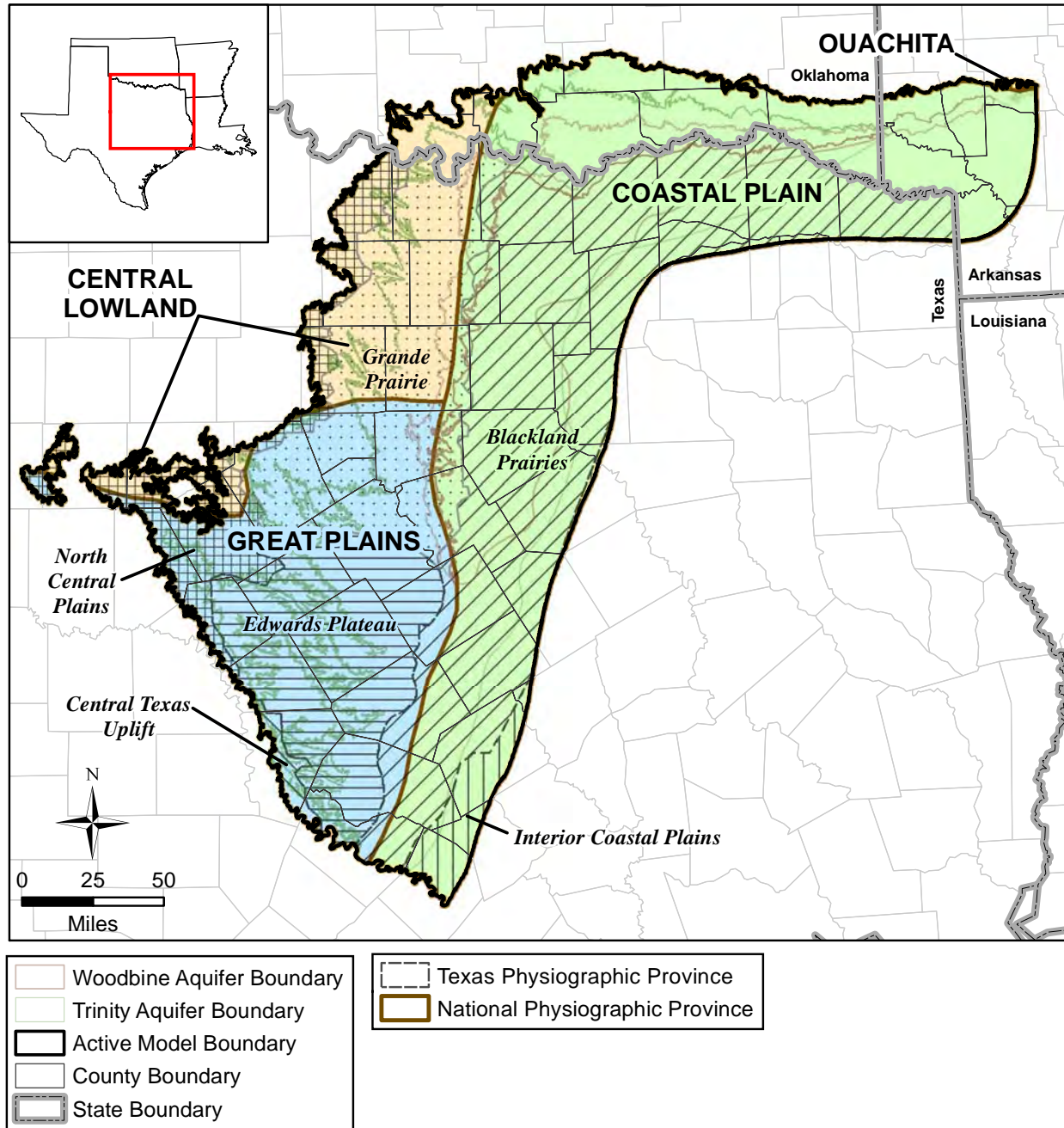
Figure 2.1.1   **Physiographic provinces in the study area.**
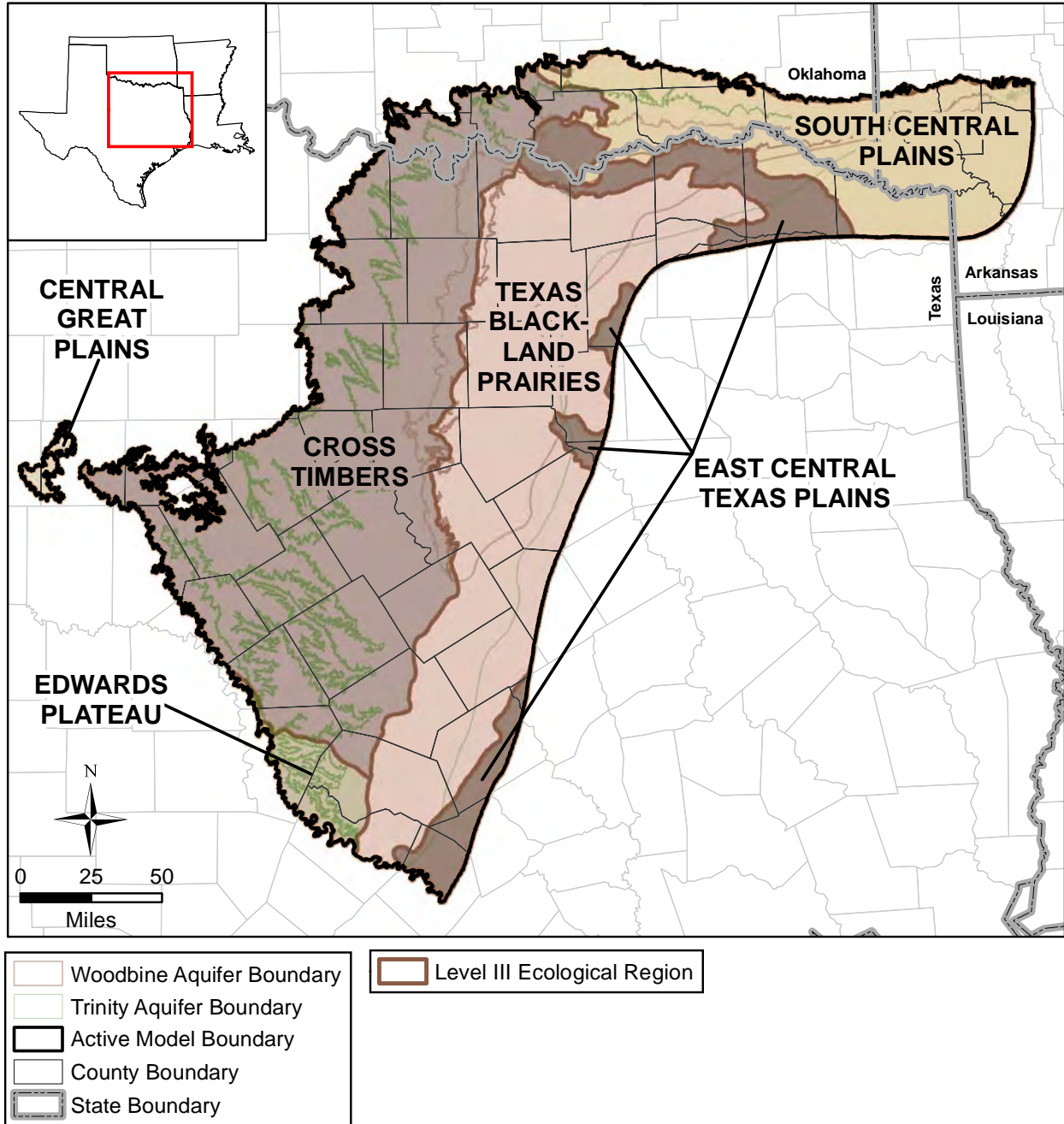
Figure 2.1.2   Level III ecological regions in the study area.
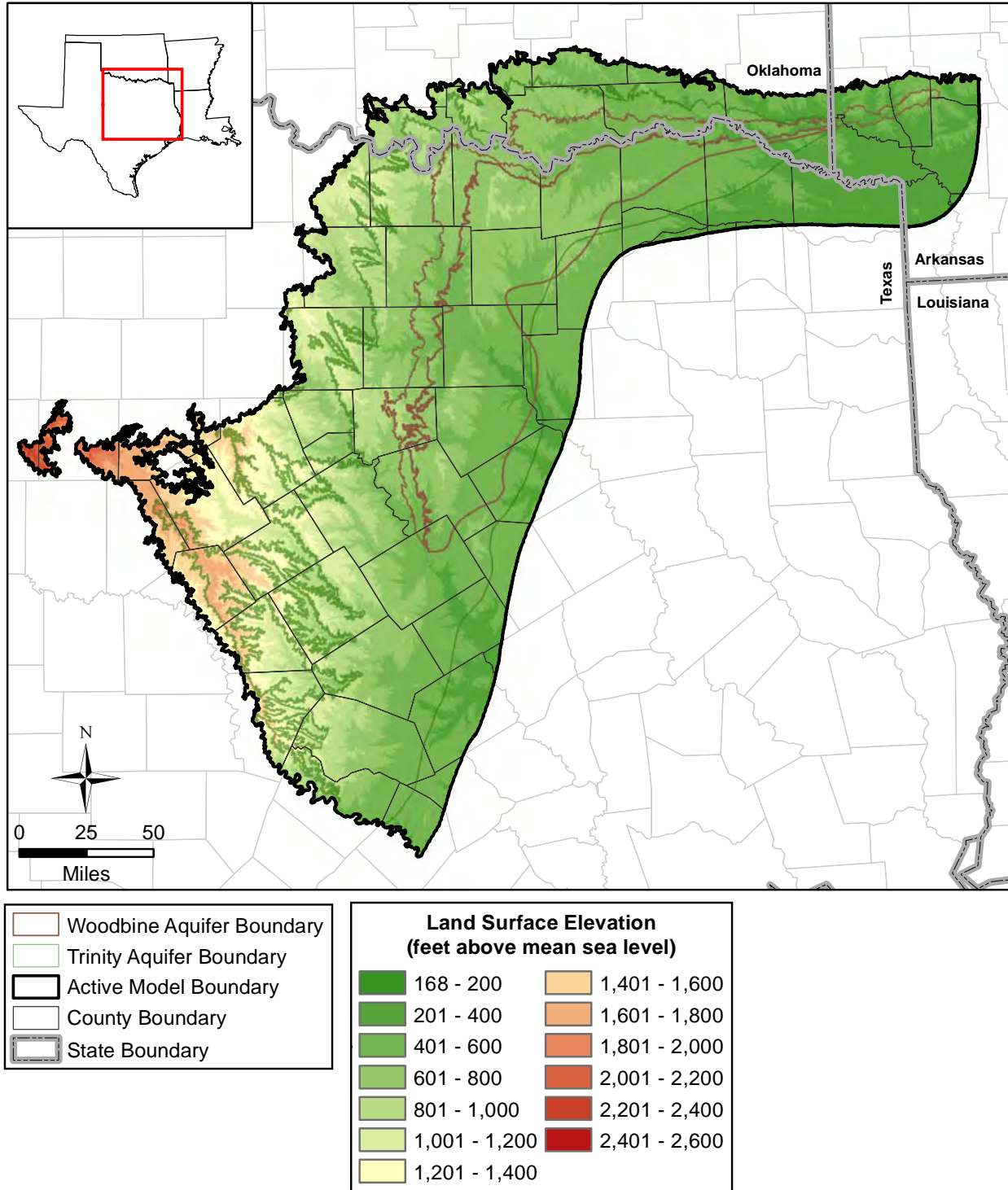
Figure 2.1.3   Topographic map of the study area showing land surface elevation in feet above mean sea level (amsl).
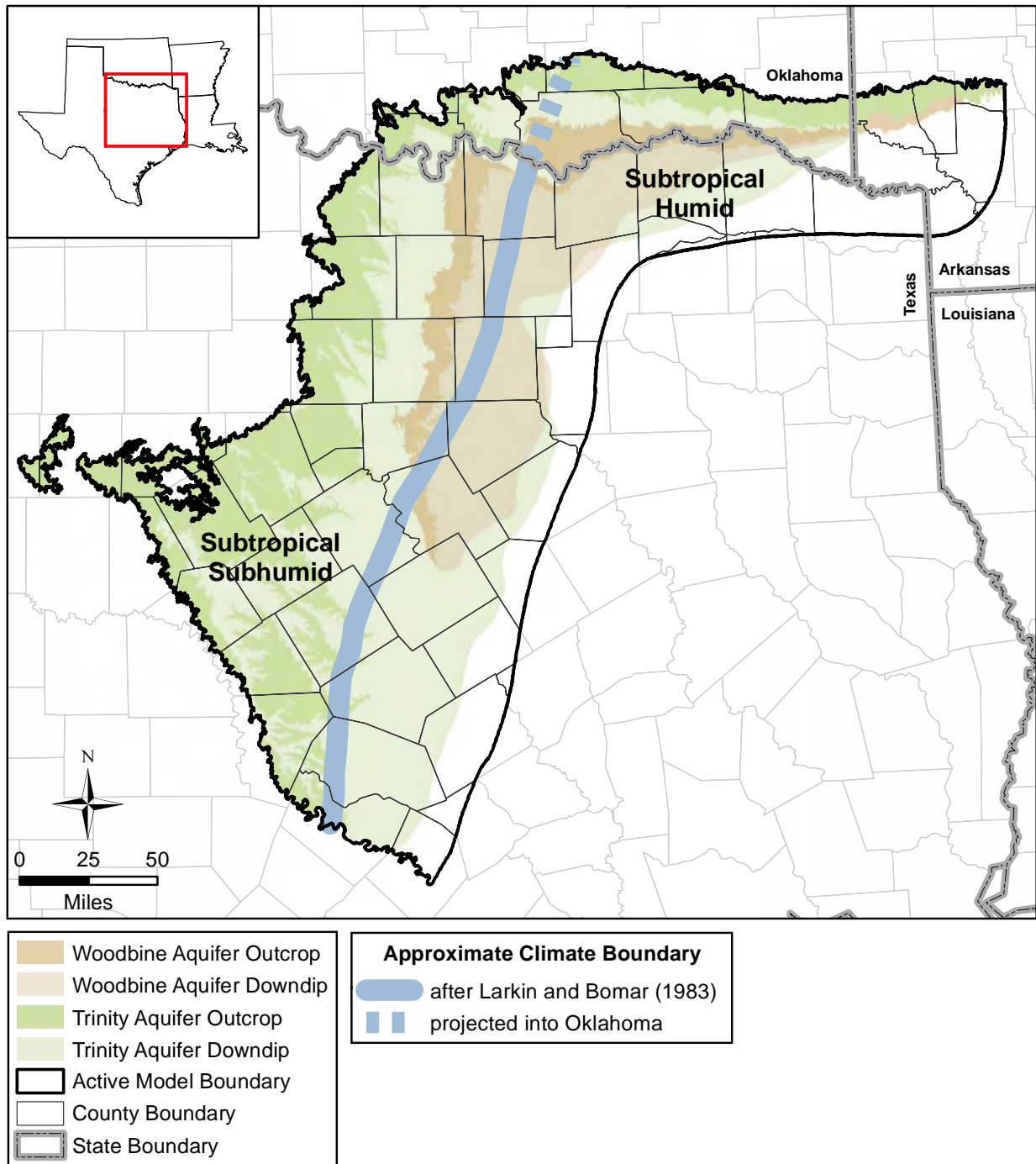
Figure 2.1.4   Climate classifications in the Texas portion of the study area.
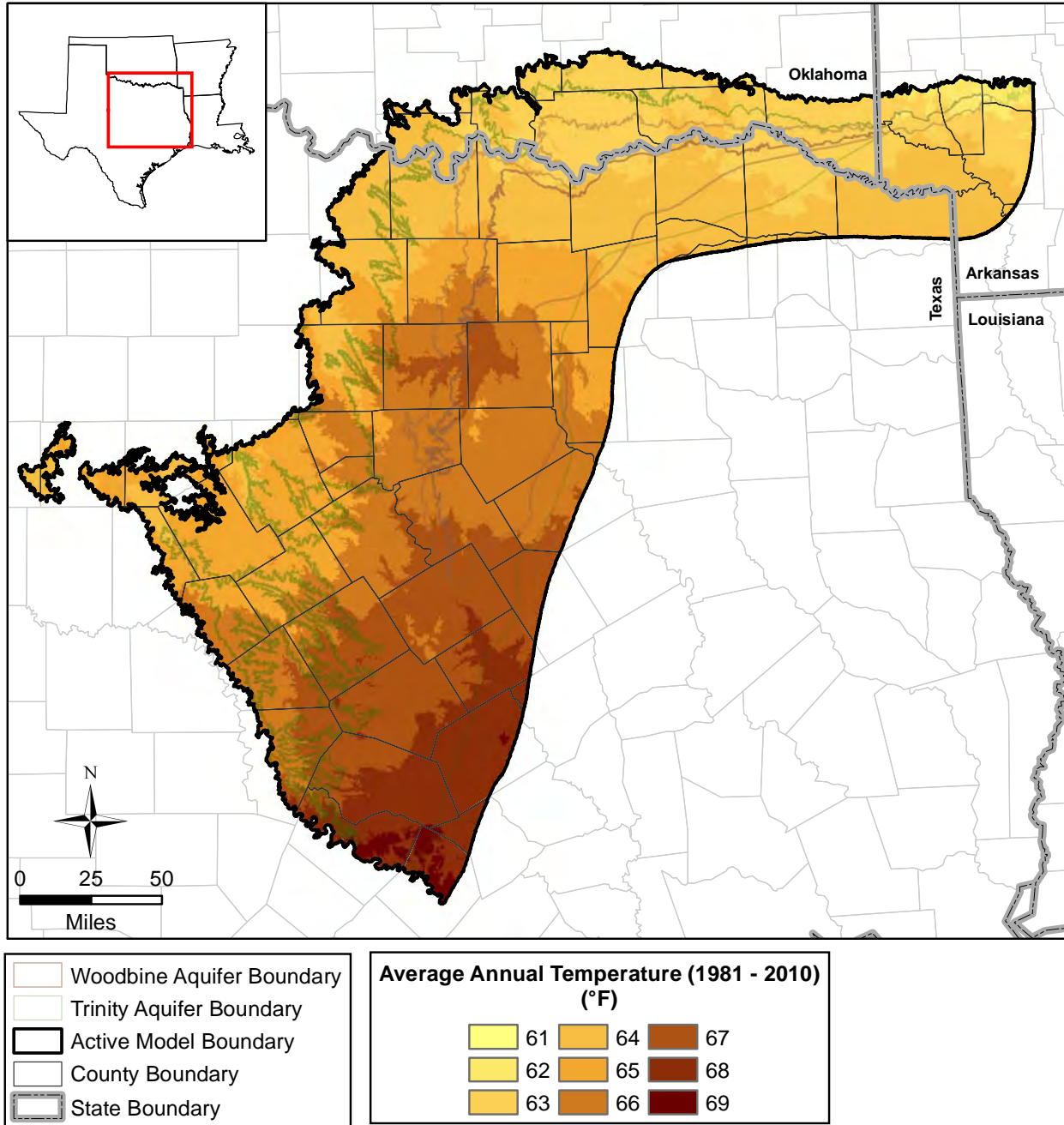
Figure 2.1.5   **Average annual air temperature in degrees Fahrenheit for the study area for the time period 1981 to 2010 (PRISM Climate Group, 2014).**
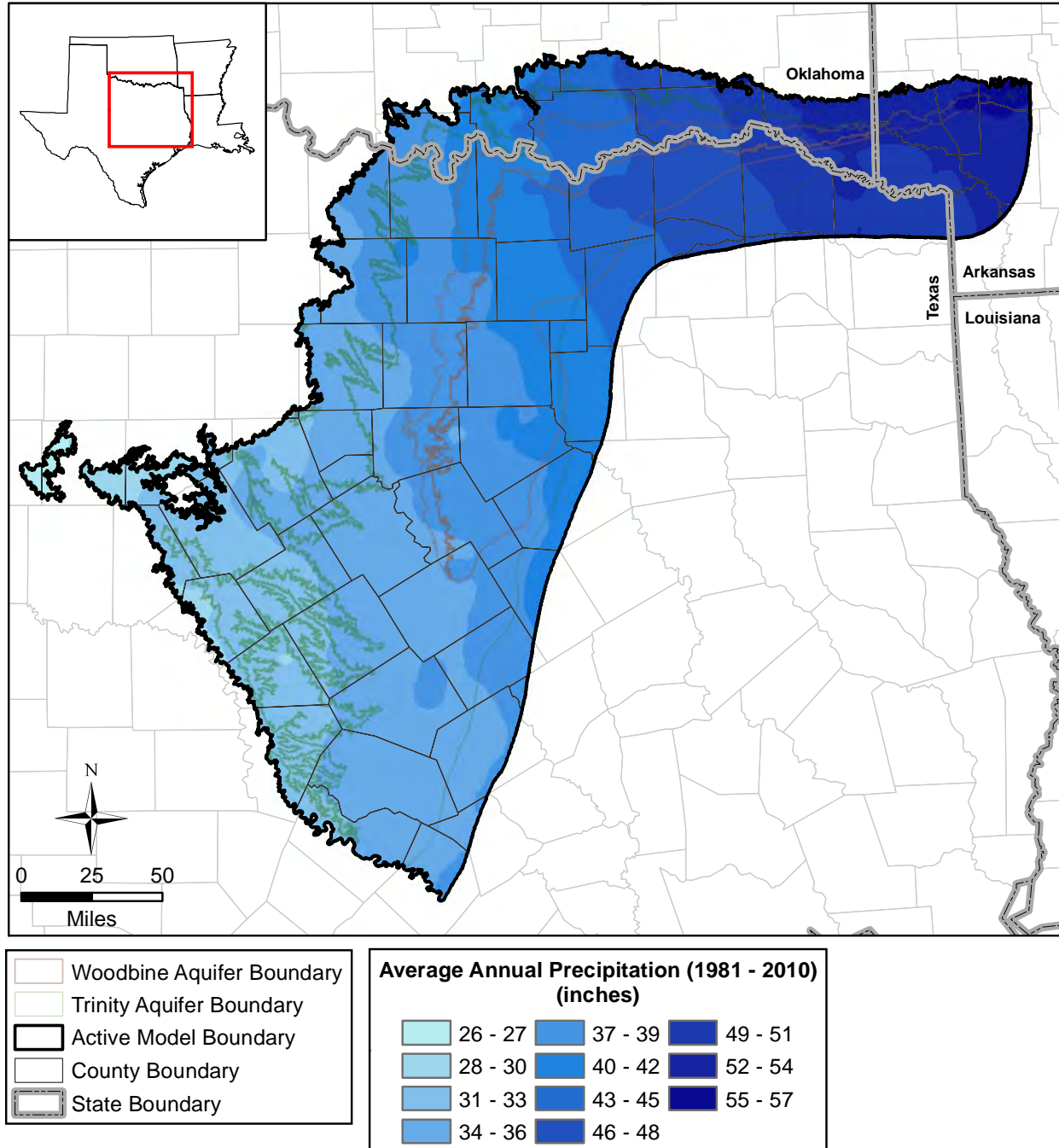
Figure 2.1.6 **Average annual precipitation in inches per year for the study area for the time period 1981 to 2010 (PRISM Climate Group, 2014).**
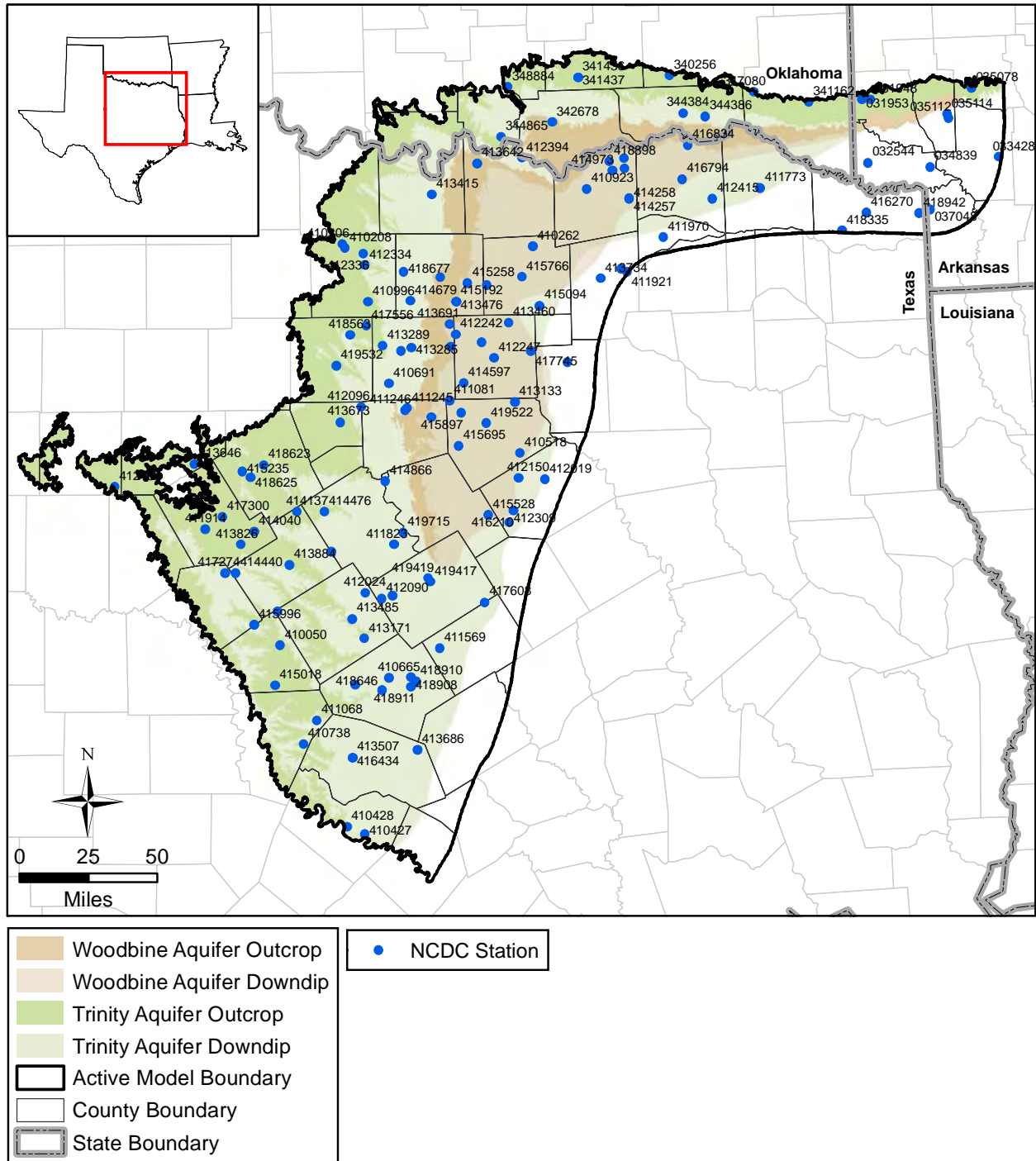
Figure 2.1.7 Location of National Climatic Data Center (NCDC) precipitation gages in the study area.
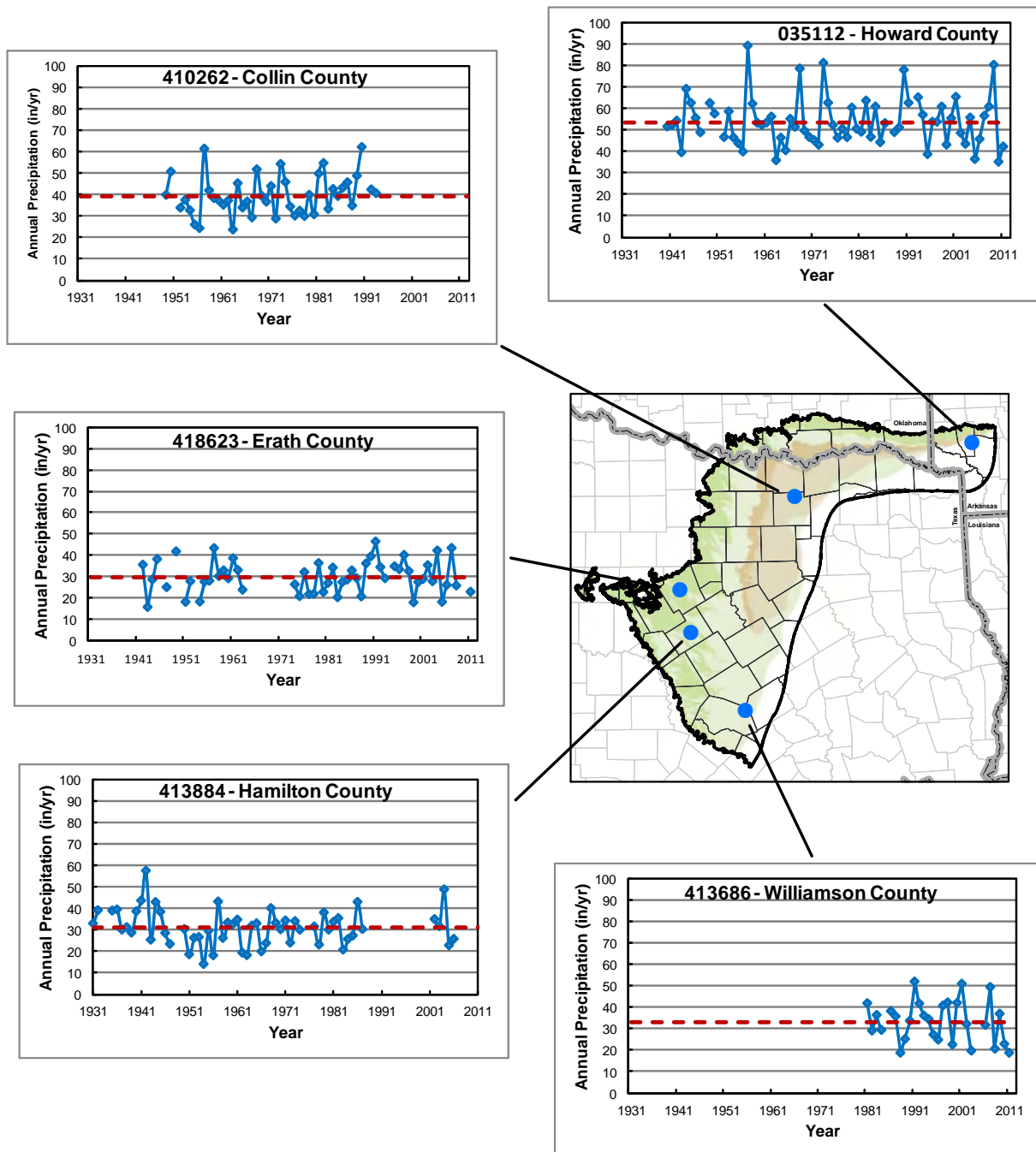
Figure 2.1.8 Selected time series of annual precipitation in inches per year at selected gages in the study area. (A discontinuous line indicates a break in the data. The dashed red line represents the mean annual precipitation).
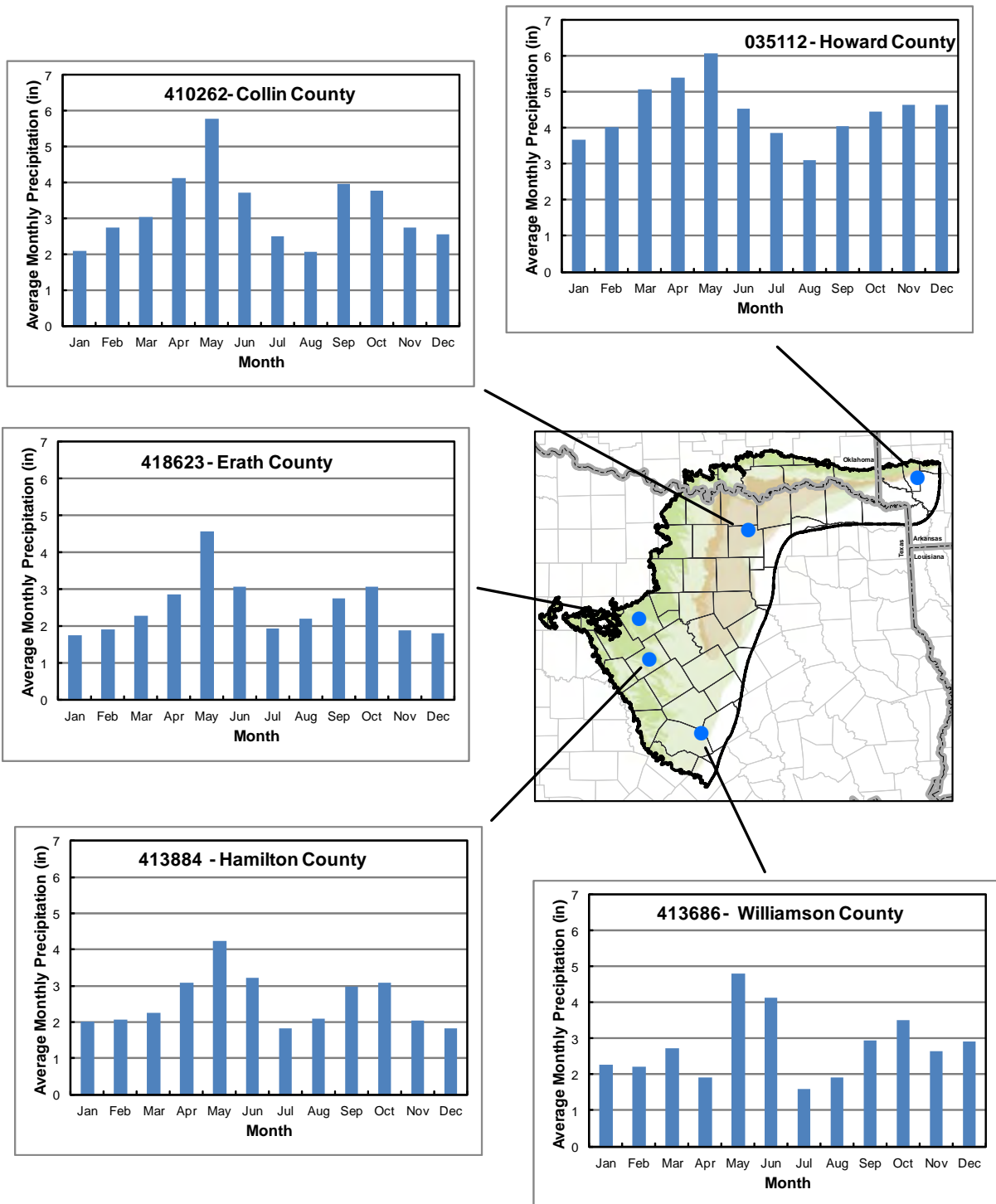
Figure 2.1.9 **Long-term monthly average precipitation in inches per month at selected gages in the study area.**
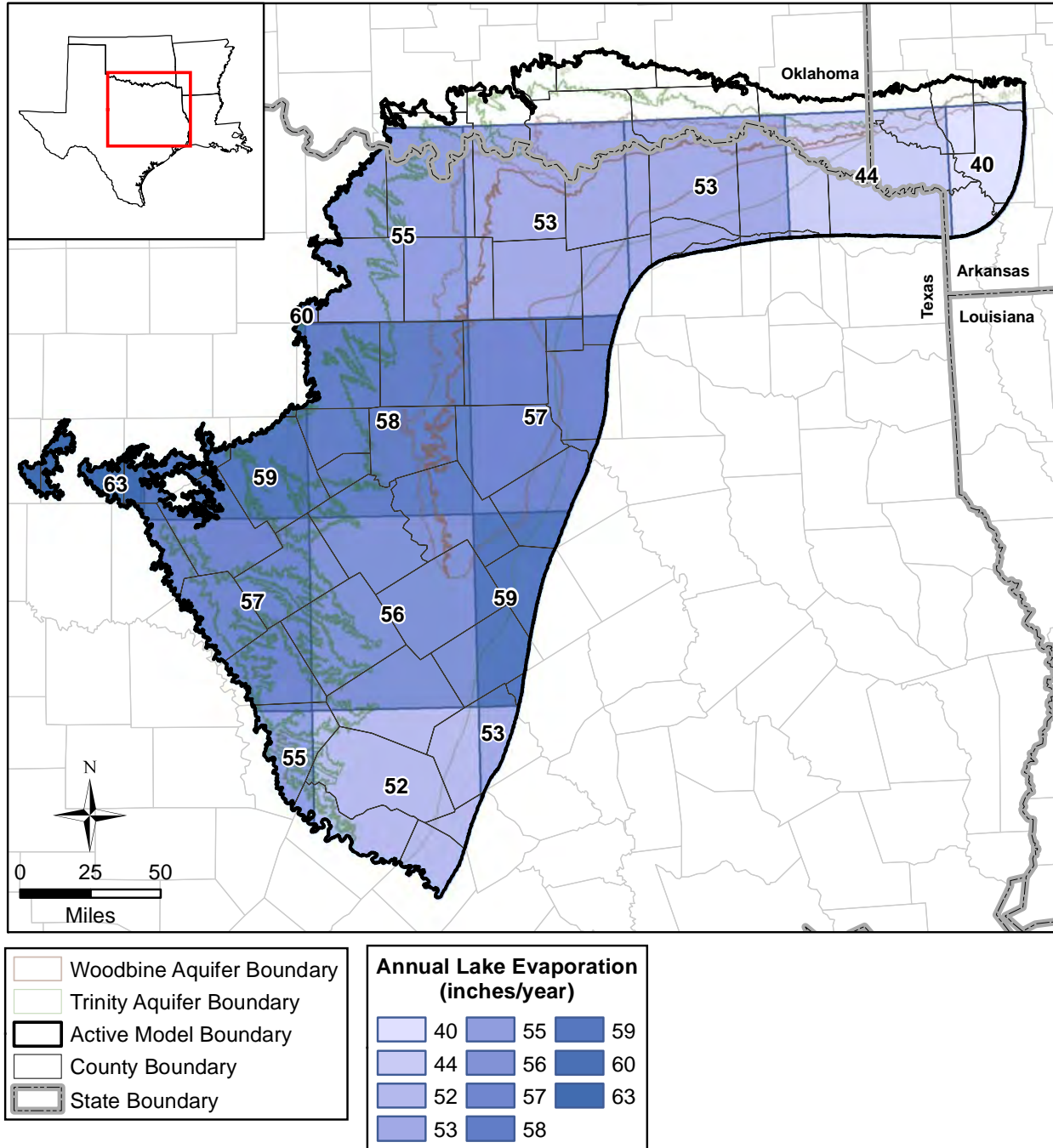
Figure 2.1.10   Average annual net pan evaporation rate in inches per year in the study area.
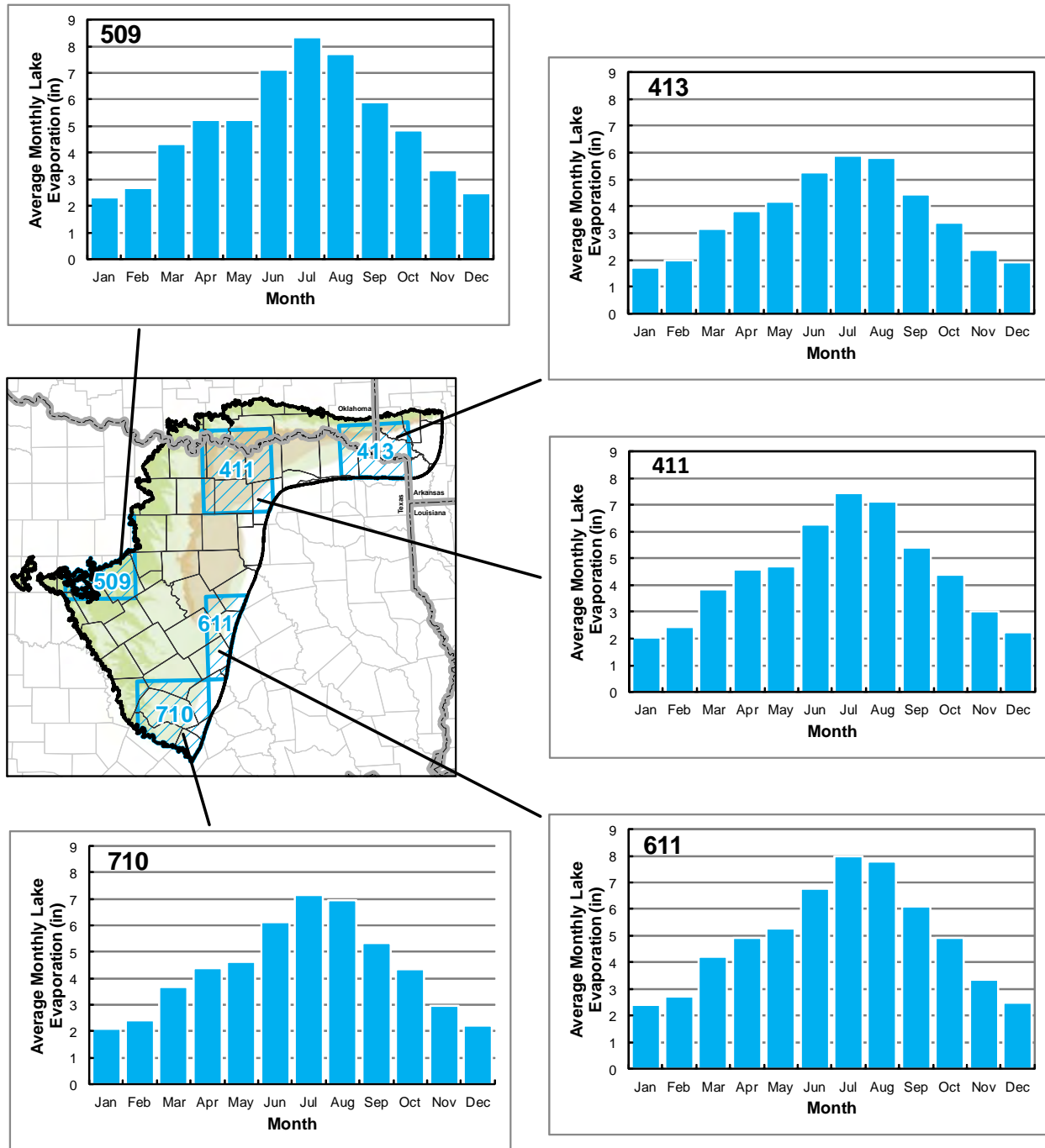
Figure 2.1.11 Average monthly lake surface evaporation in inches at selected locations in the study area.

2.2   Geology

The rocks and sediments that comprise the northern Trinity and Woodbine aquifers are contained in the northern Trinity and Woodbine groups deposited during the geologic time period known as the Cretaceous Period, which lasted from about 145 to 65 million years ago. Cretaceous-age strata are exposed at the surface across broad areas of Texas. The geologic units that make up the northern Trinity and Woodbine groups extend from the Colorado River near Austin north to southern Oklahoma and into far southwestern Arkansas. Cretaceous-age stratigraphic units in north and central Texas lie on the northwestern margin of the Gulf of Mexico Basin. Through geologic time, the Gulf of Mexico Basin has progressively filled from the margins toward the center until achieving the shoreline configuration that exists today. Cretaceous-age strata are the oldest part of the Gulf of Mexico Basin fill that is still exposed at the surface.

The Cretaceous-age sediments were unconformably deposited on an erosional surface of Paleozoic-age strata of predominantly Permian and Pennsylvanian age and dip and thicken towards the East Texas Basin to the east. This indicates that the basin was subsiding during the Cretaceous Period while the sediments were being deposited. The sediments deposited during the Cretaceous Period are subdivided, from oldest to youngest, into the Trinity, Fredericksburg, Washita, Woodbine, Eagle Ford, Austin, Taylor, and Navarro groups (Hill, 1901) (Table 2.2.1). For the aquifers considered in the current study, only the Trinity through Woodbine groups are of interest. As discussed in Section 4.1, the sediments of the northern Trinity and Woodbine groups were deposited in a variety of terrestrial and marine depositional environments including coastal plain fluvial and interfluve, deltaic shoreline, and marine shelf environments. This complexity in depositional environments resulted in a complex system of formations that can be mapped in the subsurface but have a wide variation in lithology from sand and gravel dominated systems to shale and off shore limestone units. This large degree of variability has led to a very complex geologic nomenclature (see Table 2.2.1).

As previously noted, the Cretaceous-age strata were deposited unconformably on Paleozoic-age strata, which were deposited on the eastern shelf of the Permian Basin. The Paleozoic-age sediments underlying the northern Trinity Group are comprised, from oldest to youngest, of the Strawn, Canyon, Cisco, Bowie, and Wichita groups. The Strawn Group is primarily a fluvial-

deltaic system comprised of several sandstone units inter-layered with shales. The Canyon

Group is a fluvial-deltaic system composed of sandstones and shales, but which also has

limestones reflecting a lower energy depositional environment. The Cisco Group is composed of

fluvial-deltaic and marine deposits. The Cisco Group contains many intermittent sandstone units

that are poorly mapped and extensive limestone units (Brown and others, 1990). The Bowie

Group represents a continental depositional facies and is typically composed of more coarse

grained sediments than the underlying Cisco Group. The Wichita Group is also a continental

deposit and is composed of highly heterogeneous deposits of sand, gravel, and shale. The

Paleozoic-age strata generally dip in a westerly direction, while the northern Trinity Group dips

to the east-southeast.

The nomenclature of the formations in the northern Trinity Group varies across the study area as

shown in Table 2.2.1. In the northern and western portions of the study area, the northern Trinity

Group consists of the undifferentiated sediments of the Antlers Formation. Nordstrom (1982,

1987) describes the Antlers Formation as consisting of an upper sand and sandstone with some

clay lenses; a middle section composed of sandy clay with sandstone, siltstone, and clayey sand

streaks; and a lower section of conglomerate, gravel, sand, and sandstone, with some clay lenses.

In the central and southern portions of the study area, the northern Trinity Group is divided into

three formations: the uppermost Paluxy Formation and a middle Glen Rose Formation in both

portions and lower Twin Mountains and Travis Peak formations in the central and southern

portions, respectively (see Table 2.2.2). Fisher and Rodda (1966) make a distinction between the

differences in the facies in the portion of the northern Trinity Group located below the Glen Rose

Formation. They describe a more clastic facies in the central portion of the study area (the Twin

Mountains Formation) and a more carbonate facies in the southern portion of the study area (the

Travis Peak Formation).

The Travis Peak Formation consists of three units. The lowermost unit is the Hosston/Sligo

Member. These two members of the Travis Peak Formation were deposited generally at the

same time but the Sligo Member consists of finer grained sediments that were deposited in an off

shore or marine environment generally in the eastern portions of the study area near the Mexia-

Talco Fault Zone. The Hosston Member is a bedded sandstone with high sand percentages

(greater than 60 percent) across its extent. The entirety of the Hosston Member in the study area was deposited in a fluvial coastal plain depositional environment. In the west, this lower unit is named the Sycamore Member and "is a conglomerate consisting of limestone and dolomite pebbles with a calcareous cement" (Klemt and others, 1975).

The middle unit of the Travis Peak Formation consists of the Pearsall/Cow Creek/Hammett Members. These members are carbonate and clay rich sediments deposited primarily in a marine shelf environment and composed of limestone and shale in the southern part of the study area transitioning to deltaic and coastal plain sediments to the north. The Cow Creek Member (predominately limestone) and Hammett Member (predominately shale) occur to the east. The limestones of the Cow Creek Member thin and gradually pinch out to the west. Where this occurs, shale in the Cow Creek Member and the shale of the Hammett Member coalesce to form the Pearsall Member (Klemt and others, 1975).

The Pearsall Member is overlain by the Hensell Member of the Travis Peak Formation, which Hill (1901) identified as the uppermost sand of the Travis Peak Formation. Like the Hosston Member, the Hensell Member is predominantly a sandstone unit with nearly its entire extent being composed of at least 50 percent sandstone or greater. Bené and others (2004) point out that the Hensell Member differs from other Cretaceous-age sandstone units in the northern Trinity Group in that it does not thicken toward the East Texas Basin. The Hensell Member was deposited primarily in coastal plain and deltaic environments with lower energy marine shelf depositional environments in the far east of the study area near the Mexia-Talco Fault Zone.

In the central portion of the study area, the Travis Peak Formation is called the Twin Mountains Formation based on the nomenclature change recommended by Fisher and Rodda (1966). The Hosston, Pearsall, and Hensell members of the Travis Peak Formation tend to become more dominantly sand to the north and comprise the members of the Twin Mountains Formation.

The Glen Rose Formation is a limestone unit that conformably overlies the Twin Mountain and Travis Peak formations and was deposited on an extensive shallow-marine shelf. The formation is composed of dense, finely crystalline limestone with inter-bedded shale, sandy-shale and anhydrite.

The Paluxy Formation, composed of upper sands in the northern Trinity Group, was deposited in a coastal plain environment in the northeast and western portions of the study area and transitions in central Texas to a deltaic shoreline depositional environment and to a marine shelf environment in the southern study area. As a result, the thickest net sand is found in the northeast and northern portions of the formation and essentially no sand is found in the southernmost portion of the formation. Where the Paluxy Formation is predominantly a sand unit, it is characterized as being composed of fine-grained, friable quartz sand, which is poorly cemented and exhibits cross bedding (Klemt and others, 1975).

The northern Trinity Group is overlain by the Fredericksburg and Washita groups (see Table 2.1.1 and Figure 2.2.3). The nomenclature of these two groups is complex. In general, they are composed of limestone, dolomite, marl, and shale (Leggat, 1957). The Fredericksburg and Washita groups comprise a significant percentage of the land surface (outcrop) in the central and southern portion of the study area (see Figure 2.2.2) and separate the northern Trinity and Woodbine groups.

The Woodbine Group was deposited in late Cretaceous time. Both a sand facies and a shale facies are found in the Woodbine Group. The sand facies occurs in the outcrop and in the subsurface in and north of Hill County. The shale facies occurs in the subsurface south of Hill County. In general, the sand facies of the Woodbine Group consists of sand and sandstone with some interbedded shale and clay. Typically, the lower portion of the Woodbine Group contains less clay and shale than the upper portion of the group. The sand facies of the Woodbine Groups was deposited in a deltaic shoreline depositional environment. This portion of the group is composed of two members; the lower Dexter Member and the upper Lewisville Member. The shale facies of the Woodbine Group is referred to as the Pepper Shale. The Woodbine Group is unconformably overlain by shale of the Eagle Ford Group.

Figures 2.2.1 and 2.2.2 show the generalized surface geology for the northern and southern portions of the study area, respectively. The relationship between the terminology used on these figures and the stratigraphic column is provided in Table 2.2.1. Figure 2.2.3 shows structural cross sections of the stratigraphic units in north and central Texas (George and others, 2011;

Bené and others, 2004; Nordstrom, 1982; Klemt and others, 1975). On this figure, the unit

identified as "Younger formations" corresponds to Tertiary- and Quaternary-age sediments.

Table 2.2.1   Stratigraphic column for the study area.

Period	Group	North and West Formation	Central Formation	Central Member	South Formation	South Member	Terminology for Generalized Surface Geology in Figures 2.2.1 and 2.2.2
Quaternary		differentiation not necessary for this study					Alluvium
Tertiary		differentiation not necessary for this study					Tertiary System
Cretaceous	Navarro	differentiation not necessary for this study					Cretaceous above the Woodbine Group
	Taylor	differentiation not necessary for this study					
	Austin	differentiation not necessary for this study					
	Eagle Ford	differentiation not necessary for this study					
	Woodbine	Lewisville	Lewisville		Pepper Shale		Woodbine Group
		Dexter	Dexter				
	Washita	Grayson Marl	Buda, Del Rio		Buda, Del Rio		Washita Group
		Mainstreet, Pawpaw, Weno, Denton	Georgetown		Georgetown		
		Fort Worth, Duck Creek					
	Fredericksburg	Kiamichi	Kiamichi		Kiamichi		Fredericksburg Group
		Goodland	Edwards		Edwards		
			Comanche Peak		Comanche Peak		
		Walnut Clay	Walnut Clay		Walnut Clay		

Table 2.2.1, continued

Period	Group	North and West	Central		South		Terminology for Generalized Surface Geology in Figures 2.2.1 and 2.2.2
		Formation	Formation	Member	Formation	Member	
Cretaceous (continued)	Trinity	Antlers	Paluxy		Paluxy		Antlers Formation (north and west) or Paluxy Formation (central and south)
			Glen Rose		Glen Rose		Antler Formation (north and west) or Glen Rose Formation (central and south)
			Twin Mountains	Hensell	Travis Peak	Hensell	Antlers Formation (north and west) or Hensell Member (south)
				Pearsall		Pearsall/ Hammett/ Cow Creek	Antlers Formation (north and west), Twin Mountains Formation (central), Travis Peak Formation (south), or Cow Creek Member (south)
				Hosston		Sycamore /Hosston/ Sligo	Antlers Formation (north and west), Twin Mountains Formation (central), Travis Peak Formation (south), or Sycamore Member (south)
Permian	Wichita	differentiation not necessary for this study					na
	Bowie	differentiation not necessary for this study					
Pennsylvanian	Cisco	differentiation not necessary for this study					
	Canyon	differentiation not necessary for this study					
	Strawn	differentiation not necessary for this study					

na - Permian- and Pennsylvanian-age groups do not outcrop in the study area
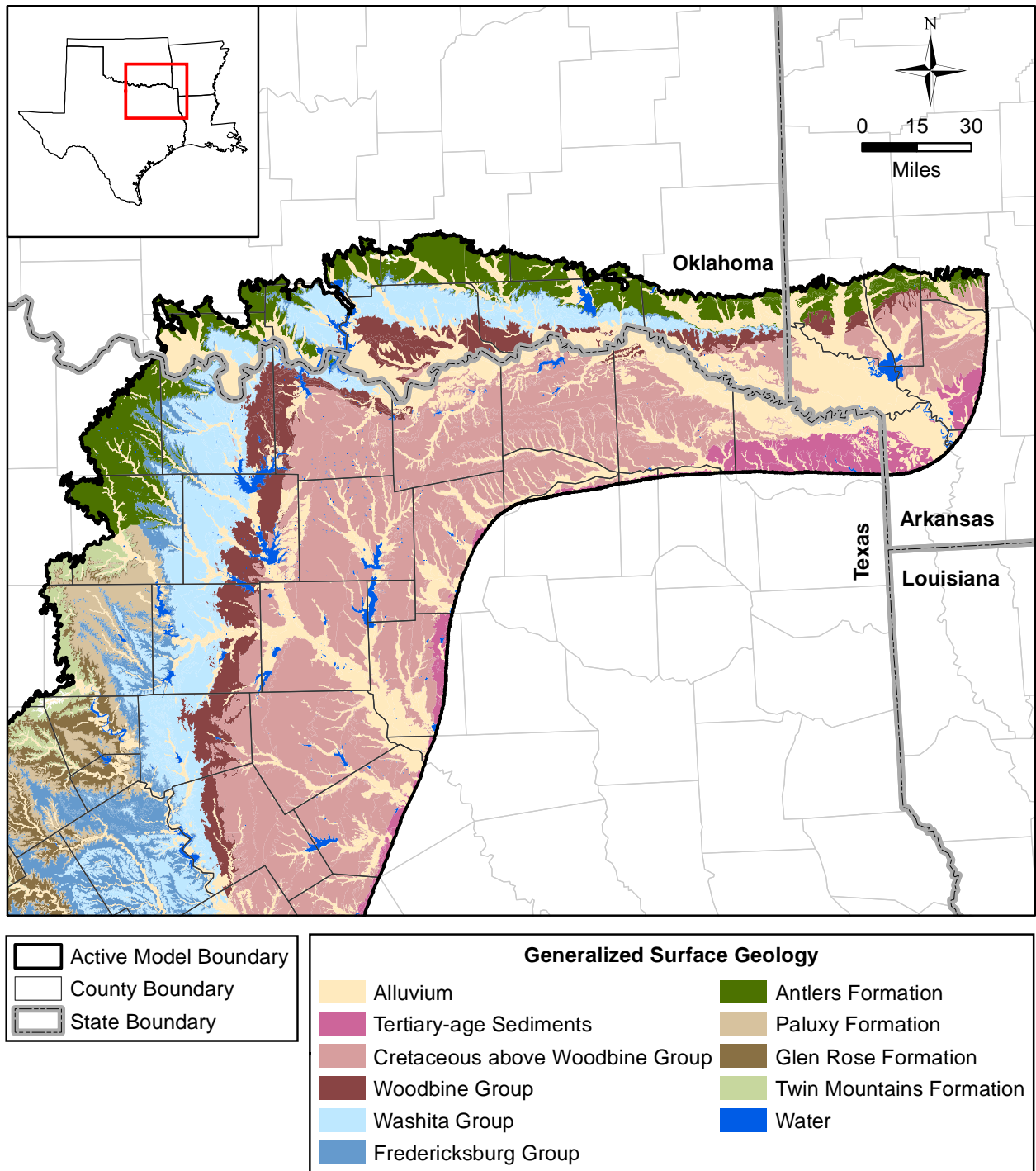
**Figure 2.2.1   Generalized surface geology for the northern portion of the study area (Bureau of
Economic Geology, 2012).**
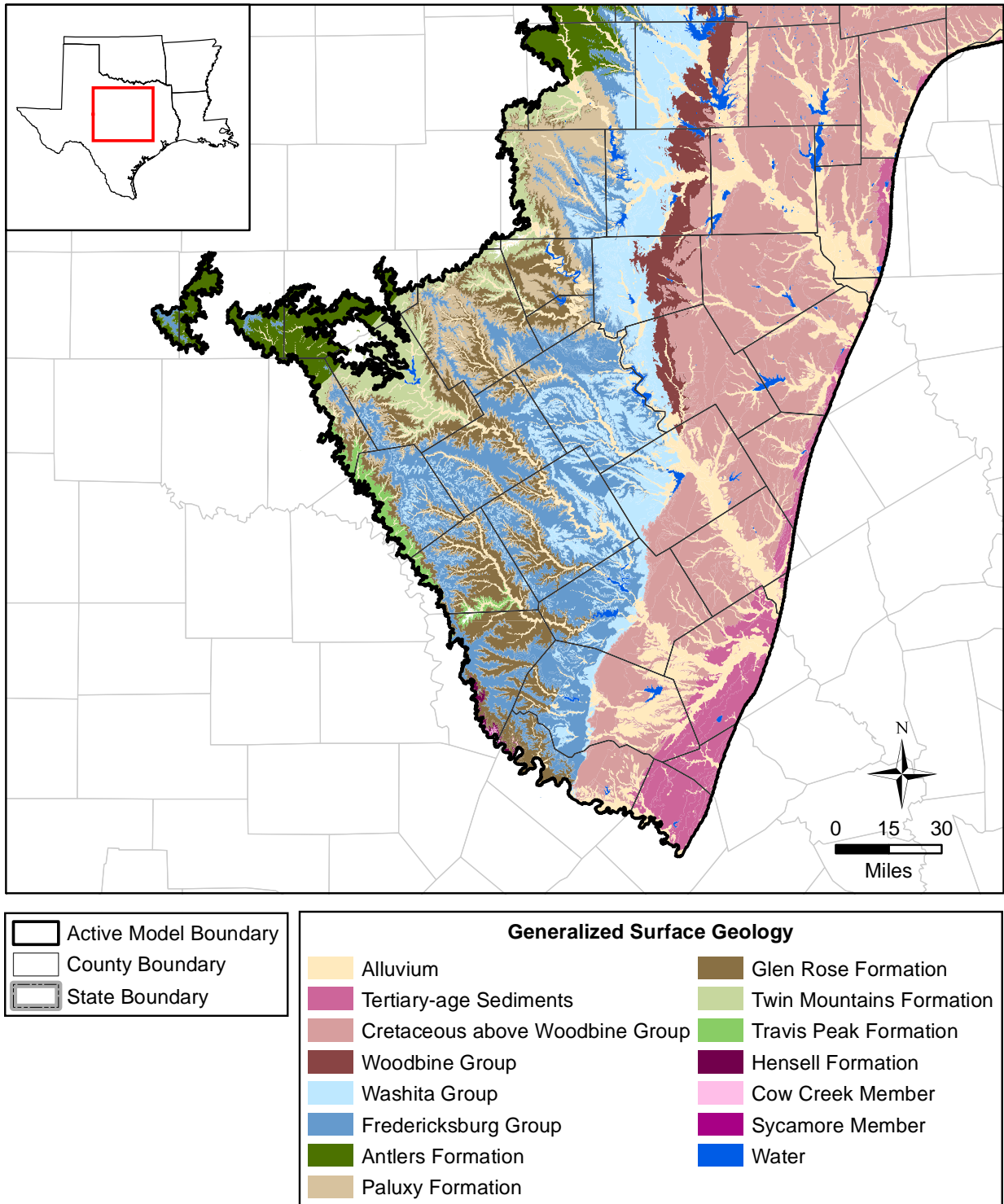
Figure 2.2.2   Generalized surface geology for the southern portion of the study area (Bureau of Economic Geology, 2012).
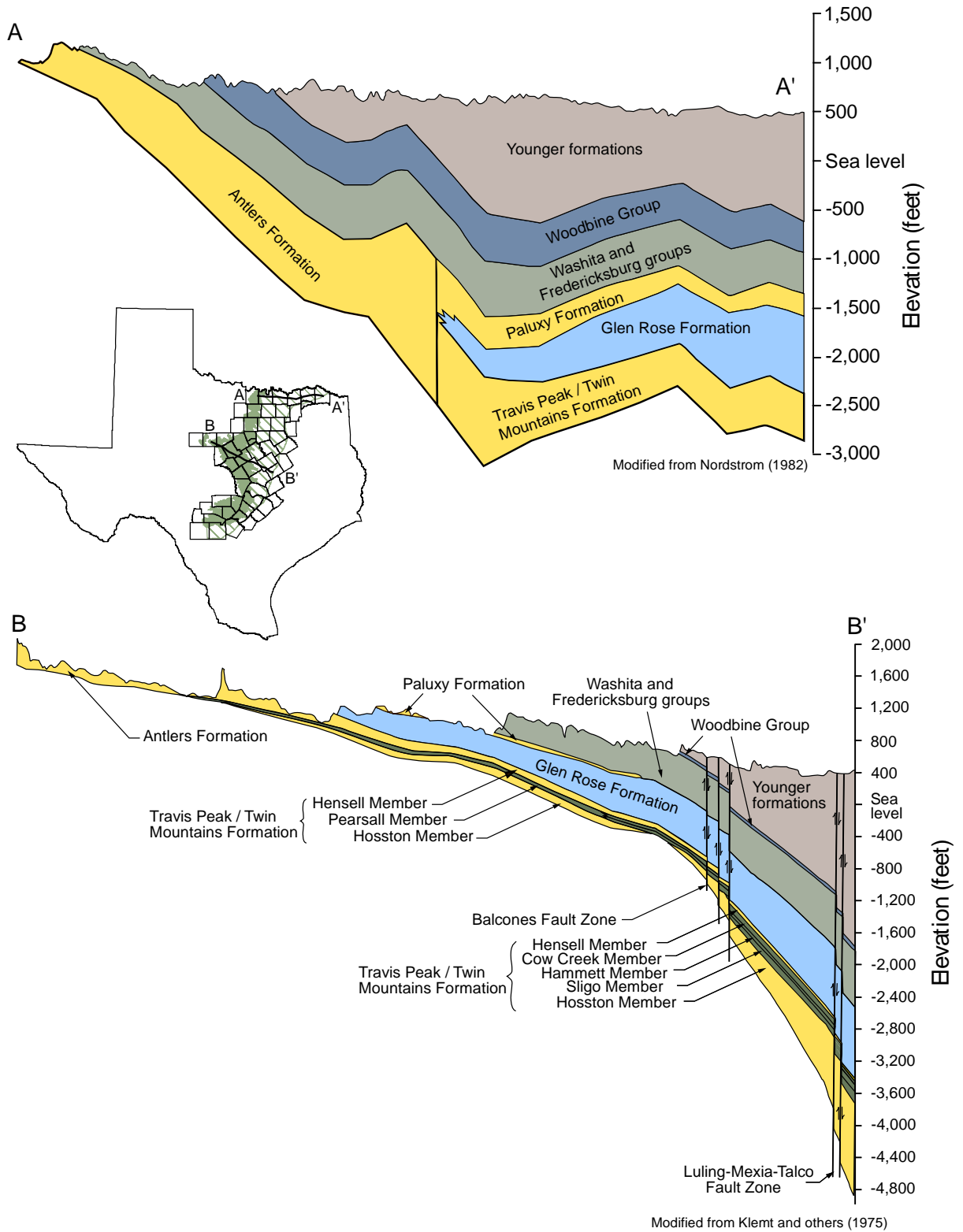
Figure 2.2.3 Cross sections of the stratigraphic units in the study area (after George and others, 2011; Bené and others, 2004; Nordstrom, 1982; Klemt and others, 1975).

3.0   Previous Investigations

Reports and papers documenting previous investigations of the formations composing the northern Trinity and Woodbine aquifers are prolific and a complete review of this body of literature is beyond the scope of this report. As a result, this section provides a review of the previous investigations documented in the literature focusing on seminal works and/or investigations directly relevant to this report. Appendix B contains an extended literature database for the aquifers in the study area.

Previous investigations of the formations composing the northern Trinity and Woodbine aquifers can be divided into three general categories; those related to geology, those related to hydrogeology, and those documenting numerical models. Based on these general distinctions, this section is divided into three subsections containing discussions of the three types of previous investigations. Those investigations that include discussion of more than one area are covered in the appropriate subsections.

3.1   Previous Geologic Investigations

Investigations of Cretaceous-age rocks in Texas began as early as the mid-1800s. Some of these early reports include Shumard (1860), which describes observations on the Cretaceous-age strata of Texas, and Taff (1892), which reports on Cretaceous-age strata located north of the Colorado River. The first comprehensive description of the Cretaceous-age rocks in central and north-central Texas is provided in Hill (1901), which documents investigations conducted by Hill independently or with others beginning in 1882. Hill (1901) states that he treated the Cretaceous-age rocks with greater detail than earlier writings "in order that they may be more readily recognized and that a knowledge of them may be of service to the public." Hill (1901) presents a discussion of defects of earlier classifications of these formations and provides a refinement of the nomenclature. This refinement includes dividing the Cretaceous-age rocks into a lower Comanche Series and an upper Gulf Series, identifying groups within each series, and naming formations based on several local stratigraphic sections. Many of his formation names, and group and series divisions and names, are still in use. Hill (1901) also provides detailed descriptions of the formations.

Numerous county-specific geologic investigations have been conducted for counties in the study area. For Texas counties, these reports, in general, describe the topography, physiography, stratigraphy, structure, and mineral resources/economic geology of the county. Some reports provide additional information such as petroleum development (e.g., Cooke County), paleontology (e.g., Bell and Tarrant counties), and well data (e.g., Bell and McLennan counties). The Oklahoma Geological Survey published a series of bulletins on the geology and groundwater resources of various counties in that state. These include Bullard (1925) for Love County, Bullard (1926) for Marshall County, Davis (1960) for McCurtain County, Huffman and others (1975) for Choctaw County, Huffman and others (1978) for Bryan County, and Huffman and others (1987) as an update to Bullard (1926) for Marshall County. In Arkansas, hydrogeological assessments have been performed and documented for most of the counties in the study area, including Hempstead, Lafayette, Little River, Miller and Nevada counties (Ludwig, 1973) and Pike and Howard counties (Thornton, 1992). The available geological and groundwater resources reports for counties in the study area are provided in Table 3.1.1.

In addition, numerous geologic and stratigraphic investigations involving Cretaceous-age rocks in the study area have been conducted. Examples include, but are not limited to, studies of the upper Cretaceous-age formations of southwestern Arkansas (Dane, 1929); the Mesozoic Systems in Texas (Adkins, 1933); the stratigraphy of the Woodbine Group (Dodge, 1952; Adkins and Lozo, 1951; Bryan, 1951; Price, 1951; Lee, 1958; Hamman, 2001), the lower Cretaceous-age Paluxy Sand in central Texas (Atlee, 1962), the northern Trinity Group deposits of central Texas (Boone, 1968; Stricklin and others, 1971), rocks of the Comanchean series of central Texas (Hayward and Brown, 1967), the Glen Rose Limestone in Texas (Rodgers, 1967), the Cretaceous-age and pre-Cretaceous-age strata in north-central Texas (Bain, 1973), the Comanchean Series in east central Texas (Mostellar, 1970), and the Paluxy sand in north-central Texas (Owen, 1979).

As a result of historical use of confusing and sometimes inappropriate geologic nomenclature, Fisher and Rodda (1966) developed a revised nomenclature for the basal Cretaceous-age rocks in the area between the Red and Colorado rivers and on the Callahan Divide in Texas. They divide these units geographically into three distinctive lithologic outcrop sequences corresponding to north-central Texas, north and west-central Texas, and central Texas and one subsurface

sequence in north-central Texas. The stratigraphic nomenclature applied by Fisher and Rodda
(1966) is summarized in Table 3.1.2. They present the addition of a new formation name, the
Twin Mountains Formation, in north-central Texas because the basal Cretaceous-age rocks in
that area have a facies distinct from that of the Travis Peak Formation in central Texas. Their
nomenclature has been adopted by most modern groundwater availability studies in the study
area.

The depositional systems in the Woodbine Group and Glen Rose Formation in northeast Texas
are presented in Oliver (1971) and Davis (1974), respectively. Investigation of the depositional
systems in the Paluxy Formation for application to oil, gas, and groundwater resources are
presented in Caughey (1977). Hall (1976) presents the depositional systems and facies in lower
Cretaceous-age sandstones in north-central Texas and discusses their hydrogeological
significance. A discussion of the depositional systems of the Cretaceous-age strata in central and
north-central Texas are also discussed in numerous other reports

Table 3.1.1   Summary of geological and groundwater resources reports for counties in the study area.

County	Geological Report	Groundwater Resources Report
Texas		
Bell	Adkins and Arick (1930)	Duffin and Musick (1991)
Bosque		
Bowie		
Brown		Thompson (1967a)
Burnet		Duffin and Musick (1991)
Callahan		Price and others (1983)
Collin		
Comanche		
Cooke	Bybee and Bullard (1927), Bradfield (1957)	
Coryell	Caskey (1961)[a]	
Dallas	Shuler (1918)	
Delta		
Denton	Winton (1925)	
Eastland		
Ellis		Thompson (1967b)
Erath		
Falls		
Fannin		
Franklin		Broom and others (1965)
Grayson	Bullard (1931), Bradfield (1957)	Baker (1960)
Hamilton		
Hill		
Hood		
Hopkins		
Hunt		
Johnson	Winton and Scott (1922)	Thompson (1969)
Kaufman		
Lamar		
Lampasas		
Limestone		Rettman (1987)
McLennan	Adkins (1923)	
Milam		
Mills		
Montague	Bullard and Cuyler (1930)	Bayha (1967)
Navarro		Thompson (1972)

Table 3.1.1, continued

County	Geological Report	Groundwater Resources Report
Parker	Hendricks (1957)	Stramel (1951)
Rains		White (1973)
Red River		
Rockwall		
Somervell		
Tarrant	Winton and Adkins (1919)	Leggat (1957)
Taylor		Taylor (1978)
Titus		Broom and others (1965)
Travis		Brune and Duffin (1983); Duffin and Musick (1991)
Williamson		Duffin and Musick (1991)
Wise	Scott and Armstrong (1932)	
Oklahoma		
Bryan	Huffman and others (1978)	
Choctaw	Huffman and others (1975)	
Love	Bullard (1925)	
Marshall	Huffman and others (1987)	
McCurtain	Davis (1960)[b]	Davis (1960)[b]
Arkansas		
Hempstead		Ludwig (1973)
Howard		Thornton (1992)
Little River		Ludwig (1973)
Miller		Ludwig (1973)
Pike		Thornton (1992)
Sevier		

[a] western Coryell County only
[b] southern McCurtain County only

Table 3.1.2   Fisher and Rodda (1966) nomenclature.

North Texas and West-central Texas		North-Central Texas			Central Texas	
		Outcrop		Subsurface	Northeast Side of Llano Uplift	Travis County
Antlers Formation	upper unit	Paluxy Formation		Glen Rose Limestone	Paluxy Formation	Glen Rose Limestone
	middle unit	Glen Rose Formation			Glen Rose Formation	
	lower unit	Twin Mountains Formation	upper unit	Hensell Formation	Travis Peak Formation	Hensell Formation
			middle unit	Pearsall Formation		Cow Creek Limestone
						Hammett Shale
			lower unit	Sligo Formation		Sycamore Sand
				Hosston Formation		

3.2   Previous Hydrogeological Investigations

The earliest systematic investigation of groundwater in the study area is documented in Hill (1901). As discussed in Section 3.1, Hill (1901) provides detailed descriptions of the geology of the Cretaceous-age rocks in the study area. In addition, he conducted detailed investigations of the artesian waters in these rocks. Earlier wells drilled into the Paluxy Formation and the northern Trinity Group encountered artesian conditions and, in many instances, pressures were sufficient to cause wells to flow at the surface. Hill (1901) set forth in his study to identify the formations from which artesian waters could be obtained, the depths of those waters, and the height to which water in those formations would rise in an effort to provide information useful for future well development. He provides descriptions of the northern Trinity and Woodbine aquifers, existing knowledge of the chemistry of the groundwater in these aquifers, and estimated locations where the pressure in the aquifers was sufficient to result in flowing wells. He also includes well schedules for select wells and some information on aquifer yield and surface flow rates.

In response to the concern of residents regarding the cessation of flowing conditions in wells, Fiedler (1934) conducted an investigation of the artesian water in Somervell County, Texas. His investigation "comprised a study of the use and waste of artesian water, the safe yield of artesian reservoirs, underground leakage of wells, methods of constructing wells, and other related features necessary for the formulation of a conservation program" (Fiedler, 1934).

County- or multicounty-based studies of geology and groundwater resources have been conducted for several counties in the study area by past and present Texas state agencies responsible for water resources. In general, a main objective of those investigations was the assessment of groundwater resources in the county. The counties with a report related to groundwater resources and the citation for that report are provided in Table 3.1.1.

During 1942 and 1943, several local investigations were conducted to evaluate groundwater availability and estimate the impact of future pumping in association with war efforts related to selecting locations for military facilities or providing water for war related industries. Sundstrom and Barnes (1942) report on groundwater resources in the vicinity of Gatesville, Texas;

Livingston and Hastings (1942) report on a test well drilled at a proposed army camp southeast of Gatesville, Texas; and Guyton and George (1943) and Rose (1943) present results of pumping tests conducted in wells at Camp Hood and the Tank Destroyer Center, respectively, located near Gatesville, Texas. Investigations of groundwater resources in the vicinity of Belton, Texas and McGregor, Texas, made at the request of the military, are documented in Bennett (1942) and Livingston and Bennett (1942), respectively. The evaluation of groundwater resources for the military in selected areas in Erath, Hood, and Hamilton counties are summarized in Rose and George (1942) and in the vicinity of Burnet, Texas and Bertram, Texas are summarized in George (1942). In anticipation of an influx of workers for war industries, an investigation of groundwater resources in Fort Worth and vicinity was conducted by George and Rose (1942). Additional reports related to groundwater supplies for war or post-war purposes include the results of aquifer pumping tests conducted on wells in Waco, Texas (George and Barnes, 1945), groundwater resources at Sherman, Texas (Livingston, 1945), and results of aquifer pumping tests on city wells at Waxahachie, Texas (Sundstrom, 1948). An investigation conducted for the city of Burnet, Texas in response to well failures during the drought of the early 1950s is discussed in Mount (1962).

Winslow and Kister (1956) report on the saline water resources of Texas, which includes a discussion of the northern Trinity and Woodbine aquifers. The purpose of their report was "to outline the occurrence, quantity, and quality of saline water available in Texas; to discuss and identify aquifers containing saline water, with emphasis on those capable of yielding large quantities; and to delineate areas in which a considerable amount of saline surface water is available." As part of a statewide program to assess groundwater supplies and availability, reconnaissance investigations of principal aquifers where conducted in the Sabine River basin (Baker and others, 1963a), the Red River, Sulphur River, and Cypress Creek basins (Baker and others, 1963b); the Trinity River basin (Peckham and others, 1963); and the Brazos River basin (Cronin and others, 1973). These investigations were conducted on the basis of river basins because the approach to state water planning at that time was by river basins. Two studies of groundwater availability were conducted by the TWDB or a predecessor agency at the request of city officials for Whitney, Texas (Mount, 1963) and Commerce, Texas (Baker, 1971). Both of these investigations focused on the possibility of producing water from the northern Trinity Aquifer.

Leggat (1957), in his investigation of groundwater in Tarrant County, estimated that Lake Worth recharges the Paluxy Formation at a rate of about 650 acre-feet per year (AFY) and that recharge from Eagle Mountain Lake is likely similar. Based on comparisons of levels in Lake Grapevine and groundwater elevations in the Woodbine Group, Leggat (1957) indicates that recharge of the group by the lake is likely small. Baker (1960) suggests that, prior to development, natural discharge occurred from the Antler Formation along the crest and southern flank of the Preston Anticline and along the Red River in Grayson County. He suggests that groundwater movement in the Antlers Formation in the county was towards the Red River prior to significant development and the impoundment of Lake Texoma. Afterwards, however, he suggests that the Preston Anticline became a recharge area for the Antlers Formation. Cross-formational flow is also given as a natural discharge mechanism in the downdip portions of the Antlers Formation and the Woodbine Group in Grayson County by Baker (1960).

Regional studies of groundwater resources of the northern Trinity and Woodbine aquifers are documented in Klemt and others (1975) and Nordstrom (1982; 1987). Klemt and others (1975) studied the Antlers and Travis Peak formations in portions of central Texas. The counties included in their investigation, either wholly or partially, are Bell, Bosque, Brown, Burnet, Callahan, Comanche, Coryell, Eastland, Erath, Falls, Hamilton, Hill, Lampasas, Limestone, McLennan, Milam, Mills, Somervell, Travis, and Williamson. The portions of their report that discuss groundwater movement are summarized here.

Klemt and others (1975) suggest that the movement of groundwater downdip from the outcrop areas may be significantly restricted by the Balcones Fault Zone and Mexia-Talco Fault Zone. Groundwater movement may also be restricted in the vicinity of the McGregor High, located in Coryell County, due to thinning of the lower Cretaceous-age sediments. They suggest that the impact of this high is likely most significant for the Hosston Member of the Travis Peak Formation. They also estimate that groundwater movement in the Antlers and Travis Peak formations is impacted by thicker accumulations of sand in valleys of the pre-Cretaceous Period surface and thinner accumulations on the ridges.

Klemt and others (1975) state that the basal sediments in the Travis Peak and Antlers formations are hydraulically connected, having the same potentiometric surface and water quality. They

state that the most important aquifers in the study area are, first, the Hosston Member of the

Travis Peak Formation and, second, the Hensell Member of the Travis Peak Formation. The

Hensell Member is the source for most domestic wells in the study area of Klemt and others

(1975). The Glen Rose Formation provides small quantities of water to predominately domestic

and stock wells in localized areas on and adjacent to its outcrop. Downdip, the groundwater in

the Glen Rose Formation becomes highly mineralized. Small to moderate amounts of

groundwater are supplied by the Paluxy Formation in the northern and central areas of Klemt and

others' (1975) investigation. In their study area, the Woodbine Group is an important source of

groundwater only in the northeast, in Hill County. The Woodbine Group provides groundwater

for many domestic and stock wells and several small towns and industries.

The sources of recharge to the Travis Peak and Antlers formations are precipitation in the

outcrop areas, seepage from some lakes, particularly Proctor Lake and Lake Travis, some

streams, particularly the Lampasas, Leon, and Sabine rivers, seepage from ponds, and irrigation

return flow (Klemt and others, 1975). They estimate that recharge to the Travis Peak Formation

through infiltration of precipitation is less in Burnet, Lampasas, Mills, and Brown counties due

to tight soils in the outcrops and well cemented sediments in the subsurface. Due to interbedded

sands and shales in the outcrop areas of the Travis Peak and Antlers formations, perched water

locally occurs in these two formations. Before development of groundwater in the Travis Peak

Formation, the pressure in the formation was sufficient to drive water to the ground surface in

wells drilled in topographic lows downdip of the outcrop area. Klemt and others (1975) indicate

that groundwater in the Travis Peak and Antlers formations moved downdip from the recharge

area in the outcrops prior to development. They report that natural discharge from these two

formations occurs in the outcrops through seeps, springs, and evapotranspiration (ET) and in the

downdip areas along faults and through cross-formational flow.

Recharge to the Woodbine Group occurs through infiltration of precipitation in the outcrop and

seepage from streams (Klemt and others, 1975). The movement of groundwater in this group is

from the outcrop area to the downdip area. They indicate that natural discharge from the

Woodbine Group is through seeps, springs, and ET in the outcrop area and cross-formation flow

in the downdip area. One of the main objectives of the Klemt and others (1975) investigation

was numerical simulation of predicted future water-level declines. That modeling is discussed in Section 3.3.1.

Nordstrom (1982) discusses groundwater resources in the Cretaceous-age strata of north-central Texas. His report includes a discussion of the geology of the study area as it relates to the occurrence of groundwater; the stratigraphy of the water-bearing formations; the groundwater chemistry as related to use; the occurrence and development of groundwater resources, including hydraulic characteristics and historical water-level declines; the availability of groundwater, and well construction. His study included all or parts of Collin, Cook, Dallas, Delta, Denton, Ellis, Fannin, Grayson, Hood, Hunt, Johnson, Kaufman, Lamar, Montague, Navarro, Parker, Red River, Rockwall, Tarrant, and Wise counties. The most prolific aquifers in his study area are the Antlers, Twin Mountains, and Paluxy aquifers. Groundwater is also provided by the Woodbine Group in the eastern portion of his study area. Although well yields in the Twin Mountains and Antlers formations are higher than those in the shallower Paluxy Formation, the area over which development has occurred is greater for the Paluxy Formation. In Nordstrom's (1982) study area, the Twin Mountains Formation is the most prolific aquifer and the Woodbine Group is the most important over large parts of the area. He reports that the basal portions of the Twin Mountains and Antlers formations are hydraulically connected. Production from the upper portion of the Antlers Formation is less than that from the lower portion. In the Twin Mountains Formation, well yields are lower in the outcrop area and increase downdip, and are generally lower in the southern portion of his study area and increase to the north (Nordstrom, 1982). Well yields in the Paluxy Formation are also greater downdip than in the outcrop area. Large yields can be obtained from the Woodbine Group in portions of both the outcrop and downdip areas.

Nordstrom (1987) discusses the groundwater resources in the outcrop areas of the Antlers and Travis Peak formations in north-central Texas. His study included all or parts of Brown, Callahan, Comanche, Eastland, Erath, and Hamilton counties. He states that the primary sources of groundwater in this area are the formations of the northern Trinity Group. The Paluxy Formation provides small quantities of water to domestic and stock wells, predominantly along the edge of the outcrop. Although the Glen Rose Formation can supply small quantities of water, some of the water from this formation is of poor quality. Beyond this information, Nordstrom (1987) does not discuss these two formations, but rather focuses on the Travis Peak and Antlers

formations, which are the principal sources of groundwater in his study area. Like Klemt and others (1975), Nordstrom (1987) indicates that the potentiometric surface of the lower sediments in the Antlers Formation is equivalent to that in the Hosston Member of the Travis Peak Formation. He also states that the Hensell Member of the Travis Peak Formation is hydraulically separate from the lower Hosston Member based on both water levels and water chemistry. The principal source of groundwater in his study area is the Hosston Member and the second most important is the Hensell Member. Nordstrom (1987) also indicates that the Hensell Member is tapped by most of the small-capacity wells in his study area.

Nordstrom (1987) reports that groundwater in the Travis Peak and Antlers formations is recharged through the infiltration of precipitation on the outcrops, stream loss, and irrigation return flow. The predevelopment movement of groundwater in these two formations is in the downdip direction. Natural discharge in the outcrop area of the Twin Mountains and Antlers formations occurs through seeps, springs, and ET. This description is consistent with that given by Klemt and others (1975). Through an evaluation of transient water-level data, Nordstrom (1987) concluded that, in general, recharge in the outcrops is sufficient for the formations to recover from the summer pumping conducted for irrigation purposes.

Duffin and Musick (1991) report on their evaluation of groundwater resources in Bell, Burnet, Travis, Williamson, and parts of adjacent counties. Structural features impacting groundwater are the erosional pre-Cretaceous Period surface, which resulted in thicker sediments in valleys and thinner sediments on ridges; and the Balcones Fault Zone and Mexia-Talco Fault Zone, across which groundwater movement might be blocked or restricted. They proposed that these fault systems could also be conduits of groundwater from deeper formations. Duffin and Musick (1991) indicate that in their study area, the northern Trinity Group produces water from the Hosston Member, small amounts from the Cow Creek Member in or near its outcrop, and the Hensell Member of the Travis Peak Formation, and from the Glen Rose Formation in localized areas on or adjacent to its outcrop. The aquifers of the Hosston and Hensell members of the Travis Peak Formation are separated by the Hammett Shale Member. The Paluxy Formation is present only in the eastern and northeastern portions of Burnet County and is not tapped by any wells. The Edwards Formation and associated limestone are the principal aquifer in their area, and are referred to as the Edwards BFZ Aquifer. In some portions of the area studied by Duffin

and Musick (1991), they found that the pressure in the Hosston Member was sufficient to cause

the groundwater to flow at the surface. Wells completed into the Hensell Member were also

observed to flow in some areas, such as along Lake Austin and in the city of Austin. Duffin and

Musck (1991) indicate that, where it is present, the Paluxy Formation is hydraulically connected

to the upper portion of the underlying Glen Rose Formation. They found no evidence of springs

issuing from the northern Trinity Group.

Dutton and others (1996) present the results of numerical modeling of the Twin Mountains and

Paluxy formations and the Woodbine Group in north-central Texas. That modeling is described

in Section 3.3. In addition, they provide discussions on the regional hydrogeological setting; the

stratigraphy and depositional systems of the formations; and the hydrogeological framework of

the formations, including historical conditions, hydraulic heads, detailed investigation of

hydraulic properties, recharge, discharge, and groundwater velocity.

In response to the passage of House Bill 2 by the Texas Legislation in 1985, which required the

"identification and study of critical ground-water areas in the State", the hydrogeological

conditions of the northern Trinity Aquifer and other aquifers in part of central Texas are

presented in Baker and others (1990a) and in part of north-central Texas in Baker and others

(1990b). The purpose of these investigations was the identification of "problems related to

pumping over-drafts and contamination of ground water as they exist or are expected to occur."

Updated investigations conducted by the TWDB evaluating changes in groundwater conditions,

demands, and availability in the northern Trinity and Woodbine aquifers are provided in Bradley

(1999) for portions of central Texas and for the northern Trinity, Woodbine, and other aquifers

are provided in Langley (1999) for portions of north-central Texas.

The TWDB published two reports compiling results of aquifer pumping tests conducted in wells

throughout Texas. The first was published in 1969 by Myers 1969) and the second in 2012 by

Christian and Wuerch (2012). These reports contain analysis of aquifer pumping test data

contained in the TWDB groundwater database and include analyses of tests conducted in wells

completed into the northern Trinity and Woodbine aquifers. An investigation into the regional

trends in transmissivity and hydraulic conductivity in the lower Cretaceous-age sands in north-

central Texas is presented in MacPherson (1983). This investigation was conducted in relation

to a series of studies investigating the potential of the lower Cretaceous-age sands in north-central Texas for use as low temperature geothermal groundwater resources. Other studies related to those investigations are documented in Woodruff and McBride (1979), Woodruff and others (1983), and Woodruff and others (1984). Dutton and others (1996) performed a detailed analysis of aquifer pumping tests and specific capacity tests in the northern Trinity and Woodbine aquifers in north-central Texas as part of the development of a groundwater flow model. Most recently, the TWDB funded a study to extract all aquifer pumping test data for Public Water Supply (PWSs) wells from the TCEQ PWS records (Young and others, 2012) and scan them into a central database.

The geology and hydrology of the Antlers Formation in Oklahoma is presented in two hydrologic atlases prepared cooperatively by the Oklahoma Geological Survey and the USGS. Hart (1974) covers the Ardmore and Sherman quadrangles, covering approximately the western half of the Antlers Aquifer in Oklahoma, and Marcher and Bergman (1983) cover the McAlester and Texarkana quadrangles, covering the eastern half of the Antlers Aquifer in Oklahoma. Davis and Hart (1978) was the first major study focusing entirely on the Antlers Aquifer in Oklahoma and they document hydrological data for the aquifer including well characteristics, water quality, several springs, and low-flow discharge from area streams.

Several investigations related to the chemistry of groundwater in the northern Trinity and/or Woodbine aquifers have been published. A detailed investigation of the chemistry and temperature of groundwater in the Woodbine Group in northeast Texas and the relationship to abnormal structure and oil pools was conducted by Plummer and Sargent (1931). At the request of the city of Sherman, Texas, an investigation was conducted to determine the source of chloride contamination in wells completed into the Woodbine Aquifer and located several miles east of the city (White, 1961). The investigation concluded that the source of contamination was local at the well and not areally extensive. Henningsen (1962) investigated the water diagenesis of sands in the Hensell and Hosston members of the Travis Peak Formation in central Texas. The objective of his investigation was to "interpret the diagenesis of the water and its effects upon the aquifer, as well as provide areal data to predict the quality of water at any point in the region." All of the county reports on groundwater resources (see Table 3.1.1) contain a

discussion of groundwater quality. Taylor (1976) contains tabulated water quality analyses for samples from observations wells in northeast Texas.

As part of the TWDB's program to monitor water quality in aquifers in the state, an investigation was conducted to evaluate the quality of groundwater in the northern Trinity Aquifer in Erath County and portions of surrounding counties (Beynon, 1991). This portion of the northern Trinity Aquifer was selected for study because it corresponded to the area other agencies were studying in an effort to minimize groundwater and surface water impacts from dairy facilities. The water-quality results from sampling 78 wells completed into the Woodbine Aquifer from 1993 through 1995 are summarized in Hopkins (1996). One of the first study areas in the National Water-Quality Assessment Program implemented by the USGS in 1991 was an urban area in Tarrant County, Texas. The results of that study, which investigated the impact of residential and commercial land use on shallow groundwater in the Woodbine Aquifer, are documented in Reutter (1996).

Hudak and Sanmanee (2003) used Geographic Information Systems (GIS) technology to map patterns of nitrate, chloride, sulfate, and fluoride in the Woodbine Aquifer of north Texas. Recently, Holland (2011) completed a Master's Thesis at the University of North Texas investigating water quality in the northern Trinity Aquifer of Texas using multivariate statistics. In 2013, Texas Agri-Life Research published an investigation of changes in water levels and water quality within the northern Trinity and Woodbine aquifers around the Dallas-Fort Worth Metroplex (Chaudhuri and Ale, 2013).

This page intentionally left blank.

3.3   Previous Numerical Modeling Studies

Four previous modeling studies have been conducted in the study area (see Figure 3.3.1). The first was performed in the early 1970s for the TWDB and considered the Travis Peak Formation over a large part of central Texas (Klemt and others, 1975). The second model simulated groundwater flow in the Antlers Aquifer in southeastern Oklahoma and northeastern Texas (Morton, 1992). The third was performed in association with the investigation of the Superconducting Super Collider Site and considered the regional aquifers in north-central Texas (Dutton and others, 1996). The fourth was a groundwater availability model of the northern Trinity and Woodbine aquifers performed for the TWDB (Bené and others, 2004). A discussion of each of these models is provided in the following subsections.

3.3.1   Model Documented in Klemt and others (1975)

The model documented in Klemt and others (1975) considered the Travis Peak Formation over a large part of central Texas. The estimated extent of the model, which is assumed to be coincident with the area they studied, is shown on Figure 3.3.1. The purpose of the modeling was to simulate future drawdown in the Travis Peak Formation due to estimated projected pumping in order to provide a mechanism for evaluating the aquifer's ability to meet anticipated future groundwater demands. The model consisted of 584 total nodes with half simulating conditions in the Hensell Aquifer and the other half simulating conditions in the Hosston Aquifer. The two members were connected using a vertical leakage value designed to represent the Pearsall Member or the Hammett and Cow Creek members of the Travis Peak Formation. The Balcones Fault Zone was assumed to be a barrier to flow and given lower transmissivity values than in the rest of the model. Recharge in the outcrop area was estimated to be about 3 percent of the annual precipitation.

The modeling study consisted of three parts. First, the model was calibrated to drawdowns calculated from subtracting observed water levels in the spring of 1967 from estimated 1900 water levels. Second, predicted water-level declines for the periods spring 1967 to 1975, spring 1967 to 1990, and spring 1967 to 2020 were simulated for both the Hensell and Hosston aquifers using estimated projected pumping. Third, simulations were conducted to estimate the annual pumping required to lower the water level in the Hensell and Hosston aquifers to between 400

and 500 feet below land surface or to the top of the water-bearing sand in 2020. This reduction in water levels was considered to occur only in the portions of the aquifers between the outcrop and the downdip limit of fresh to saline water. The model results indicated tremendous water-level declines in heavily pumped areas, including one area with predicted dewatering of the Hosston Aquifer, and provided a means for estimating the available groundwater from downdip areas of the aquifers.

Conclusions from model predictions documented in Klemt and others (1975) include:

- Tremendous water-level declines would occur in areas of the model with heavy pumping based on pumping projections obtained from resource planning studies. These areas include the vicinity of Belton, Gatesville, Hillsboro, McGregor, Stephenville, and Waco.
- Dewatering of the Hosston Aquifer is possible by 2020 in the area of Stephenville.
- Water-level declines in excess of 1,000 feet by 2020 are possible in the area of Waco.

3.3.2 The Model of Morton (1992)

Morton (1992) developed a two-dimensional model of the Antlers Aquifer in southeastern Oklahoma and northeastern Texas. The model boundary is shown in Figure 3.3.1. The purposes of the modeling were to predict the effects of increased pumping through 2040 on water levels and well yields and to gain an improved understanding of the aquifer, including hydraulic properties, recharge, flow, and connectivity to overlying confining units. The model, developed using MODFLOW, consisted of grid blocks with a dimension of 2 miles in the north-south direction and 3 miles in the east-west direction across the northern 85 percent of the modeled region. In the southern 15 percent of the modeled region, the size of the grid blocks was incrementally increased in the north-south direction. The model encompassed an area of about 10,000 square miles. In the confined portion of the aquifer, the overlying confining units were modeled using a specified-head boundary representing the water table. Constant-head boundaries were used to represent selected lakes and head-dependent flux boundaries were used to represent selected larger streams.

At the time the model was developed, there was little pumping from the aquifer and historical water levels indicate little to no long term change. Therefore, a steady-state calibration of the model was conducted using observed heads from 1970. The calibrated model had recharge of

0.32 inches per year on about the western two-thirds of the outcrop and 0.96 inches per year on about the eastern one-third of the outcrop, a hydraulic conductivity of 5.74 feet per day in the northern two-thirds of the model and 0.57 feet per day in the southern one-third of the model, and a uniform hydraulic conductivity of 2.07×10^{-4} feet per day for the overlying confining unit. The preceding values for hydraulic conductivity were taken from the text in the main body of the report. However, different values are given in the summary and conclusions section of the report. The summary section indicates that aquifer hydraulic conductivity ranged from 0.87 to 3.75 feet per year and that the vertical hydraulic conductivity of the confining units was 1.5×10^{-4} feet per day.

Morton (1992) conducted a sensitivity analysis on the calibrated model to evaluate the sensitivity of model results to the calibration parameters, which were recharge, aquifer hydraulic conductivity, and vertical conductivity of the overlying confining units. Projection simulations were conducted using estimated future pumping to predict drawdown by decade from 1990 to 2040. The predictive simulations used an average storage coefficient of 0.0005 for the confined portion of the aquifer and a specific yield of 0.17 for the aquifer outcrop.

Conclusions reported by Morton (1992) include:

- The simulated results are consistent with the conclusion that that Antlers Aquifer is in steady state as indicated by groundwater hydrologic data.
- Because a transient calibration was not performed due to minimal pumping in the Antlers Aquifer, the head changes predicted by the projection simulations are estimates only.
- The projection simulations show little change in storage in the aquifer for the assumed future pumping volumes.

3.3.3 The Model of Dutton and Others (1996)

Dutton and others (1996) document modeling conducted near the Superconducting Super Collider site in north-central Texas. They constructed two models that focused on the Twin Mountains, Paluxy, and Woodbine aquifers. Dutton and others (1996) first developed a two-dimensional cross-section model that included the aquifers and the confining layers. The purpose of this model was to "evaluate model boundary conditions and the vertical hydrologic properties of the confining layers" (Dutton and others, 1996). They then developed a three-

dimensional model of the aquifers using results and insights gained from the cross-sectional model. The primary purpose of the three-dimensional model was prediction of the effects of future groundwater production. Dutton and others (1996) indicate that the two models "developed in this study were used as tools to estimate amounts of recharge and discharge, evaluate uncertain hydrologic characteristics of confining layers and aquifer boundaries, and quantitatively estimate how water levels will respond to future pumping rates."

For use in their models, Dutton and others (1996) developed formation structure using about 1,200 geophysical logs. Hydraulic conductivity for the aquifers was assigned based on results of aquifer pumping test and specific capacity tests and sandstone distributions. The transmissivity distributions for the Woodbine, Paluxy, and Twin Mountains aquifers indicate lower values near the center of the aquifers, as a result of less sandstone in those areas, and higher values in and near the outcrop and along the Mexia-Talco Fault Zone. Vertical hydraulic conductivity in the aquifer units was assumed to be a factor of ten lower than the horizontal hydraulic conductivity. The horizontal hydraulic conductivity for the confining units was developed based on results of aquifer pumping tests or literature values and estimated sand/shale percentages. A single value was used for the confining units. The vertical hydraulic conductivity in the confining units was assumed to be a factor of 100 less than the horizontal value. Dutton and others (1996) state that "storativity initially was assigned as a covarying function of depth and transmissivity and constrained by the mean and range of values determined from aquifer tests."

Dutton and others (1996) used over 22,000 water-level measurements for calibration. They used information from numerous historical reports to estimate historical pumping from 1891 to 2000 on a county basis. This pumping was distributed in the counties on a random basis at the start of each 10-year stress period using "a binomial probability density function controlled by the number of blocks per county and total pumping in the county" (Dutton and others, 1996). The projected future pumping for 2000 to 2050 was obtained from the TWDB. MODFLOW was used for both the cross-sectional and three-dimensional models.

The cross-sectional model of Dutton and others (1996) included the aquifers of the Twin Mountains and Paluxy formations and the Woodbine Group, as well as the confining units of the Glen Rose Formation and the Fredericksburg, Washita, Eagle Ford, Austin, Taylor, and Navarro

groups. The model consists of 54 columns extending a distance of 111 miles and 10 layers that
extend from ground surface to the base of the Twin Mountains Formation. A steady-state
calibration of the model to water-level measurements reported in Hill (1901) was conducted by
adjusting hydraulic properties. A general head boundary condition was applied at the top surface
of the model and a no-flow boundary was applied to the bottom surface of the model. Several
different types of boundary conditions were applied at the downdip limit of the model, which
corresponded to the Mexia-Talco Fault Zone, to evaluate the nature of this boundary. The
boundary condition types evaluated were no-flow, specified head assuming hydrostatic
conditions, and no-flow with a column of high vertical hydraulic conductivity.

The best model calibration for the cross-sectional model was obtained using the specified head
boundary condition at the fault zone. The results of the model suggest that "ground water exits
the aquifers through the Mexia-Talco Fault Zone" and "cross-formational flow between the
aquifers is not an important control on ground-water movement compared to the discharge
through the fault zone" (Dutton and others, 1996). The initial horizontal hydraulic conductivities
were adjusted during model calibration. The resultant hydraulic conductivities indicate
increasing values in the downdip direction in all three aquifers. The cross-sectional model
predicted recharge rates of 0.11 inches per year for the Twin Mountains Aquifer, 0.25 inches per
year for the Paluxy Aquifer, and 0.017 inches per year for the Woodbine Aquifer (Dutton and
others, 1996).

The three-dimensional model of Dutton and others (1996) was developed based on insights
gained from the cross-sectional model. This model included three layers representing the Twin
Mountains, Paluxy, and Woodbine aquifers and vertical conductance factors representing the
confining units. Uniform grid-block dimensions of 2 miles by 2 miles were used over the
30,600 square mile modeled region. The model extent is illustrated on Figure 3.3.1. A head-
dependent boundary condition was assigned to the top of the model to represent recharge and
discharge in the outcrop area and vertical leakage in the confined area. A no-flow boundary was
assigned at the bottom of the model. After trying several boundary conditions at the Mexia-
Talco Fault Zone, the final one used was the Drain Module of MODFLOW to simulate vertical
discharge from the aquifers at the location of the fault zone. The hydraulic conductivity
distributions were not adjusted during model calibration.

The calibrated model overestimated heads as compared to those given in Hill (1901) for all three aquifer units. The overestimates were considered to be acceptable considering the fact that the water levels in Hill (1901) reflected the effects of pumping and free-flowing wells in the late 1800s. The three-dimensional steady-state model predicted recharge rates of 2.7 inches per year for the Woodbine Aquifer and approximately 4.4 inches per year for the Twin Mountains and Paluxy aquifers. Almost all of this recharge exited head boundaries within the outcrop representing stream, spring, and groundwater ET losses. In steady-state, the model predicted an effective (deep recharge to the confined section) recharge rate of 0.04 inches per year.

The calibrated model was then used to simulate historical conditions from 1891 to 2000 and projected future conditions from 2001 through 2050. The transient model results were compared to selected historical hydrographs and potentiometric surfaces from 1900 and 1990 for all three aquifers, but the transient model was not calibrated. They also present predicted potentiometric surfaces in 2050 based on the assumed projected future pumping in the model. Effective recharge increased from 0.04 inches per year in the steady-state simulation to 0.3 inches per year by 1990 as a result of pumping. The authors questioned whether this induced increase in effective recharge was realistic or an artifact of the boundary conditions employed and suggested further study towards that point.

Conclusions reached by Dutton and others (1996) include:

- Net sand distributions provide an excellent guide for interpreting regional patterns of transmissivity and storativity.
- Predevelopment water levels were very high in the outcrop areas (at or near surface) and were above surface in many areas of the confined portions of the aquifers.
- The free discharge of groundwater from flowing wells in the early twentieth century depressurized large portions of the aquifer and removed significant quantities of water from storage. Discharge rates from flowing well declined as hydraulic head was lowered until approximately the 1940s when pumping accelerated.
- Most water recharged in the aquifer outcrop exits through surficial discharge mechanisms. They estimated that recharge to the confined aquifer system was approximately 25,000 AFY which they noted was far less than annual groundwater production.

3.3.4 2004 Northern Trinity and Woodbine Aquifers GAM by Bené and others (2004)

Bené and others (2004) present the first GAM developed for the northern Trinity and Woodbine aquifers. As the first GAM under the TWDB GAM program, that model was developed to evaluate the availability of groundwater in the aquifers over a 50-year planning period and evaluate aquifer response to projected future pumping and a potential drought. The model was developed using MODFLOW-96 and consisted of seven layers representing four primary aquifer units and three confining units. The model layers are:

- Layer 1 – Woodbine Group - aquifer
- Layer 2 – Fredericksburg/Washita groups – confining unit
- Layer 3 – Paluxy Formation - aquifer
- Layer 4 – Glen Rose Formation – confining unit
- Layer 5 – Hensell Member - aquifer
- Layer 6 – Pearsall/Cow Creek/Hammett members - confining unit
- Layer 7 – Hosston Member - aquifer

The model extended from the western and northern edges of the northern Trinity Aquifer outcrop downdip to the Mexia-Talco Fault Zone and south to the Colorado River (see Figure 3.3.1). The dimensions of all grid blocks in the model are 1 mile by 1 mile. The total number of grid blocks was 694,351, made up of 281 rows and 353 columns. The number of active grid blocks was 220,858.

Structure for the model layers was developed by Bené and others (2004) through interpretation of over 1,000 geophysical logs. The logs were also used to obtain net sand thickness for the aquifer layers. The hydraulic parameters input to the model were horizontal and vertical hydraulic conductivity and storage coefficients. The initial distributions and magnitudes of horizontal hydraulic conductivity in the aquifer units were developed using several steps. First, a statistical correlation factor between transmissivity determined from aquifer pumping tests and net sand thicknesses was developed for each aquifer unit. A surface representing net sand thickness was then developed for each aquifer unit. Third, the net sand distributions were multiplied by the correlation factors to generate transmissivity distributions. Finally, the

transmissivity distributions were divided by layer thicknesses to obtain the hydraulic conductivity distribution for each aquifer layer.

The initial horizontal hydraulic conductivity distributions were modified during model calibration, typically by modifying the correlation factor for the aquifer layers. Horizontal hydraulic conductivity for the confining units determined through calibration consisted of one value assigned in the updip portions and another value assigned in the southern portion of Layers 2 and 4 and a single value assigned for all of Layer 6. The values determined through calibration were generally lower than the initial values assigned to the confining units. A single value for vertical hydraulic conductivity was initially assigned to all model layers. During model calibration, the vertical hydraulic conductivity for Layer 2 was reduced, and Layers 4 and 6 were divided into two areas and two different vertical hydraulic conductivities were assigned to the layers, both of which were lower than the initial value. A single value was initially assigned for the specific storage in the outcrop areas and the storage coefficient in the downdip areas for all model layers. The storage coefficient in the downdip area was slightly lowered in model Layers 1, 2, 4, and 6 during the calibration process.

Recharge in the outcrop areas was calculated as a function of precipitation, soil permeability, land use, and outcropping aquifer characteristics. Long-term average simulated recharge rates in the Texas portions of the aquifers ranged from a high of 0.88 inches per year for the Woodbine Aquifer to 0.31 inches per year in the Hensell Aquifer. Effectively all of the recharge in the outcrop was discharged either through the MODFLOW River Package or the groundwater ET Package discussed below. Therefore, the effective recharge or recharge to the deep confined portions of the aquifer was simulated to be effectively zero.

The boundary conditions for the Bené and others (2004) model consisted of the following. The MODFLOW-96 River Package was used to represent reservoirs and the Streamflow-Routing Package was used to represent interaction between streams and groundwater. Streambed conductances were modified during model calibration. Discharge to streams not represented with the Streamflow-Routing Package, seeps and springs, and groundwater ET were represented with the MODFLOW-96 ET Package. The units overlying the Woodbine Aquifer were represented using the General Head Boundary Package as was interaction between the northern

Trinity Aquifer and the Colorado River. The general head boundary representing the overlying units was modified to improve model calibration. The Horizontal Flow Barrier Package was used to represent faulting in the Mexia-Talco Fault Zone. A no-flow boundary was placed at the base of the model.

Bené and others (2004) developed what they refer to as a steady-state/transitional model and a transient calibration/verification model. Development and calibration of the steady-state/transitional model consisted of two parts. First, initial heads were developed by conducting a quasi-steady-state simulation with no pumping that was run until the simulated model heads changed little or not at all with time. The resultant simulation time was greater than 100,000 years. The results of that quasi steady-state simulation were then used as initial conditions for a second transitional model that simulated the time period from 1880 to 1980. Pumping for this simulation was assumed to be zero in 1880 and to increase linearly through time to pumping estimates from the TWDB for 1980. Recharge for the transitional model was calculated using the average precipitation from 1960 to 2000. The results from the transitional simulation were calibrated to water-level and estimated base flow data for 1980. The parameters used to calibrate the transitional model were storage in all layers in the artesian portion of the aquifers, vertical hydraulic conductivity in all model layers, the horizontal hydraulic conductivity in all layers, and the general head boundary condition used to represent the units overlying the Woodbine Aquifer. Resultant heads from the steady-state/transitional model were assigned as initial conditions for the transient calibration/verification model.

The transient calibration/verification model simulated the time period from 1980 to 2000 and was calibrated to water-level and estimated base flow data in 1990 and verified against water-level and estimated base flow data in 2000. Recharge and pumping were input on a yearly basis in this model. Bené and others (2004) state little calibration was necessary for the calibration/verification model because of how the initial conditions were developed using the steady-state/transitional model. The only changes made to the calibration/verification model were minor in nature and the result of identifying errors in input parameter values.

A sensitivity analysis was conducted using the calibrated calibration/verification model. This analysis consisted of varying the value for one parameter at a time and observing the changes in

model results. Twelve different parameters were investigated with the sensitivity analysis. The analysis indicated that the model is most sensitive to horizontal hydraulic conductivity, vertical hydraulic conductivity, storativity, and pumping. In addition, results in Layer 1, representing the Woodbine Aquifer, showed some sensitivity to the general head boundary used to simulate the overlying formations.

The calibration/verification model was used to predict future heads in the aquifer units based on projected future groundwater demands. This simulation considered the time period from 2000 to 2050 and used a constant recharge rate that was developed from the average precipitation for 1960 to 2000. The model was also used to evaluate aquifer responses to a future drought of record for five simulation scenarios. The precipitation assumed for the projected drought of record was taken from precipitation recorded in 1954 to 1956 during the historical drought of record. All five simulations began in 2000 and simulated to 2010, 2020, 2030, 2040, or 2050. The projected future pumping was used for each simulation. The simulations used recharge calculated using the average 1960 to 2000 precipitation for all years except for the last 3 years, which had recharge assigned based on precipitation during the drought of record.

Primary conclusions reached by Bené and others (2004) were:

- Historical drawdown in major pumping centers in Tarrant, Dallas, and McLennan counties are as much as 800 to 1,000 feet.
- Despite these large drawdown cones in the confined section of the aquifer, they conclude that water levels in the outcrop have been very stable over the last 50 years and, therefore, storage in the aquifers has been relatively constant over the last 50 years.
- The model predicts that effectively all recharge in the predevelopment model discharges in the outcrop through the mechanisms of stream discharge, spring flow, and groundwater ET (rejected recharge) and they conclude that, while uncertain, rejected recharge is likely a large part of the groundwater budget.
- Simulated water levels in the aquifer units are relatively insensitive to recharge from which they concluded that the aquifer was relatively resistant to drought conditions.

- Simulated water levels in the artesian portions of the aquifer units will recover in the future in response to reduced pumping. However, they concluded that this prediction was uncertain because of the high potential for continued growth in the Interstate 35 corridor.
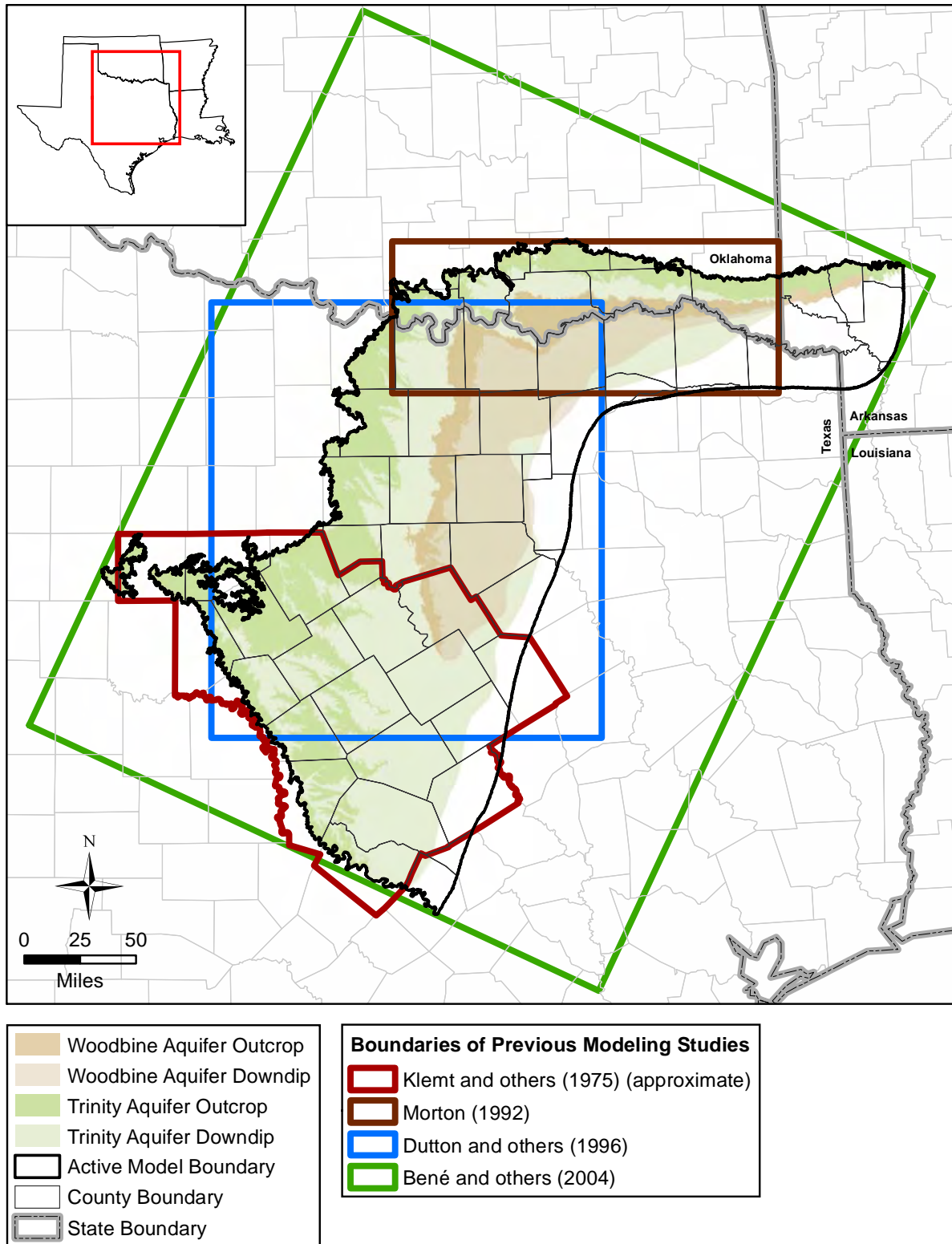
Figure 3.3.1   Boundaries of previous models in the study area.

4.0 Hydrogeologic Setting

This section details the data compilation and analyses used to support development of the conceptual model for the northern Trinity and Woodbine aquifers. This information, in total, defines the hydrogeologic setting and it includes a discussion of hydrostratigraphy, hydraulic properties, hydraulic heads, water quality, recharge, natural aquifer discharge, and pumping.

4.1 Hydrostratigraphy of the Northern Trinity and Woodbine Aquifers

In this subsection, the hydrostratigraphy of the northern Trinity and Woodbine aquifers is discussed, including structure, lithology, and depositional environment. In addition, this subsection includes an introductory discussion of water quality based on geophysical log analyses. The analysis of water quality is expanded in Section 4.4 through the analysis of groundwater quality samples from wells.

4.1.1 Introduction

The rocks and sediments that host the northern Trinity and Woodbine aquifers formed during the geologic time period known as the Cretaceous Period, which lasted from about 145 to 65 million years ago. Cretaceous-age strata are exposed at the surface across broad areas of Texas (Figure 4.1.1). The most abundant rock type in the Cretaceous-age strata in Texas is limestone, which covers the Edwards Plateau (see Figure 2.1.1) and much of central Texas. Light colored limestone road cuts are a common sight along highways in these areas. However, with the exception of the limestone of the Edwards BFZ Aquifer, the most important aquifers in the study area are composed of sand and sandstone of Cretaceous age. Sandstones in the Trinity Group form major aquifers in the Hill Country, Edwards Plateau, and north-central Texas and minor aquifers under the High Plains of west Texas. Sandstones in the Woodbine Group and Nacatoch and Blossom formations host minor aquifers in northeast Texas (George and others, 2011). The focus of the northern Trinity and Woodbine aquifers GAM are the sand-dominated aquifers in the geologic formations of the northern Trinity and Woodbine groups in central and north-central Texas north of the Colorado River (Figure 4.1.2).

Cretaceous-age stratigraphic units in north-central Texas lie on the northwestern margin of the Gulf of Mexico Basin. To the west are Paleozoic-age strata, which were deposited in the Fort Worth and Permian basins (Figure 4.1.1). These older oceanic basins existed prior to the

opening of the Gulf of Mexico. To the east are younger Tertiary- and Quaternary-age strata, which record sedimentary infilling of the Gulf of Mexico Basin. Through geologic time, the Gulf of Mexico Basin has progressively filled from the margins toward the center until achieving the shoreline configuration that exists today (Figure 4.1.3). Cretaceous-age strata are the oldest part of the Gulf of Mexico Basin fill exposed at the surface. Freshwater aquifers occupy only the uppermost few thousand feet of Cretaceous-age strata.

4.1.2   Previous Studies

R.T. Hill conducted the first geologic and hydrogeologic studies of the Trinity and Woodbine groups and aquifers in Texas (Hill, 1891, 1894, 1901). Hill named the various formations and established their stratigraphic relationships to each other. The nomenclature for Cretaceous-age formations is complex and varies between outcrop and subsurface and from north to south (Figure 4.1.2). This complication arises from lithologic and stratigraphic variability, as formations thin, thicken, or merge together. Lithologies change from limestone-dominated in the south to sandstone-dominated in the north. Fisher and Rodda (1966, 1967) revised Trinity Group stratigraphy based on the distribution of limestone in the Glen Rose Formation and lithologic changes that occur between outcrop and subsurface. A comprehensive volume of papers on lower Cretaceous-age stratigraphy (Hendricks, 1957) further documented lithology, paleontology, and stratigraphy, defining three geologically distinctive regions in north and central Texas (Figure 4.1.2). Subsequent studies focused on depositional patterns of sandstone in the Trinity Group (Boone, 1968; Hall, 1976; Caughey, 1977). The understanding of stratigraphy and depositional environments for the Woodbine Group was refined by Dodge (1968, 1969) and Oliver (1971). Nordstrom (1982) in the north and Klemt and others (1975) in the south provide two key hydrogeologic studies relating stratigraphic and lithologic variability to aquifer development.

4.1.3   Overview of Hydrostratigraphy

Stratigraphy and lithology are fundamental properties of aquifers and primary controls on groundwater flow rates and volumes and on groundwater quality and chemical composition. This section describes the stratigraphy and lithology of the formations of the northern portion of the Trinity Group and the Woodbine Group as these properties relate to aquifer development. Stratigraphy is essentially the arrangement of layers in sedimentary rocks. Sediments (gravel, sand, silt, and clay particles) are typically transported by currents in rivers and oceans and

deposited in horizontal layers. Depositional layering is preserved in stratified rocks, imparting

directionality to rock properties. Hydraulic conductivity, for example, is commonly much

greater in the horizontal direction than in the vertical direction. Lithology is also more persistent

in the horizontal direction. A sandstone formation, such as the Hosston Formation, extends

laterally across many counties relatively unchanged, but in the vertical direction, sandstone in the

Hosston Formation changes to shale abruptly across a stratigraphic boundary only a few feet

thick. These properties of stratified rocks result in a system composed of lithologically

contrasting layers (aquifers and aquitards) that extend from shallow recharge areas to deeply

buried areas, providing conduits for regional groundwater flow.

Lithologic changes in the horizontal direction, although more gradational than vertical changes,

result in regional differences in formation properties. Based on geologic variations, the northern

Trinity Group can be divided into five regions in the study area based on stratigraphic and

lithologic similarities (Figure 4.1.4). Stratigraphic layers are physically continuous across the

regions, but layer thicknesses, lithologies, and formation names, as well as corresponding aquifer

names, change. Figure 4.1.5 shows a cross section composed of typical digital geophysical logs

transecting Regions 1 through 5. The digital logs show the spontaneous potential curve on the

left and a resistivity (short normal) curve on the right.

Region 1 encompasses the western and northwestern portions of the study area in Texas as well

as Oklahoma and Arkansas (see Figure 4.1.4). In this region, the northern Trinity Group consists

of undifferentiated sandstones and shales referred to as the Antlers Formation, which is an

aquifer in this region and locally referred to as the Antlers Aquifer. Region 2 lies south and east

of Region 1. In this region, limestones of the Glen Rose Formation separate the sandstones in

the upper portion of the northern Trinity Group from the undifferentiated sandstones and shales

in the lower portion of the northern Trinity Group. In this region, the upper sandstones are

referred to as the Paluxy Formation and make up the Paluxy Aquifer and the undifferentiated

lower sandstones and shales are referred to as the Twin Mountains Formation. The water-

bearing sandstones in the Twin Mountains Formation are locally referred to as the Twin

Mountains Aquifer. Region 3 is stratigraphically similar to Region 2, the main distinctions being

a somewhat arbitrary name change and more shale and limestone in the lower portion of the

northern Trinity Group. In Region 3, the upper sandstones are also referred to as the Paluxy

Formation and make up the Paluxy Aquifer and the undifferentiated sandstones, shales, and limestones in the lower portion of the northern Trinity Group are referred to as the Travis Peak Formation. The water-bearing sandstones in the Travis Peak Formation are locally referred to as the Travis Peak Aquifer.

In Regions 4 and 5, located in the southern portion of the study area, the Glen Rose Formation is thicker than in Regions 2 and 3 and the stratigraphic layers in the lower portion of the northern Trinity Group can be differentiated into individual formations. In these two regions, the stratigraphy above the Glen Rose Formation is also referred to as the Paluxy Formation. These two regions are distinguished by the presence of sandstone in the Paluxy Formation in Region 4, which makes up the Paluxy Aquifer, and the absence of sandstone in the Paluxy Formation in Region 5, corresponding to an absence of the Paluxy Aquifer.

In Region 4, the stratigraphy of the northern Trinity Group underlying the Glen Rose Formation (i.e., the Twin Mountains Formation) is divisible into sandstones of the Hensell and Hosston members separated by limestones and shales of the Pearsall Member. In Region 5, the stratigraphy of the northern Trinity Group underlying the Glen Rose Formation (i.e., the Travis Peak Formation) is also divided into three units. The upper unit consists of sandstones of the Hensell Member. The middle unit consists of the Pearsall/Cow Creek/Hammett members. The limestones of the Cow Creek Member and shales of the Hammett Member occur to the east and coalesce to form the Pearsall Member in the west. The lower unit consists of limestones and dolomites of the Sycamore Member in the outcrop area to the west, sandstones of the Hosston Member to the east and downdip, and shales of the Sligo Member, which overly the Hosston Member in the vicinity of the Mexia-Talco Fault Zone. In both Regions 4 and 5, the sandstones of the Hensell and Hosston members are referred to as the Hensell and Hosston aquifers, respectively.

The Woodbine Group is separated from the northern Trinity Group by the limestone and shale of the Washita/Fredericksburg groups (Figures 4.1.5 and 4.1.6). Across the entire study area, sandstones are rare to absent in the Washita/Fredericksburg groups. In the south (Bell, Williamson, and Travis counties), the Fredericksburg Group includes the Edwards BFZ Aquifer (Jones, 2003). The Woodbine Group is not present west or north of its outcrop, which extends

through the middle of the study area (Figure 4.1.4). In the southern portion of Region 4 and all of Region 5, sandstone is absent in the Woodbine Group (Figure 4.1.5).

For the model, the Woodbine, Washita/Fredericksburg, and northern Trinity groups in the study area were divided into seven layers based on significant differences in geologic properties. These are the Woodbine Aquifer, Washita/Fredericksburg groups, Paluxy Aquifer, Glen Rose Formation, Hensell Aquifer, Pearsall Formation, and Hosston Aquifer (Figure 4.1.6). Generally, the layering differentiates between sandstone-dominated layers that are aquifers and shale- and limestone-dominated layers that are typically confining units. Shales have low hydraulic conductivities and include soluble mineral salts that decrease groundwater quality. Most limestones in the study area possess similar properties. Sand and sandstone, in contrast, typically have high hydraulic conductivities and are composed of relatively insoluble quartz and feldspar grains. The presence of seven contrasting layers does not occur everywhere in the study area. For example, in Region 1 there are only two or three contrasting layers; the sandstones of the Antlers Formation, the shale and limestone of the Washita/Fredericksburg groups, and the sandstone of the Woodbine Group, where present. In fact, all seven contrasting layers are present together only in portions of Region 4. Vertically adjacent model layers can have similar hydraulic properties, and subdividing a thick sandstone sequence, such as the Antlers Formation, adds resolution to the model.

For modeling purposes, all seven layers shown in Figure 4.1.6 were extended throughout the study area. This was done because it was not feasible to distinguish the complex nomenclature used across the study area in the model and the groundwater code used requires that model layers be continuous over the entire model domain. The nomenclature for Region 4 was selected for use because it has the greatest number of divisions that require implementation as individual layers in the model. Mapping of the model layers to the Antlers, Twin Mountains, and Travis Peak aquifers in Regions 1, 2, and 3, respectively, can be done using the cross section in Figure 4.1.5 and the chart in Figure 4.1.6. For example, the Paluxy Aquifer maps to the upper sands of the Antlers Aquifer in Region 1 and the Hosston Aquifer maps to the lower sands of the Travis Peak Aquifer in Region 3, the lower sands of the Twin Mountains Aquifer in Region 2, and the lower sands of the Antlers Aquifer in Region 1. The layer terminology shown in Figure 4.1.6 is used throughout the remainder of this report.

4.1.4 Structural Features

Structural geology deals with structural changes to sedimentary rocks after deposition in horizontal layers. Most rock formations have been structurally deformed by compressive forces within the Earth's crust or by subsidence. Subsidence of the Gulf of Mexico Basin caused Cretaceous-age formations to tilt (dip) toward the southeast (Figure 4.1.3). Formations at land surface in the west are thousands of feet below surface in the east. The structural dip of the strata in the northern Trinity and Woodbine groups is regular and concentric to the East Texas Basin, which is an embayment (now filled with sediment) of the Gulf of Mexico Basin (Figure 4.1.7). Structural dip increases toward the center of the East Texas Basin (to the southeast). The lowest dips (15 feet per mile) occur in the southwest outcrop area. In the northwest outcrop area, dips are 25 to 30 feet per mile. Along the downdip margin of the study area, dips range from 250 to 350 feet per mile (Figure 4.1.7). Along with lithology and stratigraphy, structural dip is another key property of layered aquifers, because it enables downward groundwater flow.

Subsidence also impacts sedimentary thicknesses. Without subsidence of the land surface, sediments would not be able to accumulate to form sedimentary rocks. The opposite of subsidence is uplift. Sediments are eroded in uplifted areas (plateaus and mountains) and deposited in subsided areas (river valleys and ocean basins). Gulfward increasing subsidence has resulted in the formation of sedimentary wedges that thicken Gulfward (Figure 4.1.3). The stratigraphic intervals of the northern Trinity and Woodbine groups in the study area thicken southeastward in a regular pattern, which parallels the structural dip (compare Figures 4.1.7 and 4.1.8).

The same structural forces that tilt stratigraphic layers also break them along surfaces of discontinuity called faults or fractures. A fault displaces the broken layer so that the two sides are no longer fully in contact. Fault displacements range from a few feet to hundreds of feet. In the latter case, a faulted layer may be completely disconnected. Fractures are breaks in layers without displacement. Both faults and fractures are generally oriented vertically and provide opportunities for vertical groundwater flow. Fault locations and properties in the study area were compiled from the geologic literature in Ewing (1990, 1991). These documented faults represent the largest faults (most laterally extensive and largest vertical displacements) in the study area that disrupt Cretaceous-age strata (Figure 4.1.7). Small faults and fractures are common in most geologic formations, and have been mapped in outcrops of the Cretaceous-age strata and

excavated tunnels (Nance and others, 1994). These localized structures are typically less than 1 mile long, have displacements less than 10 feet, and are subvertically oriented (cross cutting horizontal bedding). Many small faults drip or even flow water into excavated tunnels, indicating that they form pathways for vertical groundwater flow.

Faults tend to occur in closely spaced groups (fault zones) in response to geographically focused structural forces. The study area includes three regions of large-scale faulting and structural deformation. The Balcones Fault Zone extends into the study area from the south through Travis, Bell, McLennan, and Hill counties (Figure 4.1.7). Displacements across faults in this fault zone range from 100 to 400 feet, which are sufficient to completely disconnect some layers (Klemt and others, 1975). Faults in the Balcones Fault Zone are mostly down to the east, with the disconnected layer deeper on the east side of the fault relative to its position on the west side. The Mexia-Talco Fault Zone is a complex zone of interweaving faults that extends along the entire length of the downdip boundary of the study area (Figure 4.1.7). Individual faults in this fault zone have as much as 700 feet of displacement (Ewing, 1990). Fresh groundwater in the aquifers in the study area does not extend beyond the Mexia-Talco Fault Zone (Klemt and others, 1975).

An area of faulted and folded strata occurs in Cooke and Grayson counties and extends northwest into Oklahoma (Figure 4.1.7). This structurally deformed area is commonly known as the Sherman Syncline and Preston Anticline. In some cases, strata that experience compressive forces will fold instead of break along faults. Near the city of Sherman in Grayson County, there are several faults that parallel the southeast-trending folds (Figure 4.1.7). Structural complexity in the Sherman area is mainly confined to underlying Paleozoic-age strata, but is manifested in overlying Cretaceous-age strata as gentle folds. The thickness patterns in the Cretaceous-age strata also reflect the folds (Figure 4.1.8), indicating that structural movement occurred during deposition in the Cretaceous Period. The structures in the area of Sherman, Texas lie at the hinge between north-oriented outcrops to the south and east-oriented outcrops through Oklahoma (Figure 4.1.7). These large-scale trends resulted from continental breakup that preceded formation of the Gulf of Mexico Basin.

4.1.5 Paleogeography and Depositional Environment

Paleogeography and depositional environment affect the properties of sedimentary rocks. Paleogeography is the configuration of landforms and water bodies that existed at the time of deposition. Depositional environment is the specific setting of sediment accumulation, such as a river or a marine shoreline. A depositional system, introduced later in this section, is a three-dimensional body of rock or sediments deposited in a specific depositional environment. Paleogeography is reconstructed from the rocks themselves (the rock record), which involves comparison of properties of rocks of the same age across broad regions. Missing rocks indicate that an area was uplifted (nondeposition or erosion). Fossils are important to paleogeographic reconstruction because the habitats of specific plant and animal species are generally understood. Fossils of marine shellfish are ubiquitous in Cretaceous-age limestones, for example. Paleogeography provides a context for interpreting depositional environments, which are more specific and localized. A marine shoreline (sandy) is different from a marine bay (muddy). Sandstones are deposited where currents are strong, such as river channels and shorelines; shales are deposited in quiet water, such as bays and lagoons. Understanding depositional environments allows prediction of rock properties where data are discontinuous (in between wells). Depositional environments for all formations in the northern Trinity and Woodbine groups were interpreted and used to infer rock properties and directionality of those properties as discussed in Section 4.2.

Paleogeographic reconstructions of North and Central America during the Cretaceous Period provide a starting point and context for the exploration of depositional history and environments for the northern Trinity and Woodbine groups. The Cretaceous Period was characterized by long-term rising sea level and flooding of the continents. At the beginning of the Cretaceous Period, most of North America was covered by terrestrial landforms, much like today (Figure 4.1.9a). The ancestral Gulf of Mexico was in a similar position as it is today, and rivers carried sediment from mountainous areas in the northwest across north-central Texas to depositional sites farther southeast. Figure 4.1.9a is a schematic representation of the eroded surface of the Paleozoic-age strata upon which basal sands in the Trinity Group were deposited (Boone, 1968).

Later in the early Cretaceous Period, rising sea level caused the Gulf of Mexico shoreline to move west and north, flooding east Texas and changing north-central Texas into a low-lying

coastal area (Figure 4.1.9b). Basal sands (Hosston Aquifer) of the northern Trinity Group, which were deposited in river channels, represent the first Cretaceous-age depositional system to develop along that coast. The shoreline coincided approximately with the downdip boundary of the study area (Figure 4.1.9b). Following deposition of the Hosston Aquifer, the coastal plain partly flooded, and the shales and limestones of the Pearsall Formation were deposited in the south and east. Pearsall Formation deposition was followed, in turn, by another sandy coastal plain system (Hensell Aquifer). Glen Rose Formation limestones and Paluxy Aquifer sandstones record yet another episode of rising sea level followed by shoreline progradation.

In the late Cretaceous Period, sea levels continued to rise, eventually flooding the northern Trinity Group coastal plain and creating marine conditions across most of Texas as well as the central portion of North America (Figure 4.1.9c). Limestones and shales of the Washita and Fredericksburg groups were deposited at this time in shallow marine waters similar to the modern Florida Keys. By late Cretaceous time, renewed input of sand-rich sediments from land areas to the north formed the depositional systems of the Woodbine Group in a variety of near-shore environments.

Rising sea levels in the Cretaceous Period were periodically offset by input of sand-rich sediment. Each episode of sand deposition built up the coastal plain and pushed the shoreline back toward the southeast. Sand was supplied discontinuously by episodic uplift in the north and west. During times when the supply of sand was low, the study area flooded and limestones and shales were deposited. Thus, fluctuating paleogeographic conditions resulted in vertical alternation of sandstone-rich and limestone-rich sedimentary formations. The western and northwestern portions of the study area, which were always farthest from the coast, are sand dominated, whereas the eastern and southern portions are limestone and shale dominated.

4.1.6 Methods and Data

Data compilation and quality control represent major tasks in creating the hydrostratigraphic framework. Previous geologic studies did not cover the entire study area and were not focused on data compilation. Furthermore, hydrostratigraphic frameworks used to construct previous groundwater models were not preserved. In addition to developing a well-documented hydrostratigraphic framework for the GCDs in GMA 8, another goal was to build an equally well-documented, publically available database, encompassing all raw data and interpretations

used to complete this study. This database will provide a firm foundation for further studies and future work in a large and complex aquifer system.

The stratigraphic and lithologic study presented here was based on geophysical logs. Geophysical logs are required for correlating stratigraphic boundaries. Lithologic descriptions from previous studies were used to calibrate geophysical logs, but standard logging principles provided the basis for interpreting lithology from spontaneous potential and resistivity log responses. Although there is some uncertainty where limestone and sandstone are interbedded in a freshwater environment, an attempt was made to reduce this uncertainty by referring to published descriptions.

Geophysical well logs were used to correlate boundaries, map lithologies, interpret depositional environments, and estimate water quality in each layer of the northern Trinity and Woodbine aquifers. Large amounts of time and effort were spent searching for, evaluating the quality of, and depth calibrating geophysical well logs. When that work was complete, a database comprising 1,498 geophysical well logs distributed across the study area was compiled. During the progress of the study, some of those logs were eliminated from the database owing to problems with log quality or incomplete vertical coverage. The final database includes 1,302 logs, which represent the best available coverage of Cretaceous-age formations across the study area (Figure 4.1.10). Almost all logs in the final database are electric logs, meaning they include spontaneous potential and resistivity curves. Some wells also have gamma-ray and other log types, but for consistency and comparability, only the spontaneous potential and resistivity curves were used. The final database includes 408 geophysical logs from water wells and 894 geophysical logs from oil and gas wells.

The well log database is primarily composed of electronic image files, such as TIFF or JPEG, which are typically referred to as rasters. Before the advent of desktop computing, well logs were printed on long, folded paper. Rasters are scanned versions of those paper logs. The commercially available Petra software (IHS, Inc.) was used to prepare and interpret logs and display results. Petra is a GIS-type program that specializes in spatial data from wells. Raster versions of well logs are just images with no attached quantitative information. Petra provides functions for visually examining the images and recording observations at specific depths.

Raster logs were used to correlate stratigraphic boundaries and interpret lithologies. Geologic formation boundaries were defined in outcrop and traced into the subsurface using standard well log correlation techniques. The work documented here established that formation definitions in various portions of the study area are essentially correct; no significant changes are necessary. This study focused on regional consistency and connecting layers across lithologic changes. For example, it was confirmed that the Paluxy and Glen Rose formations in the south are at the same stratigraphic level as the upper part of the Antlers Formation in the north (Figure 4.1.5). In other words, strata in the Paluxy and Glen Rose formations are physically connected to strata in the upper Antlers Formation even though lithologies differ. In contrast, strata in the Fredericksburg Group everywhere overlie strata in the Antlers or Paluxy formations. Actual stratigraphic details are complicated, however, and most formation boundaries are gradational to some extent. The layer definitions and well-to-well correlations establish a regionally consistent stratigraphic framework while preserving as much local detail as possible.

Lithology interpretations were based on geophysical well logging principles supported by limited well sample information and best professional judgment. Lithologic interpretation was conducted on 988 geophysical logs. Electrical properties, as measured in wells, provide information about both lithology and fluid saturation. If fluid saturation is relatively homogeneous (as is expected in an aquifer), then lithology has a pronounced effect on electric log responses. Shales are relatively conductive (low resistivity), whereas limestones generally have high resistivities. Sandstones display intermediate resistivities, which are partly controlled by pore fluid composition (salinity). Shales display distinctive responses on electric logs and can be interpreted with high confidence. Sandstones and limestones can be distinguished from each other with less confidence, especially in a freshwater environment. The spontaneous potential log, which under certain conditions provides a qualitative measure of hydraulic conductivity, is useful for distinguishing permeable sandstone from impermeable limestone. Knowledge of local lithologies from previous studies provides a context for lithologic interpretation. Using Petra functions, a foot-by-foot continuous vertical record of lithology for each electric log was constructed. Lithologies (sandstone, shale, limestone) were then summed by layer and mapped.

Electric logs in digital format were used to interpret water quality and for graphical display (Figure 4.1.11). Whereas raster images are just pictures, digital logs are computer files of measured log responses. Digital logs are tables of measured values, generally having one log

value for every half foot of depth. Information can be extracted wholesale from digital logs

without painstaking log-by-log measurement. Digital log values can be analyzed statistically and

used in equations to create derivative logs. Unfortunately, the availability of digital logs is

limited, and the cost is high. For older wells, and most water wells, log curves must be manually

traced using digitizing software. A distribution of 109 digital electric logs across the study area

was compiled. The locations of the digital logs are shown in red on Figure 4.1.10.

4.1.7 Lithologic Character of Enclosing Formations

Prior to the onset of deposition during the Cretaceous Period, north-central Texas was covered

by eroded landforms comprising three different geologic provinces. These underlying rocks

possess differing hydraulic properties that may influence groundwater flow in the aquifers.

Where log depths permitted, lithologies of underlying rocks extending 300 feet below the base of

the Cretaceous-age strata were interpreted. Paleozoic-age strata underlie the western and

northwestern portions of the study area (Figure 4.1.12). Paleozoic-age strata are composed of

sandstone, shale, and limestone similar to the overlying Cretaceous-age strata (Brown and others,

1990). Paleozoic-age sandstones are potential aquifers and may be in hydraulic communication

with Cretaceous-age sandstones where the two are superimposed.

Deformed rocks of the Ouachita fold belt underlie Cretaceous-age sandstones east of the

Paleozoic-age terrain (Figure 4.1.12). Ouachita rocks are also Paleozoic in age, but have a

different history. Ouachita rocks were squeezed between two continental plates (ancestral North

and South America) during a collision that took place during the Paleozoic Era (Flawn and

others, 1961). During that collision, Ouachita rocks experienced high pressures and

temperatures, which destroyed whatever hydraulic conductivity they originally possessed.

Ouachita rocks in the study area are aquitards.

Jurassic-age sandstones (Cotton Valley Group) underlie Cretaceous-age sandstones along the

downdip margin of the study area (Figure 4.1.12). Sandstones of the Cotton Valley Group and

overlying Hosston Aquifer are lithologically similar and in hydraulic communication.

Black shales of the Eagle Ford Group overlie the sandstones of the Woodbine Group, forming an

effective aquitard and top seal across the eastern portion of the study area. Additional low

hydraulic conductivity rocks of the Austin Chalk overlie Eagle Ford shales. Somewhat higher in

the stratigraphic section, sandstones forming minor aquifers are present in uppermost

Cretaceous-age strata (Nacatoch and Blossom aquifers). These overlying formations are only present east of the Woodbine Aquifer outcrop. Through the TWDB, a GAM has been developed and is available for the Nacatoch Aquifer (Beach and others, 2009) and a GAM is currently under development for the Blossom Aquifer.

4.1.8   Regional Sandstone Distribution and Depositional Systems

Sandstones in the northern Trinity and Woodbine groups record a major pulse of sediment input in the face of rising sea levels during the Cretaceous Period (Figure 4.1.9). Within that overall sandy interval, smaller scale pulses of sand deposition alternated with marine flooding. This back and forth fluctuation formed the layered system of aquifers and aquitards in the northern Trinity and Woodbine groups in the study area, which is the focus of this report. This section describes regional lithologic properties and sandstone depositional systems of each layer in the Woodbine, Washita/ Fredericksburg, and northern Trinity groups (see Figure 4.1.6). Sandstone distribution, geometry, and orientation are illustrated using net and percent sandstone maps. Depositional systems interpretations are also illustrated on maps. Sandstone and depositional systems maps are shown on Figures 4.1.13 through 4.1.30 by layer from deepest to shallowest. Net sandstone maps show total sandstone thickness in the layer, which is sensitive to the gross layer thickness, whereas the percent sandstone maps show a measure of sandstone concentration without regard to absolute thickness. Where sandstone percentages are high, individual sandstone beds are thick and interbedded shales are thin. Together, the two types of sandstone maps delineate fairways where potential for groundwater flow is greatest.

Figures 4.1.31 through 4.1.37 are schematic, reduced-scale cross sections showing depths, lithologies, and water quality in profile. The cross sections were developed using high-resolution digital electric logs. Large-format versions of the cross sections, showing the digital logs, are included in Appendix C.

Depositional systems maps are based largely on sandstone patterns in paleogeographic context and further emphasize sandstone geometries and orientations. Sandstones in the northern Trinity and Woodbine groups were deposited in two contrasting environments settings: fluvial and shoreline. Fluvial environments include river channels and valleys, whereas shoreline environments include coastal barrier and near offshore areas. The term "fluvial" is also used here for rivers in coastal plains and delta plains. The term "deltaic shoreline" is used here for

coastal barrier and near offshore areas and on adjacent to river deltas. Both fluvial and shoreline environments produce sandstone bodies having elongated external geometries, but orientations vary. Both of these environments produce sandstone bodies having elongated external geometries, but orientations vary. Fluvial sandstones are elongated in the direction of river flow, mainly toward the coast, whereas shoreline sandstones are elongated parallel to the coast. In the northern Trinity and Woodbine depositional systems, fluvial sandstones are oriented mainly northwest-southeast, whereas shoreline sandstone are oriented mainly southwest-northeast. Sandstone geometry and orientation are important because they influence groundwater flow directions. The following discussion is presented by layer from deepest to shallowest.

The specific depositional environments and systems described here are based on previous studies. The depositional systems of the Hensell and Hosston aquifers and the Antlers Aquifer equivalent are documented by Boone (1968) and Hall (1976). The depositional systems of the Paluxy Aquifer are documented by Caughey (1977) and those of the Woodbine Aquifer are documented by Dodge (1968, 1969) and Oliver (1971). Along the downdip margin of the study area, the depositional systems of the Hosston Member of the Travis Peak Formation are documented by McGowen and Harris (1984). The work conducted for this study supports these earlier studies and adds detail relevant to groundwater modeling.

Hosston Aquifer

The Hosston Aquifer is sand-dominated across the entire study area. The aquifer is relatively thin (less than 100 feet) in western outcrops but thickens greatly (500 to 1,000 feet) in downdip areas to the east (see Figures 4.1.31 through 4.1.35). Net sandstone thickness ranges from less than 50 feet to greater than 800 feet along the downdip margin of the study area (Figure 4.1.13). The percent sandstone map displays the opposite pattern, with highest sandstone percentages occur in the west (Figure 4.1.14). High percentage sandstone lobes extend eastward from the outcrop. Net sandstone patterns show relatively thicker sandstones at and near the outcrop, which coincide with high sandstone percentages (compare Figures 4.1.13 and 4.1.14). Two broad high-sand trends dominate the study area: one in the north from Cooke to Parker counties and extending downdip to Dallas and Collin counties and another one in the south centered on Comanche and Erath counties and extending downdip to Bell, McLennan, and Hill counties. The Hosston Aquifer typically has a sharp lower contact with the underlying Paleozoic-age strata

and is sandiest in its lower part. Individual sandstones range from a few feet to about 100 feet thick and average 20-feet thick.

Based on the orientation of sand-rich trends (Figure 4.1.14) and paleogeographic context (Figure 4.1.9b), sandstones of the Hosston Aquifer were deposited in a fluvial environment. Major rivers (channel axes) entered the study area from the west and flowed east and southeast into the East Texas Basin (Figure 4.1.15). Based on the concentration of sand (percent sandstone), the coastal plain must have contained several broad sandy rivers. These rivers were not confined in steep-walled valleys but were free to migrate laterally, depositing sand in wide, coalescing belts. Thus, individual sandstones in the Hosston Aquifer display broad, sheet-like geometries, which are elongated toward the southeast (Figure 4.1.14). These rivers supplied abundant sand to deltaic shoreline systems located beyond the study area in the East Texas Basin (McGowen and Harris, 1984). Increased subsidence in the Mexia-Talco Fault Zone along the eastern boundary of the study area allowed sand to accumulate in thick sequences (Figure 4.1.13).

Pearsall Formation

The Pearsall Formation is composed of sandstone and shale in the north and limestone and shale in the south (see Figures 4.1.36 and 4.1.37). Sandstone is best developed in northwestern counties extending south into Collin and Dallas counties (Figure 4.1.16). Thickest sandstone is located mainly downdip in northeastern counties. Unlike the Hosston Aquifer, sandstones in the Pearsall Formation do not display strong west-east orientation, rather, they are oriented mainly north-south (Figure 4.1.16). The Pearsall Formation is not a sand-dominated sequence; percent sand is less than 50 percent in most wells (Figure 4.1.17). Limestone dominates in downdip counties in the southern half of the study area (see Figures 4.1.33 through 4.1.35).

The Pearsall Formation was deposited during a transgressive episode. The supply of abundant sand that fed fluvial systems in the Hosston Aquifer was shut off, and the marine waters flooded (transgressed) the south. Sand deposition persisted in the north where a deltaic shoreline system formed (Figure 4.1.18). Relatively small rivers supplied sand to the delta from source areas to the north and northeast. Sand-poor coastal plain environments flanked the small rivers. South of the sandstone area, limestone and shale were deposited in offshore marine environments. In summary, shallow marine environments encroached the area from the southeast in response to

rising sea level, while coastal plain and shoreline environments persisted in the north
(Figure 4.1.18).

Hensell Aquifer

The Hensell Aquifer is another sand-dominated interval. This aquifer, which is generally
relatively thin (less than 120 feet), is thickest in outcrop areas and thins downdip (Figures 4.1.31
through 4.1.35). Net sandstone thickness ranges from 0 to 100 feet, averaging 50 feet
(Figure 4.1.19). Percent sandstone is greater than 50 percent across most of the study area
(Figure 4.1.20). Several high sandstone trends extend directly away from the outcrop and are
west-east oriented in the south but become more north-south oriented to the north
(Figure 4.1.20). Most high sandstone trends terminate before reaching the downdip margin of
the study area. In more downdip areas, sandstones display north to northeast orientations
(Figure 4.1.20). Individual sandstones in the Hensell Aquifer are thickest (15 to 25 feet) within
the high percent sandstone trends.

The Hensell Aquifer was deposited in fluvial and deltaic shoreline systems that migrated
(prograded) into the study area mainly from the west and northwest. Broad sandy rivers flowed
eastward and merged with an equally broad sandy shoreline system (Figure 4.1.21). The Hensell
Aquifer coastal plain and shoreline never extended as far southeast as they did in the Hosston
Aquifer. In effect, the Hosston Aquifer constructed a platform of sand that completely covered
the study area, and Hensell Aquifer depositional systems never reached the edge of that stable
platform. Thus, the Hensell Aquifer never experienced large-scale subsidence in downdip areas
and, consequently, does not thicken downdip. Along the downdip margin of the area, the
Hensell Aquifer was deposited in shale-dominated offshore marine systems. Uppermost sands in
the Hensell Aquifer were partly reworked during the marine transgression that deposited the
limestones of the overlying Glen Rose Formation.

Glen Rose Formation

The Glen Rose Formation is limestone dominated across most of the study area except in the
northwest. Limestones in the Glen Rose Formation range from 0 to 400 feet thick in the outcrop
and 300 to 1,300 feet thick in downdip areas (Figures 4.1.31 through 4.1.37). The Glen Rose
Formation includes a northeast-oriented lobe of sandstone in the northwest, which reaches
200 feet in thickness (Figure 4.1.22) and consist of 40 to 60 percent sandstone (Figure 4.1.23).

Individual sandstones in the Glen Rose Formation are thinner than those in the Hensell and Hosston aquifers, averaging only 8-feet thick. Thus, the Glen Rose Formation is composed of thick limestones across most of the study area and thinly interbedded sandstone and shale in the northwest.

Limestones in the Glen Rose Formation record a marine transgressive episode, which was more extensive than the transgression during deposition of the Pearsall Formation. Shallow marine waters covered most of the study area, although sand deposition persisted in the northwestern corner (Figure 4.1.24). Based on sandstone geometries and bed thicknesses, sandstones in the Glen Rose Formation were deposited in marginal marine environments, including small fluvial systems, coastal lowlands, and shorelines. In summary, deposition of the Glen Rose Formation was coincident with another sea level rise and another flooded coastal plain. Shallow marine limestones covered much of the study area, but marginal marine and shoreline environments persisted in the northwest.

Paluxy Aquifer

The Paluxy Aquifer is a sandstone-dominated interval centered in the north. The aquifer is thickest (greater than 400 feet) in the northeast and thins to the south (Figure 4.1.37). Net sandstone is also thickest in the northeast (Figure 4.1.25). Net sandstone is closely related to interval thickness, so the percent sandstone map shows that the Paluxy Aquifer is commonly sand-dominated even where it is thin (Figure 4.1.26). The Paluxy Aquifer is shale dominated in a thin remnant in the southeast and in the far northeast. Sandstones in the Paluxy Aquifer display elongate trends that enter the study area from the north, northwest, and west (Figure 4.1.26). In the north, sandstone trends in the aquifer extend completely across the study area, exiting to the southeast. However, in the south, sandstones in the aquifer thin to zero thickness before reaching the eastern boundary of the study area (Figure 4.1.26). Within high percent sandstone trends (greater than 60 percent), individual sandstones in the Paluxy Aquifer average 20 feet in thickness. In areas with lower percent sandstone, individual sandstones average 10 to 15 feet in thickness.

During deposition of the Paluxy Aquifer, fluvial systems converged on the study area from the north, northwest, and west. Rivers flowed east to southeast across most of the study area but flowed directly south in the northeast portion of the area (Figure 4.1.27). In the north, the

shoreline was beyond the downdip boundary of the study area but, in the south, a broad sandy shoreline extended from Coryell County northeast to Dallas County (Figure 4.1.27). A shale-dominated marine shelf existed south and east of the shoreline system. Fluvial sandstones in the Paluxy Aquifer are elongated directly away from the outcrop (sandstone orientation perpendicular to outcrop orientation). In summary, deposition of the Paluxy Aquifer was coincident with major sediment input from the north, northwest, and west, which constructed broad sandy coastal plain and shoreline deposits. The offshore marine environments in the south resulted in shale-dominated deposits.

Washita/Fredericksburg Groups
The Washita/Fredericksburg groups are composed of limestone and shale across the entire study area (Figures 4.1.31 through 4.1.5.) The Washita/Fredericksburg groups are exposed at the surface in between the northern Trinity and Woodbine group outcrops. The Washita/Fredericksburg groups thicken downdip from about 400 feet near the outcrop to 800 feet along the downdip boundary of the study area. The thickness of the Washita/Fredericksburg groups is relatively constant from north to south (Figure 4.1.37). The deposition of the Washita/Fredericksburg groups records a major marine transgression similar to the Glen Rose Formation, but even more extensive. There were no significant sources of sand during the Washita/Fredericksburg depositional episode; shallow marine conditions prevailed across the area.

Woodbine Aquifer
The Woodbine Aquifer is sandstone dominated from Hill County in the south to Fannin County in the north, but is shale dominated in the far northeast and in the south (Figure 4.1.28). This aquifer is not present west or north of its outcrop. Net sandstone is thickest in the area where outcrop trends change from north to east oriented, forming a lobe of sandstone greater than 300-feet thick (Figure 4.1.28). Sandstone concentration (percent sandstone) is actually greater to the south of this net sandstone maximum (Figure 4.1.29). Sandstones in the Woodbine Aquifer are generally elongated to the northeast, paralleling outcrop trends. Thick sandstones are concentrated in the lower half of the interval. In the area where the Woodbine Aquifer includes greater than 200 feet of net sandstone (Figure 4.1.28), individual sandstones in the lower part of the interval average 20 feet in thickness. In Collin County, individual sandstones reach 80 feet in

thickness. South of Hill County, the Woodbine Aquifer is thin (less than 20 feet) and composed entirely of shale (Figure 4.1.37).

The Woodbine Aquifer records the final progradation of sandy depositional systems into the study area. Subsequent to deposition of the Woodbine Aquifer, the entire area was covered by an offshore marine, shale-dominated environment. Depositional systems in the Woodbine Aquifer were primarily deltaic marine shorelines and related coastal lowlands (Figure 4.1.30). Small fluvial systems may be present in Grayson County and in Oklahoma. Thick stacks of marine shoreline sandstones cover eastern Collin and western Hunt counties (Figure 4.1.28). Ellis and Dallas counties are covered by thinner but more concentrated shoreline sandstones (Figure 4.1.29). In summary, sandstones in the Woodbine Aquifer were deposited primarily in deltaic shoreline environments.

4.1.9   Water Quality from Resistivity Logs

Groundwater quality in sandstone aquifers can be estimated using electric log resistivities. Freshwater is more resistive to the flow of electrical current than is saline water. Therefore, in general, higher sandstone resistivity coincides with better quality groundwater. Empirical relationships have been established between groundwater salinity, as determined by chemical analysis, and resistivity of the corresponding saturated sandstone (Jones and Buford, 1951; Alger, 1966; Fogg and Blanchard, 1984; Hamlin and others, 1988; Collier, 1993). Lithology, bed thickness, porosity, water composition, and temperature among other variables also influence measured resistivities. Specific resistivity cutoffs for fresh or slightly saline groundwater are usually only valid in limited geographic areas where formation properties are relatively constant (Collier, 1993). Resistivity was mapped in selected sandstone-dominated layers without attempting to quantify corresponding groundwater salinities. Instead, resistivity maps and descriptions are presented in terms of relatively lower and higher groundwater salinities. Using digital electric logs, average (median) resistivity in the aquifers was calculated. To reduce bed thickness effects, only sandstones greater than 10-feet thick were included in the averaging process. The resistivity maps show trends that can be related, at least in part, to groundwater salinity changes. The approximate downdip limit of freshwater in each sandstone layer is marked on the cross sections in Figures 4.1.31 through 4.1.35. These downdip limits of freshwater, which is also general and qualitative, were based on resistivities, previous studies

(Klemt and others, 1975; Nordstrom, 1982), and the groundwater quality data in water wells presented in Section 4.4 of this report.

Low salinity groundwater extends deepest and farthest downdip in the Hosston Aquifer. Low salinity groundwater is present at depths of 3,500 to 5,000 feet below land surface in Collin, Dallas, and Ellis counties and at depths of 2,500 to 3,500 feet in Hill and McLennan counties (Figures 4.1.31 through 4.1.34). Farther south, low salinity groundwater in the Hosston Aquifer extends less than 2,000 feet below land surface (Figure 4.1.35). Resistivities in the Hosston Aquifer are relatively high in areas coincident with high percent sandstone trends (compare Figures 4.1.14 and 4.1.38), suggesting that recharging (low salinity/high resistivity) groundwater preferentially flows along these high conductivity pathways. Exceptionally high resistivities in the south are probably caused by high bicarbonate concentrations (Collier, 1993). Resistivities in the Hosston Aquifer are uniformly low in the far northeast, indicating generally high groundwater salinities in that region.

Groundwater in the Hensell Aquifer has relatively low salinity in and near the outcrop area, but the lower salinity groundwater does not extend as far downdip in the Hensell Aquifer as in the Hosston Aquifer. Higher salinity groundwater in the Hensell Aquifer commonly overlies lower salinity groundwater in the Hosston Aquifer, an example of decreasing salinity with depth (Figures 4.1.31 through 4.1.35). Resistivities in the Hensell Aquifer also show some geographic coincidence with high percent sandstone trends (compare Figures 4.1.19 and 4.1.39). As in the Hosston Aquifer, resistivities in the Hensell Aquifer are uniformly low in the northeast.

In the northern portion of the study area, relatively low salinity groundwater in the Paluxy Aquifer extends as far or farther downdip than it does in the Hosston Aquifer, although not as deep (Figures 4.1.31 and 4.1.32). Except in the far northeast, areas of high sandstone coincide with higher resistivities in the Paluxy Aquifer (compare Figures 4.1.26 and 4.1.40).

Resistivities in the sandstones of the Woodbine Aquifer are lower than in the sandstones of the Paluxy, Hensell, and Hosston aquifers. Formation-specific properties unrelated to water quality probably cause these resistivity differences within the Woodbine Aquifer, however, downdip decreasing resistivities reflect increasing groundwater salinity (Figure 4.1.41). High resistivities (low salinities) extend further downdip in two areas: in the south, where the Woodbine Aquifer is thin but the sandstone percentage is high (Figure 4.1.29), and, in the north, where the net

sandstone in the Woodbine Aquifer is high (Figure 4.1.28). In the Woodbine Aquifer, low salinity groundwater is best developed in Collin, Dallas, and Ellis counties, coinciding with greater concentrations of sandstone in those counties (compare Figures 4.1.29, 4.1.31, and 4.1.32). Even in this area, however, low salinity groundwater in the Woodbine Aquifer does not extend deeper than about 2,000 feet below land surface.

Resistivity maps were not constructed for other layers, owing to the effects of mixed lithologies, but approximate downdip limits of lower salinity groundwater are shown on cross sections. The Pearsall Formation generally contains higher salinity groundwater than do the other sandstone-bearing layers (Figures 4.1.31 through 4.1.35). The Glen Rose Formation contains low salinity groundwater in the northwest where it is sandstone-dominated (Figure 4.1.31).

4.1.10 Hydrostratigraphy for the GCDs Comprising the Inter-local Agreement

Hydrostratigraphy specific to each of the GCDs comprising the inter-local agreement (Prairielands, North Texas, Northern Trinity, and Upper Trinity GCDs) is provided in this subsection. Included are cross sections and discussions of aquifer characteristics in the GCDs. The following discussion is organized by GCD location from east to west and north to south.

4.1.10.1 Upper Trinity GCD

The Upper Trinity GCD is located almost entirely in the outcrop of the northern Trinity Aquifer (Figure 4.1.42). The northern Trinity Aquifer is missing where Paleozoic-age strata are exposed at the surface in the western portions of Montague, Wise, and Parker counties. The Woodbine Aquifer is not present in the Upper Trinity GCD. Two digital electric log cross sections were constructed to display the stratigraphy and sandstone development in the northern Trinity Aquifer in the Upper Trinity GCD (Figures 4.1.43 and 4.1.44). On these cross sections, both the layer terminology for the model (see Figure 4.1.6) and the local terminology of the Antlers Aquifer are given. In the west, the northern Trinity Aquifer extends from land surface down to 100 to 300 feet below land surface (Figure 4.1.43) and includes only the Hensell Aquifer, Pearsall Formation, and Hosston Aquifer. In the eastern portion of the Upper Trinity GCD, the northern Trinity Aquifer extends from land surface down to as much as 700-feet deep. The Paluxy Aquifer and Glen Rose Formation, as well as the Hensell Aquifer, Pearsall Formation, and Hosston Aquifer, are present in the southeast (Figure 4.1.44).

The northern Trinity Aquifer is sandstone-dominated across most of the Upper Trinity GCD. Shallow sandstones, 30- to 50-feet thick, are common in the west (Figure 4.1.43). Most of these thick sandstones correspond to the Hosston and Hensell aquifers. The Pearsall Formation is more shale dominated. The underlying Paleozoic-age sediments also include thick sandstones, which are in hydrologic communication with the Hosston Aquifer in some areas. In the eastern portion of the Upper Trinity GCD, sandstones are thickest in Montague County (Figure 4.1.44). In southern Parker and Hood counties, limestones of the Glen Rose Formation occupy a large part of the northern Trinity Aquifer, but sandstones of the Paluxy Aquifer are well developed above the Glen Rose Formation at depths less than 250 feet (Figure 4.1.44). Sandstones are thick locally below the Glen Rose Formation at depths ranging from 200 to 700 feet. Groundwater quality is generally good throughout the Upper Trinity GCD.

4.1.10.2 North Texas GCD

The North Texas GCD is located mostly east of the northern Trinity Aquifer outcrop, but the Woodbine Aquifer outcrop extends through the center of the District (Figure 4.1.45). Two digital electric log cross sections were constructed to display the stratigraphy and sandstone development in the northern Trinity and Woodbine aquifers in the North Texas GCD (Figures 4.1.46 and 4.1.47). In the western portion of Cooke and Denton counties, limestones of the Washita/Fredericksburg groups are exposed at the surface, overlying 500 to 800 feet of sandstones in the northern Trinity Aquifer. Limestones of the Glen Rose Formation are present in southern Denton County (Figure 4.1.46). In Collin County, sandstones in the northern Trinity Aquifer are present at much greater depths than in Denton County, owing to the eastward dipping stratigraphy (Figure 4.1.47). Sandstones in the Hosston Aquifer are found at depths greater than 5,000 feet in eastern Collin County. Sandstones in the Woodbine Aquifer range from 300- to 3,000-feet deep in Collin County. Sandstones in the Paleozoic-age sediments underlie the northern Trinity Aquifer locally in western Cooke County, but in most of the North Texas GCD, the northern Trinity Aquifer is underlain by shale and limestone. In southeastern Collin County, the Jurassic-age sandstones of the Cotton Valley Formation underlie and are in hydrologic communication with the Hosston Aquifer (Figure 4.1.47).

Sandstones in the Woodbine, Paluxy, Hensell, and Hosston aquifers are well developed in the North Texas GCD. Maximum sandstone thicknesses (summing all aquifers/formations across the study area) containing good quality groundwater are located in the North Texas GCD and in

adjacent Grayson and Dallas counties. Multiple, sandstone-dominated, fluvial and shoreline depositional systems are superimposed in the North Texas GCD. The western portion of the North Texas GCD includes thick sequences of northern Trinity Aquifer sandstones and relatively minor shales and limestones (Figure 4.1.46). In the eastern portion of the North Texas GCD in Collin County, sandstones in the northern Trinity Aquifer, although more deeply buried, are thicker than in the western portion of the North Texas GCD (Figure 4.1.47). In the Hosston Aquifer, the base of low salinity groundwater is 5,000-feet deep or deeper in parts of Collin County. The Woodbine Aquifer comprises 200 to 350 feet of sandstone having low to moderate salinity groundwater in Collin County.

4.1.10.3 Northern Trinity GCD

The Northern Trinity GCD is located east of the northern Trinity Aquifer outcrop, but the Woodbine Aquifer outcrop extends through the eastern portion of the District (Figure 4.1.48). Two digital electric log cross sections were constructed to display stratigraphy and sandstone development in the northern Trinity and Woodbine aquifers in the Northern Trinity GCD (Figures 4.1.49 and 4.1.50). On these cross sections, both the layer terminology used for the model and the local terminology of Twin Mountains Aquifer are given. The limestones of the Glen Rose Formation and the Washita/Fredericksburg groups are well developed confining layers throughout the Northern Trinity GCD. Sandstones of the Hensell and Hosston aquifers range in depth from about 500 feet in the west to 2,000 feet in the east (Figure 4.1.50). Sandstones in the Paluxy Aquifer range in depth from 100 to 1,000 feet. Sandstones in the Woodbine Aquifer are present at the surface to about 400 feet in the eastern portion of the District. The northern Trinity Aquifer is underlain by Paleozoic-age sandstone, shale, and limestone sediments throughout the Northern Trinity GCD, which are generally thin bedded and shale dominated (Figure 4.1.49).

The sandstones of the Paluxy, Hensell, and Hosston aquifers are well developed in the Northern Trinity GCD. The Paluxy Aquifer is composed of greater than 60 percent sandstone everywhere except in the northwest corner of Tarrant County. Major, east-oriented, fluvial channel axes in the Paluxy Aquifer are expressed as thick-bedded sandstone (Figure 4.1.49). The Hosston and Hensell aquifers also contain greater than 60 percent sandstone. The sandstones of the Paluxy and Hosston aquifers form the most hydraulically conductive and transmissive layers in the Northern Trinity GCD. In the channelized fluvial depositional systems of the Paluxy, Hensell,

and Hosston aquifers, however, well-to-well variability is high. Thick, river-channel sandstones are enclosed in shale-dominated interchannel areas. The abrupt sandstone-shale transitions are well displayed on the cross sections in Figures 4.1.49 and 4.1.50. Groundwater quality is good throughout the Northern Trinity GCD.

4.1.10.4 Prairielands GCD

The Prairielands GCD covers a broad region in the center of the study area. The western portion of the Prairielands GCD is located in the northern Trinity Aquifer outcrop, and the Woodbine Aquifer outcrop extends through the center (Figure 4.1.51). Both aquifers are deeply buried in the eastern portion of the Prairielands GCD. Three digital electric log cross sections were constructed to display the stratigraphy and sandstone development in the northern Trinity and Woodbine aquifers in the Prairielands GCD (Figures 4.1.52 through 4.1.54). In Somervell County, limestones of the Glen Rose Formation overlie sandstones in the Hensell and Hosston aquifers, which range in depth from about 250 to 700 feet. The Pearsall Formation is mostly shale in Somervell County. Sandstones in the Paluxy Aquifer are exposed at the surface in the southern and eastern portions of Somervell County (Figure 4.1.52). In portions of Johnson and western Hill counties, sandstones in the Woodbine Aquifer are exposed at the surface. Thick sequences of limestones in the Washita/Fredericksburg groups and Glen Rose Formation confine the Paluxy, Hensell, and Hosston aquifers (Figure 4.1.53). Sandstones of the Paluxy Aquifer are buried at depths ranging from 300 to 1,000 feet in Johnson and western Hill counties. Sandstones in the Hensell and Hosston aquifers range in depth from 1,000 to 2,000 feet (Figure 4.1.53). Ellis and eastern Hill counties include the full suite of sandstones in the northern Trinity and Woodbine aquifers (Figure 4.1.54). Sandstones in the Hosston Aquifer are underlain by shale- and limestone-dominated strata of Paleozoic age.

Sandstones in the northern Trinity and Woodbine aquifers are variably developed across the Prairielands GCD. Sandstones in the Woodbine and Paluxy aquifers are thick and concentrated (high sandstone percentages) in the northern portions of Ellis and Johnson counties, but thin southward, reaching essentially zero thickness in southern Hill County (Figures 4.1.53 and 4.1.54). Sandstones in the Hensell Aquifer are thick in Somervell and Johnson counties but are much thinner in Ellis and eastern Hill counties. Sandstones in the Hosston Aquifer, however, are well developed and contain low salinity groundwater throughout the Prairielands GCD. The Woodbine and Paluxy aquifers contain low salinity groundwater in Johnson and western Ellis

counties, whereas low salinity groundwater in the Hensell Aquifer is mainly restricted to Johnson and Somervell counties.

4.1.11 Summary of Northern Trinity and Woodbine Aquifers Hydrostratigraphy

Cretaceous-age sandstones in the northern Trinity and Woodbine groups in central and north-central Texas are important sources of groundwater and comprise the northern Trinity and Woodbine aquifers. The stratigraphy of the Cretaceous-age strata consists of interbedded sandstones, limestones, and shales. Cretaceous-age strata thicken and dip toward the East Texas Basin where they are overlain by thousands of feet of younger strata. Only along the western and northern margins of the East Texas Basin are Cretaceous-age sandstones saturated with fresh groundwater. The northern Trinity and Woodbine aquifers extend from the Edwards Plateau, through the Hill Country, and to the northeast into Oklahoma and Arkansas.

The Cretaceous Period (145 to 65 million years ago) was characterized by rising sea level and episodic input of sandy sediment. Limestones were deposited in shallow marine waters, whereas sandstones were deposited mainly in rivers on sandy coastal plains and along marine shorelines. Depositional environment controls sandstone geometry and orientation, which in turn, influence groundwater flow directions. Geographically fluctuating shorelines resulted in stratigraphic interlayering of sandstone and limestone (shale is interbedded with both). Sandstones form the aquifer units, and limestones form the confining units in the northern Trinity, Washita/Fredericksburg, and Woodbine groups. The hydrostratigraphy of the northern Trinity and Woodbine aquifers is based on this lithologic interlayering. The Woodbine, Paluxy, Hensell and Hosston aquifers are sandstone-dominated, the Glen Rose and Pearsall formations are mixed lithology, and the Washita/Fredericksburg groups are limestone-dominated.

At the regional level, geologic structure is relatively simple in the Cretaceous-age strata of north-central Texas. Stratigraphic dips range from eastward in the south to southward in the northeast. Gently folded strata are present in the northwest, and large, northeast-oriented fault zones are present in the south (Balcones Fault Zone) and along the eastern margin of the study area (Mexia-Talco Fault Zone). Faults in the Balcones Fault Zone displace aquifer sandstones by several hundred vertical feet and have the greatest potential to influence vertical groundwater flow within the freshwater interval. Faults in the Mexia-Talco Fault Zone are located downdip from the freshwater interval. Smaller, more localized faults and fractures are known to be

abundant in Cretaceous-age strata, but their effects on groundwater flow and quality have not been documented.

The northern Trinity Aquifer is sandstone-dominated in the northwest, where it is locally referred to as the Antlers Aquifer. In the rest of the study area, limestones of the Glen Rose Formation separate the lower portion of the northern Trinity Aquifer (i.e., sandstones of the Hosston and Hensell aquifers and the Pearsall Formation) from the sandstones in the upper portion of the northern Trinity Aquifer (i.e., Paluxy Aquifer). Sandstones in the Woodbine Aquifer are separated from the underlying northern Trinity Aquifer by limestones and shales in the Washita/and Fredericksburg groups. The Hosston Aquifer, which is the stratigraphically lowest sandstone layer, is the most widespread and best developed aquifer in the system. The Hosston Aquifer includes greater net sandstone and thicker individual sandstones than any other layer. The Hensell Aquifer is well developed in western portions of the study area, but thins and becomes increasingly shale dominated to the east. The Pearsall and Glen Rose formations include sandstones only in the north. The Paluxy Aquifer is dominated by thick sandstones across broad areas, where it rivals the Hosston Aquifer, but thins across the southern one-third of the study area. The Woodbine Aquifer includes thick sandstones in the east-central and northeastern portions of the study area.

With two exceptions, the distribution of low salinity groundwater in the northern Trinity and Woodbine aquifers coincides in a general way with sandstone development. Low salinity groundwater extends deepest and farthest southeast in widespread sandstones of the Hosston Aquifer. In the other aquifers/formations, low salinity groundwater is more limited geographically, coinciding with areas of maximum sandstone thickness. One exception is in the counties in northeastern Texas located east of Fannin County. Sandstones in the northern Trinity and Woodbine aquifers are present in this area, but contain poor quality groundwater. The second exception occurs along the eastern boundary of the study area at depths below the base of the low salinity groundwater.
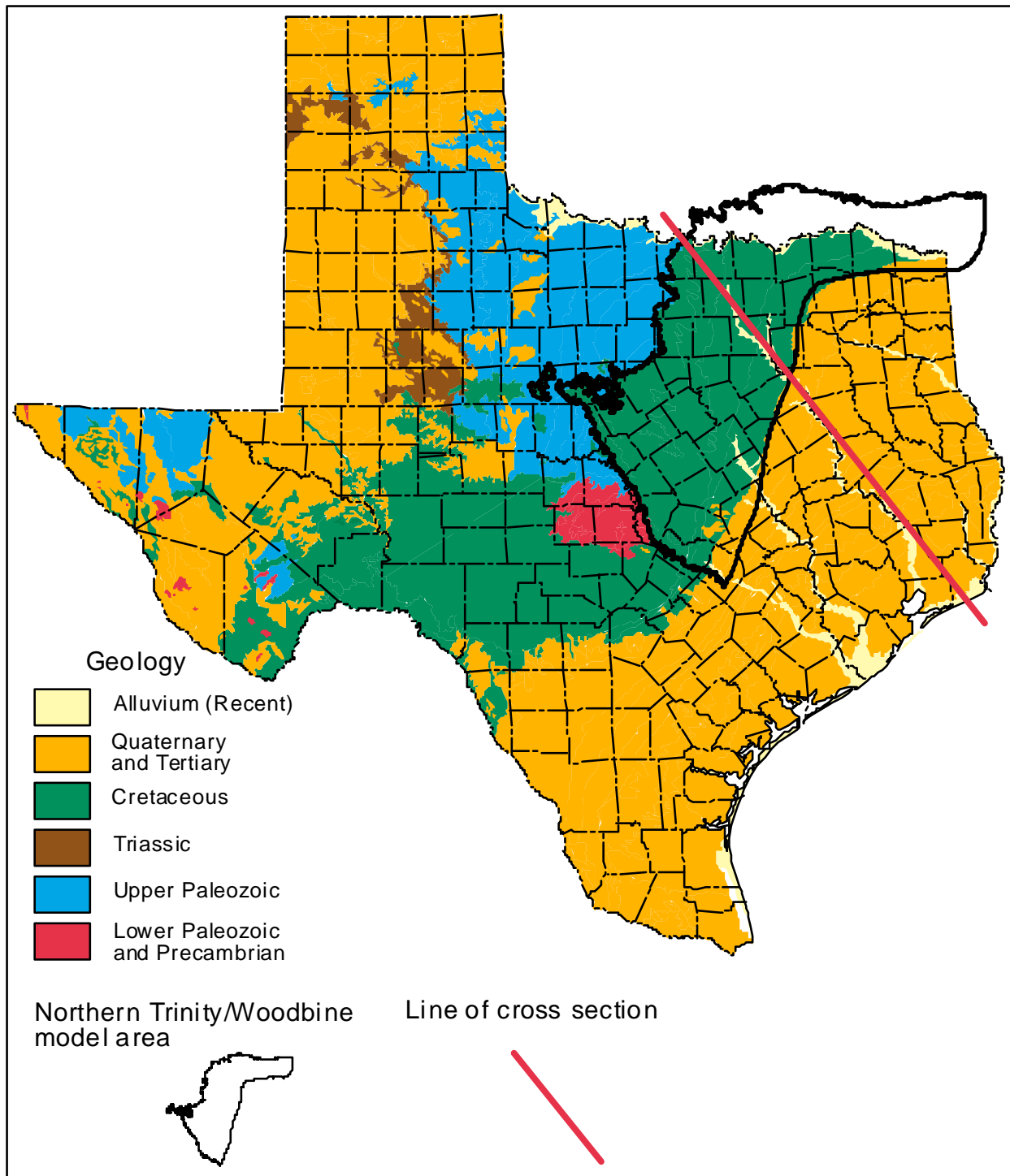
Figure 4.1.1   Simplified surface geology of Texas showing the study area and the location of the cross section in Figure 4.1.3 (modified from Bureau of Economic Geology, 1992).

Age m.y	Period	Group	Formations		
			North and West	Central	South
65	Upper Cretaceous	Eagle Ford	not present	undifferentiated	undifferentiated
		Woodbine	not present	undifferentiated	undifferentiated
		Washita	Grayson Mainstreet Pawpaw Weno Denton Fort Worth Duck Creek	Buda Del Rio Georgetown	Buda Del Rio Georgetown
100	Lower Cretaceous	Fredericksburg	Kiamichi Goodland Walnut	Kiamichi Edwards Comanche Peak Walnut	Kiamichi Edwards Comanche Peak Walnut
		Trinity / Antlers	Twin Mountains — Hensell Pearsall Hosston	Paluxy Glen Rose — Travis Peak: Hensell Pearsall/Cow Creek/Hammett Hosston/Sligo	Paluxy Glen Rose

Figure 4.1.2 **Stratigraphic correlation showing Cretaceous-age stratigraphy in various portions of the study area (modified from Fisher and Rodda, 1966, 1967; Salvador and Muneton 1989; Walker and Geissman, 2009).**
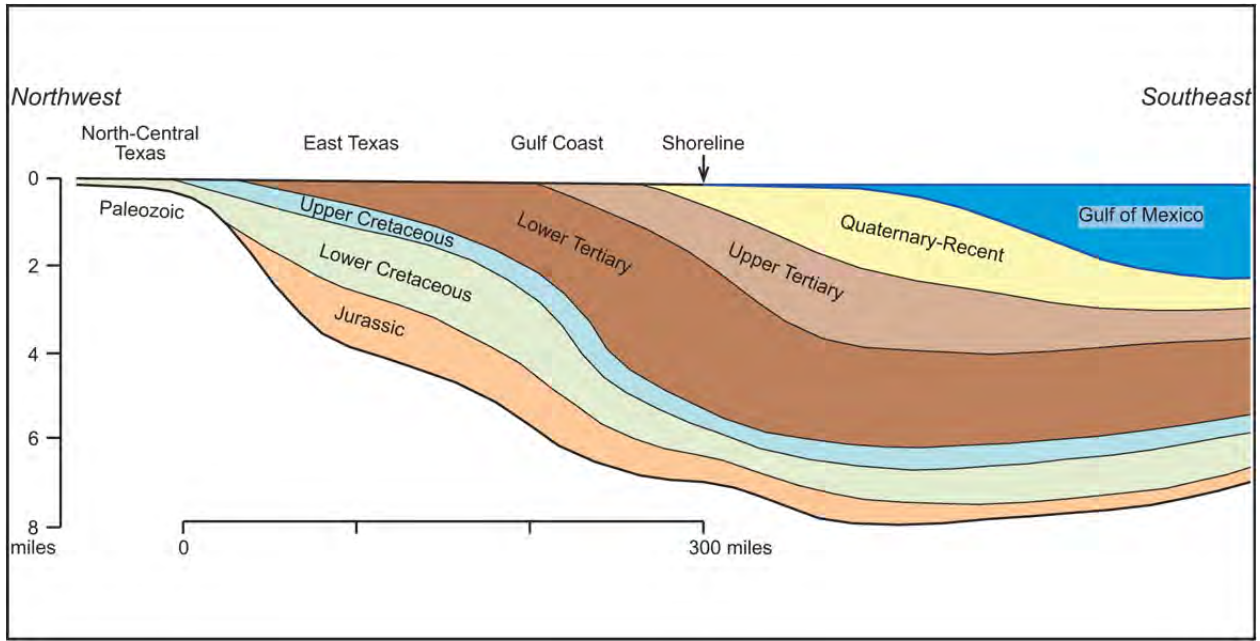
Figure 4.1.3   Schematic cross section showing sedimentary fill of the Gulf of Mexico Basin (modified from Salvador, 1991).
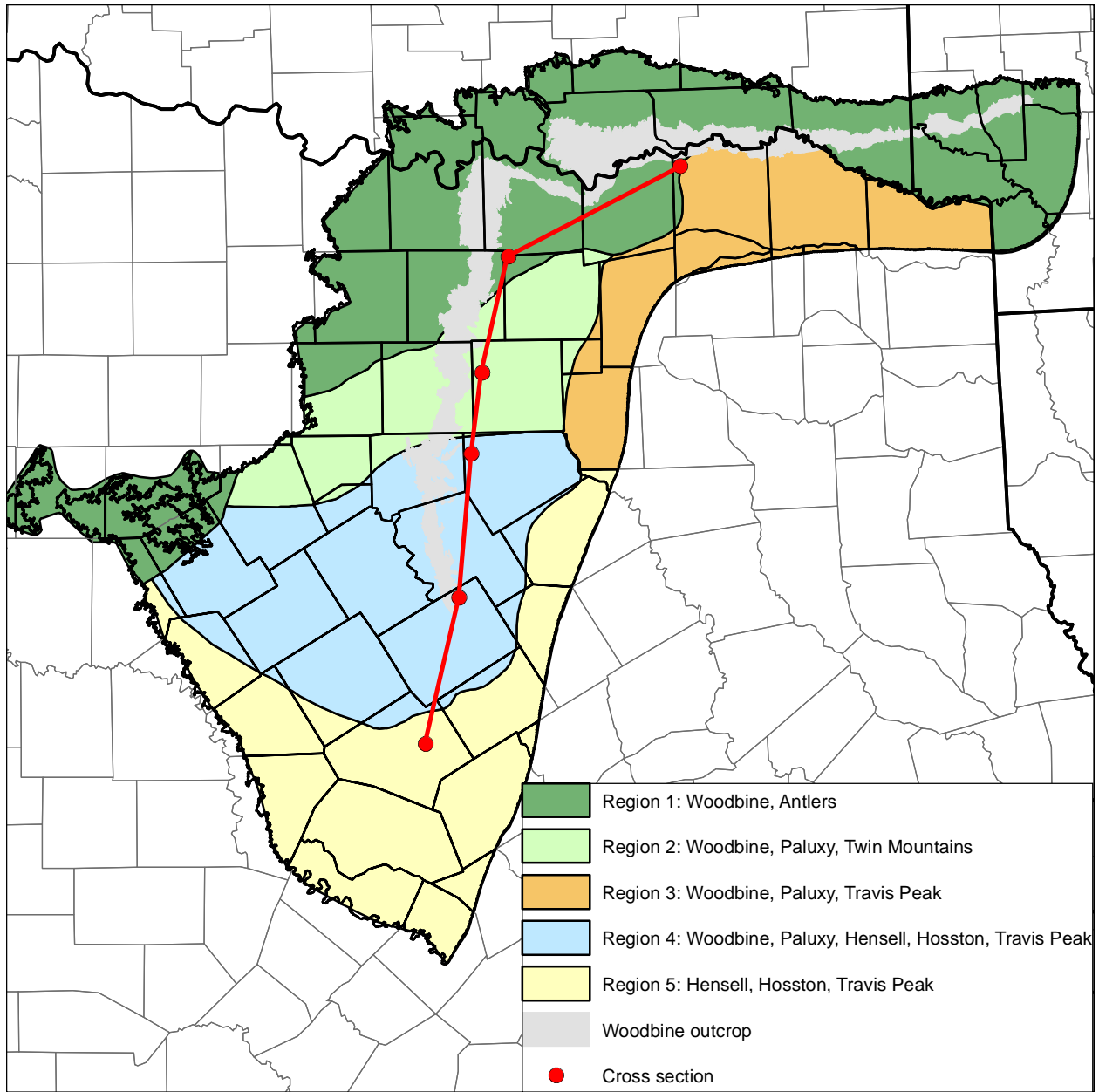
Figure 4.1.4   Study area showing regions defined by stratigraphic and lithologic similarities and aquifer names common to each region, and the location of the cross section shown in Figures 4.1.5.

yellow = greater than 50 percent sandstone, blue = greater than 50 percent limestone, brown = greater than 50 percent shale
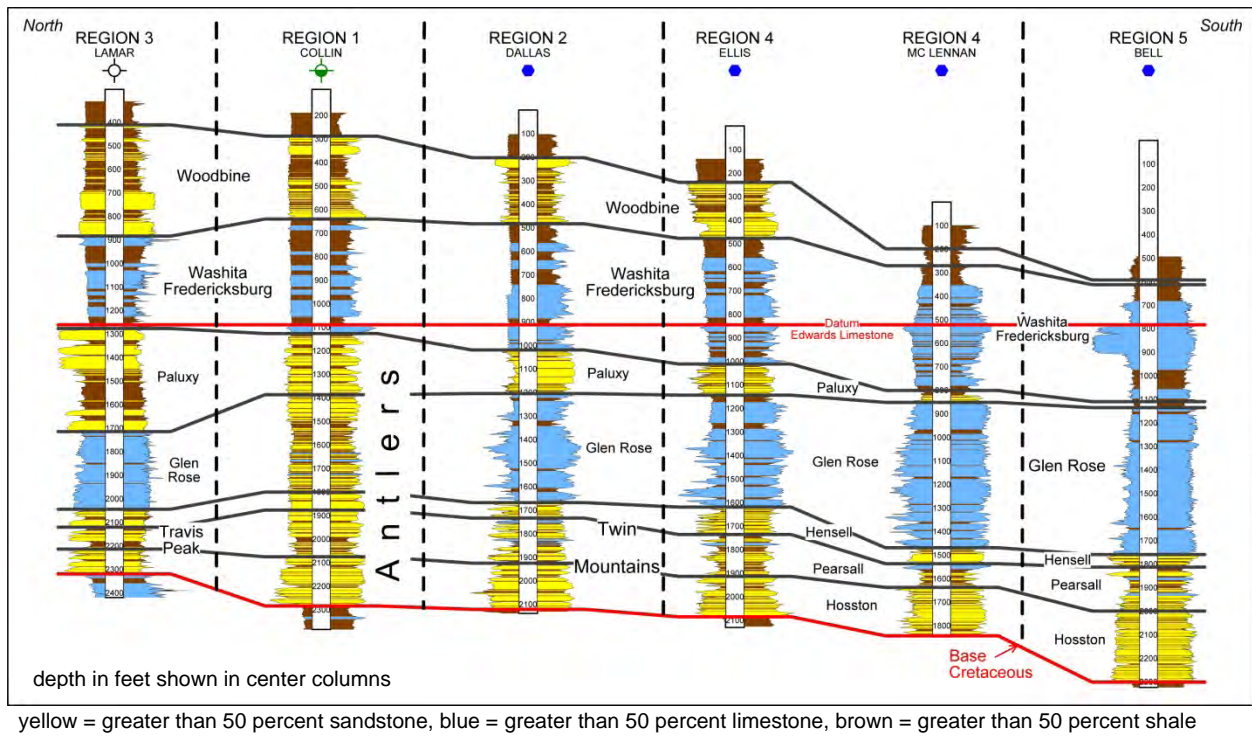
Figure 4.1.5   Cross section composed of typical electric logs in Regions 1 through 5 showing digital spontaneous potential curve on the left and a resistivity (short normal) curve on the right and aquifer names common to each region.

Model Terminology	Region 1	Region 2	Region 3	Region 4	Region 5
Woodbine Aquifer	Woodbine	Woodbine	Woodbine	Woodbine	Woodbine (no sand)
Washita/ Fredericksburg Groups	Washita/ Fredericksburg	Washita/ Fredericksburg	Washita/ Fredericksburg	Washita/ Fredericksburg	Washita/ Fredericksburg
Paluxy Aquifer	Antlers	Paluxy	Paluxy	Paluxy	Paluxy (no sand)
Glen Rose Formation	Antlers	Glen Rose	Glen Rose	Glen Rose	Glen Rose
Hensell Aquifer	Antlers	Twin Mountains	Travis Peak	Hensell/ Travis Peak	Hensell/ Travis Peak
Pearsall Formation	Antlers	Twin Mountains	Travis Peak	Pearsall/ Sligo	Pearsall/ Sligo
Hosston Aquifer	Antlers	Twin Mountains	Travis Peak	Hosston/ Travis Peak	Hosston/ Travis Peak

yellow = sandstone aquifers

Figure 4.1.6   Chart showing model terminology and corresponding formation names and aquifer names common to each region.
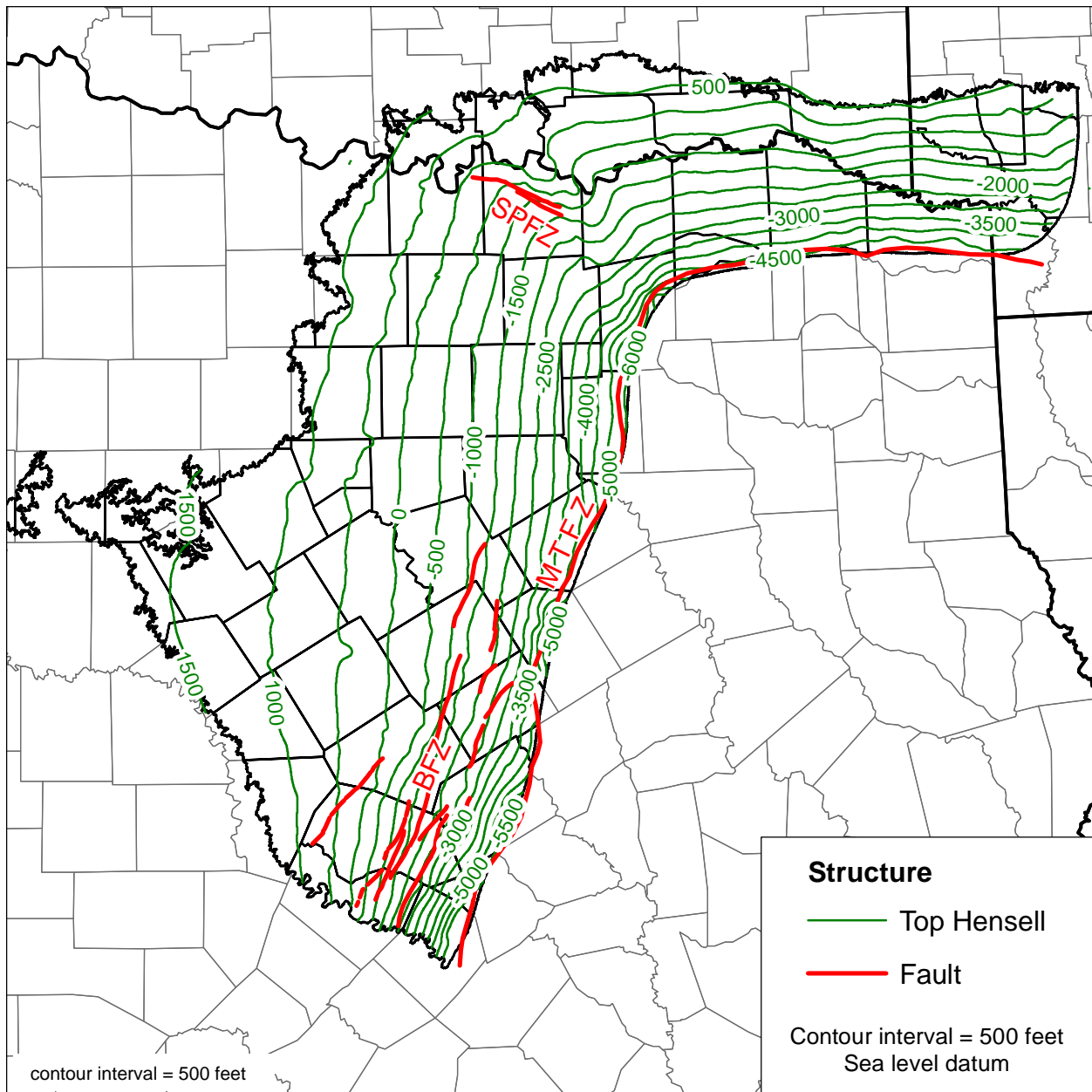
BFZ = Balcones Fault Zone
MTFZ = Mexia-Talco Fault Zone (numerous closely spaced faults are represented by a single line)
SPFZ = Sherman/Preston Fault Zone

Figure 4.1.7 **Top of the Hensell Aquifer in feet above mean sea level and locations of faults that displace Cretaceous-age strata (from Ewing, 1990, 1991).**
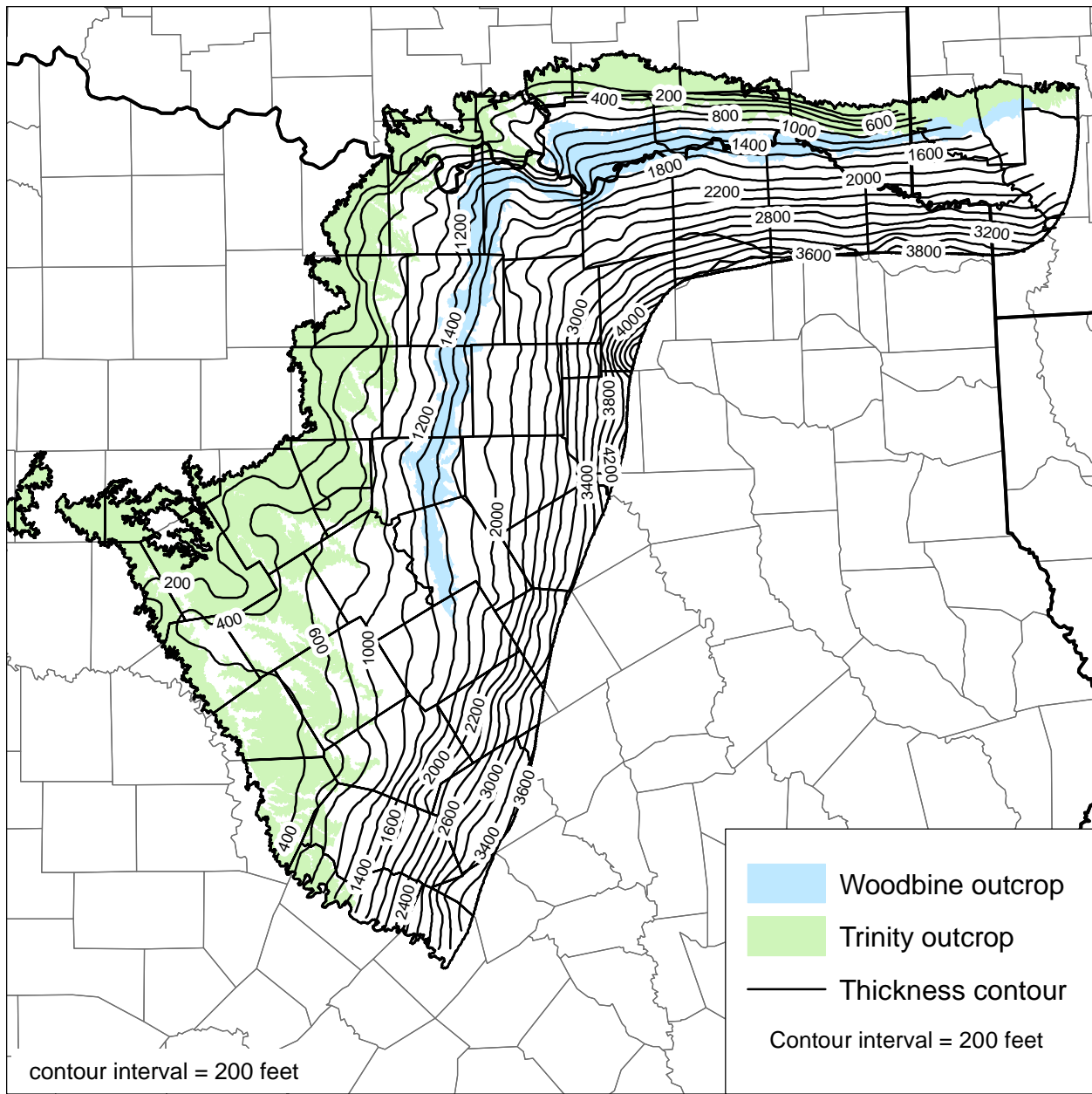
Figure 4.1.8 **Isopach (thickness) map in feet from the base of the Cretaceous-age strata to the top of the Woodbine Aquifer.**
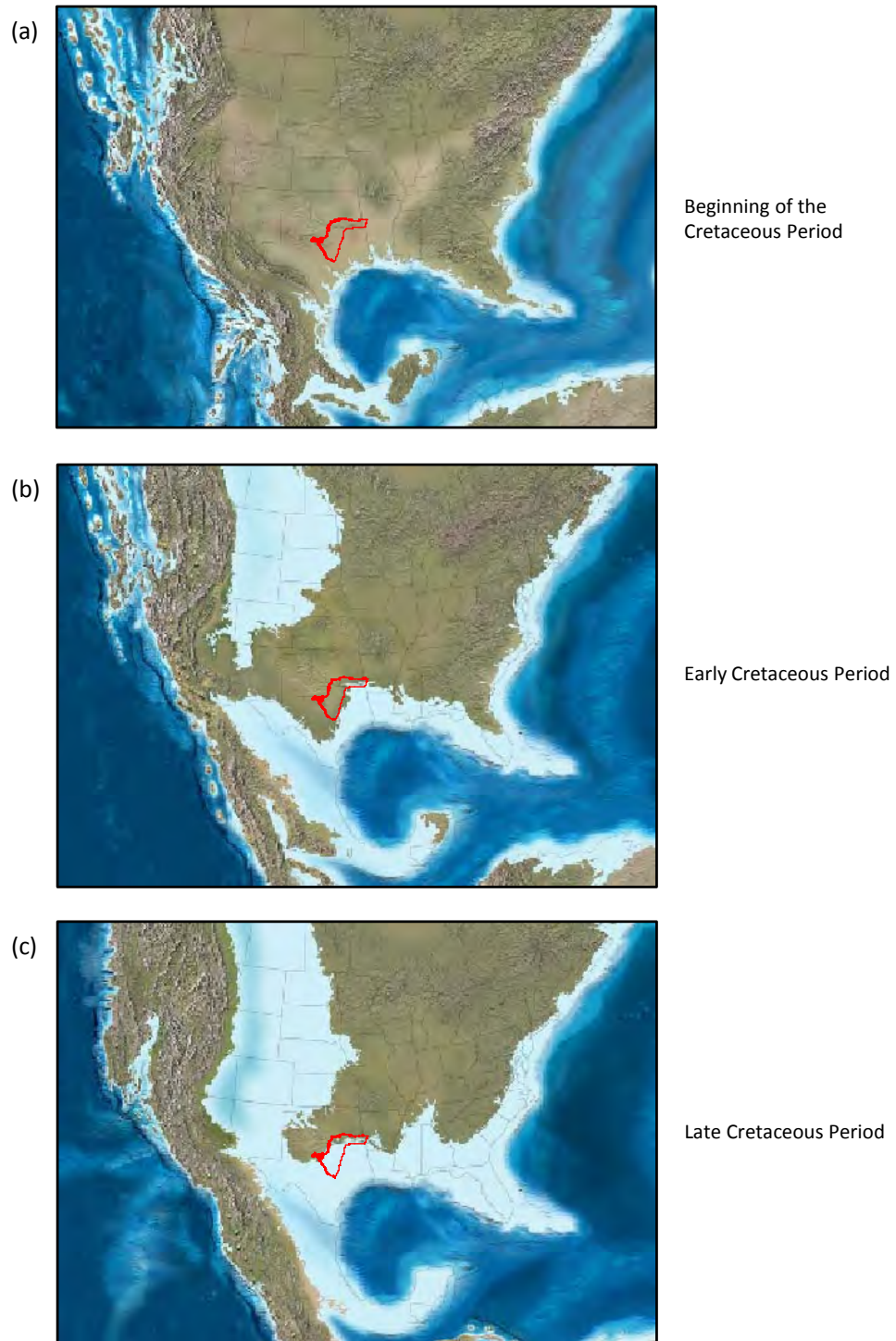
Figure 4.1.9 **Paleogeographic reconstructions showing (a) the beginning of the Cretaceous Period prior to deposition of the northern Trinity Group, (b) the early Cretaceous Period during deposition of the lower northern Trinity Group sandstones, and (c) the late Cretaceous Period during deposition of the Woodbine Group sandstones (modified from Blakey, 2011). (Brown areas represent land, light blue areas represent shallow marine water, and dark blue areas represent deep marine water.)**
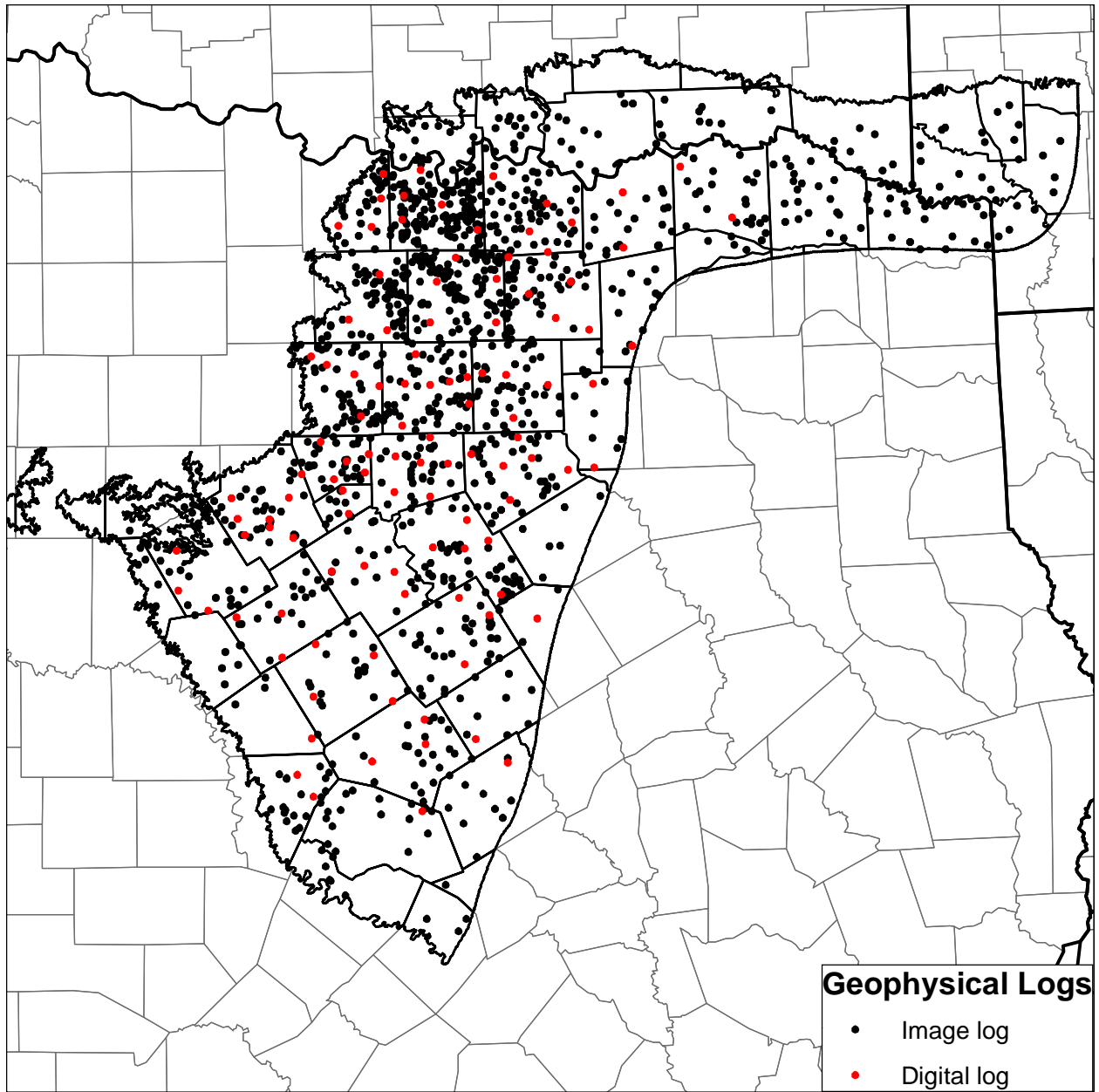
Figure 4.1.10   Location of geophysical well log data used for this study distinguishing between the 1,193 image logs and the 109 digital logs.

yellow = greater than 50 percent sandstone, blue = greater than 50 percent limestone, brown = greater than 50 percent shale
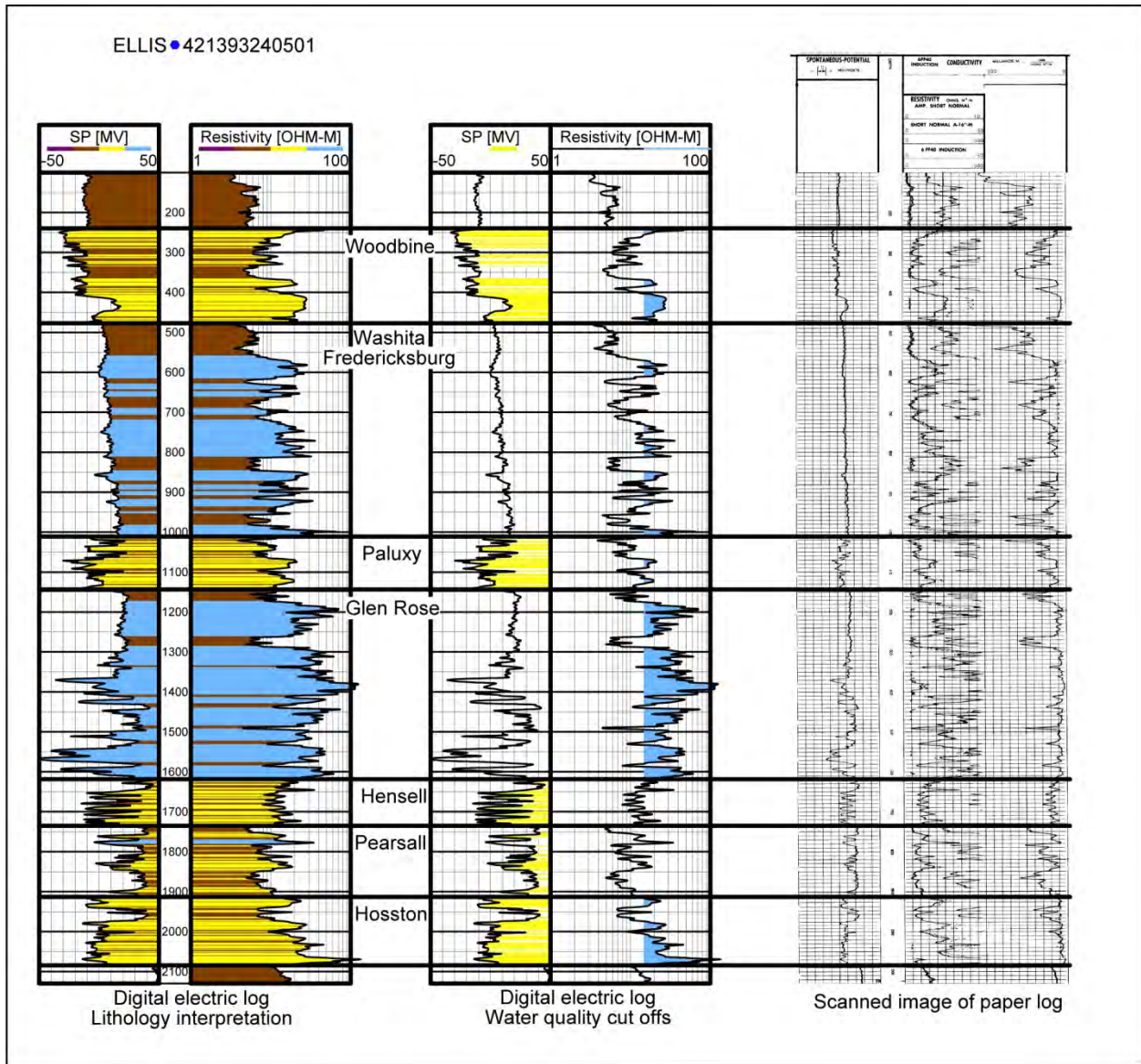
Figure 4.1.11   Example electric log from a well in Ellis County showing differences between digital logs and image (raster) logs from the same well.
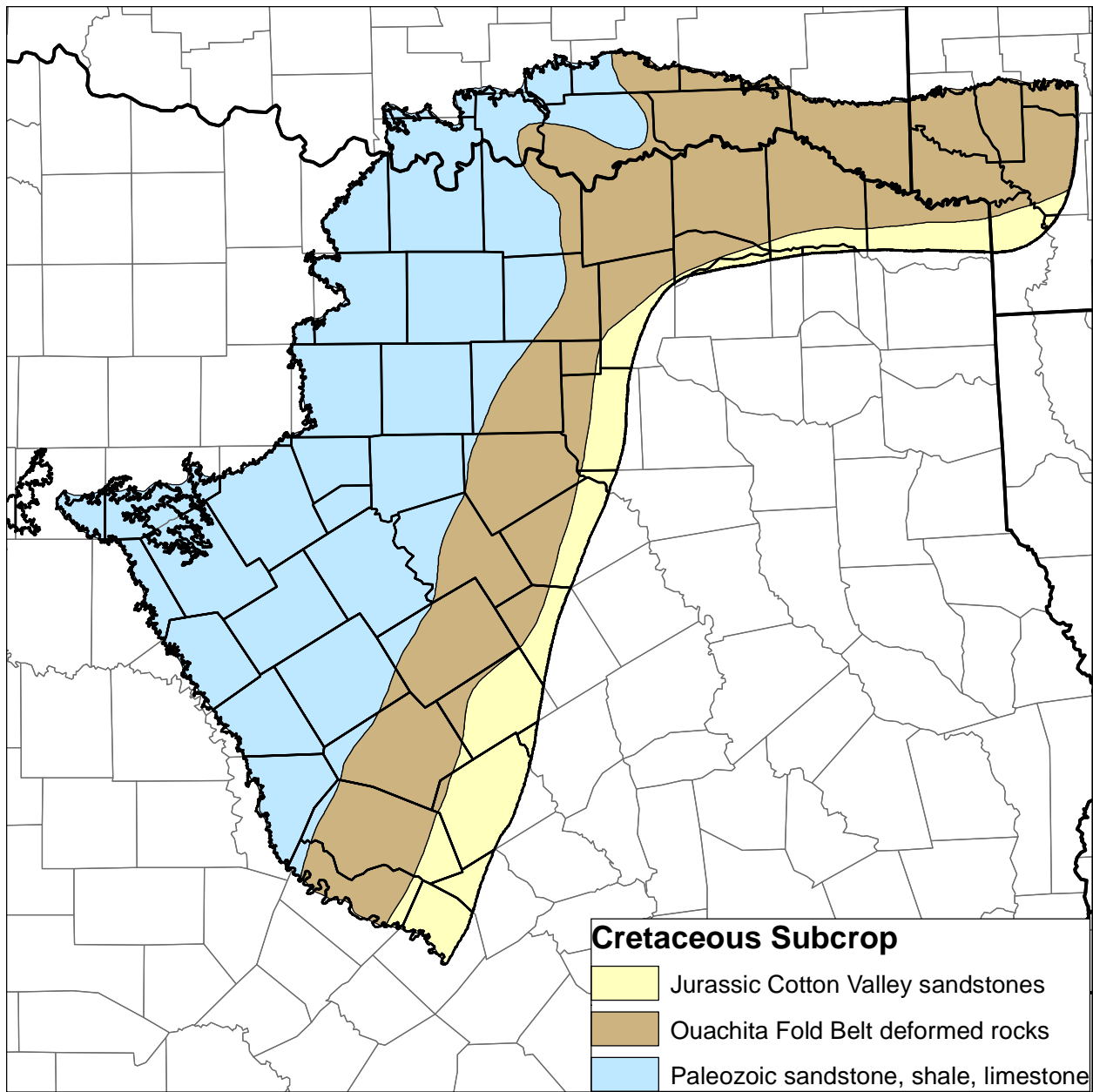
Figure 4.1.12   Geologic terrains underlying Cretaceous-age strata in the study area (modified from Ewing, 1990).
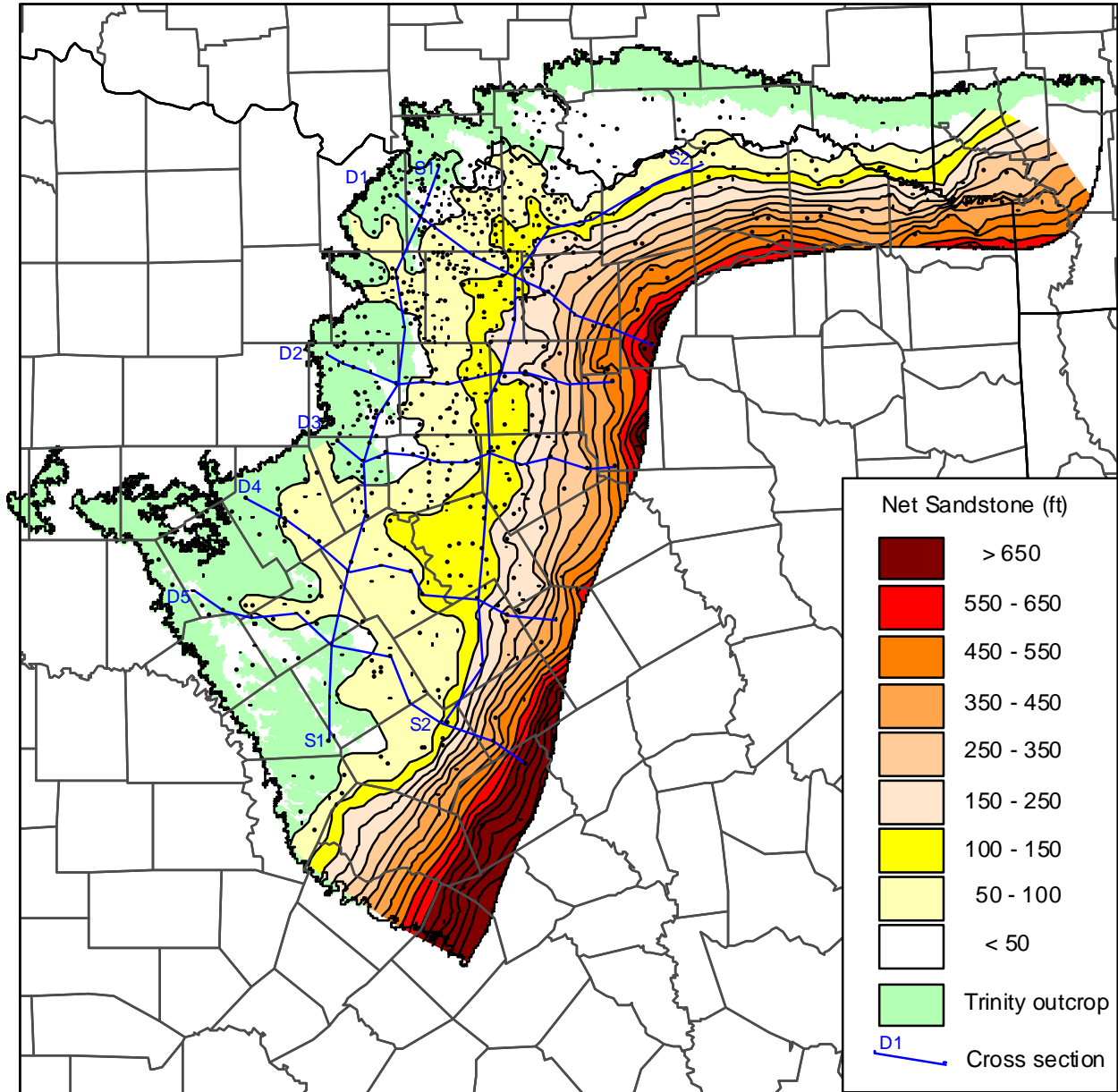
Figure 4.1.13   Net sandstone in the Hosston Aquifer in feet and location of cross sections shown in Figures 4.1.31 through 4.1.37.
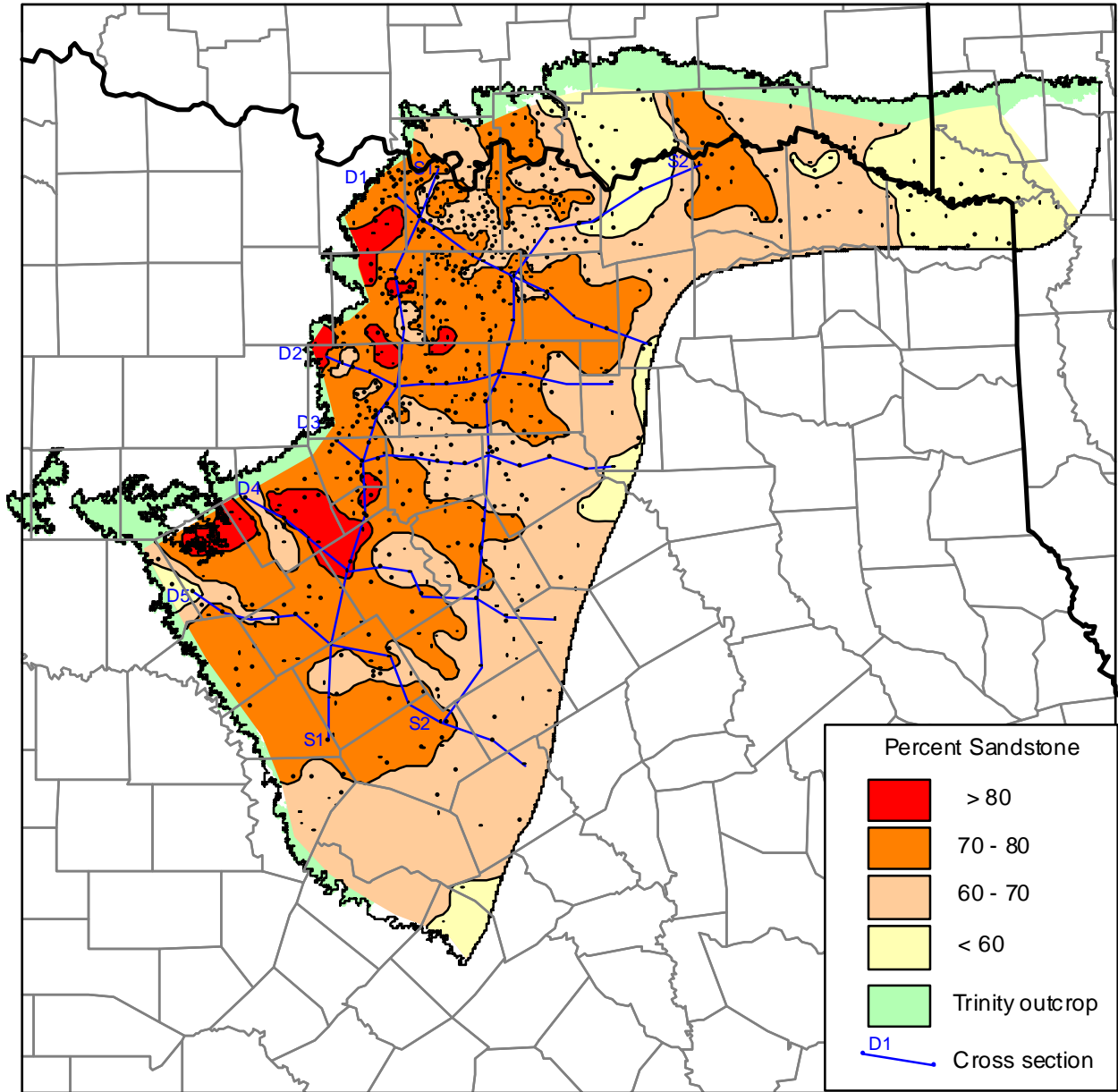
Figure 4.1.14   Percent sandstone in the Hosston Aquifer and location of cross sections shown in Figures 4.1.31 through 4.1.37.
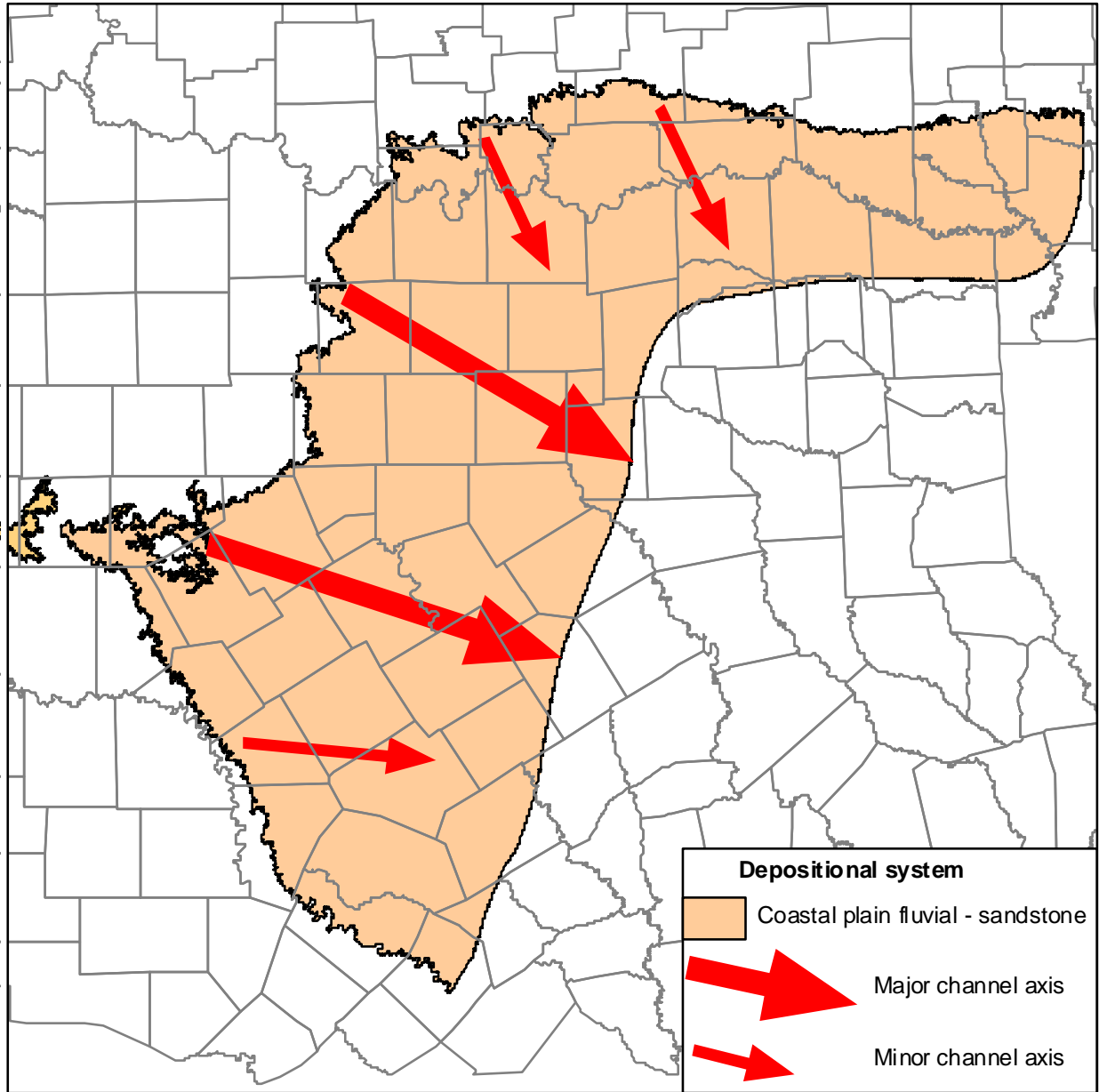
Figure 4.1.15   Depositional systems of the Hosston Aquifer showing locations where larger rivers persisted.
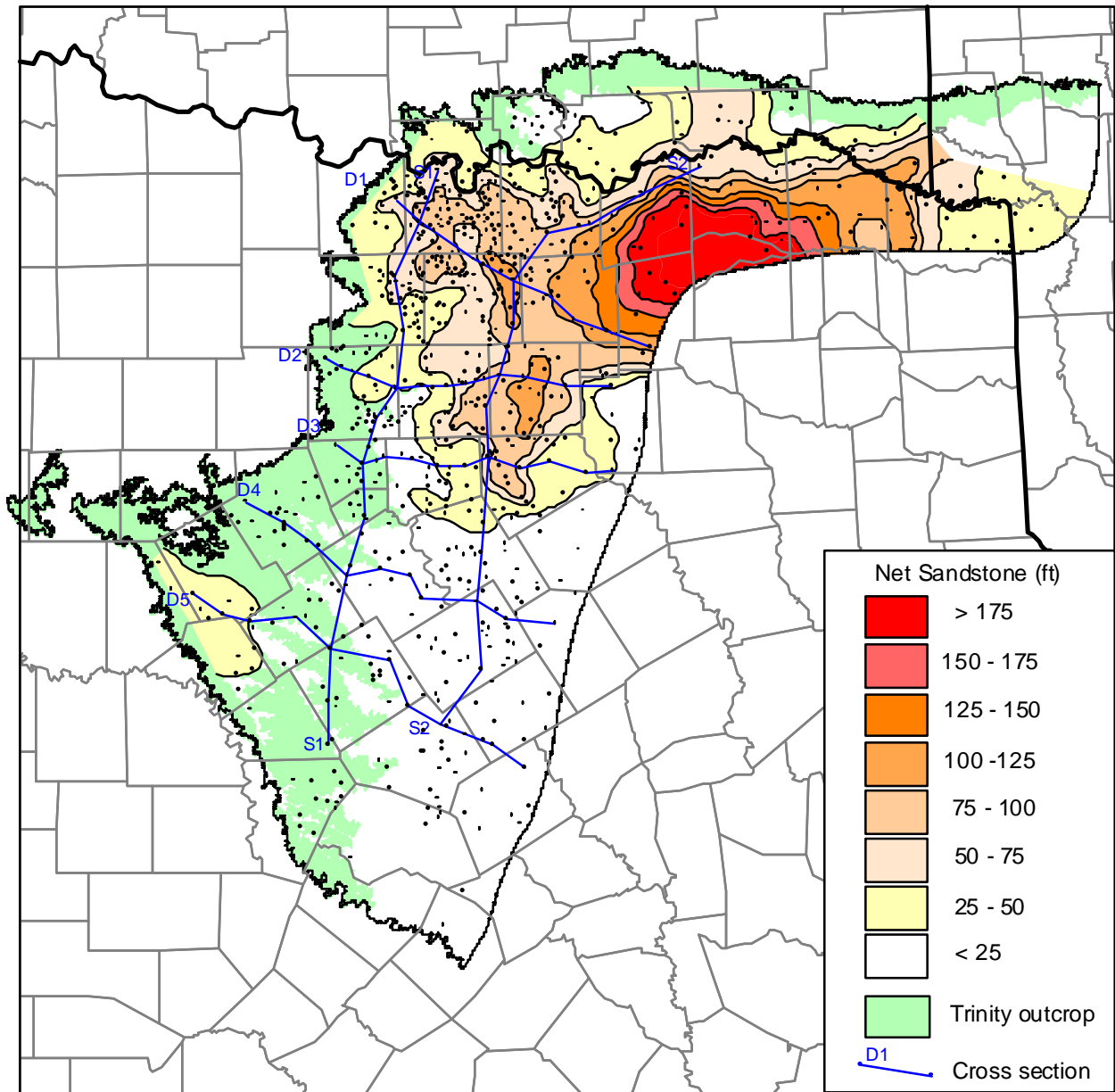
Figure 4.1.16   Net sandstone in the Pearsall Formation in feet and locations of cross sections shown in Figures 4.1.31 through 4.1.37.
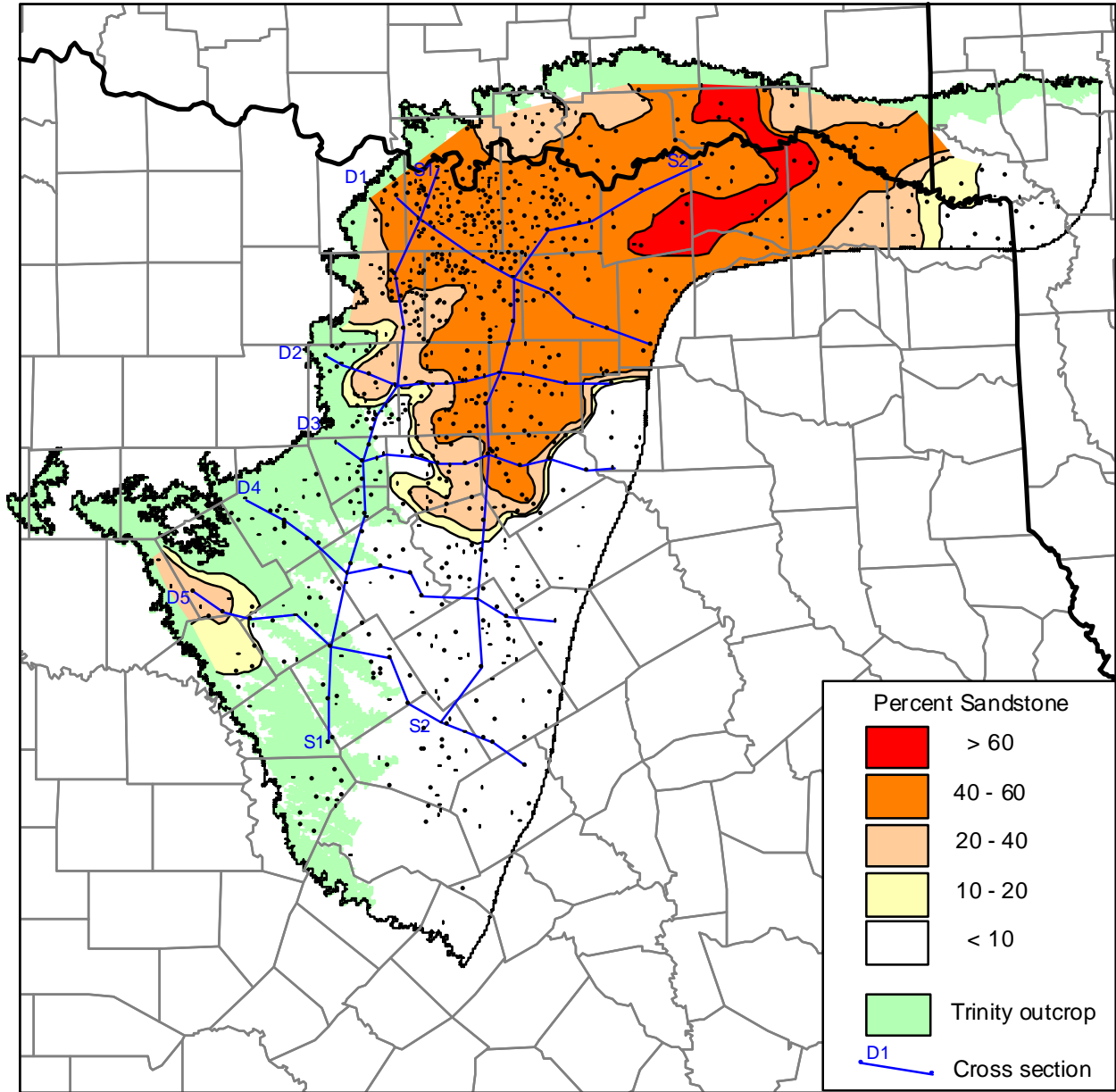
Figure 4.1.17   Percent sandstone in the Pearsall Formation and locations of cross sections shown in Figures 4.1.31 through 4.1.37.
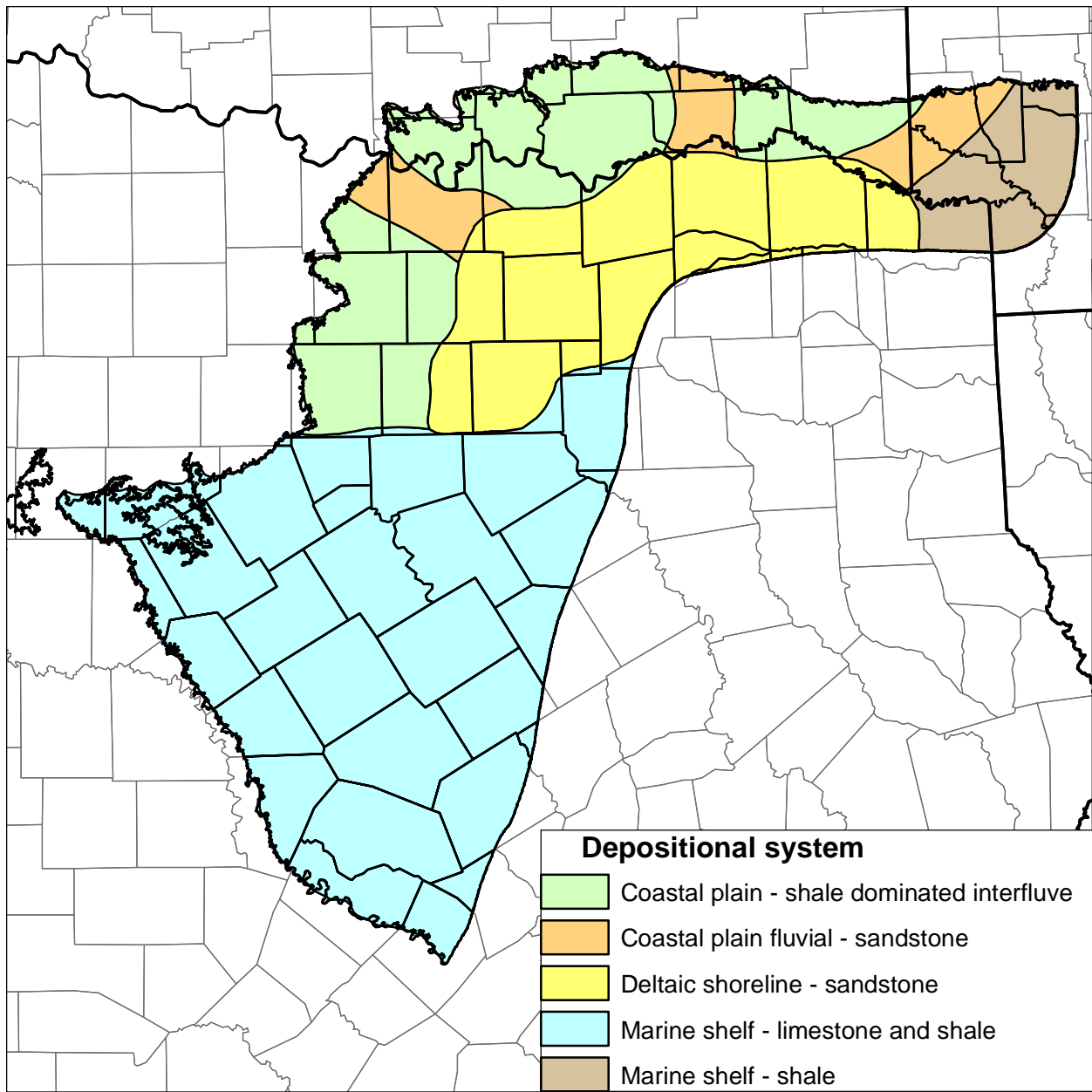
Figure 4.1.18   Depositional systems of the Pearsall Formation.
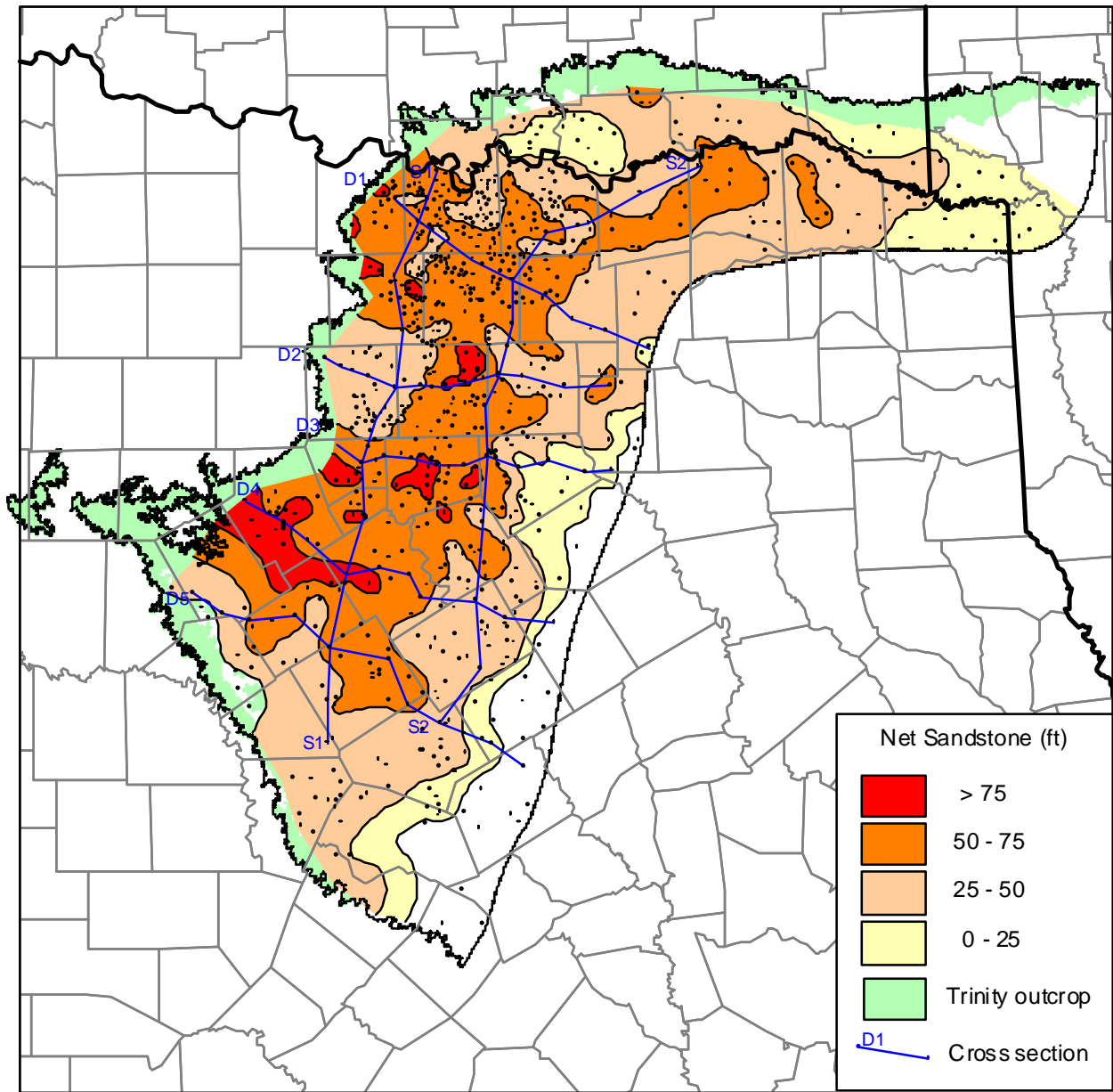
Figure 4.1.19   Net sandstone in the Hensell Aquifer in feet and locations of cross sections shown in Figures 4.1.31 through 4.1.37.
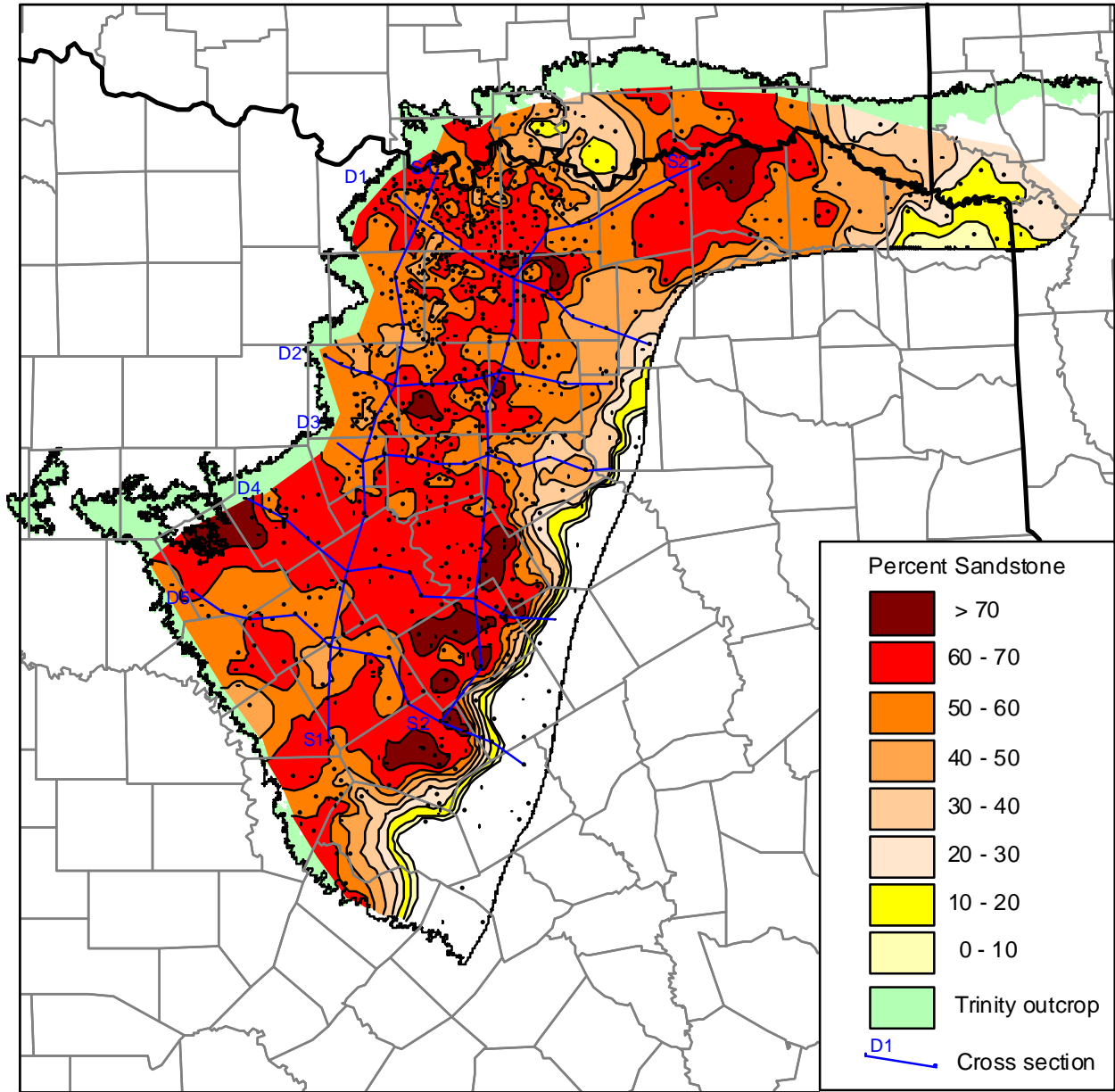
Figure 4.1.20 **Percent sandstone in the Hensell Aquifer and locations of cross sections shown in Figures 4.1.31 through 4.1.37.**
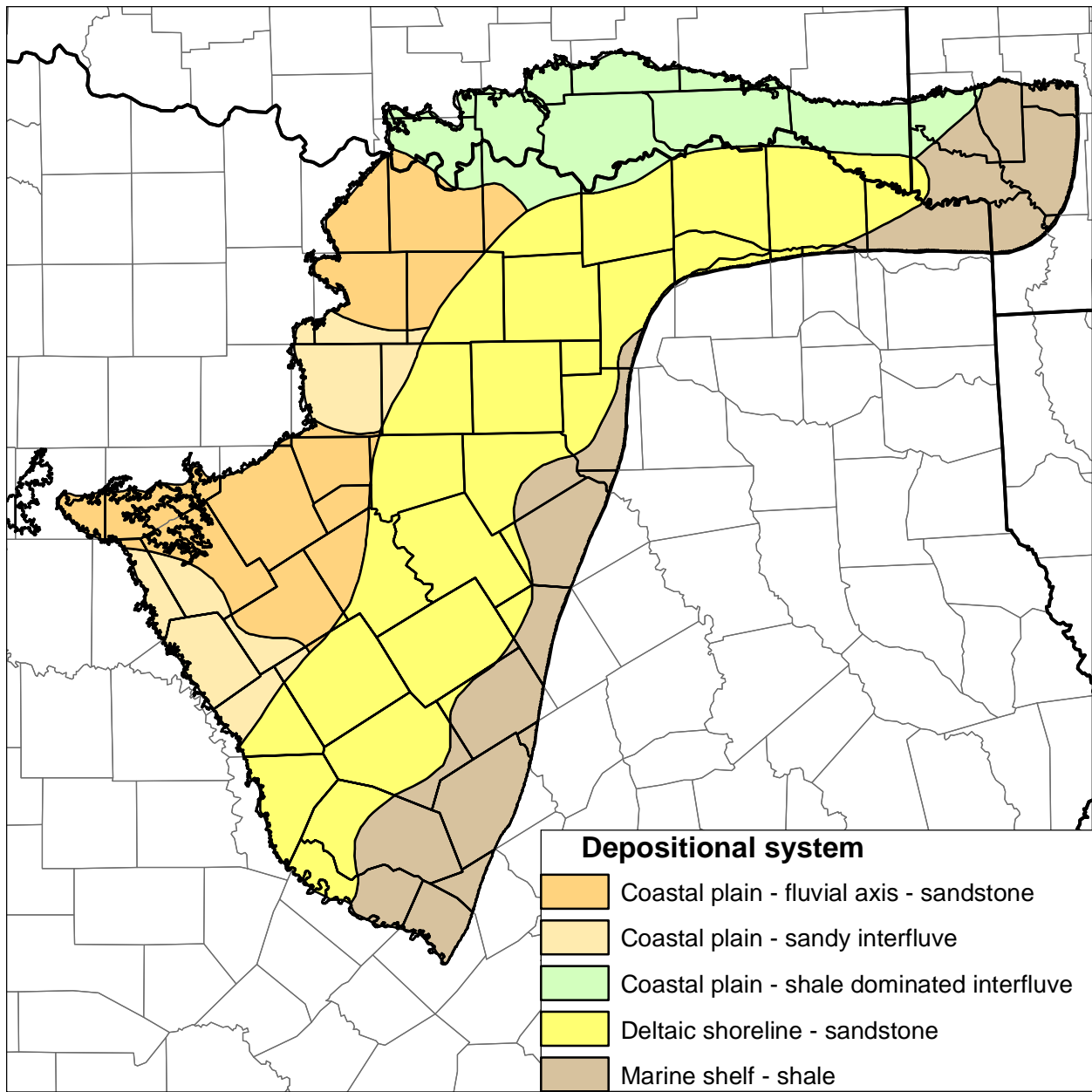
Figure 4.1.21   Depositional systems of the Hensell Aquifer.
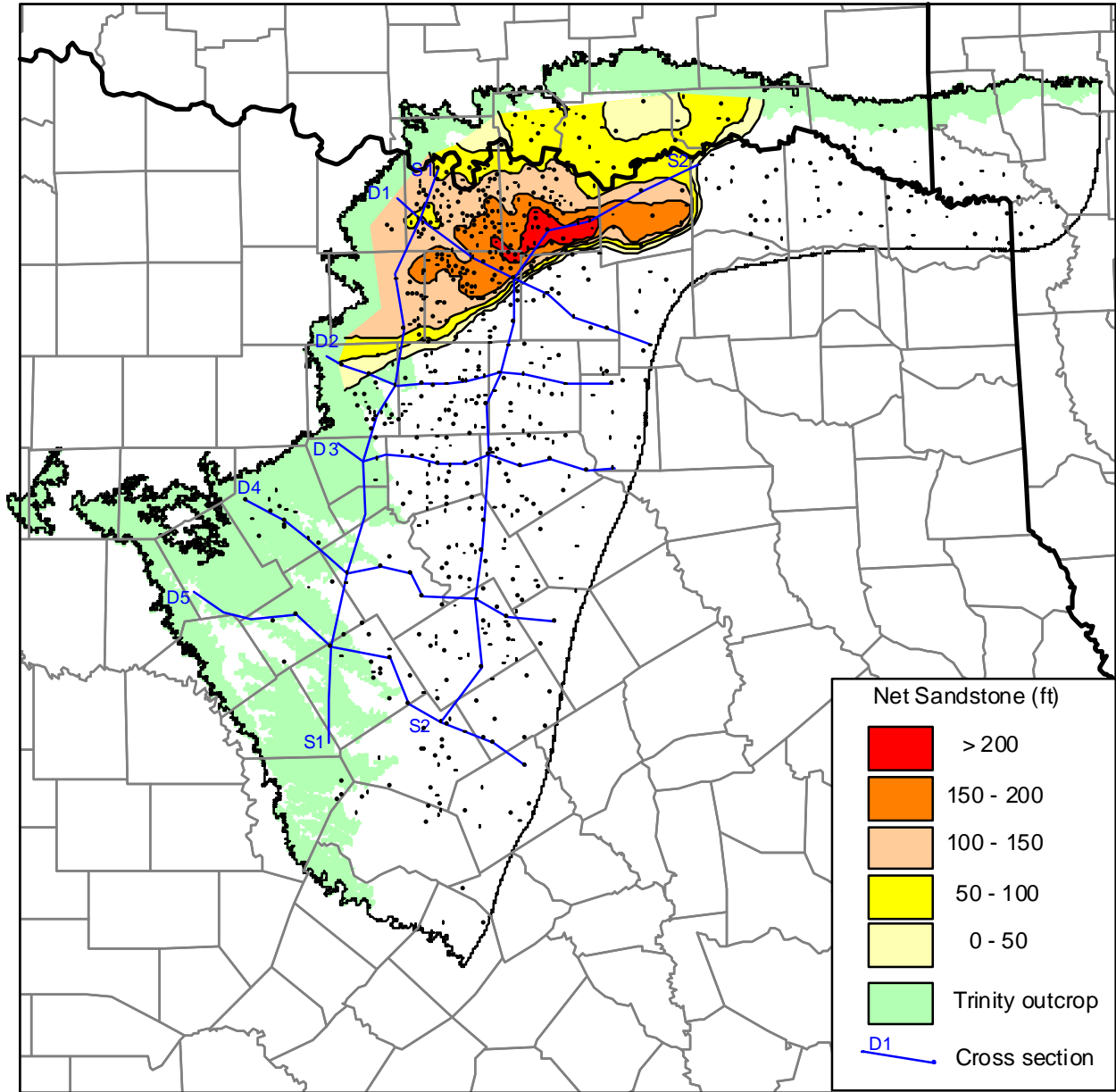
Figure 4.1.22　　Net sandstone in the Glen Rose Formation and locations of cross sections shown in Figures 4.1.31 through 4.1.37.
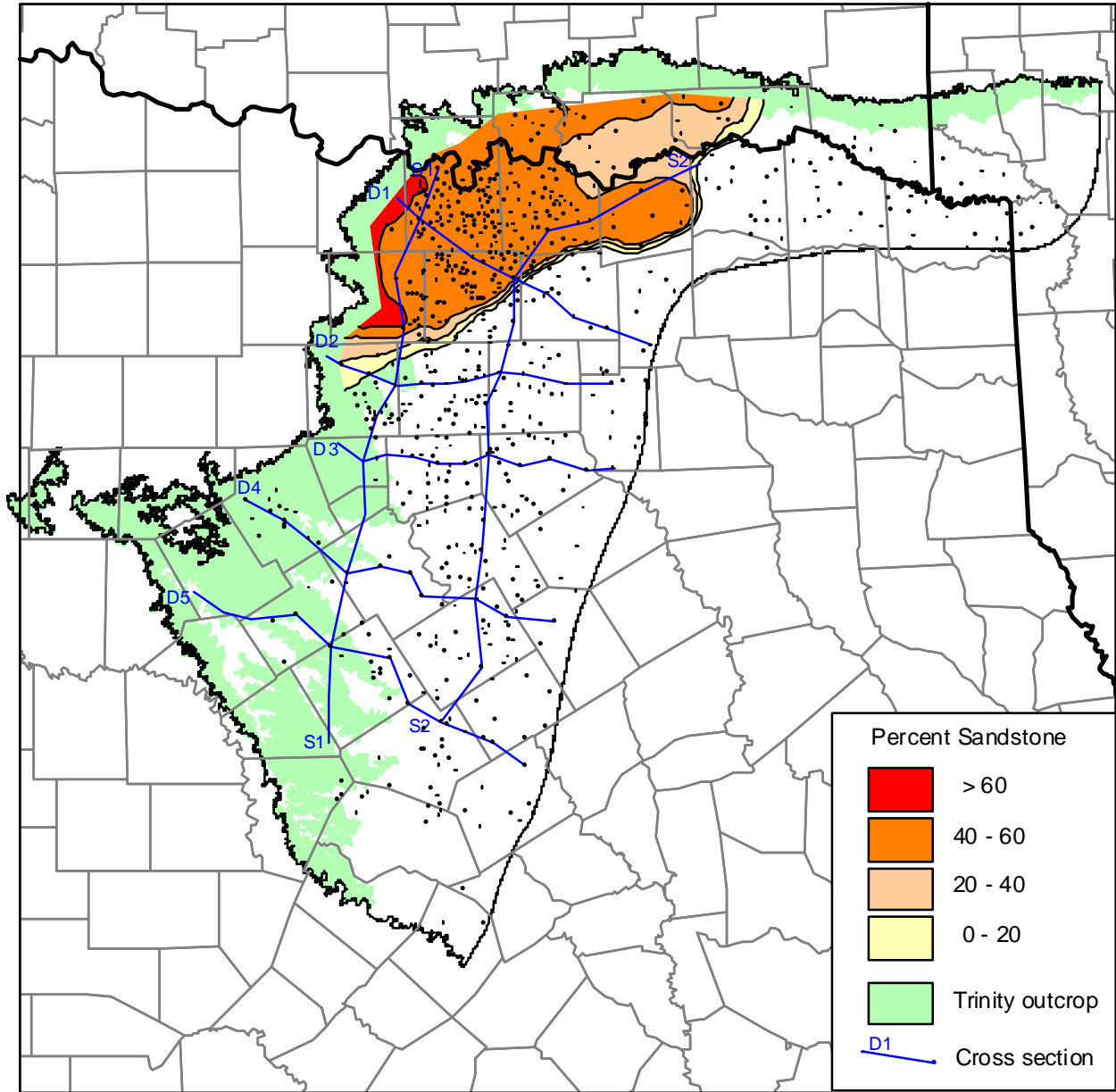
Figure 4.1.23   Percent sandstone in the Glen Rose Formation and locations of cross sections shown in Figure 4.1.31 through 4.1.37.
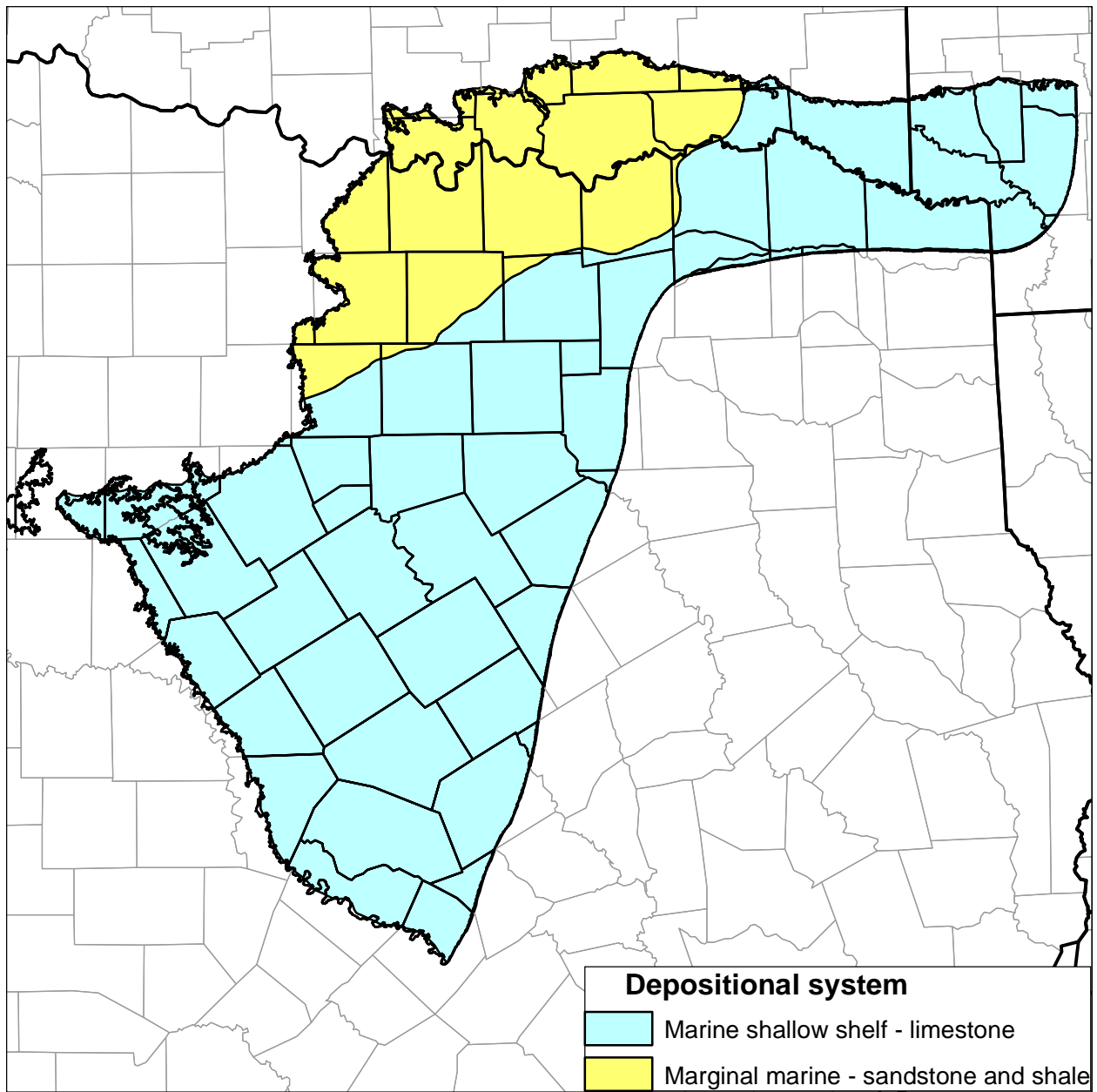
Figure 4.1.24   Depositional systems of the Glen Rose Formation.
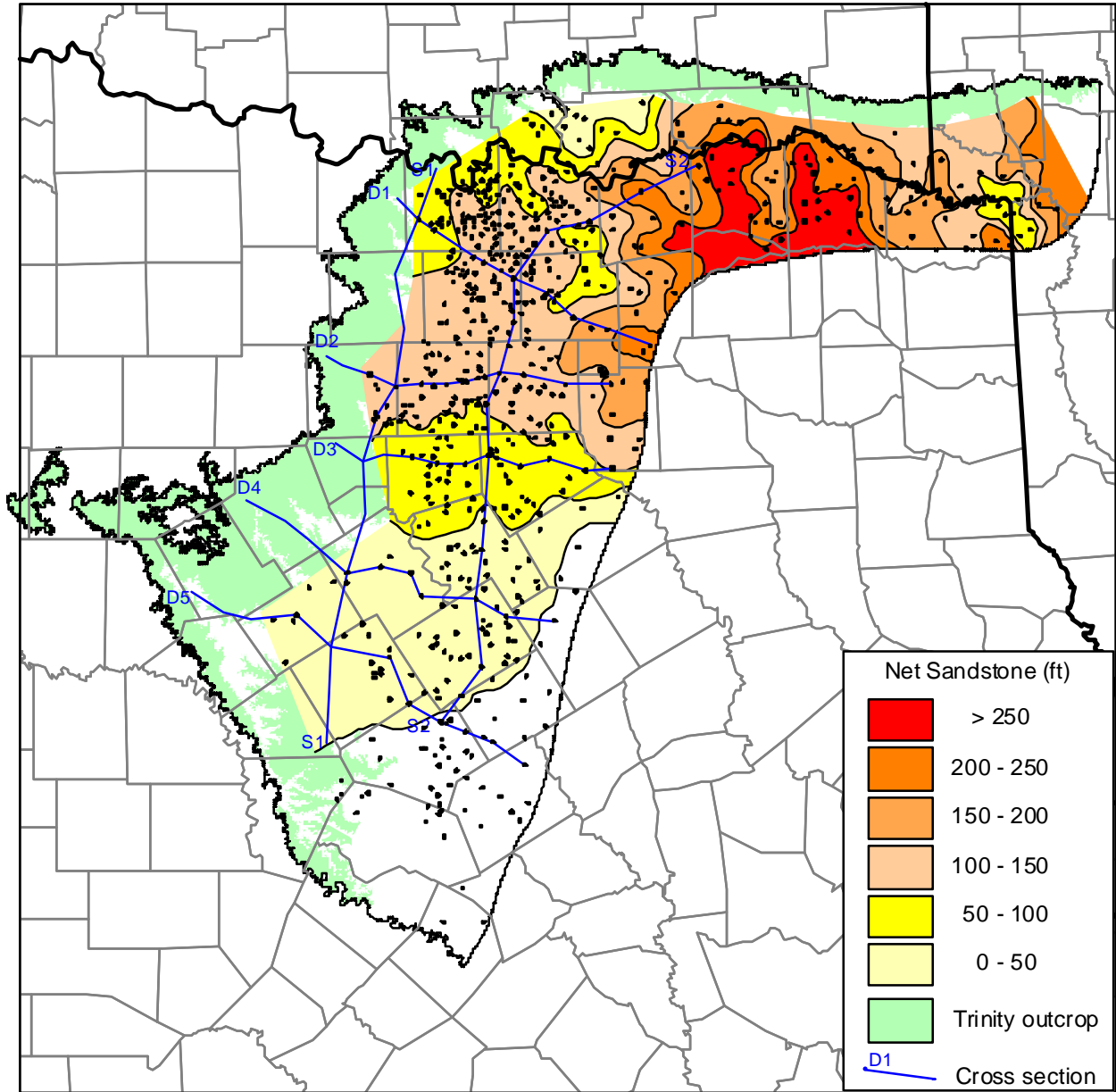
Figure 4.1.25   Net sandstone in the Paluxy Aquifer in feet and locations of cross sections shown in Figures 4.1.31 through 4.1.37.
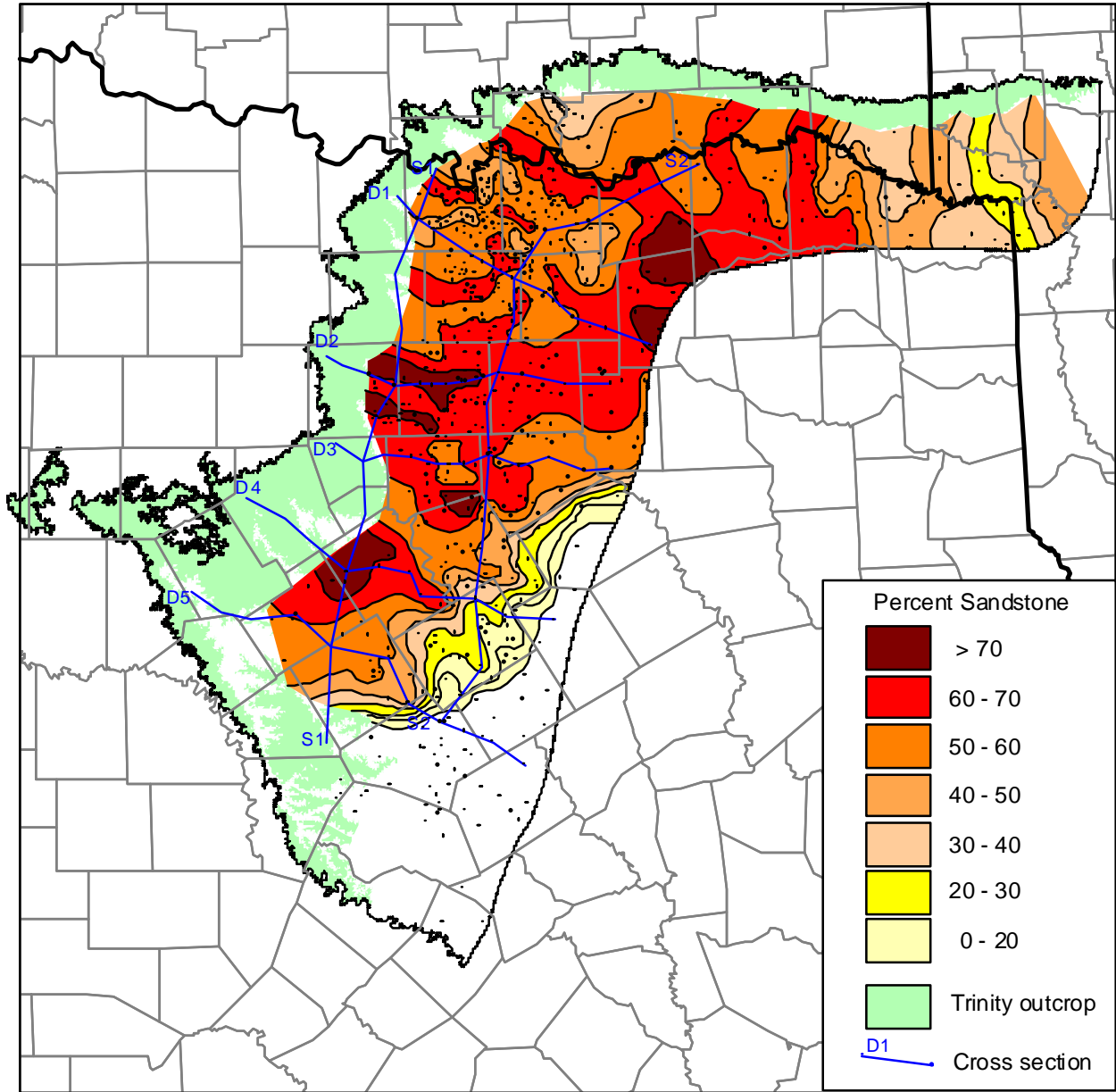
Figure 4.1.26 **Percent sandstone in the Paluxy Aquifer and locations of cross sections shown in Figures 4.1.31 through 4.1.37.**
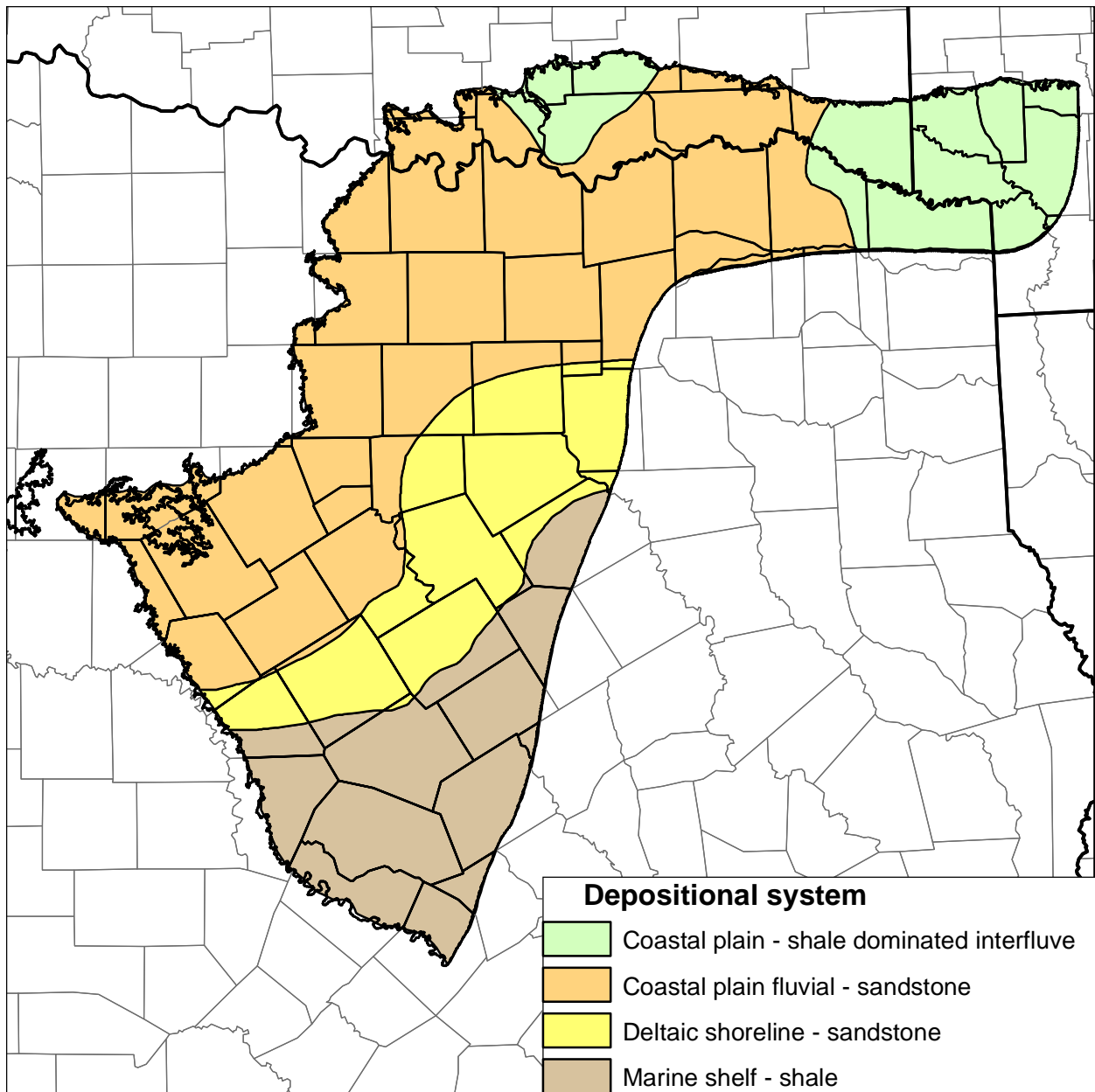
Figure 4.1.27   Depositional systems of the Paluxy Aquifer.
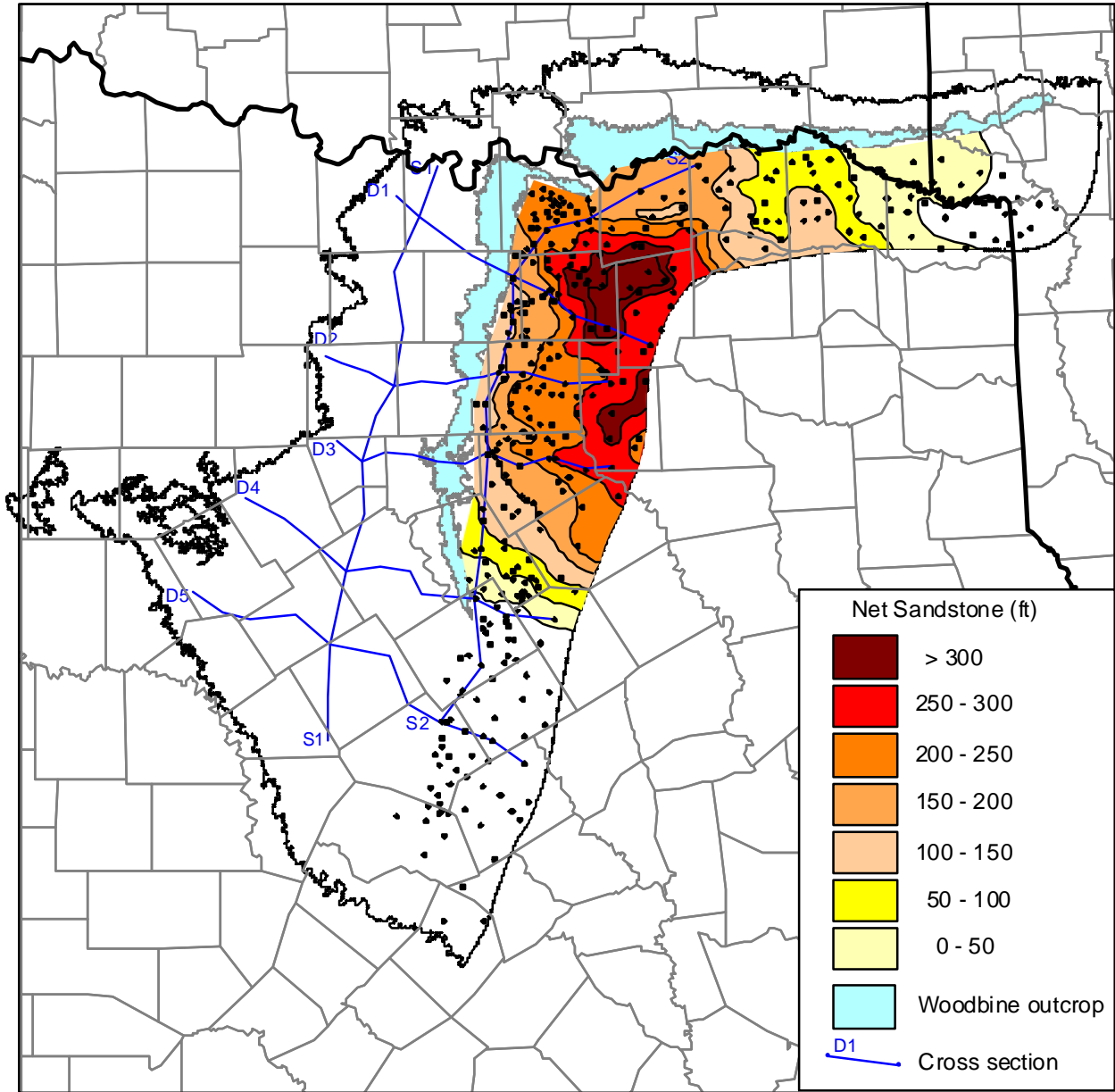
Figure 4.1.28 Net sandstone in the Woodbine Aquifer in feet and locations of cross sections shown in Figures 4.1.31 through 4.1.37.
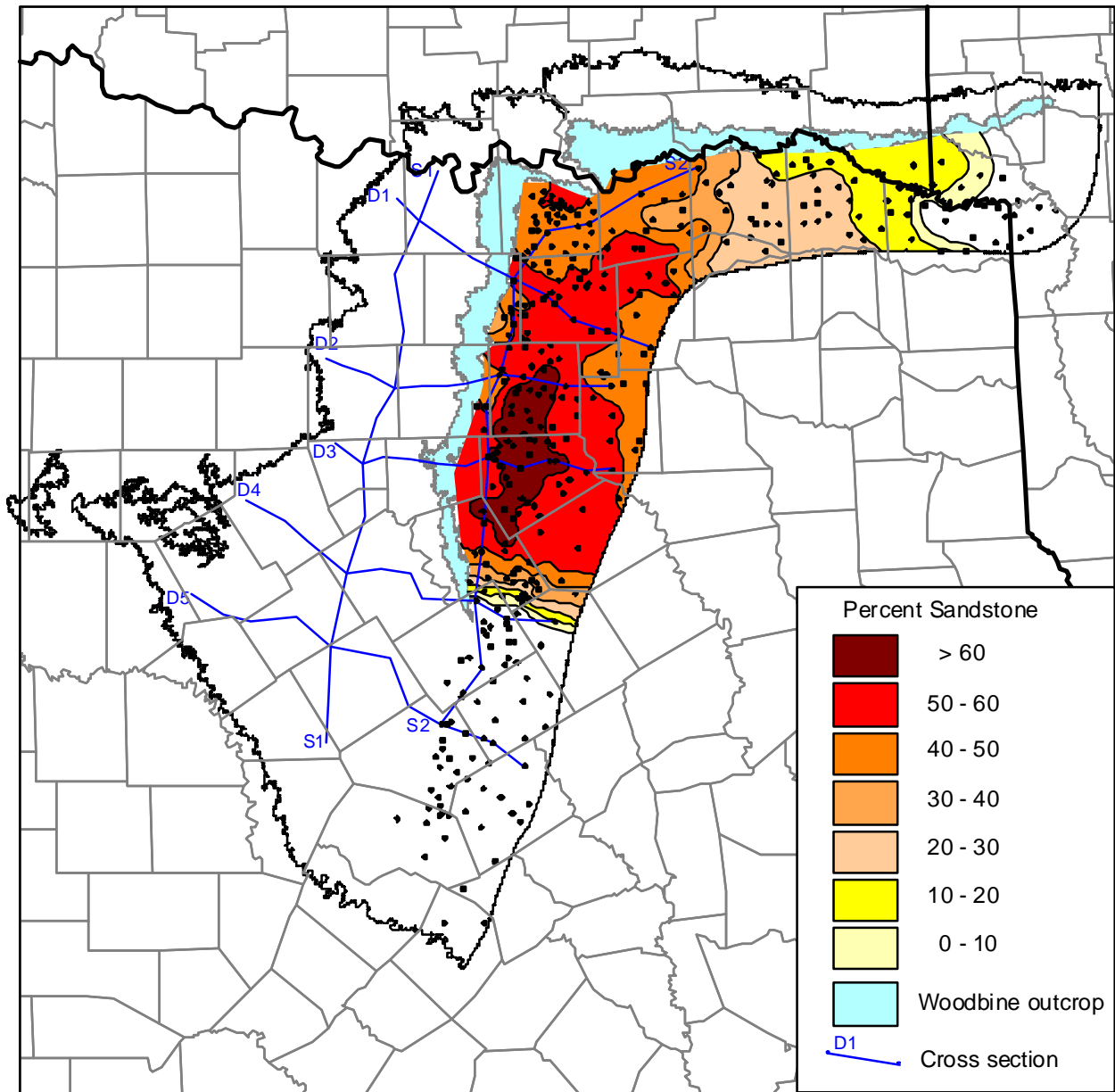
Figure 4.1.29   Percent sandstone in the Woodbine Aquifer and locations of cross sections shown in Figures 4.1.31 through 4.1.37.
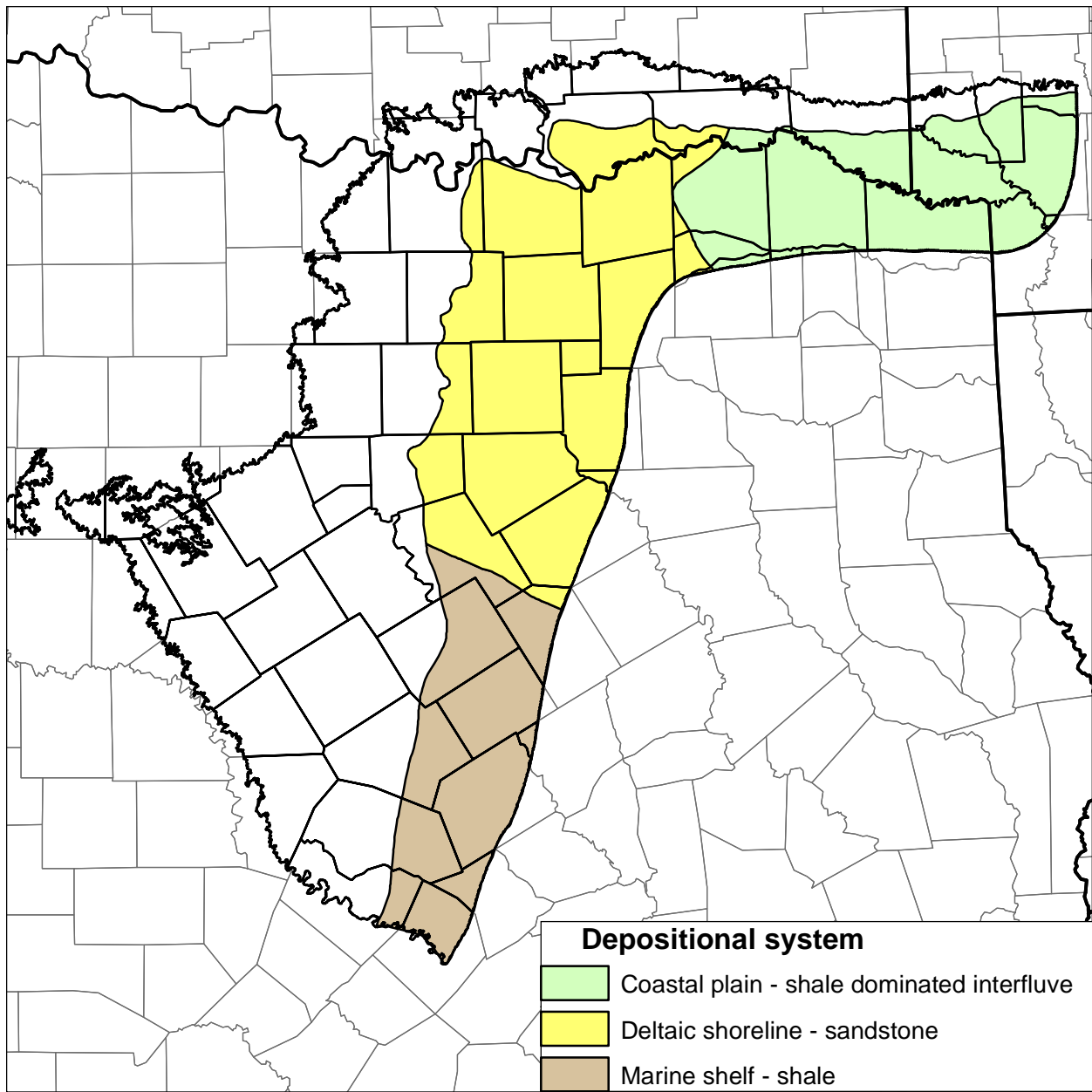
Figure 4.1.30 Depositional systems of the Woodbine Aquifer.
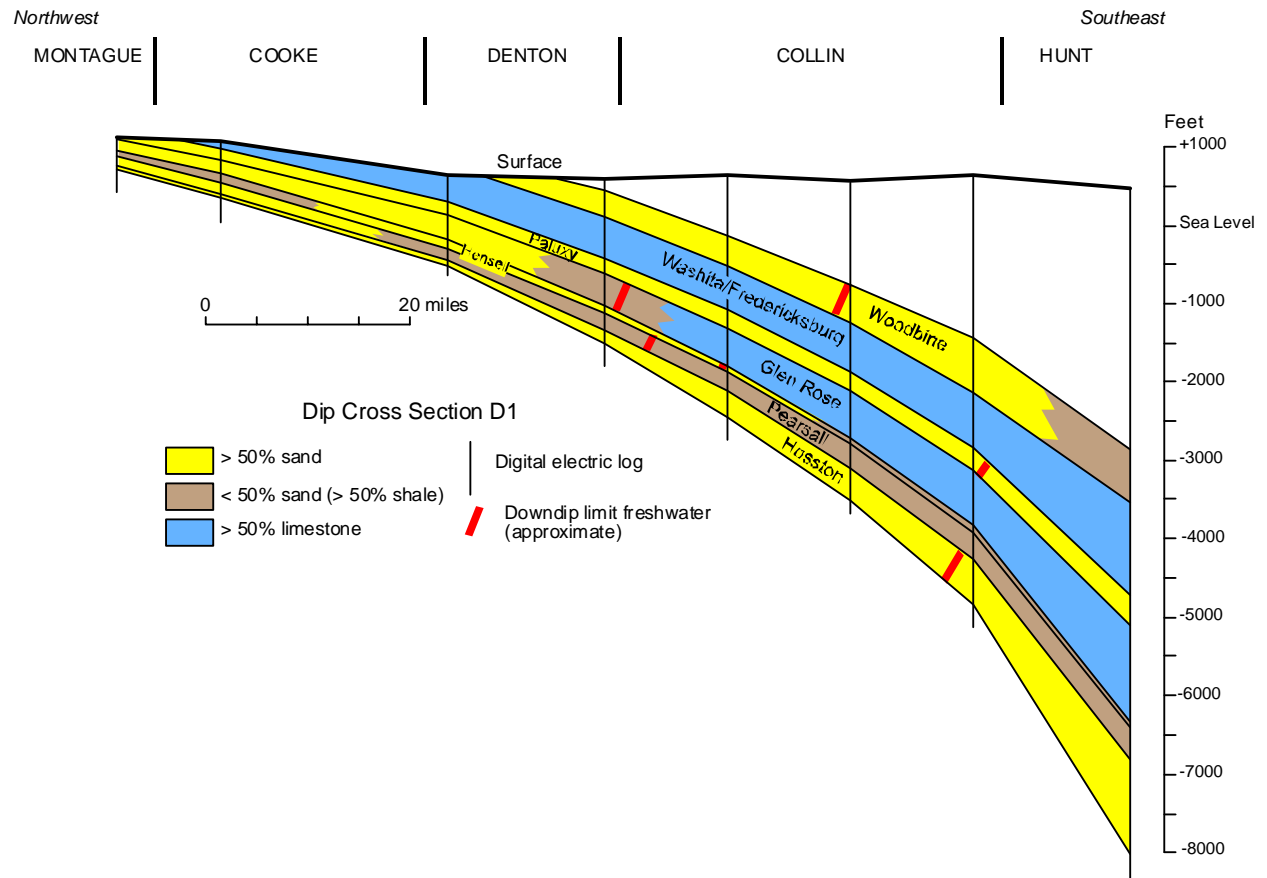
Figure 4.1.31   Dip-oriented cross section D1 showing stratigraphic boundaries, dominant lithologies, depths in feet, and downdip limits of freshwater in sandstone and shale layers.
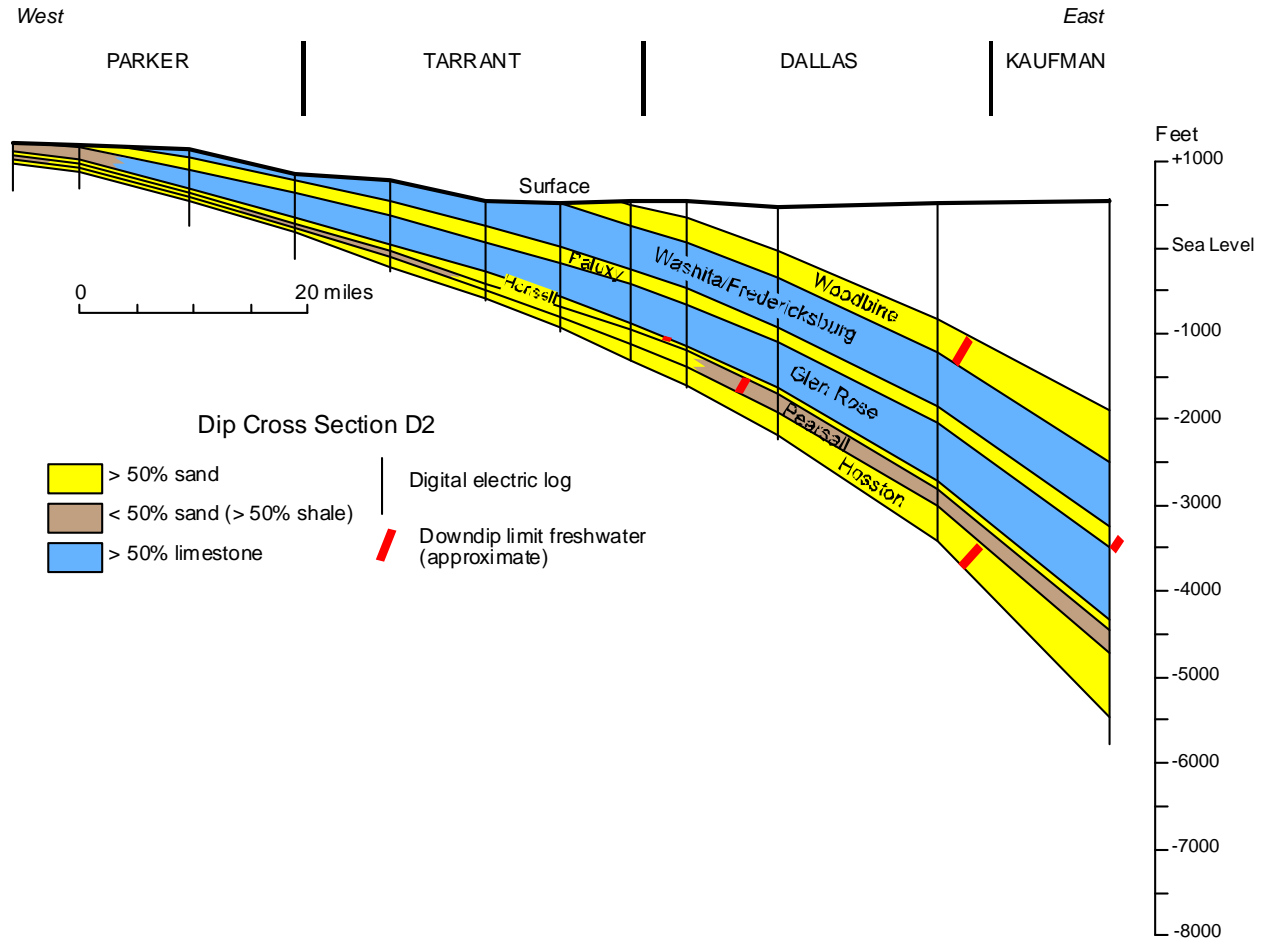
**Figure 4.1.32   Dip-oriented cross section D2 showing stratigraphic boundaries, dominant
lithologies, depths in feet, and downdip limits of freshwater in sandstone and shale
layers.**
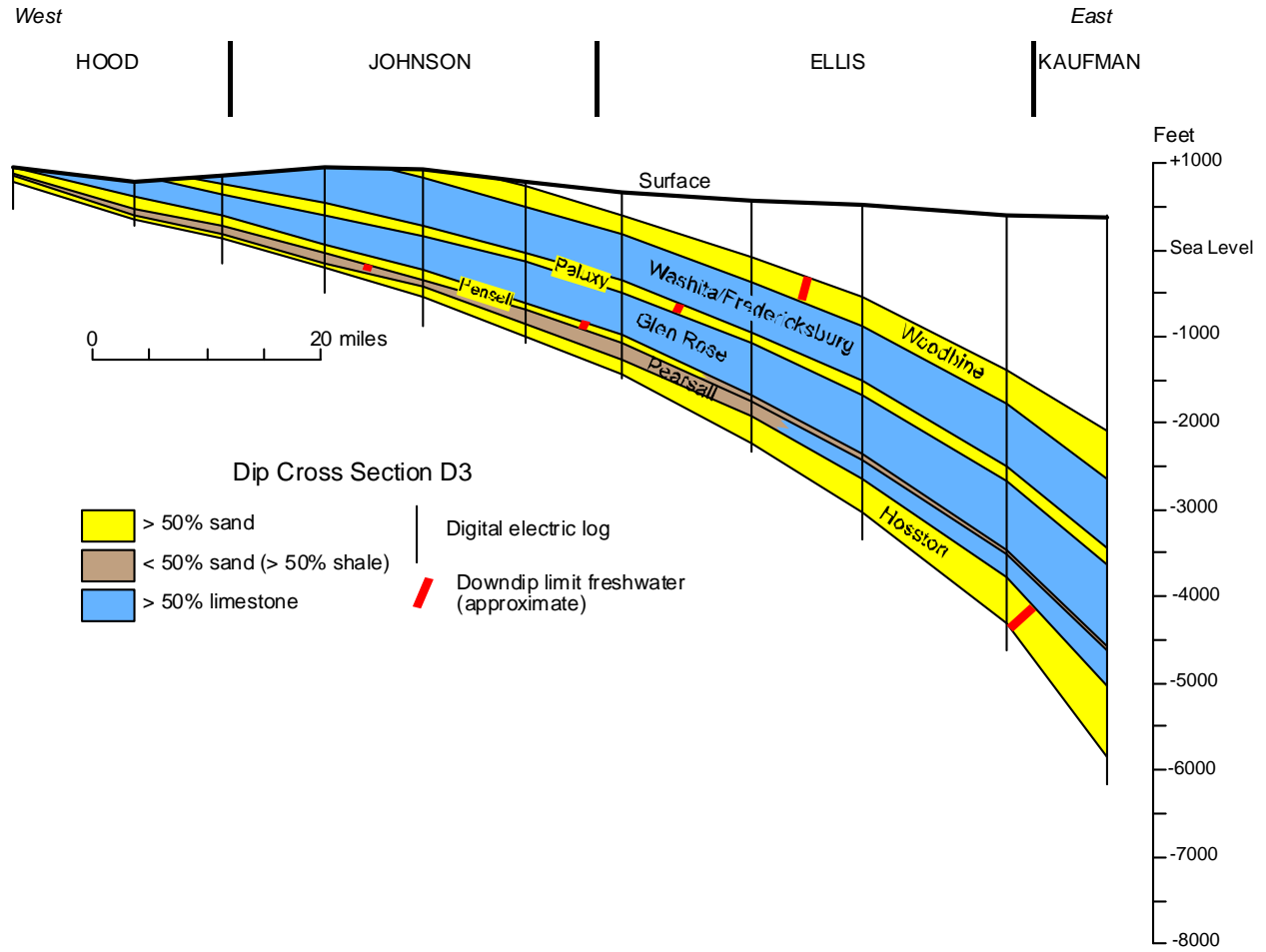
Figure 4.1.33   Dip-oriented cross section D3 showing stratigraphic boundaries, dominant lithologies, depths in feet, and downdip limits of freshwater in sandstone and shale layers.
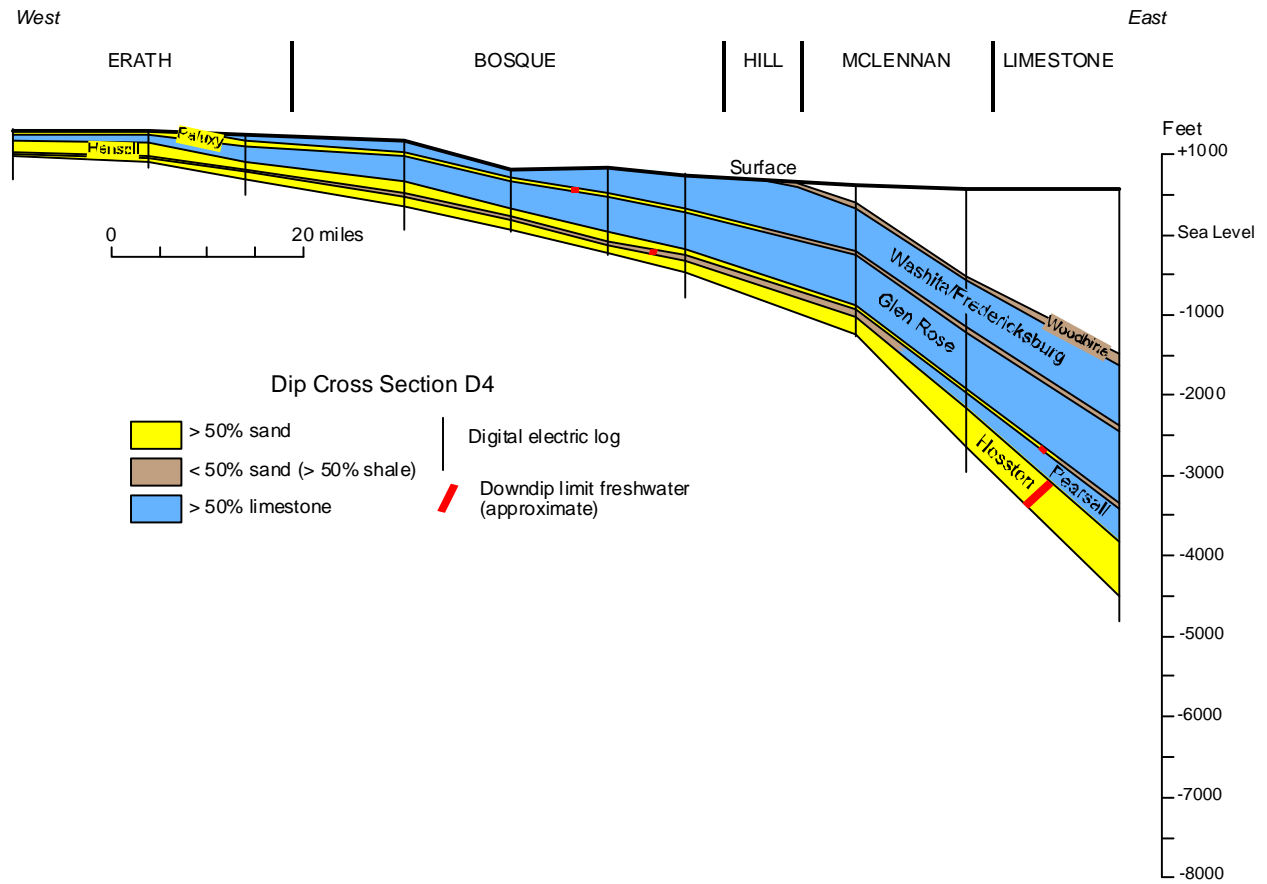
Figure 4.1.34 **Dip-oriented cross section D4 showing stratigraphic boundaries, dominant lithologies, depths in feet, and downdip limits of freshwater in sandstone and shale layers.**
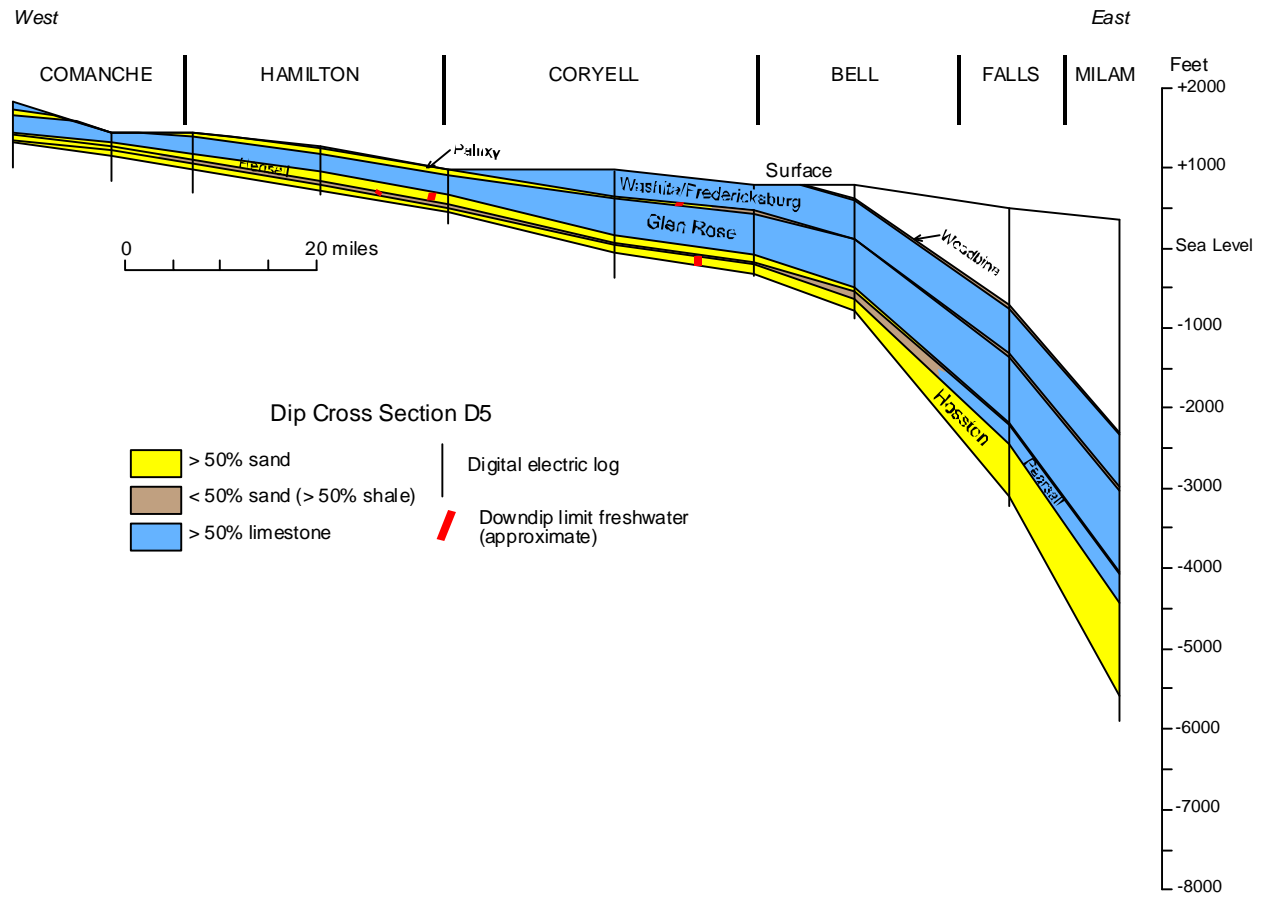
Figure 4.1.35   Dip-oriented cross section D5 showing stratigraphic boundaries, dominant lithologies, depths in feet, and downdip limits of freshwater in sandstone and shale layers.
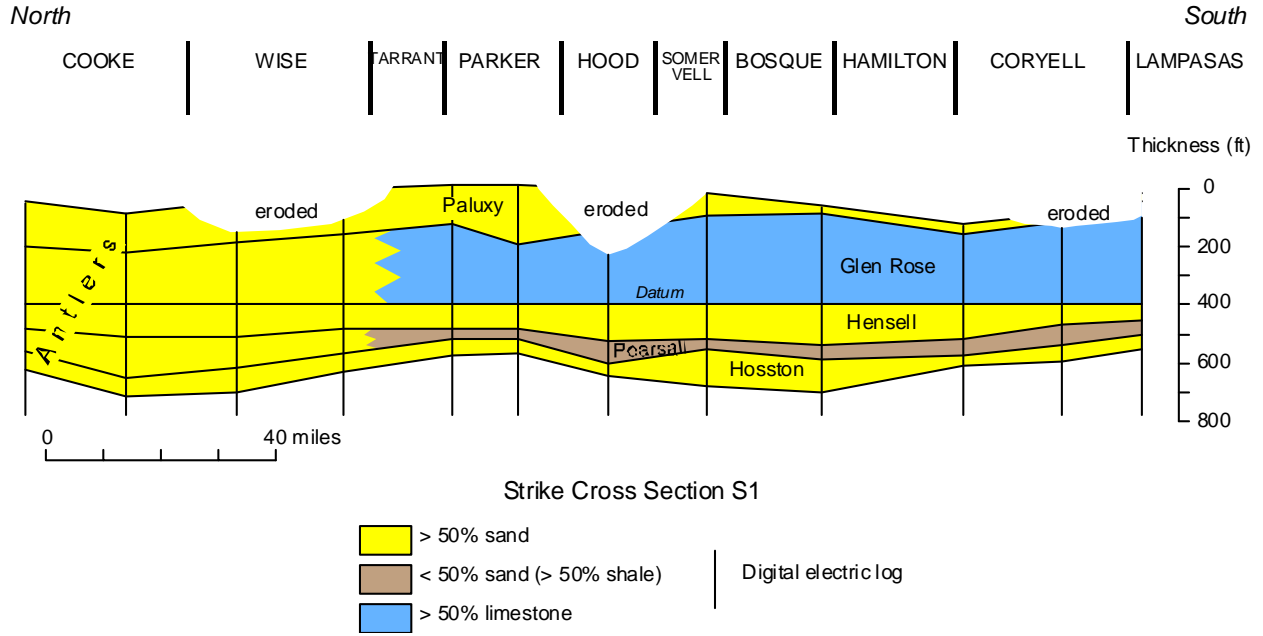
Figure 4.1.36   Strike-oriented cross section S1 showing stratigraphic boundaries, dominant lithologies, and thicknesses in feet.
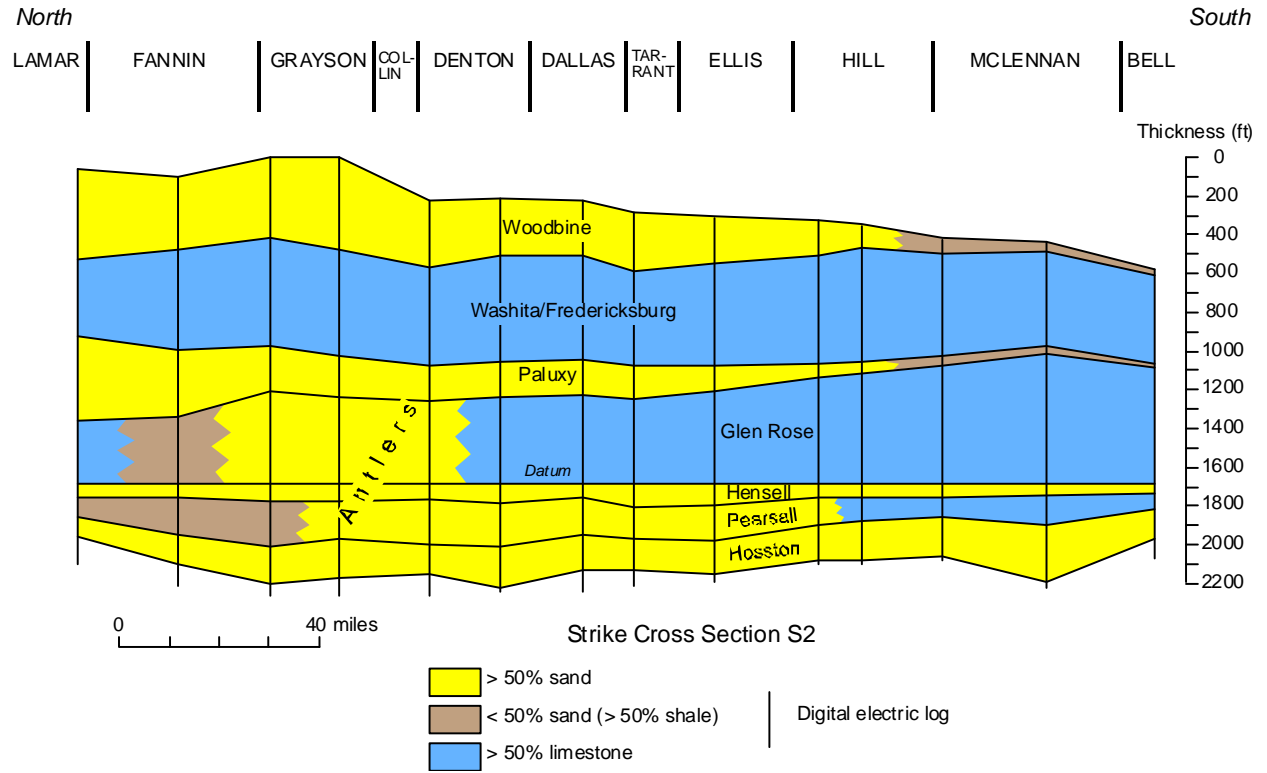
Figure 4.1.37   **Strike-oriented cross section S2 showing stratigraphic boundaries, dominant
lithologies, and thicknesses in feet.**
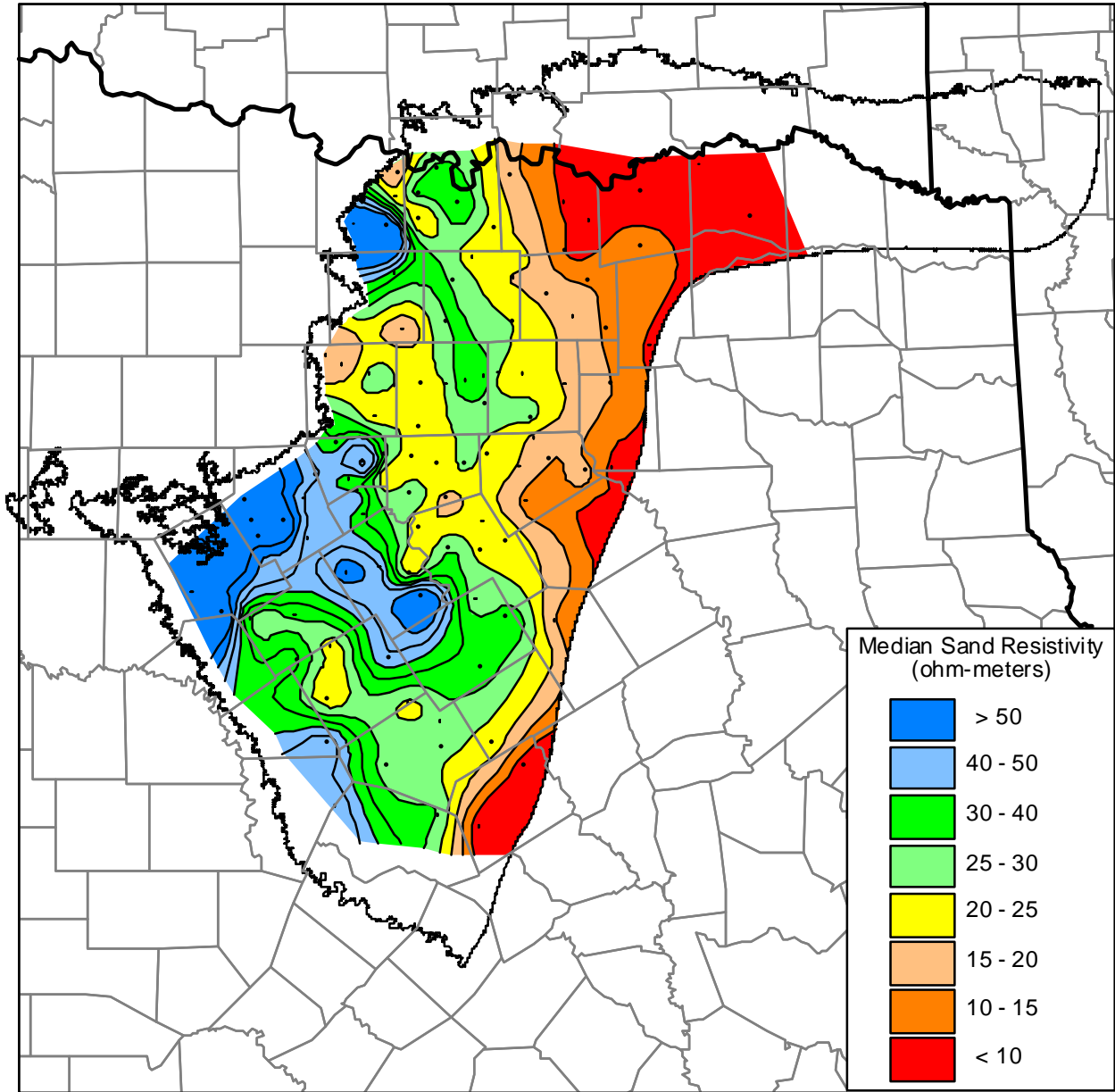
Figure 4.1.38   Median resistivity of sandstones greater than 10-feet thick in the Hosston Aquifer.
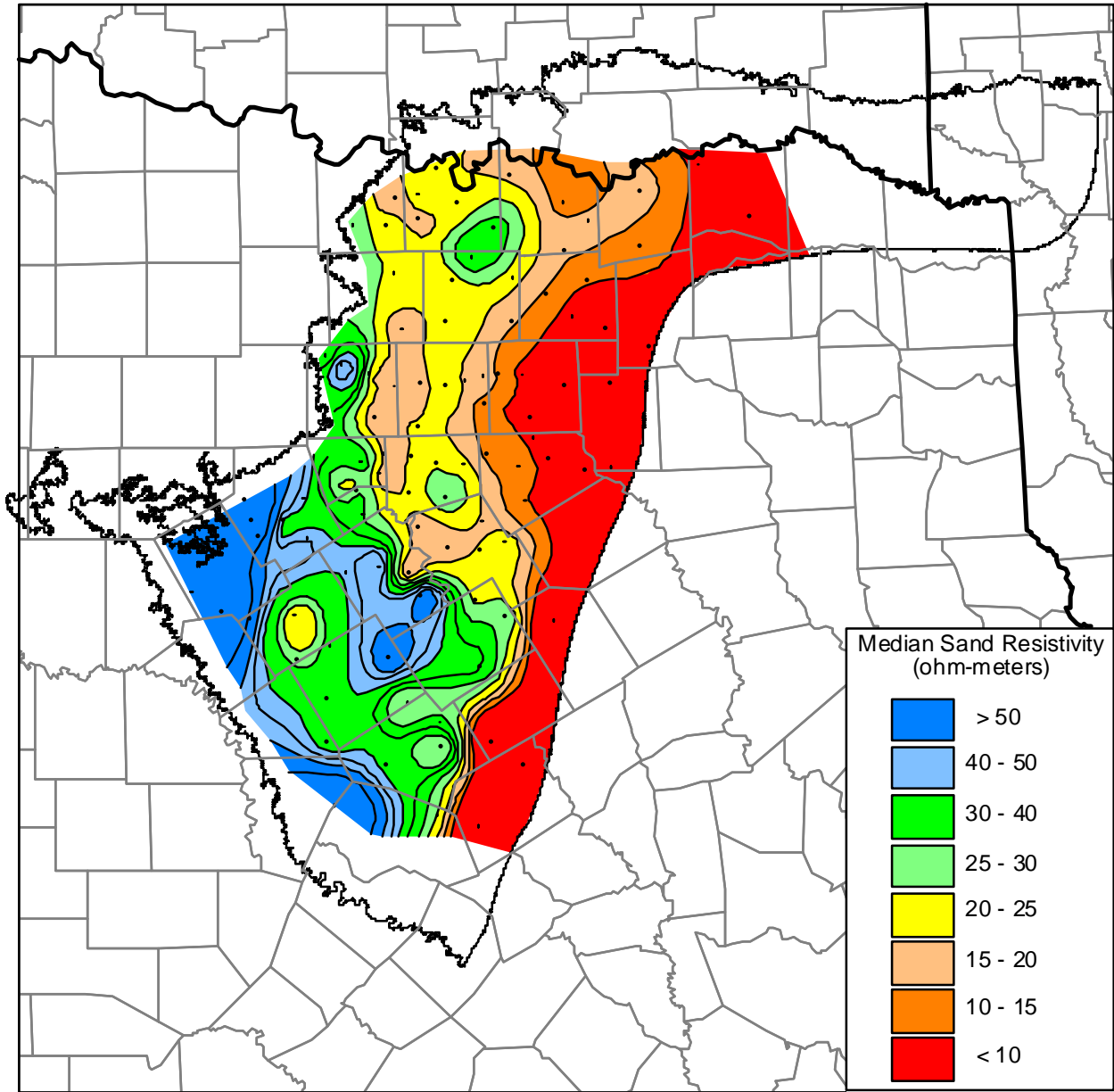
Figure 4.1.39   Median resistivity of sandstones greater than 10-feet thick in the Hensell Aquifer.
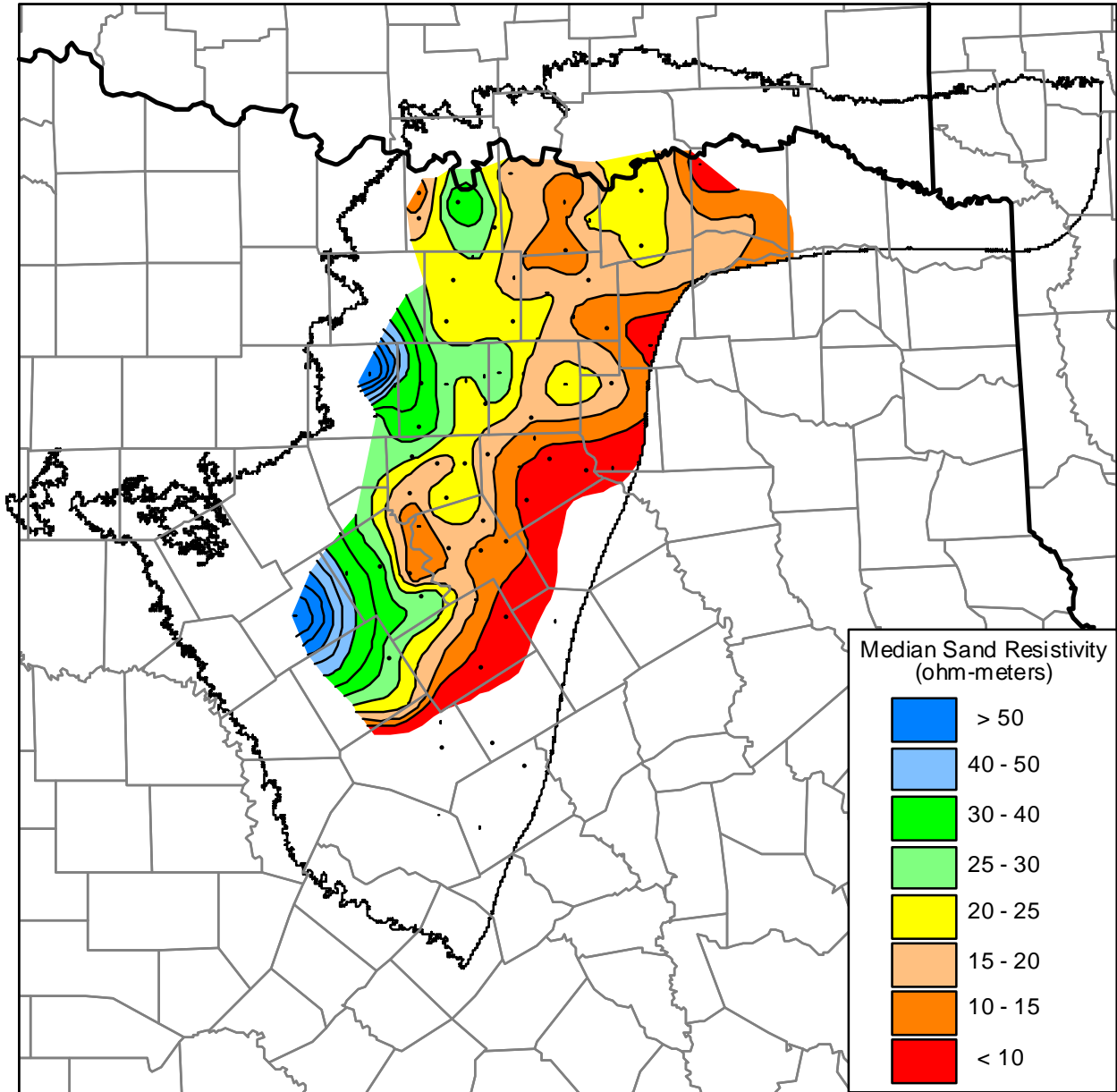
Figure 4.1.40   Median resistivity of sandstones greater than 10-feet thick in the Paluxy Aquifer.
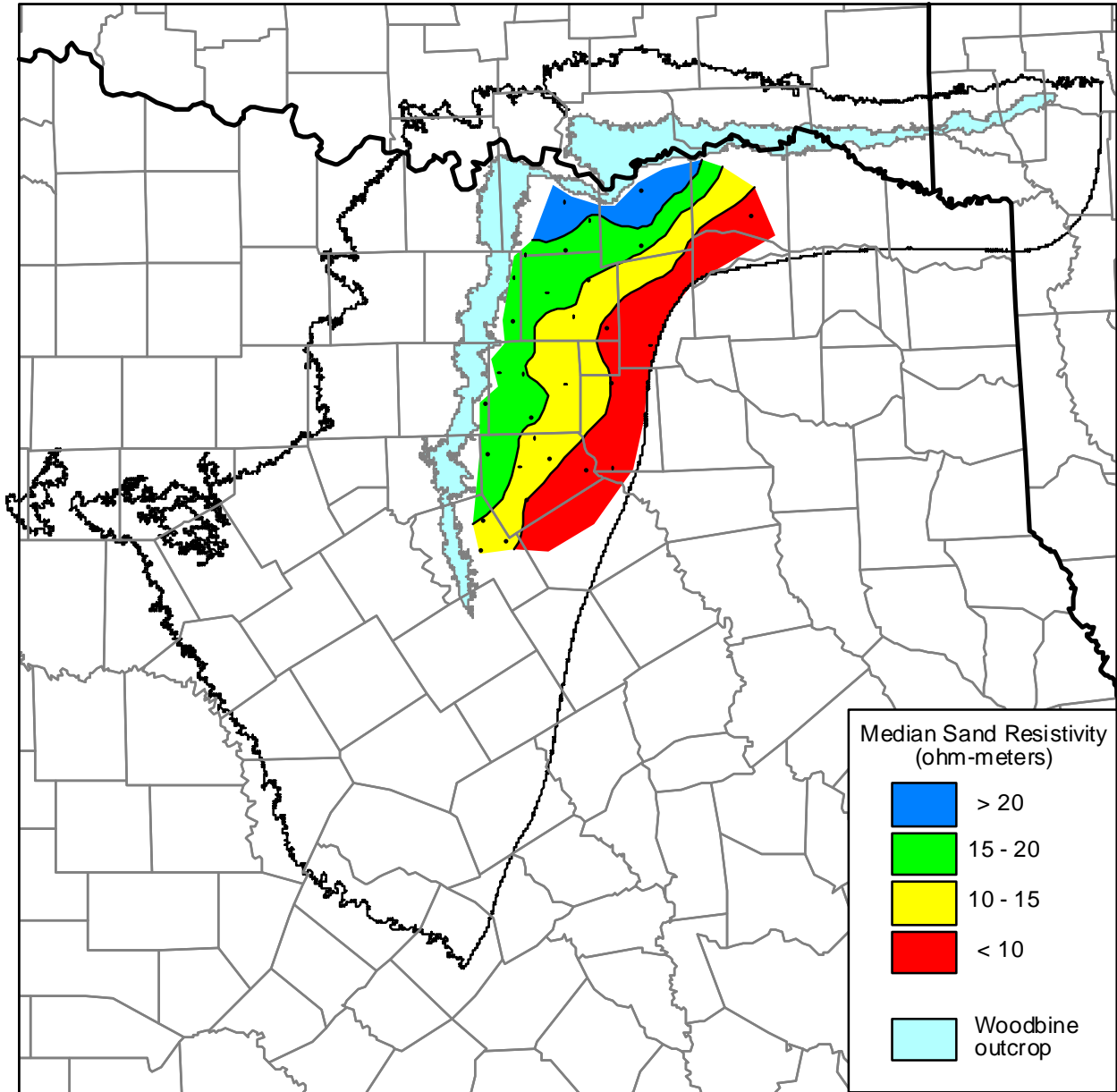
Figure 4.1.41 Median resistivity of sandstones greater than 10-feet thick in the Woodbine Aquifer.
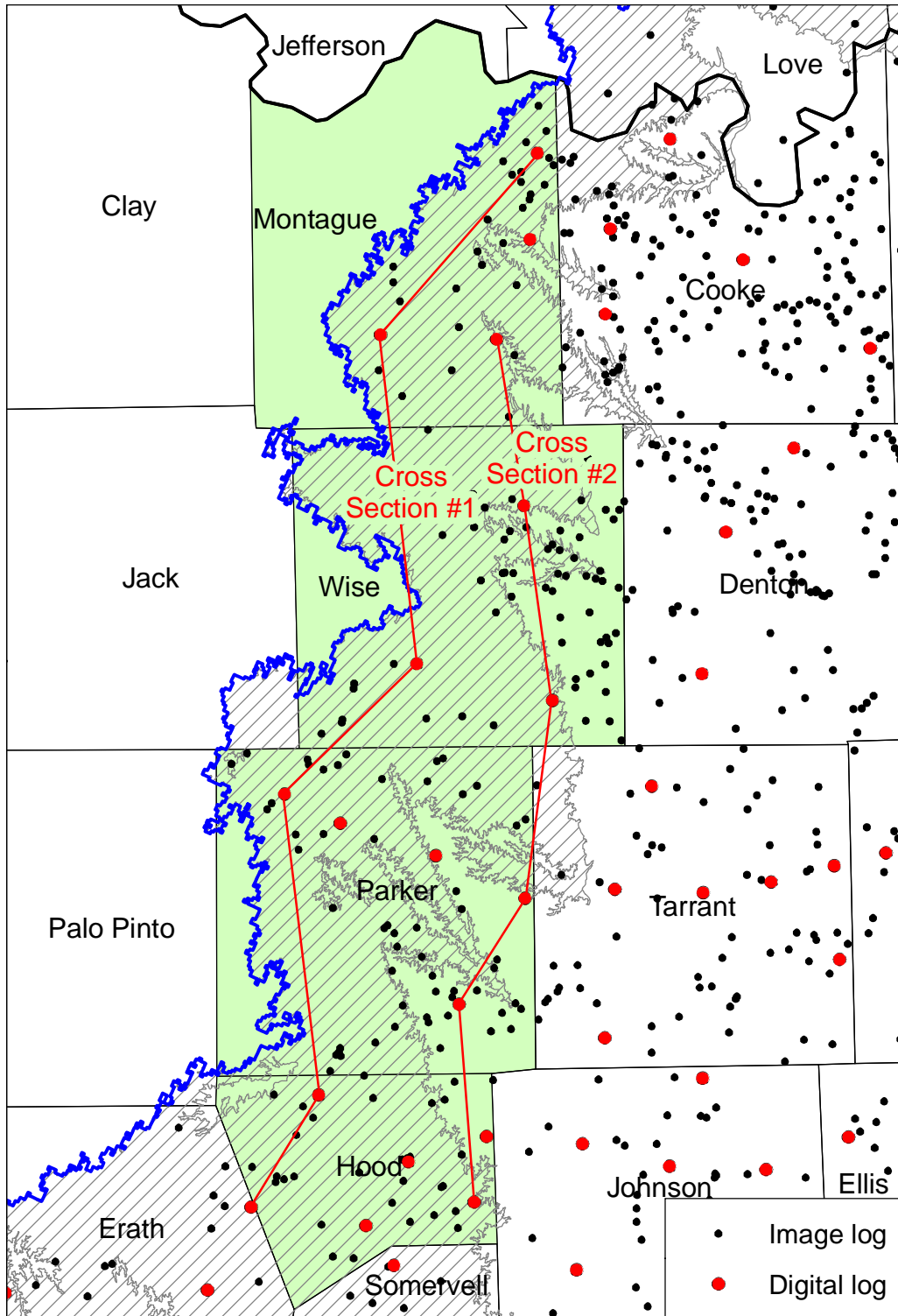
Figure 4.1.42 **Upper Trinity GCD (green) showing the northern Trinity Aquifer outcrop (grey cross hatching), locations of geophysical well logs, and locations of cross sections shown in Figures 4.1.43 and 4.1.44.**

yellow = greater than 50 percent sandstone, brown = greater than 50 percent shale
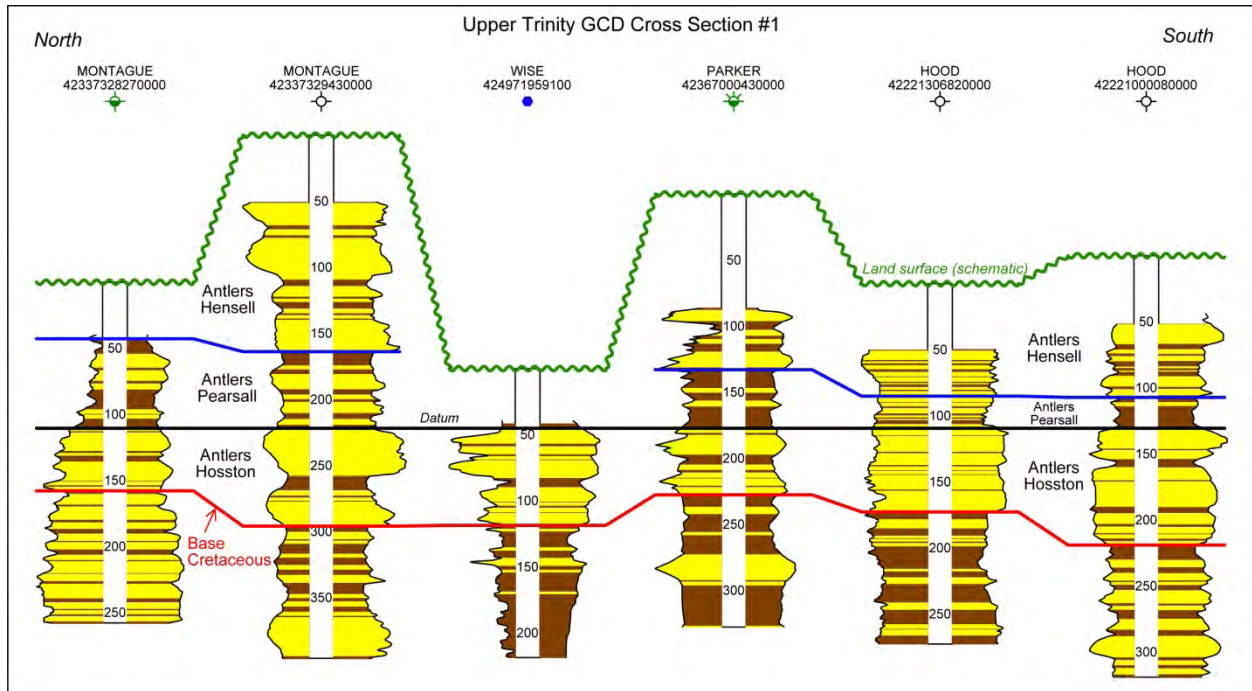
Figure 4.1.43   Upper Trinity GCD digital cross section # 1 with stratigraphic layers flattened on the top of the Hosston Aquifer (datum), so true elevations relative to sea level are not shown.

yellow = greater than 50 percent sandstone, blue = greater than 50 percent limestone, brown = greater than 50 percent shale
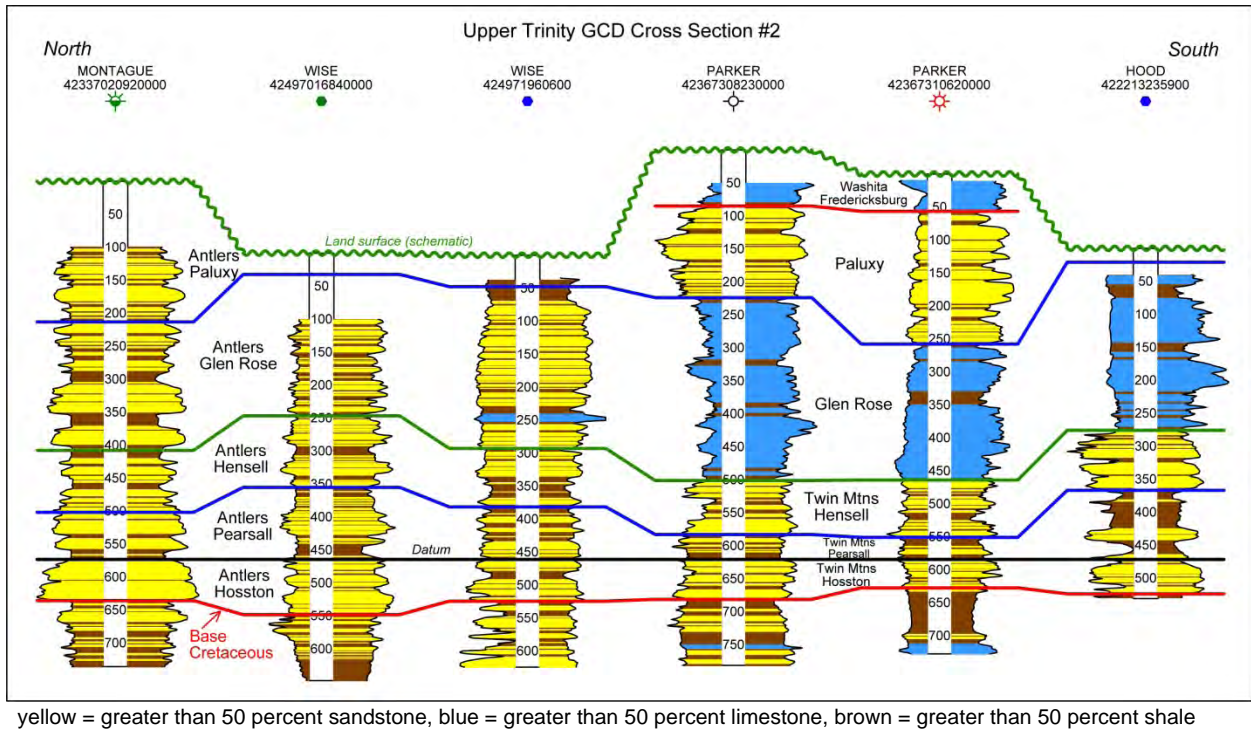
Figure 4.1.44   Upper Trinity GCD digital cross section # 2 with stratigraphic layers flattened on the top of the Hosston Aquifer (datum), so true elevations relative to sea level are not shown.
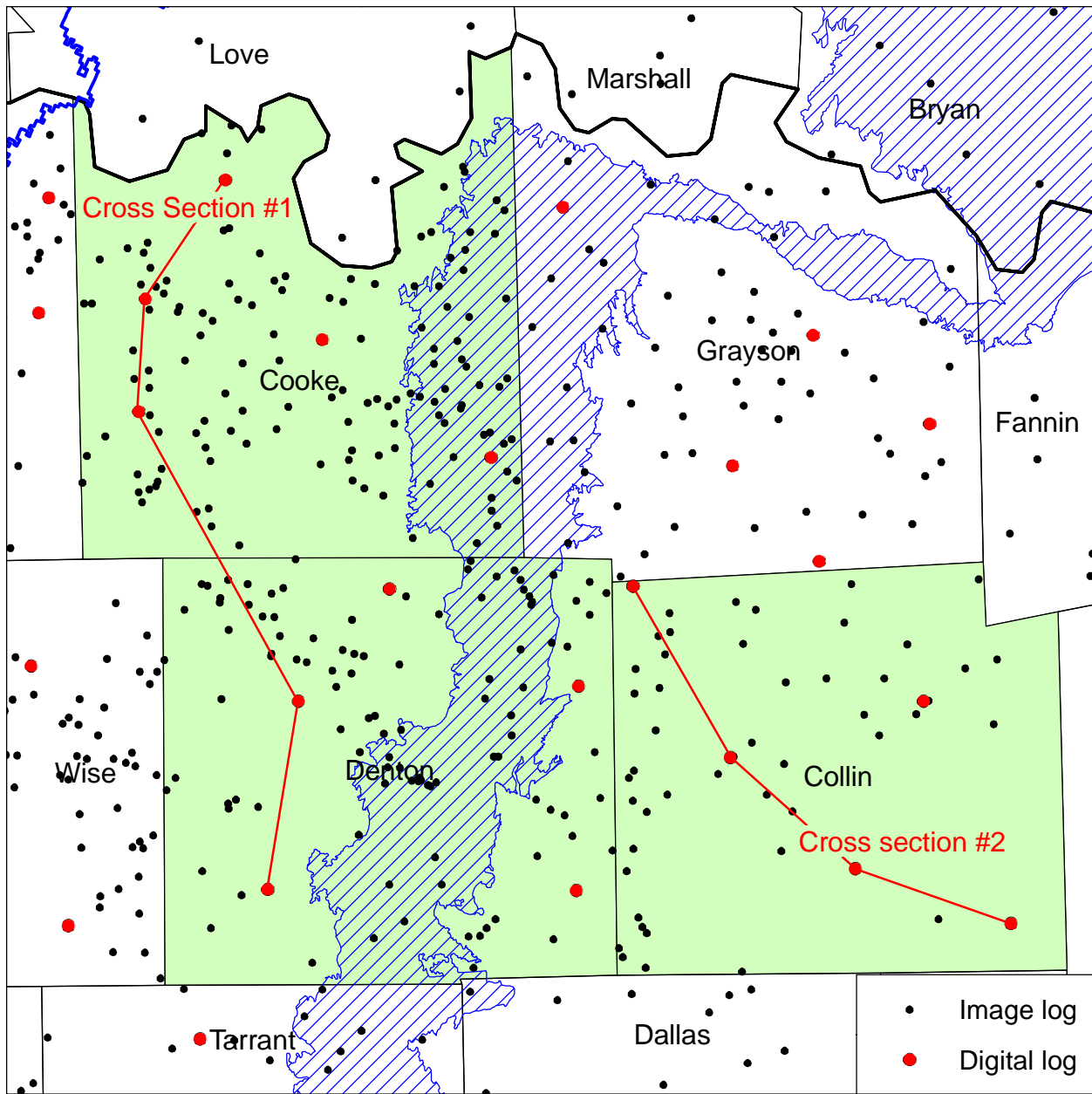
Figure 4.1.45   **North Texas GCD (green) showing the Woodbine Aquifer outcrop (blue cross hatching), locations of geophysical well logs, and locations of cross sections shown in Figures 4.1.46 and 4.1.47.**
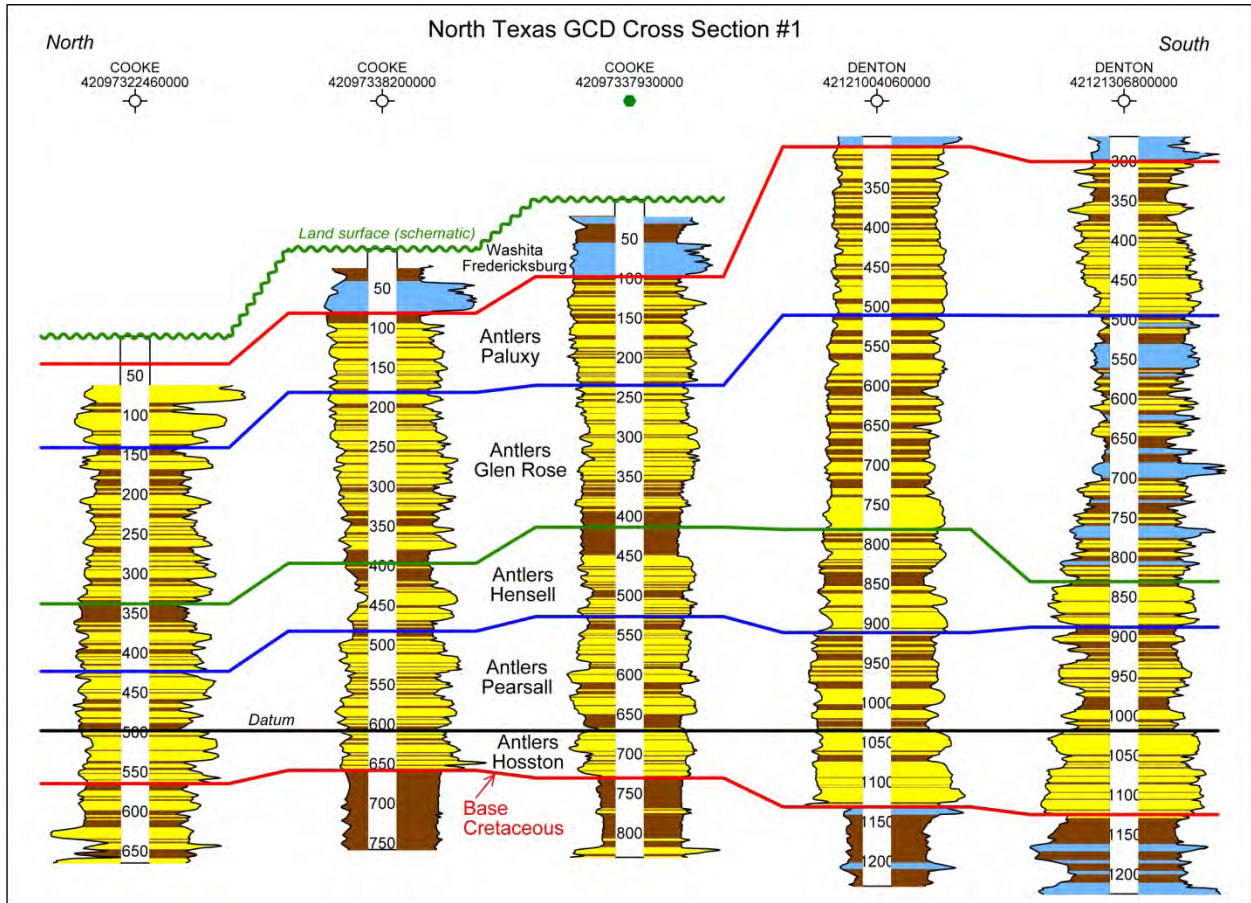
yellow = greater than 50 percent sandstone, blue = greater than 50 percent limestone, brown = greater than 50 percent shale

Figure 4.1.46   North Texas GCD digital cross section # 1 with stratigraphic layers flattened on the top of the Hosston Aquifer (datum), so true elevations relative to sea level are not shown.

yellow = greater than 50 percent sandstone, blue = greater than 50 percent limestone,
brown = greater than 50 percent shale
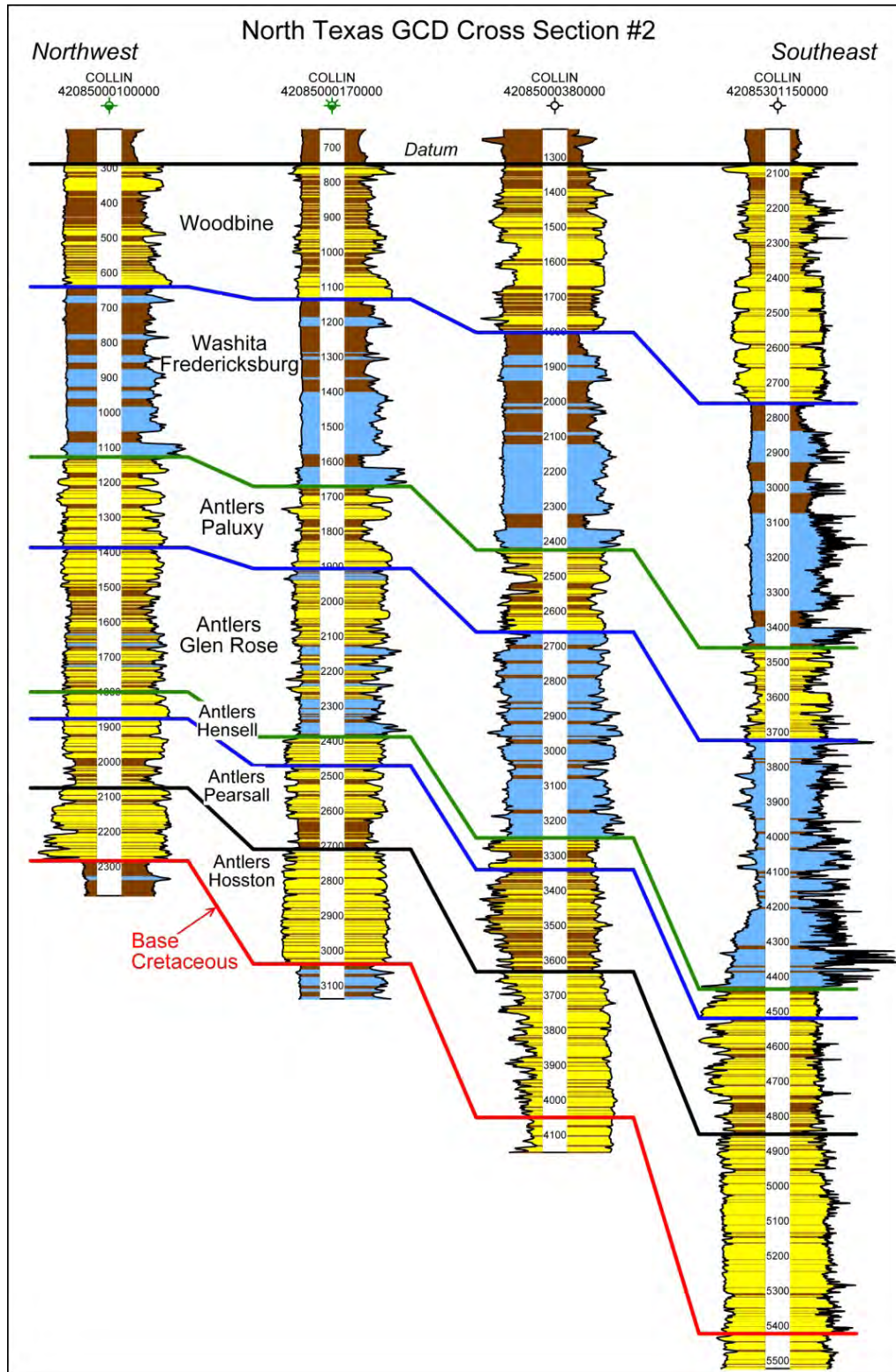
Figure 4.1.47   North Texas GCD digital cross section # 2 with stratigraphic layers flattened on the top of the Woodbine Aquifer (datum), so true elevations relative to sea level are not shown.
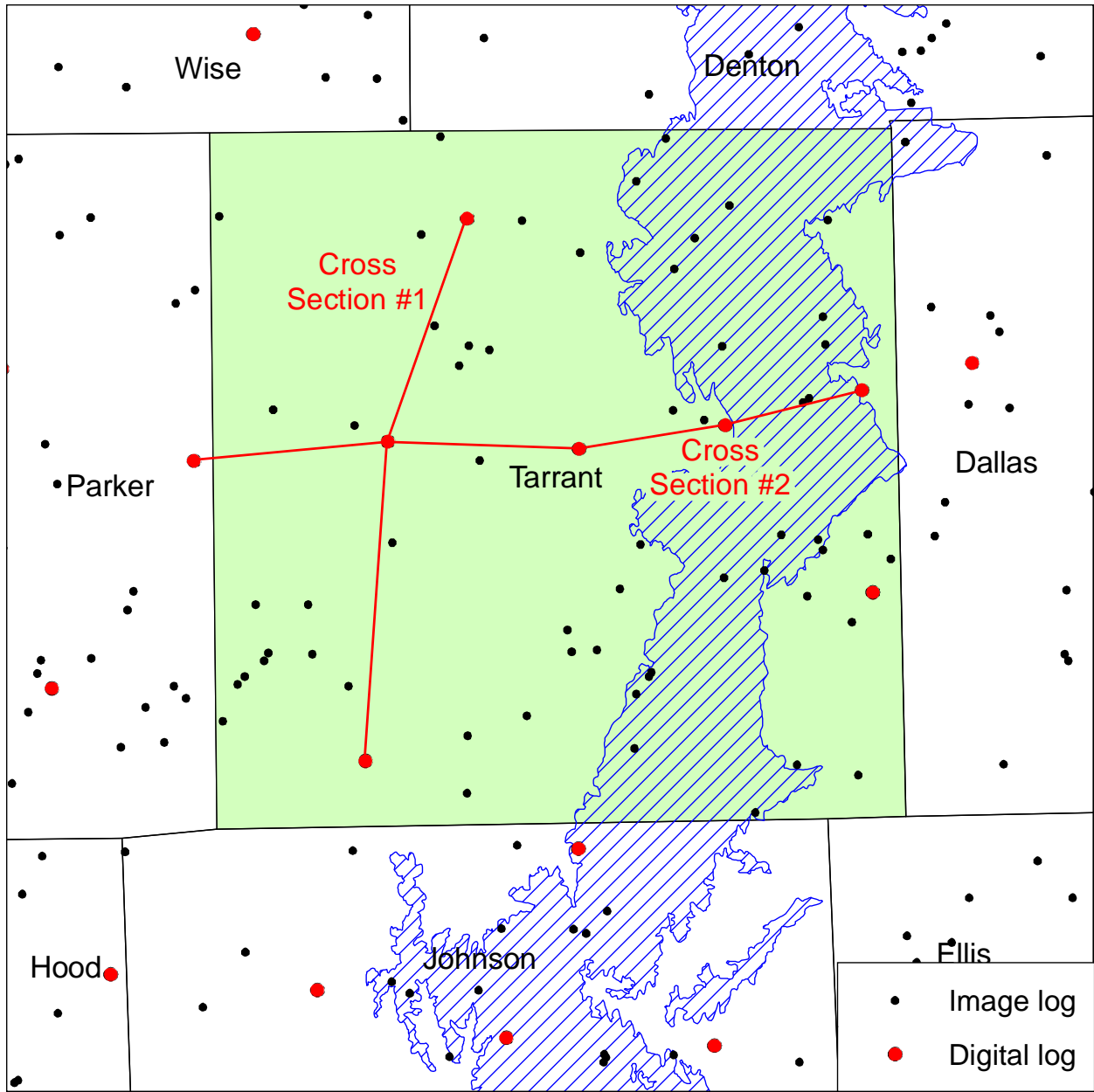
Figure 4.1.48   Northern Trinity GCD (green) showing the Woodbine Aquifer outcrop (blue cross hatching), locations of geophysical well logs, and locations of cross sections shown in Figures 4.1.49 and 4.1.50.
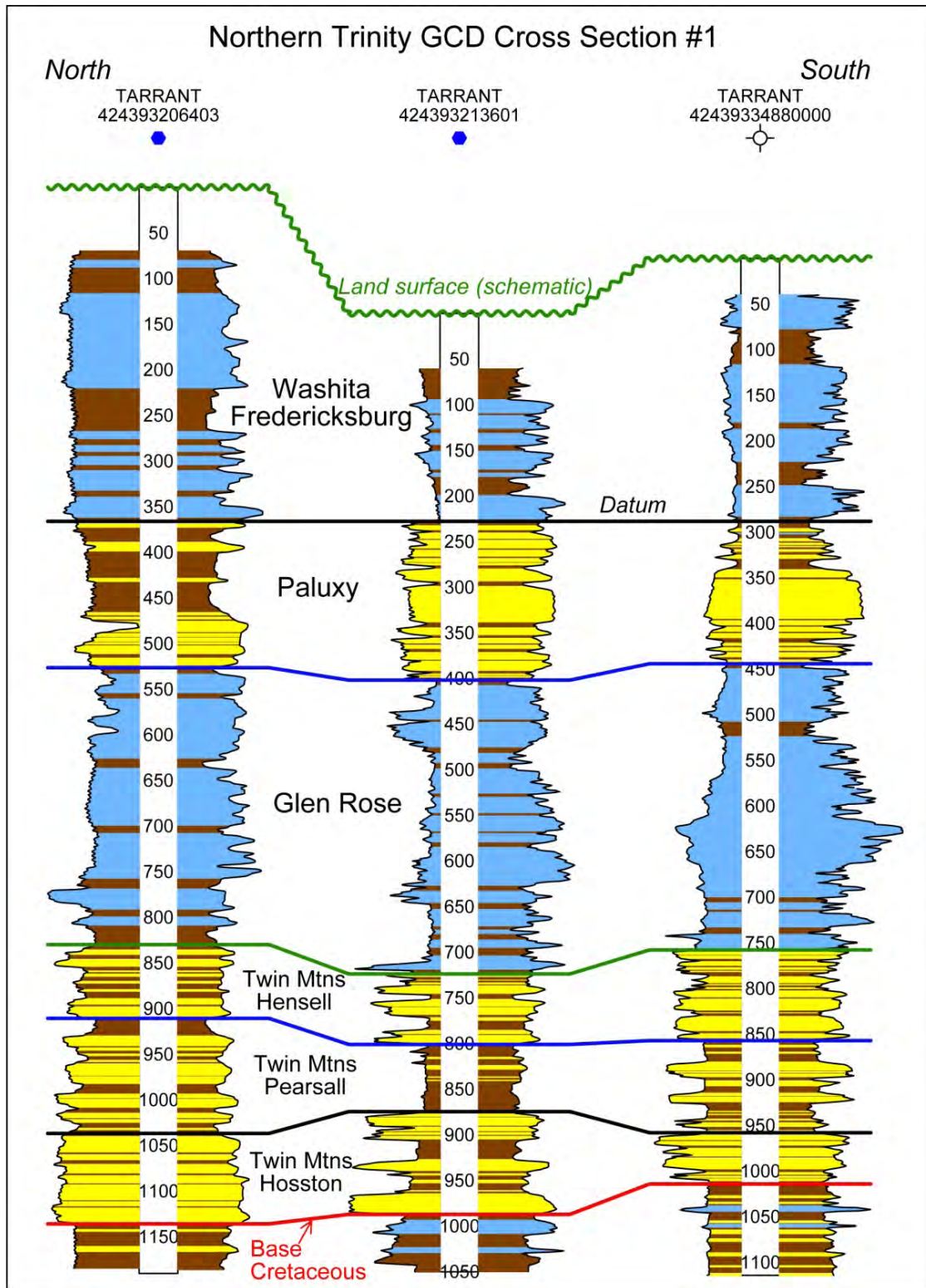
yellow = greater than 50 percent sandstone, blue = greater than 50 percent limestone,
brown = greater than 50 percent shale

Figure 4.1.49   Northern Trinity GCD digital cross section # 1 with stratigraphic layers flattened on the top of the Paluxy Aquifer (datum), so true elevations relative to sea level are not shown.
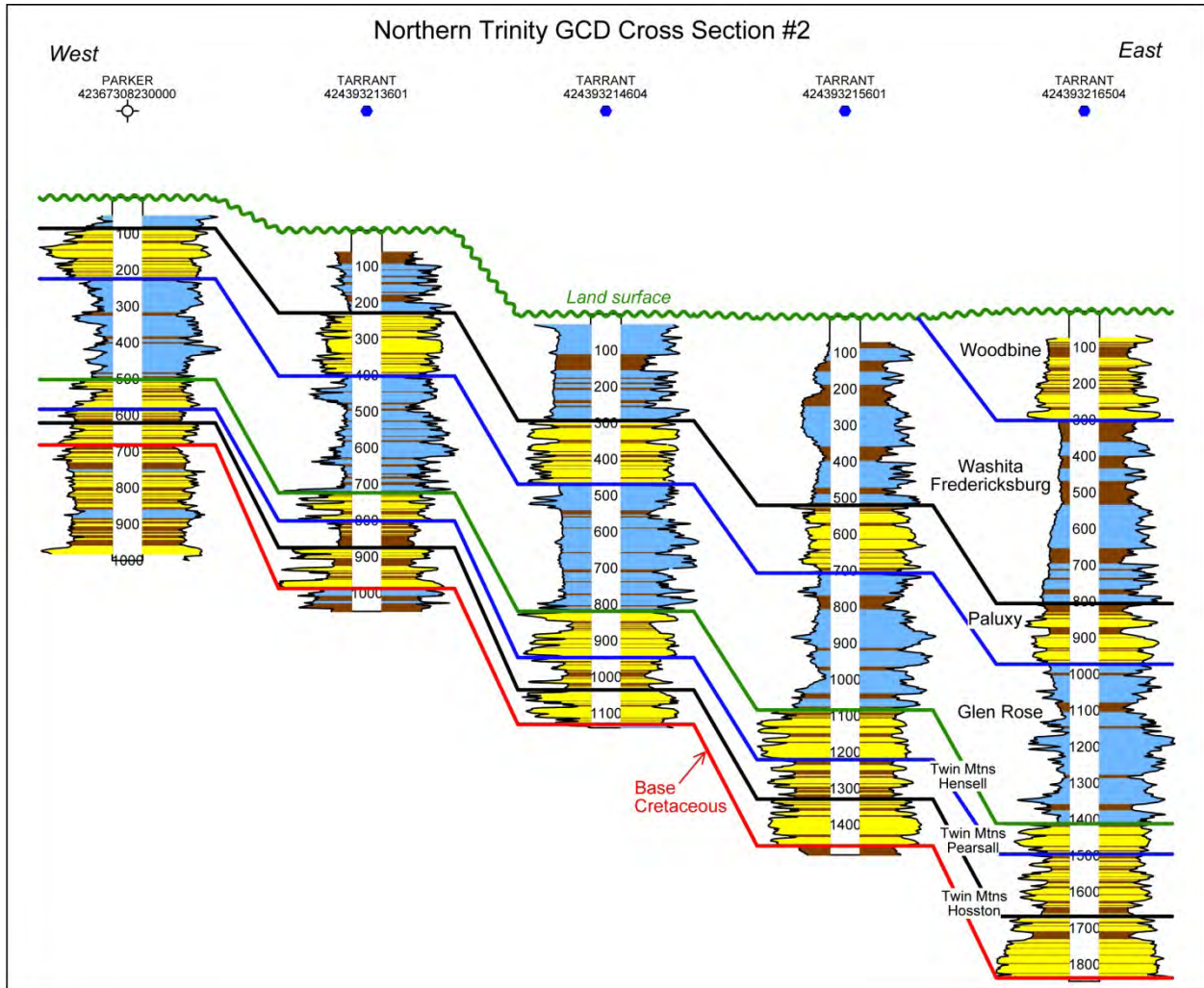
yellow = greater than 50 percent sandstone, blue = greater than 50 percent limestone, brown = greater than 50 percent shale

Figure 4.1.50   Northern Trinity GCD digital cross section # 2 with stratigraphic layers and land surface shown as true depths relative to sea level.
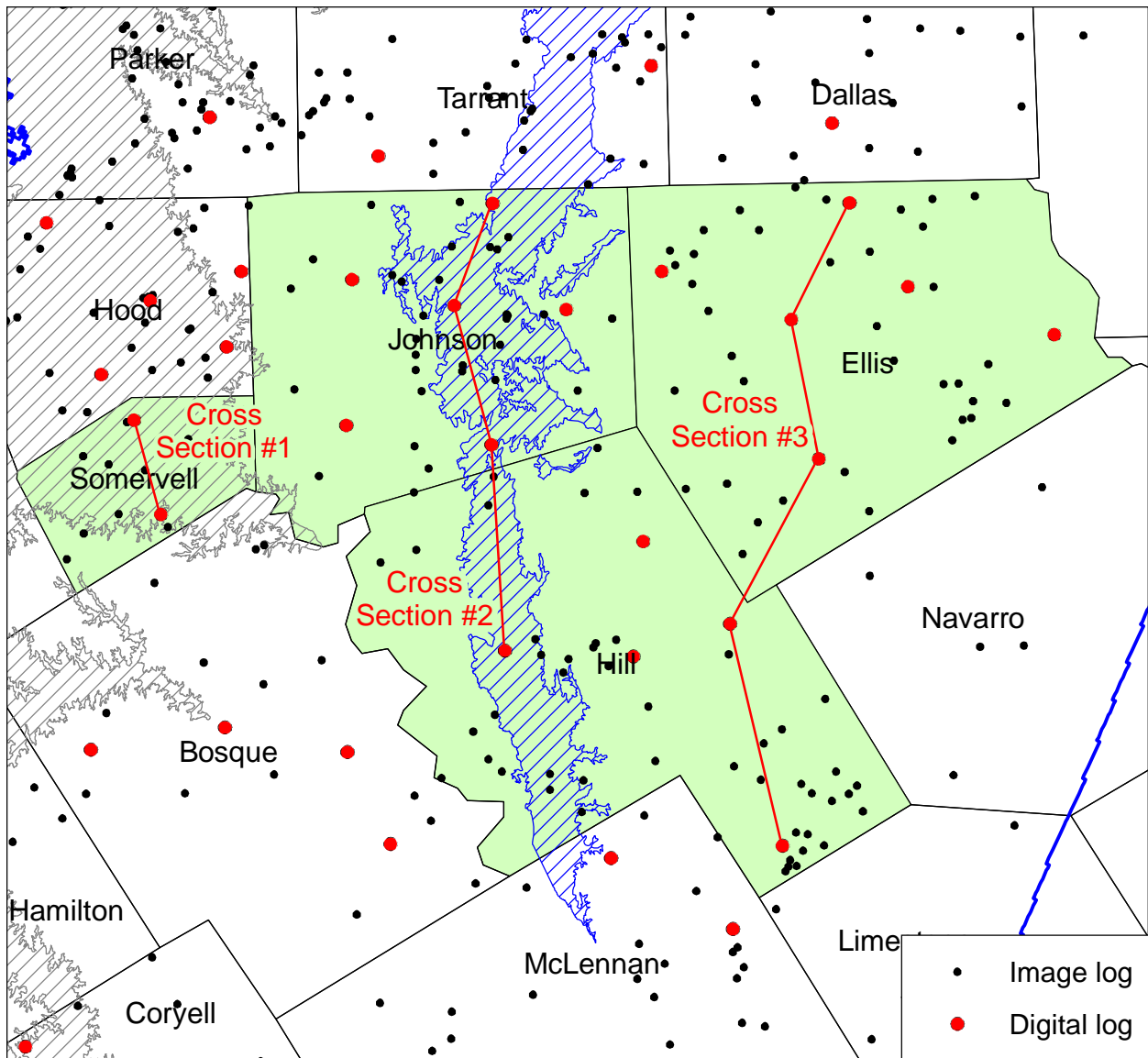
Figure 4.1.51 **The Prairielands GCD (green) showing the northern Trinity and Woodbine aquifer outcrops (grey and cross hatching, respectively), locations of geophysical well logs, and locations of cross sections shown in Figures 4.1.52 and 4.1.54.**

yellow = greater than 50 percent sandstone, blue = greater than 50 percent limestone,
brown = greater than 50 percent shale
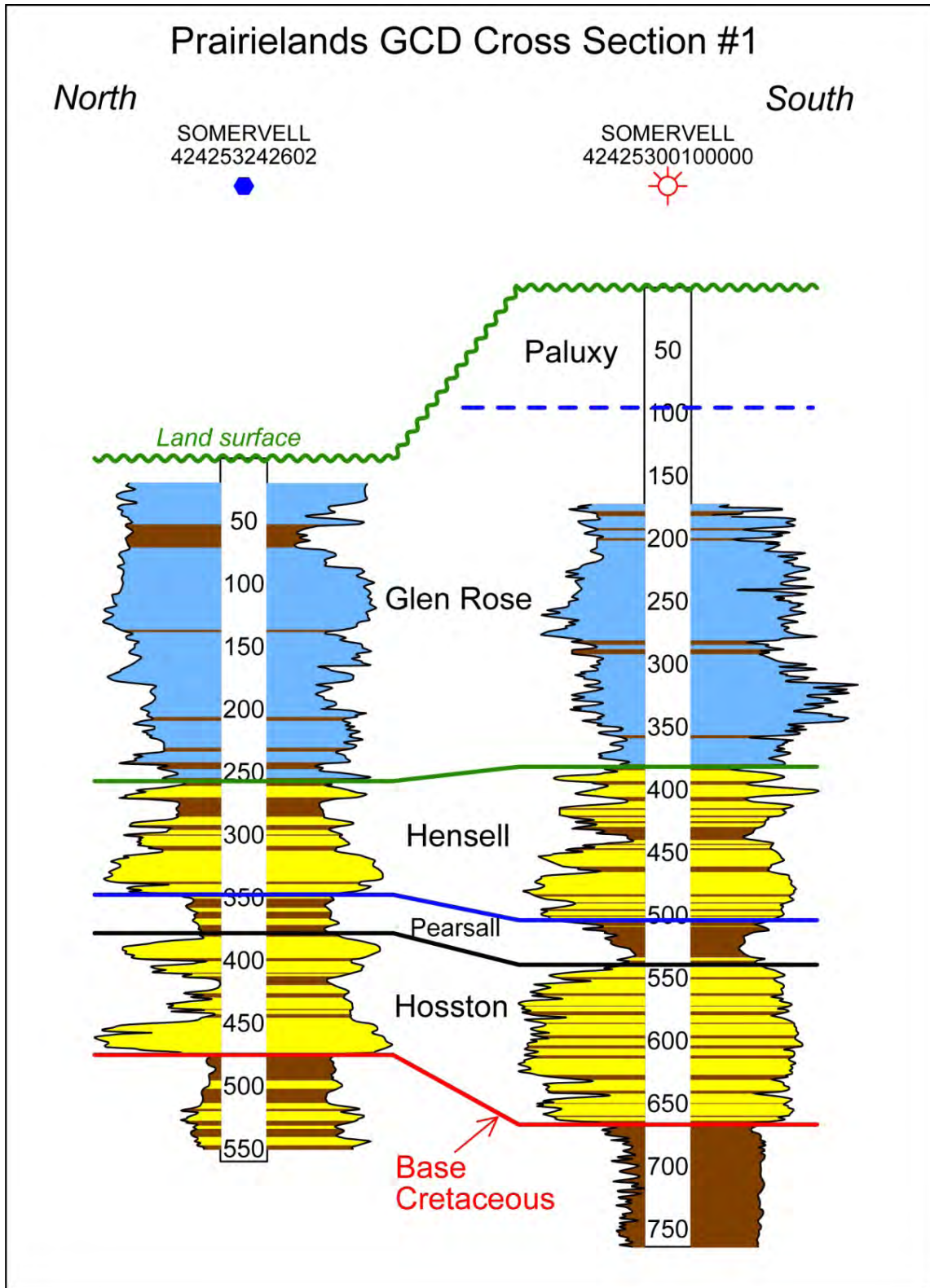
Figure 4.1.52   Prairielands GCD digital cross section # 1 with stratigraphic layers and land surface shown as true depths relative to sea level.
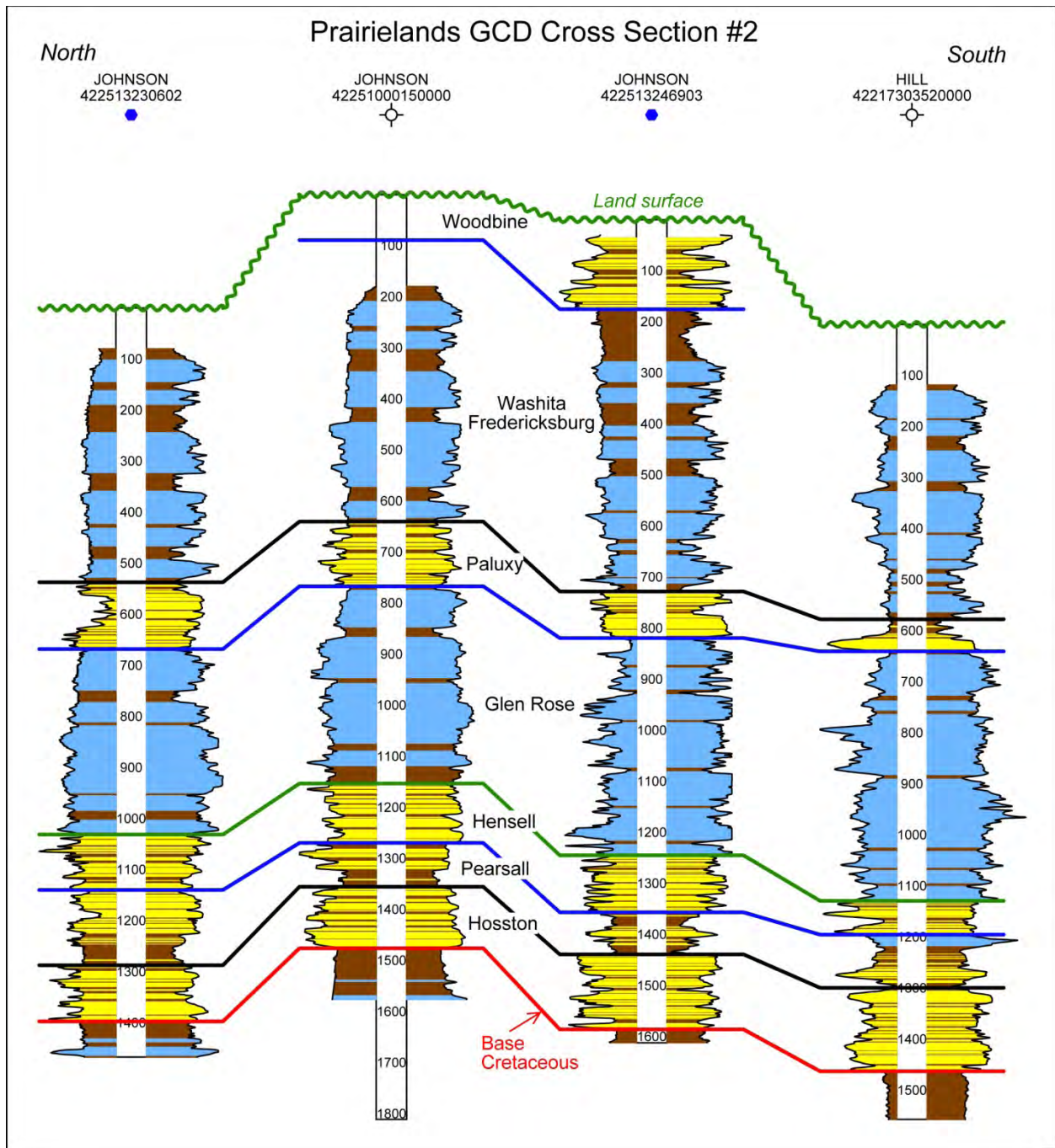
yellow = greater than 50 percent sandstone, blue = greater than 50 percent limestone, brown = greater than 50 percent shale

Figure 4.1.53   Prairielands GCD digital cross section # 2 with stratigraphic layers and land surface shown as true depths relative to sea level.
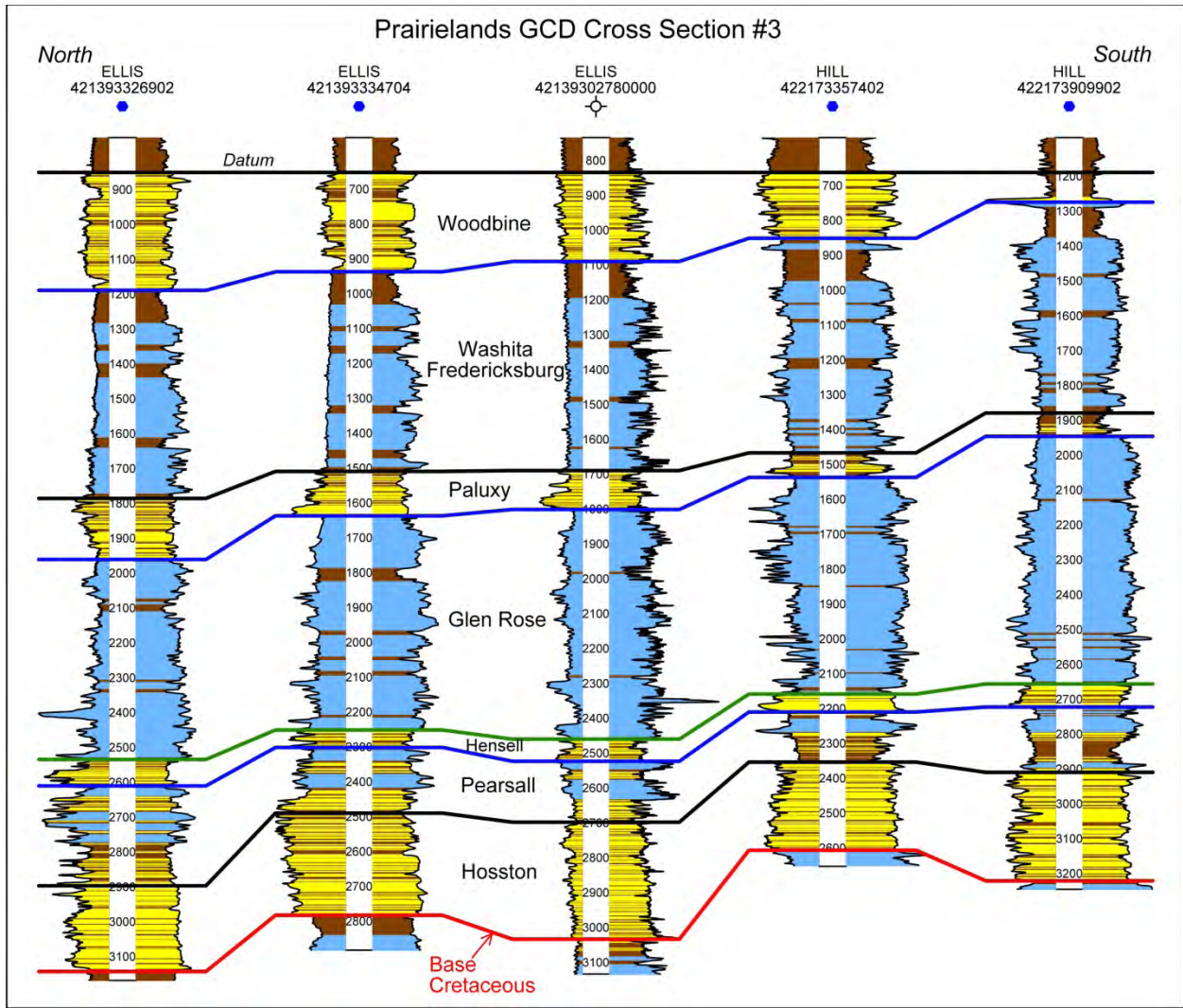
yellow = greater than 50 percent sandstone, blue = greater than 50 percent limestone, brown = greater than 50 percent shale

Figure 4.1.54   Prairielands GCD digital cross section # 3 with stratigraphic layers flattened on the top of the Woodbine Aquifer (datum), and so true elevations relative to sea level are not shown.

4.2   Aquifer Hydraulic Properties

This section discusses the collection and analysis of aquifer test data and the development of a conceptual geohydrostratigraphic (GHS) model for estimating aquifer hydraulic properties. The GHS model combines depositional and lithological information from Section 4.1 with the aquifer test information in this section to provide a framework for estimating hydraulic properties across the seven model layers representing the Woodbine Aquifer, Washita/Fredericksburg groups, and Trinity Aquifer. The GHS model was used to provide an initial set of aquifer parameters for model calibration and to guide the adjustment of aquifer parameters during model calibration.

4.2.1   Aquifer Flow Concepts and Terminology

The construction of a GHS model required the integration of depositional, lithological, and hydraulic data and concepts. Section 4.1 introduced and provided a foundation for understanding the key concepts and terminology associated with depositional, lithological, and hydraulic information and data. The purpose of this subsection is to introduce several important terms and concepts associated with groundwater hydrology.

4.2.1.1   Horizontal Hydraulic Conductivity and Transmissivity

Hydraulic conductivity, symbolically represented as "K", is a property of an aquifer that describes the ease with which a fluid (usually water) can move through pore spaces or fractures. It depends on the pore structure of the aquifer deposits and on the degree of saturation, and on the density and viscosity of the fluid. Hydraulic conductivity has units with dimensions of length per time (e.g., feet per day).

In the mid-1800s, the French engineer Henry Darcy successfully quantified several factors controlling groundwater movement. These factors are expressed in an equation commonly known as Darcy's Law (Freeze and Cherry, 1979):

$$Q = -KA\frac{dh}{dl} \qquad (4.2.1)$$

where:

Q = discharge (volume of water per time)

K = hydraulic conductivity (volume of water per area per time)

A = cross-sectional area (at right angle to the groundwater flow direction)

dh/dl = hydraulic gradient (change of water-level expressed as hydraulic head per unit

distance)

The hydraulic gradient term in Darcy's equation can be thought of as the slope of the water table

(which is the change of the water pressure) divided by the distance over which that change takes

place. Darcy's equation is the principal equation solved by groundwater models to predict the

direction and magnitude of groundwater flow.

For many practical problems in water resources, transmissivity is a term often used by drillers

and engineers. Transmissivity is the aquifer parameter used to describe the transmissive

properties of the aquifer at a given location. Transmissivity is calculated by multiplying the

saturated thickness of the aquifer by the hydraulic conductivity (Freeze and Cherry, 1979):

$$T = Kb \tag{4.2.2}$$

where:

T = transmissivity (volume of water per width per time)

b = thickness of the aquifer (length)

K= hydraulic conductivity (volume of water per area per time)

Two terms commonly used to describe the spatial variability in an aquifer's hydraulic parameters

are homogeneous and heterogeneous. Homogeneous aquifers are those considered to have

similar hydraulic conductivity distributions throughout the entire aquifer and to be generally void

of large scale patterns or trends in the magnitude of their hydraulic conductivity values.

Typically, a homogeneous aquifer is characterized by a single depositional system (see

Section 4.1). Heterogeneous aquifers are those considered to have variable hydraulic

conductivity distributions across their domain. Typically, aquifers characterized by significant

spatial variability contain sediments deposited by multiple depositional environments.

4.2.1.2   Vertical Hydraulic Conductivity and Vertical Anisotropy

In circumstances where the value of hydraulic conductivity is dependent on direction, the

hydraulic conductivity is anisotropic. In most aquifers, the vertical hydraulic conductivity is less

than the horizontal hydraulic conductivity. Vertical anisotropy is caused mainly by bedding

planes and laminae (small layering) within a sequence of sediment layers but may also be

affected by fractures and sedimentary structures. Vertical anisotropy is often represented as the

ratio of horizontal hydraulic conductivity (K_h) to vertical hydraulic conductivity (K_v), or K_h/K_v.

Vertical anisotropy ratios of hydraulic conductivity measured on core samples are typically on the order of 2:1 to 10:1. At the field scale, vertical anisotropic ratios of conductivity in layered geologic media may be at as large as 100:1 or greater (Maidment, 1992). Many of the GAM models have vertical anisotropy values for major aquifers in the range of 10:1 to 10,000:1.

4.2.1.3   Scale-Dependency of Hydraulic Conductivity Measurements

Numerous studies (Rovey and Cherkauer, 1995; Bradbury and Muldoon, 1990; Keller and others, 1986; Schulze-Makuch and others, 1999) demonstrate that measured hydraulic conductivity values are a function of the sample size of the measurement. In particular, these researchers discovered that hydraulic conductivity values tend to increase as measurement scale increases. Figure 4.2.1 illustrates an example of the scale-dependency of hydraulic conductivity measurements. The figure shows that as the size of the aquifer sample becomes larger, the estimate of its hydraulic conductivity inferred either through direct measurements or numerical modeling increases. In Figure 4.2.1, the data show that over a four-order-of-magnitude scale of measurement (from 0.1 to 10,000 meters), the geometric mean of the measured hydraulic conductivity increases from 0.01 meters per day to more than 1,000 meters per day. Based on evidence assembled from 39 different aquifers, Schulze-Makuchk and others (1999) demonstrate that the relationship of hydraulic conductivity to the scale of measurement is a function of the type of fluid flow present in the medium (i.e., fractured, porous media, conduit) and the degree of heterogeneity in the medium. Based on their data, Schulze-Makuch and others (1999) discovered that measured hydraulic conductivity increases by about a factor of ten with each order of magnitude increase in the scale of measurement.

The task of inferring regional hydraulic conductivity for large aquifers, such as the northern Trinity Aquifer, has been declared "among the most significant challenges in basin hydrology" by Bethke (1989). Dagan (1986) emphasizes in his classic paper of scale dependence that, in order to properly model groundwater flow, the scale of both the measurement and analysis of field data must be considered. In short, scale dependence of hydraulic conductivity has profound implications for data acquisition, and the collection of hydraulic data for the development of computer models for simulating regional groundwater flow. As illustrated in Figure 4.2.1, the best available data set for a estimating hydraulic conductivity at the regional aquifer scale is through the analysis of aquifer pumping tests.

4.2.1.4   Scale Dependent Heterogeneity

With regard to construction of a GHS model for estimating aquifer hydraulic properties, the hierarchical concept of heterogeneity developed by petroleum geologists and engineers is relevant. They recognize four scales of heterogeneity, which are: microscopic, mesoscopic, macroscopic, and megascopic (Alpay, 1972). Megascopic heterogeneity is of primary importance to the development of regional groundwater availability models. Megascopic heterogeneity is a product of variability across depositional systems and is reflected as field-wide differences in effective properties at the scale of several thousand feet or more (Tyler and Finley, 1991).

4.2.1.5   Aquifer Pumping Tests and Specific Capacity Tests

An aquifer pumping test is conducted by pumping groundwater from a well completed in the aquifer and observing the aquifer's "response" by measuring drawdown in the well or in nearby wells. Drawdown can be defined as the change in water level or water elevation (hydraulic head) from a baseline water level measured at some earlier time. For aquifer pumping tests, drawdown is measured from the observed water level prior to the start of pumping. The most common type of aquifer pumping test is a constant rate test in which the aquifer is pumped at a steady rate and the data collection activities focus on collecting drawdown values over time. One of the largest sets of existing aquifer pumping test data in the state is managed by the TCEQ Public Water Supply (PWS) program. The TCEQ has amassed numerous aquifer pumping tests because a long-term aquifer pumping test of about 36 hours is required by statute to demonstrate the production capacity of a public water supply well.

The approach for analyzing an aquifer pumping test and the representativeness of the resulting calculated transmissivity value depend on both the complexity of the aquifer hydrogeology and the design of the aquifer pumping test. In general, the uncertainty and error with estimating aquifer hydraulic parameters increases with increased spatial heterogeneity in the aquifer, increased cross-flow communication among adjacent aquifers, and the degree of penetration of the well screen (i.e., the fraction of the aquifer thickness contacted by the screen). Most analytical methods, such as the Theis solution (Theis, 1935) and the Cooper-Jacob solution (Cooper and Jacob, 1946) are based on the assumption of radial flow in a homogeneous aquifer. In order for ideal radial flow to occur, the well needs to fully penetrate the aquifer and the aquifer needs to be fairly homogeneous.

Specific capacity is a measure of the productivity of a well and is calculated by dividing the total pumping rate by the drawdown (Freeze and Cherry, 1979):

$$S_C = \frac{Q}{s}$$ (4.2.3)

where:

      S_C = specific capacity (volume of water per time per length)

      Q = pumping rate (volume of water per time)

      s = drawdown in the well (length)

Specific capacity is generally reported as gallons per minute per foot. However, by converting to consistent units, specific capacity can be expressed as square feet per minute. Water-well drillers have historically used specific capacity to quantify the productivity of a well. Several researchers have shown that there is a theoretical linear relationship between specific capacity and transmissivity. However, in practical applications, caution is needed when using specific capacity values to estimate transmissivity. Specific capacity does not adequately account for potentially important field variables such as the condition of the well, the size of the well, and the partial penetration of the well into an aquifer.

4.2.2 Description of a Geohydrostratigraphic (GHS) Model

The goal of a GHS model is to create a framework for estimating the hydraulic conductivity and transmissivity field for the entire aquifer system based on principals and ideas independent of the process of groundwater modeling. That is, a GHS model should allow the groundwater availability model to be calibrated within a framework consistent with the conceptualization of the aquifer hydrostratigraphy and constrained to avoid unrealistic parameter values or combinations of parameter values. In order to build a GHS model, multiple types of data are necessary: stratigraphy, lithology, depositional environments/systems, and measurements of aquifer hydraulic properties.

- Stratigraphy consists of the surface boundaries (i.e., the tops and bottoms) for the geological formations and aquifers of interest. The seven aquifers and formations of interest for this study are, from oldest to youngest, the Hosston Aquifer, Pearsall Formation, Hensell Aquifer, Glen Rose Formation, Paluxy Aquifer, Washita/Fredericksburg groups, and Woodbine Aquifer.

- Lithology consists of continuous profiles of the same sediment type (i.e., sand, shale, and limestone) and their thicknesses (or beds) at each geophysical log location.

- Depositional Environments/Systems consist of a series of system maps (see Section 4.1.8) that describes the type of environment (fluvial versus marine) and the type of deposit (sandstone versus shale) that comprise the aquifer or formation. Thus, facies maps can be used as secondary data in developing maps of lithology for an aquifer or formation.

- Measurements of hydraulic properties include results from any aquifer pumping tests performed on the aquifer or formation to determine transmissivity or hydraulic conductivity.

The process of building a GHS model involves developing relationships among the different data sets such that hydraulic properties can be associated to each type of lithology that exists within each aquifer or formation. Once this has been accomplished, every continuous profile of lithology can be transformed via the GHS model to a continuous profile of hydraulic properties. This transformation allows assignment of hydraulic properties on the finer scale of the lithology data, rather than at the coarser scale of the aquifer pumping test data. Hence, if the 988 geophysical logs analyzed for lithology (see Section 4.1) intersect all seven aquifers/formations, a continuous profile of hydraulic properties at each geophysical log location would produce 5,600 locations where hydraulic properties are estimated. Examples of the use of this procedure to estimate hydraulic properties from geophysical and driller's logs can be found in Young and others (2003, 2009), Young and Budge (2002), and LBG Guyton Associates and INTERA (2012).

Previous GHS models developed in Texas have ranged from the size of an Air Force base (Young and Tu, 2001), to a single county (LBG-Guyton Associates and INTERA, 2012), to a regional groundwater flow system (Young and Kelley, 2006). The success of GHS models hinges on the quality of the hydrogeologic data. The two most important types of data required are lithology and transmissivity values from aquifer pumping tests.

The primary process of developing a GHS model is to use well locations where both lithology and transmissivity of an aquifer are known and, based on that data, develop a model capable of estimating aquifer transmissivity based on knowledge of lithology alone. The objective in

developing a GHS model is to enable the estimation of hydraulic properties, such as aquifer transmissivity, for portions of an aquifer where little or no aquifer pumping test data exist using available lithology data. Through this process, entire depositional systems within aquifers or formations can be parameterized with lithologic data constrained by available aquifer pumping test data. Development of a GHS model requires the following:

1. Development of transmissivity values from aquifer pumping tests.
2. Development of lithologic profiles from sand, shale, and limestone data.
3. Assignment of hydraulic properties to each lithology type based on good aquifer pumping tests.
4. Development of continuous profiles of hydraulic conductivity at all points where lithology is defined.
5. Create transmissivity maps for each aquifer or formation.
6. Evaluate the GHS model results using transmissivity values derived from specific capacity tests.
7. Discuss the approach for using the GHS model as a framework for development of the numerical groundwater model.

4.2.3 Transmissivity Values from Aquifer Pumping Test Data

The primary hydraulic information required for development of the GHS model is aquifer pumping test data. Ideally, these tests need to be well documented with respect to the well construction and completion, as well as the time-drawdown and time-pumping rate data associated with the test. As discussed below, a high priority was placed on finding and evaluating aquifer pumping tests based on these criteria.

4.2.3.1 Published Transmissivity Values

The search for transmissivity values included reviewing the relatively large amount of historical hydrogeological work performed by state and federal agencies. Among notable sources reviewed and providing useful transmissivity values are Klemt and others (1975), Brune and Duffin (1983), Nordstrom (1987), Dutton and others (1996), and Christian and Wuerch (2012). Approximately 200 transmissivity values were found in published reports. The most comprehensive and useful report for transmissivity data was Myers (1969). Myers (1969) provides well-screen information, time-drawdown data for the aquifer pumping test, and

graphically shows how the analysis was performed on the drawdown data to calculate transmissivity values.

4.2.3.2   Aquifer Pumping Test Elapsed Time-Drawdown Data

In addition to published literature data, the primary source of data for the aquifer pumping test analyses is the data files prepared from PWS aquifer pumping test data in GMA 8 described by Young and others (2012). Young and others (2012) provide information from approximately 900 aquifer pumping tests that were assembled from the paper files from the TCEQ's PWS Program. The project was funded by the TWDB in anticipation of improving the GAM for the northern Trinity and Woodbine aquifers. The TCEQ has a repository of aquifer pumping test data as part of its enforcement authority over the Texas public water system's compliance with the Safe Drinking Water Act and its amendments. As part of this program, TCEQ maintains an electronic database and a set of paper records to manage information regarding the location, construction, borelog lithology, and data from a 36-hour aquifer pumping tests for each public supply well.

After analyses of the PWS aquifer pumping test data were performed, areas where data were sparse or non-existent were identified. These areas included the following counties: Bell, Bosque, Brown, Burnet, Callahan, Comanche, Coryell, Dallas, Delta, Eastland, Falls, Hamilton, Hill, Hopkins, Hunt, Johnson, Kaufman, Lamar, Lampasas, Limestone, McLennan, Milam, Mills, Navarro, Red River, Rockwall, Somervell, Tarrant, and Williamson. Two additional sources of data not contained in the GMA 8 PWS data set were investigated. These were aquifer pumping tests in TWDB well records and PWSs located in the counties with sparse data. A search of approximately 7,400 TWDB well records for wells completed in the northern Trinity or Woodbine aquifers in the selected counties yielded 62 aquifer pumping test records that had been scanned and archived in PDF format. The data from each of these aquifer pumping tests were transcribed and used in the pumping test analyses.

A contact list was developed consisting of 43 PWS entities located in the counties with sparse data and having wells completed in the northern Trinity or Woodbine aquifers not previously represented in the GMA 8 PWS data set. Out of these 43 PWS entities, 14 were no longer in existence. The remaining 29 entities were contacted and requests for aquifer pumping test data were made. Three tests were provided as a result of this effort; however, none were determined

to be useful for analysis based on a lack of variation in pumping level data throughout the test. Table 4.2.1 documents the contacts and responses from the 29 entities.

The third source of aquifer pumping test information is from GCDs located in GMA 8. The search through GCD files produced approximately 40 aquifer pumping tests. Most of the aquifer pumping tests found in the scanned files had already been identified through the search of the TCEQ and TWDB databases. Approximately 15 new aquifer pumping tests were used from the GCD data.

The aquifer pumping test data for each test was transferred into an elapsed time-drawdown file. The elapsed time-drawdown file format was created for this project to facilitate data analysis and visualization. A time-consuming part of creating the elapsed time-drawdown files was determining the start and end of pumping. After the start and end times of pumping were chosen, the pumping period data were selected and elapsed time in minutes since pumping began was calculated for each record of the pumping period. The drawdown was calculated as the difference in the pumping water level and the static water level. Table 4.2.2 is an example of an elapsed time-drawdown file.

The first three columns in the elapsed time-drawdown file provide the elapsed time since the start of pumping, the change in the water level, and the measured pumping rate. The fourth column of data is a Boolean input to indicate whether or not to include the data point in the calculation of transmissivity. As part of the quality check and evaluation of the suitability of the data for calculating a transmissivity value, the data were graphically displayed using plots like those shown in Figure 4.2.2.

4.2.4 *Analysis of Aquifer Pumping Test Elapsed Time-Drawdown Data*

The aquifer pumping test data were analyzed using the Cooper-Jacob approximation to the Theis nonequilibrium well equation (Cooper and Jacob, 1946). After well bore storage effects have dissipated based on the calculated threshold times provided by Papadopulos and Cooper (1967), the Cooper-Jacob analysis is applied. This analysis method involves fitting a logarithmic model to the elapsed time-drawdown data for the test, selecting drawdown points one log cycle apart, and applying the equation:

$$T = \frac{35.3Q}{\Delta s} \tag{4.2.4}$$

where

T = Transmissivity (square feet per day)

Q = Flow (gallons per minute)

Δs = Change in drawdown over one log cycle (feet)

The green line in Figure 4.2.2b is the straight-line fit and the red dots on the green line mark the location where change in drawdown was calculated. In addition to the data plots, an analysis data record for each test was prepared with the following fields:

- Test identification number (PWS source ID-test# or State Well Number).

- Data point count.

- Average flow rate in the portion of the test selected for Cooper-Jacob analysis.

- Calculated transmissivity.

- Slope, intercept, and drawdown points used in the Cooper-Jacob fit.

- R-squared value of the data as compared to the Cooper-Jacob fit.

- First and last flow, drawdown, and specific capacity in the test.

After the initial plotting and analysis of the elapsed time-drawdown files, arithmetic and semilog plots were visually inspected to detect any remaining errors in the elapsed time-drawdown file preparation process. These were corrected and the analysis was performed again on the corrected data. The plots and analysis data were then evaluated with respect to usefulness of the test data to the Cooper-Jacob analysis. The usefulness was assigned a category from 1 to 5 in order of increasing usefulness. The descriptions of the test analysis categories are:

- *Category 1*: Aquifer pumping test data are not useful for analysis - there is no meaningful change in water level, or the water level change does not exhibit a useful trend.

- *Category 2*: Aquifer pumping test data are not useful for analysis - flow rate is not relatively constant over a significant portion of the test.

- *Category 3*: Aquifer pumping test data are useful, but significant adjustment to the plotted semilog data was necessary. Examples of cases where data would require adjustment are: if the aquifer pumping test was a step test and only a portion of the data should be used; if recovery data was improperly included in the semilog drawdown curve; if only a portion of the semilog data appears valid due to a flow rate change.

- *Category 4*: Aquifer pumping test data are useful, and only a small adjustment in the plotted semilog data was necessary.

- *Category 5*: Aquifer pumping test data are useful, no adjustment to the plotted semilog data was necessary.

Only analysis categories 3, 4, and 5 were considered useful for Cooper-Jacob analysis. Once the data were categorized, the elapsed time-drawdown files in categories 3, 4, and 5 were adjusted as necessary to obtain the best fit to the data for the Cooper-Jacob analysis. All of the category 3 and 4 data were then re-calculated and re-plotted. The completed analyses were compiled into a geo-referenced table for use in other aspects of the conceptual model development.

Appendix D contains plots for approximately 820 aquifer pumping tests. The data for these tests were assembled from the TCEQ PWS data files, the TWDB groundwater data, and scanned pumping test data from GCDs in GMA 8. Out of 820 aquifer pumping tests, only 430 tests are considered to have credible transmissivity values calculated from the elapsed time-drawdown file. However, out of these 430 good aquifer pumping tests, about 90 are screened either above the Woodbine Aquifer or below the base of the Hosston Aquifer. Thus, 340 of the good aquifer pumping tests from the PWS wells are located in the northern Trinity or Woodbine aquifers. The elapsed time-drawdown files for all 820 aquifer pumping tests are included in the attached geodatabase (see Appendix J).

A review of the plots and the corresponding statistics for the 340 good aquifer pumping tests shows that the vast majority of the tests are very high quality. The average number of data points used for each Cooper-Jacob fit is more than 25 and the average coefficient of determination (R^2), which is a measure of linearity, of all of the fits is greater than 0.97. In addition, all of the wells have known screened elevations. In addition to the transmissivity values obtained from the 340 aquifer pumping tests, an additional 160 transmissivity values were obtained from the literature search. Table 4.2.3 provides the breakdown of the 500 transmissivity values by aquifer/formation.

Figure 4.2.3 shows the spatial distribution and source for the 500 transmissivity values. These data are concentrated in about 13 counties that cover the central and southern portion of the study area. The least amount of coverage occurs in the northeast and southwest portions of the study area. Each aquifer pumping test was assigned to the aquifer or formation that intersects the

largest amount of well screen. Figures 4.2.4 through 4.2.10 show the wells assigned to each aquifer or formation unit and their transmissivity values. In some areas where data are clustered, relatively large differences in transmissivity values occurs.

Also, shown on Figures 4.2.4 through 4.2.10 are the depositional systems for the aquifer/formation as presented in Section 4.1.8. A depositional system was not developed for the Washita/Fredericksburg groups because it consists primarily of carbonate without significant sandstone. The Hosston Aquifer in the study area is composed of a single depositional system – coastal plain fluvial sandstone.

Table 4.2.4 provides the mean and standard deviation for the calculated transmissivity values for each aquifer/formation. Despite a wide range of sampling locations, four of the seven aquifers/formations have mean transmissivity values within about 10 percent of each other. The information in Table 4.2.4 supports the following observations:

- The most transmissive aquifer is the Hosston Aquifer with a mean transmissivity of 841 square feet per day.

- The least transmissive aquifer is the Paluxy Aquifer with a mean transmissivity of 289 square feet per day.

- The Woodbine Aquifer, Washita/Fredericksburg group, Hensell Aquifer, and Pearsall Formation have very similar mean transmissivity values which are within 10 percent of 650 square feet per day.

- A comparison of the mean value and standard deviation values for transmissivities indicates that there is considerable overlap in the transmissive properties for the seven aquifers/formations.

4.2.5 *Sand, Shale, and Limestone Profiles from Lithologic Analyses*

As described in Section 4.1, 1,302 geophysical logs were analyzed to develop tops and bottoms for the Hosston Aquifer, Pearsall Formation, Hensell Aquifer, Glen Rose Formation, Paluxy Aquifer, and Woodbine Aquifer. Based upon log quality, 988 geophysical logs were also analyzed to generate continuous profiles of sand, shale, and limestone. Figure 4.2.11 shows the locations of the geophysical logs used for this lithologic analysis. For each aquifer/formation, Table 4.2.5 provides the number of geophysical logs analyzed for lithology that include the

aquifer/formation. Furthermore, depositional systems for each aquifer and formation were developed and mapped (see Section 4.1.8).

In order to more precisely define differences in the characteristics of the strata that comprise the seven aquifers and formations in the GHS model, a 10 litho-unit classification system was developed for describing the arrangement and thicknesses of the sands, shales, and limestone that comprise each aquifer or formation. The 10 litho-unit system, shown on Table 4.2.6, was tailored after the 8 litho-unit classification system used by Young and Kelley (2006) to describe the lithology of the Chicot and Evangeline aquifers of the Texas Gulf Coast.

For this study, 10 litho-units were constructed based on a minimum limit of 4 feet for both sands and shales. This minimum limit was selected based on professional judgment after a statistical evaluation of the distribution of bed thicknesses. Values of 4, 6, and 8 feet were considered. Four feet was selected because it provided the best statistical fit and due to the need to characterize aquifer layers that were sometimes less than 20-feet thick. All profiles that consisted of continuous sands were translated into one of four litho-units: 4 to 8-foot sand, 8 to 14-foot sand, 14 to 25-foot sand, and greater than 25-foot sand. Any sand contained in a bed less than 4-feet thick was lumped with shales/clays to create a sand-clay mixture. As shown in Table 4.2.6, the sand percentages used to create the sand-clay mixtures were 10 to 30 percent, 30 to 50 percent, and 50 to 80 percent sand.

One reason for developing litho-units was to facilitate the assignment of hydraulic properties beyond the basic lithologic descriptions of sand, shale, and limestone. Numerous studies (Folk, 1980; Carmen, 1939; Lambe and Whitman, 1969; Masch and Denny, 1966; Cade and others, 1994) show that lithology can be a useful and reliable estimator of hydraulic conductivity and other aquifer hydraulic properties. With other factors being equal, in a mixture of sands and clays, the hydraulic conductivity of a deposit will increase with increasing percentage of sand, increasing average size of the sand grains, and as a result of the sorting of the deposits.

At the macroscopic scale, important factors in determining the effective properties of an aquifer are both the amount of sand and the connectivity among the different sand bodies (Fogg, 1986; Fogg and Kreitler, 1982). The potential for connectivity among aquifer sand bodies can be shown to be a function of the distribution of their sizes and their orientation. A consideration that should affect the ability of one sand deposit to connect with another sand deposit is its

thickness. As discussed in Section 4.2.1.3, the factors affecting flow at the scale of aquifer pumping tests and regional flow systems are heavily weighted to the factors affecting the interconnection among the many deposits.

Two additional factors affecting flow at different scales are depositional system and thickness of litho-units within a depositional system. Both of these factors were used by Hall and Turk (1975) to understand the hydrogeological factors controlling flow in the northern Trinity Aquifer. Based on their work in the Hosston Aquifer in north Texas, Hall and Turk (1975) concluded that delineation of major depositional systems and their lithology are useful in predicting regional aquifer properties such as hydraulic conductivity distribution and vertical anisotropy.

The GHS developed for the northern Trinity and Woodbine aquifers is composed of 21 different depositional systems. To assist in quantifying the variability in lithology between the depositional systems, they were evaluated in terms of their lithologic composition based on 10 litho-units. This evaluation is shown graphically in Figures 4.2.12 and 4.2.13. To perform this analysis, a computer program was developed to implement the rules associated with constructing the 10 litho-units described in Table 4.2.6. The computer program partitions the continuous lithologic profile within a given aquifer or formation and calculates the occurrence of each of the 10 litho-units within a single depositional system. The result is quantification of the percent of each litho-unit that composes an individual depositional system within an aquifer or formation. A minimum thickness of 4 feet was used to force a change in litho-unit as the lithologic profile was being analyzed.

Figures 4.2.12 and 4.2.13 show the depositional systems that contain more than 50 percent sand and 50 percent shale, respectively. The depositional systems are arranged by aquifer or formation. The value for the average hydraulic conductivity for each litho-unit is discussed in the next section. The distributions in Figures 4.2.12 and 4.2.13 show significant differences, as well as some similarities, among some of the depositional systems. To help illustrate the difference percentages among the litho-units, the percentage scale on the x-axis is not the same among the different plots. Figure 4.2.14 shows the percentages for only the major litho-units (i.e., sands, sand-clay mixtures, and limestone and shale) (see Table 4.2.6). This figure shows that there are relatively similar distributions of sand and shale among most of the major sandy

depositional systems, which are clastic deposits composed primarily of silica. The Hosston
Aquifer averages about 10 percent more sand than any other aquifer or formation.

4.2.6 Assignment of Hydraulic Conductivity Values to Litho-Units

The process of assigning a hydraulic conductivity value to each litho-unit involved the solution
of a suite of equations containing the thickness of the litho-units as input and their hydraulic
conductivity values as outputs. Although conceptually simple, there are several potential
challenges associated with implementation of a process of assigning a hydraulic conductivity
value to each litho-unit. These are discussed in the following description of the process used to
assign hydraulic conductivity.

The locations of the transmissivity values used for the analyses are those shown in Figure 4.2.3.
Each of the 500 transmissivity values was assigned to a single aquifer or formation based on
where the majority of the well is screened. Because the geophysical log locations in
Figure 4.2.11 are not at the same location as the water well locations with transmissivity data, the
thicknesses of the litho-units were interpolated to the water well locations. The interpolation of
the litho-units was performed for each aquifer and formation. The average distance between a
water well and its closest geophysical log location is about 1.5 miles.

4.2.6.1   Estimating Hydraulic Properties from Aquifer Pumping Tests

A typical approach to calculating hydraulic conductivity from an aquifer pumping test involves
dividing the estimated transmissivity value either by the total screened interval of the well or by
the total thickness of the aquifer. For the case where the well fully intersects the aquifer, a
calculation using either the well screen length or the aquifer thickness will yield the same result.
In the absence of detailed site information, the decision of how to convert transmissivity to
hydraulic conductivity is difficult when the well screen partially penetrates the aquifer.

Figure 4.2.15 illustrates some challenges associated with calculating hydraulic conductivity by
dividing the transmissivity by the length of the well screen. In this figure, groundwater flows
toward four different well screens in a layered aquifer consisting of two clay layers, a fine sand
layer, and a coarse sand layer. Well 1 partially penetrates the center region of the most
permeable aquifer zone. For Well 1, the calculated hydraulic conductivity (calculated by
division of transmissivity by the well screen length) will be significantly higher than the average
aquifer hydraulic conductivity because of (1) the contribution of water from above and below the

well screen and (2) pumping is occurring only in the most permeable portion of the aquifer.
Well 2 intersect the entire thickness of the aquifer's most permeable zone. For Well 2, the
calculated hydraulic conductivity will again be higher than the average due to the second reason
(i.e., the lower conductivity layers are ignored in the estimation). Well 3 penetrates a moderately
transmissive zone and a zone of low hydraulic conductivity in the aquifer. For Well 3, the
calculated hydraulic conductivity will underestimate the average hydraulic conductivity because
most of the well screen lies in zones of relatively low hydraulic conductivity. Well 4 intersects
all of the aquifer zones and will provide the best estimate of an average hydraulic conductivity
for the aquifer since all of the zones are considered in the pump test.

The potential importance of well screen length for estimating hydraulic conductivity from
transmissivity values was demonstrated by Young and Kelley (2006). Figure 4.2.16 shows that
the calculated hydraulic conductivity decreases as a function of screen length from values greater
than 200 feet per day for screen lengths less than 25 feet to values less than 20 feet per day for
screen lengths greater than 600 feet. This asymptotic-like relationship is expected because, as
the well screen length increases, the length approaches the total thickness of the aquifer. The
bias towards high hydraulic conductivity values for partially penetrating screens occurs because
short well screens tend to be placed preferentially in areas of high sand percentages and because
pumping a short well screen causes converging, not radial, flow toward the well.

Figure 4.2.17 shows the same type of sensitivity analysis performed for the current study.
Calculated hydraulic conductivities demonstrate the same sensitivity to screen length as in the
Young and Kelley (2006) study. The average calculated hydraulic conductivity for all aquifers
and formations is about 16 feet per day for a screen length interval of 0 to 50 feet and is about
3 feet per day for a screen length interval of greater than 200 feet.

Besides well screen length, two other factors were investigated as potential sources for bias in
estimating hydraulic conductivity from transmissivity. The first of these is the percentage of the
well screen that is in an aquifer or formation. This factor is of concern because, if the well is
screened across multiple aquifers and/or formations, then the calculated transmissivity at that
well is affected by the hydraulic properties of the non-targeted aquifer or formation. The second
factor is the percentage of the aquifer or formation that is screened. This factor is of concern
because, if only a small percentage is screened, the calculated transmissivity may not be

representative of the entire aquifer or formation thickness. The criteria in Table 4.2.7 were used to select wells for the analyses. These criteria were determined primarily through trial and error. When considering these criteria, the percent limits were balanced against the change in the number of available wells meeting the criteria.

4.2.6.2   Assignment of Hydraulic Conductivities

Young and Kelley (2006) demonstrated a successful approach for calculating hydraulic conductivity for two litho-units (sand and clay) in the Gulf Coast Aquifer using transmissivities from aquifer pumping tests. As part of their approach, they applied the following equation across the total interval of the well screen.

$$K_{GHS} = \frac{T}{Z_T} = \frac{(K_{sand}*Z_{sand}+K_{clay}*Z_{clay})}{Z_T} \qquad (4.2.5)$$

where:

K_{GHS} = hydraulic conductivity for the GHS model (feet per day)

T = total transmissivity (square feet per day)

Z_T = total thickness of well screen (feet)

K_{sand} = hydraulic conductivity of sand (feet per day)

Z_{sand} = sand thickness (feet)

K_{clay} = hydraulic conductivity of clay (feet per day)

Z_{clay} = clay thickness (feet)

Using Equation 4.2.5, the total length of sands and clays for each well equaled the total thickness of the well screen. Young and Kelley (2006) applied this approach to more than 100 wells in the Houston area and demonstrated a relatively good match between measured and simulated transmissivity for the sand litho-group in the Chicot and Evangeline aquifers.

For the current study, the approach of Young and Kelley (2006) was modified and expanded to accommodate the 10 litho-units described in Table 4.2.6. The calculations were implemented in Microsoft Excel. The hydraulic conductivity values for each litho-unit were adjusted manually with the goal of improving the match between K_{AQ} and K_{LITH}.

where:

- K_{AQ} represents the best estimate of hydraulic conductivity for the aquifer/formation calculated by dividing the Cooper-Jacob transmissivity by the average of the well screen interval and the aquifer thickness.

- K_{LITH} represents the best estimate of hydraulic conductivity based on the estimated hydraulic conductivity of each litho-unit at the geophysical log location, calculated as:

$$K_{LITH} = \frac{\sum_{i=1}^{10} K_i Z_i}{Z_T} \qquad (4.2.6)$$

where:

        i = index of litho-units

        K = hydraulic conductivity of litho-unit (feet per day)

        Z = thickness of litho-unit (feet)

The estimation of average hydraulic conductivity values for the different litho-units primarily consisted of adjusting their values and monitoring the improvement in the comparison between K_{LITH} and K_{AQ}. K_{AQ} was taken from the nearest well with an aquifer pumping test. Table 4.2.8 shows the comparisons for wells matching the well screen criteria given in Table 4.2.7. A set of litho-unit hydraulic conductivity values was considered acceptable if over 50 percent of the K_{LITH} - K_{AQ} pairs were within a factor of two of each other. An exact match to K_{AQ} could only be achieved if the number of matches between K_{AQ} and K_{LITH} was less than the number of litho-units, which is 10. Because there were many more matches than 10, an exact match was not possible. The set of hydraulic conductivities for the litho-units is not unique. However, in developing the hydraulic conductivity values for the litho-units, constraints were imposed to produce reasonable magnitudes and relative differences among the 10 litho-units.

In summary, the process can be summarized as:

1. Analyzed well logs and assigned depth intervals for each aquifer/formation.
2. Assigned litho-units within each aquifer/formation.
3. Estimated hydraulic conductivity for each litho-unit.
4. Calculated the transmissivity for each litho-unit as the product of the litho-unit thickness and the assigned litho-unit hydraulic conductivity. Summed the litho-unit transmissivities to obtain the total transmissivity for the aquifer/formation. Divided the total transmissivity by the aquifer/formation thickness to obtain K_{LITH}.

5. Compared K_{LITH} to K_{AQ}. If the difference was greater than a factor of two, adjusted the litho-unit hydraulic conductivity and recalculated until the difference between K_{LITH} and K_{AQ} was less than a factor of two.

Table 4.2.9 summarizes the resulting estimates of hydraulic conductivity for each litho-unit and aquifer/formation. These assigned estimates established a baseline hydraulic conductivity distribution for each aquifer/formation.

4.2.7 *Application and Refinement of the GHS Model*

In this section, spatially distributed hydraulic conductivity and transmissivity estimates generated using the GHS model are presented. In addition, the approach for using the GHS model to estimate values of vertical hydraulic conductivity and specific storage during calibration of the numerical model is presented.

4.2.7.1   Hydraulic Conductivity Fields for Aquifers/Formations

Figures 4.2.18 through 4.2.24 provide maps of the estimated hydraulic conductivity field for the Woodbine Aquifer, Washita/Fredericksburg groups, Paluxy Aquifer, Glen Rose Formation, Hensell Aquifer, Pearsall Formation, and Hosston Aquifer, respectively. The maps were generated by:

1. Calculating an average hydraulic conductivity for each aquifer/formation at each geophysical log location.
2. Interpolating the average hydraulic conductivity at each geophysical well location using kriging.

Table 4.2.10 provides a statistical summary of the hydraulic conductivity field for each aquifer/formation. These results show that the Hosston Aquifer is the most permeable unit in the northern Trinity and Woodbine aquifers. The Hosston Aquifer has average and median hydraulic conductivity values of 4.9 and 6.8 feet per day, respectively. The two aquifers with the lowest hydraulic conductivity averages are the Woodbine and Paluxy aquifers. Both of these aquifers have average conductivity values near 1 foot per day and median hydraulic conductivity values between 2.0 and 2.5 feet per day. Across the majority of the area covered by each aquifer/formation, the hydraulic conductivity is fairly uniform. However, at or near several of the edges or boundaries of the mapped depositional systems, variations of up to several feet per day are present. In the Hosston Aquifer, at the locations where two major fluvial channels were

identified, the hydraulic conductivity values are at relative highs and the bands of localized
higher hydraulic conductivity are oriented in the same direction as the two fluvial channels.

Table 4.2.11 summarizes the hydraulic conductivities by litho-unit and depositional system for
each aquifer/formation. Note that there is only one limestone litho-unit and this unit is used to
represent all of the limestone in the Washita/Fredericksburg groups and the Glen Rose
Formation. The basic geological makeup of both the Washita/Fredericksburg groups and the
Glen Rose Formation indicates that their limestone could have significant variability in
transmissive properties. However, information was insufficient to justify and quantify a second
limestone type, so only one limestone type was used in the analysis. Development of the GHS
model indicated that the calculated average hydraulic conductivity was relatively insensitive to
the estimated hydraulic conductivity value for shale as long as it remained below 0.01 feet per
day. So the value of 0.001 feet per day for shale shown in Table 4.2.11 does not affect the
calculated horizontal hydraulic conductivity.

4.2.7.2 Transmissivity Fields for Aquifers/Formations

Figures 4.2.25 through 4.2.31 show the estimated transmissivity fields for the Woodbine
Aquifer, Washita/Fredericksburg groups, Paluxy Aquifer, Glen Rose Formation, Hensell
Aquifer, and Hosston Aquifer, respectively. The transmissivity fields were generated by
multiplying the hydraulic conductivity field by the aquifer/formation thickness. The highest
transmissivity values occur in the downdip region of the Hosston Aquifer. A review of the
transmissivity field for the Hosston Aquifer shows large increases in the transmissivity values
south of Bell, McLennan, and Hill counties. In that area, the Hosston Aquifer appears to
represent the vast majority of the transmissivity of the lower portion of the northern Trinity
Aquifer (i.e., the Hensell Aquifer, Pearsall Formation, and Hosston Aquifer). In the updip area
and across the outcrop areas of the lower portion of the northern Trinity Aquifer, the Hensell
Aquifer has the largest transmissivity. Figure 4.2.27 shows that the transmissivity of the Paluxy
Aquifer is highest in the northeast region in the vicinity of Red River and Lamar counties. In the
southern region, the transmissivity of the Paluxy Aquifer reduces from about 100 square feet per
day to about 10 square feet per day across Hill County. The transmissivity fields for both the
Washita/Fredericksburg groups and the Glen Rose Formation show a relatively uniform increase
in transmissivity in the downdip direction. The transmissivity of the Woodbine Aquifer reaches

1,000 square feet per day in portions of the northern region, which covers an approximate 11-county area.

4.2.7.3   Vertical Hydraulic Conductivity

Groundwater flow through an aquifer is influenced by the orientation of the grains at the microscale, the stacking of different types of deposits at the mesoscale, and changes in the depositional system and lithology at the macroscale. At each of these scales, these factors affect the vertical and hydraulic conductivities differently. At the very small scale of a few millimeters, the differences between vertical and horizontal hydraulic conductivities may be very small. However, at the large scale of 500 to 1,000 feet, the differences between the vertical and horizontal hydraulic conductivities can be very large. One of the principal causes for large differences between the horizontal and vertical hydraulic conductivities is aquifer heterogeneity that includes layering of relatively low-permeable materials. Field measurements of vertical hydraulic conductivity are not available at the vertical scale of the model grids, which is typically greater than 300 feet. Because vertical hydraulic conductivity is not measurable at the scale of greater than hundreds of feet, it is generally a model calibrated parameter.

Typical vertical anisotropy ratios are on the order of 1:1 to 1,000:1, as determined from model applications (Anderson and Woessner, 2002). Vertical anisotropy values as high as 50,000:1 have been used in some groundwater models. Williamson and others (1989) reported that the vertical anisotropy in the Gulf Coast Aquifer System in Texas and Louisiana could be much greater than a ratio of 1,000:1 because of the relative abundance of clayey deposits.

For the northern Trinity and Woodbine aquifers, the vertical hydraulic conductivity was not calculated by dividing the horizontal hydraulic conductivity by an anisotropy value. Rather, like horizontal hydraulic conductivity, the magnitude of the vertical hydraulic conductivity was developed based on the theoretical analysis for determining the effective hydraulic conductivity based on one-dimensional vertical flow through layered media (Freeze and Cherry, 1979). This approach has previously been used in the development of several groundwater models, including those by (Deeds and others (2003), Dutton and others (2003), and Young and others (2009). For one-dimensional flow, the effective vertical hydraulic conductivity is the weighted harmonic mean of the hydraulic conductivity of the different layers. For a two-layer aquifer consisting of a

sand layer and a shale layer, the weighted effective vertical hydraulic conductivity is calculated
as:

$$K_v = \frac{B}{b_s/K_{vs} + b_{sh}/K_{vsh}} \qquad (4.2.7)$$

where:

K_v = effective vertical hydraulic conductivity (feet per day)

b_s = total thickness of sand layer (feet)

K_{vs} = vertical hydraulic conductivity of sand layer (feet per day)

b_{sh} = total thickness of shale layer (feet)

K_{vsh} = vertical hydraulic conductivity of shale layer (feet per day)

B = total aquifer thickness (feet)

The harmonic mean is more greatly influenced by the lowest hydraulic conductivity values in the
averaging process. To illustrate this point, the effective vertical hydraulic conductivity was
calculated for several idealized two-layer aquifer systems. As shown in Table 4.2.12, the
magnitude of the effective vertical hydraulic conductivity is largely determined by the magnitude
of the lowest vertical hydraulic conductivity and not the thickness of the layer with the lowest
hydraulic conductivity. The calculations in Table 4.2.12 show that the impact of 50 feet of
0.1 feet per day shale is significantly greater on reducing the vertical hydraulic conductivity of
500 feet of sand than the impact of 500 feet of 1 feet per day shale. While the former produces a
vertical hydraulic conductivity of 1.1 feet per day for the sand-shale deposit, the latter produces a
vertical hydraulic conductivity of 2.0 feet per day.

The methodology for estimating vertical hydraulic conductivity during numerical model
calibration was based on application of this harmonic mean, along with adjustments for depth of
burial and (potentially) temperature. A decrease in vertical hydraulic conductivity with depth is
predominantly the result of the compression of clays due to overburden and is typically modeled
as an exponential function of depth (Loucks and others, 1984; Evans and others, 1997; Zhang
and others, 2007; Magara, 1978).

4.2.7.4 Storativity, Specific Storage, and Specific Yield

The terms storativity, specific storage, and specific yield are terms used to define the amount of
water that can physically be removed from, or added to, an aquifer when the water level in the
aquifer changes. In general terms, when water is removed from an aquifer by pumping or is

added to an aquifer by recharge, the amount of water stored in the aquifer changes. The concept of stored water in an aquifer is similar to the concept of stored water in a lake. In a lake, the amount of water removed from the lake per foot of decline in the lake level is typically calculated as the change in water level multiplied by one square foot. Because aquifers are comprised of both water and sediment, the calculation of the change in stored water per foot of water-level change is significantly more complicated than it is for a lake.

Storativity is defined as the volume of water that an aquifer releases from storage under a unit decline in hydraulic head (Freeze and Cherry, 1979). Because of physical differences between unconfined and confined aquifers, storativity is defined differently for the two aquifer conditions. For a confined aquifer, the storativity is equal to the product of specific storage and aquifer thickness. In an unconfined aquifer, the aquifer storativity is equal to the sum of the specific yield and the product of specific storage and aquifer thickness. Specific storage values account for the way changes in the hydraulic pressure change the density of the water and for changes in the arrangement and bulk density of the aquifer matrix. Specific yield values account for the amount of water that drains from the aquifer pores following a drop in the water level.

For most unconsolidated aquifers, reported values for specific yield for calibrated regional models fall within a relatively narrow range, between 0.10 and 0.3. Unlike specific yield, specific storage values typically have a range of several orders of magnitude. Factors that affect the specific storage values are lithology and depth of burial. Lithology is a factor because clay materials are more compressible than sand and, therefore, are more susceptible to changes in porosity with changes in pressure. Depth of burial is a factor because the compressibility of unconsolidated deposits is a nonlinear function of pressure.

The conceptual model for estimating specific storage was based on the model of Shestakov (2002), who postulated a relationship based on geomechanical considerations as follows:

$$Ss = \frac{A}{D+z0} \qquad (4.2.8)$$

where:

Ss = specific storage

A = calibration parameter (per foot)

D = depth (feet)

$z0$ = calibration parameter

Shestakov (2002) showed that A varied in the narrow range between 0.00018 and 0.00091 per foot for sandy rocks and between 0.003 and 0.03 per foot for clayey rocks. The Shestakov model assumes a power-law relationship between porosity and depth, where the decrease is more pronounced at shallower depths. This is consistent with the Magara (1978) observation that the rate of porosity decrease is fast at shallow depths and slows down with greater burial. Young and Kelley (2006) provide an example of how the Shestakov (2002) approach can be used to calculate storage values for a groundwater model.

4.2.8   Collection and Analysis of Specific Capacity Tests

The primary source of data used for calculating specific capacity values was drillers' logs. These logs are submitted to the state as part of the regulatory process when drilling a new well. After an exhaustive search of more than 80,000 driller's logs, 12,300 driller's logs containing the information required to calculate specific capacity were identified. The requisite information includes a top and bottom depth for the well screen, a pumping rate, and a non-zero drawdown. Approximately 300 logs recorded zero for the drawdown. Based on professional judgment, these drawdowns were dismissed as unrealistic. Because many of the driller's logs do not contain well coordinates, the information from the driller's logs were grouped and organized by Texas state well grid number. A state well grid represents a square with a length of about 3 miles on a side. In the analysis of the specific capacity data, the mid-point of the state well grid was assigned as the location for all wells identified for the grid.

In order to develop an equation for estimating transmissivity from specific capacity, the time-drawdown data from the 340 aquifer pumping tests assembled primarily from PWS wells in GMA 8 (see Section 4.2.3.2) were used. The specific capacity was plotted as a function of the transmissivity calculated by the Cooper and Jacob (1946) equation (see discussion in Section 4.2.4). If a well has at least 80 percent of its screen in a single aquifers/formations, the well was assigned to that aquifer/formation. Figure 4.2.32 shows specific capacity versus transmissivity by aquifer/formation. It appears that a single relationship may be appropriate for general use. However, in order to properly account for possible differences among the aquifers/formations, separate relationships were constructed for each.

4.2.8.1   Relationship between Specific Capacity Tests and Transmissivity

Figures 4.2.33 and 4.2.34 show the relationship between specific capacity and transmissivity for each aquifer/formation. The data in these figures are plotted on log-log scales, with a best-fit line and the equation for that line shown on the plot. Each set of data contains two types of points. The larger symbols in the plots represent data for wells that meet the 80 percent coverage criteria for the well screen. The smaller symbols represent data for wells that do not meet the 80 percent criteria. The potential importance of the 80 percent criteria is illustrated by the large difference in the trends for the Hensell Aquifer (Figure 4.2.34a). As can be inferred by the relatively few large symbols, the majority of the wells that intersect the Hensell Aquifer are screened across more than one aquifer/formation.

Figure 4.2.35 shows the areal distribution of about 12,300 specific capacity measurements that were assembled and reviewed. Development of transmissivity values from specific capacity values for each aquifer/formation involved a three-step process. The first step was to assign each well to a single unit based on the aquifer/formation with the greatest screen intersection. The second step was to calculate the specific capacity from the available data in the driller's log. The third step was to calculate the transmissivity from the specific capacity based on the equations in Figures 4.2.33 and 4.2.34. Table 4.2.13 provides the means and standard deviations for the calculated transmissivity values for each aquifer/formation from both specific capacity and aquifer pumping test data.

The following observations can be made regarding the data in Table 4.2.13:

- The mean transmissivity values for the aquifers/formations are considerably more variable for the specific capacity tests than for the aquifer pumping tests.
- A large difference in the mean transmissivity values between the two data sets occurs for the Glen Rose Formation. For the Glen Rose Formation, the mean value from the specific capacity data is about 2.9 times higher than the mean value from the aquifer pumping test data.
- There are about 20 times more specific capacity tests than aquifer pumping tests.
- The two sets of transmissivity values are generally within a factor of two for the sandy aquifers.

Figures 4.2.36 through 4.2.49 consist of a pair of figures for each aquifer/formation. The first figure shows the number of specific capacity tests conducted in the aquifer/formation by state well grid. The second figure shows the average transmissivity value for all of the transmissivity values calculated from specific capacity tests associated with the state well grid. The transmissivity values associated with the higher counts of specific capacity values are presumed to be more precise than the transmissivity values associated with lower counts.

The following observations are noted based on a review of these figures:

- The areal coverage for the specific capacity measurements is much greater than the aquifer pumping test coverage. The areal coverage for the specific capacity tests is focused primarily in the updip regions for all aquifers/formations. The aquifer pumping tests tend to occur further downdip than do the specific capacity tests.

- The specific capacity tests in the Glen Rose Formation show transmissivity values greater than 1,000 square feet per day in the vicinity of Somervell, Hood, and Parker counties with other 1,000 square feet per day transmissivity estimates scattered across the Washita/Fredericksburg groups and Trinity Aquifer outcrops. The aquifer pumping test data set has no transmissivity values above 1,000 square feet per day for the Glen Rose Formation.

- The specific capacity tests in the Washita/Fredericksburg groups have numerous measurements less than 25 square feet per day. There are no aquifer pumping tests with transmissivity values less than 500 square feet per day.

- The test locations are significantly different for the specific capacity tests and the aquifer pumping tests for some aquifers/formations. In the Hosston Aquifer, for example, the majority of the specific capacity tests were performed in the outcrop area while the majority of the aquifer pumping tests were performed in the downdip confined section. Many of the specific capacity test locations are in the updip region of the Hosston Aquifer where transmissivity is expected to be low. It appears plausible that the discrepancy between the mean and standard deviation of the two sets of transmissivity values (specific capacity versus aquifer pumping test) for the Hosston Aquifer is largely caused by the difference in locations where testing was performed.

Figures 4.2.50 and 4.2.51 provide the cumulative distribution functions for the transmissivity values calculated from aquifer pumping tests and specific capacity tests by aquifer/formation. The following observations are notable based on a review of these two figures.

- There are no aquifer pumping tests with transmissivity value less than 10 square feet per day for any of the aquifers/formations. However, the number of transmissivity values from specific capacity tests that are less than 10 square feet per day is about 15 percent for the Washita/Fredericksburg groups and about 10 percent for the Glen Rose Formation.

- For the Hosston Aquifer, approximately 30 percent of the aquifer pumping tests yield transmissivity values greater than 1,000 square feet per day but there are no specific capacity tests where transmissivities are greater than 1,000 square feet per day.

- The transmissivity distribution for the Paluxy Aquifer is almost identical for the two data sets after the 30th percentile. Prior to the 30th percentile, the transmissivity values from specific capacity tests are considerably less than from aquifer pumping tests.

- For the Woodbine, Paluxy, Hensell, and Hosston aquifers, the relationship between transmissivity from the two data sets has the least scatter for the Paluxy Aquifer.

4.2.8.2   Assessment of Transmissivity Values from Specific Capacity Tests

The assessment of the transmissivity values calculated from specific capacity tests provides useful and complimentary information to the transmissivity values yielded by aquifer pumping tests. As a result, the transmissivity values calculated from specific capacity tests were useful for consideration in model calibration. The approach was to analyze the specific capacity data in aggregate for each aquifer/formation, identify issues of interest and vet the issues as they were discovered. The benefits that the specific capacity data brings to the project compared to the transmissivity data from aquifer pumping test are the following:

- Different lower transmissivity threshold for sampling. The analysis suggests that one of the reasons the specific capacity tests show a cumulative distribution with lower transmissivity values may be a result of sampling bias. For the aquifer pumping tests, which are performed on PWS wells, there is a lower transmissivity threshold below which a well is not economical and would not be installed. This lower threshold appears to be about 10 square feet per day in the study area. Because individual well owners

typically do not require production rates on the order of a PWS well, the thresholds will be lower for specific capacity tests.

- Different sampling areas. A review of the location and frequency of wells in the outcrop areas indicates that individual well owners are more likely to drill wells in the outcrop area compared to industry or major water suppliers. The difference in the mean transmissivity values for the Hosston Aquifer may be largely caused by the sampling bias resulting from this difference.

- Different sampling size (numbers of tests). Specific capacity tests are orders of magnitude cheaper to perform than aquifer pumping tests. As a result, they are more than 10 times more common than aquifer pumping tests. When the aquifer pumping tests are analyzed in aggregate with the specific capacity tests, the large population size can be used to help vet trends and patterns that appear in the data. The large sampling size is attributed to the identification of numerous transmissivity values above 1,000 square feet per day in the Glen Rose Formation. These transmissivity values could be evidence of significant secondary porosity features that could affect or confirm the conceptual model of recharge and shallow flow zone.

4.2.8.3   Potential Changes to the GHS Model Baseline for Hydraulic Conductivity

Figures 4.2.52 through 4.2.58 show the ratio of hydraulic conductivity values generated from specific capacity data (K_{SC}) and from aquifer pumping test data (K_{AQ}) to hydraulic conductivity values estimated from lithologic data (K_{LITH}) predicted by the GHS model. For example, if K_{SC} equals 2.0 feet per day and K_{LITH} equals 1.0 feet per day, the ratio (K_{SC}/K_{LITH}) is equal to 2.0 and the GHS model under predicts the measured hydraulic conductivity. An error/uncertainty tolerance limit for this analysis was set at a factor of three for the difference between measured hydraulic conductivity values from aquifer pumping test and specific capacity test data and hydraulic conductivity values predicted by the GHS model.

The comparison results shown in Figure 4.2.52 through 4.2.58 are color coded. Grey points indicate that the comparison is within the error/uncertainty tolerance. Points that are either green or blue indicate regions where the hydraulic conductivity predicted by the GHS model is more than a factor of three greater than or less than, respectively, the measured hydraulic conductivity from aquifer pumping test or specific capacity test data. These figures also show areas where the

GHS model under or over predicts hydraulic conductivity. The zones marked as over predicting hydraulic conductivity represent regions where there are a concentrated number of specific capacity tests that have estimated hydraulic conductivity values that are lower than the values predicted by the GHS model. The zones marked as under predicting hydraulic conductivity represent regions where there are a concentrated number of specific capacity tests that have estimated hydraulic conductivity values that are higher than the values predicted by the GHS model.

The following observations are made regarding the comparisons shown in Figures 4.2.52 through 4.2.58.

- The transmissivity values from specific capacity test are in general agreement with the GHS model hydraulic conductivity estimates for the Woodbine and Paluxy aquifers and the Pearsall Formation.

- For the Washita/Fredericksburg groups, the specific capacity tests suggest that across much of the region the transmissivity values from the GHS model are too high. This result suggests that although there are locations that are sufficiently transmissive to support a PWS well, there are many locations that cannot.

- The specific capacity tests suggest that the transmissivity in the Glen Rose Formation is considerably more varied than indicated by the GHS model. Of particular concern is the area with dark blue squares in Figure 4.2.55, where secondary porosity features may be augmenting recharge.

- The specific capacity tests suggest that there is a zone of relatively high hydraulic conductivity in the Hosston Aquifer in the vicinity of Parker and Hood counties.

A key conclusion from these observations is that the hydraulic conductivities from the GHS model tend to over predict hydraulic conductivity for the Washita/Fredericksburg groups and the Glen Rose Formation. As such, the hydraulic conductivities from the GHS model were considered to be too high for most of the area covered by these two units. In addition, the hydraulic conductivities from the GHS model may not be applicable for all of the updip areas of the Hosston Aquifer, as they are higher than observed values.

Table 4.2.1   List of PWS entities contacted for aquifer pumping test data.

County	Entity	Response
Brown	City of Blanket	No records provided.
Brown	May WSC	No records available
Brown	Lake Brownwood Christian Retreat	Left message on 11/16/12
Callahan	City of Cross Plains	No records provided.
Callahan	Iron Hand Mobile Park	No answer, no machine
Comanche	City of Gustine	No records available.
Comanche	Sidney ISD	No records available.
Coryell	Coryell City Water Supply District	No records available.
Coryell	City of Evant	No answer, no machine
Eastland	City of Rising Star	No records provided.
Erath	City of Dublin	Left message 11/16/12
Erath	City of Stephenville	Left message 11/19/12
Hamilton	City of Hico	No records provided.
Hamilton	Dutchmans Hidden Valley Store	No records available.
Hamilton	Hamilton Inn	Left message 11/19/12
Hamilton	Alexander Moulding Mill	Sent log of well drilled in 1994, limited data
Hamilton	Cedar Hill Water Association	No records available.
Lamar	Pattonville WSC	No records available.
Lampasas	LCRA Lometa Regional Water System	No records available.
Lampasas	Kempner WSC	No records available.
Lampasas	Woodland Acres Water Association	Left message 11/19/12
Mills	City of Goldthwaite	Test data received from three wells
Mills	Priddy WSC	No records provided.
Mills	Jope Thurman Lodge & Livery Inc	No records available.
Mills	Mullin ISD	No answer, no machine
Mills	Star ISD	No answer, no machine
Mills	Minute Stop	TCEQ lists as inactive, phone number disconnected
Red River	City of Detroit	No answer, no machine
Red River	Red River County WSC	No records provided.

WSC = water supply corporation
ISD = independent school district

Table 4.2.2   Example elapsed time-drawdown file.

Elapsed Time (minutes)	Water-Level change (feet)	Pumping Rate (gallons per minute	Indicator[a]
2	25.0	45	T
4	33.0	45	T
6	43.5	45	T
8	48.5	45	T
10	52.4	45	T
15	58.0	45	T
20	60.7	43	T
25	62.5	43	T
30	63.8	42	T
45	66.3	42	T

[a]Boolean input to indicate whether or not to include the data point in the calculation of transmissivity

Table 4.2.3   Number of transmissivity values calculated from PWS aquifer pumping test data and obtained from the literature by aquifer and formation.

Aquifer/Formation	Number of PWS Transmissivity Values	Number of Transmissivity Values from Other Sources	Total Number of Transmissivity Values
Woodbine Aquifer	53	27	80
Washita/Fredericksburg Groups	19	2	21
Paluxy Aquifer	36	8	44
Glen Rose Formation	41	24	65
Hensell Aquifer	29	22	51
Pearsall Formation	53	20	73
Hosston Aquifer	109	57	166
Total	340	160	500

Table 4.2.4   **Mean and standard deviation of transmissivity values by aquifer/formation.**

Aquifer/Formation	Transmissivity (square feet per day)		Count
	Mean	Standard deviation	
Woodbine Aquifer	623	684	80
Washita/Fredericksburg Groups	660	686	21
Paluxy Aquifer	289	250	44
Glen Rose Formation	446	386	65
Hensell Aquifer	638	556	51
Pearsall Formation	680	629	73
Hosston Aquifer	841	953	166

Table 4.2.5   **Number of geophysical logs analyzed for lithology that include the aquifer/formation.**

Aquifer/Formation	Number of Geophysical Logs
Woodbine Aquifer	406
Washita/Fredericksburg Groups	587
Paluxy Aquifer	671
Glen Rose Formation	749
Hensell Aquifer	782
Pearsall Formation	797
Hosston Aquifer	784

Table 4.2.6   **Descriptions of the 10 litho-units.**

Major Lithologies	Litho-Unit	Description[a]
Sands	25+ ft Sand	Sand bed with thickness greater than 25 feet
	14-25 ft Sand	Sand bed with thickness between 14 and 25 feet
	8-14 ft Sand	Sand bed with thickness between 8 and 14 feet
	4-8 ft Sand	Sand bed with thickness between 4 and 8 feet
Sand-Clay Mixtures	Well Sorted Sands	Sand and shale mixture, 50 to 80 percent sand
	Poorly Sorted Sands	Sand and shale mixture, 30 to 50 percent sand
	Clayey Sands	Sand and shale mixture, 10 to 30 percent sand
Shales and Limestones	Limestone	Limestone bed of any thickness
	Shaley Limestone	Combination of shales and limestone
	Shale	Shale with thicknesses greater than 4 feet

[a] Sand and limestone beds are defined as a stratigraphic layer composed of nearly 100 percent sand or 100 percent limestone, respectively, as interpreted from geophysical logs.

Table 4.2.7   **Criteria for well selection.**

Aquifer/Formation	Criteria for Well Selection		Number of Wells Meeting Criteria
	Percentage of the Well Screen in the Aquifer/Formation	Percentage of the Aquifer/Formation in the Well Screen	
Woodbine Aquifer	70	40	16
Washita/Fredericksburg Groups	70	20	8
Paluxy Aquifer	70	72	13
Glen Rose Formation	70	30	17
Hensell Aquifer	50	40	9
Pearsall Formation	55	55	21
Hosston Aquifer	65	65	58

**Table 4.2.8   Comparison of hydraulic conductivities (feet per day) calculated from
transmissivity values (K_{AQ}) and estimated for the litho-units (K_{LITH}).**

Well ID	Latitude	Longitude	K_{AO} (feet per day)	K_{LITH} (feet per day)	K_{AQ} to K_{LITH} Ratio
Woodbine Aquifer					
344	32.433	-96.685	1.36	2.20	0.6
347	32.536	-96.813	1.07	2.07	0.5
348	33.604	-96.146	1.31	1.62	0.8
349	32.504	-96.909	1.93	2.56	0.8
361	32.466	-96.830	2.64	2.00	1.3
363	32.527	-96.934	3.89	2.01	1.9
365	32.481	-96.865	3.50	2.20	1.6
370	32.532	-96.782	3.89	1.25	3.1
1019	33.349	-96.548	0.78	1.70	0.5
1104	33.547	-96.603	1.40	1.65	0.8
1107	33.823	-96.876	16.57	2.57	6.4
1111	33.708	-96.667	0.20	1.32	0.2
1113	33.638	-96.620	1.09	1.13	1.0
1118	33.586	-96.604	3.10	1.36	2.3
1121	33.423	-96.576	4.11	1.31	3.1
1122	33.423	-96.576	3.28	0.97	3.4
Washita/Fredericksburg Groups					
37	33.617	-96.357	0.29	1.22	0.2
40	30.744	-97.600	1.07	1.50	0.7
44	30.787	-97.629	1.90	1.59	1.2
45	30.612	-97.640	1.22	1.60	0.8
46	30.603	-97.610	1.60	1.60	1.0
47	30.613	-97.639	1.56	1.60	1.0
48	30.635	-97.638	2.31	1.59	1.5
51	30.713	-97.647	3.60	1.57	2.3
Paluxy Aquifer					
238	33.632	-96.472	0.45	1.26	0.4
240	33.244	-96.783	0.53	1.80	0.3
242	32.407	-97.100	1.06	1.90	0.6
244	32.412	-97.100	1.08	1.90	0.6
245	33.356	-96.551	0.70	1.79	0.4
253	33.233	-96.783	0.73	1.82	0.4
256	32.428	-97.312	1.82	1.33	1.4
257	33.234	-96.797	1.23	1.90	0.6
260	32.765	-96.959	1.59	2.30	0.7
264	32.902	-96.565	1.92	2.15	0.9
1020	33.244	-96.783	0.56	1.80	0.3
1166	32.703	-97.156	3.44	2.20	1.6
1168	32.736	-97.054	4.96	1.71	2.9

Table 4.2.8, continued

Well ID	Latitude	Longitude	K_{AO} (feet per day)	K_{LITH} (feet per day)	K_{AQ} to K_{LITH} Ratio
Glen Rose Formation					
65	32.760	-97.698	0.59	1.69	0.3
66	32.740	-97.681	0.70	1.67	0.4
69	32.757	-97.687	0.82	1.70	0.5
71	33.170	-97.440	0.94	1.88	0.5
73	32.854	-97.613	1.30	1.78	0.7
74	32.780	-97.739	1.42	1.75	0.8
77	33.432	-96.577	0.91	2.89	0.3
79	32.739	-97.689	1.56	1.67	0.9
80	32.763	-97.692	1.83	1.70	1.1
88	32.767	-97.699	3.29	1.70	1.9
89	32.752	-97.689	3.11	1.69	1.8
92	33.424	-96.645	1.68	2.70	0.6
1070	32.739	-97.114	1.74	1.68	1.0
1071	32.787	-97.111	2.07	1.62	1.3
1072	32.728	-97.109	3.09	1.68	1.8
Hensell Aquifer					
105	33.338	-97.120	1.29	2.65	0.5
112	32.388	-97.740	1.23	3.13	0.4
114	33.302	-96.994	4.22	3.76	1.1
117	32.347	-97.677	3.48	3.49	1.0
118	32.422	-97.815	4.45	2.65	1.7
119	32.493	-97.777	4.70	3.01	1.6
1073	33.467	-96.913	5.41	3.56	1.5
1087	32.166	-98.194	9.56	3.24	3.0
1129	32.139	-97.393	9.83	4.71	2.1
Pearsall Formation					
278	32.411	-97.658	0.41	1.30	0.3
286	33.461	-97.221	0.92	3.06	0.3
292	33.681	-96.847	1.33	3.74	0.4
294	33.461	-97.221	1.69	3.06	0.6
295	32.416	-97.668	2.33	1.28	1.8
296	32.419	-97.205	2.08	2.02	1.0
297	32.419	-97.205	2.08	2.02	1.0
300	32.446	-97.669	3.07	1.15	2.7
307	33.649	-97.035	3.22	3.50	0.9
310	33.704	-97.015	3.39	4.04	0.8
312	32.666	-96.278	4.65	3.55	1.3
313	33.587	-97.024	4.90	3.00	1.6
315	33.584	-97.023	5.15	3.00	1.7
318	33.305	-96.938	6.54	3.37	1.9
319	33.652	-96.914	8.50	2.70	3.1

Table 4.2.8, continued

Well ID	Latitude	Longitude	K_{AO} (feet per day)	K_{LITH} (feet per day)	K_{AQ} to K_{LITH} Ratio
320	33.083	-97.059	9.49	2.83	3.4
321	33.664	-96.902	15.26	2.87	5.3
1040	33.608	-97.140	5.64	3.03	1.9
1043	33.626	-97.124	13.91	3.17	4.4
1102	32.656	-97.908	4.26	2.96	1.4
1123	33.656	-96.907	3.42	3.34	1.0
Hosston Aquifer					
134	32.412	-97.261	1.04	4.47	0.2
143	32.228	-97.300	1.17	5.97	0.2
145	31.793	-97.519	1.70	5.64	0.3
150	31.983	-97.210	1.26	5.63	0.2
152	31.925	-97.322	1.90	5.67	0.3
153	32.246	-97.304	2.00	5.50	0.4
156	30.656	-97.921	1.19	6.32	0.2
157	31.962	-97.326	1.91	5.58	0.3
158	32.348	-97.215	1.55	4.83	0.3
163	32.042	-97.403	2.87	5.51	0.5
165	31.575	-96.966	0.85	4.72	0.2
168	32.319	-97.032	2.30	5.40	0.4
169	32.162	-97.140	2.21	6.05	0.4
170	32.284	-97.273	2.67	4.68	0.6
171	32.053	-97.363	2.98	5.70	0.6
172	32.978	-97.207	3.78	5.74	0.7
173	32.735	-97.004	2.52	5.93	0.4
176	31.308	-97.357	2.77	4.28	0.7
177	30.720	-97.444	1.71	7.29	0.2
178	31.949	-97.322	2.86	5.48	0.5
183	32.346	-96.930	3.13	5.28	0.6
184	32.539	-96.956	3.09	5.46	0.6
187	31.265	-97.363	4.07	4.86	0.8
193	32.425	-96.945	3.86	5.69	0.7
203	33.142	-97.301	8.09	6.27	1.3
204	32.309	-97.015	5.31	5.42	1.0
207	32.460	-97.000	5.80	4.75	1.2
208	33.079	-97.345	8.63	6.05	1.4
212	33.161	-97.079	8.65	6.24	1.4
213	32.296	-97.790	9.92	6.52	1.5
215	32.372	-96.955	7.18	5.96	1.2
217	32.817	-97.198	9.54	4.87	2.0
218	32.817	-97.197	9.54	4.87	2.0
222	31.785	-97.572	14.73	5.62	2.6
223	32.418	-97.010	11.62	5.48	2.1

Table 4.2.8, continued

Well ID	Latitude	Longitude	K_{AO} (feet per day)	K_{LITH} (feet per day)	K_{AQ} to K_{LITH} Ratio
226	32.723	-97.021	11.47	6.10	1.9
229	30.721	-97.444	9.55	7.29	1.3
230	33.085	-96.885	21.13	7.22	2.9
232	32.574	-96.976	27.37	5.96	4.6
1013	31.785	-97.571	13.44	5.62	2.4
1052	32.972	-96.912	10.79	6.25	1.7
1053	32.960	-96.874	9.84	6.01	1.6
1054	32.842	-96.972	9.56	6.71	1.4
1056	32.816	-96.976	9.42	6.64	1.4
1058	32.829	-96.958	13.63	6.77	2.0
1060	32.636	-96.919	3.46	6.67	0.5
1061	32.626	-96.804	9.08	6.54	1.4
1062	32.603	-96.874	6.59	6.22	1.1
1063	32.605	-96.840	7.88	6.27	1.3
1081	32.435	-97.010	7.64	4.99	1.5
1082	32.477	-96.999	4.71	4.61	1.0
1142	32.229	-97.300	0.97	5.76	0.2
1145	31.821	-97.089	2.06	2.21	0.9
1147	31.639	-97.078	2.08	6.23	0.3
1149	31.646	-97.066	2.70	5.52	0.5
1170	32.729	-97.224	8.51	4.66	1.8
1171	32.726	-97.216	9.87	4.99	2.0
1172	32.733	-97.224	10.98	1.71	6.4

Table 4.2.9   Hydraulic conductivity estimates by litho-unit and aquifer/formation for the GHS model.

Aquifer/Formation	Hydraulic Conductivity (feet per day)									
	Sands				Sand/Clay Mixtures			Shales and Limestones		
	4-8 ft Sand	8-14 ft Sand	14-25 ft Sand	25+ ft Sand	Clayey Sands	Poorly Sorted Sands	Well Sorted Sands	Shale[a]	Limestone	Shaley-Limestone[a]
Woodbine Aquifer	2	3	5	5	0.2	0.25	0.6	0.001	2	0.1
Washita/Fredericksburg Groups	2	3	5	5	0.2	0.25	0.6	0.001	2	0.1
Paluxy Aquifer	2	3	5	5	0.2	0.25	0.6	0.001	2	0.1
Glen Rose Formation	2	3	5	5	0.1	0.25	0.6	0.001	2	0.1
Hensell Aquifer	6	7	7	7	0.2	1	2	0.001	2	0.1
Pearsall Formation	7	9	10	10	0.2	1	3	0.001	2	0.1
Hosston Aquifer	7	9	10	10	0.2	1	3	0.001	2	0.1

[a] Shale and shaley limestone are estimates that could not be informed by the GHS model with existing data

Table 4.2.10   Basic statistics for hydraulic conductivity by aquifer/formation.

Aquifer/Formation	Hydraulic Conductivity (feet per day)							
	Mean	Standard Deviation	Median	Percentiles				
				5	25	50	75	95
Woodbine Aquifer	0.9	0.7	2.2	0.2	1.1	2.2	3.3	4.2
Washita/Fredericksburg Groups	1.4	0.3	2.1	0.6	1.1	2.1	3.1	4.0
Paluxy Aquifer	1.1	0.6	2.5	0.2	1.2	2.5	3.7	4.7
Glen Rose Formation	1.7	0.4	2.3	0.5	1.1	2.3	3.4	4.3
Hensell Aquifer	2.7	1.1	3.8	0.4	1.9	3.8	5.7	7.2
Pearsall Formation	2.7	1.2	5.4	0.5	2.7	5.4	8.1	10.2
Hosston Aquifer	4.9	1.1	6.8	0.7	3.5	6.8	10.2	13.0

Table 4.2.11   Statistical breakdown of hydraulic conductivities by depositional system and litho-unit for each aquifer/formation.

Aquifer/Formation	Depositional System	Area (sq. miles)	Shale	Shaly Limestone	Limestone	Sandy Clay	Clayey Sand	Poorly-sorted Sand	4-8 ft Sand	8-14 ft Sand	14-25 ft Sand	25+ ft Sand	Average K (ft/d)
Woodbine Aquifer	K (feet per day)		0.001	0.1	2	0.1	0.25	0.5	1.5	3	4	6	
	coastal shale interfluve	5414	24%	0%	1%	55%	3%	0%	5%	4%	4%	3%	0.6
	deltaic sand	9603	13%	0%	0%	30%	15%	0%	13%	11%	8%	6%	1.2
	marine shelf shale	4392	63%	0%	3%	25%	4%	0%	3%	2%	1%	2%	0.3
Washita/ Fredericksburg Groups	K (feet per day)		0.001	0.1	2	0.1	0.25	0.5	1.5	3	4	6	
	shelf lime	20178	34%	3%	60%	2%	0%	0%	0%	0%	0%	2%	1.3
Paluxy Aquifer	K (feet per day)		0.001	0.1	2	0.1	0.25	0.6	2	3	5	5	
	coastal fluvial sand	19059	13%	0%	1%	16%	21%	2%	15%	14%	10%	3%	1.5
	coastal shale interfluve	5262	14%	0%	1%	41%	13%	1%	8%	7%	7%	4%	1.0
	deltaic sand	6394	16%	0%	1%	12%	23%	1%	16%	13%	9%	3%	1.4
	marine shelf shale	7132	56%	0%	13%	27%	2%	0%	2%	0%	0%	1%	0.4
Glen Rose Formation	K (feet per day)		0.001	0.1	0.1	0.1	0.25	0.6	2	3	5	5	
	marine shelf lime	29461	10%	0%	87%	1%	1%	0%	0%	0%	0%	1%	0.2
	marine shoreline sand	8395	10%	0%	4%	15%	36%	2%	18%	11%	3%	4%	1.1
Hensell Aquifer	K (feet per day)		0.001	0.1	2	0.1	1	2	6	7	7	7	
	coastal fluvial sand	6479	11%	0%	0%	13%	28%	2%	18%	16%	9%	3%	3.4
	coastal sandy interfluve	2801	16%	0%	1%	8%	32%	2%	21%	14%	5%	3%	3.2
	coastal shale interfluve	5014	14%	0%	1%	19%	26%	1%	16%	12%	7%	2%	2.8
	deltaic sand	16021	13%	0%	1%	12%	26%	1%	19%	13%	10%	2%	3.2
	marine shelf shale	7514	26%	2%	21%	29%	13%	0%	6%	2%	0%	1%	1.2
Pearsall Formation	K (feet per day)		0.001	0.1	2	0.1	1	3	7	9	10	10	
	coastal fluvial sand	2231	9%	0%	0%	17%	33%	2%	19%	12%	5%	2%	3.5
	coastal shale interfluve	7317	11%	0%	0%	20%	32%	2%	17%	12%	4%	3%	3.4
	deltaic sand	7286	14%	0%	6%	23%	22%	1%	14%	12%	6%	4%	3.4
	marine shelf lime shale	18926	18%	1%	30%	19%	16%	0%	9%	5%	2%	1%	2.2
	marine shelf shale	2172	34%	5%	51%	4%	3%	0%	1%	1%	0%	1%	1.4
Hosston Aquifer	K (feet per day)		0.001	0.1	2	0.1	1	3	7	9	10	10	
	coastal fluvial sand	37643	15%	0%	1%	8%	17%	2%	17%	20%	14%	3%	4.9

Table 4.2.12   Calculated vertical hydraulic conductivities for a two-layer aquifer consisting of sand and shale.

Sand Properties		Shale Properties		Aquifer Properties	
Thickness (ft)	K_v (ft/day)	Thickness (ft)	K_v (ft/day)	Thickness (ft)	K_v (ft/day)
500	100	500	1	1000	2.0
500	100	50	1	550	10.0
500	100	500	0.1	1000	0.2
500	100	50	0.1	550	1.1

ft = feet
ft/day = feet per day

Table 4.2.13   Mean and standard deviation of transmissivity values calculated from specific capacity tests and aquifer pumping test for each aquifer/formation.

Aquifer/Formation	Transmissivity (square feet per day)				Transmissivity Count	
	Mean		Standard Deviation			
	Specific Capacity Test	Aquifer Pumping Test	Specific Capacity Test	Aquifer Pumping Test	Specific Capacity Test	Aquifer Pumping Test
Woodbine Aquifer	239	623	325	684	1,226	80
Washita/Fredericksburg Groups	272	660	1,484	686	888	21
Paluxy Aquifer	357	289	808	250	2,614	44
Glen Rose Formation	1,279	446	13,005	386	3,335	65
Hensell Aquifer	384	638	272	556	2,173	51
Pearsall Formation	783	680	1,053	629	140	73
Hosston Aquifer	392	841	572	953	1,988	166
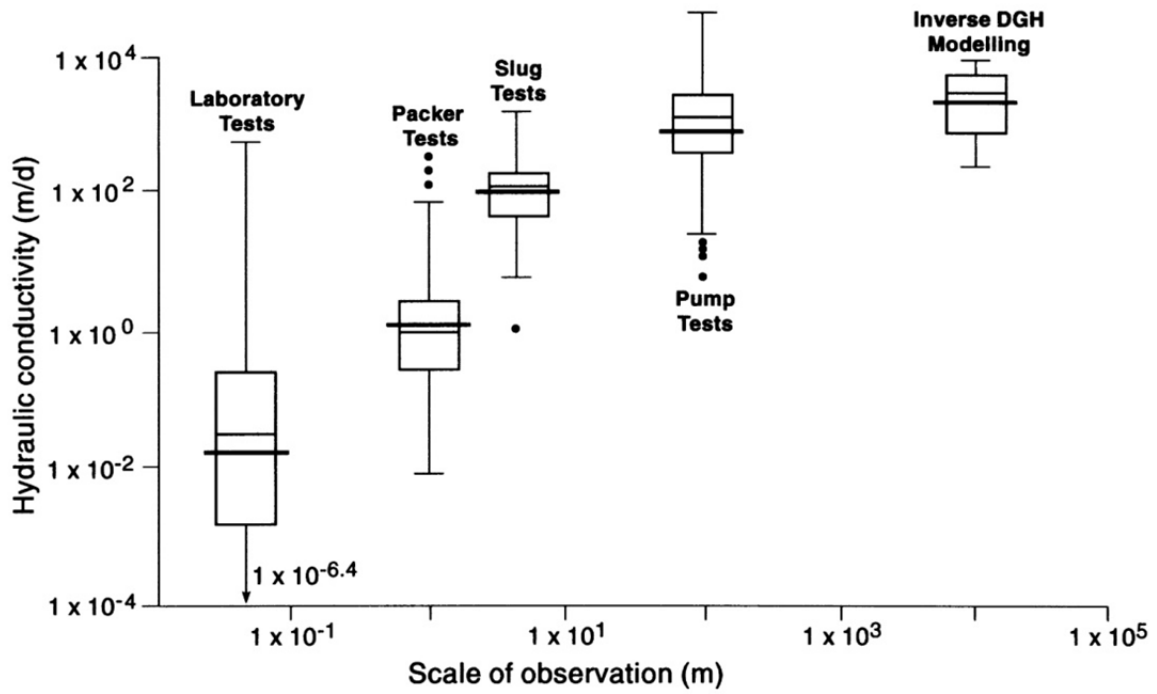
Figure 4.2.1   Box plots showing the scale dependence of hydraulic conductivity measurements in carbonate Pleistocene aquifers (from Whitaker and Smart, 2000). Heavy lines are geometric means.
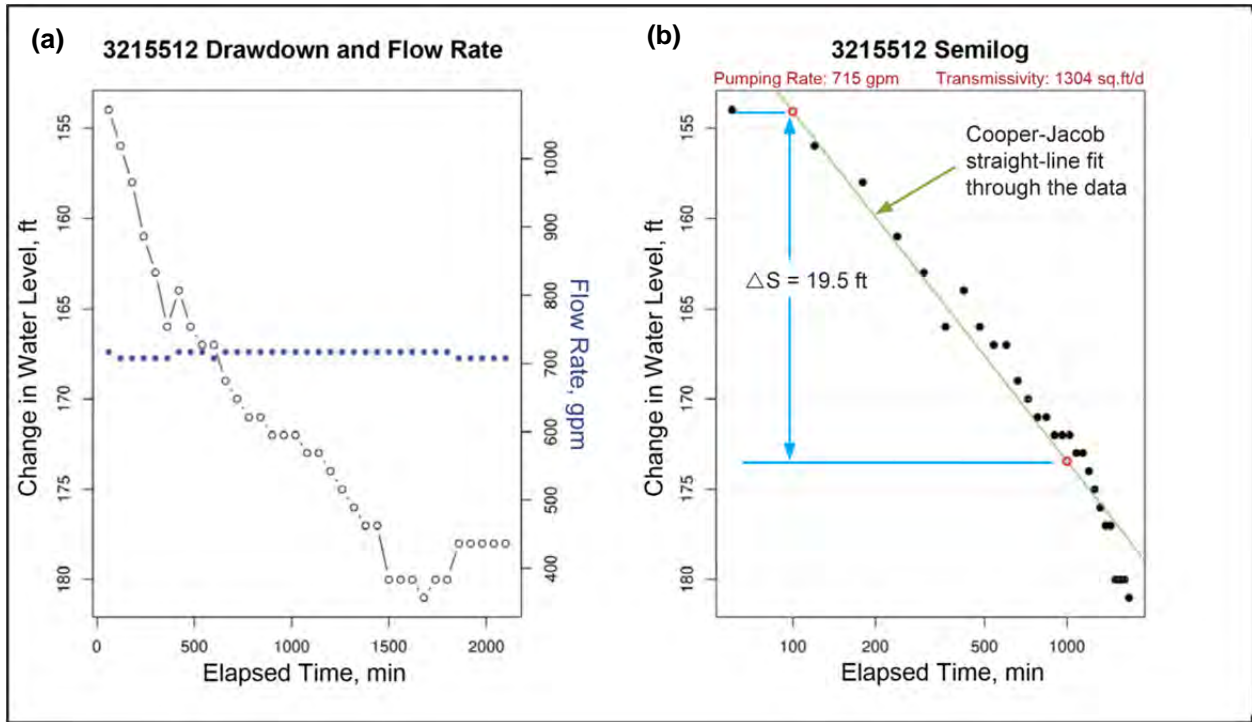
Figure 4.2.2   **Plots used to display and analyze the aquifer pumping test data in the elapsed time-drawdown files showing (a) the measured pumping rate and drawdown values over time and (b) a semi-log plot of elapsed water-level change over time.**
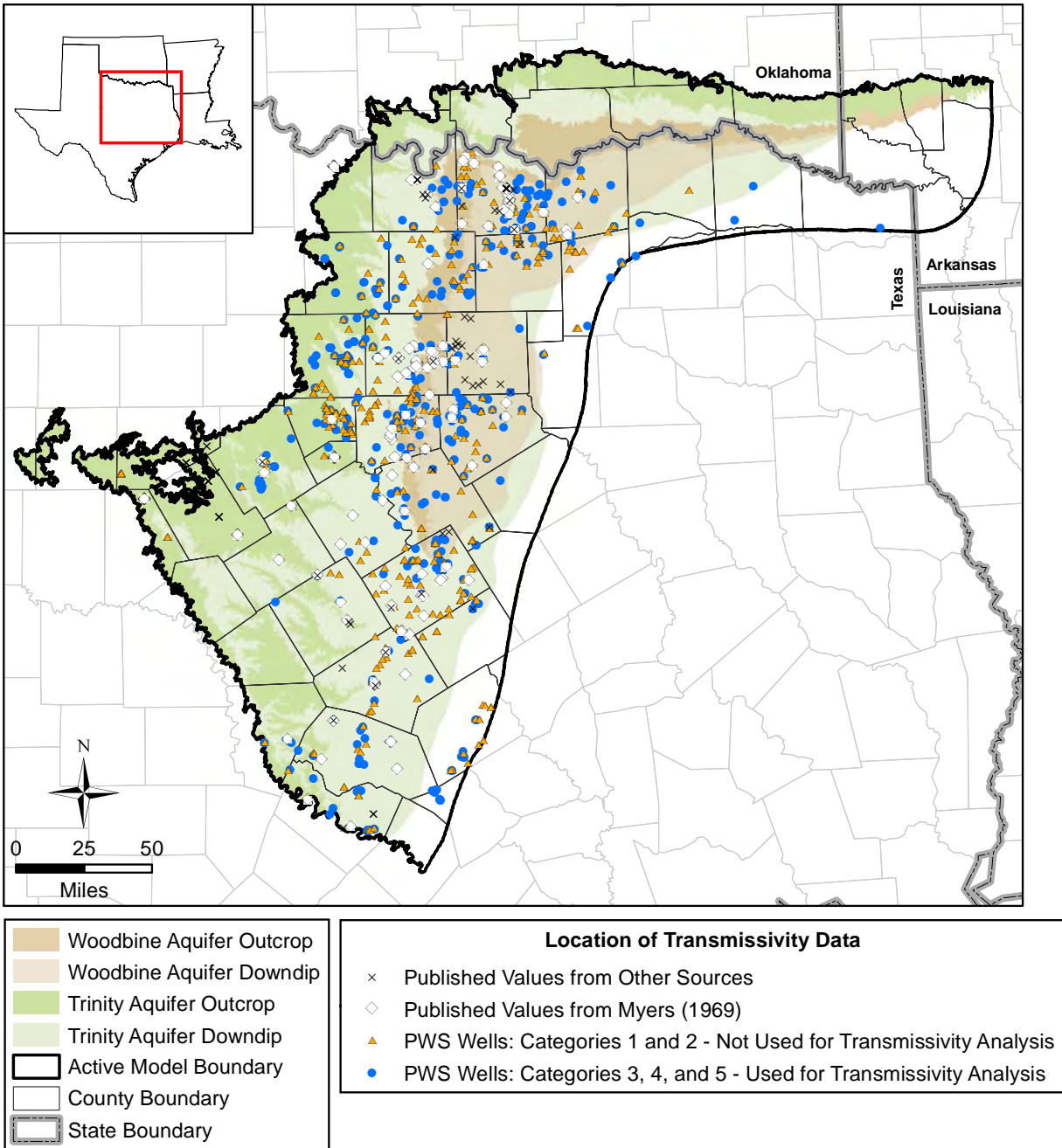
Figure 4.2.3   Spatial distribution of transmissivity data from PWS aquifer pumping tests and the literature.
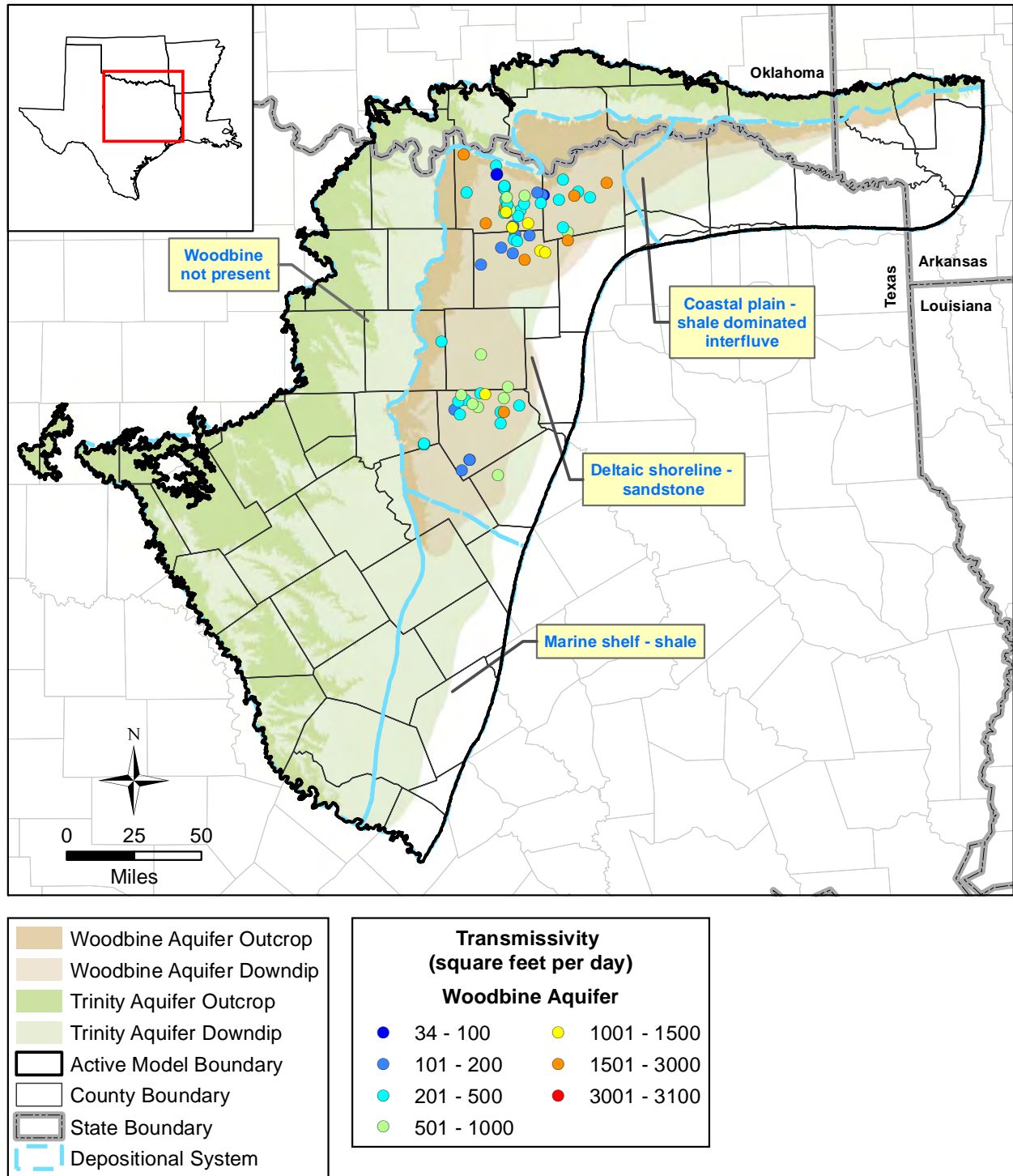
Figure 4.2.4 Spatial distribution of transmissivity values from aquifer pumping tests for the Woodbine Aquifer.
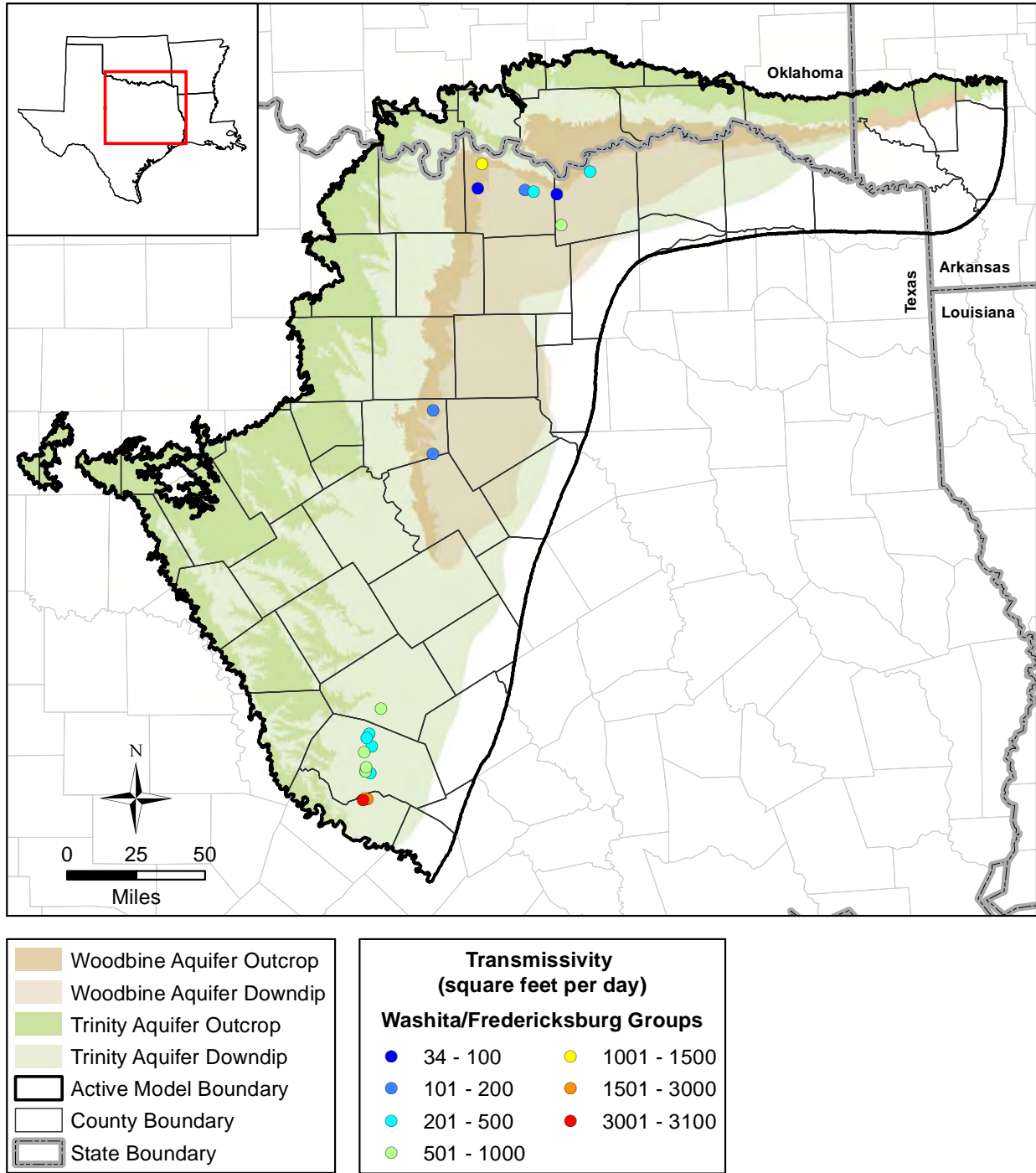
Figure 4.2.5 **Spatial distribution of transmissivity values from aquifer pumping tests for the Washita/Fredericksburg groups.**
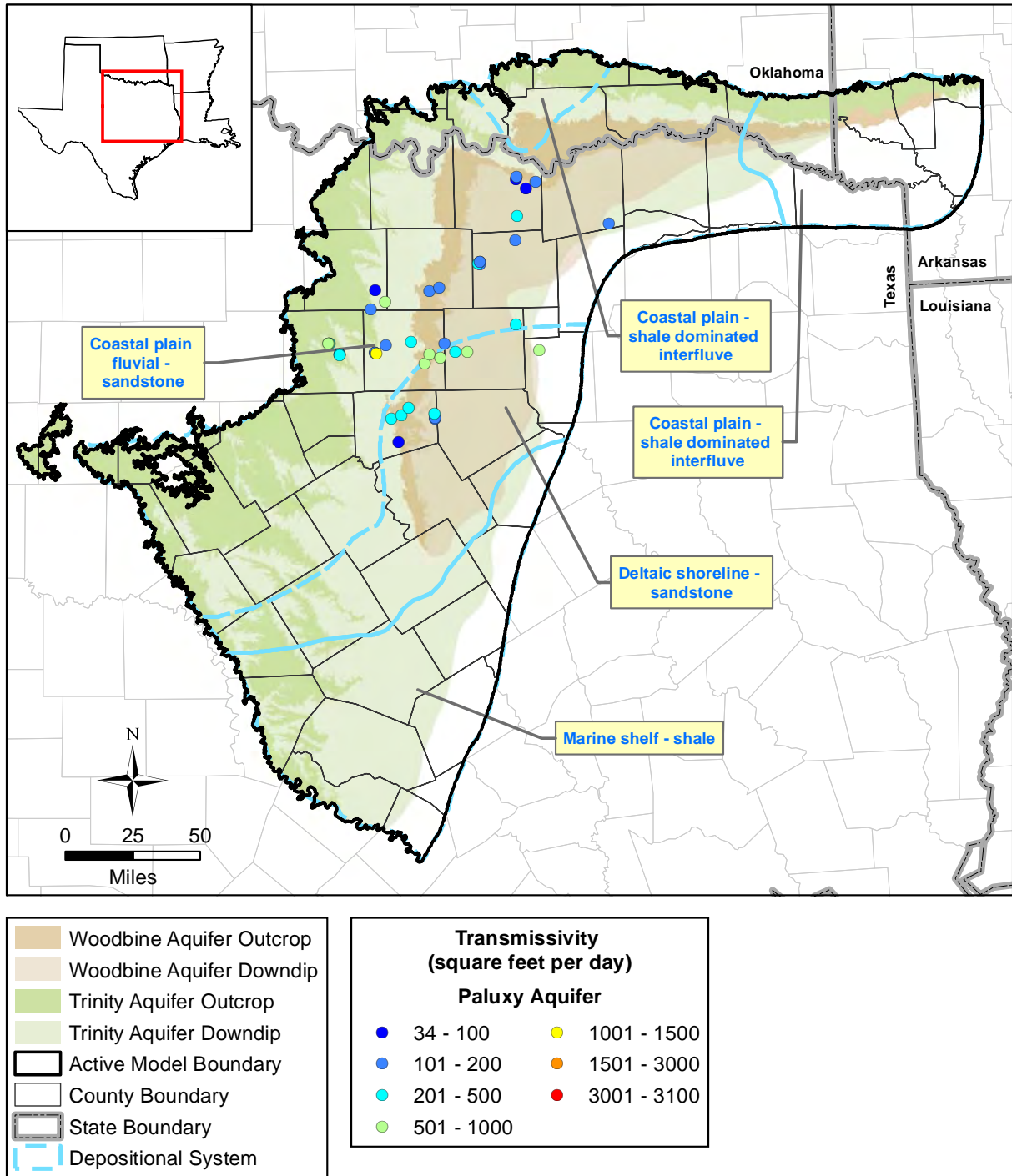
Figure 4.2.6 **Spatial distribution of transmissivity values from aquifer pumping tests for the Paluxy Aquifer.**
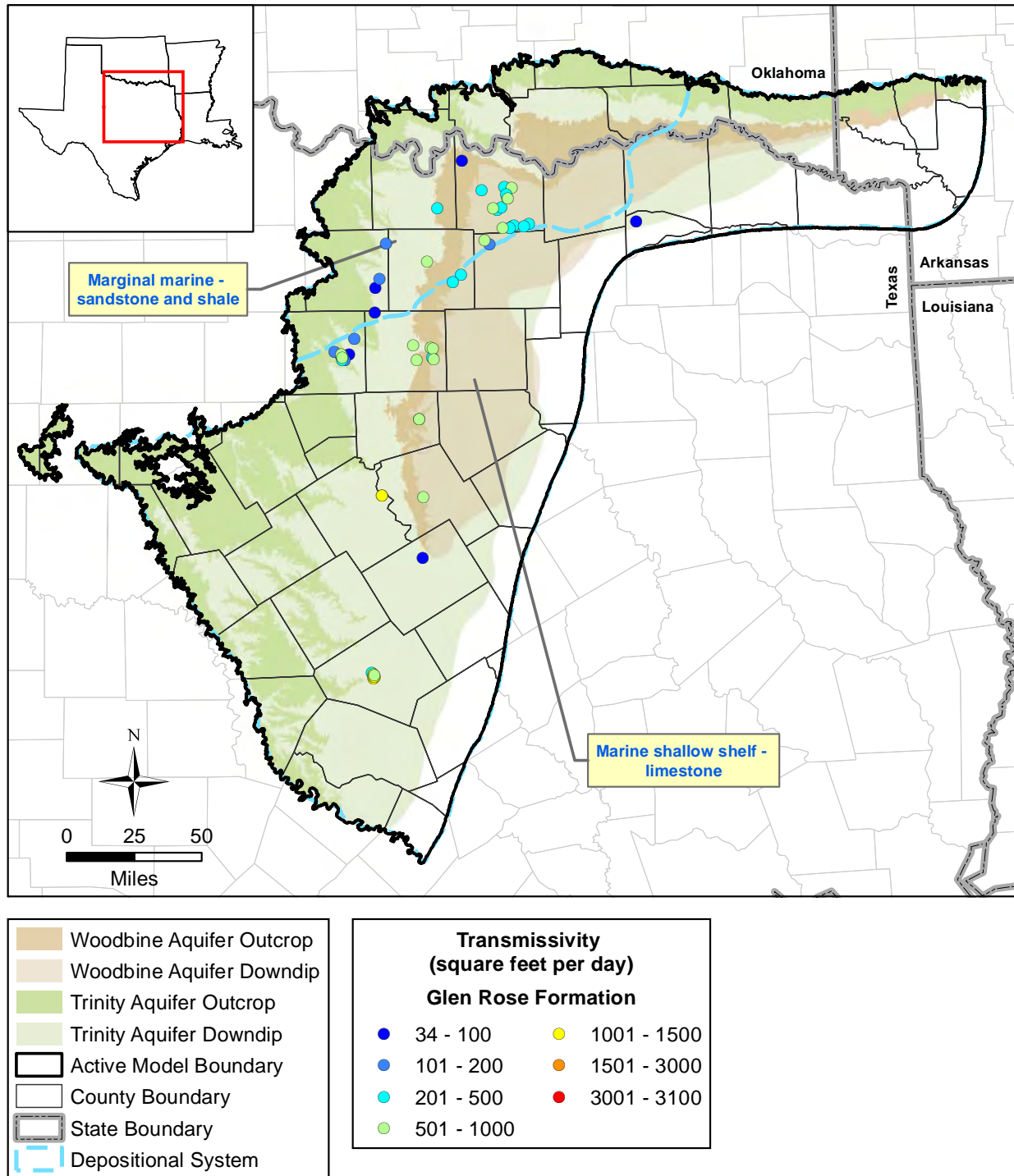
Figure 4.2.7 **Spatial distribution of transmissivity values from aquifer pumping tests for the Glen Rose Formation.**
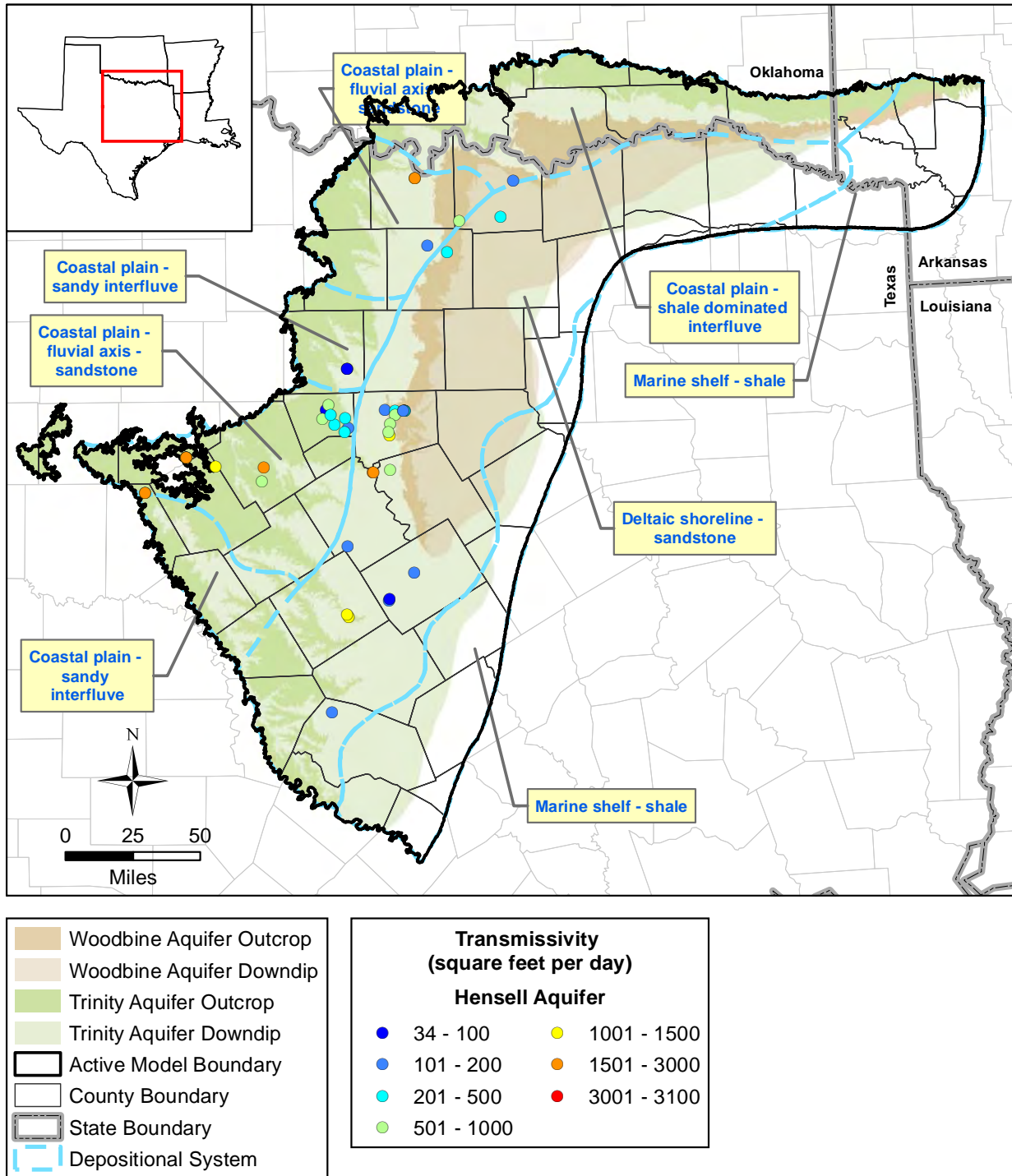
Figure 4.2.8 Spatial distribution of transmissivity values from aquifer pumping tests for the Hensell Aquifer.
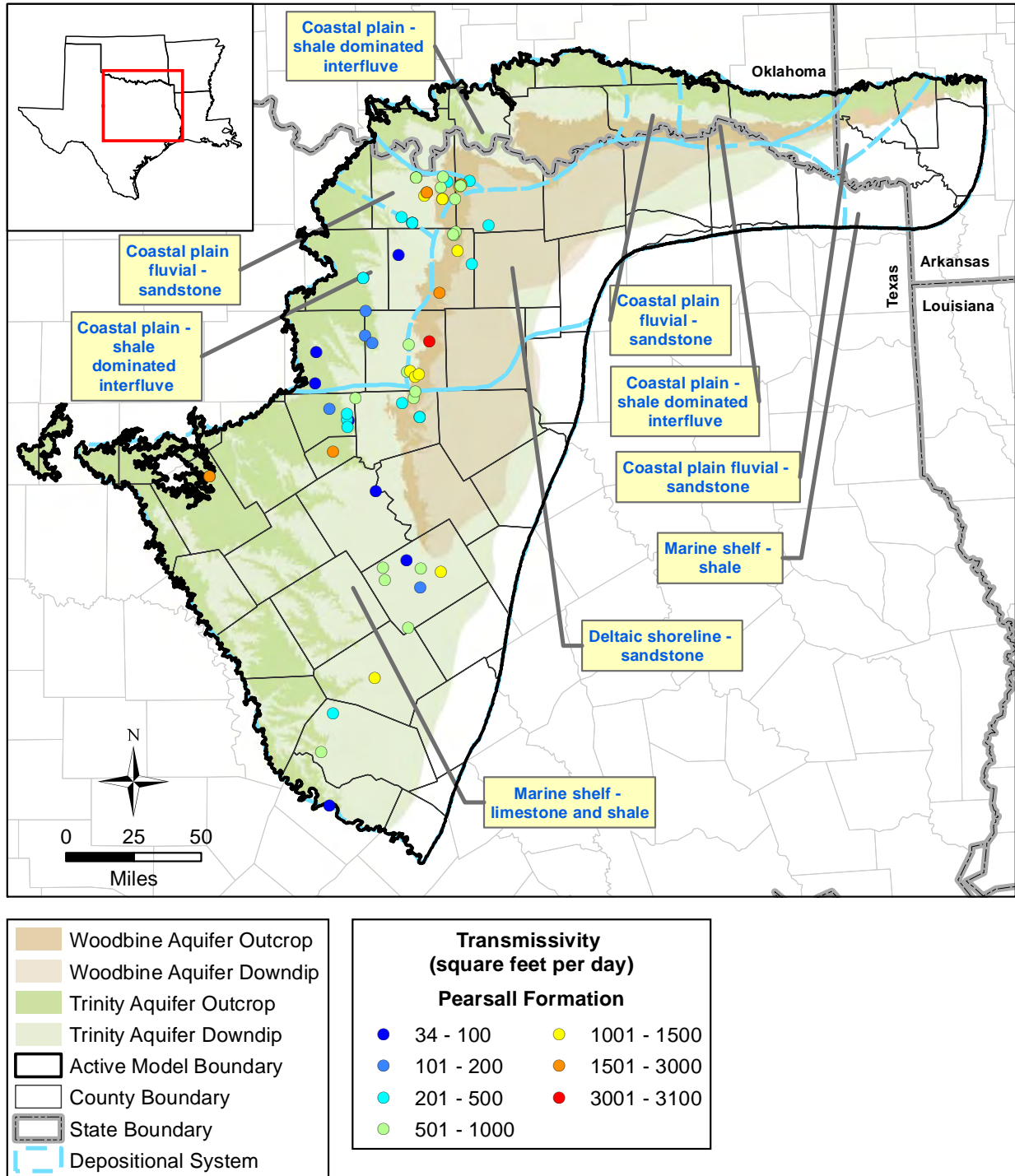
Figure 4.2.9 **Spatial distribution of transmissivity values from aquifer pumping tests for the Pearsall Formation.**
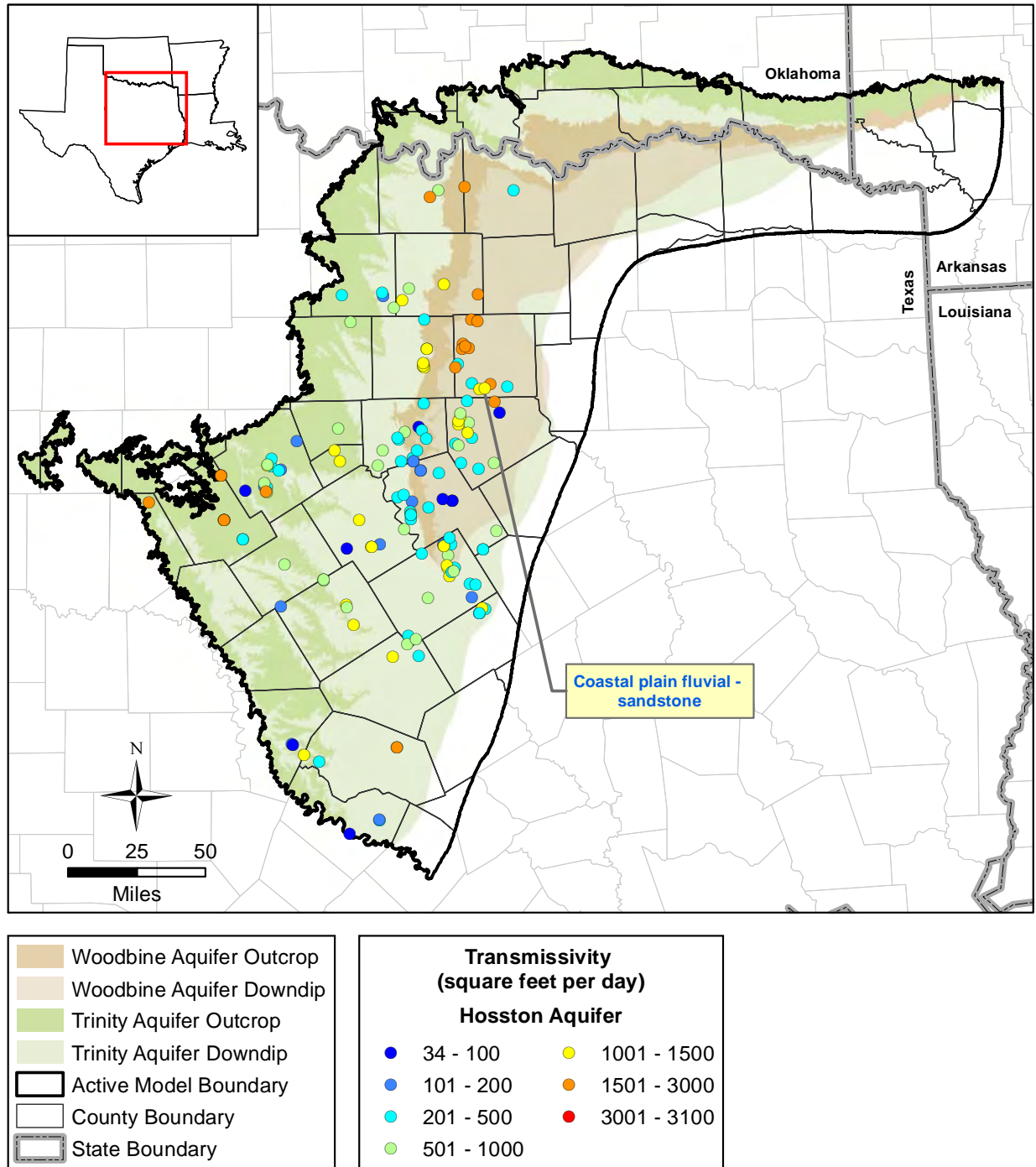
Figure 4.2.10 **Spatial distribution of transmissivity values from aquifer pumping tests for the Hosston Aquifer.**
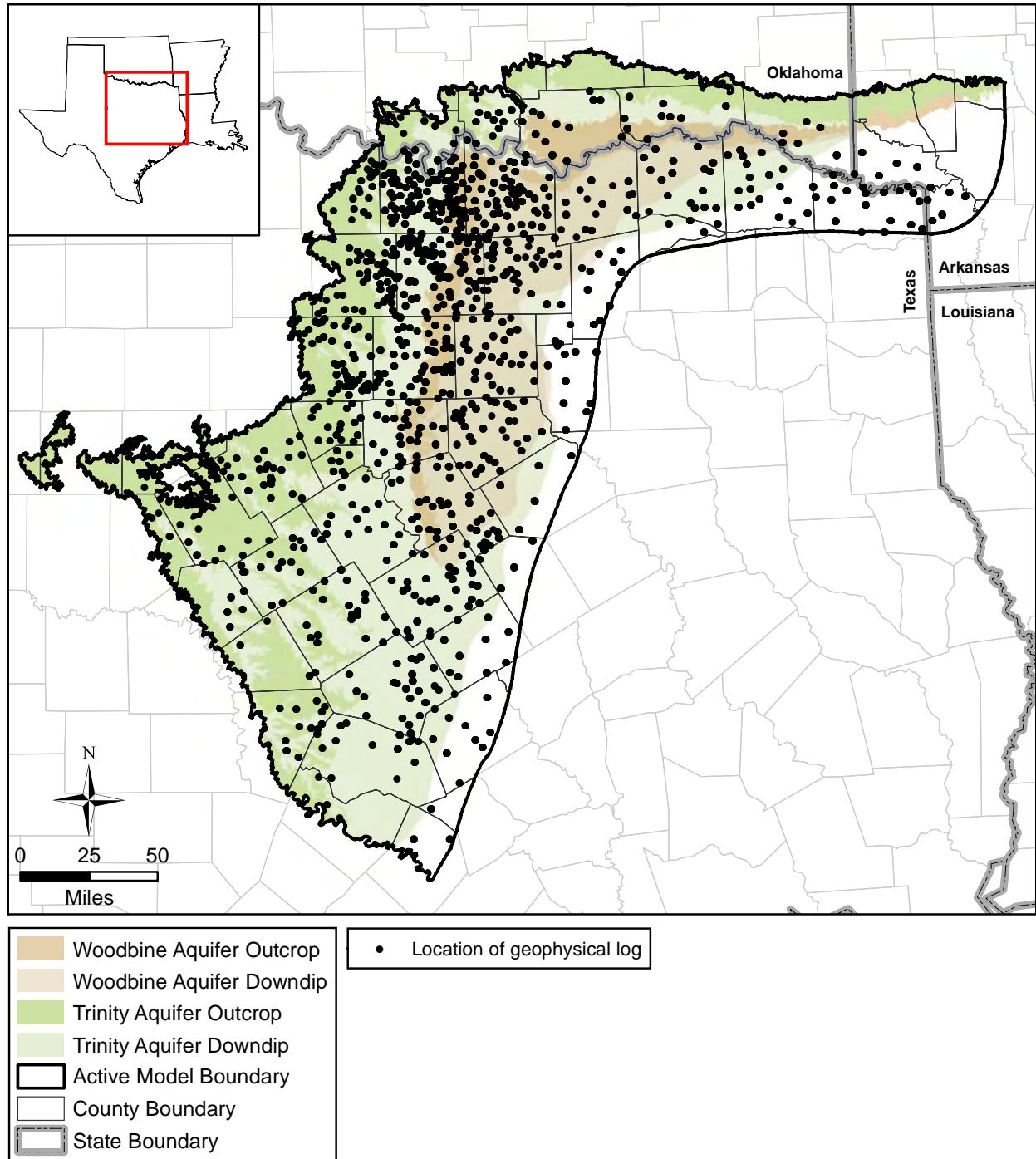
Figure 4.2.11   Location of geophysical logs used to calculate lithology profiles.
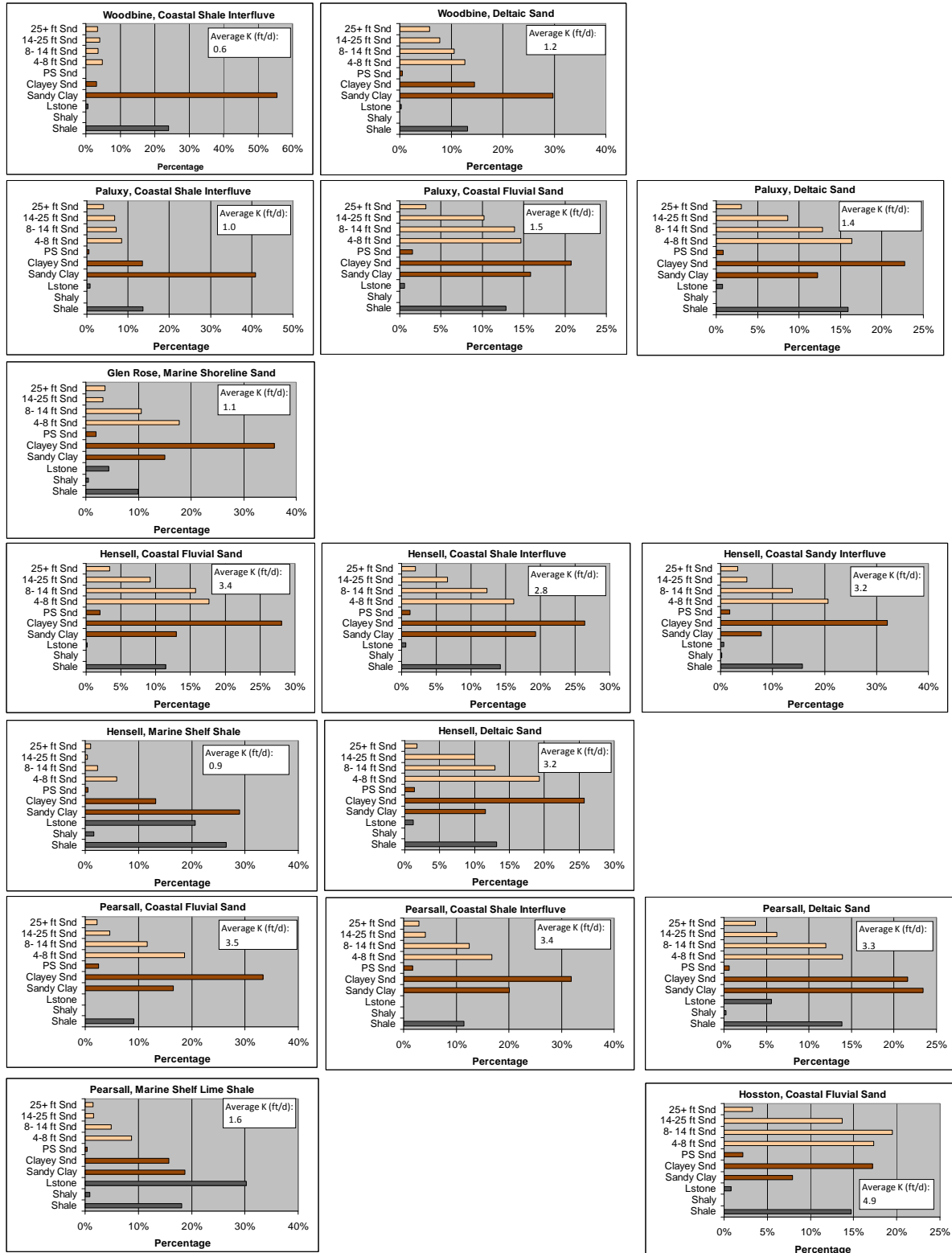
K(ft/d) = hydraulic conductivity in feet per day

Figure 4.2.12 **Percent distribution of the 10 litho-units (see Table 4.2.6) in the sandy depositional systems associated with the Woodbine, Paluxy, Hensell, and Hosston aquifers and the Glen Rose and Pearsall formations.**
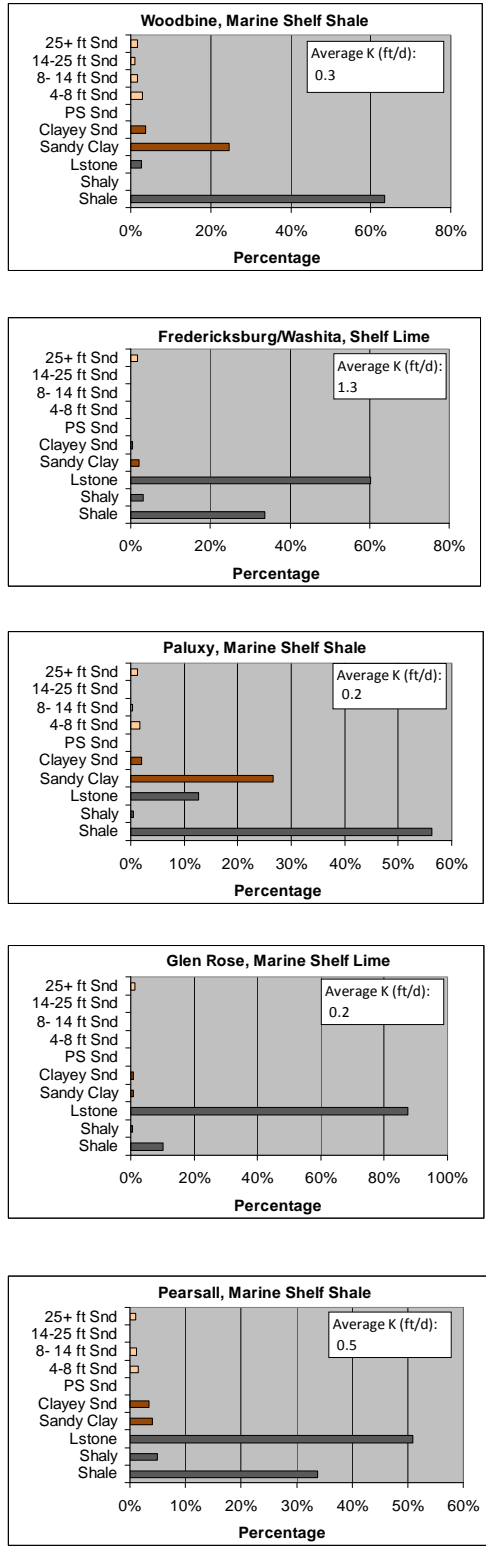
K(ft/d) = hydraulic conductivity in feet per day

Figure 4.2.13   Percent distribution of the 10 litho-units (see Table 4.2.6) in the shaley depositional systems association with the Woodbine Aquifer, Washita/Fredericksburg groups, Paluxy Aquifer, Glen Rose Formation, and Pearsall Formation.
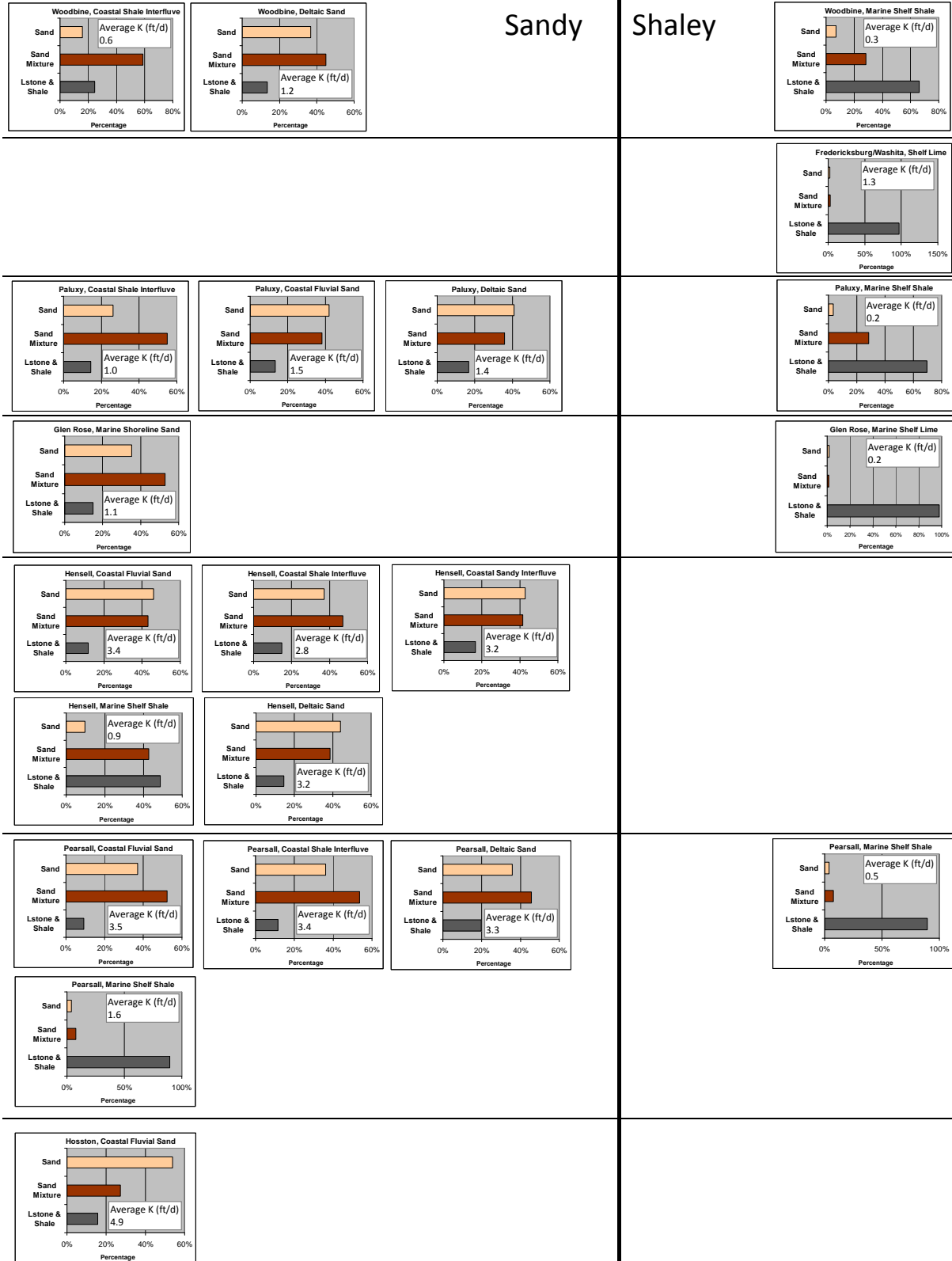
K(ft/d) = hydraulic conductivity in feet per day

Figure 4.2.14   Percent distribution of three major litho-units in the sandy and shaley depositional systems associated with the aquifers/formations.
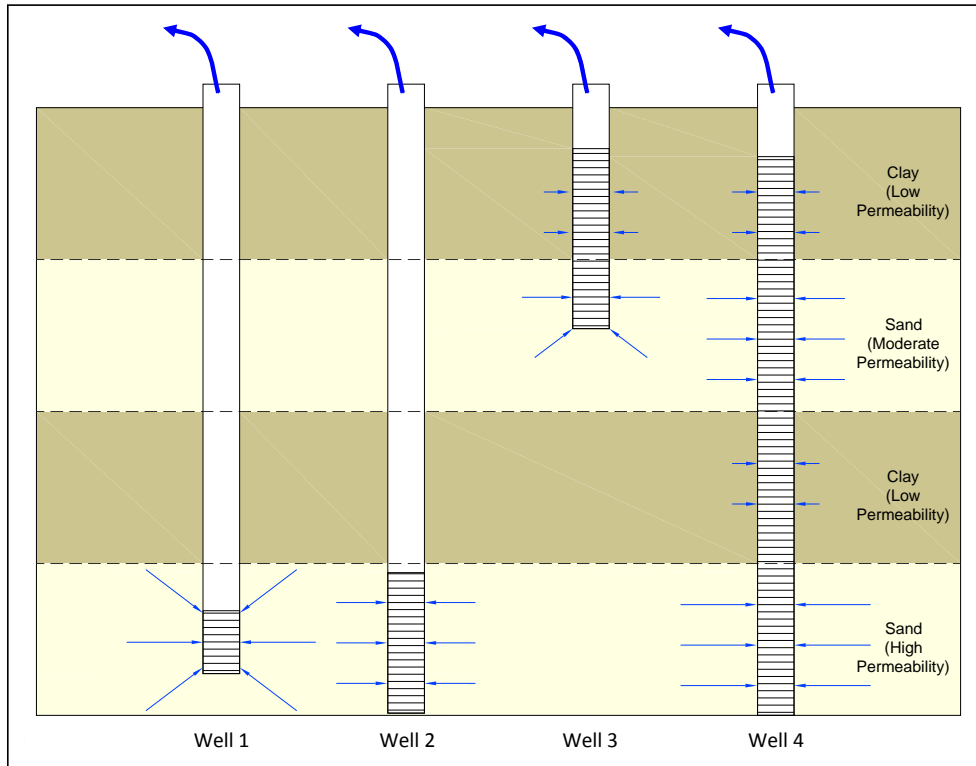
Figure 4.2.15   Schematic showing groundwater flow to four wells screened across different intervals of an aquifer.
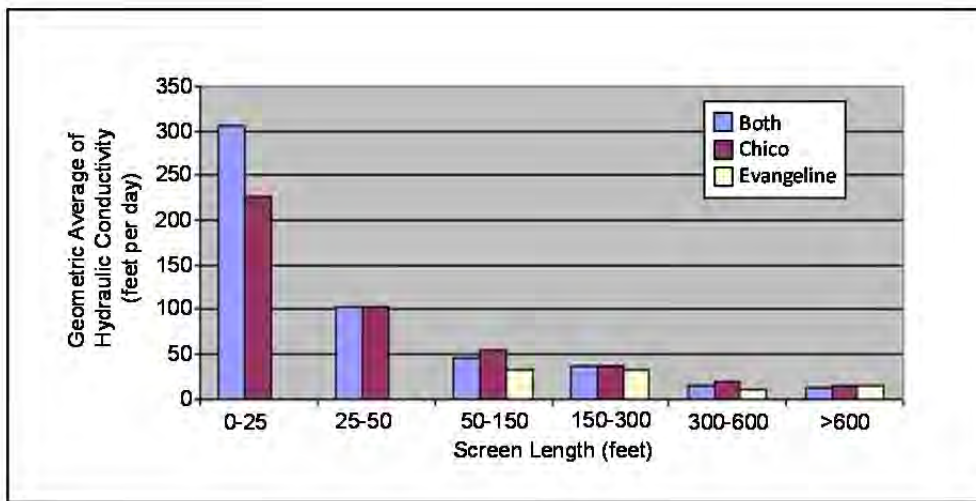
Figure 4.2.16   Sensitivity of hydraulic conductivity calculated from transmissivity and well screen length to screen length (modified from Young and Kelley, 2006).
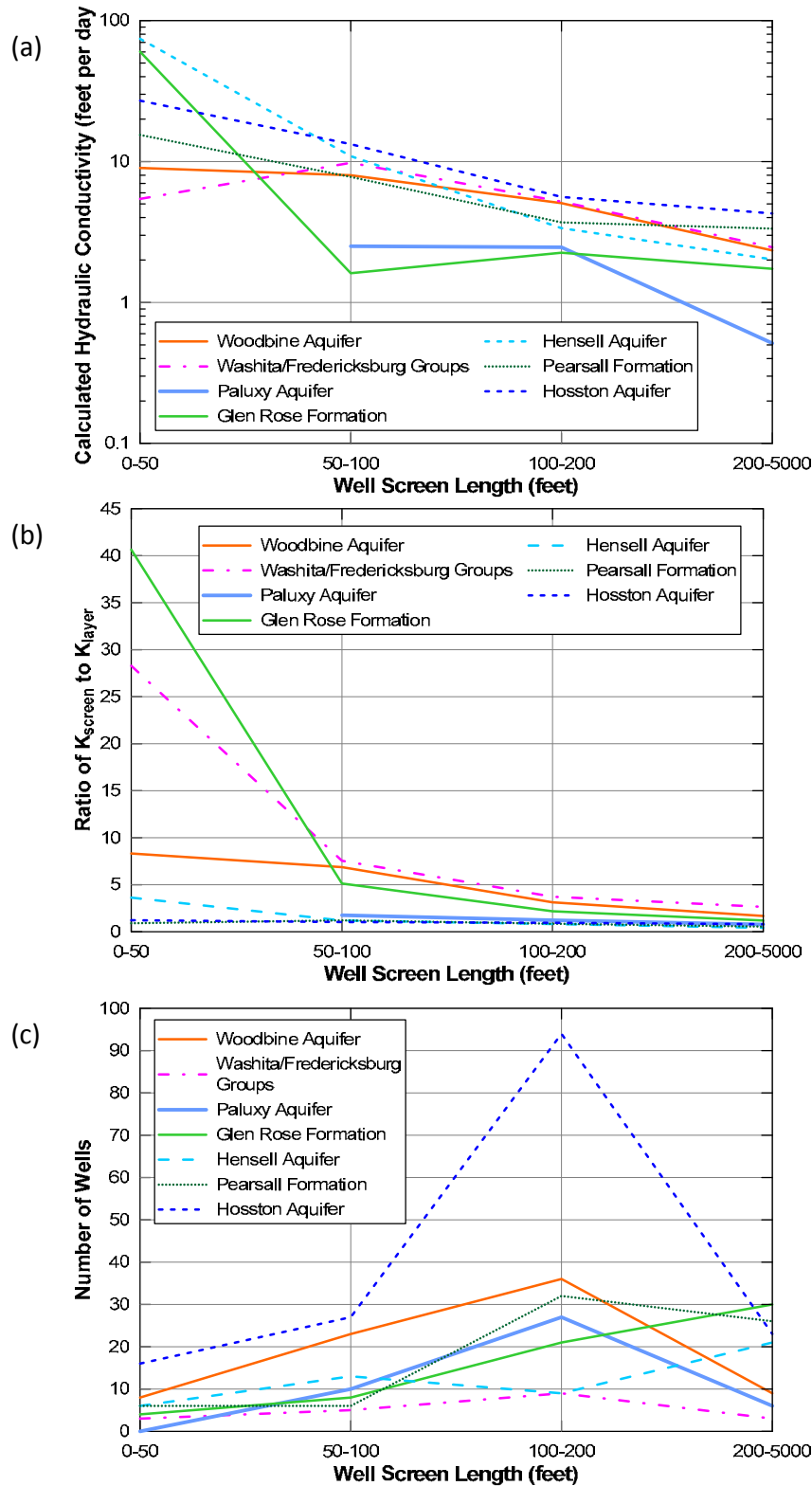
Figure 4.2.17 **From aquifer pumping tests for this study, (a) sensitivity of calculated hydraulic conductivity values to length of well screen interval, (b) sensitivity of K_{screen} to K_{layer} to length of well screen interval, and (c) number of wells per of well screen interval lengths.**
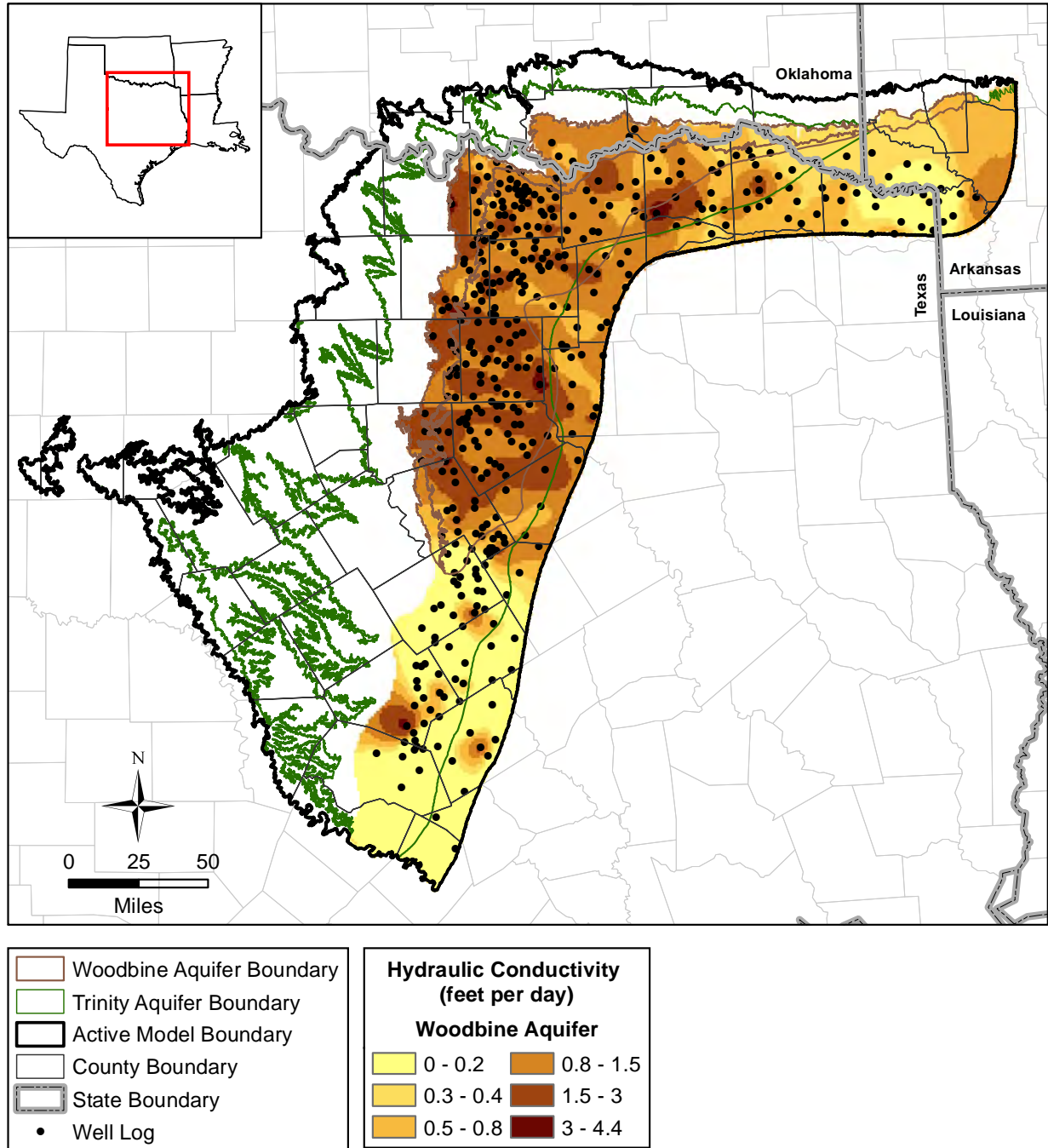
**Figure 4.2.18   Baseline estimate of the hydraulic conductivity distribution for the Woodbine
Aquifer from the GHS model.**
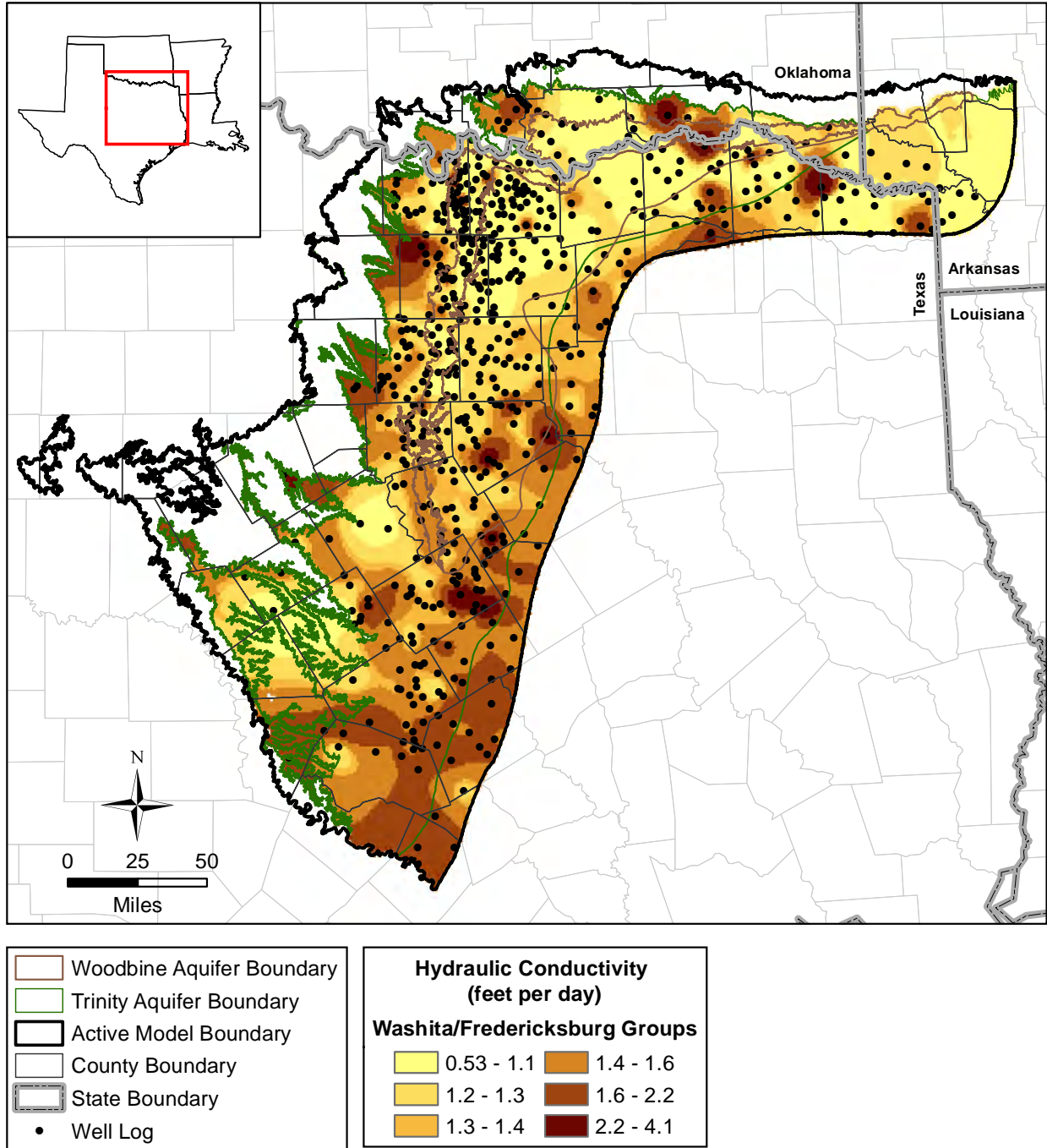
Figure 4.2.19 **Baseline estimate of the hydraulic conductivity distribution for the Washita/Fredericksburg groups from the GHS model.**
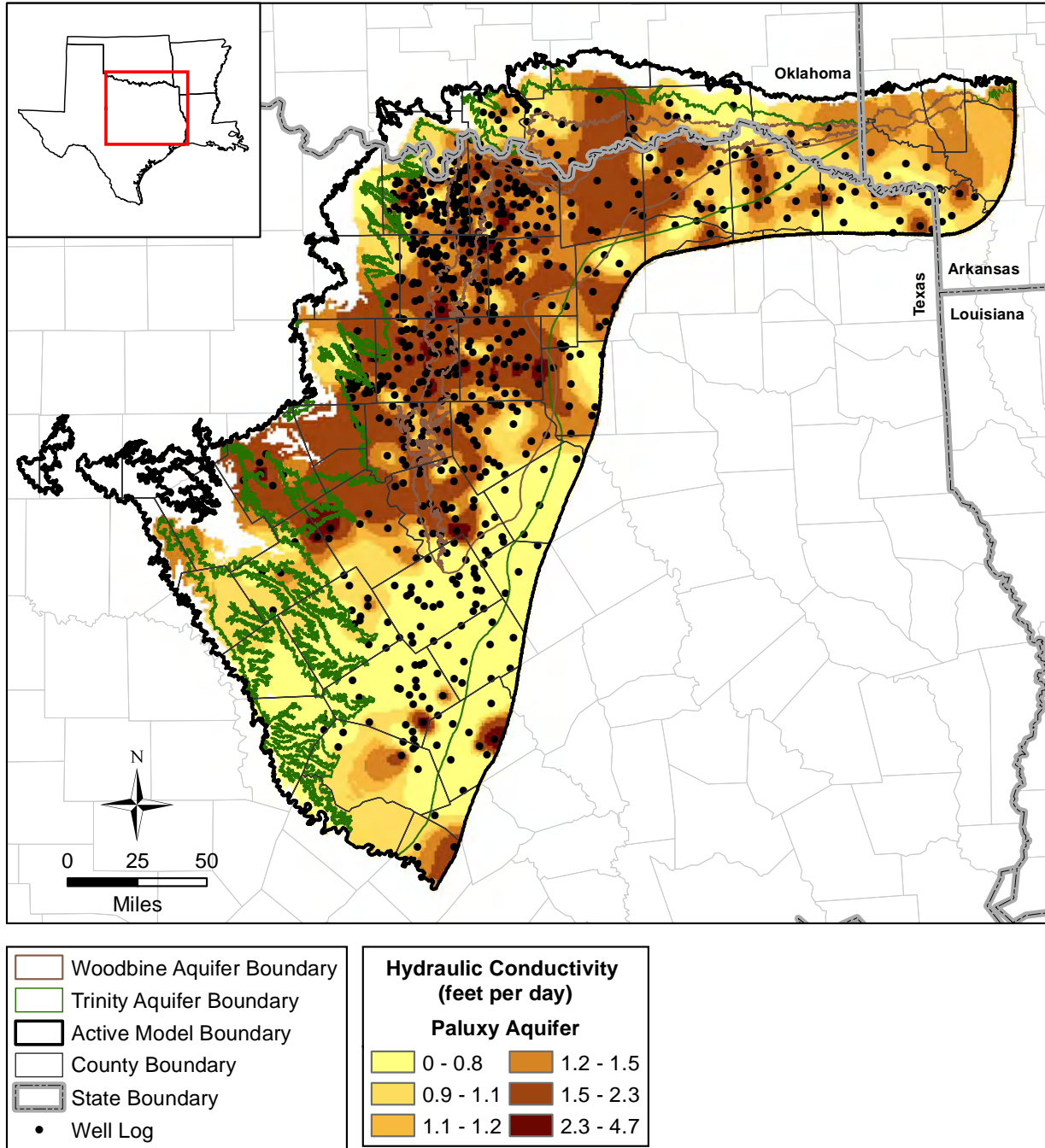
**Figure 4.2.20   Baseline estimate of the hydraulic conductivity distribution for the Paluxy Aquifer
from the GHS model.**
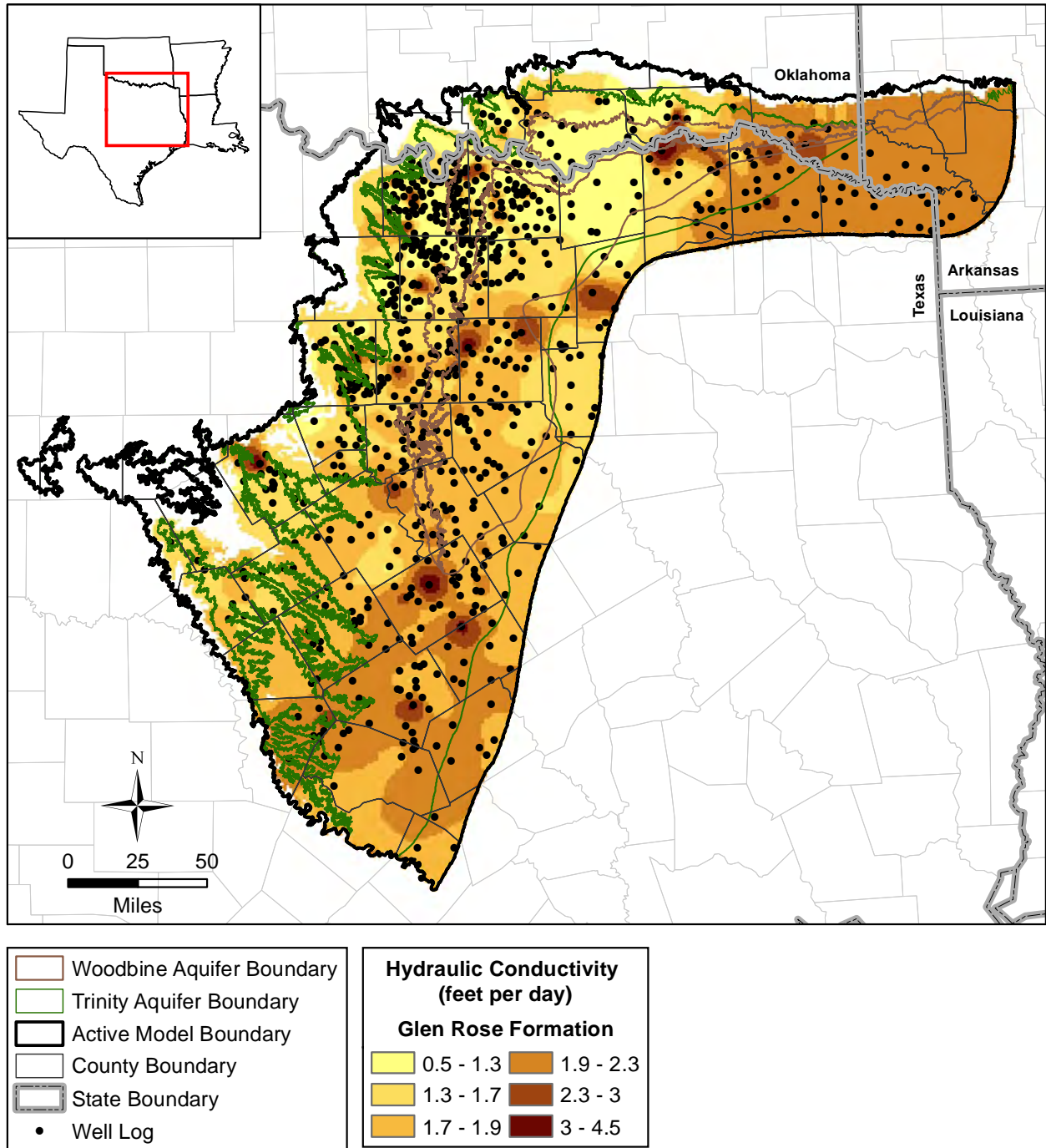
Figure 4.2.21   Baseline estimate of the hydraulic conductivity distribution for the Glen Rose Formation from the GHS model.
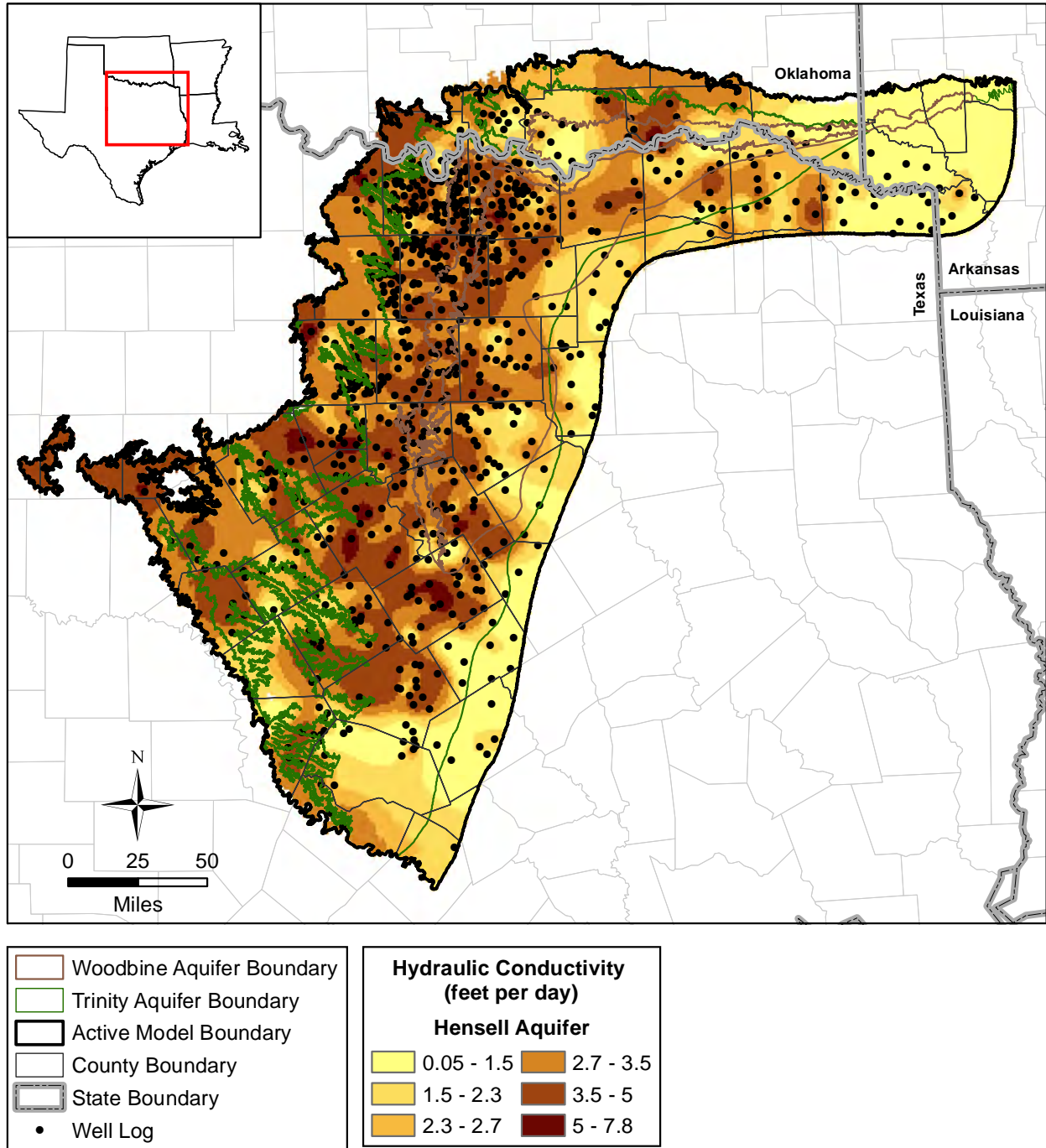
Figure 4.2.22   Baseline estimate of the hydraulic conductivity distribution for the Hensell Aquifer from the GHS model.
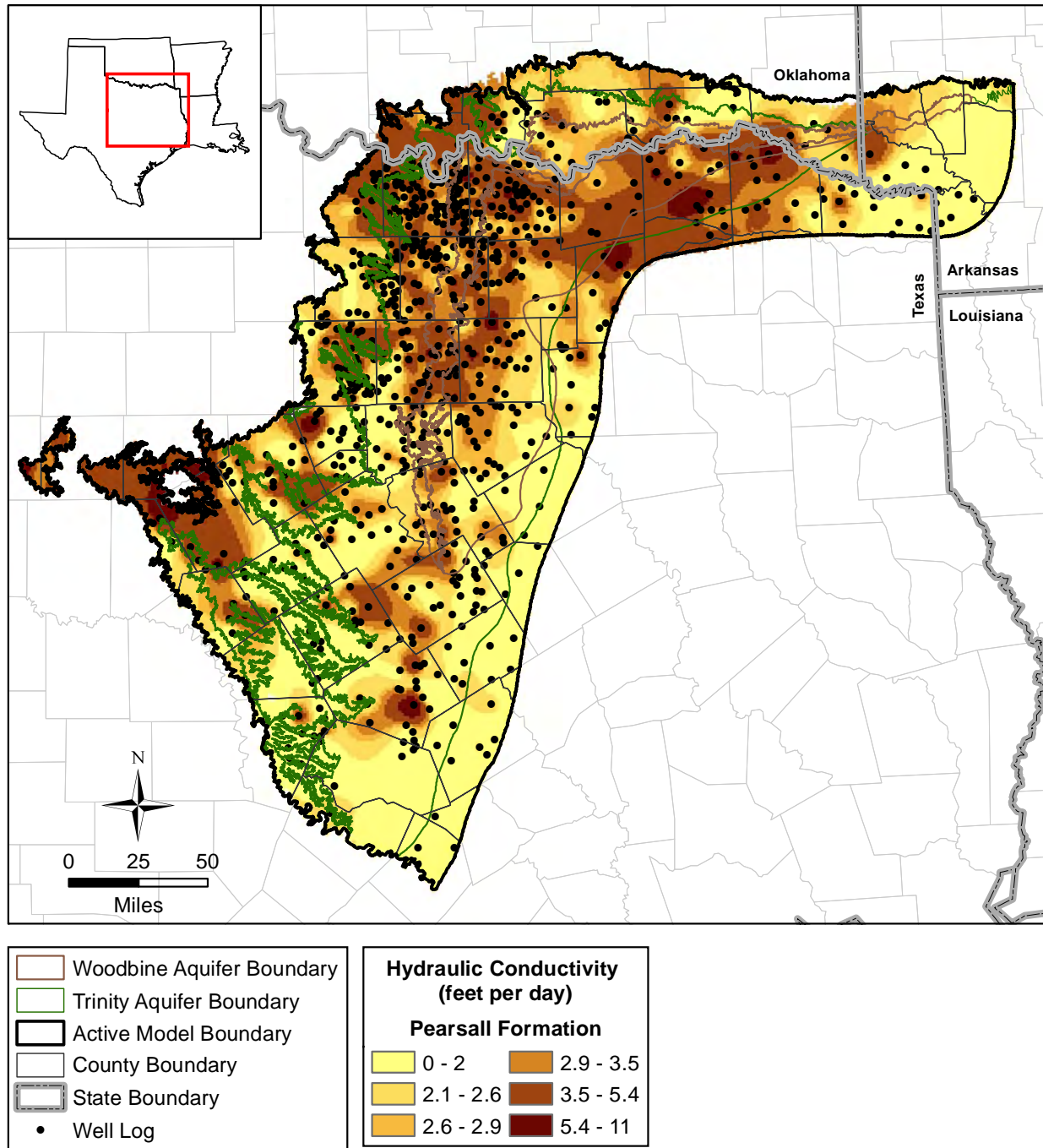
Figure 4.2.23   Baseline estimate of the hydraulic conductivity distribution for the Pearsall Formation from the GHS model.
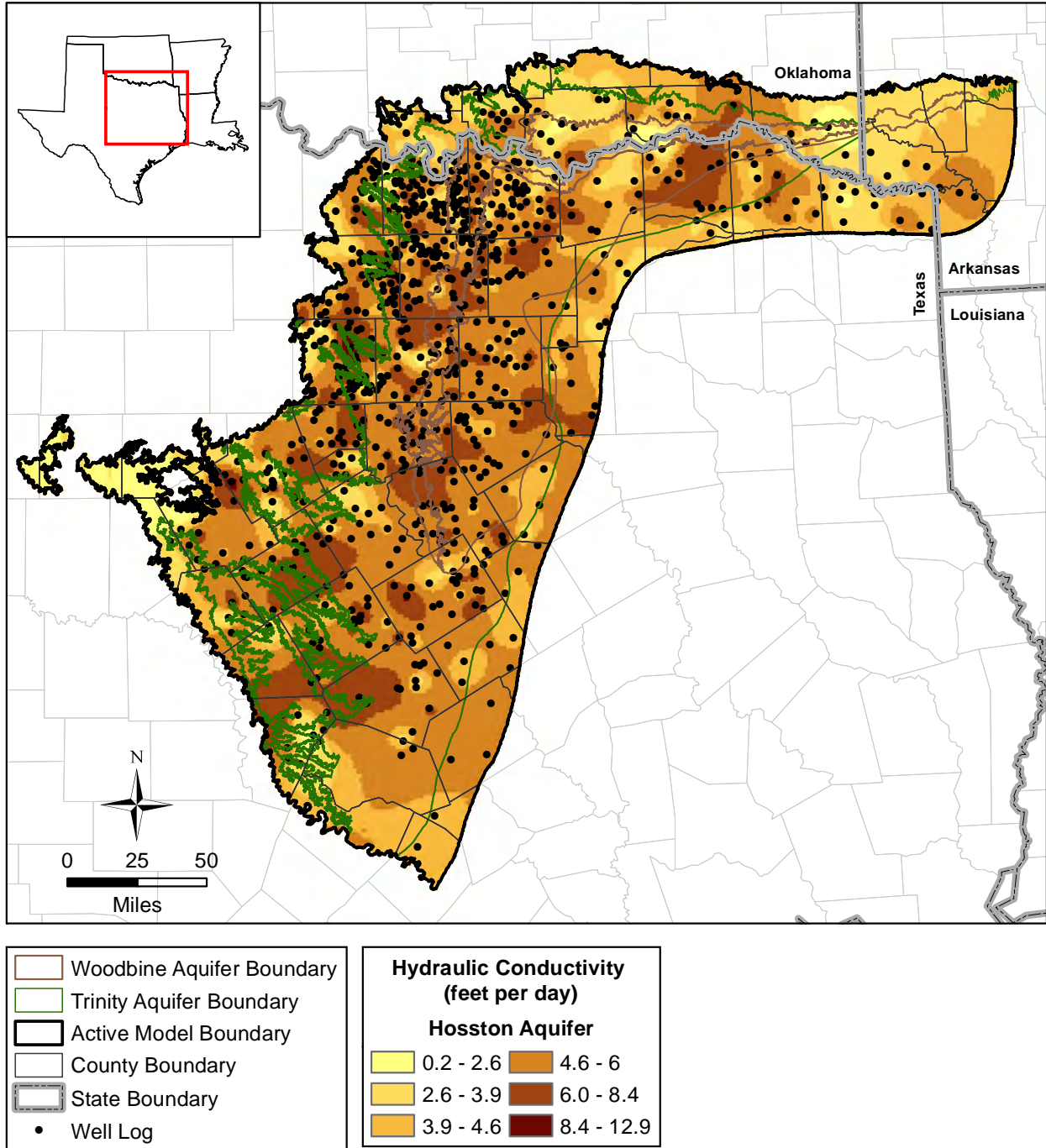
Figure 4.2.24 **Baseline estimate of the hydraulic conductivity distribution for the Hosston Aquifer from the GHS model.**
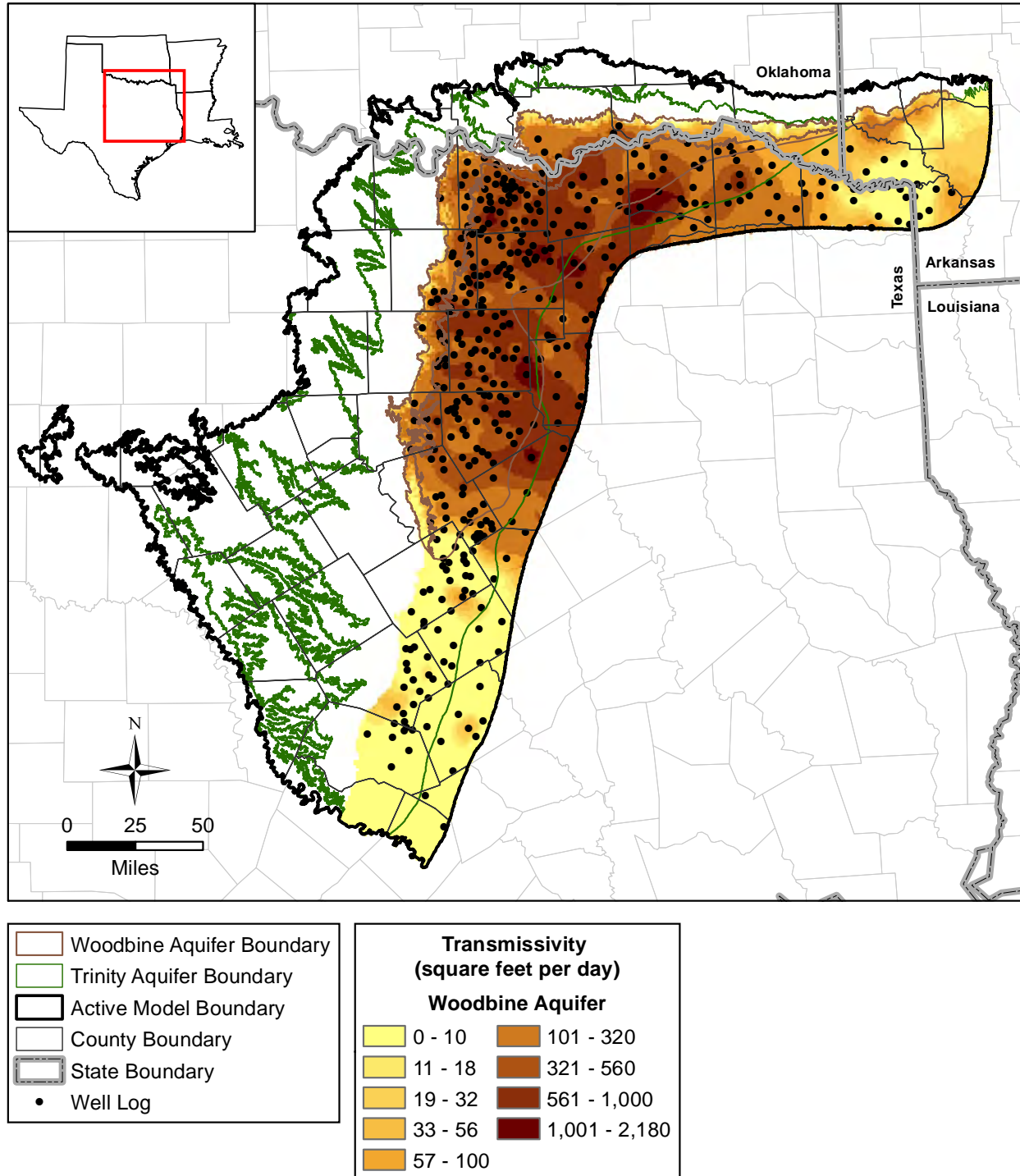
Figure 4.2.25   Baseline estimate of the transmissivity distribution for the Woodbine Aquifer from the GHS model.
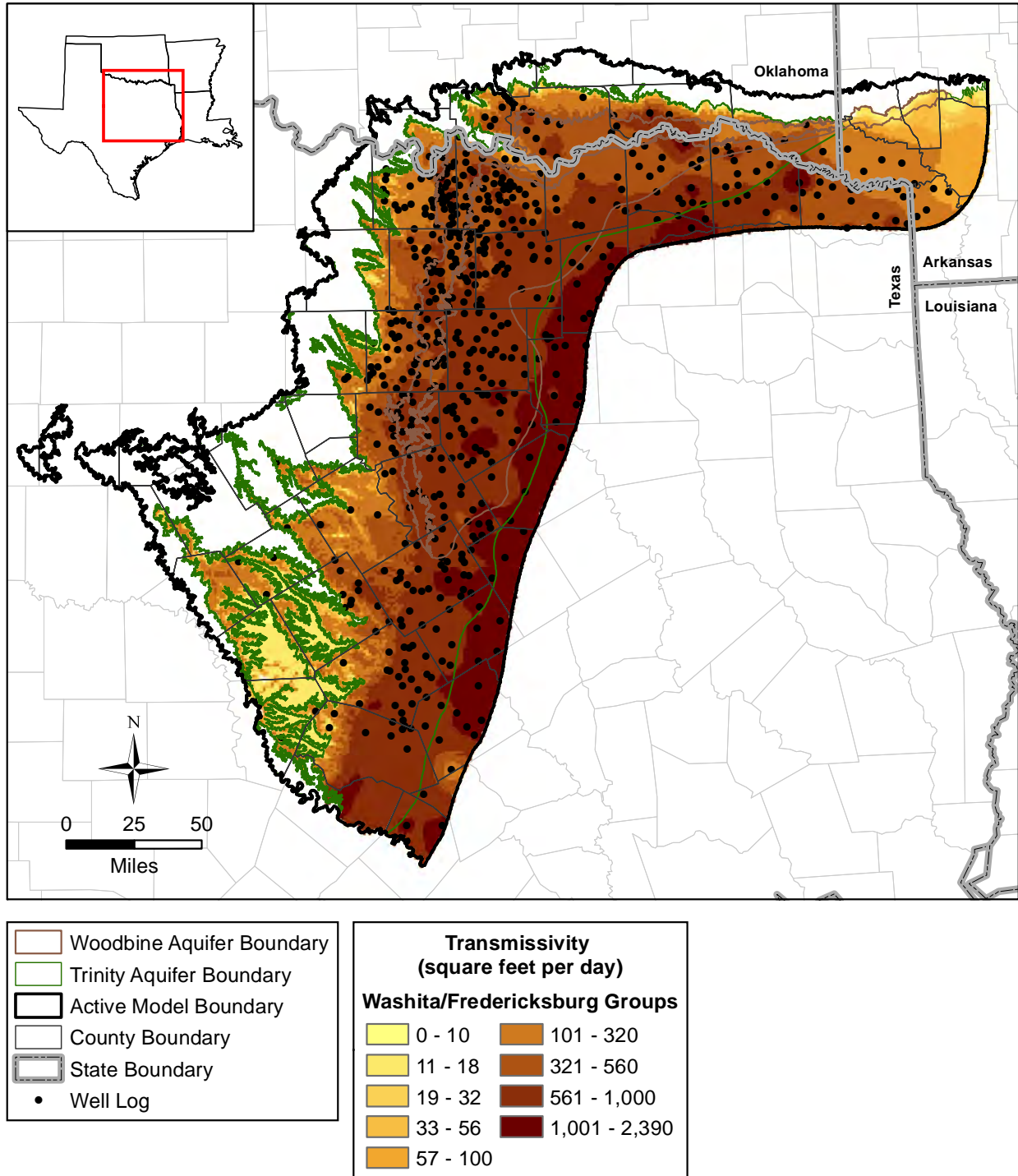
Figure 4.2.26   Baseline estimate of the transmissivity distribution for the Washita/Fredericksburg groups from the GHS model.
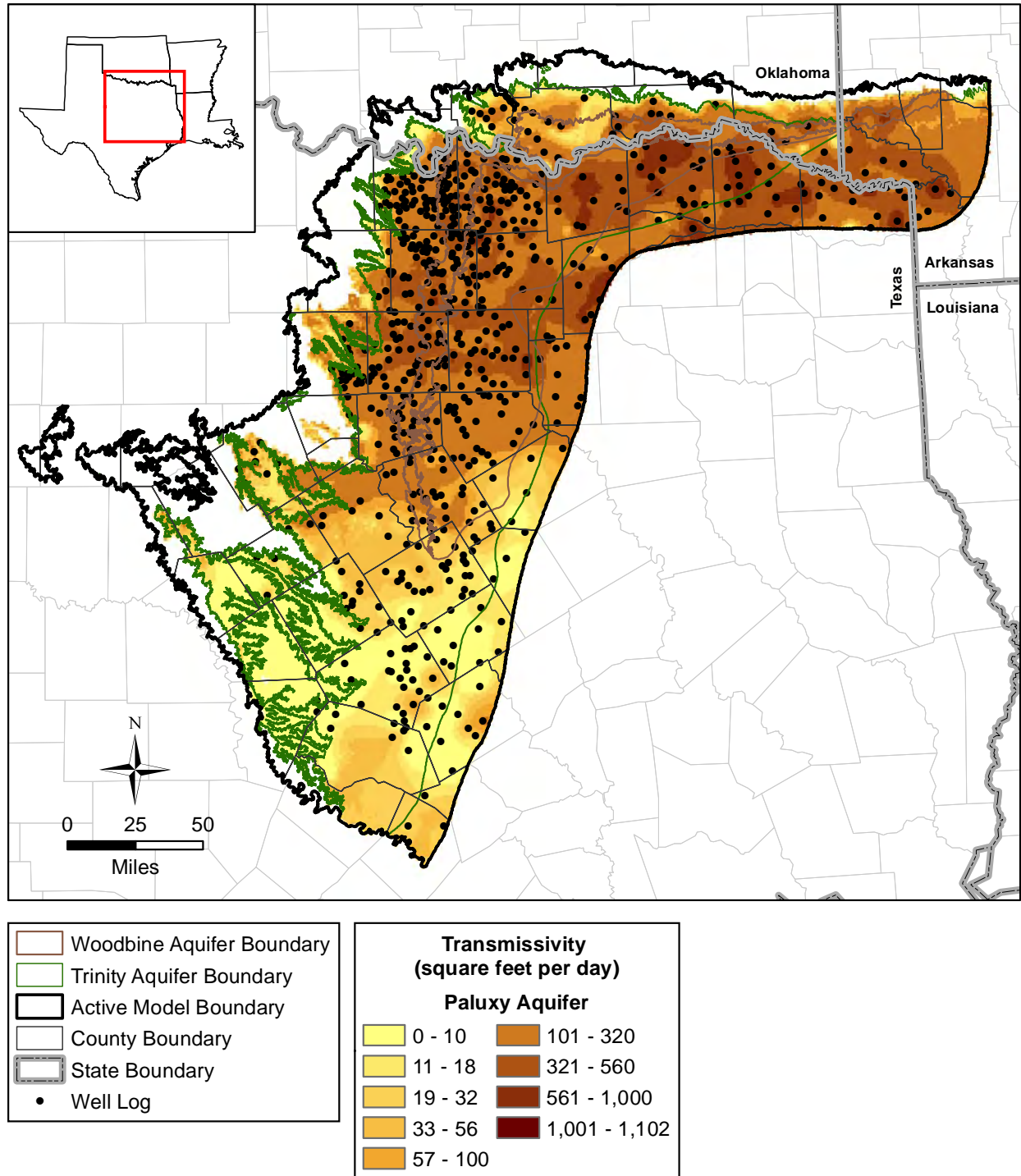
Figure 4.2.27 **Baseline estimate of the transmissivity distribution for the Paluxy Aquifer from the GHS model.**
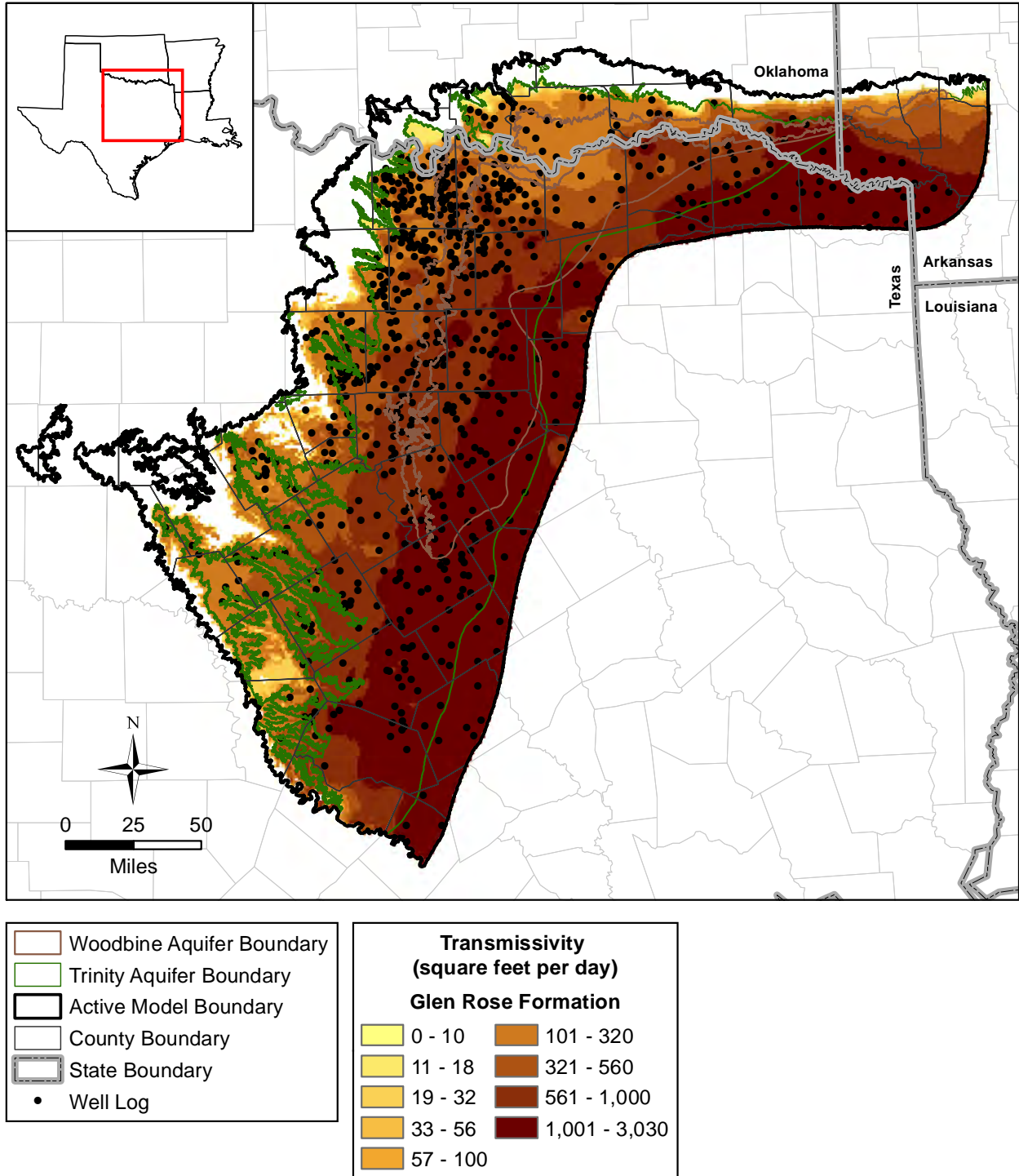
Figure 4.2.28 **Baseline estimate of the transmissivity distribution for the Glen Rose Formation from the GHS model.**
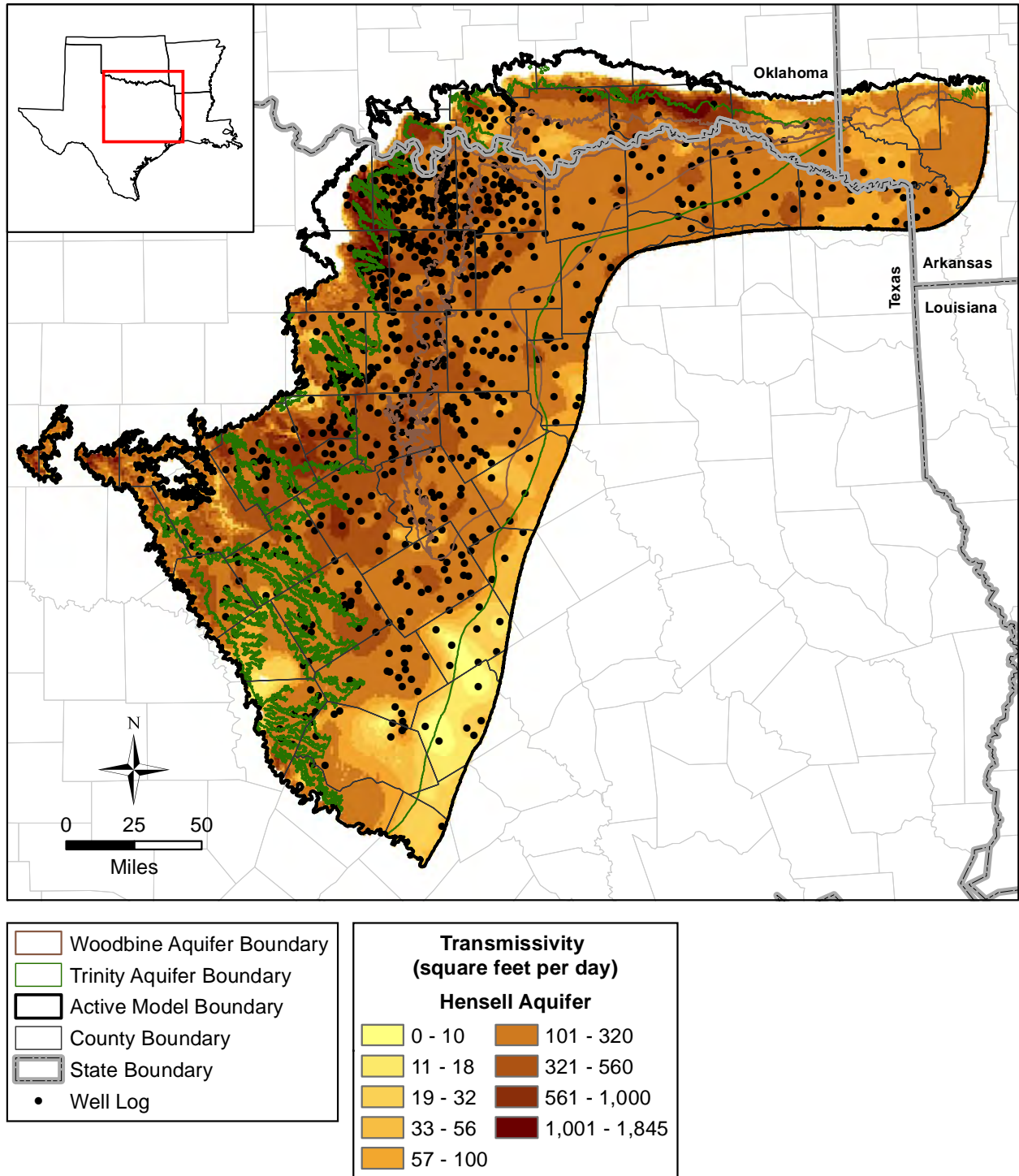
Figure 4.2.29   Baseline estimate of the transmissivity distribution for the Hensell Aquifer from the GHS model.
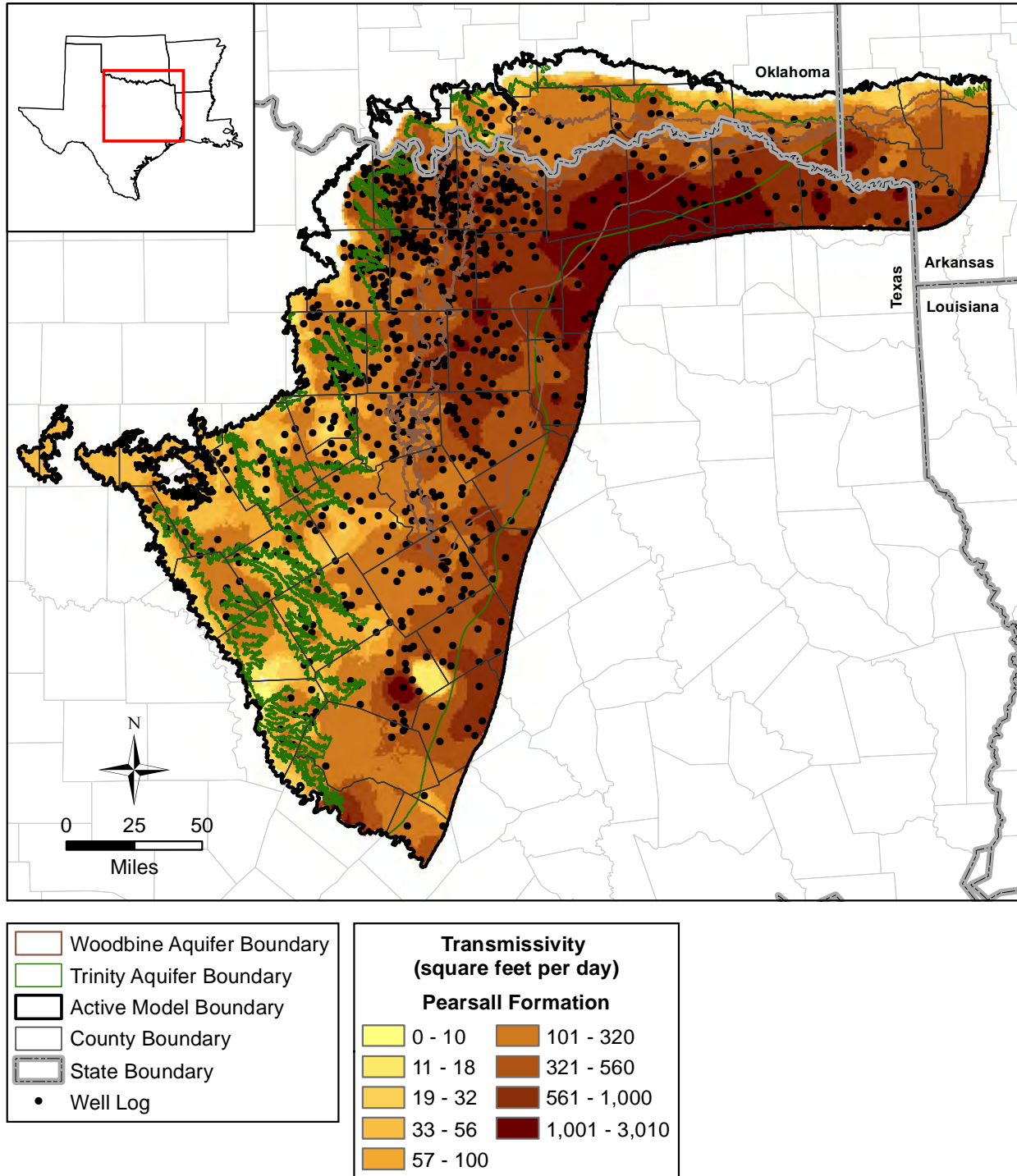
Figure 4.2.30 **Baseline estimate of the transmissivity distribution for the Pearsall Formation from the GHS model.**
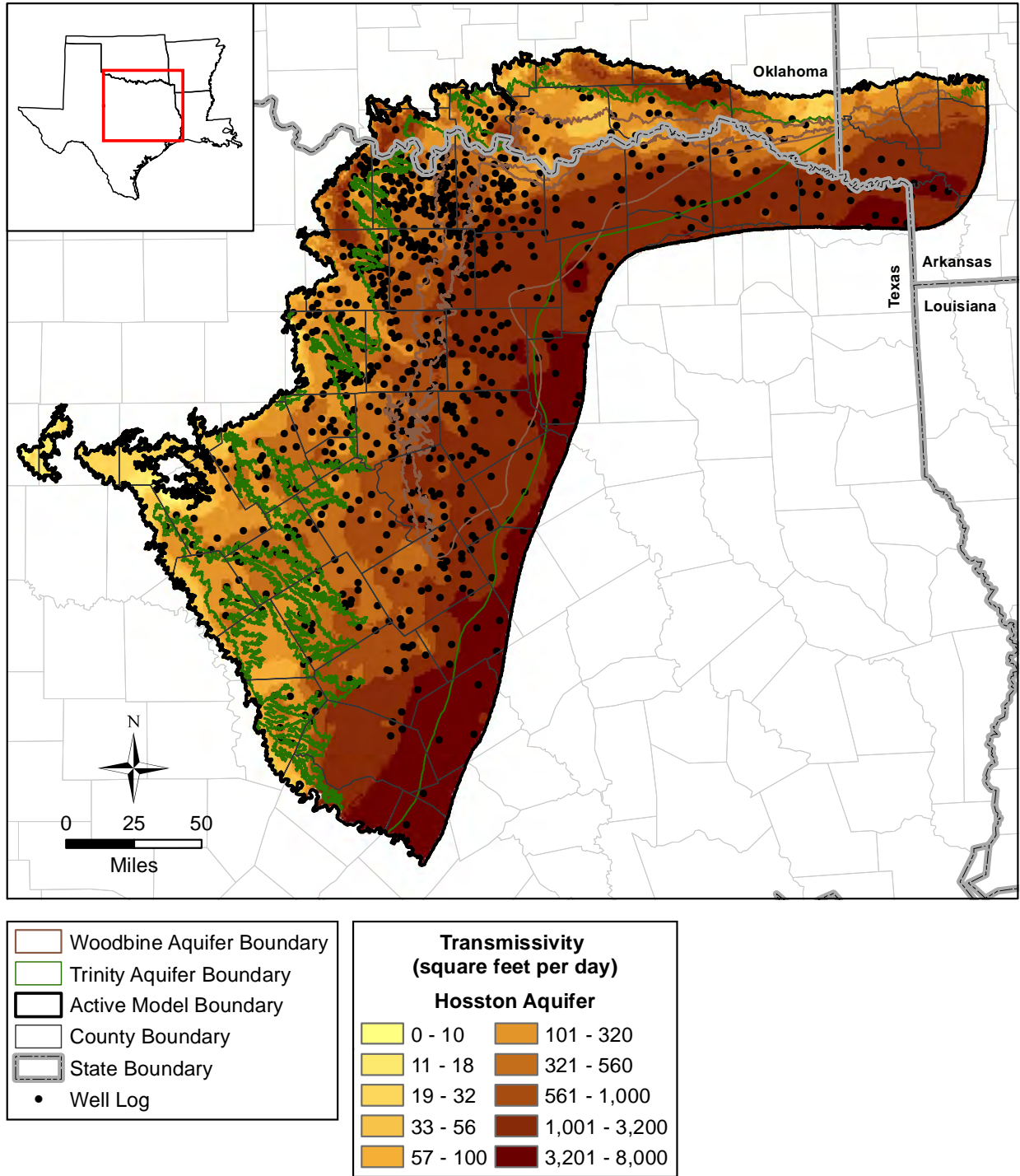
Figure 4.2.31   Baseline estimate of the transmissivity distribution for the Hosston Aquifer from the GHS model.
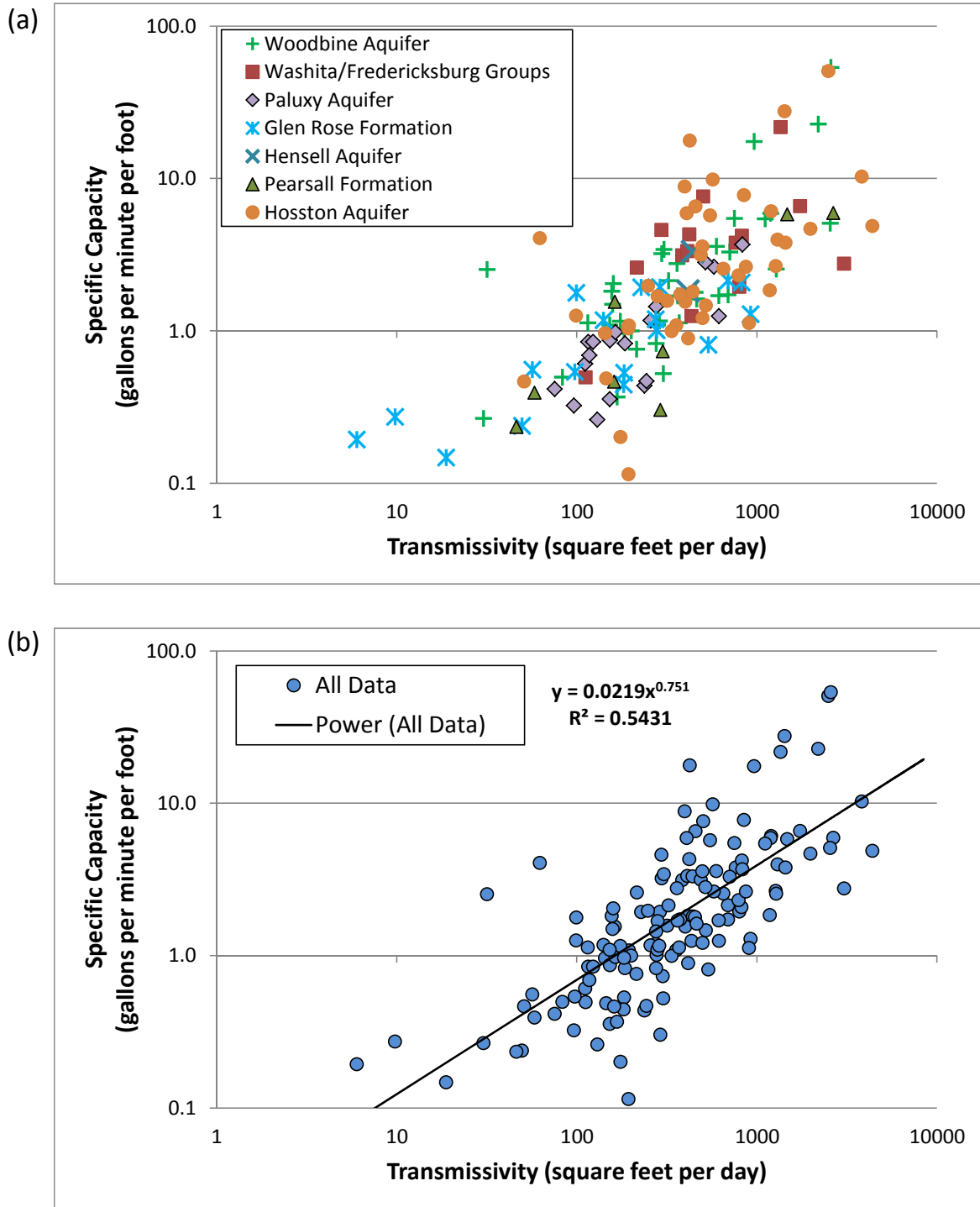
Figure 4.2.32 **Relationship between specific capacity and transmissivity (a) by aquifer/formation and (b) for all data combined.**
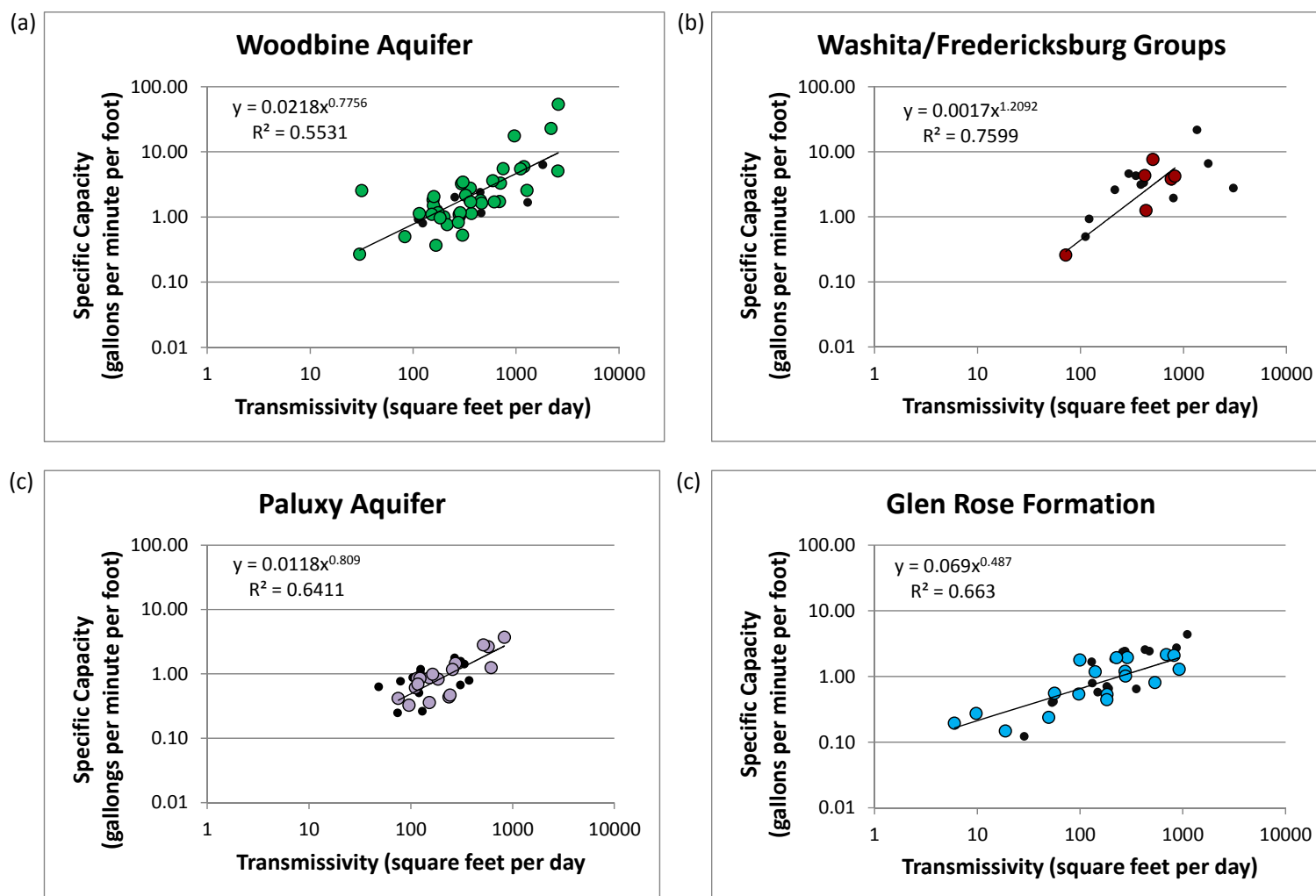
Figure 4.2.33 **Relationship between specific capacity and transmissivity for the (a) Woodbine Aquifer, (b) Washita/Fredericksburg groups, (c) Paluxy Aquifer, and (d) Glen Rose Formation. The large symbols represent data for wells meeting the 80 percent coverage criteria and the small symbols represent data for wells not meeting the 80 percent coverage criteria.**
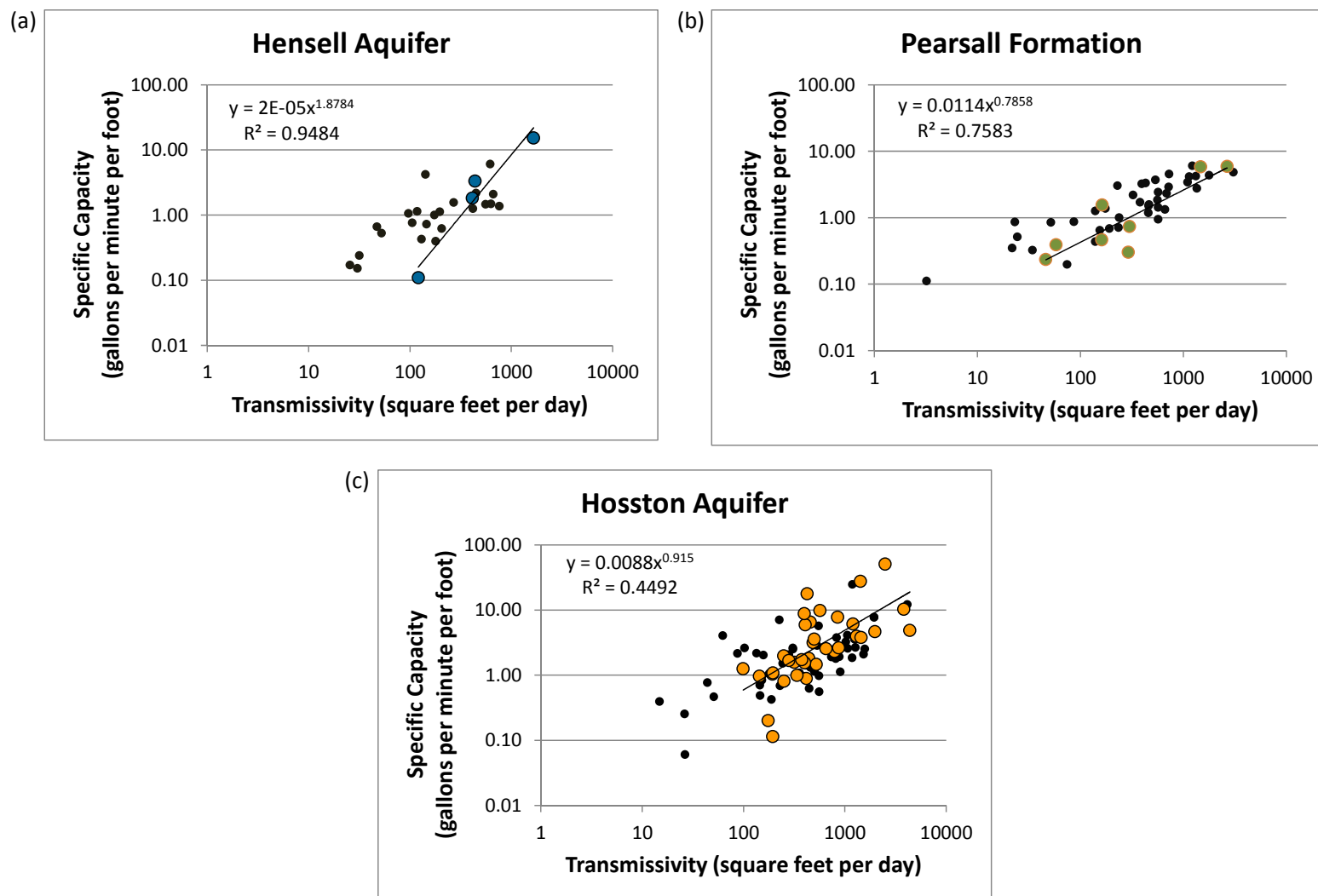
Figure 4.2.34 **Relationship between specific capacity and transmissivity for the (a) Hensell Aquifer, (b) Pearsall Formation, and (c) Hosston Aquifer. The large symbols represent data for wells meeting the 80 percent coverage criteria and the small symbols represent data for wells not meeting the 80 percent coverage criteria.**
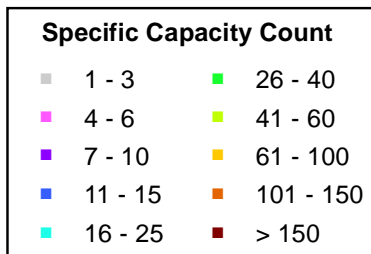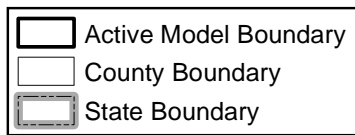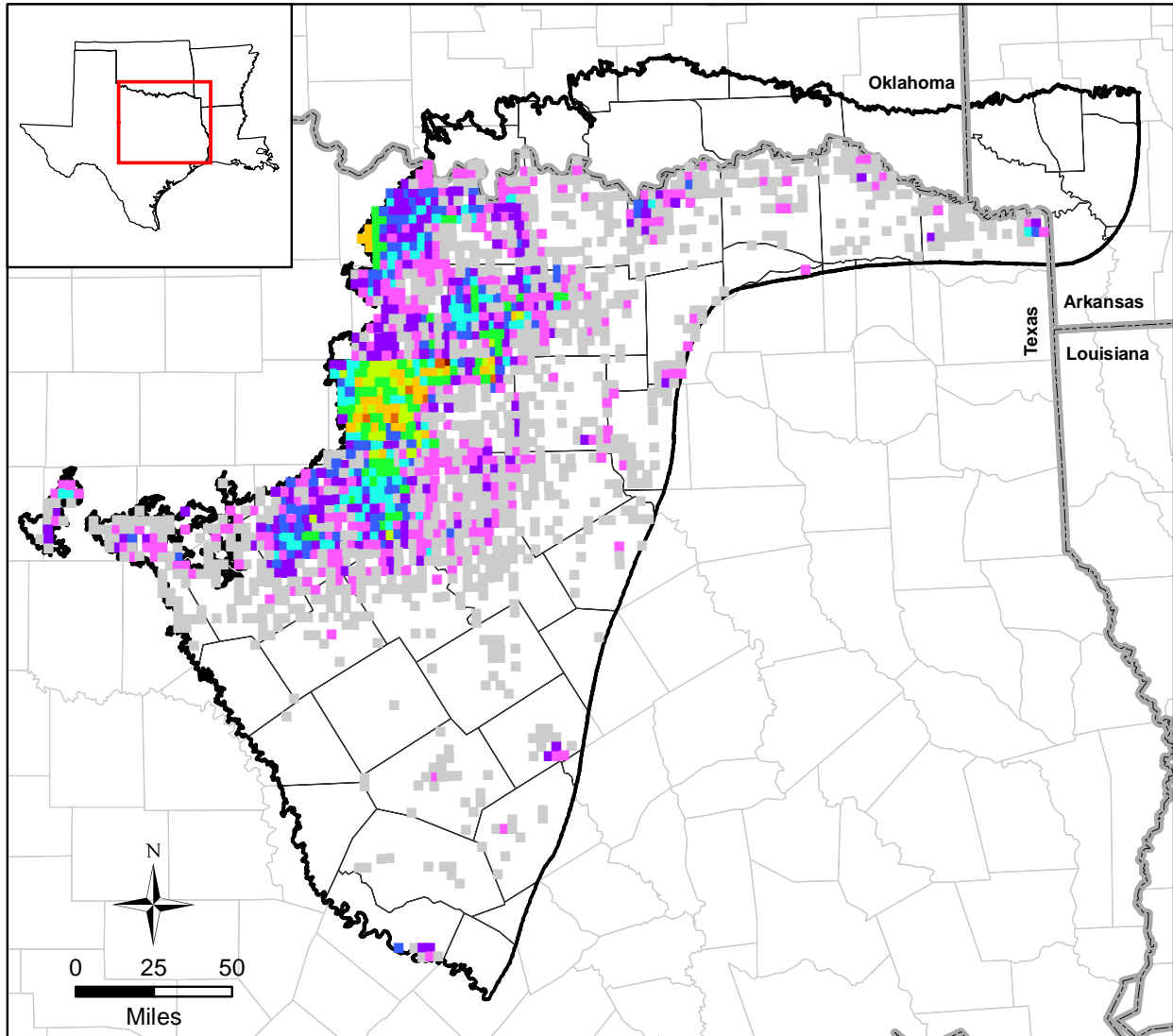
Figure 4.2.35 **Spatial distribution of specific capacity values for all aquifers/formations by state well grid.**
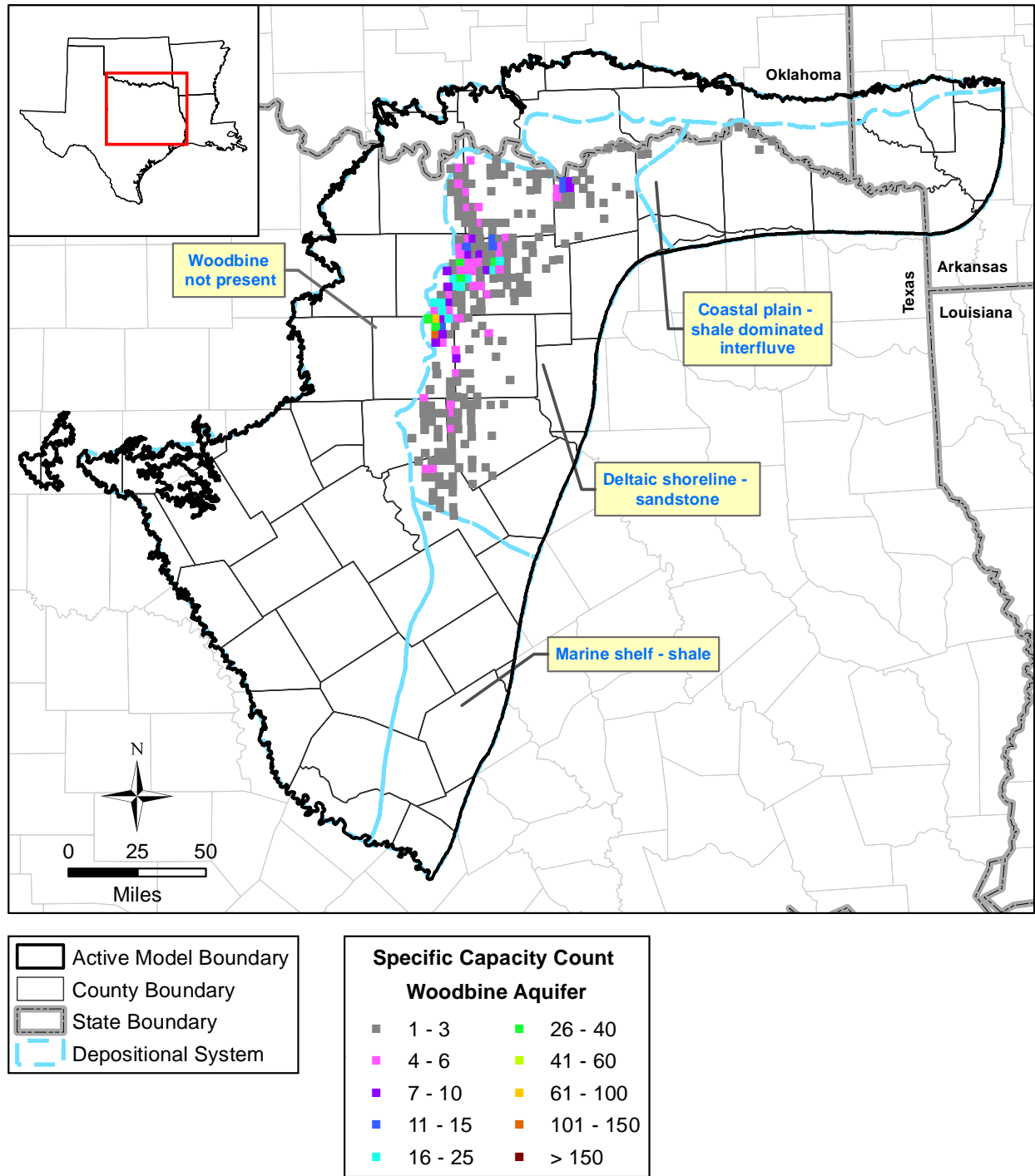
Figure 4.2.36 **Spatial distribution of the number of specific capacity values for the Woodbine Aquifer by state well grid.**
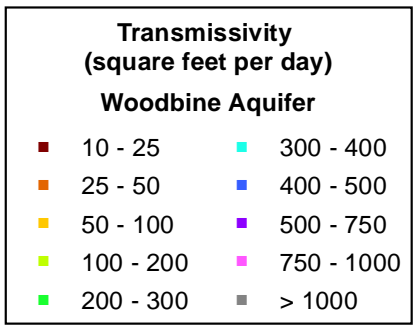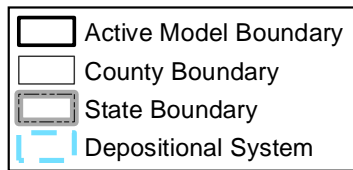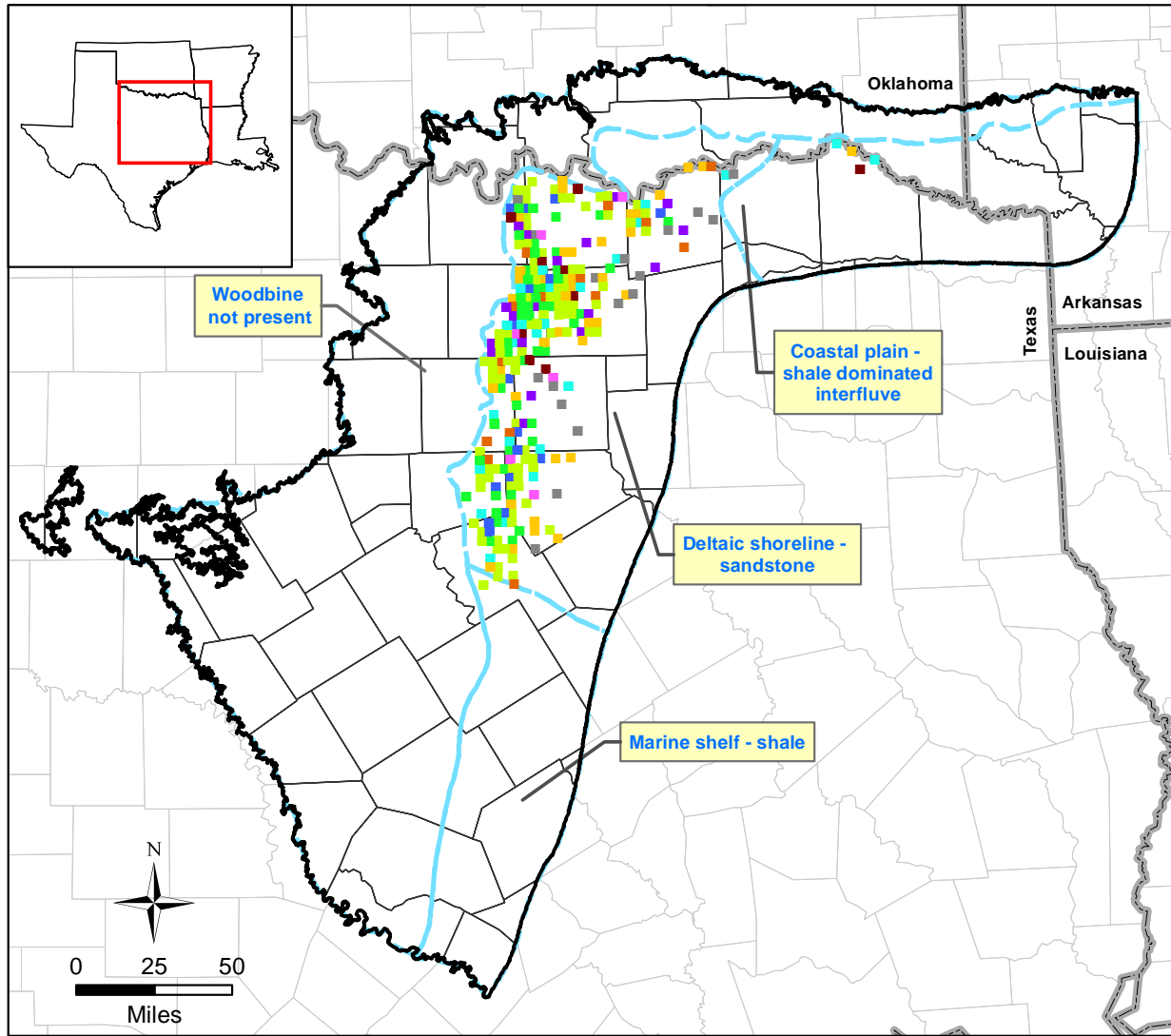
Figure 4.2.37 **Spatial distribution of mean transmissivity values calculated from specific capacity data for the Woodbine Aquifer by state well grid.**
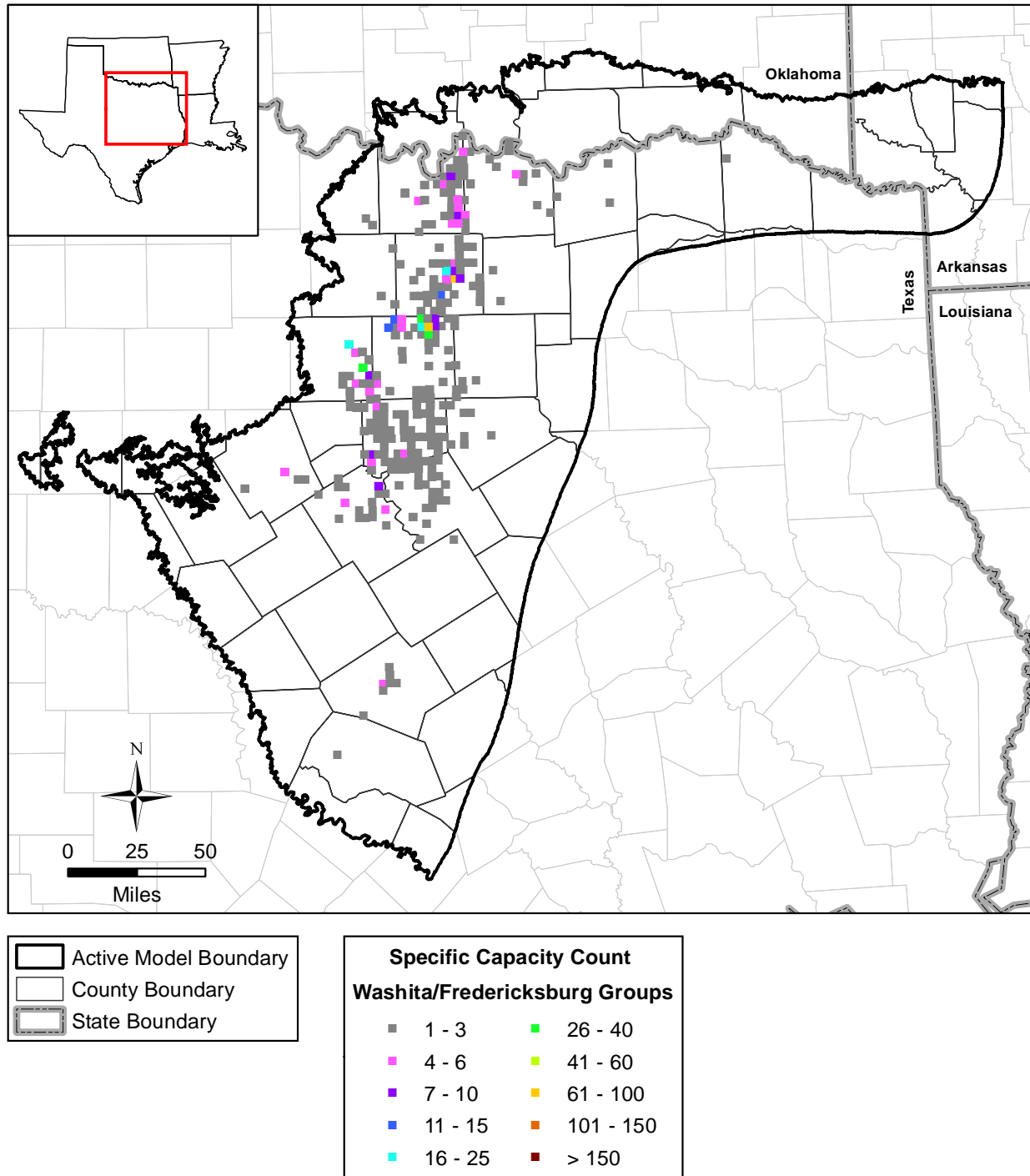
Figure 4.2.38 **Spatial distribution of the number of specific capacity values for the Washita/Fredericksburg groups by state well grid.**
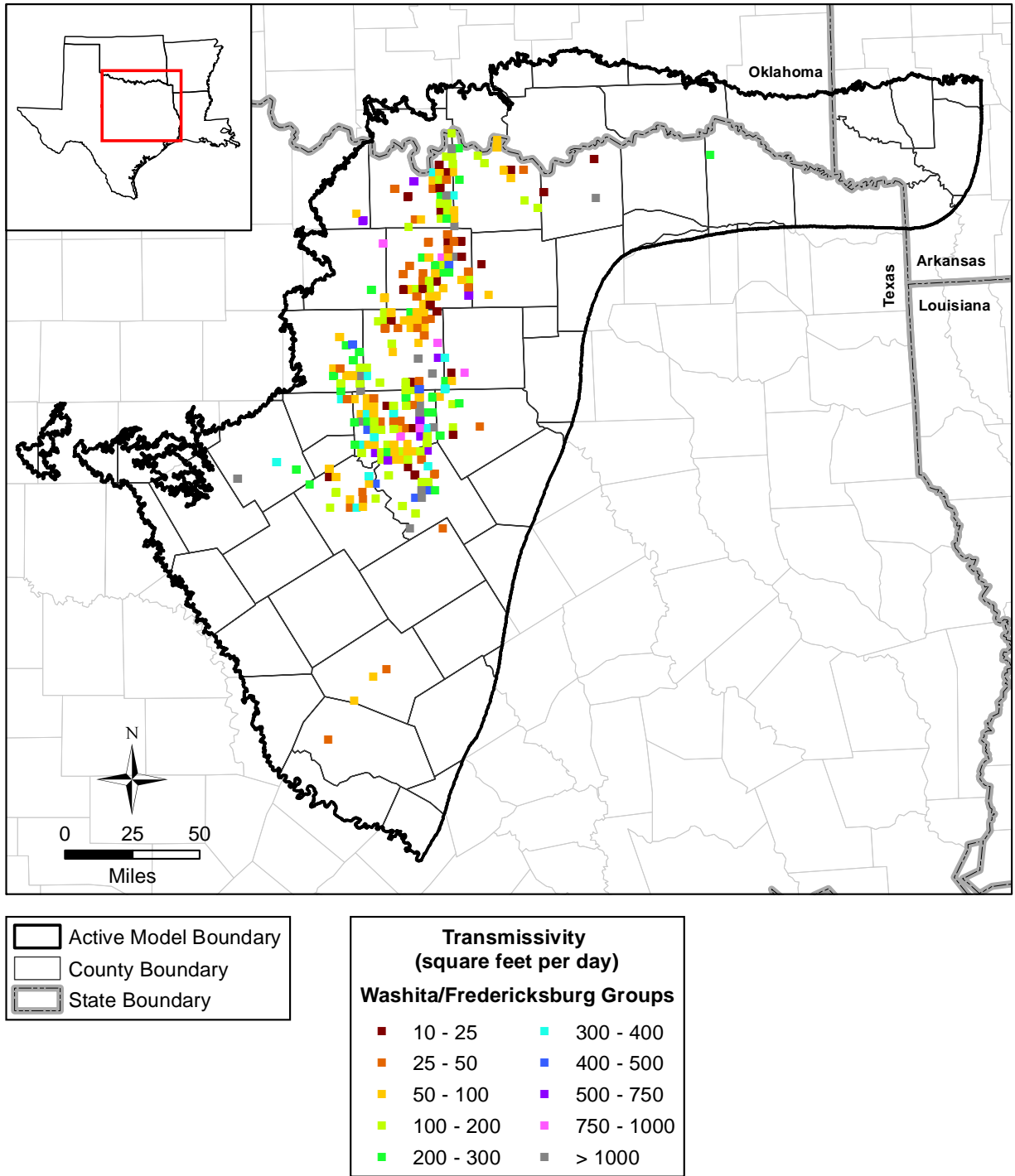
Figure 4.2.39 **Spatial distribution of mean transmissivity values calculated from specific capacity data for the Washita/Fredericksburg groups by state well grid.**
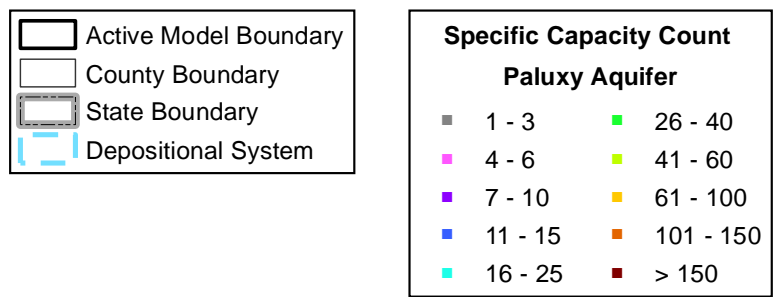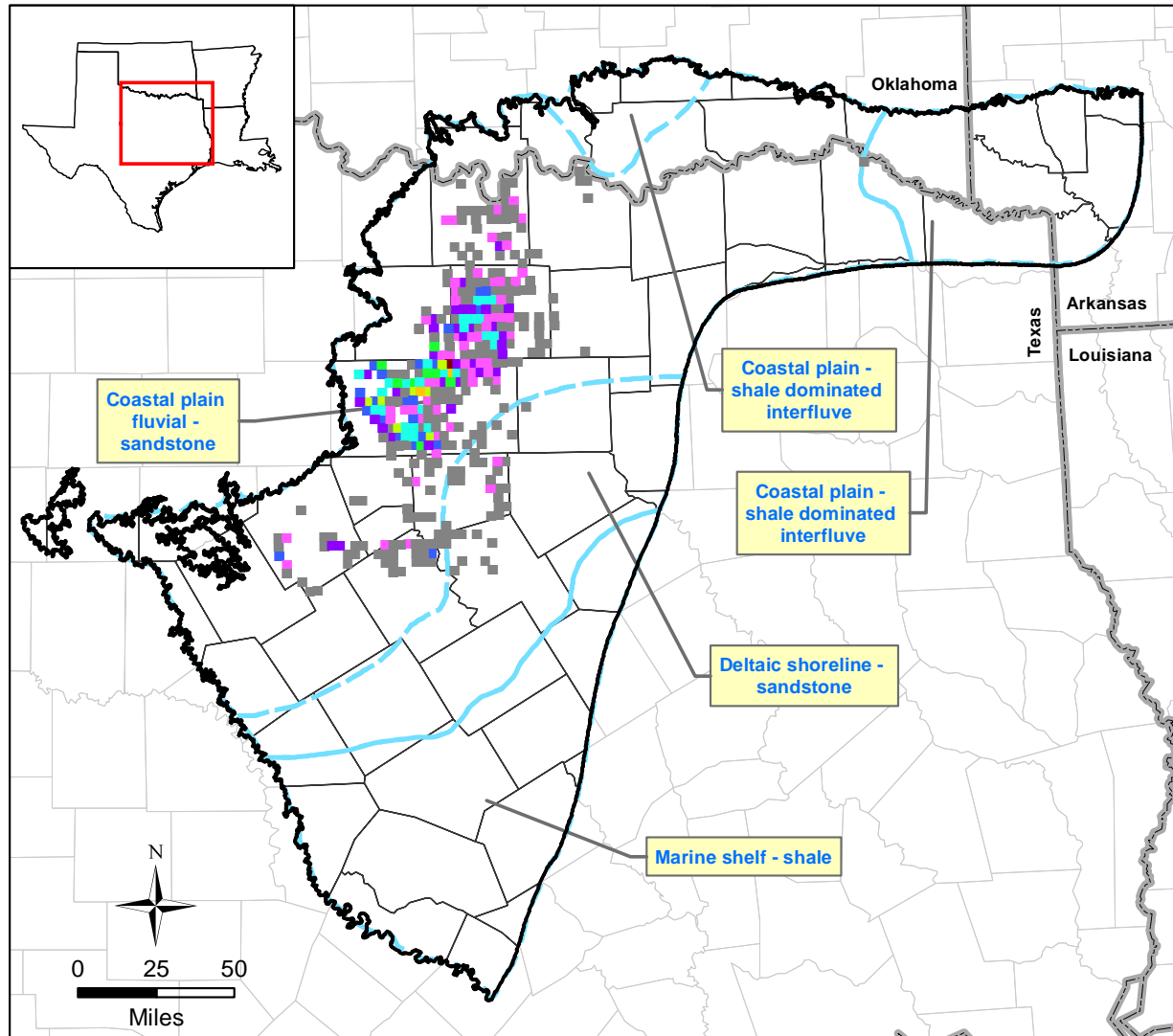
Figure 4.2.40   Spatial distribution of the number of specific capacity values for the Paluxy Aquifer by state well grid.
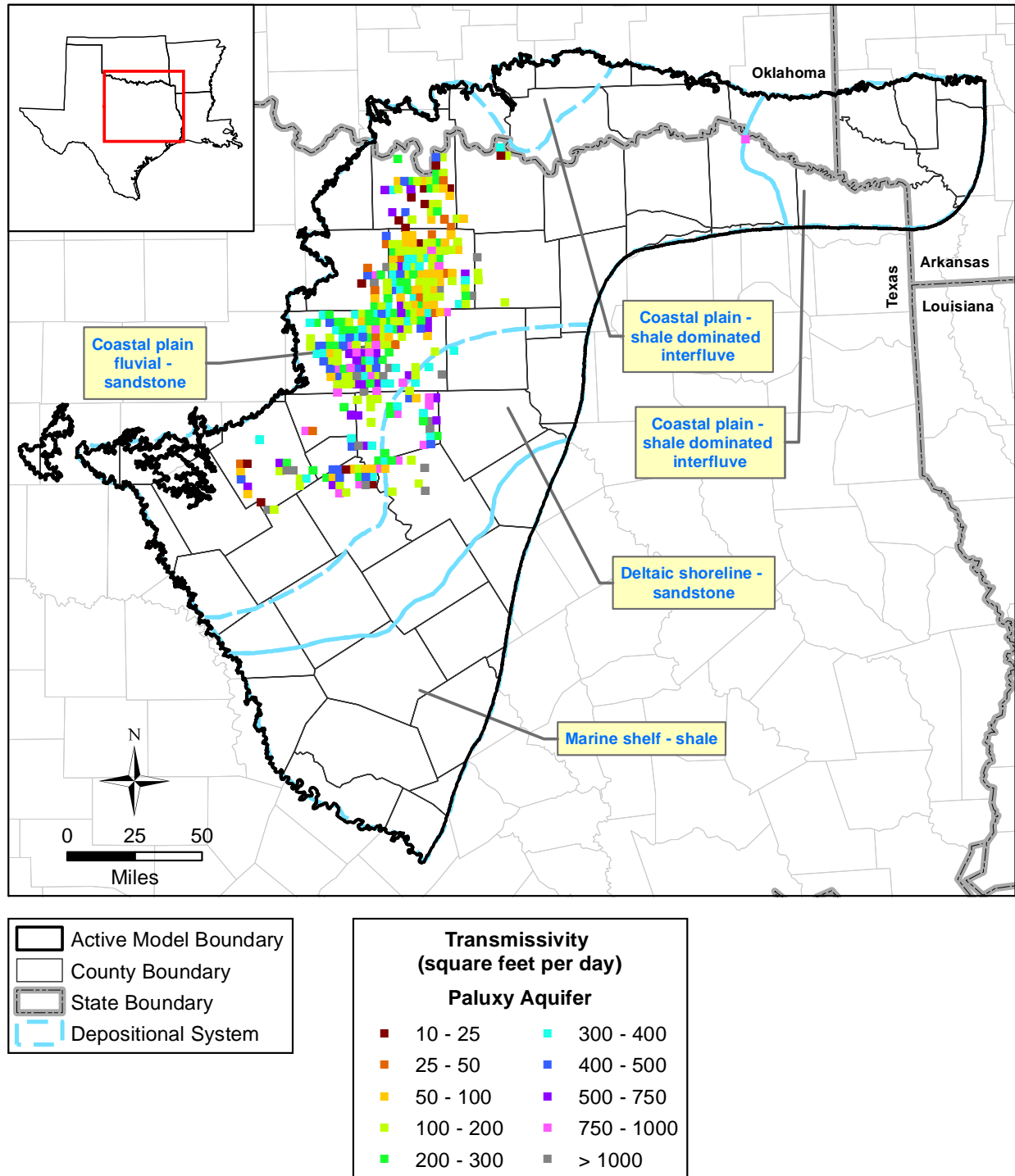
Figure 4.2.41   Spatial distribution of mean transmissivity values calculated from specific capacity data for the Paluxy Aquifer by state well grid.
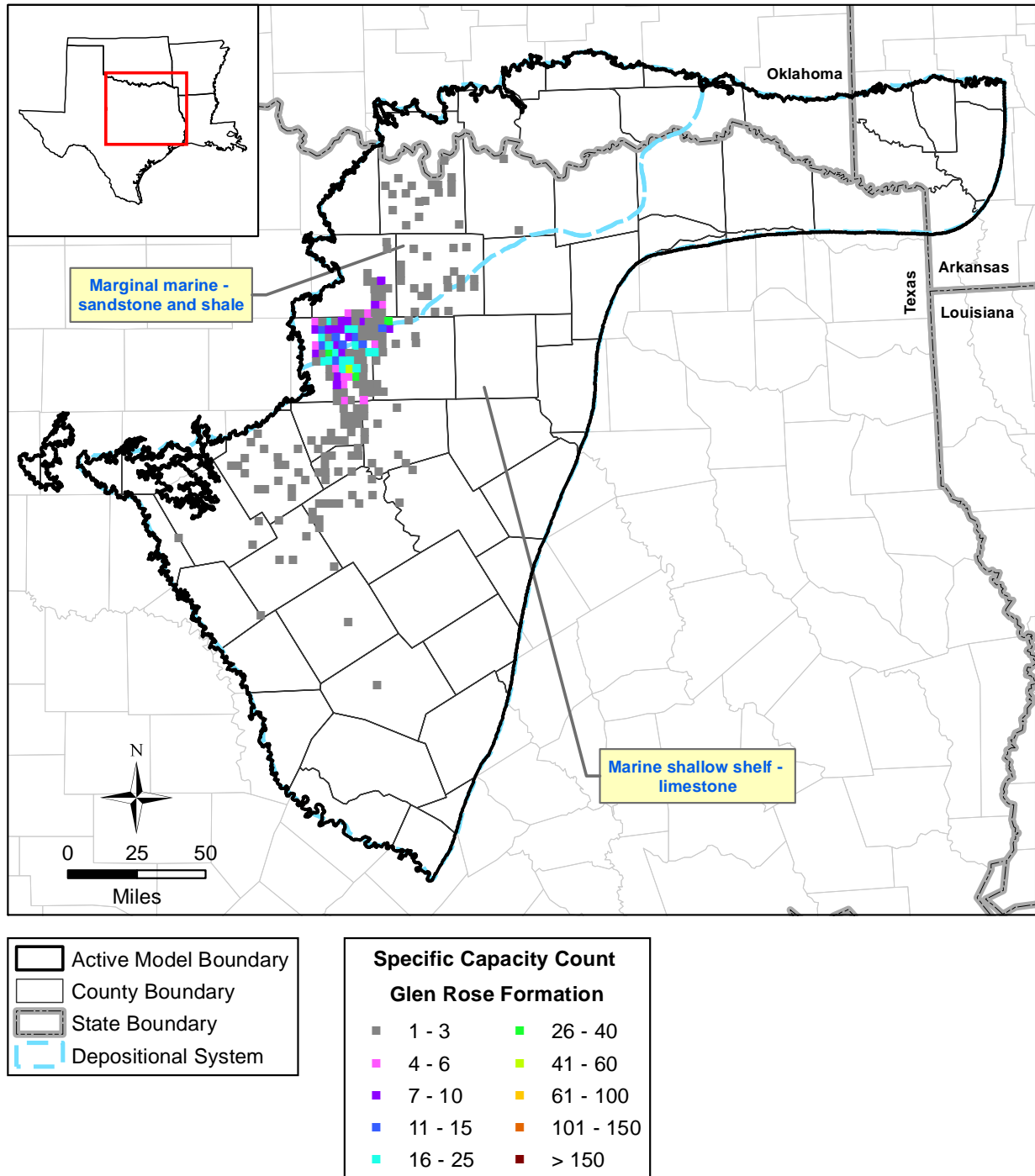
Figure 4.2.42   Spatial distribution of the number of specific capacity values for the Glen Rose Formation by state well grid.
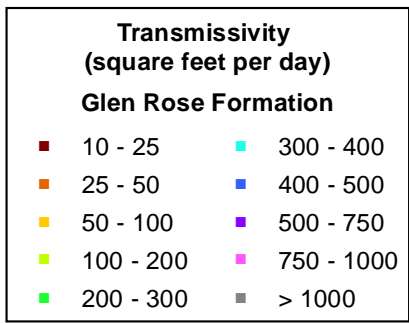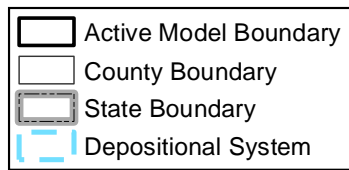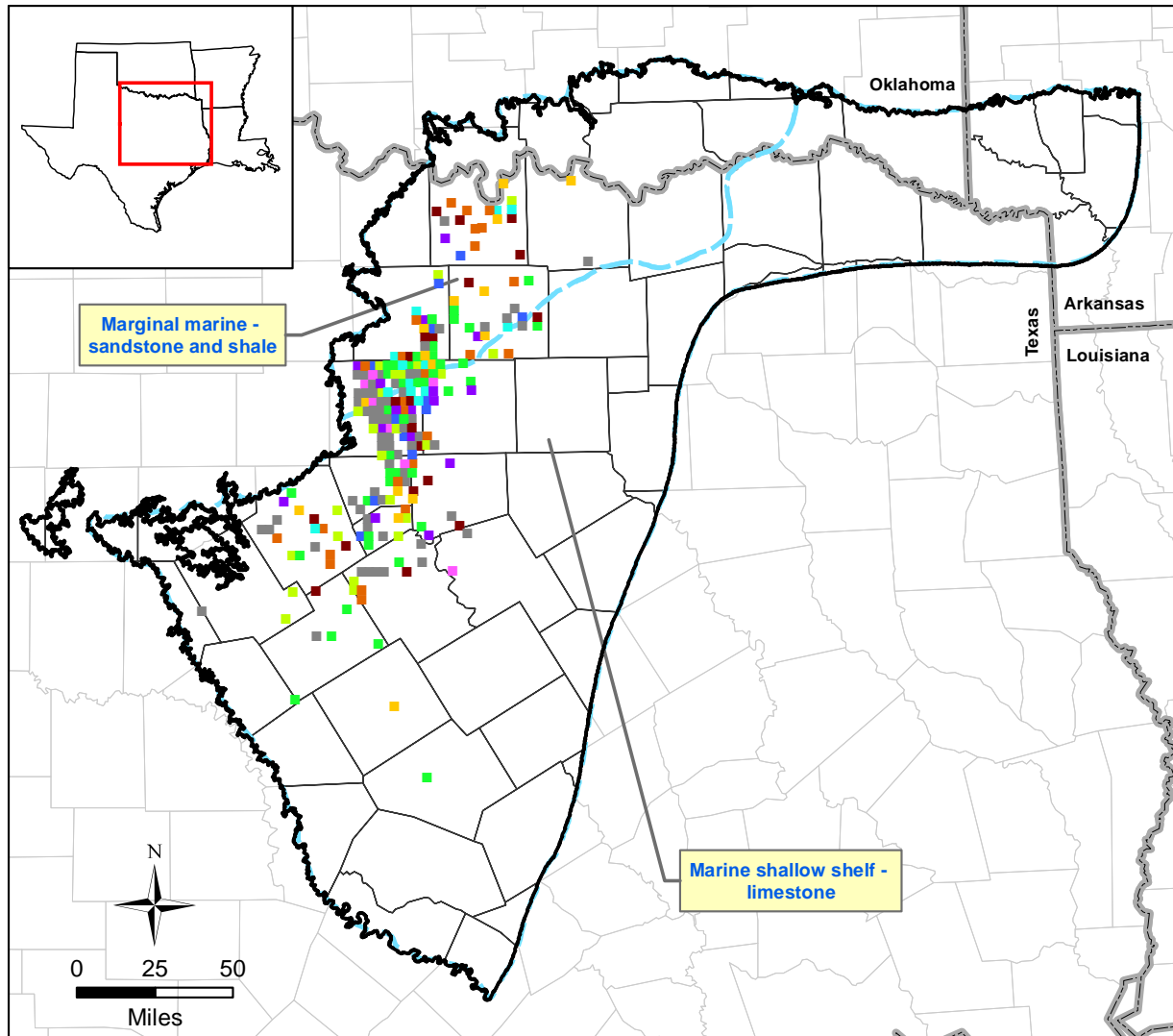
Figure 4.2.43 **Spatial distribution of mean transmissivity values calculated from specific capacity data for the Glen Rose Formation by state well grid.**
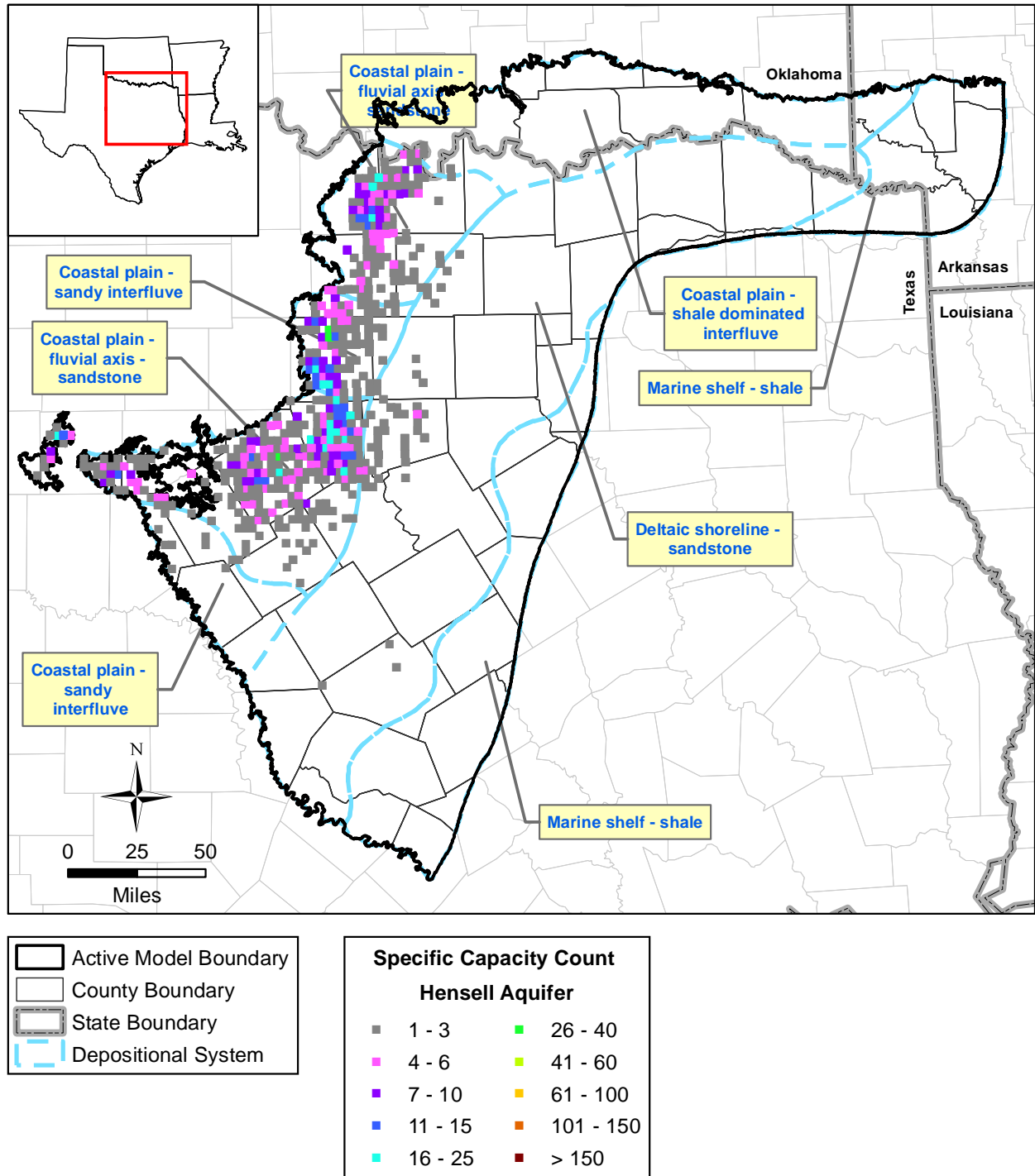
Figure 4.2.44 **Spatial distribution of the number of specific capacity values for the Hensell Aquifer by state well grid.**
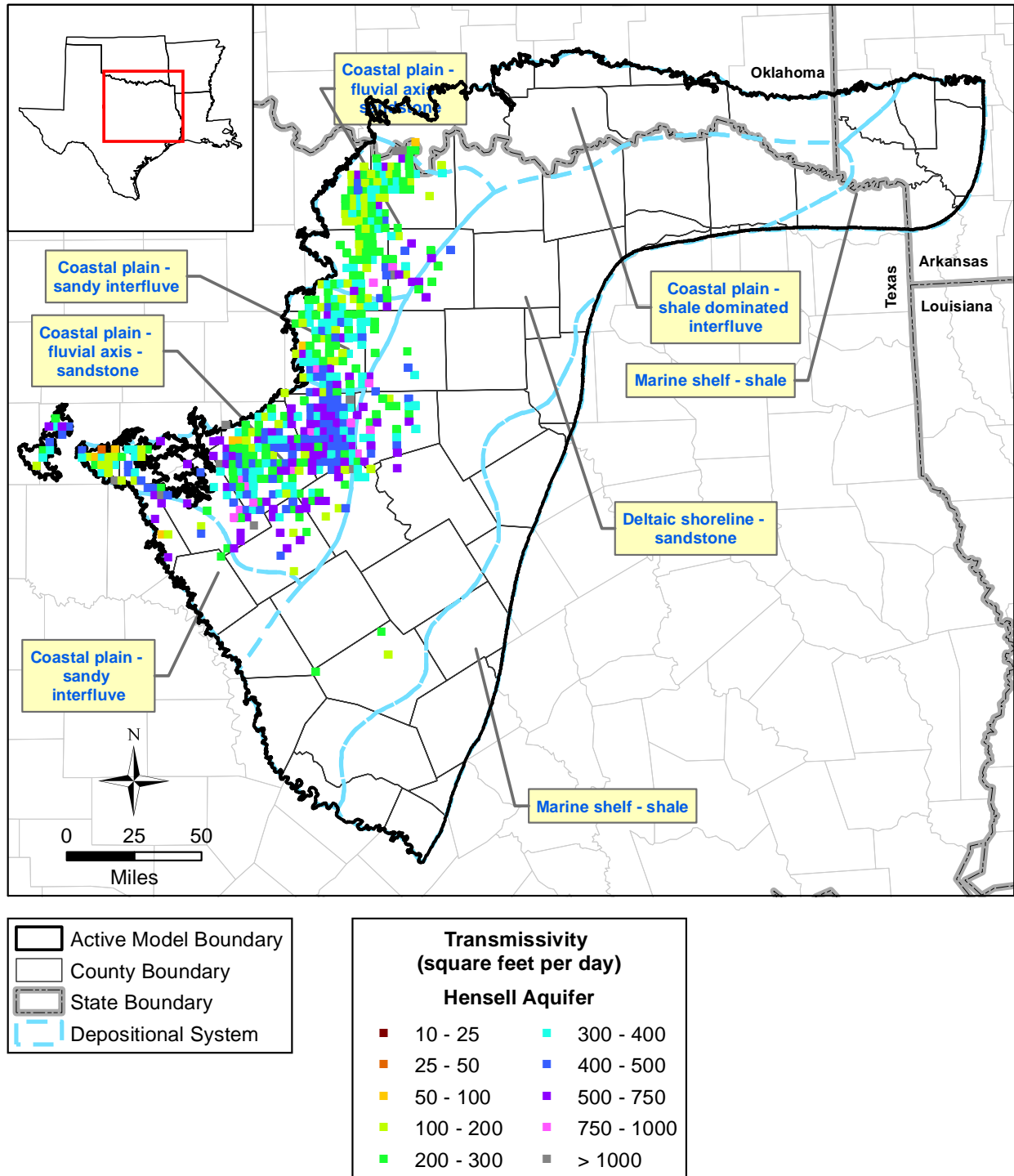
Figure 4.2.45   Spatial distribution of mean transmissivity values calculated from specific capacity data for the Hensell Aquifer by state well grid.
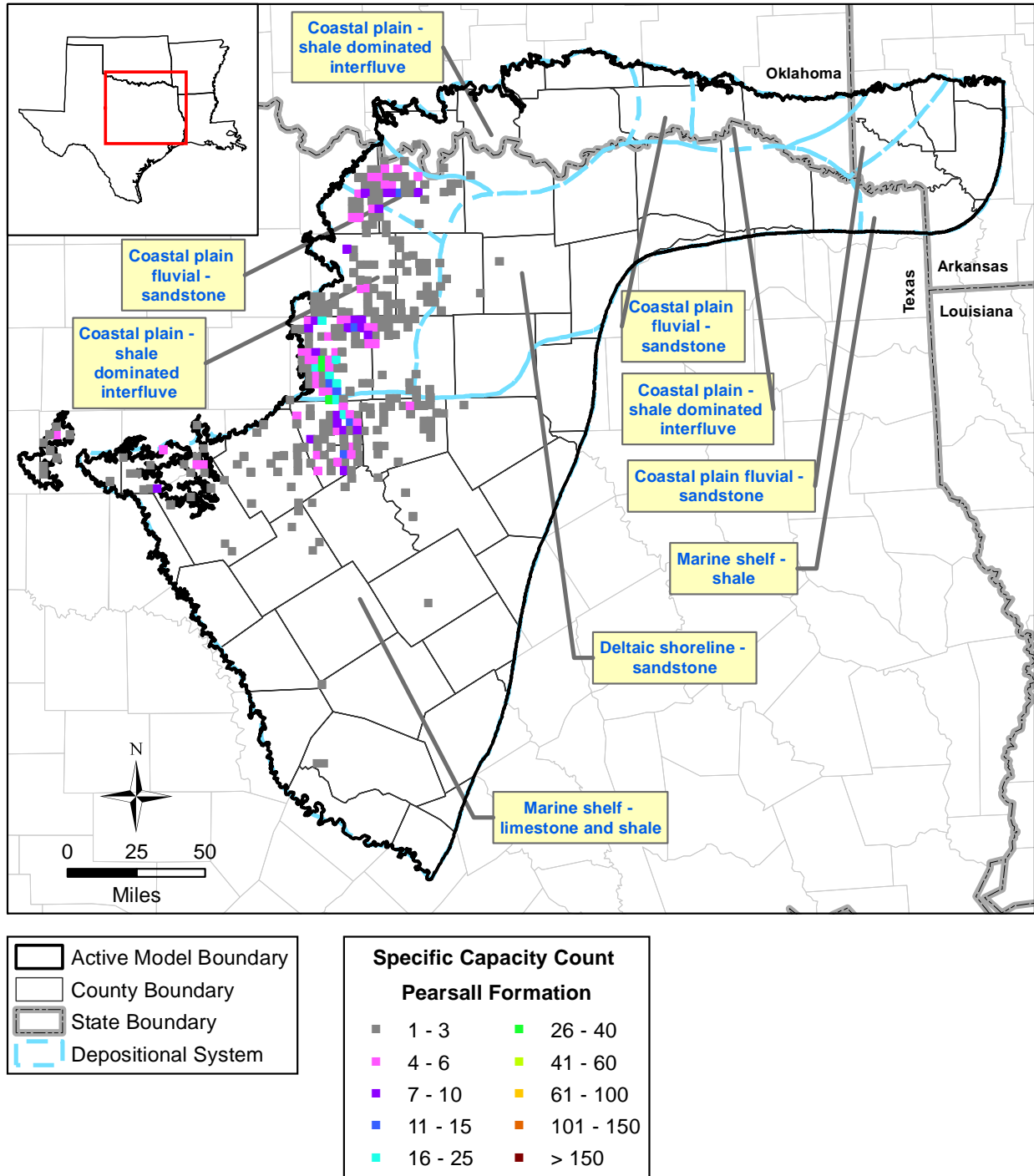
Figure 4.2.46   **Spatial distribution of the number of specific capacity values for the Pearsall Formation by state well grid.**
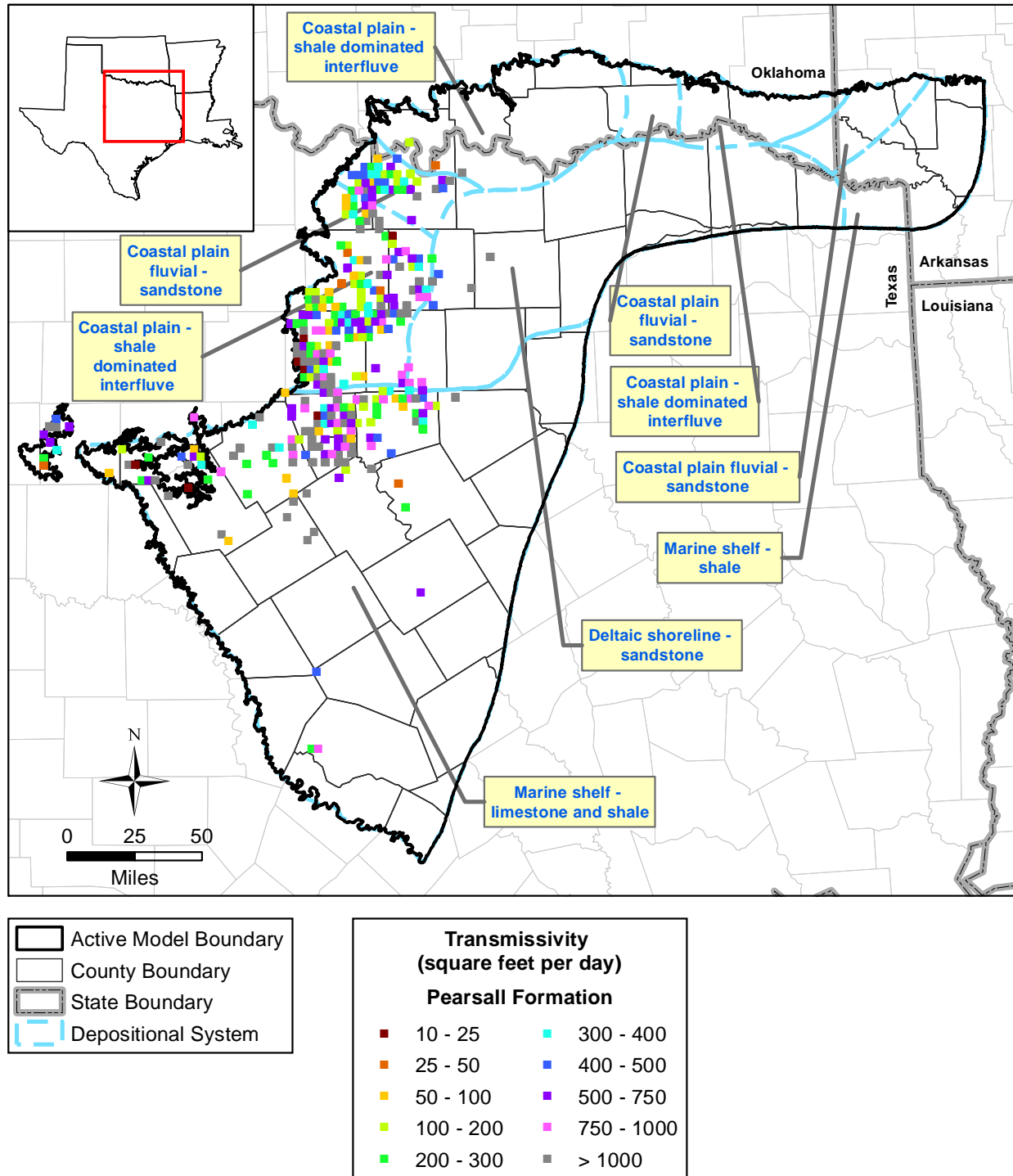
Figure 4.2.47   Spatial distribution of mean transmissivity values calculated from specific capacity data for the Pearsall Formation by state well grid.
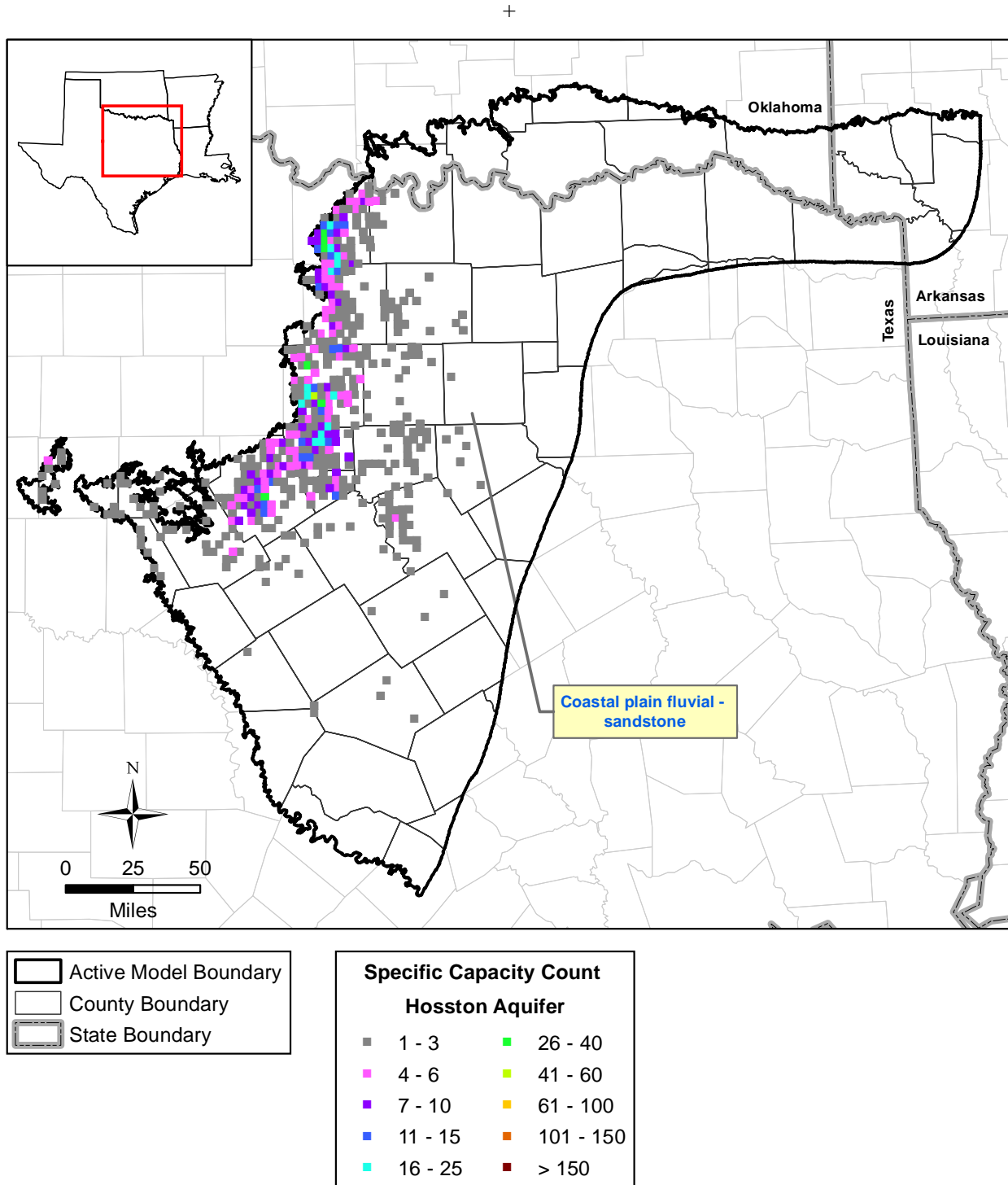
Figure 4.2.48   Spatial distribution of the number of specific capacity values for the Hosston Aquifer by state well grid.
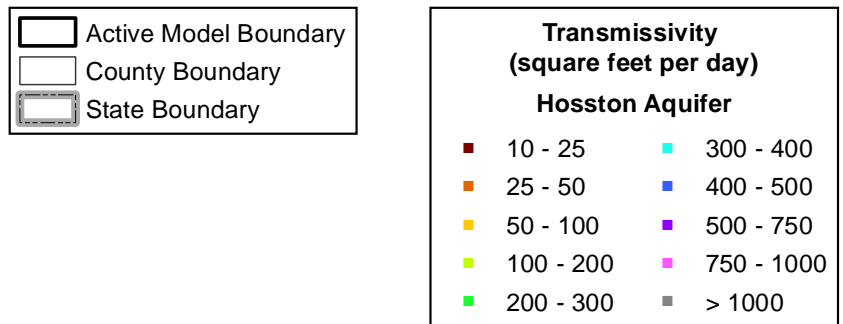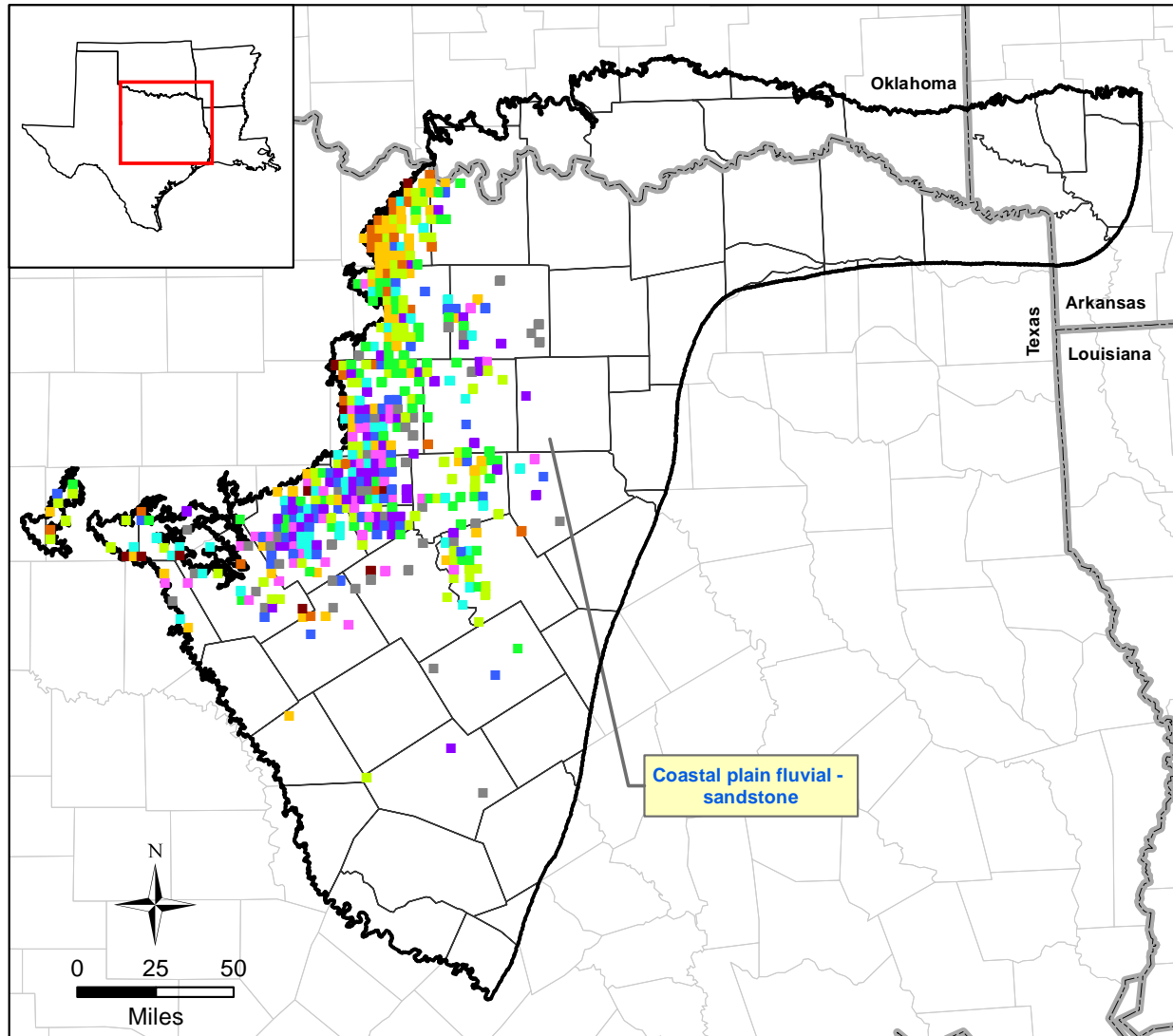
Figure 4.2.49   Spatial distribution of mean transmissivity values calculated from specific capacity data for the Hosston Aquifer by state well grid.

(a)

Woodbine Group	Mean	Standard deviation	Count
Pumping Test based	623	684	80
Specific Capacity based	239	325	1226

(b)

Washita/Fredericksburg Groups	Mean	Standard deviation	Count
Pumping Test based	660	686	21
Specific Capacity based	272	1,484	888

(c)

Paluxy Formation	Mean	Standard deviation	Count
Pumping Test based	289	250	44
Specific Capacity based	357	808	2614

(d)

Glen Rose Formation	Mean	Standard deviation	Count
Pumping Test based	446	386	65
Specific Capacity based	1,279	13,005	3335

Figure 4.2.50   Cumulative distribution function for transmissivity from aquifer pumping tests and specific capacity tests for the (a) Woodbine Aquifer, (b) Washita/Fredericksburg groups, (c) Paluxy Aquifer, and (d) Glen Rose Formation.

(a)

(b)

(c)
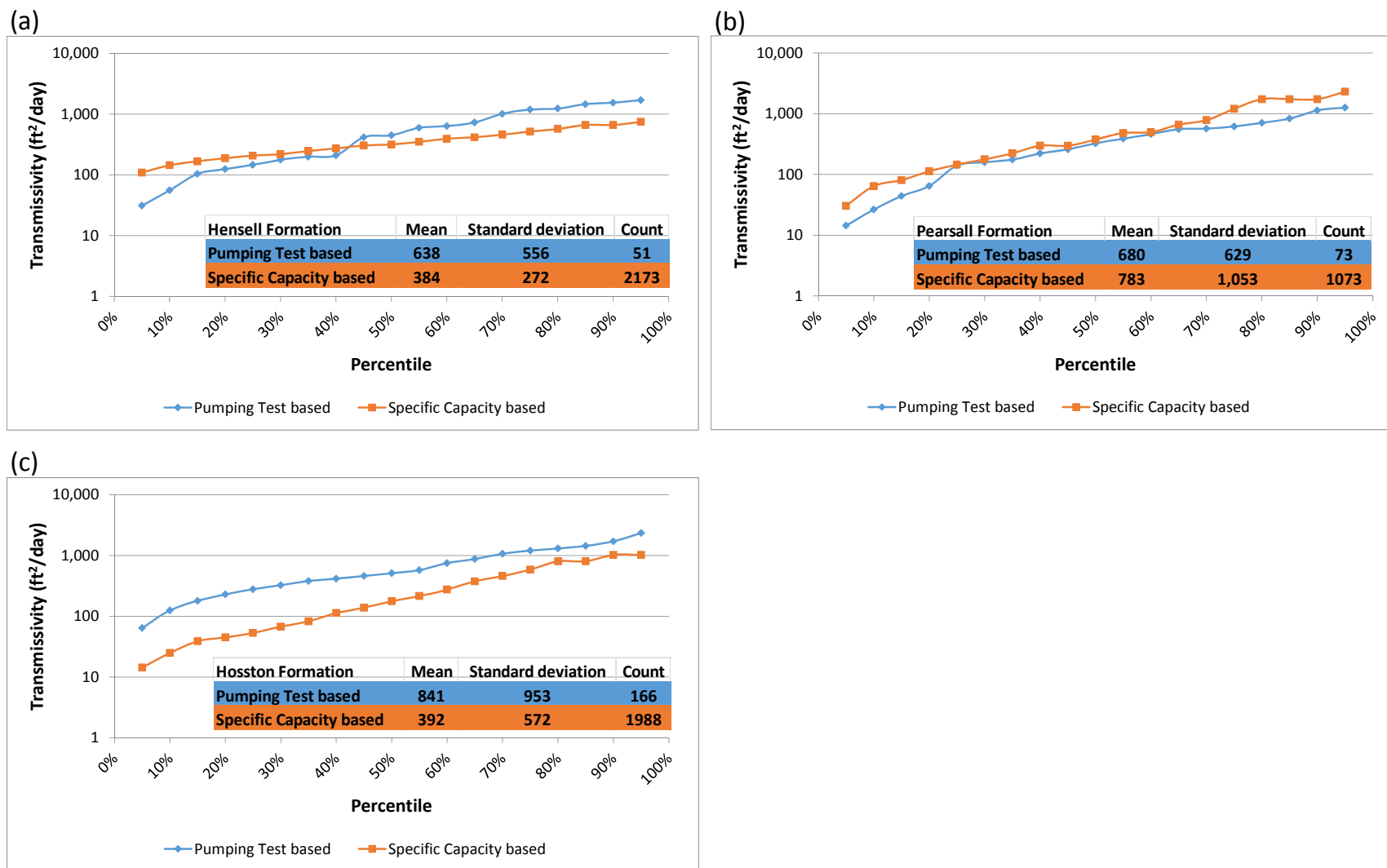
Figure 4.2.51   Cumulative distribution function for transmissivity from aquifer pumping tests and specific capacity test for the (a) Hensell Aquifer, (b) Pearsall Formation, and (c) Hosston Aquifer.
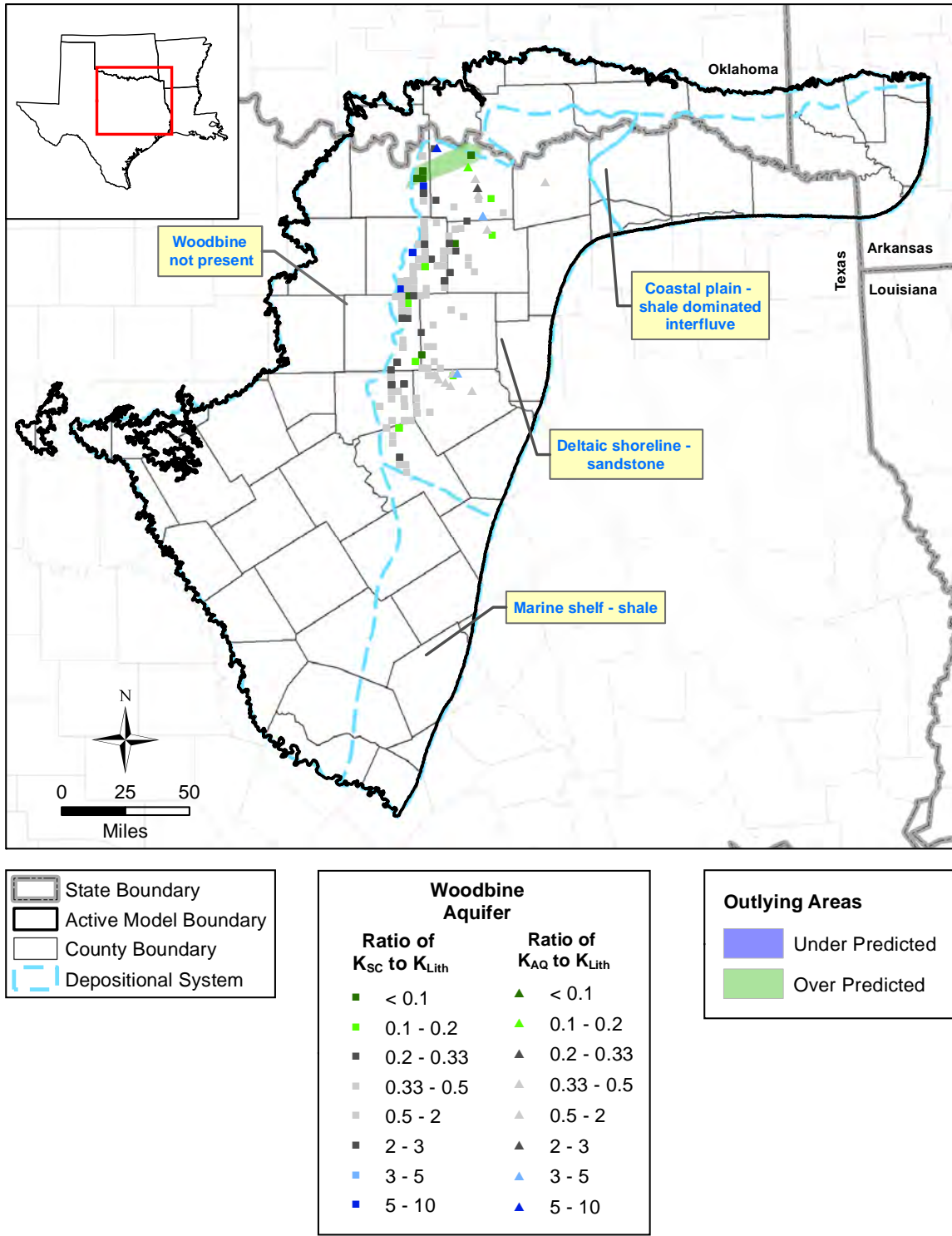
Figure 4.2.52 **Comparison of hydraulic conductivity values for the Woodbine Aquifer generated from lithology data (K_{LITH}) to hydraulic conductivity values estimated from specific capacity data (K_{SC}) and from aquifer pumping test data (K_{AQ}). Outlying areas identify regions where the GHS model appears to be under or over predicting hydraulic conductivity.**
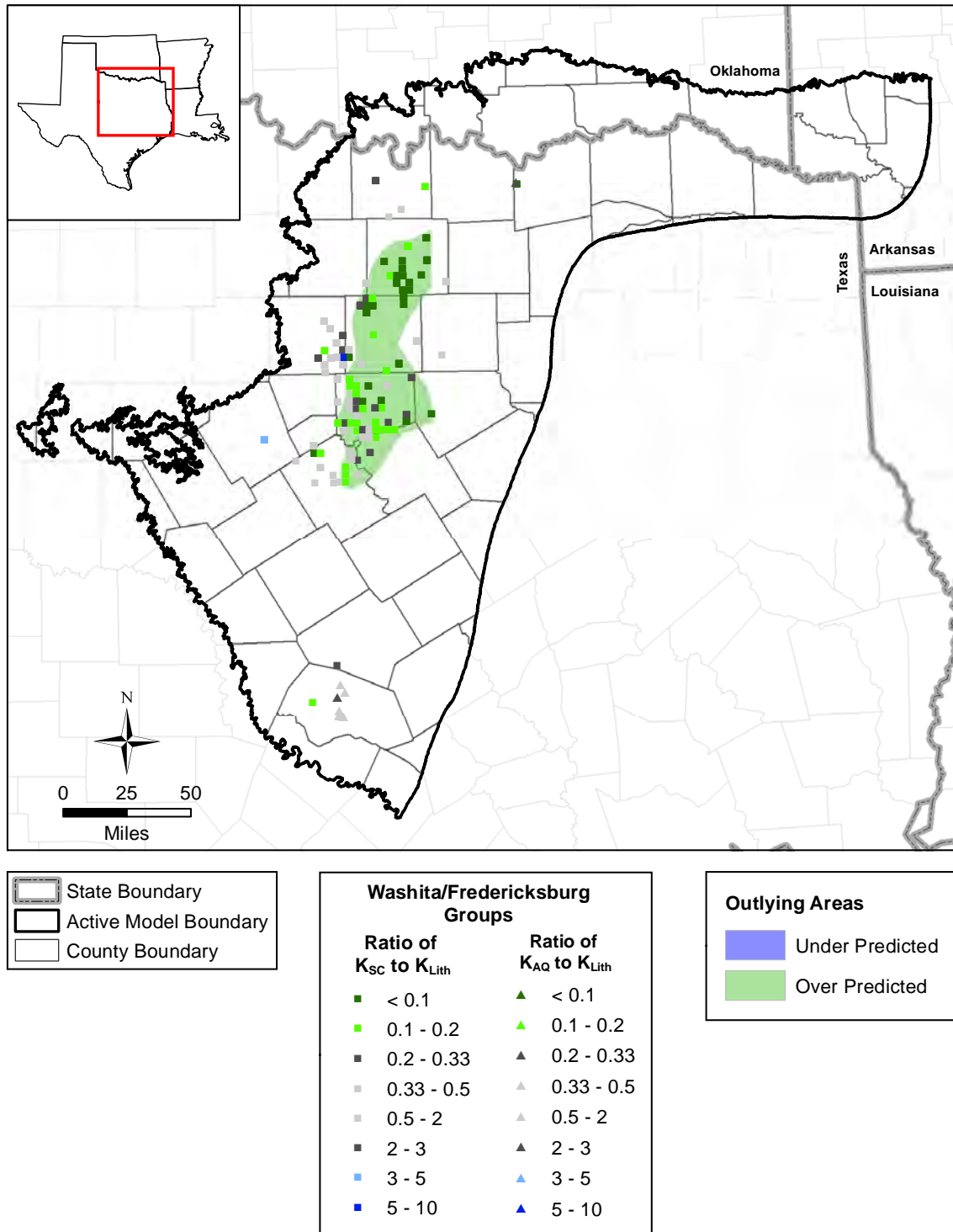
Figure 4.2.53 Comparison of hydraulic conductivity values for the Washita/Fredericksburg groups generated from lithology data (K_{LITH}) to hydraulic conductivity values estimated from specific capacity data (K_{SC}) and from aquifer pumping test data (K_{AQ}). Outlying areas identify regions where the GHS model appears to be under or over predicting hydraulic conductivity.
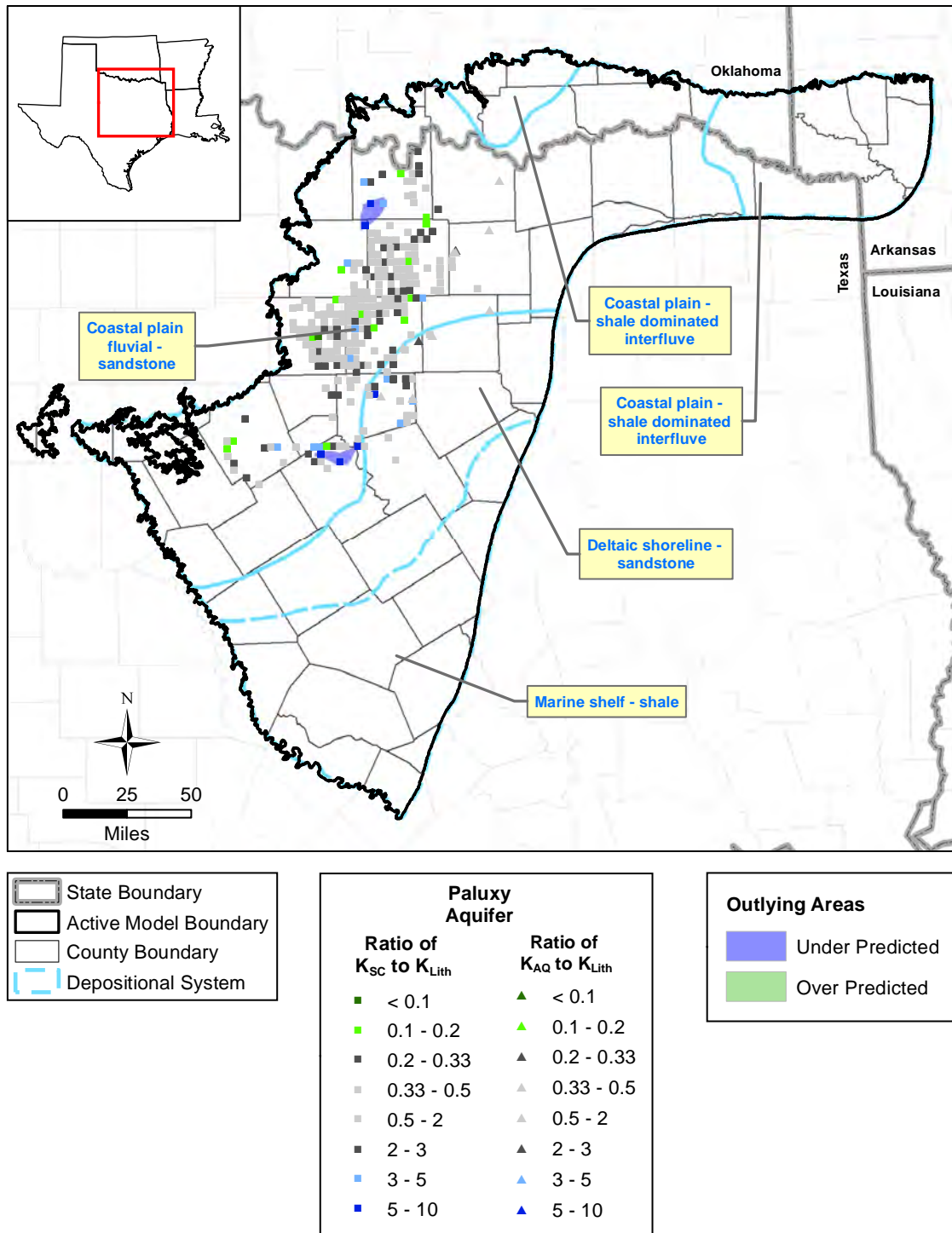
Figure 4.2.54 **Comparison of hydraulic conductivity values for the Paluxy Aquifer generated from lithology data (K_{LITH}) to hydraulic conductivity values estimated from specific capacity data (K_{SC}) and from aquifer pumping test data (K_{AQ}). Outlying areas identify regions where the GMS appears to be under or over predicting hydraulic conductivity.**
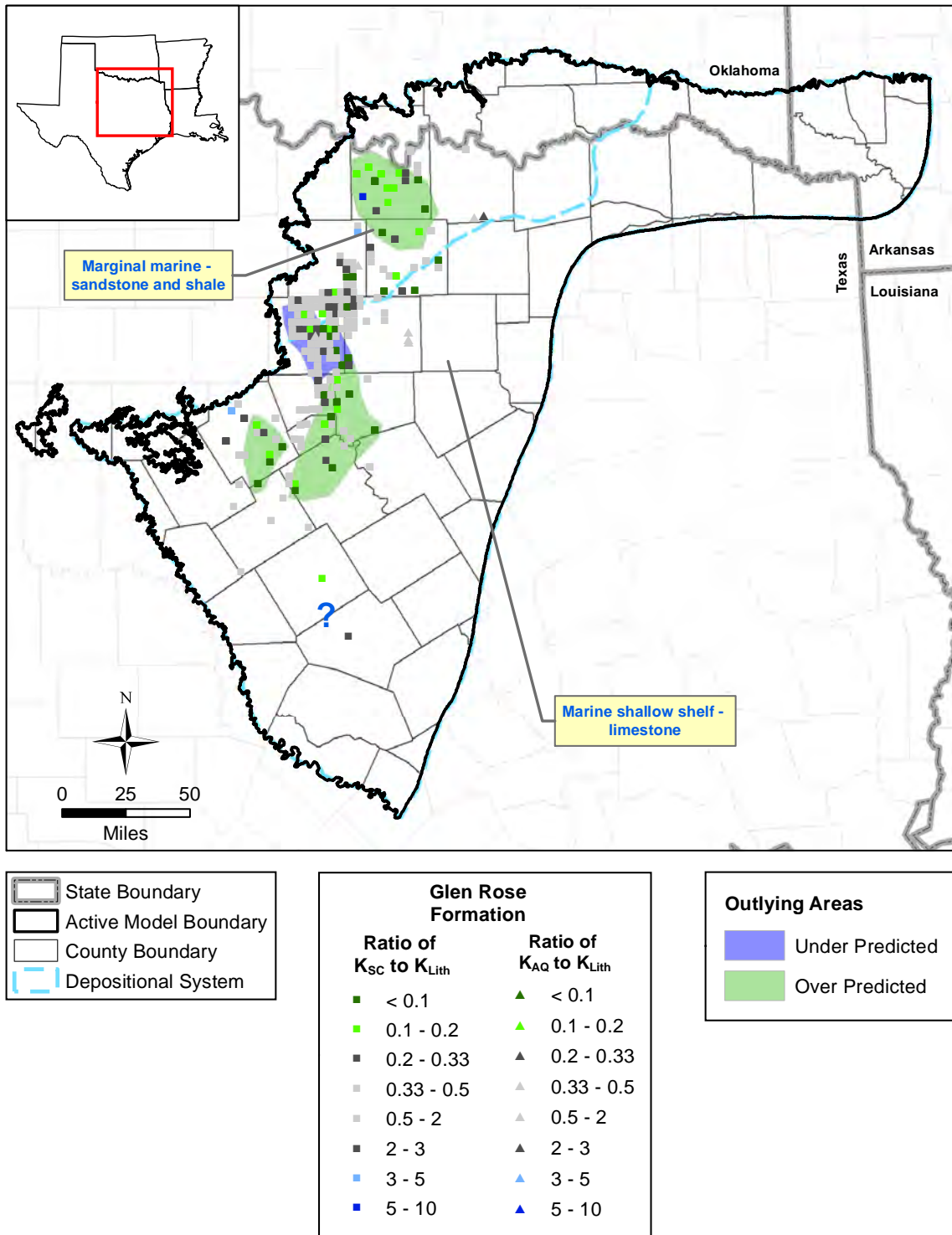
Figure 4.2.55   Comparison of hydraulic conductivity values in the Glen Rose Formation generated from lithology data (K_{LITH}) to hydraulic conductivity values estimated from specific capacity data (K_{SC}) and from aquifer pumping test data (K_{AQ}). Outlying areas identify regions where the GHS model appears to be under or over predicting hydraulic conductivity.
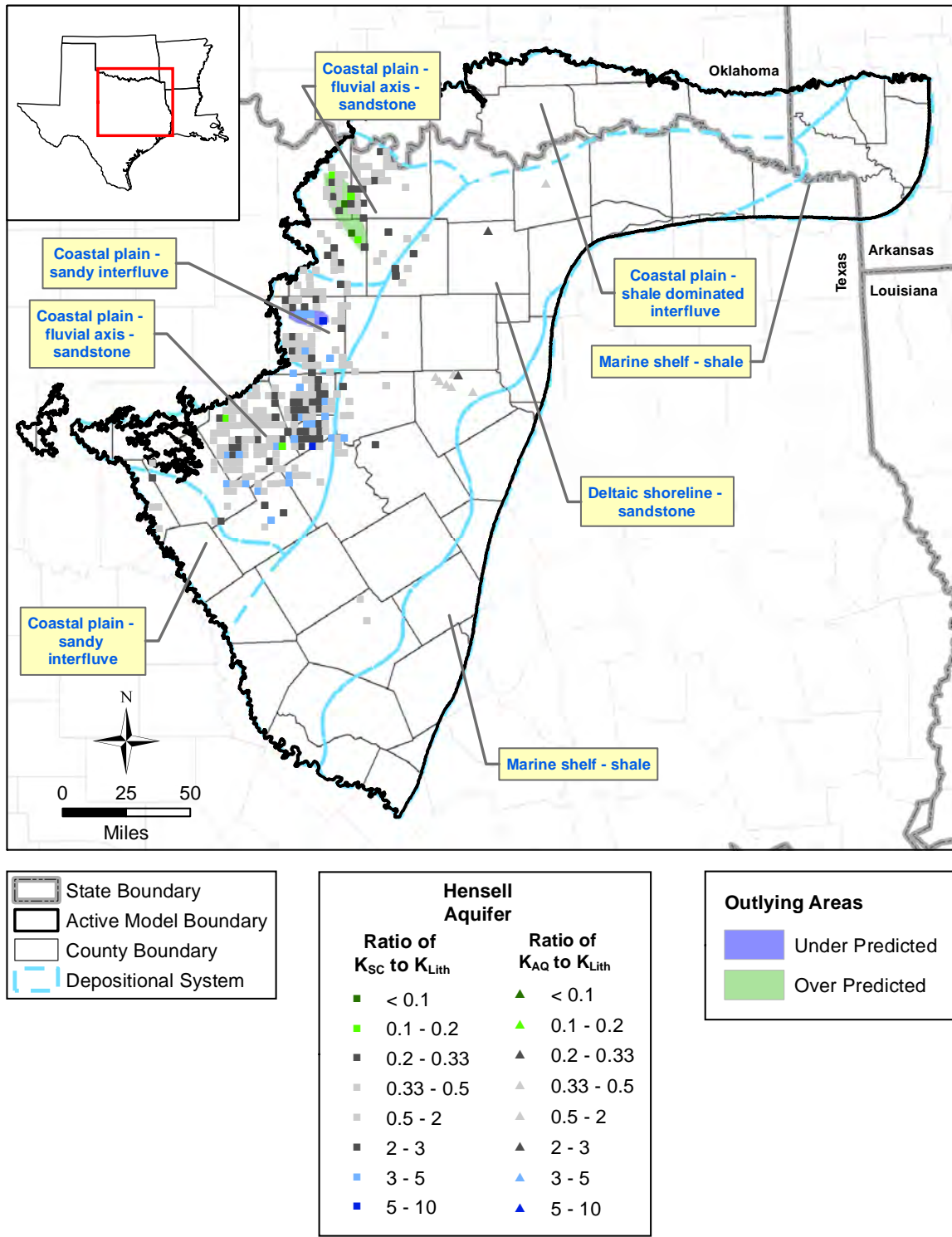
Figure 4.2.56   Comparison of hydraulic conductivity values for the Hensell Aquifer generated from lithology data (K_{LITH}) to hydraulic conductivity values estimated from specific capacity data (K_{SC}) and from aquifer pumping test data (K_{AQ}). Outlying areas identify regions where the GHS model appears to be under or over predicting hydraulic conductivity.
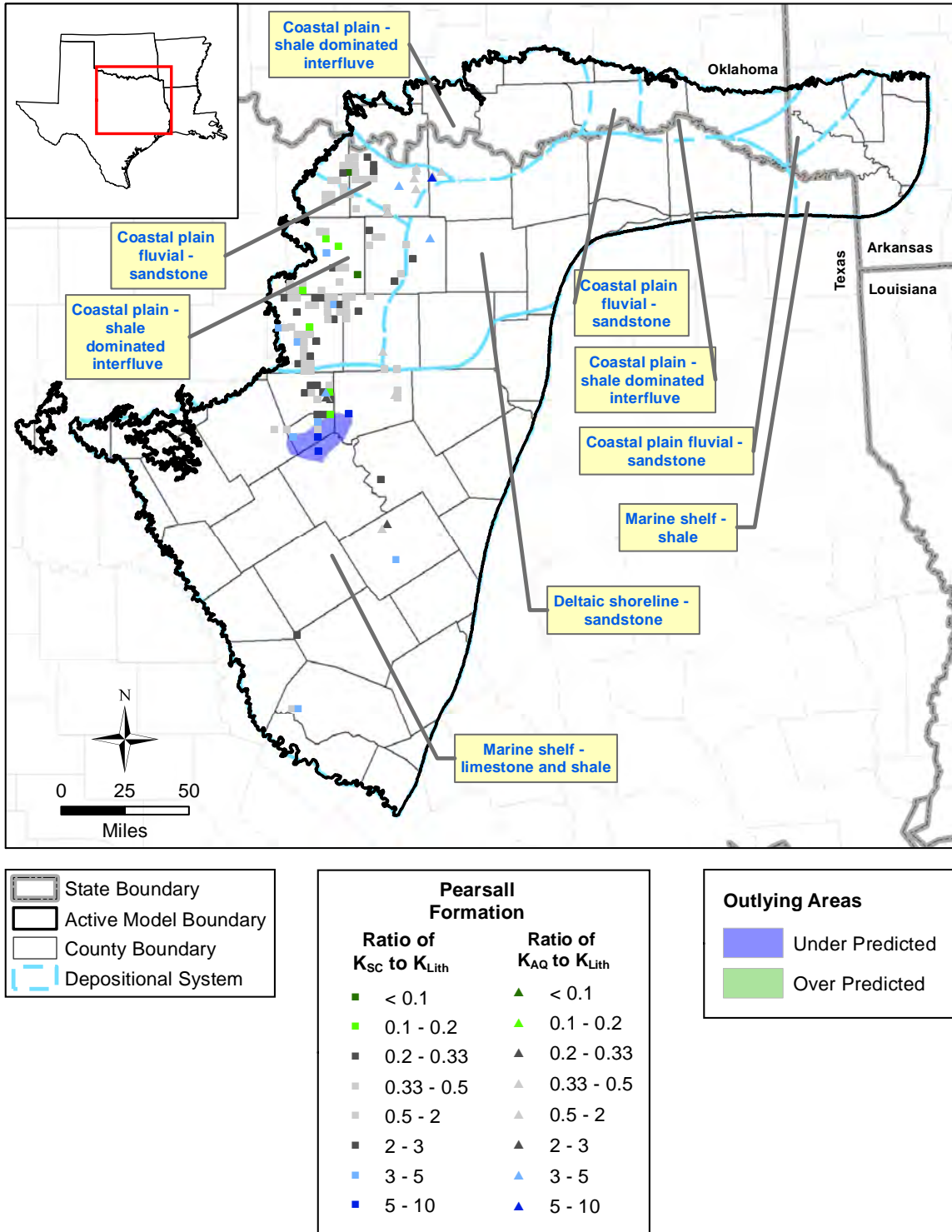
Figure 4.2.57   Comparison of hydraulic conductivity values for the Pearsall Formation generated from lithology data (K_{LITH}) to hydraulic conductivity values estimated from specific capacity data (K_{SC}) and from aquifer pumping test data (K_{AQ}). Outlying areas identify regions where the GHS model appears to be under or over predicting hydraulic conductivity.
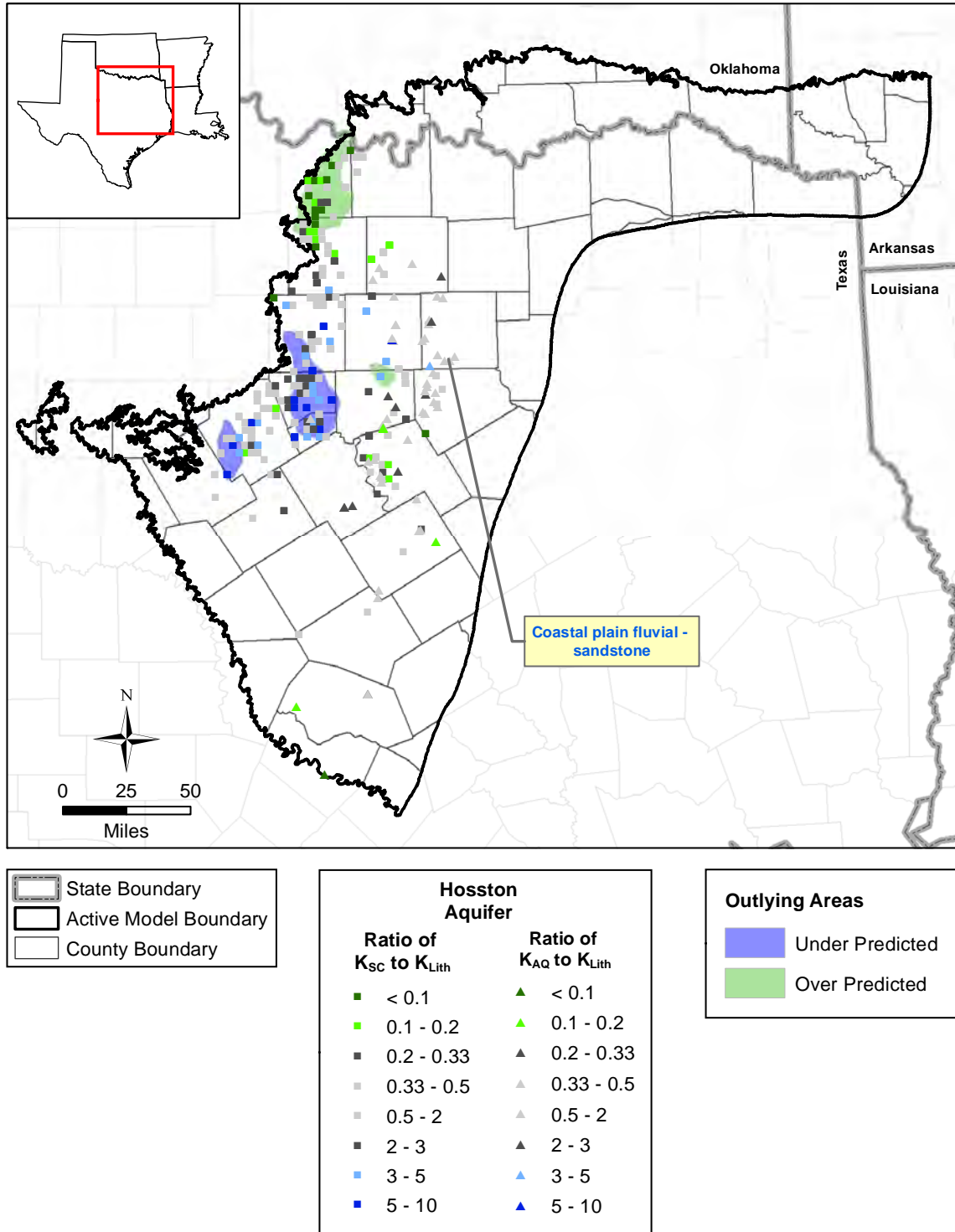
Figure 4.2.58 **Comparison of hydraulic conductivity values for the Hosston Aquifer generated from lithology data (K_{LITH}) to hydraulic conductivity values estimated from specific capacity data (K_{SC}) and from aquifer pumping test data (K_{AQ}). Outlying areas identify regions where the GHS model appears to be under or over predicting hydraulic conductivity.**

4.3   Hydraulic Heads and Groundwater Flow

Hydraulic head is the elevation of the groundwater level in an aquifer and is generally measured in a well. Hydraulic head is a direct measure of the potential energy of groundwater. Groundwater flows from high hydraulic heads to low hydraulic heads (see Equation 4.2.1). Hydraulic head data were collected for the northern Trinity and Woodbine aquifers in the study area in order to estimate historical hydraulic head surfaces and hydraulic head declines, evaluate the transient behavior of hydraulic heads observed in wells, identify hydraulic head calibration targets for the model, and investigate vertical hydraulic head gradients. The following subsections provide the sources used to compile hydraulic head data for the study area and describe the compiled data, discuss and present an estimate of predevelopment hydraulic heads, discuss transient hydraulic head data and present selected transient data throughout the study area, present historical hydraulic head surfaces, discuss hydraulic head calibration targets, and investigate vertical gradients in hydraulic heads.

4.3.1   Data Sources and Description

Hydraulic head data for the study area were obtained from the following sources organized below by state:

- Texas
  - Historical groundwater reports
  - The TWDB groundwater database
  - Hard copies of driller's logs from TCEQ well files
  - The TWDB driller's logs database
  - Data received from GCDs
  - USGS online data
- Oklahoma
  - Oklahoma Water Resources Board online data
  - USGS online data
- Arkansas
  - USGS online data

Hill (1901) provides information on artesian water in the northern Trinity and Woodbine aquifers in Texas prior to 1900 across most of the study area. His data includes water-level measurements, locations where wells completed in the northern Trinity and Woodbine aquifers flowed, estimates of locations where wells were likely to flow if drilled, and estimates of water levels above ground surface for some flowing wells. The coordinates for wells in the Hill (1901) report are uncertain because they were determined by digitizing well locations from a map in his report. Although the map was georeferenced as accurately as possible, the locations of reference points on Hill's map created in 1898 are different from the more accurate locations available today, resulting in uncertain well locations. The water-level measurements from Hill (1901) consist of one measurement per well.

Water-level measurements given in historical reports published by the TWDB and predecessor agencies were collected for selected counties in the Texas portion of the study area. The reports reviewed were those whose data had not already been entered into the TWDB groundwater database, which is an electronic database maintained by the TWDB containing well, water-level, and water quality data for selected wells in the State (TWDB, 2013a). The criteria used to select water-level data from historical reports was measurements made prior to 1960 for counties with few measurements during that time from other sources. Historical water-level measurements were obtained for Brown (Davis, 1938), Dallas (Cumley, 1943), Grayson (Baker, 1960), and Williamson (Cumley and others, 1942) counties. In addition, it appeared that not all of the early water-level measurements reported in the Tarrant County report (Leggatt, 1957) are included in the TWDB groundwater database. Since this county experienced significant water-level declines prior to 1950, some early measurements were obtained from that report. A few historical water-level measurements from the early 1900s were collected from a USGS report on artesian water in Somervell County (Fiedler, 1934). Typically, the water-level data in the historical reports consists of a single measurement or, in a few instances, several measurements for a well. The water-level data from historical reports span the time period from 1895 through 1960. For the selected historical reports, well coordinates were determined by digitizing well locations off of georeferenced report maps. These locations are likely more accurate than those digitized off the Hill (1901) map, but were still considered to be uncertain.

The TWDB groundwater database (TWDB, 2013a) was queried to obtain water-level data for the counties in the study area. The water-level data obtained from the TWDB groundwater database range in date from 1900 through 2012, with the majority having dates after 1950. This database is the most significant source of transient water-level data available. The TWDB groundwater database contains coordinates for each well. Therefore, the well locations from these data were considered to have a high degree of certainty.

Water-level measurements in Texas from driller's logs were obtained from two sources: scanned logs from TCEQ well files and the TWDB's driller's log database (TWDB, 2013b). Measurements from the TCEQ scanned files range in date from 1916 through 2009 and measurements from the TWDB driller's log database range in date from 1999 through 2013. The latter contains only recent measurements because electronic collection of driller's logs by the TWDB began in 2001. Water levels from both sources of driller's logs consist of only one measurement per well.

Well coordinates are given in the TWDB driller's log database. Therefore, the well locations from these data are considered to have a high degree of certainty. The only location information contained on the scanned driller's logs from the TCEQ well files is the number from the Texas water well numbering grid for the grid-block in which the well is located and, in some cases, a hand drawn map showing the well's location within the grid block. The grid blocks consist of a 2.5-minute by 2.5-minute area. It was not feasible, if not possible, to determine exact well locations from the available information. Therefore, all wells within a grid block were assigned coordinates consistent with the coordinates of the centroid of the grid block. Consequently, the location for the wells with water-level data obtained from the scanned driller's logs in the TCEQ well files were considered to be uncertain.

Water-level data were received from several of the GCDs in the study area. Data for dates ranging from 1961 to 2012 were obtained from the Central Texas GCD, from 1996 to 2012 from the Clearwater UWCD, from 2001 to 2010 from the Northern Trinity GCD, from 1965 to 2012 from the Prairielands GCD, from 1962 to 1988 from the Southern Trinity GCD, and from 1964 to 2013 from the Upper Trinity GCD. Care was taken to eliminate duplicate measurements in the data from the GCDs and that in the TWDB groundwater database. In addition, data from

both sources for a well were integrated. The water levels received from GCDs include some

transient data consisting of several water-level measurements over time. Coordinates for wells

were provided by the GCDs, so well locations were considered to have a high degree of

certainty.

Water-level data for Oklahoma, Arkansas, and portions of Texas were obtained from Oliver and

others (2013), who conducted a modeling study of the Antlers Aquifer in Oklahoma. Their

sources were online data from the USGS National Water Information System and the Oklahoma

Water Resources Board. The data they obtained from the USGS consisted of measurements

from 1960 to 2012 for Texas, from 1944 to 2010 for Oklahoma, and from 1900 to 1994 for

Arkansas. Water-level data in Texas from Oliver and others (2013) and the TWDB groundwater

database were compared and duplicate measurements were eliminated. Data from the Oklahoma

Water Resource Board from Oliver and others (2013) consisted of water-level measurements

from 1956 to 2011. Coordinates for wells are included in the USGS and Oklahoma Water

Resources Board data, so well locations from Oliver and others (2013) were considered to have a

high degree of certainty.

Table 4.3.1 provides a summary of the water-level data and includes the number of wells

obtained from each source, the total number of water-level measurements associated with those

wells, and the first and last years of the water-level measurements. This table indicates that the

source for the largest number of wells is the TWDB driller's log database. These data, however,

include only one water-level measurement per well for dates that cover only a small portion of

the time period of interest for the model. The source for the largest number of water-level

measurements is the TWDB groundwater database. The total number of wells identified within

the study area was 45,526, which combine for a total of 98,036 water-level measurements.

An effort was made to collect all available water-level data and evaluate those data for use in the

updated northern Trinity and Woodbine aquifers GAM. The data were evaluated and selected

based on the following criteria:

- Water-level measurements in the TWDB groundwater database with a non-
  publishable flag were not used.

- Water-level measurements in the TWDB groundwater database with a remark indicating the measurement was questionable were not used.

- The date of the water-level measurement was compared to the date that the well was completed. In many instances, reported water levels were measured during the drilling process. Water-level measurements with a date prior to the well completion data were not used.

- The depth to water was compared to the total depth of the well and, if it was greater, the water-level measurement was not used.

- Available information and notes were reviewed to evaluate whether the reported water level was affected by pumping in the well or in a nearby well. Water levels determined to be affected by pumping were not used.

- When identified, anomalous data for a well were not used.

Further censoring of the hydraulic head calibration targets occurred during model calibration as discussed in Section 9.

Using completion data, which are available for many wells but not the majority of wells, the aquifer(s)/formation(s) across which the wells are completed was estimated by comparing the completion interval(s) to the structure data. Table 4.3.2 summarizes the available completion information for the wells with water-level measurements. This table summarizes, by source, the percentage of wells with completion information, or partial completion information, and the percentage where only a total depth was provided by the source. Completion information consists of the depth to the top and bottom of each screen in the well. The number of screens in a well varied from one to 20, with the majority of the wells having one or two screens. Partial completion information consists of the depth to the top of the uppermost screen, either the depth to the top or bottom of the screen, but not both, or the depth to the top and bottom of the gravel pack. In some cases, the two percentages in Table 4.3.2 do not sum to 100 percent because neither completion information nor total depth are available for some wells.

The spatial distribution of the types of completion information available for the wells with water-level data in the study area is illustrated in Figure 4.3.1a. As seen on this figure, completion information is available for the majority of the wells in the northern and western portions of the

study area, and the majority of the wells with total depth only are located in the southern portion of the study area. Completion information for wells located in the North Texas, Northern Trinity, Prairielands, and Upper Trinity GCDs is shown in Figure 4.3.1b.

Table 4.3.3 summarizes the number of wells and water-level measurements by estimated completion interval. For wells with completion information, it was possible to identify the aquifer(s)/formation(s) across which the well is completed. For wells with only total depth information, the completion interval was estimated when possible based on the predominate aquifer(s)/formation(s) present shallower than the total depth at the location of the well and the aquifer or aquifer code given in the source data, if available. This approach was most successful for shallow wells.

In many cases, wells are completed within a single aquifer or formation, as listed under Group 1 in Table 4.3.3. The spatial location of these wells is shown in Figure 4.3.2a for the study area and Figure 4.3.2b for the North Texas, Northern Trinity, Prairielands, and Upper Trinity GCDs. A well was considered completed in a single aquifer/formation if 90 percent or more of the screen interval was across that aquifer/formation. Many other wells are completed across multiple aquifers and/or formations within the northern Trinity and Woodbine aquifers, as shown under Group 2 in Table 4.3.3. Table 4.3.4 explains the terminology used in Table 4.3.3 for completions across three or more aquifers/formations in the northern Trinity Aquifer. The spatial distribution of wells in Group 2 is shown in Figure 4.3.3a for the study area and Figure 4.3.3b for the North Texas, Northern Trinity, Prairielands, and Upper Trinity GCDs.

Group 3 in Table 4.3.3 summarizes estimated completions across multiple aquifers/formations but not exclusively within the northern Trinity Aquifer (i.e., the completion interval includes portions of the northern Trinity Aquifer as wells as portions of the Washita/Fredericksburg groups and/or Paleozoic-age sediments). The majority of wells with this type of completion are those for which only a total depth is available or those with completion information that indicates the well screen includes Paleozoic-age sediments. Also included in Group 3 are completions exclusively outside of the northern Trinity and/or Woodbine aquifers [i.e., completions in younger sediments, the Washita/Fredericksburg groups (other than the Edwards BFZ Aquifer), or Paleozoic-age sediments]. The spatial distribution of wells in Group 3 is shown in

Figure 4.3.4a for the study area and Figure 4.3.4b for the North Texas, Northern Trinity, Prairielands, and Upper Trinity GCDs.

In Table 4.3.3, the Group 4 completions represent those given for wells with potentially "mixed formation" completions that include the Washita/Fredericksburg groups as well as the northern Trinity and/or Woodbine aquifers, deep wells with large completion intervals or total depth information only for which a completion interval was not determined, and wells with an unknown completion interval because completion information for the well was not found. Many of the wells in the study area have multiple screens or, in the case of old wells, long open hole intervals, as the objective of the well was to access as much producing sand as possible. Although many of the wells for which completion information are available included one or two screens, it was not uncommon to find wells with five to ten screened intervals. The maximum number of screens identified for a well in the study area was 20. Since many of the wells with an undetermined completion are thousands of feet deep and could potentially be screened across multiple aquifers and/or formations, no specific completion interval was estimated for these wells. The spatial distribution of wells in Group 4 is shown in Figure 4.3.5a for the study area and Figure 4.3.5b for the North Texas, Northern Trinity, Prairielands, and Upper Trinity GCDs.

The temporal distribution of water-level measurements for wells completed in a single aquifer or formation in the study area is shown in Figures 4.3.6 through 4.3.9 as the number of water-level measurements each year from 1900 through 2013. Note that the scale of the y-axis varies from plot to plot in these figures depending on the number of water-level measurements. In all figures of this type in this section of the report the y-axis, denoting number of water-level measurements, is not the same. In general, few measurements are available prior to 1950 for any aquifer/formation. Peaks in the number of water-level measurements are observed around 1970 and 2005 for the Woodbine and Hensell aquifers and the Pearsall Formation, around 1980 and 2005 for the Edwards BFZ Aquifer, about 1955 and 2005 for the Paluxy Aquifer, and in about 2008 for the Hosston Aquifer. Refer to Table 4.3.3 for the total number of water-level measurements for each aquifer or formation. The temporal distribution of water-level measurements for wells completed across multiple aquifers/formations in the northern Trinity Aquifer are shown in Figures 4.3.10 through 4.3.12 as the number of water-level measurements per year from 1900 through 2013. Again, few measurements are available prior to 1950. In

general, the largest number of measurements is available around 1970 and after 2000. Refer to Table 4.3.3 for the total number of water-level measurements for the multi-completed wells in the northern Trinity Aquifer.

The temporal distribution of water-level measurements for wells completed in a single aquifer or formation or multiple aquifers and/or formations in the northern Trinity Aquifer are shown in Figures 4.3.13 and 4.3.14 for the North Texas GCD, Figures 4.3.15 and 4.3.16 for the Northern Trinity GCD, Figures 4.3.17 and 4.3.18 for the Prairielands GCD, and Figures 4.3.19 and 4.3.20 for the Upper Trinity GCD. These figures show the number of water-level measurements every 5 years from 1900 through 2013. Note that the scale of the y-axis varies from plot to plot in these figures depending on the number of water-level measurements. All of these figures show a general absence of water-level measurements prior to about 1950. The total number of water-level measurements associated with these figures is summarized in Table 4.3.5.

4.3.2 Predevelopment Hydraulic Head Surfaces

Predevelopment conditions are defined as those existing in an aquifer(s) before the natural flow of groundwater was disturbed by artificial discharge via pumping. Typically, predevelopment conditions represent steady-state conditions in the aquifer; where aquifer recharge is balanced by natural aquifer discharge. Under predevelopment conditions, the general direction of flow in the northern Trinity and Woodbine aquifers was from the outcrop areas towards the East Texas Basin. Predevelopment flow within the aquifers generally moved from the outcrop areas to the downdip portions of the aquifers. The outcrop areas of the northern Trinity and Woodbine aquifers trend northeast-southwest in Texas and east-west in Oklahoma and Arkansas. The direction of flow during the predevelopment period was generally eastward and southeastward in Texas. In Oklahoma and Arkansas, subcrop flow in the northern Trinity Aquifer may have been eastward parallel to the outcrop based on results from Morton (1992). Flow was diverted from the general downdip direction towards major rivers in the outcrop areas.

The earliest available information on hydraulic heads in the northern Trinity and Woodbine aquifers is provided by Hill (1901). He presents an extensive geologic study of the Black and Grand prairies of Texas with emphasis on artesian waters in the northern Trinity and Woodbine aquifers. Hill (1901) indicates that by the time of his investigation, significant development of

the aquifers had already occurred. Appendix E provides a brief summary of the development history of the northern Trinity and Woodbine aquifers based on Hill (1901) and other historical reports. Development of the northern Trinity and Woodbine aquifers began in the late 1800s with most of that occurring in the 1890s.

High hydraulic pressures resulted in flowing conditions for early wells drilled into the northern Trinity and Woodbine aquifers in many portions of the study area. By 1900, there were many wells drilled to the Hensell Aquifer in the vicinity of Waco, Texas and to the Paluxy and Hensell aquifers in the vicinity of Fort Worth, Texas. In fact, Waco was advertised as "Geyser City" in the late 1800s due to the presence of numerous wells drilled to the Hensell Aquifer having pressure sufficient to cause water to rise tens of feet above ground surface. Fiedler (1934) reports that the first flowing well in Somervell County was drilled in 1880. He estimates that over 250 wells were drilled in that county prior to 1900. Hill (1901) sent out inquiries requesting information on artesian wells in the Black and Grand prairies as part of his investigation. This area includes 34 of the counties within the study area. Based on the results of those inquires, he estimated 964 artesian wells, with 458 of them being flowing wells and 506 being non-flowing wells, with the flow rate in the flowing wells varying from about 1 to 700 gallons per minute. Many of the flowing wells were allowed to flow freely for years, resulting in significant loss of water. Several of the historical reports indicate substantial reductions in flow rates over short periods of time due to the drilling of numerous wells. Leggat (1957) reports that well fields developed by the city of Fort Worth in the 1890s and 1905 were abandoned in 1914 and the city switched to surface water supplies because the wells had stopped flowing. Similar reductions in pressure were observed in the Hensell Aquifer near Waco, resulting in the city converting to surface water in 1930.

Historical reports indicate that development of the northern Trinity and Woodbine aquifers began in the late 1800s resulting in reduced pressures prior to the availability of early water-level measurements. In addition, these reports indicate that significant reductions in hydraulic heads occurred in the aquifers in the early part of the 1900s. As a result, the predevelopment hydraulic head surfaces presented here are estimated surfaces based on the best available data.

Predevelopment hydraulic head surfaces were developed for the Woodbine, Paluxy, Hensell, and Hosston aquifers generally using water-level data for wells estimated to be completed exclusively in each aquifer. The predevelopment hydraulic head surfaces were estimated using the known locations of wells that flowed when drilled, water-level measurements from Hill (1901), and maximum water levels in wells located in the outcrop areas regardless of time. These hydraulic head surfaces are considered to be an under estimation of the predevelopment hydraulic heads, with the hydraulic heads in the outcrop areas expected to be closer to predevelopment conditions than hydraulic heads in the downdip portions of the aquifers.

The known locations of wells in the northern Trinity and Woodbine aquifers that flowed when drilled are shown in Figure 4.3.21. These wells were identified from historical reports, predominantly Hill (1901) and Fiedler (1934), and are wells with water-level measurements above ground surface in the TWDB groundwater database and TWDB driller's log database. In developing the estimated predevelopment hydraulic head surfaces, the elevation of the water level in flowing wells was calculated based on measured values when available and estimated to be at ground surface when measured levels are not available. The ground surface elevation at the location of every flowing well shown in Figure 4.3.21 was not used in estimating the predevelopment surfaces. In instances where the ground surface elevation at the location of a flowing well appeared low relative to the trend in the estimated hydraulic head contours, that ground surface elevation was not used. Since the ground surface elevation was used for most of the flowing wells, the estimated predevelopment surfaces underestimate predevelopment conditions at the location of the flowing wells.

Available data for estimating predevelopment hydraulic heads generally do not exist throughout the spatial extent of the aquifers in the study area. No attempt was made to estimate hydraulic heads representative of predevelopment conditions where data are not available. Therefore, the estimated predevelopment surfaces do not always cover the entire extent of the aquifers.

The hydraulic heads estimated to be representative of predevelopment conditions in the Woodbine Aquifer are shown in Figure 4.3.22. In the outcrop area, data are available in the portion that trends north-south. Data in the downdip portion are available in approximately the

southern half of the aquifer. This surface indicates eastward flow from the outcrop to the downdip portion of the aquifer.

The estimated predevelopment hydraulic head surfaces for the Paluxy, Hensell, and Hosston aquifers are shown in Figures 4.3.23, 4.3.24, and 4.3.25, respectively. The majority of the data from which the predevelopment surface for the Paluxy Aquifer was estimated are located in or near the outcrop area. In general, this surface shows eastward flow from the outcrop to the downdip area in Texas, which is the expected direction of flow because it mimics the regional topographic gradient in most of the study area. The direction of flow is also shown to be towards the east in western Oklahoma and to the southeast in eastern Oklahoma and Arkansas. Few data are available to estimate the hydraulic head surface in the Hensell Aquifer under predevelopment conditions and, consequently, the surface is developed in a small portion of the aquifer (see Figure 4.3.24). This surface indicates eastward flow from the outcrop area to the East Texas Basin. A few data points in both the outcrop and downdip portions of the Hosston Aquifer were available for estimating the predevelopment hydraulic head surface (see Figure 4.3.25). The direction of predevelopment flow indicated by this surface is the expected direction in Texas (i.e., eastward toward the East Texas Basin). The eastward direction in Oklahoma and Arkansas is consistent with subcrop hydraulic heads in Morton (1992).

The estimated predevelopment hydraulic head surfaces for the aquifers present general regional patterns of west to east flow in the Texas portion of the aquifers. It is expected that the predevelopment hydraulic heads in the outcrop regions of the aquifers varied significantly and were a subdued replica of the topography with higher hydraulic heads in higher elevation regions and lower hydraulic heads in lower elevation regions as described by Toth (1963). To be able to reproduce such a surface requires a much denser array of monitoring points than in a confined aquifer setting. Data are insufficient to estimate local hydraulic heads or the complex localized flow systems in the outcrop portions of the aquifers during predevelopment.

4.3.3 *Transient Hydraulic Head Data (Hydrographs)*

An evaluation of the transient behavior of hydraulic heads was conducted using transient water-level data in wells. In general, transient data were considered to be more than five water-level measurements. However, if only a couple of measurements are available for a well, but at least

one of those was taken prior to 1950, those data were included in the evaluation if they provided

information on change in hydraulic heads in the early part of the 1900s. In some instances, data

from a well consists of more than five water-level measurements, but the measurements were

taken within a very short time period. Those data were not included in the evaluation because

they provide little information on the transient behavior of hydraulic head trends.

The evaluation presented here discusses observed trends in transient hydraulic heads for wells

identified as completed in the:

- Woodbine Aquifer.

- Paluxy Aquifer.

- Hensell Aquifer.

- Hosston Aquifer.

- Paluxy Aquifer and Glen Rose Formation.

- Hensell Aquifer and Glen Rose Formation, Hensell Aquifer and Pearsall Formation, or
  Hensell Aquifer and Glen Rose and Pearsall formations (i.e., wells with a middle-Trinity
  completion).

- Hosston Aquifer and Pearsall Formation.

- Glen Rose Formation.

- Pearsall Formation.

- Edwards BFZ Aquifer.

The locations of wells with transient hydraulic head data are shown in Figure 4.3.26a for the

study area and Figure 4.3.26b for the North Texas, Northern Trinity, Prairielands, and Upper

Trinity GCDs. The remainder of this section presents and discusses select hydrographs. The

scale for years on the x-axis is from 1900 to 2013 for all hydrographs. The scale for the water-

level elevation on the y-axis is variable from hydrograph to hydrograph depending on the range

of the observe data, however, the division of the y-axis is consistent at 25 feet.

Due to the large volume of transient hydraulic head data available for wells in the study area, all

hydrographs could not be presented and discussed in this section. However, an appendix is

included with this report that contains hydrographs for wells with transient data (Appendix M).

Section M.1 of this appendix provides large size plates of transient hydrographs for the counties

comprising the North Texas, Northern Trinity, Prairielands, and Upper Trinity GCDs.
Section M.2 provides transient hydrographs in the study area organized by state, county, and
completion. This appendix includes hydrographs for wells regardless of completion and includes
the wells where the completion interval was not determined or was unknown.

Figure 4.3.27 through 4.3.36 show select hydrographs by completion. Hydrographs shown in
these figures were selected based on several criteria. First, a review of all hydrographs was
conducted in order to select those with a long-term record or data that provide information on
early water-level declines. Second, hydrographs were selected based on spatial location in an
effort to show transient conditions across the study area. Third, an effort was made to select
hydrographs with sufficient data to define a hydraulic head trend. In the discussions below, the
hydrograph for specific wells mentioned in the text are shown in the cited figures.

The hydrograph plots shown in Figures 4.3.27 through 4.3.36 include a label indicating the well
number, the county in which the well is located, and the estimated completion for the well. In
most instances, the well number is the state well number as given in the TWDB groundwater
database. A few of the hydrographs show data obtained from historical reports written prior to
the establishment of the state well number system. In those cases, an arbitrary well number was
given to the well that includes the county in which the well is located and the number given in
the historical report that contains the water-level data for the well. For example, well Dallas_343
shown on Figure 4.3.27 corresponds to well 343 from a historical report on water-level
measurements in Dallas County. The county name was included in this arbitrary well number
because common well numbers were used in multiple historical reports that provide water-level
data for different counties.

Woodbine Aquifer

Select hydrographs for wells completed in the Woodbine Aquifer are shown in Figure 4.3.27.
Several trends in hydraulic head data are observed in this aquifer. In general, hydraulic heads in
the outcrop area show little change over time (wells 3238602 and 1814906). However, local
declines up to about 100 feet are observed in some outcrop areas (wells 3231301, 1841201, and
1825301). The data show declining hydraulic heads throughout the downdip portion of the
aquifer. The greatest decline is about 450 feet in a well in Dallas County (well Dallas_343). In

Grayson County, the recovery of hydraulic heads starting in about 1990 is observed in many wells (well 1828402). Although the hydraulic heads in these wells are recovering, they have not yet reached their pre-decline level. The trend in several wells in Fannin, Ellis, and Johnson counties show a decrease in the rate of decline starting in about 1980 to 1990 (well 3248501). The hydraulic heads in a couple of wells located in the outcrop show an overall increase over the period of record of about 25 feet. In the downdip portion of the aquifer, overall declines in hydraulic heads range from about 10 to 450 feet and observed rates of decline range from 0.5 to 13.2 feet per year. Table 4.3.6 summarizes the overall declines in hydraulic heads and rates of decline observed in wells completed in the Woodbine Aquifer and located in the downdip portion of the aquifer by county. Because transient hydraulic head data are not available everywhere, the declines shown in this table likely do not reflect declining conditions throughout the aquifer.

Paluxy Aquifer

Select hydrographs for wells completed in the Paluxy Aquifer are shown in Figure 4.3.28. In general, hydraulic heads in the outcrop area have remained constant over time (well 3218201). In a few outcrop wells, an overall increase or decrease in hydraulic heads of less than about 25 feet is observed (well 3162108). In the downdip portion of the aquifer, decreasing trends are observed throughout the aquifer with declines ranging from about 4 to 378 feet and rates of decline ranging from 0.3 to 23.3 feet per year. The rate of decline has been relatively constant in many wells (wells 1833301 and 3319303) but began to slow in about 1980 to 1990 in many other wells (wells 1961301 and 3214610). A few wells show temporary recovery in hydraulic heads imposed on an overall declining trend (well 1963601) and a few wells show some recovery in hydraulic heads since the early 1970s (well 3215504). Typically, however, periods of recovery are not observed in most wells located in the downdip portion of the aquifer. Table 4.3.6 summarizes the overall declines in hydraulic heads and rates of decline observed in wells completed in the Paluxy Aquifer and located in the downdip portion of the aquifer by county. Because transient hydraulic head data are not available everywhere, the declines shown in this table likely do not reflect declining conditions throughout the aquifer.

Hensell Aquifer

Select hydrographs for wells completed in the Hensell Aquifer are shown in Figure 4.3.29. In general, hydraulic heads in the western outcrop area have remained constant (wells 3046701 and 4112201) or slightly fluctuated, with changes less than 25 feet, over time (well 3152303). In a few wells in the western outcrop area, overall declines in hydraulic heads of less than 10 feet are observed as well as overall increases of less than 10 feet. In the northern and central areas of the outcrop in Montague, Wise, and Hood counties, observed hydraulic heads generally show a declining trend of up to about 75 feet (wells 1943603 and 3242403). However, a relatively constant trend is observed in one well in Montague County (well 1920801) and periods of recovery are observed in one well each in Montague and Hood counties (wells 1928804 and 3234609, respectively). In the downdip portion of the Hensell Aquifer, overall declining trends in hydraulic heads are observed. In general, the declines have been constant with time (wells 4011602, 3262701, and 3251104). A maximum decline of 300 feet is observed for well 4011602 in Bosque County. One well in Coryell County shows an initially declining trend followed by a rising trend since about 1990 (well 4033102). Table 4.3.6 summarizes the overall declines in hydraulic heads and rates of decline observed in wells completed in the Hensell Aquifer and located in the downdip portion of the aquifer by county. Because transient hydraulic head data are not available everywhere, the declines shown in this table likely do not reflect declining conditions throughout the aquifer.

Hosston Aquifer

Select hydrographs for wells completed in the Hosston Aquifer are shown in Figure 4.3.30. In general, hydraulic heads in the outcrop area have remained constant through time (wells 1912605 and 3140101). Declining trends in hydraulic heads are observed in the downdip portion of the aquifer. Observed declines range from 44 to 832 feet and average 247 feet. The largest declines are found in Hill County, where declines over 800 feet have been observed (well 3326902), and Ellis and McLennan counties, where declines over 600 feet have been observed. Over the available periods of record, observed hydraulic heads continually declined at a fairly constant rate (well 4064101). In some wells, relatively short periods of recover are observed on the overall declining trend (wells 4016404, 3246907, and 3909201) while longer-term periods of recovery are observed in other wells (wells 5844201 and 3319101). After initially declining, one

well in Dallas County (well 3309701) and two wells in Bosque County show hydraulic heads that have recovered to near or greater than the initial measurement. Hydraulic heads in several wells have been fairly stable over the last 30 to 40 years after initial large declines (wells 3213601 and 5829603). Table 4.3.6 summarizes the overall declines in hydraulic heads and rates of decline observed in wells completed in the Hosston Aquifer and located in the downdip portion of the aquifer by county. Because transient hydraulic head data are not available everywhere, the declines shown in this table likely do not reflect declining conditions throughout the aquifer.

Paluxy Aquifer and Glen Rose Formation

Select hydrographs for wells completed in both the Paluxy Aquifer and the Glen Rose Formation are shown in Figure 4.3.31. In general, the composite hydraulic heads observed in these wells show little change with time in the outcrop area (well 3227402) and slightly declining trends in the shallow subcrop (wells 3212503 and 3228301). A few wells in the outcrop area show periods of both slightly declining and slightly rising hydraulic heads, with the magnitude of the declines and rises less than 25 feet (wells 3210201 and 3234803). Deeper in the subcrop, declining hydraulic heads are observed in most wells (wells 3207106, 1829302, and 3239701). A large (175-foot) increase in hydraulic heads is observed in well 4028402 in Coryell County. Table 4.3.6 summarizes the overall declines in hydraulic heads and rates of decline observed in wells completed in both the Paluxy Aquifer and the Glen Rose Formation and located in the downdip area. Because transient hydraulic head data are not available everywhere, the declines shown in this table likely do not reflect declining conditions throughout the aquifer and formation.

Hensell Aquifer and/or Glen Rose and Pearsall Formations

Select hydrographs for wells completed in the Hensell Aquifer and Glen Rose Formation, Hensell Aquifer and Pearsall Formation, or Hensell Aquifer, Glen Rose Formation, and Pearsall Formation (middle-Trinity completions) are shown in Figure 4.3.32. In general, hydraulic heads in the outcrop area have remained fairly stable through time (well 1951901) or slightly decreased (wells 3218701, 3055503, and 3162803). One well in Brown County shows a rising trend in hydraulic heads over its period of record. In the northern portion of the study area, hydraulic

heads observed in wells with this type of completion show overall declining trends at a fairly constant rate in the downdip portions of these aquifer/formations (wells 1938301, 1915701, and 3243805). In some of these northern wells with declining trends, hydraulic heads are observed to have temporarily recovered for an extended period of time (wells 4014602 and 4037501). A significant decrease in the rate of hydraulic head decline is observed in one well in Somervell County (well 3243046). An increase in hydraulic heads of about 60 feet over the period of record from the mid-1980s to present is observed in one well in McLennan County. In Coryell, Burnet, and Bell counties, cycles of both declining and rising hydraulic heads are observed in several wells (wells 4140903 and 5724101). Table 4.3.6 summarizes the overall declines in hydraulic heads and rates of decline observed in wells completed in the Hensell Aquifer and/or Glen Rose and Pearsall formations and located in the downdip area. Because transient hydraulic head data are not available everywhere, the declines shown in this table likely do not reflect declining conditions throughout the aquifer and formations.

Hosston Aquifer and Pearsall Formation

Select hydrographs for wells completed in both the Hosston Aquifer and the Pearsall Formation are shown in Figure 4.3.33. In general, hydraulic heads in the outcrop area have remained fairly stable through time (wells 4105105 and 4164604) or slightly declined (less than 25 feet). Wells in the downdip area show declining hydraulic heads over their periods of record. Essentially continually declining trends are observed in some wells (wells 1932302, 3224101, and 4048201), while temporary periods of recovery are observed in other wells (wells 3222903, 4061703, 3239057). Table 4.3.6 summarizes the overall declines in hydraulic heads and rates of decline observed for wells completed in both the Hosston Aquifer and Pearsall Formation and located in the downdip area. Because transient hydraulic head data are not available everywhere, the declines shown in this table likely do not reflect declining conditions throughout the aquifer and formation.

Glen Rose Formation

Select hydrographs for wells completed in the Glen Rose Formation are shown in Figure 4.3.34. In general, hydraulic heads in the shallow subcrop area of the formation have remained constant through time (well 3250802). A few wells in the shallow outcrop show rising hydraulic heads

with time (well 4128401). Several wells located in the shallow subcrop show declining trends with time. The magnitude of those declines ranges from about 25 to 75 feet (wells 3243402, 1923701, and 4124301). Deeper in the subcrop in McLennan, Bosque, and Bell counties, significant declines of 253 to 405 feet are observed (wells 4038101 and 4014702). The observed hydraulic heads in a few wells in Wise, Parker, Johnson, and Hamilton counties show temporary periods of recovery (wells 3211702, 1945301, and 3237702). Table 4.3.6 summarizes the overall declines in hydraulic heads and rates of decline observed for wells completed in the Glen Rose Formation and located in the downdip area of the formation. Because transient hydraulic head data are not available everywhere, the declines shown in this table likely do not reflect declining conditions throughout the formation.

Pearsall Formation

Select hydrographs for wells completed in the Pearsall Formation are shown in Figure 4.3.35. In general, hydraulic heads in the outcrop area of the formation have been constant through time (wells 1958401 and 4112902). The hydraulic heads for wells in the shallow subcrop show declining trends, with the magnitude of the declines ranging from about 25 to 50 feet (well 5715601). Deeper in the subcrop, declines ranging from about 100 to 325 feet are observed (wells 1817902, 4048801, and 5805403). The hydraulic heads in a few wells initially declined and then stabilized. In some cases, the hydraulic heads have remained stable and in other cases recent data show additional declines (well 5810303). Several of the wells completed in the Pearsall Formation are located in Burnet, Williamson, and Bell counties. Typically, wells are not expected to be completed in this formation in these areas. However, the available data on completion information for the wells and formation hydrostratigraphy indicate that these well are completed in the Pearsall Formation. Table 4.3.6 summarizes the overall declines in hydraulic heads and rates of decline observed for wells completed in the Pearsall Formation and located in the downdip area of the formation. Because transient hydraulic head data are not available everywhere, the declines shown in this table likely do not reflect declining conditions throughout the formation.

Edwards BFZ Aquifer

Select hydrographs for wells completed in the Edwards BFZ Aquifer are shown in Figure 4.3.36. In Bell County, observed hydraulic heads are predominately relatively stable (well 5804801) and a few wells show an overall rising trend (well 5804620). In Travis and Williamson counties, hydraulic heads are observed to be relatively stable in some wells (well 5834601) and widely fluctuating over relatively short time periods in other wells (wells 5835701 and 5835201). The magnitude of the fluctuations ranges from about 50 to 125 feet in Travis County and about 25 to 75 feet in Williamson County. In some areas in Williamson County, overall declining trends are observed in the aquifer (wells 5820101 and 5820403). The hydrograph for well 5827814 in Figure 4.3.36 is atypical in that the hydraulic heads are observed to decline and rise gradually over time rather than widely fluctuating over a short time period as observed in most wells. Based on the hydrograph data, they hydraulic head trends in the Edwards BFZ Aquifer appear to be widely variable over short horizontal distances consistent with a carbonate aquifer where flow is dominated by secondary porosity and karst features (Jones, 2003).

Summary

A review of the hydrographs data for wells completed in the Woodbine, Paluxy, Hensell, and Hosston aquifers suggests the following general trends. For all aquifers, hydraulic heads in the outcrop area have generally either remained fairly stable or increased or decreased less than about 25 feet over the period of record, which is much shorter than the period over which aquifer development has occurred. However, in areas of the outcrop located adjacent to areas of large decline in the downdip portion of the aquifers, declines greater than 25 feet have occurred. Large declines in hydraulic heads have occurred in the downdip portions of all aquifers during the early part of the 1900s and continuing through current day. In a few areas, the declining trend has reversed, or temporarily reversed, and the hydraulic heads have recovered slightly or are declining at a slower rate. For the majority of the wells in the downdip areas, hydraulic heads at the end of the period of record are significantly less than at the beginning of the record. Based on the available transient hydraulic head data, the largest declines have occurred in the Hosston Aquifer predominately in Tarrant, Johnson, Ellis, Hill, and McLennan counties.

4.3.4   Historical Hydraulic Head Data and Hydraulic Head Declines

Historical hydraulic head surfaces for the Woodbine, Paluxy, Hensell, and Hosston aquifers were estimated for 1950, 1970, 1990, and 2010. In addition, the declines in hydraulic heads from predevelopment to 1950 and from predevelopment to 2010 were estimated. The surfaces were estimated only in areas with data.

The decline in hydraulic heads in the outcrop areas of the aquifers is not well defined using the historical hydraulic head surfaces due to the lack of predevelopment data in the outcrop. Therefore, an analysis was conducted to look at hydraulic head trends in the outcrop areas using available transient data. The discussion of this analysis can be found after the discussion of the historical hydraulic head surfaces.

Historical Hydraulic Head Surfaces

Water-level data are not available at regular time intervals in every well. Therefore, the coverage of water-level data for a particular month or even a year is sparse. Since the amount of water-level data available are typically not sufficient for a particular year of interest, the historical hydraulic head surfaces were developed based on data from a few years before and a few years after the year of interest. Generally, data from the year of interest and one year prior to and one year after the year of interest were used. On occasion, the range was expanded if there were insufficient data and narrowed if there were sufficient data. The ranges of years used to develop the historical hydraulic head surfaces are summarized in Table 4.3.7. If a well had only one water-level measurement during the date range, that measurement was used. If a well had several water-level measurements during the date range, the average of the water levels was used. Because few data are available in the early part of the 20th century, the large declines in hydraulic heads illustrated by the hydrographs shown in Section 4.3.3 are not always captured by these surfaces. For example, the 450-foot decline in hydraulic heads in the Woodbine Aquifer between 1910 and 1942 observed at well Dallas_343 in Dallas County (see Figure 4.3.27) is not captured by the historical surface. This is because only two measurements are available for this well, and they do not coincide with the time interval used to develop the 1950 hydraulic head surface for this aquifer.

The estimated hydraulic head surfaces for the Woodbine Aquifer in 1950 and 1970 are shown in Figure 4.3.37 and in 1990 and 2010 in Figure 4.3.38. A very small cone of depression is present in Grayson County in 1950. A much larger region of lowered hydraulic heads is shown in this area in 1970, in addition to a cone of depression in Dallas County. The cone of depression in Grayson County is more defined in 1990 and 2010, due to an increase in available hydraulic head data.

Figure 4.3.39a shows an estimated decline in hydraulic heads of about 100 to 150 feet in the downdip portion of the Woodbine Aquifer between predevelopment and 1950. The greatest decline is a little over 200 feet in Collin County. However, the exact location of this decline is uncertain due to the paucity of data for both predevelopment and 1950. The decline of 200 feet in the northern portion of the outcrop in Texas is a function of the lack of data control in this portion of the aquifer in 1950, rather than an actual decline. The plot of hydraulic head decline from predevelopment to 2010 (Figure 4.3.39b) shows essentially very little, if any decline in hydraulic heads on the western edge of the outcrop and a decline of about 50 to 100 feet on the eastern edge of the outcrop. Declines in the downdip portion of the aquifer range from 200 to over 500 feet, with the latter located in Grayson, Collin, and Ellis counties.

The figure of hydraulic heads in the Paluxy Aquifer in 1950 (Figure 4.3.40a) shows the presence of a significant low in hydraulic heads in the vicinity of Tarrant and Dallas counties. A significant cone of depression is observed in Tarrant and Dallas counties and surrounding counties in 1970, 1990, and 2010 (Figures 4.3.40b and 4.3.41). Based on the available data identified as representing the Paluxy Aquifer, no other areas with cones of depression are present in the aquifer. The hydraulic head decline in the Paluxy Aquifer in the vicinity of Dallas and Tarrant counties was over 400 feet by 1950 and over 700 feet by 2010 (Figure 4.3.42).

The historical surfaces for the Hensell Aquifer (Figures 4.3.43 and 4.3.44) do not show any large cones of depression within this aquifer. The data available for 1990 suggest a small cone of depression in Johnson and Hill counties and the data available for 2010 suggest a small cone of depression in Wise County. The hydraulic head decline ranges from 10 feet in the outcrop area to about 150 feet in the downdip area for the time period from predevelopment to 1950 and from

about 25 feet in the outcrop area to over 400 feet in the downdip area for the time period from predevelopment to 2010 (Figure 4.3.45).

The presence of a large regional cone of depression centered in Tarrant County is illustrated on the 1950 hydraulic head surface for the Hosston Aquifer (Figure 4.3.46a). By 1970, this cone of depression had deepened and another cone of depression had developed centered in McLennan County (Figure 4.3.46b). The surfaces for 1990 and 2010 show that these two cones of depression had merged, resulting in a large regional low in hydraulic heads in the aquifer extending from north of Tarrant County to McLennan County (Figure 4.3.47). The deepest portion of this cone is in Johnson and Ellis counties. In Tarrant County, the estimated hydraulic head decline was over 700 feet between predevelopment and 1950 and over 1,200 feet between predevelopment and 2010 (Figure 4.3.48).

Water-Level Trend Analysis in Aquifer Outcrop Areas

Using the available transient water-level data, an analysis was conducted to calculate historical trends in hydraulic heads in the outcrop areas of the northern Trinity and Woodbine aquifers in the Texas portion of the study area. This analysis consisted of calculating the rate of water-level change (in feet per year) between the first measured water level and the last measured water level. The analysis for the Woodbine Aquifer considered only wells located in the outcrop and completed in that aquifer, since those are the ones representative of the water table. For the northern Trinity Aquifer, all wells located in the aquifer outcrop with a total depth less than 200 feet were included, since the aquifer is comprised of many aquifers/formations and the water level in the shallower wells likely represents water-table conditions.

The data were divided into the following four time periods for the analysis:
- First measurement before 1950 and last measurement in or after 2000.
- First measurement between 1950 and 1974 and last measurement in or after 2000.
- First measurement between 1975 and 1999 and last measurement in or after 2000.
- First and last measurement in or after 2000.

The time frames for the first measurement were selected based on:
- Sufficient data to evaluate long-term historical trends; thus, the selection of pre-1950.
- Data to evaluate recent trends versus historical trends; thus the selection of 2000 or later.

- Dividing the time between 1950 and 2000 into two equal periods.

The time frame for the last measurement was after 2000 in all cases so that trends through current conditions could be evaluated. The purpose of separating the data into these four time bins was to evaluate whether the overall rate of change has increased in recent years.

The analysis did not consider the rate of change for wells where the time frame between the first and last water-level measurement was less than one year. For instances when only two measurements are available for a well, the trend of the data could not be evaluated to determine whether both of the measurements represent undisturbed conditions in the aquifer. Therefore, data for wells with only two measurements were not used for the analysis. For some wells with multiple water-level measurements, the value of the first measurement was anomalous with respect to the other measurements. In those cases, the second measurement rather than the first measurement was used for the analysis.

The results of the analysis for the Woodbine Aquifer outcrop are shown in Figure 4.3.49 and summarized in Table 4.3.8. In this figure and table, a negative value represents decreasing hydraulic heads and a positive value represents increasing hydraulic heads. Data with a first water-level measurement prior to 1950 and a last measurement in or after 2000 and data with a first and last water-level measurement in or after 2000 are not available for wells in the outcrop of the Woodbine Aquifer. The change in water level ranged from a decline of 2.2 feet per year to a rise of 0.4 feet per year based on data with a first measurement between 1950 and 1974 and a last measurement in or after 2000. The available data in Fannin, Grayson, and Cooke counties indicate only decreasing hydraulic heads during this time period. Both decreasing and increasing trends were observed in the data in Denton, Tarrant, and Johnson counties over this time period. The maximum observed rate of decline occurred in Denton County and the maximum observed rate of rise occurred in Johnson County.

The rate of change in hydraulic heads varied from a decline of 0.1 feet per year to an increase of 0.05 feet per year for data with a first water-level measurement between 1974 and 1999 and a last measurement in or after 2000. These data were from two wells located in Denton County. Consistently declining hydraulic heads are observed in the Woodbine Aquifer outcrop in Fannin, Grayson, Cooke, and northern Denton counties. These declines are likely due to the declines in

the downdip portion of the aquifer illustrated by the cone of depression centered in Grayson County. In the remainder of the outcrop, both rising and declining trends are observed. Due to limited data, no conclusion was reached regarding changes in hydraulic head trends between the two time periods with data for the Woodbine Aquifer outcrop.

The results of the analysis for the northern portion of the northern Trinity Aquifer outcrop are shown in Figure 4.3.50a and summarized in Table 4.3.8. Date for the time period from before 1950 to in or after 2000 are available only in Parker County. Those data show trends ranging from a decline of 0.2 feet per year to an increase of 0.09 feet per year. Data for numerous wells are available for the time period from between 1950 and 1974 to in or after 2000. These data show that the trend in hydraulic heads was declining at 60 percent of the wells analyzed and rising at 40 percent of the wells analyzed. The largest declining trend of 1.7 feet per year is observed in Wise County and the largest rising trend of 0.8 feet per year is observed in Montague County. All wells with available data from between 1974 and 1999 to in or after 2000 indicate declining hydraulic heads. Data for wells with first and last water-level measurements both in or after 2000 indicate a maximum declining rate of 2.9 feet per year in Cooke County and a maximum rising rate of 1.4 feet per year in Parker County.

A comparison of the results for the four different time periods investigated indicates the largest rates of decline for data with a first and last measurement in or after 2000, the largest rates of rise for data with a first measurement between 1950 and 1974 and a last measurement in or after 2000, and only declining trends for data with a first measurement between 1974 and 1999 and a last measurement in or after 2000. There does not appear to be any spatial trend in the distribution of rising and declining hydraulic heads in the outcrop area in Montague, Wise, and Parker counties (see Figure 4.3.50a). In Hood County, only declining trends are observed. A spatial trend cannot be determined for Somervell County since there are data at only one location in that county.

The results of the analysis of water-level data at wells located in the western portion of the northern Trinity Aquifer outcrop are shown in Figure 4.3.50b and summarized in Table 4.3.8. For all time periods investigated, the hydraulic head trend was decreasing in 58 percent of the wells analyzed and increasing in 42 percent of the wells analyzed. The largest rate of decline

was 1.6 feet per year at a well located in Hamilton County and the largest rate of rise was 1 foot

per year at a well located in Comanche County. There does not appear to be any spatial trend in

the locations of wells with declining and rising trends in the western outcrop area. The largest

rates of change are observed for data with a first measurement between 1950 and 1974 and a last

measurement in or after 2000.

4.3.5   *Transient Hydraulic Head Calibration Targets*

The primary means by which a groundwater model is calibrated is by comparing model predicted

hydraulic heads to observed hydraulic heads. The observed hydraulic heads used for this

comparison are referred to as hydraulic head targets, or more precisely, hydraulic head

calibration targets. The greater the number of hydraulic head calibration targets, in both time

and space, the more informed the calibration. Hydraulic head calibration targets are used both

individually (i.e., single hydraulic heads) and in time series to evaluate model performance.

Because many measurements of water levels are made only one or two times at the same well,

individual hydraulic head calibration targets are combined into a single data set, and comparisons

to simulated hydraulic heads are predominantly statistical, where summary statistics of fit are

used to describe calibration performance. For wells where multiple measurements have been

made over a long period of time, both quantitative and qualitative comparisons can be made to

simulated results, where the trends in hydraulic heads at a particular well can be compared to the

simulated trends in head at the same location.

Potential individual hydraulic head calibration targets for the transient model include all water-

level measurements. However, hydraulic head data for wells in which a completion interval

could be determined are more useful as calibration targets than data for wells where a completion

interval could not be determined. This is because the aquifer/formation associated with the

observed data is unknown and, therefore, uncertain. In addition, hydraulic head data for wells

which are completed across few aquifers/formations are more desirable than those for wells

completed across many aquifers/formations. This is because the model does not simulate

composite hydraulic heads but, rather, simulates hydraulic heads on an individual model layer

bases only. Therefore, assessment of model calibration through comparison of observed

composite hydraulic heads and simulated aquifer/formation specific hydraulic heads is

challenging. The most useful hydraulic head data for use as calibration targets are those for

wells completed into a single aquifer/formation. In this case, the observed hydraulic heads are directly comparable to simulated hydraulic heads for that aquifer/formation. The number of individual hydraulic heads for wells completed in a single aquifer/formation are shown by county and decade in Table 4.3.9. This table is organized by county and aquifer with Texas counties listed first followed by Oklahoma then Arkansas counties. The location of wells completed into a single/aquifer formation can be found in Figure 4.3.2a for the study area and Figure 4.3.2b for the North Texas, Northern Trinity, Prairielands, and Upper Trinity GCDs.

As with individual hydraulic head data, the most useful long-term transient hydraulic head data for use as calibration targets are also those for wells completed into a single aquifer/formation. With transient data, the length of the transient record and the number of measurements in the record are also of interest. Records over a short time period, such as less than 5 years, are basically equivalent to individual calibration targets, and are less useful for assessing model calibration. Wells single or multi-completed within the northern Trinity and Woodbine aquifers with transient hydraulic head data having five or more measurements over greater than 5 years can be found in Figure 4.3.26a for the study area and in Figure 4.3.26b for the North Texas, Northern Trinity, Prairielands, and Upper Trinity GCDs. Also included in these figures are the locations of wells with less than five water-level measurements if one of those measurements was taken prior to 1950. Data for these wells were considered to be potential transient calibration targets because they provide information on changes in aquifer conditions early in the development period. On Figure 4.3.26a, wells completed in the Edwards BFZ Aquifer with five or more water-level measurements over 5 years are more are also shown. The hydraulic head calibration targets used for the transient model are discussed in Section 9.1.1.

4.3.6 Vertical Hydraulic Gradients

The outcrops of the northern Trinity and Woodbine aquifers are at higher elevations than their subcrops and at higher elevations than sediments of younger age. In addition, within the northern Trinity Aquifer itself, older aquifers and formations, such as the Hosston Aquifer, generally outcrop at higher elevations than younger aquifers and formations, such as the Paluxy Aquifer. These types of dipping aquifers are generally conceptualized as having higher hydraulic heads in the outcrop areas that provide hydraulic drive to move groundwater into the confined portions of the aquifers. The groundwater that flows into the deep confined portions of

the aquifers is conceptualized as ultimately discharging to younger, overlying aquifers/formations through diffuse cross-formational flow and/or through major fault zones (Dutton and others, 1996; Bené and others, 2004). Rapp (1988) proposes that downward flow occurred from the Glen Rose Formation to the Hosston Aquifer in areas west of Waco, where the structural dip of the northern Trinity Aquifer is very low.

The conceptual model proposed for elevation drive to the subsurface results in a condition where vertical gradients in hydraulic heads are upward in predevelopment times. This fact is well documented by Hill (1901) who reports increasing hydraulic heads with depth in the northern Trinity Aquifer. Once development begins, vertical gradients can be altered and downward gradients to zones with significant drawdown, such as the Hosston Aquifer, can develop.

This section uses hydraulic head data collected years after development of the aquifers began to investigate trends in vertical hydraulic gradients in the historical period when good hydraulic head data are available. Two methods were used to evaluate the vertical hydraulic gradient between the aquifers and formations in the northern Trinity and Woodbine aquifers. The first consisted of comparing the estimated historical hydraulic head surfaces for predevelopment and 2010 to evaluate the vertical gradient direction prior to significant development of the aquifers and under current conditions. The second method consisted of comparing hydraulic heads in nearby wells completed in different aquifers or formations. The remainder of this section discusses the first method used to investigate vertical hydraulic gradients and then discusses the second method.

Comparison of Historical Hydraulic Head Surfaces

A comparison of the estimated predevelopment hydraulic head surfaces for the Woodbine and Paluxy aquifers (Figures 4.3.22 and 4.3.23, respectively) indicate higher hydraulic heads in the Paluxy Aquifer than in the Woodbine Aquifer, indicating an upward vertical gradient prior to significant development of the aquifers. Due to larger historical hydraulic head declines in the Paluxy Aquifer than in the Woodbine Aquifer, the vertical gradient is currently downward due to higher hydraulic heads in the Woodbine Aquifer than in the Paluxy Aquifer as shown by the 2010 hydraulic head surfaces in Figures 4.3.38b and 4.3.41b, respectively.

Where data are available for both aquifers, the estimated predevelopment hydraulic head surfaces for the Paluxy and Hensell aquifers indicate a downward vertical gradient from higher hydraulic heads in the Paluxy Aquifer to lower hydraulic heads in the Hensell Aquifer (see Figures 4.3.23 and 4.3.24, respectively). The hydraulic heads in the Paluxy Aquifer are also higher than that in the Hensell Aquifer in 2010 (see Figures 4.3.41b and 4.3.44b, respectively) indicating no change in the direction of the vertical gradient between these two aquifers from predevelopment conditions. This suggests that either the estimated predevelopment hydraulic head surface for the Hensell Aquifer shows the effects of pumping and is not representative of predevelopment conditions in the aquifer or that recharge to deeper units through cross-formational flow is an important process in the southwestern portion of the aquifer consistent with Rapp (1988).

Based on the available data, the estimated predevelopment hydraulic head surfaces indicate an upward vertical gradient from the Hosston Aquifer to the Hensell and Paluxy aquifers during predevelopment (see Figures 4.3.25, 4.3.24, and 4.3.23, respectively). This conclusion is consistent with that found by Hill (1901). With the exception of western portions of the outcrop area, the 2010 hydraulic heads in the Hosston Aquifer are less than those in the Hensell Aquifer (see Figures 4.3.47b and 4.3.44b, respectively), indicating a reversal of the vertical gradient between predevelopment conditions and conditions in 2010. Currently, the vertical gradient is downward from the Hensell Aquifer to the Hosston Aquifer. The same reversal in vertical gradient is also observed between the Hosston and Paluxy aquifers due to lower hydraulic heads in the Hosston Aquifer than in the Paluxy Aquifer in 2010 (see Figures 4.3.47b and 4.3.41b, respectively).

Comparison of Hydraulic Heads in Nearby Wells Completed to Different Aquifers/Formations

At several locations in the study area, wells located relatively closely to each other are completed in different aquifers or formations. For these wells, the hydraulic heads were compared for the purpose of evaluating the direction of the vertical hydraulic head gradients between the aquifers and formations. Note on the figures that both the year scale on the x-axis and the water-level elevation scale on the y-axis vary from plot to plot.

A comparison of hydraulic heads in the Woodbine Aquifer and overlying younger formations is shown in Figure 4.3.51. The specific formation into which the well in the younger formation is completed was not determined because the purpose of the comparison was to evaluate, in general, whether the vertical gradient was upward from the Woodbine Aquifer into the younger formations or downward from the younger formations to the Woodbine Aquifer. At a location near the Red River in northern Fannin County, observed hydraulic heads in the younger formation are greater than those in the Woodbine Aquifer by about 400 to 600 feet. Significantly higher hydraulic heads in the younger formations than in the Woodbine Aquifer are also observed at locations in Grayson and Collin counties. The hydraulic heads at these three locations indicate a downward vertical gradient from the younger formations to the Woodbine Aquifer. The large difference in hydraulic heads between the younger formations and the Woodbine Aquifer at these three locations is likely the result of historical declines in the hydraulic heads in the Woodbine Aquifer in Grayson County as illustrated by the cone of depression in this region of the aquifer (see Figure 4.3.38). For wells at a location in southern Fannin County, the comparison shows very similar hydraulic heads, within about 12 feet.

A comparison of hydraulic heads in the Woodbine Aquifer only at the four locations shown in Figure 4.3.51 shows that the recent hydraulic heads at three of the locations are about 200 feet amsl and at the fourth location are about 484 feet amsl. This suggests that the well with the higher hydraulic heads may be completed in the upper portion of the Woodbine Aquifer and the wells with the lower hydraulic heads may be completed in the lower portion of the aquifer.

A comparison of hydraulic heads in the Woodbine Aquifer and the underlying Washita/Fredericksburg groups is shown for two locations in Figure 4.3.52. At the location in northern Grayson County, the hydraulic heads in the Woodbine Aquifer were initially lower than those in the Washita/Fredericksburg groups and became higher in about 1980. This switch was the result of hydraulic heads in the Woodbine Aquifer increasing after 1970 and hydraulic heads in the Washita/Fredericksburg groups decreasing with time. At the location in Johnson County, the difference in hydraulic heads in the two units remained fairly constant at about 30 feet, with the hydraulic heads in the Woodbine Aquifer being lower than those in the Washita/Fredericksburg groups. These hydraulic heads indicate a upward vertical gradient from the Washita/Fredericksburg groups to the Woodbine Aquifer.

Also illustrated in Figure 4.3.52 is a comparison of hydraulic heads in the Paluxy Aquifer and the overlying Washita/Fredericksburg groups, also at a location in Johnson County. This comparison shows significantly higher hydraulic heads in the Washita/Fredericksburg groups than in the Paluxy Aquifer, suggesting a downward vertical gradient.

A comparison of hydraulic heads in the Woodbine Aquifer and the underlying Paluxy Aquifer at five locations is shown in Figure 4.3.53. At the two locations each in Collin and Johnson counties, hydraulic heads in the Woodbine Aquifer are greater than those in the Paluxy Aquifer, indicating a downward vertical gradient. Data for the Paluxy Aquifer at one of the locations in Collin County are available from about 1925 to 1955 (well 1842602). During this time period, the difference in hydraulic heads between the two aquifers was about 20 feet. At a nearby location with data from about 40 years later (wells 1850301 and 1850205), the difference in hydraulic heads between the two aquifers had increased to between 100 to 350 feet. The largest difference is a result of increasing hydraulic heads in the Woodbine Aquifer over a portion of this time. For both of these aquifers, hydraulic heads in about 1925 were between 500 and 600 feet amsl. By about 2000, hydraulic heads in the Woodbine Aquifer had declined to about 350 feet amsl and those in the Paluxy Aquifer had declined to about sea level, or declines of about 150 feet in the Woodbine Aquifer and about 500 feet in the Paluxy Aquifer.

At the two locations in Johnson County, hydraulic heads in the Woodbine Aquifer are about 400 to 450 feet higher than those in the Paluxy Aquifer, indicating a downward vertical gradient. This large difference in hydraulic heads between the two aquifers is likely due to historically stable hydraulic heads in the outcrop of the Woodbine Aquifer at this location and large historical hydraulic head declines of about 700 feet in the Paluxy Aquifer observed in this area (see Figure 4.3.42).

At the fifth location on Figure 4.3.53 in Dallas County, hydraulic heads in the Woodbine Aquifer are generally lower than those in the Paluxy Aquifer, with the difference ranging from about 100 feet in 1955 to about 10 feet in 1982. Based on the overall decreasing trend for the hydraulic heads in the well completed in the Paluxy Aquifer and the stabilizing hydraulic heads for the well completed in the Woodbine Aquifer, it is likely that the hydraulic heads in the Woodbine Aquifer are now higher than those in the Paluxy Aquifer at this location.

A comparison of hydraulic heads between the Paluxy Aquifer and the underlying Glen Rose Formation is available at four locations (Figure 4.3.54). At all but one location, the hydraulic heads in the Paluxy Aquifer are greater than those in the Glen Rose Formation, suggesting a downward vertical gradient. At the other location, hydraulic heads are similar in the two units for the time period with available data.

Figure 4.3.54 also shows a comparison between hydraulic heads in the Glen Rose Formation and the underlying Hensell Aquifer at one location in Somervell County. At this location, hydraulic heads in both units are essentially identical where the two have overlapping periods of record, suggesting that the two units could be hydraulically connected in this area. This connection could be the result of a poor well completion. This plot also shows about a 150-foot decline in hydraulic heads in the Hensell Aquifer between about 1965 and 2010 at this location.

A comparison of hydraulic heads in the Paluxy and Hosston aquifers at two locations in Tarrant County show higher heads in the Paluxy Aquifer than in the Hosston Aquifer (Figure 4.3.55). The time period for both of these comparisons starts in the 1940s. At this time, the difference in hydraulic heads was about 100 feet at one location and almost 200 feet at the other location, suggesting local impacts of pumping. The difference in hydraulic heads increased with time at one location. At the other location, the hydraulic head trends in the two wells completed in the Hosston Aquifer are very similar during about the first 10 years of the record but diverge starting in about 1955. The hydraulic heads in one well continued to decrease while the hydraulic heads in the other well appear to have remained stable for about 20 years and then increased during the last 10 years of the record. The different trends of the hydraulic heads in these two wells suggest the likelihood that they are completed in different sands within the Hosston Aquifer.

The difference in hydraulic heads between the Hensell and Hosston aquifers for one location in the outcrop area in Montague County is also shown in Figure 4.3.55. This plot shows fairly stable hydraulic heads in both aquifers over the period of record, and hydraulic heads in the Hensell Aquifer about 250 to 275 feet higher than those in the Hosston Aquifer, indicating a downward vertical gradient.

At one location each in Williamson and Bell counties, hydraulic heads in the Pearsall Formation were compared to those in the underlying Hosston Aquifer (Figure 4.3.56). At the location in

Williamson County, the hydraulic heads in the Hosston Aquifer are higher than those in the Pearsall Formation, suggesting an upward vertical gradient. Hydraulic heads in both these wells declined over the period of record, but the rate of decline was greater at the well completed in the Pearsall Formation than at the well completed in the Hosston Aquifer. Therefore, the difference in hydraulic heads between the two formations increased with time. At the location in Bell County, hydraulic heads in the Pearsall Formation are greater than those in the Hosston Aquifer, suggesting a downward vertical gradient. Over the period of record, the difference was initially small, but increased with time due to increasing hydraulic heads in the well completed in the Pearsall Formation and declining hydraulic heads in the well completed in the Hosston Aquifer.

Also shown in Figure 4.3.56 are comparisons of hydraulic heads in the Hosston Aquifer and the underlying Paleozoic-age strata at one location in Bosque County and another location in Wise County. At both locations, the hydraulic heads are higher in the Hosston Aquifer than in the Paleozoic-age strata, suggesting a downward vertical gradient. The difference in hydraulic heads is about 300 feet at the location in Bosque County and about 30 feet at the location in Wise County.

The hydraulic heads for wells completed in both the Paluxy Aquifer and Glen Rose Formation and wells completed in both the Hensell Aquifer and Pearsall Formation are compared at three locations in Figure 4.3.57. At all three locations, the hydraulic heads in the wells completed in the Paluxy Aquifer and Glen Rose Formation are higher than those in the wells completed in the Hensell Aquifer and Pearsall Formation, with the difference about 200 feet in Mills County, about 350 feet in Somervell County, and about 300 feet in Hood County. These plots show relatively stable hydraulic heads in the wells at these three locations, and suggest a vertical downward gradient from the Paluxy Aquifer and Glen Rose Formation (i.e., upper portion of the northern Trinity Aquifer) to the Hensell Aquifer and Pearsall Formation (i.e., middle portion of the northern Trinity Aquifer).

Figure 4.3.58 shows the difference in hydraulic heads between wells completed in both the Hensell Aquifer and Pearsall Formation or in the Hensell Aquifer, Glen Rose Formation, and Pearsall Formation (i.e., the middle portion of the northern Trinity Aquifer) and wells completed in both the Hosston Aquifer and Pearsall Formation (i.e., the lower portion of the northern

Trinity Aquifer) at four locations. At the location in Cooke County, the hydraulic heads in the middle and lower portions of the northern Trinity Aquifer are very similar, as is the historical trend in the hydraulic heads. The hydraulic heads in these wells were essentially identical in the time period from about 1935 to 1950. After that time, the hydraulic heads in the wells completed in the middle portion of the northern Trinity Aquifer were lower than those in the wells completed in the lower portion of the northern Trinity Aquifer, with the difference increasing from about 25 feet in 1960 to generally about 50 feet in 2005. At the location in Hood County, the hydraulic heads in the wells completed in the middle portion of the northern Trinity Aquifer are about 40 to 50 feet higher than those in the wells completed in the lower portion of the northern Trinity aquifer. The hydraulic heads in the wells completed in the Hensell Aquifer and Pearsall Formation are also higher than those in the wells completed in the Hosston Aquifer and Pearsall Formation at the location in Burnet County, with the difference being about 125 feet in 1955 and about 200 feet in 1965. At the location in Somervell County, hydraulic heads in the well completed in the Hosston Aquifer and Pearsall Formation lie between the hydraulic heads in two wells completed in the Hensell and Glen Rose Formation. Therefore, it is not possible to estimate the direction of the vertical gradient at this location. The difference in hydraulic heads between the two wells completed in the Hensell Aquifer and Glen Rose Formation (wells 3250306 and 3250307) is almost 30 feet and the trend in the hydraulic heads in these two wells is essentially identical.

Summary

The two methods used to evaluate the vertical hydraulic head gradients between aquifers consisted of comparing the estimated historical hydraulic head surfaces for predevelopment and 2010 and comparing hydraulic heads in nearby wells completed in different aquifers. From a comparison of conditions based upon predevelopment hydraulic head surfaces, vertical gradients were generally upward consistent with previous conceptual models for dipping aquifers and the study of Hill (1901). The exception was the gradient between the Hensell and Paluxy aquifers in central Texas. In this area, the estimated predevelopment hydraulic heads are lower in the deeper Hensell Aquifer than in the shallower Paluxy Aquifer, indicating a downward vertical gradient. This observation is inconsistent with the conceptualization of upward cross-formation flow in dipping aquifers prior to the onset of aquifer development. Consequently, the estimated

hydraulic head surface for the Hensell Aquifer may show the effects of pumping and not be representative of predevelopment conditions in the aquifer. However, the downward vertical gradient indicated by the predevelopment hydraulic head surfaces may be correct as it is consistent with Rapp (1988), who indicates recharge to deeper units through cross-formation flow in the southwestern portion of the aquifer.

Using available transient hydraulic head data from the historical period, vertical hydraulic head gradients during the post-development period were downward from the Woodbine Aquifer to the Paluxy Aquifer, downward from the Paluxy Aquifer to the Hosston Aquifer, and downward from the Hensell Aquifer to the Hosston Aquifer. These results suggest that the upward vertical gradient between these aquifers during predevelopment were significantly altered and in many areas reversed as a result of development in the early 1900s. No data were available at nearby wells completed in the Paluxy and Hensell aquifers. Therefore, the only data with which to estimate the vertical gradients between these two aquifers are the historical surfaces, which indicate a downward vertical gradient under current conditions.

In general, the range in hydraulic heads and the differing temporal trends between the aquifers and formations that comprise the northern Trinity and Woodbine aquifers suggest that the northern Trinity Aquifer is a vertically heterogeneous system and that hydraulic heads in both aquifers have been significantly altered by pumping. In both aquifers, the vertical hydraulic conductivity appears to be sufficiently low to allow large differences in hydraulic heads for very long time periods over relatively short vertical distances between aquifers/formations.

Table 4.3.1   Summary of water-level data by source.

Source	Number of Wells with Water-Level Data	Number of Water-Level Measurements	First Year of Water-Level Data	Last Year of Water-Level Data
TWDB groundwater database	8,646	46,727	1900	2012
TWDB driller's logs database	23,578	23,578	1999	2013
USGS Texas (non duplicates[a])[b]	44	3,304	1960	2012
GCD	765	10,803	1961	2014
Historical Reports	629	765	1895	1960
Oklahoma Water Resources Board[b]	19	478	1956	2011
TCEQ well records	11,731	11,731	1916	2009
USGS Arkansas[b]	16	195	1900	1994
USGS Oklahoma[b]	98	455	1944	2012
Total[c]	**45,526**	**98,036**	**1895**	**2014**

[a] wells and/or water-level measurements not also in the TWDB groundwater database
[b] obtained from Oliver and others (2013)
[c] total number for wells and water-level measurements and minimum first year and maximum last year for water-level dates

Table 4.3.2   Available completion information for wells with water-level measurements.

Source	Number of Wells with Water-Level Data	Number of Wells with Completion Information[a]	Number of Wells with Partial Completion Information[b]	Percentage with Completion Information[c]	Percentage with Total Depth Only[c]
TWDB groundwater database	8,646	3,489		**40%**	58%
TWDB driller's logs database	23,578		18,219	**77%**	20%
USGS Texas (non duplicates[d])	44	21		**48%**	48%
GCD	765	670	30	88%	4%
Historical Reports	629	245		39%	61%
Oklahoma Water Resources Board	19		11	58%	42%
TCEQ well records	11,731	10,777		92%	8%
USGS Arkansas	16	0		0%	94%
USGS Oklahoma	98	0		0%	93%
Total	**45,526**	**15,202**	**18,260**		

[a] completion information consists of the depth to the top and bottom of each screen in the well

[b] partial completion information consists of depth to top of uppermost screen; depth to top or bottom of screen, but not both; gravel pack top and bottom

[c] the two percentages may not sum to 100 percent because some wells do not have completion information or total depth

[d] wells not in the TWDB groundwater database

Table 4.3.3   Summary of wells and water-level measurements by completion interval.

Completion Interval	Number of Wells	Number of Water-Level Measurements
Group 1- completed in a single aquifer/formation		
Woodbine Aquifer	3,125	6,057
Paluxy Aquifer	3,065	5,966
Glen Rose Formation	2,708	3,863
Hensell Aquifer	2,847	6,595
Pearsall Formation	404	876
Hosston Aquifer	1,271	7,051
Edwards BFZ Aquifer	1,137	9,120
Group 2- multi-completed in the northern Trinity and/or Woodbine aquifers		
Woodbine & Paluxy Aquifers	2	4
Paluxy Aquifer & Glen Rose Formation	4,208	5,166
Glen Rose & Pearsall Formations	23	23
Hensell Aquifer & Glen Rose Formation	1,331	2,094
Hensell Aquifer & Pearsall Formation	1,900	4,609
Middle-Trinity Completion (Glen Rose Formation, Hensell Aquifer & Pearsall Formation)[a]	900	1,225
Upper-Middle Trinity Completion (Paluxy Aquifer, Glen Rose Formation, Hensell Aquifer & Pearsall Formation)[a]	177	400
Hensell & Hosston Aquifers	87	1,411
Middle-Lower Trinity Completion (Glen Rose Formation, Hensell Aquifer, Pearsall Formation & Hosston Aquifer)[a]	2,983	7,210
Hosston Aquifer & Pearsall Formation	935	3,388
Trinity Group Completion (Paluxy Aquifer, Glen Rose Formation, Hensell Aquifer, Pearsall Formation & Hosston Aquifer)[a]	35	82
Group 3 - not exclusively completed in the northern Trinity Aquifer or exclusively completed outside the northern Trinity Aquifer		
younger sediments[b]	3,945	6,844
Washita/Fredericksburg Groups (other than Edwards BFZ Aquifer)	1,382	2,625
Hensell Aquifer & Paleozoic-age Sediments	12	30
Middle-Lower Trinity Completion & Paleozoic-age Sediments	1,629	2,384
Hosston Aquifer, Pearsall Formation & Paleozoic-age Sediments	1,650	3,692
Hosston Aquifer & Paleozoic-age Sediments	792	1,618
Trinity Group Completion & Paleozoic-age Sediments	11	48
Paleozoic-age Sediments	2,313	3,318
Group 4 - mixed formations, undetermined, or unknown completion		
Mixed Formations[c]	2,369	3,684
Undetermined Completion[d]	3,459	7,059
Unknown Completion[e]	826	1,594

[a]   see Table 4.3.4

[b]   Quaternary-, Tertiary-, and upper Cretaceous-age sediments deposited after deposition of the Woodbine Aquifer

[c]   wells identified as potentially completed in the Washita/Fredericksburg groups as well as the northern Trinity and/or Woodbine aquifers

[d]   wells for which a completion interval was not determined

[e]   wells with no total depth or completion interval information

Table 4.3.4   Description of terminology for completions in multiple aquifers/formations in the northern Trinity Aquifer.

Aquifer/Formation	Description of Multi-Completion Terminology			
Paluxy Aquifer		Upper-Middle Trinity Completion		Trinity Group Completion
Glen Rose Formation	Middle-Trinity Completion			
Hensell Aquifer			Middle-Lower Trinity Completion	
Pearsall Formation				
Hosston Aquifer				

Table 4.3.5   Number of water-level measurements for Group 1 and Group 2 wells located in the North Texas, Northern Trinity, Prairielands, and Upper Trinity GCDs.

Completion Interval	Number of Water-Level Measurements			
	North Texas GCD	Northern Trinity GCD	Prairielands GCD	Upper Trinity GCD
Group 1 – completed in a single aquifer/formation				
Woodbine Aquifer	1,429	894	1,476	na
Paluxy Aquifer	769	3,039	338	993
Glen Rose Formation	271	210	352	1,853
Hensell Aquifer	169	3	340	1,090
Pearsall Formation	106	7	67	196
Hosston Aquifer	165	181	596	1,054
Group 2 - multi-completed in the northern Trinity Aquifer				
Paluxy Aquifer & Glen Rose Formation	333	1,206	217	2,750
Glen Rose & Pearsall Formations	0	0	1	4
Hensell Aquifer & Glen Rose Formation	94	13	226	476
Hensell Aquifer & Pearsall Formation	213	14	158	789
Middle-Trinity Completion[a]	41	19	106	293
Hensell & Hosston Aquifers	0	0	36	33
Hosston Aquifer & Pearsall Formation	205	358	154	462
Upper-Middle Trinity Completion[a]	35	3	21	191
Middle-Lower Trinity Completion[a]	83	130	400	798
Trinity Group Completion[a]	4	1	30	16

[a] see Table 4.3.4 for explanation of terminology

Table 4.3.6   **Summary of overall declines in hydraulic heads and rates of decline observed in the subcrop.**

County[a]	Range in Overall Decline (feet)	Range in Rate of Decline (feet per year)	Average Rate of Decline (feet per year)
Woodbine Aquifer			
Grayson	10 - 215	0.5 - 12.2	4.3
Fannin	23 - 239	1.6 - 8.9	4.7
Lamar	46	2.4	2.4
Denton	68	3.4	3.4
Collin	39 - 238	2.0 - 12.7	5.3
Hunt	63	1.5	1.5
Dallas	20 - 450	1.1 - 13.2	6.1
Kaufman	41 - 65	1.6 - 2.9	2.0
Johnson	40	0.9	0.9
Ellis	25 - 244	2.2 - 11.9	5.3
Hill	53	5.4	5.4
Navarro	104	4.6	4.6
Paluxy Aquifer			
Cooke	31 - 80	5.3 - 5.9	5.6
Grayson	378	7.3	7.3
Fannin	84 - 166	3.0 - 4.3	3.6
Lamar	23 - 69	1.5 - 1.7	1.6
Red River	116	4.6	4.6
Wise	16 - 32	0.4 - 0.8	0.6
Denton	66 - 267	2.8 - 11.8	6.4
Collin	43 - 276	2.3 - 10.7	5.1
Tarrant	4 - 225	0.3 - 23.3	5.5
Dallas	90 - 203	5.8 - 7.7	6.7
Johnson	16 - 254	0.3 - 6.2	3.4
Hill	26	1.1	1.1
Hensell Aquifer			
Cooke	30	2.2	2.2
Grayson	106	14.7	14.7
Bosque	25 - 293	3.3 - 7.4	5.7
Hill	97 - 231	6.5 - 9.1	7.5
McLennan	108	8.9	8.9
Coryell	31 - 127	1.8 - 6.0	3.9
Hosston Aquifer			
Denton	182 - 348	5.5 - 7.4	6.7
Collin	62 - 328	3.2 - 10.8	7.3
Tarrant	105 - 580	2.8 - 45.7	15.7
Dallas	132 - 340	4.6 - 21.9	10.4
Johnson	342 - 532	10.2 - 17.8	12.6
Ellis	101 - 651	3.1 - 16.0	10.4

Table 4.3.6, continued

County[a]	Range in Overall Decline (feet)	Range in Rate of Decline (feet per year)	Average Rate of Decline (feet per year)
Hosston Aquifer, continued			
Bosque	150 - 366	5.4 - 9.2	7.6
Hill	108 - 832	3.2 - 18.3	12.1
McLennan	87 - 608	5.4 - 21.0	10.2
Coryell	64 - 213	3.3 - 8.0	5.0
Falls	237 - 286	4.4 - 6.3	5.6
Bell	37 - 215	2.4 - 5.5	4.4
Burnet	44	1.1	1.1
Williamson	17 - 248	1.1 - 5.8	3.7
Travis	118	1.7	1.7
Paluxy Aquifer and Glen Rose Formation			
Grayson	102 - 385	3.6 - 38.6	18.2
Denton	255	11.6	11.6
Parker	67	2.5	2.5
Tarrant	14 - 28	1.6 - 2.6	2.0
Dallas	25 - 145	2.8 - 9.7	6.2
Rockwall	180	8.1	8.1
Hood	37	1.1	1.1
Johnson	29 - 311	1.2 - 14.4	5.8
Bosque	67	1.6	1.6
Hill	22	2.8	2.8
Middle-Trinity Completions			
Cooke	76 - 412	1.9 - 7.0	4.6
Grayson	103 - 118	3.2 - 5.0	4.1
Denton	190 - 216	10.1 - 16.3	13.2
Collin	343 - 367	9.1 - 24.4	16.8
Bosque	170 - 219	5.3 - 7.6	6.1
Hill	260 - 298	5.6 - 7.7	6.6
McLennan	235 - 456	7.3 - 19.0	12.0
Coryell	50 - 85	1.4 - 8.5	4.4
Bell	35 - 94	3.4 - 18.0	9.5
Williamson	30 - 61	1.5 - 8.4	4.3
Hosston Aquifer and Pearsall Formation			
Cooke	74 - 360	1.8 - 7.8	4.8
Denton	127 - 364	7.0 - 10.1	8.7
Collin	186	5.0	5.0
Tarrant	170 - 472	4.1 - 30.2	15.7
Dallas	10 - 158	0.9 - 5.6	3.4
Johnson	149 - 726	5.5 - 21.7	13.0
Hill	120 - 552	5.0 - 14.0	9.5
McLennan	257 - 364	5.7 – 16.9	13.2

Table 4.3.6, continued

County[a]	Range in Overall Decline (feet)	Range in Rate of Decline (feet per year)	Average Rate of Decline (feet per year)
Hosston Aquifer and Pearsall Formation, continued			
Bell	63 - 156	3.6 - 4.3	4.0
Milam	172	5.2	5.2
Williamson	148 - 191	4.7 - 20.8	11.7
Glen Rose Formation			
Cooke	48	2.1	2.1
Wise	24 - 38	0.6 - 0.8	0.7
Parker	41	1.0	1.0
Tarrant	142	13.6	13.6
Johnson	34	2.6	2.6
Bosque	405	9.7	9.7
McLennan	253 - 315	10.3 - 11.1	10.7
Bell	74 - 272	4.0 - 5.2	4.6
Pearsall Formation			
Grayson	25 - 209	1.1 - 4.9	2.9
Denton	123 - 204	10.0 - 12.8	11.4
Hood	76	3.1	3.1
Mills	49	4.3	4.3
Falls	315	7.1	7.1
Bell	205	4.4	4.4
Williamson	220 - 311	6.7 - 7.0	6.8

[a] counties listed in order from west to east and north to south
[b] wells completed in the Hensell Aquifer and Glen Rose Formation, the Hensell Aquifer and Pearsall Formation, or
     the Hensell Aquifer, Glen Rose Formation, and Pearsall Formation

**Table 4.3.7   Summary of years averaged to obtain data for constructing historical hydraulic
head surfaces.**

Aquifer	Year Range Used to Obtain Data for Historical Hydraulic Head Surfaces			
	1950 surface	1970 surface	1990 surface	2010 surface
Woodbine Aquifer	1946-1954	1968-1972	1988-1992	2009-2011
Paluxy Aquifer	1946-1954	1968-1972	1988-1992	2008-2012
Hensell Aquifer	1941-1959	1970	1988-1992	2009-2011
Hosston Aquifer	1941-1959	1970	1988-1992	2009-2011

Table 4.3.8   Outcrop trend results.

County	Trend in Water-Level Change (feet per year)			
	< 1950 to ≥2000	1950-1974 to ≥2000	1975-1999 to ≥2000	both ≥2000
Woodbine Aquifer				
Cooke		-0.3		
Denton		-2.2 to 0.3	-0.1 to 0.05	
Fannin		-0.07		
Grayson		-0.8		
Johnson		-0.6 to 0.06		
Tarrant		-0.4 to 0.4		
Northern Trinity Aquifer				
northern outcrop				
Cooke				-2.9 to -0.01
Hood		-0.3 to 0.05	-1.2 to -0.9	
Jack			0.0	
Montague		0.01 to 0.8		-2.1 to 0.05
Parker	-0.2 to 0.09	-0.04 to 0.2		1.4
Somervell				0.2
Wise		-1.7 to 0.7	-1.9 to -1.1	-1.9 to -1.8
western outcrop				
Brown	-0.1	-1.2 to 0.1		
Burnet	-0.2			-0.8
Callahan	-0.04 to 0.02	-0.2 to 0.2		
Comanche		-0.7 to 1.0	-0.7	-0.5 to 0.3
Eastland	-0.07 to 0.04	-0.2 to 0.1		0.7
Erath		-0.03 to 0.1	0.4	
Hamilton		-1.6		
Lampasas		-0.09 to 0.1		
Mills		-0.4 to -0.09		
Taylor		-0.08 to 0.0		

Table 4.3.9   Number of hydraulic heads by decade for wells completed in a single aquifer/formation by county.

County and Aquifer/Formation[a]	Decade											
	1900s	1910s	1920s	1930s	1940s	1950s	1960s	1970s	1980s	1990s	2000s	2010s
BELL												
Glen Rose Formation	6				3	2	8	27	7	34	29	69
Hensell Aquifer								1		1	4	
Pearsall Formation						1	10	42	5	13	31	11
Hosston Aquifer					1	6	75	47	25	16	20	69
Total	**6**				**4**	**9**	**93**	**117**	**37**	**64**	**84**	**149**
BOSQUE												
Paluxy Aquifer	1		1			11	46	29	16	17	14	4
Glen Rose Formation	2						15	26	30	29	20	1
Hensell Aquifer	2				1		49	80	42	44	36	22
Pearsall Formation							3	1	2	8	2	
Hosston Aquifer					1		8	4	9	19	21	22
Total	**5**		**1**		**2**	**11**	**121**	**140**	**99**	**117**	**93**	**49**
BROWN												
Paluxy Aquifer							1					
Glen Rose Formation							7	1			2	
Hensell Aquifer				8			52	20	13	10	3	11
Hosston Aquifer								4				
Total				**8**			**60**	**25**	**13**	**10**	**5**	**11**
BURNET												
Glen Rose Formation							2				2	3
Hensell Aquifer							2	8	2		154	950
Pearsall Formation							4	12	6	12	11	3
Hosston Aquifer						1	1	9	3	4	152	945
Total						**1**	**9**	**29**	**11**	**16**	**319**	**1,901**
CALLAHAN												
Hensell Aquifer					28	17	34	355	53	40	113	59
Total					**28**	**17**	**34**	**355**	**53**	**40**	**113**	**59**
COLLIN												
Woodbine Aquifer	1		1	5	3	6	12	84	74	72	234	26
Paluxy Aquifer			2		1	1		10	11	12	10	2
Glen Rose Formation							1	2				
Hosston Aquifer					1	2	1	11	9	8	8	
Total	**1**		**3**	**5**	**5**	**9**	**14**	**107**	**94**	**92**	**252**	**28**

Table 4.3.9, continued

County and Aquifer/Formation[a]	Decade											
	1900s	1910s	1920s	1930s	1940s	1950s	1960s	1970s	1980s	1990s	2000s	2010s
COMANCHE												
Paluxy Aquifer									2			
Glen Rose Formation							4	19	18	10	4	2
Hensell Aquifer				1		5	95	266	131	111	203	70
Pearsall Formation								13	10	15	29	6
Hosston Aquifer								19	9	31	33	2
Total				**1**		**5**	**99**	**317**	**170**	**167**	**269**	**80**
COOKE												
Woodbine Aquifer							1	39	32	14	24	3
Paluxy Aquifer	6					1	6	34	24	15	14	4
Glen Rose Formation	1						3	27	30	46	20	
Hensell Aquifer				1			4	33	23	15	28	7
Pearsall Formation						1	4	17	16	20	9	1
Hosston Aquifer							2	5	2		1	2
Total	**7**			**1**		**2**	**20**	**155**	**127**	**110**	**96**	**17**
CORYELL												
Paluxy Aquifer							3	5				3
Glen Rose Formation	2						1	3			8	1
Hensell Aquifer					1		4	30	28	21	232	76
Hosston Aquifer						1	11	13	2	295	254	76
Total	**2**				**1**	**1**	**19**	**51**	**30**	**316**	**494**	**156**
DALLAS												
Woodbine Aquifer	14	3	5	23	9	103	95	88	46	13	37	11
Paluxy Aquifer				3	3	5	2	13	2			
Hosston Aquifer					1	9	14	151	212	233	211	29
Total	**14**	**3**	**5**	**26**	**13**	**117**	**111**	**252**	**260**	**246**	**248**	**40**
DELTA												
Paluxy Aquifer								6	6	7	2	2
Total								**6**	**6**	**7**	**2**	**2**
DENTON												
Woodbine Aquifer	1				1	1	41	123	131	116	345	46
Paluxy Aquifer	8		1	1	2	4	30	84	123	140	153	17
Glen Rose Formation									18	65	52	
Hensell Aquifer							3	8	1		8	

Table 4.3.9, continued

County and Aquifer/Formation[a]	Decade											
	1900s	1910s	1920s	1930s	1940s	1950s	1960s	1970s	1980s	1990s	2000s	2010s
DENTON, continued												
Pearsall Formation								17	10	1	1	
Hosston Aquifer						3	4	22	14	34	25	3
Total	**9**		**1**	**1**	**3**	**8**	**78**	**254**	**297**	**356**	**584**	**66**
EASTLAND												
Hensell Aquifer				38	1		124	290	48	60	98	34
Pearsall Formation									4			
Total				**38**	**1**		**124**	**290**	**52**	**60**	**98**	**34**
ELLIS												
Woodbine Aquifer	2			3	8	27	119	145	111	75	100	24
Paluxy Aquifer						2	3	1	1			
Hosston Aquifer						1	6	16	9	7	43	9
Total	**2**			**3**	**8**	**30**	**128**	**162**	**121**	**82**	**143**	**33**
ERATH												
Paluxy Aquifer								18	12	59	79	22
Glen Rose Formation							1	8	12	33	39	10
Hensell Aquifer			1			2	37	89	50	90	202	33
Pearsall Formation								3			1	
Hosston Aquifer								16	26	42	242	79
Total			**1**			**2**	**38**	**134**	**100**	**224**	**563**	**144**
FALLS												
Glen Rose Formation								1				
Pearsall Formation							5	3	2	9	2	1
Hosston Aquifer							1	31	51	27	20	23	7
Total							**1**	**36**	**55**	**29**	**29**	**25**	**8**
FANNIN												
Woodbine Aquifer		1	1	4	11	16	17	119	119	75	57	10
Paluxy Aquifer							1	9	10	12	9	
Total		**1**	**1**	**4**	**11**	**16**	**18**	**128**	**129**	**87**	**66**	**10**
GRAYSON												
Woodbine Aquifer	6			7	11	98	27	173	80	141	379	98
Paluxy Aquifer							2	20	10	9	7	4
Glen Rose Formation						1	1			1	1	
Hensell Aquifer							2	6				

Table 4.3.9, continued

County and Aquifer/Formation[a]	Decade											
	1900s	1910s	1920s	1930s	1940s	1950s	1960s	1970s	1980s	1990s	2000s	2010s
GRAYSON, continued												
Pearsall Formation				1	1	4	1	3		4	8	1
Total	**6**			**8**	**12**	**103**	**33**	**202**	**90**	**155**	**395**	**103**
HAMILTON												
Paluxy Aquifer							2			1	2	
Glen Rose Formation						1	17	30	31	28	56	14
Hensell Aquifer						1	43	103	22	7	12	2
Pearsall Formation							7	5	1		1	
Hosston Aquifer							1	2			12	3
Total						**2**	**70**	**140**	**54**	**36**	**83**	**19**
HILL												
Woodbine Aquifer	2			2	2	3	99	138	43	35	30	15
Paluxy Aquifer							7	2	12	5	4	
Glen Rose Formation	1						1	7	8	13	4	
Hensell Aquifer							32	59	8	6	1	
Pearsall Formation									2			
Hosston Aquifer				1		1	44	56	31	29	37	12
Total	**3**			**3**	**2**	**4**	**183**	**262**	**104**	**88**	**76**	**27**
HOOD												
Paluxy Aquifer								8		1	4	
Glen Rose Formation						1	2	18	20	35	52	26
Hensell Aquifer						2	20	74	54	64	120	26
Pearsall Formation							1	11	14	15	14	1
Hosston Aquifer						1		15	8	35	31	1
Total						**4**	**23**	**126**	**96**	**150**	**221**	**54**
HUNT												
Woodbine Aquifer					2		2	6	1	7	7	1
Paluxy Aquifer									2	2		
Total					**2**		**2**	**8**	**3**	**7**	**7**	**1**
JOHNSON												
Woodbine Aquifer	3			1	1	2	57	102	98	74	131	42
Paluxy Aquifer		1		2	2	8	112	42	52	7	25	19
Glen Rose Formation							11	20	10	4	27	7
Hensell Aquifer									2	2	1	

Table 4.3.9, continued

County and Aquifer/Formation[a]	Decade											
	1900s	1910s	1920s	1930s	1940s	1950s	1960s	1970s	1980s	1990s	2000s	2010s
JOHNSON, continued												
Pearsall Formation									1	3	1	
Hosston Aquifer							3	14	8	8	24	11
Total	**3**	**1**		**3**	**3**	**10**	**183**	**178**	**171**	**98**	**209**	**79**
KAUFMAN												
Woodbine Aquifer		2			2		1	9	6			
Paluxy Aquifer								6	6	2		
Total		**2**			**2**		**1**	**15**	**12**	**2**		
LAMAR												
Woodbine Aquifer						1	3	11	9	8	3	
Paluxy Aquifer							2	15	15	23	16	2
Total						**1**	**5**	**26**	**24**	**31**	**19**	**2**
LAMPASAS												
Glen Rose Formation						1	21	36	19	13	12	4
Pearsall Formation					1							
Total					**1**	**1**	**21**	**36**	**19**	**13**	**12**	**4**
MCLENNAN												
Glen Rose Formation	3				2		4	10	10	11	12	4
Hensell Aquifer							22	9				
Pearsall Formation								1				
Hosston Aquifer					2	4	155	165	148	214	52	15
Total	**3**				**4**	**4**	**181**	**185**	**158**	**225**	**64**	**19**
MILAM												
Hosston Aquifer					1							
Total					**1**							
MILLS												
Glen Rose Formation							5	10	7	9	12	6
Hensell Aquifer							5	7			13	4
Pearsall Formation					4	7					1	
Hosston Aquifer											1	
Total					**4**	**17**	**17**	**7**	**9**	**27**	**10**	
MONTAGUE												
Glen Rose Formation									2	1	1	
Hensell Aquifer							11	70	87	69	155	83

Table 4.3.9, continued

County and Aquifer/Formation[a]	Decade											
	1900s	1910s	1920s	1930s	1940s	1950s	1960s	1970s	1980s	1990s	2000s	2010s
MONTAGUE, continued												
Pearsall Formation							1	6	11	7	11	1
Hosston Aquifer					1		16	56	68	83	165	47
Total					**1**		**28**	**132**	**168**	**160**	**332**	**131**
NAVARRO												
Woodbine Aquifer	2	1		1		2	6	14	16	9	10	3
Total	**2**	**1**		**1**		**2**	**6**	**14**	**16**	**9**	**10**	**3**
PARKER												
Paluxy Aquifer	1				31	12	10	77	92	118	468	100
Glen Rose Formation					7		3	122	138	270	801	112
Hensell Aquifer					3	6	1	3	13	33	56	4
Pearsall Formation					4	3	1	6	6	12	40	3
Hosston Aquifer					1			3	3	4	5	
Total	**1**				**46**	**21**	**15**	**211**	**252**	**437**	**1,370**	**219**
RED RIVER												
Woodbine Aquifer								3	1		4	
Paluxy Aquifer						2		8	10	16	2	
Total						**2**		**11**	**11**	**16**	**6**	
SOMERVELL												
Paluxy Aquifer								2	3	1	2	
Glen Rose Formation	1		3		1	43	44	63	34	26	17	4
Hensell Aquifer	1						30	56	73	30	33	7
Pearsall Formation							1	6	23	28	1	1
Hosston Aquifer							3	44	35	95	262	83
Total	**2**		**3**		**1**	**43**	**78**	**171**	**168**	**180**	**315**	**95**
TARRANT												
Woodbine Aquifer	3				17	14	36	116	33	68	509	103
Paluxy Aquifer	4	1	2	11	67	367	111	541	347	488	917	155
Glen Rose Formation					4	6		4	23	47	105	19
Hensell Aquifer										2		
Pearsall Formation									1	4	1	
Hosston Aquifer					8	89	7	21	11	16	24	5
Total	**7**	**1**	**2**	**11**	**96**	**476**	**154**	**682**	**415**	**625**	**1,556**	**282**

Table 4.3.9, continued

County and Aquifer/Formation[a]	Decade											
	1900s	1910s	1920s	1930s	1940s	1950s	1960s	1970s	1980s	1990s	2000s	2010s
TAYLOR												
Hensell Aquifer								15	1	6	14	3
Total								**15**	**1**	**6**	**14**	**3**
TRAVIS												
Glen Rose Formation					3	9	1	14	1	14	203	1
Hensell Aquifer							1		1		1	1
Pearsall Formation						1	5	13	12	13	16	3
Hosston Aquifer				1	2		1	11	8	10	7	1
Total				**1**	**5**	**10**	**8**	**38**	**22**	**37**	**227**	**6**
WILLIAMSON												
Glen Rose Formation					15			4	4		14	4
Hensell Aquifer					1							
Pearsall Formation					1		19	47	12	20	6	1
Hosston Aquifer					3	3	34	37	33	50	236	73
Total					**20**	**3**	**53**	**88**	**49**	**70**	**256**	**78**
WISE												
Paluxy Aquifer	1							18	20	25	70	9
Glen Rose Formation							1	42	33	31	112	30
Hensell Aquifer							1	36	15	11	82	23
Pearsall Formation								8	7	9	13	1
Hosston Aquifer							5	69	32	27	82	8
Total	**1**						**7**	**173**	**107**	**103**	**359**	**71**
ATOKA, OK												
Hosston Aquifer								8	17	16	17	3
Total								**8**	**17**	**16**	**17**	**3**
BRYAN, OK												
Woodbine Aquifer								1	1		9	2
Total								**1**	**1**		**9**	**2**
CARTER, OK												
Hosston Aquifer					1		1					
Total					**1**		**1**					
CHOCTAW, OK												
Paluxy Aquifer					3		1	11	10			
Glen Rose Formation								1				

Table 4.3.9, continued

County and Aquifer/Formation[a]	Decade											
	1900s	1910s	1920s	1930s	1940s	1950s	1960s	1970s	1980s	1990s	2000s	2010s
CHOCTAW, OK, continued												
Hensell Aquifer								8				
Hosston Aquifer								5				
Total					**3**		**1**	**25**	**10**			
JOHNSTON, OK												
Hensell Aquifer							1					
Hosston Aquifer					1							
Total					**1**		**1**					
LOVE, OK												
Hensell Aquifer							3					
Hosston Aquifer					1		5	2	10	9	2	
Total					**1**		**8**	**2**	**10**	**9**	**2**	
MCCURTAIN, OK												
Woodbine Aquifer							7	81	48	29		
Paluxy Aquifer						7	73	4	16	20	20	4
Total						**7**	**80**	**85**	**64**	**49**	**20**	**4**
PUSHMATAHA, OK												
Hosston Aquifer									9	10	16	4
Total									**9**	**10**	**16**	**4**
SEVIER, AR												
Paluxy Aquifer						13	21	20	12	3		
Total						**13**	**21**	**20**	**12**	**3**		
GRAND TOTAL	**74**	**9**	**17**	**114**	**278**	**939**	**2,182**	**5,448**	**3,698**	**4,567**	**9,076**	**4,006**

[a] only aquifers and formations with at least one hydraulic head value in the county are listed
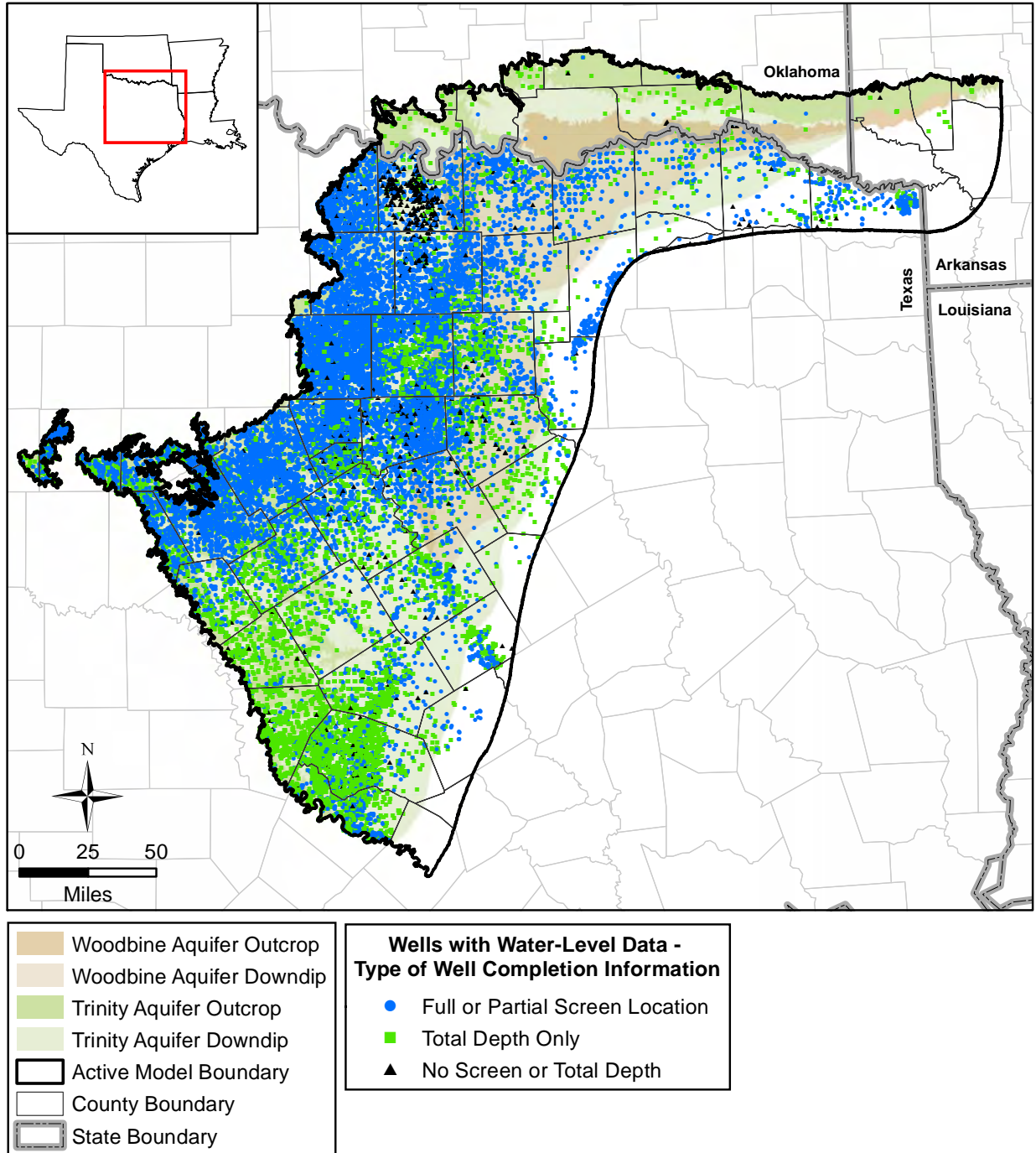
Figure 4.3.1a   Location of wells in the study area with water-level data showing type of completion information.

Figure 4.3.1b **Location of wells in the North Texas, Northern Trinity, Prairielands, and Upper Trinity GCDs with water-level data showing type of completion information.**
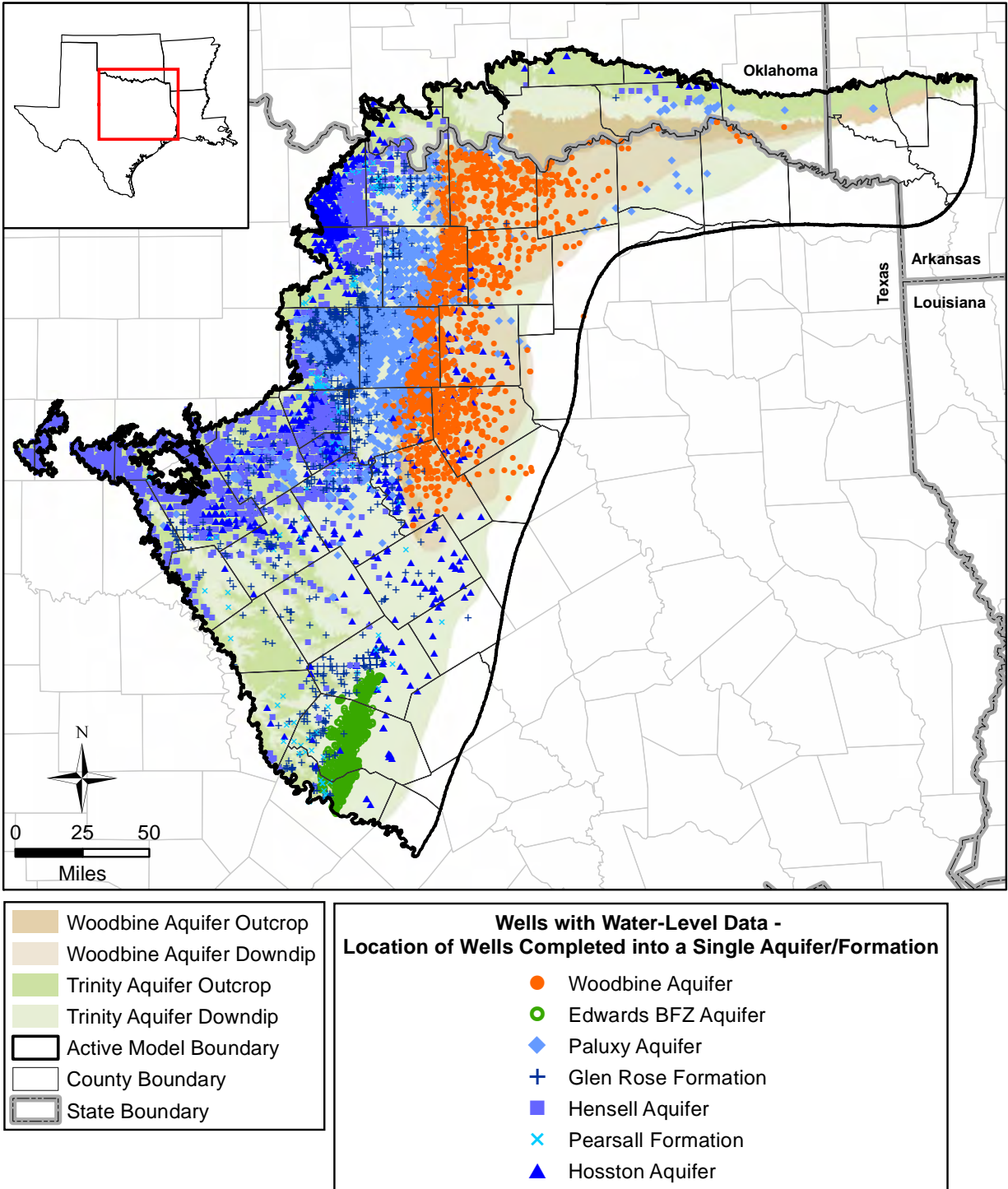
Figure 4.3.2a   Location of wells completed in a single aquifer or formation in the study area (Group 1 wells in Table 4.3.3).
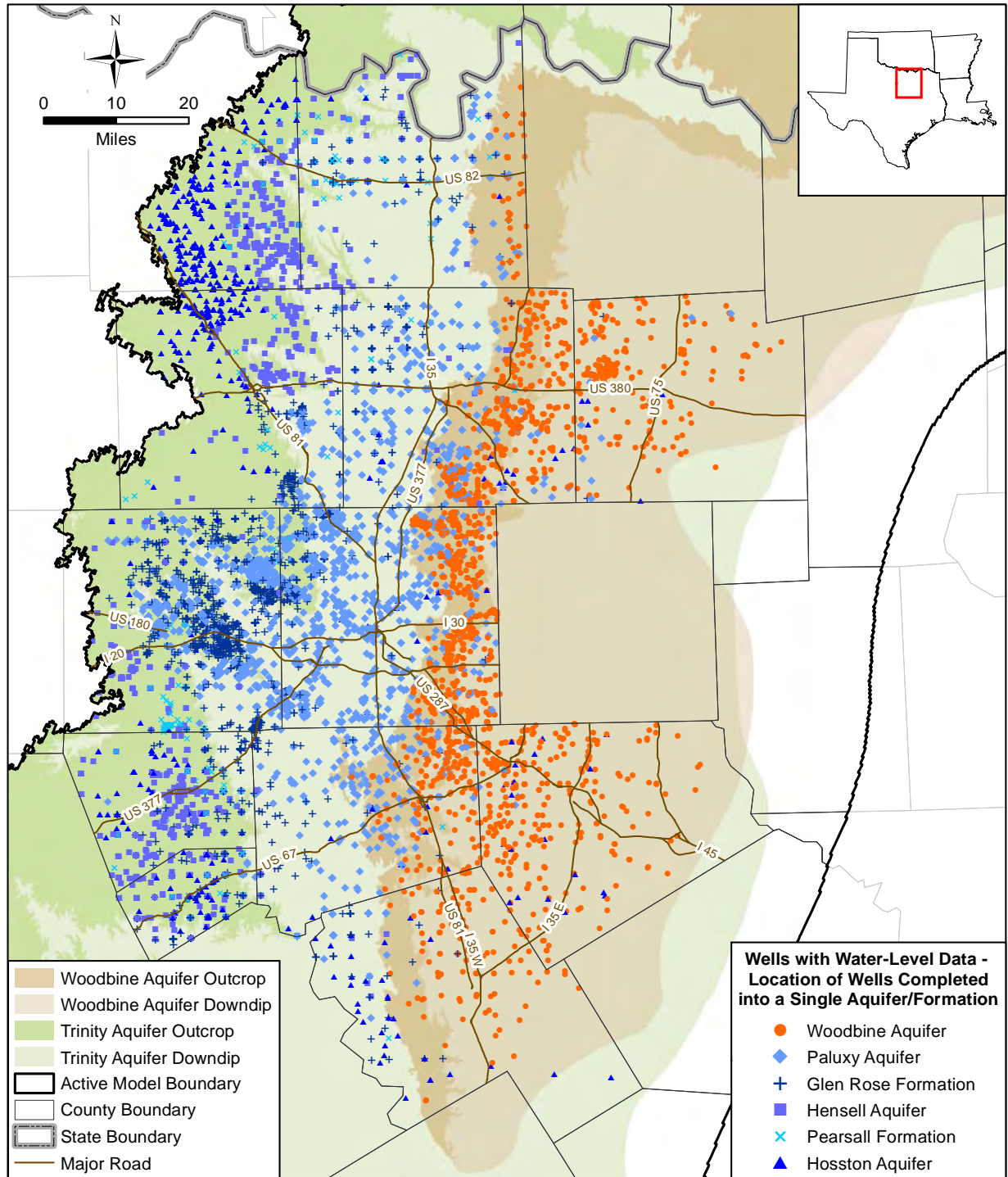
Figure 4.3.2b   Location of wells completed in a single aquifer or formation for the North Texas, Northern Trinity, Prairielands, and Upper Trinity GCDs (Group 1 wells in Table 4.3.3).
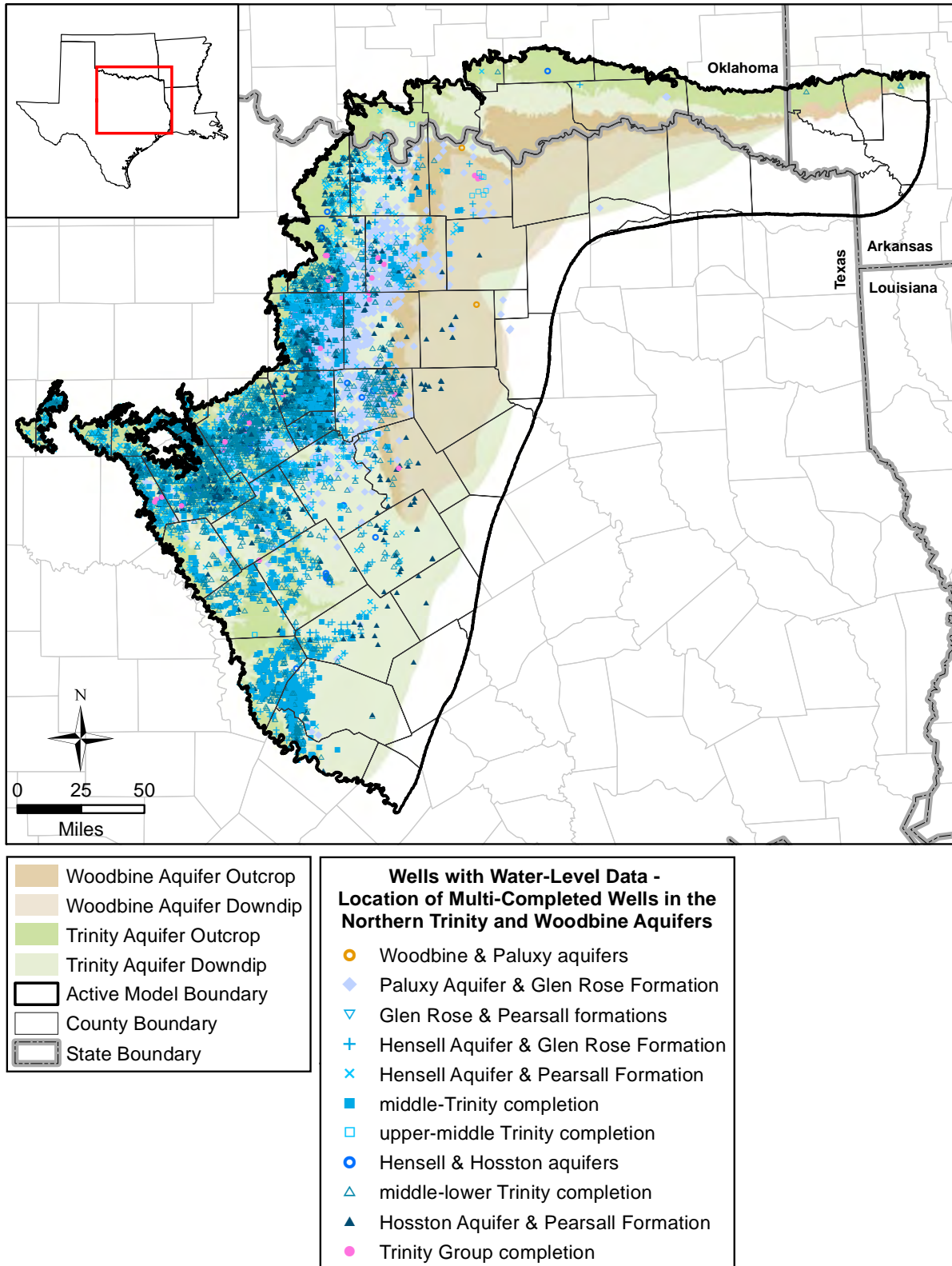
Figure 4.3.3a   **Location of multi-completed wells in the northern Trinity and/or Woodbine aquifers in the study area (Group 2 wells in Table 4.3.3).**
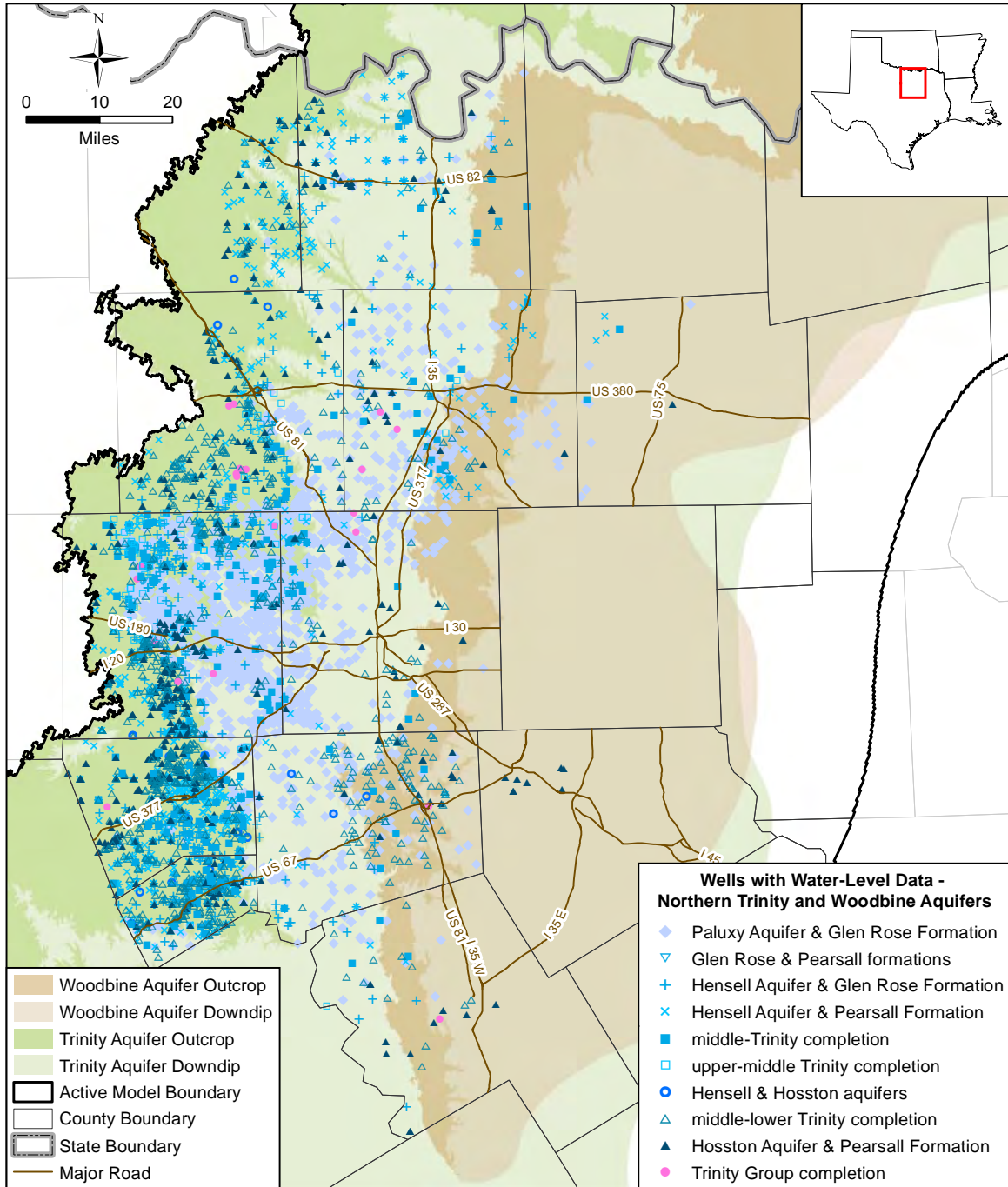
Figure 4.3.3b   **Location of multi-completed wells in the northern Trinity Aquifer in the North Texas, Northern Trinity, Prairielands, and Upper Trinity GCDs (Group 2 wells in Table 4.3.3).**
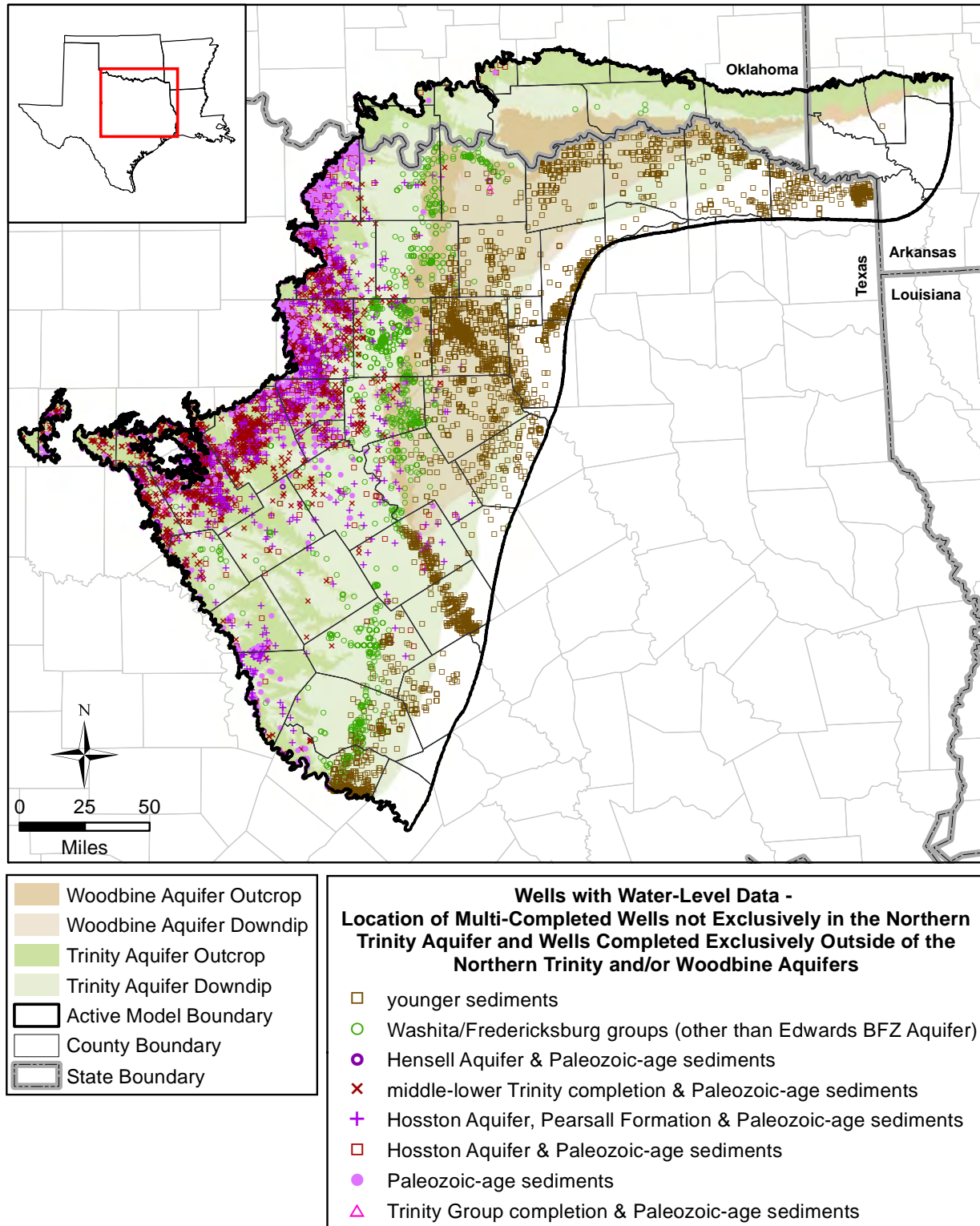
Figure 4.3.4a Location of multi-completed wells not exclusively in the northern Trinity Aquifer
and wells completed exclusively outside of the northern Trinity and/or Woodbine
aquifers in the study area (Group 3 wells in Table 4.3.3).
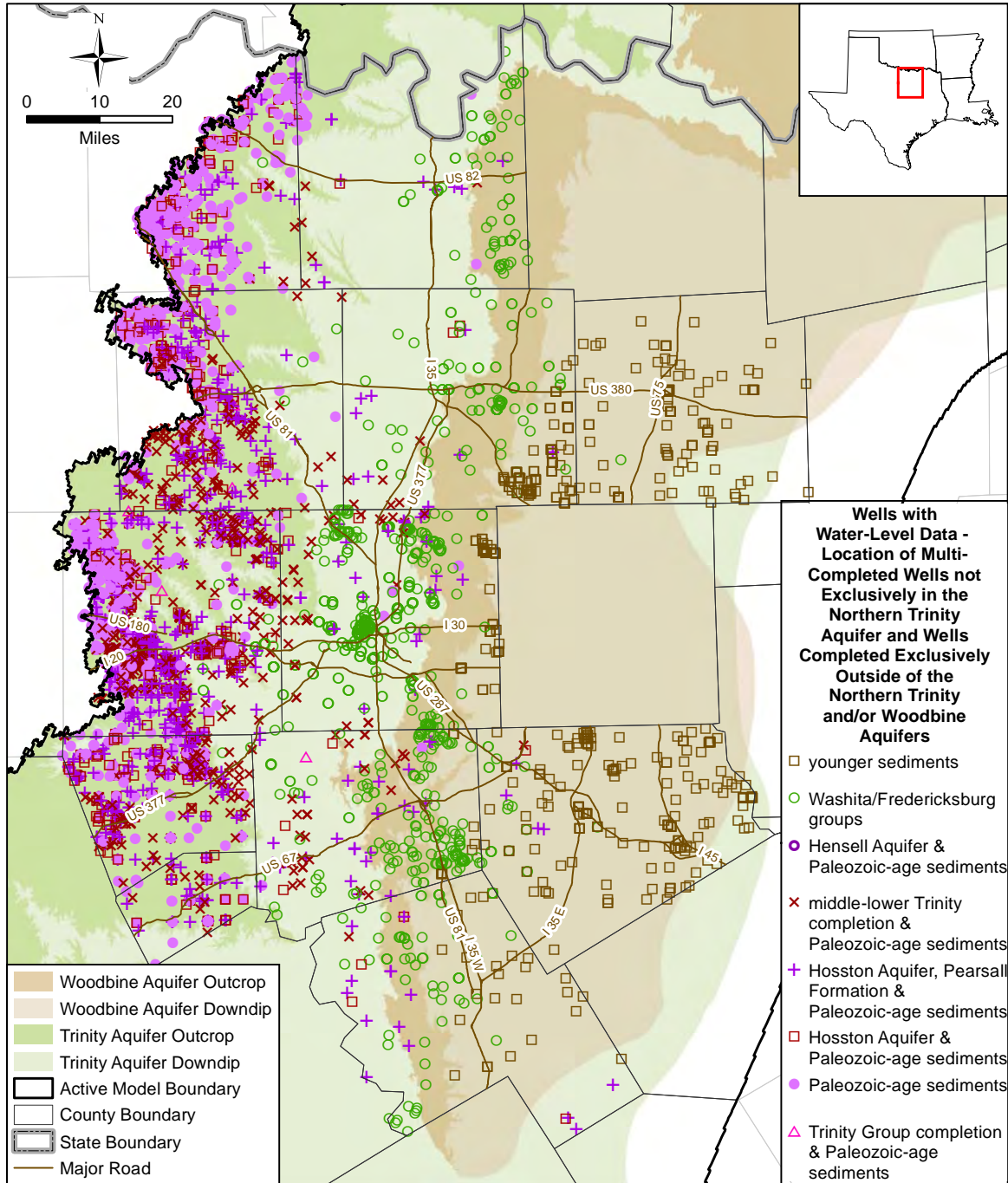
Figure 4.3.4b **Location of multi-completed wells not exclusively in the northern Trinity Aquifer and wells completed exclusively outside of the northern Trinity and/or Woodbine aquifers in the North Texas, Northern Trinity, Prairielands, and Upper Trinity GCDs (Group 3 wells in Table 4.3.3).**
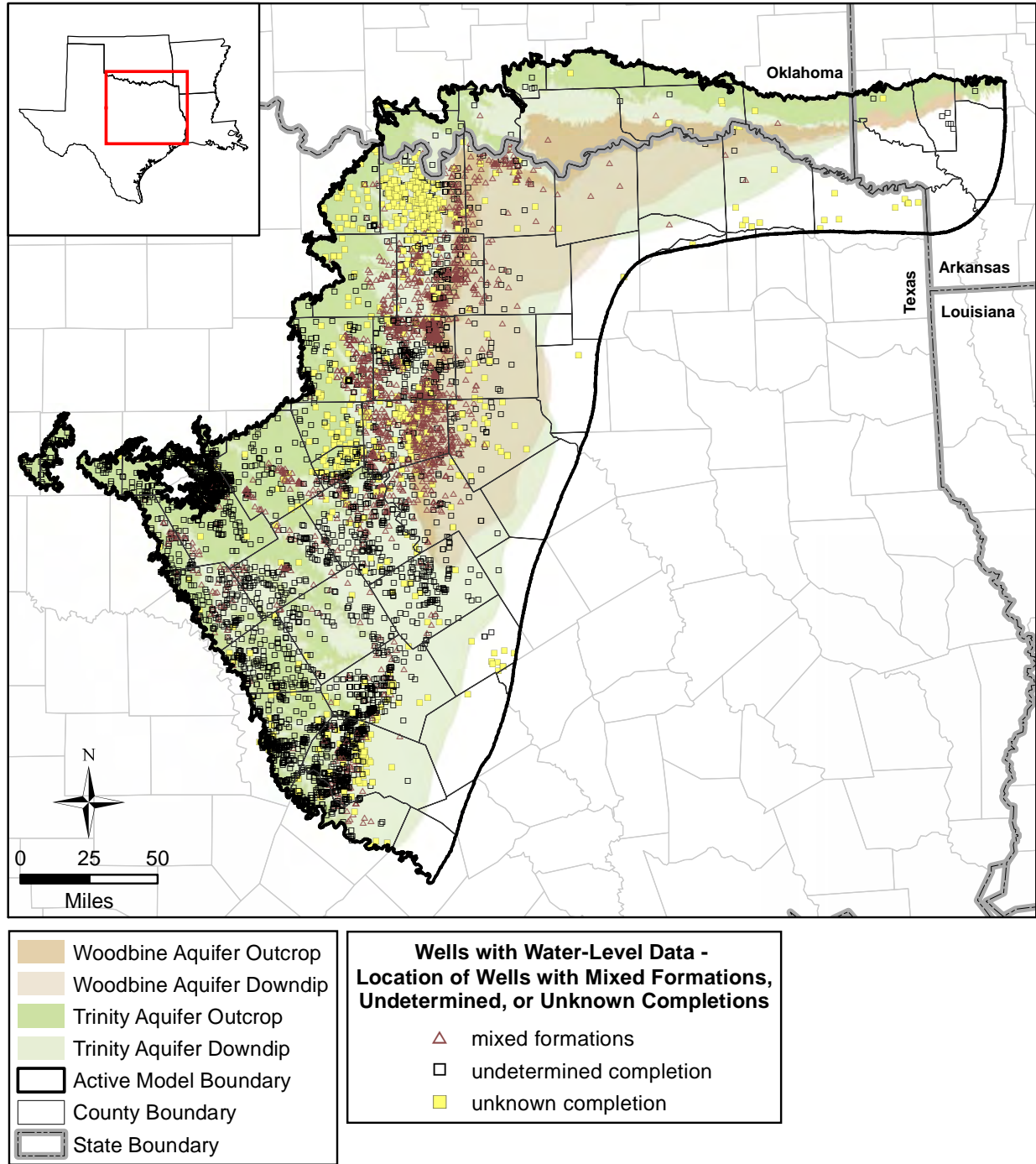
Figure 4.3.5a Location of wells with mixed formations, undetermined, or unknown completions in the study area (Group 4 wells in Table 4.3.3).
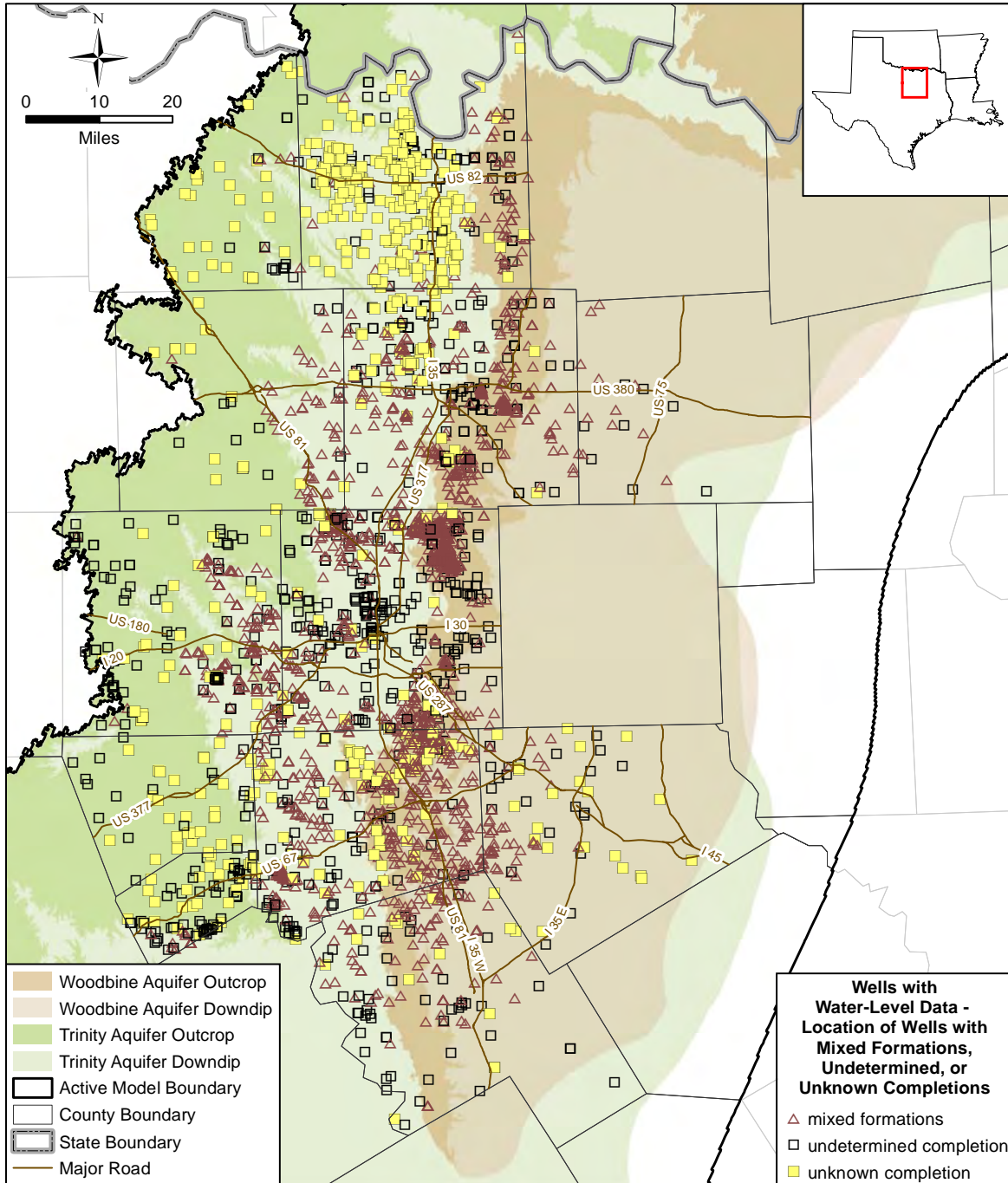
Figure 4.3.5b   **Location of wells with mixed formations, undetermined, or unknown completions in the North Texas, Northern Trinity, Prairielands, and Upper Trinity GCDs (Group 4 wells in Table 4.3.3).**
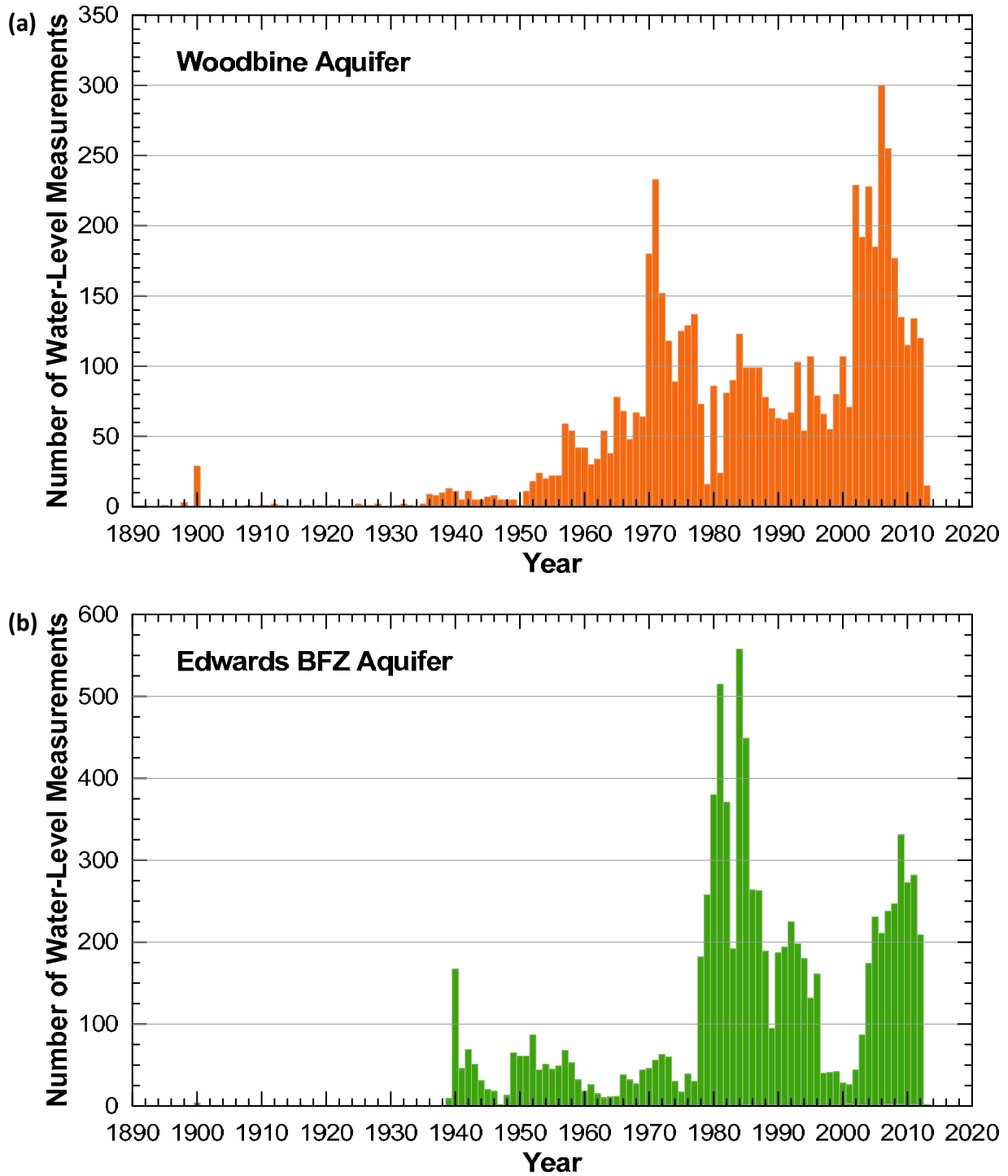
Figure 4.3.6   Temporal distribution of water-level measurements in the study area for the
            (a) Woodbine Aquifer and (b) Edwards BFZ Aquifer.
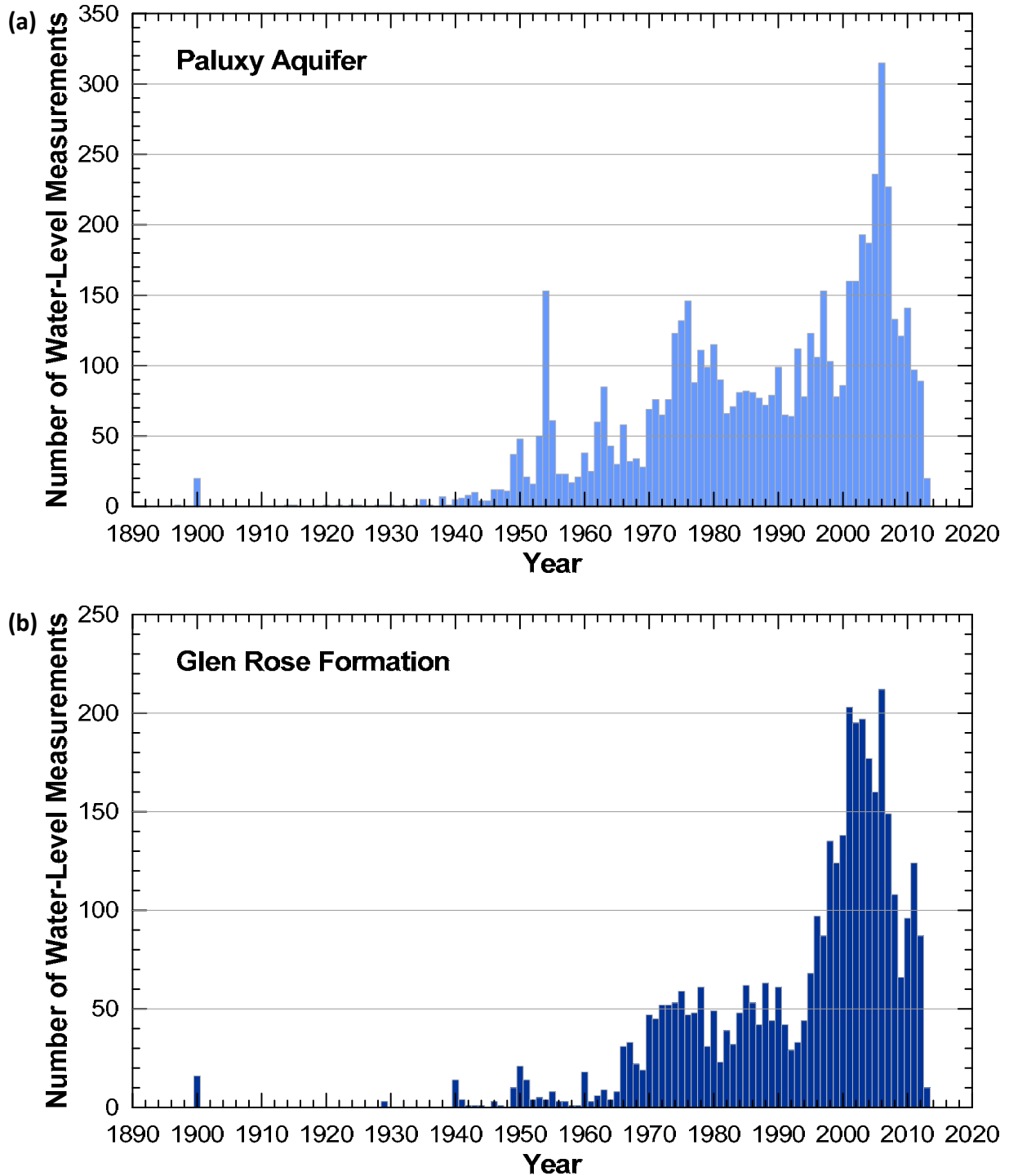
Figure 4.3.7   **Temporal distribution of water-level measurements in the study area for the (a) Paluxy Aquifer and (b) Glen Rose Formation.**
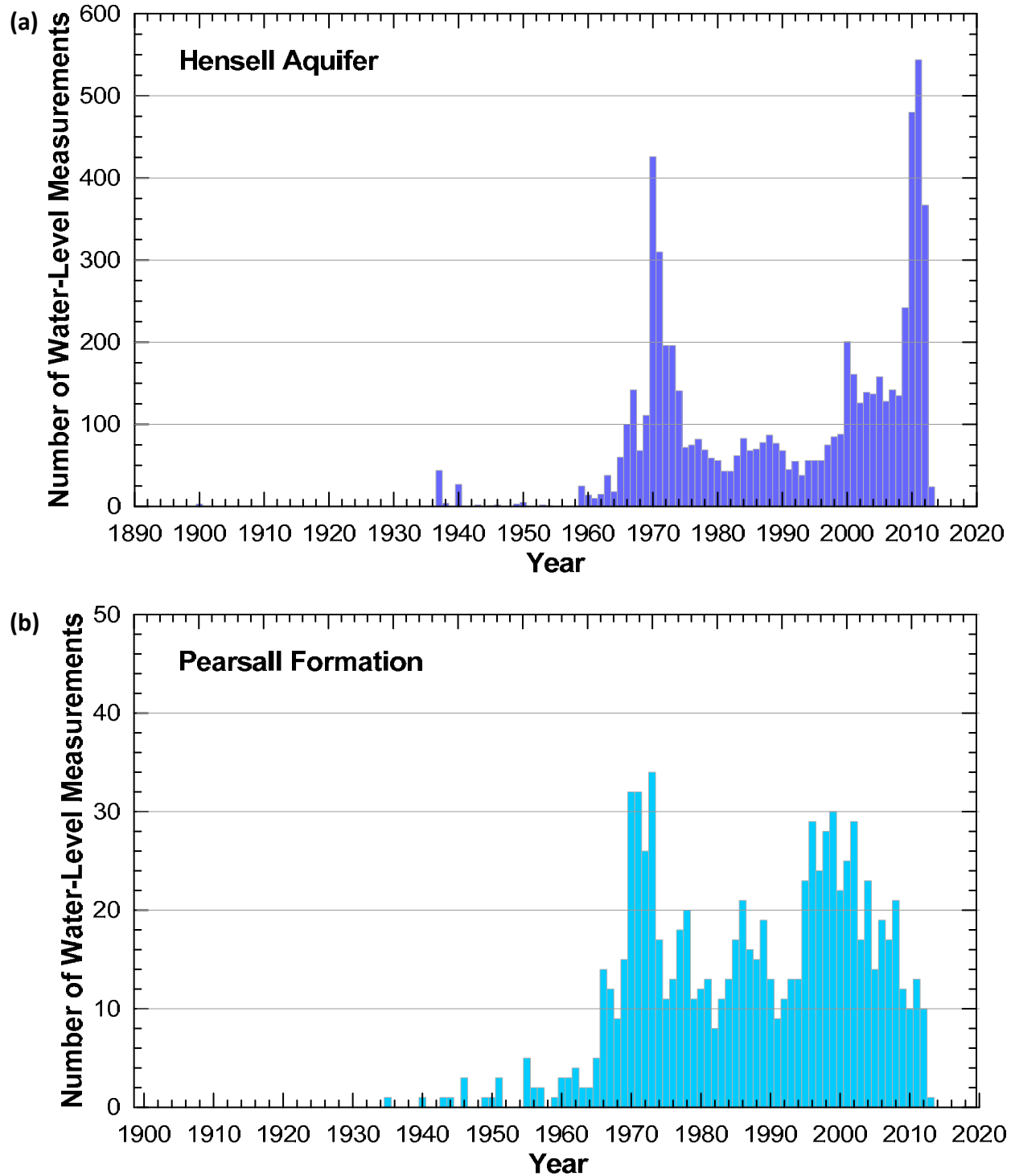
Figure 4.3.8 Temporal distribution of water-level measurements in the study area for the (a) Hensell Aquifer and (b) Pearsall Formation.
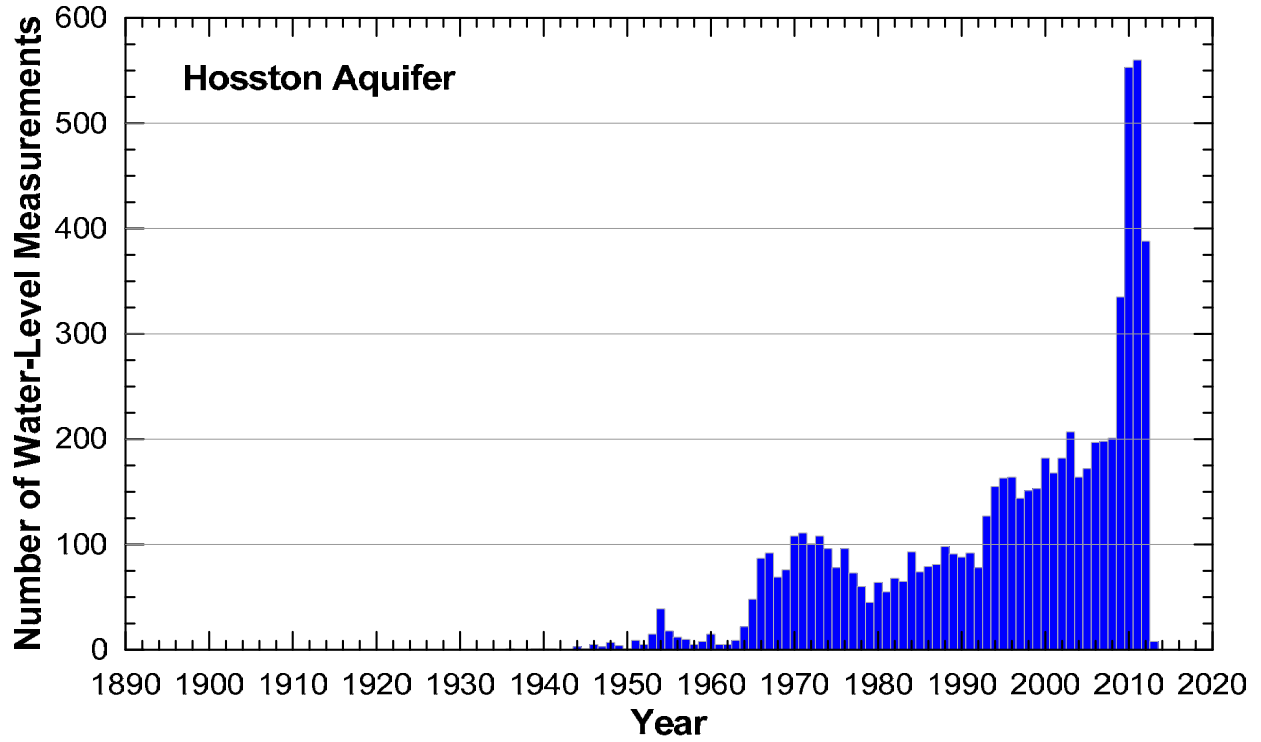
**Figure 4.3.9   Temporal distribution of water-level measurements in the study area for the
(a) Hosston Aquifer.**
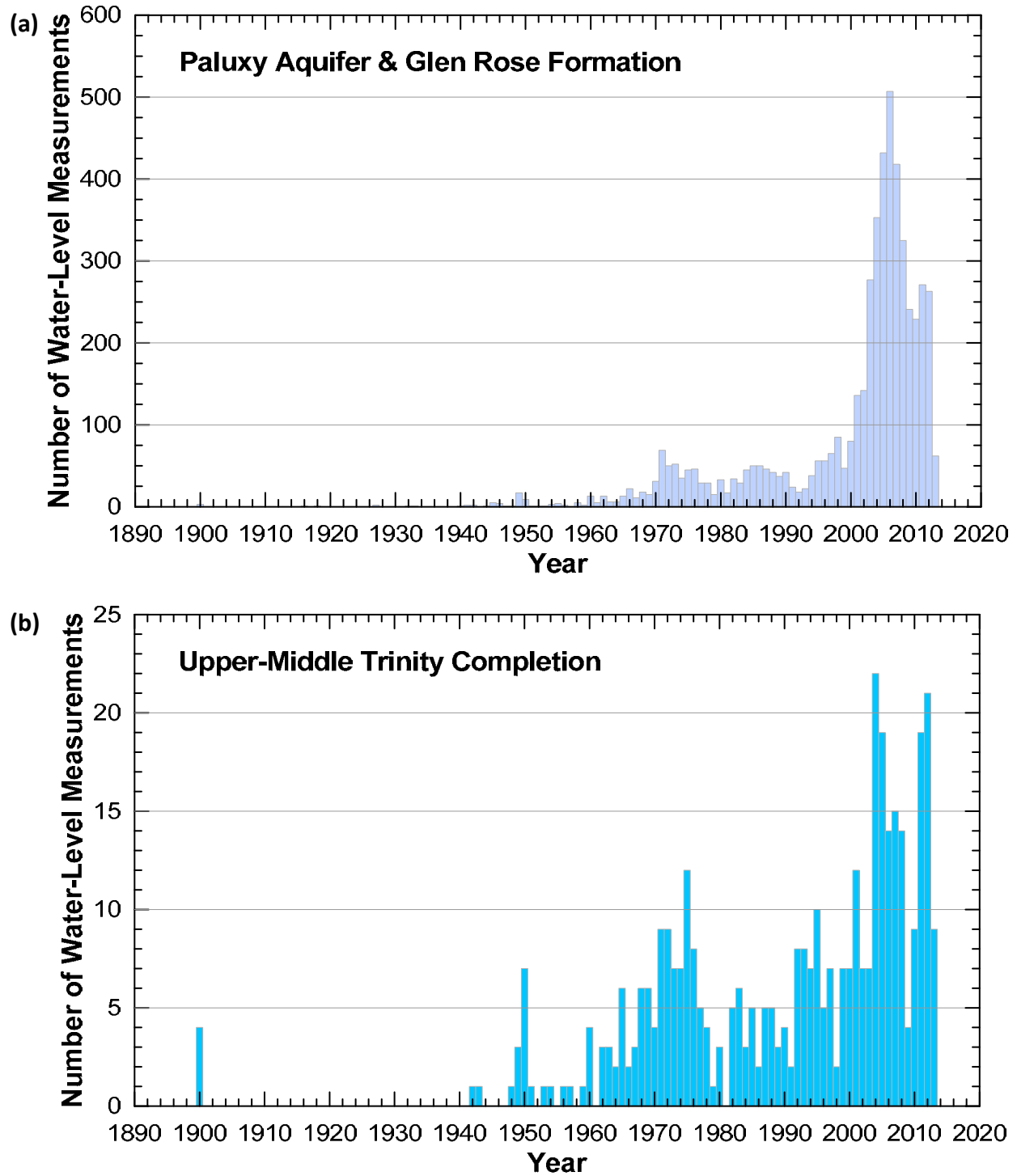
Figure 4.3.10 Temporal distribution of water-level measurements in the study area for wells (a) completed in the Paluxy Aquifer and Glen Rose Formation and (b) with an upper-middle Trinity completion.
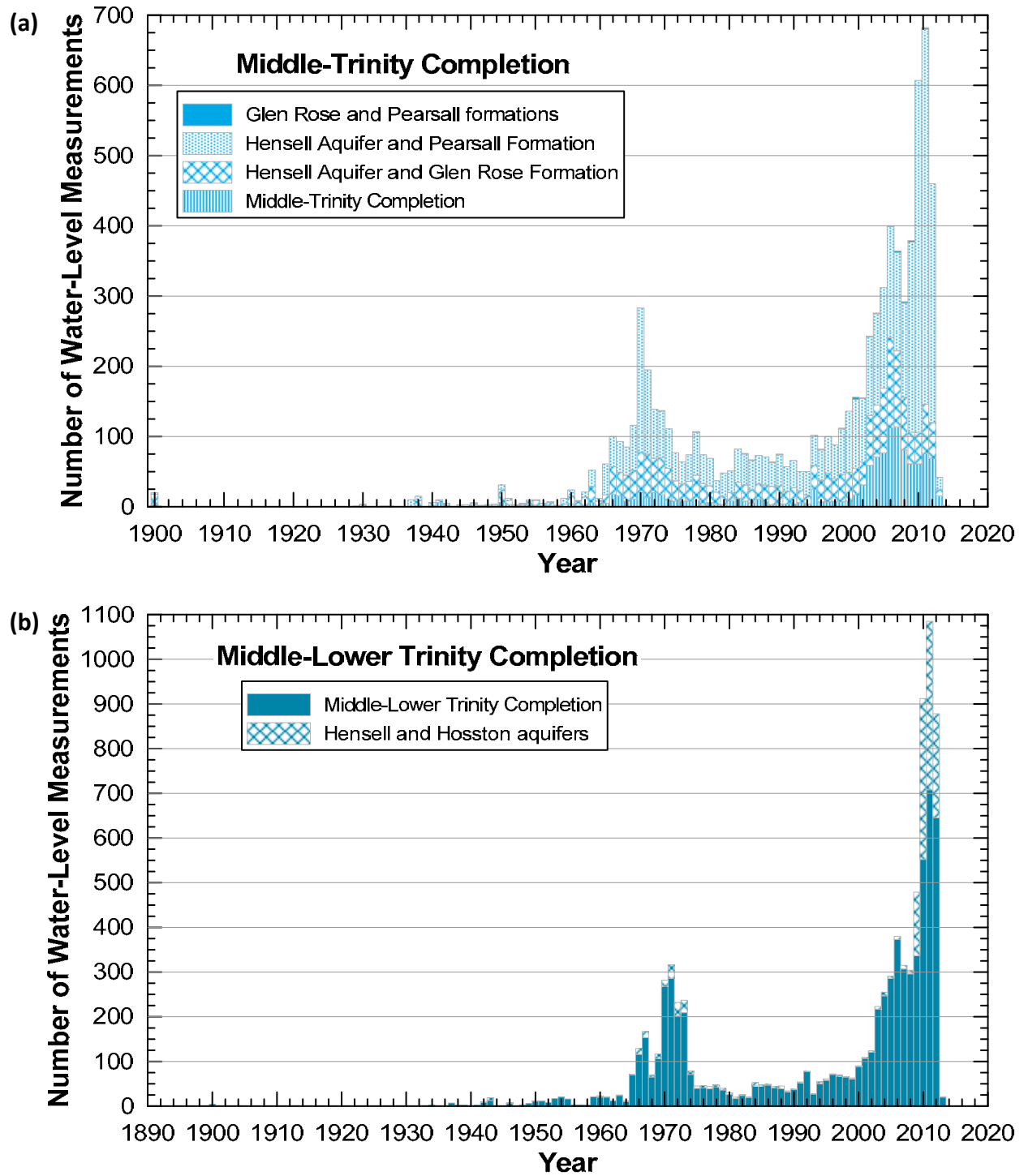
Figure 4.3.11 Temporal distribution of water-level measurements in the study area for wells
(a) completed in the Hensell Aquifer and Glen Rose Formation, Hensell Aquifer and
Pearsall Formation, or with a middle-Trinity completion and (b) completed in the
Hensell and Hosston aquifers or with a middle-lower Trinity completion.
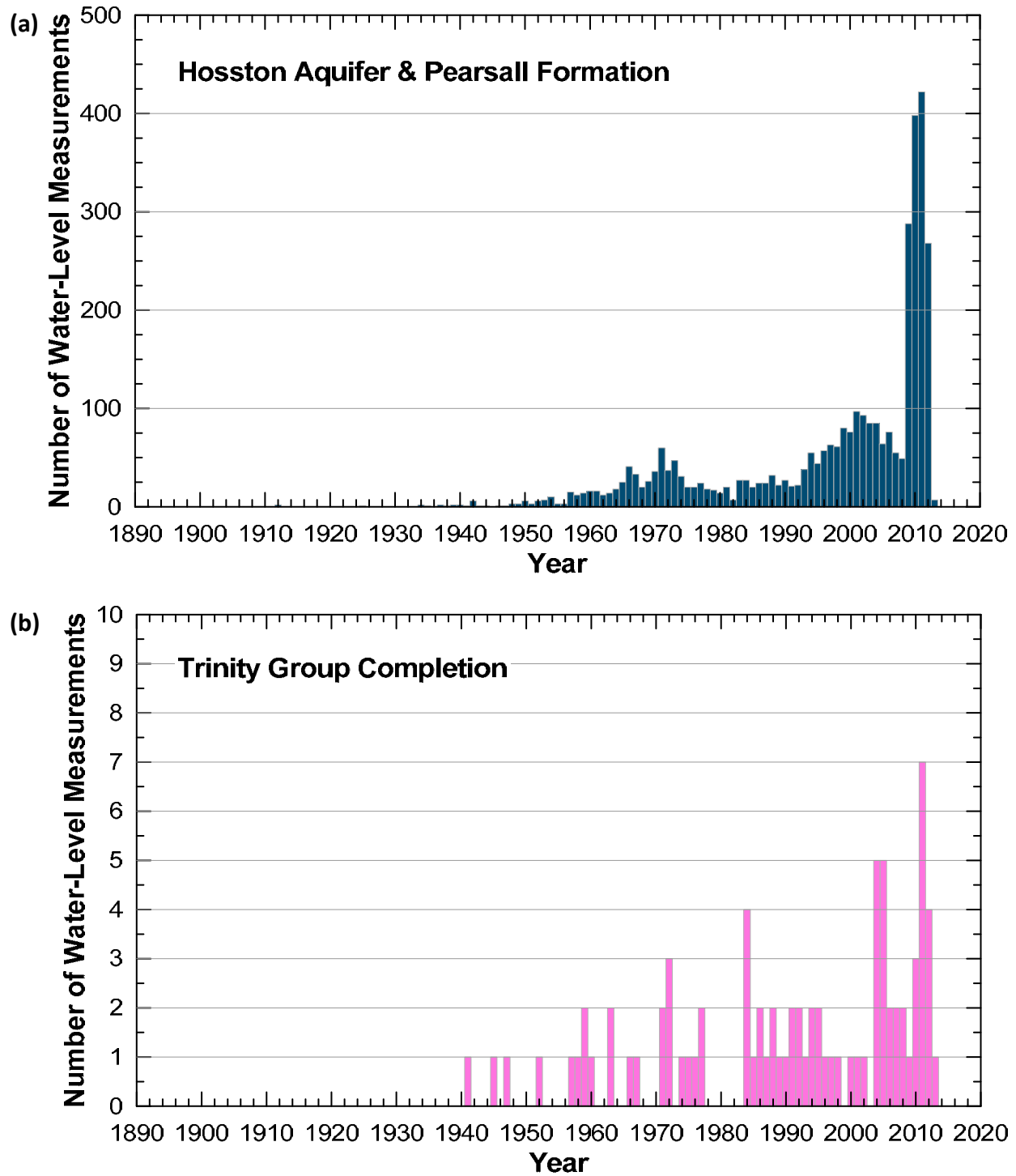
Figure 4.3.12 Temporal distribution of water-level measurements in the study area for wells
(a) completed in the Hosston Aquifer and Pearsall Formation and (b) with a Trinity
Group completion.
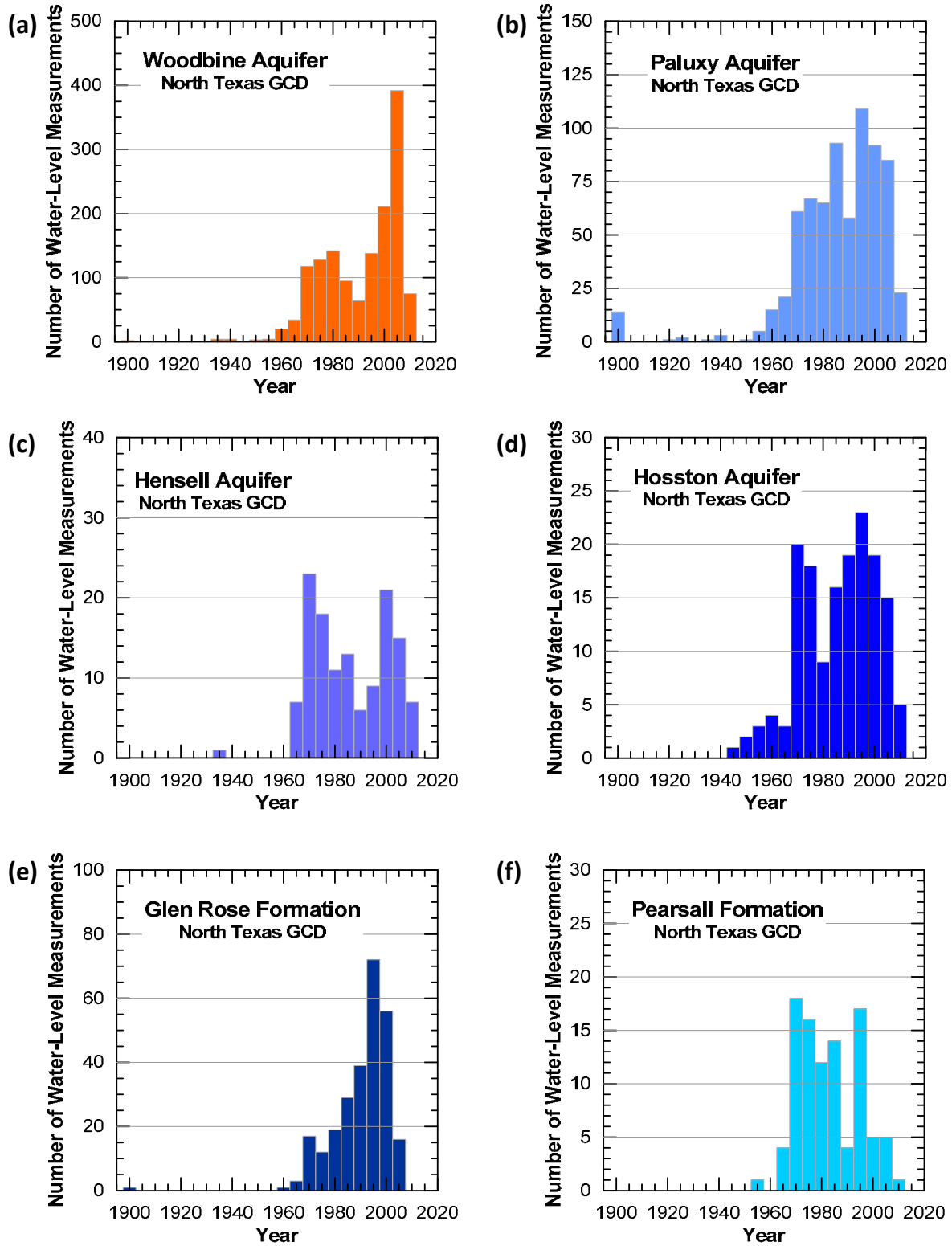
Figure 4.3.13 **Temporal distribution of water-level measurements in the North Texas GCD for the
(a) Woodbine Aquifer, (b) Paluxy Aquifer, (c) Hensell Aquifer, (d) Hosston Aquifer,
(e) Glen Rose Formation, and (f) Pearsall Formation.**
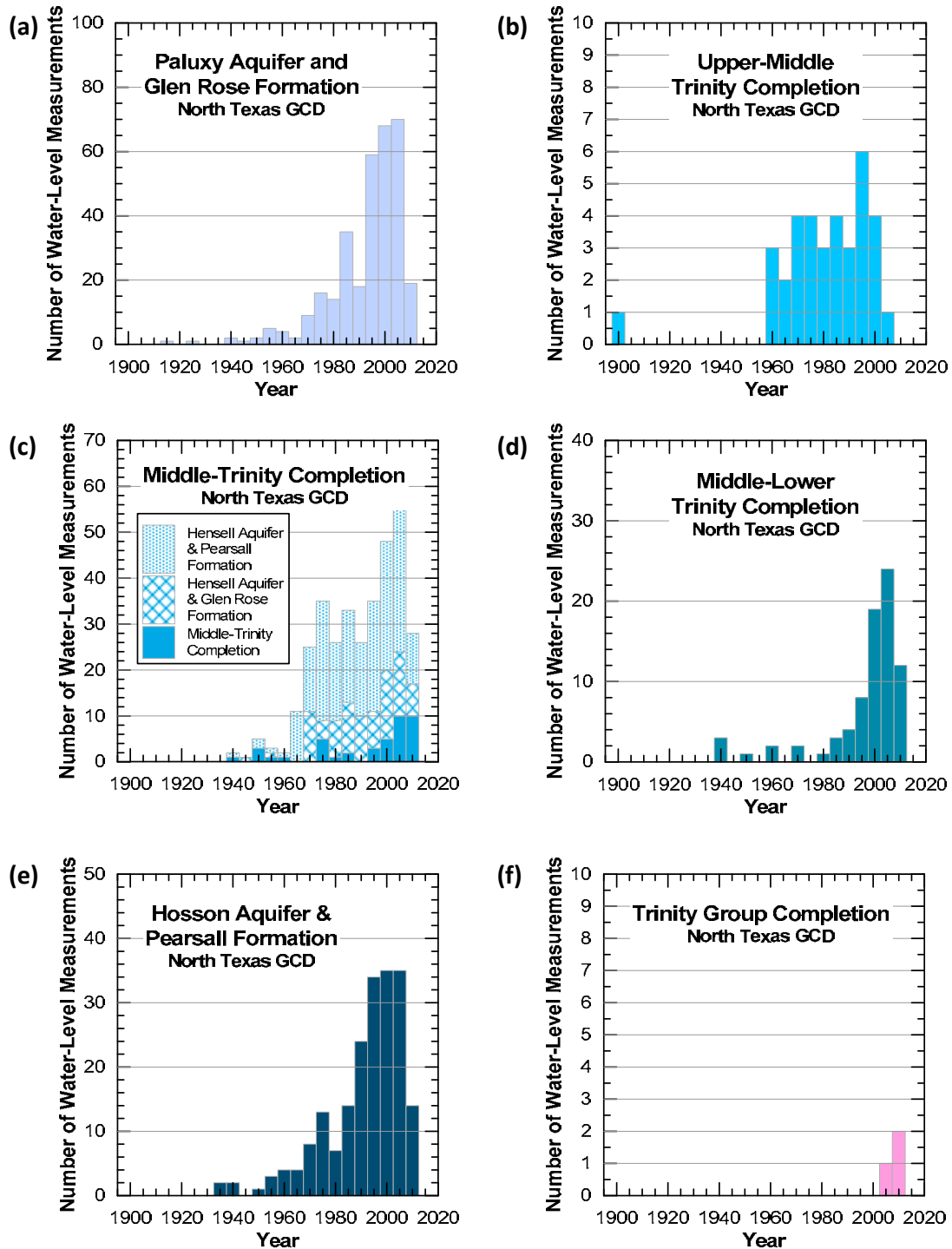
Figure 4.3.14 Temporal distribution of water-level measurements in the North Texas GCD for wells (a) completed in the Paluxy Aquifer and Glen Rose Formation, (b) with an upper-middle Trinity completion, (c) completed in the Hensell Aquifer and Glen Rose Formation, Hensell Aquifer and Pearsall Formation, or with a middle-Trinity completion, (d) with a middle-lower Trinity completion, (e) completed in the Hosston Aquifer and Pearsall Formation, and (f) wells with a Trinity Group completion.
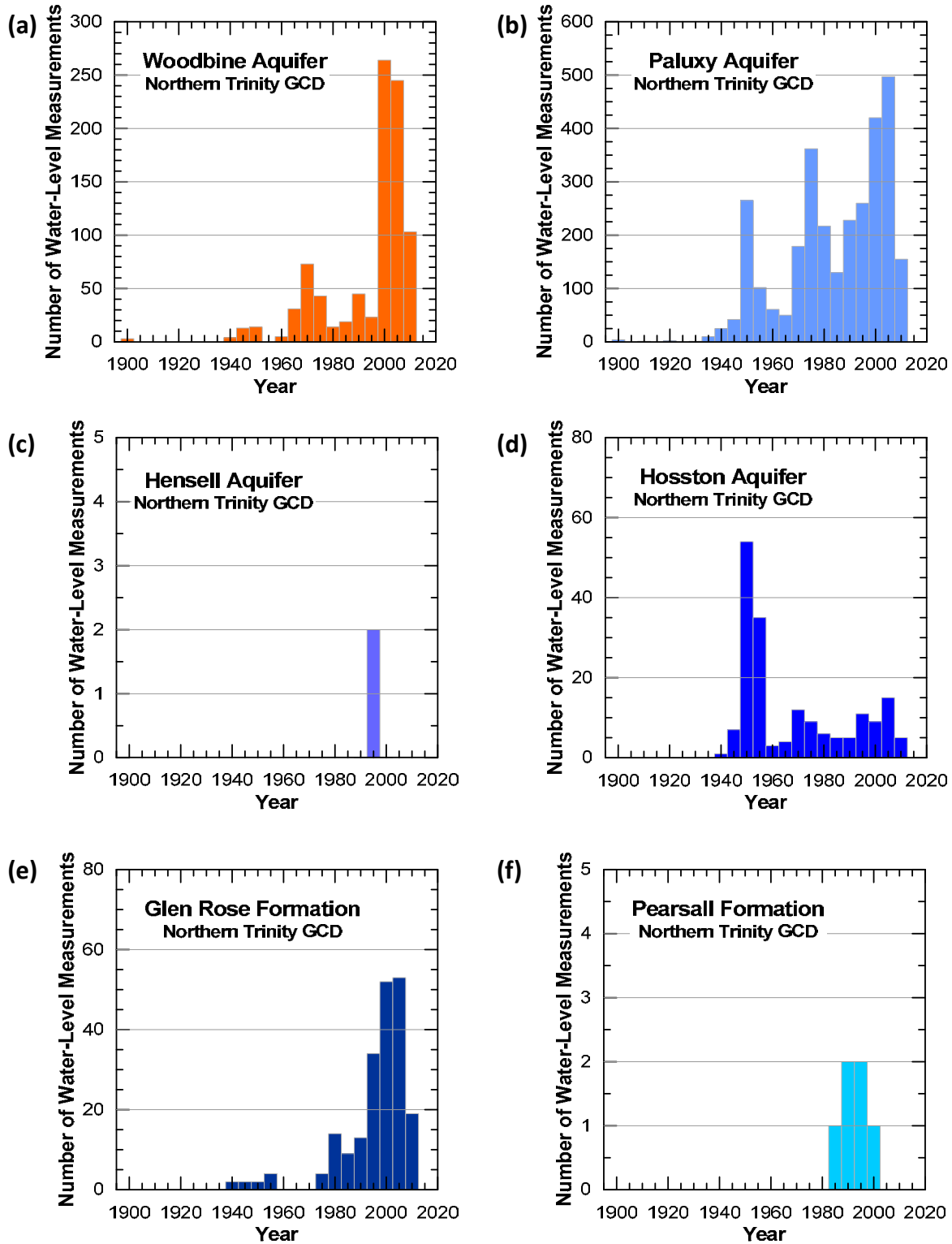
Figure 4.3.15 Temporal distribution of water-level measurements in the Northern Trinity GCD for the (a) Woodbine Aquifer, (b) Paluxy Aquifer, (c) Hensell Aquifer, (d) Hosston Aquifer, (e) Glen Rose Formation, and (f) Pearsall Formation.
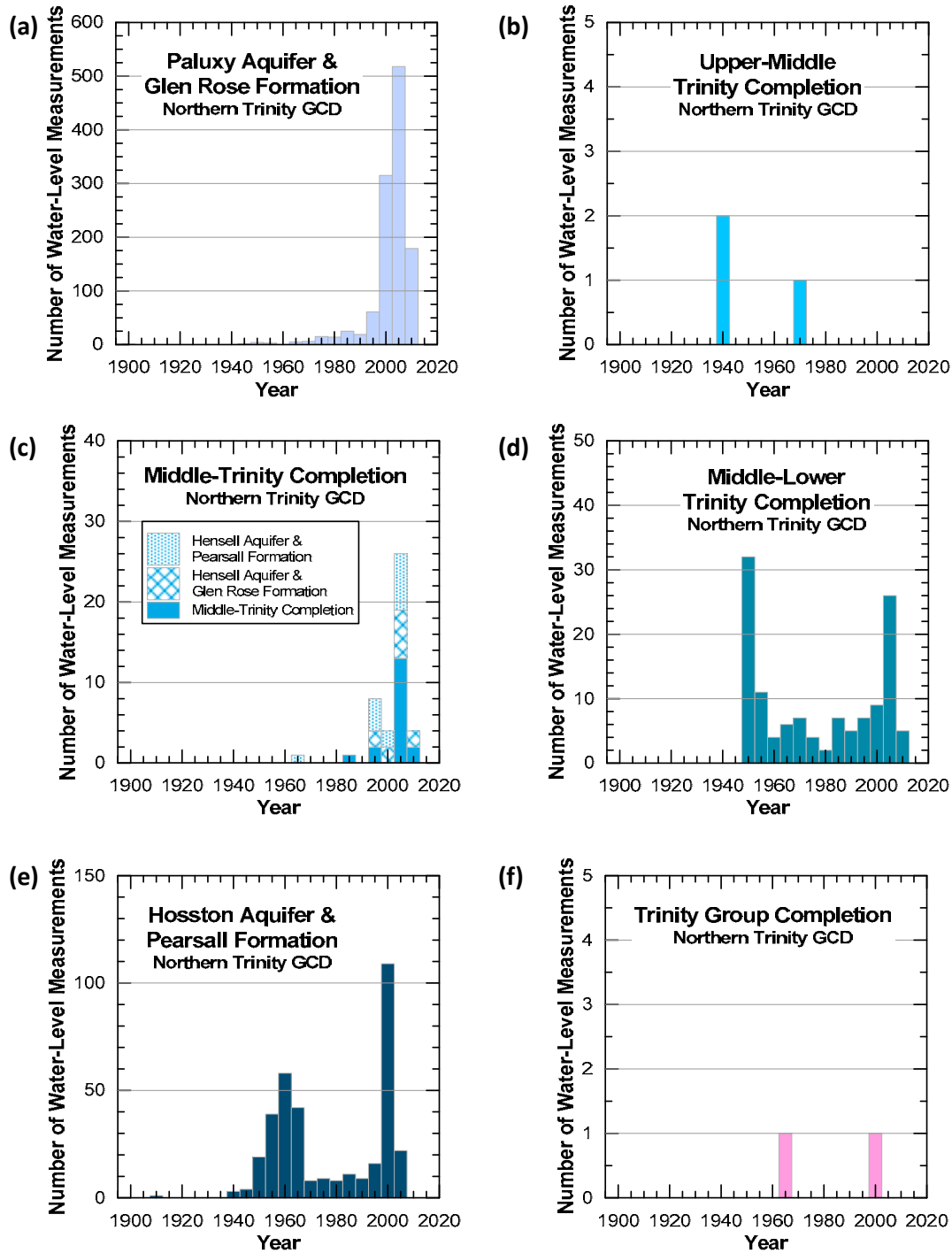
Figure 4.3.16   Temporal distribution of water-level measurements in the Northern Trinity GCD
for wells (a) completed in the Paluxy Aquifer and Glen Rose Formation, (b) with an
upper-middle Trinity completion, (c) completed in the Hensell Aquifer and Glen
Rose Formation, Hensell Aquifer and Pearsall Formation, or with a middle-Trinity
completion, (d) with a middle-lower Trinity completion, (e) completed in the
Hosston Aquifer and Pearsall Formation, and (f) wells with a Trinity Group
completion.
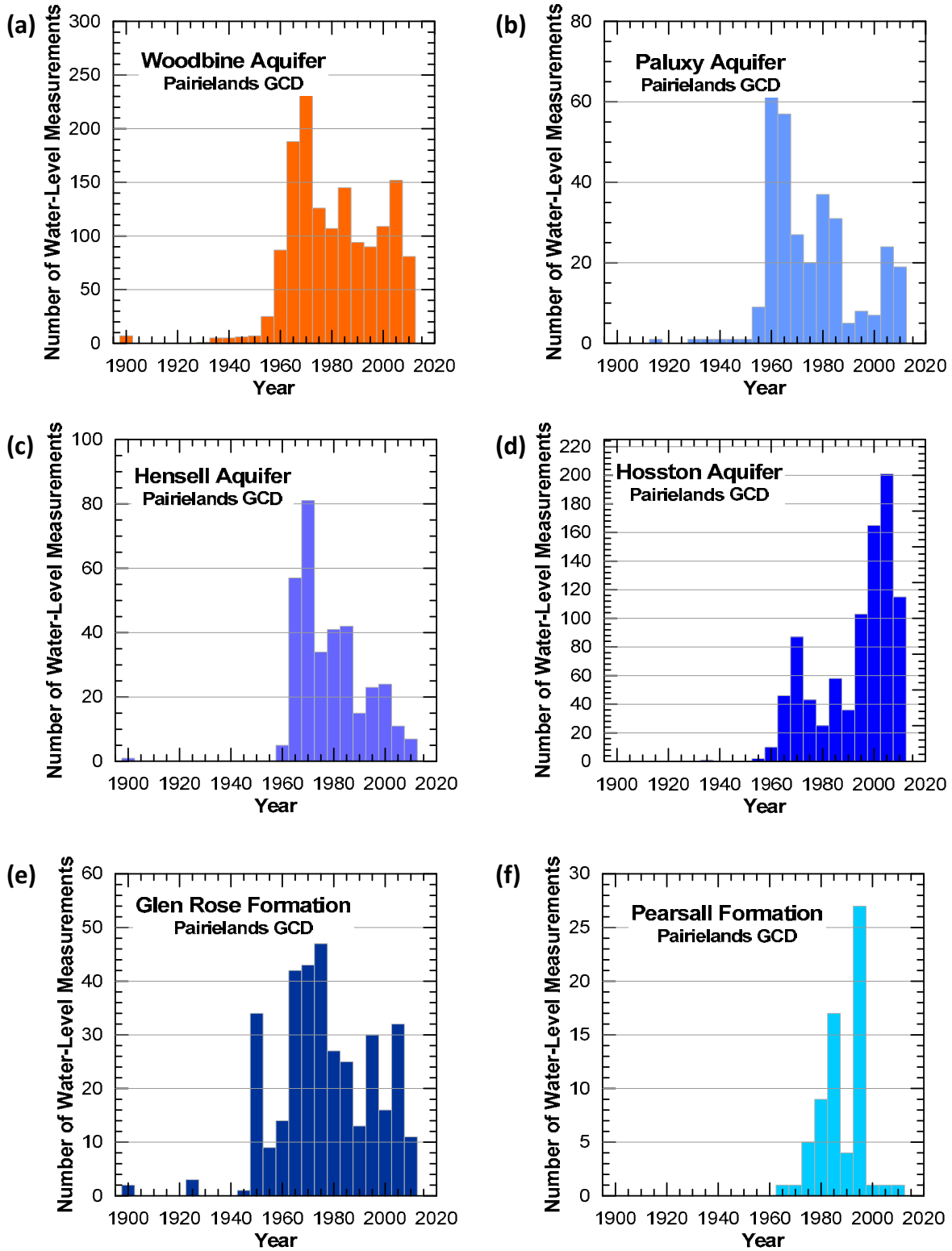
Figure 4.3.17   Temporal distribution of water-level measurements in the Prairielands GCD for the
(a) Woodbine Aquifer, (b) Paluxy Aquifer, (c) Hensell Aquifer, (d) Hosston Aquifer,
(e) Glen Rose Formation, and (f) Pearsall Formation.
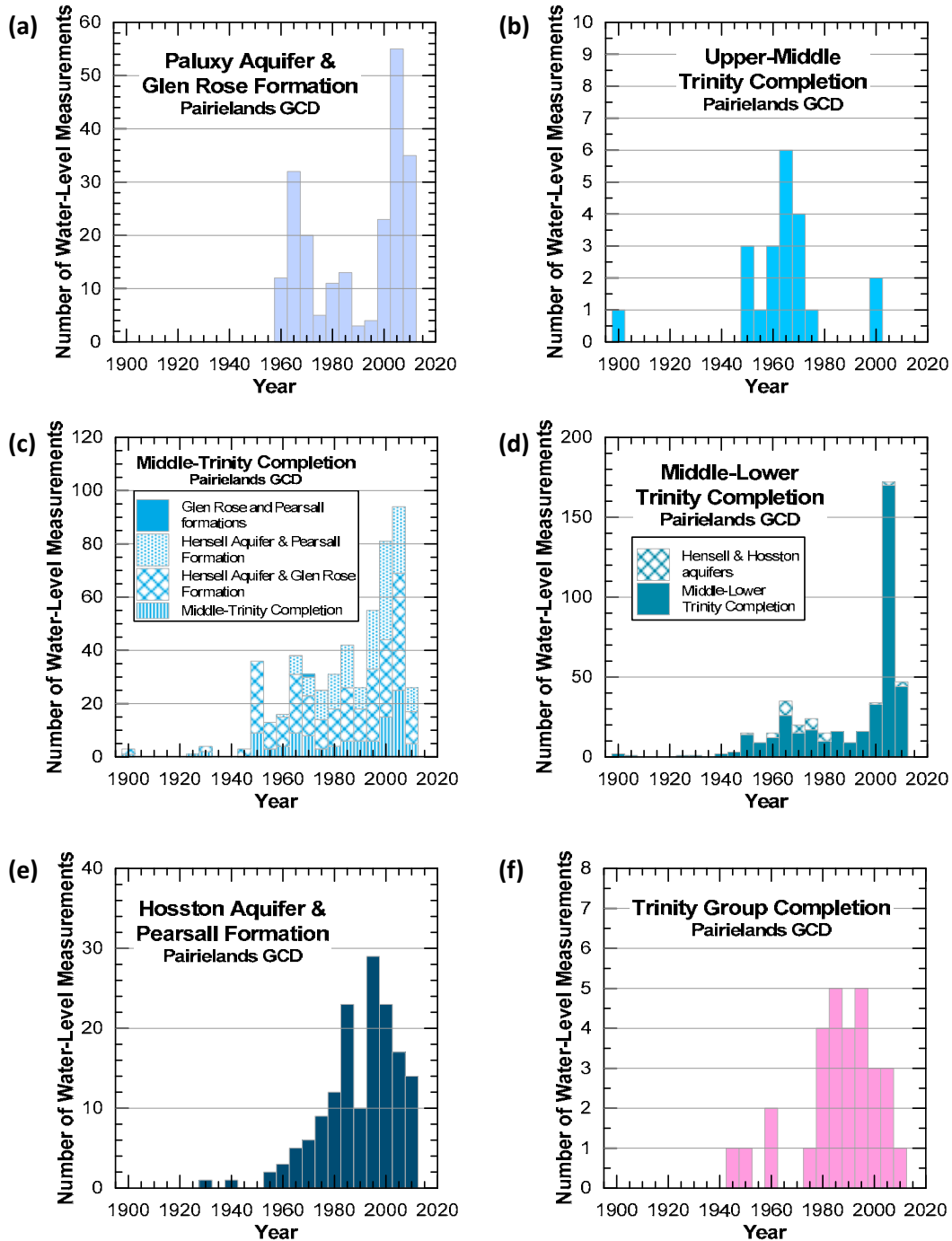
Figure 4.3.18   Temporal distribution of water-level measurements in the Prairielands GCD for wells (a) completed in the Paluxy Aquifer and Glen Rose Formation, (b) with an upper-middle Trinity completion, (c) completed in the Hensell Aquifer and Glen Rose Formation, Hensell Aquifer and Pearsall Formation, Glen Rose and Pearsall formations, or with a middle-Trinity completion, (d) completed in the Hensell and Hosston aquifers or with a middle-lower Trinity completion, (e) completed in the Hosston Aquifer and Pearsall Formation, and (f) wells with a Trinity Group completion.
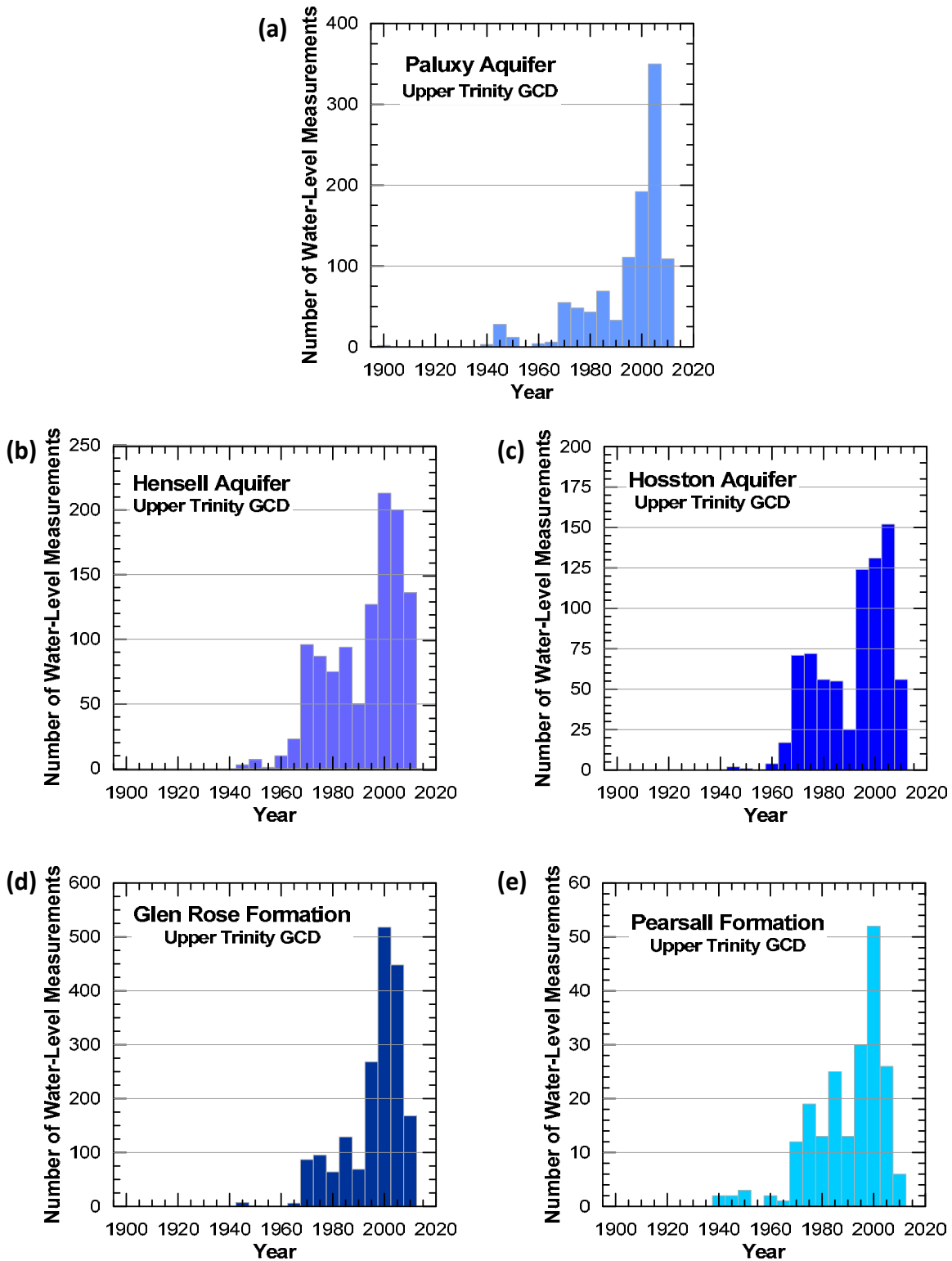
Figure 4.3.19 Temporal distribution of water-level measurements in the Upper Trinity GCD for the (a) Paluxy Aquifer, (b) Hensell Aquifer, (c) Hosston Aquifer, (d) Glen Rose Formation, and (e) Pearsall Formation.
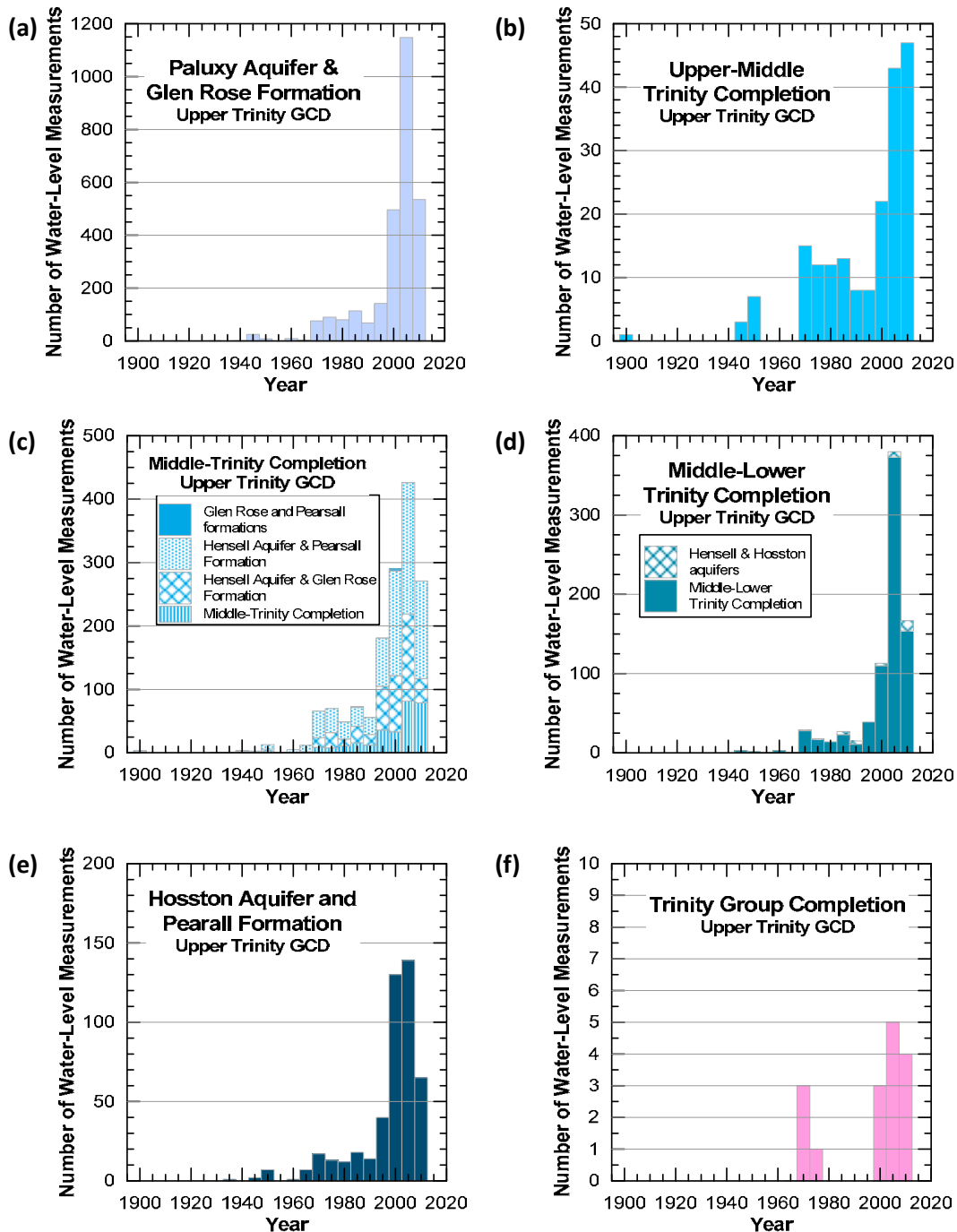
Figure 4.3.20 Temporal distribution of water-level measurements in the Upper Trinity GCD for wells (a) completed in the Paluxy Aquifer and Glen Rose Formation, (b) with an upper-middle Trinity completion, (c) completed in the Hensell Aquifer and Glen Rose Formation, Hensell Aquifer and Pearsall Formation, Glen Rose and Pearsall formations, or with a middle-Trinity completion, (d) completed in the Hensell and Hosston aquifers or with a middle-lower Trinity completion, (e) completed in the Hosston Aquifer and Pearsall Formation, and (f) wells with a Trinity Group completion.
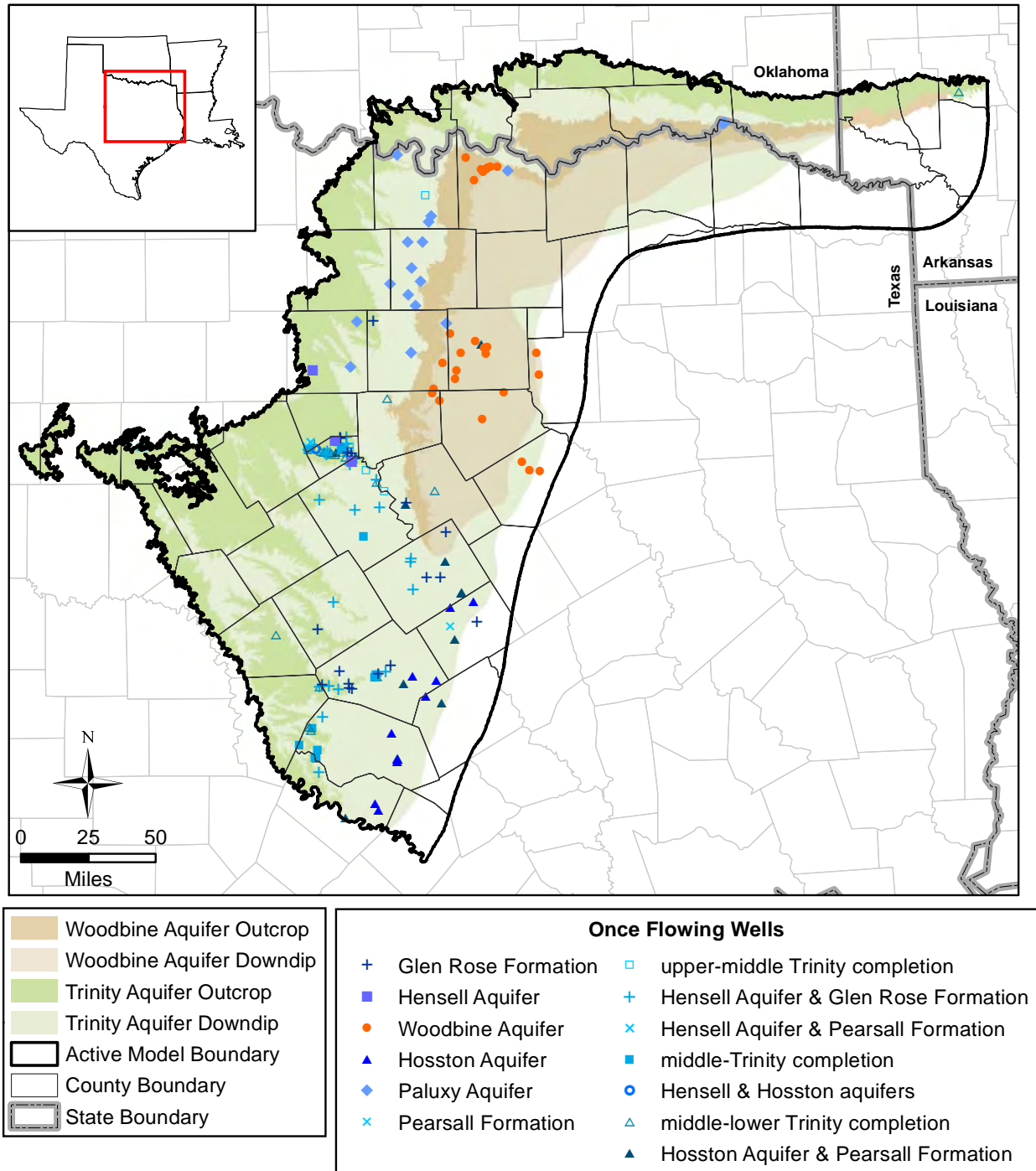
Figure 4.3.21   Known locations of wells that flowed when drilled.
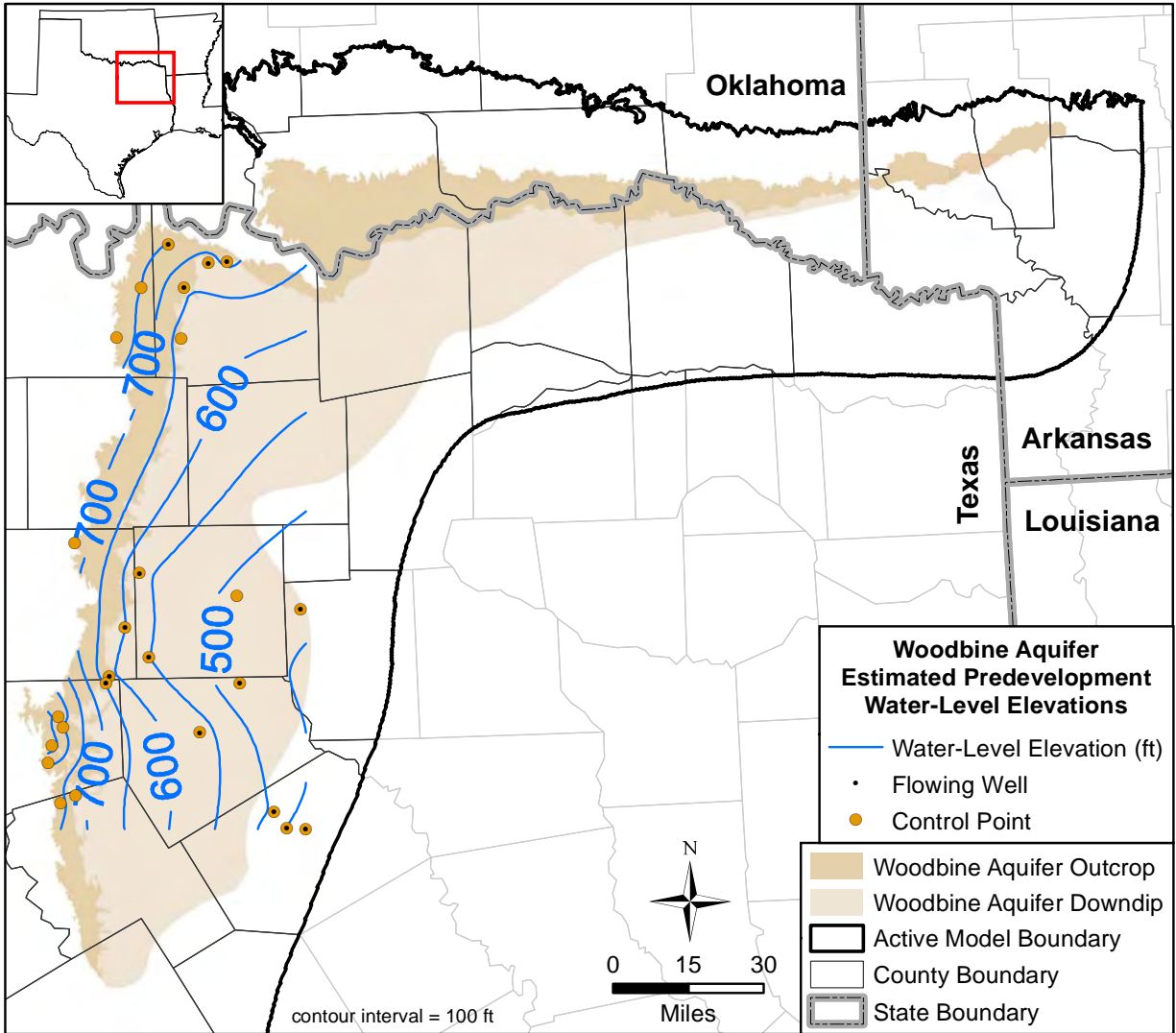
Figure 4.3.22   Estimated predevelopment water-level elevation (hydraulic head) contours in feet amsl for the Woodbine Aquifer.
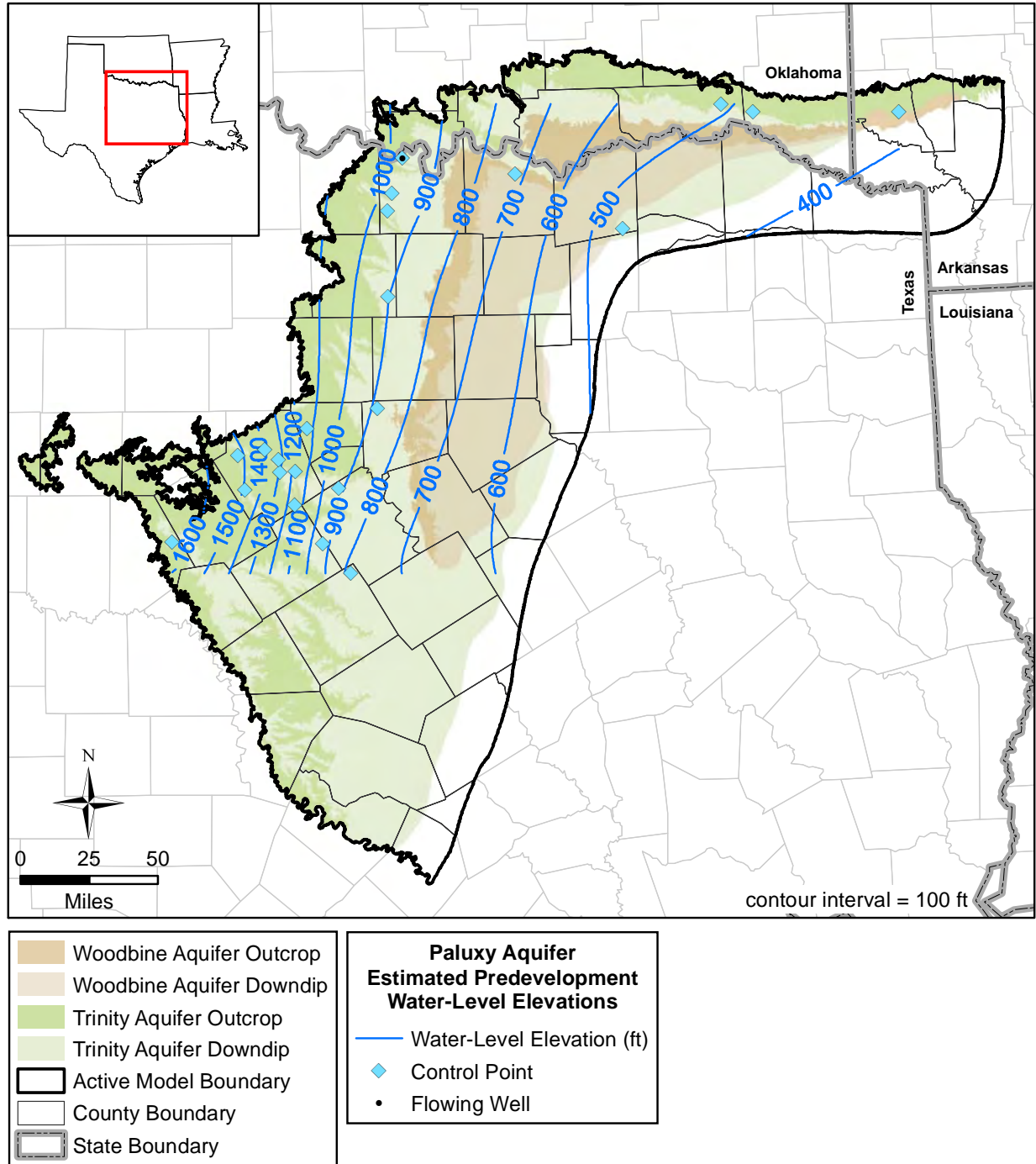
Figure 4.3.23   Estimated predevelopment water-level elevation (hydraulic head) contours in feet amsl for the Paluxy Aquifer.
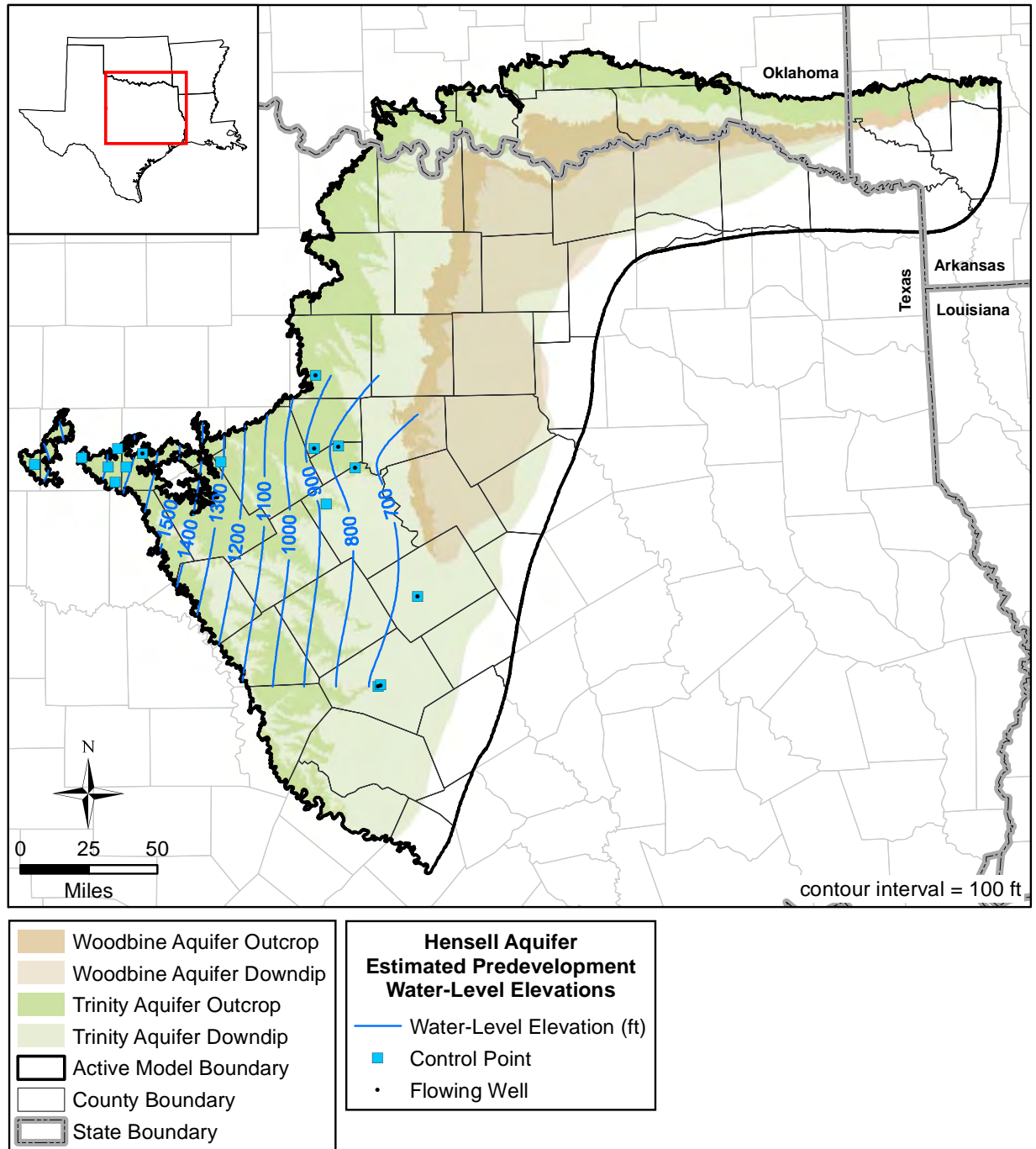
Figure 4.3.24   Estimated predevelopment water-level elevation (hydraulic head) contours in feet amsl for the Hensell Aquifer.
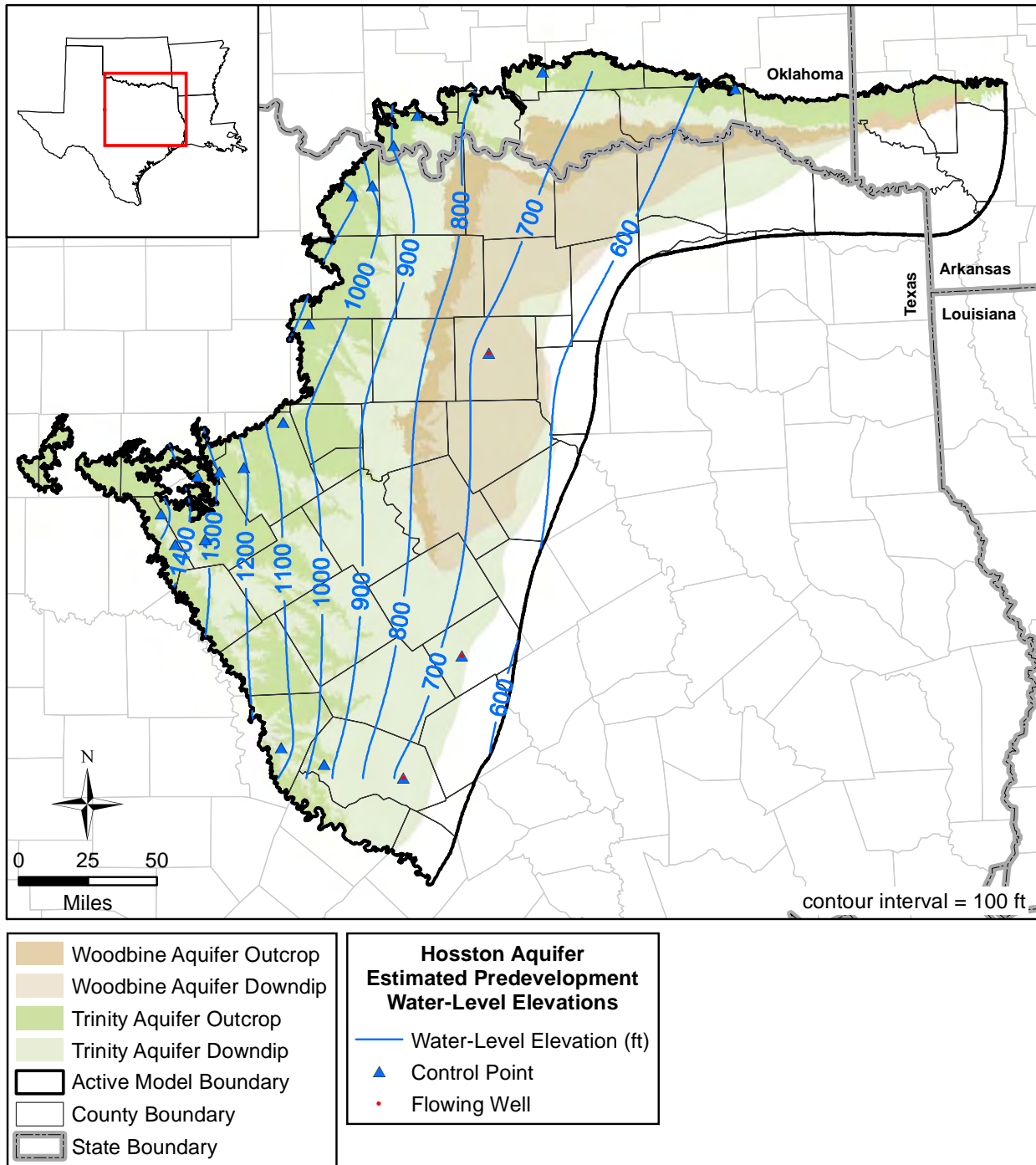
Figure 4.3.25   Estimated predevelopment water-level elevation (hydraulic head) contours in feet amsl for the Hosston Aquifer.
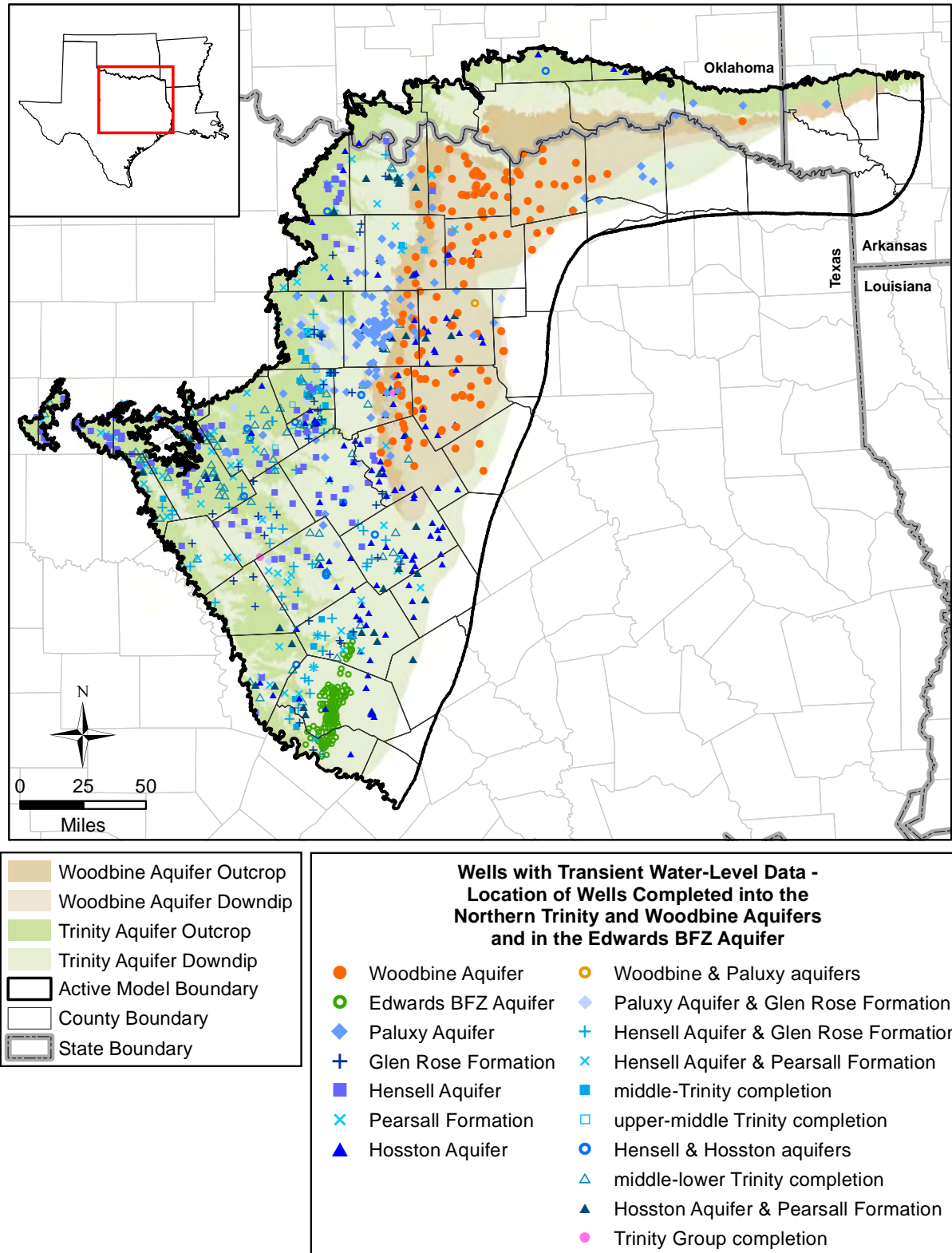
Figure 4.3.26a Locations of wells completed in the northern Trinity and/or Woodbine aquifers with transient water-level data in the study area.
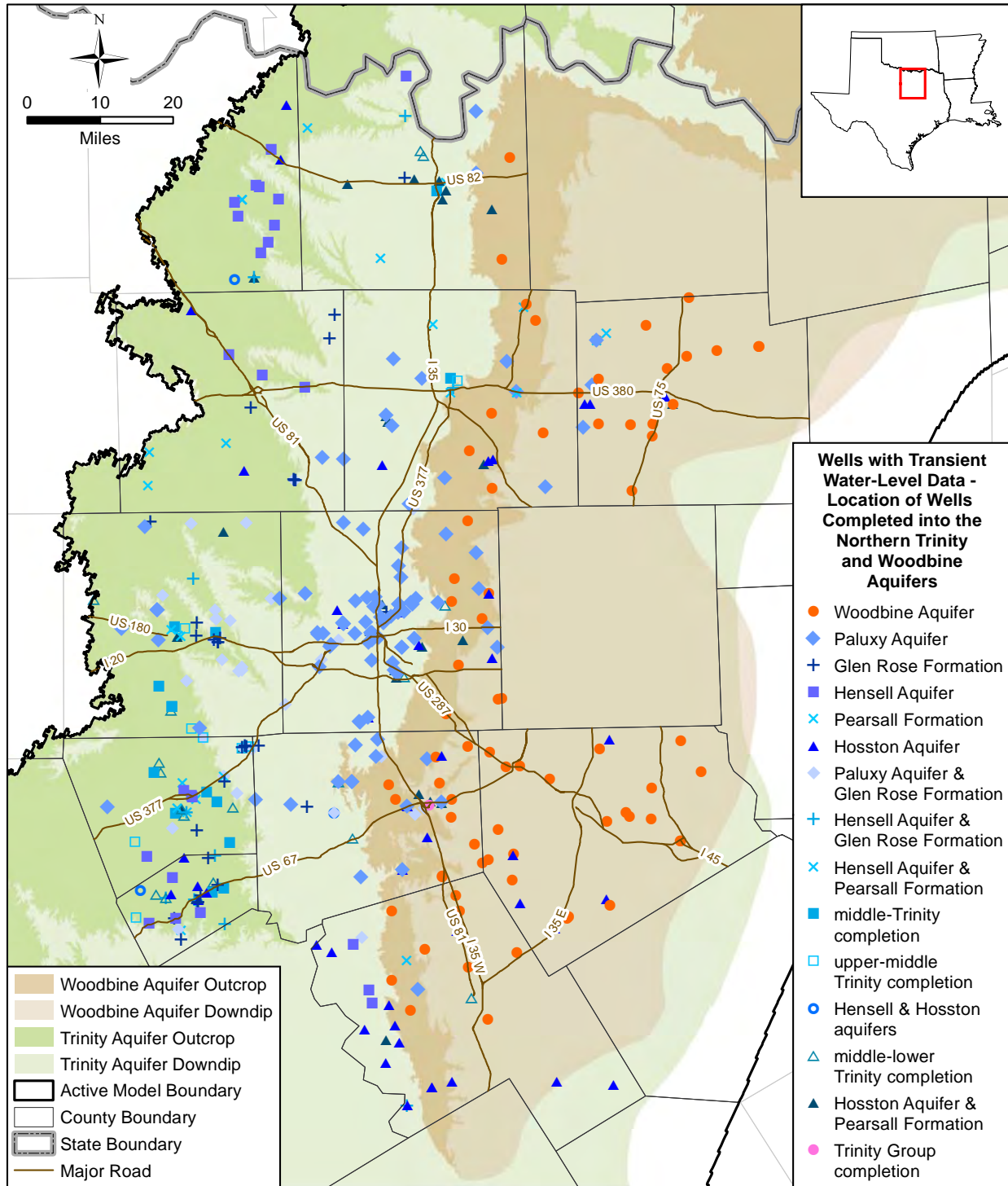
Figure 4.3.26b Locations of wells completed in the northern Trinity and Woodbine aquifers with transient water-level data in the North Texas, Northern Trinity, Prairielands, and Upper Trinity GCDs.

This page intentionally left blank.
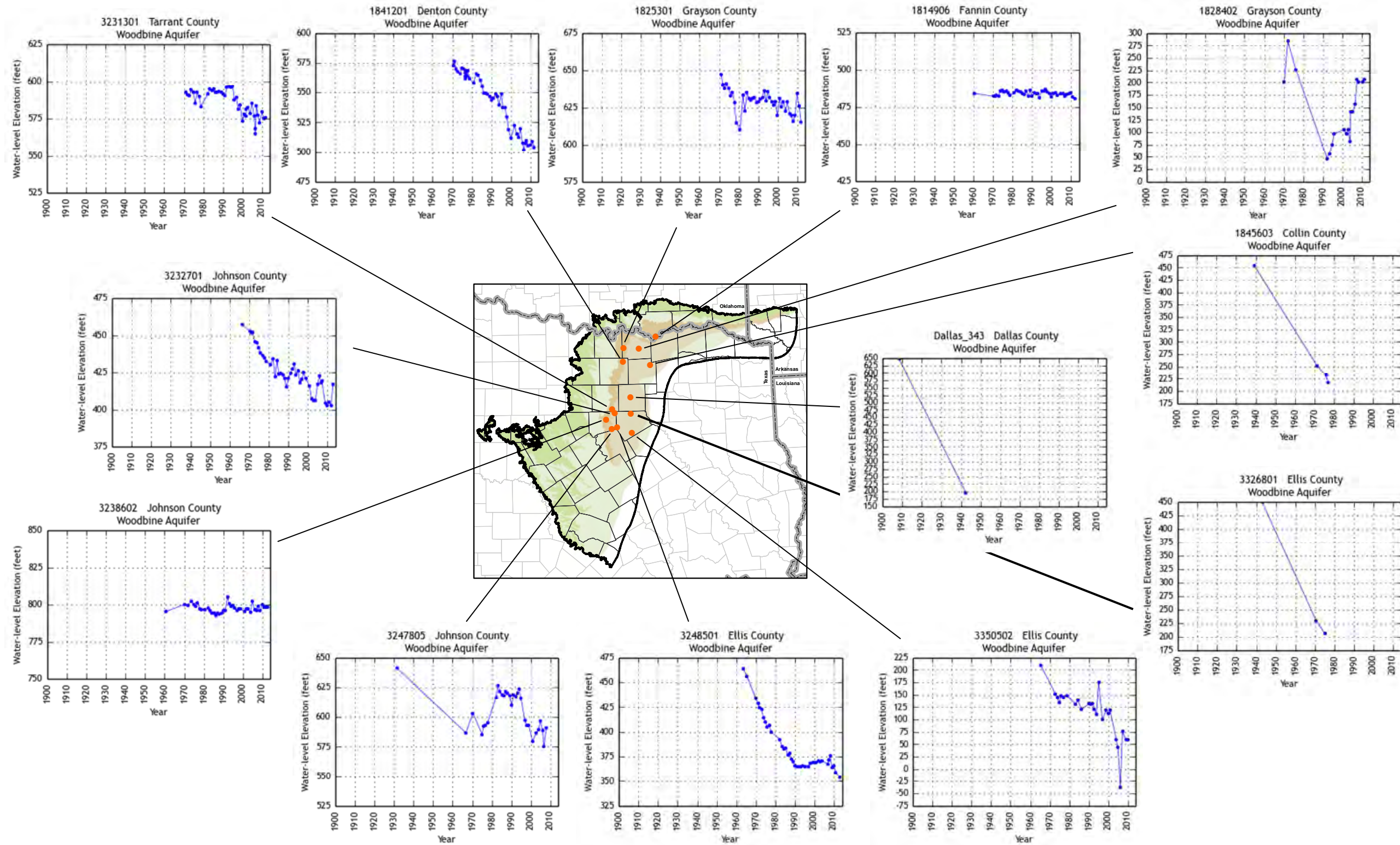
Figure 4.3.27   Select hydrographs showing water-level elevations (hydraulic heads) in feet amsl for wells completed in the Woodbine Aquifer.
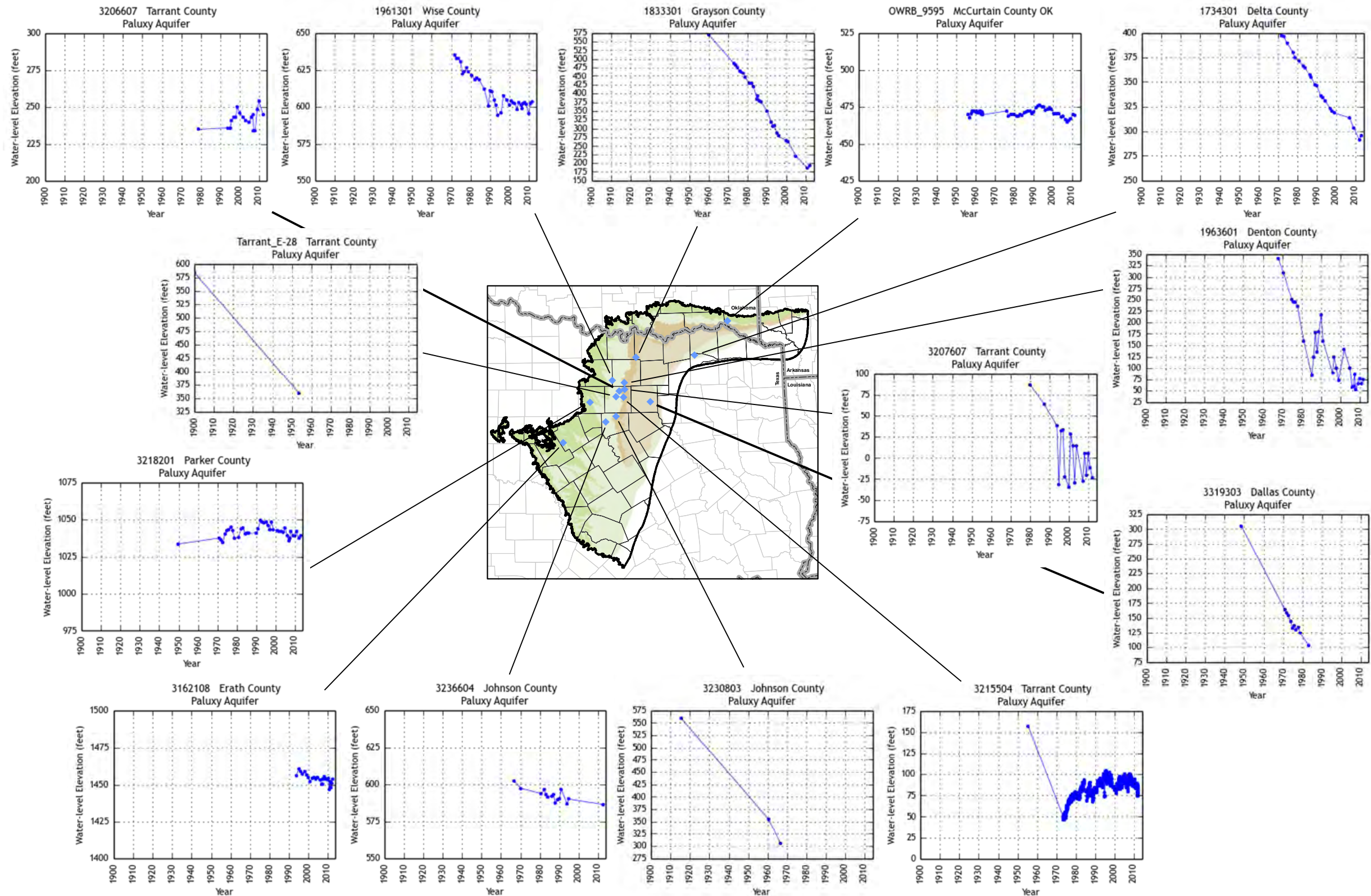
Figure 4.3.28   Select hydrographs showing water-level elevations (hydraulic heads) in feet amsl for wells completed in the Paluxy Aquifer.
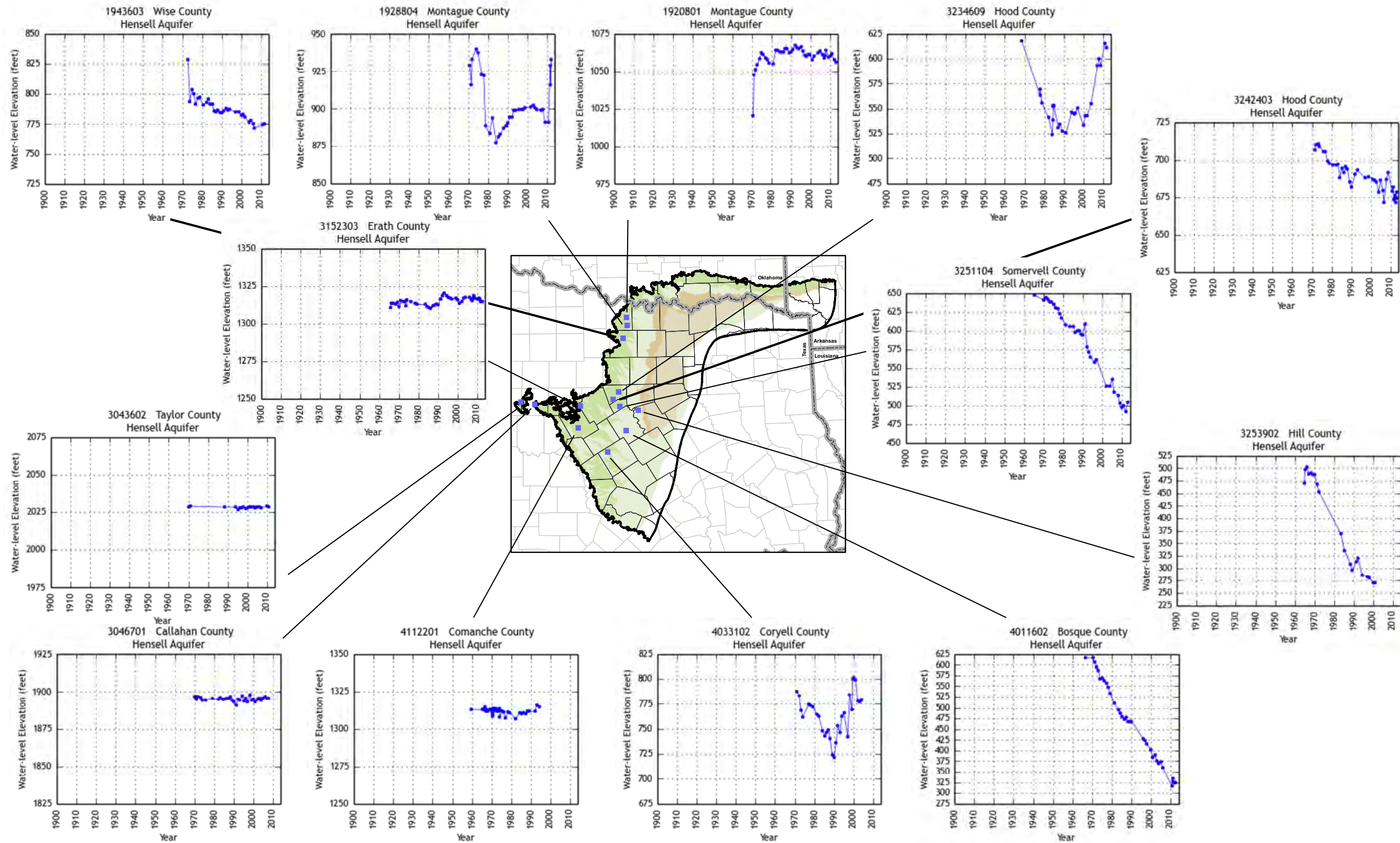
**Figure 4.3.29   Select hydrographs showing water-level elevations (hydraulic heads) in feet amsl
for wells completed in the Hensell Aquifer.**
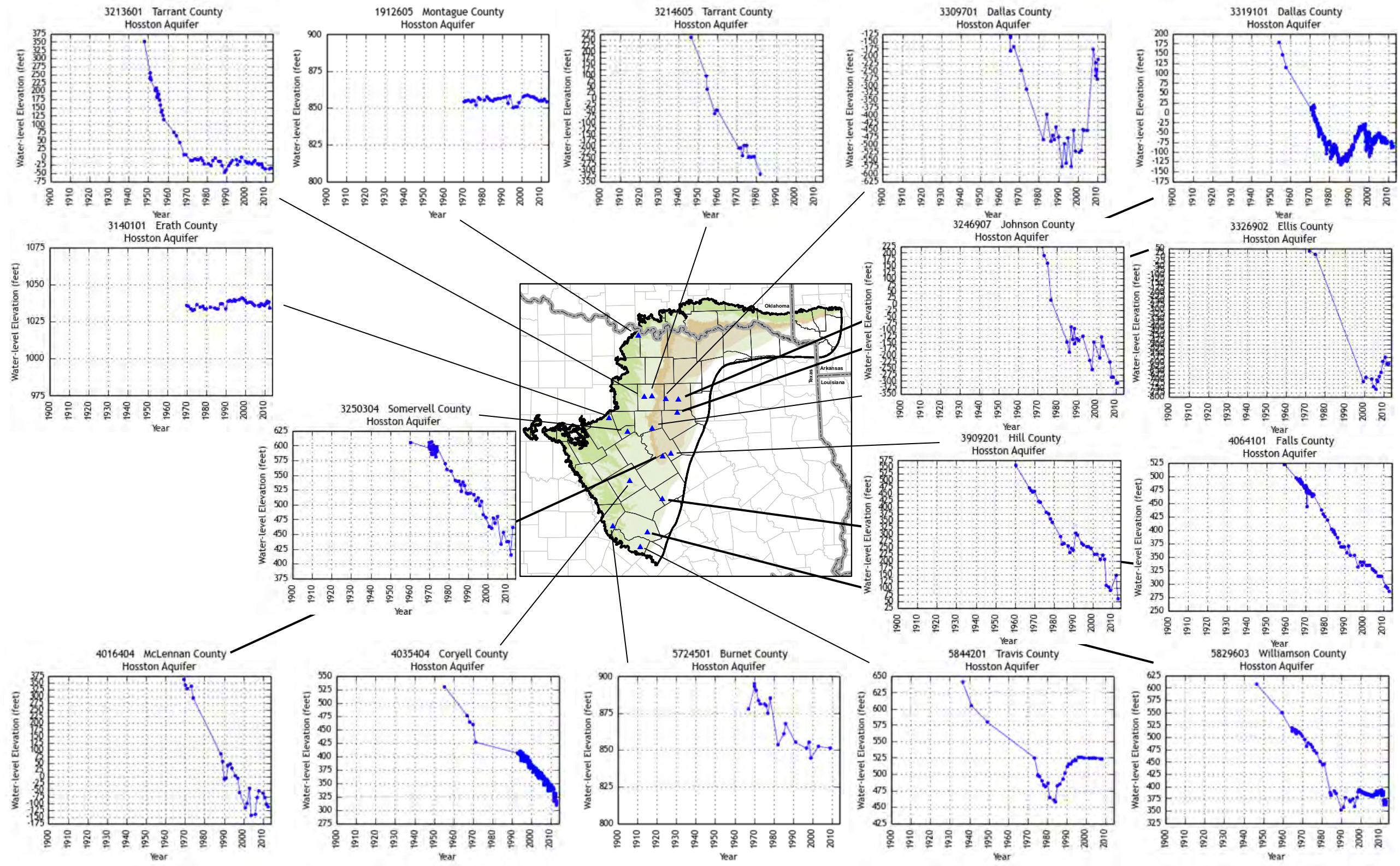
Figure 4.3.30   Select hydrographs showing water-level elevations (hydraulic heads) in feet amsl for wells completed in the Hosston Aquifer.
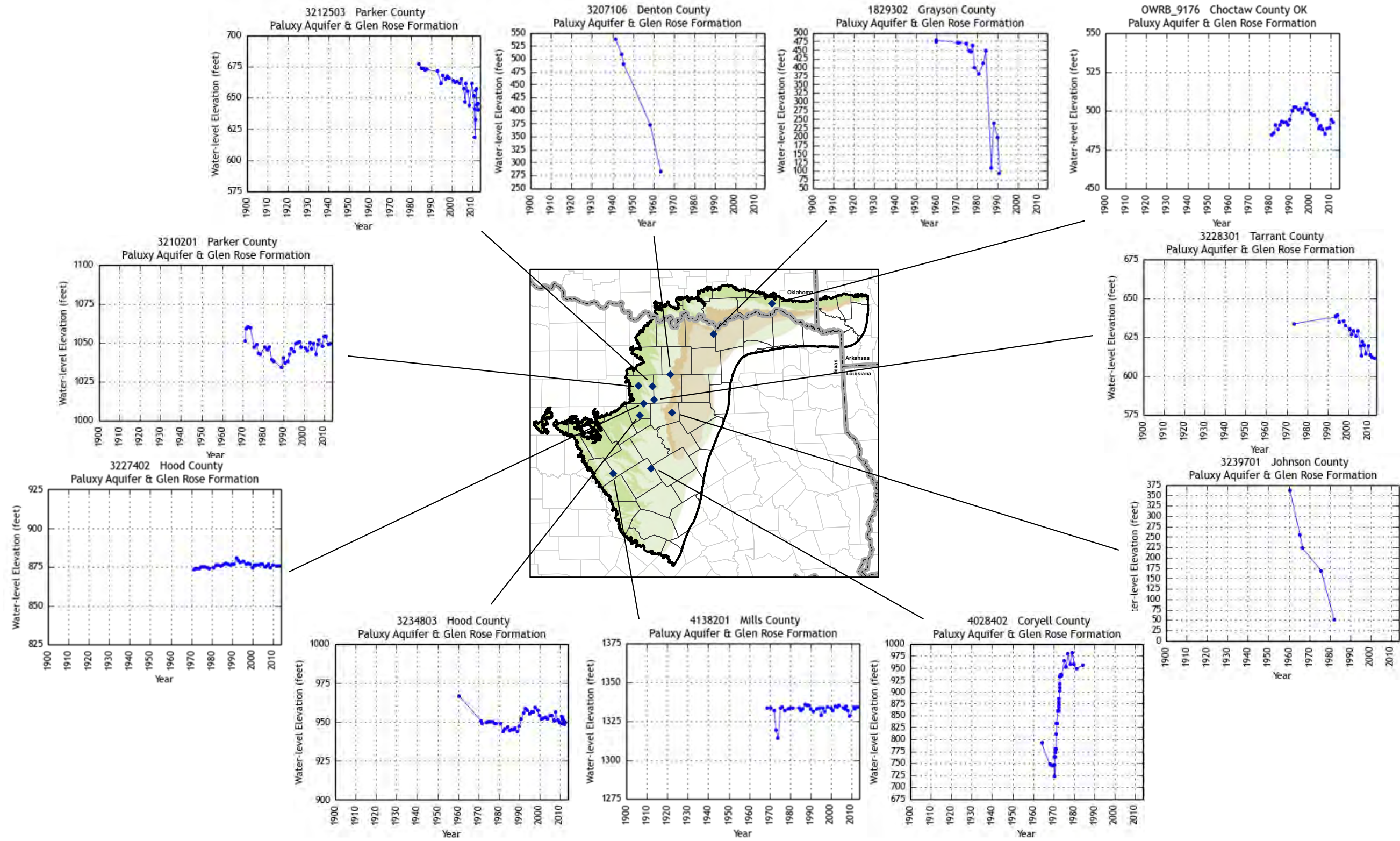
**Figure 4.3.31   Select hydrographs showing water-level elevations (hydraulic heads) in feet amsl
for wells completed in both the Paluxy Aquifer and Glen Rose Formation.**
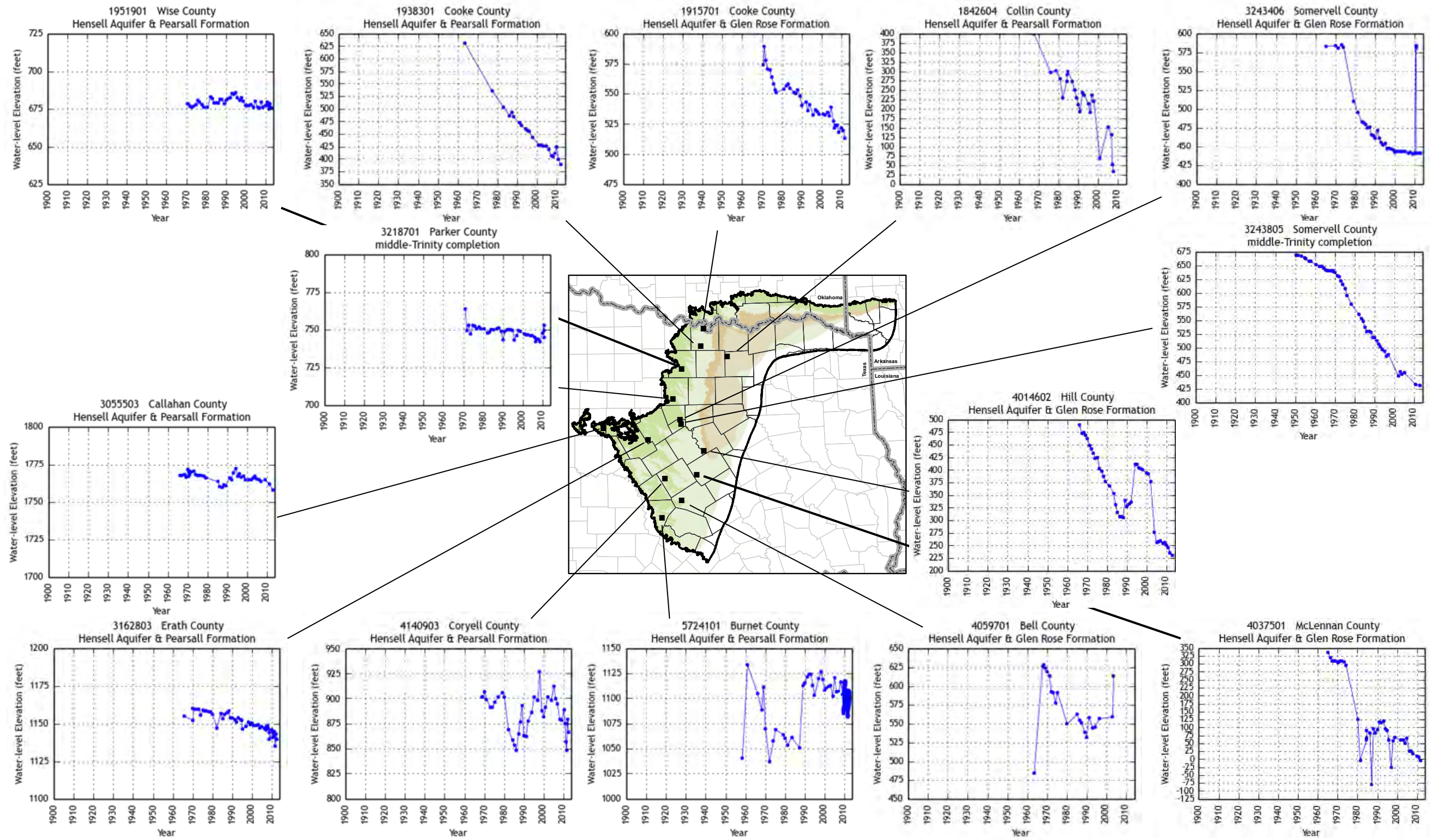
Figure 4.3.32   Select hydrographs showing water-level elevations (hydraulic heads) in feet amsl
for wells completed in the Hensell Aquifer and Glen Rose Formation, Hensell
Aquifer and Pearsall Formation, or with a middle-Trinity completion.
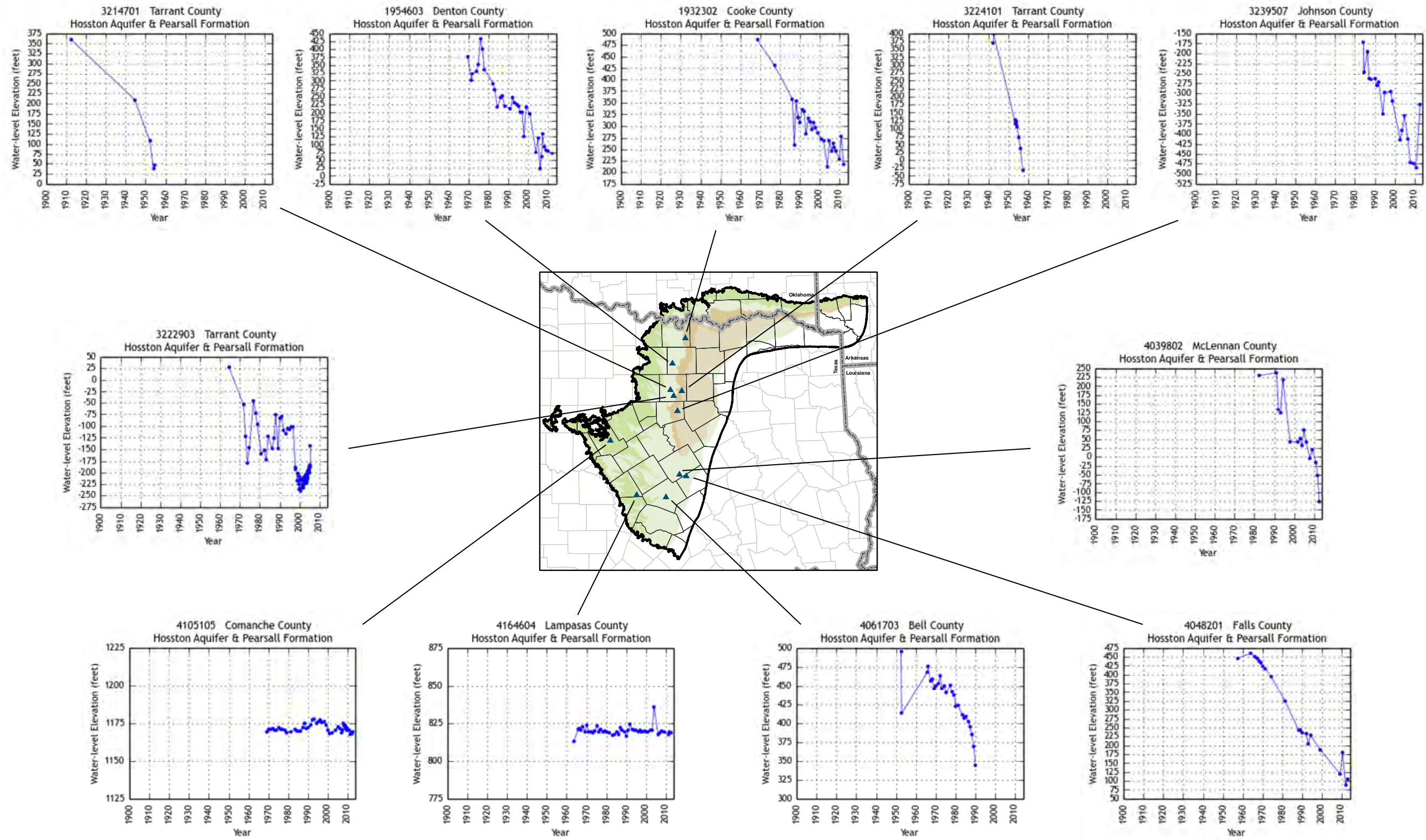
Figure 4.3.33 Select hydrographs showing water-level elevations (hydraulic heads) in feet amsl for wells completed in both the Hosston Aquifer and Pearsall Formation.
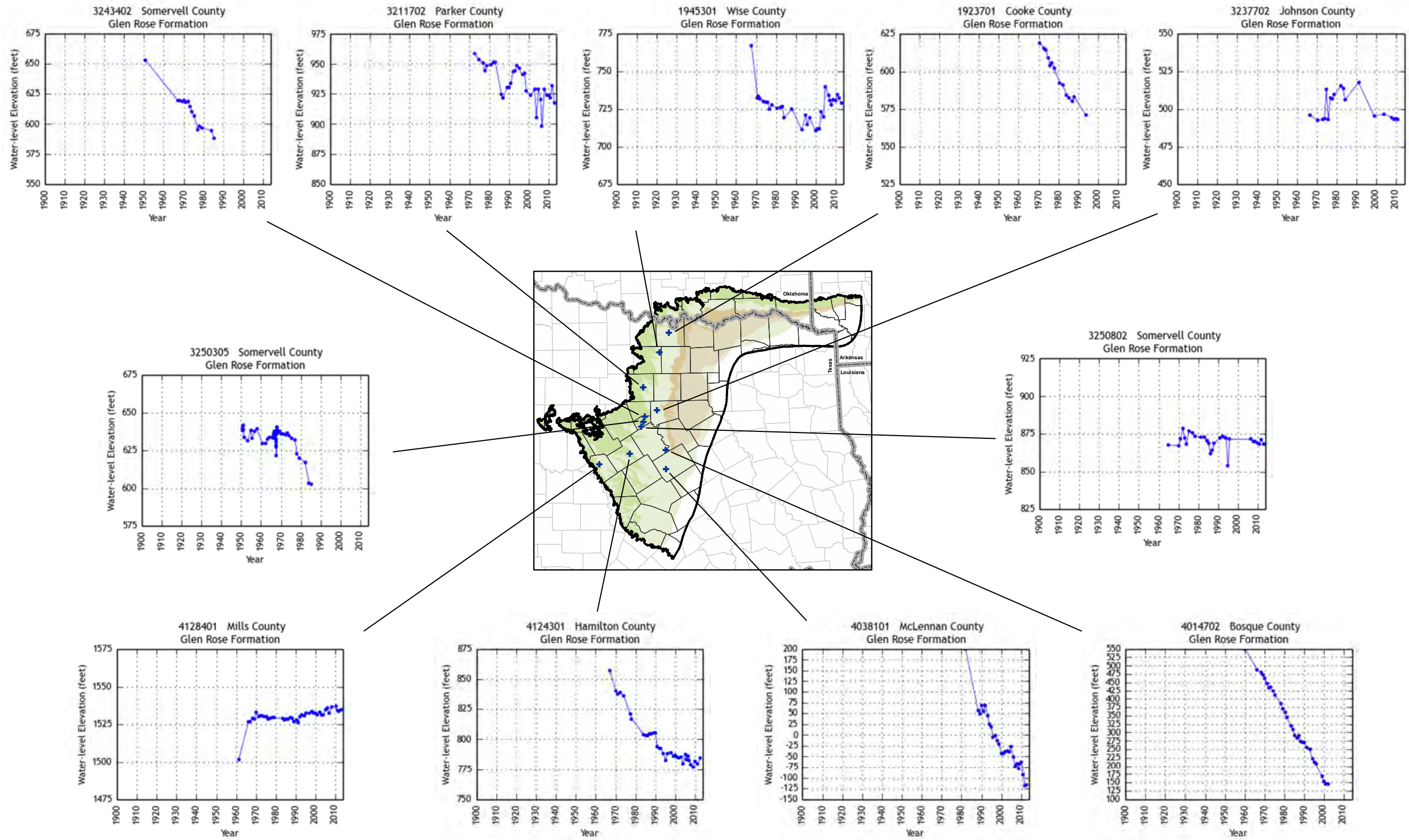
Figure 4.3.34 Select hydrographs showing water-level elevations (hydraulic heads) in feet amsl for wells completed in the Glen Rose Formation.
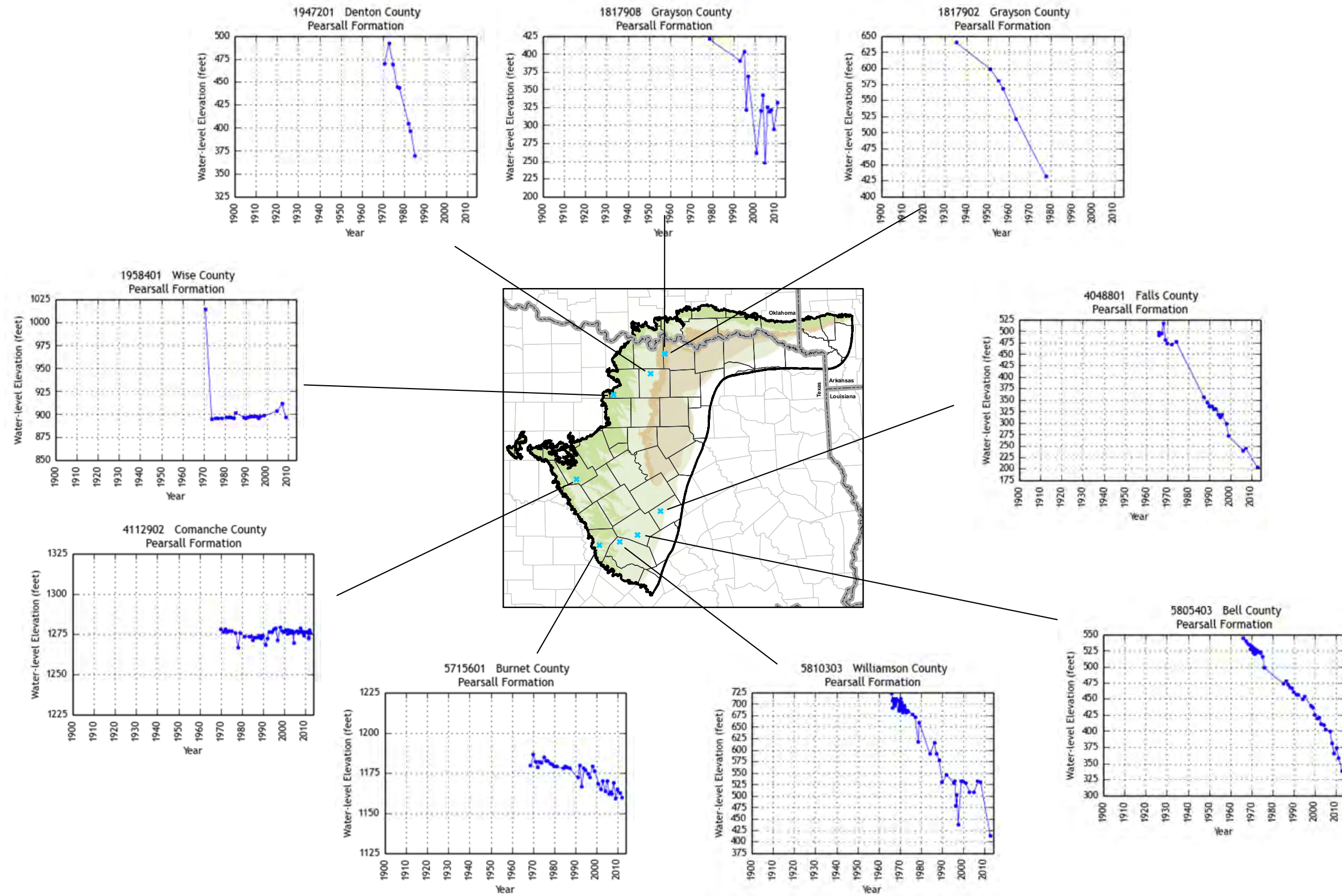
Figure 4.3.35 Select hydrographs showing water-level elevations (hydraulic heads) in feet amsl for wells completed in the Pearsall Formation.
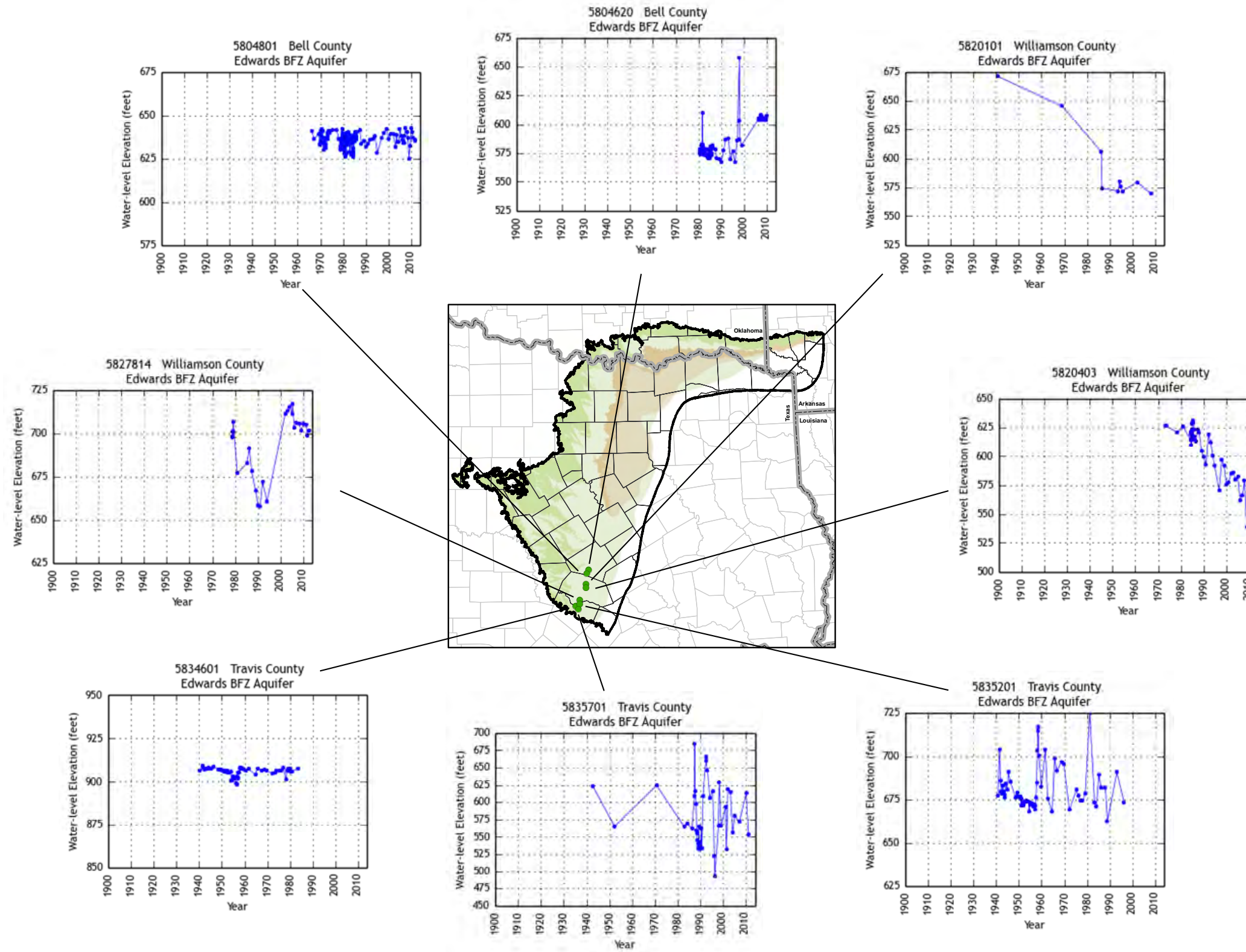
Figure 4.3.36   Select hydrographs showing water-level elevations (hydraulic heads) in feet amsl for wells completed in the Edwards BFZ Aquifer.
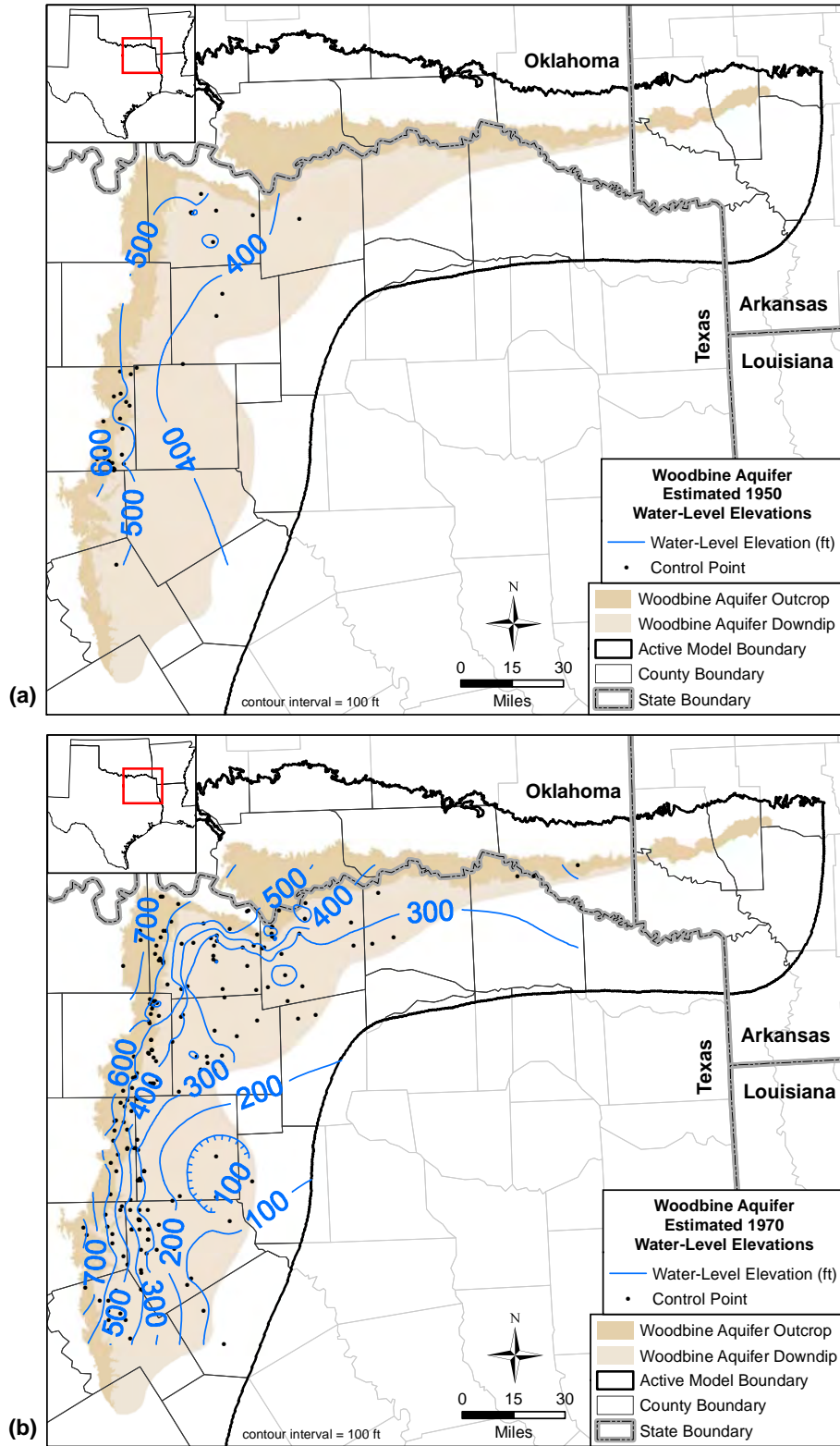
Figure 4.3.37   Estimated water-level elevation (hydraulic head) contours in feet amsl for the Woodbine Aquifer in (a) 1950 and (b) 1970.
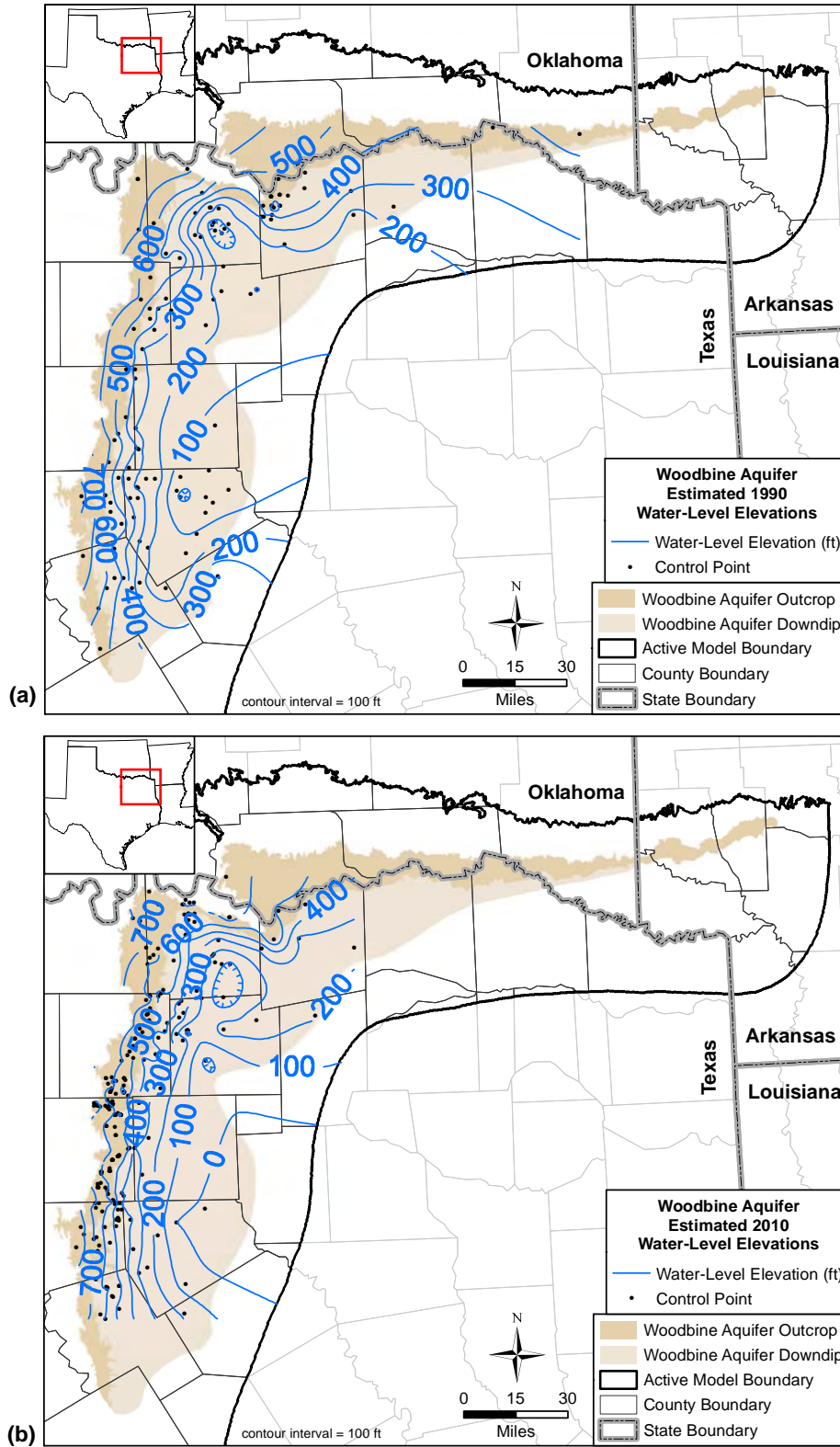
Figure 4.3.38   **Estimated water-level elevation (hydraulic head) contours in feet amsl for the Woodbine Aquifer in (a) 1990 and (b) 2010.**
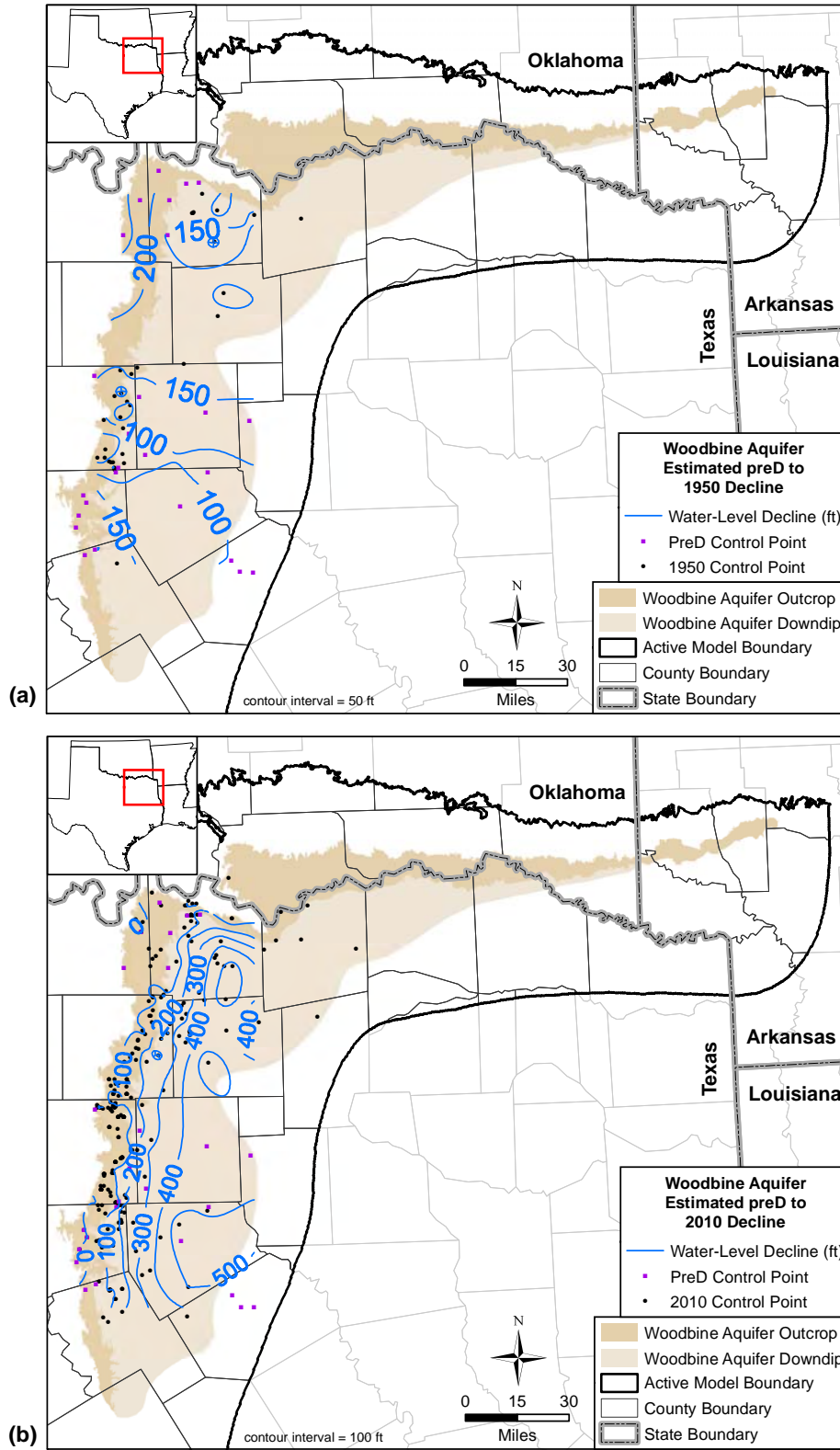
Figure 4.3.39   Estimated water-level (hydraulic head) declines in feet in the Woodbine Aquifer from (a) predevelopment to 1950 and (b) predevelopment to 2010.
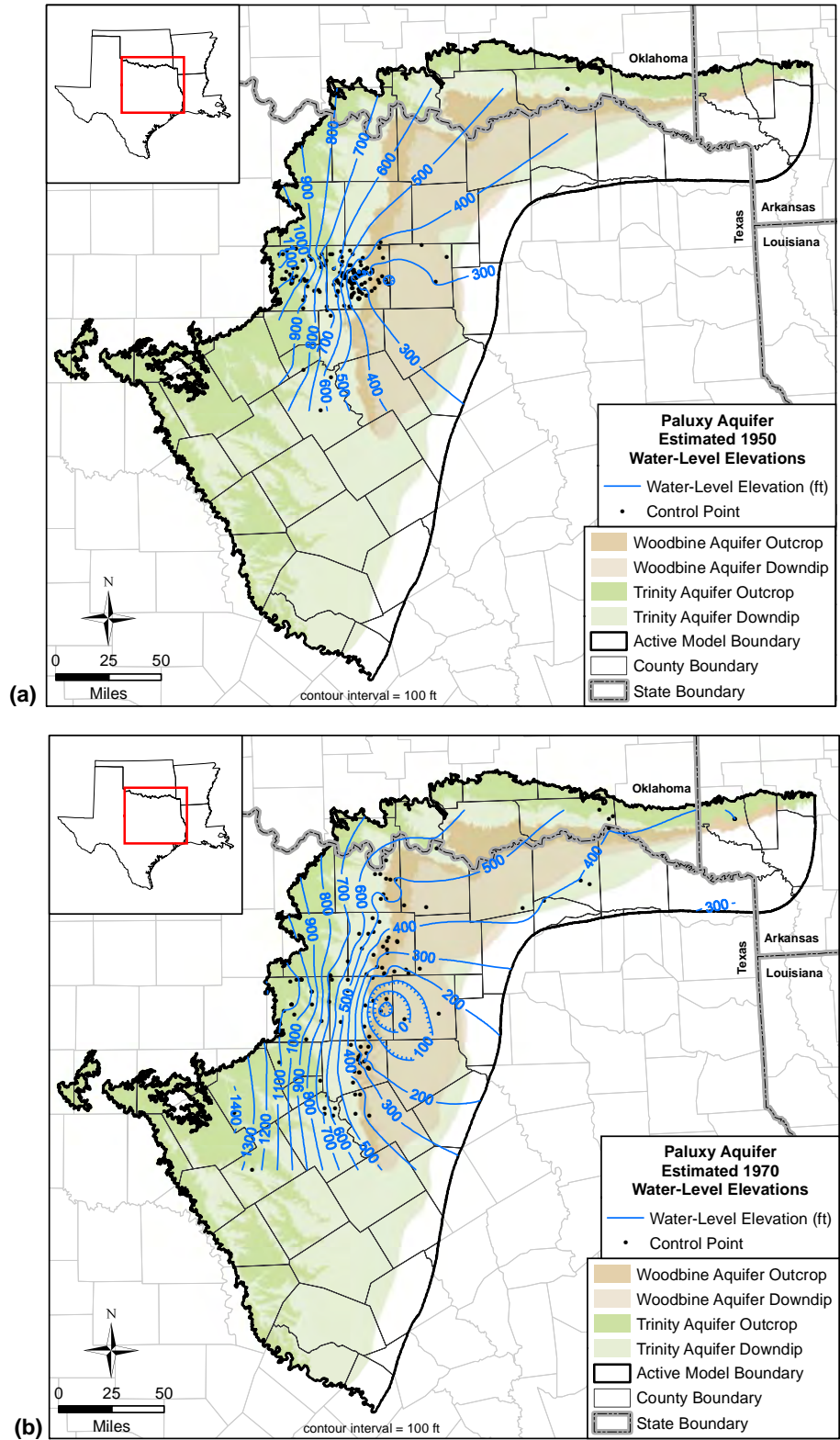
Figure 4.3.40   **Estimated water-level elevation (hydraulic head) contours in feet amsl for the Paluxy Aquifer in (a) 1950 and (b) 1970.**
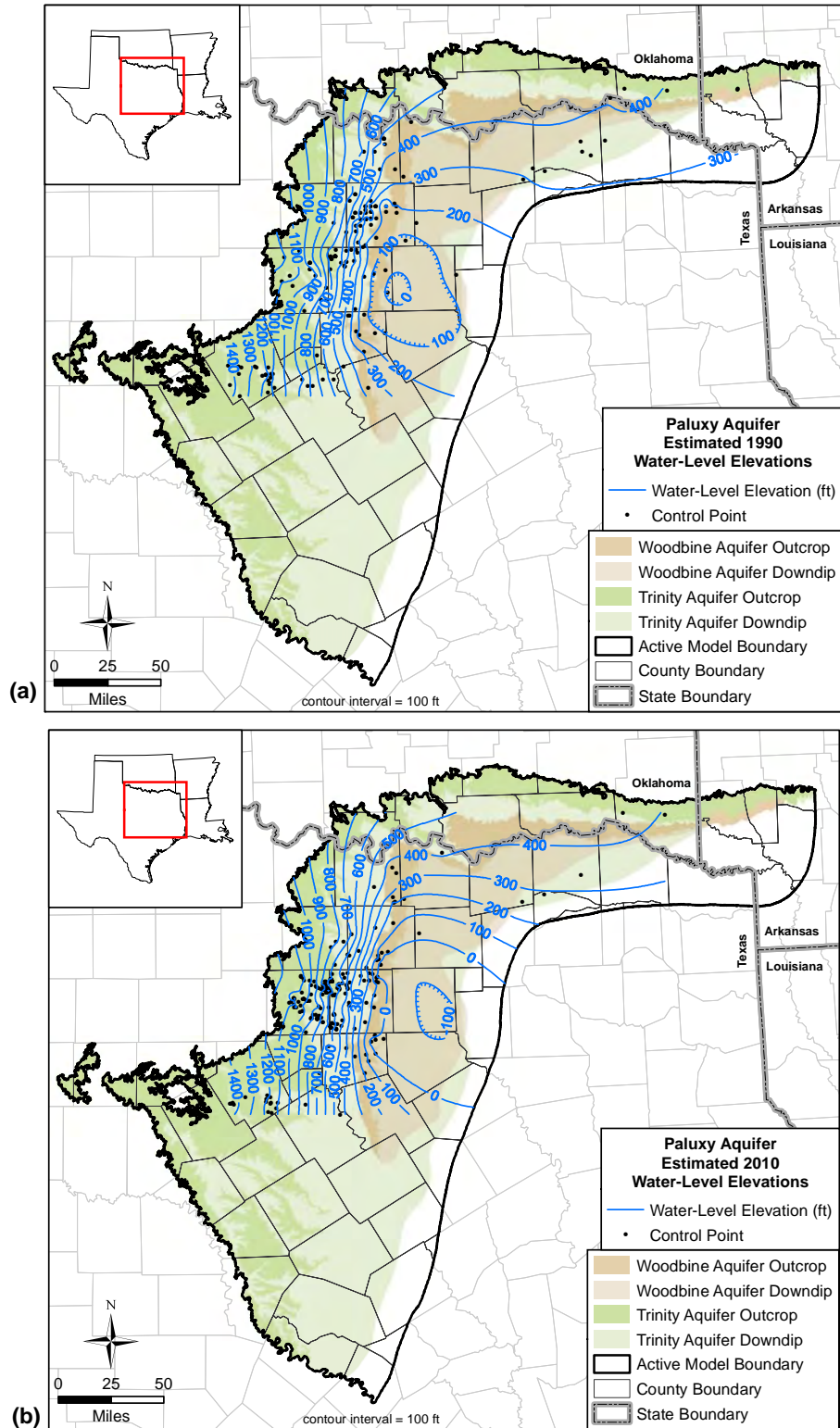
**Figure 4.3.41   Estimated water-level elevation (hydraulic head) contours in feet amsl for the
Paluxy Aquifer in (a) 1990 and (b) 2010.**
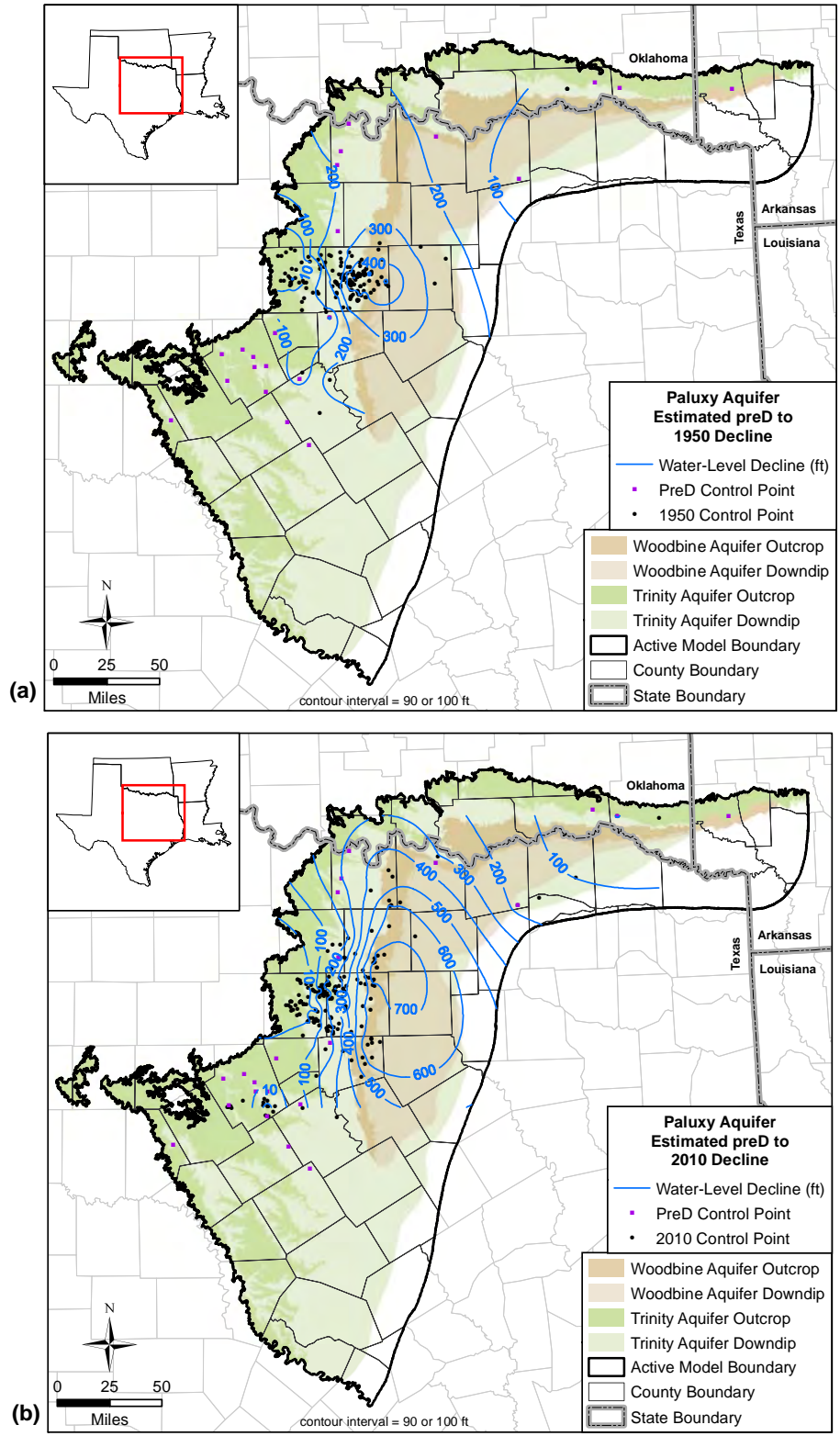
Figure 4.3.42 **Estimated water-level (hydraulic head) declines in feet in the Paluxy Aquifer from (a) predevelopment to 1950 and (b) predevelopment to 2010.**
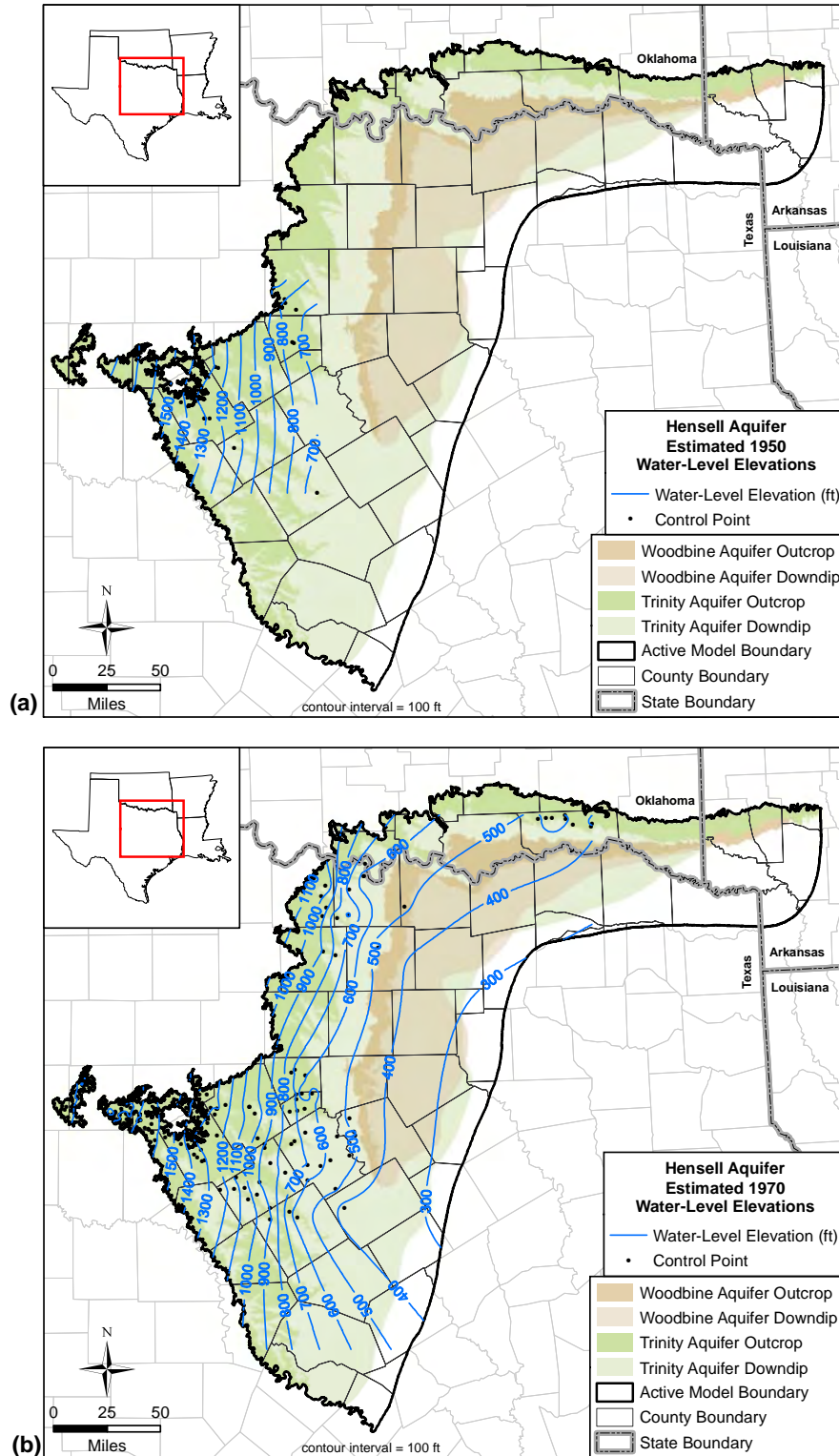
Figure 4.3.43   Estimated water-level elevation (hydraulic head) contours in feet amsl for the Hensell Aquifer in (a) 1950 and (b) 1970.
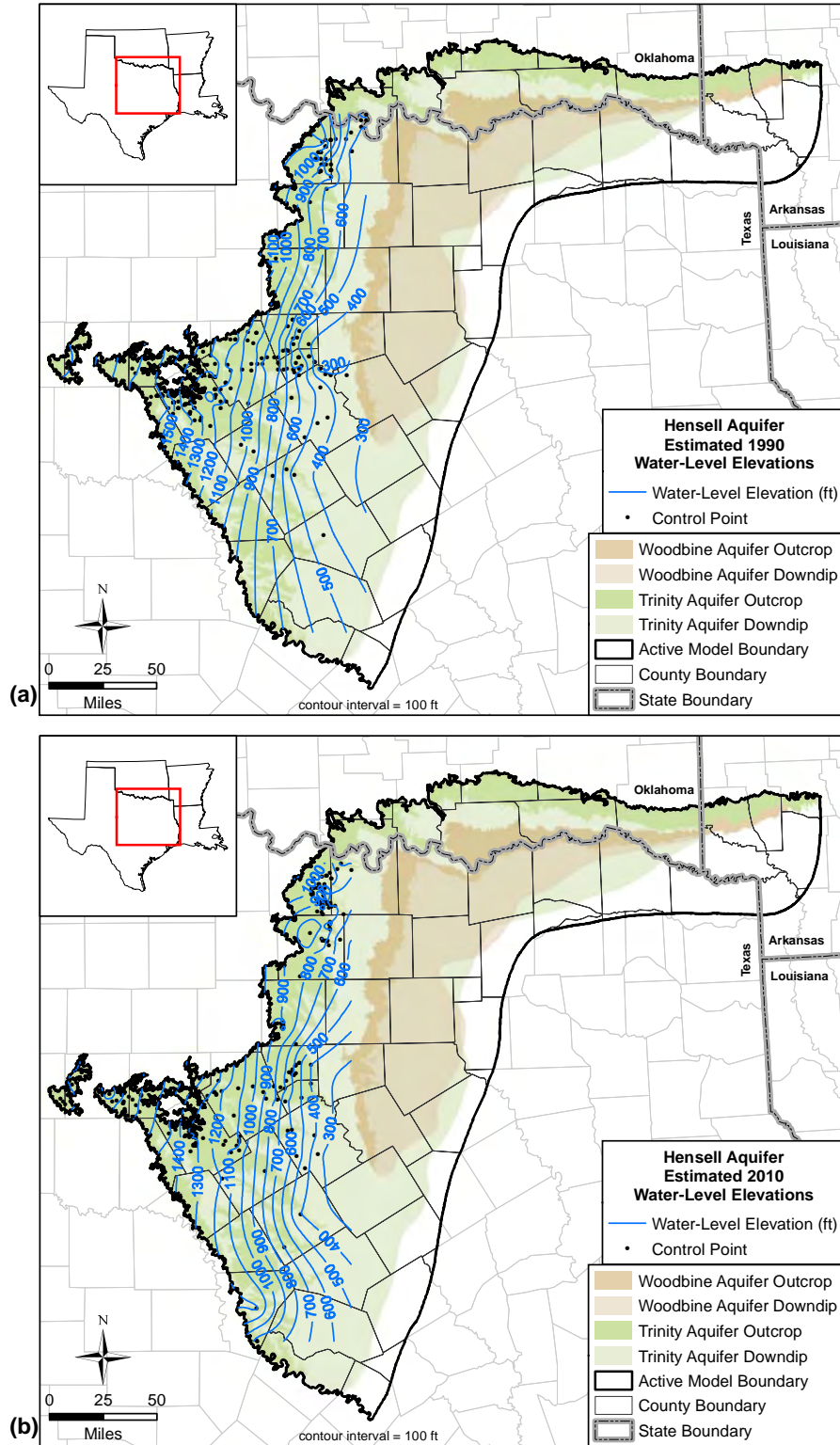
**Figure 4.3.44   Estimated water-level elevation (hydraulic head) contours in feet amsl for the
Hensell Aquifer in (a) 1990 and (b) 2010.**
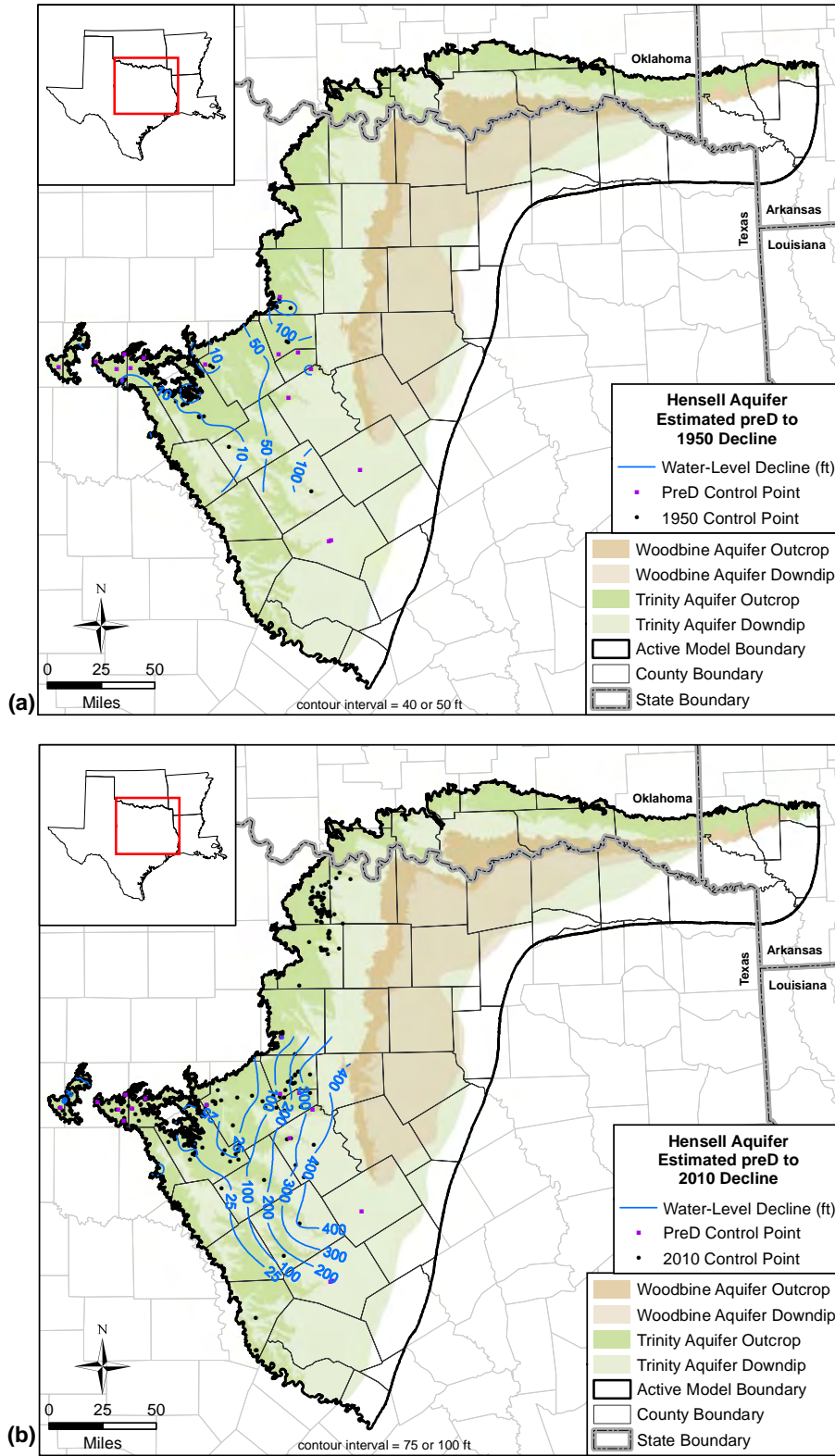
Figure 4.3.45 Estimated water-level (hydraulic head) declines in feet in the Hensell Aquifer from (a) predevelopment to 1950 and (b) predevelopment to 2010.
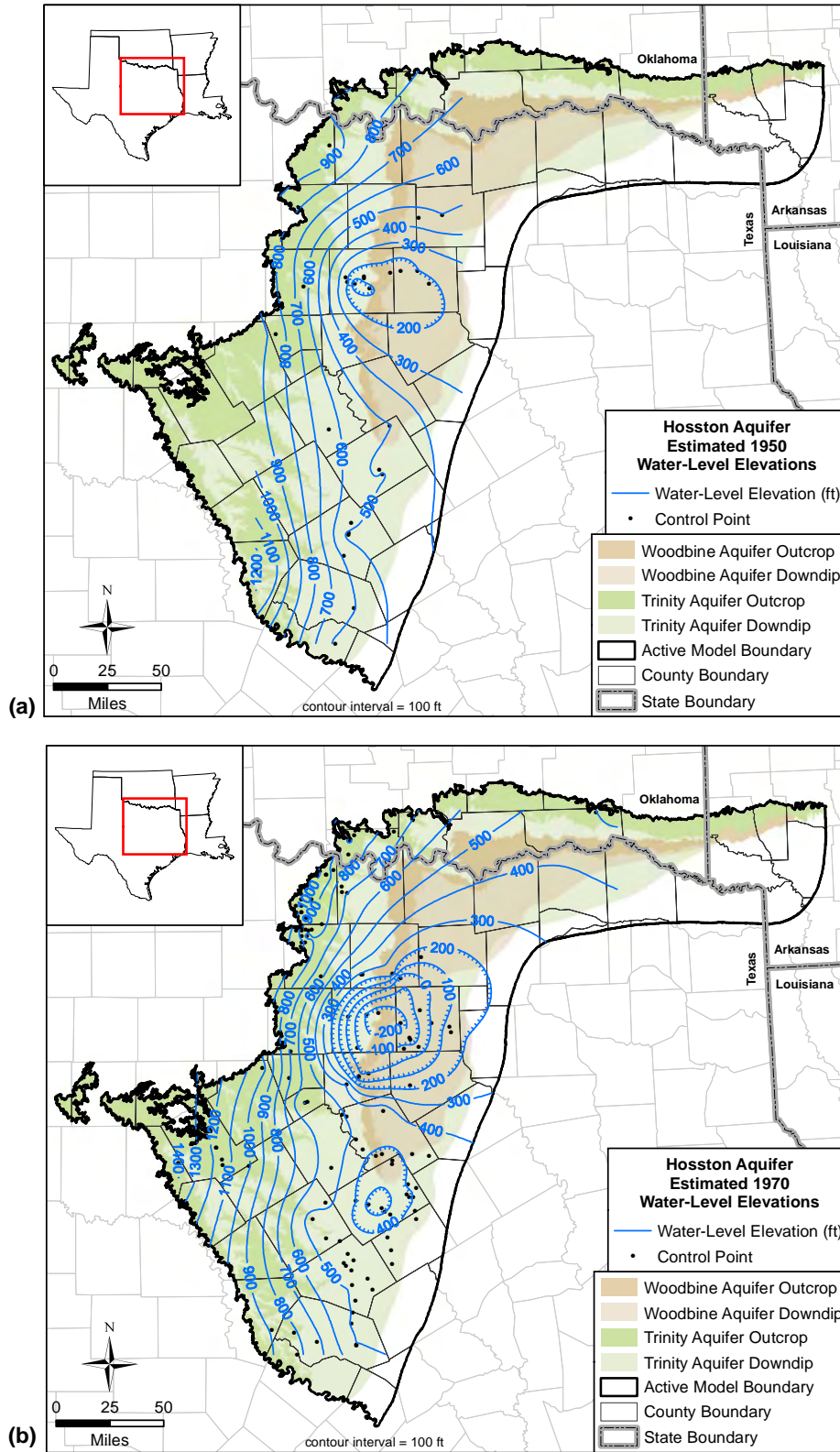
Figure 4.3.46   Estimated water-level elevation (hydraulic head) contours in feet amsl for the Hosston Aquifer in (a) 1950 and (b) 1970.
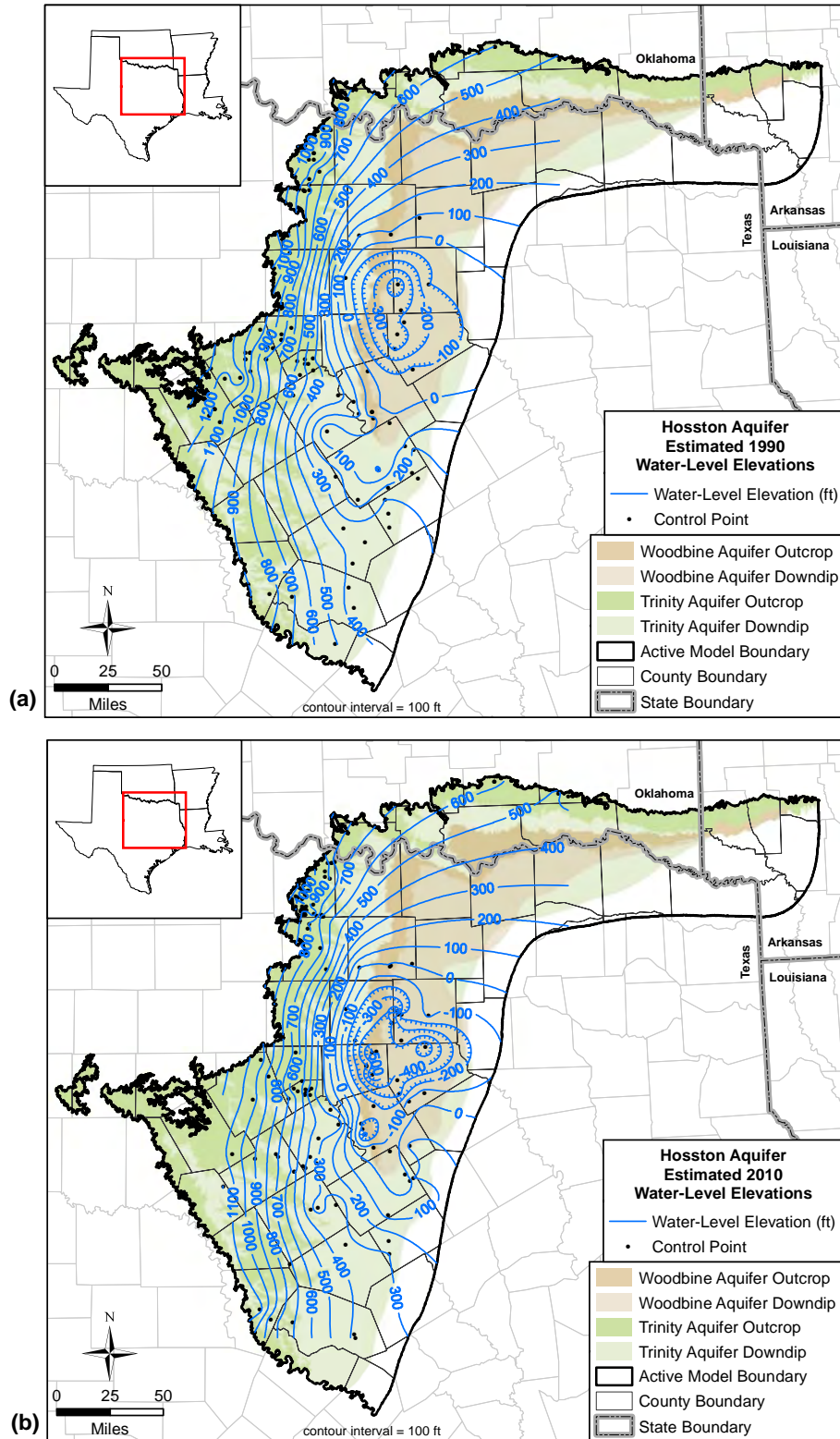
Figure 4.3.47 Estimated water-level elevation (hydraulic head) contours in feet amsl for the Hosston Aquifer in (a) 1990 and (b) 2010.
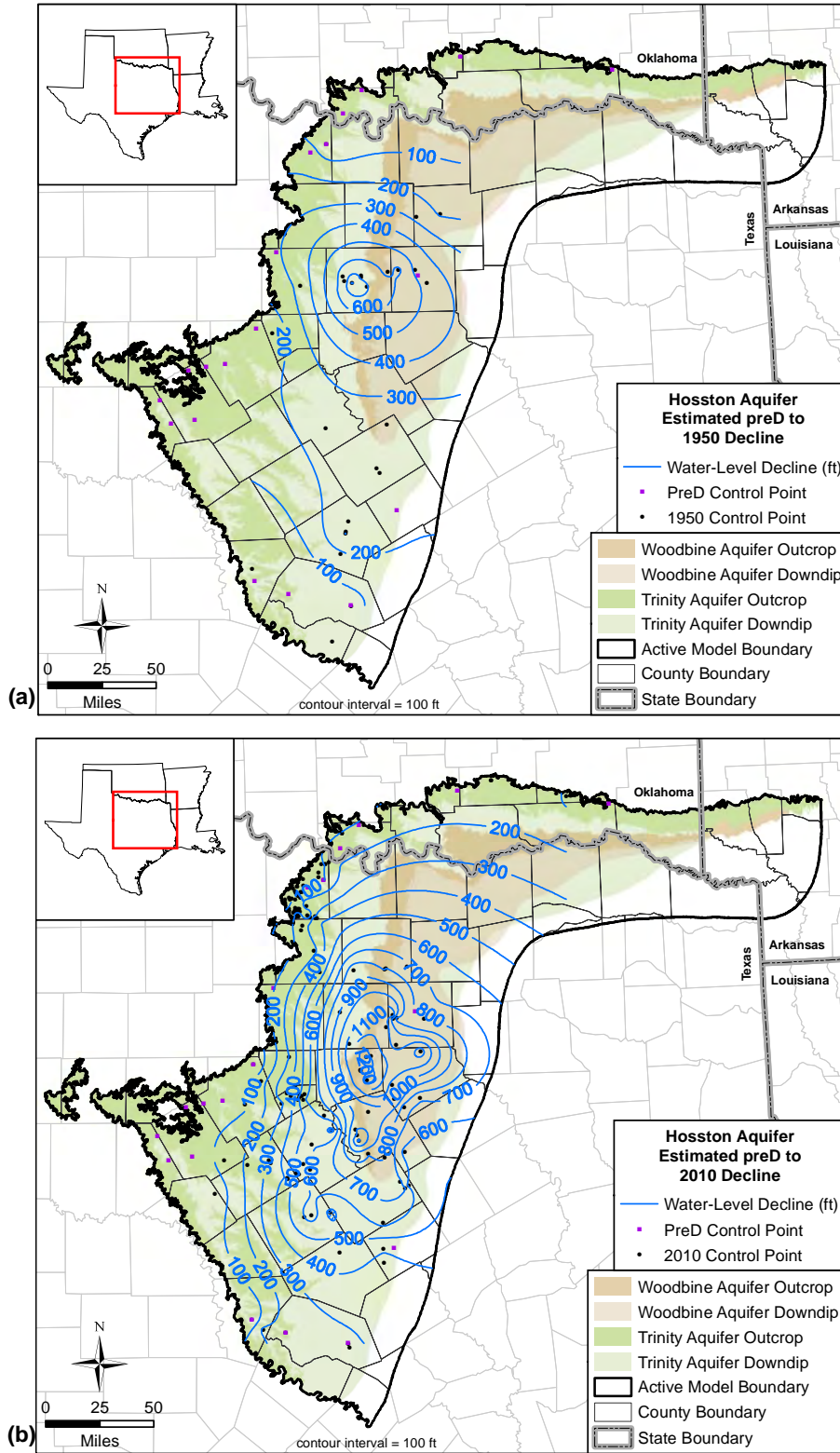
Figure 4.3.48 **Estimated water-level (hydraulic head) declines in feet in the Hosston Aquifer from (a) predevelopment to 1950 and (b) predevelopment to 2010.**
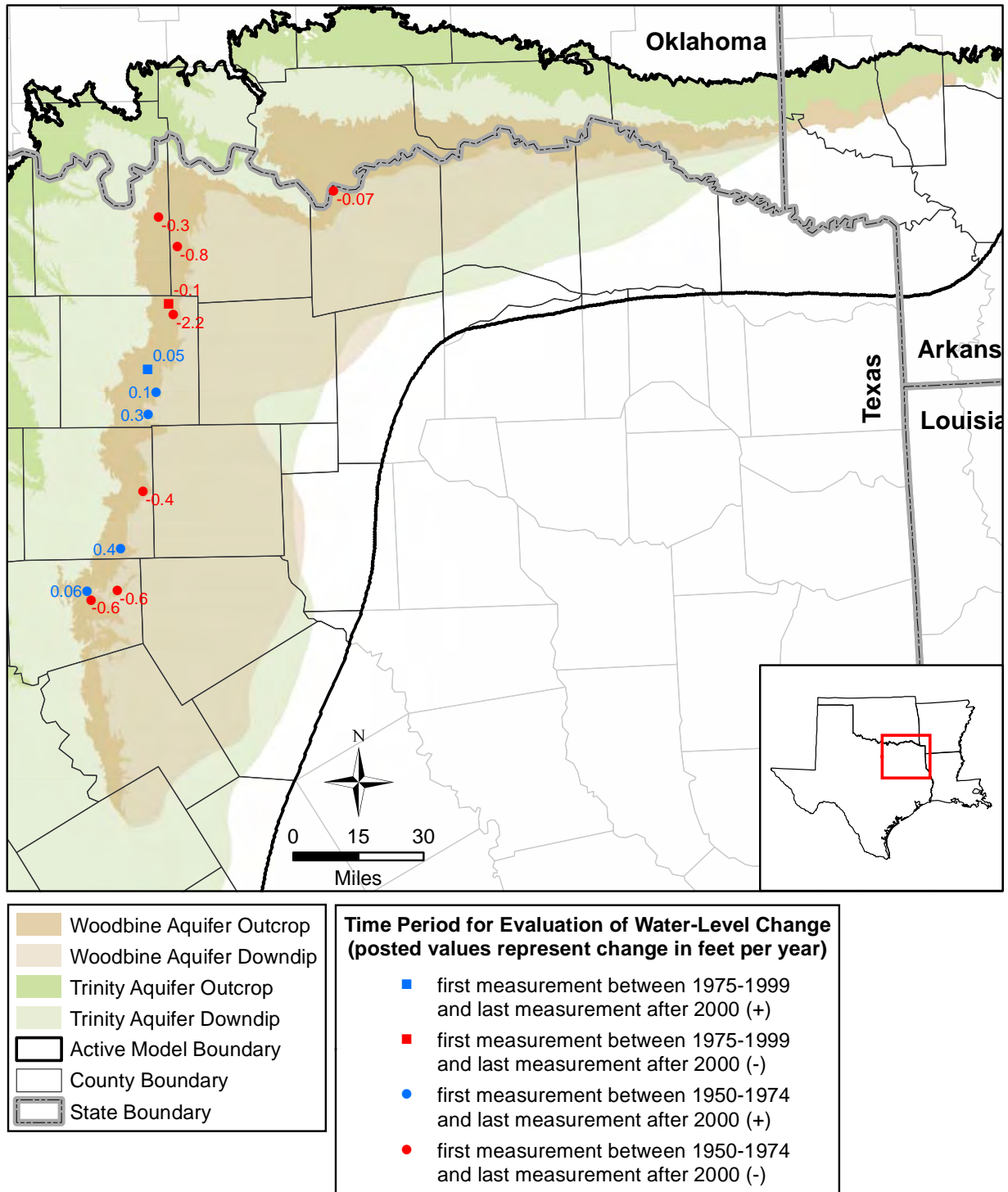
Figure 4.3.49   Results of water-level trend analysis in the Woodbine Aquifer outcrop.
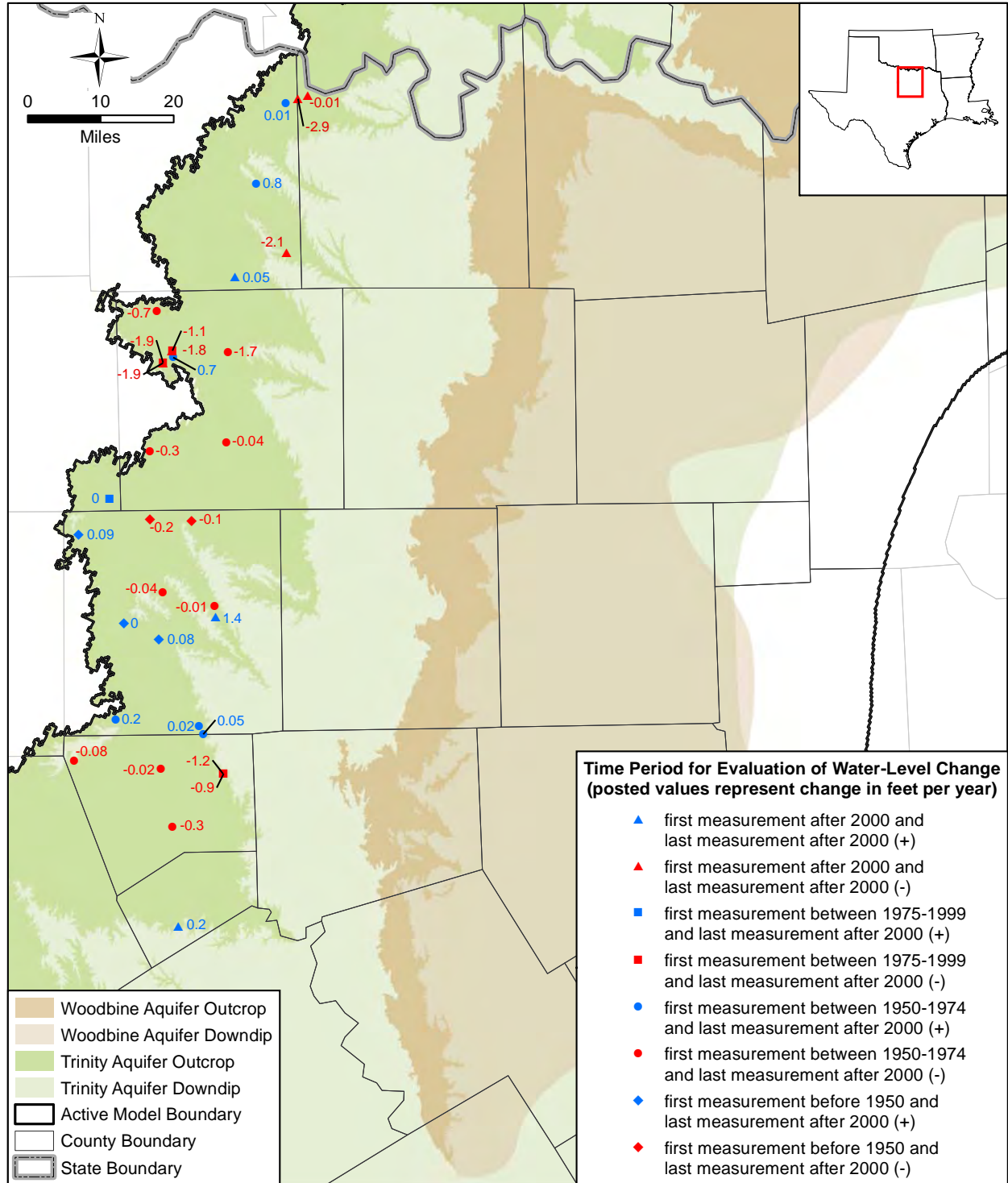
Figure 4.3.50a Results of water-level trend analysis in the northern portion of the northern Trinity Aquifer outcrop.
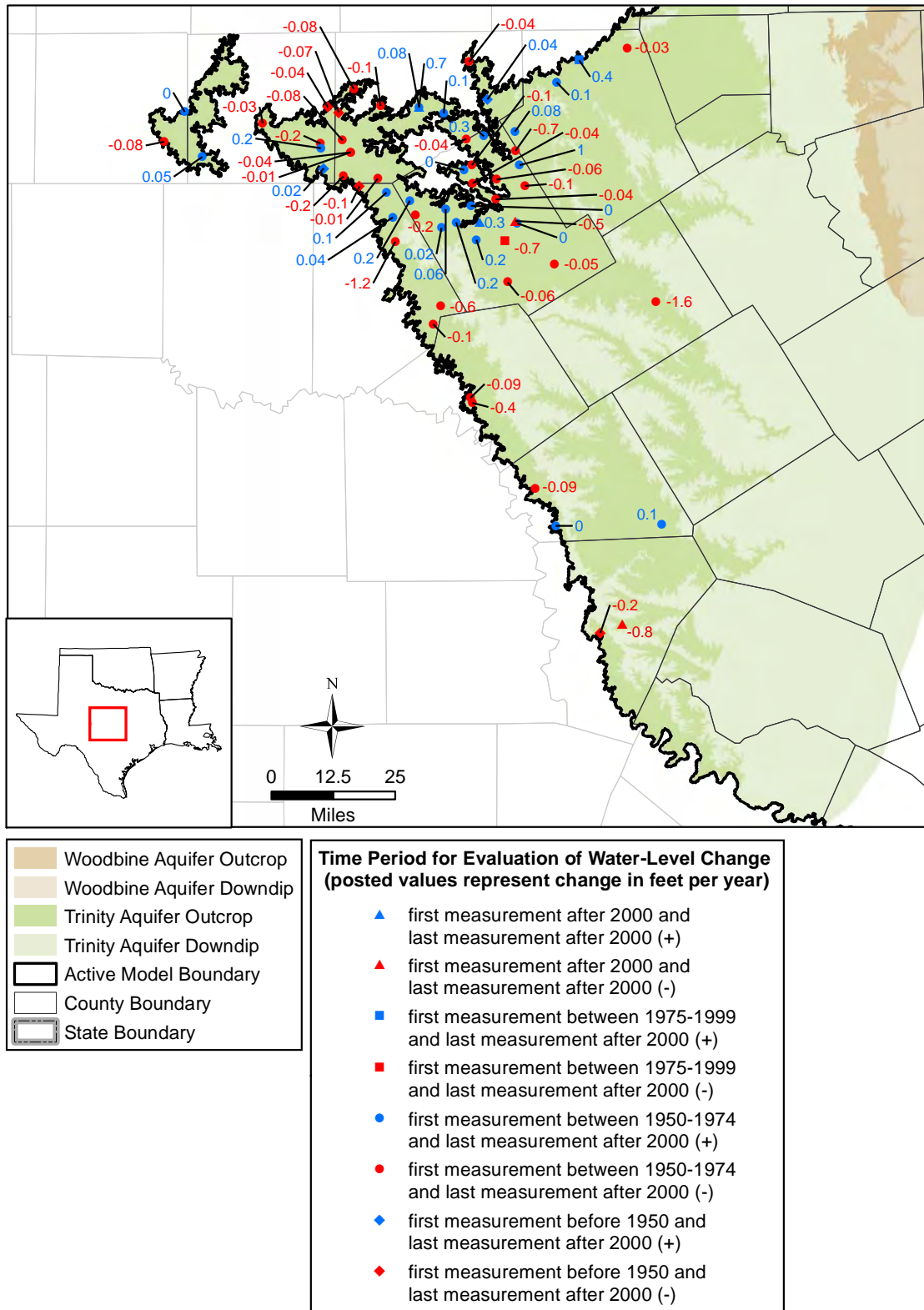
Figure 4.3.50b Results of water-level trend analysis in the western portion of the northern Trinity Aquifer outcrop.
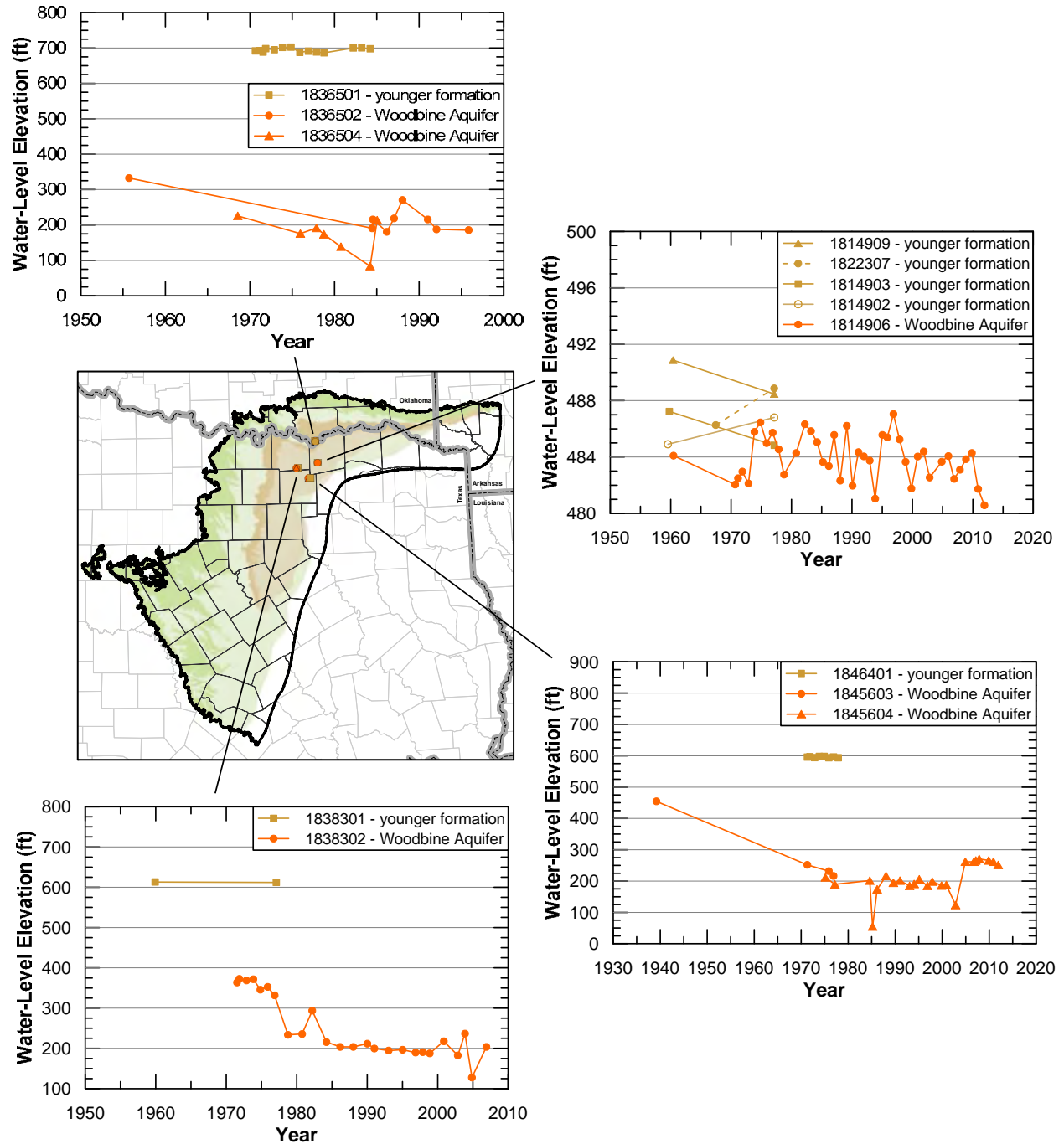
Figure 4.3.51   Comparison of water-level elevations (hydraulic heads) in feet amsl in the younger formations and the Woodbine Aquifer.
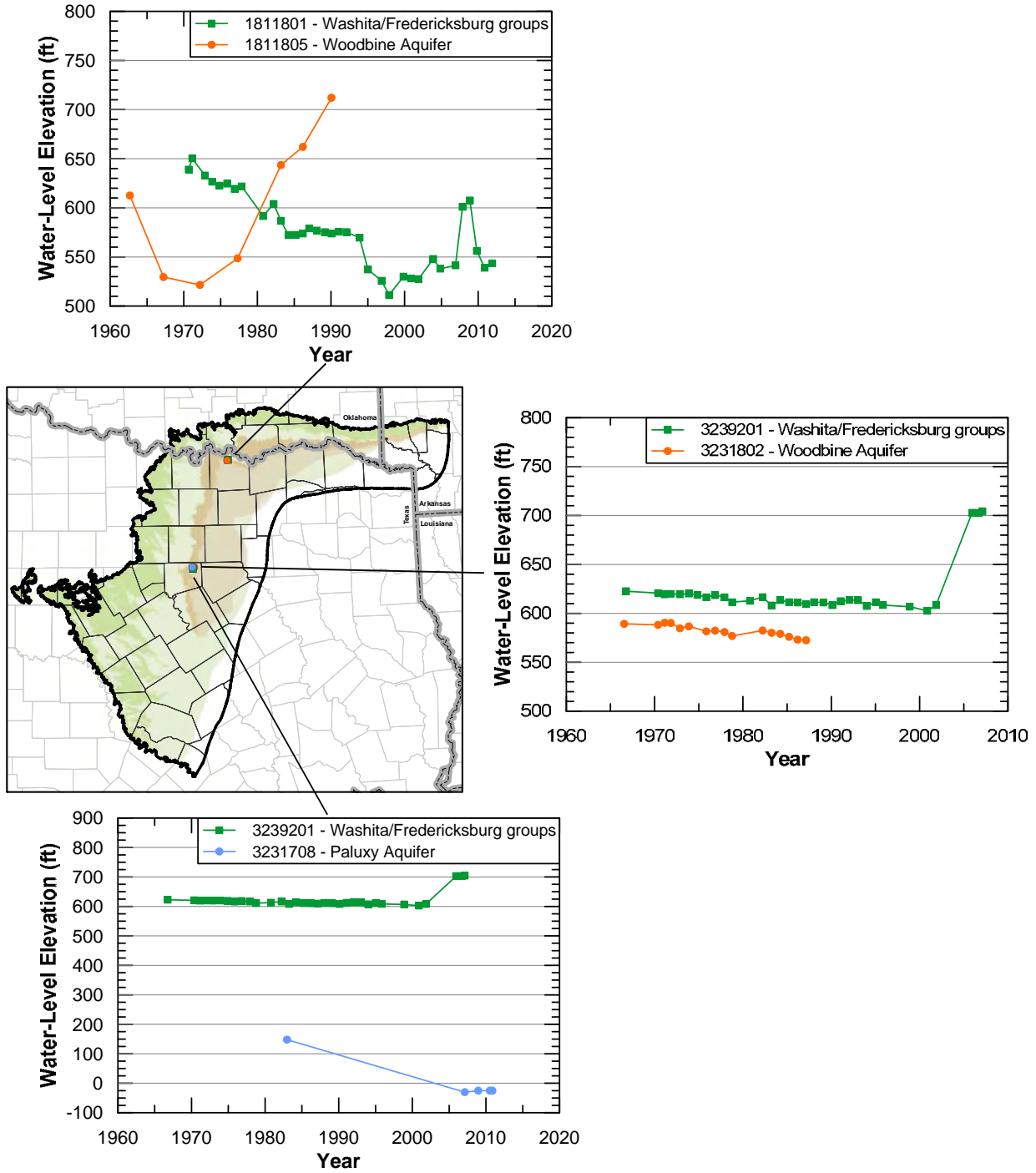
Figure 4.3.52 **Comparison of water-level elevations (hydraulic heads) in feet amsl in the Woodbine Aquifer and the Washita/Fredericksburg groups and in the Washita/Fredericksburg groups and the Paluxy Aquifer.**
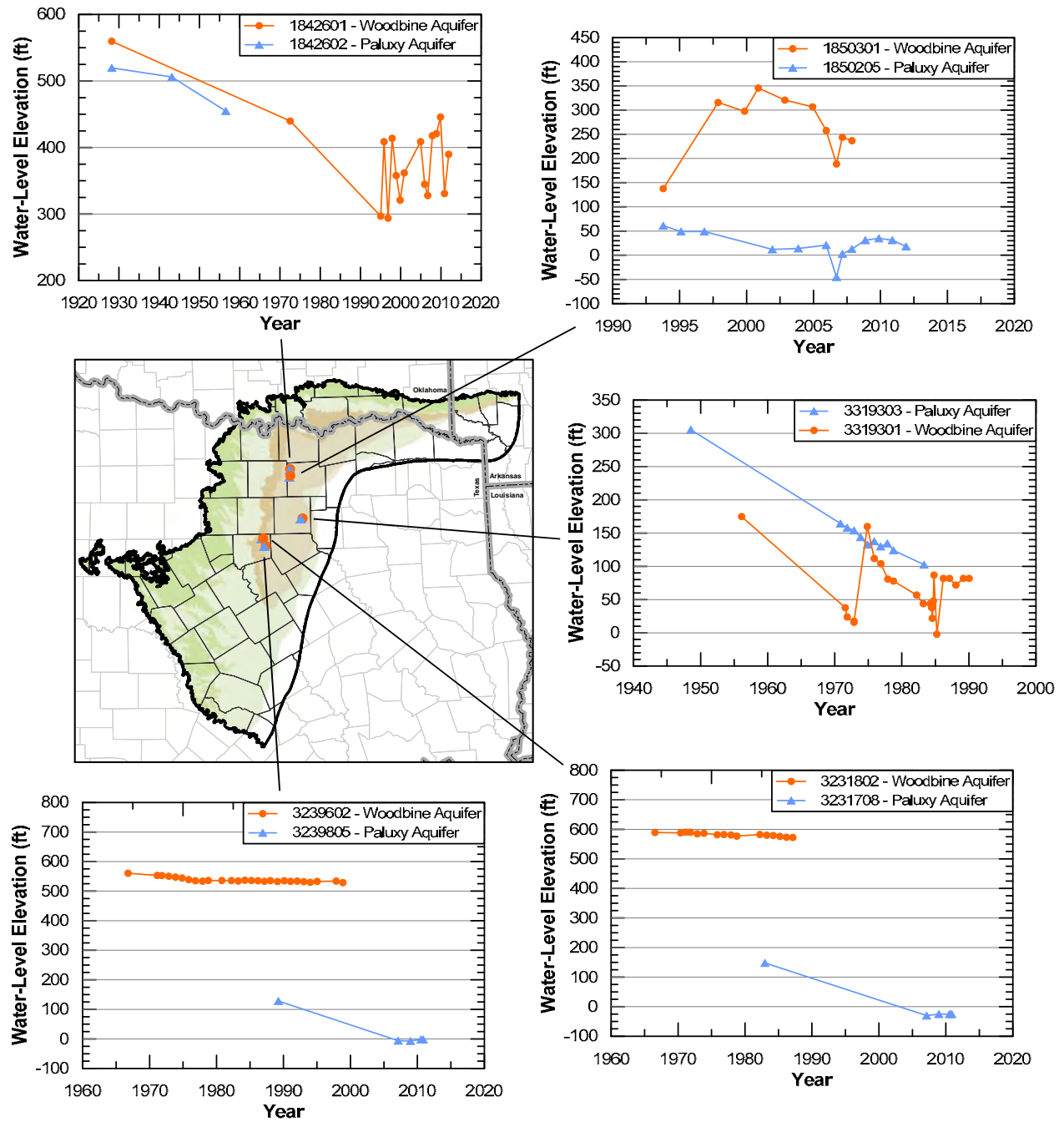
Figure 4.3.53   Comparison of water-level elevations (hydraulic heads) in feet amsl in the Woodbine and Paluxy aquifers.
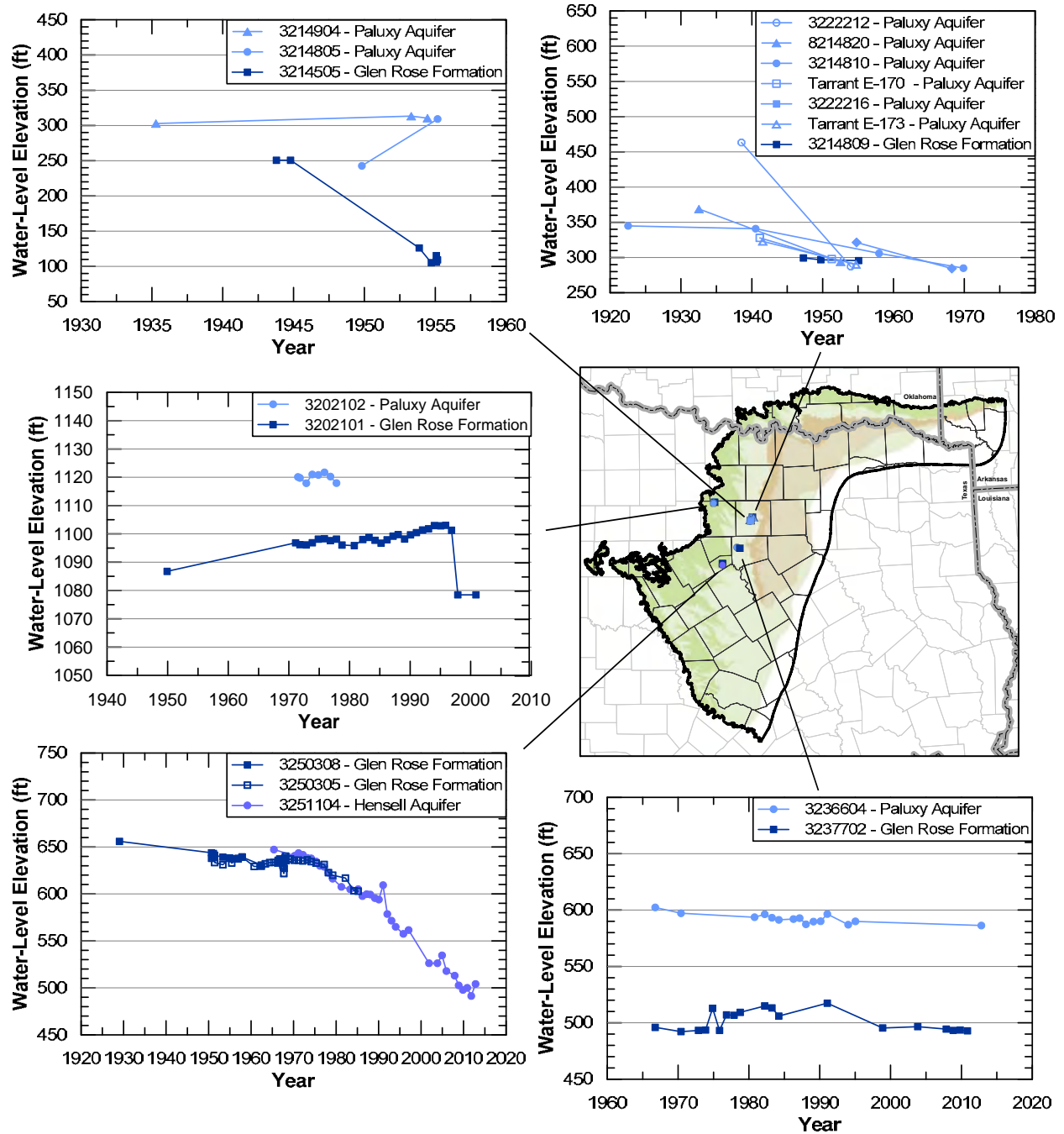
Figure 4.3.54   Comparison of water-level elevations (hydraulic heads) in feet amsl in the Paluxy Aquifer and the Glen Rose Formation and in the Glen Rose Formation and the Hensell Aquifer.
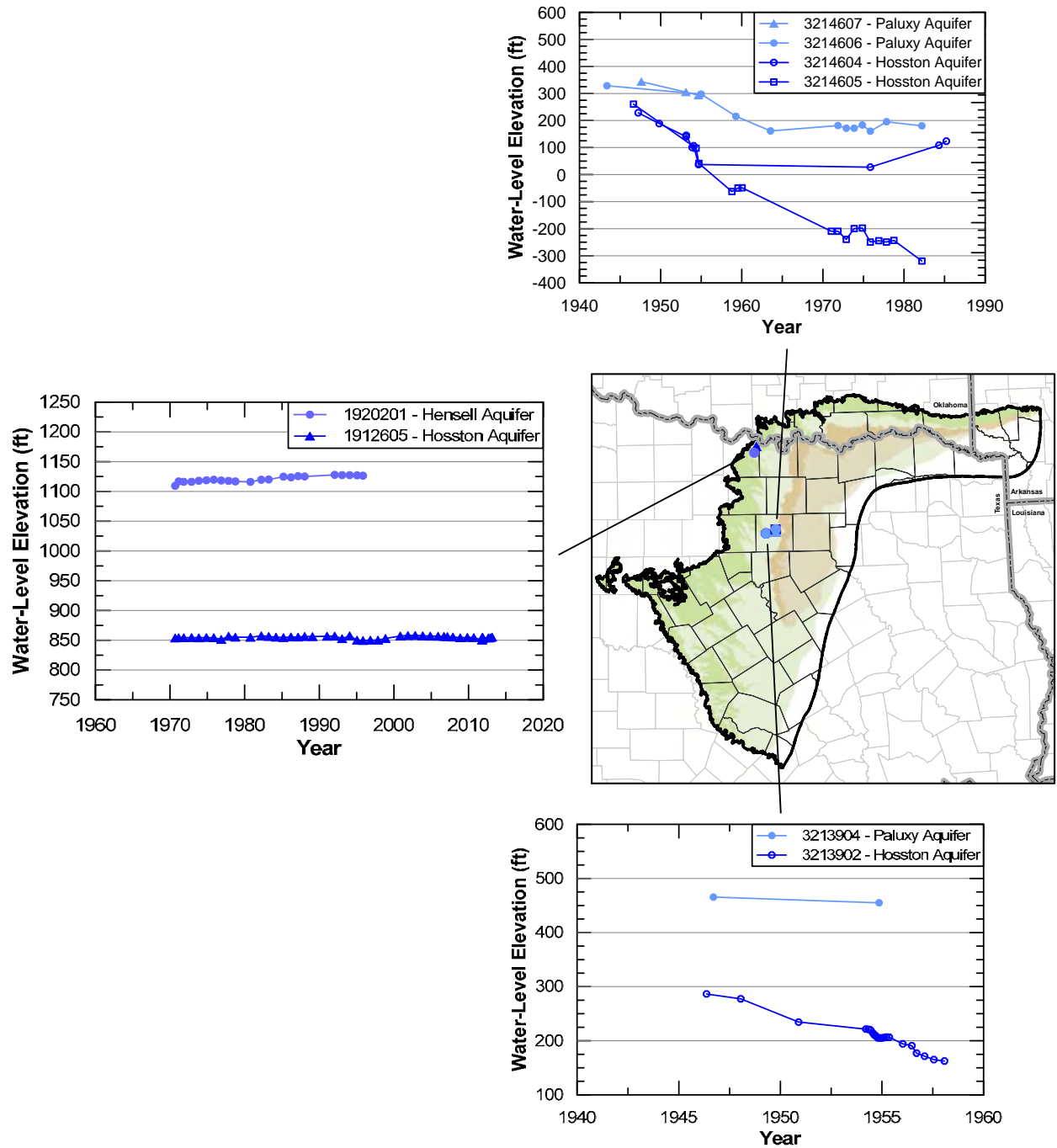
Figure 4.3.55   Comparison of water-level elevations (hydraulic heads) in feet amsl in the Paluxy and Hosston aquifers and in the Hensell and Hosston aquifers.
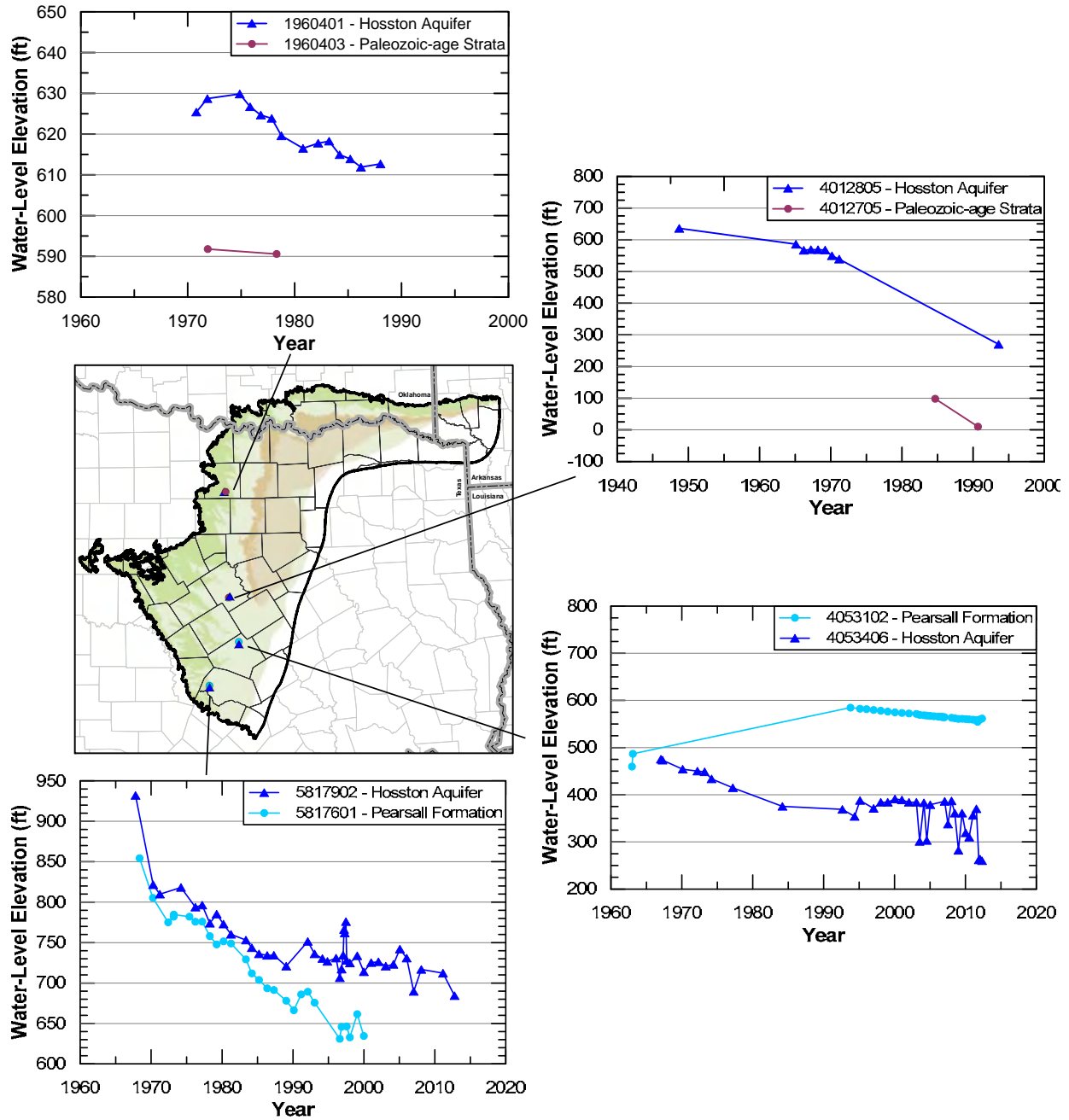
Figure 4.3.56 Comparison of water-level elevations (hydraulic heads) in feet amsl in the Hosston Aquifer and the Pearsall Formation and in the Hosston Aquifer and the Paleozoic-age strata.
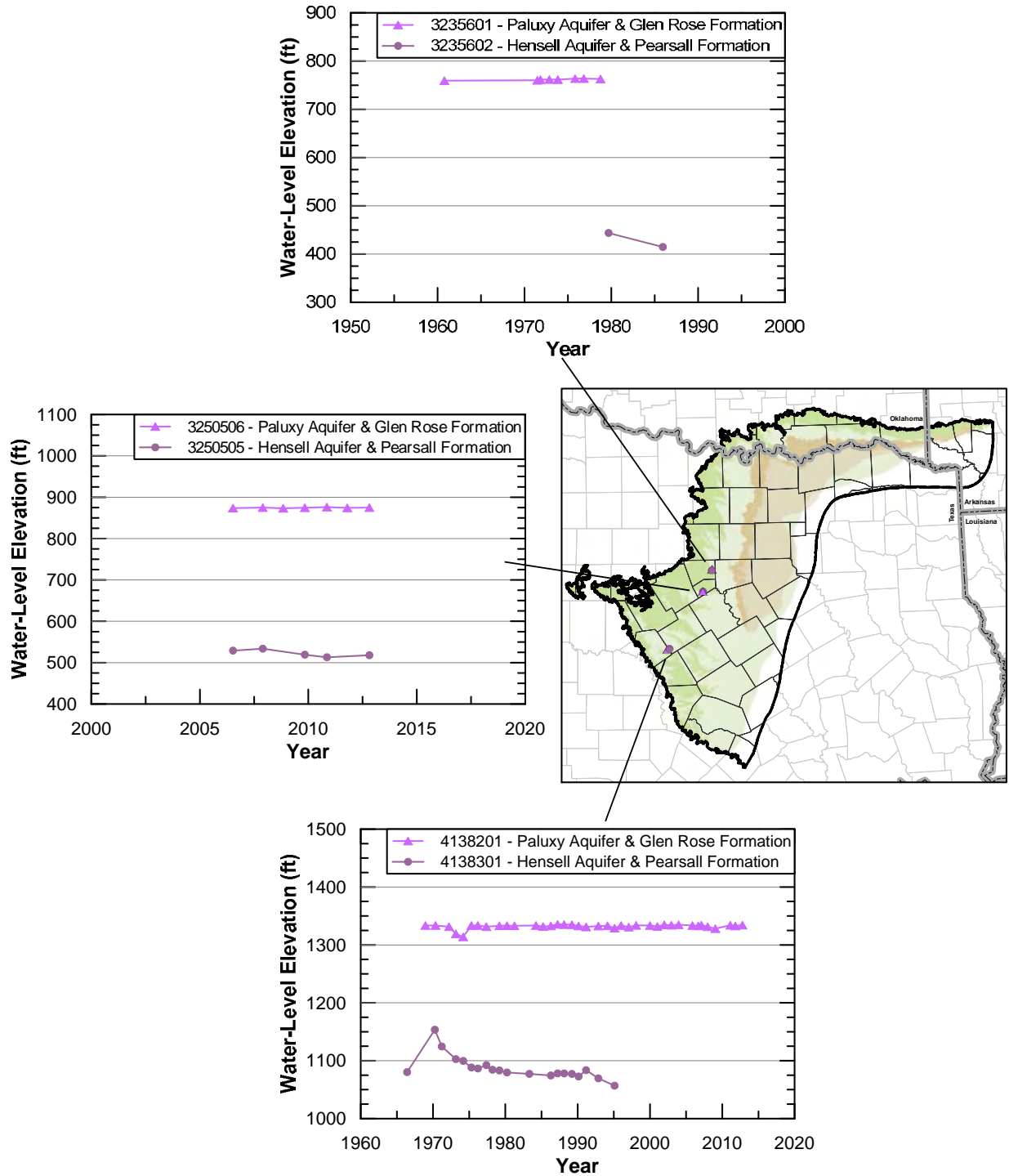
Figure 4.3.57 **Comparison of water-level elevations (hydraulic heads) in feet amsl for wells completed in both the Paluxy Aquifer and Glen Rose Formation and wells completed in both the Hensell Aquifer and Pearsall Formation.**
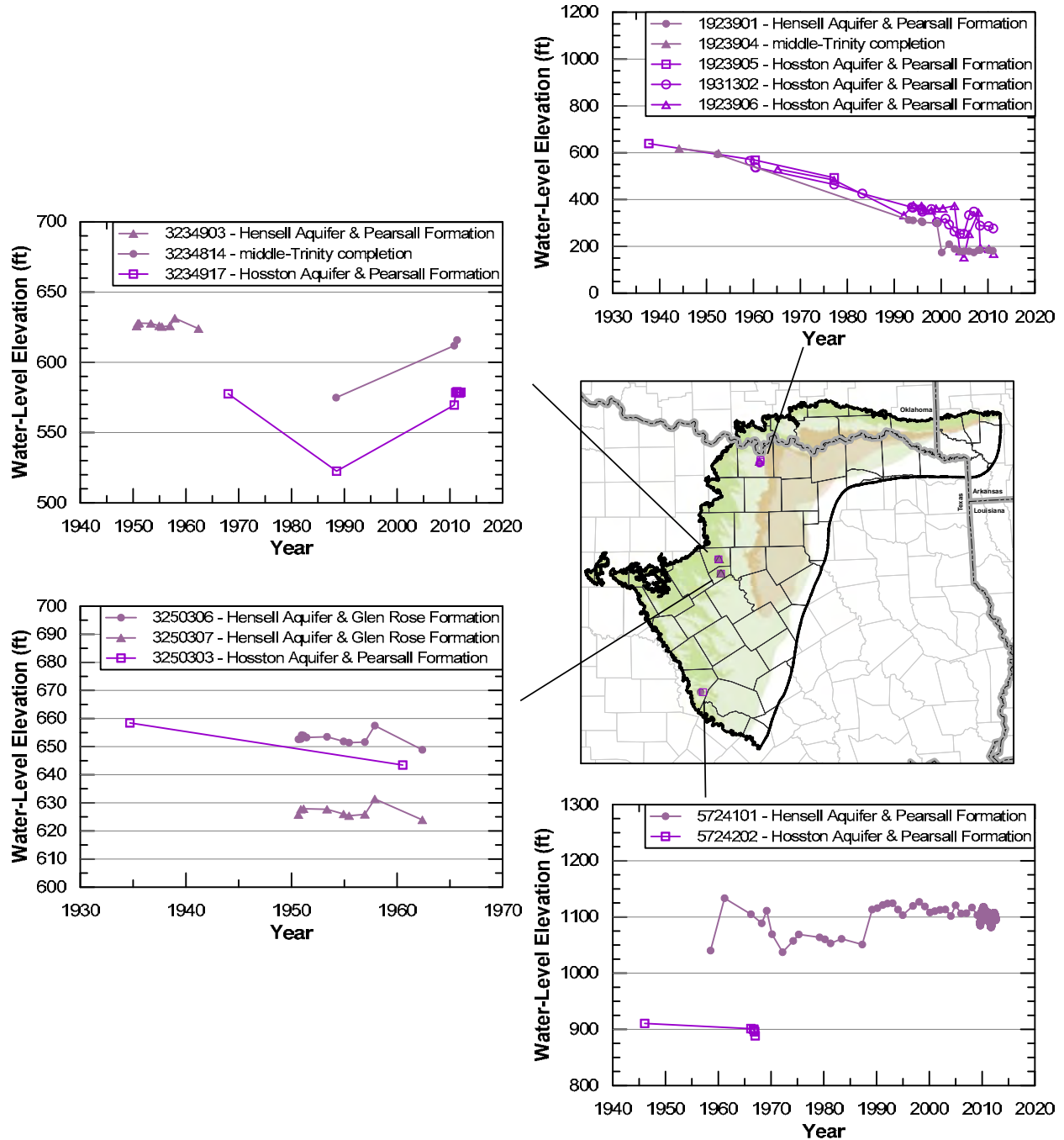
Figure 4.3.58 **Comparison of water-level elevations (hydraulic heads) in feet amsl for wells completed in both the Hensell Aquifer and Pearsall Formation or with a middle-Trinity completion and wells completed in both the Hosston Aquifer and Pearsall Formation.**

This page intentionally left blank.

4.4   Groundwater Quality

The groundwater quality of the northern Trinity and Woodbine aquifers has been studied extensively. This section does not seek to reproduce the large number of studies that have been performed for these aquifers. Rather, it provides a review of the relevant literature and presents an analysis focusing on hydrochemical facies, total dissolved solids (TDS), and chloride to attempt to better describe and understand the hydrodynamics of the aquifers.

4.4.1   Relevant Previous Work

There has been a significant body of work documenting the water quality of the northern Trinity and Woodbine aquifers starting with the early work of Hill (1901). Almost every county report in the study area (see Table 3.1.1) provides water quality data and some form of analysis. Regional studies of groundwater quality have been performed by the TWDB and predecessor agencies (Klemt and others, 1975; Nordstrom, 1982, 1987; Baker and others, 1990b; Duffin and Musick, 1991; Hopkins, 1996; Bradley, 1999; Langley, 1999; Ridgeway and Petrini, 1999; Bené and others, 2004).

Several factors affect the water quality in the northern Trinity and Woodbine aquifers. The dominant process is the natural dissolution of minerals and geochemical evolution that occurs as groundwater moves from the recharge areas in the outcrop through local and regional pathways to discharge areas. In general, groundwater becomes more mineralized as the residence time increases. The Woodbine Aquifer contains lignite beds in southern Tarrant and Johnson counties that increase the sulfate concentrations (Bradley, 1999). Another natural factor that affects water quality in the northern Trinity and Woodbine aquifers is deep-seated geologic structural features. The most important of these include the Mexia-Talco Fault System, the Balcones Fault System, the Sherman Syncline, and the Preston Anticline (Klemt and others, 1975; Hall and Turk, 1975; Ambrose, 1990; LBG-Guyton, 2003). Water quality has also been impacted by anthropological factors that include oil field brine disposal, irrigation, and septic systems (Nordstrom, 1987; Ambrose, 1990; Bradley, 1999; Reedy and others, 2011). Contamination due to pit disposal of oil field brines as well as nitrate contamination associated with agricultural and septic systems is generally isolated to the outcrop counties from Montague County in the north to Comanche and Callahan counties in the southwest. Many investigators have postulated that the poor water quality in the individual clastic aquifers within the northern Trinity Aquifer is the result of cross-

formational flow, generally from the Glen Rose Formation (Klemt and others, 1975; Rapp, 1988; Ambrose, 1990; Diehl, 2011). The northern Trinity Aquifer has many wells that are completed across multiple stratigraphic units and, as such, allow inter-formational flow. Many researchers have suggested that excessive drawdown in the northern Trinity Aquifer has caused significant cross-formational flow that has led to degradation of water quality. Ambrose (1990) attributed fingers of high TDS (sulfate rich) water in the Hosston Aquifer in the Dallas area to excessive drawdown, which caused cross-formational flow from the Glen Rose Formation.

Two recent studies looked specifically at the issue of trends in water quality. A study by Diehl (2011) focused on McLennan County. Chaudhuri and Ale (2013) conducted a more regional study of the northern Trinity and Woodbine aquifers generally coinciding with the Central Texas – Trinity Aquifer and North-Central Texas – Trinity and Woodbine aquifers Priority Groundwater Management Areas (PGMAs).

Diehl (2011) noted a large number of dual completed wells connecting the Hensell and Hosston aquifers in McLennan County. She found that the TDS increased with depth in the county, with the slope of that relationship steeper for the Hensell Aquifer than for the Hosston Aquifer. Her research noted a slight decrease in initial sulfate concentrations measured in wells drilled between 1938 and 2006, but she credited that downward trend to improved targeting of better water-quality zones and better completion methods. She documented an upward trend (with a great deal of scatter) in sulfate concentrations in four Hensell Aquifer wells that had measurements from the early 1950s through the mid-2000s. Another important conclusion of her work was that water levels were declining in the Hensell and Hosston aquifers at a rate of over 10 feet per year in McLennan County.

Chaudhuri and Ale (2013) characterize changes in groundwater levels and groundwater quality from 1960 to 2010 in an 18-county area using statistical and graphical methods. Their study combined groundwater samples from the Trinity Aquifer across the vertical extent of the aquifer, which could obfuscate trends in both water levels and water quality. However, they make a compelling case that groundwater levels in the 18 counties continually declined from 1960 through 2010. They also make the statistical case that water quality improved through time in the aquifers, which is conceivable in the outcrop area since disposal of drilling brine has been better regulated since the 1960s. Their conclusions may be impacted by the sample size, which

is not included in the study. Groundwater sampling performed by the state peaked in the 1960s, when approximately 2,500 samples were collected and analyzed in a given year, declining to less than 500 by 2010. The study by Chaudhuri and Ale (2013) delineated two clusters of counties based upon water-level and water quality trends separating the outcrop counties from the downdip counties.

4.4.2 Regional-scale Flow Observations Inferred from Geochemistry Data

Groundwater is subject to multiple geochemical processes (see Figure 4.4.1) as soon as rainwater infiltrates the land surface and moves as groundwater from a recharge area to a discharge area. As a result of being modified by geochemical processes, the groundwater chemical signature evolves along a groundwater flow path. Changes in the chemical signature are often similar to those observed by Chebotarev (1955). Chebotarev (1955) reviewed more than 10,000 chemical measurements from water wells in Australia and concluded that groundwater tends to evolve chemically toward the composition of seawater and that this evolution typically includes the following regional changes in dominant anion species:

Travel along flow path: --►

$$HCO_3^- \rightarrow HCO_3^- + SO_4^{2-} \rightarrow SO_4^{2-} + \ HCO_3^- \rightarrow SO_4^{2-} + \ Cl^- \rightarrow Cl^- + SO_4^{2-} \rightarrow Cl^-$$

Increasing Age: --►
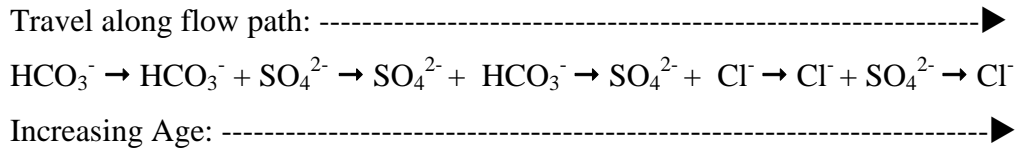
where HCO_3^- is bicarbonate, SO_4^{2-} is sulfate, and Cl^- is chloride

For a large sedimentary basin, the anion-evolution sequence described by Chebotarev (1955) can be described by three main zones, which correlate in a general way with depth (Domenico, 1972; Freeze and Cherry, 1979).

1. The upper zone – characterized by active groundwater flushing through relatively well-leached rocks. Water in this zone has bicarbonate as the dominant anion and is low in TDS.

2. The intermediate zone – with less active groundwater circulating and higher TDS. Sulfate is normally the dominant anion in this zone.

3. The lower zone – with very sluggish groundwater flow. Highly soluble minerals are commonly present in this zone because very little groundwater flushing has occurred. High chloride concentrations and high TDS are characteristic of this zone.

For large aquifer systems, Chebotarev (1955) suggests that salinity should generally increase with (1) depth, (2) distance from the recharge area, (3) nearness to the sea (where applicable), and (4) duration of contact with aquifer minerals, which can also be referred to as residence time as measured from time of recharge. Ophori and Toth (1989) and Back (1966) are among the notable studies that document the anion-evolution sequence of Chebotarev (1955). Ophori and Toth (1989) show that the spatial distribution of ions in the Ross Creek Basin in Alberta, Canada show good correlation with basin flow regimes. In that study, low TDS, high calcium to magnesium ratios, low sulfate, and high bicarbonate coincide and occur in recharge areas. Whereas, high TDS, low calcium to magnesium ratios, high sulfate, and low bicarbonate mark the discharge areas. Similarly, in his study of groundwater flow patterns in the northern Atlantic Coastal Plain, Back (1966) identified highest concentrations of calcium and magnesium in the recharge areas underlained by calcareous clays and highest sodium concentrations in discharge areas, the latter a result of ion exchange and salt-water intrusion. As a result of his findings, Back (1966) proposed the concept of hydrochemical facies as a means for detection of regional relations between the chemical character of groundwater, lithology, and regional flow patterns.

4.4.3 Hydrogeochemical Facies

Freeze and Cherry (1979) define hydrogeochemical facies as distinct zones that have cation and anion concentrations describable within defined composition categories. The nomenclature for hydrogeochemical facies can vary among studies. As a general rule, the name of a hydrogeochemical facies includes the name of the major cations and/or the name of the major anions. Example hydrogeochemical facies names are sodium-chloride facies, calcium-bicarbonate-chloride facies, and calcium-magnesium facies.

To develop hydrochemical facies for this study, the concentrations of the major ions were expressed into terms of equivalents, which is a unit of charge. In order to convert the distribution of the ions into a suitable form for evaluating charge balances, the mass of each chemical, which is expressed as milligrams per liter, is converted to a charge concentration, which is expressed as milliequivalents per liter. This conversion is performed by dividing the mass of the chemical by its equivalent weight, which is calculated by dividing the chemical's atomic weight by its valence. For instance, calcium has an atomic weight of 40.08 milliequivalents per milligram, and a valence of 2^+, so it has an equivalent weight of

20.04 milligrams per milliequivalents. Thus, a calcium concentration of 100 milligrams per liter is equivalent to about 5 milliequivalents per liter.

The hydrogeochemical facies the Woodbine Aquifer, Washita/Fredericksburg groups, Paluxy Aquifer, Glen Rose, Formation, Hensell Aquifer, Pearsall Formation, and Hosston Aquifer are shown in Figures 4.4.2 through 4.4.8, respectively, using color coded circles. The quadrants on the left side of the circle represent the major cation(s) and the quadrants on the right side of the circle represent the major anions. If an ion represents 66 percent or more of the total amount of positive or negative charge equivalents in solution, then the ion occupies half of the circle. If an ion represents 35 percent or more, but less than 66 percent, of the total amount of positive or negative equivalents in solution, then the ion occupies a single quadrant of the circle. The chemical data used to generate the hydrochemical facies was obtained from the TWDB groundwater database (TWDB, 2013a). Wells were assigned to the aquifer or formation in which its well screen terminated. Table 4.4.1 lists the number of calculated hydrogeochemical facies, the number of TDS measurements and the number of chloride measurements for each aquifer/formation.

The spatial sequence of hydrogeochemical facies in Figures 4.4.2 through 4.4.8 is consistent with the findings of Chebotarev (1955). As suggested by Chebotarev (1955) and others (Ophori and Toth, 1989; Back, 1966), the occurrence of magnesium and calcite facies can be indicators for recharge areas. The mapping of recharge areas based on magnesium and calcium facies is based on the ability of carbon dioxide to act as a weak acid in groundwater and cause the weathering of minerals, which in turns changes the chemistry of the groundwater. After precipitation infiltrates the soil, the carbon dioxide concentration of the infiltrating rainwater increases as a result of carbon dioxide produced by plant respiration and microbiological degradation of soil organic matter. Because of plant respiration and microbial activity, the carbon dioxide partial pressure in the soil unsaturated zone is usually much higher than that of the earth's atmosphere. In soil, a carbon partial pressure in the range of 10^{-3} to 10^{-2} bars is typical (Freeze and Cherry, 1979), whereas in the atmosphere, the carbon dioxide partial pressure is 3×10^{-4} bars.

Two common reactions that occur with carbon dioxide are the dissolution of calcite and dolomite to form calcium and magnesium, and the weathering of silicate minerals to form clays. For a carbon partial pressure between 10^{-3} to 10^{-2} bars, calcite and dolomite readily dissolve and

produce calcium and magnesium ions in the range of 100 to 600 milligrams per liter. However, once the groundwater has migrated beyond the zone where carbon dioxide is being added to the groundwater system, the dissolution of calcite and/or magnesium is slowed and calcium and magnesium ions are gradually removed from the groundwater for two reasons. One reason is that, with depth, the groundwater temperature increases as a result of the geothermal gradient (increased temperatures with depth) so that the solubility of carbon dioxide is decreased. Another reason is that ion exchange reactions cause calcium and magnesium ions to replace sodium ions on clay surfaces, which adds sodium to the solution and removes calcium and magnesium from the solution.

The areal extents of the calcium and calcium-magnesium facies for the Paluxy Aquifer, Glen Rose Formation, Hensell Aquifer, Pearsall Formation, and Hosston Aquifer in Figures 4.4.4 through 4.4.8, respectively, coincide with the mapped outcrop of the northern Trinity Aquifer. This overlap confirms that the outcrop is an active zone of recharge in the northern Trinity Aquifer as would be expected. Furthermore, the similar areal extent of calcium and calcium-magnesium facies for the aquifers and formations from Brown to Wise counties suggests that similar groundwater flow patterns or considerable cross-flow exists among the aquifers/formations. The similarity in the spatial distribution of the facies is most evident among the Hensell Aquifer, Pearsall Formation, and Hosston Aquifer in Comanche, Erath, and Hamilton counties. This similarity in chemical facies may reflect the fact that there are well-connected shallow flow systems that allow mixing of groundwater from older aquifers/formations with groundwater in younger aquifers/formations. Other processes that can contribute to vertical mixing are high pumping rates, large irrigation amounts, and conduits, either through well completions or fractures, providing a path for leakage through the upper aquifers/formations.

For both the Woodbine Aquifer and the Washita/Fredericksburg groups, the calcium and calcium-magnesium facies occur a few miles from the mapped outcrops. In Figure 4.4.2, calcium and calcium-magnesium facies are coincident with the Woodbine Aquifer outcrop. In Figure 4.4.3, the number of wells available to document the occurrence of calcium and calcium-magnesium facies are numerous in the southeast corner of the Washita/Fredericksburg groups outcrop (bounded by the outcrop of the northern Trinity and Woodbine aquifers) but significantly decreases in frequency northward. There is only one mapped calcareous facies north of Bosque County in the Washita/Fredericksburg groups. However, in the Paluxy Aquifer,

there are about 10 well locations directly underlying the Washita/Fredericksburg groups outcrop that are characterized by calcareous facies (see Figure 4.4.4). At these wells, the calcareous facies may be caused either by migration of groundwater enriched with carbon dioxide from the northern Trinity Aquifer outcrop and/or from vertical leakage through the Washita/Fredericksburg groups outcrop. Rapp (1988) suggests that the latter is a primary mechanism for recharge to the northern Trinity Aquifer.

The dominant anion for all of the aquifers/formations is the bicarbonate facies. Within most aquifers/ formations, the occurrence of either a chloride or sulfate facies appears to have occurred more as a result of mixing with other water or a change in the subsurface mineralogy than as a result of natural evolution of groundwater chemistry along a flow path. Previous researchers (Hall and Turk, 1975; Chaudhuri and Ale, 2013) suggest that one of the reasons for changes in the facies composition across the northern Trinity and Woodbine aquifers is a change in depositional system. In order to explore this hypothesis and possible correlations between hydrogeochemical facies and depositional systems, the outlines of the depositional systems are included in Figures 4.4.2 through 4.4.8. Introduction of the depositional systems is given in Section 4.1.8. Depositional systems were not developed for the Washita/Fredericksburg groups because it consists primarily of carbonate without significant sandstones. The Hosston Aquifer in the study area is composed of a single depositional system - coastal plain fluvial sandstone. There is some evidence of a correlation between depositional system and hydrogeochemical facies. For example, Figure 4.4.5 shows a change from dominant bicarbonate to some sulfate moving north to south across the depositional system boundary in the Glen Rose Formation. Correlations between hydrogeochemical facies and depositional systems are the result of changes in the mineralogy of the deposits, the amount of carbon dioxide in solution, the duration of contact/age of the groundwater, and/or the mixing of groundwater between aquifers.

In the hydraulically confined regions of the Woodbine Aquifer, sulfate facies are scattered at variable distances from the outcrop. This is likely due to the variability in the distribution of deposits containing sulfate minerals, such as lignite coal, gypsum, clay, and volcanic ash, in the aquifer (Peckham and others, 1963) rather than groundwater residence time. The sulfate facies are accompanied by chloride facies in Dallas, Rockwall, and southern Collin counties. The cause for the chloride facies in the Woodbine Aquifer is unknown. Possible sources for the high

chlorides, which are over 1,000 milligrams per liter, are anthropogenic contamination (Hopkins, 1996).

The Glen Rose Formation consists of two depositional systems: a marginal marine sandstone and a marine shelf limestone. Sulfate facies only occur in the marine shelf limestone depositional system. The sources of the sulfates are evaporite beds and deposits of anhydrite and gypsum. The sulfate facies are most prevalent south of McLennan County, but also occur as far west as Hamilton County and as far north as Denton County (Figure 4.4.5). Reasons for the higher frequency of sulfate facies south of the McLennan County include a high density of sulfate sources and/or longer residence time of groundwater in the downdip region of the Glen Rose Formation.

The importance of groundwater residence time and its impact on the development of hydrogeochemical facies is explained well by Domenico (1972). He states that the evolutionary development of the bicarbonate-sulfate-chloride sequence identified by Chebotarev (1955) can be compared with the process of mineral formation by evaporation of surface-water bodies:

> "With evaporation, concentration of the soluble salts occurs, and when super saturation with any salt is achieved, that salt is precipitated. The least soluble salts are precipitated first, and the most soluble last, with the order being calcite (bicarbonate), gypsum (sulfate), and halite (chloride). Halite remains in solution until its normal marine salinity of 35,000 ppm has increased to 337,000 ppm. Whereas evaporation is the mechanism of concentration in surface-water bodies, the relative solubility of the rocks in a dynamic flow system is the responsible factor in groundwater basins. With evaporation, a vertical zonation of evaporite deposits is anticipated; with groundwater flow it is the chemical constituents in solution that reflect zonation."

The spatial distribution of sulfate facies in the Glen Rose Formation is similar to the spatial distribution of sulfate facies in the Hensell Aquifer and Pearsall Formation (see Figures 4.4.6 and 4.4.7, respectively) and to a lesser degree in the Hosston Aquifer (see Figure 4.4.8). A reason that could partially account for this similarity is provided by Rapp (1988), who concluded that significant recharge to the lower portion of the northern Trinity Aquifer (i.e., the Hensell Aquifer, Pearsall Formation, and Hosston Aquifer) occurs through the Glen Rose Formation.

Thus, some, if not an appreciable amount, of the sulfate in the Hensell Aquifer and Pearsall Formation originated in the Glen Rose Formation. To support this conclusion, Rapp (1988) shows that, although the northern Trinity Aquifer is semi-confined below the Glen Rose Formation, water-level data indicate that the flow component is downward from the Paluxy Aquifer, across the Glen Rose Formation, and into the lower portion of the northern Trinity Aquifer.

One of the notable observations in the Hosston Aquifer (see Figure 4.4.8) is the occurrence of sodium-chloride facies in Denton and Collin counties and in northern Williamson, Bell, and Coryell counties. In these two areas, chloride concentrations between 100 and 500 milligrams per liter have been measured, which are about two to three times higher than the chloride concentrations measured in most of the other wells in the Hosston Aquifer. Potential sources of the elevated chloride concentrations may be the upwelling of small amounts of brines along faults and/or the upward migration of chlorides from the underlying Paleozoic-age sands.

4.4.4 TDS and Chloride Concentrations and Limits of Freshwater

Figures 4.4.9 through 4.4.15 show the TDS concentrations at well locations for the Woodbine Aquifer, Washita/Fredericksburg groups, Paluxy Aquifer, Glen Rose Formation, Hensell Aquifer, Pearsall Formation, and Hosston Aquifer, respectively. Each of the maps has an estimated downdip extent of freshwater based on the water quality information and the analysis of the geophysical logs presented in Section 4.1.10. The federal secondary drinking water standard for TDS is 500 milligrams per liter. The TCEQ secondary drinking water standard for TDS is 1,000 milligrams per liter. The major ions that comprise TDS for the northern Trinity and Woodbine aquifers include silica, calcium, magnesium, sodium, chloride, bicarbonate, sulfate, and carbonate. Secondary ions typically included as part of TDS are fluoride, nitrate, potassium, manganese, iron, and aluminum.

Table 4.4.2 divides groundwater into five classes based on TDS (Collier, 1993). LGB-Guyton and NRS Consulting (2003) grouped the classes of slightly saline and moderately saline water under the general category of brackish groundwater. Thus, brackish groundwater by that definition has a TDS between 1,000 and 10,000 milligrams per liter, and freshwater has a TDS less than 1,000 milligrams per liter. Water with a TDS greater than 10,000 milligrams per liter is classified as being saline water (LGB-Guyton and NRS Consulting, 2003).

Figures 4.4.16 through 4.4.22 show the chloride concentrations for the Woodbine Aquifer, Washita/Fredericksburg groups, Paluxy Aquifer, Glen Rose Formation, Hensell Aquifer, Pearsall Formation, and Hosston Aquifer, respectively. These figures are provided primarily to support the interpretation of the hydrogeochemical facies and TDS data. The federal secondary drinking water standard for chloride is 250 milligrams per liter. The TCEQ secondary drinking water standard for chloride is 300 milligrams per liter. Chloride concentrations in rainwater in GMA 8 likely range between 2 and 10 milligrams per liter (Hem, 1985; Sharpley and others, 1985). After precipitation enters the soil, evaporation and evapotranspiration tend to concentrate the chloride in soil water to levels ten or more times their original concentration. Rock-water interactions, such as mineral dissolution of chloride and desorption of chloride from clays within the soil zone, can further increase chloride concentrations.

The largest source of chloride in the Earth's crust is the mineral halite in evaporite deposits, which formed over geologic time by the evaporation of seawater. Chloride is also found in other less common salts (e.g., potassium chloride and calcium chloride) associated with these evaporite deposits. Because halite and other chloride salts are extremely soluble, they are not found in areas where there is active circulation of freshwater. Chloride is usually a minor constituent of sedimentary rocks such as limestone, sandstone, and shale (as well as granitic rocks) and typically occurs at low concentrations. Krauskopf (1979) reported typical chloride concentrations of 150, 10, and 200 milligrams per liter for limestone, sandstone, and shale, respectively. Chloride is also present within some minerals as fluid inclusions and can have very high concentrations comparable to those of a concentrated brine; however, fluid inclusions are typically very small (a few microns in diameter) and impart very little chloride to circulating groundwater.

Salt domes are a localized but major source of chloride in the subsurface in Texas. Salt domes are halite, or sodium chloride, deposits that grow and develop as sediments are deposited around them (Seni and Jackson, 1984; Halbouty, 1979). The salt that comprise the domes originally formed bedded evaporite deposits in the ancestral Gulf of Mexico during the Jurassic Period. Salt, which is a low-density, ductile mineral, is gravitationally mobilized by sediment loading and can form a variety of upwelling structures, one of which is cylindrical salt domes. Along the Texas Gulf Coast, salt domes have intruded to with several thousand feet of land surface. In such instances, the dissolution of halite can significantly impact the chloride concentration of

meteoric groundwater. Ewing (1990) and Jackson (1982) provide maps of salt domes and other features across Texas. In the study area, salt domes and related formations occur primarily east of the Mexia-Talco Fault Zone.

Examination of the TDS and chloride data led to the following observations:

- The Hosston Aquifer has the farthest downdip extent of freshwater documented by measured TDS in wells (see Figure 4.4.15). In Falls County, the 1,000 milligrams per liter contour is located about 100 miles southeast from the aquifer outcrop area due to numerous freshwater wells located in McLennan County. Factors that likely contribute to the relatively far downdip extent of freshwater are well connected sand units along dip from the recharge area toward Falls County combined with a deep groundwater discharge mechanism. Possible discharge mechanisms include cross-formational flow to other aquifers/formations, vertical flow along the fault zones near the southeast boundary of the northern Trinity Aquifer, and discharge and leakage through wells.

- For the Hensell Aquifer, Pearsall Formation, and Hosston Aquifer, the 1,000 milligrams per liter contour has a similar updip turn in the area of Bell and Coryell counties. The similar TDS measurements in these two counties of between 1,000 and 3,000 milligrams per liter suggest that there is considerable amount of cross-formational flow between the units or similar mineralogy in their deposits. In addition, the similar water quality may be the result of flow between the Hensell Aquifer, Pearsall Formation, and Hosston Aquifer due to multi-completed wells and/or leaking along well annulus. The hydrogeochemical facies and chloride maps indicate that the increased TDS is a result of both increases in chloride and sulfate. Among the possible sources for elevated chloride are upwelling of brine, leakage from abandoned and older wells (Hudak and Wachal, 2001), and cross-formational flow from the Glen Rose Formation and Paleozoic-age deposits.

- The Woodbine Aquifer has the least downdip penetration of freshwater (see Figure 4.4.9). The 1,000 milligrams per liter TDS contour is about 20 miles from the aquifer outcrop in most of the southern portion of the aquifer but is less than 5 miles from the outcrop area in Dallas County. The short distance to brackish water is attributed primarily to the prevalence of deposits of lignite, anhydrite, and gypsum in the Woodbine

Aquifer. In the northern portion of the Woodbine Aquifer (middle of Denton County), the location of the 1,000 milligrams per liter TDS contour occurs considerable farther downdip than it does in the southern portion of the aquifer.

- Localized contamination of all of the aquifers/formations has occurred and is evident from the spatial distribution of the TDS and chloride concentrations. In the outcrop or shallow confined areas, leakage from open brine pits likely contributed to elevated and anomalously high values of chlorides. In the deeper confined regions, leakage along abandoned or improperly constructed oil/gas or water wells may have contributed to localized areas of high TDS.

- There is no compelling evidence to suggest that faults with offsets of 100 feet or less have significantly hindered groundwater flow in the confined portions of the aquifers/formations.

4.4.5 Implications for Recharge Boundaries

The water quality analyses suggest that the occurrence of calcium and calcium-magnesium facies is an indicator of groundwater recharge. The maps of hydrogeochemical facies provide a spatial distribution of calcium and calcium-magnesium facies that is consistent with the mapped outcrop locations for the seven aquifers/formations. The spatial distribution of the hydrogeochemical facies maps suggest that recharge occurring in the outcrops of the Washita/Fredericksburg groups and the Glen Rose Formation is also providing recharge to the Hensell Aquifer, Pearsall Formation, and Hosston Aquifer. This conclusion is consistent with Rapp (1988) who states:

> "Recharge to the covered Trinity aquifer from the leakage through the overlying Glen Rose Limestone and the Fredericksburg Group contributes 20,000 acre-ft/year, or 80 percent of the effective recharge to the artesian Trinity aquifer."
> "Recharge [to the Trinity Aquifer] occurs through leakage from overlying formations as well as on the Trinity sands outcrop belt. Leakage from overlying units adds 75 percent more recharge area in this study."

4.4.6 Implications for Discharge Boundaries

The conceptual model for discharge is based on the spatial distribution of TDS shown in Figures 4.4.9 through 4.4.15. The downdip penetration of freshwater in the Hosston Aquifer extends into McLennan and Falls counties. The ability for freshwater to migrate such a distance

from the outcrop area suggests that groundwater is discharging from the Hosston Aquifer east of Falls County. The conceptual model for this discharge consists of cross-formational flow between aquifers as the primary discharge mechanism and localized discharge through preferential flowpaths created by faults as a secondary discharge mechanism. East of Falls County, the conceptual model presumes that vertical flow in the Mexia-Talco Fault Zone is acting as a regional area of discharge for the Hosston Aquifer. In addition, reduction in the effective horizontal flow along the aquifer was assumed to occur as a result of the offsets and disconnections in sand beds produced by the faults.

A vertical upward hydraulic gradient from the Hosston Aquifer to the Pearsall Formation and Hensell Aquifer during the predevelopment period was assumed. At some locations, faults were expected to enhance vertical mixing, with the amount of that mixing depending on the magnitude of the vertical gradient, the conductance of the vertical flow paths, and the transmissivity of the aquifers/formations near the faults. An area where transmissivity variations were expected to be important is the southeastern portion of the Hensell Aquifer near the transition between the deltaic shoreline-sandstone depositional system, which is primarily sand, and the marine shelf-shale depositional system, which is primarily clay.

Prior to pumping in the northern Trinity Aquifer, groundwater flow from the Hosston Aquifer upward toward the Hensell Aquifer was assumed to have occurred along faults that cut through the Pearsall Formation. Vertical flow from the Hosston Aquifer into the Hensell Aquifer was presumed to be much greater where the Hensell Aquifer is comprised primarily of sands, which corresponds to the area covered by the deltaic shoreline-sandstone depositional system, than where the Hensell Aquifer is comprised primarily of shales, which corresponds to the area covered by the marine shelf-shale depositional system. A comparison of Figures 4.4.13 and 4.4.15 shows a good correlation between the location of the transition between the sand and shale depositional systems in the Hensell Aquifer and the downdip extend of freshwater in the Hosston Aquifer in Falls, McLennan, and Limestone counties. One of the reasons for this correlation was attributed to a reduction in downdip horizontal flow in the Hosston Aquifer due to reduced discharge from the Hosston Aquifer to the Hensell Aquifer east of where the Hensell Aquifer transitions from a sandy depositional system to a shaley depositional system.

A similar downdip extent of freshwater is observed in the Hensell Aquifer, Pearsall Formation, and Hosston Aquifer in the southern portion of the study area. This is attributed to good vertical communication as a result of cross-formational flow, vertical flow along faults, and vertical flow in the annulus and screens of wells completed across the Hosston Aquifer and overlying aquifers/formations. Most of the wells in this portion of the study area are multi-completed across the Hosston Aquifer and overlying aquifers/formations and, thus, mixing among the aquifers/formations was assumed to occur if there is a vertical hydraulic gradient in the well.

There is an absence of freshwater in the Hosston Aquifer, Pearsall Formation, and Hensell Aquifer in Coryell and Bell counties. Two scenarios were considered to explain this absence. First, the transmissivity of the Hosston Aquifer is reduced by the numerous faults along the groundwater pathways from Comanche and Erath counties to Coryell County, which prevents the downdip flow of freshwater in the aquifer beyond Hamilton County. Second, faults and/or wells in this area provide a mechanism for vertical connection between the Glen Rose Formation and the Hosston Aquifer and, after the onset of pumping in the Hosston Aquifer, a downward vertical gradient was established that resulted in the flow of high TDS groundwater from the Glen Rose Formation into the underlying aquifers, including the Hosston Aquifer.

Table 4.4.1   Number of wells in the TWDB groundwater database used to determine hydrogeochemical facies and TDS and chloride concentrations.

Aquifer/Formation	Number of Wells		
	Hydrogeochemical Facies	TDS	Chloride
Woodbine Aquifer	232	233	239
Washita/Fredericksburg groups	268	271	283
Paluxy Aquifer	128	127	146
Glen Rose Formation	211	211	229
Hensell Aquifer	213	218	220
Pearsall Formation	267	271	271
Hosston Aquifer	368	368	377
Total	1687	1699	1765

Table 4.4.2.   Groundwater classifications based on TDS.

Class		TDS (milligrams per liter)	Example of Use
Collier (1993)	LBG-Guyton and NRS Consulting (2003)		
Freshwater	Freshwater	0 to 1,000	Drinking and all other uses
Slightly saline water	Brackish water	more than 1,000 to 3,000	Drinking, if freshwater is unavailable, irrigation, industrial, mineral extraction and oil and gas production
Moderately saline water		more than 3,000 to 10,000	Potential future drinking and limited livestock watering and irrigation if fresh or slightly saline water is unavailable; mineral extraction and oil and gas production
Very saline water	Saline water	more than 10,000 to 100,000	Mineral extraction and oil and gas production
Brine water		more than 100,000	Mineral extraction and oil and gas production
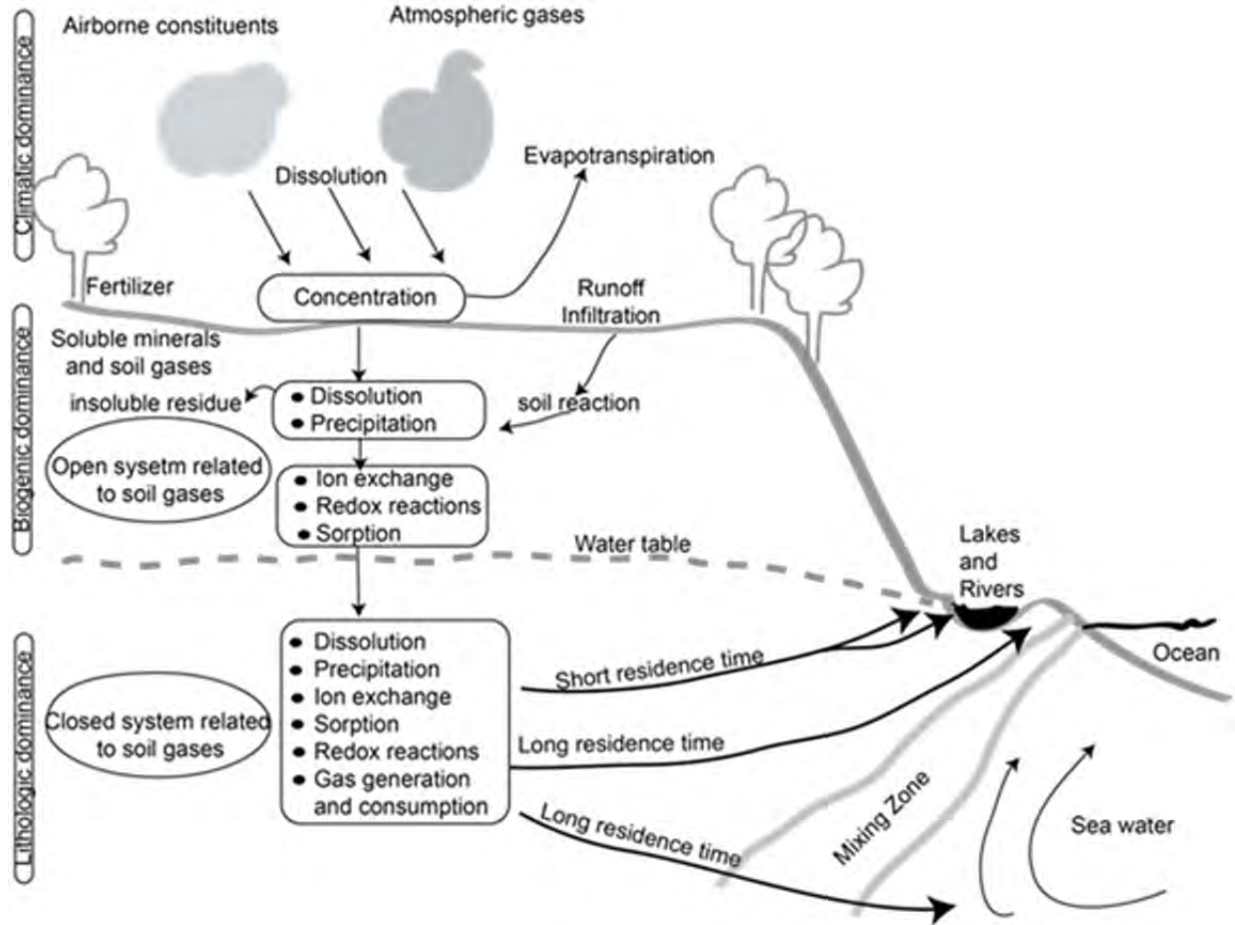
Figure 4.4.1   Conceptualized groundwater flow system incorporating hydrochemical processes that affect reactions and transport involving major ions (modified after Back and others, 1983; Herczeg and Edmunds, 2000). Distinction between open and closed system is based on whether the aquifer is connected or not to atmospheric gases such as carbon dioxide and oxygen.
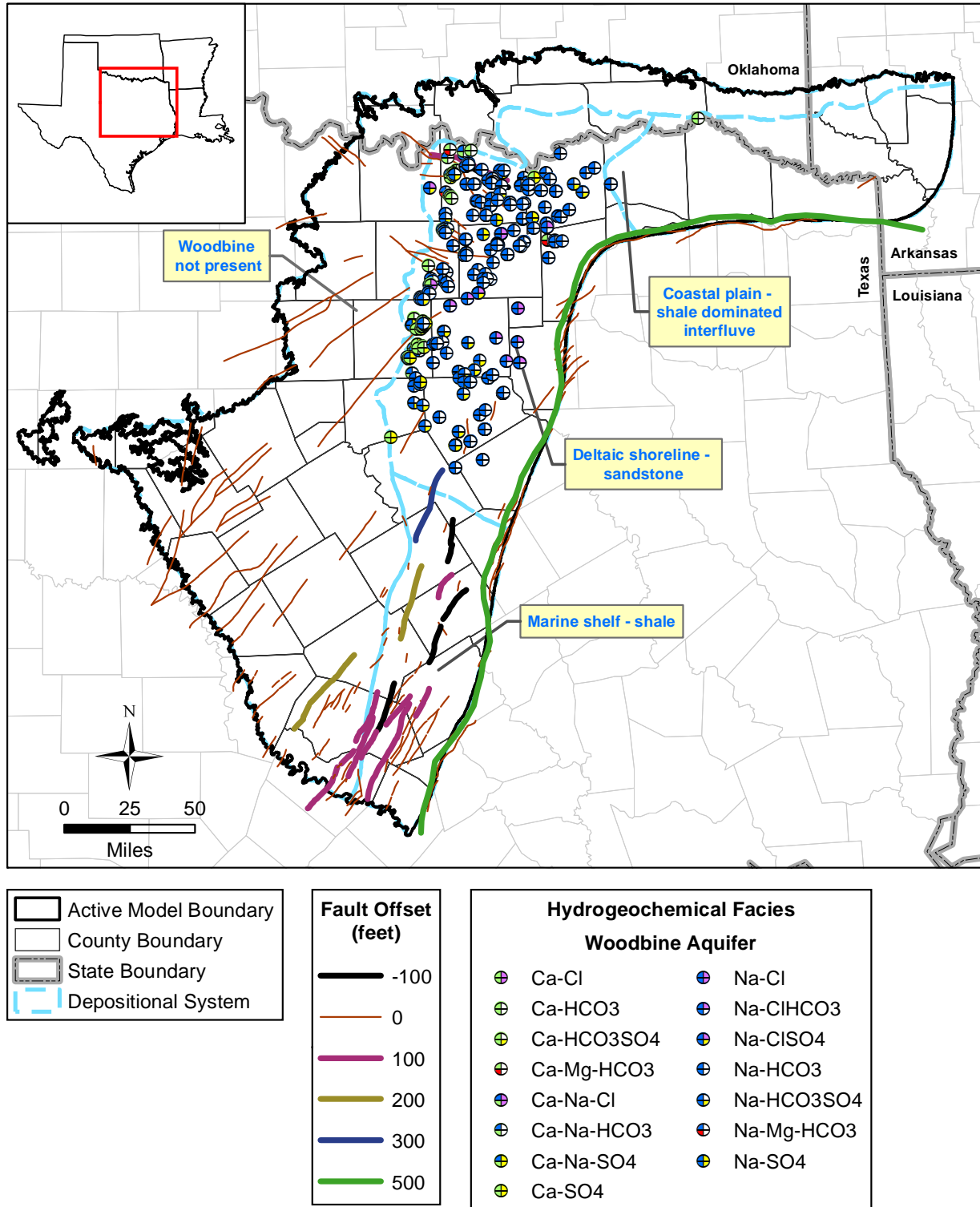
Figure 4.4.2   Hydrogeochemical facies at well locations in the Woodbine Aquifer.
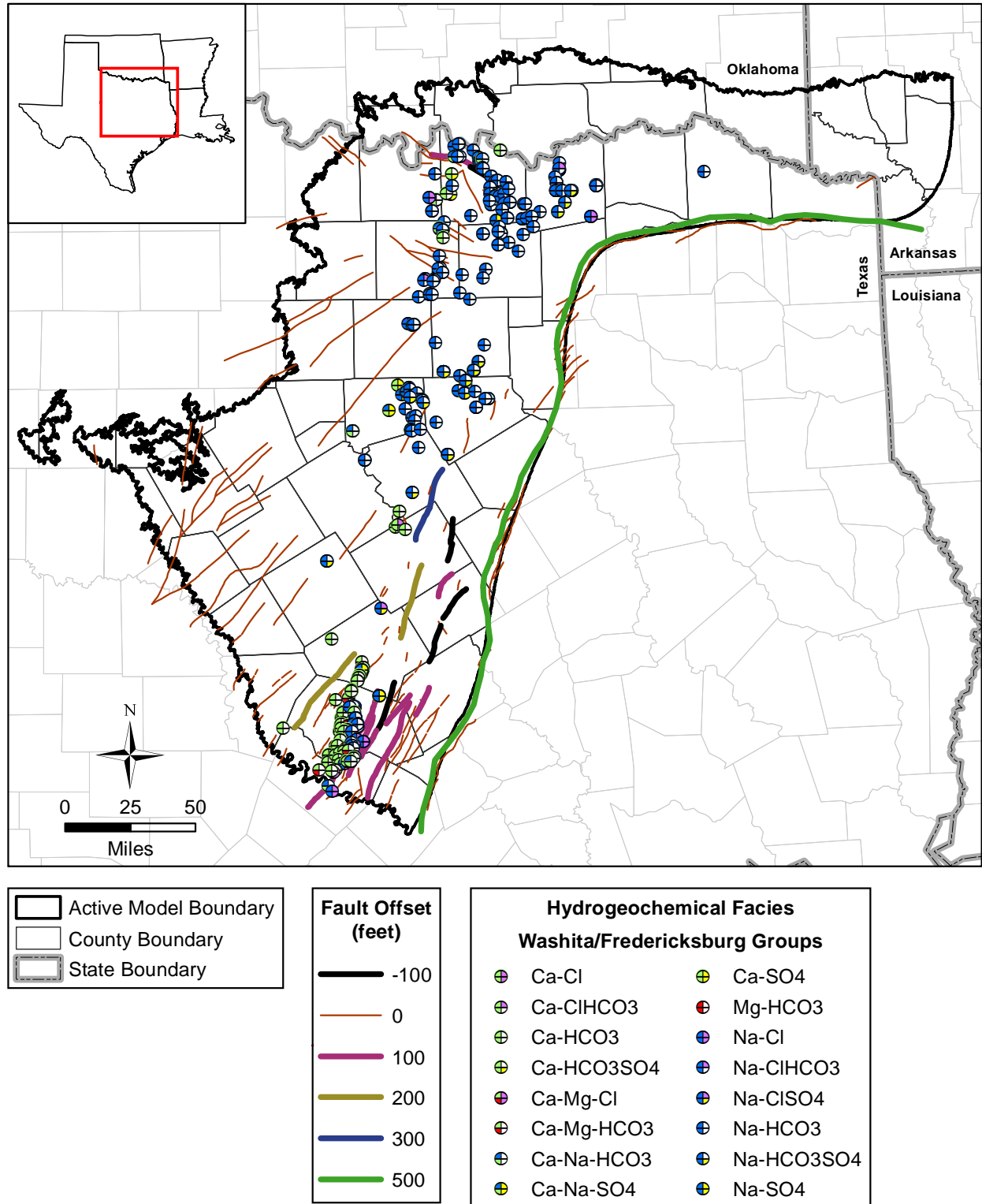
Figure 4.4.3 **Hydrogeochemical facies at well locations in the Washita/Fredericksburg groups.**
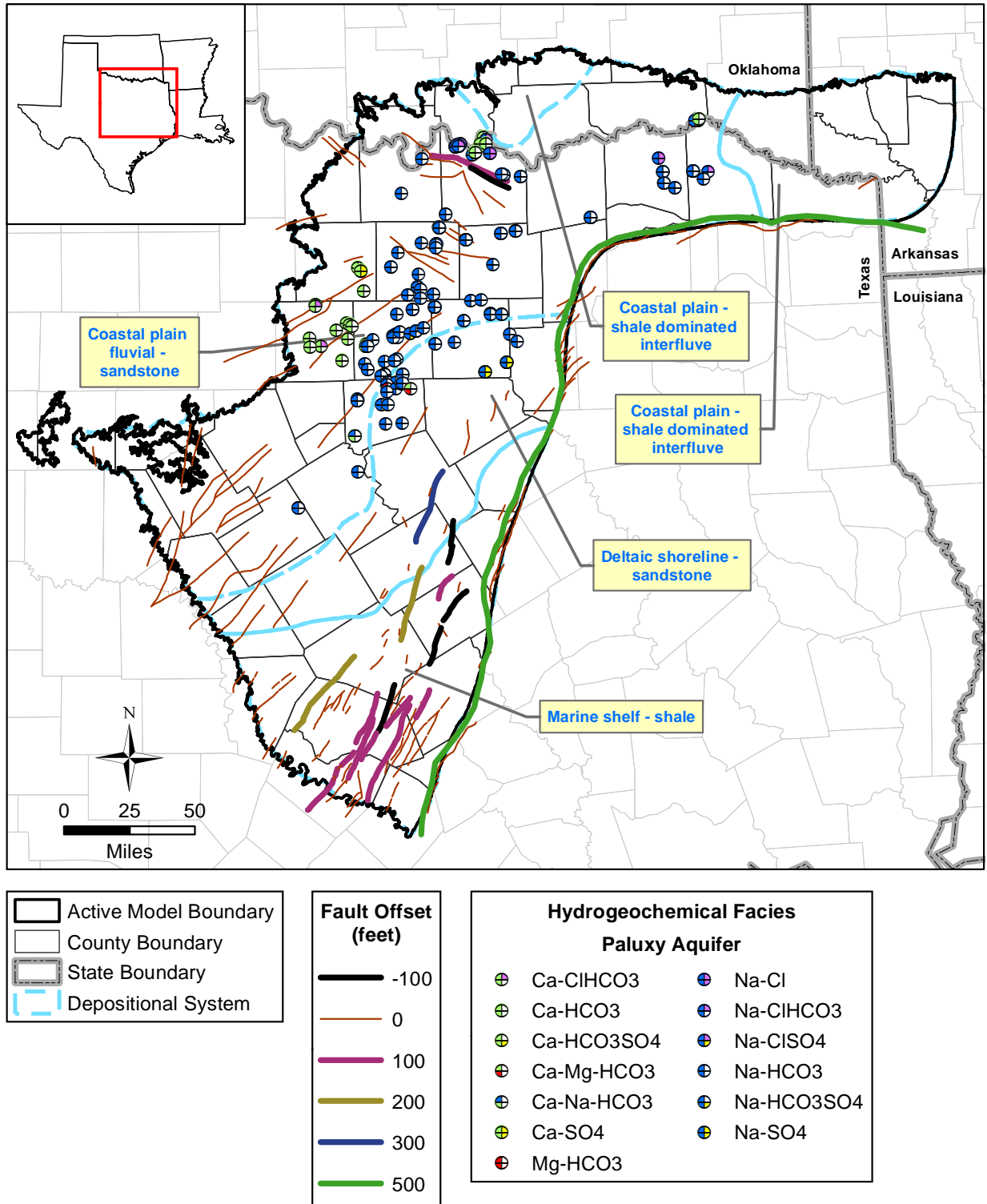
Figure 4.4.4   Hydrogeochemical facies at well locations in the Paluxy Aquifer.
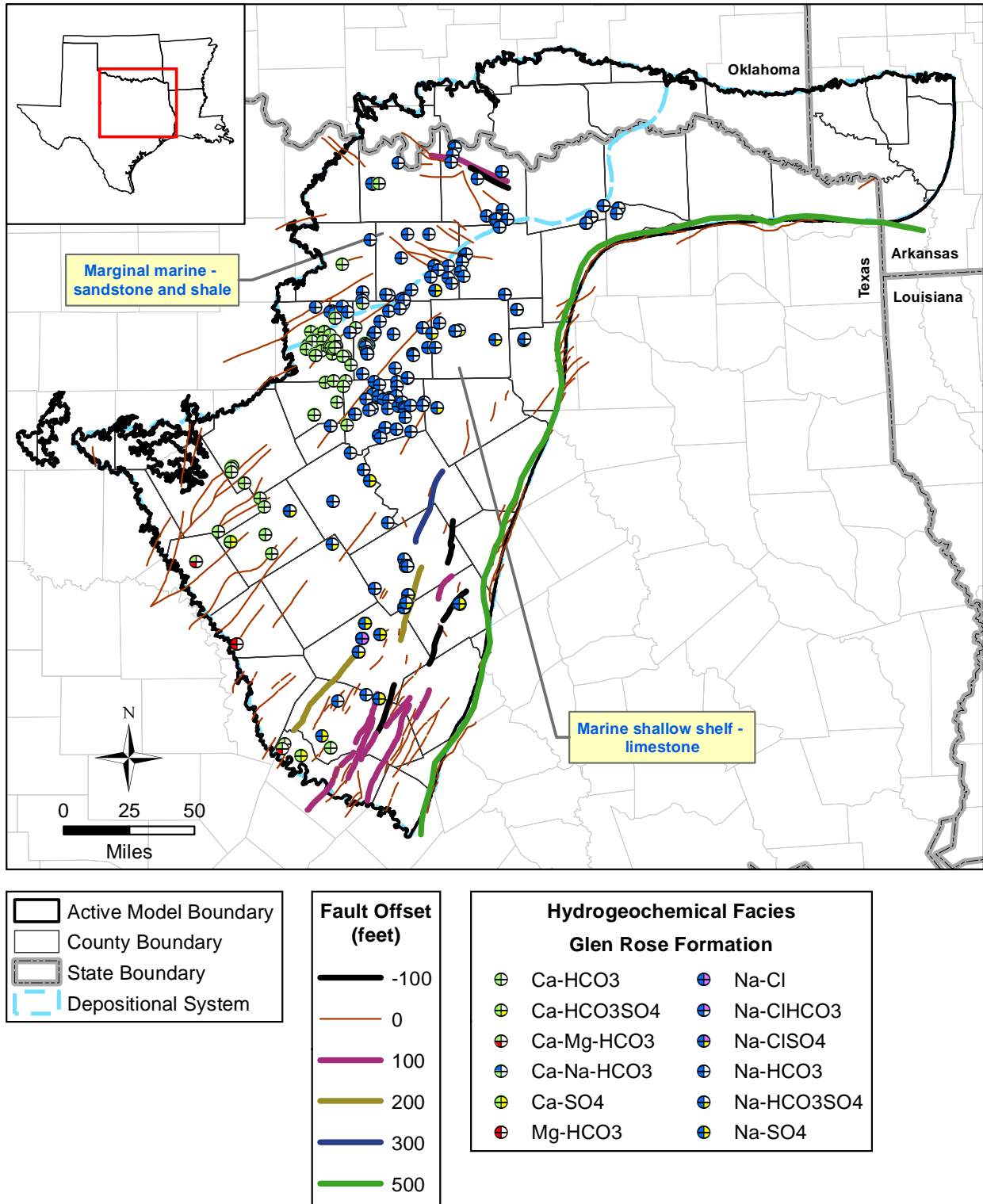
Figure 4.4.5 **Hydrogeochemical facies at well locations in the Glen Rose Formation.**
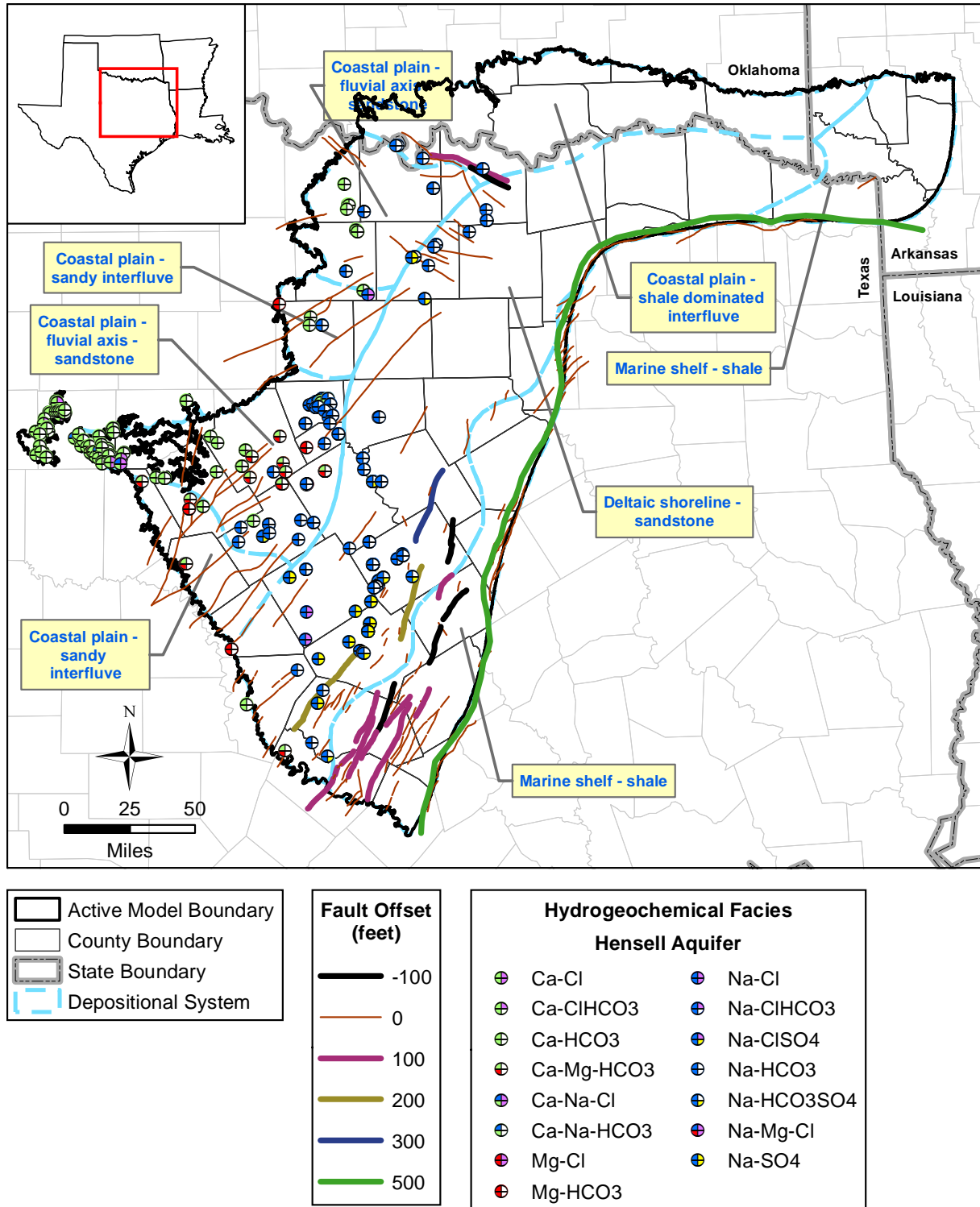
Figure 4.4.6   Hydrogeochemical facies at well locations in the Hensell Aquifer.
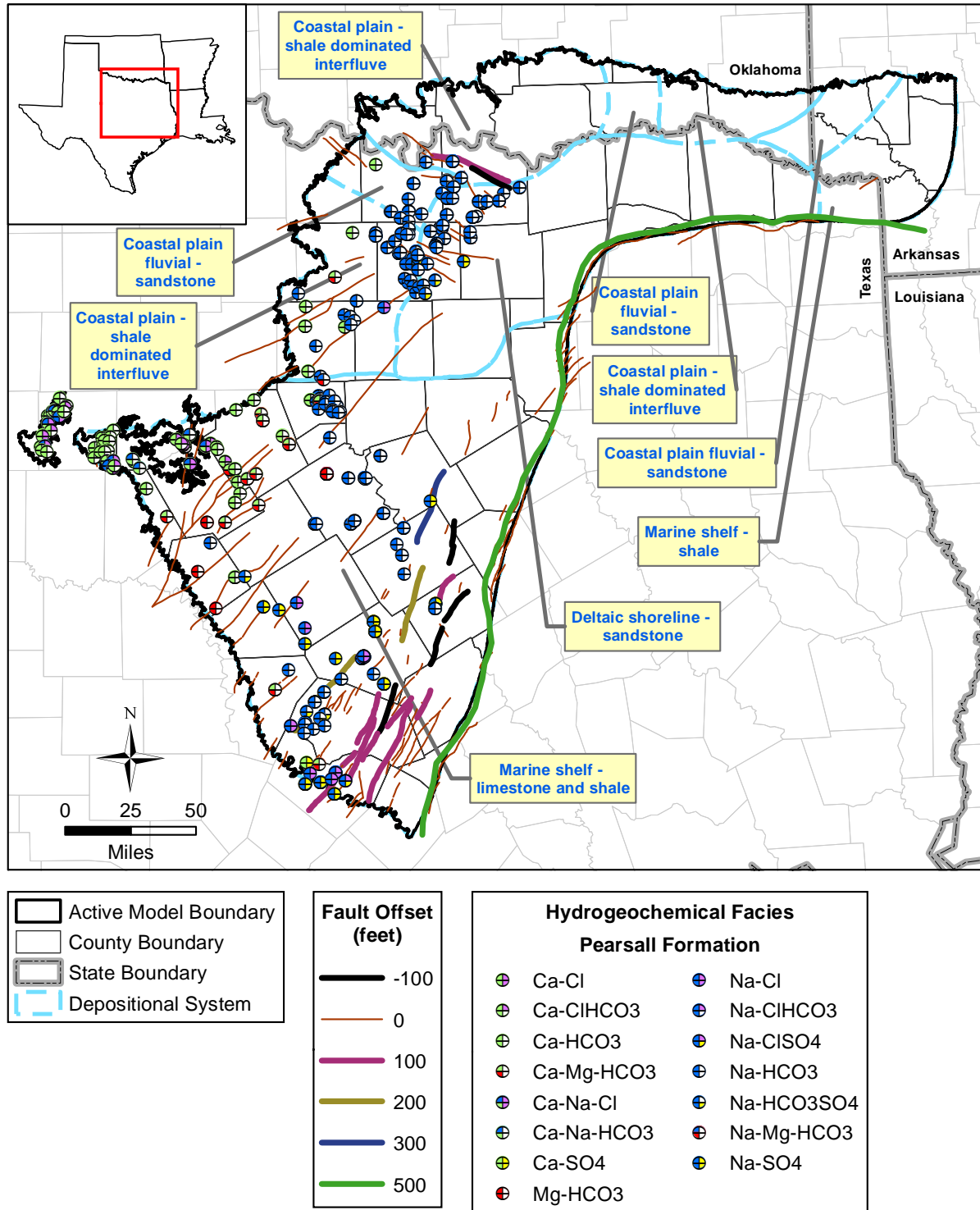
Figure 4.4.7   Hydrogeochemical facies at well locations in the Pearsall Formation.
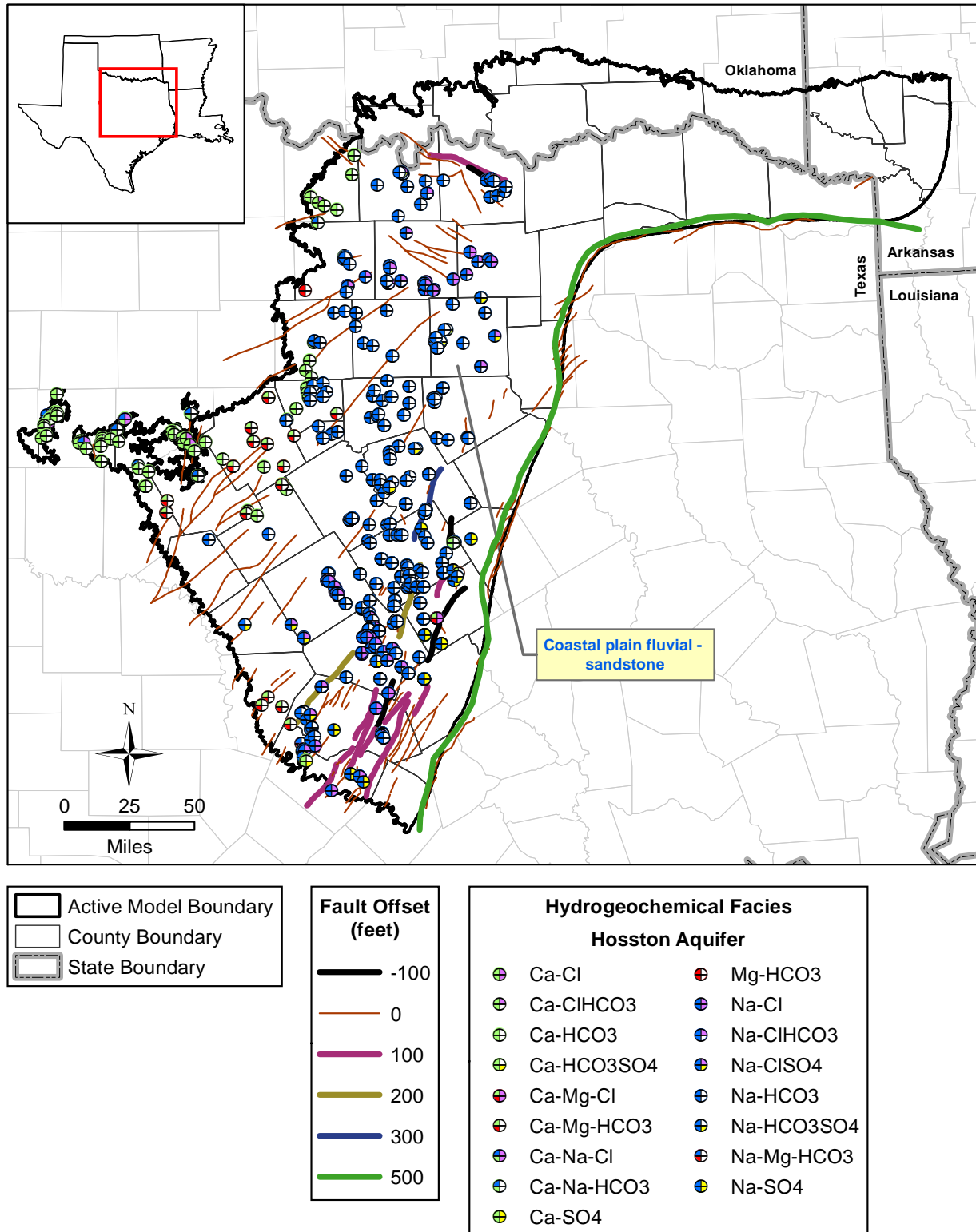
Figure 4.4.8   Hydrogeochemical facies at well locations in the Hosston Aquifer.
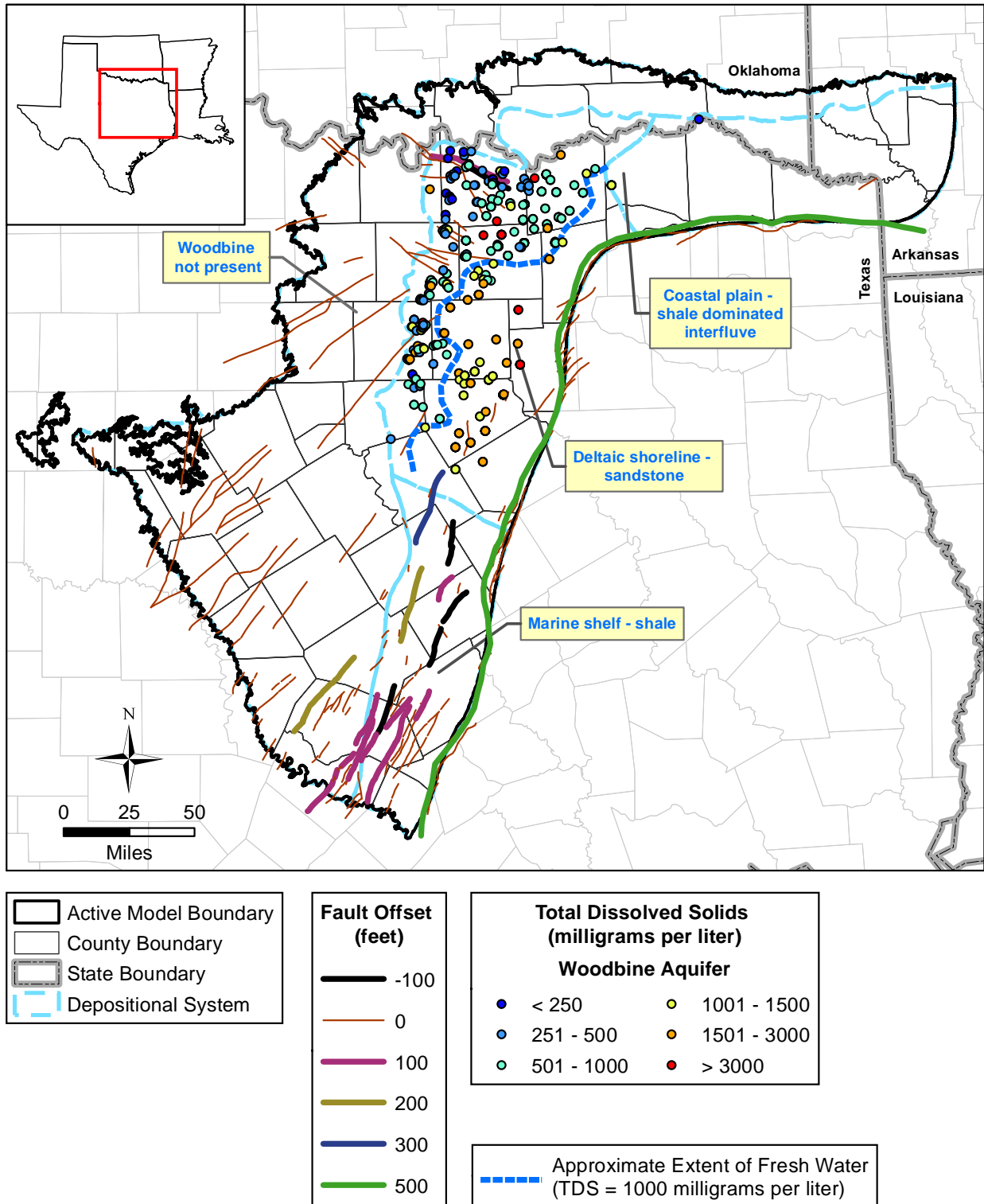
Figure 4.4.9   TDS concentration at well locations in the Woodbine Aquifer.
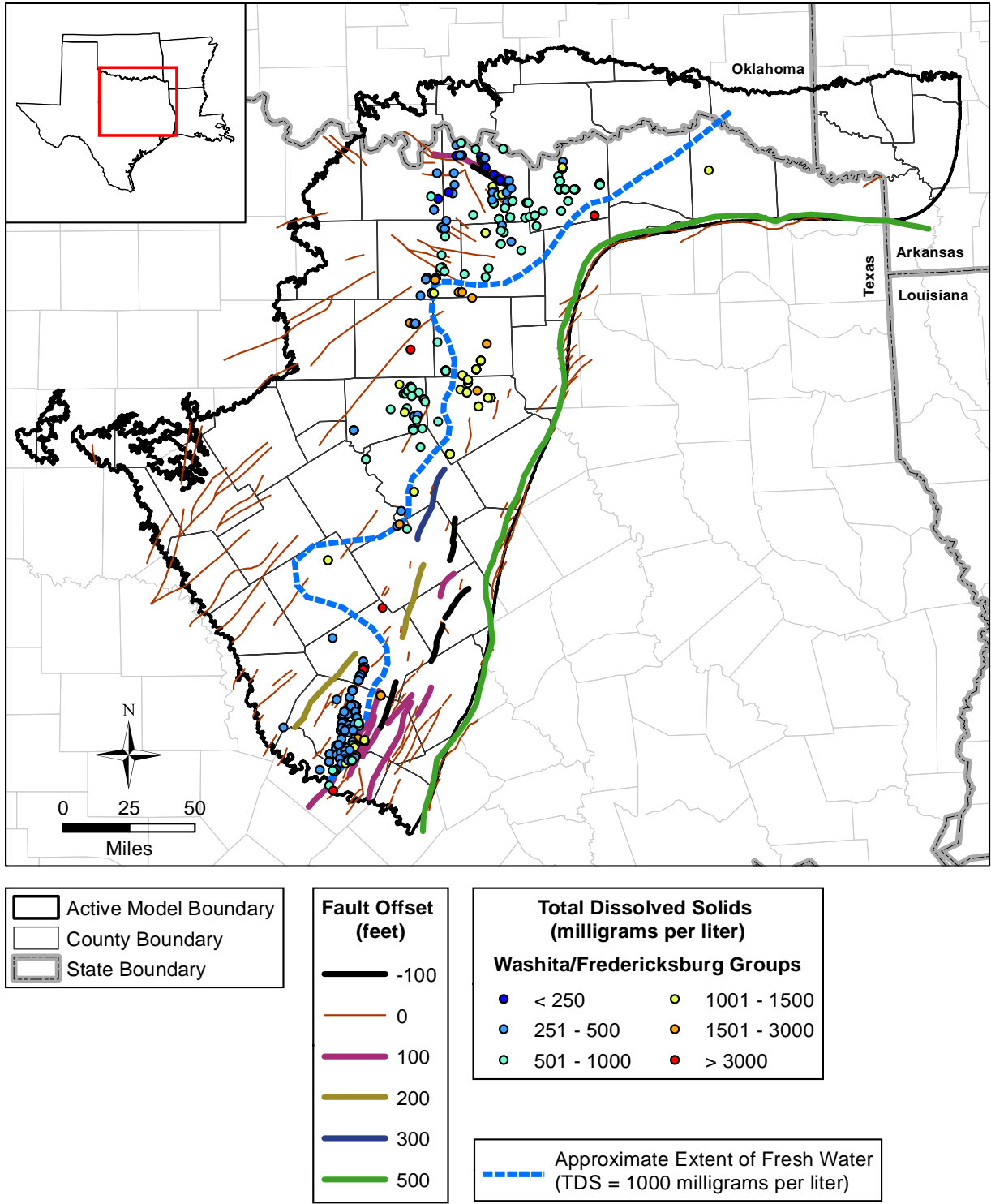
Figure 4.4.10   TDS concentration at well locations in the Washita/Fredericksburg groups.
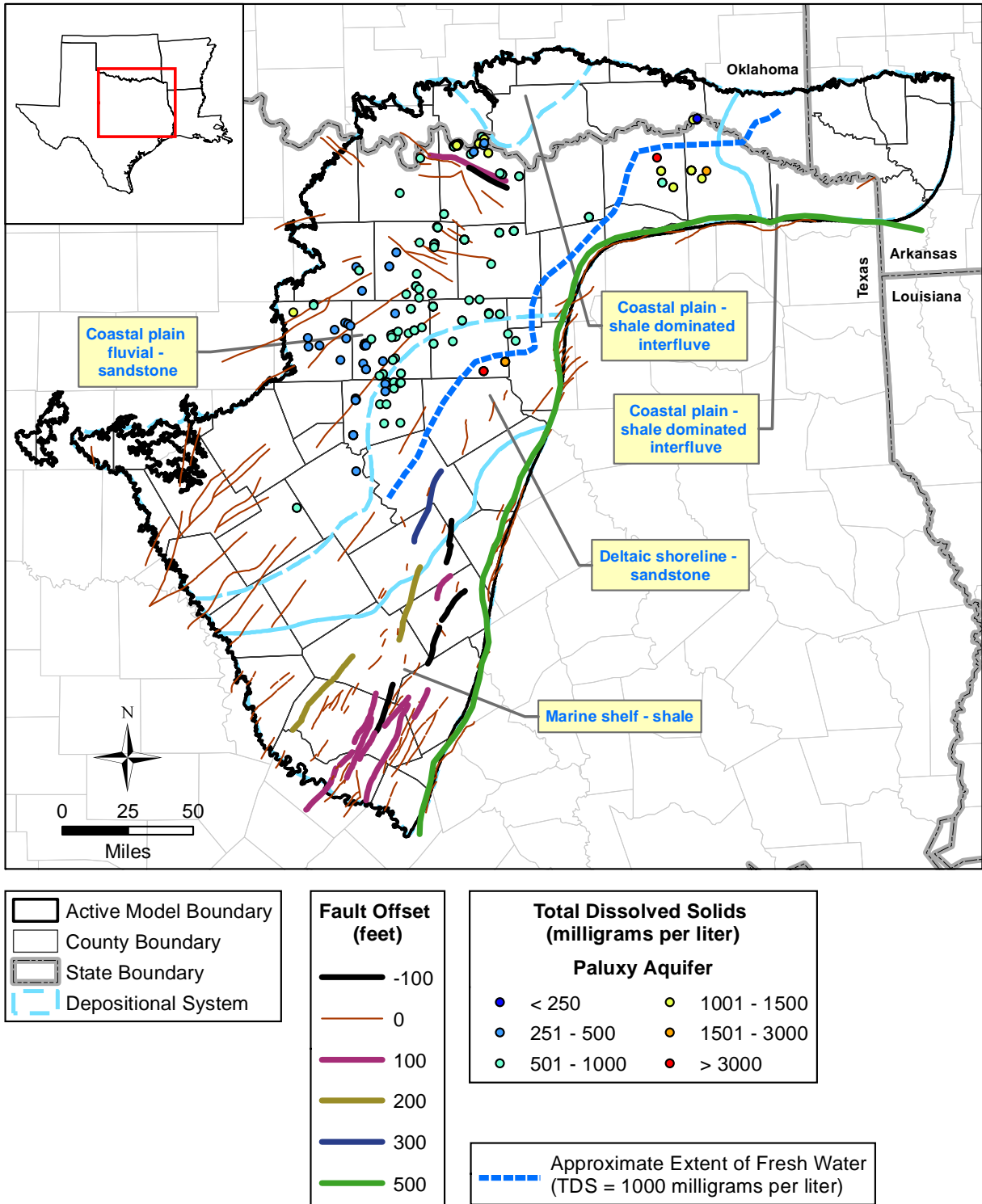
Figure 4.4.11   TDS concentration at well locations in the Paluxy Aquifer.
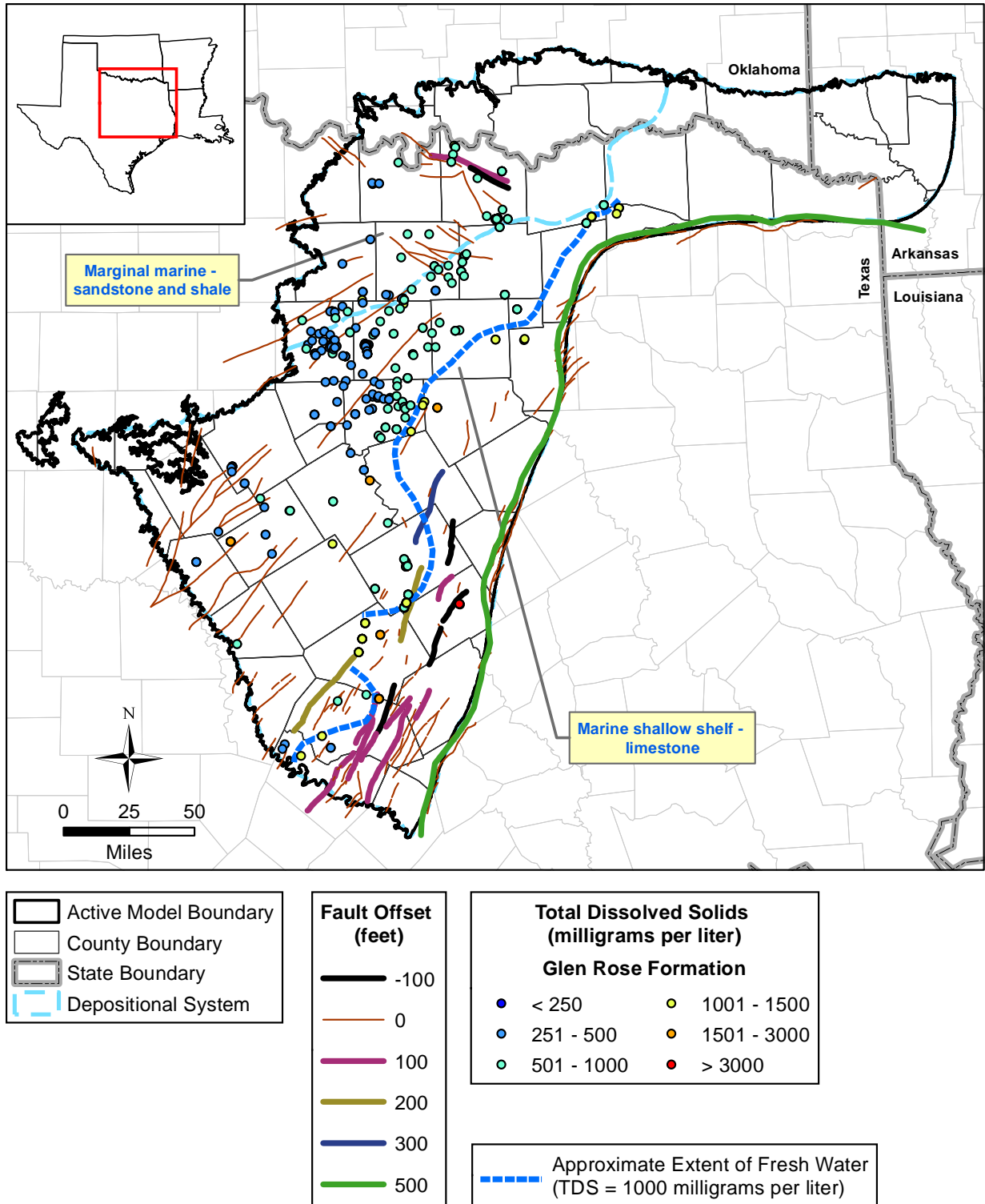
Figure 4.4.12   TDS concentration at well locations in the Glen Rose Formation.
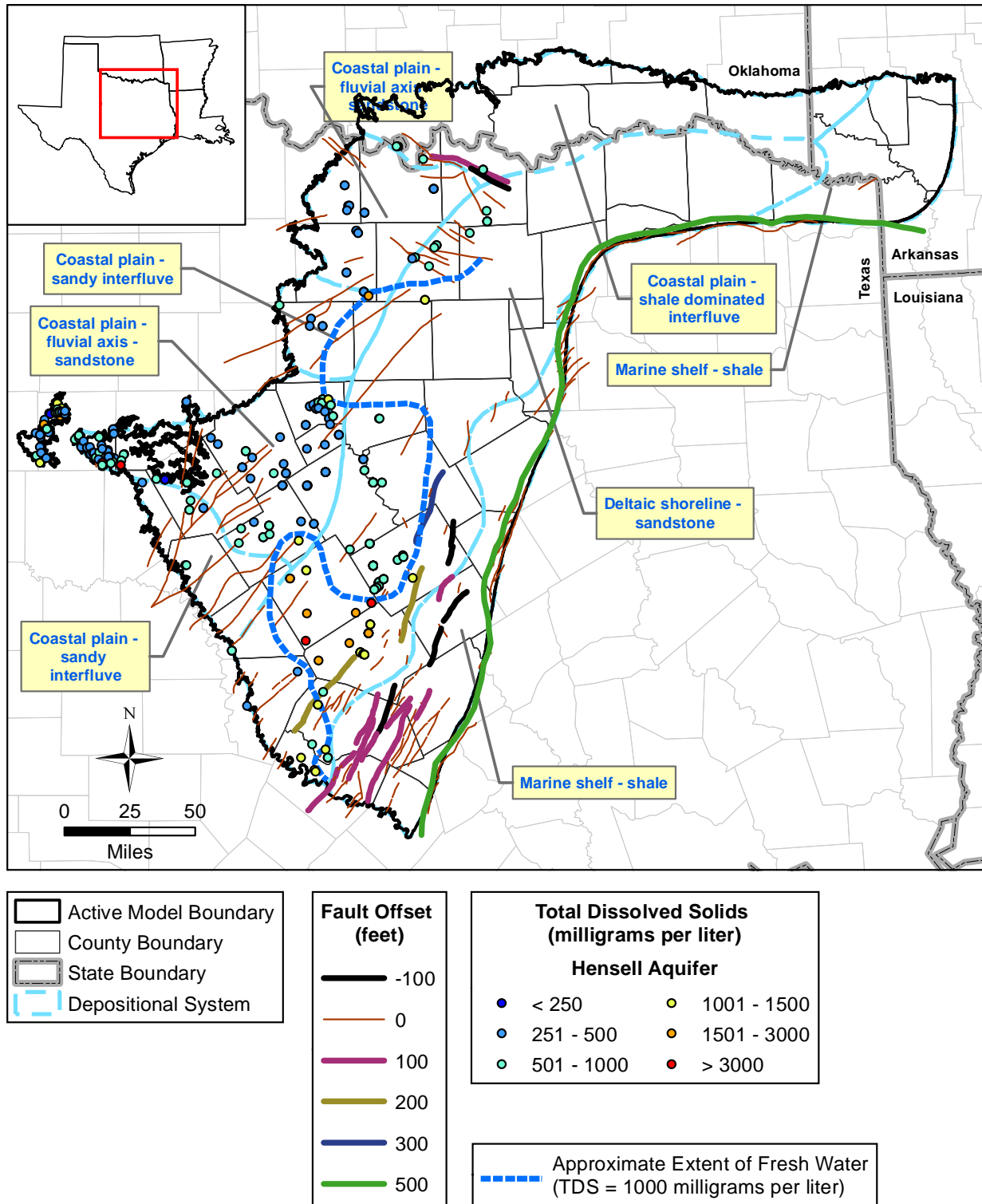
Figure 4.4.13   TDS concentration at well locations in the Hensell Aquifer.
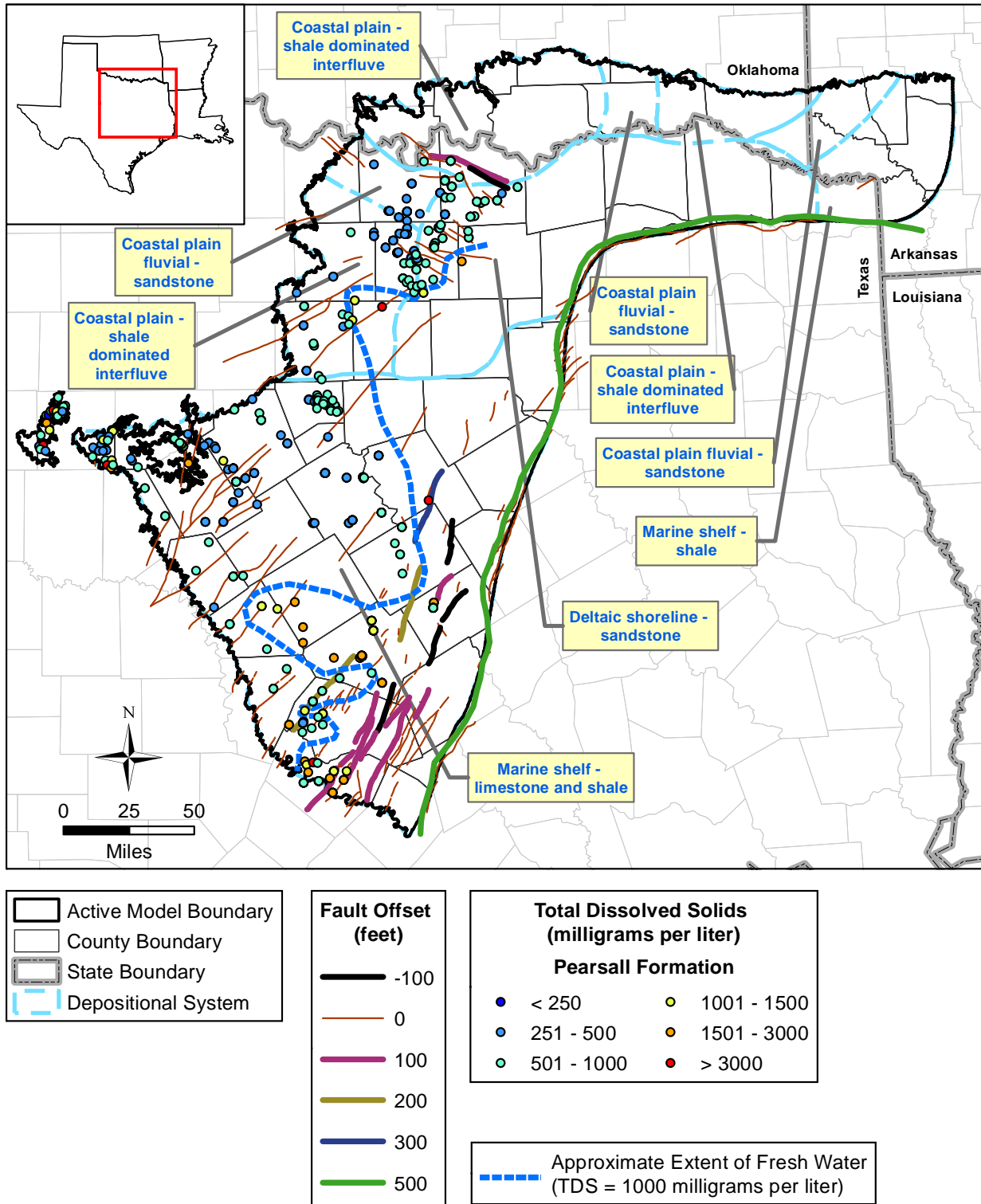
Figure 4.4.14   TDS concentration at well locations in the Pearsall Formation.
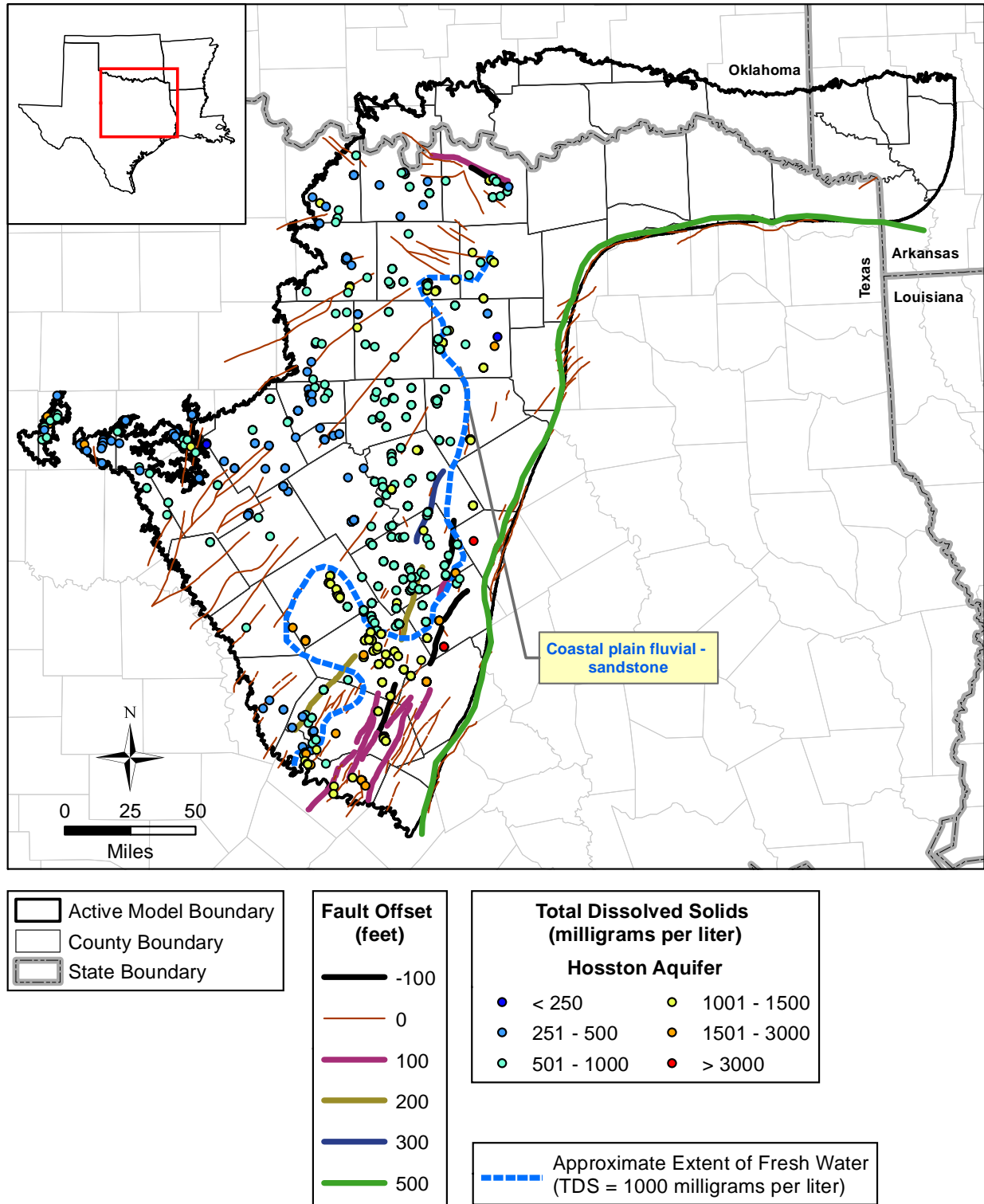
Figure 4.4.15   TDS concentration at well locations in the Hosston Aquifer.
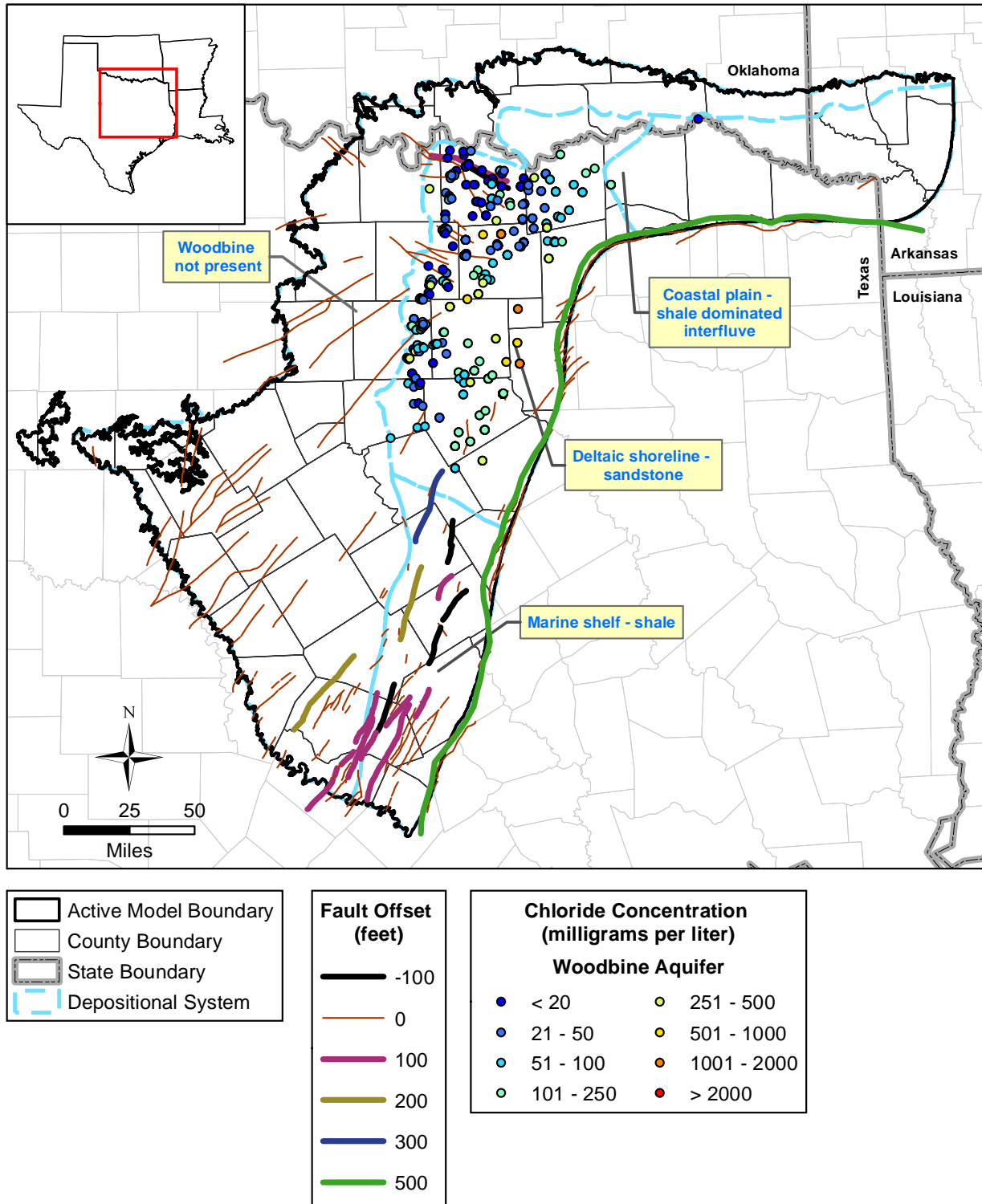
Figure 4.4.16   Chloride concentration at well locations in the Woodbine Aquifer.
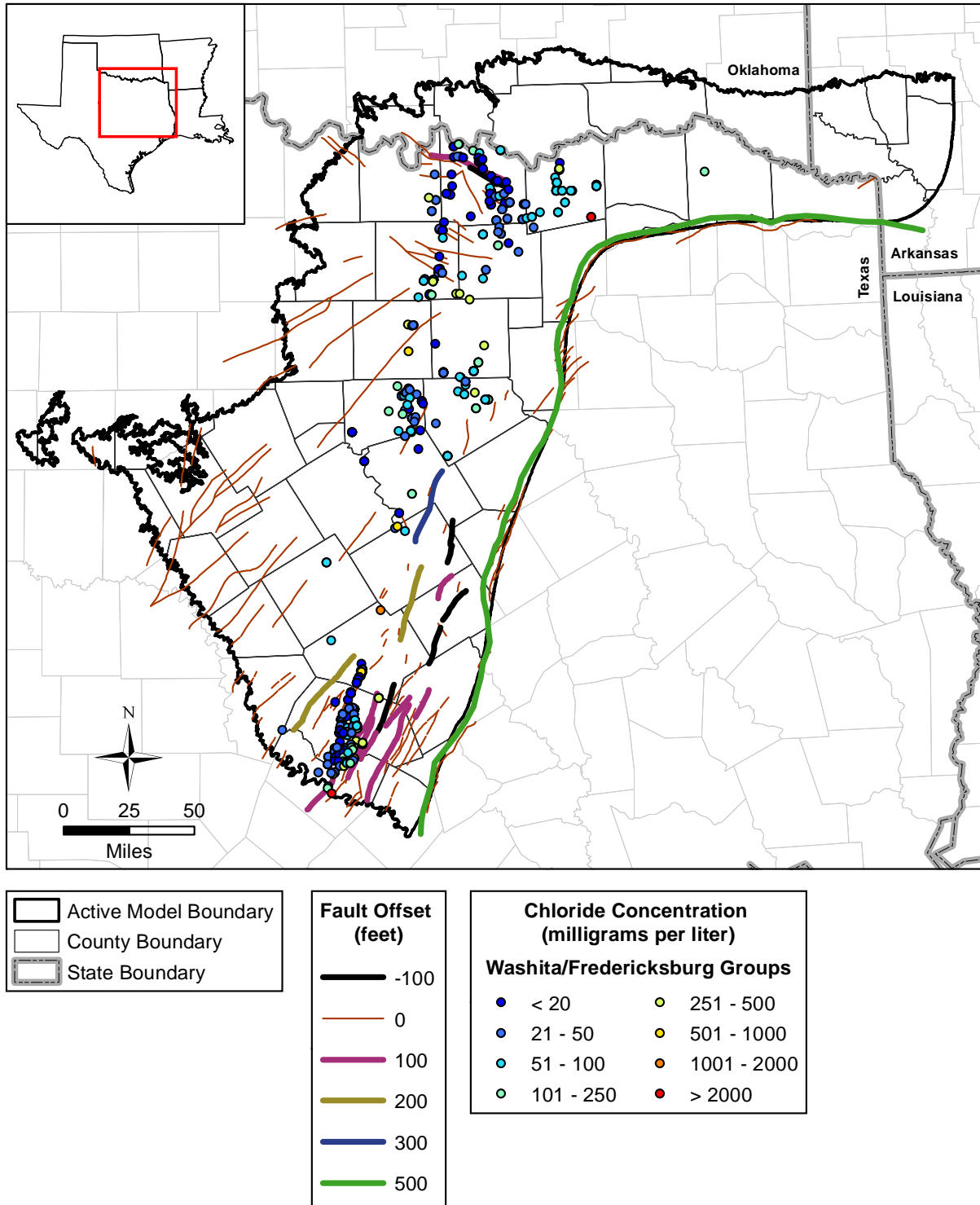
Figure 4.4.17   Chloride concentration at well locations in the Washita/Fredericksburg groups.
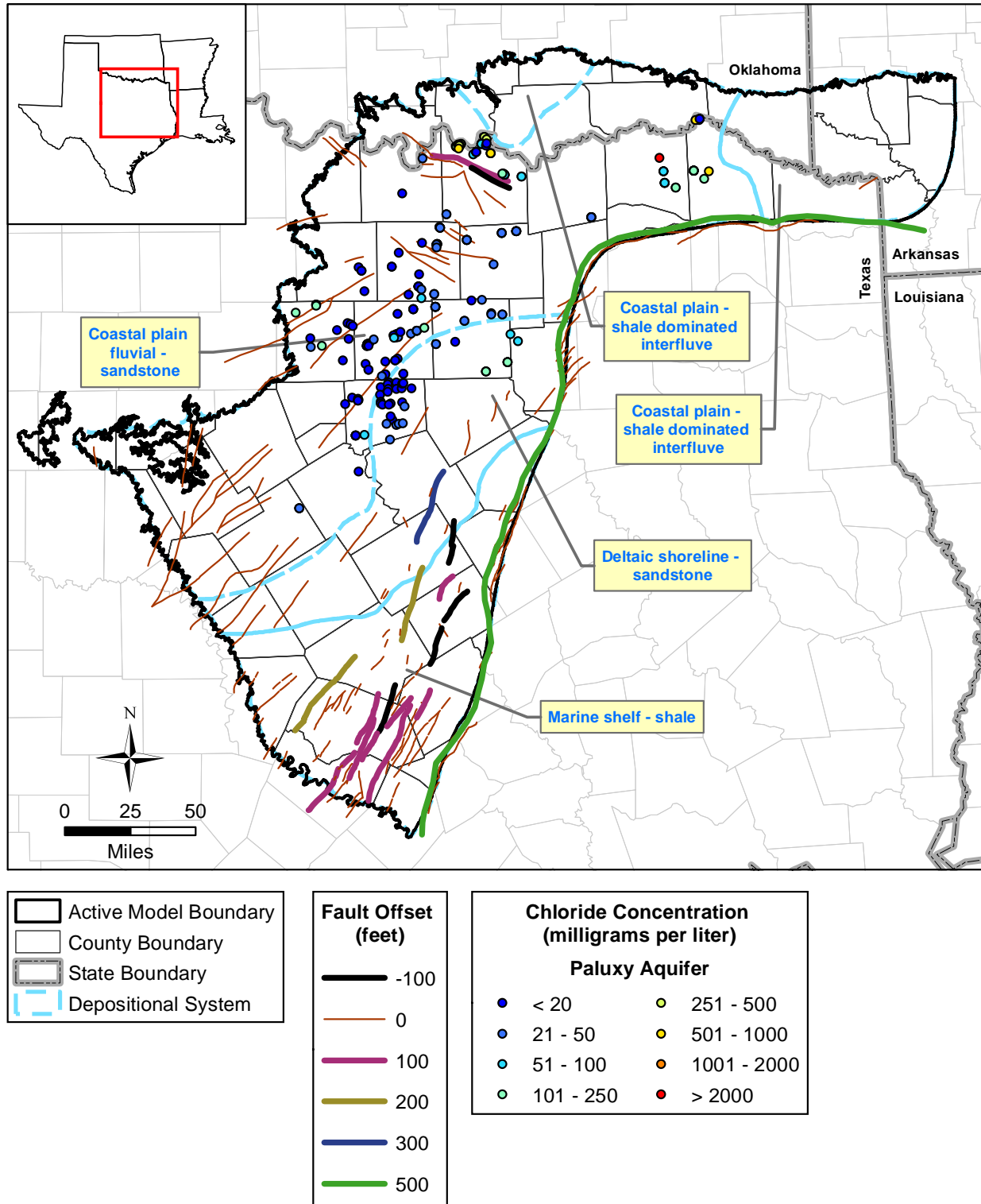
Figure 4.4.18   Chloride concentration at well locations in the Paluxy Aquifer.
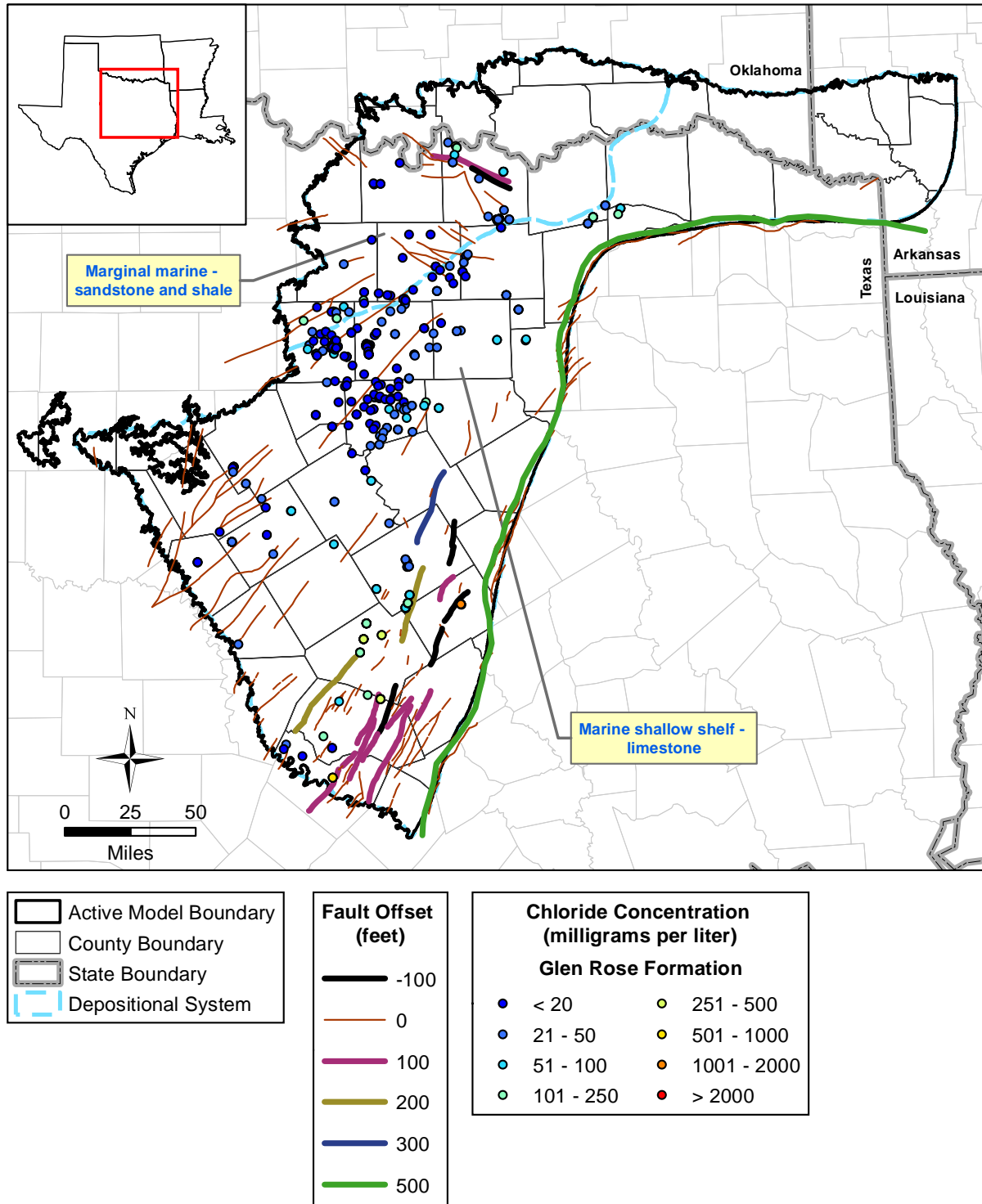
Figure 4.4.19   Chloride concentration at well locations in the Glen Rose Formation.
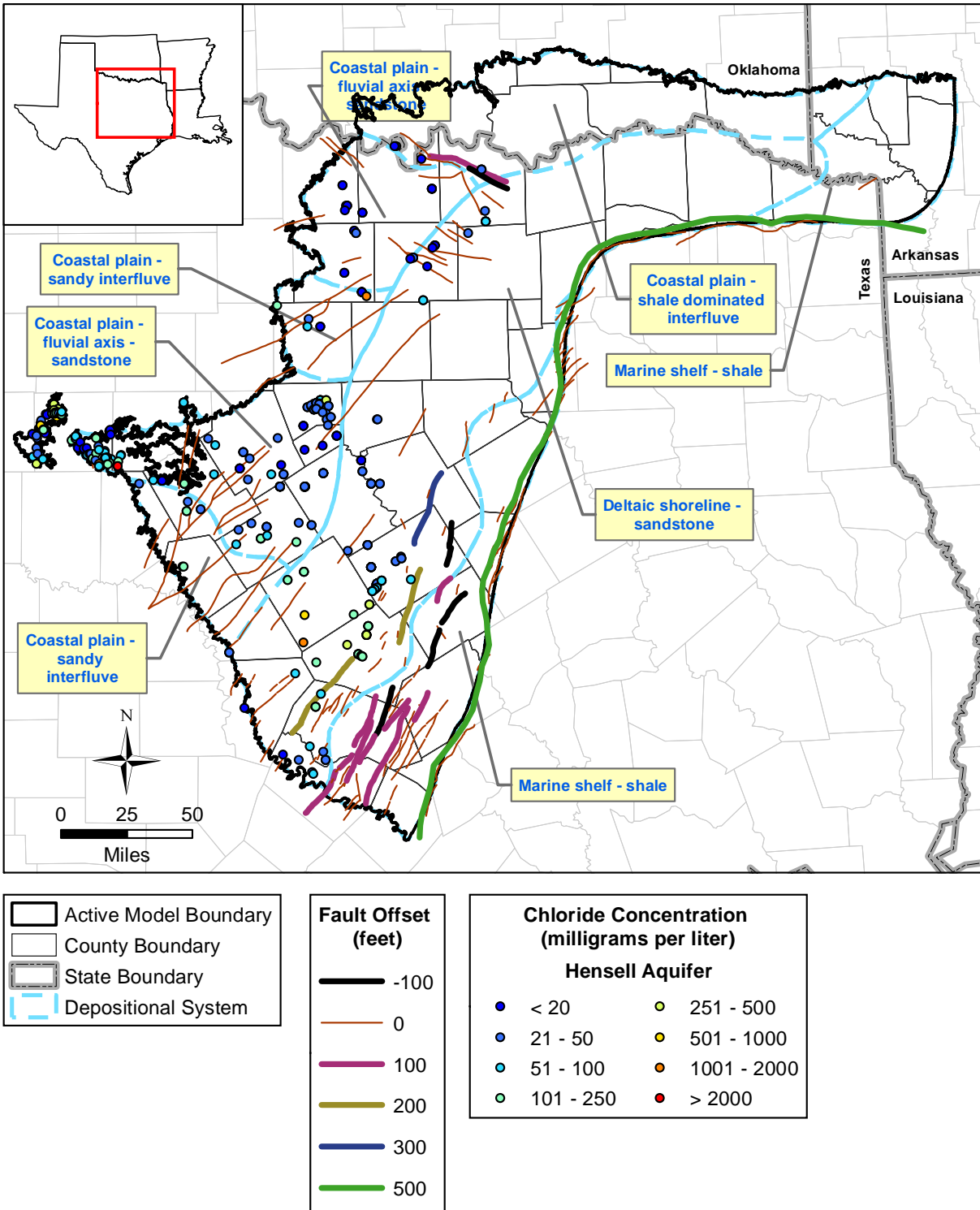
Figure 4.4.20 Chloride concentration at well locations in the Hensell Aquifer.
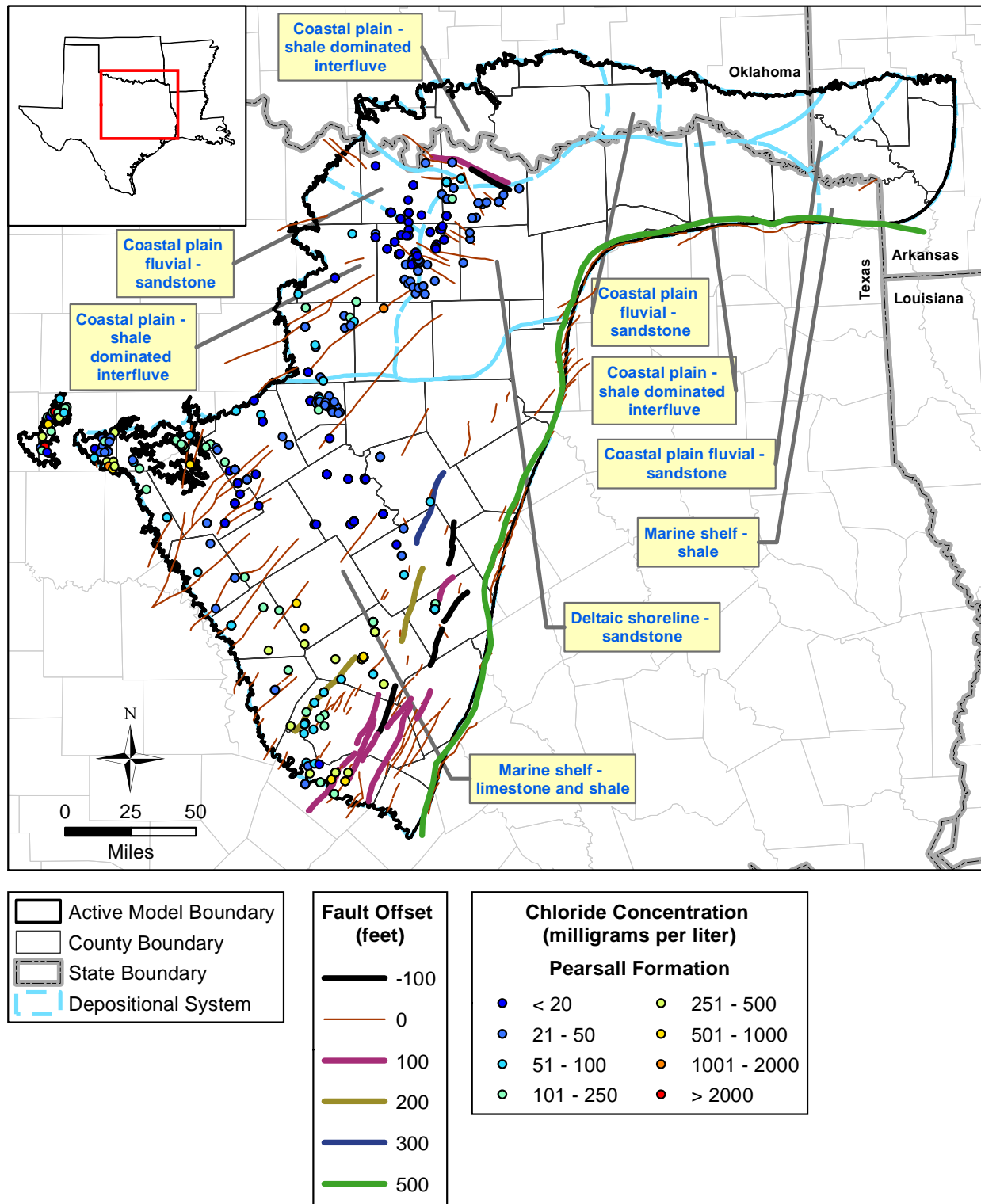
Figure 4.4.21   Chloride measurements at well locations in the Pearsall Formation.
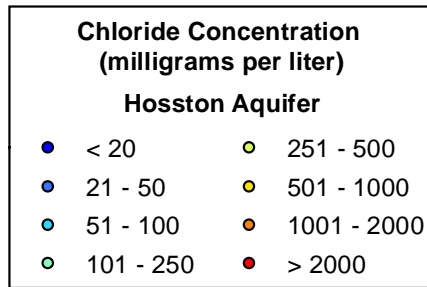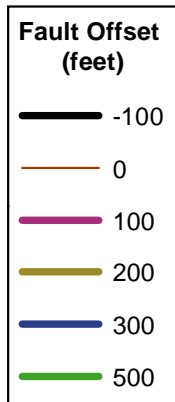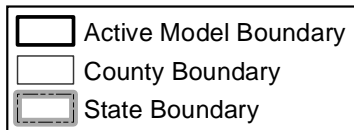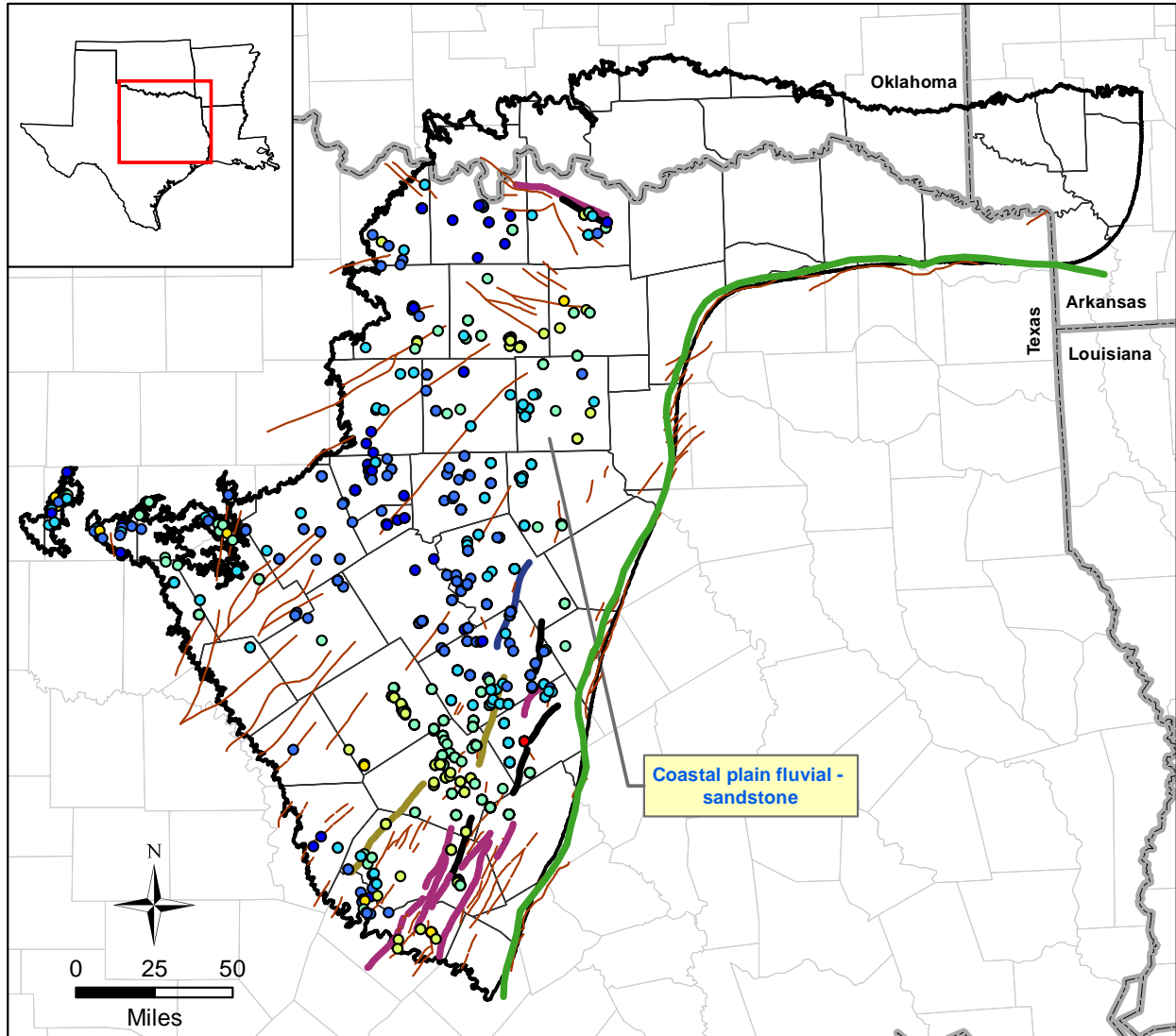
Figure 4.4.22   Chloride measurements at well locations in the Hosston Aquifer.

This page intentionally left blank.

4.5   Recharge

Recharge is defined in this study as the downward flow of water reaching the water table and increasing groundwater storage (Healy, 2010). Recharge represents the inflow to an aquifer which constrains the water balance of the system under predevelopment conditions (i.e., prior to pumping). Recharge is generally considered a rate or flux, with units of length over time similar to precipitation, and is generally reported in inches per year. The following subsections describe the conceptual understanding of recharge as it pertains to the study area; review recharge estimates from previous studies that include the study area; discuss the controls in aquifer recharge; present recharge estimated using various methods; compare recharge estimates from the various methods; and present conceptual strategies for distributing recharge spatially and temporally in the study area.

4.5.1   Conceptual Understanding of Recharge

The dominant controls on recharge include precipitation, vegetation/land use, and soil type (Keese and others, 2005). Potential sources of recharge to an aquifer include precipitation, irrigation return flow, and stream/reservoir leakage. Recharge is defined as diffuse if it is areally distributed, such as that derived from precipitation and irrigation return flow. In contrast, focused recharge occurs in localized areas, such as river or reservoir leakage. Several authors have documented or estimated reservoir leakage to the northern Trinity and Woodbine aquifers (Leggat, 1957; Klemt and others, 1975; Nordstrom, 1982). Nordstrom (1982) found evidence that the northern Trinity Aquifer was being recharged directly by leakance from Lake Texoma.

Precipitation falling on the land surface partitions into evaporation from bare soil and transpiration from vegetation, runoff, and infiltration into the soil profile. Most of the infiltrated water is lost through bare soil evaporation near the surface or from transpiration through vegetation and, generally, a small fraction of the water moves below the root zone of the vegetation to recharge the aquifer.

In subhumid regions, such as the study area for the northern Trinity and Woodbine aquifers, groundwater recharge occurs in the outcrop zone of the aquifers and groundwater discharge occurs at streams through base flow and as ET by riparian vegetation along streams. In dipping unconfined/confined aquifer systems, much of the recharge remains in the unconfined outcrop area and quickly discharges in nearby streams. However, some fraction of recharge may

penetrate deeper into the confined portion of the aquifer in the outcrop area before discharging to surficial features. A small fraction of recharge moves deeper into the confined portion of the aquifer located downdip of the aquifer outcrop area and regionally discharges through younger overlying sediments or through structural features such as faults. This smaller fraction of recharge to the confined downdip portions of an aquifer is often referred to as effective recharge.

Figure 4.5.1 is a conceptual block diagram of how precipitation may partition into the various components of the water balance described above under predevelopment conditions. This figure is generally representative of the study area and conceptual in nature. Precipitation defines the total input to the water balance and all other components shown in Figure 4.5.1 are provided as a percent of precipitation. In this schematic, only a small percentage (5 percent) of precipitation actually drains below the root zone and becomes aquifer recharge. Recharge occurs in the outcrop of the aquifer and initially is stored in the unconfined portions of the aquifer closest to ground surface. The vast majority of recharge discharges locally in the outcrop area to streams and/or springs, as groundwater ET, and/or through pumping after development begins. A small percentage of recharge (2 percent of precipitation in Figure 4.5.1) moves down into the semi-confined and confined portions of the aquifer in the outcrop area before it discharges back to surface as local discharge. A much smaller percent of recharge (less than 0.5 percent in Figure 4.5.1) flows into the confined portion of the aquifer downdip of the outcrop area and discharges regionally as diffuse discharge through younger overlying sediments or through structural features such as faults. Only a small percentage of the recharge reaches the deep aquifer. While there are various methods for estimating recharge, which are discussed below in Section 4.5.4, it is difficult to estimate how much recharge reaches the confined portions of the aquifer.

The northern Trinity Aquifer has a large outcrop area (7,634 square miles), while the Woodbine Aquifer has a smaller outcrop area (1,726 square miles). The Washita/Fredericksburg groups crop out between the northern Trinity and Woodbine aquifers with an area of 7,869 square miles. While the Washita/Fredericksburg groups are considered a confining unit over much of the study area, recharge does occur in this unit. Recharge rates are considered to be lower than for the more permeable outcrops of the northern Trinity and Woodbine aquifers. A potential exception is the Edwards BFZ Aquifer.

4.5.2 *Previous Investigations of Recharge in the Study Area*

There is limited information on measured recharge rates in the northern Trinity and Woodbine aquifers. Table 4.5.1 summarizes recharge estimates available in the literature. Recharge rates were compiled by Scanlon and others (2002a) for major aquifers in Texas. That report, however, referenced only two estimates of recharge in the northern Trinity Aquifer, with rates ranging from 0.02 to 4.4 inches per year, both of which are given in Dutton and others (1996). These estimates were based on groundwater modeling. Other references on recharge in the northern Trinity and Woodbine aquifers generally assumed a specific rate [e.g., less than 1 inch per year in Nordstrom (1982) and 0.5 inches per year in Thompson (1969) for sandy portions of the aquifer in Johnson County]. Others assumed recharge as a percentage of mean annual precipitation [i.e., 3 percent of mean annual precipitation in Klemt and others (1975), 1.5 percent of mean annual precipitation in Muller and Price (1979) and Duffin and Musick (1991)]. Klemt and others (1975) also report an estimated regional recharge to the confined portion of the Paluxy Aquifer of 0.13 inches per year (0.3 percent of precipitation) and to the confined portion of the Woodbine Aquifer of 0.3 inches per year (0.75 percent precipitation). Most of these studies do not provide information on the methods used to estimate recharge. For example, the recharge estimate by Klemt and others (1975) was simply an assumption for a model developed for the northern Trinity Aquifer.

Rapp (1988) studied recharge processes in the northern Trinity Aquifer in central Texas in the Leon, Lampasas, and Paluxy river basins. His study suggests that approximately 20 percent of recharge (5,000 AFY or 0.12 inches per year) to the northern Trinity Aquifer is derived from sandy parts of the outcrop area, representing about 25 percent of the aquifer outcrop area. He attributed the remaining 80 percent (20,000 AFY or 0.16 inches per year) of recharge to cross-formational flow through the overlying Glen Rose Formation and Fredericksburg Group based on groundwater head data and chemistry data.

Annual groundwater recharge was also estimated using a water budget approach based on remote sensing estimates of actual ET for a 50-year time period (1960 to 2009) over about a 50,000 square mile area corresponding to GMA 8 (Kirk and others, 2012). These recharge estimates are discussed in greater detail in Section 4.5.4.2.

In Oklahoma, where the northern Trinity Aquifer is termed the Antlers Aquifer, several investigators have estimated recharge through low-flow studies. Hart and Davis (1981) used low-flow discharge from Davis and Hart (1978), Westfall and Cummings (1963), and Laine and Cummings (1963) to estimate that it would require recharge of approximately 3.2 inches per year to account for the observed flows in creeks draining portions of the Antlers Aquifer outcrop. They then increased that value to account for ET and cross-formational flow, resulting in a total recharge value of 6 inches per year for the Antlers Aquifer outcrop in Oklahoma and western Arkansas.

Many estimates of recharge in the northern Trinity and Woodbine aquifers have been determined through calibration of groundwater models. When considering estimates of recharge from modeling studies, it is important to recognize what Johnston (1997) calls "the scale problem." As a general rule, for properly constrained groundwater models, the scale of the horizontal model grid and the scale and number of model layers impact the estimate of recharge that a model may predict. The model grid size is the model spatial integration scale and, if it is very large, the possibility of properly modeling recharge and discharge processes becomes problematic. As a result, very large models typically have calibrated recharge estimates that are smaller than those of finer-scale models. This is particularly true if a hydrologic system consists of significant near surface flow components, such as areas with large topographic variability and multiple small ephemeral streams and seeps. As a rule, Johnson (1997) found that the larger the model grid, the more likely that recharge would be underestimated through model calibration.

Klemt and others (1975) performed a study of the groundwater resources of a 20-county area of central Texas. As part of that study, they present an early digital groundwater model of the Hensell and Hosston aquifers. The applied recharge in the model was approximately 3 percent of precipitation. Although they did not model these aquifers, they also reported an estimated recharge rate for the Paluxy and Woodbine aquifers of 0.13 and 0.3 inches per year, respectively. Klemt and others (1975) assumed that their recharge estimates were more representative of recharge to the confined portions of the aquifer and were not representative of total recharge.

Morton (1992) developed a groundwater model of the Antlers Aquifer (northern Trinity Aquifer equivalent) in Oklahoma and Arkansas. Calibrated recharge rates ranged from 0.32 to 0.96 inches per year. Dutton and others (1996) developed two models of the northern Trinity

Aquifer near the Superconducting Super Collider site in north-central Texas. The two models focused on the Twin Mountains, Paluxy, and Woodbine aquifers. Dutton and others (1996) first developed a two-dimensional cross-section model that included the aquifers and the confining layers. The purpose of this model was to "evaluate model boundary conditions and the vertical hydrologic properties of the confining layers" (Dutton and others, 1996). The range in simulated recharge from the cross-sectional model was 0.02 to 0.5 inches per year. Because this model effectively cut out the outcrop and shallow confined portions of the aquifer, the recharge estimates would be representative of recharge to the confined portions of the aquifer downdip of the outcrop. They then developed a three-dimensional model of the aquifers using results and insights gained from the cross-sectional model. The range in recharge for that model was 2.7 to 4.4 inches per year. However, in the steady-state model, the effective recharge to the confined section downdip of the outcrop was only 0.04 inches per year.

Bené and others (2004) developed the original state GAM for the northern Trinity and Woodbine aquifers. The simulated recharge rates from the calibrated model range from 0.21 to 3.5 inches per year. Ninety-six percent of the recharge in the model discharges through groundwater ET (which was simulated to represent groundwater ET and shallow mechanisms of discharge, such as small streams and springs). Approximately 4 percent of recharge in the model discharges through simulated streams and rivers and basically zero recharge moves to the deep confined portion of the aquifer downdip of the outcrop in predevelopment conditions. The recharge numbers used in Bené and others (2004) appear reasonable given the literature.

Keese and others (2005) estimated recharge for Parker County using one-dimensional unsaturated flow modeling. There best estimate of recharge rate assuming a vegetated, texturally variable soil profile was 1.1 inches per year. The modeling analysis in their study showed the importance of soil texture and vegetation in reducing recharge because recharge as a function of precipitation alone (mean annual precipitation of 34 inches per year in the model) in bare sandy soils was as high as 16.7 inches per year. The impact of vegetation alone resulted in a recharge rate of 7.6 inches per year for vegetated sandy soils. Therefore, finer textured soils, soil textural layering, and vegetation have a large impact on actual recharge rates.

4.5.3 Controls on Aquifer Recharge

The primary controls on aquifer recharge include precipitation, soil type/surface geology, and vegetation and land use. The following describes these controls.

4.5.3.1 Precipitation

Long-term mean annual precipitation for the study area was estimated from Parameter-elevation Regressions on Independent Slopes Model (PRISM) based on gridded data (1 by 1 kilometer) for the 50-year period from 1960 through 2009 (PRISM Climate Group, 2013). This period was selected because it is the same as that considered in the recent GMA 8 recharge study conducted by HydroBio (Kirk and others, 2012). However, the HydroBio study developed kriged estimates of precipitation from the Digital Climate Atlas (TWDB, 2009) because they found that the spatial distribution of precipitation from kriging the Digital Climate Atlas data was smoother than that derived from the Parameter-elevation Regressions on Independent Slopes Model (PRISM) data. The time series from the Parameter-elevation Regressions on Independent Slopes Model (PRISM) data and the kriged Digital Climate Atlas data are highly correlated [coefficient of determination (R^2) = 0.99] (Figure 4.5.2). The following description focuses on the Parameter-elevation Regressions on Independent Slopes Model (PRISM) data because it covers the entire study area, whereas, the kriged Digital Climate Atlas data developed by Kirk and others (2012) does not extend into Oklahoma and Arkansas.

Based on the 50-year period from 1960 through 2006, precipitation contours trend north to south with increasing precipitation from west to east (Figure 4.5.3). Long-term mean annual precipitation for the entire outcrop area averages about 36 inches per year and ranges from about 26 inches per year in the westernmost outcrop areas to about 55 inches per year in the easternmost outcrop areas of Arkansas (Table 4.5.2). Mean annual precipitation values for the aquifer outcrop areas are 34 inches per year for the northern Trinity Aquifer, 35 inches per year for the Washita/Fredericksburg groups, and 40 inches per year for the Woodbine Aquifer.

4.5.3.2 Soil Physical Properties

Soil properties can have a significant impact on recharge because of their impact on runoff, infiltration, and ET. Sandy soils typically allow more infiltration for a given precipitation event than clay soils. Also, clay soils tend to retain water, allowing more time for ET by vegetation.

Information on soil texture is available from two separate sources, the State Soil Geographic (STATSGO) database (U.S. Department of Agriculture, 1994) and Soil Survey Geographic (SSURGO) database (U.S. Department of Agriculture, 1995). The spatial resolution of these products differs with a resolution of 1:250,000 for the STATSGO data and about 1:24,000 for the SSURGO data, with STATSGO representing a generalization of the more detailed SSURGO mapping. The recharge study conducted by HydroBio (Kirk and others, 2012) used permeability and depth to bedrock data from STATSGO. In this study, the higher resolution SSURGO data were used.

Important soil physical properties that can impact recharge include clay content, thickness, and permeability. In the SSURGO database, values for each of these parameters are associated with individual soil horizons (layers), with generally from 1 to 4 soil horizons constituting a soil series (or component). Individual soil series are generally represented as a single mapped polygon area (map unit), though multiple soil series (generally less than or equal to three) may also be grouped together within a map unit polygon area. The soil clay contents (expressed as a percent) and thicknesses generated for the analysis presented here represent composite values for all soil horizons in a given map unit polygon area. This was done by first vertically averaging soil series attributes using an average weighted by layer thickness within each map unit polygon area. Then the vertical composite values for each soil series were spatially averaged within a map unit polygon area weighted by the percentage each series comprised of the map unit polygon area. Mean and minimum soil permeability values represent the geometric mean of all horizons and the minimum horizon value, respectively, within each soil series spatially averaged within a map unit polygon area. Soil properties were estimated for both the outcrop areas and for the USGS gage drainage basins as they intersect those outcrop areas.

Mean soil clay content, mean soil thickness, geometric mean vertical soil permeability, and minimum soil permeability are shown in Figures 4.5.4 through 4.5.7, respectively. The lowest clay contents are observed in the northern Trinity Aquifer outcrop and in Quaternary alluvium sediments, followed by the Woodbine Aquifer and Washita/Fredericksburg groups outcrop areas (Table 4.5.3). Soil thickness is generally lower in the outcrop area of the Washita/Fredericksburg groups (mean 4.1 feet) than in the other northern Trinity and Woodbine aquifer outcrops and the Quaternary alluvium sediments (mean 5.0 to 5.9 feet). Mean soil permeability is also lowest in the Washita/Fredericksburg groups (1.8 feet per day), intermediate

in the northern Trinity and Woodbine aquifer outcrops (4 to 4.5 feet per day), and highest in the
Quaternary alluvium sediments (7.2 feet per day).

4.5.3.3   Land Use/Land Cover

Current land use/land cover for the study area is based on the 2006 National Land Cover Data
(NLCD) coverage (Fry and others, 2011) (Figure 4.5.8). An estimate of irrigated areas was
determined by Ozdogan and Gutman (2008) based on Moderate Resolution Imaging
Spectroradiometer (MODIS) satellite imagery (Figure 4.5.9). The northern Trinity Aquifer
outcrop area is dominated by natural or semi-natural vegetation, including grassland, forest, and
shrubland, which accounts for about 80 percent of the entire outcrop region. Agricultural areas
include pasture/hay (about 11 percent) and cultivated crops (about 4 percent) (Table 4.5.4).
Cultivated croplands are primarily located in Eastland, Erath, and Comanche counties and
represent the only significant irrigated agriculture in the study area. Irrigated areas also account
for about 4 percent of the northern Trinity Aquifer outcrop area, and are primarily focused in the
same counties as the cultivated croplands.

The same land cover types that dominate the northern Trinity Aquifer outcrop area also dominate
the Washita/Fredericksburg groups outcrop area in similar proportions, with about 75 percent
native or semi-native vegetation, about 9 percent pasture/hay, and about 4 percent crops.
However, there is less forest and shrubland and more grassland relative to the northern Trinity
Aquifer outcrop. Croplands in the Washita/Fredericksburg groups outcrop are located in the area
north of Fort Worth in Denton and Cooke counties and also in the southeast along the edge of the
outcrop area in Hill, McLennan, Coryell, and Bell counties. Irrigated areas represent only
2.2 percent of the outcrop area and are generally dispersed evenly throughout the region.

The Woodbine Aquifer outcrop is the most urban area, with about 18 percent of the outcrop area
classified as developed land, primarily the Fort Worth metropolitan area. Forests and grasslands
combine to account for about 54 percent of the outcrop area while pasture/hay represents about
24 percent. This large percentage of pasture mostly reflects the Oklahoma portion of the
outcrop, which, like the other outcrop areas outside of Texas, is dominated by pasture/hay and
forest. The percentage of forest increases and pasture/hay decreases toward the east in the
Woodbine Aquifer outcrop in Oklahoma and Arkansas. Very little of the Woodbine Aquifer
outcrop is cultivated. Most of the cultivated cropland and irrigated areas are located in a narrow

band along the Red River, which is obscured by the state boundary line symbology in
Figures 4.5.8 and 4.5.9.

Developed land, generally the result of urbanization, is a potentially important land use when
considering recharge to an aquifer. The outcrops of the Woodbine Aquifer and the
Washita/Fredericksburg groups are most impacted. Urbanization undoubtedly changes the
recharge and runoff patterns of previously undeveloped land; however, quantifying that effect on
groundwater recharge is difficult. Generally, increasing impervious surfaces leads to higher run-
off and "flashier" streamflow, while decreasing groundwater recharge and groundwater
contributions to streamflow (Leopold, 1968; Dunne and Leopold, 1978; Harbor, 1994).
However, secondary urbanization effects, such as leaking water distribution and wastewater
systems, increased irrigation, or infiltration through retention ponds, can actually increase urban
groundwater recharge (Lerner, 2002; Garcia-Fresca, 2006). Leakage from old or poorly
constructed water supply and sewage systems is particularly pronounced in developing countries
(e.g., Al-Sefry and Sen, 2006) but can be significant even in water distribution systems in the
U.S. (Garcia-Fresca and Sharp, 2005). Removing woodland and vegetation during development
reduces the amount of water lost to evapotranspiration, which can also lead to an additional
increase in urban groundwater levels (Forman, 2014).

These conflicting impacts result in a heavy dependence on the individual characteristics of a
particular urban area when quantifying the net effect of that urbanization on groundwater
recharge. Calculating the effect of urbanization on recharge involves large amounts of uncertain
data that can vary first with location, due to differences in water distribution infrastructure and
land surface, and second with time, due to changes in climate or land use (Lerner, 2002).
Urbanization has, therefore, been considered the cause of both increased urban groundwater
recharge (Appleyard and others, 1999; Hooker and others, 1999; Garcia-Fresca, 2006) as well as
decreased urban groundwater recharge (Rose and Peters, 2001; Bosch and others, 2003). Lerner
and others (1990) also note that in some areas, the increase in urban recharge can essentially
offset the loss of recharge due to impervious surfaces, resulting in little or no net impact on
groundwater recharge.

Without detailed investigation of the urban areas in the study area, quantifying the net change to
groundwater recharge due to urbanization is difficult. Therefore, for the purposes of this study,

the simplified relationship presented in U.S. Environmental Protection Agency (EPA) (1993) was used to represent the changes to the water cycle imposed by urbanization. Even though some of the urban areas in the study area are very densely developed, the least developed option in the U.S. Environment Protection Agency relationship (10 to 20 percent impervious surface) was chosen in order to account for the size variation between the developed areas in the study area. This also offers the most conservative estimate of the reductive impact of impervious surfaces, since this may be counteracted by artificial urban recharge. This scenario limits changes to a 10 percent increase in runoff, a 2 percent decrease in ET, and 4 percent reductions to shallow and deep infiltration (U.S. Environmental Protection Agency, 1993).

4.5.4 Methods of Recharge Estimation

Recharge can be estimated using a variety of different methods. The following subsections provide estimates of recharge using various methods. In each case, the limits of the method are discussed.

4.5.4.1 Stream Hydrograph Separation Method

Stream hydrograph separation analysis (sometimes referred to as base flow analysis) was conducted on 36 stream gages and associated watersheds intersecting the outcrop of the northern Trinity and Woodbine aquifers and the Washita/Fredericksburg groups. Of these 36, 34 stream gage records and associated base flow estimates were considered robust. A complete discussion of the hydrograph separation analysis can be found in Section 4.6.1.4. Aquifer discharge to streams, or base flow, is considered to be a lower bound estimate of aquifer recharge because aquifer recharge discharges through other processes including groundwater ET, spring discharge, cross-formational flow in the regional confined section downdip of the outcrop, and pumping capture. Therefore, the stream hydrograph separation method is considered to provide a lower bound for aquifer recharge.

An estimate of the amount of recharge required to sustain the base flow of a stream was calculated by dividing the average volumetric base flow (i.e., base flow in AFY) by the drainage area to obtain base flow in inches per year. The average annual recharge estimates from the hydrograph separation analysis are given in Table 4.5.5. Recharge estimates ranged from 0.2 to 2.9 inches per year. Figure 4.5.10 shows the estimated average recharge by watershed for the gages analyzed by hydrograph separation. In Texas, these values compare favorably to Scanlon

and others (2002a), which places average recharge to the northern Trinity Aquifer at 0.1 to

2 inches per year based on a compilation of past studies in the Texas portion of the study area. A

quick review of Figure 4.5.10 shows that the recharge values tend to be higher in the wetter

northern portion of the study area as compared to the southern and southwestern portions of the

study area. The range in average annual precipitation for the northern watersheds is 37 to

57 inches per year, whereas the range in average annual precipitation for the southern watersheds

is 31 to 36 inches per year. This trend of higher recharge in areas of higher precipitation is in

agreement with the positive correlation expected between recharge and precipitation.

Figure 4.5.11 plots the annual base flow (log scale) as a function of precipitation (linear scale)

for two stream gages analyzed in the study area, which confirms this relationship.

The process of hydrograph separation uses the stream discharge records of a stream gage. The

estimate of base flow is associated with the area of the entire watershed upstream of the gage. A

review of Figure 4.5.10 shows that the watersheds that feed many of the gages in Oklahoma and

Arkansas largely fall north of the northern extent of the study area. Therefore, there is greater

uncertainty in the applicability of the recharge estimates for these watersheds because they

represent an integrated average recharge estimate for all formations within the watershed

upstream of the stream gage. Therefore, the recharge estimates for these watersheds are

considered to provide an upper bound for recharge.

4.5.4.2   Water Balance Method

Water balance methods are widely used to estimate recharge (Scanlon and others, 2002b).

However, uncertainties in each of the water balance components accumulate in the recharge

estimate and the uncertainty can often exceed the recharge rate (Gee and Hillel, 1988). A

detailed water budget approach was used by Kirk and others (2012) to estimate annual

groundwater recharge over about a 50,000 square mile area corresponding to GMA 8. Their

analysis was conducted using precipitation, stream discharge, and actual ET from remote sensing

over a 50-year time period (1960 to 2009). The equation they used to estimate groundwater

recharge is:

$$GWr = P - Q - ET_a \qquad\qquad\qquad\qquad (4.5.1)$$

where

GWr = groundwater recharge

P = precipitation

Q = total discharge

ET_a = actual ET

Total discharge includes runoff and base flow to streams (rejected recharge in the outcrop area); therefore, the estimated recharge is the residual recharge for the confined part of the aquifer downdip of the outcrop.

Kirk and others (2012) estimated annual actual ET using the Remotely-sensed Dual Coefficient (RDC) method based on Moderate Resolution Imaging Spectroradiometer (MODIS) data for wet and dry conditions. The range of actual ET was estimated for a record wet year (2007 with precipitation of 48.7 inches) and a record dry year (2005 with precipitation of 24.3 inches). Surface water and soil moisture storage changes were assumed to be negligible at annual timescales. Kirk and others (2012) estimated reference or potential ET using either Moderate Resolution Imaging Spectroradiometer (MODIS) for years with sufficient meteorological data or using a regression between precipitation and reference ET interpolated across the study area. They also estimated runoff from precipitation and estimated infiltration from precipitation and calculated runoff. The methodology they used for estimating reference ET, runoff, and infiltration are provided in Appendix A of Kirk and others (2012).

Actual ET was estimated by Kirk and others (2012) using a remotely sensed dual coefficient method:

$$ET_a = \sum (K_{cb} \times ET_0 + K_e \times ET_0)\, tn \tag{4.5.2}$$

where

K_{cb} = canopy factor

ET_0 = reference or potential ET

K_e = soil surface factor

n = crop type

t = time step

Normalized Difference Vegetation Index (NDVI) was used to relate the canopy factor and the soil surface factor based on data for a dry year (2005) and a wet year (2007) using Moderate Resolution Imaging Spectroradiometer (MODIS) and Landsat images. Kirk and others (2012)

calibrated actual ET against ground-based estimates of actual ET from the AmeriFlux network. They estimated reference ET from the meteorological data at flux towers using the Food and Agriculture Organization of the United Nations (FAO) Penman-Monteith method (Allen and others, 1998). Regressions were performed for different types of vegetation coverages, including (1) woody perennial vegetation (e.g., forests and shrubland), (2) non-woody perennial vegetation (e.g., grasslands and savannahs), and (3) cultivated crops (both irrigated and nonirrigated). Actual ET for other years was estimated by simpler interpolation based on precipitation.

Kirk and others (2012) used kriged precipitation data from the Digital Climate Atlas (DCA) (TWDB, 2009) rather than data from Parameter-elevation Regressions on Independent Slopes Model (PRISM) because of local spatial variability in the Parameter-elevation Regressions on Independent Slopes Model (PRISM) data. Runoff was calibrated for selected unregulated watersheds and then extrapolated to the entire GMA 8 region using permeability data from STATSGO.

Results from the Kirk and others (2012) study for the entire study area show that reference ET, which is controlled by meteorological forcing, is high, ranging from 50.4 inches per year (2007) to 61.2 inches per year (1963) (see Figure 4.5.2). Inter-annual variability in reference ET is relatively low. Reference ET is inversely correlated with precipitation [coefficient of determination $(R^2) = 0.98$]. Inter-annual variability in annual mean precipitation is high, ranging from 21.5 inches per year in 1963 to 48.7 inches per year in 2007. The years 2005 (24.3 inches per year) and 2007 (48.7 inches per year) represent almost the entire range in observed mean annual precipitation in the study area, both temporally and spatially. Differences in area-averaged precipitation from kriged Digital Climate Atlas (DCA) and Parameter-elevation Regressions on Independent Slopes Model (PRISM) data are minor (0.84 inches per year). Actual ET estimated by Kirk and others (2012) is plotted on Figure 4.5.2 and, as would be expected, is much lower than reference ET, ranging from 35 percent in 1963 to 68 percent in 2007. Actual ET is also highly correlated with precipitation [coefficient of determination $(R^2) = 0.93$]. Other estimates of actual ET are available from the National Aeronautics and Space Administration (NASA) National Land Data Assimilation System (NLDAS) models (Mosaic and Noah) (see Figure 4.5.2). Mitchell and others (2004) provide a summary of these data sets and methods. These methods are referred to as Land Surface Models and they simulate ET using an energy water budget approach. ET from the MOSAIC and NOAH models compare well with the

estimates of Kirk and others (2012). As a water balance component, variability in annual actual ET is relatively low (standard deviation 2.8 inches; coefficient of variation 0.09).

Recharge estimates from the water budget equation used in Kirk and others (2012) represent net recharge to the confined portion of the aquifer downdip of the outcrop because their total discharge (see Equation 4.5.1 above) represents total streamflow, including base flow or rejected recharge in the outcrop zone. Recharge to the confined portions of an aquifer downdip of the outcrop is not an input to a numerical groundwater model but can be used as a constraint in calibration. Kirk and others (2012) include maps of recharge for their entire study region for 2005 (Figure 4.5.12), representing the driest year during their study period, and for 2007 (Figure 4.5.13), representing the wettest year during their study period. During 2005, the results of the HydroBio study indicate essentially no recharge throughout the entire study area with the exception of a very few isolated locations in the south. During 2007, their study results indicate recharge occurred over wide portions of the study area, though with a patchwork distribution and with apparently no recharge occurring over much of the northern Trinity Aquifer outcrop regions in Texas, Oklahoma, and Arkansas. With regard to the outcrop areas of the current study, most recharge during this wet year was focused in only the central outcrop areas in Oklahoma, in the Woodbine Aquifer outcrop area in Texas, and generally in the southern outcrop areas of the northern Trinity Aquifer and Washita/Fredericksburg groups.

The distribution of mean annual recharge for the entire period of the study for Kirk and others (2012) (Figure 4.5.14) is generally similar to the 2007 map, though with somewhat overall lower values and generally more widespread recharge in Oklahoma, Arkansas, and northeast Texas. However, the Kirk and others (2012) study results also indicate zero mean recharge for much of the northern Trinity Aquifer outcrop area in Texas. Most recharge in Texas generally ranges between 0.25 and 2 inches per year and occurs primarily in the southern Washita/Fredericksburg groups outcrop area, with generally lower amounts in the Woodbine Aquifer outcrop area south of the Red River. Mean annual recharge rates in the Oklahoma and Arkansas outcrop area generally range from 1to 4 inches per year, transitioning to a small region of zero recharge in the far west.

The water budget approach was also applied to the watersheds where recharge was estimated using base flow in this study. Actual ET from Kirk and others (2012) is only available for 1960

through 2009 and the time periods for hydrograph separation for individual watersheds were often prior to this period because the streams were unregulated at these earlier times. However, inter-annual variability in actual ET is generally low (see Figure 4.5.2); therefore, applying average actual ET should provide an estimate of recharge for the watersheds. In 50 percent of the basins, however, annual mean actual ET exceeded annual mean precipitation (Table 4.5.5).

Table 4.5.5 shows the difficulty in using the water balance method to estimate recharge. Ideally, runoff and actual ET could be subtracted from precipitation to obtain an estimate of total recharge minus the consideration of groundwater ET, which is considered small relative to actual ET. From Table 4.5.5, it can be seen that this calculation gives a negative result in every case, suggesting that the long-term actual ET error has a magnitude far larger than the recharge rate. In addition to the inherent difficulty in estimating recharge by this method, other factors of the Kirk and others (2012) analysis add to uncertainty and the apparent non-physical results. For instance, the actual years where base flow and runoff were calculated do not match with the years that were averaged to estimate actual ET. Also, if the analysis was performed on a smaller time step (i.e., monthly or even daily), periods of the year when the water balance results in a recharge surplus might be expected. This could be interpreted to be times when recharge to the confined portion of the units downdip of the outcrop would be possible. However, actual ET was only available on an annual basis from Kirk and others (2012).

Kirk and others (2012) concluded their study with a series of recommendations for future analysis of groundwater recharge and for treatment of groundwater recharge in future groundwater models. Some of the key recommendations based on their study and potential applicability to the current study are (Kirk and others, 2012):

- They suggest moving away from using precipitation as the primary climatic forcing function for recharge and use precipitation divided by reference ET. As shown later in this section, reference and actual ET are highly correlated variables and recharge as estimated from hydrograph separation was most highly correlated to precipitation.
- They suggest incorporating a memory function for soil moisture to enable antecedent soil moisture conditions to affect recharge variation. This is a good idea but very difficult to apply to a groundwater model with an annual time step. Without detailed vadose zone modeling and field study, this estimate of soil moisture would be totally unconstrained.

- They also suggested that there be an evaluation of the effect of the 2011 die-off of cedar as a result of the bark beetle and drought and for a re-assessment of groundwater recharge (recharge to the deep confined portion downdip of the outcrop in their study) within urbanized areas using high resolution remote sensing data and local scale calibration. Both of these ideas may have merit, but are outside the scope of this study.

4.5.4.3   Chloride Mass Balance (CMB) Method

Groundwater chloride concentrations can be used to estimate recharge rates using the following equation (Scanlon and others, 2002b):

$$R = P \times \frac{Cl_P}{Cl_{gw}} \tag{4.5.3}$$

where

R = recharge

P = mean annual precipitation

Cl_P = chloride concentration in precipitation

Cl_{gw} = chloride concentration in groundwater

Precipitation data representing the mean from 1980 to 2010 were obtained from Parameter-elevation Regression on Independent Slopes Model (PRISM) data (PRISM Climate Group, 2013). Data on chloride concentrations in precipitation were obtained from the National Atmospheric Deposition Program (2013) that has been operating a national network of precipitation monitoring stations beginning in the late 1970s through the present, including 23 stations in Texas, Oklahoma, Arkansas, and Louisiana surrounding the study area.

Several sources of data were used for groundwater chloride concentrations (Table 4.5.6). The primary source with by far the most data was the TWDB groundwater database (TWDB, 2013a), which provided significant numbers of data points on groundwater quality in the Texas portions of the northern Trinity Aquifer (4,360 wells) and Woodbine Aquifer (770 wells). In the northern Trinity Aquifer, water-quality analysis was limited to shallow wells completed at depths less than or equal to 150 feet (1,325 wells) to limit the influence of potential mixing with water from greater depths. The samples used represent the latest available for a given well, with sample dates ranging from 1923 to 2007 and having an average sample date of 1975.

Information on groundwater quality in the Oklahoma and Arkansas portions of the study area was limited to a small number of samples in the USGS National Water Inventory System (NWIS) database (USGS, 2013a) (12 samples) and to sample data for 54 wells published in Hart and Davis (1981). The USGS NWIS database also provided sample data for the northern Trinity Aquifer (30 wells) and Woodbine Aquifer (8 wells) in Arkansas, most completed in the confined sections to the south of the outcrop areas. Where completion data were not available for a well [all of the Hart and Davis (1981) data and six wells in the USGS NWIS database], wells were assigned to the aquifer outcrop associated with their physical location.

Kriging was used to generate separate continuous grid coverages of CMB recharge rates for the Texas portions of the northern Trinity and Woodbine aquifer outcrop areas. There were insufficient data to perform kriging in the Texas outcrop area of the Washita/Fredericksburg groups and for all aquifer outcrop areas in Oklahoma and Arkansas. CMB recharge rates for these data are shown for the well point locations.

Northern Trinity Aquifer CMB Recharge

Kriging results for the Texas outcrop area of the northern Trinity Aquifer yield a mean recharge rate of 0.76 inches per year, ranging from 0.03 to 6.4 inches per year (Figure 4.5.15). The spatial mean recharge rate is greater than the mean of the well point data used to generate the grid coverage (0.48 inches per year). This may reflect the effects of well clustering. In general, CMB recharge rates are lower along the western edge of the outcrop area and increase toward the east. The largest area with the greatest recharge rates is located in Parker, Hood, Somervell, and Erath counties, where rates generally range from 0.5 to 2.0 inches per year. A similar range of recharge rates is found in the eastern outcrop area in Montague and Wise counties in the north and in Burnet and Travis counties, adjacent to the Colorado River, in the south.

Chloride data for the northern Trinity Aquifer are comparatively limited in the Oklahoma and Arkansas outcrop area. However, the available data indicate much higher CMB recharge rates in this region, with an overall mean recharge rate of 2.9 inches per year, ranging from 0.04 to 8.9 inches per year. Recharge rates are lower in the western regions of the Oklahoma outcrop area (about 0.5 to 1.0 inches per year) and increase toward the east (about 2 to 4 inches per year), with highest mean recharge rates in the Arkansas area (about 9 inches per year).

Woodbine Aquifer CMB Recharge

Kriging results for the Texas outcrop area of the Woodbine Aquifer yield a mean recharge rate of 0.70 inches per year, ranging from 0.04 to 1.6 inches per year (Figure 4.5.15), slightly higher and generally more uniformly distributed than in the northern Trinity Aquifer outcrop area. The spatial mean recharge rate is identical to the mean of the well point data used to generate the grid coverage (0.70 inches per year). In general, CMB recharge rates are higher to the north and south of the urban (Fort Worth) regions of the outcrop area and decrease again toward the north approaching the Red River.

Groundwater chloride data are even more limited in the Woodbine Aquifer outcrop area than the northern Trinity Aquifer outcrop area in Oklahoma and Arkansas. The available data, only six wells in Oklahoma and nine wells in Arkansas, also suggest much higher CMB recharge rates in these areas than in Texas, averaging 1.7 inches per year and ranging from 0.02 to 5.0 inches per year, with lower recharge rates in the Oklahoma outcrop area (about 0.6 inches per year) increasing toward the east with higher mean recharge rates in the Arkansas area (about 2.6 inches per year).

Washita/Fredericksburg Groups CMB Recharge

Groundwater sample data in the TWDB database for wells in the Washita/Fredericksburg groups are limited to 21 wells, almost entirely in the southern portion of the outcrop area in Texas (Figure 4.5.15). The CMB recharge rates are relatively high, with a mean of about 1.5 inches per year and range from 0.05 to 3.8 inches per year. The 32 wells located in the outcrop area in Oklahoma indicate a mean recharge rate of 1.3 inches per year, ranging from 0.12 to 7 inches per year, again showing a general increasing pattern from west to east.

4.5.4.4 Evaluation of Other Sources of Chloride to Groundwater

Application of the CMB method generally involves the assumption that chloride is derived solely from precipitation; however, previous studies suggest additional sources of chloride in the study area. One of the earliest studies by Klemt and others (1976) provides a map of areas contaminated with brine and tabulates data on brine disposal from the Railroad Commission of Texas. Nordstrom (1982) lists historic concentrations of chloride in individual geological units and cites the source as most likely oil field brines. Nordstrom (1987) assumed oil field brines contributed to measured chloride in Brown, Callahan, Eastland, and Comanche counties. Water-

quality improvements over time in some wells in the recharge areas were attributed to flushing caused by recharge. O'Rourke and others (2011) report on anthropogenic contamination for all Texas aquifers and identify several areas within the northern Trinity and Woodbine aquifers that have been impacted by human activity. The predominant contaminants were chloride and nitrate.

Prior to 1969 (and since the 1920s), produced brine in connection with oil and gas was disposed in unlined open pits in porous and permeable sands of the northern Trinity Aquifer. TDS values as high as 100,000 to 200,000 milligrams per liter were found in adjacent water wells. Baker and others (1990a) noted leakage from the overlying Glen Rose Formation contributing chloride to groundwater and suggested oil field brine as the most likely source. A more recent study by Chauduri and Ale (2013) characterized groundwater quality, showing increases in chloride along the groundwater flow path from the recharge area of the northern Trinity Aquifer downdip to the confined region of the aquifer. They attributed the degradation of water quality primarily to natural processes, including mineral weathering and ion-exchange. Increases in chloride concentrations along the flow path also coincide with changes from fluvial to deltaic depositional conditions. Shallow chloride sources were assumed to be associated with past oil and gas activities, industrial and domestic effluents, septic tanks, and sewage disposal practices commonly associated with urban development.

Other potential sources of chloride in the study area, in addition to oil and gas activities, include halite dissolution and upward flow from deeper aquifers having more saline water. In the High Plains Aquifer of Texas in areas northeast of Amarillo, chloride to sulfate ratios much greater than one are spatially associated with upwelling of saline water from deeper units (Scanlon and others, 2010). Long term mean chloride to sulfate mass ratios (milligrams per liter chloride divided by milligrams per liter sulfate) in wet precipitation in the study area generally range from 0.1 to 0.25 based on sampling data provided by National Atmospheric Deposition Program (2013). Chloride to sulfate ratios vary widely in the outcrops in the study area, with values ranging generally between 2 to 4 in the western outcrop area of the northern Trinity Aquifer with decreasing ratios generally toward the east. Ratios in the Woodbine Aquifer are generally less than one and are more consistent with ratios in precipitation (Figure 4.5.16).

Though the cause of the noted west to east trend from generally higher to generally lower chloride to sulfate ratios is unclear, these ratios do not seem to suggest pervasive cross-formational flow and mixing of deeper, saline rich water. The large area of high ratios in the western most northern Trinity Aquifer outcrop area is generally associated with the densest region of cultivated agriculture in the study area. Increased recharge following conversion from natural to agricultural land uses has been shown to mobilize salt inventories in the unsaturated zone that may have been accumulated over thousands of years (Scanlon and others, 2010). Chloride is more mobile than sulfate under these conditions, which would lead to an increase in groundwater chloride concentrations relative to sulfate concentrations resulting from increased recharge following land use conversion (Scanlon and others, 2007).

Additionally, nitrate-N in groundwater is generally associated with and results from surface or near surface anthropogenic activity and is particularly associated with agricultural fertilizers, concentrated animal feeding operations, and septic systems. Figure 4.5.17 plots the probability of exceeding the nitrate-N groundwater standard of 4 milligrams per liter based upon water quality samples from wells less than or equal to 150 feet in depth. The method used to determine the probability is non-parametric which offers two advantages. It does not assume a normal distribution of nitrate-N concentrations and the method can also use detection limits in the analysis as long as they are below the exceedance level one is analyzing. For this data set, the method offers an advantage over looking at raw concentrations. The relative spatial distribution of elevated (greater than 4 milligrams per liter) groundwater nitrate-N concentrations generally parallels that of the chloride to sulfate ratio distribution (Figure 4.5.17), suggesting that both may have resulted from relatively recent anthropogenic activity.

Leakage from brine disposal pits and mud pits related to oil and gas well drilling activity was evaluated, particularly that which occurred prior to regulation requiring lining of these pits in 1969. A simple calculation shows that mixing a regional groundwater sample having 20 milligrams per liter of chloride with only 0.1 percent oil field brine having a typical concentration of 50,000 milligrams per liter of chloride would increase the chloride in the sample to 70 milligrams per liter. The chloride to sulfate ratio would increase by a factor of 2.5, and the calculated CMB recharge rate would decrease by the same factor. Data from the Information Handling Services well database (Information Handling Services, 2013) indicate that 23,470 oil and gas wells have been drilled in the northern Trinity Aquifer outcrop (Information Handling

Services, 2013). Regions with high density well drilling activity with up to about two to 10 wells per square mile include the western most northern Trinity Aquifer outcrop area in Callahan, Eastland, Brown, and Comanche counties, generally coincident with the region of densest cultivated agriculture (Figure 4.5.18). A second area of high density well drilling activity occurred further north in regions of Jack, Wise, Montague, and Cooke counties. The oil and gas well density distribution also parallels the distribution of elevated chloride to sulfate ratios. The Information Handling Services database also indicates that 6,851 oil and gas wells were drilled in the Woodbine Aquifer outcrop, with the highest well density in eastern Cooke County, also coincident with the greatest chloride to sulfate ratios in that region.

Application of the CMB method to estimating recharge rates is complicated by anthropogenic activity in different regions of the aquifer outcrop areas, as supported by co-location of increased chloride to sulfate ratios in groundwater with areas of higher density oil and gas drilling activity and with agricultural activity and by co-location of elevated nitrate-N in groundwater with regions having the most intensive cultivated agriculture. CMB recharge rates in these regions would, therefore, represent minimum values and higher CMB recharge rates in regions removed from these activities may, therefore, be more representative of the outcrop areas in general.

4.5.4.5   Tritium Concentrations in the Northern Trinity and Woodbine Aquifers

Tritium concentrations alone cannot be used directly to calculate recharge rates. However, the presence of elevated tritium concentrations in groundwater indicates that a component or percentage of that groundwater was recharged since the 1952 to 1963 period when atmospheric nuclear weapons testing resulted in increased atmospheric tritium concentrations and fallout in precipitation. The TWDB database has 129 analyses for tritium concentrations in the northern Trinity and Woodbine aquifers for wells located in the Texas region of the study area, with analysis dates ranging from 1990 to 2006 (TWDB, 2013a) (Figure 4.5.19). Values are reported in the database in both picocuries per liter and tritium unit units (1 tritium unit equals 3.22 picocuries per liter). For this analysis, tritium units are used and analyses that are generally in excess of about 0.5 tritium units are considered to have a component of "young" water present in the sample.

There are 87 tritium samples in the northern Trinity Aquifer in the study area (Figure 4.5.19). Unfortunately, the earliest sampling campaign in 1990, consisting of 48 samples collected from

shallow wells (mean depth of 122 feet and range of 50 to 333 feet) completed in the northern Trinity Aquifer in Erath County, used an analytical method with a very poor detection limit of 1,000 tritium units, which is orders of magnitude greater than required to obtain useable information for recharge estimation. The remaining 39 samples were obtained in 2003 from wells completed over a wide spatial area of the aquifer in both outcrop and downdip areas at depths ranging from 48 to 3,366 feet (mean 1,259 feet). A component of young water was indicated for eight of these samples, all taken from wells located along the western edge of the northern Trinity Aquifer outcrop area and completed at depths ranging from 48 to 200 feet (mean 117 feet). Tritium concentrations in these wells ranged from 0.71 to 7.42 tritium units. All of the remaining wells had concentrations ranging from -0.14 to 0.14 tritium units.

Tritium sampling of the Woodbine Aquifer is spatially very limited. A sampling campaign was conducted in 1993 in two small portions of the Woodbine Aquifer outcrop area located within the Fort Worth urban area. A total of 38 shallow wells were sampled, with a mean depth of 57 feet and a range from 14 to 225 feet. A component of young water was found in 23 (61 percent) of these wells, with values ranging from 2.2 to 11.2 tritium units, while the remaining 15 wells had values less than or equal to 0.3 tritium units. Four deep wells completed downdip in the confined portion of the Woodbine Aquifer at depths ranging from 700 to 1,475 feet were later sampled in 2006 and no component of young water was indicated, with reported tritium concentrations ranging from -0.04 to 0.05 tritium units.

4.5.5   Results and Discussion

The following discussions provide a comparison of estimated recharge rates using the methods discussed in Section 4.5.4. The first subsection compares recharge estimates from the hydrograph separation analysis to those using the CMB method. The second subsection compares recharge estimates from the hydrograph separation analysis to those using the SSURGO soil data and precipitation.

4.5.5.1   Comparison of Recharge Estimates from the Hydrograph Separation Analysis and the CMB Method

Comparison of the recharge rates based on different methods indicates that, in general, recharge rates derived from the CMB method are higher than those derived from the hydrograph separation analysis, with only a few individual basins in the northern Trinity Aquifer outcrop area showing close agreement between the two methods (Table 4.5.7, Figure 4.5.20). This may

be due in part to poor coincidence of the respective analysis areas, with the CMB method generally covering only a relatively small percentage of the drainage areas. Greater variability in estimates using the CMB method as compared to the hydrograph separation analysis is expected.

An alternate way to compare the recharge estimates from the hydrograph separation analysis and the CMB method is to review the simple statistics of range and arithmetic average between the two methods. Table 4.5.8 provides such a comparison. A review of this table shows that the CMB method predicts a mean recharge rate of 0.76 inches per year in Texas for the northern Trinity Aquifer as compared to 1.0 inches per year from the hydrograph separation analysis. In both instances, the average is probably biased low. In the case of the CMB method, this would be the result of anthropogenic contaminants. In the case of the hydrograph separation analysis, this is because the gages analyzed in Texas are all located south of Hood County. The CMB method predicts a mean recharge rate of 1.7 inches per year in Oklahoma and Arkansas for the northern Trinity Aquifer as compared to 3.6 inches per year for the hydrograph separation analysis. The hydrograph separation analysis in Oklahoma and Arkansas is considered to have higher uncertainty than the Texas gage analyses because of the relatively small percentage of northern Trinity Aquifer outcrop represented by many of the gage watersheds analyzed. Both methods show an increase in average recharge from south to north. The ranges associated with the CMB method are higher than for the hydrograph separation analysis, which is to be expected given the nature of the scale of measurement between the two.

A review of Table 4.5.8 shows that the CMB method predicts a mean recharge rate of 0.76 inches per year in Texas for the Woodbine Aquifer as compared to 0.37 inches per year from the hydrograph separation analysis. It is possible that the average from the CMB method is biased low as a result of urbanization in the north and anthropogenic contaminants. In the case of the hydrograph separation analysis, the estimates are biased low because the three gages analyzed in the Woodbine Aquifer outcrop are all located south of southern Tarrant County. The Woodbine Aquifer becomes thinner and less transmissive due to a thinning of sands and a corresponding increase in clay content.

The CMB method predicted an average recharge for the Woodbine Aquifer in Oklahoma and Arkansas of 2.9 inches per year. This area is largely non-urban, so the expectation for anthropogenic sources of chloride is minimal. This compares reasonably well with the

hydrograph separation average recharge estimate for the northern Trinity and Woodbine aquifers in Oklahoma and Arkansas of 3.8 inches per year.

4.5.5.2   Comparison of Recharge Estimates from the Hydrograph Separation Analysis and from the SSURGO Soil Parameters and Precipitation

Multiple linear regression models were constructed using the SSURGO soil and precipitation data in Table 4.5.9. The variables reference ET and actual ET from the HydroBio study are highly correlated with precipitation. As such, it is not appropriate to include more than one of these variables in a single model. Substitution of either reference ET or actual ET for precipitation in the regression models produces similar results, though precipitation produces the highest statistical significance. Results indicate that if precipitation and the soil variables are all included in the model, only precipitation and mean soil thickness contribute significantly to predicting hydrograph separation recharge, though the inclusion of soil thickness only marginally increases model predictability by about 5 percent and precipitation alone accounts for 76 percent of variation of hydrograph separation recharge. Alternatively, if only the three SSURGO soil parameters are incorporated into a model, mean soil permeability is the only significant parameter, explaining 59 percent of variation of hydrograph separation recharge.

The dominance of precipitation as the important variable controlling groundwater recharge, as opposed to surface infiltration, is perhaps most clearly shown through a single multiple-linear regression analysis assuming recharge is the dependent variable and precipitation and the SSURGO soil properties are independent variables. This analysis of the data in Table 4.5.9 shows that with 95 percent confidence that the dominant factor influencing recharge is precipitation. The only other variable that shows any statistically significant importance is the mean soil column thickness but it is shown to be relatively unimportant compared to precipitation. These results indicated that precipitation is the dominant regional variable controlling recharge, with soil thickness playing a secondary role at a more local scale.

4.5.6   Spatial and Temporal Recharge Model

This section discusses the conceptual framework for the recharge model. The approach ultimately implemented in model calibration is discussed in Section 6.3.4of this report. The previous sections discussed the conceptual basics of recharge and some of the potential variables that can influence recharge, such as precipitation, soil properties, underlying geology, and land

use. This information was used to develop a conceptual framework for the application of recharge in the model from both a spatial and a temporal sense.

There are many potential spatial variables that may impact recharge. The discussion in Section 4.5.5.2 shows that the most important spatial variable is precipitation, which spatially varies significantly across the study area (see Figure 4.5.3). Soil thickness (see Figure 4.5.5) and perhaps to a lesser degree soil permeability (see Figures 4.5.6 and 4.5.7) can influence recharge at the more local scale. Soil texture, permeability, and thickness are related to the parent geologic material at the ground surface. In isolated areas of the study area, land use is considered an important spatial variable. Based upon the highest nitrate-N concentrations being spatially in the counties with some of the most irrigated acreage, return flows are also considered as a recharge factor in these counties (especially Callahan, Eastland, Brown, and Comanche counties). The degree of urbanization in the Dallas-Fort Worth Metroplex would be expected to have an impact on recharge during post development.

The strongest spatial and temporal variable considered in the recharge model was precipitation. The spatial range of long-term average precipitation (Figure 4.5.3) is nearly matched by the average annual precipitation in the study area (Figure 4.5.2). The range in annual average precipitation in the outcrop areas is approximately 29 inches and the inter-annual variability in annual average precipitation in the study area is approximately 27 inches per year (Kirk and others, 2012). A review of Figures 4.5.10 and 4.5.11 shows that the average recharge predicted by stream gage hydrograph separation is strongly correlated to annual average precipitation. As a result, the recharge estimates from the stream gage hydrograph separation analysis (presented in detail in Section 4.6.1.4) was used as the fundamental basis of the spatial, and temporal, model for recharge. Recharge determined from this method certainly has uncertainty and that uncertainty, is believed to be greatest in the watersheds in eastern Oklahoma (see Section 4.5.4.1). The advantage of hydrograph separation estimates of recharge is that they provide an integrated recharge estimate over a large area of outcrop. In that sense, they average local natural variability in recharge that is often poorly understood without local field studies and which would be averaged in a regional groundwater model anyway.

As discussed in Section 4.5.4.1, the northern watersheds resulted in higher recharge estimates than the southern watersheds. This trend is also observed in average annual precipitation. This

observation suggests that any relationship between precipitation and recharge should have a spatial component. For the purposes of developing a recharge model, the study area was divided into northern and southern areas, which generally coincide with areas where good hydrograph separation data are available (Figure 4.5.21). The area between the northern and southern area, where hydrograph separation data are not available, is termed the central area. A relationship between precipitation and recharge for the northern portion of the study area and the southern portion of the study area was developed using data only from that portion (Figure 4.5.21).

A linear regression was fit to recharge as a function of precipitation for the northern and southern portions of the study area. That regression fit results in the relationship:

$$\log(\text{recharge}) = m(\text{precipitation}) + b \tag{4.5.4}$$

The log transformation of recharge (base flow in inches per year) was performed because the empirical trend (see Figure 4.6.15) looks linear on a semi-log plot. The results for the slope and intercept of the regression for all watersheds analyzed in the northern portion are shown in Table 4.5.10. The results for the slope and intercept of the regression for all watersheds analyzed in the southern portion are shown in Table 4.5.11.

Using the mean slope and intercept, a simple relationship was constructed for the northern and southern portions of the study area between recharge (base flow) and precipitation. The initial relationship derived by just using the mean slope and intercept for the northern portion is:

$$\log(\text{base flow}) = 0.02(\text{precipitation}) - 0.27 \tag{4.5.5}$$

The initial relationship derived by just using the mean slope and intercept for the southern portion is:

$$\log(\text{base flow}) = 0.05(\text{precipitation}) - 1.87 \tag{4.5.6}$$

Both relationships are plotted in Figure 4.5.22. These relationships are considered valid within their range of fit values, which is covered by the maximum and minimum annual average recharge plotted.

In the central portion of the study area, no unregulated perennial stream gages with greater than 10 years of continuous data are available (see Section 4.6.1.4). As a result, a spanning relationship between the northern and southern portions of the study area had to be developed. To do this, a weight that would determine the reliance on the southern relationship versus the

northern relationship was used. Exactly in the middle of the central portion of the study area the
equation would be:

$$\log(\text{base flow}) = 0.5(0.02(\text{precipitation}) - 0.27) + 0.5(0.05(\text{precipitation}) - 1.87) \quad (4.5.7)$$

The weights in Equation 4.5.7 are 0.5, representing a half and half mix. The convention to
define the weights was to set it at zero at the southern edge of the central portion of the study
area and one at the northern edge of the central portion of this study area. The generic equation
for estimated shallow recharge in the central portion is:

$$\log(\text{base flow}) = (1\text{-Weight}) (0.02(\text{precipitation}) - 0.27) + \text{Weight} (0.05(\text{precipitation}) - 1.87) \quad (4.5.8)$$

In Figure 4.5.22, two vertical lines, corresponding to the range in average annual precipitation,
where each equation was used are shown. The equation for the southern portion was used for
annual average precipitation values less than 32 inches per year. The equation for the northern
portion was used for annual average precipitation greater than 44 inches per year. Between these
two precipitation values, a mix of these two relationships was used in the central portion of the
study area.

Figure 4.5.23 plots the estimated average annual recharge based upon the hydrograph separation
analysis. This figure shows that it ranges from approximately 5.4 inches per year in the north to
a low of less than 0.5 inches per year in the west. Based upon the developed recharge model,
there are average annual precipitation values in the extreme northeastern portion of the study
area that would predict greater than 7 inches of annual average recharge. This amount of
recharge was considered extreme. For this reason, the high end of recharge in the northern
portion was restricted to the highest value derived from the hydrograph separation analysis.

Figure 4.5.24 plots a color-flood showing the regression slope of each watershed for the
relationship of log recharge (derived from base flow) versus watershed precipitation rate (both in
inches per year). This spatial representation of the slopes clearly shows distinct differences in
the slopes of these relationships between the northern and southern watersheds. This again
confirms the approach of treating the northern and southern data sets separately with two
different recharge regression models. The difference in the regression slopes very likely has
significance regarding the hydrology of the two regions. The northern portion has lower slopes
to the relationship between recharge as a function of precipitation. This could imply that

watersheds and recharge reacts less strongly or directly to changes in precipitation than those in the south. In drier climates, streams might be expected to be flashier and for streamflows, and base flows, to be more variable and more directly tied to variability in precipitation.

Equation 4.5.8 defines the initial recharge model for the updated northern Trinity and Woodbine aquifers GAM. The single most important variable for recharge rate is precipitation. Other spatial variables considered secondary in importance, such as soil properties, land use or outcropping geologic formation, were also considered in model calibration.

Precipitation varies not only spatially, but as a function of time. Because the recharge function is derived from regressions between recharge and precipitation, this function allows recharge to be varied as a function of time as climate varies. The approach used to develop the base recharge model averages the variability within any given watershed between precipitation and calculated base flow. As a result, the model generally produces lower variability in simulated base flow than observed in the raw data.

The volume of recharge associated with an assumed recharge rate is calculated as the recharge rate multiplied by the area over which the recharge rate occurs. Assuming a typical county area of 900 square miles, a recharge rate of 0.5 inches per year equates to a recharge volume of 24,000 AFY. Assuming the county receives the annual average precipitation for the study area (36.4 inches per year), this recharge rate is approximately 1.4 percent of the annual average precipitation. The math is linear, so a recharge rate of 1.5 inches per year over a typical county area equates to 72,000 AFY of recharge representing 4.1 percent of the average annual precipitation.

Table 4.5.1   Summary of recharge rates from the literature for the northern Trinity and Woodbine aquifers.

Recharge Rate (in/yr)	Range in Recharge Rate (in/yr)	Method[a]	Percent of Precipitation	Reference
NR	≤ 1	Water Balance	NR	Nordstrom (1982)
0.5	NR	Water Balance	NR	Thompson (1969)
1.2	0.13 to 1.2	Water Balance	0.3 to 3	Klemt and others (1975)
NR	NR	Water Balance	1.5	Muller and Price (1979)
NR	0.12 – 0.16	Darcy Flow	NR	Rapp (1988)
NR	NR	Water Balance	1.5	Duffin and Musick (1991)
1.1	NR	Vadose Modeling	NR	Keese and others (2005)
NR	-0 to 0.25 and 2 in/yr. (TX) 1 to 4 in/yr. (OK & AR)	Water Balance – areally distributed across TX, OK, & AR	Mapped values	Kirk and others (2012)
NR	NR	GIS Analysis – Water Balance	Mapped values	Wolock (2003b)
NR	NR	BF / Water Balance	4	Ashworth (1983)
NR	NR	BF / Water Balance	11	Kuniansky (1989)
NR	NR	BF / Water Balance	6.7	Bluntzer (1992)
NR	NR	BF	6.6	Mace and others (2000)
6	NR	Adjusted low flow studies in OK	NR	Hart and Davis (1981)
NR	0.32 – 0.96	GW Model	NR	Morton (1992)
NR	0.02 to 0.5	GW Model - Cross-sectional model	NR	Dutton and others (1996)
NR	2.7 – 4.4	GW Model - 3D groundwater model	NR	Dutton and others (1996)
NR	0.21 – 3.5	GW Model	NR	Bené and others (2004)
NR	NR	GW Model	7	Kuniansky and Holligan (1994)
NR	NR	GW Model	4	Mace and others (2000)

[a] method used to estimate recharge

NR = not reported
OK = Oklahoma
BF = Stream hydrograph separation (base flow) analysis

GW = Ground Water
AR = Arkansas

TX = Texas
in/yr = inches per year

Table 4.5.2   Outcrop areas and minimum, maximum, mean, and median annual precipitation within those areas for the period 1960 to 2009 based on Parameter-elevation Regressions on Independent Slopes Model (PRISM) data (PRISM Climate Group, 2013).

Outcrop	Area (mi[2])	Area (Percent of Total)	Minimum (in/yr)	Maximum (in/yr)	Mean (in/yr)	Median (in/yr)
Northern Trinity Aquifer	7,634	36.9	25.5	55.0	34.3	32.2
Wash/Fred groups	7,869	38.0	25.5	51.0	34.8	34.2
Woodbine Aquifer	1,726	8.3	34.6	53.5	40.3	38.7
Quaternary	3,057	14.8	27.9	54.5	39.5	37.6

Wash/Fred = Washita/Fredericksburg   mi[2] = square miles
Quaternary = Quaternary-age sediments   in/yr = inches per year

Table 4.5.3   Weighted mean SSURGO soil parameters in the outcrop areas.

Outcrop	Clay Content[a] (percent)	Thickness[a] (feet)	Mean Permeability[a] (feet per day)	Minimum Permeability[a] (feet per day)
Northern Trinity Aquifer	31 (17-46)	5.0 (1.8-6.7)	4.5 (0.4-17)	4.1 (0.3-17)
Wash/Fred groups	40 (24-51)	4.1 (1.2-6.7)	1.8 (0.1-6.5)	1.7 (0.1-6.3)
Woodbine Aquifer	34 (19-47)	5.7 (3.9-6.7)	4.0 (0.1-15)	3.6 (0.1-15)
Quaternary	31 (11-50)	5.9 (4.3-6.7)	7.2 (0.1-25)	6.9 (0.1-24)

[a] Values in parenthesis represent the 5th to 95th percentile range.
Wash/Fred = Washita/Fredericksburg
Quaternary = Quaternary-age sediments

Table 4.5.4   Land use/land cover percentages for the entire outcrop area and the individual outcrop areas.

Category	All areas	Northern Trinity Aquifer	Wash/Fred Groups	Woodbine Aquifer	Other[a]
Developed	9.1	6.6	10.8	17.5	6.5
Forest	23.5	27.8	19.1	24.6	23.6
Grassland	36.9	35.5	45.1	29.3	25.2
Shrubland	10.8	16.8	10.8	0.2	2.5
Barren	0.2	0.1	0.2	0.1	0.5
Water	2.4	0.4	0.4	0.9	11.8
Wetland	1.4	0.6	0.7	1.1	5.2
Pasture	11.3	8.6	8.0	24.2	18.4
Crops	4.4	3.5	4.9	2.1	6.3
Irrigated	3.6	4.2	2.2	2.1	6.0

[a] Sum of all Quaternary-age alluvium, younger, and water covered regions
Wash/Fred = Washita/Fredericksburg

Table 4.5.5   Comparison of base flow (i.e., recharge estimate from hydrograph separation analysis), runoff, precipitation, and actual ET for selected gaged drainage basins.

USGS Gage ID	Site Name	Drainage Area (mi²)	Base flow[a] (in/yr)	Runoff (in/yr)	Precipitation (in/yr)	Actual ET (in/yr)
07332500	Blue River near Blue, OK	477	2.5	9.0	40.9	33.8
08048970	Village Creek at Everman, TX	85	0.5	6.4	34.2	30.7
08049700	Walnut Creek near Mansfield, TX	63	0.3	4.9	34.8	31.6
08091500	Paluxy River at Glen Rose, TX	410	0.6	2.3	28.0	29.9
08093500	Aquilla Creek near Aquilla, TX	308	0.4	5.3	34.3	31.9
08095000	North Bosque River near Clifton, TX	968	0.5	2.8	29.0	30.6
08095300	Middle Bosque River near McGregor, TX	182	1.6	5.8	30.5	29.6
08095400	Hog Creek near Crawford, TX	78	1.6	6.2	32.5	29.4
08099500	Leon River near Hasse, TX	1261	0.2	1.8	26.3	29.5
08100500	Leon River at Gatesville, TX	2342	0.4	1.6	24.8	29.5
08101000	Cowhouse Creek at Pidcoke, TX	455	0.7	3.0	28.9	28.9
08102500	Leon River near Belton, TX	3582	0.7	2.5	27.0	29.5
08103800	Lampasas River near Kempner, TX	818	0.9	2.6	27.5	28.5
08104000	Lampasas River at Youngsport, TX	1240	1.1	3.1	28.5	28.5
08104700	North Fork San Gabriel River near Georgetown, TX	248	1.8	4.7	30.0	28.9
08104900	South Fork San Gabriel River at Georgetown, TX	133	2.0	5.4	32.5	29.5
08105000	San Gabriel River at Georgetown, TX	405	1.9	4.5	28.3	29.1
08105100	Berry Creek near Georgetown, TX	83	1.6	4.1	32.3	29.2
08154700	Bull Creek at Loop 360 near Austin, TX	22	2.9	8.5	32.3	30.8

[a] Base flow in inches per year provides the estimated recharge rate from a hydrograph separation analysis

TX = Texas   mi² = square miles
OK = Oklahoma   in/yr = inches per year

Table 4.5.6   Source of groundwater chloride concentration data.

Aquifer	Number of Samples		
	TWDB (2013a)	USGS (2013a)[a]	Hart and Davis (1981)[b]
Northern Trinity Aquifer	1325	35	
Woodbine Aquifer	769	8	
Wash/Fred Groups	21	1	
Unknown	-	6	54

[a] 12 wells in Oklahoma and 38 wells in Arkansas
[b] data did not include information indicating the producing aquifer

Wash/Fred = Washita/Fredericksburg groups

Table 4.5.7   Comparison of hydrograph separation recharge rates with intersecting outcrop area groundwater CMB recharge rates.

Gage ID	Outcrop Area	Analysis Area (mi^2)	Mean CMB (in/yr)	Drainage Area (mi^2)	Percent Area Analyzed	Hyd. Sep. Rech.[a] (in/yr)
08091000	northern Trinity	765	2.2	25,818	3	0.1
08091500	northern Trinity	366	1.7	410	89	0.6
08095000	northern Trinity	369	2.0	968	38	0.5
08099500	northern Trinity	732	1.4	1,261	58	0.2
08100500	northern Trinity	220	1.0	2,342	9	0.4
08101000	northern Trinity	162	0.7	455	36	0.7
08102500	northern Trinity	26	0.3	3,582	1	0.7
08103800	northern Trinity	440	1.0	818	54	0.9
08104000	northern Trinity	258	0.9	1,240	21	1.1
08104700	northern Trinity	114	0.9	248	46	1.8
08104900	northern Trinity	45	0.7	133	34	2.1
08154700	northern Trinity	5	1.2	22	24	2.9
08048970	Woodbine	35	1.3	85	41	0.5
08049700	Woodbine	53	0.8	63	84	0.3
08093500	Woodbine	115	0.5	308	37	0.4

[a] hydrograph separation recharge estimate

Trinity = Trinity Aquifer   in/yr = inches per year
Woodbine = Woodbine Aquifer   mi^2 = square miles

Table 4.5.8   Comparison of range and mean recharge rates (inches per year) as determined from the hydrograph separation analysis and the CMB method.

Recharge Estimation Method	Northern Trinity Aquifer - Texas		Northern Trinity Aquifer - Oklahoma/Arkansas		Woodbine Aquifer – Texas		Woodbine Aquifer – Oklahoma/Arkansas	
	Mean (in/yr)	Range (in/yr)	Mean (in/yr)	Range (in/yr)	Mean (in/yr)	Range (in/yr)	Mean (in/yr)	Range (in/yr)
Chloride Mass Balance	0.76	0.03-6.4	1.7	0.04-8.9	0.76	0.04-1.6	2.9	0.02-5
Hydrograph Separation	1.01	0.12-2.9	3.6	0.6-5.4	0.37	0.28-0.47	NA	NA

NA = not applicable
in/yr = inches per year

Table 4.5.9 **Hydrograph separation analysis estimated recharge, Parameter-elevation Regressions on Independent Slopes Model (PRISM) precipitation, and mean soil thickness, permeability, and clay content for USGS gage drainage areas intersected with study outcrop areas.**

USGS Gage ID	Hyd. Sep. Recharge[a] (in/yr)	PRISM Precipitation (in/yr)	SSURGO Mean Thickness (feet)	SSURGO Mean Perm (ft/day)	SSURGO Mean Clay (percent)	HydroBio[b] P/ET$_0$ (ratio)	HydroBio[b] ET$_a$ (in/yr)
7332400	4.71	40.4	5.7	11.5	25.9	0.84	33.6
7332500	2.55	42.6	5.2	7.6	34.4	0.85	33.8
7335000	1.25	41.7	5.5	10.2	33.2	0.88	32.8
7336500	2.71	49.7	5.7	18.1	23.1	1.04	31.7
7337500	3.65	51.7	5.4	18.0	23.1	1.15	33.3
7338000	4.24	52.2	5.4	9.4	25.9	1.10	34.8
7338500	3.75	50.9	5.4	8.0	28.7	1.08	35.1
7339000	4.81	55.2	5.1	12.8	24.6	1.11	36.5
7339500	3.78	54.9	5.7	8.7	31.5	1.13	36.0
7340000	4.88	51.5	5.8	8.5	28.3	1.09	36.4
7340500	4.63	56.8	5.2	10.0	26.5	1.15	35.6
7341000	4.12	56.3	5.9	9.0	24.0	1.16	36.3
7341200	3.37	53.3	5.8	9.8	25.6	1.14	37.5
7360800	3.24	54.2	6.0	8.6	28.8	1.15	34.8
7361000	5.39	58.0	6.4	14.0	24.2	1.17	35.3
8048970	0.47	34.6	5.9	1.3	37.3	0.63	30.7
8049700	0.28	35.3	5.8	1.3	37.5	0.66	31.6
8091000	0.12	22.6	4.8	2.0	31.3	0.55	30.2
8091500	0.58	31.5	4.1	1.7	35.7	0.55	29.9
8093500	0.37	35.7	6.2	2.5	31.4	0.65	31.9
8095000	0.53	32.7	4.1	1.4	37.9	0.58	30.5
8095300	1.62	34.3	4.1	1.3	40.2	0.60	29.7
8095400	1.63	34.1	3.9	0.9	42.5	0.60	29.3
8099500	0.22	29.3	5.1	1.4	29.9	0.49	29.5
8100500	0.37	31.7	5.3	1.9	33.0	0.56	29.5
8101000	0.67	30.3	4.7	2.1	34.6	0.52	28.9
8102500	0.72	34.0	4.3	2.5	37.5	0.61	30.9
8103800	0.92	30.0	4.7	2.1	35.9	0.51	28.5
8104000	1.10	31.7	4.4	1.9	39.6	0.54	28.6
8104700	1.77	32.3	2.9	1.6	40.0	0.56	28.9
8104900	2.05	32.7	3.0	1.5	42.0	0.57	29.5
8105000	1.89	34.9	3.4	1.4	50.3	0.62	29.6
8154700	2.88	32.8	2.7	3.5	36.5	0.60	31.1

[a] hydrograph separation recharge estimate
[b] Kirk and others (2012)

P = precipitation   ET$_a$ = actual ET   ET$_0$ = reference ET
in/yr = inches per year   ft/day = feet per day

Table 4.5.10 Regression data for each stream gage in the northern portion of the study area.

Gage	Lag (months)	R²	Intercept	Slope
7332400	3	0.62	-0.06	0.02
7332500	3	0.70	-0.61	0.02
7335000	3	0.56	-0.88	0.02
7336500	0	0.57	-0.44	0.02
7337500	1	0.82	-0.50	0.02
7338000	0	0.60	-0.07	0.01
7338500	1	0.81	-0.43	0.02
7339000	0	0.62	-0.11	0.01
7339500	1	0.59	-0.16	0.01
7340000	1	0.74	-0.20	0.02
7341000	1	0.67	-0.22	0.01
7340500	1	0.71	-0.03	0.01
7341200	1	0.66	-0.50	0.02
7360800	1	0.58	-0.13	0.01
7361000	1	0.43	0.28	0.01
Average	**1.2**	**0.65**	**-0.27**	**0.02**

R^2 = coefficient of determination

Table 4.5.11 Regression data for each stream gage in the southern portion of the study area.

Gage	Lag (months)	R²	Intercept	Slope
8048970	3	0.62	-1.55	0.03
8049700	4	0.29	-2.19	0.04
8091500	3	0.45	-1.52	0.04
8093500	2	0.42	-2.04	0.04
8095000	3	0.42	-2.58	0.07
8099500	4	0.63	-2.79	0.07
8100500	3	0.69	-3.61	0.10
8102500	0	0.51	-2.27	0.07
8095400	2	0.65	-1.64	0.05
8095300	2	0.63	-1.33	0.04
8101000	4	0.54	-2.59	0.07
8103800	3	0.30	-1.05	0.03
8104000	3	0.61	-2.00	0.06
8105100	3	0.70	-1.70	0.05
8104700	4	0.59	-1.10	0.04
8105000	4	0.52	-1.78	0.06
8104900	3	0.68	-1.38	0.05
8154700	2	0.80	-0.60	0.03
Average	**2.9**	**0.56**	**-1.87**	**0.05**

R^2 = coefficient of determination
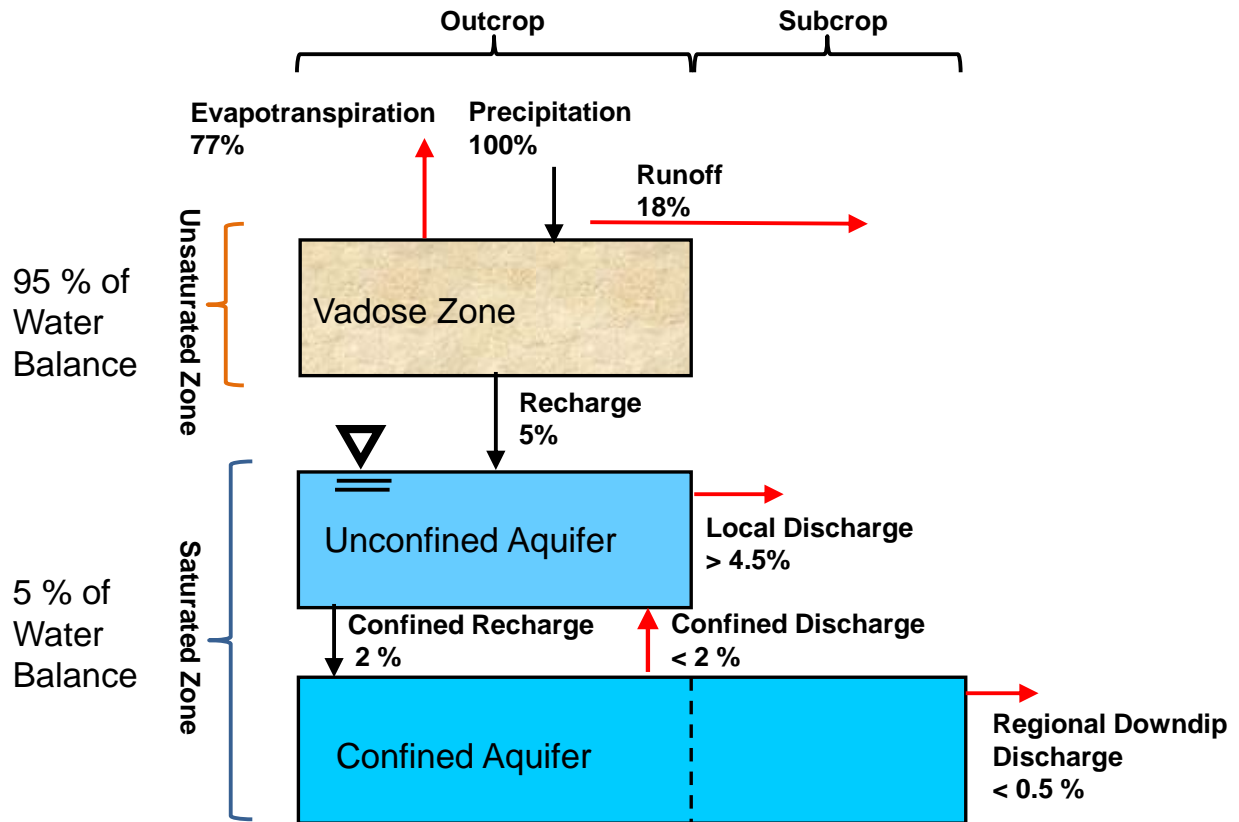
Figure 4.5.1   **Conceptual block diagram of a representative average water balance in the study area showing the partitioning of precipitation flux into the other components of the hydrologic system.**
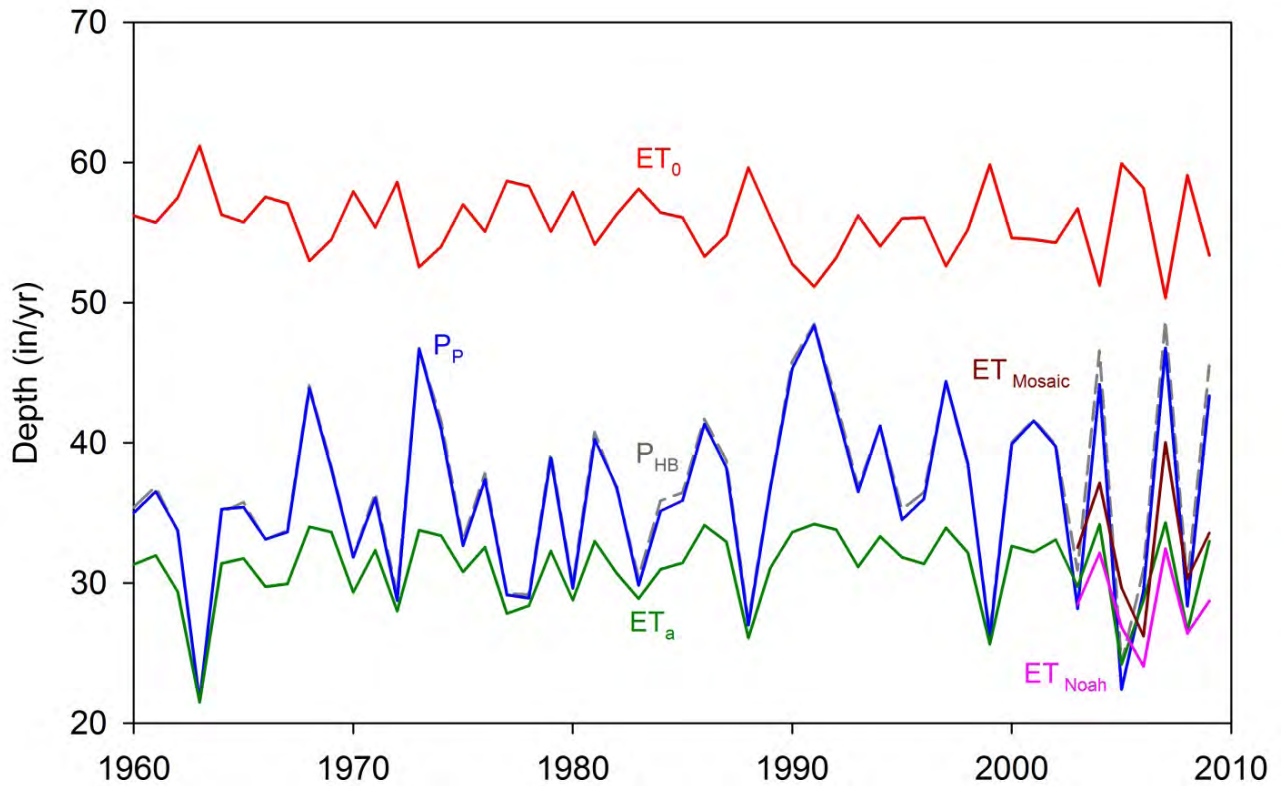
ET_0 = reference ET
P_P = precipitation from Parameter-elevation Regressions on Independent Slopes Model (PRISM) data
(solid blue line)
P_{HB} = precipitation from Kirk and others (2012) (dashed gray line)
ET_a = actual ET from Kirk and others (2012)
ET_{Mosaic}= ET from National Aeronautics and Space Administration (NASA) Mosaic model
ET_{Noah} = ET from National Aeronautics and Space Administration (NASA) Noah model
in/yr = inches per year

**Figure 4.5.2   Temporal variation in regional annual precipitation (P), actual ET (ETa), and
reference or potential ET (ET$_0$) depths.**
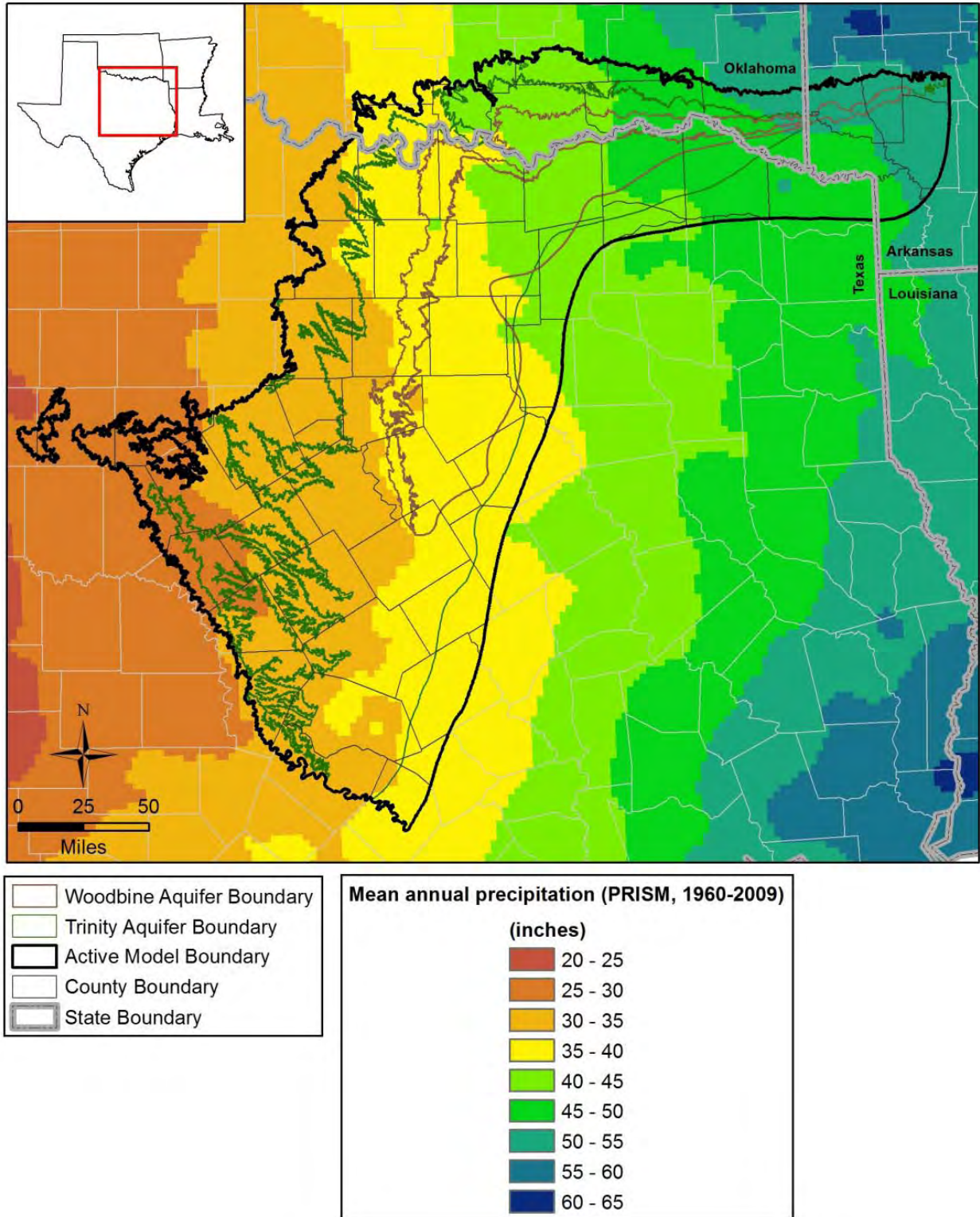
Figure 4.5.3 **Mean annual precipitation in the study area and vicinity (PRISM Climate Group, 2013).**
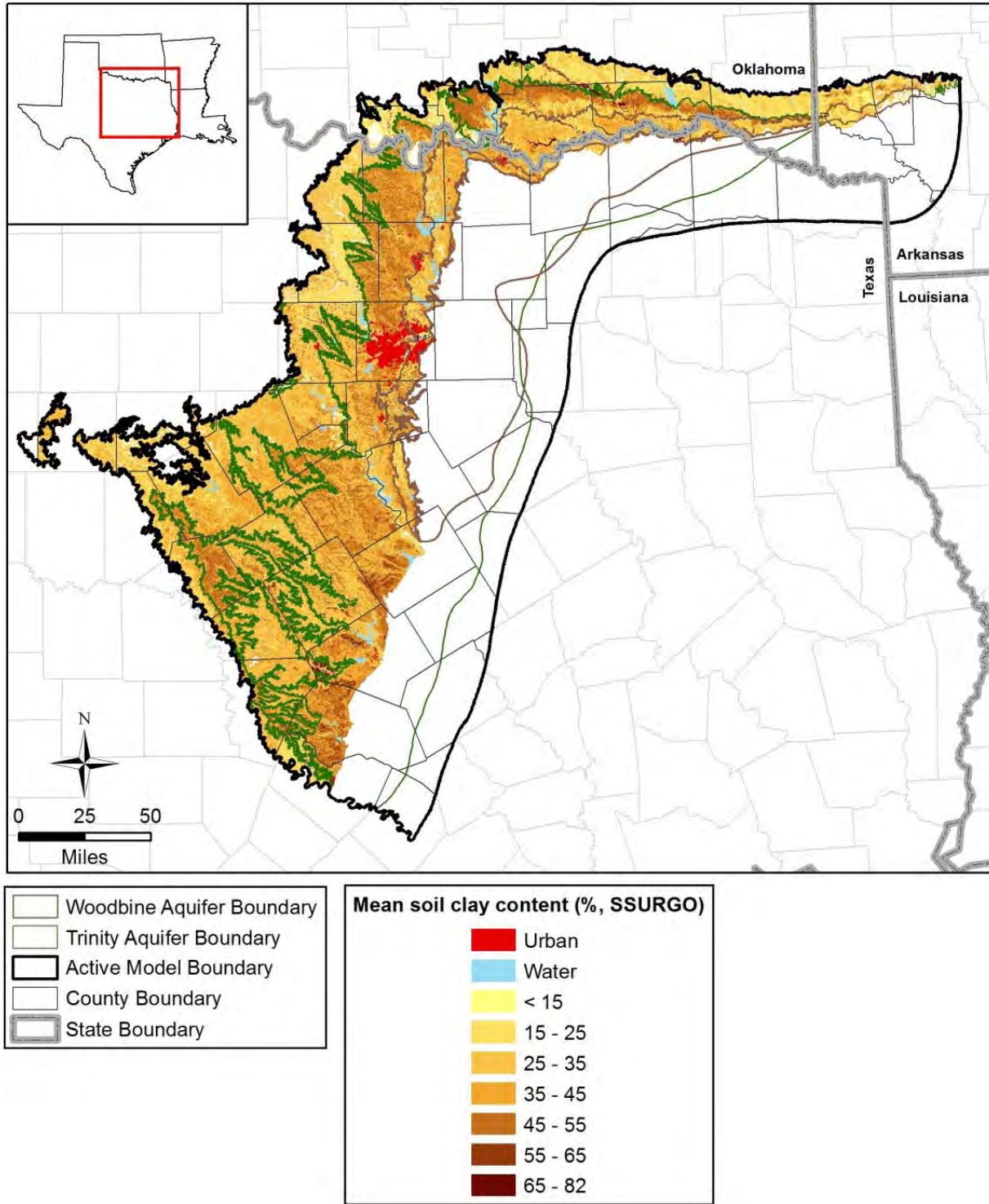
Figure 4.5.4   Mean soil clay content in percent in the combined outcrop areas of the northern Trinity Aquifer, Washita/Fredericksburg groups, and Woodbine Aquifer in the study area based on SSURGO data (U.S. Department of Agriculture, 1995).
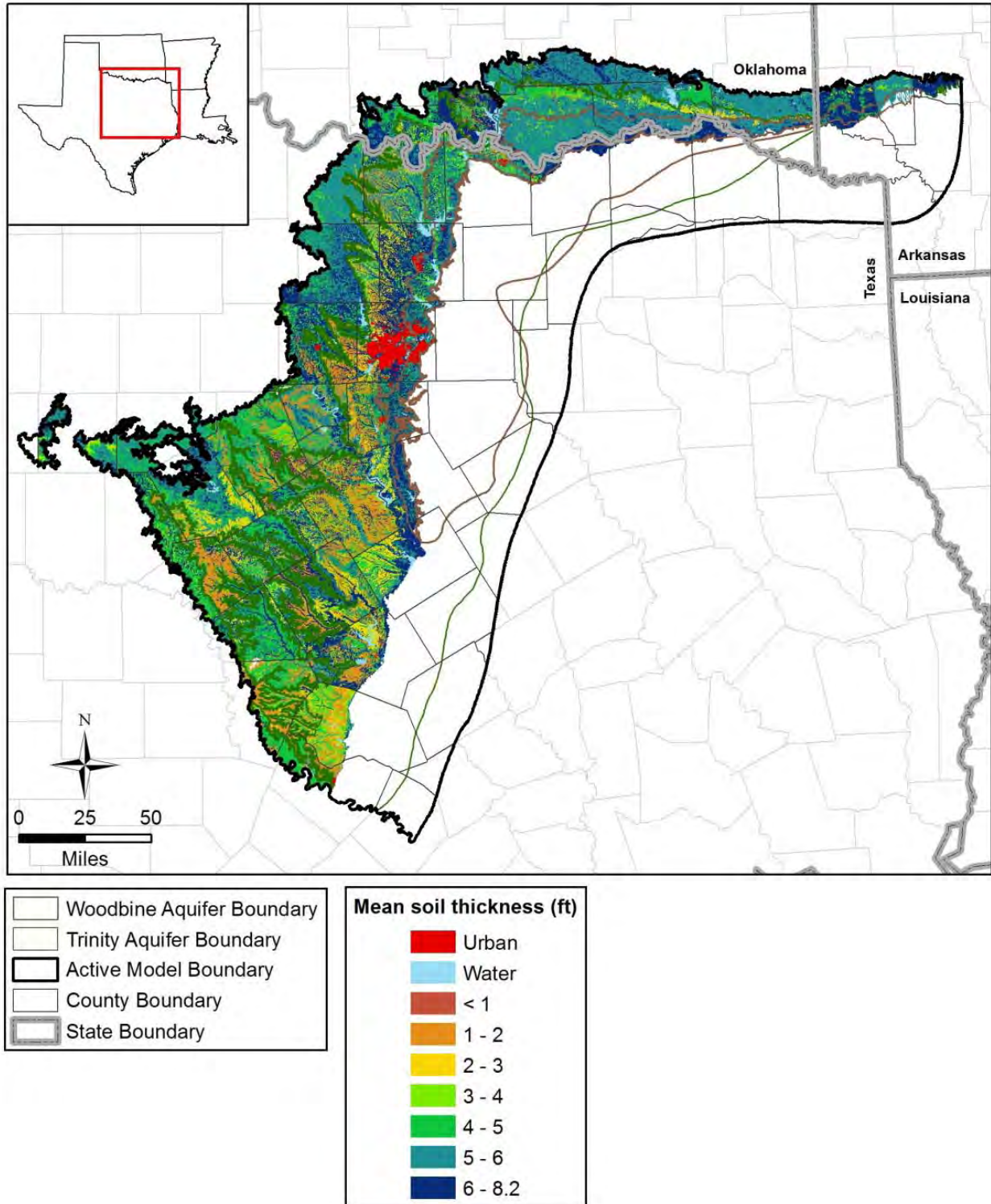
Figure 4.5.5   Mean soil thickness in feet in the combined outcrop areas of the northern Trinity Aquifer, Washita/Fredericksburg groups, and Woodbine Aquifer in the study area based on SSURGO data (U.S. Department of Agriculture, 1995).
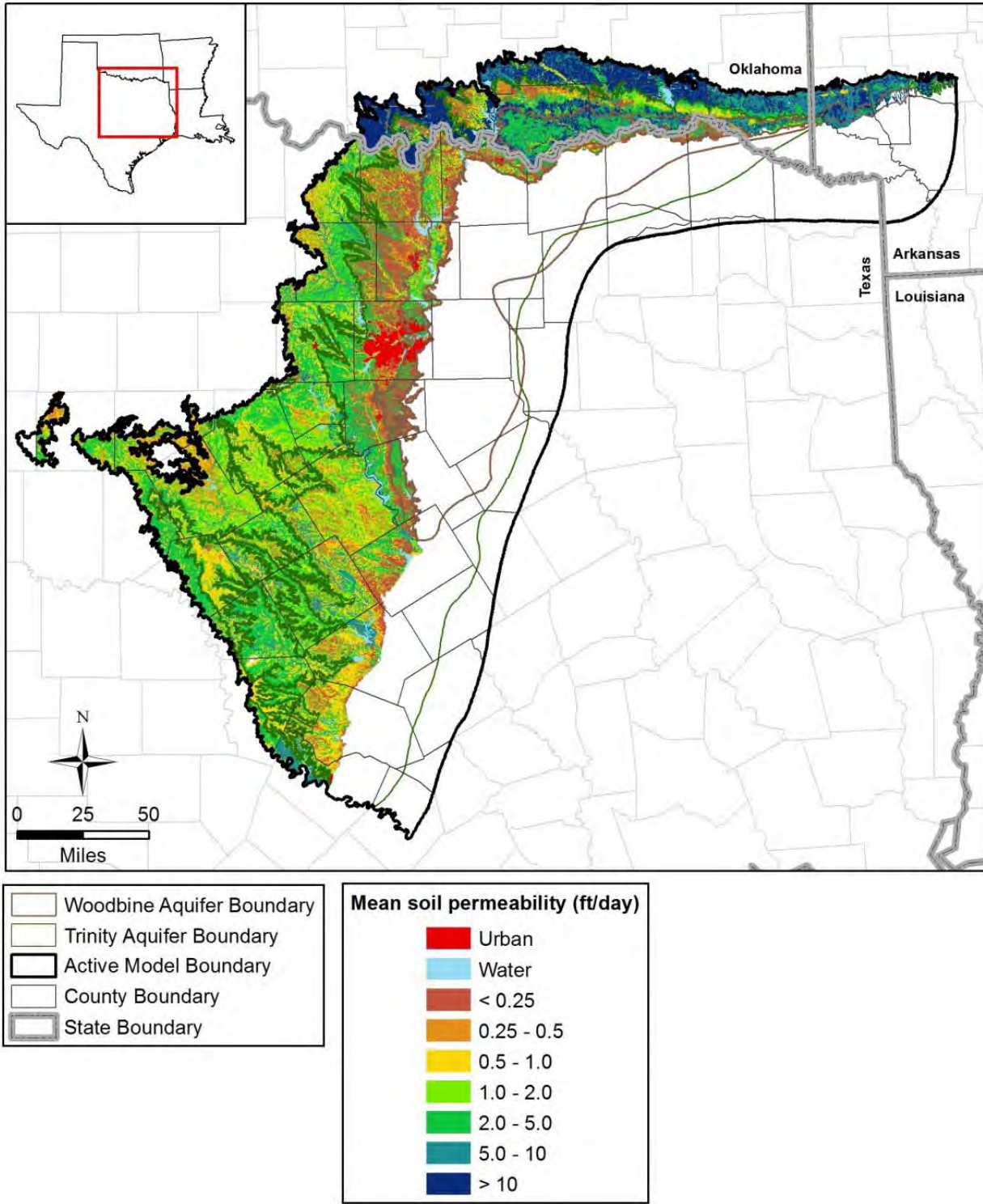
Figure 4.5.6   Geometric mean vertical soil permeability in feet per day in the combined outcrop areas of the northern Trinity Aquifer, Washita/Fredericksburg groups, and Woodbine Aquifer in the study area based on SSURGO data (U.S. Department of Agriculture, 1995).
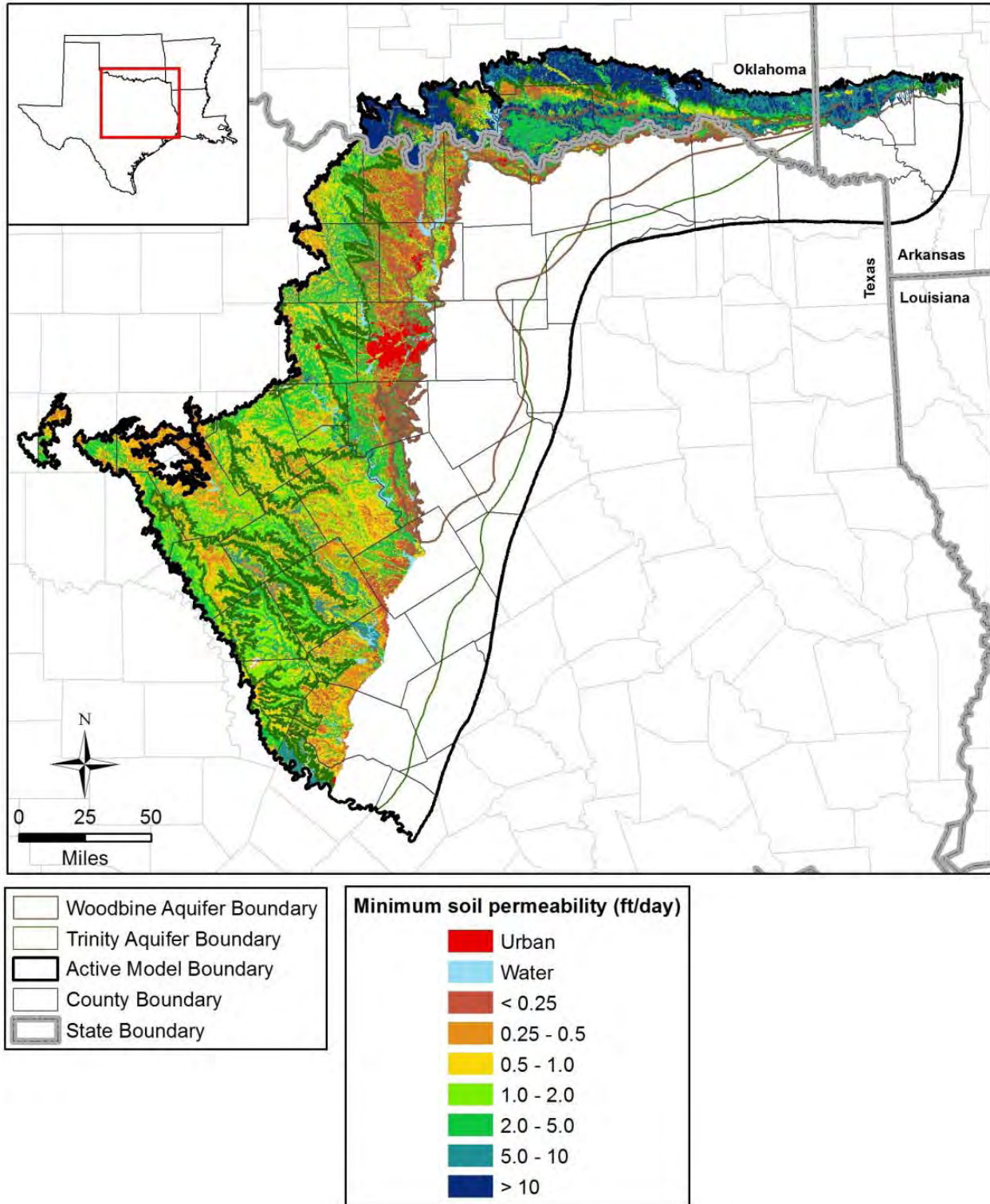
Figure 4.5.7   **Minimum soil horizon permeability in feet per day in the combined outcrop areas of the northern Trinity Aquifer, Washita/Fredericksburg groups, and Woodbine Aquifer in the study area based on SSURGO data (U.S. Department of Agriculture, 1995).**
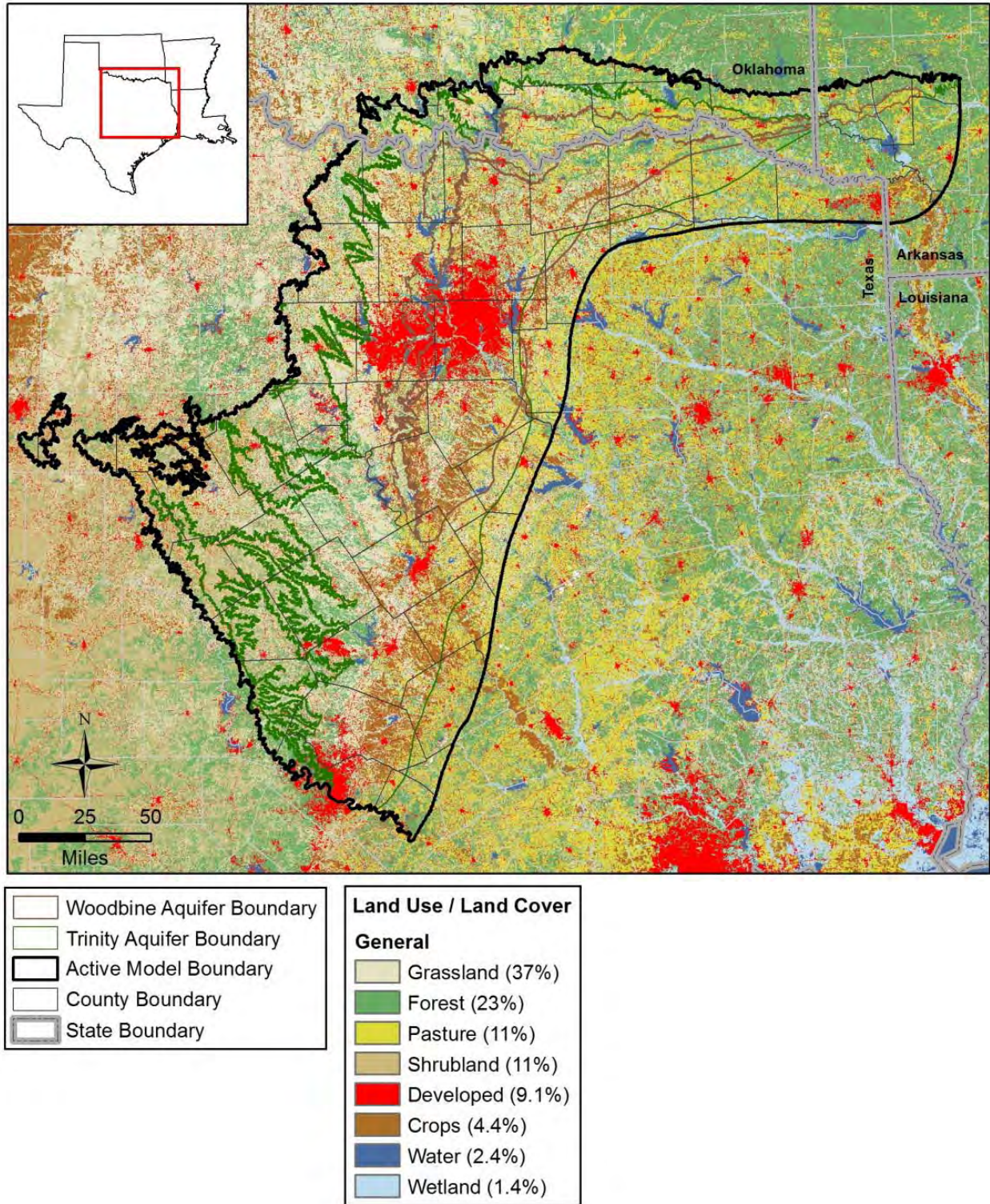
Figure 4.5.8   Land use/land cover in the study area and vicinity based on National Land Cover Data (NLCD) data from 2006 (Fry and others, 2011).
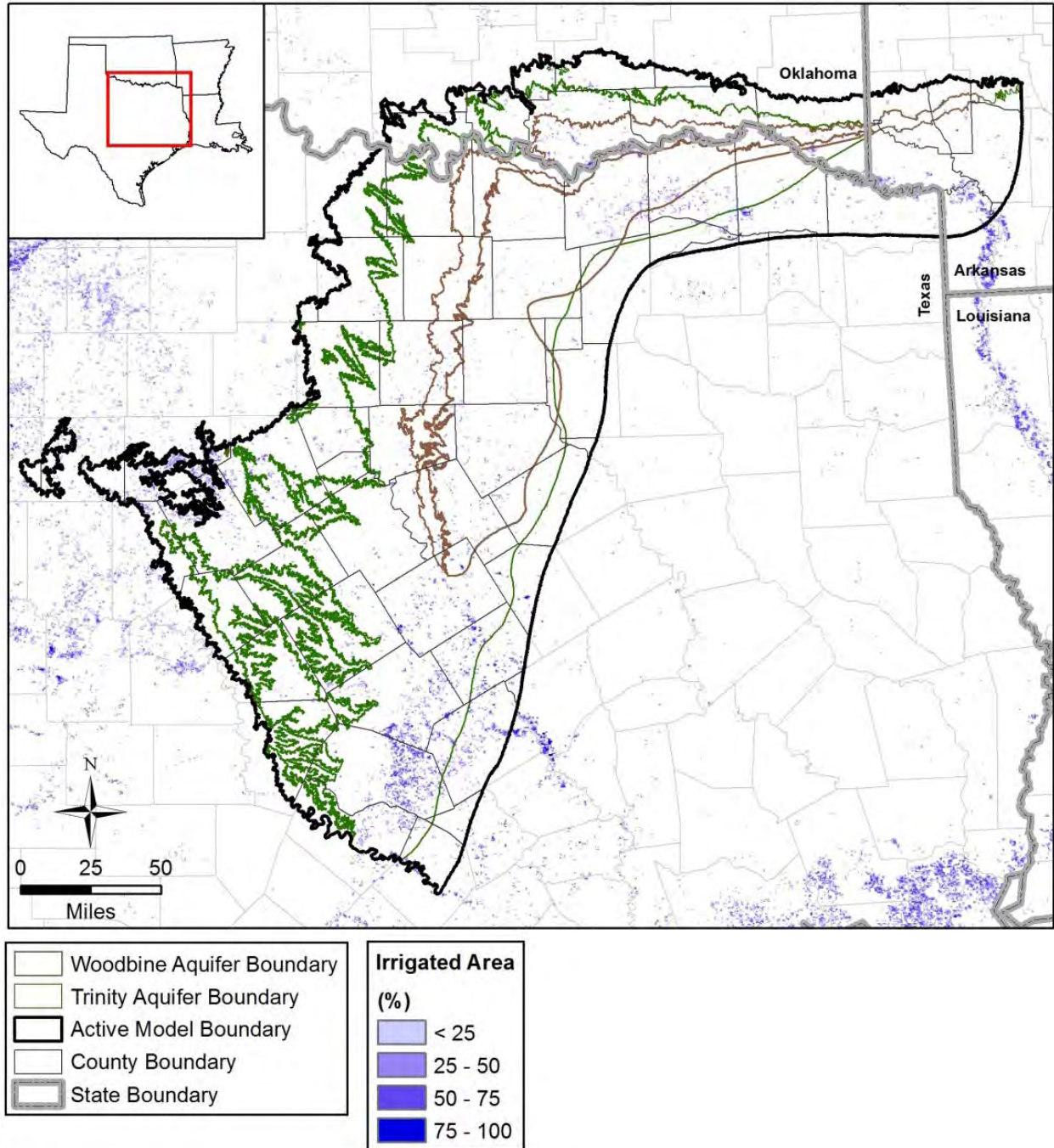
Figure 4.5.9 **Distribution of irrigation in the study area and vicinity based on Moderate Resolution Imaging Spectroradiometer (MODIS) data (Ozdogan and Gutman, 2008).**
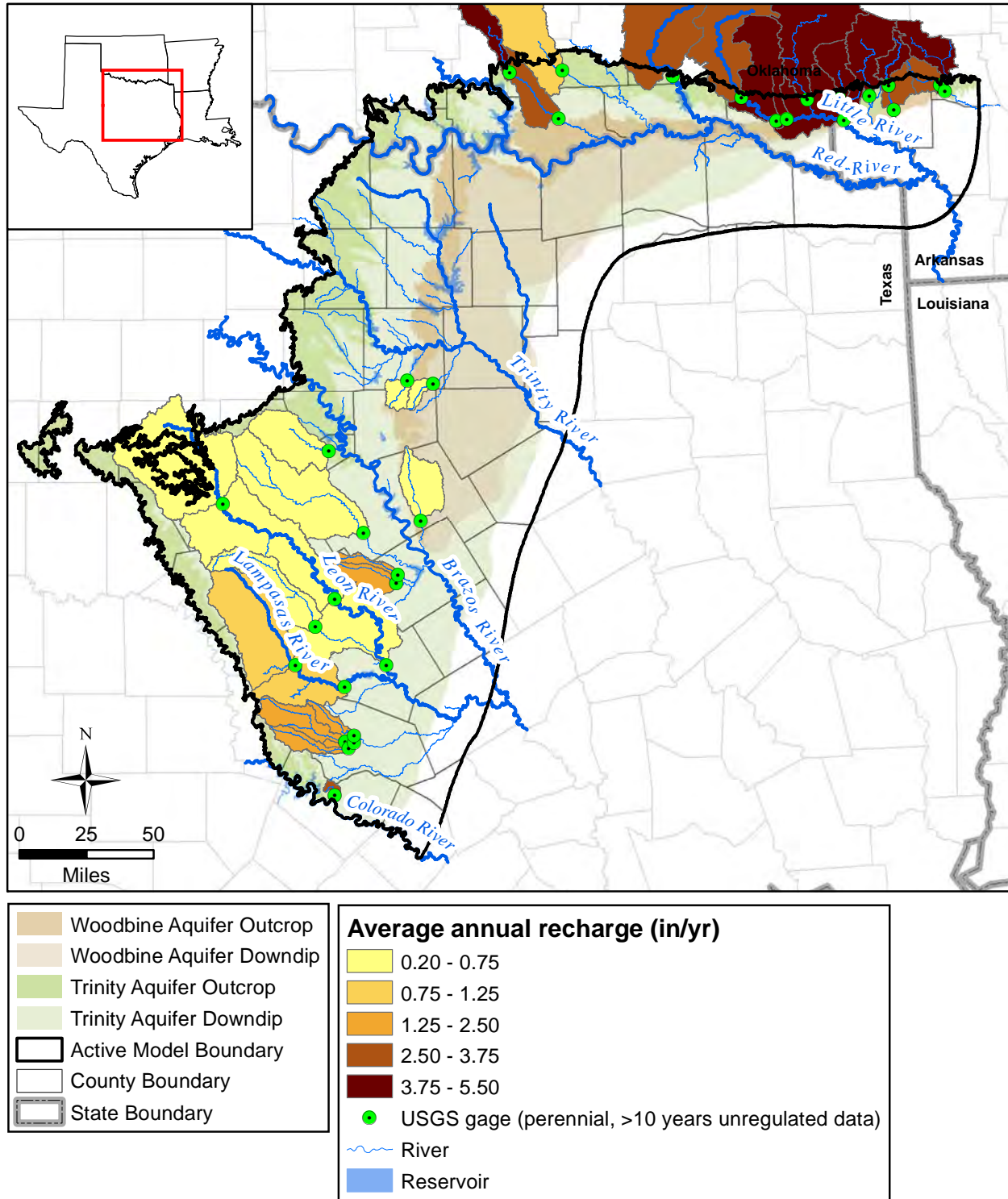
Figure 4.5.10 **Estimated average annual recharge in inches per year by watershed from the stream hydrograph separation analysis.**
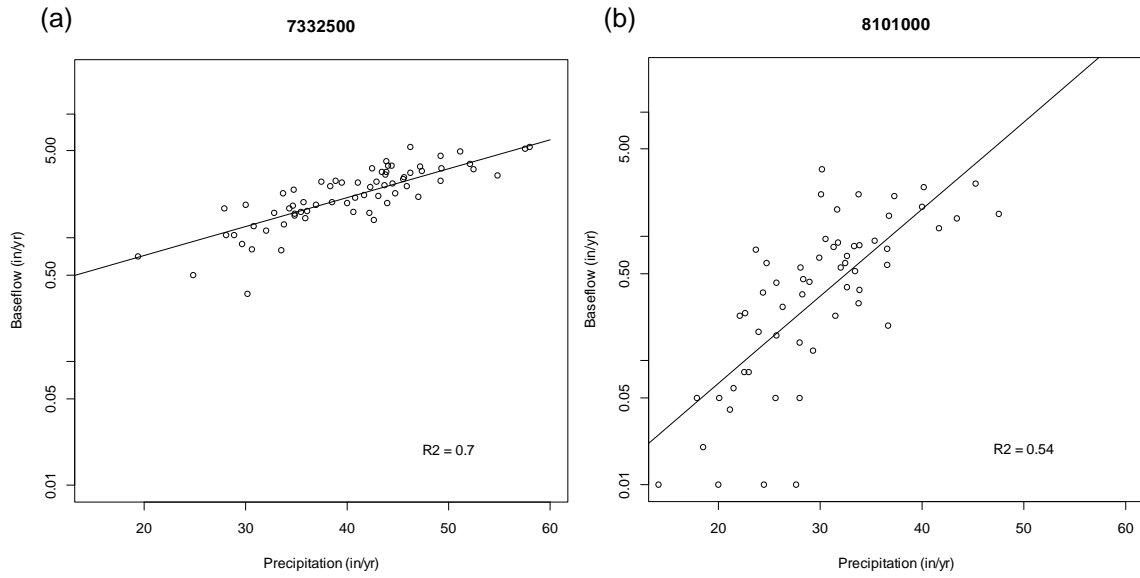
ln/yr = inches per year

**Figure 4.5.11   Scatter plot of log annual recharge versus annual precipitation for select stream
gages in the study area.**
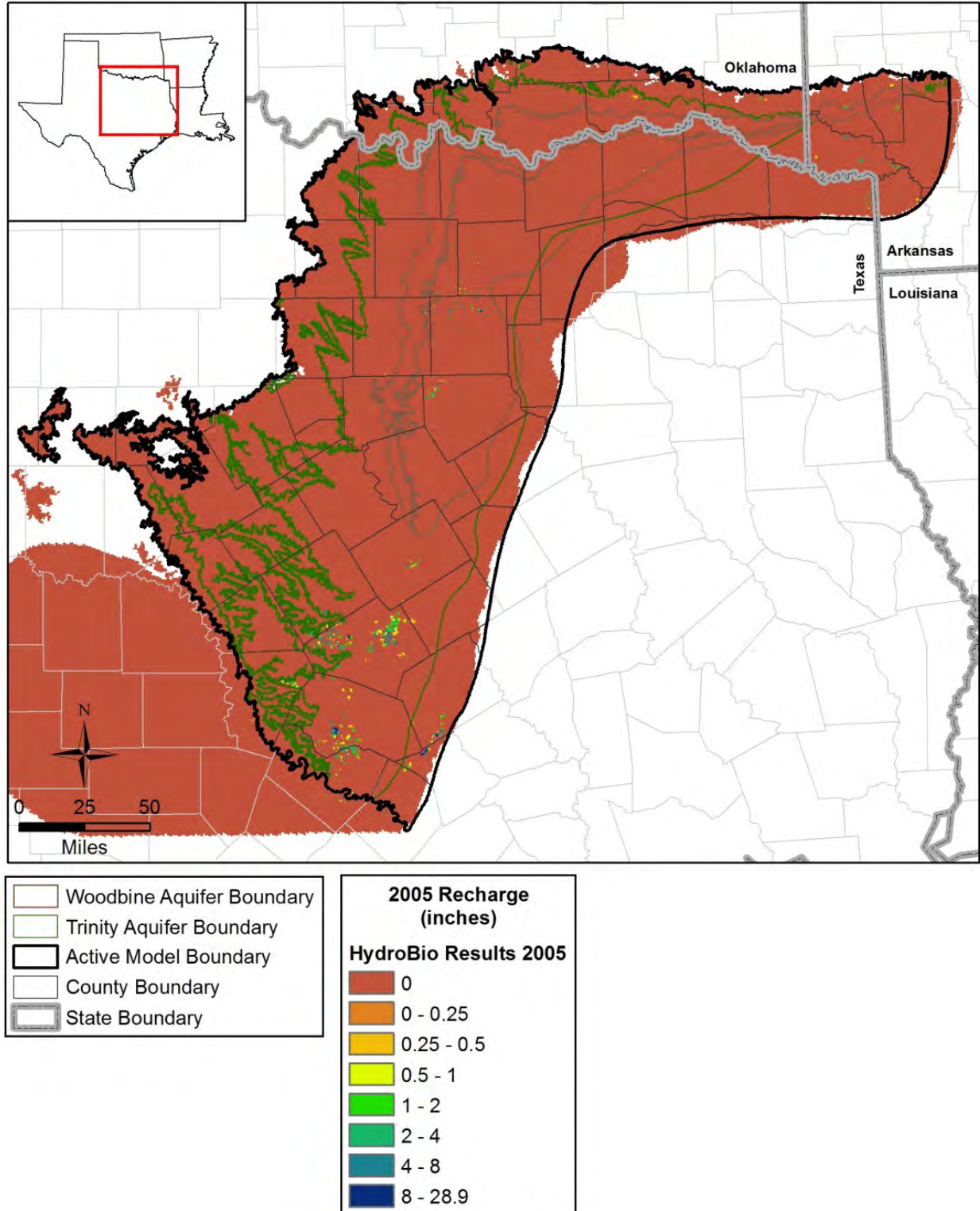
**Figure 4.5.12   Groundwater recharge for 2005 (dry year) in the study area and vicinity based on
results of the HydroBio water balance study (Kirk and others, 2012).**
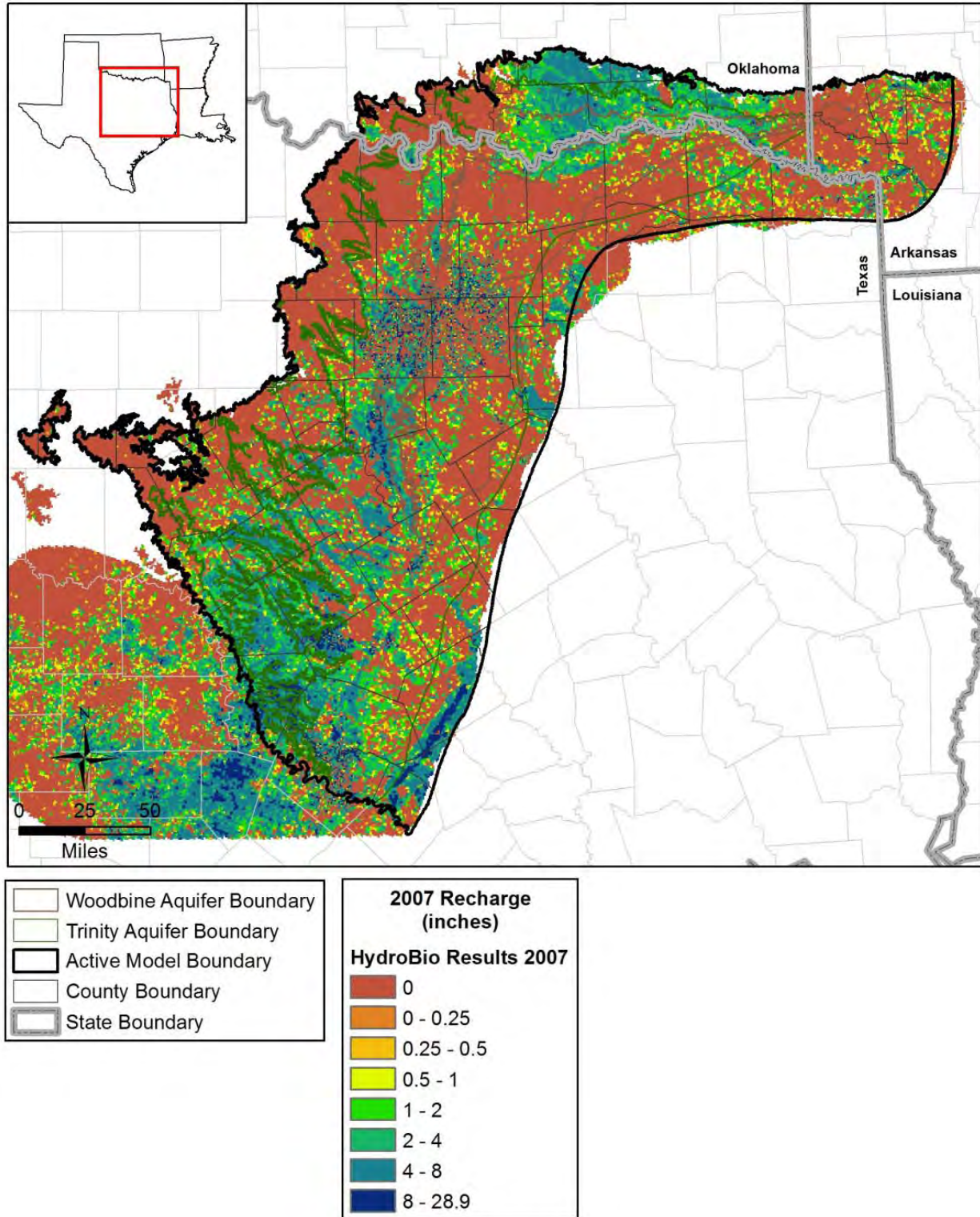
Figure 4.5.13 **Groundwater recharge for 2007 (wet year) in the study area and vicinity based on results of the HydroBio water balance study (Kirk and others, 2012).**
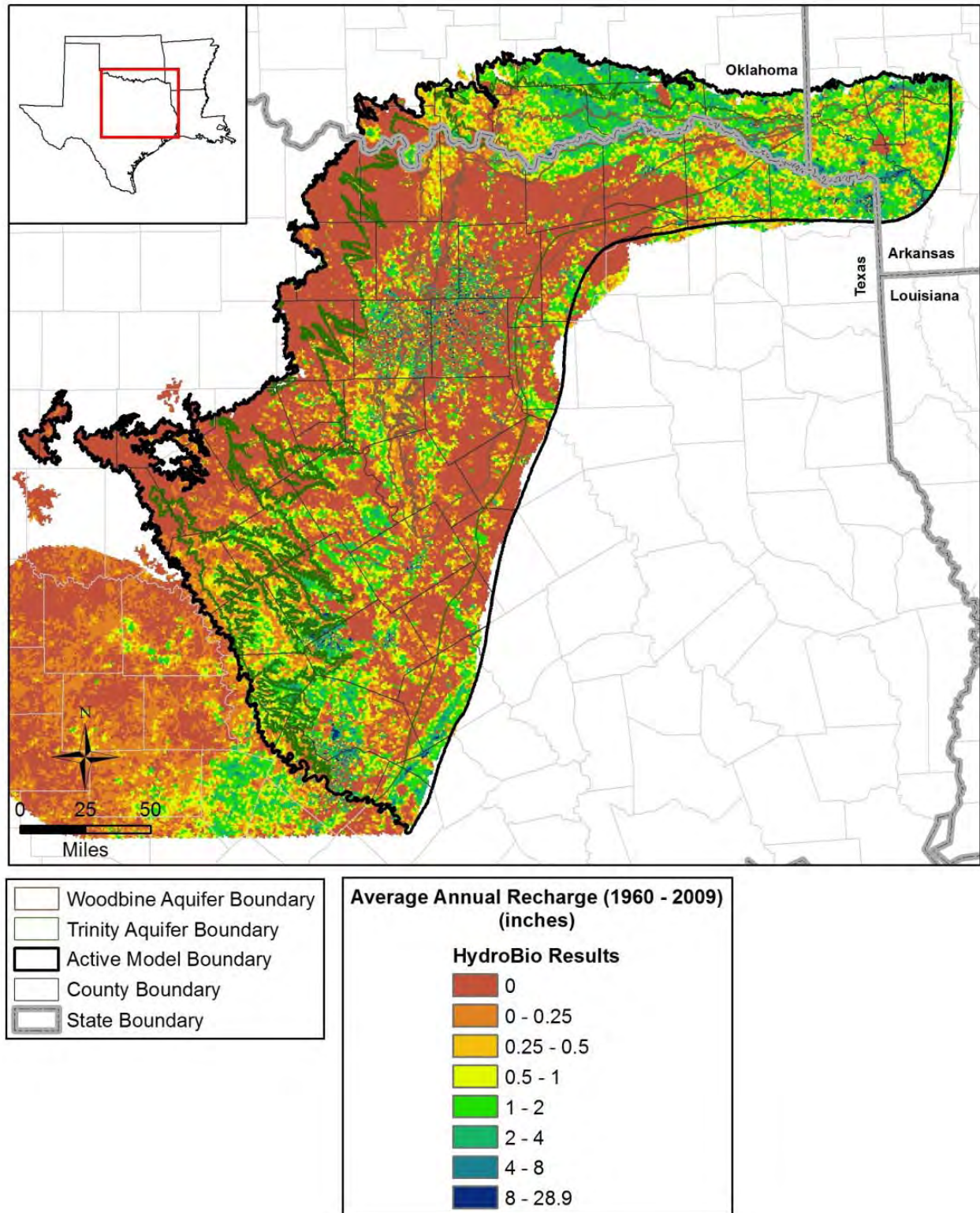
Figure 4.5.14 **Average annual groundwater recharge for the period 1960 to 2009 in the study area and vicinity based on results of the HydroBio water balance study (Kirk and others, 2012).**
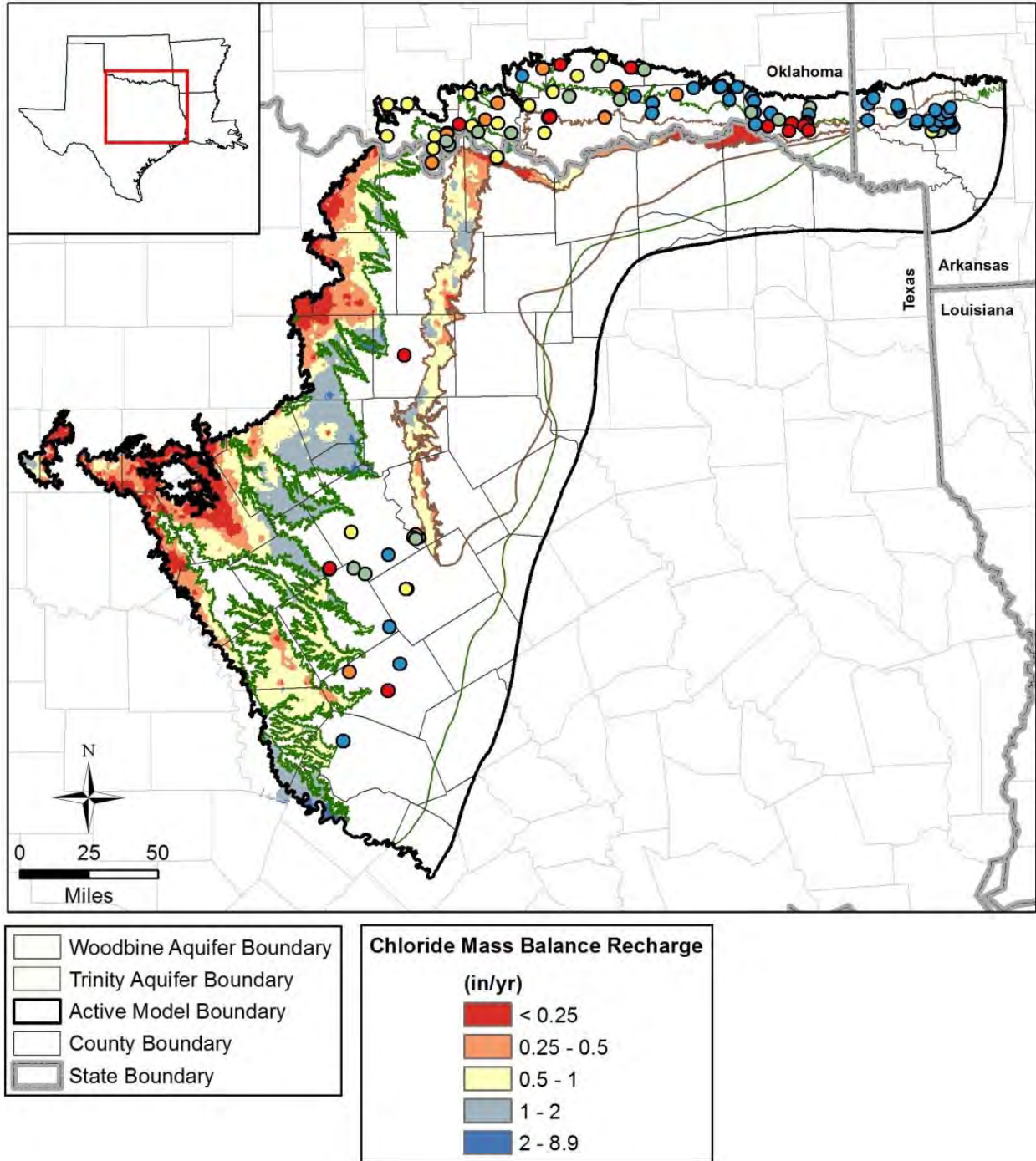
Figure 4.5.15 **Estimated groundwater recharge rates in inches per year in the study area based on the CMB method.**
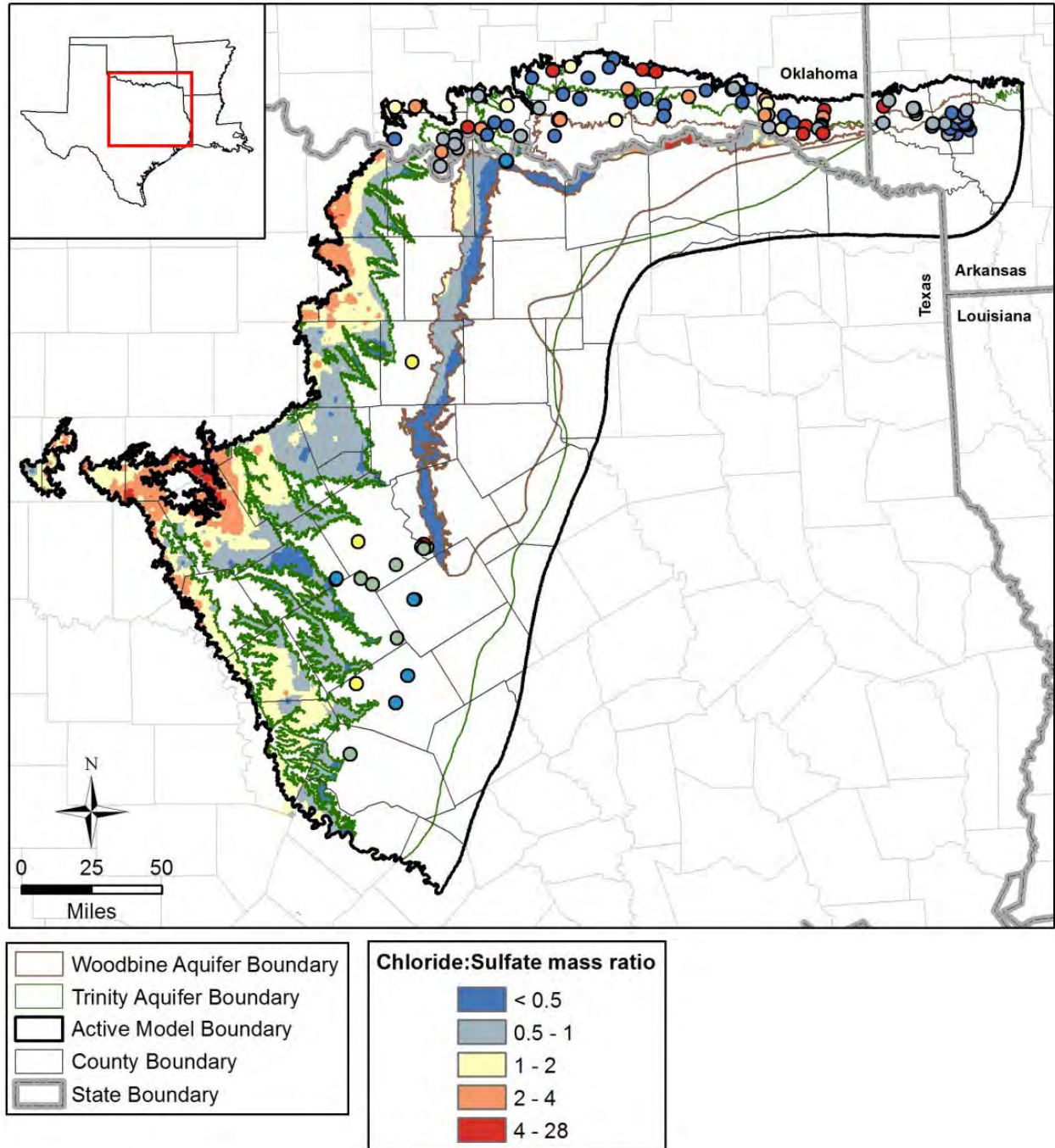
Figure 4.5.16   Distribution of groundwater chloride to sulfate mass ratios in the study area.

Legend:
- Trinity Aquifer Boundary
- Active Model Boundary
- County Boundary
- State Boundary

Trinity nitrate-N

Probability of Nitrate-N > 4 mg/L (%)
- < 10
- 10 - 25
- 25 - 50
- 50 - 75
- 75 - 100
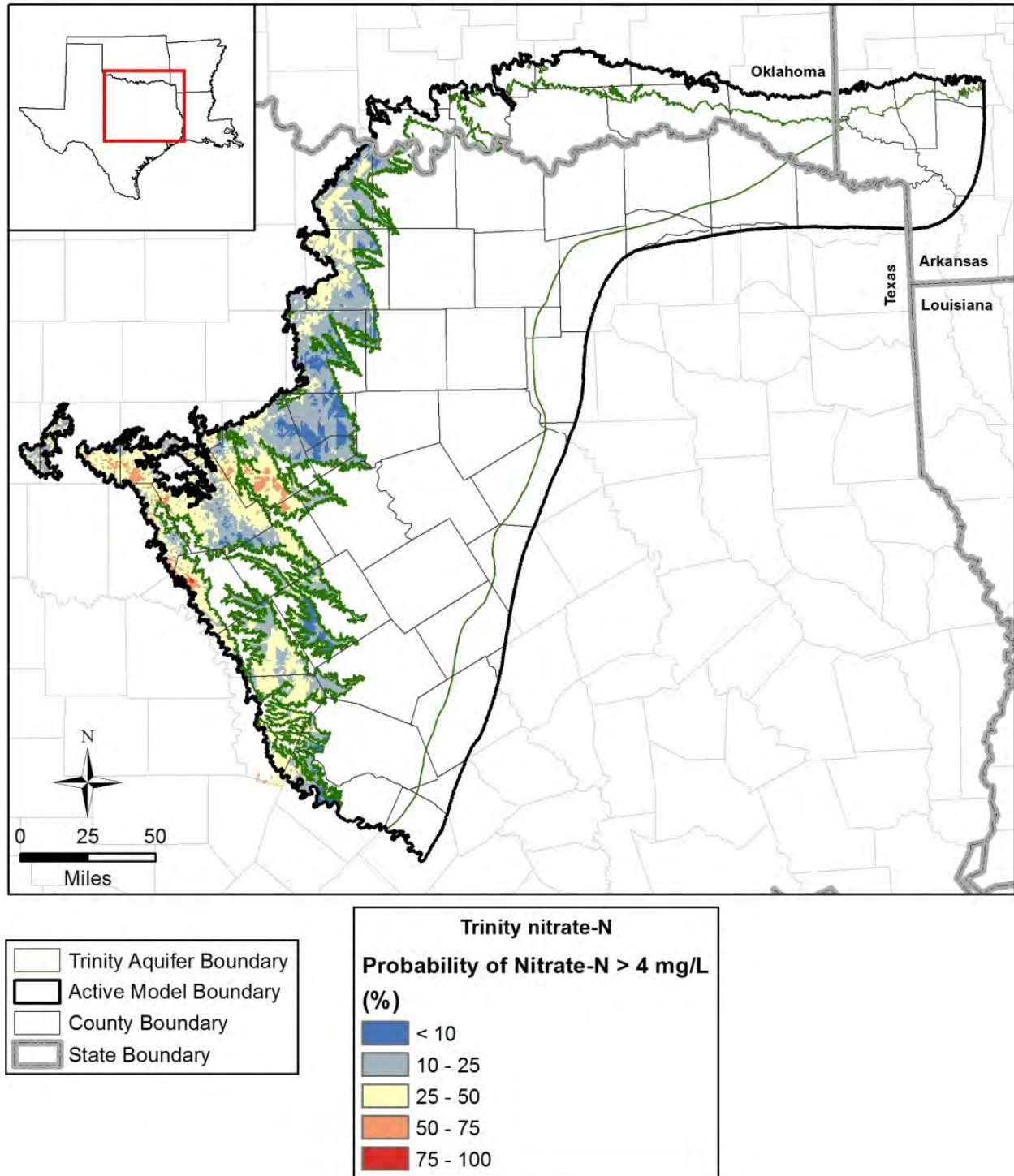
**Figure 4.5.17   Probability distribution of groundwater nitrate-N (N) exceeding a nominal
background concentration of 4 milligrams per liter in the northern Trinity Aquifer
outcrop in the Texas portion of the study area based on samples from wells
completed at depths less than or equal to 150 feet.**
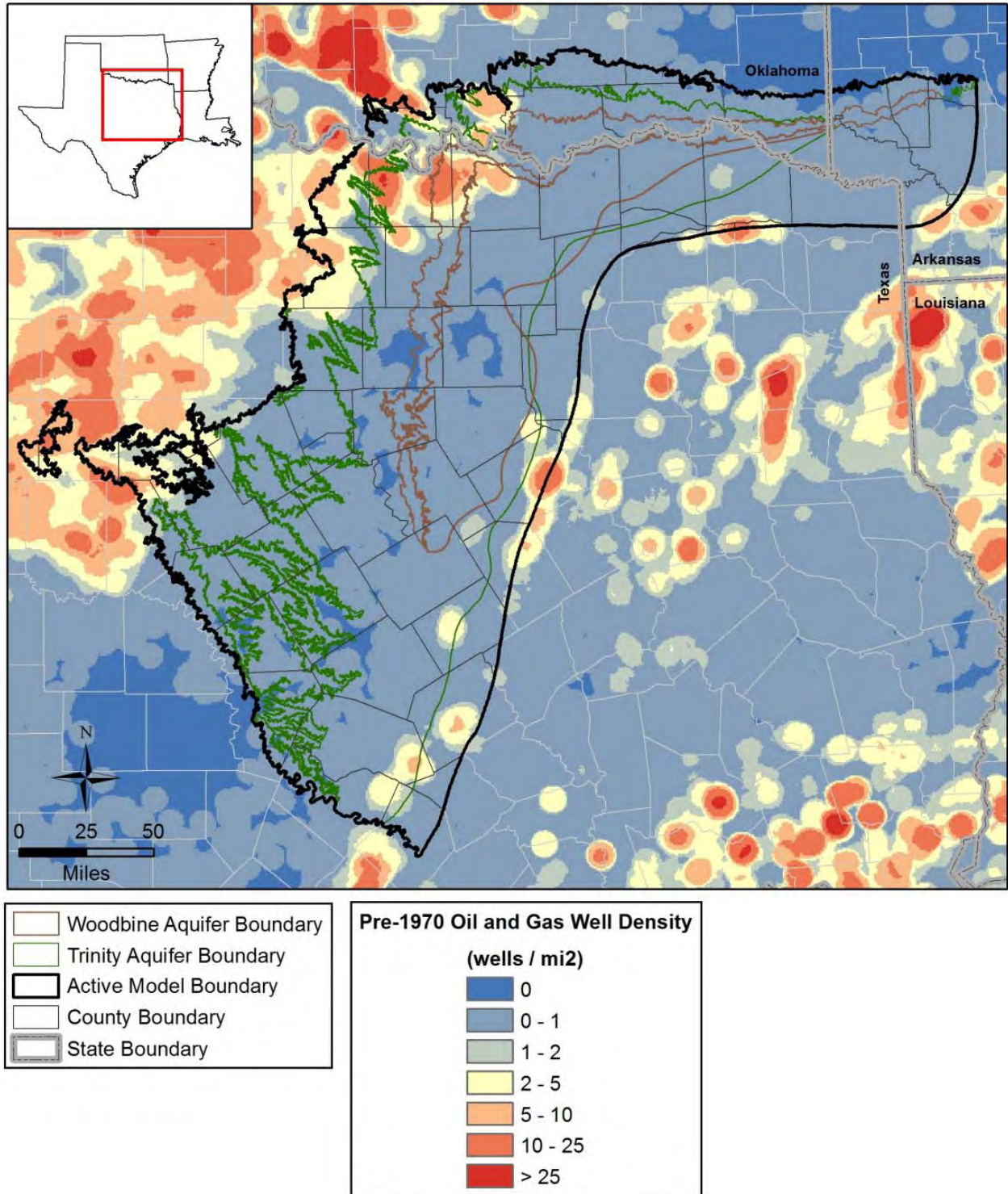
Figure 4.5.18   Density distribution of oil and gas wells in wells per square mile drilled prior to brine disposal regulation in the study area and vicinity.
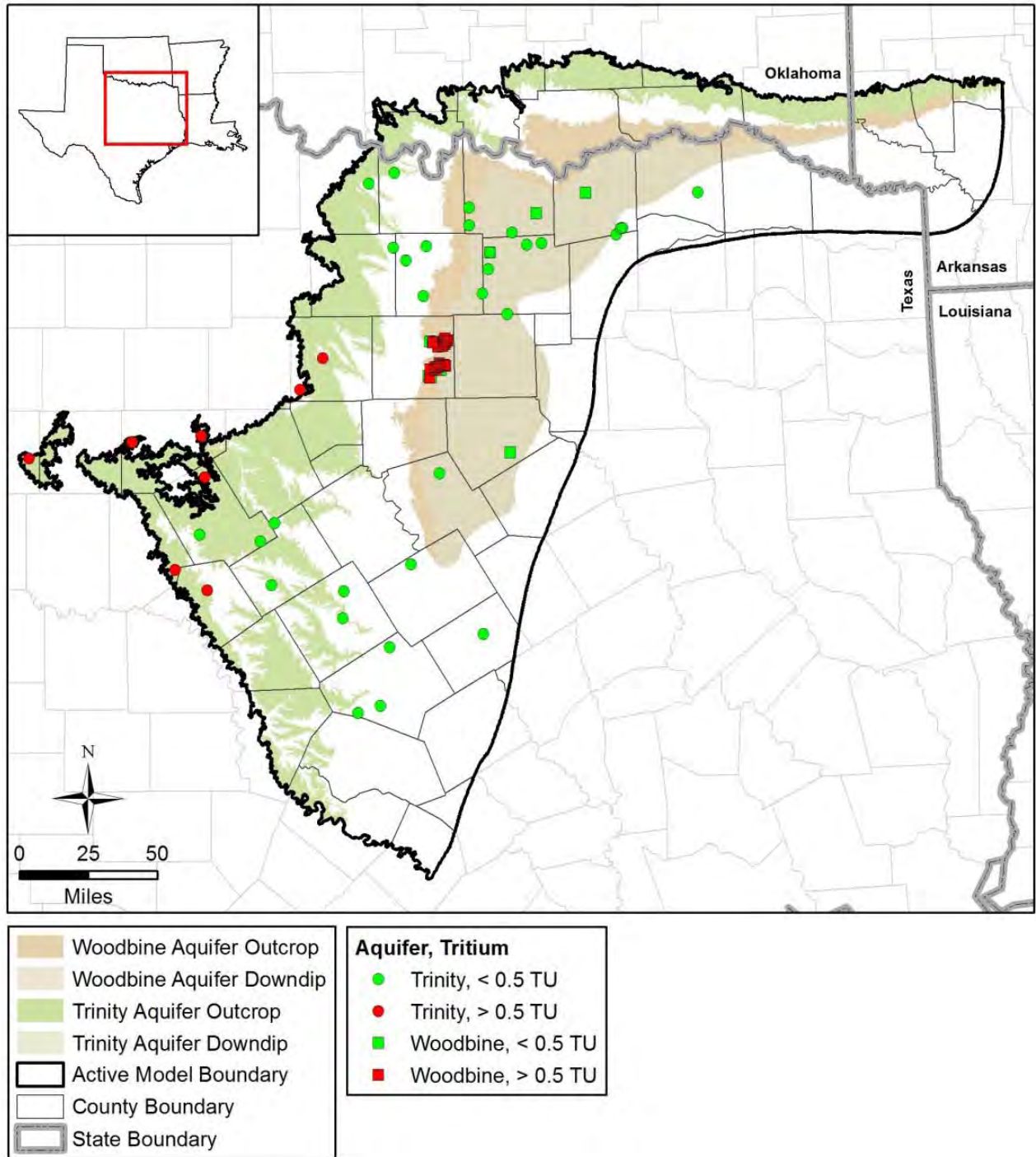
Figure 4.5.19   Locations and results of tritium sampling in tritium units in the northern Trinity and Woodbine aquifers in the study area.
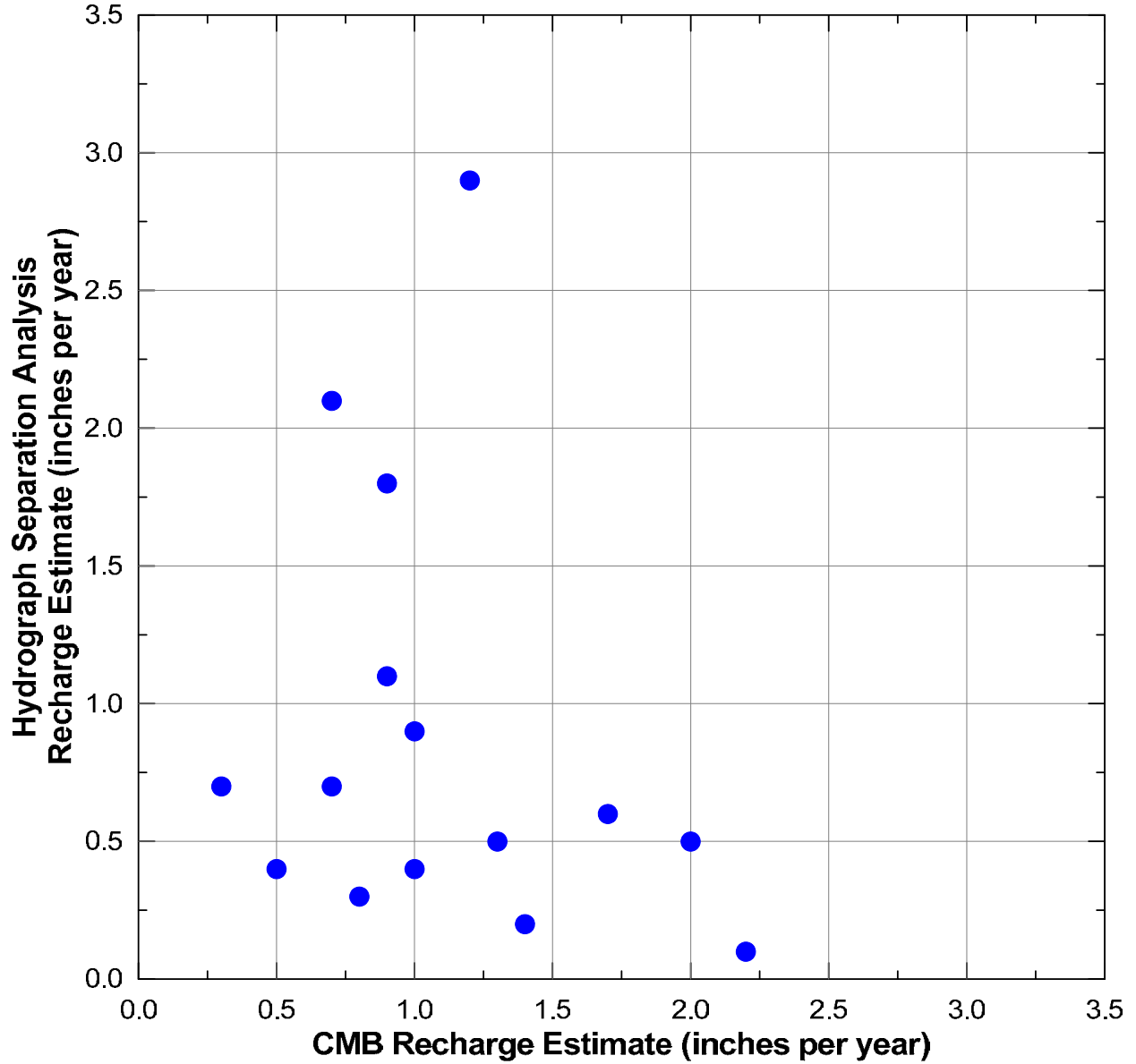
Figure 4.5.20 **Relationship between recharge rates in inches per year determined using the CMB method and from the hydrograph separation analysis for drainage basins intersecting outcrop areas of the northern Trinity and Woodbine aquifers.**
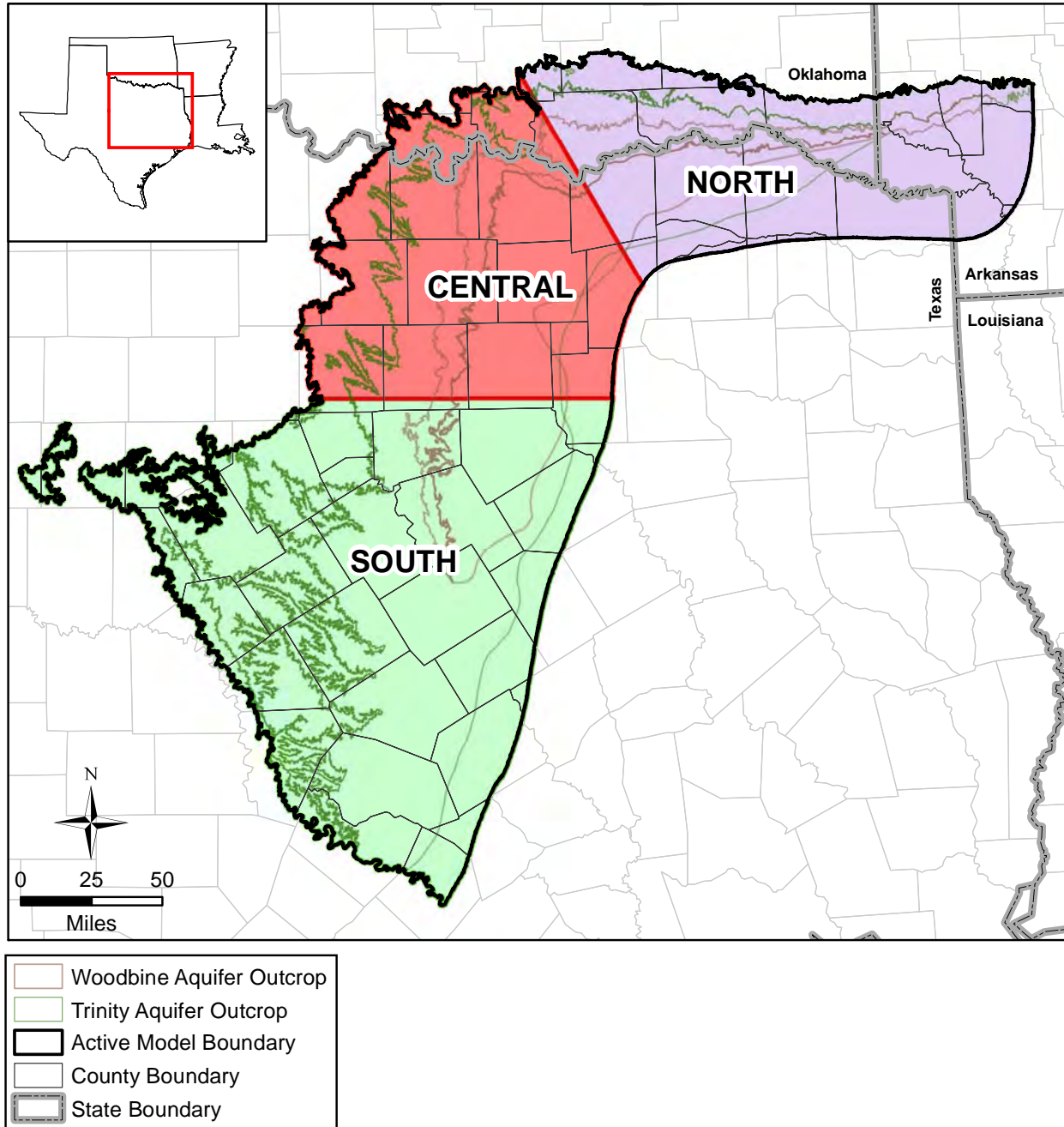
Figure 4.5.21   Recharge regions in the study area based on the hydrograph separation analysis.
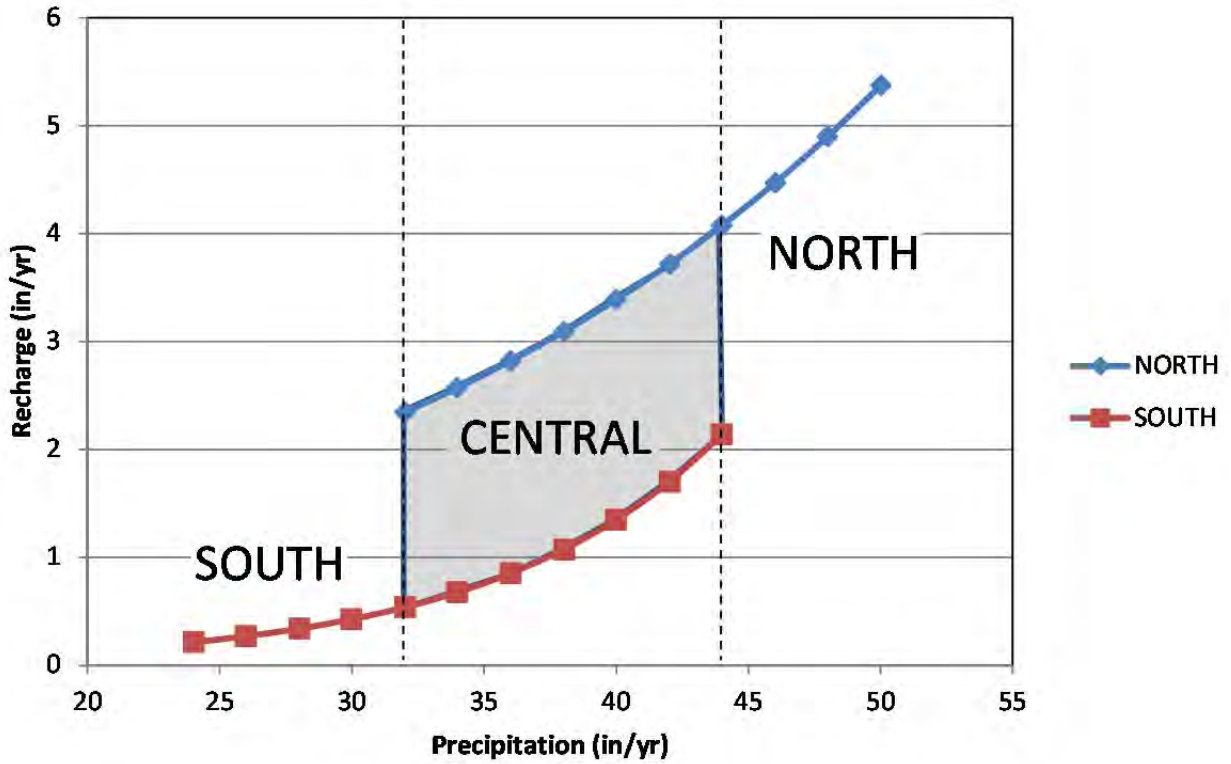
Figure 4.5.22   Relationships between average estimated recharge versus annual average precipitation in inches per year for the northern and southern portions of the study area.
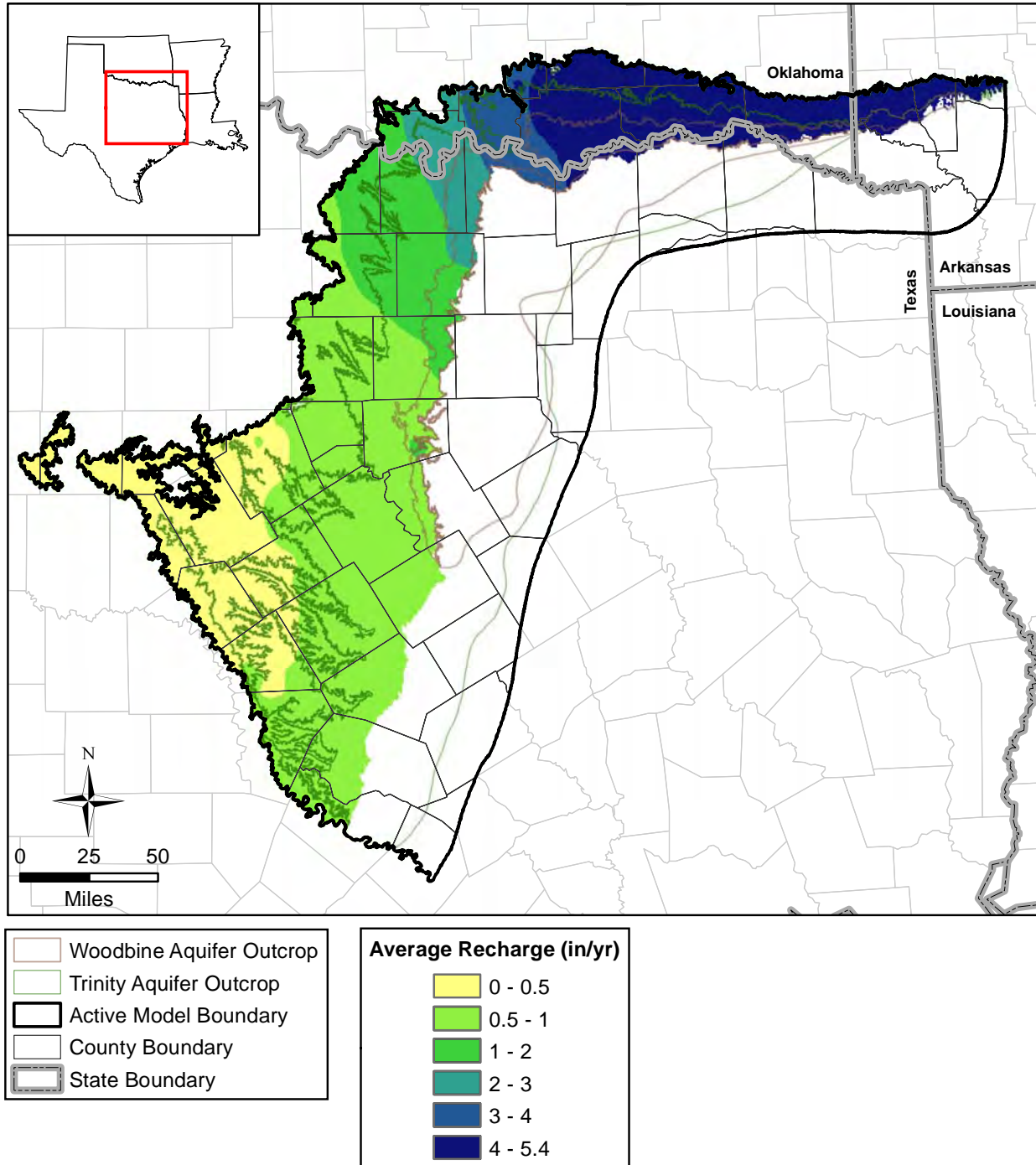
Figure 4.5.23   Average estimated annual recharge in inches per year in the study area based on relationships derived from the hydrograph separation analysis.
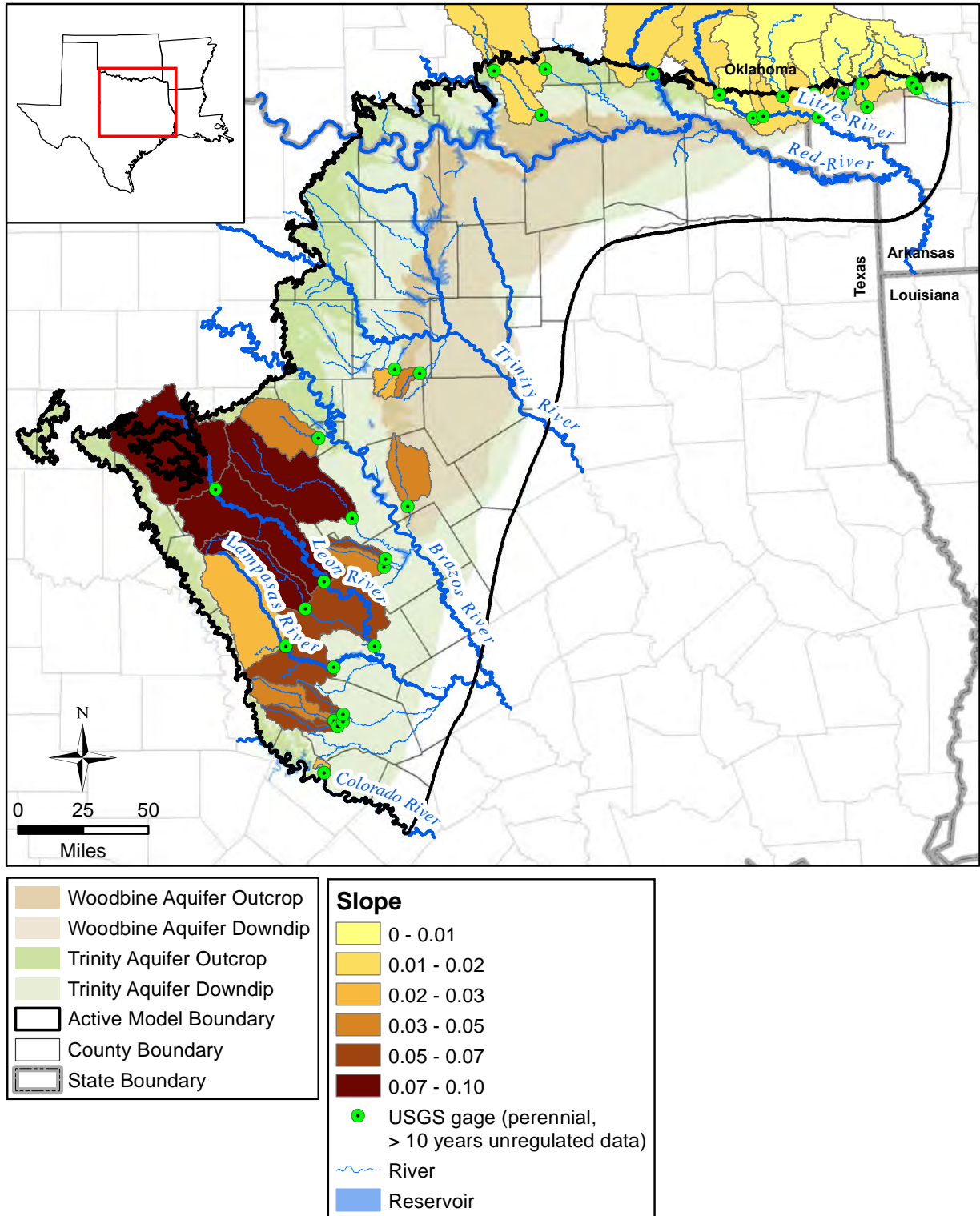
Figure 4.5.24   Slope of the regression between the log average annual recharge versus the average annual precipitation by watershed analyzed.

4.6   Natural Aquifer Discharge

Natural aquifer discharge occurs through many mechanisms including stream discharge, groundwater ET, wetland discharge, spring discharge, and cross-formational flow. The interaction between groundwater and surface water occurs primarily where a surface water body, such as a river, stream, or lake, intersects an aquifer outcrop. Rivers and streams can either lose water to the underlying aquifer, resulting in aquifer recharge, or gain water from the underlying aquifer, resulting in aquifer discharge. Lakes, like rivers and streams, may provide a potential site of focused recharge when the water table is below the elevation of the lake, or may gain water from the aquifer when the water table is above the elevation of the lake. Discharge from an aquifer also occurs where the water table intersects the ground surface at springs or seeps. Under steady-state conditions (predevelopment), the long-term average aquifer discharge is equal to aquifer recharge. In the post-development period, aquifer discharge includes pumping in addition to the natural mechanisms of discharge. Pumping initially pulls water from aquifer storage, but in the very long term, as the groundwater system comes to equilibrium, the volume pumped will be balanced by a decrease in aquifer discharge (termed pumping capture). As a result, aquifer discharge mechanisms are a very important process in defining how an aquifer responds to development.

This section discusses stream-aquifer interaction, groundwater ET, spring discharge, lakes, and cross-formational flow. Where possible, the amount of aquifer discharge attributable to each process is quantified. Section 4.7 discusses aquifer discharge from pumping.

4.6.1   Stream-Aquifer Interaction

Under predevelopment conditions, groundwater flow in the northern Trinity and Woodbine aquifers is elevation-driven, with the majority of flow occurring in the near outcrop regions in response to elevation differences and a minor percentage of flow moving downdip, also in response to elevation differences between the outcrop and the downdip portions of the aquifer. Most major streams in the region are perennial and flow year round in a year of average climate, indicating that they are likely naturally gaining streams. A gaining stream has a stage that is at a lower elevation than the local water table. Under gaining-stream conditions, the stream is a discharge boundary for groundwater. Some smaller tributaries in the region are intermittent, indicating that they are naturally losing streams on an average basis. A losing stream has a stage

that is at a higher elevation than the local water table and, as a result, surface water is a source of recharge to the groundwater. It is possible that a stream can vary from gaining to losing conditions along its course. Gaining and losing conditions can also change as a result of seasonal climate variations. After significant development of groundwater in the vicinity of gaining streams, it is also possible that shallow groundwater elevations (heads) can be lowered, creating less stream base flow or even reversing the hydraulic gradient between the stream and the aquifer creating a losing stream condition.

The factors controlling the volumetric flux between the stream and the groundwater are the hydraulic gradient and the hydraulic conductance between the stream bed and the aquifer. The equation describing flow between the aquifer and the stream in MODFLOW can be written as (Prudic and others, 2004):

$$Q_L = \frac{KwL}{m}(h_s - h_a) \qquad (4.6.1)$$

where

Q_L = volumetric flow between a given section of stream and volume of aquifer (volume per time)

K = hydraulic conductivity of stream bed sediments (length per time)

w = representative width of stream (length)

L = length of stream corresponding to a volume of aquifer (length)

m = thickness of the stream bed deposits (length)

h_s = head in the stream (length)

h_a = head in the aquifer beneath the stream bed (length)

It is the interaction between aquifers and streams that necessitates the study and characterization of streams in the study area and the implementation of streams into the groundwater model. Aquifer water levels have the potential to alter streamflows, especially in drought periods. Stream-aquifer interaction is also important to understand because in regions where the streams are gaining, the base flow component of streamflow (i.e., streamflow that originates from groundwater) provides a lower-bound estimate for recharge (see Section 4.5). Stream-aquifer interaction was investigated in the outcrop portions of the northern Trinity Aquifer, Washita/Fredericksburg groups, and Woodbine Aquifer, which lie between the updip edge of the northern Trinity Aquifer outcrop and the downdip edge of the Woodbine Aquifer and

Washita/Fredericksburg groups outcrops (Figure 4.6.1). This outcrop area where surface water/groundwater interaction occurs in the model is referred to in this section as the study outcrop area.

4.6.1.1   Streamflow Characteristics

The northern Trinity and Woodbine outcrops are intersected by 10 major rivers: the Colorado, Lampasas, Leon, Brazos, West Fork Trinity, Elm Fork Trinity, Washita, Kiamichi, Little and Red rivers and numerous smaller rivers and streams (Figure 4.6.2). Figure 4.6.3 shows the location of stream gages that are part of the USGS national stream gage network and have daily streamflow data. Note that only the gages located in the study outcrop area are shown on this figure. The gages in Figure 4.6.3 are distinguished by the properties of the stream (perennial or intermittent and regulated or unregulated) and the number of continuous years of available data. The purpose of these distinctions is discussed in Section 4.6.1.4. Figure 4.6.4 shows several example stream hydrographs across the study outcrop area. These hydrographs show annual streamflow for selected streams as they cross or exit either the northern Trinity or Woodbine aquifer outcrops.

Stream gage data can be used to characterize streamflow rates and determine aquifer-stream interaction through comparisons of stream stage height and shallow groundwater elevations, low-flow or stream gain/loss studies and hydrograph separation studies. The following subsections discuss each of these methods for investigating stream-aquifer interaction.

4.6.1.2   Groundwater Level/Stage Relationships

Historical groundwater levels in relatively shallow wells within 2 miles of USGS stream gaging stations in the study outcrop area are compared to stream stage (gage height) records to infer whether groundwater hydraulic gradients in the vicinity of the gaging stations are generally directed toward or away from the streams (i.e., whether the streams are gaining water through base flow or losing water to groundwater recharge).

Water-level data were taken from the TWDB groundwater database (TWDB, 2013a), and stream gage data are taken from the USGS National Water Information System (USGS, 2013b). Groundwater elevations are taken directly from the TWDB data, and surface water elevations were calculated by adding the stage height (from the "daily data" or "field measurements" in the USGS data) to the gage datum (from the "site information" in the USGS data).

Comparisons were made between well data and stream gage data at 10 locations within the study outcrop area. Eight of the locations were selected on the basis of the stream gage station being located within 2 miles of at least one well with a total depth of 100 feet or less. Two additional locations (stream gages 08050800 and 08091500) were chosen due to a paucity of streamflow data in their vicinities, although all wells within 2 miles of these two stations exceed 100-feet total depth. Upon selection of these 10 gaging stations, all wells within 2 miles with depths less than 200 feet were selected for comparison. However, data from wells deeper than 100 feet were not considered if sufficient information was available from shallower wells. Wells with no reported depth or a depth of zero were excluded from the analysis.

Plots of stream gage elevations and groundwater elevations from nearby wells in the northern, central, and southern portions of the study outcrop area are given in Figures 4.6.5 through 4.6.7, respectively. The total depth and approximate distance from the stream gaging station are given for each well in the plot legends. This information was useful in evaluating whether the stream is gaining or losing. Shallow wells completed a short distance from a stream gage are more likely than deeper wells or wells further away to reflect near-surface groundwater conditions in the vicinity of the stream gaging station.

Comparisons for three stream gaging locations in the northern portion of the study outcrop area within Texas are shown in Figure 4.6.5. The northernmost of these stations is at Timber Creek near Collinsville (gage 08050800). A single, relatively deep (190 feet) well completed in the Woodbine Aquifer is located about 1.8 miles west-southwest of this gage. The water-level elevations for the two measurements in the well are higher than the stream water elevations, suggesting a gradient from the groundwater to the stream. However, the depth of the well and its distance from the stream result in uncertainty in this conclusion. If one or more shallow, relatively low-permeability confining layers are present, the deeper water level in the well would not be representative of shallower groundwater conditions. This comparison was included due to a general lack of data in this portion of the study outcrop area.

Another set of stream/groundwater data for the Woodbine Aquifer outcrop area are available for the Rush Creek at Woodland Park Boulevard station (gage 080949240); however, the data are limited and ambiguous (see Figure 4.6.5). The well nearest to the stream gage location is 25-feet deep and located roughly 0.5 mile west-southwest of the stream gage station. A single

measurement in the well shows a groundwater elevation over 20 feet lower than the water level in the stream, suggesting that the stream is losing water to groundwater recharge. However, two other wells located at a greater distance (1.4 and 1.9 miles) to the east of the gaging station indicate groundwater elevations, taken at roughly the same time, exceeding the water level in the stream by over 15 feet and roughly 60 feet, respectively. All wells are at similar shallow depths, 21 to 25 feet below ground surface. However, the two wells to the east of the gaging station are located at land surface elevations exceeding the elevation of the stream gaging station by over 50 feet to nearly 100 feet, while the land surface elevation at the closer well to the west exceeds the gage elevation by less than 20 feet. Since unconfined phreatic surfaces generally mimic patterns in the surface topography, it is reasonable to postulate that the relatively high groundwater elevations to the east are less representative of shallow groundwater conditions near the stream than the well to the west, which is nearer to the gaging station both laterally and vertically. This best available data point indicates that the stream is losing water in this area.

The other stream/groundwater comparison shown on Figure 4.6.5 is for the Big Sandy Creek gaging station near Bridgeport (gage 08044000). Multiple measurements between 1970 and 1994 in two wells completed at depths of 80 and 102 feet, located approximately 1.8 and 1.2 miles from the station, respectively, exceed the water level in the stream by roughly 30 to 85 feet. Although the surface elevation of these two wells exceed that of the gaging station by 106 and 76 feet, respectively, the available information indicates that the stream is likely gaining in this area.

Figure 4.6.6 shows stream/groundwater comparisons in the vicinity of four USGS stream gaging stations in the central portion of the study outcrop area. For the northernmost of these stations (Paluxy River at Glen Rose, gage 08091500), groundwater data for shallow wells located nearby are lacking. However, data are available for three deeper wells (120 to 128 feet) located 1.5 to 2.0 miles from the station. For this gage, the "field measurement" data for the stage height levels seems inconsistent with the "daily" data, which begins in 1989. Measurements from two of the wells in the early 1950s are insufficient to conclude the relationship between the groundwater and the stream. Measurements from the 120-foot deep well completed in the Glen Rose Formation and located a distance of 1.5 mile from the gaging station indicate a significant decline in groundwater elevations between the mid-1970s and the late 1980s, likely due to pumping withdrawals. It is not possible with the available data to determine whether the

drawdown cone for this well is localized or impacts groundwater levels proximal to the stream. Therefore, data at this location do not provide adequate certainty to determine whether the stream is gaining or losing.

More clear-cut information is available for the gaging station at the Leon River near Hasse (gage 08099500). Although lateral distances between wells and the station generally exceed 1 mile, the wells with shallower depths (68 to 100 feet) likely represent near-surface groundwater conditions. Further, the water-level data are consistently higher than the stream level data by over 20 feet. This suggests that the river, at this location, is gaining base flow from the groundwater.

Roughly 25 miles downstream of the above station lies the Leon River near Hamilton station (gage 08100000). Two measurements are available for a 50-foot deep well located a short distance (roughly 225 feet) from the station. The groundwater elevation at the location of this well is 25 feet higher than that of the stream gage. The water levels in the well and in the stream are very similar and, due to the limited number of water-level measurements in the well, a conclusion regarding whether the stream is gaining or losing could not be drawn.

The comparison of shallow groundwater to the stream elevation at the station at the Brazos River near Aquilla (gage 08093100) is straightforward, despite the low number of groundwater level observations (see Figure 4.6.6). The wells near this station are both shallow (37 and 12 feet) and are relatively near the station (0.4 and 1.2 miles). Stream stage data prior to the commencement of daily data acquisition in 1987 seem biased toward high-flow events, but the two shallow groundwater level measurements exceed these by several tens of feet. The well elevations exceed the stream gage elevation by significant amounts (86 and 98 feet). The shallow depths and relatively close proximities of the wells to the gaging station indicate the presence of shallow groundwater at a height above the stream within a relatively short distance. Despite the limited amount of well data, it is reasonable to infer that the stream is gaining base flow from groundwater at this location.

Figure 4.6.7 shows stream/groundwater relationships in the vicinity of four USGS stream gaging stations in the southern portion of the study outcrop area. The northernmost of the three gaging stations is the Lampasas River near Kempner station (gage 08103800). Three wells with depths ranging between 70 and 80 feet are located less than 1 mile from the stream gage. The well with

the greatest amount of water-level data is located roughly 0.2 miles from the gaging station. Water-level measurements for all three wells are very similar to the stream level data. Therefore, no conclusion could be drawn as to whether the stream is gaining or losing at this location.

A relatively large number of shallow (less than 100-foot deep) wells are located between 0.5 and 0.6 miles from the Berry Creek near Georgetown station (gage 08105100). With the exception of a relatively recent measurement in a well completed at a depth of 72 feet in the Edwards BFZ Aquifer, groundwater elevations in these wells typically exceeds that of the stream level. With the exception of the most recent measurement in the Edwards BFZ Aquifer well, water levels in that well tend to be a few feet lower than the water levels in the other wells. The data at this location suggest that the stream was likely gaining water from base flow prior to about 1995 but at some point after that time local pumping likely reversed this condition and the stream became a losing stream.

The South Fork San Gabriel River at Georgetown station (gage 08104900) is located a little over 3 miles south-southwest of the station discussed directly above (see Figure 4.6.7). Water levels from two wells in the vicinity of this station show water-level elevations higher than the stream level. The data suggest that the stream is likely gaining water from base flow at this location.

The analysis of stream-aquifer interaction using stream stage and water-level measurements in wells indicate that:

- At the Timber Creek near Collinsville station (08050800), the stream appears to be gaining from base flow, based on two measurements from a 190-foot deep Woodbine Aquifer well located 1.8 miles away.
- At the Rush Creek at Woodland Park station (08049240), the stream appears to be losing water to groundwater based on a single measurement from a shallow well located 0.5 miles away. Two other shallow wells located at a greater distance in the opposite direction provide contradictory measurements.
- At the Big Sandy Creek near Bridgeport station (08044000), the stream appears to be gaining from base flow.
- At the Paluxy River at Glen Rose station (08091500), the stream appears to have transitioned from a gaining stream to a losing stream between the mid–1970s to the late

1980s. However, the wells used to make this inference are deeper than ideal for characterizing near-surface groundwater conditions.

- At the Leon River near Hasse station (08099500), the stream appears to be gaining from base flow.

- At the Leon River near Hamilton station (08100000), data are insufficient to conclude whether the stream is gaining or losing.

- At the Brazos River near Aquilla station (08093100), the stream appears to be gaining from base flow.

- At the Lampasas River near Kempner station (08103800), local groundwater levels are very similar to the stream level. Therefore, no conclusion was drawn as to whether the stream is gaining or losing at this location.

- At the Berry Creek near Georgetown station (08105100), the stream appears to generally be a gaining, although a relatively recent water-level measurement suggests the possibility that the stream is now losing.

- At the South Fork San Gabriel River at Georgetown station (08104900), the stream appears to be gaining from base flow.

4.6.1.3   Gain/Loss Studies

Gain-loss or low-flow studies have traditionally been used to estimate gaining or losing conditions in a stream. These methods basically perform a flow balance between two stream control points. The net gain, or loss, of flow between the two control points is assumed to be a result of stream gain or loss, depending upon the sign of the difference in measured flows. The key to assessing stream conditions using this method is the assumption that surface runoff is negligible and, therefore, the studies are performed at low-flow conditions. It is also important to characterize all diversions and return flows occurring over the period of the study in terms of timing, quantity, and downstream propagation. A literature review of gain/loss studies conducted in the study outcrop area was performed. Three reports were reviewed and summarized for gain/loss studies performed in Oklahoma (Laine and Cummings, 1963; Westfall and Cummings, 1963; Davis and Hart, 1978). Two reports documenting historical stream gain/loss studies were reviewed and summarized for Texas. The first was Slade and others (2002), who compiled the results of USGS gain/loss studies conducted in Texas, and the second was Baldys and Schalla (2011), who studied aquifer-stream interaction on the Brazos River.

USGS Gain/Loss Studies in Oklahoma (Laine and Cummings, 1963; Westfall and Cummings, 1963; Davis and Hart, 1978)

The USGS conducted a series of gain/loss studies focused on the Muddy Boggy River (Westfall and Cummings, 1963) and the Kiamichi River (Laine and Cummings, 1963), both of which cross the northern Trinity Aquifer outcrop in Oklahoma. Within the study outcrop area, Westfall and Cummings (1963) provide 46 low-flow measurements from 1939 to 1963 at six stations (Table 4.6.1). Laine and Cummings (1963) provide eight measurements from 1962 at three stations (Table 4.6.2). A later gain/loss study by Davis and Hart (1978) focused on low-flow contributions specifically from the Antlers Aquifer. Their study documents 16 measurements from 1975 to 1976 at four stations (Table 4.6.3).

USGS Gain/Loss Studies in Texas (Slade and others, 2002)

A comprehensive compilation of gain/loss studies in Texas is provided by Slade and others (2002). This compilation contains the results of 366 gain/loss studies conducted since 1918, which include 249 individual stream reaches throughout Texas. They document 29 gain/loss studies in the study outcrop area (Figure 4.6.8). These studies are all located in the southern portion of the study outcrop area (Leon River and south) and include reaches crossing the northern Trinity and Edwards BFZ aquifer outcrops. Table 4.6.4 summarizes the results of these studies and detailed characteristics of the studies are tabulated in Appendix F.1. Slade and others (2002) do not document gain/loss studies intersecting the Woodbine Aquifer outcrop.

According to the studies documented in Slade and others (2002), the only river that is generally losing over the northern Trinity Aquifer outcrop is the Lampasas River. However, while the Lampasas River does have negligible flow for a small portion of the year, its near perennial flow indicates it may historically have been a consistently gaining stream. This inconsistency could be attributed to the fact that gain/loss studies represent a snapshot of the river at a given time, rather than a long-term average. Streams can typically gain and lose across the same year and depending upon the reach of stream. Groundwater flow models generally try to reproduce the average stream-aquifer interaction that may be integrated over a season or even a year.

With gain/loss studies, the analyzed measurements are typically recorded over a relatively short period of time, whereas stream base flow has a strong climatically driven temporal component. For example, four studies on the same stretch of the North Fork San Gabriel River [(studies 14 to

17 in Slade and others (2002)], conducted in different years and seasons, yielded significantly different values for gain/loss estimates. Studies on Berry Creek (studies 1 to 4) show that the stream was gaining with the exception of one time period. Therefore, results from gain/loss studies were used only to inform evaluation of stream-aquifer interaction in the model.

USGS Gain/Loss Studies for the Brazos River (Baldys and Schalla, 2011)

The USGS conducted gain/loss studies in 2010 and base flow analyses for 1966 to 2009 along the Brazos River and its tributaries (Baldys and Schalla, 2011). The study extended from the New Mexico-Texas state line to Waco. The gages they analyzed that lie within the study outcrop area are shown in Figure 4.6.9 and summarized in Table 4.6.5 with the results of their analysis. The results of their gain/loss studies are discussed here and the results of their base flow analyses are discussed in Section 4.6.1.4.

Seasonal measurements of discharge and specific conductance were made in June and October 2010 along the Brazos River and its tributaries in order to characterize the gaining or losing nature of the stream. Those measurement values are included in Table 4.6.5. The study found most of the North Bosque River to be gaining, with the exception of the upstream site on the North Fork North Bosque River north of Stephenville, Texas (site NB–1on Figure 4.6.9), which had no flow in either season. Streamflow values on the North Bosque River were generally much lower in October than in June, as would be expected from precipitation patterns. The stream reach from site NB–1 to site NB–2 was thought to gain base flow from the northern Trinity Aquifer, but treated effluent from Stephenville, Texas might have also been a source. The gain in streamflow on the stretch between sites NB–3 and NB-5 was also thought to be from the underlying northern Trinity Aquifer, since the East Bosque River (site NB–4), the largest tributary, contributes very little inflow. Downstream, the North Bosque River continues to gain water, likely from groundwater inflows, but not necessarily from the northern Trinity Aquifer.

Baldys and Schalla (2011) report that they were unable to conclusively determine whether the main stem of the Brazos River was gaining or losing. Flow in the reach from downstream of Lake Granbury to Lake Whitney (characterized by site BMS-7) increased due to input from the Paluxy River (BMST-8), Squaw Creek (BMST-9), and Nolan River (BMST-10) and, also potentially, from the northern Trinity Aquifer. The reach from Lake Whitney to the mouth of the North Bosque River (characterized by site BMS-8) increased due to input from Aquilla Creek

(BMST-12 and BMST- 14), Cobb Creek (BMST-13), and Childress Creek (BMST-11) and, also potentially groundwater inputs. However, the actual amount of groundwater input to these two reaches is very uncertain. Each reach only had one measurement site on the main stem and so data were insufficient to conclusively characterize those sections of the Brazos River as gaining. In addition, the measurements could have potentially been affected by reservoir releases.

4.6.1.4   Hydrographic Separation Studies

Hydrograph separation is a methodology whereby streamflow hydrograph data are analyzed and surface runoff is partitioned from the stream base flow component. The basic premise of this method is that the sharp peaks in the streamflow hydrograph represent surface runoff events, and the smooth, constant portion of the streamflow hydrograph represents base flow. The base flow for a stream is then assumed to be flow supplied by groundwater. There are several automated methods available to perform hydrograph separation. The hydrograph separation code Base Flow Index (Wahl and Wahl, 1995) was used for the analyses in this study. Figure 4.6.10 shows an example of this technique for streamflow gage 08091000 located on the Brazos River near Glen Rose, Texas in Somervell County. This figure shows a relatively steady base flow component across orders of magnitude changes in overall flow. Once base flow is estimated using hydrograph separation, an estimated areal recharge flux (a rate with units of length per unit time) can be calculated by dividing the estimated base flow rate by the drainage area upstream of the gage.

The following discussion briefly summarizes historical hydrograph separation analyses conducted in the study outcrop area and then presents the analyses conducted for this study. Historical hydrograph separation analyses include those of Wolock (2003a), Bené and others (2004), Baldys and Schalla (2011), and Kirk and others (2012).

USGS Conterminous U.S. Hydrograph Separation Study (Wolock, 2003a, b)

In 2003, the USGS published a study for the entire conterminous U.S. that estimated the base flow component of streamflow at more than 19,000 USGS stream gages (Wolock, 2003a). These point estimate values were then used to interpolate a 1-kilometer grid raster data set of base flow index values that could be used to estimate base flow index values even for streams with no gaged data (Wolock, 2003b). The base flow index is the ratio of base flow to total

streamflow, expressed as a percentage. His estimates of stream base flow were calculated using the Base Flow Index code (Wahl and Wahl, 1995).

From the base flow index grid, a raster data set of groundwater recharge can be estimated by multiplying the base flow index grid by a grid of average annual run off. The approach used by Wolock (2003b) has two underlying assumption; long-term average groundwater recharge is equal to long-term average groundwater discharge, and the base flow index provides a basic long-term estimate of the percentage of groundwater discharge comprising streamflow. Like all hydrographic separation methods, this method likely underestimates recharge. Wolock (2003b) reported that his method underestimates recharge in areas of high irrigation and areas where ET is high. Another issue related to the Wolock (2003a) study is that it did not discriminate between regulated and unregulated gages, so reservoir releases and other human related return flows appear as base flow.

Figure 4.6.11 plots the gage estimated base flow index ratios in the study outcrop area after Wolock (2003a, b). The base flow index provides an estimate of the percent of long-term streamflow that is contributed by aquifer discharge. The base flow index values are almost all greater than zero, consistent with the conceptual model that most streams in the region are, on average and over the long term, gaining streams. The base flow index values are highest in the vicinity of the Lampasas and Leon rivers in the southern portion of the study outcrop area. The higher base flow index values imply that base flow is a high percentage of average river flow in these areas. Intermediate base flow index values occur in a large portion of Texas between the northern Trinity and Woodbine aquifer outcrops and in Oklahoma and Arkansas. The lowest values are found in the westernmost portion of the northern Trinity Aquifer outcrop and in eastern Tarrant County near the West Fork of the Trinity River. These lower values imply a smaller contribution from groundwater.

Because the Wolock (2003a, b) studies did not discriminate between regulated and unregulated gages and used a somewhat one-size fits all approach, the results from his studies were not relied on in a quantitative sense.

2004 Northern Trinity/Woodbine Aquifers GAM (Bené and others, 2004)

The GAM constructed in 2004 for the northern Trinity and Woodbine aquifers estimated base flow the hydrograph separation analyses using the Base Flow Index code of Wahl and Wahl

(1995) (Bené and others, 2004). The USGS streamflow gages used in their analysis are shown in Figure 4.6.12. Table 4.6.6 summarizes the results from their analysis, which they used to calibrate aquifer discharge to streams in the GAM. They observed no decrease in base flow over the period of record. The median base flow at all gages was positive with five sites on Denton Creek and the Paluxy, North Bosque, Leon, and Lampasas rivers exceeding 5 cubic feet per second median base flow. The Lampasas River at Youngsport, Texas had the largest median base flow at 25 cubic feet per second. Most of the streamflow data analyzed by Bené and others (2004) were also used for the current analyses described in Section 4.6.1.4. However, four of the gages they used were not included in the current study as indicated in Table 4.6.6 and explained in Table 4.6.9.

USGS Hydrograph Separation Analyses for the Brazos River (Baldys and Schalla, 2011)

The hydrograph separation analyses of Baldys and Schalla (2011) calculated yearly base flow indexes (base flow divided by total streamflow) for four gages with historical streamflow data located in the study outcrop area. Their calculated base flow indexes range from 0.19 to 0.35 (see Table 4.6.5) and generally increase from west to east. This suggests that the portion of streamflow contributed by the underlying aquifer increases from west to east. Baldys and Schalla (2011) found that gage 08090800 (BMS-6 on Figure 4.6.9) had statistically significant increases in base flow over time but, since regulated years of data were included, it was uncertain whether or not this increase might have been influenced by reservoir releases. Three of the gages used by Baldys and Schalla (2011) were used in the current hydrograph separation analysis. The fourth gage was not used because the watershed lies predominately outside of the study outcrop area.

Hydrograph Separation Analysis as Part of Recharge Study for GMA 8 (Kirk and others, 2012)

Kirk and others (2012) conducted a large-scale study for the TWDB using remote sensing technology to develop a groundwater recharge model for GMA 8 in Texas. As part of that study, they conducted a hydrograph separation analysis on 24 select USGS gages in order to calibrate the annual shallow stream discharge in their water balance model. The locations of these gages are shown in Figure 4.6.12. Table 4.6.7 provides the base flow values they estimate for these gages using the USGS streamflow partitioning program PART (Rutledge, 1998). Several of

their base flow estimates are based on time periods during which the representative gage is regulated, or affected by an unknown degree by upstream diversions or reservoirs. Therefore, the base flow estimates for those gages cannot be used to estimate recharge.

Current Hydrograph Separation Study

Hydrograph separation is relatively easy to perform; however, obtaining appropriate gage data can be difficult. Gages and their corresponding data should meet certain criteria before being used for analysis. The primary criteria considered in the current study are:

- The gage should be on a stream considered to be primarily gaining.
- The majority of the catchment area for the gage must be unregulated (i.e., not influenced by reservoir discharge). If the gage is paired with an upstream gage, the unregulated periods must have a significant overlapping record.
- The catchment area for the gage should be primarily in the outcrop of interest.

The first criterion ensures that the hydrograph separation calculation can be accomplished. For a river with perennial flow (i.e., a gaining river), a large percent of the basin yield can come from base flow, indicating that a large portion of rainfall infiltrates into the basin as groundwater recharge and reaches the stream as subsurface flow (Chow and others, 1988). However, for a gage located on an intermittent stream, an estimate of base flow would only be valid for times when the stream was flowing. The second criterion ensures that estimated gains to the system are due to groundwater sources rather than discharge from reservoirs or return flows. The third criterion ensures that results are valid for the aquifer of interest.

The second criterion is difficult to overcome, since many of the major rivers in Texas are highly regulated (i.e., influenced by reservoir discharge). In some cases, analysts attempt to use local knowledge of river management to account for regulation of the river. This is a difficult and time-consuming approach that is not tractable for the current study given the regional nature of the model. Instead, regulated periods of record were not considered for the current analysis. Estimates of the time periods when a stream was regulated are available in Slade and others (2002) for Texas and Lewis and Esralew (2009) for Oklahoma. These reports list beginning and ending years of regulation for many active and discontinued streamflow gaging stations in the study outcrop area. Calculations of base flow were made based on the unregulated years as provided in these reports. Since a gage's "unregulated" status could only be considered valid up

to each report's publication date, individual gage information available from the USGS National Water Information System database (USGS, 2013b) was used to confirm unregulated status up to the current year. Gages were rejected if they were classified as "urbanized" in either report, as the calculated base flow values would reflect anthropogenic influences rather than natural recharge conditions.

Flow Duration Curves

The first step in conducting the hydrograph separation analysis is the calculation of flow duration curves to indicate the relative perennial nature of a particular gaged stream segment, thus addressing the first criterion that the stream is gaining. Example flow duration curves are presented in Figure 4.6.13. The flow duration curve for gage 8050800 (Figure 4.6.13a) indicates that the gaged portion of the stream is intermittent, as evidenced by the curve terminating near 60 percent. This indicates that the streamflows 60 percent of the time and does not flow 40 percent of the time. The flow duration curve for gage 7340000 terminates near 100 percent, which is characteristic of a perennial stream (Figure 4.6.13b). Flow duration curves were calculated for all unregulated, un-urbanized gages. For the purposes of this analysis, a stream was considered intermittent if it flowed less than 90 percent of the time. All calculated flow duration curves are provided in Appendix F.2.

Hydrograph Separation Analysis

Once perennial streams were identified using the calculated flow duration curves, the gages in those streams were evaluated to determine if they included more than 10 years of unregulated data. This was done to satisfy criterion 2. The contributing drainage area for these gages as reported in the USGS National Water Information System database (USGS, 2013b) was then determined. For those gages with the contributing area not noted, the total drainage area was used. To meet criterion 3, only those gages with the majority of the contributing area located in the study outcrop area of were used. This resulted in 36 gages for which hydrograph separation was performed.

Table 4.6.8 summarizes the results of the hydrograph separation analysis. Dividing the average base flow by the drainage area yields the rate of recharge required to sustain the base flow. These recharge estimates are discussed in detail in Section 4.5. The average base flow volume in AFY and the average base flow rate in inches per year are provided in Table 4.6.8. Calculated

base flow rate estimates are in the range of 0.12 to 5.39 inches per year with a median value of 1.7 inches per year. These values compare favorably to recharge rates reported by Scanlon and others (2002a), which places average recharge to the northern Trinity Aquifer at 0.1 to 2 inches per year based on a compilation of literature values in the study area. Base flow estimates tended to be higher in the wetter northern portion of the study outcrop area where precipitation is higher. Figure 4.6.14 shows the gages and watersheds analyzed with the estimated average base flow expressed as a rate in inches per year. Table 4.6.9 summarizes the unused gages in the area and the reason for their rejection.

Temporal Trends in Base Flow

The yearly estimates of base flow produced by the Base Flow Index code (Wahl and Wahl, 1995) provided an opportunity to examine base flow trends through time. Because streamflow and shallow aquifer levels change due to climate, base flow is expected to change with time. To the degree that groundwater pumping impacts shallow water levels, it can also have an effect. Figure 4.6.15 shows examples of long-term base flow estimates for gages in the study outcrop area (long-term trends for all gages used in the base flow analysis are shown in Appendix F.2). The long-term base flow estimates were used to calculate an average base flow and areal recharge value for each gage. Averages were only calculated for perennial gages with greater than 10 years of unregulated data. In general, the trends are mixed, showing no consistent evidence of either an increase or decrease with time since considerable scatter exists in the data.

Correlation between Precipitation and Base Flow

In a natural environment, a correlation between the amount of rainfall in the drainage area and base flow is expected. As rainfall increases, the groundwater table should rise, increasing the hydraulic gradient and causing increased flows to streams. In order to determine the amount of rainfall that the drainage area for each gage received over time, monthly total precipitation data was used with ArcGIS and the Spatial Analyst Tool. With ArcGIS, it was possible to calculate the average total precipitation over each watershed and create a monthly time series for each gage. Using this time series, along with the calculated base flow, a linear regression of 12-month average precipitation versus 12-month average log (base flow) was created. Since the lag time between precipitation events and discharge to a stream is unknown, time lags between 1 and 6 months were analyzed for each case. The lag that produced a regression with the highest

coefficient of determination (R^2 value) was selected for that gage. For perennial streams with greater than 10 years of unregulated data, the average optimal lag time was a little over 2 months. Figure 4.6.16 provides examples of this regression relationship along with the calculated coefficient of determination for the gages shown in Figure 4.6.15. The coefficient of determination was used as a metric to judge the strength of the relationship between the two variables. Therefore, while both gages show the expected positive correlation between base flow and the amount of precipitation, gage 7332500 shows a stronger correlation ($R^2 = 0.7$) than gage 08101000 ($R^2 = 0.54$). In areas where there was little correlation between precipitation and base flow (low R^2 value), it could be possible that external factors are influencing the estimate of base flow. The slope for gage 08101000 is steeper (see Figure 4.6.16b), indicating a stronger sensitivity of base flow to changes in precipitation. The shallower slope seen for gage 7332500 is common in the northern section of the study outcrop area, where precipitation is higher (see Figure 4.5.24). This indicates that the base flow for northern streams (wetter climate) is less sensitive to precipitation fluctuations then the streams in the drier, southern portion of the study outcrop area. The regression plots for all unregulated, non-urbanized gages are provided in Appendix F.2. For the purposes of this analysis, an R^2 value of less than 0.3 was assumed to indicate influence from factors other than climate.

Diversions

The analysis of gage data was done with the understanding that the hydrographs are affected by diversions related to irrigation water use in the study outcrop area. However, total diversions are estimated on a larger scale than many of the watersheds analyzed here. Therefore, it was extremely difficult to accurately attribute a diversion amount to a particular USGS gage watershed. In addition, the timing of the diversions is largely unknown, meaning it was not known if the diversion occurred during runoff events or during times where base flow provided a significant portion of the overall streamflow. Since omitting the effect of diversions might bias the results towards lower recharge, the calculated values from the hydrograph separation analyses should be considered lower limits for areal recharge values.

Basins Originating Outside the Study Region

When quantifying stream-aquifer interaction, ideally the watersheds of the analyzed gages should fall largely on the aquifer outcrops of interest, as noted in the third criterion at the

beginning of this section. However, several of the watersheds shown in Figures 4.6.14 do not

originate in the study outcrop area and large portions fall outside the northern Trinity and

Woodbine aquifer outcrop areas. This is true of most of the northern rivers that flow through

southern Oklahoma, as well as the Brazos and Leon Rivers in the southern portion of the study

outcrop area. The analysis of gages in these basins was made with the understanding that the

cumulative effects from catchment areas further upstream and outside the study outcrop area are

present in the results. Theoretically, a gage just upstream of the study outcrop area boundary can

be analyzed, and the results subtracted from gages inside the study outcrop area, to determine the

incremental addition of base flow that occurs inside the study outcrop area. In practice, it is

difficult to determine what portion of the base flow originates in the study outcrop area for these

rivers, since the incremental addition of base flow in the study outcrop area may be small

compared to the overall inflow. Therefore, while these gages are useful in demonstrating the

general spatial trends of recharge in the study outcrop area, they were used cautiously as

recharge estimates specific to the northern Trinity and Woodbine aquifers.

4.6.1.5   Calibration Targets for Streams

In addition to calibrating the model to hydraulic head data as described in Section 4.3.5, the

model was also calibrated to streamflow data by comparing model predicted stream-aquifer

interaction with observed stream-aquifer interaction. The calibration targets for streams were

taken from observed base flow based on the current hydrograph separation analyses. These

calibration targets are summarizes in Table 4.6.10. Because base flow is typically a cumulative

measurement (the result of the addition of water in all contributing areas upstream), the targets

are expressed as an average annual volumetric flow rate (AFY) expected at that point in the

stream. The percentage of each watershed that falls within the study outcrop area was

calculated. The calibration targets presented in Table 4.6.10 were determined by weighting the

base flow estimates from the hydrograph separation analysis by this percentage. This was done

in an effort to minimize the inclusion of base flow that is coming from formations other than

those that outcrop in the study outcrop area. Because all of these estimates vary in the amount of

supporting data and the timing of the measurements upon which they were based, they have

considerable uncertainty as strict calibration targets. Still, they provide a guideline for

constraining base flow in the groundwater model.

4.6.2 Groundwater ET, Springs, and Reservoirs

The following subsections discuss natural aquifer discharge via groundwater ET, springs, and reservoirs.

4.6.2.1   Groundwater ET

ET is the combined process of soil water evaporation near the land surface and the uptake in the root zone and subsequent transpiration of water by vegetation. For the purposes of groundwater modeling, two types of ET are distinguished: vadose zone ET and groundwater ET. ET in the vadose zone captures infiltrating water before it reaches the water table. Groundwater ET is plant uptake or surface evaporation of groundwater. Here, the focus is groundwater ET, since it is the type implemented in the groundwater model. Vadose zone ET is already accounted for in the recharge estimate.

Groundwater ET occurs primarily in riparian areas adjacent to streams (Scanlon and others, 2005). Riparian zones are not specifically mapped in Texas. Two methods can be used for defining the location of groundwater ET in the study outcrop area. Either a fixed buffer around the streams can be defined as riparian areas, or the topographically lower areas can be assumed to be likely regions of groundwater ET. In general, the goal is to limit the potential for groundwater ET to regions where the water table is near ground surface. Some potential for groundwater ET is expected in the outcrop of the northern Trinity and Woodbine aquifers near the rivers and streams that occur in the outcrop.

Scanlon and others (2005) summarize the conceptual approach to estimating groundwater ET. In general, if water tables are very near the surface, ET will be close to the potential ET, assuming there is some type of vegetative cover. Potential ET and reference ET are terms often used interchangeably. Reference ET is defined as the ET rate from a reference vegetation, often a short grass, that has unlimited available water. Potential ET should not be confused with "pan evaporation", which is the rate of water evaporation from an open pan. Potential ET can be related to pan evaporation by the use of pan coefficients; however, since potential evaporation can be estimated with basic climate data, pan evaporation is not used in the calculation of potential ET.

When the water table is below ground surface, but still in the main vegetation root zone, ET will occur at the unhindered vegetative evapotranspiration rate. This can be estimated by (Scanlon and others, 2005):

$$ETVmax = PET * Kc \qquad (4.6.2)$$

where

> $ETVmax$ = unhindered vegetative evapotranspiration rate (length per time)
>
> Kc = vegetation coefficient
>
> PET = potential ET (length per time)

Thus, to parameterize groundwater ET, three parameters must be estimated: potential ET, vegetation coefficient, and rooting depth. Rooting depth and vegetation coefficient are specific to the type of vegetation, so a necessary prerequisite is some knowledge of the types of vegetation in the riparian areas in the study outcrop area. The following paragraphs discuss how the types of vegetation in the study outcrop area were estimated, the corresponding vegetation coefficients and rooting depths, and potential evaporation in the area.

Borrelli and others (1998) provide an estimate of long-term potential ET in Texas, based on the Penman-Monteith method, as reproduced in Figure 4.6.17 for the study outcrop area. This figure shows that the long-term average potential ET ranges from about 53 to 66 inches per year and generally increasing from east to west. Although ET varies considerably with seasons, it does not vary significantly from year to year (annual average basis). For this reason, the assumption is made that potential ET is constant throughout a transient simulation, where annual stress periods are used.

The 2006 National Land Cover Database (Fry and others, 2011) provides detailed land use data for the entire conterminous U.S. (see Figure 4.5.8 for the study area and vicinity). Figures 4.6.18 through 4.6.21 show land use coverage in greater detail for the study outcrop area in the North Texas, Northern Trinity, Prairielands, and Upper Trinity GCDs, respectively. Unfortunately, this national land cover data set does not specifically identify riparian vegetation or riparian zones. However, relevant parameters for groundwater ET can be estimated from Scanlon and others (2005), which provides a database of estimates of vegetation coefficient and rooting depths for many types of vegetation. Table 4.6.11 shows estimates for several vegetation types relevant to

the study outcrop area. The estimates of potential ET, vegetation coefficient, and rooting depth can be used to estimate groundwater ET parameters on a cell-by-cell basis in the model.

4.6.2.2   Springs

A spring is a location where groundwater flows out of the ground due to the aquifer hydraulic head (an elevation of the water level) exceeds the land surface elevation and a pathway to the surface exists. Springs typically occur in topographically low areas in river valleys or in areas of the outcrop where hydrogeologic conditions preferentially reject recharge. Four sources were used to find spring data: the TWDB groundwater database (TWDB, 2013a), a database of Texas springs compiled by the USGS and reported in Heitmuller and Reece (2003), the USGS National Water Information System database (USGS, 2013b), and Brune (2002). Figure 4.6.22 shows the locations of springs in the outcrops of the northern Trinity and Woodbine aquifers and the Washita/Fredericksburg groups in the study outcrop area. Springs found in Brune (2002) are included on the map with approximate locations based upon the accuracy of Brune (2002).

The literature review identified 336 springs or groups of springs in the study outcrop area, of which 90 flow out of the northern Trinity Aquifer, 23 out of the Woodbine Aquifer, and 122 out of the Washita/Fredericksburg groups. The remainder flow from alluvium, formations younger than the Woodbine Aquifer, formations older than the northern Trinity Aquifer, or unknown sources and are not further discussed. Information on all springs in the study outcrop area is included in Appendix F.3. Twenty-one springs do, or at one time did, discharge at a rate greater than 0.22 cubic feet per second (100 gallons per minute). The available measured spring flow rates range from the springs being dry to a high of 35 cubic feet per second (15,850 gallons per minute) at Salado Creek and Springs in Bell County. Brune (2002) states that this group of springs is fed through faults in the Edwards and associated limestones and rise under artesian pressure. The highest discharge was measured in 1961 and discharge was still high as of the last measurement in 1973.

Throughout much of Texas, including the study outcrop area, spring flows have shown a general decline over time. However, most information regarding spring declines for minor springs is anecdotal and undocumented. Table 4.6.12 shows that, of the springs issuing from the northern Trinity and Woodbine aquifers, 26 have records of spring flow, but only one has more than two measurements. Most have one or zero measurements, making it impossible to construct long-

term trends of spring flow in the area. Swimming Pool Springs, issuing from the northern
Trinity Aquifer in Lampasas County, the one spring with 13 measurements, does not show a
declining trend over time. However, the annual data does not extend beyond 1975 and so does
not necessarily represent the current condition of the spring.

4.6.2.3 Lakes and Reservoirs

There are no natural lakes in the study outcrop area. However, 25 reservoirs intersect the
outcrops of the northern Trinity Aquifer, Washita/Fredericksburg groups, or Woodbine Aquifer,
13 of which have a surface area of over 5,000 acres. Table 4.6.13 lists the names, owners,
surface area, and year impounded for the reservoirs in the study outcrop area with a surface area
greater than 1 square mile (640 acres). Figure 4.6.23 shows the locations of these reservoirs.
Figure 4.6.24 and Table 4.6.14 show the historical lake stage elevations for four of the reservoirs
in the study outcrop area. Reservoir stage data for all reservoirs in the study outcrop area was
collected for implementation in the model. The water-level time series from 1960 to 2012 for
Lake Texoma, located on the Texas/Oklahoma border, shows annual elevation fluctuations from
about 605 to 620 feet above mean sea level with an average value of about 616 feet above mean
sea level. The water-level time series from 1987 to 2012 for Lake Granbury, located in Hood
County, shows almost no inter-annual elevation fluctuation, with water level varying from about
690 to 693 feet above mean sea level, with an average value of about 692 feet above mean sea
level.

4.6.3 Groundwater Discharge to Younger Formations

Groundwater within the northern Trinity and Woodbine aquifers occurs under water table
conditions in the shallow outcrop areas and confined (artesian) conditions downdip of the aquifer
outcrop belts. Groundwater flow within the outcrop areas is naturally controlled by local
topography, flowing from higher elevation areas and discharging in lower elevation areas
(streams and riparian corridors). As discussed in Section 4.5, the bulk of the groundwater
recharge and discharge stays confined to the outcrop areas with only a small percent of the total
recharge flowing downdip into the confined portions of the aquifers. This recharge is deep
recharge and is generally referred to as effective recharge in the literature. Effective recharge
under predevelopment conditions discharges the aquifers through cross-formational flow and
potentially through structural features.

The force which moves groundwater from the outcrop to the downdip portions of the aquifer is derived from the difference in elevation between the outcrop and the downdip area. The outcrop area of the aquifers in the study area is at a higher elevation than the downdip portions of the aquifers. Under natural conditions, the hydraulic head (elevation of the water level and a direct measure of potential energy of groundwater) of the aquifer in the outcrop is higher than in the downdip area. This condition creates a downdip hydraulic gradient that results in flow to the deep confined portions of the aquifers. If the aquifers are of relatively high transmissivity, groundwater can flow tens of miles into the subsurface without losing significant energy.

This condition has existed within the northern Trinity and Woodbine aquifers of north-central Texas as documented by Hill (1901). Hill (1901) documented very high artesian heads in the subsurface in north-central Texas and he also documented many flowing wells within the study area. A review of groundwater quality (see Section 4.4) also provides distinct evidence of fresh connate groundwater moving from the outcrop into the subsurface. Groundwater with TDS less than 1,000 milligrams per liter can extend as much as 40 miles downdip in the northern Trinity Aquifer. The extent of fresh groundwater in the Woodbine Aquifer is generally closer to the outcrop, especially south of central Collin County. South of north McLennan County, the Woodbine Aquifer does not exist as a clastic aquifer.

While there is good evidence for significant downdip movement of groundwater from the outcrop to the subcrop, there is not good evidence of how much moves to the subcrop and how it is discharged. To constrain downdip flow to the confined section downdip of the outcrop requires good estimates of groundwater age data in these portions of the aquifer. From age data, a groundwater Darcy velocity can be estimated and used to calculate volumetric flow. This type of data is generally lacking for the northern Trinity and Woodbine aquifers.

Several studies have considered this issue in general terms (Plummer and Sargent, 1931; Klemt and others, 1975; Nordstrom 1982, 1987; Rapp, 1988; Baker and others, 1990a, b), but few have tried to quantify how confined groundwater discharges. Plummer and Sargent (1931) were likely the first to note relationships between water quality and structure in an aquifer. They noted that chloride concentrations within the Woodbine Aquifer were elevated in the vicinity of the Preston Anticline. Klemt and others (1975) stated that discharge of confined groundwater in the lower

portion of the northern Trinity Aquifer was through the mechanisms of cross-formational flow and through vertical flow at faults, such as the Mexia-Talco Fault Zone.

Dutton and others (1996) developed two groundwater models of the northern Trinity and Woodbine aquifers in a 20-county area of north-central Texas. The purpose of their cross-sectional model was to investigate, among other things, the vertical conductance of the units being modeled and the sensitivity of the flow system to potential discharge at the Mexia-Talco Fault Zone. Based upon the results from the cross-sectional flow model, they concluded that cross-formational flow was not important as compared to discharge through the fault zone. The three-dimensional model of Dutton and others (1996) estimated that flow to the deep confined section was approximately 1 percent of recharge. The 2004 GAM for the northern Trinity and Woodbine aquifers (Bené and others, 2004) may under predict deep confined recharge. That GAM predicts that approximately 5,000 AFY of deep confined flow occurs as compared to 1.23 million AFY of recharge in the Texas portion of the model. Greater than 99 percent of the total recharge in the Texas portion of their model discharges in the outcrop.

Published estimates of effective recharge in the northern Trinity and Woodbine aquifers provide some guidance for assessing deep confined flow rates. From Table 4.5.1, the range in effective or deep recharge is approximately 0.12 to 0.5 inches per year. Given the surface area of the outcrop and this range of possible effective recharge rates, effective recharge volumes can be estimated. The assumption is that confined recharge must discharge to overlying younger units through diffuse discharge or through focused discharge at fault systems. The northern Trinity Aquifer has a relatively flat and broad outcrop region over a large portion of Texas (see Figures 4.1.32 and 4.1.33 as an example). As a result, a high percentage of recharge that occurs in these outcrop areas can penetrate to the lower confined portions of the aquifer yet discharge to regional sinks represented by rivers and streams. Consequently, a small percent of recharge may actually flow into the deep confined portions of the aquifer and discharge to overlying younger units through diffuse discharge or through focused discharge at fault systems.

An assumed effective deep recharge rate of 0.1 inches per year consistent across the outcrops of the northern Trinity Aquifer, Washita/Fredericksburg groups, and Woodbine Aquifer equates to a deep recharge of approximately 102,500 AFY. Considering only the northern Trinity and

Woodbine aquifer outcrops, the effective recharge would be approximately 62,500 AFY.

Effective recharge is poorly known and, therefore, poorly constrained for model calibration.

Table 4.6.1   Low-flow stream discharge measurements from Westfall and Cummings (1963).

Station Name	Drainage Area (mi²)	Date	Discharge (cfs)	Discharge (AFY per mi²)	Estimated Drainage Area Recharge (in/yr)
Muddy Boggy Creek southwest of Sand Bluff, OK	1198	12/12/1957	297	180	3.37
		4/8/1958	304	184	3.45
		2/7/1963	102	62	1.16
Clear Boggy Creek north of Caney, OK	656	12/12/1957	139	154	2.88
Caney Creek north of Caney, OK	61.9	2/25/1958	13.6	159	2.98
		4/7/1958	18.7	219	4.10
		9/19/1962	0	0	0.00
		12/19/1962	8.68	102	1.90
		2/8/1963	4.58	54	1.01
Clear Boggy Creek north of Boswell, OK	973	12/15/1939	0.1	0	0.00
		1/11/1940	0.1	0	0.00
		1/16/1940	0.1	0	0.00
		2/23/1940	77.7	58	1.08
		3/1/1940	19.8	15	0.28
		3/8/1940	7.77	6	0.11
		3/27/1940	6.25	5	0.09
		4/22/1940	91.3	68	1.27
Clear Boggy Creek northwest of Boswell, OK	1001	12/12/1957	267	193	3.62
		2/26/1958	232	168	3.15
		4/8/1958	339	245	4.60
		5/17/1962	82.7	60	1.12
		7/11/1962	38.6	28	0.52
		8/15/1962	14.4	10	0.20
		9/19/1962	261	189	3.54
		2/7/1963	124	90	1.68
		2/8/1963	119	86	1.61

Table 4.6.1, continued

Station Name	Drainage Area (mi^2)	Date	Discharge (cfs)	Discharge (AFY per mi^2)	Estimated Drainage Area Recharge (in/yr)
		6/12/1936	152	48	0.91
		6/16/1936	60.3	19	0.36
		6/20/1936	37.5	12	0.22
		6/25/1936	10.4	3	0.06
		7/8/1936	172	55	1.03
		10/2/1936	208	66	1.24
		10/19/1936	51	16	0.30
		11/13/1936	114	36	0.68
		11/20/1936	58	18	0.35
Muddy Boggy River west of Soper, OK	2273	11/23/1936	48	15	0.29
		11/30/1936	34	11	0.20
		12/14/1936	109	35	0.65
		2/23/1937	261	83	1.56
		3/1/1937	224	71	1.34
		2/14/1962	117	37	0.70
		5/17/1962	159	51	0.95
		7/11/1962	65.7	21	0.39
		8/15/1962	22.8	7	0.14
		2/7/1963	232	74	1.39
		2/8/1963	223	71	1.33

OK = Oklahoma
mi^2 = square miles
cfs = cubic feet per second
in/yr = inches per year

Table 4.6.2   Low-flow stream discharge measurements from Laine and Cummings (1963).

Station Name	Drainage Area (mi^2)	Date	Discharge (cfs)	Discharge (AFY per mi^2)	Estimated Drainage Area Recharge (in/yr)
Kiamichi River near Apple, OK	1589	7/10/1962	47.9	22	0.41
		8/14/1962	15.7	7	0.13
		8/22/1962	9.41	4	0.08
		12/1/1962	422	192	3.61
Gates Creek near Fort Townson, OK	18.4	2/14/1962	10.3	406	7.60
Gates Creek near Lake Raymond Gary dam	55.7	7/10/1962	10.2	133	2.49
		8/14/1962	4.1	53	1.00
		9/20/1962	1.54	20	0.38

OK = Oklahoma
mi^2 = square miles
cfs = cubic feet per second
in/yr = inches per year

Table 4.6.3   Low-flow stream discharge measurements from Davis and Hart (1978).

Station Name	Drainage Area (mi^2)	Date	Discharge (cfs)	Discharge (AFY per mi^2)	Estimated Drainage Area Recharge (in/yr)
Little Huauni Creek near Lebanon, OK	25.0	10/28/75	2.7	78	1.47
		11/17/75	2.6	75	1.41
		12/11/75	3.0	87	1.63
		1/21/76	3.3	96	1.79
Davis Creek at Caney, OK	14.2	10/29/75	0.4	20	0.38
		11/17/75	0.6	31	0.57
		12/11/75	1.1	56	1.05
		1/21/76	1.1	56	1.05
Dumpling Creek near Antlers, OK	24.2	10/29/75	0.7	21	0.39
		11/18/75	2.4	72	1.35
		12/12/75	4.8	144	2.70
		1/22/76	4.2	126	2.36
West Branch of Gates Creek near Fort Towson, OK	18.9	10/29/75	3.5	134	2.52
		11/18/75	4.0	153	2.88
		12/12/75	5.2	199	3.74
		1/22/76	4.7	180	3.38

OK = Oklahoma
mi^2 = square miles
cfs = cubic feet per second
in/yr = inches per year

Table 4.6.4   **Summary of gain/loss studies from Slade and others (2002) in the study outcrop area.**

Study	Date	Gain or Loss (-) in Subreach (cfs)	Length of Subreach (river mile)	Aquifers(s)[a]	Total Gain or Loss (-) per Mile of Reach (cfs/mi)[b]
Berry Creek - Briggs to mouth (northeast of Georgetown)					
1	4/21-24/1978	0	13.6	--	0.000
1	4/21-24/1978	-0.79	13.3	Edwards	-0.059
1	4/21-24/1978	3.04	3.2	--	0.950
Berry Creek - Briggs to mouth (northeast of Georgetown)					
2	8/15/1978	0	13.6	--	0.000
2	8/15/1978	-0.21	13.3	Edwards	-0.016
2	8/15/1978	0	3.2	--	0.000
Berry Creek - Briggs to mouth (northeast of Georgetown)					
3	2/15/1979	18.12	13.6	--	1.332
3	2/15/1979	-0.33	13.3	Edwards	-0.025
3	2/15/1979	13.5	3.2	--	4.219
Berry Creek - Briggs to mouth (northeast of Georgetown)					
4	8/14-15/1979	2.53	13.6	--	0.186
4	8/14-15/1979	8.23	13.3	Edwards	0.619
4	8/14-15/1979	10.99	3.2	--	3.434
Brushy Creek - northwest of Leander to 4 miles east of Round Rock					
5	4/17-18/1978	0.38	2.6	--	0.146
5	4/17-18/1978	2.71	13.2	Edwards	0.205
5	4/17-18/1978	-1.03	1	--	-1.030
Brushy Creek - northwest of Leander to 4 miles east of Round Rock					
6	8/17-18/1978	0	2.6	--	0.000
6	8/17-18/1978	-0.08	13.2	Edwards	-0.006
6	8/17-18/1978	0.15	5	--	0.030
Brushy Creek - northwest of Leander to 4 miles east of Round Rock					
7	2/13-14/1979	3.77	2.6	--	1.450
7	2/13-14/1979	30.06	13.2	Edwards	2.277
7	2/13-14/1979	14.22	5	--	2.844
Brushy Creek - northwest of Leander to 4 miles east of Round Rock					
8	8/13-14/1979	0.9	2.6	--	0.346
8	8/13-14/1979	2.89	13.2	Edwards	0.219
8	8/13-14/1979	2.78	5	--	0.556
Lampasas River - northeast of Lampasas to mouth					
10	6/3-6/1963	-3.95	46.3	Trinity	-0.085
10	6/3-6/1963	0.3	14.6	--	0.021
10	6/3-6/1963	-1.85	18.9	Edwards	-0.098
Lampasas River - Stillhouse Hollow Dam site to confluence with Little River					
11	1/16/1968	15.88	15.7	Edwards	1.011
Leon River - Belton Dam to Little River					
12	1/16-17/1968	2.48	9	--	0.276

Table 4.6.4, continued

Study	Date	Gain or Loss (-) in Subreach (cfs)	Length of Subreach (river mile)	Aquifers(s)[a]	Total Gain or Loss (-) per Mile of Reach (cfs/mi)[b]
Leon River - southeast of Eastland to near Hasse					
13	3/13-14/1951	0.23	10.3	Trinity	0.022
North Fork San Gabriel River - above US 183 to Country Club Road at Georgetown					
14	4/26-27/1978	1.08	8.4	Trinity	0.129
14	4/26-27/1978	2.57	8.6	Edwards	0.299
North Fork San Gabriel River - above US 183 to Country Club Road at Georgetown					
15	8/16-26/1978	0.03	8.4	Trinity	0.004
15	8/16-26/1978	0.04	8.6	Edwards	0.005
North Fork San Gabriel River - above US 183 to Country Club Road at Georgetown					
16	2/13-15/1979	18.26	8.4	Trinity	2.174
16	2/13-15/1979	15.48	8.6	Edwards	1.800
North Fork San Gabriel River - above US 183 to Country Club Road at Georgetown					
17	8/13-15/1979	5.35	8.4	Trinity	0.637
17	8/13-15/1979	4.05	8.6	Edwards	0.471
North Fork San Gabriel River - north of Leander to mouth					
18	3/16-18/1964	-0.35	4.6	Trinity	-0.076
18	3/16-18/1964	2.33	9.8	Edwards	0.238
Salado Creek - northwest of Florence to Salado					
19	4/24/1978	15.29	26.2	Edwards	0.584
Salado Creek - northwest of Florence to Salado					
20	8/14/1978	8.96	26.2	Edwards	0.342
Salado Cr - northwest of Florence to Salado					
21	2/16/1979	63	26.2	Edwards	2.405
Salado Creek - northwest of Florence to Salado					
22	8/15/1979	49.09	26.2	Edwards	1.874
San Gabriel River - Georgetown (08105000) to mouth					
24	3/17-18/1964	-2.06	9	--	-0.229
South Fork San Gabriel River - US 183 to SH 29 at Georgetown					
25	3/16/1964	1.38	12.8	Edwards	0.108
South Fork San Gabriel River - near Bertram to Georgetown					
26	4/19-21/1978	1.4	16.7	Trinity	0.084
26	4/19-21/1978	-0.07	2.8	--	-0.025
26	4/19-21/1978	3.76	10.2	Edwards	0.369
South Fork San Gabriel River - near Bertram to Georgetown					
27	8/17/1978	20.01	16.7	Trinity	1.198
27	8/17/1978	-20.01	2.8	--	-7.146
27	8/17/1978	0.01	10.2	Edwards	0.001
South Fork San Gabriel River - near Bertram to Georgetown					
28	2/13-15/1979	16.75	16.7	Trinity	1.003
28	2/13-15/1979	6	2.8	--	2.143
28	2/13-15/1979	10.47	10.2	Edwards	1.026

Table 4.6.4, continued

Study	Date	Gain or Loss (-) in Subreach (cfs)	Length of Subreach (river mile)	Aquifers(s)[a]	Total Gain or Loss (-) per Mile of Reach (cfs/mi)[b]
South Fork San Gabriel River - near Bertram to Georgetown					
29	8/13-15/1979	3.81	16.7	Trinity	0.228
29	8/13-15/1979	1.41	2.8	--	0.504
29	8/13-15/1979	3.37	10.2	Edwards	0.330
Sulphur Creek - Lampasas to 1.5 miles downstream from Burleson Creek					
30	6/30/1942	2.7	0.53	Trinity/Marble Falls	5.094
30	6/30/1942	12.5	3.14	Trinity	3.981
Sulphur Creek - Lampasas to 1.5 miles downstream from Burleson Creek					
31	8/10/1942	1.8	0.53	Trinity/Marble Falls	3.396
31	8/10/1942	9.9	3.14	Trinity	3.153
Colorado River - Robert Lee to Barton Springs (08155500)					
53	4/7-24/1925	1	31	Edwards, Trinity	0.032
Colorado River - Robert Lee to mouth					
54	8/7-14/1918	1.4	13	Trinity	0.108

[a] Texas major or minor aquifer over which the river segment lies; -- indicates that the segment does not lie on a major or minor Texas aquifer

[b] The gain/loss estimate is for the portion of the river reach located over the study outcrop area.

cfs = cubic feet per second

cfs/mi = cubic feet per second per mile

Table 4.6.5 **Summary of Baldys and Schalla (2011) gain/loss study and hydrograph separation analyses results for gages located in the study outcrop area.**

Gage Number[a]	Station Name	Station Identifier	Gain/Loss Study Discharge (cfs)[b]		BFI from Hydrograph Separation Analyses[c]	Used in Current Hydrograph Separation Analyses
			June 6-9, 2010	Oct 16-19, 2010		
8090800	Brazos River near Dennis, TX	BMS-6	192	172	0.27	No[d]
8091000	Brazos River near Glen Rose, TX	BMS-7	99	62.4	0.19	Yes
8093100	Brazos River near Aquilla, TX	BMS-8	252	252		
324151097581900	Grindstone Creek at I-20 near Brock Junction, TX	BMST-7	0.05	0.06		
8091500	Paluxy River at Glen Rose, TX	BMST-8	35.4	9.84	0.35	Yes
8091750	Squaw Creek near Glen Rose, TX	BMST-9	15.6	4.45		
8092000	Nolan River at Blum, TX	BMST-10	6.63	8.76		
314220097174100	Childress Creek at FM 2490 near Waco, TX	BMST-11	3.54	4.33/5.02		
8093360	Aquilla Creek above Aquilla, TX	BMST-12	2.26	14		
315300097114200	Cobb Creek near Aquilla, TX	BMST-13	0	no flow		
8093560	Aquilla Creek at FM 1858 near Ross, TX	BMST-14	15.5	22.1		
321513098133100	North Fork North Bosque River at State Route 108 near Stephenville, TX	NB-1	0	no flow		
8094800	North Bosque River at Hico, TX	NB-2	11.7	4.16		
315839097534200	North Bosque River at Hwy 6 near Iredell, TX	NB-3	14.2	4.85		
320106097465700	East Bosque River at FM 927 near Walnut Springs, TX	NB-4	0.87	0.26		
315510097394300	North Bosque River at Hwy 22 at Meridian, TX	NB-5	26.1	7.60/7.59		
314842097364100	Meridian Creek at Hwy 6 near Clifton, TX	NB-6	0	3.70/3.52		
8095000	North Bosque River near Clifton, TX	NB-7	47.9	17.6	0.30	Yes
314136097320700	Neils Creek at Hwy 6 near Valley Mills, TX	NB-8	18.2	6.84		
8095200	North Bosque River at Valley Mills, TX	NB-9	86.7	39.1		

Table 4.6.5, continued

Gage Number[a]	Station Name	Station Identifier	Gain/Loss Study Discharge (cfs)[b]		BFI from Hydrograph Separation Analyses[c]	Used in Current Hydrograph Separation Analyses
			June 6-9, 2010	Oct 16-19, 2010		
313830097220100	North Bosque River near China Springs, TX	NB-10	0	41.4		

[a] Note that all gages with a 15-digit number were created solely for the purpose of the Baldys and Schalla (2011) study, so no historical data are available.
[b] Results from the gain/loss study; two given discharge values indicate replicate measurements.
[c] Results from the hydrograph separation analyses; BFI is the base flow index calculated as the base flow divided by the total streamflow.
[d] Watershed falls mostly outside the study outcrop area.
TX – Texas
FM = farm to market road
Hwy = highway

Table 4.6.6   USGS gages and base flow estimates from Bené and others (2004).

Gage Number	Station Name	Q_{10} (cfs)	Q_{25} (cfs)	Q_{50} (cfs)	Q_{75} (cfs)	Comment
8043950	Big Sandy Creek near Chico, TX	0.00	0.00	1.73	8.21	omitted from current analysis
8046000	Clear Fork Trinity River near Aledo, TX	0.00	0.00	0.93	5.46	omitted from current analysis
8053500	Denton Creek near Justin, TX	0.00	0.00	5.11	20.38	omitted from current analysis
8091500	Paluxy River at Glen Rose, TX	0.28	3.03	9.40	21.00	used for current analysis
8093500	Aquilla Creek near Aquilla, TX	0.00	0.15	1.25	6.24	used for current analysis
8094800	North Bosque River at Hico, TX	0.06	0.91	2.88	8.36	omitted from current analysis
8095000	North Bosque River near Clifton, TX	0.41	2.50	10.50	35.72	used for current analysis
8100500	Leon River at Gatesville, TX	0.19	0.69	5.70	45.03	used for current analysis
8101000	Cowhouse Creek at Pidcoke, TX	0.00	0.12	2.44	13.83	used for current analysis
8104000	Lampasas River at Youngsport, TX	3.62	9.58	25.00	75.94	used for current analysis

Q_{10} = flows from the 10th percentile
Q_{25} = flows from the 25th percentile
Q_{50} = flows from the 50th percentile (median flow)
Q_{75} = flows from the 75th percentile
Cfs = cubic feet per second
TX = Texas

Table 4.6.7   **Base flow estimates from Kirk and others (2012).**

USGS Number	USGS Name	Years of Record	Base Flow Average (in/yr)
08150800	Beaver Creek near Mason, TX	1964- 2008	0.41
08065800	Bedias Creek near Madisonville, TX	1968 -2009	0.84
08086290	Big Sandy Creek above Breckenridge, TX	1963-2009	0.06
08044000	Big Sandy Creek near Bridgeport, TX	1960-1964, 2005-2009	0.83[a]
07332500	Blue River near Blue, OK	1960-2009	3.31[a]
07332600	Bois D' Arc Creek near Randolph, TX	1963-1984	1.82
07344486	Brushy Creek at Scroggins, TX	1978-2003	4.53
07335000	Clear Boggy Creek near Caney, OK	1988-2009	3.15[a]
08139500	Deep Creek near Mercury, TX	1960-1972	0.19[a]
07315200	East Fork Little Wichita River near Henrietta, TX	1964-2009	0.1[a]
08109800	East Yegua Creek near Dime Box, TX	1963-2009	0.98
08094500	Green Creek near Alexander, TX	1960-1972	0.49[a]
08058500	Honey Creek near McKinney, TX	1960-1972	3.14[a]
08103800	Lampasas River near Kempner, TX	1963-2009	1.36[a]
08158700	Onion Creek near Driftwood, TX	1980-2009	4.02
08172400	Plum Creek at Lockhart, TX	1960-2009	1.79[a]

[a]   Base flow estimate is influenced by data from regulated years.
in/yr = inches per year
TX = Texas
OK = Oklahoma

Table 4.6.8   Perennial streams with greater than 10 years of unregulated data.

Site Number	Site Name	First Year	Last Year	Years Base Flow[a]	Contributing Drainage Area (mi²)	Average Base Flow (AFY)	Average Base Flow (in/yr)	R²
7332000	Red River near Colbert, OK	1923	1943	18	39777 [b]	1218510	0.58	-- [c]
7332400	Blue River at Milburn, OK	1966	1987	20	203	51049	4.71	0.62
7332500	Blue River near Blue, OK	1937	2008	70	477	64961	2.55	0.7
7335000	Clear Boggy Creek near Caney, OK	1943	1965	21	713	47577	1.25	0.56
7336500	Kiamichi River near Belzoni, OK	1926	1972	46	1423	206936	2.71	0.57
7337500	Little River near Wright City, OK	1930	1970	25	645	126240	3.65	0.82
7338000	Little River near Idabel, OK	1929	3000	16	1173 [b]	266379	4.24	0.6
7338500	Little River below Lukfata Creek, near Idabel, OK	1947	1970	22	1228	247281	3.75	0.81
7339000	Mountain Fork near Eagletown, OK	1925	1969	38	800	206172	4.81	0.62
7339500	Rolling Fork near DeQueen, AR	1949	1974	24	182 [b]	36967	3.78	0.59
7340000	Little River near Horatio, AR	1931	1979	46	2660 [b]	695616	4.88	0.74
7340500	Cossatot River near DeQueen, AR	1938	1975	35	361 [b]	89844	4.63	0.71
7341000	Saline River near Dierks, AR	1939	1972	32	124 [b]	27500	4.12	0.67
7341200	Saline River near Lockesburg, AR	1964	1976	11	256 [b]	46359	3.37	0.66
7360800	Muddy Fork Creek near Murfreesboro, AR	1940	1980	13	120 [b]	20911	3.24	0.58
7361000	Little Missouri River near Murfreesboro, AR	1927	1950	13	380 [b]	109940	5.39	0.43
8044800	Walnut Creek at Reno, TX	1996	2012	14	75.6	1910	0.47	-- [c]
8048970	Village Creek at Everman, TX	1990	2012	22	84.5	2136	0.47	0.62
8049700	Walnut Creek near Mansfield, TX	1961	2012	51	62.8	972	0.28	0.29
8091000	Brazos River near Glen Rose, TX	1924	1941	16	25818	182679	0.12	0.66[d]
8091500	Paluxy River at Glen Rose, TX	1925	1982	33	410	12815	0.58	0.45
8093500	Aquilla Creek near Aquilla, TX	1940	1983	42	308	6151	0.37	0.42

Table 4.6.8, continued

Site Number	Site Name	First Year	Last Year	Years Base Flow[a]	Contributing Drainage Area (mi²)	Average Base Flow (AFY)	Average Base Flow (in/yr)	R²
8095000	North Bosque River near Clifton, TX	1924	1968	43	968	27961	0.53	0.42
8095300	Middle Bosque River near McGregor, TX	1960	1985	29	182	15884	1.62	0.63
8095400	Hog Creek near Crawford, TX	1960	1980	19	78.2	6878	1.63	0.65
8099500	Leon River near Hasse, TX	1940	1954	13	1261	15080	0.22	0.63
8100500	Leon River at Gatesville, TX	1951	1964	12	2342	46923	0.37	0.69
8101000	Cowhouse Creek at Pidcoke, TX	1951	2012	61	455	16359	0.67	0.54
8102500	Leon River near Belton, TX	1924	1955	30	3582	139161	0.72	0.51
8103800	Lampasas River near Kempner, TX	1963	1974	10	818	40292	0.92	0.3
8104000	Lampasas River at Youngsport, TX	1925	1974	48	1240	73310	1.1	0.61
8104700	North Fork San Gabriel River near Georgetown, TX	1969	1980	10	248	23474	1.77	0.59
8104900	South Fork San Gabriel River at Georgetown, TX	1969	2012	44	133	14599	2.05	0.68
8105000	San Gabriel River at Georgetown, TX	1935	1973	38	405	41002	1.89	0.52
8105100	Berry Creek near Georgetown, TX	1968	2003	33	83.1	7270	1.63	0.7
8154700	Bull Creek at Loop 360 near Austin, TX	1979	2011	33	22.3	3445	2.88	0.8

[a] Years of base flow data may not equal the difference between starting and ending year. This difference is due to either the upstream area being regulated or because yearly flow data was occasionally incomplete.

[b] "Contributing " watershed area unavailable so "Total" watershed area was used instead.

[c] Watershed polygon area did not match the USGS watershed area value so precipitation vs. base flow analysis was not performed.

[d] Only a very small portion of the watershed falls within the outcrop area – not used for base flow calibration target.

R² = coefficient of determination

TX = Texas

OK = Oklahoma

AR = Arkansas

Table 4.6.9   Gages not used in the current hydrograph separation analysis.

Gage Number	Site Name	Reason for Rejection
7315900	Walnut Bayou near Burneyville, OK	Less than 10 years unregulated data
7316200	Mineral Creek near Sadler, TX	Less than 10 years unregulated data
7335300	Muddy Boggy Creek near Unger, OK	No unregulated years
7335500	Red River at Arthur City, TX	Urbanized (Lewis and Esralew, 2009)
7336750	Little Pine Creek near Kanawha, TX	Intermittent
8043950	Big Sandy Creek near Chico, TX	No unregulated years
8044000	Big Sandy Creek near Bridgeport, TX	Intermittent
8044135	Garrett Creek near Paradise, TX	Less than 10 years unregulated data
8044140	Salt Creek near Paradise, TX	Less than 10 years unregulated data
8044500	West Fork Trinity River near Boyd, TX	No unregulated years
8045500	West Fork Trinity River at Lake Worth Dam above Ft Worth, TX	Intermittent
8045550	West Fork Trinity River at White Settlement Road., Fort Worth, TX	No unregulated years
8045850	Clear Fork Trinity River near Weatherford, TX	No unregulated years
8045995	Clear Fork Trinity River at Kelly Road near Aledo, TX	No unregulated years
8046000	Clear Fork Trinity River near Aledo, TX	Intermittent
8047000	Clear Fork Trinity River near Benbrook, TX	Less than 10 years unregulated data
8047050	Marys Creek at Benbrook, TX	No unregulated years
8047500	Clear Fork Trinity River at Ft Worth, TX	Intermittent
8048000	West Fork Trinity River at Ft Worth, TX	No unregulated years
8048520	Sycamore Creek at IH 35 West, Ft Worth, TX	Urbanized (Slade and others, 2002)
8048530	Sycamore Creek Tributary above Seminary Street Shopping Center, Ft Worth, TX	Urbanized (Slade and others, 2002)
8048540	Sycamore Creek Tributary at IH 35 West, Ft Worth, TX	Urbanized (Slade and others, 2002)
8048543	West Fork Trinity River at Beach Street, Ft Worth, TX	No unregulated years
8048600	Dry Branch at Fain Street, Ft Worth, TX	Urbanized (Slade and others, 2002)
8048800	Big Fossil Creek at Haltom City, TX	Urbanized (Slade and others, 2002)
8048850	Little Fossil Creek at Mesquite Street, Ft Worth, TX	Urbanized (Slade and others, 2002)
8048980	Village Creek at Kennedale, TX	No unregulated years
8049000	Village Creek near Handley, TX	Intermittent
8049550	Big Bear Creek near Grapevine, TX	Intermittent
8049553	Big Bear Creek at Euless/Grapevine Road near Grapevine, TX	Less than 10 years unregulated data
8050300	Elm Fork Trinity River near Muenster, TX	No unregulated years
8050400	Elm Fork Trinity River at Gainesville, TX	No unregulated years

Table 4.6.9, continued

Gage Number	Site Name	Reason for Rejection
8050500	Elm Fork Trinity River near Sanger, TX	Less than 10 years unregulated data
8050800	Timber Creek near Collinsville, TX	Intermittent
8051000	Isle Du Bois Creek near Pilot Point, TX	Intermittent
8051130	Elm Fork Trinity River near Pilot Point, TX	No unregulated years
8051135	Elm Fork Trinity River at Greenbelt near Pilot Point, TX	No unregulated years
8051500	Clear Creek near Sanger, TX	Intermittent
8052000	Elm Fork Trinity River near Denton, TX	Less than 10 years unregulated data
8052700	Little Elm Creek near Aubrey, TX	Intermittent
8052780	Hickory Creek at Denton, TX	No unregulated years
8053500	Denton Creek near Justin, TX	Intermittent
8054000	Denton Creek near Roanoke, TX	Intermittent
8055000	Denton Creek near Grapevine, TX	Intermittent
8090905	Brazos River downstream Lake Granbury near Granbury, TX	No unregulated years
8091750	Squaw Creek near Glen Rose, TX	No unregulated years
8092600	Brazos River at Whitney Dam near Whitney, TX	No unregulated years
8093100	Brazos River near Aquilla, TX	Less than 10 years unregulated data
8093360	Aquilla Creek above Aquilla, TX	No unregulated years
8093700	North Bosque River at Stephenville, TX	Intermittent
8094500	Green Creek near Alexander, TX	No unregulated years
8095200	North Bosque River at Valley Mills, TX	Less than 10 years unregulated data
8095500	South Bosque River near Speegleville, TX	Less than 10 years unregulated data
8095600	Bosque River near Waco, TX	Less than 10 years unregulated data
8100000	Leon River near Hamilton, TX	Less than 10 years unregulated data
8101500	Cowhouse Creek near Killeen, TX	Less than 10 years unregulated data
8102600	Nolan Creek at Belton, TX	No unregulated years
8103900	South Fork Rocky Creek near Briggs, TX	Intermittent
8104100	Lampasas River near Belton, TX	Less than 10 years unregulated data
8104310	Salado Creek below Salado Springs at Salado, TX	No unregulated years
8105095	Berry Creek at Airport Rd near Georgetown, TX	Intermittent
8105886	Lake Creek at Lake Creek Parkway near Austin, TX	Less than 10 years unregulated data
810464660	North Fork San Gabriel River at Reagan Boulevard near Leander, TX	Less than 10 years unregulated data

TX = Texas
OK = Oklahoma

Table 4.6.10   Base flow calibration targets from the hydrograph separation analyses.

Gage Number	Site Name	Base Flow (AFY)	Percent of Watershed in Outcrop Area	Base Flow (AFY)
8048970	Village Creek at Everman, TX	2136	100	2136
8049700	Walnut Creek near Mansfield, TX	972	84	816
8091500	Paluxy River at Glen Rose, TX	12815	100	12815
8093500	Aquilla Creek near Aquilla, TX	6151	39	2399
8095300	Middle Bosque River near McGregor, TX	15884	100	15884
8095400	Hog Creek near Crawford, TX	6878	100	6878
8099500	Leon River near Hasse, TX	15080	63	9500
8101000	Cowhouse Creek at Pidcoke, TX	16359	100	16359
8103800	Lampasas River near Kempner, TX	40292	100	40292
8104700	North Fork San Gabriel River near Georgetown, TX	23474	100	23474
8104900	South Fork San Gabriel River at Georgetown, TX	14599	100	14599
8154700	Bull Creek at Loop 360 near Austin, TX	3445	100	3445
7332400	Blue River at Milburn, OK	51049	5	2552
7335000	Clear Boggy Creek near Caney, OK	47577	18	8564
7336500	Kiamichi River near Belzoni, OK	206936	6	12416
7337500	Little River near Wright City, OK	126240	9	11362
7339000	Mountain Fork near Eagletown, OK	206172	1	2062
7339500	Rolling Fork near DeQueen, AR	36967	6	2218
7340500	Cossatot River near DeQueen, AR	89844	4	3594
7341000	Saline River near Dierks, AR	27500	2	550
7360800	Muddy Fork Creek near Murfreesboro, AR	20911	42	8783
8095000	North Bosque River near Clifton, TX	27961	100	27961
8104000	Lampasas River at Youngsport, TX	73310	100	73310
8105000	San Gabriel River at Georgetown, TX	41002	100	41002
8105100	Berry Creek near Georgetown, TX	7270	100	7270
7332500	Blue River near Blue, OK	64961	56	36378
7338000	Little River near Idabel, OK	266379	16	42621
7341200	Saline River near Lockesburg, AR	46359	43	19934
7361000	Little Missouri River near Murfreesboro, AR	109940	17	18690
8100500	Leon Rv at Gatesville, TX	46923	80	37538
7338500	Little River below Lukfata Creek, near Idabel, OK	247281	18	44511
8102500	Leon River near Belton, TX	139161	86	119678
7340000	Little River near Horatio, AR	695616	21	146079

TX = Texas
OK = Oklahoma
Ar = Arkansas

Table 4.6.11   **Estimates of vegetation coefficient and rooting depth for several vegetation types in the study outcrop area (from Scanlon and others, 2005).**

Vegetation Type	Vegetation Coefficient	Rooting Depth (feet)
Shrubland	0.54	14
Grassland	0.70	2.5
Conifer	0.41	10
Cropland	0.6[a]	7

[a] estimated from analogs

Table 4.6.12   Springs issuing from the northern Trinity or Woodbine aquifers in the study outcrop area.

County	State Well Number (Brune Number)	Spring	Spring Source	Records[a] (Number)	Min Flow (gpm)	Date of Min Flow	Max Flow (gpm)	Date of Max Flow	Source
Callahan	3045903		northern Trinity Aquifer	2	5	not noted	20	not noted	TWDB
Callahan	3046902		northern Trinity Aquifer	2	30	not noted	40	not noted	TWDB
Grayson	(11)	Sand Springs	Woodbine Aquifer	1			3	1976	Brune
Grayson	(12)	Moss Springs	Woodbine Aquifer	1			2	1976	Brune
Hood	3241501	LY-32-41-501	northern Trinity Aquifer	1			5	not noted	Heitmuller, TWDB
Hood	(7)	Walnut Springs	northern Trinity Aquifer	1			103	7/7/1976	Brune
Lamar	(5)	Fulton Springs	Woodbine Aquifer	1			103	3/11/1976	Brune
Lampasas	4163501	Sulphur Creek Springs	northern Trinity Aquifer	2	600	1/1/1970	3097	1/21/1924	Heitmuller, TWDB
Lampasas	4163521 (3)	Swimming Pool Springs	northern Trinity Aquifer	13	90	1931	761	1901	Heitmuller, TWDB, Brune
Somervell	3243806	Porter Spring	northern Trinity Aquifer	1			50	not noted	Heitmuller, TWDB
Tarrant	(10)	Village Springs	Woodbine Aquifer	1			76	7/31/1978	Brune
Tarrant	(19)	Tonkawa Springs	northern Trinity Aquifer	1			71	7/9/1979	Brune
Travis	5732805	YD-57-32-805	northern Trinity Aquifer	1			5	8/25/1972	Heitmuller, TWDB
Travis	5732902	YD-57-32-902	northern Trinity Aquifer	1			10	5/10/1966	Heitmuller, TWDB
Travis	5740203	Cherry Spring	northern Trinity Aquifer	1			5	8/25/1972	Heitmuller, TWDB
Travis	5825102	Sheep Hollow Springs	northern Trinity Aquifer	1			30	9/6/1972	Heitmuller, TWDB
Travis	5825404	Barnes Hollow Spring	northern Trinity Aquifer	1			0	9/6/1972	Heitmuller, TWDB
Travis	5825505	Flag Spring	northern Trinity Aquifer	1			0	9/6/1972	Heitmuller, TWDB
Travis	5825602	YD-58-25-602	northern Trinity Aquifer	1			20	9/6/1972	Heitmuller, TWDB
Travis	5825603	YD-58-25-603	northern Trinity Aquifer	1			5	9/6/1972	Heitmuller, TWDB
Travis	5825702	YD-58-25-702	northern Trinity Aquifer	1			30	9/6/1972	Heitmuller, TWDB
Travis	5825703	YD-58-25-703	northern Trinity Aquifer	1			5	9/6/1972	Heitmuller, TWDB
Travis	5825704	YD-58-25-704	northern Trinity Aquifer	1			5	9/6/1972	Heitmuller, TWDB
Travis	5841304	YD-58-41-304	northern Trinity Aquifer	1			100	2/6/1973	Heitmuller, TWDB
Travis	5841305	YD-58-41-305	northern Trinity Aquifer	1			50	2/6/1973	Heitmuller, TWDB
Travis	5842309	YD-58-42-309	northern Trinity Aquifer	1			20	1/1/1973	Heitmuller, TWDB

[a] Number of discharge measurements
Min = minimum
Max = maximum
gpm = gallons per minute

TWDB = TWDB (2013a)
Brune = Brune (2002)
Heitmuller = Heitmuller and Reece (2003)

Table 4.6.13   Reservoirs in the study outcrop area with surface area greater than 1 square mile.

Reservoir Name	Owner/Controlling Authority	Surface Area (acres)	Date Impounded
Aquilla Lake[a]	US Army Corp of Engineers	3066	1983
Belton Lake[a]	US Army Corp of Engineers	12135	1954
Benbrook Lake[a]	US Army Corp of Engineers	3635	1950
Eagle Mountain Lake[a]	Tarrant County WCID #1	8694	1934
Georgetown Lake[a]	US Army Corp of Engineers	1287	1980
Grapevine Lake[a]	US Army Corp of Engineers	6707	1952
Hubert H. Moss Lake[a]	City of Gainesville	1140	1965
Hugo Lake[a]	US Army Corps of Engineers	11673	1974
Lake Arlington[a]	City of Arlington	1926	1957
Lake Granbury[a]	Brazos River Authority	7945	1969
Lake Murray[b]	State of Oklahoma	5876	1938
Lake Texoma[a]	US Army Corp of Engineers	74686	1943
Lake Travis[a]	Lower Colorado River Authority	19199	1940
Lake Weatherford[a]	City of Weatherford	1112	1957
Lake Worth[a]	City of Fort Worth	3458	1914
Lewisville Lake[a]	US Army Corp of Engineers	27175	1954
Pat Cleburne Lake	City of Cleburne, Texas	1568	1964
Pine Creek Lake[b]	US Army Corps of Engineers	3750	1969
Proctor Lake[a]	US Army Corp of Engineers	4537	1963
Ray Roberts Lake[a]	US Army Corp of Engineers	28646	1987
Squaw Creek Reservoir[a]	TXU Energy	3169	1977
Stillhouse Hollow Lake[a]	US Army Corp of Engineers	6484	1968
Valley Lake[c]	TXU Energy	1080	1960
Waco Lake[a]	US Army Corps of Engineers	8190	1965
Whitney Lake[a]	US Army Corp of Engineers	23220	1951

[a] Lake information from the latest TWDB survey available at http://www.twdb.state.tx.us/hydro_survey/
[b] Lake information from Oklahoma Water Resource Board website available at
     http://www.owrb.ok.gov/news/publications/lok/lok.php
[c] Lake information from TWDB's website at http://wiid.twdb.texas.gov/ims/ResInfo/

Table 4.6.14   Surface elevation data for selected reservoirs in the study outcrop area.

Lake Texoma[a]		Lake Hugo[b]	Lake Granbury[c]	Lake Aquilla[d]
1960	615.57*			
1961	615.80			
1962	615.47			
1963	610.52			
1964	605.07			
1965	612.16			
1966	611.98			
1967	609.22			
1968	615.90[+]			
1969	613.43*			
1970	613.29			
1971	612.09			
1972	612.12			
1973	618.45			
1974	617.27	405.10		
1975	617.10	405.40		
1976	614.44	404.27		
1977	614.66	404.79		
1978	612.51	403.52		
1979	615.25	406.47		
1980	614.03[+]	404.74		
1981	618.95*	405.25		
1982	617.70	407.66		
1983	616.36	404.32		
1984	614.71	405.50		
1985	617.07	406.95		
1986	616.68	404.95		
1987	618.07	407.95	692.40**	
1988	615.06	404.70	691.42	535.63**
1989	616.80	407.43	692.35	537.93
1990	620.53	411.29	692.40	538.38
1991	618.65	408.12	692.42	538.21
1992	617.60	406.64	692.38	539.59[++]
1993	618.46[+]	407.80[+]	692.45	
1994	618.48*	408.65*	692.48	
1995	618.24	405.02	692.44	536.85**
1996	617.13	406.08	692.18	535.97

Table 4.6.14, continued

Lake Texoma[a]		Lake Hugo[b]	Lake Granbury[c]	Lake Aquilla[d]
1997	617.95	406.57	692.44	537.91
1998	615.51	406.39	692.16	537.31
1999	615.60	405.99	692.18	536.44
2000	615.74	406.12	691.05	535.90
2001	617.30	408.12	691.56	537.57
2002	616.99	407.06	692.19	537.27
2003	614.86	406.41	692.52	537.22
2004	615.69	406.49	692.54	538.76
2005	614.77	405.37	692.41	536.57
2006	614.58	405.99	691.85	531.91
2007	620.12	410.53	692.24	536.97
2008	616.58	407.94	691.59	536.36
2009	618.00	409.95	691.12	536.60
2010	617.01	404.16	692.51	537.85
2011	613.17	405.30	690.35	534.86
2012	615.26	403.17	690.30	535.84

[a] Lake Hugo annual elevation values calculated from elevation measured at the end of the month for the period February 1974 to September 1993 (annual lake reports from USGS, WRD, Oklahoma Water Science Center) and from average monthly elevation for the period November 1994 to December 2012 (U.S. Army Corps of Engineers, 2013a).

[b] Lake Texoma annual elevation values calculated from elevation measured at the end of the month for the period October1960 to September 1993(annual lake reports from USGS, WRD, Oklahoma Water Science Center) and from average monthly elevation for the period November 1994 to December 2012 (U.S. Army Corps of Engineers, 2013b)

[c] Lake Granbury annual elevation values calculated from daily elevation at midnight for the period 10/1/1987 to 7/1/2001 and daily mean elevation from 7/2/2001 to 12/31/2012 (USGS, 2013b).

[d] Lake Aquilla annual elevation values calculated from daily elevation at midnight for the period 9/29/1988 to 7/9/2001 and from mean daily elevation for the period 7/10/2001 to 12/31/2012 (USGS, 2013b).

[+]   Average based on less than 10 months data

[*]   Average based on less than 5 months.

[++] Average based on less than 300 days data

** Average based on less than 100 days data
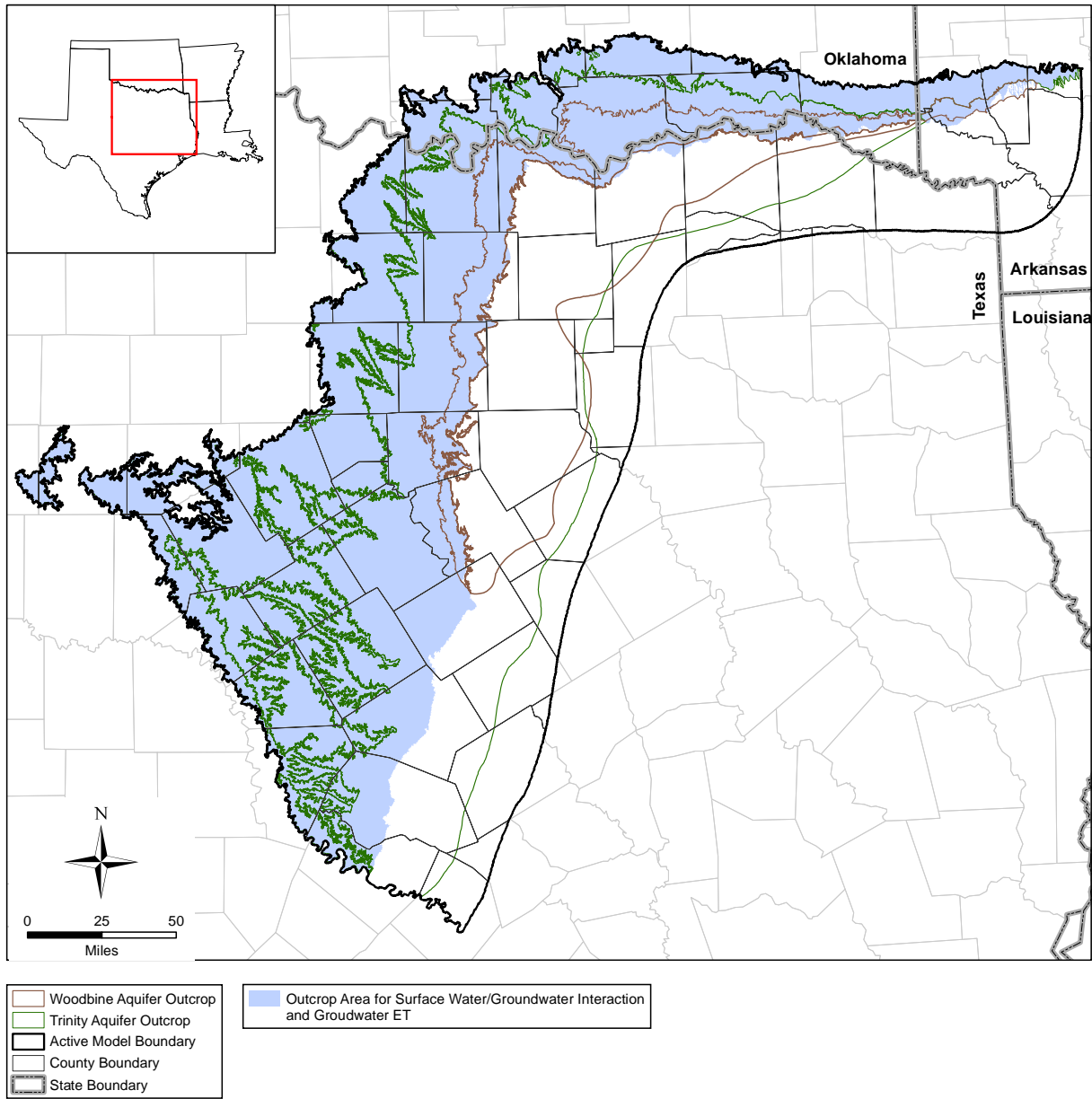
Figure 4.6.1   The study outcrop area for surface water/groundwater interaction and groundwater ET.
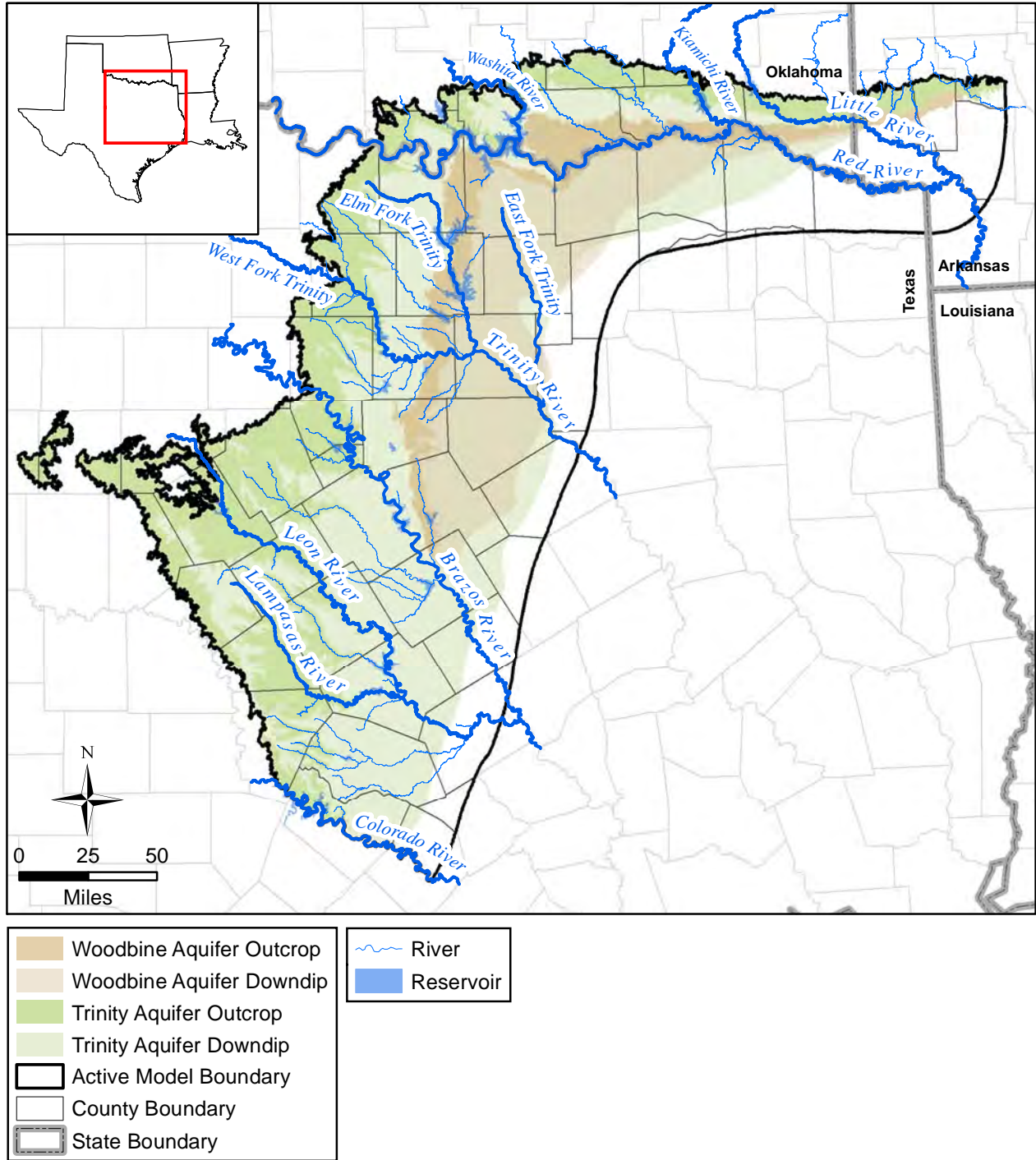
Figure 4.6.2   Major rivers and streams in the study area.
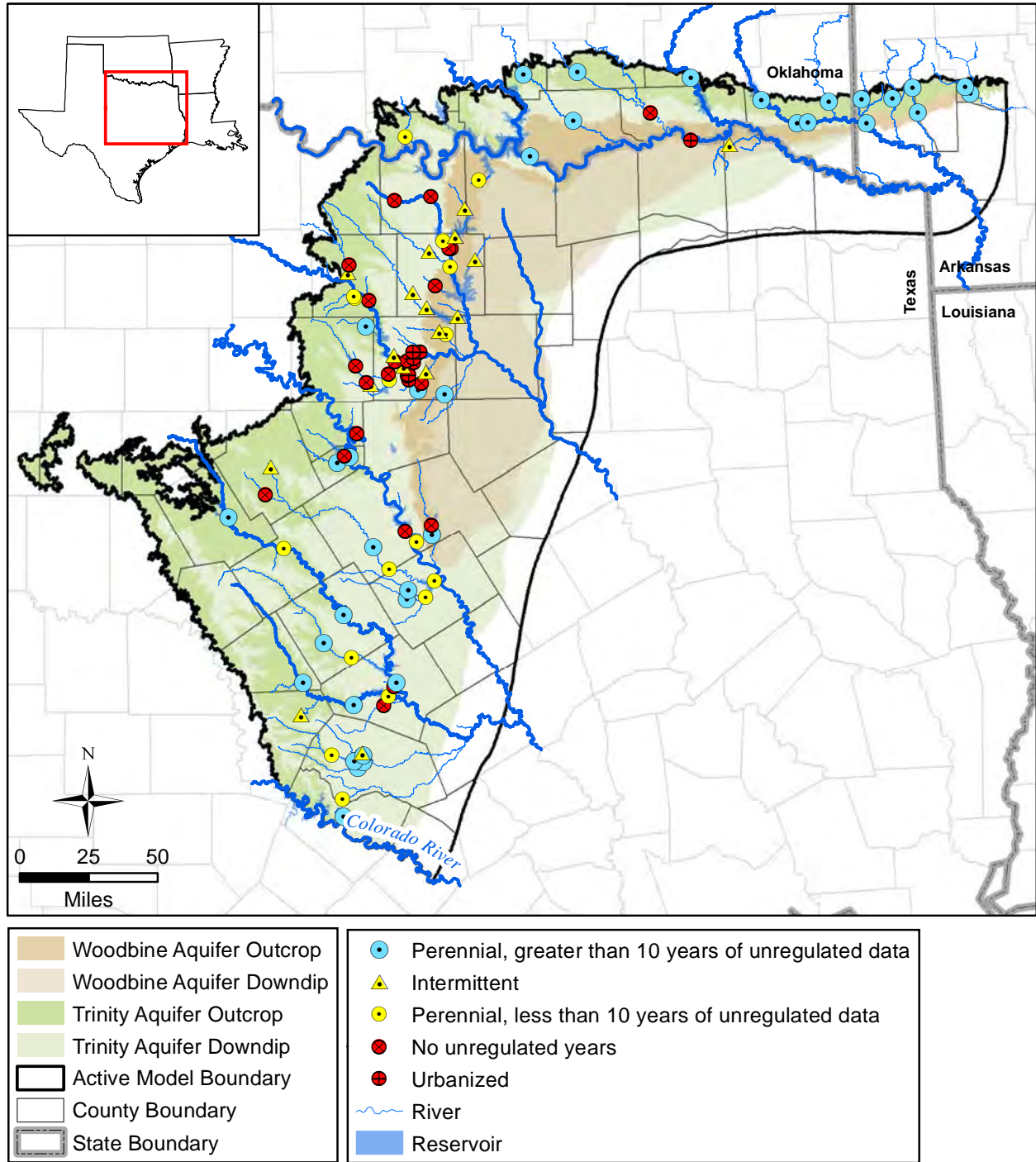
Figure 4.6.3   USGS stream-gage locations in the study outcrop area.
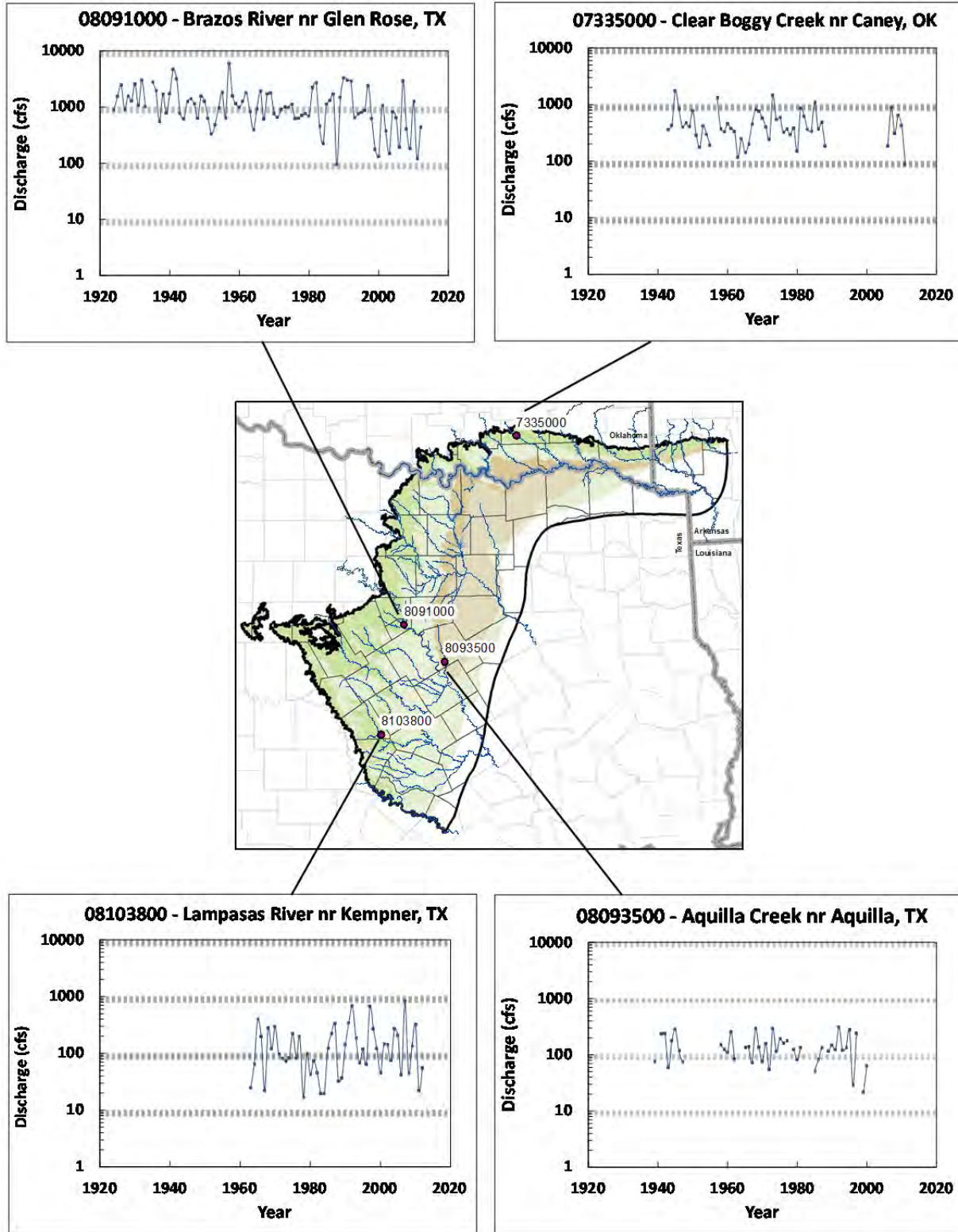
Figure 4.6.4   Example streamflow hydrographs.
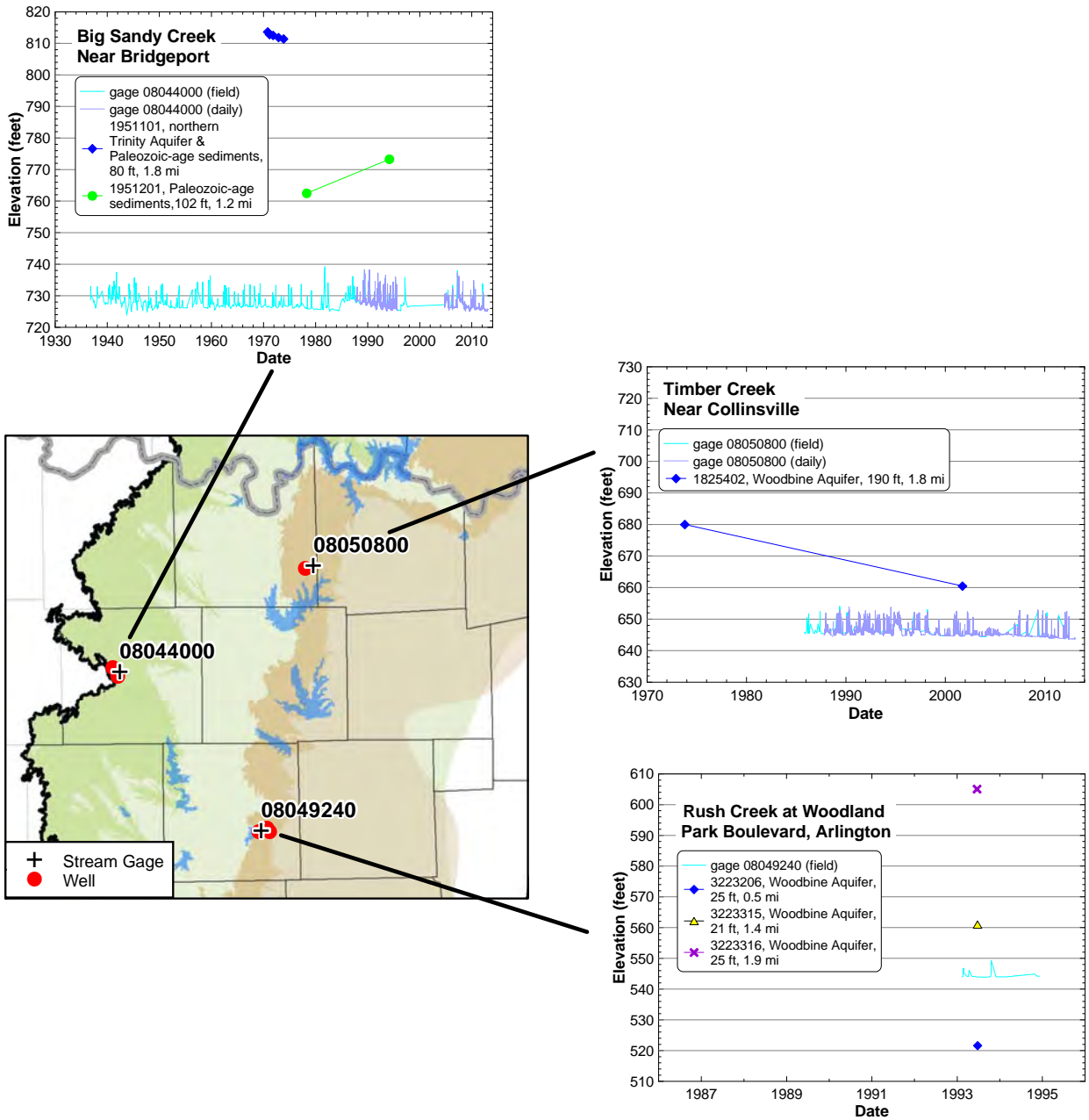
Figure 4.6.5 Stream stage elevations plotted with groundwater elevations from relatively shallow, nearby wells in the northern portion of the study outcrop area.
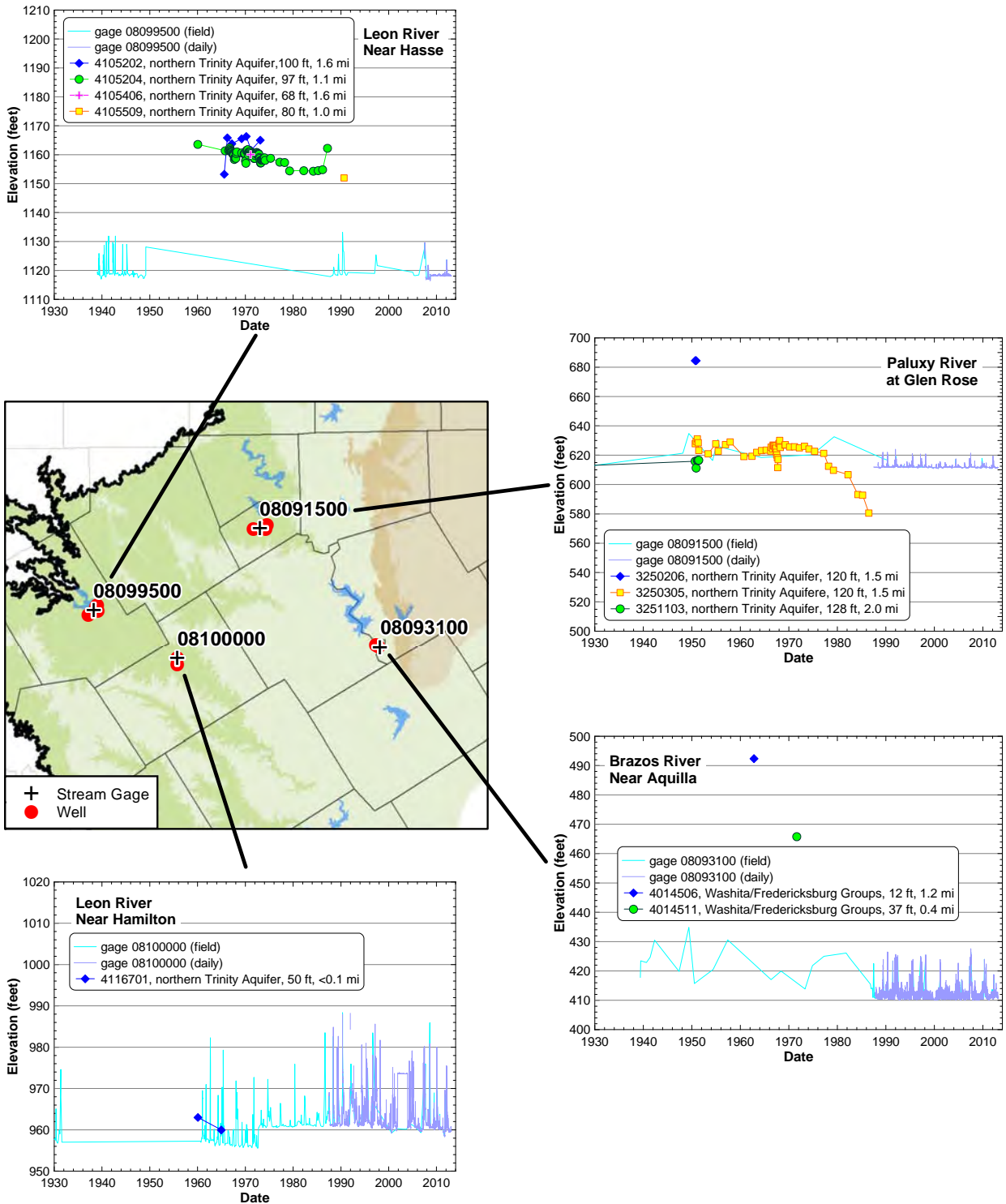
Figure 4.6.6   Stream stage elevations plotted with groundwater elevations from relatively shallow nearby wells in the central portion of the study outcrop area.
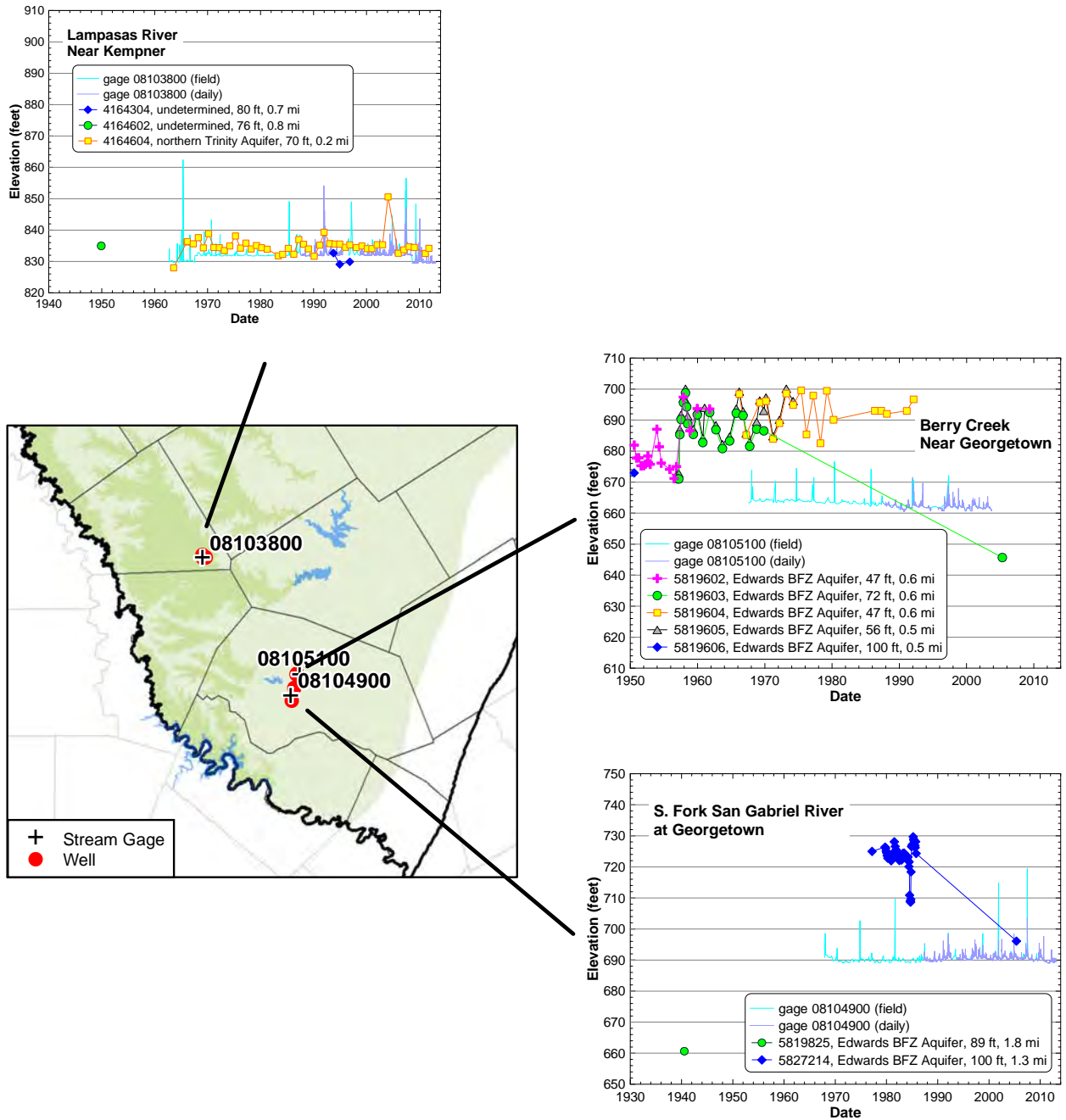
Figure 4.6.7   Stream stage elevations plotted with groundwater elevations from relatively shallow, nearby wells in the southern portion of the study outcrop area.
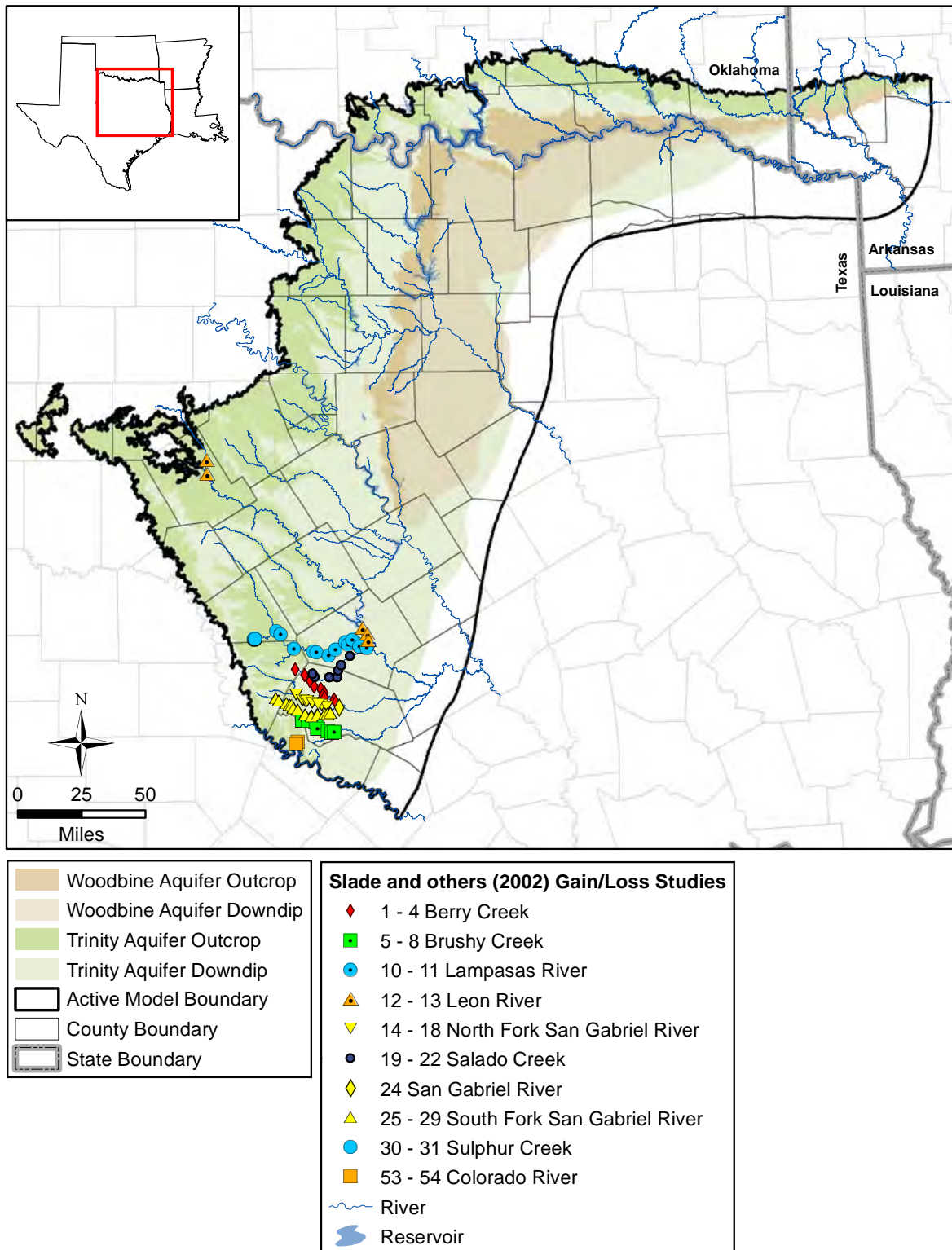
Figure 4.6.8 **Location of Slade and others (2002) stream gain/loss studies in the study outcrop area. Numbers in the legend reflect the study number given in Slade and others (2002).**
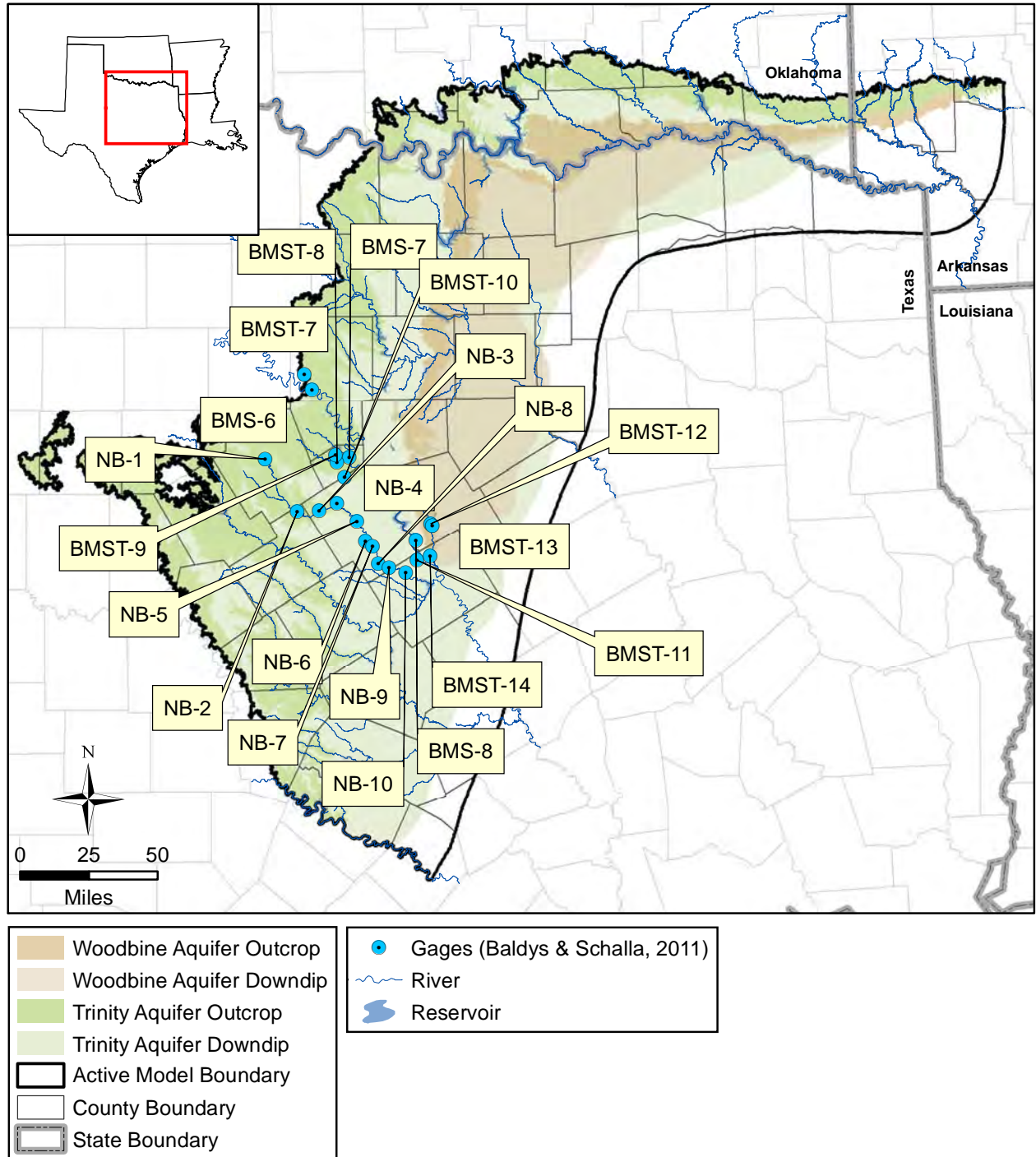
Figure 4.6.9   Location of gages used by Baldys and Schalla (2011).

(a)

(b)
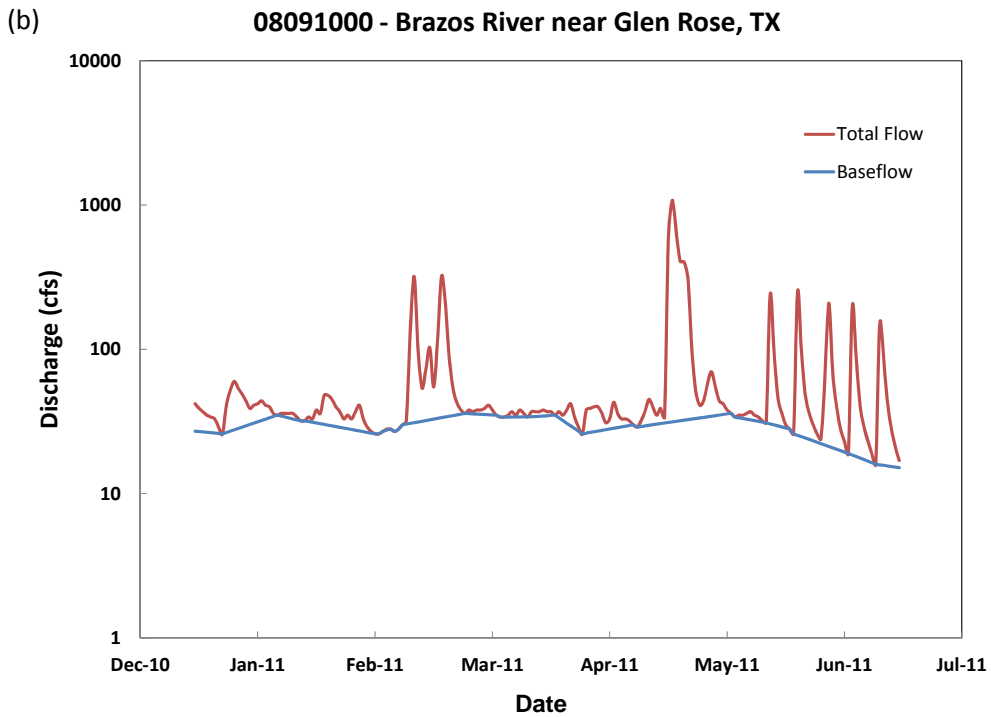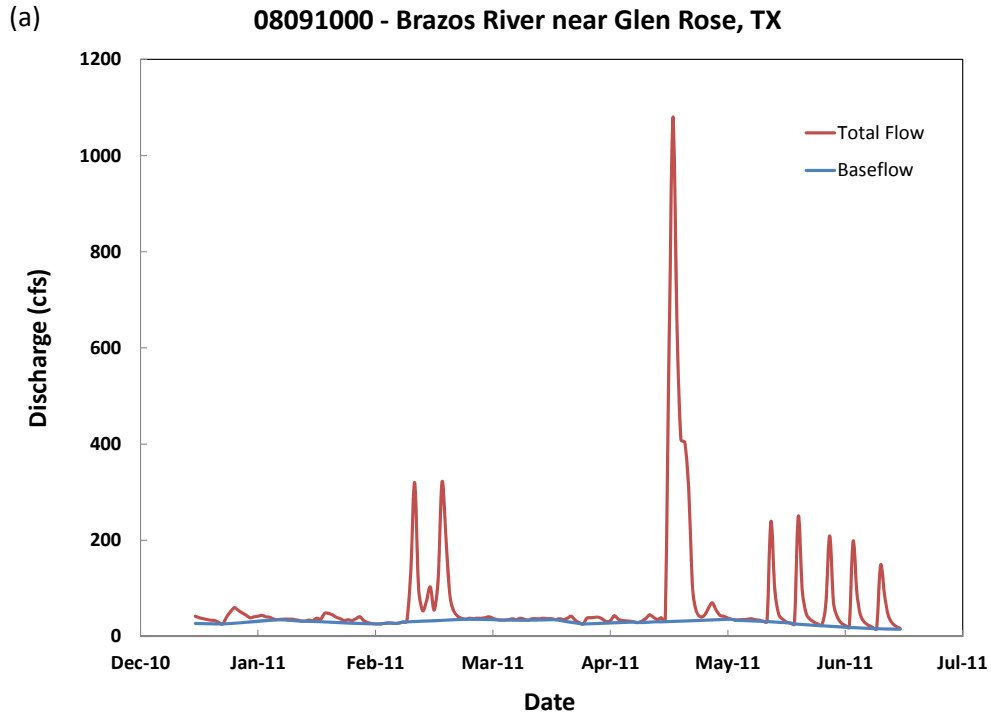
cfs = cubic feet per second

Figure 4.6.10   Example of hydrograph separation for gage 08091000 located on the Brazos River on a (a) linear and (b) log y-axis.
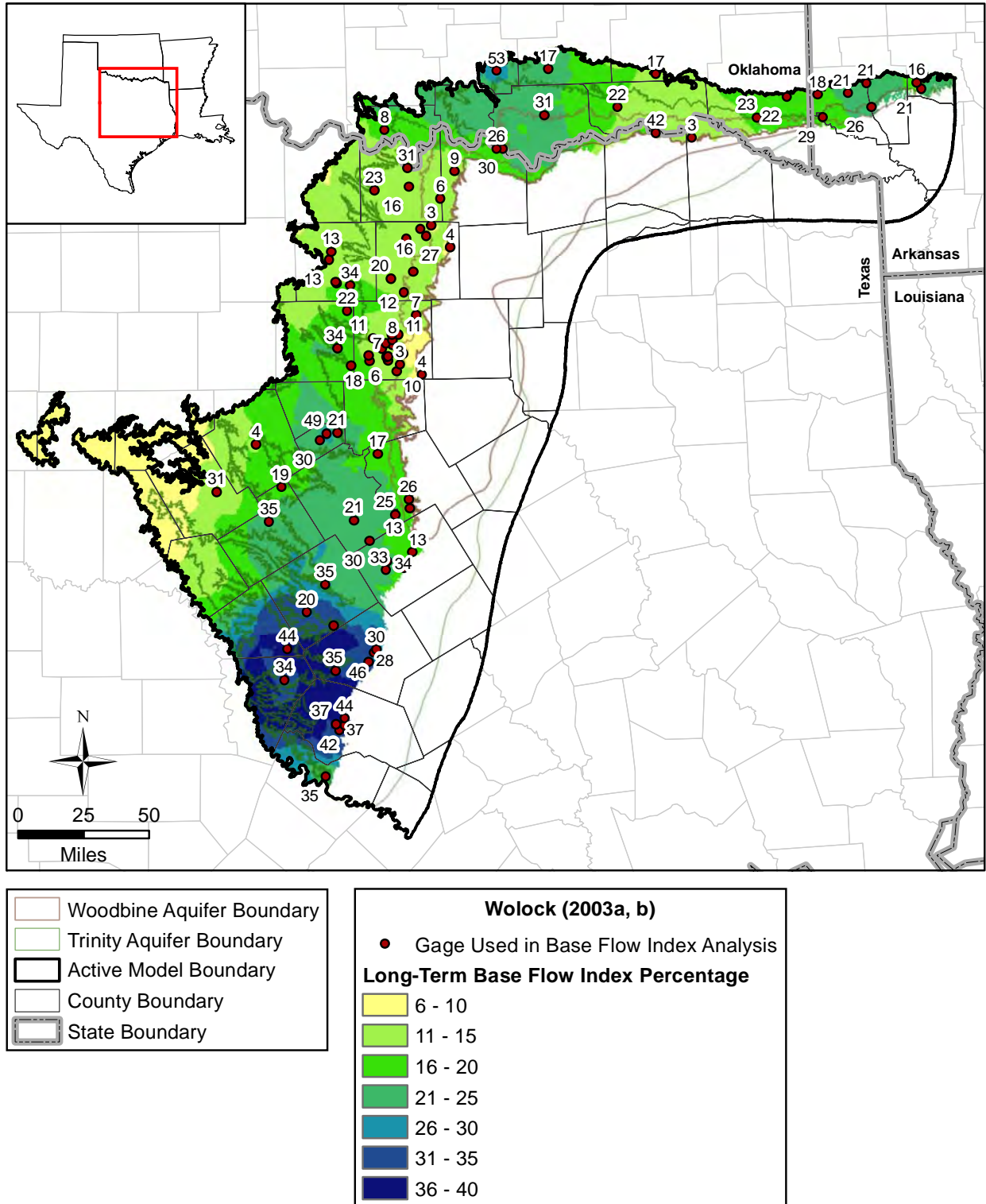
Figure 4.6.11   Base flow index values from Wolock (2003a, b).
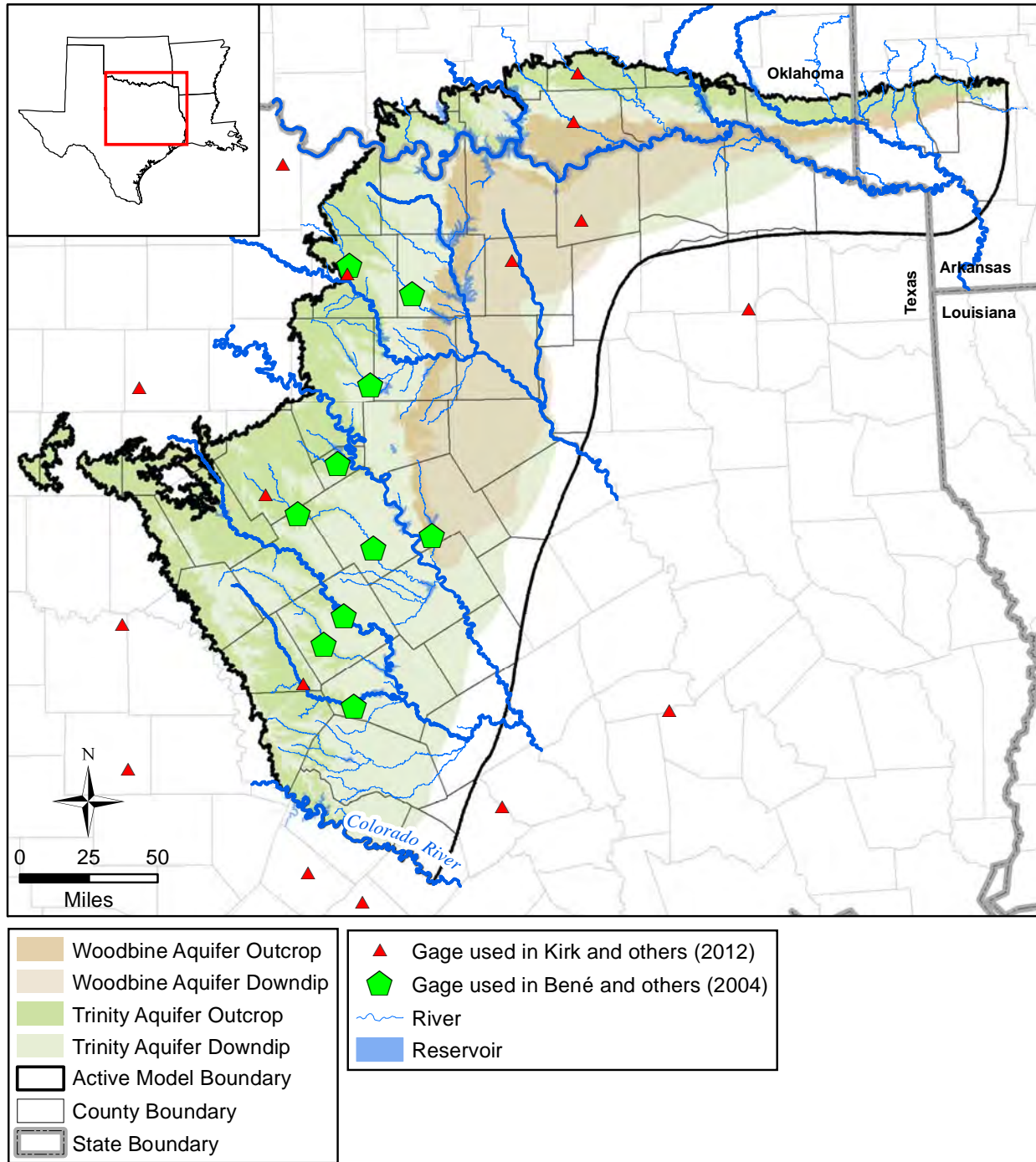
Figure 4.6.12   Gages used in Bené and others (2004) and Kirk and others (2012).

(a) 8050800 (b) 7340000
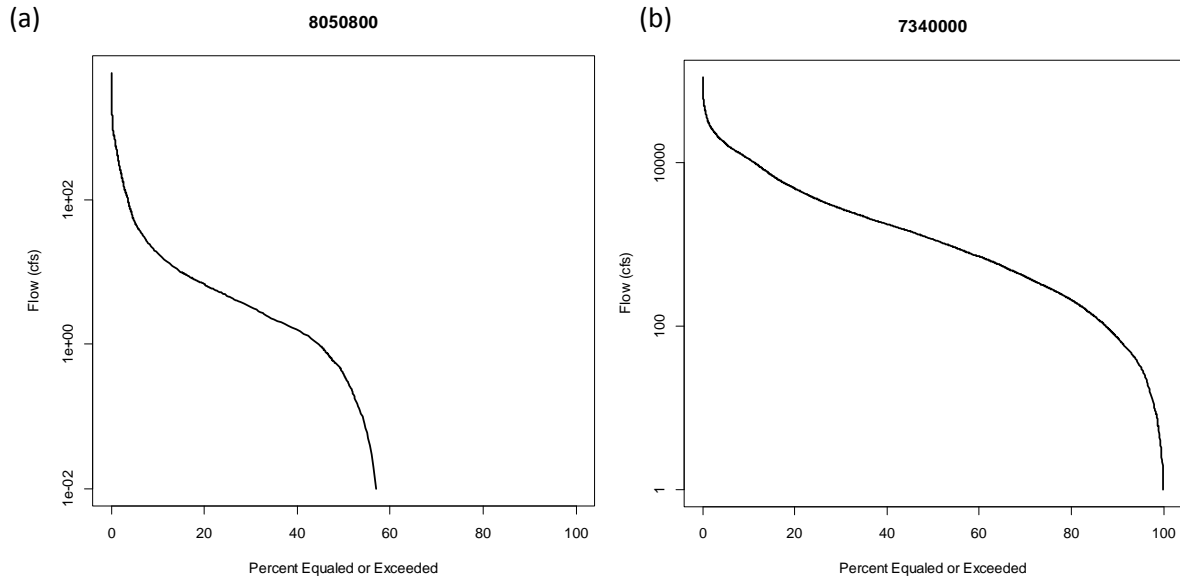
Figure 4.6.13 **Example flow duration curves for (a) an intermittent stream and (b) a perennial stream.**
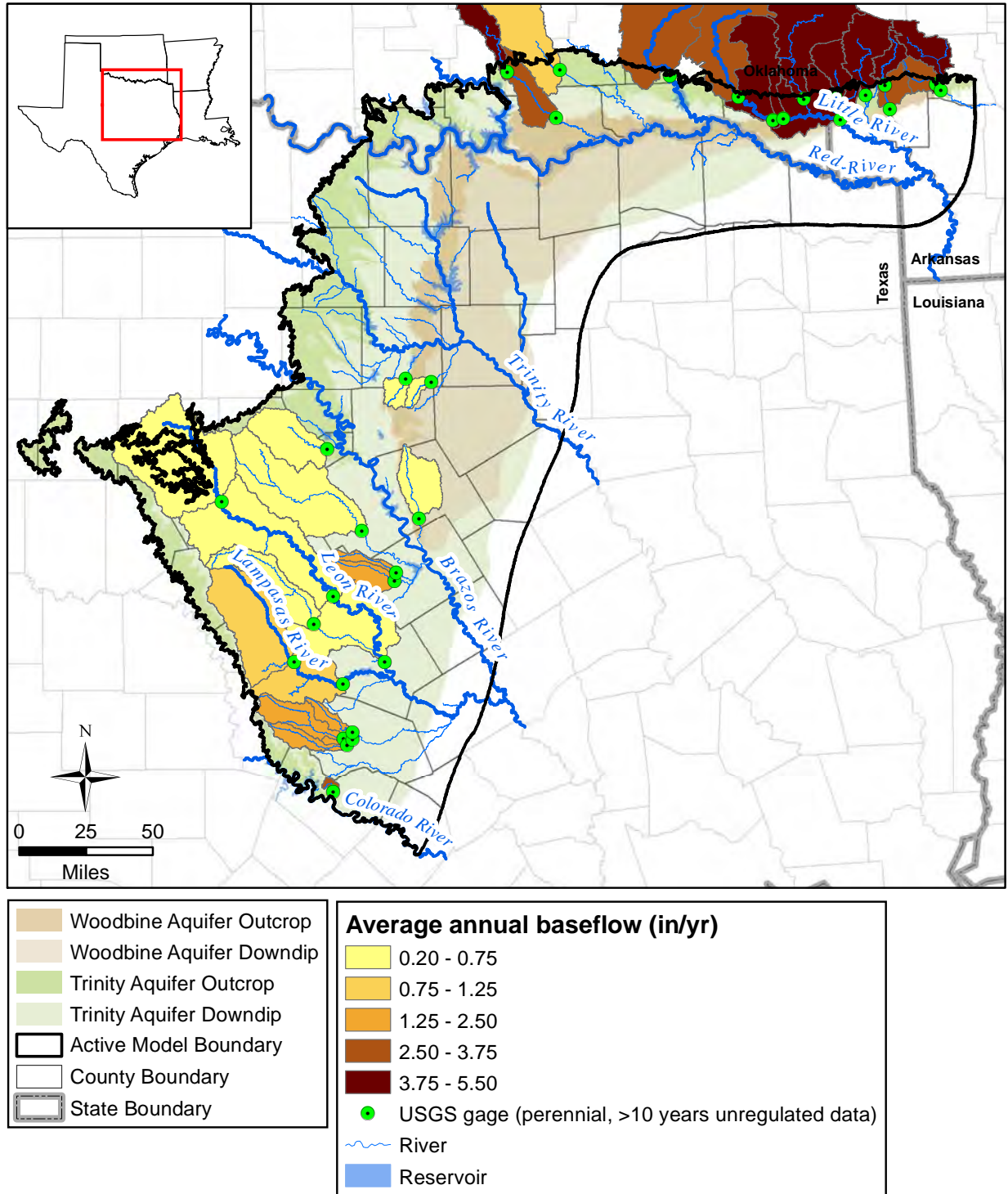
Figure 4.6.14   Gages used for base flow analysis and estimated average annual base flow in inches per year.
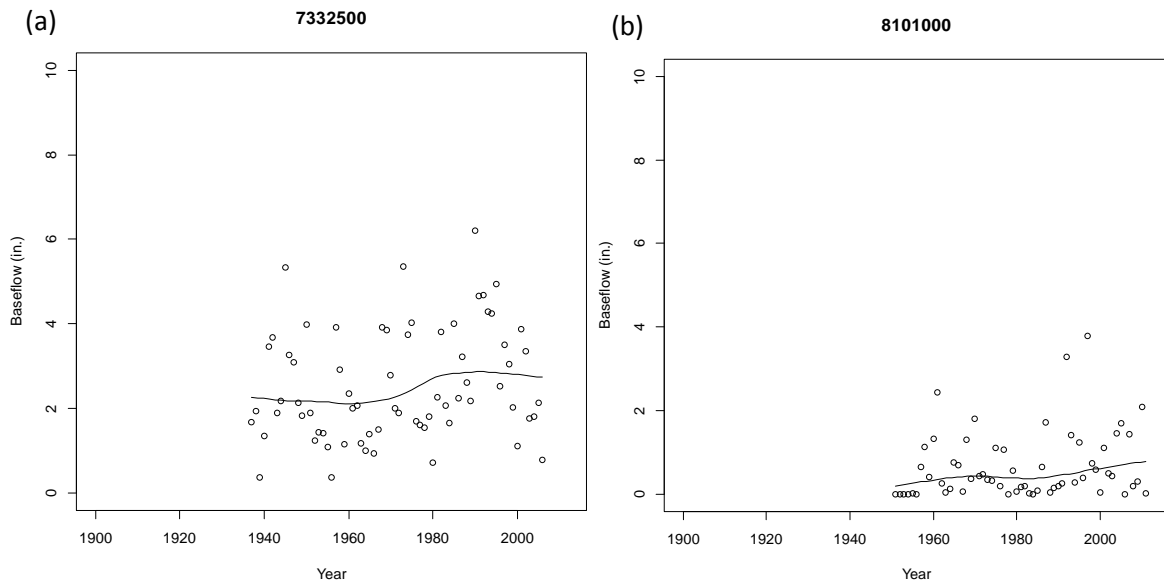
Figure 4.6.15   Example temporal base flow trends for (a) gage 7332500 and (b) gage 8101000.
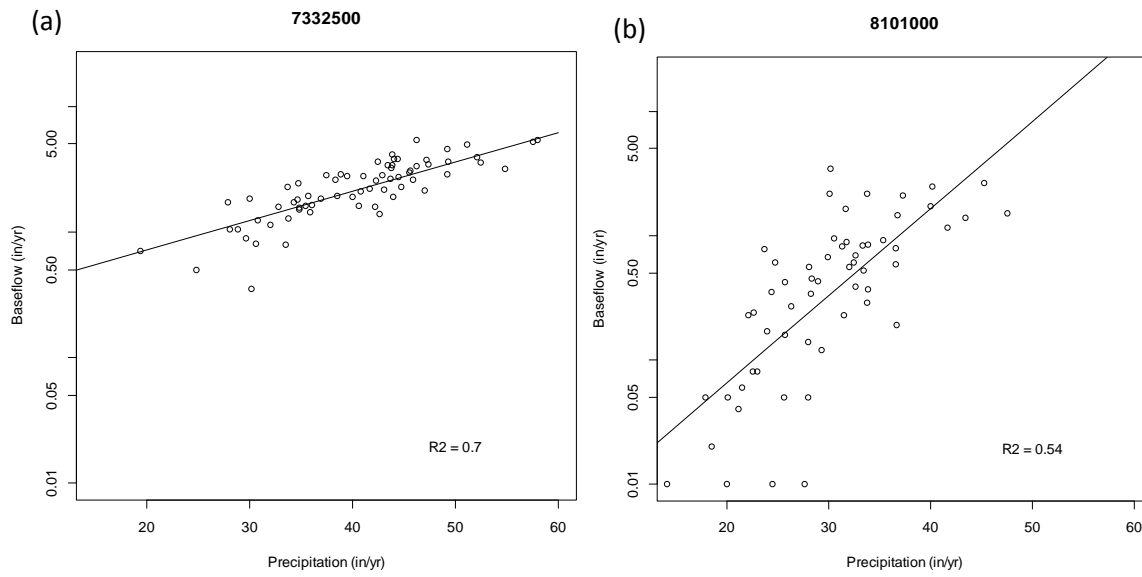
**Figure 4.6.16   Example relationships between precipitation and base flow for (a) gage 7332500 and
(b) gage 8101000.**
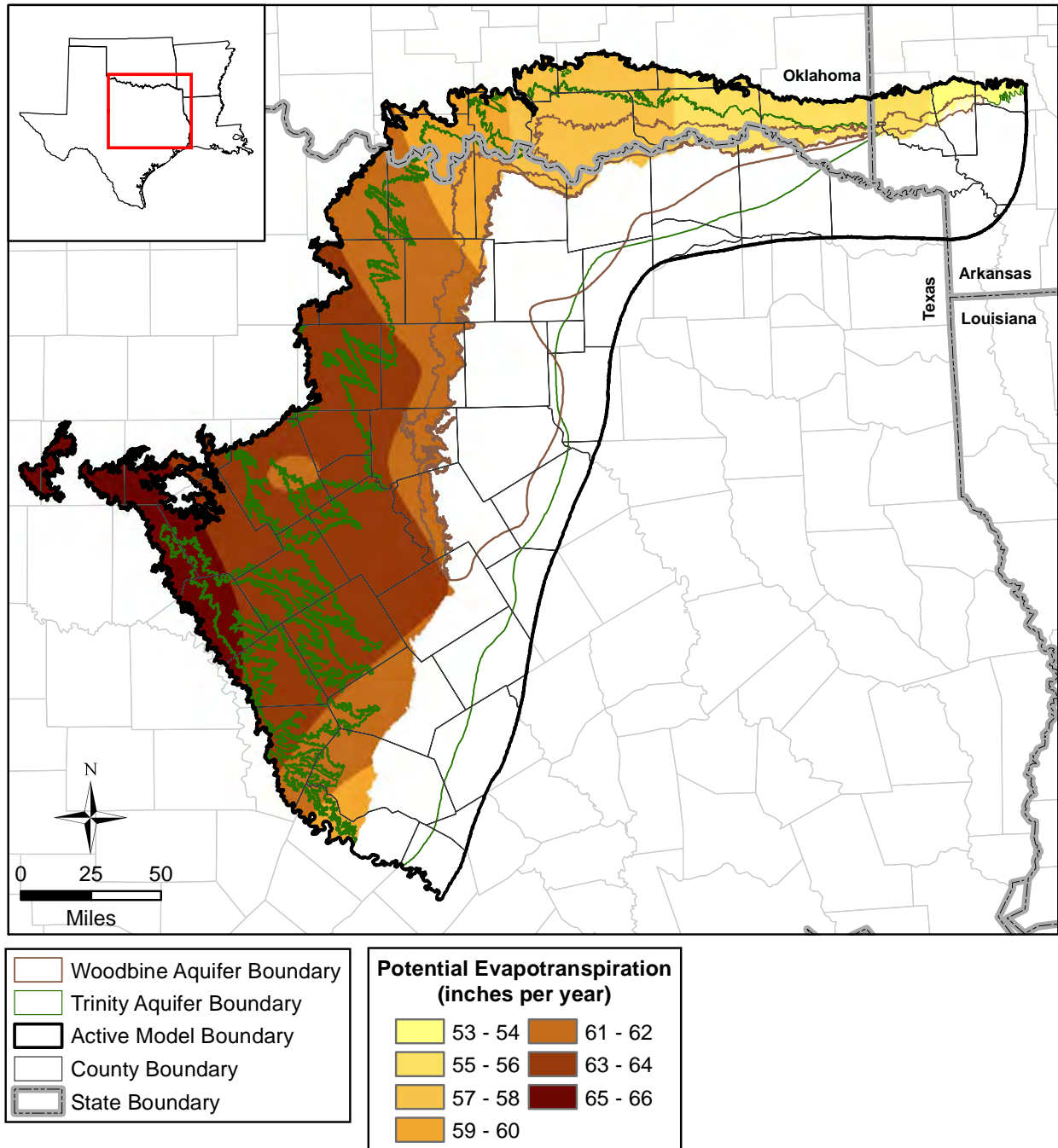
Figure 4.6.17   Potential ET in inches per year in the study outcrop area (Borrelli and others, 1998).
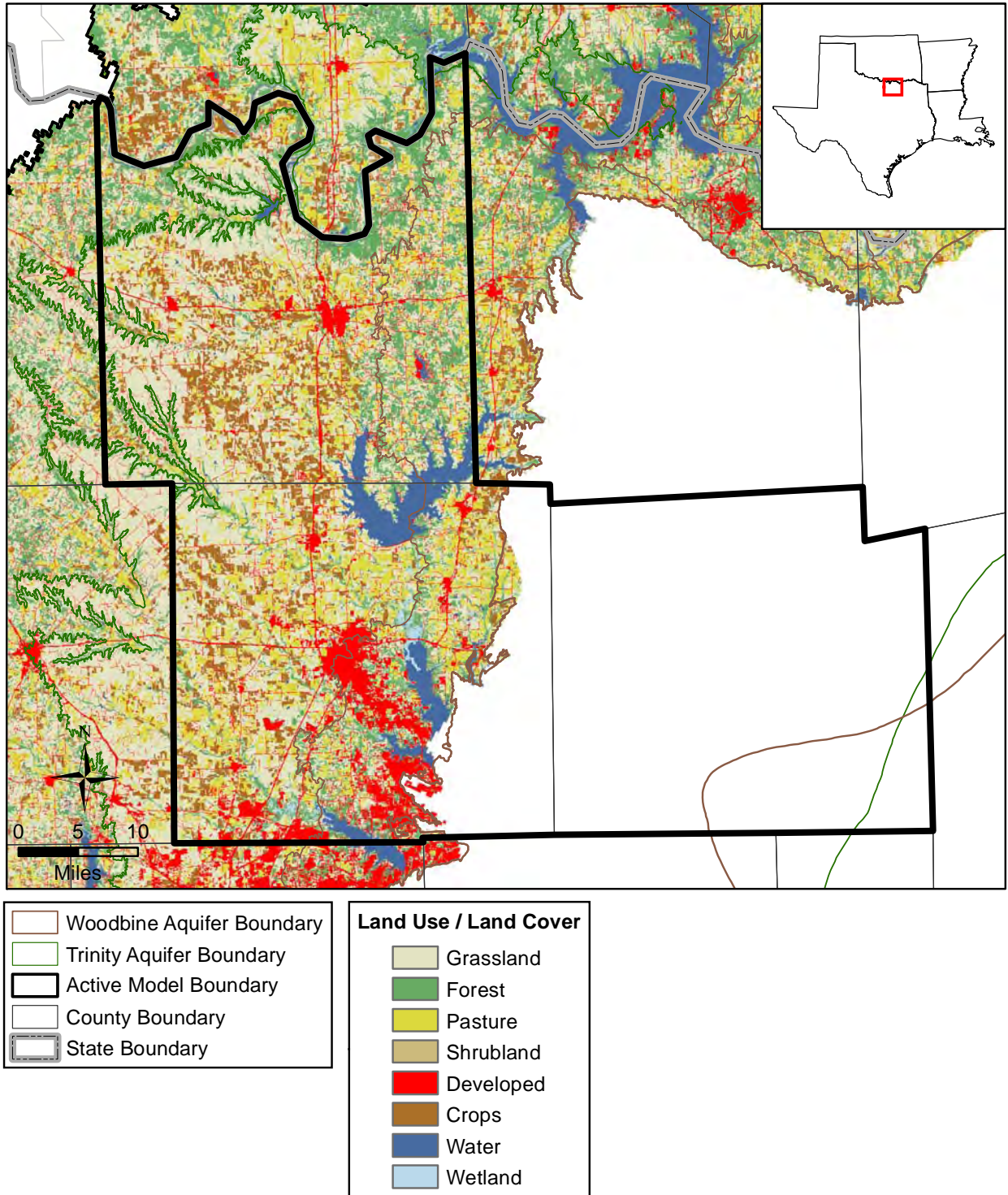
Figure 4.6.18   Land use in the study outcrop area in the North Texas GCD.
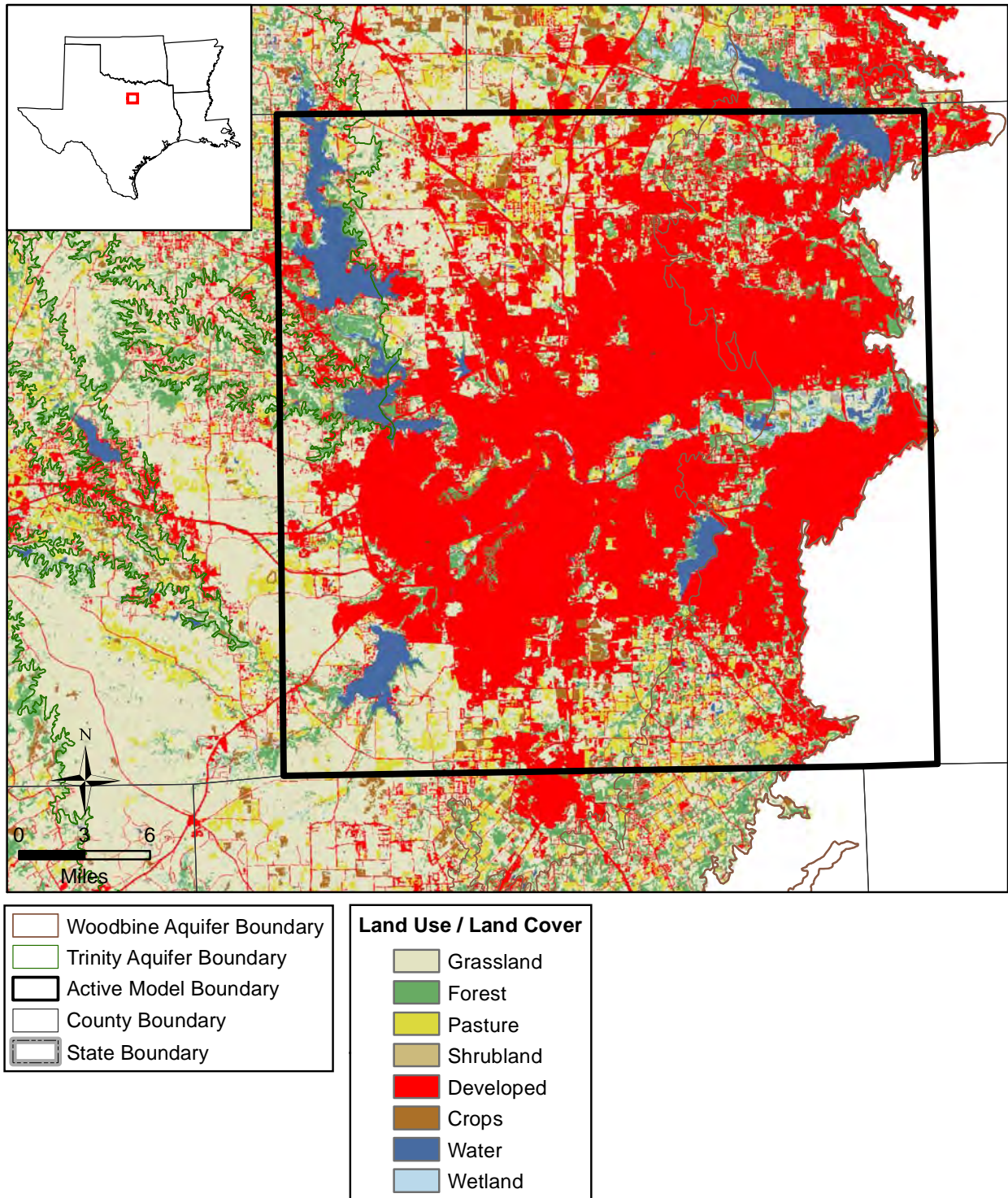
Figure 4.6.19   Land use in the study outcrop area in the Northern Trinity GCD.
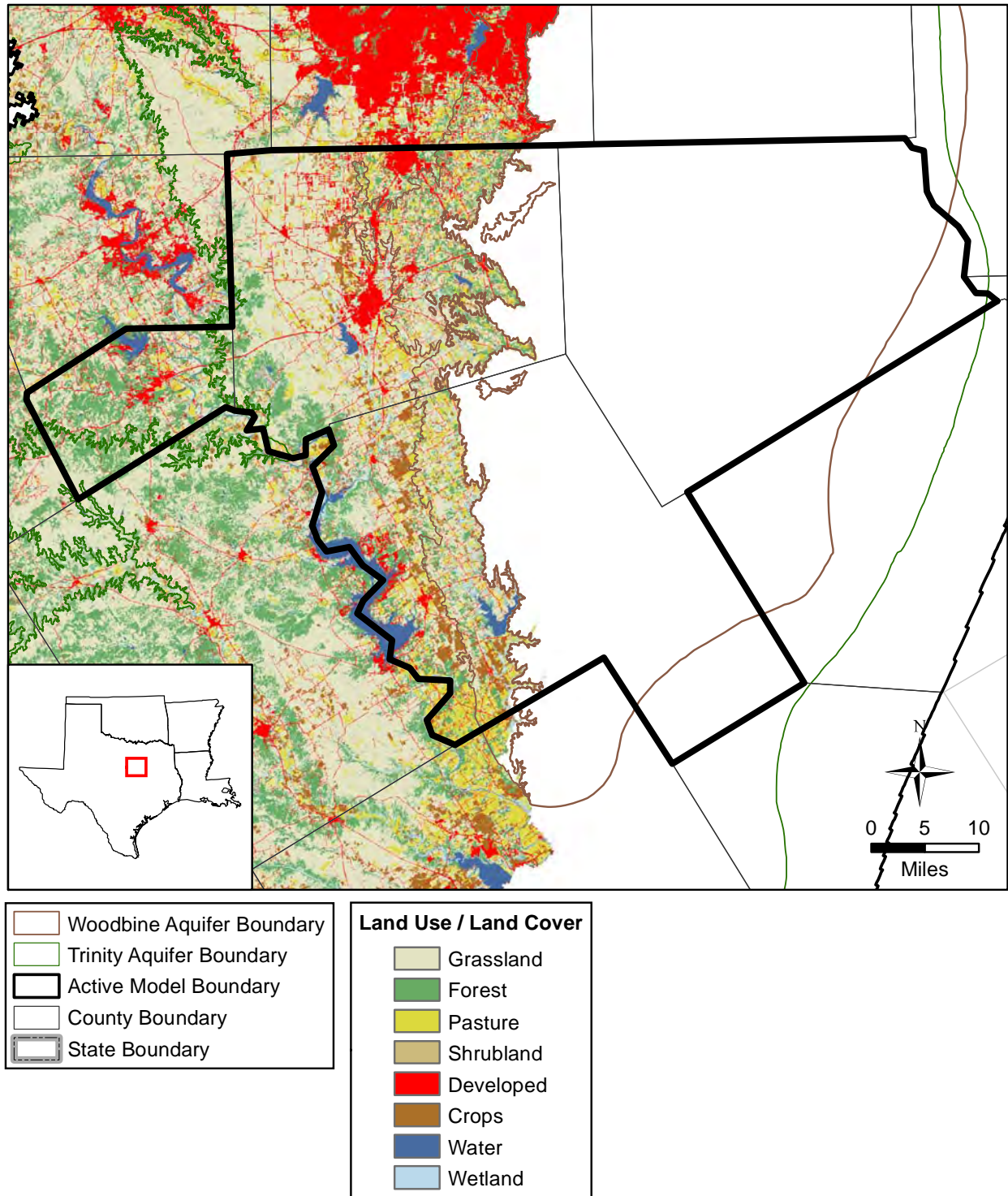
Figure 4.6.20   Land use in the study outcrop area in the Prairielands GCD.
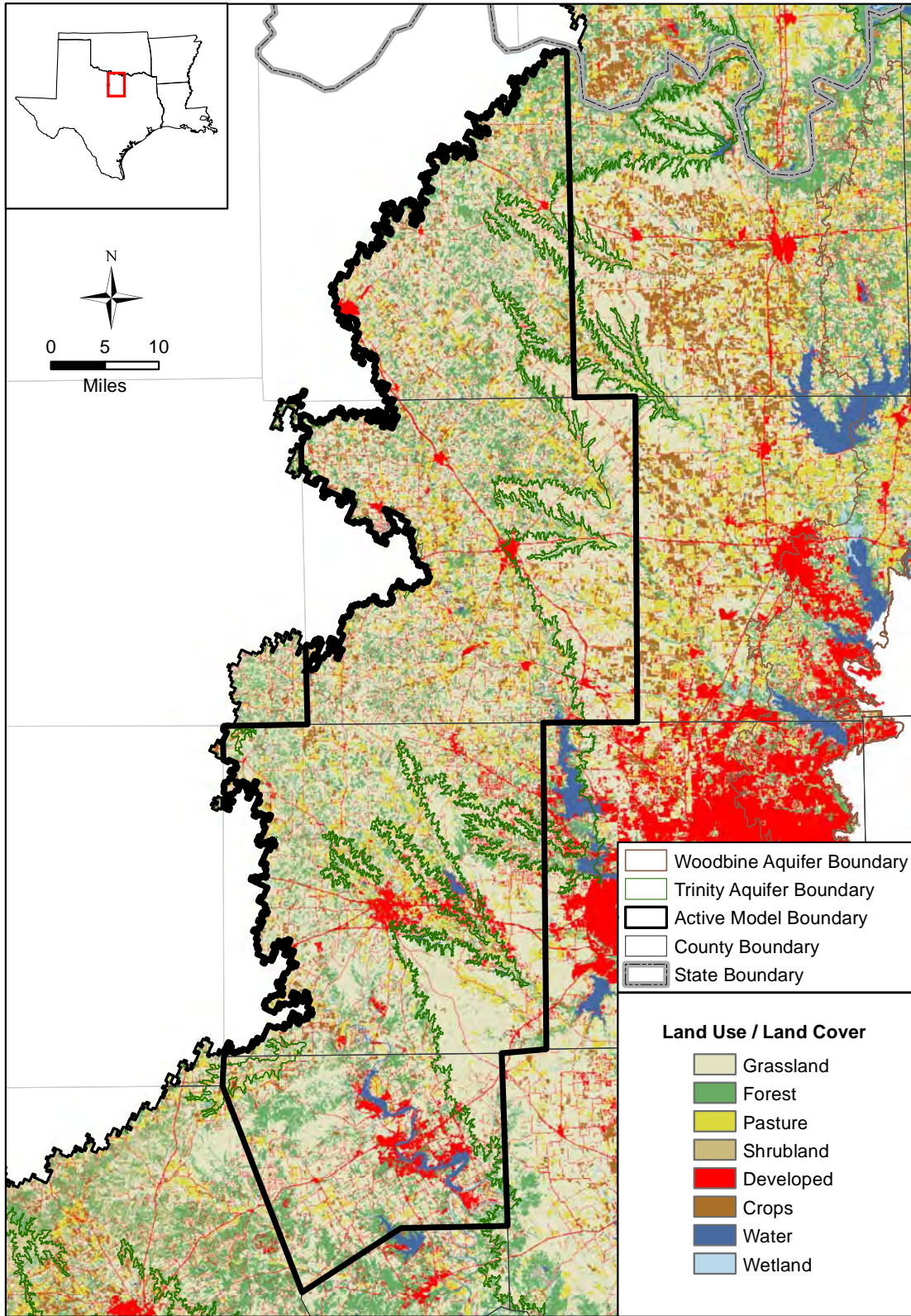
Figure 4.6.21   Land use in the study outcrop area in the Upper Trinity GCD.
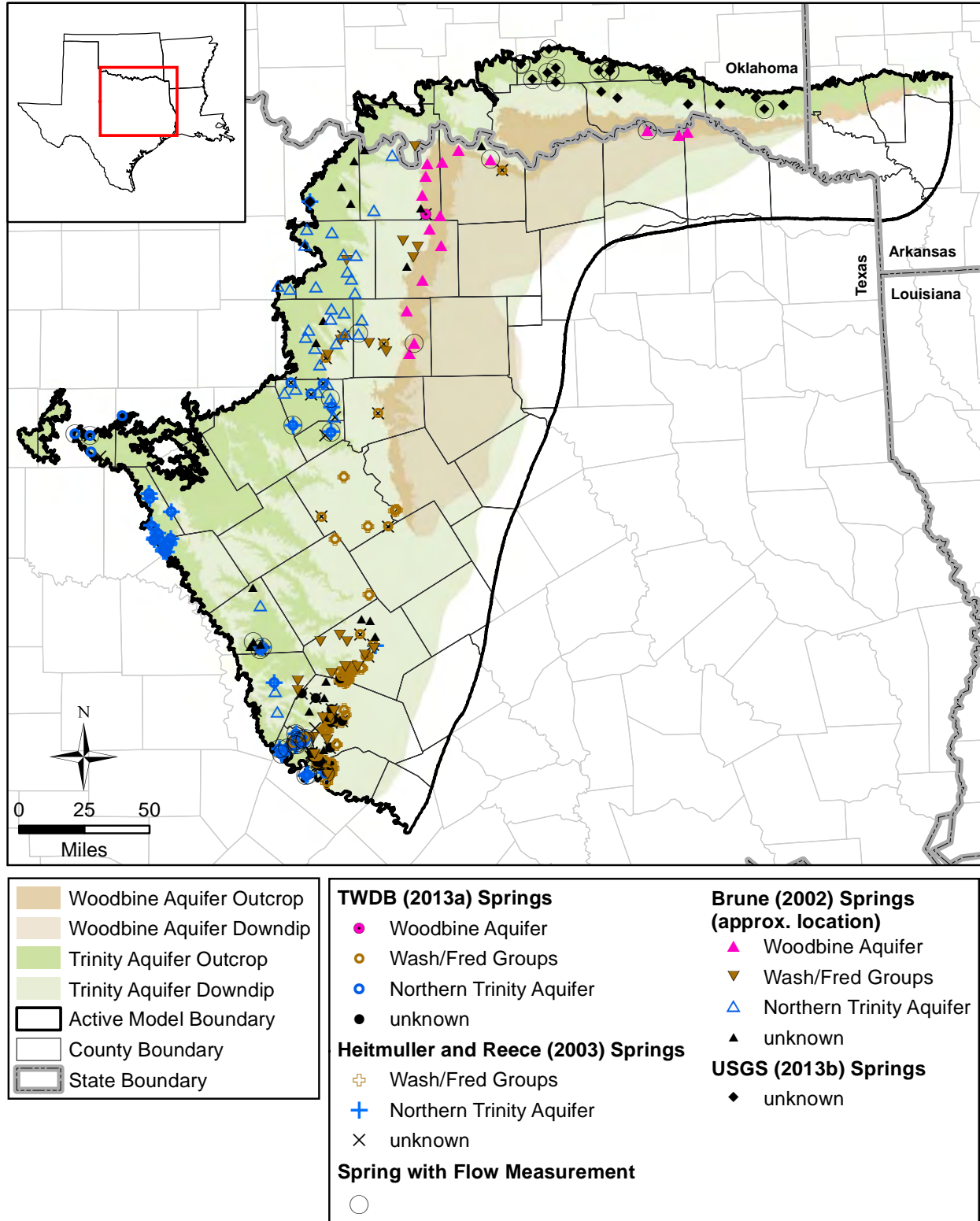
Figure 4.6.22   Select springs in the study outcrop area.
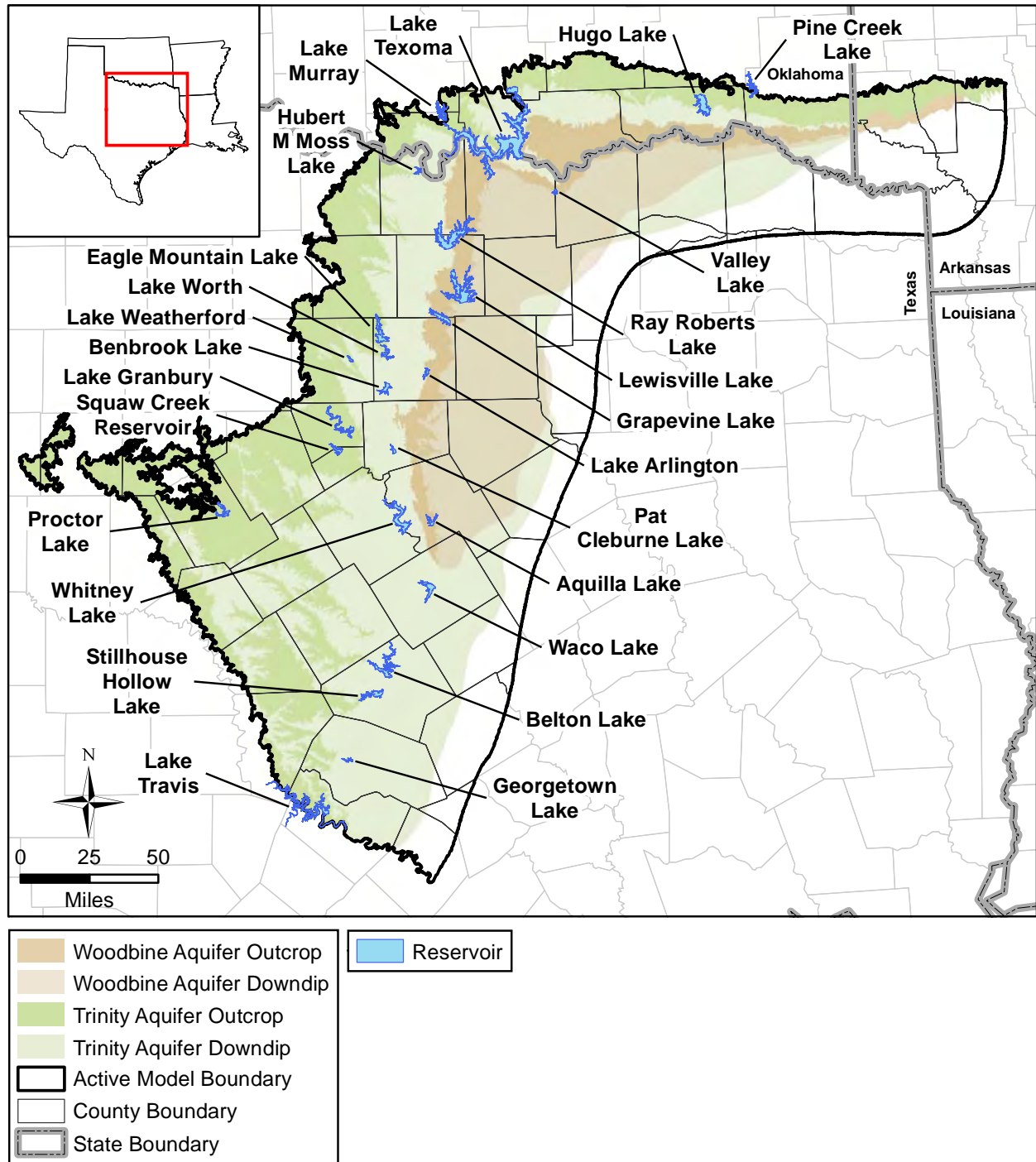
Figure 4.6.23   Reservoirs in the study outcrop area with a surface area greater than 1 square mile.
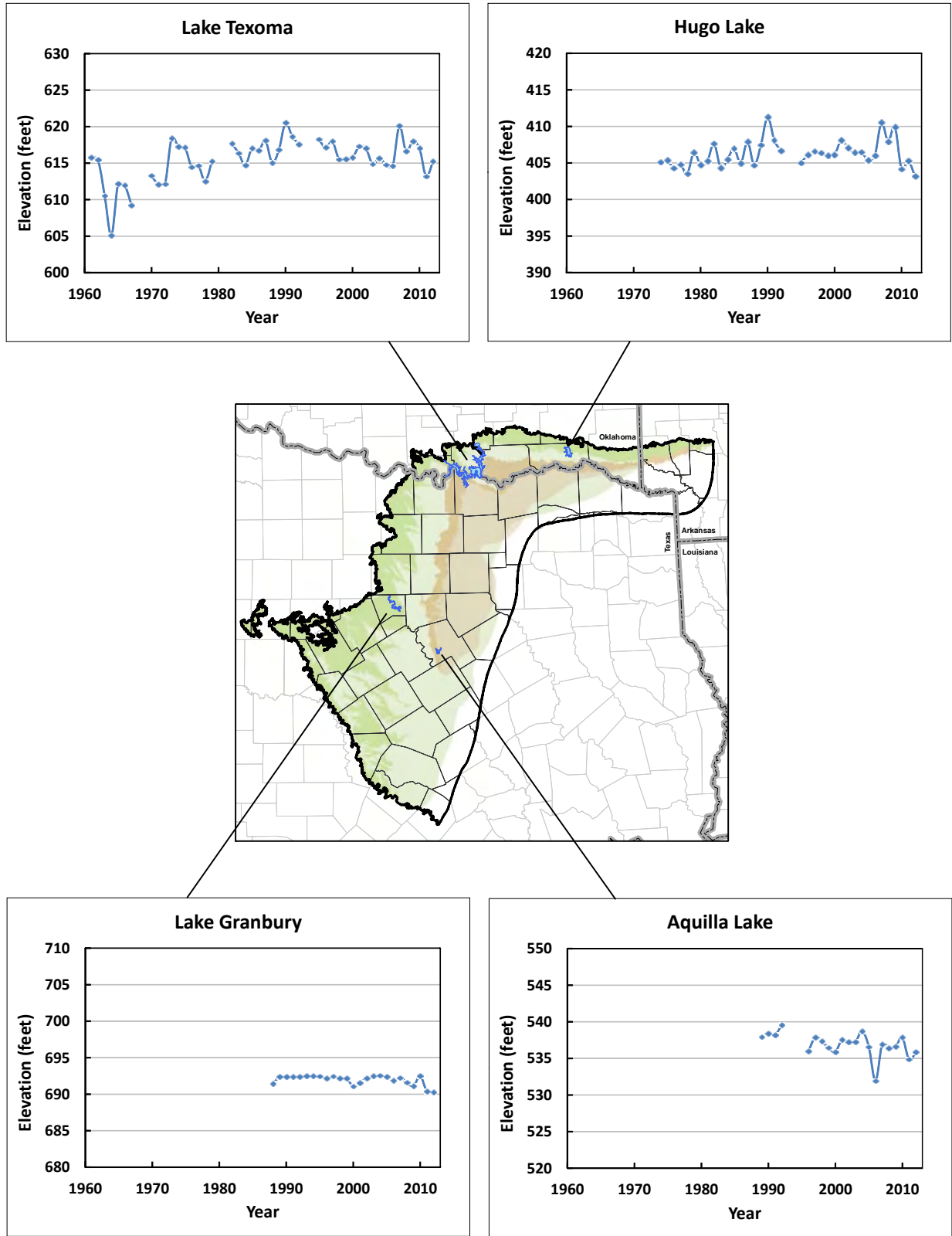
Figure 4.6.24   Elevation data for selected reservoirs in the study outcrop area.

4.7   Groundwater Pumping and Discharge from Flowing Wells

In predevelopment hydraulic conditions, a long-term dynamic equilibrium exists where aquifer recharge is balanced by aquifer discharge. This hydraulic condition is generally referred to as a steady-state flow system. Human activities alter the dynamic equilibrium of the predevelopment flow system through groundwater pumping withdrawals, changes in recharge through development and irrigation return flow, and changes in vegetation. From the groundwater perspective, groundwater withdrawals due to pumping almost always have the greatest impact on aquifer hydraulics. For the northern Trinity and Woodbine aquifers, aquifer hydraulics were also impacted by the loss of groundwater through free flowing wells during the latter part of the 1800s and the early part of the 1900s.

Groundwater removed by pumping and free flowing wells is supplied through decreased groundwater storage, reduced natural groundwater discharge, and sometimes increased recharge. The observable impact resulting from removing water from storage is declines in hydraulic heads. Hydraulic head declines have been significant in the study area historically. In an area that has experienced significant groundwater loss through pumping and free flowing wells, and associated changes in hydraulic heads, definition of pumping is an important parameter required for development of a reliable model.

For the northern Trinity and Woodbine aquifers in Texas, estimated historical pumping and discharge from flowing wells were obtained from the literature and calculated for the time period from 1900 to 1980. Water use survey data provided by the TWDB were used to obtain estimated historical pumping for use types municipal, manufacturing, mining, power, irrigation, and livestock for the time period 1980 through 2010. Note that the "mining" category includes oil and gas use. Census block data were used to estimate rural domestic pumping during this same time period. Data for mining use in 2011 were obtained from Nicot and others (2011, 2012a). Additional pumping data were received from several of the GCDs in the study area. The time period for those data ranges from 2003 to 2012. Each of these pumping estimates is discussed in the following subsections.

In Texas, the Edwards BFZ Aquifer lies within the study area and is a major aquifer. The Edwards BFZ Aquifer has a state approved GAM (Jones, 2003) and the updated northern Trinity and Woodbine aquifers GAM was not developed to replace or revise it. However, because

pumping from the Edwards BFZ Aquifer can impact hydraulic conditions in portions of the northern Trinity Aquifer, estimated pumping for the Edwards BFZ Aquifer was also developed and integrated into the pumping database for this study.

In Oklahoma and Arkansas, estimated historical pumping from the northern Trinity Aquifer equivalent, the Antlers Aquifer, was based on historical data and pumping developed for a model of the Antlers Aquifer in Oklahoma by Oliver and others (2013).

Estimates of historical groundwater withdrawals and losses via flowing wells in the study area from 1900 to 2010 for the northern Trinity and Woodbine aquifers are summarized in this section. Subsections include discussions of:

- Estimated discharge from flowing wells.

- Historical pumping estimates in Texas from 1900 through 1980.

- Estimates of pumping in Texas for 1980 through 2010 and estimates of pumping for mining use in Texas in 2011.

- Pumping data received from GCDs.

- Historical pumping for the Oklahoma and Arkansas counties located in the study area.

- Estimates of historical pumping from 1900 through 2010 for the study area.

- Implementation of pumping in the numerical model.

4.7.1 Discharge from Flowing Wells

The greatest source of groundwater loss from the northern Trinity and Woodbine aquifers in the late 1800s and early 1900s was free flowing wells rather than pumping. Common practice by early well owners was to allow water to freely discharge from flowing wells, resulting in large amounts of groundwater loss and reduction in hydraulic heads in the northern Trinity and Woodbine aquifers. Hill (1901) and Sundstrom and others (1947) estimated total discharge from the northern Trinity Aquifer in 1900 through flowing wells in Waco of 10,500 and 11,200 AFY, respectively. Flowing wells were also common in the city of Fort Worth and contributed to development of that city (Leggat, 1957). Other than the two estimates of discharge from flowing wells in Waco, the amount of water loss through this mechanism is predominately undocumented and very uncertain.

A review of the information provided in Hill (1901) was conducted to:

- Identify locations of flowing wells in the northern Trinity and Woodbine aquifer that contributed to the early decline in hydraulic heads in these two aquifers.
- Collect information on discharge rates from flowing wells.

In his report, Hill (1901) provides a discussion of artesian conditions in the Black and Grande prairies by county. Those discussions usually include a table containing the schedule of wells in the county and a small county map showing locations of wells in the county. In some cases, lithology logs and estimated discharge rates from flowing wells are also included in the discussion. Hill (1901) sent out inquires requesting information on artesian wells and the responses to those inquiries were the source of the well information he included in the county discussions. Based on the results of those inquires, he estimated 964 artesian wells, 458 of which were flowing wells and 506 of which were non-flowing wells, in his area of investigation. Hill (1901) also includes large plates showing locations of wells in what he terms the Woodbine artesian reservoirs, the Fredericksburg artesian reservoirs, the Paluxy artesian reservoirs, and the Trinity artesian reservoirs, as well as a map of artesian wells in his study area. On both the small county maps and the large plates, flowing wells are distinguished from non-flowing wells.

Locations of flowing wells based on data in Hill (1901) were obtained by two methods. First, the individual county maps in his county discussions and his large plates were georeferenced and the location of flowing wells was digitized. Second, the written descriptions of well locations given in his tables of well schedules (i.e., Bluffdale, 4 ¼ miles southeast of) were used to manually assign the location of flowing wells. In some cases, the flowing wells indicated in the tables could be matched to those shown on the figures. However, the wells in the tables could not be matched with wells in the figures in many cases. In all cases, the locations of flowing wells from Hill (1901) are uncertain. Using these two methods, 427 flowing were identified in the study area, which corresponds to about 93 percent of the total number given by Hill (1901). The number of flowing well locations by county and "artesian reservoir" determined from Hill (1901) is summarized in Table 4.7.1 and the spatial distribution of those wells is shown in Figure 4.7.1. Hill (1901) referred to the aquifers as artesian reservoirs and the terminology used by Hill (1901) is given on this table and figure. The correlation between his terminology and the terminology used for the updated northern Trinity and Woodbine aquifers GAM is:

- Woodbine artesian reservoirs – Woodbine Aquifer.

- Fredericksburg artesian reservoirs – Washita/Fredericksburg groups.

- Paluxy artesian reservoirs – Paluxy Aquifer.

- Trinity artesian reservoirs – Hensell and Hosston aquifers.

In addition to locating early flowing wells, estimates of discharge rates for flowing wells were obtained from Hill (1901). Hill (1901) provides reported discharge rates in his county discussions. Unfortunately, the lengths of time at which the wells flowed at the reported rates are not provided. In addition, a direct correlation between flowing wells and discharge rates is difficult based on the data provided by Hill (1901) because the wells for which he provides discharge rates are often not the wells shown on the figures or given in the well schedule tables. Therefore, no attempt was made to associate discharge rates with specific flowing wells. A summary of the discharge rates from flowing wells reported by Hill (1901) is given in Table 4.7.1 by county.

The locations of flowing wells in the northern Trinity and Woodbine aquifers estimated from Hill (1901) were incorporated in the transient model to provide the mechanism for simulating the early reductions in hydraulic heads resulting from discharge via free flowing wells. Implementation of this early discharge is discussed in Section 6.3.5 and discharge volumes are discussed in Section 9.2.

4.7.2   Historical Pumping for 1900 to 1980 in Texas

Two methods were used to estimate historical pumping for the northern Trinity and Woodbine aquifers for the period from 1900 to 1980. The first consisted of collecting historical pumping estimates from the literature and the second consisted of performing calculations to estimate historical pumping. Calculations were also used to estimate historical pumping from 1900 to 1980 for the Edwards BFZ Aquifer. These methods are discussed below. In addition, an integrated estimate of pumping for the period from 1900 to 1980 was developed for each aquifer by county based on the literature and calculated data.

4.7.2.1   Literature Sources of Historical Pumping Estimates

Sources reviewed for historical estimates of pumping from the northern Trinity and Woodbine aquifers in Texas include reports by the TWDB and its predecessor agencies, the USGS, the University of Texas at Austin Bureau of Economic Geologic, and the Baylor Geological Society.

A summary of these sources, including their area and time period of interest and the type of pumping estimated, is provided in Table 4.7.2. The types of historical reports include regional hydrogeologic studies, studies of groundwater resources in individual counties, summaries of historical municipal water use, investigations conducted during World War II related to water supplies, and water supply investigations conducted at the request of municipalities. Also included in the sources of historical data from the literature is a report related to a groundwater model of the northern Trinity and Woodbine aquifers as part of the investigation of the Super Conducting Super Collider site (Dutton and others, 1996) and the Hill (1901) report on artesian waters in the Black and Grande prairies of Texas.

The pumping data from historical reports is somewhat limited. In general, the earliest reports, which typically addressed a local groundwater issue, provide a pumping estimate for municipal use in a single year. The reports related to regional hydrogeologic investigations provide the most data with respect to pumping for multiple use types and estimates for multiple years. The most comprehensive source of historical pumping estimates from the literature is Dutton and others (1996), who developed pumping estimates for 1891 to 1979. The pumping estimates from Dutton and others (1996) are important in that they include estimates of discharge via flowing wells. The assumptions they used to construct their early estimates of pumping were:

- *"Hill's (1901) records of flowing and non-flowing wells provide the best basis for reconstructing average discharge rates;*
- *Discharge decreased from high levels in the late 1800s to minimum levels during the 1930s;*
- *Somervell County had the highest early production rates;*
- *Where Hill (1901) does not report well data, discharge was based on an assumed yield of 10 gallons per minutes for pumped wells and 155 gallons per minute for flowing wells;*
- *Production from counties within the artesian belt decreased rapidly when wells stopped flowing; and*
- *In the few counties where reported production from the Paluxy is grouped together with that from the Twin Mountains, production from the Paluxy was assumed to be ≤ 10 percent of the total discharge."*

4.7.2.2   Calculation of Historical Pumping Estimates for 1900 to 1980

Calculations of historical pumping were conducted to estimate values for use types municipal, rural domestic, livestock, and irrigation. An overview of the calculations is provided here and a more detailed discussion is provided in Appendix G.

The basis for the municipal and rural domestic calculations was population estimates obtained from the Texas State Historical Society (2013) and assumed per capita use rates. The total population was divided into estimates for urban and rural population assuming urban conditions for towns with a population of 500 or more. The per capita use rate was assumed to be lower in 1900 than in 1980 for both rural and urban populations. In addition, urban populations were assumed to have a higher per capita use rate than rural populations. Municipal and rural domestic calculations were performed for the time period 1900 to 1980.

Calculations of pumping estimates for livestock use were based on cattle populations obtained from agriculture census cattle population data available from the U.S. Department of Agriculture (2012). A constant animal use rate was assumed throughout time. Estimates of livestock pumping were calculated from 1940 to 1980. Estimates of irrigation use are provided for several years between 1958 and 2000 in TWDB (2001). Additional estimates were calculated for years 1939, 1949, and 1954 based on irrigated acreages in those years obtained from the agricultural census by the U.S. Department of Agriculture (2012). The calculations for these additional years used average irrigation depths estimated from the data provided in TWDB (2001) and historical precipitation.

Wells used to produce groundwater for rural domestic and livestock purposes were assumed to be relatively shallow. Therefore, calculations of pumping for these purposes were confined to the portion of the study area where the northern Trinity and Woodbine aquifers outcrop, and to the outcrop of the Washita/Fredericksburg groups. This area is shown in Figure 4.7.2. The source of groundwater for rural domestic and livestock pumping was assumed to be the aquifer or formation at land surface, as wells used to produce water for these purposes are assumed to be relatively shallow.

4.7.2.3   Summary of Historical Pumping Estimates for 1900 to 1980

Figures of the historical pumping estimates from the literature and the calculated estimates were plotted in graphical form as time-series plots in order to present, evaluate, and compare the

available data. Time-series plots were prepared for both the northern Trinity and Woodbine

aquifers, as well as the Edwards BFZ Aquifer, by county. For sources with estimates for

multiple use types, the sum of pumping for all types was plotted. The data from the various

sources often overlap in time, and in many cases, differ in magnitude. Often the differences in

magnitude are a function of the number of use types for which pumping is reported in the

literature. For example, a reported estimate for municipal pumping from one source will

typically be less than the reported pumping from another source that includes estimates for both

municipal and industrial pumping.

The historical estimates from these time-series plots were reviewed and an integrated estimate of

total pumping was developed for each aquifer by county and plotted on a second time-series plot.

The objective for developing the integrated curves was to produce a consistent time series-plot of

historical pumping from each aquifer in each county. The integrated curves provided an estimate

of historical pumping that was used as the baseline pumping data set in the model

implementation and calibration phases.

For both sets of time-series plots, the year scale on the x-axis is from 1900 to 2010. The sources

of the data on the graphs after 1980 are discussed below in Sections 4.7.3 and 4.7.4. The

pumping scale on the y-axis varies from plot to plot based on the magnitude of the pumping

estimates plotted. The source of the data on the time-series plots is provided in the legend. For

sources that contained a pumping estimate for one or two use types, those types are indicated in

the plot legend. For sources containing pumping estimates for three or more use types, refer to

Table 4.7.2 for the specific use types reported by the source. For the McLennan County plot, the

legend reports the use type as FLOW for two sources. This indicates that the value in the plot

represents an estimate of discharge from flowing wells.

As discussed above, two time-series plots were created for each aquifer in each county. Due to

the large number of counties in which the northern Trinity and Woodbine aquifers are pumped,

the number of plots created was too numerous to be included in this section. However, all of the

county time-series plots for the northern Trinity, Woodbine, and Edwards BFZ aquifers are

provided in Appendix G. Time-series plots for two representative counties with pumping from

the northern Trinity Aquifer and one representative county with pumping from the Woodbine

Aquifer are presented here. The discussion provided in this section considers only the portion of the plots from 1900 through 1979.

Figure 4.7.3 presents the historical pumping estimates and the integrated historical pumping curve for the northern Trinity Aquifer in Tarrant County. In addition to the pumping data used by Dutton and others (1996) and the calculated pumping estimates conducted for this study, estimates of historical pumping from the northern Trinity Aquifer in Tarrant County from 1900 to 1979 are available from six published reports (see Figure 4.7.3a). The majority of the sources contain estimates of municipal pumping for a single year. The two sources that contain estimates for multiple use types across multiple years are both regional studies. The estimates by Dutton and others (1996) indicate substantial pumping in 1900, which likely predominantly reflects production from free flowing wells. The integrated curve of estimated historical pumping for the northern Trinity Aquifer in Tarrant County is shown in Figure 4.7.3b. This curve was developed using the estimates from Dutton and others (1996) from 1900 to 1954 and from 1974 to 1979 and the estimates from Nordstrom (1982) from 1955 to 1973.

The historical pumping estimates and integrated historical pumping curve for the northern Trinity Aquifer in Collin County are shown in Figure 4.7.4. Both the calculated estimates and Dutton and others (1996) indicate little to no pumping from the aquifer in this county until about 1910. The calculated curve is lower than that for other sources, suggesting that the calculations of historical pumping are likely too low. The largest estimates of pumping are provided by Nordstrom (1982), who reports pumping estimates for municipal, industrial, and irrigation purposes. The integrated historical pumping curve developed for the northern Trinity Aquifer in Collin County is shown in Figure 4.7.4b. The estimates of Dutton and others (1996) were used for the time periods from 1900 to 1954 and 1974 to 1979 and the estimates from Nordstrom (1982) were used for the time period from 1955 to 1974 in developing the integrated curve.

Figure 4.7.5 shows the estimated historical pumping and integrated pumping curve for the Woodbine Aquifer in Johnson County. Historical data from five sources are available as well as the calculated estimates and those from Dutton and others (1996). Estimates from the calculations and Dutton and others (1996) are similar and consistent with the municipal estimate in 1966 from Thompson (1969), but higher than the estimates from Sundstrom and others (1947), the Texas Board of Water Engineers (1961), Taylor (1976), and Nordstrom (1982). The

integrated curve shown in Figure 4.7.5b was developed from the Dutton and others (1996) estimate for 1900 to 1965, the estimate from Thompson (1969) in 1966, and the calculated estimates from 1967 to 1979.

Plots similar to Figures 4.7.3 through 4.7.5 can be found in Appendix G for all counties in the study area for the northern Trinity Aquifer, and for the Woodbine and Edwards BFZ aquifers where applicable. For the Edwards BFZ Aquifer, only calculated data from 1900 through 1979 are included in the upper plot.

4.7.3   Historical Pumping for 1980 to 2010 and 2011 Mining Pumping in Texas

Estimates of historical pumping from 1980 to 2010 were obtained from the TWDB for water use categories municipal, manufacturing, mining, power, irrigation, and livestock. These estimates have been developed by the TWDB as a water use survey database (TWDB, 2013c) to support state water planning and the TWDB GAM program. A brief summary of the water use surveys conducted by the TWDB and the methods they used to estimate groundwater pumping is provided in this section. Estimates of historical pumping for rural domestic purposes for 1980 through 2010 were calculated using census block data and estimates of per capita use. A description of these calculations is provided below. Also included in this section is a brief discussion of pumping from the northern Trinity and Woodbine aquifers for mining purposes related to oil and gas development as estimated by Nicot and others (2011, 2012a).

4.7.3.1   TWDB Methodology for Estimating Historical Pumping

The TWDB compiles groundwater use data for supporting state water planning. Their historical groundwater pumping estimates are available by water use category on a county-by-county basis for 1980 and 1984 to 2010. The water use categories they report are municipal, manufacturing, mining, power, irrigation, and livestock.

The TWDB has performed annual surveys on groundwater and surface water use by public water suppliers and major manufacturing and power entities within Texas since 1955. The results of these surveys are used by the TWDB to develop their estimates of groundwater pumping for municipal, manufacturing, and power purposes. The TWDB uses annual survey results and estimates of water used for secondary oil and gas recovery to develop their estimates of pumping for mining use. Estimates of pumping for livestock purposes reported by the TWDB are developed using estimates of livestock populations produced by the Texas Agricultural Statistics

Service and estimated water use per animal provided by the Texas Agricultural Experiment Station. Annual crop acreage, obtained from the Natural Resources Conservation Service prior to 2001 and the Farm Service Administration in 2001 and later, and irrigation rates per acre based on potential evapotranspiration are used by the TWDB to estimate pumping for irrigation purposes. The TWDB has the final irrigation rates per acre reviewed by local authorities.

4.7.3.2   Calculation of Rural Domestic Pumping

Estimates of rural domestic pumping for 1980 to 2010 were developed using census block data from 1990, 2000, and 2010, total population data for 1980 to 2010, and an assumed per capita water use. The 1990 census block data was obtained from the TWDB as a geographic information system (GIS) coverage. Historically, the TWDB has provided this data in support of estimating rural domestic pumping for GAM models. This coverage includes an identifier in each census block that indicates whether the population in the block represents an urban or rural population. Using this identifier, the rural population was calculated for each county. The 2000 and 2010 census block data were obtained from the U.S. Census Bureau as GIS coverages (U.S. Census Bureau, 2013). In addition, coverages of urban areas for 2000 and 2010 were also obtained from the U.S. Census Bureau (U.S. Census Bureau, 2013). Using these two coverages, the rural population was calculated for each county.

Using the total county population and the calculated rural population, a ratio of rural to total populations was calculated for each county for the years 1990, 2000, and 2010. A linear interpolation was conducted using these ratios to estimate ratios for each year from 1980 through 2010 for each county. The ratios for 1980 through 1989 were set equal to those calculated for 1990. The rural population for each county was estimated by multiplying the total county population from the U.S. Census Bureau, as provided by the TWDB (Cho, 2013), by the calculated rural to total population ratio. The rural domestic pumping for each county was then calculated as the rural population times an assumed per capita use of 110 gallons per day.

The calculations of rural domestic pumping for 1980 through 2010 assumed that all water used for rural domestic purposes was supplied by shallow groundwater wells located in the outcrop of the northern Trinity, Woodbine, or Edwards BFZ aquifers or the combined outcrop of the Washita/Fredericksburg groups (excluding the Edwards BFZ Aquifer) that lies between the northern Trinity and Woodbine aquifer outcrops (see Figure 4.7.2). Therefore, the total rural

domestic pumping calculated for each county was multiplied by the fraction of the county located within this outcrop area. The rural domestic pumping for each aquifer and/or formation that outcrops in a county was then calculated based on area weighting.

4.7.3.3   Summary of Historical Pumping Estimates for 1980 through 2010

The historical pumping estimates from the water use survey data provided by the TWDB (TWDB, 2013c) were combined with the calculated rural domestic pumping estimates to obtain an estimate of total historical pumping for the time period from 1980 through 2010. These estimates were combined and are shown on the time-series plots of available historical pumping data discussed in Section 4.7.2.3. A review of these estimates of historical pumping from 1980 through 2010 is provided below; first for the northern Trinity Aquifer, second for the Woodbine Aquifer, and then for the Edwards BFZ Aquifer. For all aquifers and all counties, the combined estimates from the TWDB and rural domestic calculations were used to develop the integrated pumping curve for the period from 1980 through 2010 (see plots in Appendix G).

Northern Trinity Aquifer

Tables 4.7.3 through 4.7.9 give the estimated totals for municipal, manufacturing, power, mining, irrigation, livestock, and rural domestic pumping, respectively, for the years 1980, 1985, 1990, 1995, 2000, 2005, and 2010 for the northern Trinity Aquifer. The total estimates by county for all use categories for the northern Trinity Aquifer are provided in Table 4.7.10. Each of these tables is organized by GCD, with counties not included in a GCD listed at the bottom of the tables. Across the entire northern Trinity Aquifer, the greatest water use category is municipal, followed by irrigation and rural domestic (Table 4.7.11). The overall percentage of municipal use decreased from 64 percent in 1980 to 56 percent in 2010.

In 1980, groundwater use from the northern Trinity Aquifer was greater than 10,000 acre-feet for six counties. For these counties, the highest use category was municipal for Tarrant, Dallas, and McLennan counties and irrigation for Erath, Comanche, and Eastland counties. There were eight counties with greater than 10,000 acre-feet of pumping in 2010. The dominant use category was municipal for McLennan, Denton, Tarrant, and Hood counties and irrigation for Comanche County. In Erath County, groundwater from the aquifer was predominately used for irrigation purposes in 1980, but consisted of about equal amounts of irrigation and municipal pumping in 2010. The major use categories in Parker County in 2010 were municipal and rural domestic.

Pumping for municipal, mining, and rural domestic purposes contributed the most to the overall volume pumped in Wise County in 2010.

Tables 4.7.12 through Table 4.7.15 provide pumping and percentage of total by category for the years 1980, 1985, 1990, 1995, 2000, 2005 and 2010 for the North Texas, Northern Trinity, Prairielands, and Upper Trinity GCDs, respectively. These tables show that pumping for municipal purposes was the greatest use category in all four GCDs for the period from 1980 to 2010. The percentage of groundwater pumping for municipal purposes was greatest in the North Texas and Northern Trinity GCDs and least in the Upper Trinity GCD. The category with the second greatest use was livestock for the North Texas GCD, manufacturing for the Northern Trinity and Prairielands GCDs, and rural domestic for the Upper Trinity GCD.

Stacked bar charts of pumping by use category were developed for all counties combined and for each individual county that pumps from the northern Trinity Aquifer for the time period 1980 through 2010. These charts are useful for visualizing total pumping trends and trends of pumping for individual use categories. Because of the large number of charts involved, only the chart showing totals for the entire aquifer, one representative county, and for the North Texas, Northern Trinity, Prairielands, and Upper Trinity GCDs are shown here. However, all of the bar charts for the individual counties with pumping from the northern Trinity Aquifer can be found in Appendix G. Note in these bar charts that only rural domestic pumping is plotted for 1981 through 1983 because the TWDB reports its water use estimates for 1980 and 1984 through 2010, but not for 1981 through 1983. Recall that rural domestic pumping is only included for counties where the aquifer outcrops.

Pumping from the entire northern Trinity Aquifer in Texas by use category for the years 1980 through 2010 is shown in Figure 4.7.6a. This figure shows that the largest use category for groundwater from the northern Trinity Aquifer is municipal with irrigation use second. In general, the counties with the highest municipal pumping are those located in and around the Dallas-Fort Worth Metroplex and the city of Waco and the counties with the highest irrigation pumping are those located on the western outcrop of the aquifer. Municipal pumping remained essentially constant from 1980 through 2010. Some variability in irrigation pumping occurred, but overall pumping for this category decreased from 1984 to 2010. Use of groundwater from the northern Trinity Aquifer for power and manufacturing purposes was small. Use of the

aquifer for rural domestic pumping increased and pumping for livestock purposes decreased from 1980 through 2010. Total pumping from the aquifer in Texas varied from a low of about 164,000 acre-feet in 1980 to a high of about 196,000 acre-feet in 1988.

An example bar chart of pumping from the northern Trinity Aquifer by use category for an individual county (Hood County) is shown in Figure 4.7.6b. Municipal pumping, which was the major use category in this county, increased over this time period. Irrigation pumping was variable in the county from 1980 through 2010 and pumping for mining purposes generally increased. Little change was observed in pumping for rural domestic and livestock purposes. Total pumping from the northern Trinity Aquifer in this county increased overall from 1980 through 2010, with maximum pumping observed in 2006.

Figure 4.7.7a shows pumping in the North Texas GCD by water use category from 1980 through 2010. The majority of water pumped from the northern Trinity Aquifer in this GCD is used for municipal purposes. Pumping for all other uses is relatively small. An overall increase in pumping is observed from 1980 to 2010. However, the increase did not consist of a steady rise but, rather, periods of increases and declines.

Pumping from the northern Trinity Aquifer in the Northern Trinity GCD by use category from 1980 through 2010 is shown in Figure 4.7.7b. As illustrated in this figure, the major use of groundwater pumped from the aquifer in this GCD is for municipal purposes. Pumping for manufacturing, rural domestic, and livestock purposes remained fairly consistent throughout the 1980 through 2010 time period. The available data indicate that pumping for mining purposes occurred in 2006 through 2010 and some pumping for irrigation purposes occurred in 2009 and 2010. Overall, pumping of the northern Trinity Aquifer in the Northern Trinity GCD declined from about 19,000 acre-feet in 1980 to about 12,500 acre-feet in 2010, with a spike in pumping of about 21,400 acre-feet in 2009.

Pumping from the northern Trinity Aquifer by use category for the period 1980 through 2010 is shown in Figure 4.7.8a for the Prairielands GCD. The greatest use of groundwater pumped from the northern Trinity Aquifer in this GCD is for municipal purposes. Overall, pumping increased in this GCD from 1980 to 2010 as a result of increases in municipal and mining pumping. However, pumping peaked in 2006 and has been declining since that time.

Pumping from the northern Trinity Aquifer in the Upper Trinity GCD by use category for years 1980 through 2010 is shown in Figure 4.7.8b. Municipal and rural domestic purposes are the primary use categories in this GCD. Pumping for both of these categories increased from 1980 to 2010. The percentage of pumping for mining purposes increased by about a factor of 20 percent between the time period prior to 2006 and the time period from 2006 to 2010.

Woodbine Aquifer

Estimated pumping from the Woodbine Aquifer for municipal, manufacturing, power, mining, irrigation, livestock, and rural domestic for the years 1980, 1985, 1990, 1995, 2000, 2005, and 2010 are given in Tables 4.7.16 through 4.7.22, respectively. Total pumping from the aquifer by county in these years is given in Table 4.7.23. These tables are organized by GCD, with counties not located within a GCD listed at the bottom. The dominant use of groundwater from the Woodbine Aquifer is for municipal purposes (Table 4.7.24). The counties with the highest municipal pumping from this aquifer are Grayson, Collin, Fannin, and Ellis counties (see Table 4.7.16).

Tables 4.7.25 through 4.7.27 show pumping and percentage of total from the Woodbine Aquifer in 1980, 1985, 1990 ,1995, 2000, and 2010 for the North Texas, Northern Trinity, and Prairielands GCDs, respectively, by use category. The percentage of pumping for municipal and rural domestic purposes was similar and increased from 1980 through 2010 in the North Texas GCD. Based on the available data, the aquifer is used predominately for rural domestic purposes in the Northern Trinity GCD. Pumping for both municipal and rural domestic use increased from 1980 to 2010 in the Prairielands GCD.

Stocked bar charts of historical pumping by use category from 1980 through 2010 were also developed for the Woodbine Aquifer. Charts showing total pumping from the aquifer and totals for the North Texas, Northern Trinity, and Prairielands GCDs are shown here. The individual charts for each county with pumping from the Woodbine Aquifer can be found in Appendix G. Note in these charts that only rural domestic pumping is plotted for 1981 through 1983 because the TWDB reports its water use estimates for 1980 and 1984 through 2010, but not for 1981 through 1983. Recall that rural domestic pumping is only included for counties where the aquifer outcrops.

Figure 4.7.9a shows a bar chart of total pumping from the Woodbine Aquifer by use category from 1980 through 2010. This figure illustrates an overall increase in both municipal and rural domestic pumping over this time period. Pumping of the aquifer for irrigation purposes was variable, as was that for manufacturing and livestock purposes. Use of the aquifer for mining and power purposes was small. An overall increase in pumping is observed from about 18,000 acre-feet in 1980 to about 27,000 acre-feet in 2010.

Figure 4.7.9b shows pumping from the Woodbine Aquifer by use category for the counties in the North Texas GCD. The primary uses of groundwater pumped from the Woodbine Aquifer in this GCD are municipal and rural domestic. Irrigation pumping was also significant for some years. Pumping of the aquifer in this GCD rose relatively gradually between 1980 and 1990 and then jumped about 35 percent in 2000. From 2000 to 2005, pumping in this GCD fluctuated but remained relatively stable. Pumping then decreased until 2008 and then rose until 2010.

Pumping from the Woodbine Aquifer in the Northern Trinity GCD is shown by use category in Figure 4.7.10a. Based on the available data, use of the aquifer for all purposes increased from about 500 acre-feet in 1980 to about 1,200 acre-feet in 2010, with a spike in pumping to almost 1,500 acre-feet occurring in 2009. The majority of groundwater pumped from the Woodbine Aquifer in this GCD is used for rural domestic purposes.

Figure 4.7.10b shows pumping from the Woodbine Aquifer in the Prairielands GCD by use category. Use of the aquifer in this GCD was primarily for municipal and rural domestic purposes. Pumping for livestock and manufacturing purposes declined from 1980 to 2010. Overall, pumping of the Woodbine Aquifer remained relatively constant over the time period from 1980 to 2010 in this GCD.

Edwards BFZ Aquifer

The Edwards BFZ Aquifer underlies Bell, Williamson, and Travis counties. Estimated pumping from the aquifer by water use category for the years 1980, 1985, 1990, 1995, 2000, 2005, and 2010 is provided in Table 4.7.28. The available data indicates that the majority of the groundwater pumped from this aquifer is used for municipal purposes, very little is used for irrigation, manufacturing, and livestock purposes, and none is used for power purposes. Overall, pumping from the aquifer increased from about 17,500 acre-feet in 1980 to about 39,000 acre-feet in 2010, with the greatest increase from pumping for municipal purposes (Figure 4.7.11).

4.7.3.4   Estimates of Mining Pumping

Estimates of groundwater pumping in Texas for mining purposes in association with the oil and gas industry are provided by Nicot and others (2011, 2012a). The objective of the Nicot and others (2011) study was to estimate current and projected mining water use specifically for the oil and gas sector. Because the oil and gas exploration focus and trends (from gas to oil exploration and production) were changing quickly, the TWDB funded an update to the 2011 report (Nicot and others, 2012a). Nicot and others (2012a) updates water use estimates and projects water use estimates for oil and gas exploration and production related activities. Nicot and others (2012a) also provides projections for all other mining water uses in Texas. The data from these two reports were combined and are reported here as a single estimate in 2011. The mining pumping estimated from Nicot and others (2011, 2012a) are included in the county time-series plots provided in Appendix G.

4.7.4   Pumping Data Received from GCDs

Several types of pumping data were received from GCDs in the study area. These included pumped volumes as recorded for metered non-exempt wells, reported pumping provided on well applications, reported pumping provided on historical use permit applications, and estimates of non-exempt pumping. A summary of the types of data received from the GCDs and the time periods of the data is provided in Table 4.7.29.

The pumping data received from the GCDs are included on the county time-series plots provided in Appendix G. A comparison of the GCD data and the estimated pumping developed here for the northern Trinity Aquifer found the following. For Clearwater UWCD, the pumping data reported by the GCD is slightly lower than the estimate pumping for 2004 through 2008 but quite a bit lower for the years 2003 and 2010. For the North Texas GCD, the 2010 pumping provided by the GCD is lower than the estimated pumping for Collin and Denton counties and higher than the estimated pumping for Cooke County. This is to be expected because the North Texas GCD only collects water use estimates for non-exempt wells. The pumping data obtained from well applications provided by the Northern Trinity GCD are significantly lower than the estimated pumping. This is because the Northern Trinity GCD collects water use data on all non-exempt wells and wells related to oil and gas activities that produce over a defined pumping rate.

A direct comparison of the pumping received from the Prairielands GCD and the historical

pumping estimates developed here cannot be made because the two data sets do not overlap.

However, based on the historic trends of the estimated pumping, the data from this GCD is

consistent in Ellis and Johnson counties, higher for 1 year and consistent for the other year in

Hill County, and lower in Somervell County. This suggests that the bulk of the pumping in the

Prairielands GCD is non-exempt. The pumping data received from the Southern Trinity GCD is

slightly lower than the estimates developed here for years 2000 through 2005 and fairly

consistent for the years 2006 through 2010. For all counties in the Upper Trinity GCD, the

pumping reported by the GCD is lower than that estimated here. Again, this is because the

Upper Trinity GCD only collects water use data on non-exempt wells and wells providing water

to support oil and gas activities. Rural domestic exempt pumping is a significant percentage of

pumping in the Upper Trinity GCD.

4.7.5   Historical Pumping Estimates for Oklahoma and Arkansas

Estimates of historical pumping data for Oklahoma and Arkansas were taken from a model of the

Antlers Aquifer in Oklahoma by Oliver and others (2013). The sources of historical pumping

estimates used by Oliver and others (2013) to develop pumping from the Antlers Aquifer were

the Oklahoma Water Resources Board and Tortorelli (2009). The data available from the

Oklahoma Water Resources Board consisted of results from water use surveys conducted from

1980 through 2010. Those survey results are typically incomplete and underestimate actual

pumping. Using addition pumping data from federal, state, local, and private agencies, as well as

factors such as population and average consumption rates, Tortorelli (2009) developed adjusted

pumping estimates for the year 2005. Based on his adjusted values, the average increase in

pumping over reported survey values was 53 gallons per day per capita. This increased volume

was assumed to apply predominately to rural domestic use. The historical pumping estimates

developed by Oliver and others (2013) for Oklahoma from 1980 through 2010 used the water use

survey results reported by the Oklahoma Water Resources Board plus additional pumping

calculated based on a per capita groundwater use of 53 gallons per day per. Pumping prior to

1980 in that model was developed through calibration to hydraulic head data. Figure 4.7.12a

shows the estimated pumping for the Oklahoma counties in the study area obtained from Oliver

and others (2013).

Oliver and others (2013) reports that Holland (2007) provides pumping estimates in Arkansas by county and water user group for the year 2005. Based on these estimates, pumping on a per capita basis from the Antlers Aquifer by county was estimated to range from 6 to 30 gallons per day, which Oliver and others (2013) assumed to be low. Therefore, they developed estimates of pumping for the Arkansas counties by assuming that the majority of pumping from the aquifer in Arkansas is for rural domestic and/or livestock use, and the Oklahoma rural domestic per capita use estimate of 53 gallons per day was also applicable for Arkansas. Using census block data, Oliver and others (2013) developed historical pumping estimates in Arkansas for the years 1980 through 2010 assuming a per capita use of 53 gallons per day. As was done for Oklahoma pumping, Arkansas pumping prior to 1980 was based on model calibration to hydraulic heads. The estimated historical pumping for the Arkansas counties obtained from Oliver and others (2013) is shown in Figure 4.7.12b.

4.7.6   Combined Historical Pumping Estimates for 1900 through 2010

This section presents the combined estimated historical pumping from all sources and calculations for the time period 1900 to 2010 for the northern Trinity, Woodbine, and Edwards BFZ aquifers. These estimates consist of the integrated historical pumping curves for each county in each aquifer developed from the various sources. Also presented here are the estimated total historical volumes of groundwater removed from the northern Trinity, Woodbine, and Edwards BFZ aquifers by county. When comparing the plots discussed below, note that the scale of the x-axis is constant from 1900 to 2010 but the scale of the y-axis varies from plot to plot based on the magnitudes of the pumping rates and estimated historical volumes pumped. The following discussion is organized by aquifer with the northern Trinity Aquifer discussed first following by discussions for the Woodbine Aquifer then the Edwards BFZ Aquifer.

Northern Trinity Aquifer

Figure 4.7.13 shows the integrated pumping curves and estimated cumulative volume curves for the northern Trinity Aquifer in the counties of the North Texas and Northern Trinity GCDs. Pumping in Tarrant County has been historically greater than that in Collin, Cooke, and Denton counties (Figure 4.7.13a). The year in which peak pumping occurs varies from county to county. The changes in the slope of the cumulative volume curves in Figure 4.7.13b indicate a change in the rate of groundwater pumping. A steeper slope indicates an increase in pumping, and a

shallower slope indicates a decrease in pumping. The curves in Figure 4.7.13b indicate that the estimated total volume removed by historical pumping is over twice as much for Tarrant County than for Collin, Cooke, and Denton counties.

The integrated pumping curves and estimated cumulative volume curves for the counties in the Prairielands GCD are shown in Figure 4.7.14. Early pumping was greatest in Somervell County due to estimated discharge via free flowing wells. Since about 1950, pumping in Johnson County has been greater than that in Ellis, Hill, and Somervell counties. A significant increase in pumping occurred in Johnson County in about 1970 and in Ellis County in about 1980. Pumping in Somervell County also increased in 1970, but not to the degree observed for Johnson County. Pumping in Hill County has remained fairly stable since about 1970.

For the counties in the Upper Trinity GCD, pumping in Parker County is greater than that in Wise, Hood, and Montague counties (Figure 4.7.15). Pumping from the northern Trinity Aquifer in Montague County is substantially lower than in the other three counties in the GCD. Groundwater withdrawal increased in about 1960 and then again in about 1980 in Parker County. In Wise and Hood counties, increases in the withdrawal rate are observed in 1970 and again in 1980.

Figure 4.7.16 shows integrated pumping curves and estimated cumulative volume curves for estimated historical pumping from the northern Trinity Aquifer in Dallas, Delta, Fannin, Grayson, Hunt, Kaufman, Lamar, Red River, and Rockwall counties. For these counties, pumping from the Trinity Aquifer is greatest in Dallas County followed by Grayson County. Based on the available data, pumping in Dallas County significantly increased from about 1920 to 1955, remained fairly stable until about 1988, and significantly decreased after 1988. Pumping in Grayson County increased between about 1945 and 1970, was variable from 1970 to about 2000, decreased to about 2003, and has remained fairly stable since that time. Pumping for the remaining counties shown in this figure is relatively low, with no county have total pumping from the northern Trinity Aquifer of over 1,000 AFY, except for Red River County.

Integrated pumping curves and estimated cumulative volumes pumped are shown in Figure 4.7.17 for Bell, Bosque, Coryell, Falls, Limestone, McLennan, Milam, Navarro, Travis, and Williamson counties. For this group of counties, pumping from the northern Trinity Aquifer was greatest in McLennan County and least in Navarro, Milam, and Limestone counties.

Pumping is estimated as initially high from 1900 to 1920 followed by a rapid decline in McLennan County based on estimates of discharge from free flowing wells. The pumping rate in McLennan County was higher for the period from about 1935 to about 1980 then for the period from 1980 to 2010. The rate of groundwater pumping has remained relatively constant for Bosque, Bell, and Falls counties. An increase in the pumping rate occurred from about 1980 to 1985 in Coryell and Williamson counties.

Figure 4.7.18 shows the integrated pumping curves and estimated historical volumes pumping for Brown, Burnet, Callahan, Comanche, Eastland, Erath, Hamilton, Jack, Lampasas, Mills, and Taylor counties. In these counties, pumping from the northern Trinity Aquifer has been greatest for Comanche, Erath, and Eastland counties. Pumping in all other counties has been about equal. Pumping peaked in about 1992 in Comanche County and in about 1993 in Erath County. The rate of pumping in Eastland County significantly increased between about 1978 and 1980.

Total estimates of pumping from the northern Trinity Aquifer by county in 1950, 1980, and 2010 are shown in Figures 4.7.19, 4.7.20, and 4.7.21, respectively. In general, pumping from the aquifer is lowest in the Texas counties along the eastern boundary of the study area, in Fannin, Lamar, and Red River counties, and in Arkansas for all 3 years. Pumping totals in 1950 and 1980 are greatest in Tarrant and Dallas counties and pumping totals in 2010 are greatest in McLennan and Parker counties. With the exclusion of the counties with low pumping totals, the distribution of pumping varies between the 3 years. With the exception of Tarrant County, all counties show an increase in total pumping from the northern Trinity Aquifer with time. Pumping in Tarrant County decreased between 1980 and 2010.

Woodbine Aquifer

Integrated pumping curves and estimated cumulative volume curves are shown in Figure 4.7.22 for the counties in the North Texas and Northern Trinity GCDs. Estimated volumes of groundwater withdrawn from the Woodbine Aquifer are greatest for Denton County and least for Cooke County. Although the 1950 to 2010 pumping rates estimated for Tarrant County are less than those estimated for Denton County, the cumulative volume withdrawn is estimated to be about the same due to early losses of water from flowing wells in Tarrant County. Prior to 1990, pumping in Collin County was greatest in the years from about 1954 to 1970. Since 1990, pumping in this county has continued to increase. Pumping in Denton County peaked in about

2001 and has declined since that time. The rate of groundwater withdrawal over the historical period has varied between the four counties.

Figure 4.7.23 shows integrated pumping curves and estimated cumulative volume curves for the counties in the Prairielands GCD with pumping from the Woodbine Aquifer. The cumulative volume pumped has been greatest for Ellis County and least for Hill County. Pumping appears to have peaked in about 1960 in Ellis County and in about 1995 in Johnson County. Pumping in Hill County has remained fairly constant over the historical period.

Historical pumping from the Woodbine Aquifer in Fannin, Grayson, Hunt, Lamar, and Red River counties in the form of integrated pumping curves and estimated cumulative volume curves is shown in Figure 4.7.24. For these five counties, pumping from the Woodbine Aquifer has been greatest in Grayson and Fannin counties and least in Red River County. The rate of pumping was fairly constant for Hunt and Lamar counties. After about 1940, the rate of pumping in Grayson and Fannin counties increased, with a greater increase in Grayson County then in Fannin County.

Integrated pumping curves and estimated cumulative volume curves are shown in Figure 4.7.25 for Dallas, Kaufman, McLennan, and Navarro counties. Pumping in Dallas County peaked in about 1960, then decline until about 2002, and has increased since 2002. The volume of groundwater withdrawn from the Woodbine Aquifer in Dallas County is significantly greater than for the other three counties shown on this figure.

Figures 4.7.26, 4.7.27, and 4.7.28 show total pumping from the Woodbine Aquifer by county for the years 1950, 1980, and 2010, respectively. Counties with the lowest pumping totals are Red River and McLennan in 1950 and 1980 and these two counties, plus Lamar and Navarro counties, in 2010. Pumping of the Woodbine Aquifer does not occur in Delta and Rockwall counties. Counties with the highest pumping totals are Grayson and Dallas in 1950, Grayson and Ellis in 1980, and Grayson, Fannin, Collin, and Dallas counties in 2010.

Edwards BFZ Aquifer

Figure 4.7.29 shows integrated pumping curves and estimated cumulative volume curves for pumping from the Edwards BFZ Aquifer in Bell, Travis, and Williamson counties. In all three counties, pumping was estimated to be fairly low until about 1980. After that time, pumping

increased significantly in Williamson County, and also increased substantially in Travis County. The estimated historical pumping in Bell County shows a slight increase over the historical period.

4.7.7   *Implementation of Historical Pumping*

Pumping is the single most important stress on the aquifers in the historical period. In predevelopment time, natural aquifer discharge was dominated by discharge to streams and springs and cross-formational flow. As pumping in these aquifers increased, groundwater has been produced from aquifer storage and, in some cases, aquifer discharge capture. Understanding future drawdown require a model the can reproduce historical changes in storage and hydraulic heads.

Implementation of pumping in a groundwater model requires definition of the spatial and temporal volumetric flow rate. Spatially, pumping is distributed within active model grid blocks. Therefore, the volume of groundwater withdrawn from each grid block must be defined. Temporally, pumping must be consistent with the stress periods of the model. The estimated yearly historical pumping on a county scale for all use categories presented in Section 4.7.3 for pumping in Texas and in Section 4.7.5 for pumping in Oklahoma and Arkansas must be made consistent with the spatial and temporal scales of the groundwater model. This process is referred to as the process of pumping implementation. Implementation of pumping in the updated northern Trinity and Woodbine aquifers GAM is provided in Section 6.3.5.

4.7.8   *Pumping Volume Uncertainty*

The development history of the northern Trinity and Woodbine aquifers can be generally divided into three time periods. The first period is from approximately 1900 through 1940, during which time there are little to no pumping measurements. The second period is from 1940 through 1980, during which time data are available from several historical sources of varying scope. The third period is from 1980 through present, during which time water use data from the TWDB and data from some GCDs are available. These three periods are clearly discernible on the pumping curves developed by aquifer and county and presented in Appendix G.

A review of the hydraulic heads and drawdown through 1940 (see Section 4.3) demonstrate that during this time a significant reduction in hydraulic heads had occurred in the aquifers. By 1940, an estimate of 1.6 million acre-feet of groundwater had been extracted from the northern Trinity

Aquifer in Texas. A review of the transient hydraulic head data (see Figures 4.3.28
through 4.3.35) shows that little is known regarding hydraulic heads in the period from 1900
through 1940. As a result, and because of the large volume of free-flowing wells between the
late 1800s and 1930, artificial discharge during early development of the aquifers is very
uncertain

Historical data on pumping volumes are greater for the time period from 1940 to 1980 than for
the pre1940 period. In addition, 1980 estimates of pumping developed by the TWDB can be
used to check consistency in the pumping time series as it approaches 1980. During the period
from 1940 to 1980, pumping uncertainty may be captured by the variability observed in
historical pumping estimates provided in multiple sources. This variability could average 20 to
25 percent and, in some counties, reach 50 percent.

For the final period, 1980 through present, estimates of historical pumping are available from the
TWDB water use survey data and from GCD production data. A comparison of those two
sources of data was conducted for the Upper Trinity GCD, from whom detailed production data
are available, to evaluate the uncertainty in pumping estimates for this time period. Groundwater
pumping from the northern Trinity Aquifer in the Upper Trinity GCD in 2011 was estimated
from actual metered data for non-exempt wells used for municipal and manufacturing purposes
and mining purposes as it relates to oil and gas exploration. Rural domestic pumping was
estimated based on census block data. Livestock, power, and irrigation pumping was based on
the TWDB water use survey estimates for 2010. Table 4.7.30 shows the comparison between
those GCD estimates and the water use survey data obtained from the TWDB. This comparison
shows that the total pumping estimates differ by 19 percent. The largest difference is observed
for manufacturing pumping, which is a small percentage of total pumping in the GCD, followed
by municipal pumping, which, in most cases, is metered by the Upper Trinity GCD. Although
this comparison represents a single data point in one portion of the study area, it suggests that
even for the current time period from 1980 through 2011, pumping estimates are uncertain and
could exceed 20 percent.

Table 4.7.1   Number of identified flowing wells and reported flow rates from Hill (1901).

County	Number of Identified Flowing Wells							Reported Flow Rates (gpm)
	Woodbine Artesian Reservoirs	Fredericksburg Artesian Reservoirs	Fredericksburg or Paluxy Artesian Reservoirs	Paluxy Artesian Reservoirs	Trinity Artesian Reservoirs	Not Reported	Total	
Bell		19	2	1	75		97	50 - 700
Bosque					60		60	0.5 - 60
Collin					1		1	
Cooke				1	12		13	
Coryell					19	3	22	2 - 3
Dallas	32			1			33	69
Ellis						20	20	6 - 75
Erath						2	2	
Grayson	11						11	
Hamilton						2	2	
Hill	4				16		20	4 - 160
Hood					7	3	10	
Johnson					13		13	18 - 200
McLennan	1			1	50		52	5 - 690
Navarro	4						4	190
Parker					5		5	
Somervell					24		24	10 - 300
Tarrant	8			7	1		16	3 -485
Travis					9		9	100 - 175
Williamson					8	4	12	100
Wise						1	1	
Total	**60**	**19**	**2**	**11**	**300**	**35**	**427**	**0.5 - 690**

gpm = gallons per minute

Table 4.7.2   Summary of historical pumping sources.

Source	Data Location	Data Period of Record	Use[a]
TEXAS			
Literature Sources for 1900 to 1980 Pumping Data			
Baker (1960)	Grayson County	1957	IND, IRR, MUN, STK
Baker and others (1963a)	Hunt County	1960	MUN
Baldwin (1974)	Bell, Falls, Hill, and McLennan counties	1967-1970	MUN, IND
Dutton and others (1996)	multiple counties	1891-1991	all
George and Barnes (1945)	McLennan County	1945	MUN
George and Broadhurst (1943)	Dallas County	1943	MUN
George and Rose (1942)	Tarrant County	1942	MUN
Guyton and George (1943)	Bell County	1942	MUN
Hill (1901)	McLennan County	1900	discharge from flowing wells
Klemt and others (1975)	McLennan County	1967	MUN
Leggat (1957)	Tarrant County	1940, 1941, 1944, 1946, 1951-1954	MUN
Livingston (1945)	Grayson County	1933-1941 1942- 1944	IND MUN
Nordstrom (1982)	multiple counties	1955-1976 1970-1977	MUN, IND IRR
Nordstrom (1987)	Brown, Callahan, Comanche, Eastland, Erath and Hamilton counties	1970	IND, IRR, MUN, RD, STK
Price and others (1983)	Callahan County	1954-1978	RD, IRR, MUN, STK
Rose (1943)	Coryell County	1943	MUN
Sundstrom and others (1945)	multiple counties	1940	MUN
Sundstrom and others (1947)	multiple counties	1940	MUN, discharge from flowing wells
Sundstrom (1948)	McLennan County	1940-1947	MUN
Taylor (1976)	multiple counties	1955-1972	IND, MUN
Thompson (1967b)	Ellis County	1955 1964	RD RD, IND, IRR, MUN, STK
Thompson (1969)	Johnson County	1966	MUN
Thompson (1972)	Navarro County	1968	IND, MUN
TBWE (1961)	multiple counties	1955-1959	MUN
Sources of Data for Pumping Estimate Calculations			
TWDB (2001)	all counties of interest	1958, 1964, 1969, 1974, 1984, 1989, 1994, 2000	IRR
Literature Sources for 1980 to 2011 Pumping Data			
Nicot and others (2011, 2012a)	multiple counties	2011	MIN
TWDB (2013c)	all counties of interest	1980-2010	MIN, MFG, PWR, IRR, MIN, STK
OKLAHOMA and ARKANSAS			
Oliver and others (2013)	all counties of interest	1900-2010	all

[a]   all = all uses, IND = industrial, IRR = irrigation, MFG = manufacturing, MIN = mining, MUN = municipal, PWR = power, RD = rural domestic, STK = livestock

Table 4.7.3 **Summary of municipal pumping in acre-feet from the northern Trinity Aquifer by Texas county for the years 1980, 1985, 1990, 1995, 2000, 2005, and 2010.**

County	1980	1985	1990	1995	2000	2005	2010
Central Texas GCD							
Burnet	921	1,606	675	567	755	553	706
Clearwater UWCD							
Bell	2,516	516	677	528	620	596	1,272
Fox Crossing WD							
Mills	423	360	346	326	350	379	308
Middle Trinity GCD							
Bosque	1,887	1,996	2,154	2,064	2,618	2,876	2,683
Comanche	727	808	869	845	901	522	647
Coryell	3,198	3,548	549	142	205	1,492	2,056
Erath	3,487	3,533	3,760	3,656	4,271	4,066	4,169
District Total	**9,299**	**9,885**	**7,332**	**6,707**	**7,995**	**8,956**	**9,555**
North Texas GCD							
Collin	1,068	967	1,829	1,207	1,401	1,655	1,853
Cooke	4,852	4,481	4,493	5,207	5,385	5,433	2,862
Denton	7,175	7,427	8,067	8,464	12,021	9,587	11,681
District Total	**13,095**	**12,875**	**14,389**	**14,878**	**18,807**	**16,675**	**16,396**
Northern Trinity GCD							
Tarrant	17,765	16,581	13,832	12,113	13,709	11,942	9,308
Prairielands GCD							
Ellis	2,038	3,759	4,104	1,991	2,976	4,863	4,055
Hill	2,495	2,210	2,272	2,302	1,806	2,675	3,108
Johnson	5,314	6,620	5,995	6,305	8,092	7,971	5,690
Somervell	660	708	769	750	1,022	1,113	1,202
District Total	**10,507**	**13,297**	**13,140**	**11,348**	**13,896**	**16,622**	**14,055**
Red River GCD							
Fannin	102	487	580	598	582	325	267
Grayson	5,573	10,568	11,903	8,669	10,890	6,829	6,406
District Total	**5,675**	**11,055**	**12,483**	**9,267**	**11,472**	**7,154**	**6,673**
Saratoga UWCD							
Lampasas	661	814	378	530	700	301	82
Southern Trinity GCD							
McLennan	10,657	10,220	10,893	12,201	14,651	14,617	14,647
Upper Trinity GCD							
Hood	2,362	3,100	3,449	3,144	3,793	5,329	6,708
Montague	124	126	101	103	108	133	152
Parker	3,250	3,891	4,880	5,545	7,094	5,667	7,522
Wise	1,773	2,095	2,517	2,920	3,555	1,769	4,098
District Total	**7,509**	**9,212**	**10,947**	**11,712**	**14,550**	**12,898**	**18,480**

Table 4.7.3, continued

County	1980	1985	1990	1995	2000	2005	2010
No GCD							
Bastrop	0	0	0	0	0	0	0
Bowie	0	0	0	0	0	0	0
Brown	95	145	548	227	142	224	349
Callahan	752	815	661	764	820	375	374
Dallas	14,487	15,788	8,603	2,266	5,011	1,263	1,645
Delta	191	142	149	81	82	131	0
Eastland	707	425	125	268	177	341	444
Falls	669	577	658	541	615	1,638	1,782
Hamilton	702	659	637	614	680	609	1,048
Hunt	0	0	0	0	0	166	250
Jack	3	4	4	5	5	1	7
Kaufman	50	0	13	0	0	0	0
Lamar	206	342	274	132	124	17	7
Limestone	52	36	72	0	0	0	145
Milam	31	1	0	0	0	0	0
Navarro	0	0	0	0	0	0	0
Red River	1,136	252	238	249	284	75	55
Rockwall	0	0	0	0	0	0	0
Taylor	0	0	0	0	0	21	57
Travis	2,314	2,298	2,695	2,439	1,419	2,754	3,389
Williamson	4,014	3,927	4,965	3,376	2,737	1,304	2,221
Municipal Total	*104,437*	*111,832*	*104,734*	*91,139*	*109,601*	*99,612*	*103,255*

Table 4.7.4   **Summary of manufacturing pumping in acre-feet from the northern Trinity Aquifer by Texas county for the years 1980, 1985, 1990, 1995, 2000, 2005, and 2010.**

County	1980	1985	1990	1995	2000	2005	2010
Central Texas GCD							
Burnet	4	1	4	4	4	13	1
Clearwater UWCD							
Bell	183	245	377	368	258	0	0
Fox Crossing WD							
Mills	0	0	0	0	0	0	0
Middle Trinity GCD							
Bosque	87	586	763	675	785	695	1
Comanche	7	22	3	4	2	0	1
Coryell	0	0	0	0	0	0	0
Erath	0	16	12	138	0	14	60
District Total	**94**	**624**	**778**	**817**	**787**	**709**	**62**
North Texas GCD							
Collin	1	0	0	0	0	0	0
Cooke	0	4	0	0	0	3	75
Denton	0	0	0	0	0	32	0
District Total	**1**	**4**	**0**	**0**	**0**	**35**	**75**
Northern Trinity GCD							
Tarrant	870	730	699	790	983	756	88
Prairielands GCD							
Ellis	846	2,015	2,234	1,344	947	2,380	1,155
Hill	193	103	0	0	0	0	0
Johnson	363	315	571	707	611	52	607
Somervell	0	1	0	4	5	1,231	2
District Total	**1,402**	**2,434**	**2,805**	**2,055**	**1,563**	**3,663**	**1,764**
Red River GCD							
Fannin	0	0	0	0	0	0	0
Grayson	0	0	0	0	0	0	474
District Total	**0**	**0**	**0**	**0**	**0**	**0**	**474**
Saratoga UWCD							
Lampasas	0	0	0	0	0	0	0
Southern Trinity GCD							
McLennan	1,473	1,741	787	320	726	458	508
Upper Trinity GCD							
Hood	9	16	9	20	20	22	6
Montague	0	0	0	0	0	0	0
Parker	9	33	28	0	15	0	16
Wise	1	1	1	0	0	0	0
District Total	**19**	**50**	**38**	**20**	**35**	**22**	**22**

Table 4.7.4, continued

County	1980	1985	1990	1995	2000	2005	2010
No GCD							
Bastrop	0	0	0	0	0	0	0
Bowie	0	0	0	0	0	0	0
Brown	13	0	0	0	0	0	2
Callahan	0	9	0	0	0	0	0
Dallas	1,086	875	535	350	54	162	10
Delta	0	0	0	0	0	0	0
Eastland	0	225	1	1	1	0	0
Falls	0	0	0	0	0	0	0
Hamilton	0	9	0	2	2	2	3
Hunt	0	0	0	0	0	0	0
Jack	0	0	0	0	0	0	0
Kaufman	0	0	0	0	0	0	0
Lamar	1	1	0	0	0	0	0
Limestone	0	0	0	0	0	0	1
Milam	0	0	0	0	0	0	0
Navarro	0	0	0	0	0	0	0
Red River	0	0	0	0	0	0	0
Rockwall	0	0	0	0	0	0	0
Taylor	0	0	0	0	0	0	0
Travis	0	3	0	0	0	71	64
Williamson	0	1	1	4	0	7	1
Manufacturing Total	*5,146*	*6,952*	*6,025*	*4,731*	*4,413*	*5,898*	*3,868*

Table 4.7.5   Summary of power pumping in acre-feet from the northern Trinity Aquifer by Texas county for the years 1980, 1985, 1990, 1995, 2000, 2005, and 2010.

County	1980	1985	1990	1995	2000	2005	2010
Central Texas GCD							
Burnet	0	0	0	0	0	0	0
Clearwater UWCD							
Bell	0	0	0	0	0	0	0
Fox Crossing WD							
Mills	0	0	0	0	0	0	0
Middle Trinity GCD							
Bosque	0	0	0	0	0	0	0
Comanche	0	0	0	0	0	0	0
Coryell	0	0	0	0	0	0	0
Erath	0	0	0	0	0	0	0
District Total	**0**	**0**	**0**	**0**	**0**	**0**	**0**
North Texas GCD							
Collin	303	482	559	115	570	0	0
Cooke	0	0	0	0	0	0	0
Denton	0	0	0	0	0	0	0
District Total	**303**	**482**	**559**	**115**	**570**	**0**	**0**
Northern Trinity GCD							
Tarrant	0	0	0	1	1	0	0
Prairielands GCD							
Ellis	0	0	0	0	0	0	0
Hill	0	0	0	0	0	0	0
Johnson	0	0	0	0	0	0	0
Somervell	0	21	45	68	39	29	21
District Total	**0**	**21**	**45**	**68**	**39**	**29**	**21**
Red River GCD							
Fannin	0	0	0	0	0	0	0
Grayson	0	0	0	0	0	0	0
District Total	**0**	**0**	**0**	**0**	**0**	**0**	**0**
Saratoga UWCD							
Lampasas	0	0	0	0	0	0	0
Southern Trinity GCD							
McLennan	303	357	216	117	173	139	98
Upper Trinity GCD							
Hood	58	125	70	21	47	93	6
Montague	0	0	0	0	0	0	0
Parker	0	0	0	0	0	0	0
Wise	0	0	0	0	0	0	0
District Total	**58**	**125**	**70**	**21**	**47**	**93**	**6**

Table 4.7.5, continued

County	1980	1985	1990	1995	2000	2005	2010
No GCD							
Bastrop	0	0	0	0	0	0	0
Bowie	0	0	0	0	0	0	0
Brown	0	0	0	0	0	0	0
Callahan	0	0	0	0	0	0	0
Dallas	500	2,596	260	104	0	0	0
Delta	0	0	0	0	0	0	0
Eastland	0	0	0	0	0	0	0
Falls	0	0	0	0	0	0	0
Hamilton	0	0	0	0	0	0	0
Hunt	0	0	0	0	0	0	0
Jack	0	0	0	0	0	0	0
Kaufman	0	0	0	0	0	0	0
Lamar	0	0	0	0	0	0	0
Limestone	0	0	0	0	0	0	0
Milam	0	0	0	0	0	0	0
Navarro	0	0	0	0	0	0	0
Red River	0	0	0	0	0	0	0
Rockwall	0	0	0	0	0	0	0
Taylor	0	0	0	0	0	0	0
Travis	0	21	21	0	7	0	0
Williamson	0	0	0	0	0	0	0
Power Total	*1,164*	*3,602*	*1,171*	*426*	*837*	*261*	*125*

Table 4.7.6   Summary of mining pumping in acre-feet from the northern Trinity Aquifer by Texas county for the years 1980, 1985, 1990, 1995, 2000, 2005, and 2010.

County	1980	1985	1990	1995	2000	2005	2010
Central Texas GCD							
Burnet	0	16	14	15	29	0	0
Clearwater UWCD							
Bell	126	117	0	145	145	0	431
Fox Crossing WD							
Mills	0	0	0	0	0	0	0
Middle Trinity GCD							
Bosque	221	72	61	276	276	0	1,166
Comanche	0	79	74	80	80	0	475
Coryell	0	96	86	100	100	0	180
Erath	0	0	0	0	0	0	1,007
District Total	**221**	**247**	**221**	**456**	**456**	**0**	**2,828**
North Texas GCD							
Collin	0	0	0	0	0	0	0
Cooke	599	534	421	52	52	0	153
Denton	1	0	46	32	0	0	1,209
District Total	**600**	**534**	**467**	**84**	**52**	**0**	**1,362**
Northern Trinity GCD							
Tarrant	0	0	0	0	0	0	1,933
Prairielands GCD							
Ellis	0	0	0	0	0	0	136
Hill	0	0	0	0	0	0	593
Johnson	0	87	54	324	324	0	1,671
Somervell	0	291	261	310	384	421	691
District Total	**0**	**378**	**315**	**634**	**708**	**421**	**3,091**
Red River GCD							
Fannin	0	0	0	0	0	0	0
Grayson	0	263	197	349	349	0	0
District Total	**0**	**263**	**197**	**349**	**349**	**0**	**0**
Saratoga UWCD							
Lampasas	27	36	33	123	78	0	57
Southern Trinity GCD							
McLennan	0	0	0	0	0	0	681
Upper Trinity GCD							
Hood	0	81	73	167	167	0	1,216
Montague	36	67	55	80	80	0	616
Parker	0	56	49	55	55	0	2,450
Wise	0	606	40	173	63	94	5,322
District Total	**36**	**810**	**217**	**475**	**365**	**94**	**9,604**

Table 4.7.6, continued

County	1980	1985	1990	1995	2000	2005	2010
No GCD							
Bastrop	0	0	0	0	0	0	0
Bowie	0	0	0	0	0	0	0
Brown	0	42	45	122	122	0	418
Callahan	1	229	137	81	81	0	92
Dallas	0	0	3	1,385	1,385	4	685
Delta	0	0	0	0	0	0	0
Eastland	100	421	294	78	78	0	266
Falls	0	0	0	0	0	0	12
Hamilton	0	0	0	0	0	0	256
Hunt	0	0	0	0	0	0	2
Jack	0	0	0	0	0	0	1,681
Kaufman	0	0	0	0	0	0	0
Lamar	0	0	0	0	0	0	0
Limestone	0	0	0	0	0	0	164
Milam	0	0	0	0	0	0	0
Navarro	0	0	0	0	0	0	0
Red River	0	0	0	0	0	0	0
Rockwall	0	0	0	0	0	0	0
Taylor	0	0	0	0	0	0	20
Travis	0	0	0	0	0	0	230
Williamson	0	0	0	0	0	0	0
Mining Total	*1,111*	*3,093*	*1,943*	*3,947*	*3,848*	*519*	*23,813*

Table 4.7.7   **Summary of irrigation pumping in acre-feet from the northern Trinity Aquifer by Texas county for the years 1980, 1985, 1990, 1995, 2000, 2005, and 2010.**

County	1980	1985	1990	1995	2000	2005	2010
Central Texas GCD							
Burnet	50	432	82	0	0	136	422
Clearwater UWCD							
Bell	100	54	211	315	558	18	445
Fox Crossing WD							
Mills	300	41	395	48	38	0	1,491
Middle Trinity GCD							
Bosque	300	229	159	0	0	420	458
Comanche	10,000	22,500	25,313	25,667	13,515	16,651	9,699
Coryell	0	20	13	11	0	75	57
Erath	9,000	7,010	7,376	11,578	10,261	6,795	4,867
District Total	**19,300**	**29,759**	**32,861**	**37,256**	**23,776**	**23,941**	**15,081**
North Texas GCD							
Collin	0	0	0	0	0	614	41
Cooke	100	429	300	233	0	50	119
Denton	0	0	0	0	0	304	910
District Total	**100**	**429**	**300**	**233**	**0**	**968**	**1,070**
Northern Trinity GCD							
Tarrant	50	0	0	21	0	0	256
Prairielands GCD							
Ellis	0	0	12	20	58	20	31
Hill	0	0	0	0	0	0	0
Johnson	0	0	0	0	0	4	32
Somervell	150	396	158	126	0	35	129
District Total	**150**	**396**	**170**	**146**	**58**	**59**	**192**
Red River GCD							
Fannin	0	0	0	0	0	0	78
Grayson	0	0	0	0	0	22	1,088
District Total	**0**	**0**	**0**	**0**	**0**	**22**	**1,166**
Saratoga UWCD							
Lampasas	0	0	95	29	1	0	14
Southern Trinity GCD							
McLennan	0	0	0	0	0	75	97
Upper Trinity GCD							
Hood	0	47	208	81	10	2,626	675
Montague	19	17	21	163	60	72	299
Parker	0	219	30	52	74	357	169
Wise	75	99	140	175	147	285	773
District Total	**94**	**382**	**399**	**471**	**291**	**3,340**	**1,916**

Table 4.7.7, continued

County	1980	1985	1990	1995	2000	2005	2010
No GCD							
Bastrop	0	0	0	0	0	0	0
Bowie	0	0	0	0	0	0	0
Brown	562	708	757	1,897	2,320	33	175
Callahan	699	524	417	546	600	594	649
Dallas	0	0	0	0	0	0	1,120
Delta	0	0	0	0	0	0	0
Eastland	9,199	11,700	8,174	8,935	12,135	7,579	4,541
Falls	0	0	0	0	0	0	0
Hamilton	1,300	605	1,228	502	62	268	223
Hunt	0	0	0	0	0	0	0
Jack	0	0	0	0	0	0	0
Kaufman	0	3	0	0	0	0	0
Lamar	0	0	0	0	0	0	0
Limestone	0	0	0	0	0	0	0
Milam	0	0	0	0	0	0	0
Navarro	0	0	0	0	0	0	0
Red River	0	0	0	0	0	0	3
Rockwall	0	0	0	0	0	0	0
Taylor	0	0	0	0	0	5	0
Travis	0	0	0	0	0	523	201
Williamson	0	0	0	0	0	18	44
Irrigation Total	*31,904*	*45,033*	*45,089*	*50,399*	*39,839*	*37,579*	*29,106*

Table 4.7.8   **Summary of livestock pumping in acre-feet from the northern Trinity Aquifer by Texas county for the years 1980, 1985, 1990, 1995, 2000, 2005, and 2010.**

County	1980	1985	1990	1995	2000	2005	2010
Central Texas GCD							
Burnet	211	295	269	281	274	84	117
Clearwater UWCD							
Bell	157	88	88	92	86	159	264
Fox Crossing WD							
Mills	461	221	306	417	335	304	331
Middle Trinity GCD							
Bosque	685	592	614	677	524	247	343
Comanche	583	315	470	799	851	959	789
Coryell	579	600	588	719	670	263	180
Erath	1,216	1,377	2,949	4,914	4,660	2,134	1,842
District Total	**3,063**	**2,884**	**4,621**	**7,109**	**6,705**	**3,603**	**3,154**
North Texas GCD							
Collin	0	0	0	0	0	0	22
Cooke	869	944	1,009	1,164	881	155	137
Denton	300	232	240	243	108	107	79
District Total	**1,169**	**1,176**	**1,249**	**1,407**	**989**	**262**	**238**
Northern Trinity GCD							
Tarrant	386	502	418	403	401	29	106
Prairielands GCD							
Ellis	0	0	0	0	0	0	0
Hill	0	0	0	0	0	8	11
Johnson	326	351	475	568	520	280	247
Somervell	72	51	64	77	83	41	51
District Total	**398**	**402**	**539**	**645**	**603**	**329**	**309**
Red River GCD							
Fannin	28	26	25	28	23	0	90
Grayson	0	0	0	0	0	118	105
District Total	**28**	**26**	**25**	**28**	**23**	**118**	**195**
Saratoga UWCD							
Lampasas	458	304	315	385	1,006	193	228
Southern Trinity GCD							
McLennan	343	137	158	218	62	97	87
Upper Trinity GCD							
Hood	301	360	280	314	311	245	240
Montague	65	56	62	61	61	3	2
Parker	242	152	146	150	185	94	161
Wise	798	868	1,078	1,017	857	118	101
District Total	**1,406**	**1,436**	**1,566**	**1,542**	**1,414**	**460**	**504**

Table 4.7.8, continued

County	1980	1985	1990	1995	2000	2005	2010
No GCD							
Bastrop	0	0	0	0	0	0	0
Bowie	0	0	0	0	0	0	0
Brown	135	80	88	130	118	138	138
Callahan	94	62	101	107	98	192	258
Dallas	0	0	0	0	0	0	0
Delta	0	0	0	0	0	0	0
Eastland	150	78	91	116	112	40	54
Falls	50	62	48	48	44	0	0
Hamilton	637	611	146	206	196	235	196
Hunt	0	0	0	0	0	0	0
Jack	0	0	0	0	0	0	0
Kaufman	0	43	0	0	0	0	0
Lamar	0	0	0	0	0	0	0
Limestone	11	15	26	12	10	0	0
Milam	0	0	0	0	0	0	0
Navarro	0	0	0	0	0	0	0
Red River	101	110	97	119	132	18	21
Rockwall	0	0	0	0	0	0	0
Taylor	0	0	0	0	0	17	21
Travis	377	287	303	276	227	59	56
Williamson	149	141	128	113	114	301	250
Livestock Total	*9,784*	*8,960*	*10,582*	*13,654*	*12,949*	*6,638*	*6,527*

Table 4.7.9   Summary of rural domestic pumping in acre-feet from the northern Trinity Aquifer by Texas county for the years 1980, 1985, 1990, 1995, 2000, 2005, and 2010.

County	1980	1985	1990	1995	2000	2005	2010
Central Texas GCD							
Burnet	207	261	264	331	416	492	543
Clearwater UWCD							
Bell	219	249	265	248	215	211	214
Fox Crossing WD							
Mills	134	139	135	161	198	193	192
Middle Trinity GCD							
Bosque	96	103	108	132	153	162	166
Comanche	655	694	694	785	911	903	926
Coryell	1,228	1,300	1,392	1,044	518	501	520
Erath	910	1,036	1,131	1,199	1,277	1,419	1,578
District Total	**2,889**	**3,134**	**3,325**	**3,160**	**2,860**	**2,984**	**3,191**
North Texas GCD							
Collin	0	0	0	0	0	0	0
Cooke	235	249	263	283	342	363	370
Denton	4	6	8	11	17	17	16
District Total	**239**	**256**	**271**	**295**	**359**	**380**	**386**
Northern Trinity GCD							
Tarrant	94	114	129	163	214	199	180
Prairielands GCD							
Ellis	0	0	0	0	0	0	0
Hill	0	0	0	0	0	0	0
Johnson	43	55	61	58	58	60	60
Somervell	288	335	366	479	644	715	804
District Total	**331**	**390**	**427**	**537**	**702**	**775**	**863**
Red River GCD							
Fannin	0	0	0	0	0	0	0
Grayson	38	41	41	44	53	52	52
District Total	**38**	**41**	**41**	**44**	**53**	**52**	**52**
Saratoga UWCD							
Lampasas	499	541	562	723	829	930	1,025
Southern Trinity GCD							
McLennan	0	0	0	0	0	0	0
Upper Trinity GCD							
Hood	1,475	1,992	2,408	2,063	1,657	1,737	1,774
Montague	280	297	277	297	330	352	371
Parker	2,281	2,775	3,337	3,568	4,117	4,446	4,805
Wise	1,173	1,401	1,534	1,948	2,761	2,979	3,027
District Total	**5,209**	**6,466**	**7,556**	**7,876**	**8,866**	**9,514**	**9,977**

Table 4.7.9, continued

County	1980	1985	1990	1995	2000	2005	2010
No GCD							
Bastrop	0	0	0	0	0	0	0
Bowie	0	0	0	0	0	0	0
Brown	97	102	101	103	104	106	108
Callahan	257	298	275	248	217	225	231
Dallas	0	0	0	0	0	0	0
Delta	0	0	0	0	0	0	0
Eastland	126	133	119	153	194	198	199
Falls	0	0	0	0	0	0	0
Hamilton	232	228	215	223	260	260	266
Hunt	0	0	0	0	0	0	0
Jack	5	6	5	4	4	5	5
Kaufman	0	0	0	0	0	0	0
Lamar	0	0	0	0	0	0	0
Limestone	0	0	0	0	0	0	0
Milam	0	0	0	0	0	0	0
Navarro	0	0	0	0	0	0	0
Red River	0	0	0	0	0	0	0
Rockwall	0	0	0	0	0	0	0
Taylor	4	4	4	3	2	2	2
Travis	100	126	138	196	288	261	240
Williamson	92	133	169	179	191	208	214
Rural Domestic Total	*10,770*	*12,618*	*14,000*	*14,647*	*15,972*	*16,995*	*17,888*

Table 4.7.10   Summary of total pumping in acre-feet from the northern Trinity Aquifer by Texas county for the years 1980, 1985, 1990, 1995, 2000, 2005, and 2010.

County	1980	1985	1990	1995	2000	2005	2010
Central Texas GCD							
Burnet	1,393	2,611	1,308	1,198	1,478	1,278	1,789
Clearwater UWCD							
Bell	3,301	1,269	1,618	1,696	1,882	984	2,626
Fox Crossing WD							
Mills	1,318	761	1,182	952	921	876	2,322
Middle Trinity GCD							
Bosque	3,276	3,578	3,859	3,824	4,356	4,400	4,817
Comanche	11,972	24,418	27,423	28,180	16,260	19,035	12,537
Coryell	5,005	5,564	2,628	2,016	1,493	2,331	2,993
Erath	14,613	12,972	15,228	21,485	20,469	14,428	13,523
District Total	**34,866**	**46,533**	**49,138**	**55,505**	**42,579**	**40,193**	**33,871**
North Texas GCD							
Collin	1,372	1,449	2,388	1,322	1,971	2,269	1,916
Cooke	6,655	6,641	6,486	6,939	6,660	6,004	3,716
Denton	7,480	7,665	8,361	8,750	12,146	10,047	13,895
District Total	**15,507**	**15,756**	**17,235**	**17,012**	**20,777**	**18,320**	**19,527**
Northern Trinity GCD							
Tarrant	19,165	17,927	15,078	13,491	15,308	12,926	12,664
Prairielands GCD							
Ellis	2,884	5,774	6,350	3,355	3,981	7,263	5,377
Hill	2,688	2,313	2,272	2,302	1,806	2,683	3,712
Johnson	6,046	7,428	7,156	7,962	9,605	8,367	8,307
Somervell	1,170	1,803	1,663	1,814	2,177	3,585	2,900
District Total	**12,788**	**17,318**	**17,441**	**15,433**	**17,569**	**21,898**	**20,295**
Red River GCD							
Fannin	130	513	605	626	605	325	435
Grayson	5,611	10,872	12,141	9,062	11,292	7,021	8,125
District Total	**5,741**	**11,385**	**12,746**	**9,688**	**11,897**	**7,346**	**8,560**
Saratoga UWCD							
Lampasas	1,645	1,695	1,383	1,790	2,614	1,424	1,406
Southern Trinity GCD							
McLennan	12,776	12,455	12,054	12,856	15,612	15,386	16,118
Upper Trinity GCD							
Hood	4,205	5,721	6,497	5,810	6,005	10,052	10,625
Montague	524	563	516	704	639	560	1,440
Parker	5,782	7,126	8,470	9,370	11,540	10,564	15,123
Wise	3,820	5,070	5,310	6,233	7,383	5,245	13,321
District Total	**14,331**	**18,481**	**20,793**	**22,117**	**25,568**	**26,421**	**40,509**

Table 4.7.10, continued

County	1980	1985	1990	1995	2000	2005	2010
No GCD							
Bastrop County	0	0	0	0	0	0	0
Bowie County	0	0	0	0	0	0	0
Brown	902	1,077	1,539	2,479	2,806	501	1,190
Callahan	1,803	1,937	1,591	1,746	1,816	1,386	1,604
Dallas	16,073	19,259	9,401	4,105	6,450	1,429	3,460
Delta	191	142	149	81	82	131	0
Eastland	10,282	12,982	8,804	9,551	12,697	8,158	5,504
Falls	719	639	706	589	659	1,638	1,794
Hamilton	2,871	2,112	2,226	1,547	1,200	1,374	1,992
Hunt	0	0	0	0	0	166	252
Jack	8	10	9	9	9	6	1,693
Kaufman	50	46	13	0	0	0	0
Lamar	207	343	274	132	124	17	7
Limestone	63	51	98	12	10	0	310
Milam	31	1	0	0	0	0	0
Navarro	0	0	0	0	0	0	0
Red River	1,237	362	335	368	416	93	79
Rockwall	0	0	0	0	0	0	0
Taylor	4	4	4	3	2	45	100
Travis	2,791	2,735	3,157	2,911	1,941	3,668	4,180
Williamson	4,255	4,202	5,263	3,672	3,042	1,838	2,730
Aquifer Total	*164,316*	*192,090*	*183,544*	*178,943*	*187,459*	*167,502*	*184,582*

Table 4.7.11   Summary of pumping in acre-feet from the northern Trinity Aquifer in Texas by water use category for the years 1980, 1985, 1990, 1995, 2000, 2005, and 2010.

Water Use Category	1980	1985	1990	1995	2000	2005	2010
Pumping (acre-feet)							
Irrigation	31,904	45,033	45,089	50,399	39,839	37,579	29,106
Manufacturing	5,146	6,952	6,025	4,731	4,413	5,898	3,868
Mining	1,111	3,093	1,943	3,947	3,848	519	23,813
Municipal	104,437	111,832	104,734	91,139	109,601	99,612	103,255
Power	1,164	3,602	1,171	426	837	261	125
Rural Domestic	10,770	12,618	14,000	14,647	15,972	16,995	17,888
Livestock	9,784	8,960	10,582	13,654	12,949	6,638	6,527
Total	164,316	192,090	183,544	178,943	187,459	167,502	184,582
Percentage of Total							
Irrigation	19%	23%	25%	28%	21%	22%	16%
Manufacturing	3%	4%	3%	3%	2%	4%	2%
Mining	1%	2%	1%	2%	2%	0%	13%
Municipal	64%	58%	57%	51%	58%	59%	56%
Power	1%	2%	1%	0%	0%	0%	0%
Rural Domestic	7%	7%	8%	8%	9%	10%	10%
Livestock	6%	5%	6%	8%	7%	4%	4%

Table 4.7.12 **Summary of pumping in acre-feet from the northern Trinity Aquifer in the North Texas GCD by water use category for the years 1980, 1985, 1990, 1995, 2000, 2005, and 2010.**

Water Use Category	1980	1985	1990	1995	2000	2005	2010
Pumping (acre-feet)							
Irrigation	100	429	300	233	0	968	1,070
Manufacturing	1	4	0	0	0	35	75
Mining	600	534	467	84	52	0	1,362
Municipal	13,095	12,875	14,389	14,878	18,807	16,675	16,396
Power	303	482	559	115	570	0	0
Rural Domestic	239	256	271	295	359	380	386
Livestock	1,169	1,176	1,249	1,407	989	262	238
Total	15,507	15,756	17,235	17,012	20,777	18,320	19,527
Percentage of Total							
Irrigation	1%	3%	2%	1%	0%	5%	5%
Manufacturing	0%	0%	0%	0%	0%	0%	0%
Mining	4%	3%	3%	0%	0%	0%	7%
Municipal	84%	82%	83%	87%	91%	91%	84%
Power	2%	3%	3%	1%	3%	0%	0%
Rural Domestic	2%	2%	2%	2%	2%	2%	2%
Livestock	8%	7%	7%	8%	5%	1%	1%

Table 4.7.13   Summary of pumping in acre-feet from the northern Trinity Aquifer in the Northern Trinity GCD by water use category for the years 1980, 1985, 1990, 1995, 2000, 2005, and 2010.

Water Use Category	1980	1985	1990	1995	2000	2005	2010
Pumping (acre-feet)							
Irrigation	50	0	0	21	0	0	256
Manufacturing	870	730	699	790	983	756	881
Mining	0	0	0	0	0	0	1,933
Municipal	17,765	16,581	13,832	12,113	13,709	11,942	9,308
Power	0	0	0	1	1	0	0
Rural Domestic	94	114	129	163	214	199	180
Livestock	386	502	418	403	401	29	106
Total	19,165	17,927	15,078	13,491	15,308	12,926	12,664
Percentage of Total							
Irrigation	0%	0%	0%	0%	0%	0%	2%
Manufacturing	5%	4%	5%	6%	6%	6%	7%
Mining	0%	0%	0%	0%	0%	0%	15%
Municipal	93%	92%	92%	90%	90%	92%	74%
Power	0%	0%	0%	0%	0%	0%	0%
Rural Domestic	0%	1%	1%	1%	1%	2%	1%
Livestock	2%	3%	3%	3%	3%	0%	1%

Table 4.7.14   **Summary of pumping in acre-feet from the northern Trinity Aquifer in the Prairielands GCD by water use category for the years 1980, 1985, 1990, 1995, 2000, 2005, and 2010.**

Water Use Category	1980	1985	1990	1995	2000	2005	2010
Pumping (acre-feet)							
Irrigation	150	396	170	146	58	59	192
Manufacturing	1,402	2,434	2,805	2,055	1,563	3,663	1,764
Mining	0	378	315	634	708	421	3,091
Municipal	10,507	13,297	13,140	11,348	13,896	16,622	14,055
Power	0	21	45	68	39	29	21
Rural Domestic	331	390	427	537	702	775	863
Livestock	398	402	539	645	603	329	309
Total	12,788	17,318	17,441	15,433	17,569	21,898	20,295
Percentage of Total							
Irrigation	1%	2%	1%	1%	0%	0%	1%
Manufacturing	11%	14%	16%	13%	9%	17%	9%
Mining	0%	2%	2%	4%	4%	2%	15%
Municipal	82%	77%	75%	74%	79%	76%	69%
Power	0%	0%	0%	0%	0%	0%	0%
Rural Domestic	3%	2%	2%	3%	4%	4%	4%
Livestock	3%	2%	3%	4%	3%	2%	2%

Table 4.7.15   **Summary of pumping in acre-feet from the northern Trinity Aquifer in the Upper Trinity GCD by water use category for the years 1980, 1985, 1990, 1995, 2000, 2005, and 2010.**

Water Use Category	1980	1985	1990	1995	2000	2005	2010
Pumping (acre-feet)							
Irrigation	94	382	399	471	291	3,340	1,916
Manufacturing	19	50	10	20	35	22	22
Mining	36	810	217	475	365	94	9,604
Municipal	7,509	9,212	10,947	11,712	14,550	12,898	18,480
Power	58	125	70	21	47	93	6
Rural Domestic	5,209	6,466	7,556	7,876	8,866	9,514	9,977
Livestock	1,406	1,436	1,566	1,542	1,414	460	504
Total	14,331	18,481	20,765	22,117	25,568	26,421	40,509
Percentage of Total							
Irrigation	1%	2%	2%	2%	1%	13%	5%
Manufacturing	0%	0%	0%	0%	0%	0%	0%
Mining	0%	4%	1%	2%	1%	0%	24%
Municipal	52%	50%	53%	53%	57%	49%	46%
Power	0%	1%	0%	0%	0%	0%	0%
Rural Domestic	36%	35%	36%	36%	35%	36%	25%
Livestock	10%	8%	8%	7%	6%	2%	1%

Table 4.7.16   Summary of municipal pumping in acre-feet from the Woodbine Aquifer by Texas county for the years 1980, 1985, 1990, 1995, 2000, 2005, and 2010.

County	1980	1985	1990	1995	2000	2005	2010
North Texas GCD							
Collin	769	771	745	1,040	1,479	2,515	2,811
Cooke	0	0	0	0	0	55	35
Denton	236	419	623	847	739	612	645
District Total	1,005	1,190	1,368	1,887	2,218	3,182	3,491
Northern Trinity GCD							
Tarrant	36	9	3	1	0	134	120
Prairielands GCD							
Ellis	1,657	1,952	1,696	1,605	2,165	2,398	2,015
Hill	548	45	41	23	18	187	226
Johnson	468	298	362	518	593	759	375
District Total	2,673	2,295	2,099	2,146	2,776	3,344	2,616
Red River GCD							
Fannin	1,936	1,596	1,609	1,971	2,399	2,470	2,740
Grayson	2,095	2,769	3,134	3,380	4,082	4,702	3,384
District Total	4,031	4,365	4,743	5,351	6,481	7,172	6,124
Southern Trinity GCD							
McLennan County	0	0	0	0	0	0	0
No GCD							
Dallas	399	315	429	401	205	271	684
Hunt	261	372	387	395	465	442	935
Kaufman	50	0	0	0	0	0	785
Lamar	166	268	285	177	165	25	12
Navarro	58	54	80	72	112	0	0
Red River	0	0	0	0	0	1	0
Municipal Total	*8,679*	*8,868*	*9,394*	*10,430*	*12,422*	*14,571*	*14,767*

Table 4.7.17   Summary of manufacturing pumping in acre-feet from the Woodbine Aquifer by Texas county for the years 1980, 1985, 1990, 1995, 2000, 2005, and 2010.

County	1980	1985	1990	1995	2000	2005	2010
North Texas GCD							
Collin	0	138	59	71	138	157	199
Cooke	0	0	0	0	0	0	0
Denton	9	11	21	66	36	17	7
District Total	9	149	80	137	174	174	206
Northern Trinity GCD							
Tarrant	0	0	0	0	0	0	0
Prairielands GCD							
Ellis	971	705	628	658	55	171	160
Hill	0	0	0	0	0	0	0
Johnson	0	0	0	0	0	0	0
District Total	971	705	628	658	55	171	160
Red River GCD							
Fannin	0	0	0	0	0	0	0
Grayson	98	77	0	0	0	0	260
District Total	98	77	0	0	0	0	260
Southern Trinity GCD							
McLennan	0	0	0	0	0	0	0
No GCD							
Dallas	540	462	322	331	258	1,316	298
Hunt	0	0	0	0	0	0	0
Kaufman	0	0	0	0	0	0	146
Lamar	1	1	0	0	0	0	0
Navarro	0	0	0	0	0	0	0
Red River	0	0	0	0	0	0	0
Manufacturing Total	*1,619*	*1,394*	*1,030*	*1,126*	*487*	*1,661*	*1,070*

Table 4.7.18   Summary of power pumping in acre-feet from the Woodbine Aquifer by Texas county for the years 1980, 1985, 1990, 1995, 2000, 2005, and 2010.

County	1980	1985	1990	1995	2000	2005	2010
North Texas GCD							
Collin	0	0	0	0	0	0	0
Cooke	0	0	0	0	0	0	0
Denton	0	0	0	0	0	0	0
District Total	0	0	0	0	0	0	0
Northern Trinity GCD							
Tarrant	0	0	0	0	0	0	0
Prairielands GCD							
Ellis	0	0	0	0	0	0	0
Hill	0	0	0	0	0	0	0
Johnson	0	0	0	0	0	0	0
District Total	0	0	0	0	0	0	0
Red River GCD							
Fannin	136	359	206	314	503	71	319
Grayson	0	0	0	0	0	0	0
District Total	136	359	206	314	503	71	319
Southern Trinity GCD							
McLennan County	0	0	0	0	0	0	0
No GCD							
Dallas	166	0	0	0	0	0	0
Hunt	0	0	0	0	0	0	0
Kaufman	0	0	0	0	0	0	0
Lamar	0	0	0	0	0	0	0
Navarro	0	0	0	0	0	0	0
Red River	0	0	0	0	0	0	0
Power Total	*302*	*359*	*206*	*314*	*503*	*71*	*319*

Table 4.7.19 **Summary of mining pumping in acre-feet from the Woodbine Aquifer by Texas county for the years 1980, 1985, 1990, 1995, 2000, 2005, and 2010.**

County	1980	1985	1990	1995	2000	2005	2010
North Texas GCD							
Collin	0	0	0	0	0	0	0
Cooke	0	0	0	0	0	0	0
Denton	0	0	24	17	0	0	0
District Total	0	0	24	17	0	0	0
Northern Trinity GCD							
Tarrant	0	0	0	0	0	0	0
Prairielands GCD							
Ellis	0	87	73	90	90	0	0
Hill	0	72	0	118	118	0	0
Johnson	0	0	0	0	0	0	0
District Total	0	159	73	208	208	0	0
Red River GCD							
Fannin	0	0	0	0	0	19	1
Grayson	10	281	309	466	466	20	37
District Total	10	281	309	466	466	39	38
Southern Trinity GCD							
McLennan	0	0	0	0	0	0	0
No GCD							
Dallas	0	29	0	0	0	0	0
Hunt	0	0	0	0	0	0	9
Kaufman	0	0	0	0	0	0	18
Lamar	0	0	0	0	0	0	0
Navarro	0	0	0	0	0	0	0
Red River	0	0	0	0	0	0	0
Mining Total	*10*	*469*	*406*	*691*	*674*	*39*	*65*

Table 4.7.20 **Summary of irrigation pumping in acre-feet from the Woodbine Aquifer by Texas county for the years 1980, 1985, 1990, 1995, 2000, 2005, and 2010.**

County	1980	1985	1990	1995	2000	2005	2010
North Texas GCD							
Collin	0	0	0	0	0	68	68
Cooke	0	0	0	0	0	23	3
Denton	200	500	750	670	2,108	911	56
District Total	200	500	750	670	2,108	1,002	127
Northern Trinity GCD							
Tarrant	0	0	0	0	0	0	334
Prairielands GCD							
Ellis	0	0	0	0	0	10	15
Hill	0	0	0	0	0	0	0
Johnson	50	0	0	0	0	13	97
District Total	50	0	0	0	0	23	112
Red River GCD							
Fannin	0	906	362	0	0	0	946
Grayson	2,303	4,033	1,501	2,361	2,972	562	597
District Total	2,303	4,939	1,863	2,361	2,972	562	1,543
Southern Trinity GCD							
McLennan	0	0	0	0	0	0	0
No GCD							
Dallas	0	0	0	0	0	0	1,642
Hunt	0	0	0	0	0	0	0
Kaufman	0	2	0	0	0	0	0
Lamar	0	0	0	0	0	0	0
Navarro	0	0	0	0	0	0	0
Red River	0	0	0	0	0	0	0
Irrigation Total	*2,553*	*5,441*	*2,613*	*3,031*	*5,080*	*1,587*	*3,758*

Table 4.7.21   Summary of livestock pumping in acre-feet from the Woodbine Aquifer by Texas county for the years 1980, 1985, 1990, 1995, 2000, 2005, and 2010.

County	1980	1985	1990	1995	2000	2005	2010
North Texas GCD							
Collin	0	0	0	0	0	0	37
Cooke	0	0	0	0	0	78	68
Denton	570	449	464	468	207	215	160
District Total	570	449	464	468	207	293	265
Northern Trinity GCD							
Tarrant	0	0	0	0	0	57	1
Prairielands GCD							
Ellis	146	92	105	131	78	18	26
Hill	231	117	128	143	140	49	73
Johnson	338	364	493	588	539	178	157
District Total	715	573	726	862	757	245	256
Red River GCD							
Fannin	124	115	109	124	103	0	1,093
Grayson	211	110	101	131	130	235	208
District Total	335	225	210	255	233	235	1,301
Southern Trinity GCD							
McLennan	0	0	0	0	0	0	0
No GCD							
Dallas	81	42	53	52	48	98	108
Hunt	20	4	2	3	3	0	0
Kaufman	97	41	80	82	97	0	0
Lamar	75	72	63	77	34	23	21
Navarro	0	0	0	0	0	0	0
Red River	0	0	0	0	0	0	0
Livestock Total	*1,893*	*1,406*	*1,598*	*1,799*	*1,379*	*951*	*1,952*

Table 4.7.22   Summary of rural domestic pumping in acre-feet from the Woodbine Aquifer by Texas county for the years 1980, 1985, 1990, 1995, 2000, 2005, and 2010.

County	1980	1985	1990	1995	2000	2005	2010
North Texas GCD							
Collin	0	0	0	0	0	0	0
Cooke	376	399	420	453	547	581	593
Denton	385	568	743	1,039	1,557	1,585	1,442
District Total	761	967	1,164	1,492	2,104	2,166	2,035
Northern Trinity GCD							
Tarrant	390	472	533	677	888	823	744
Prairielands GCD							
Ellis	0	0	0	0	0	0	0
Hill	141	151	153	185	233	251	265
Johnson	1,029	1,323	1,480	1,408	1,396	1,443	1,445
District Total	1,170	1,474	1,632	1,593	1,629	1,694	1,709
Red River GCD							
Fannin	18	18	18	19	22	24	26
Grayson	512	541	542	589	703	698	692
District Total	530	559	560	608	725	722	719
Southern Trinity GCD							
McLennan	9	10	10	13	16	16	17
No GCD							
Dallas	0	0	0	0	0	0	0
Hunt	0	0	0	0	0	0	0
Kaufman	0	0	0	0	0	0	0
Lamar	7	7	7	8	8	8	8
Navarro	0	0	0	0	0	0	0
Red River	5	5	4	4	3	3	3
Rural Domestic Total	*2,871*	*3,495*	*3,911*	*4,393*	*5,374*	*5,432*	*5,233*

Table 4.7.23   Summary of total pumping in acre-feet from the Woodbine Aquifer by Texas county for the years 1980, 1985, 1990, 1995, 2000, 2005, and 2010.

County	1980	1985	1990	1995	2000	2005	2010
North Texas GCD							
Collin	769	909	804	1,111	1,617	2,740	3,115
Cooke	376	399	420	453	547	737	699
Denton	1,400	1,947	2,625	3,107	4,647	3,340	2,310
District Total	2,545	3,255	3,850	4,671	6,811	6,817	6,124
Northern Trinity GCD							
Tarrant	426	481	536	678	888	1,014	1,199
Prairielands GCD							
Ellis	2,774	2,836	2,502	2,484	2,388	2,597	2,216
Hill	920	385	322	469	509	487	564
Johnson	1,885	1,985	2,335	2,514	2,528	2,393	2,074
District Total	5,579	5,206	5,158	5,467	5,425	5,477	4,853
Red River GCD							
Fannin	2,214	2,994	2,304	2,428	3,027	2,584	5,125
Grayson	5,229	7,811	5,587	6,927	8,353	6,217	5,178
District Total	7,443	10,805	7,891	9,355	11,380	8,801	10,304
Southern Trinity GCD							
McLennan	9	10	10	13	16	16	17
No GCD							
Dallas	1,186	848	804	784	511	1,685	2,732
Hunt	281	376	389	398	468	442	944
Kaufman	147	43	80	82	97	0	949
Lamar	249	348	355	262	207	56	41
Navarro	58	54	80	72	112	0	0
Red River	5	5	4	4	3	4	3
Aquifer Total	*17,927*	*21,432*	*19,158*	*21,784*	*25,919*	*24,312*	*27,164*

Table 4.7.24   Summary of pumping in acre-feet from the Woodbine Aquifer in Texas by water use category for the years 1980, 1985, 1990, 1995, 2000, 2005, and 2010.

Water Use Category	1980	1985	1990	1995	2000	2005	2010
Pumping (acre-feet)							
Irrigation	2,553	5,441	2,613	3,031	5,080	1,587	3,758
Manufacturing	1,619	1,394	1,030	1,126	487	1,661	1,070
Mining	10	469	406	691	674	39	65
Municipal	8,679	8,868	9,394	10,430	12,422	14,571	14,767
Power	302	359	206	314	503	71	319
Rural Domestic	2,871	3,495	3,911	4,393	5,374	5,432	5,233
Livestock	1,893	1,406	1,598	1,799	1,379	951	1,952
Total	17,927	21,432	19,158	21,784	25,919	24,312	27,164
Percentage of Total							
Irrigation	14%	25%	14%	14%	20%	7%	14%
Manufacturing	9%	7%	5%	5%	2%	7%	4%
Mining	0%	2%	2%	3%	3%	0%	0%
Municipal	48%	41%	49%	48%	48%	60%	54%
Power	2%	2%	1%	1%	2%	0%	1%
Rural Domestic	16%	16%	20%	20%	21%	22%	19%
Livestock	11%	7%	8%	8%	5%	4%	7%

**Table 4.7.25   Summary of pumping in acre-feet from the Woodbine Aquifer in the North Texas
GCD by water use category for the years 1980, 1985, 1990, 1995, 2000, 2005, and
2010.**

Water Use Category	1980	1985	1990	1995	2000	2005	2010
Pumping (acre-feet)							
Irrigation	200	500	750	670	2,108	1,002	127
Manufacturing	9	149	80	137	174	174	206
Mining	0	0	24	17	0	0	0
Municipal	1,005	1,190	1,368	1,887	2,218	3,182	3,491
Power	0	0	0	0	0	0	0
Rural Domestic	761	967	1,164	1,492	2,104	2,166	2,035
Livestock	570	449	464	468	207	293	265
Total	2,545	3,255	3,850	4,671	6,811	6,817	6,124
Percentage of Total							
Irrigation	8%	15%	19%	14%	31%	15%	2%
Manufacturing	0%	5%	2%	3%	3%	3%	3%
Mining	0%	0%	1%	0%	0%	0%	0%
Municipal	39%	37%	36%	40%	33%	47%	57%
Power	0%	0%	0%	0%	0%	0%	0%
Rural Domestic	30%	30%	30%	32%	31%	32%	33%
Livestock	22%	14%	12%	10%	3%	4%	4%

Table 4.7.26   **Summary of pumping in acre-feet from the Woodbine Aquifer in the Northern Trinity GCD by water use category for the years 1980, 1985, 1990, 1995, 2000, 2005, and 2010.**

Water Use Category	1980	1985	1990	1995	2000	2005	2010
Pumping (acre-feet)							
Irrigation	0	0	0	0	0	0	334
Manufacturing	0	0	0	0	0	0	0
Mining	0	0	0	0	0	0	0
Municipal	36	9	3	1	0	134	120
Power	0	0	0	0	0	0	0
Rural Domestic	390	472	533	677	888	823	744
Livestock	0	0	0	0	0	57	1
Total	426	481	536	678	888	1,014	1,199
Percentage of Total							
Irrigation	0%	0%	0%	0%	0%	0%	28%
Manufacturing	0%	0%	0%	0%	0%	0%	0%
Mining	0%	0%	0%	0%	0%	0%	0%
Municipal	8%	2%	1%	0%	0%	13%	10%
Power	0%	0%	0%	0%	0%	0%	0%
Rural Domestic	92%	98%	99%	100%	100%	81%	62%
Livestock	0%	0%	0%	0%	0%	6%	0%

Table 4.7.27   **Summary of pumping in acre-feet from the Woodbine Aquifer in the Prairielands GCD by water use category for the years 1980, 1985, 1990, 1995, 2000, 2005, and 2010.**

Water Use Category	1980	1985	1990	1995	2000	2005	2010
Pumping (acre-feet)							
Irrigation	50	0	0	0	0	23	112
Manufacturing	971	705	628	658	55	171	160
Mining	0	159	73	208	208	0	0
Municipal	2,673	2,295	2,099	2,146	2,776	3,344	2,616
Power	0	0	0	0	0	0	0
Rural Domestic	1,170	1,474	1,632	1,593	1,629	1,694	1,709
Livestock	715	573	726	862	757	245	256
Total	5,579	5,206	5,158	5,467	5,425	5,477	4,853
Percentage of Total							
Irrigation	1%	0%	0%	0%	0%	0%	2%
Manufacturing	17%	14%	12%	12%	1%	3%	3%
Mining	0%	3%	1%	4%	4%	0%	0%
Municipal	48%	44%	41%	39%	51%	61%	54%
Power	0%	0%	0%	0%	0%	0%	0%
Rural Domestic	21%	28%	32%	29%	30%	31%	35%
Livestock	13%	11%	14%	16%	14%	4%	5%

Table 4.7.28   Summary of pumping in acre-feet from the Edwards BFZ Aquifer by water use category for the years 1980, 1985, 1990, 1995, 2000, 2005, and 2010.

Water Use Category	1980	1985	1990	1995	2000	2005	2010
Pumping (acre-feet)							
Irrigation	12	8	18	0	0	993	1,568
Manufacturing	254	251	457	949	780	1,179	793
Mining	1,074	1,653	1,654	1,672	1,672	1,844	4,286
Municipal	13,575	16,910	15,211	19,095	21,010	28,983	30,716
Power	0	0	0	0	0	0	0
Rural Domestic	2,602	842	995	1,026	1,055	1,102	1,119
Livestock	121	160	165	149	127	552	532
Total	17,639	19,824	18,500	22,891	24,644	34,653	39,014
Percentage of Total							
Irrigation	0%	0%	0%	0%	0%	3%	4%
Manufacturing	1%	1%	2%	4%	3%	3%	2%
Mining	6%	8%	9%	7%	7%	5%	11%
Municipal	77%	85%	82%	83%	85%	84%	79%
Power	0%	0%	0%	0%	0%	0%	0%
Rural Domestic	15%	4%	5%	4%	4%	3%	3%
Livestock	1%	1%	1%	1%	1%	2%	1%

Table 4.7.29   Summary of pumping data received from GCDs.

Groundwater Conservation District	Counties	Type Data Received	Time Period of Data
Clearwater UWCD	Bell	Non-Exempt Production Reports	2003 through 2011
		Estimates of Exempt Pumping	2004 through 2011
North Texas GCD	Collin, Cooke, and Denton	Meter Data for Non-Exempt Wells	2010 and 2012
Northern Trinity GCD	Tarrant	Meter Data for Non-Exempt Wells and Oil and Gas Water Supply Wells and water Production Reports	2010 through 2012
Prairielands GCD	Ellis, Hill, Johnson, and Somervell	Meter Data	June 2011 through 2012
Southern Trinity GCD	McLennan	Production Reported on Historical Use Permit Applications	2000 through 2009 and 2012
Upper Trinity GCD	Hood, Montague, Parker, and Wise	Meter Data for Non-Exempt Wells and Oil and Gas Related Water Supply Wells	2009 through 2012

Table 4.7.30   **Comparison of pumping estimates for the northern Trinity Aquifer in the Upper Trinity GCD by water use category for the year 2011.**

Water Use Category	TWDB WUS[a]	UTGCD	Percent Difference
Pumping (acre-feet)			
Irrigation	2,132	2,294	7%
Manufacturing	26	246	89%
Mining	4,668	4,390	6%
Municipal	17,319	11,401	52%
Power	9	9	0%
Rural Domestic	9,977	10,240	3%
Livestock	540	540	0%
Total	**34,671**	**29,120**	**19%**
Percentage of Total			
Irrigation	6%	8%	
Manufacturing	0%	1%	
Mining	13%	15%	
Municipal	50%	39%	
Power	0%	0%	
Rural Domestic	29%	35%	
Livestock	2%	2%	

[a] TWDB water use survey data except rural domestic, which was estimated based on census block data
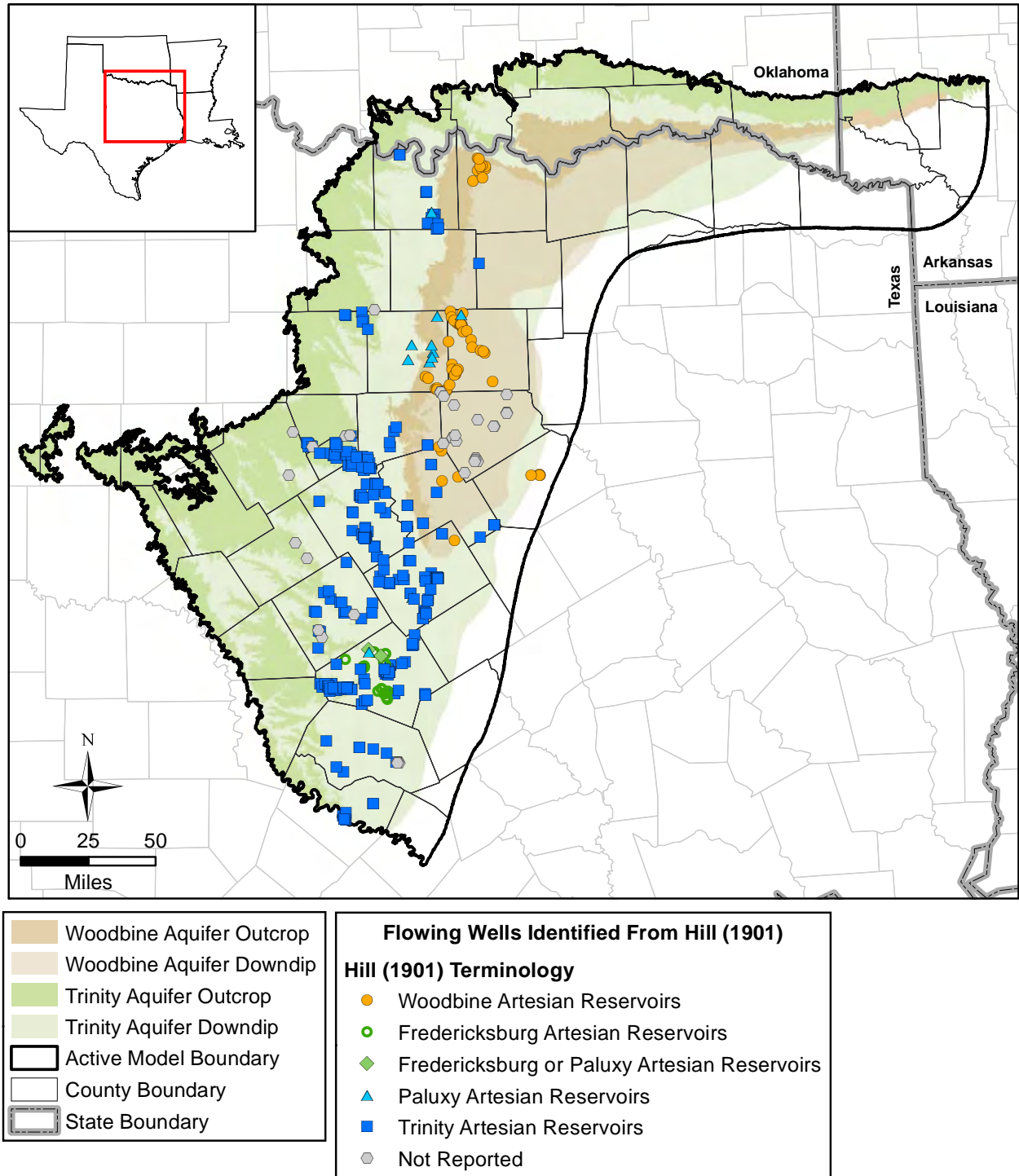
Figure 4.7.1   Estimated locations of flowing wells from Hill (1901).
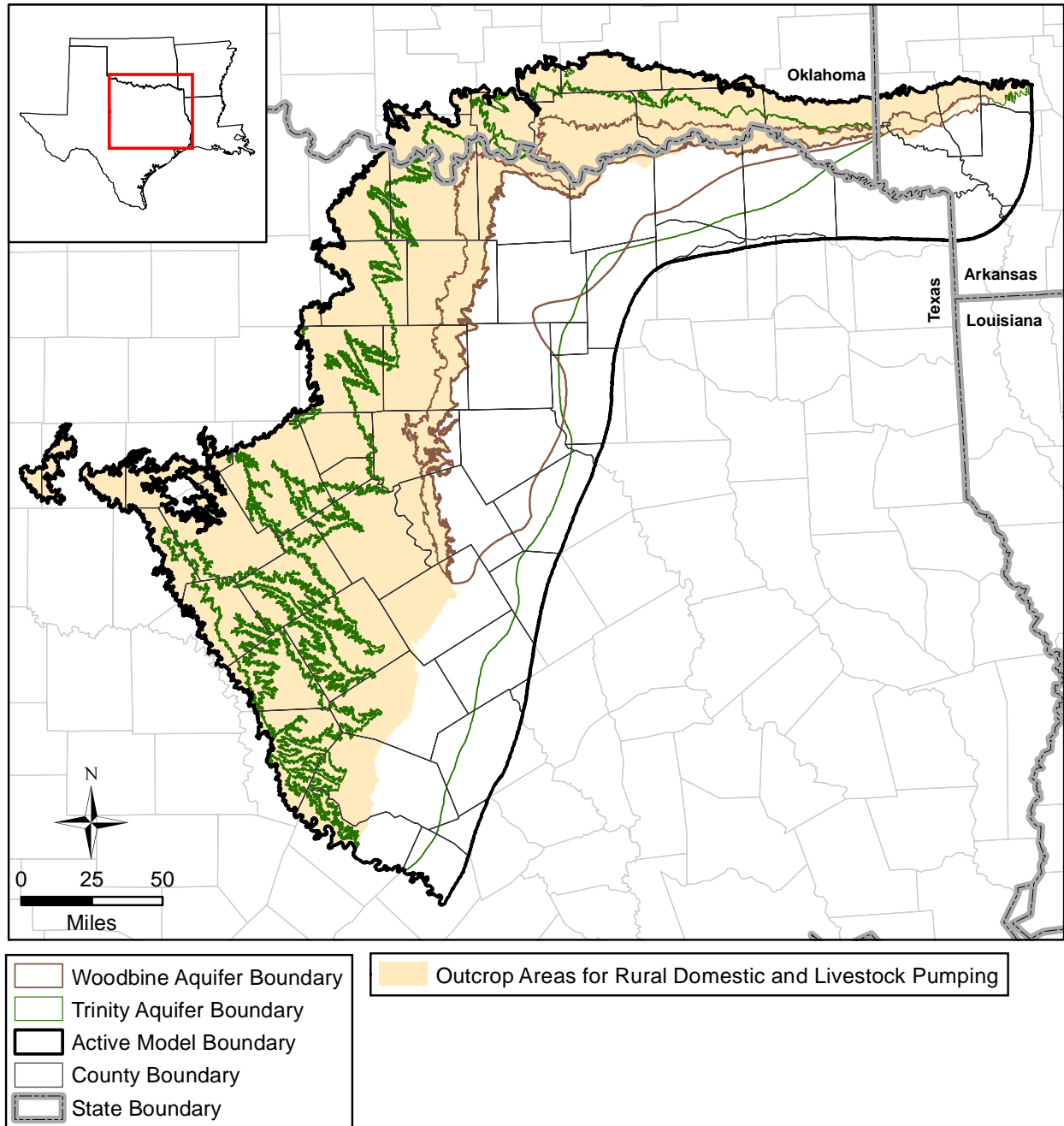
Figure 4.7.2   Outcrop areas assumed for calculations of rural domestic and livestock pumping.
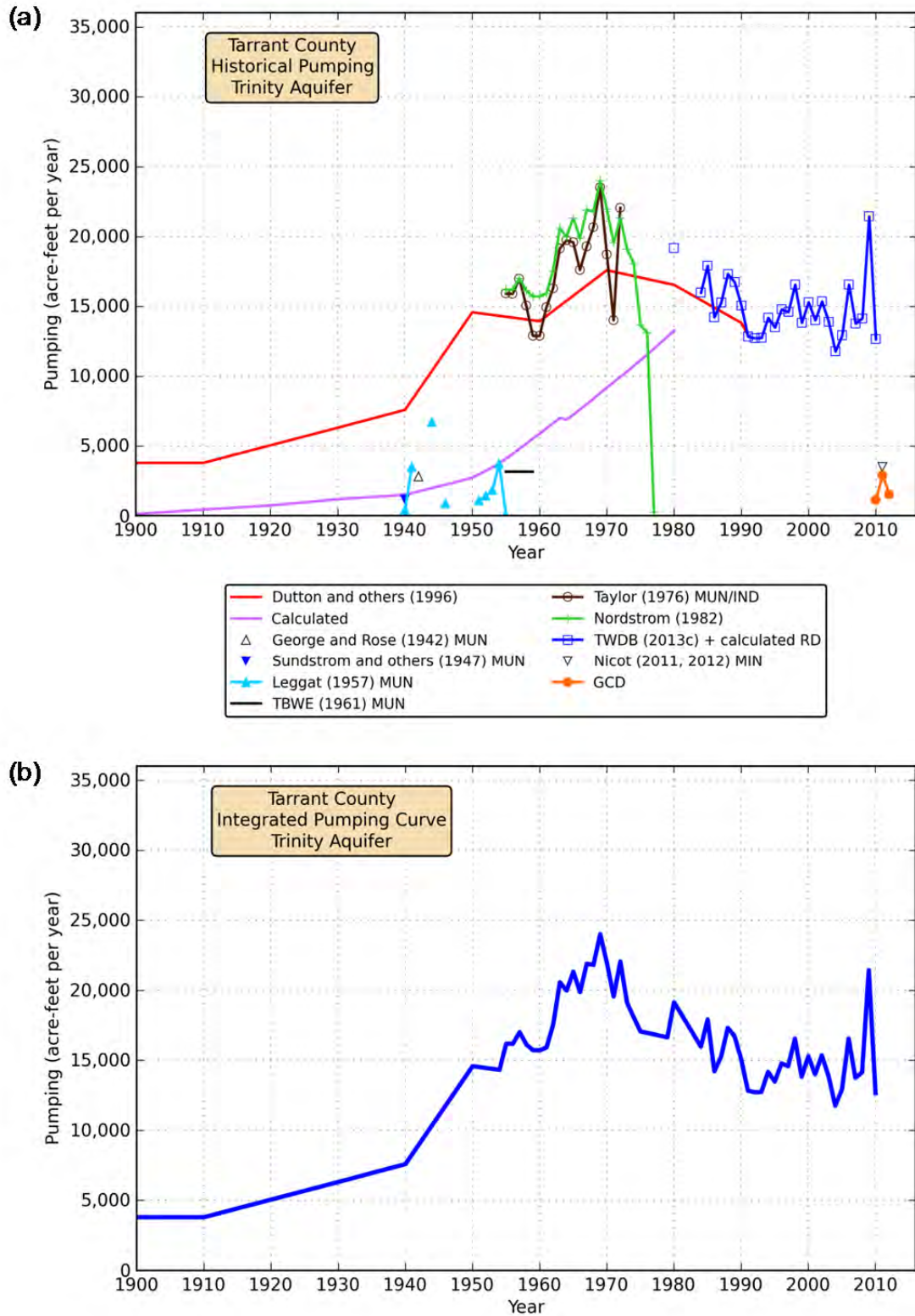
Figure 4.7.3   Plots of (a) historical pumping data and (b) integrated pumping curve for the northern Trinity Aquifer in Tarrant County.
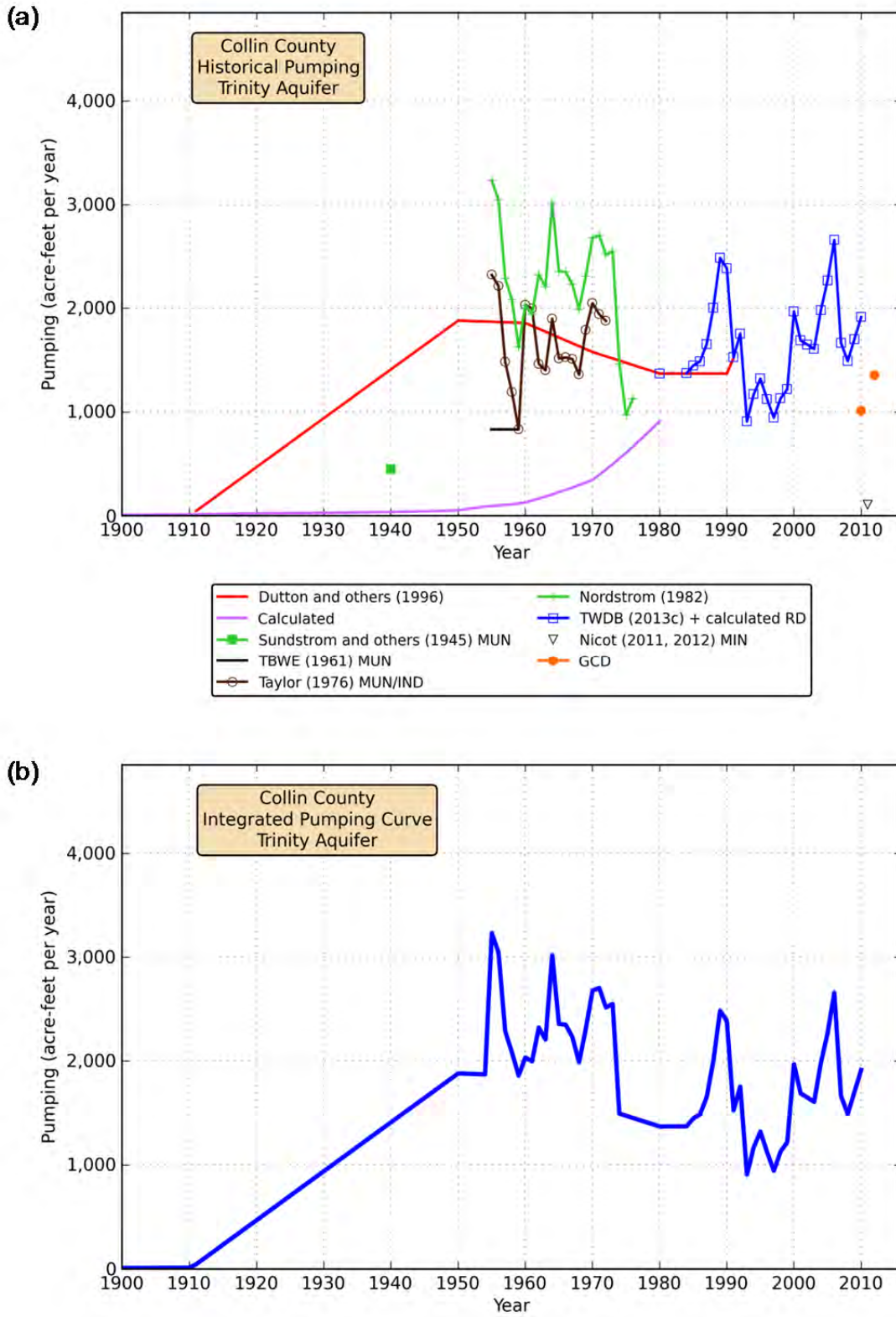
Figure 4.7.4 Plots of (a) historical pumping data and (b) integrated pumping curve for the
northern Trinity Aquifer in Collin County.
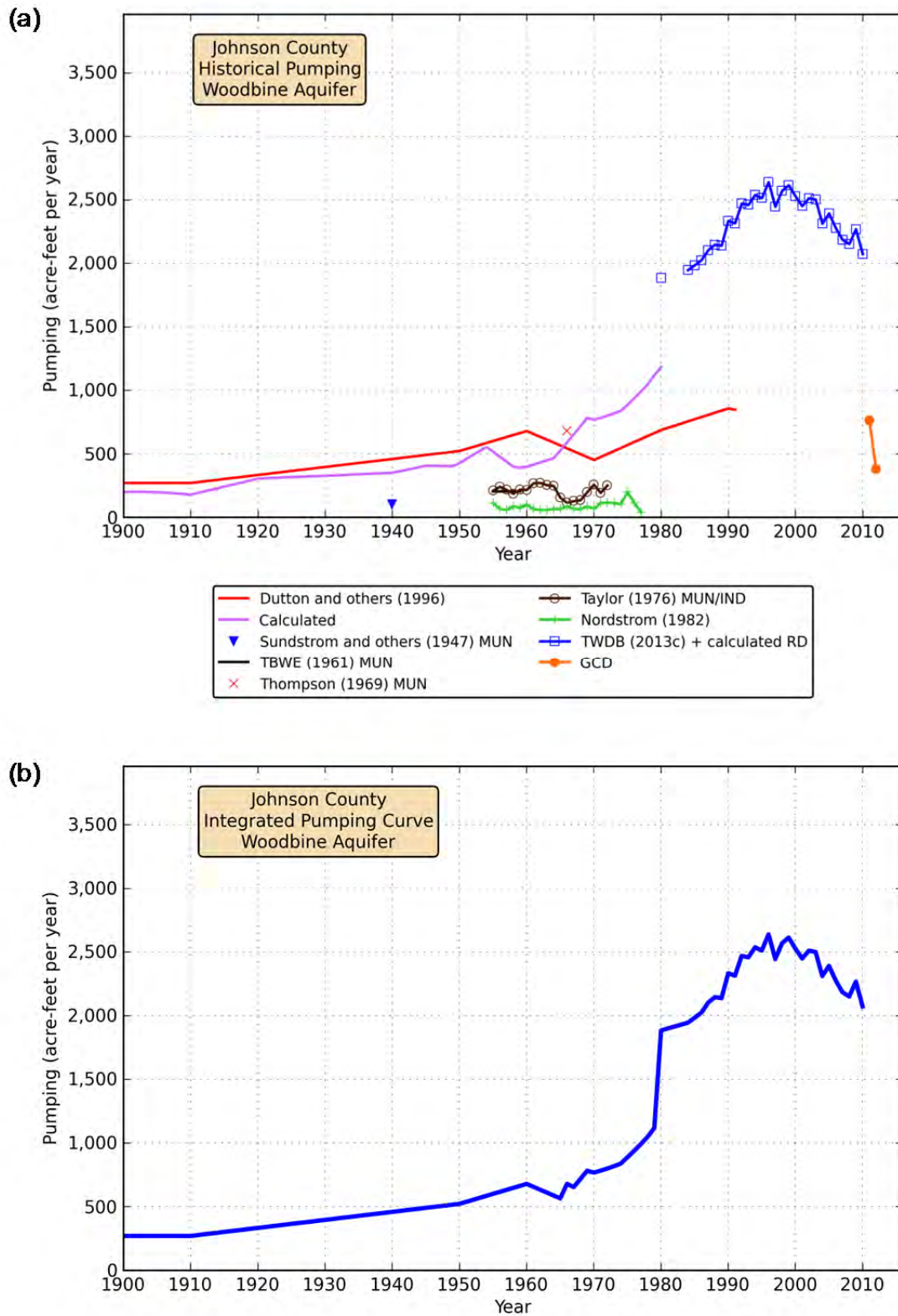
Figure 4.7.5 **Plots of (a) historical pumping data and (b) integrated pumping curve for the Woodbine Aquifer in Johnson County.**

(a)

(b)
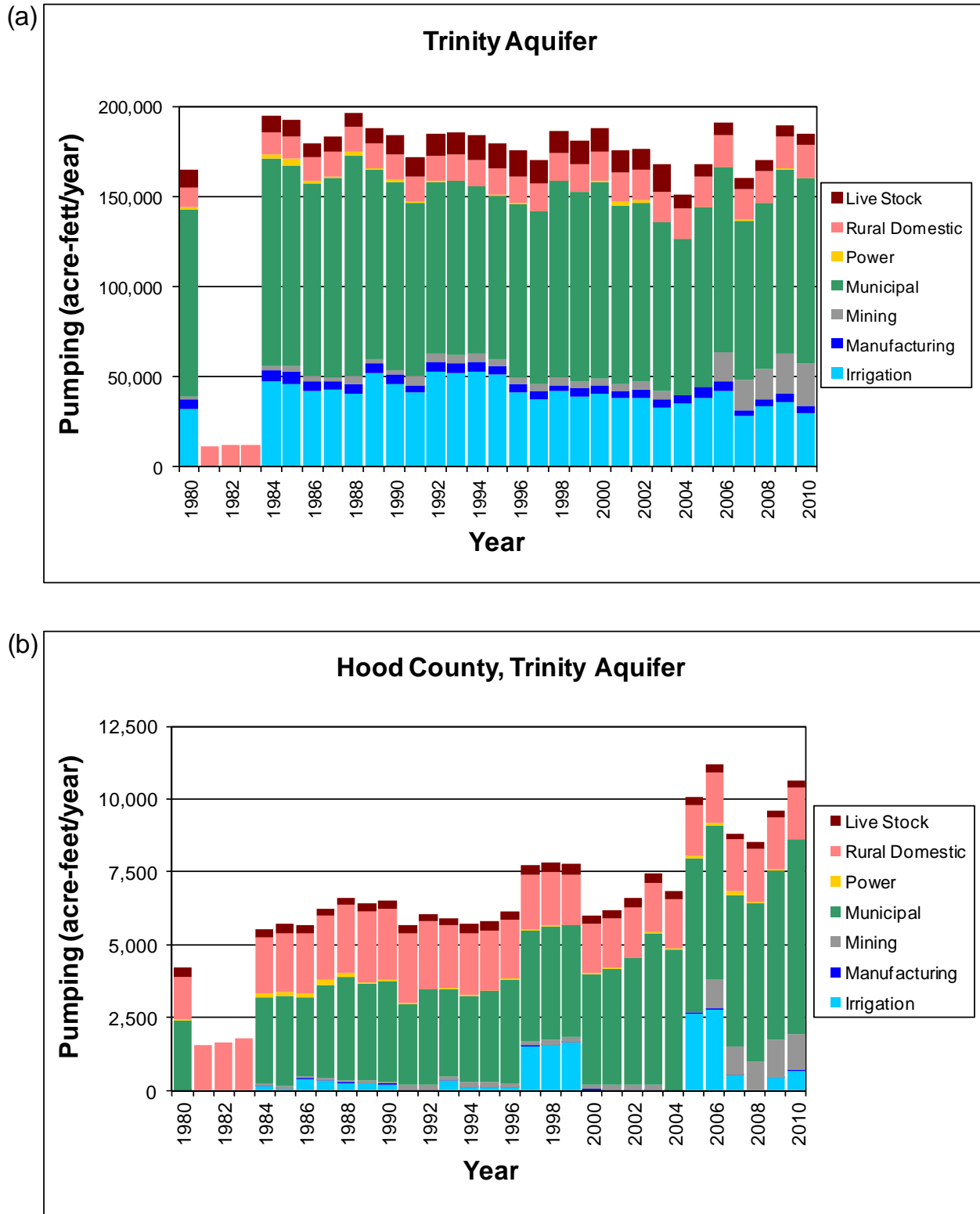
Figure 4.7.6   Bar chart of pumping from the northern Trinity Aquifer by use category from 1980 through 2010 for (a) the entire aquifer and (b) Hood County.

(a)

(b)
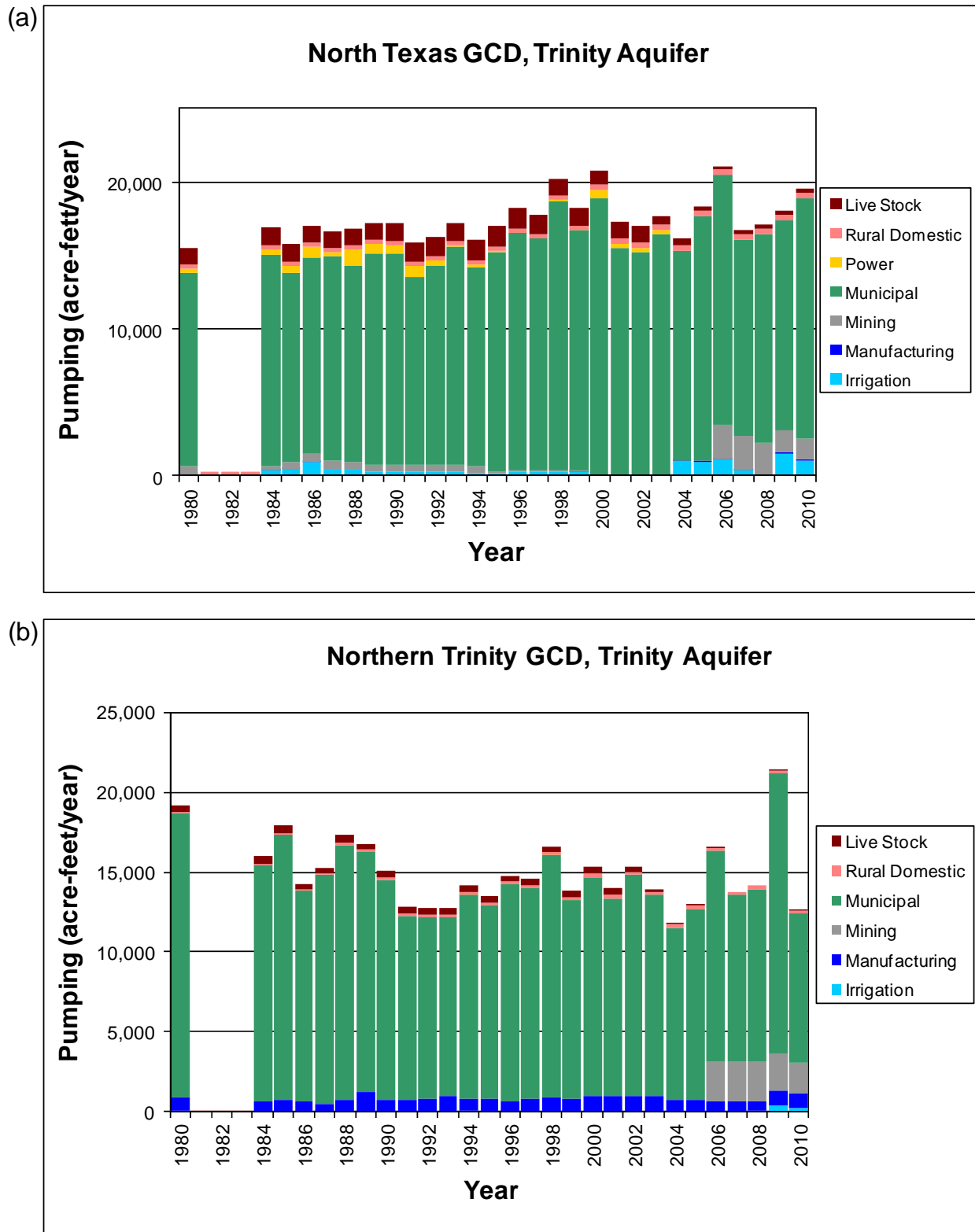
Figure 4.7.7   **Bar chart of pumping from the northern Trinity Aquifer by use category from 1980 through 2010 for (a) the North Texas GCD and (b) the Northern Trinity GCD.**
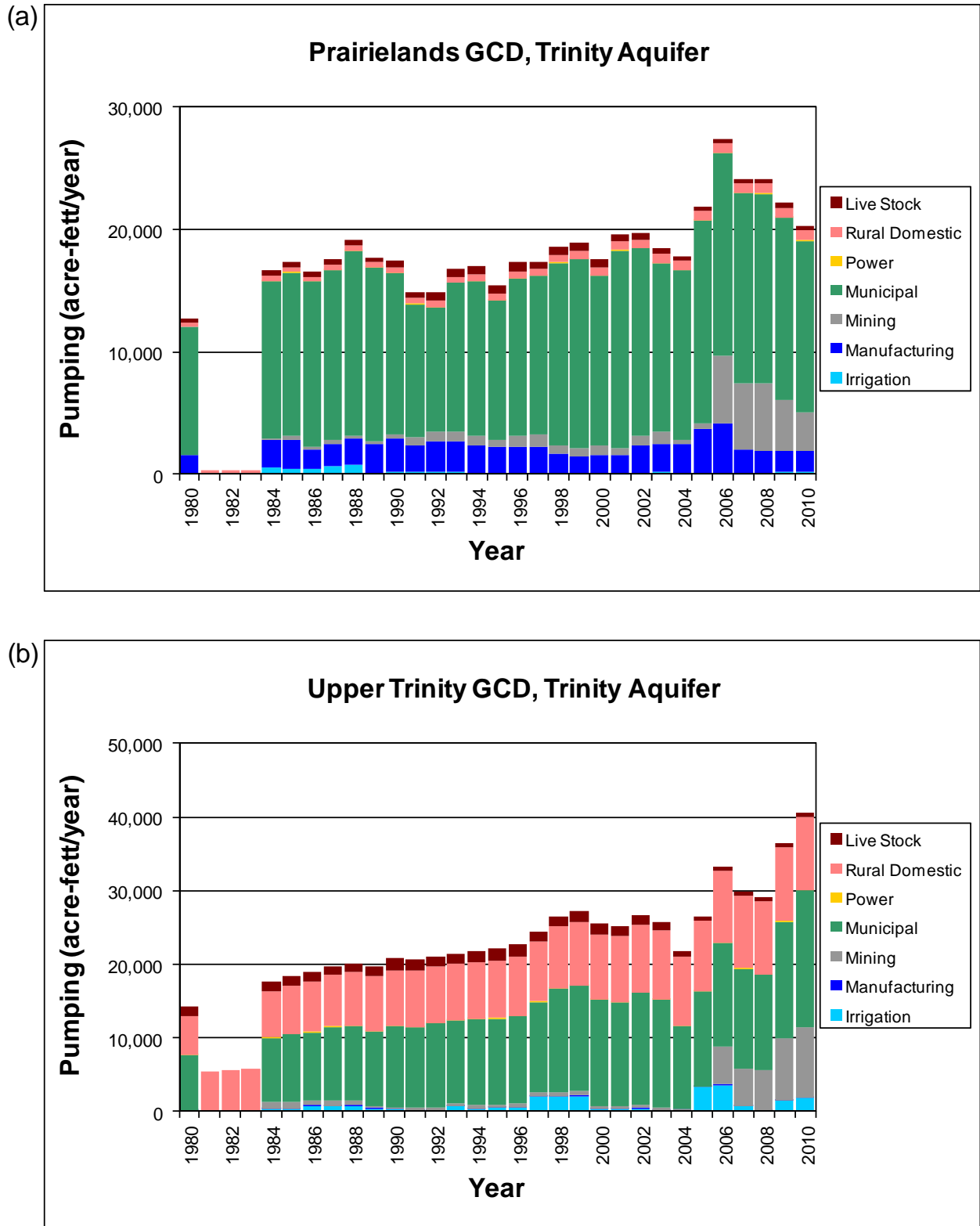
Figure 4.7.8   Bar chart of pumping from the northern Trinity Aquifer by use category from 1980 through 2010 for (a) the Prairielands GCD and (b) the Upper Trinity GCD.

(a)

(b)
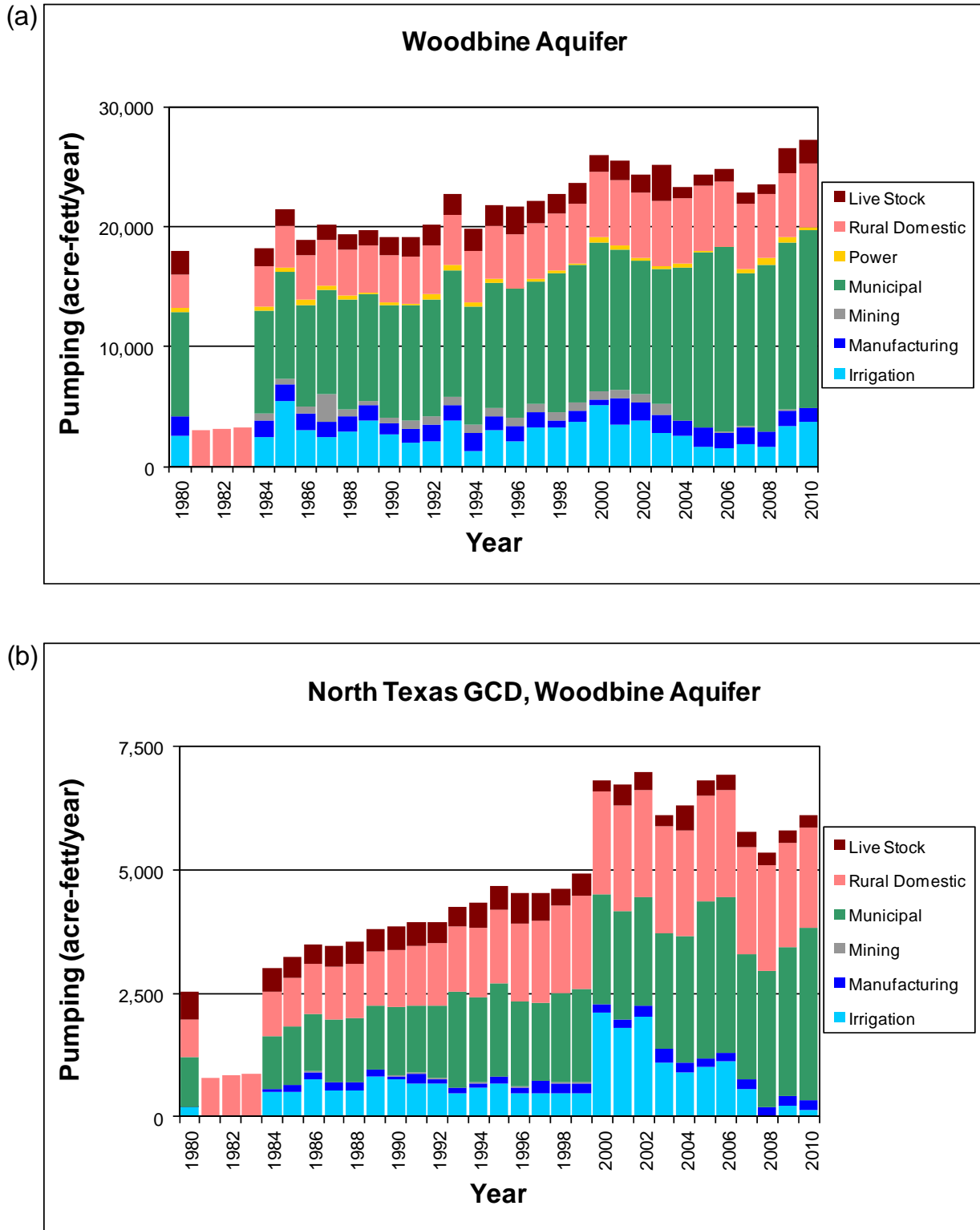
**Figure 4.7.9   Bar chart of pumping from the Woodbine Aquifer by use category from 1980
through 2010 for (a) the entire aquifer and (b) the North Texas GCD.**

(a)

(b)
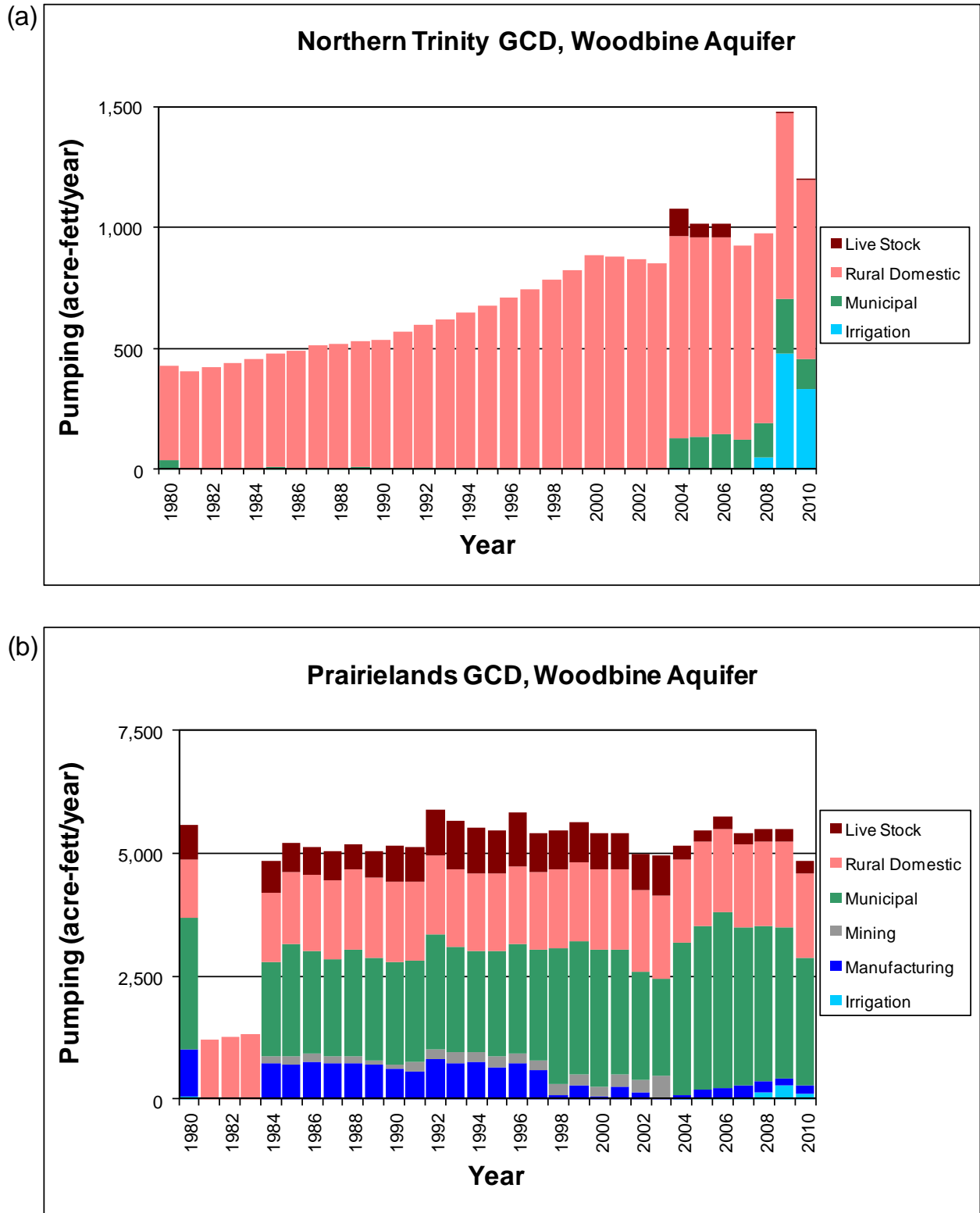
**Figure 4.7.10   Bar chart of pumping from the Woodbine Aquifer by use category from 1980
through 2010 for (a) the Northern Trinity GCD and (b) the Prairielands GCD.**
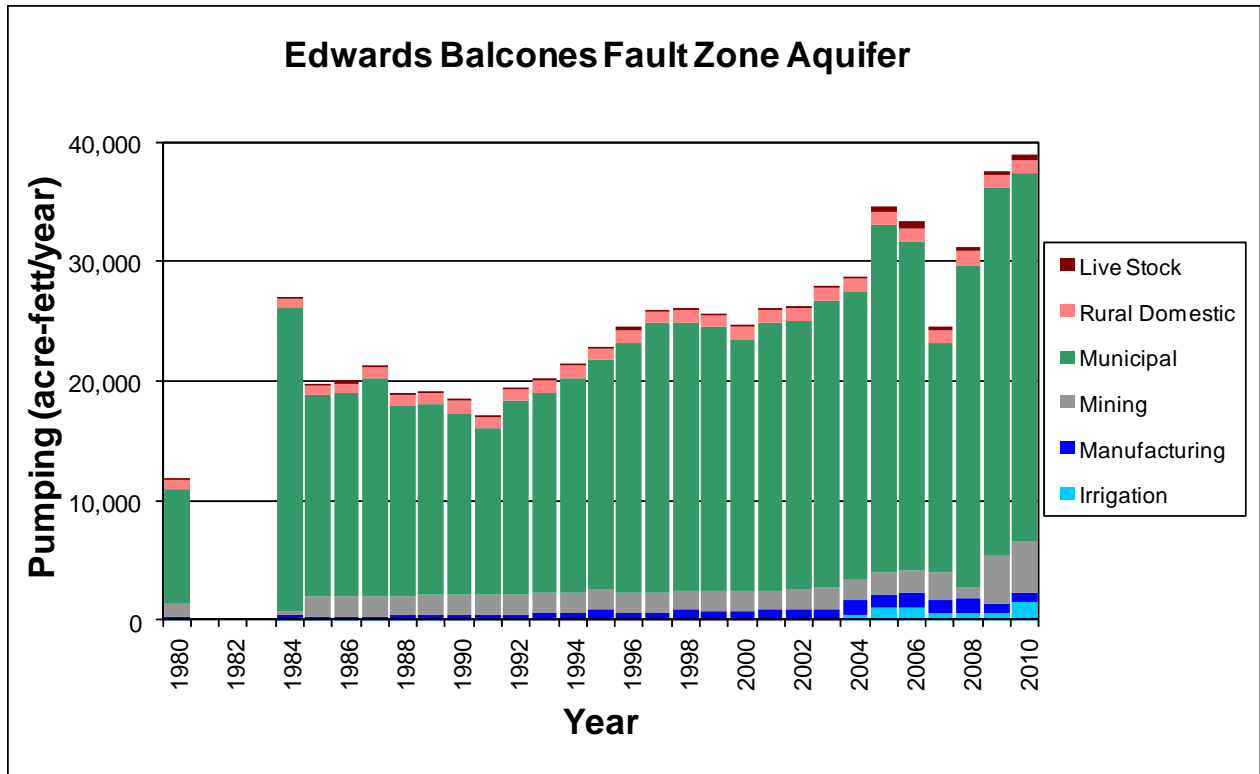
Figure 4.7.11   Bar chart of pumping from the Edwards BFZ Aquifer by use category from 1980 through 2010.
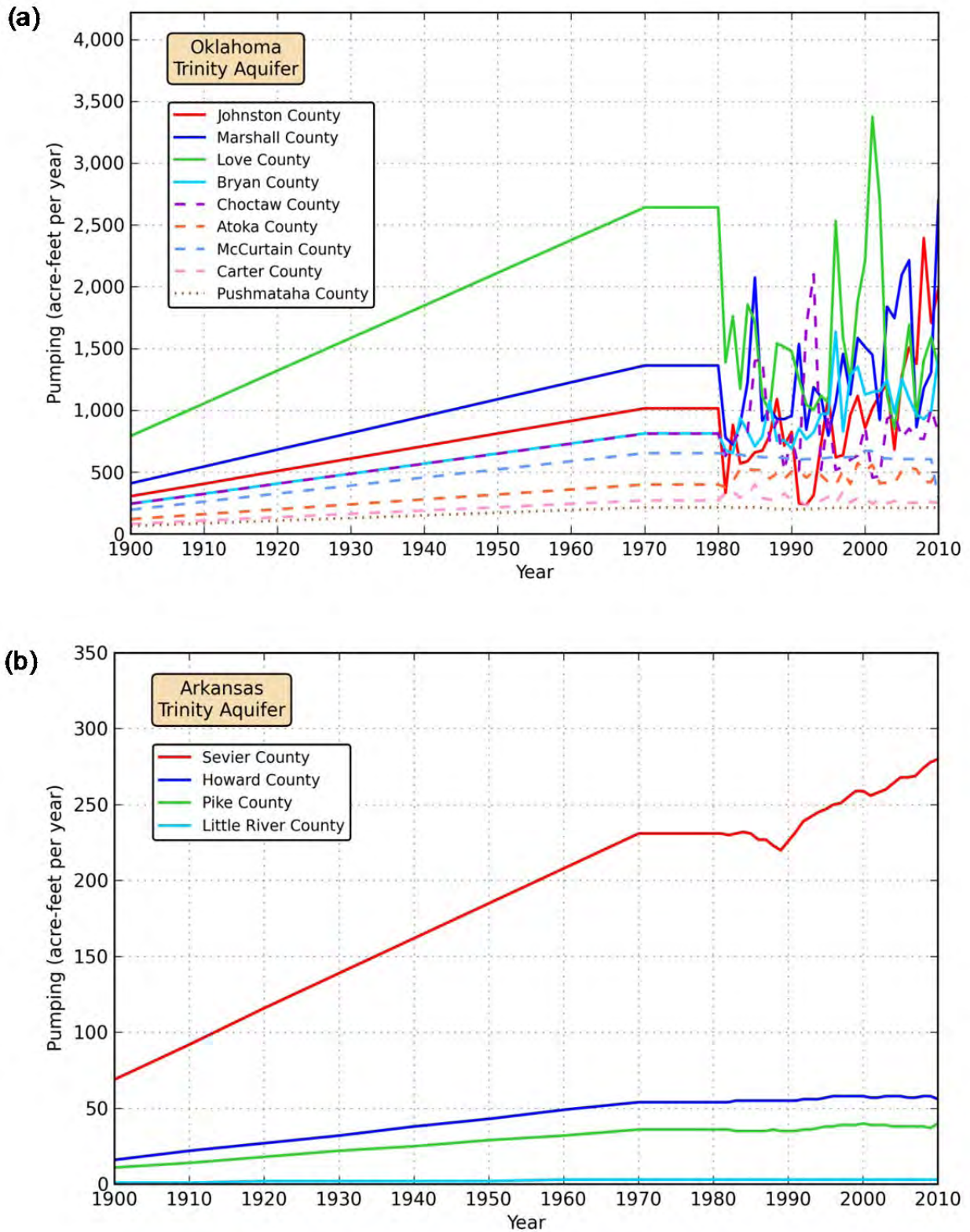
Figure 4.7.12   Estimate pumping from the northern Trinity Aquifer in (a) Oklahoma and (b) Arkansas by county.
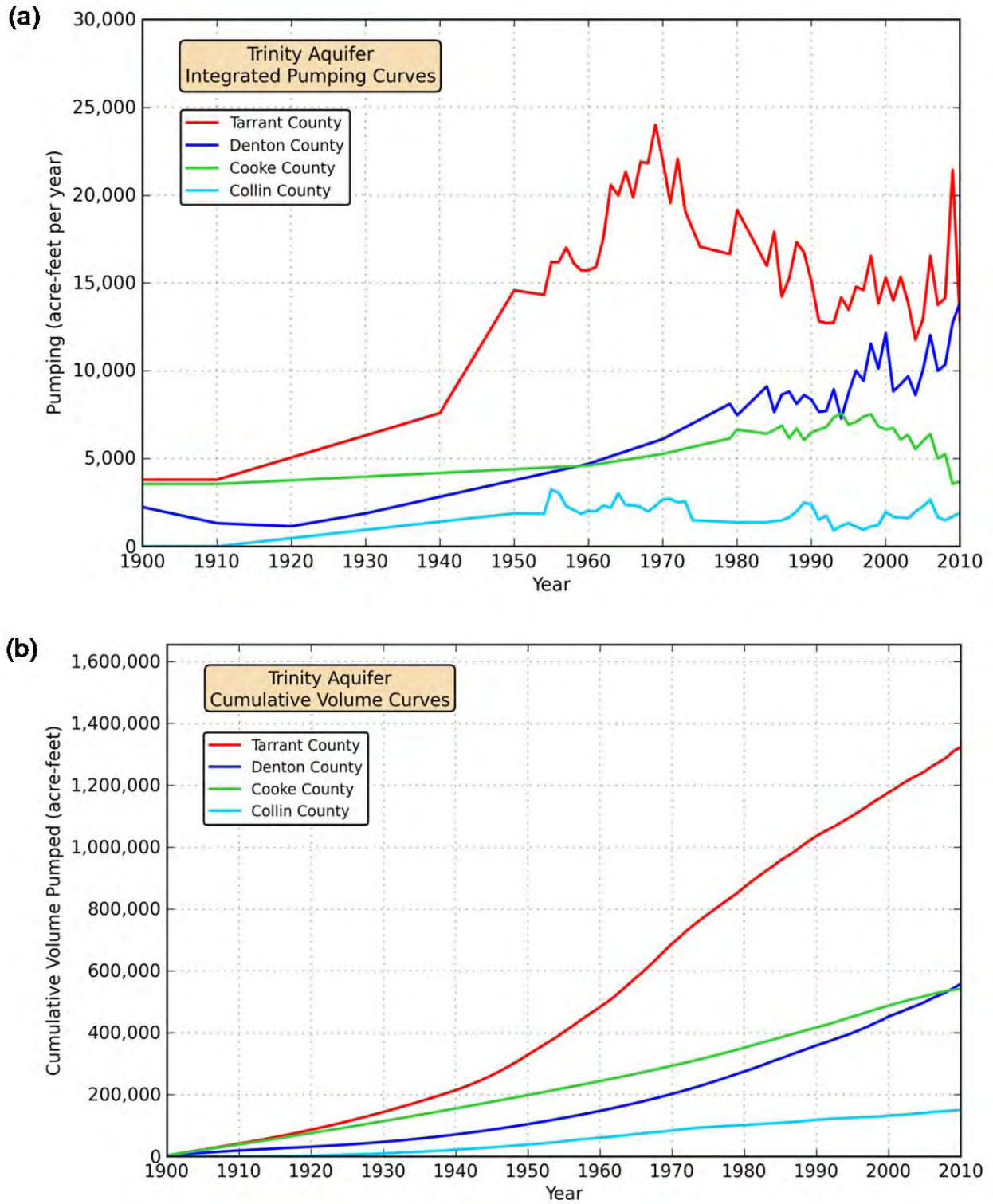
Figure 4.7.13   Times series of (a) integrated pumping curves and (b) estimated historical volumes
pumped from 1900 through 2010 for the northern Trinity Aquifer in the counties of
the North Texas and Northern Trinity GCDs.
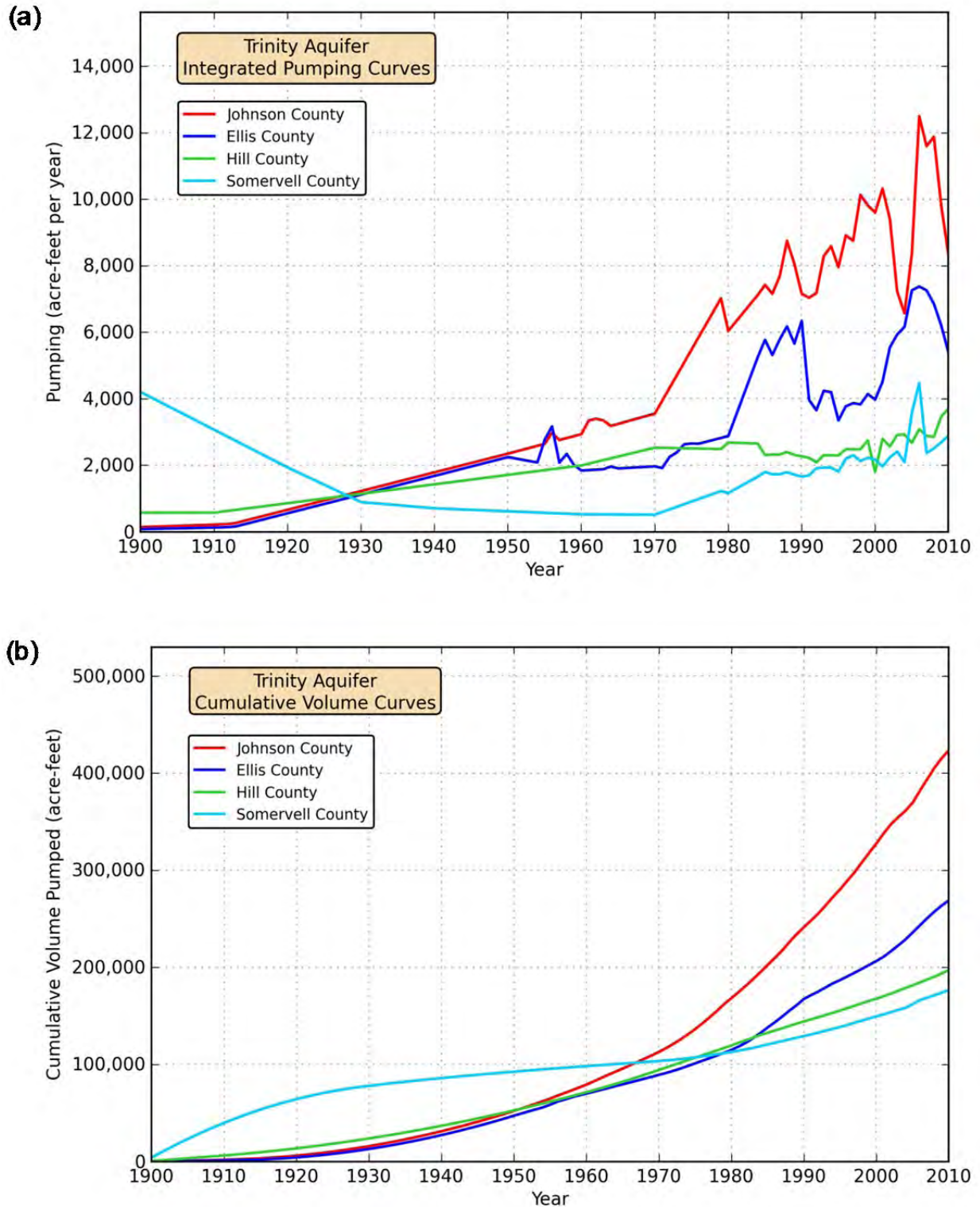
Figure 4.7.14 Times series of (a) integrated pumping curves and (b) estimated historical volumes pumped from 1900 through 2010 for the northern Trinity Aquifer in the counties of the Prairielands GCD.

(a)

(b)
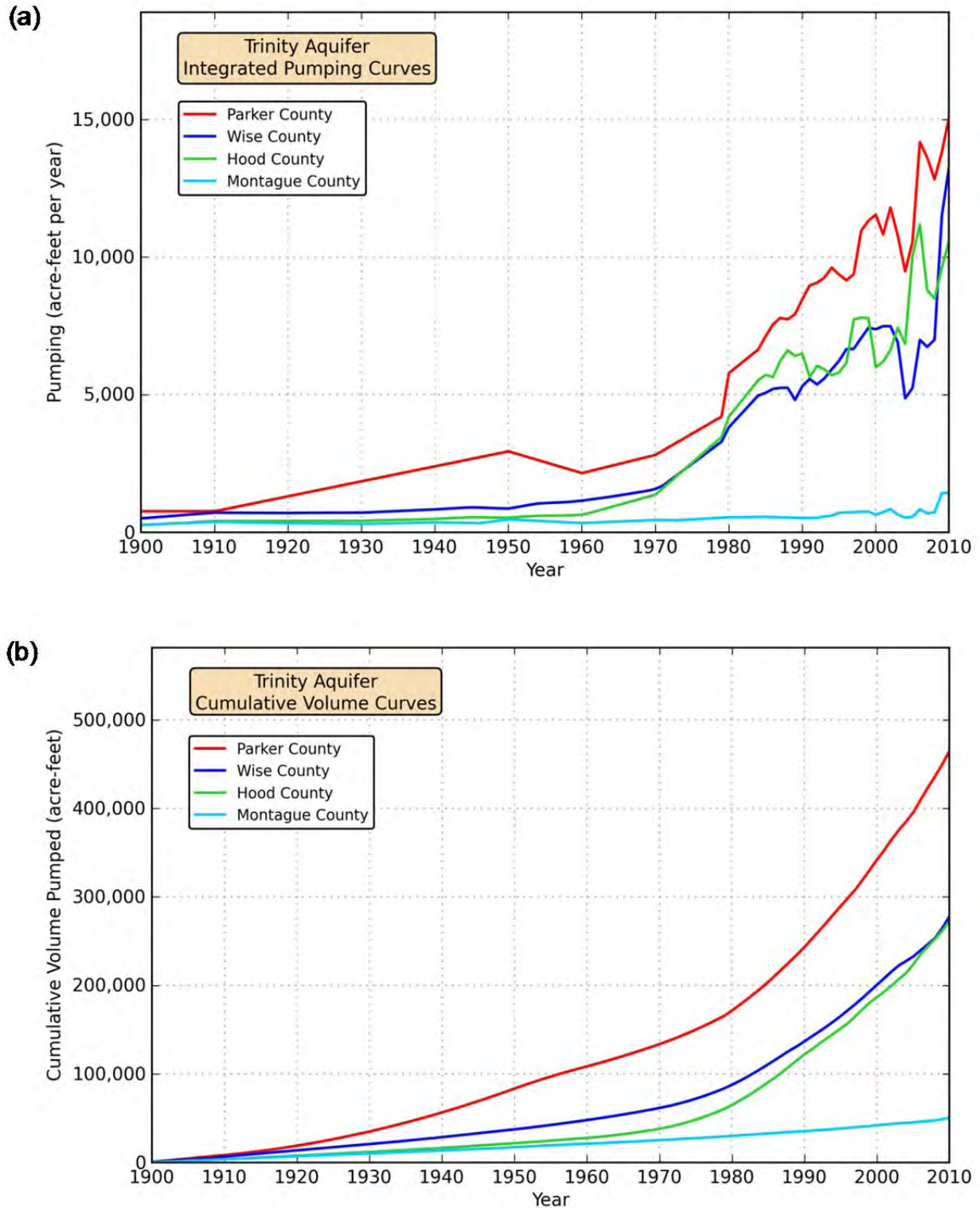
**Figure 4.7.15   Times series of (a) integrated pumping curves and (b) estimated historical volumes
pumped from 1900 through 2010 for the northern Trinity Aquifer in the counties of
the Upper Trinity GCD.**
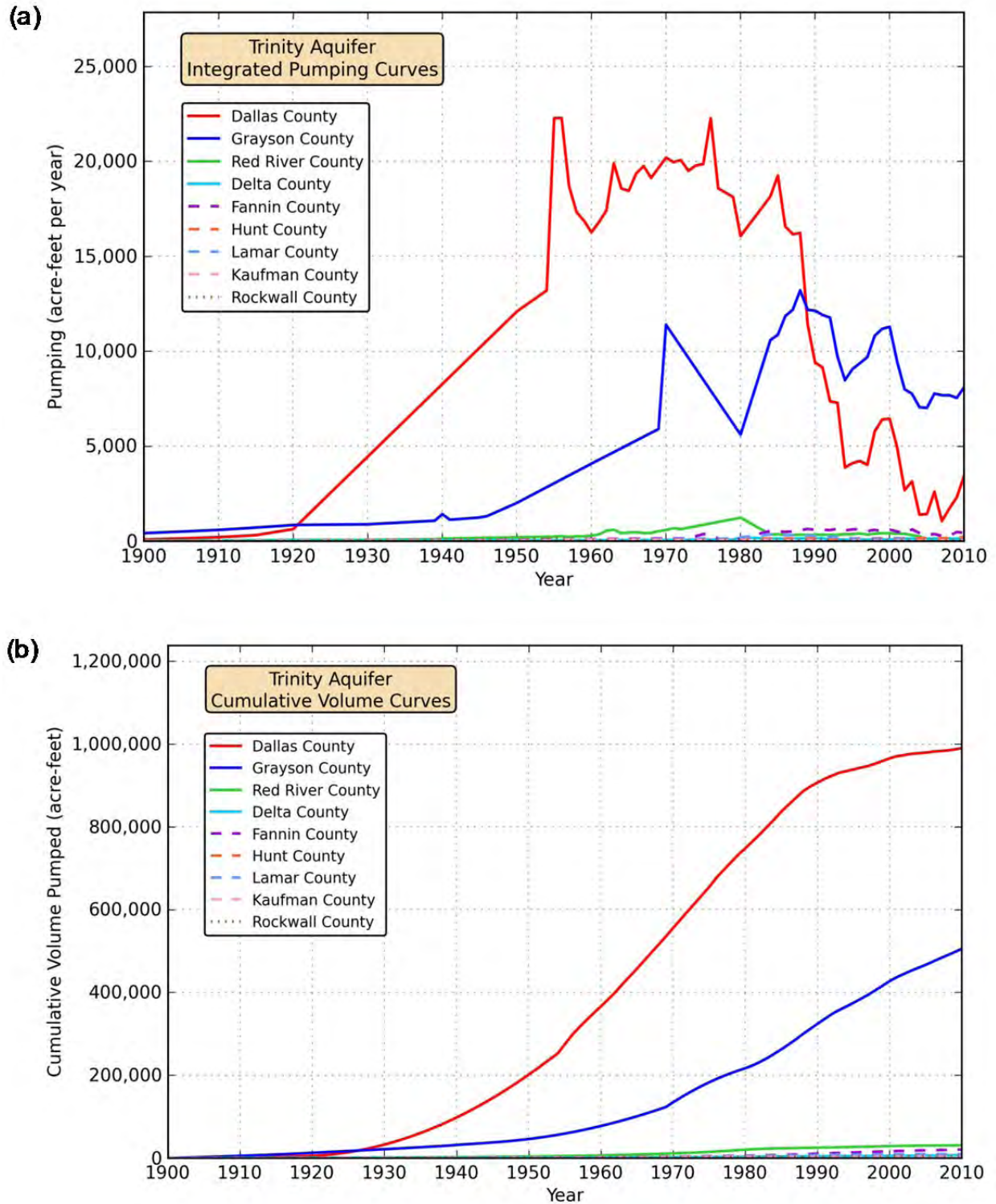
Figure 4.7.16   Times series of (a) integrated pumping curves and (b) estimated historical volumes pumped from 1900 through 2010 for the northern Trinity Aquifer in Dallas, Delta, Fannin, Grayson, Hunt, Kaufman, Lamar, Red River, and Rockwall counties.
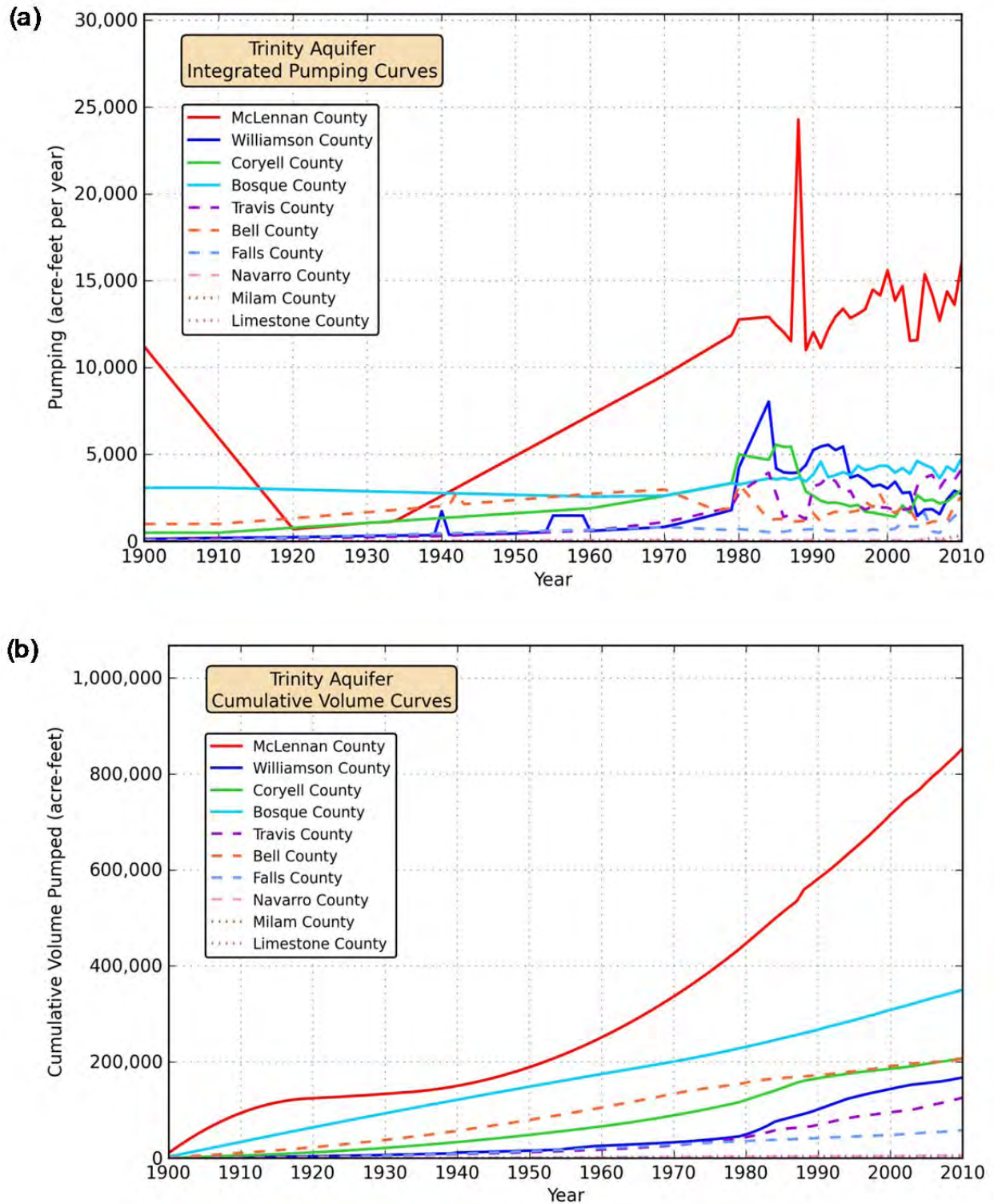
Figure 4.7.17   Times series of (a) integrated pumping curves and (b) estimated historical volumes
pumped from 1900 through 2010 for the northern Trinity Aquifer in Bell, Bosque,
Coryell, Falls, Limestone, McLennan, Milam, Navarro, Travis, and Williamson
counties.
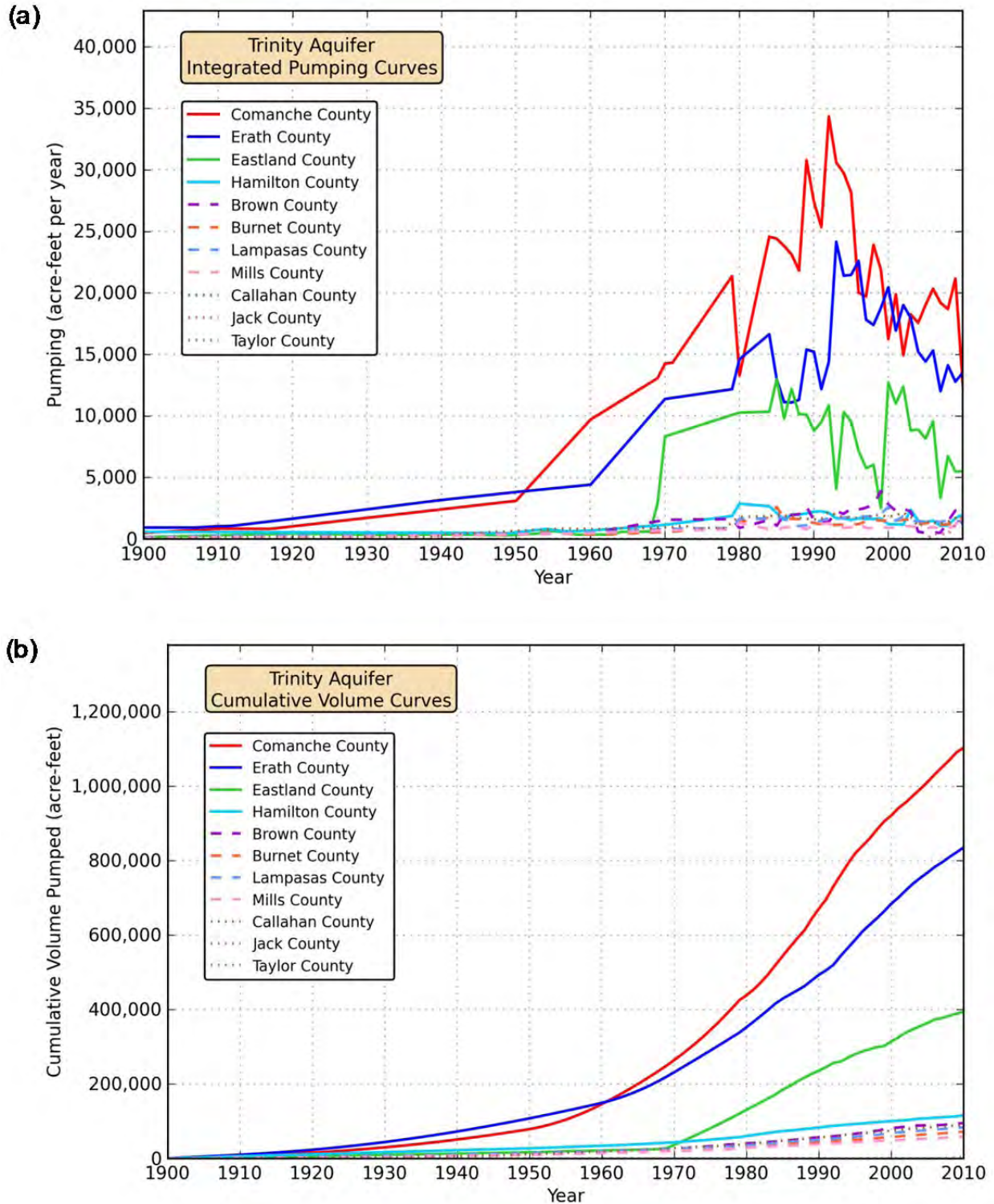
Figure 4.7.18   Times series of (a) integrated pumping curves and (b) estimated historical volumes pumped from 1900 through 2010 for the northern Trinity Aquifer in Brown, Burnet, Callahan, Comanche, Eastland, Erath, Hamilton, Jack, Lampasas, Mills, and Taylor counties.
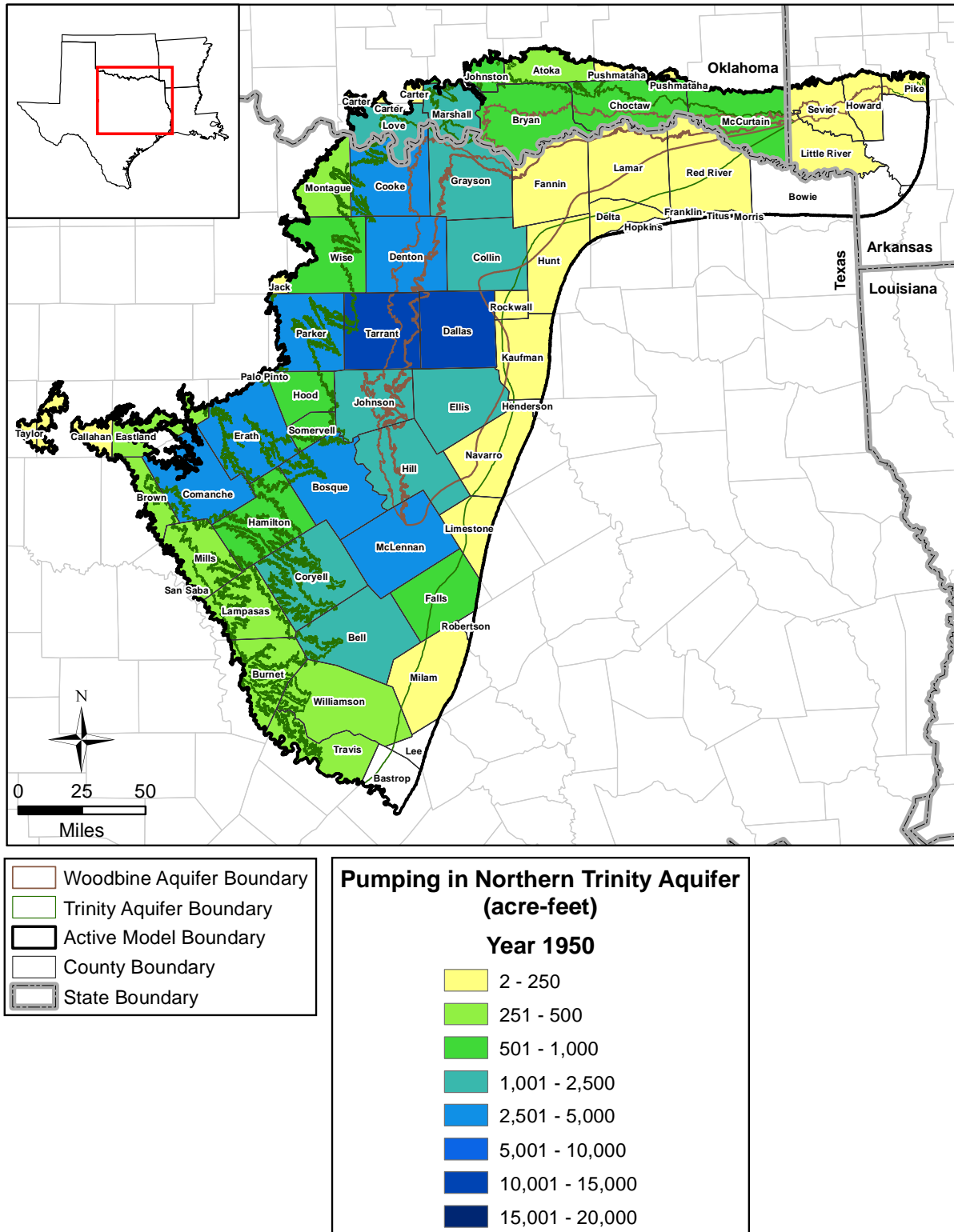
Figure 4.7.19   Estimated groundwater pumping from the northern Trinity Aquifer in 1950 by county.
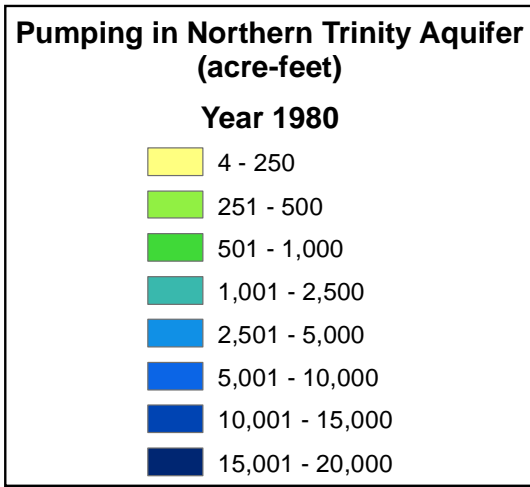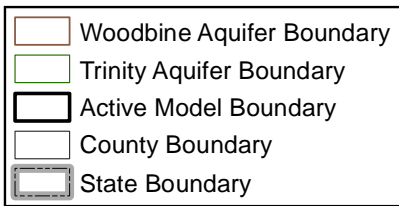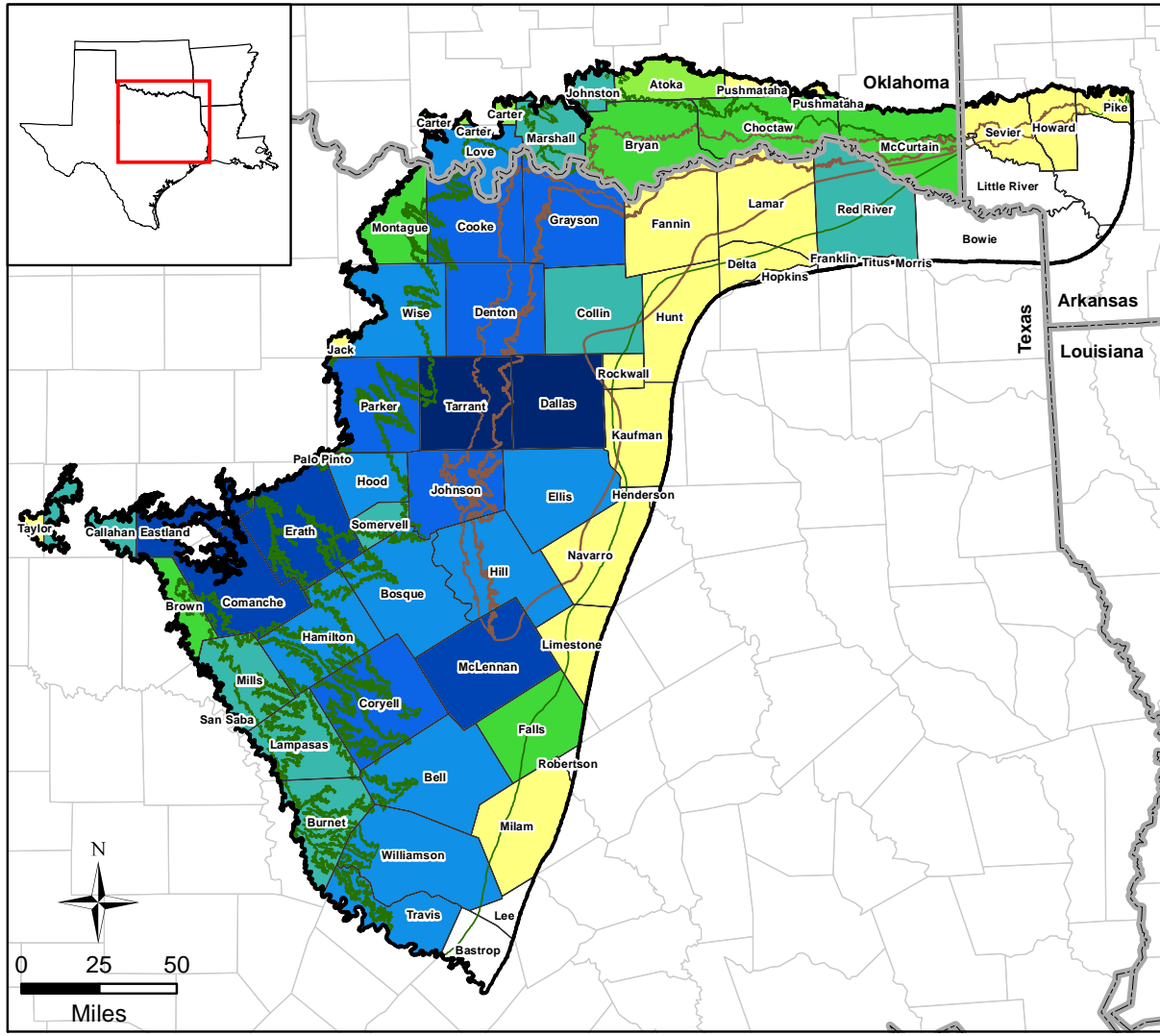
Figure 4.7.20   Estimated groundwater pumping from the northern Trinity Aquifer in 1980 by county.
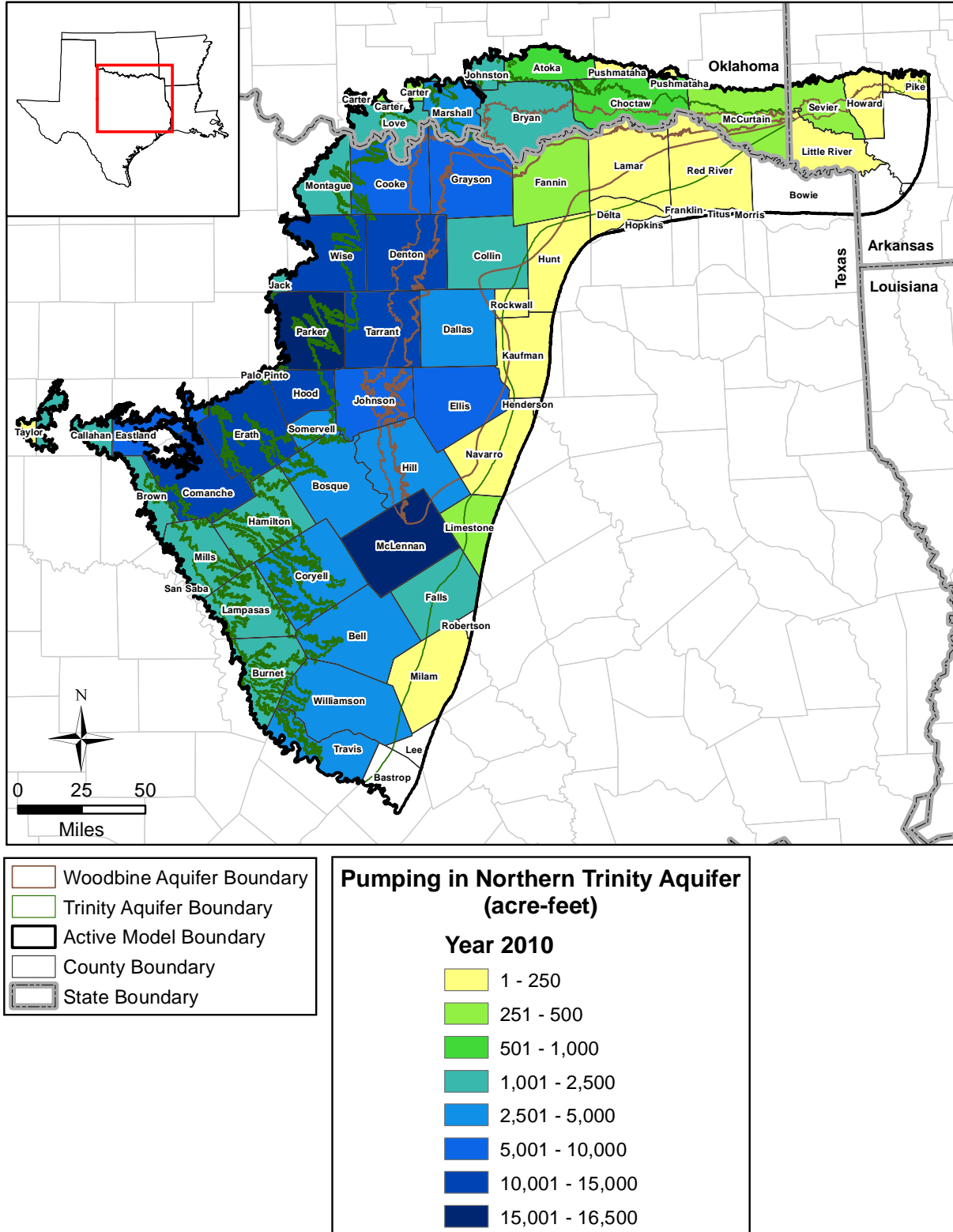
Figure 4.7.21   Estimated groundwater pumping from the northern Trinity Aquifer in 2010 by county.

(a)

(b)
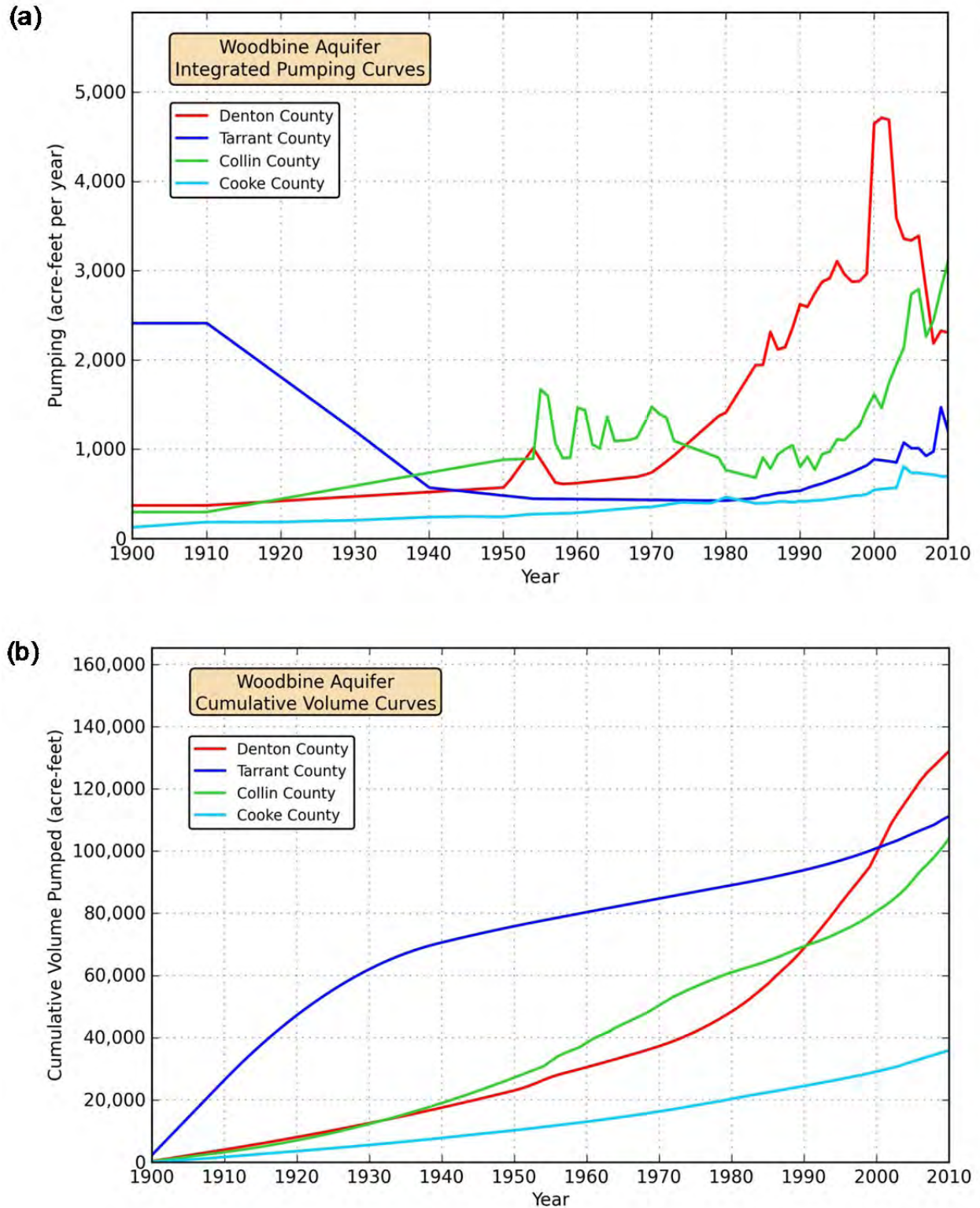
**Figure 4.7.22   Times series of (a) integrated pumping curves and (b) estimated historical volumes
pumped through 2010 for the Woodbine Aquifer in the counties of the North Texas
and Northern Trinity GCDs.**
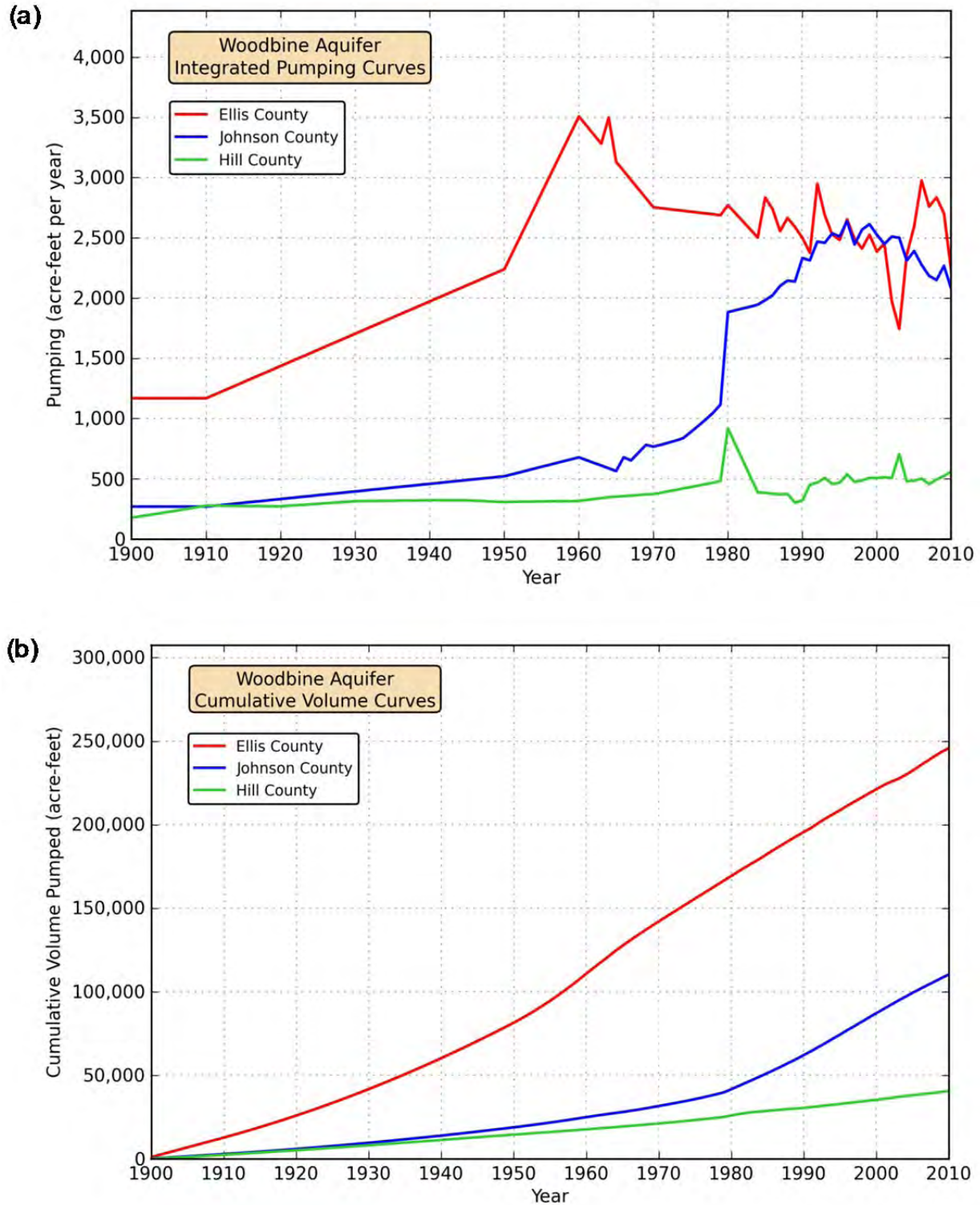
Figure 4.7.23   Times series of (a) integrated pumping curves and (b) estimated historical volumes pumped through 2010 for the Woodbine Aquifer in the counties of the Prairielands GCD.
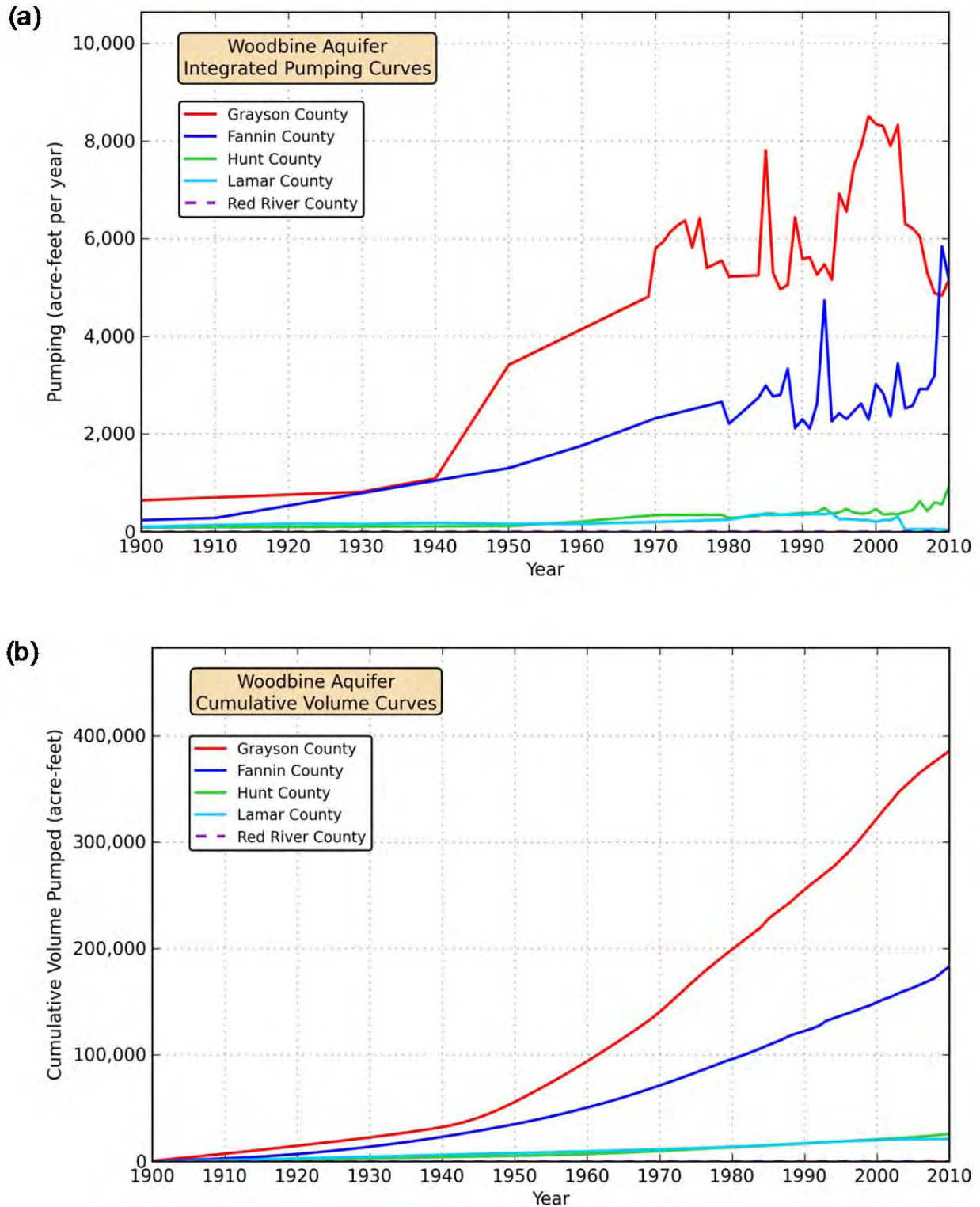
Figure 4.7.24   Times series of (a) integrated pumping curves and (b) estimated historical volumes pumped through 2010 for the Woodbine Aquifer in Fannin, Grayson, Hunt, Lamar, and Red River counties.
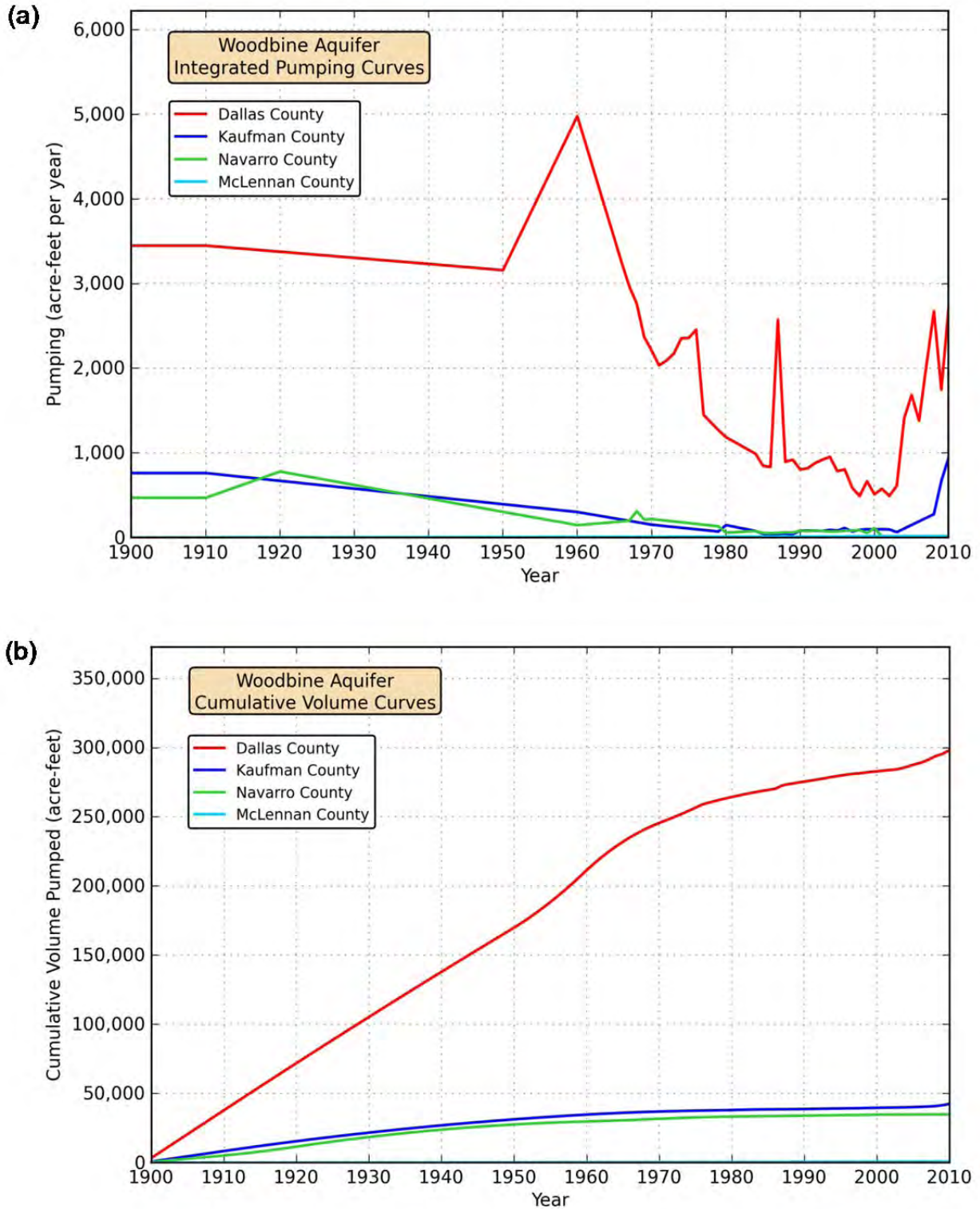
Figure 4.7.25 Times series of (a) integrated pumping curves and (b) estimated historical volumes pumped through 2010 for the Woodbine Aquifer in Dallas, Kaufman, McLennan, and Navarro counties.
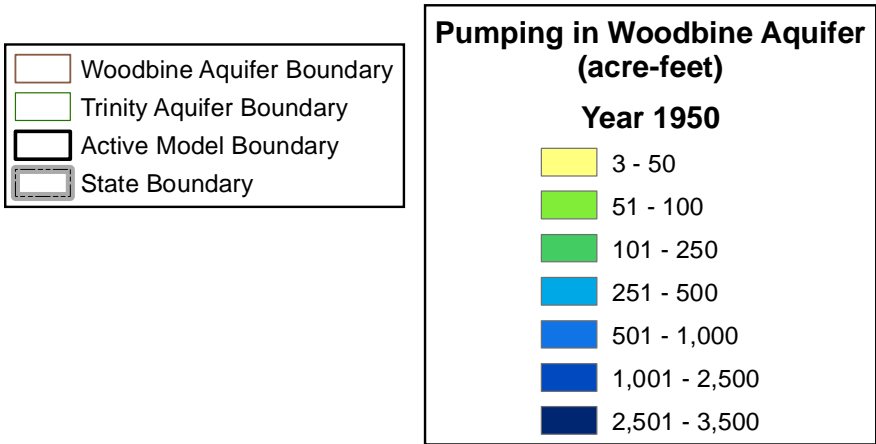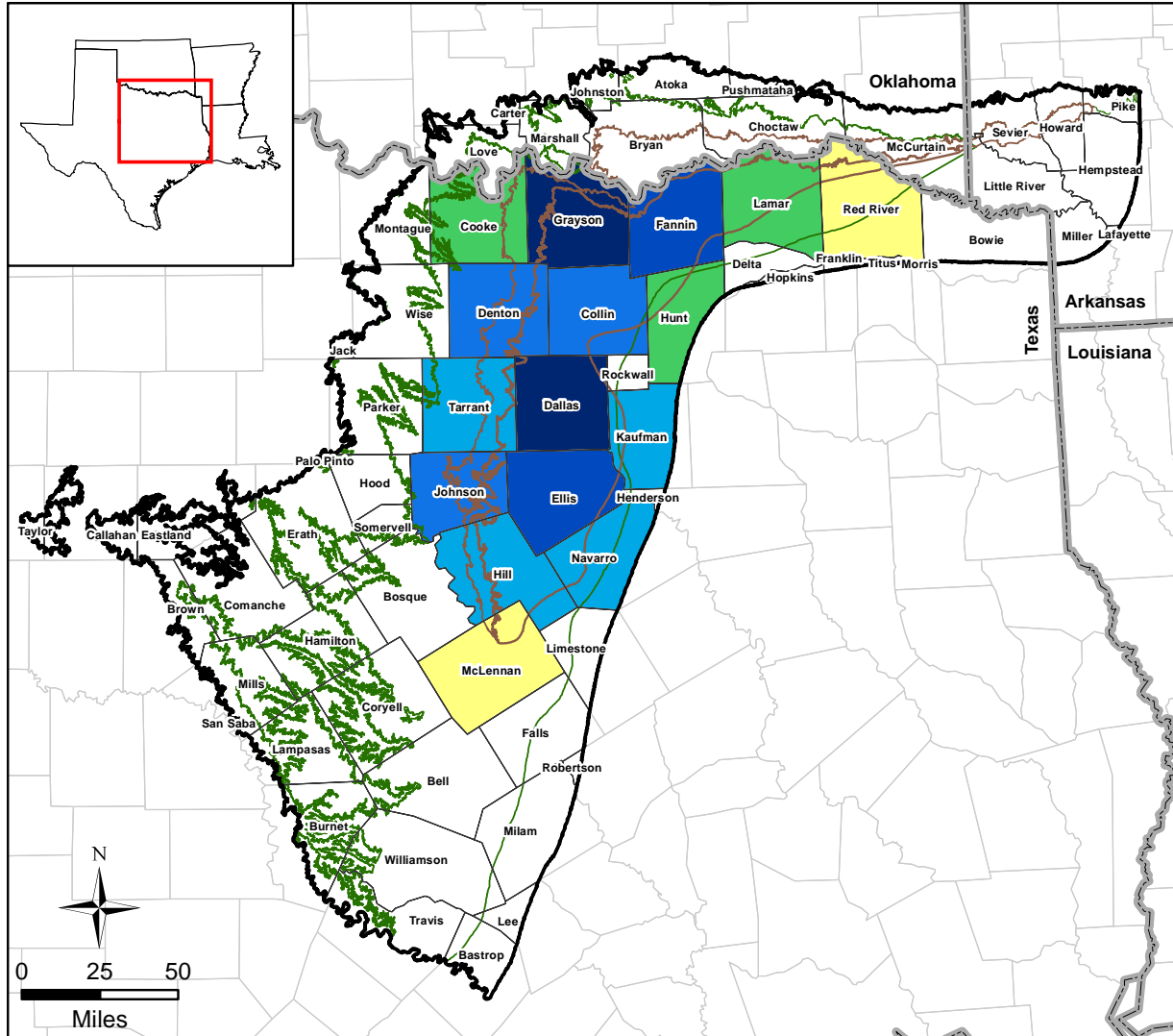
Figure 4.7.26   Estimated groundwater pumping from the Woodbine Aquifer in 1950 by county.
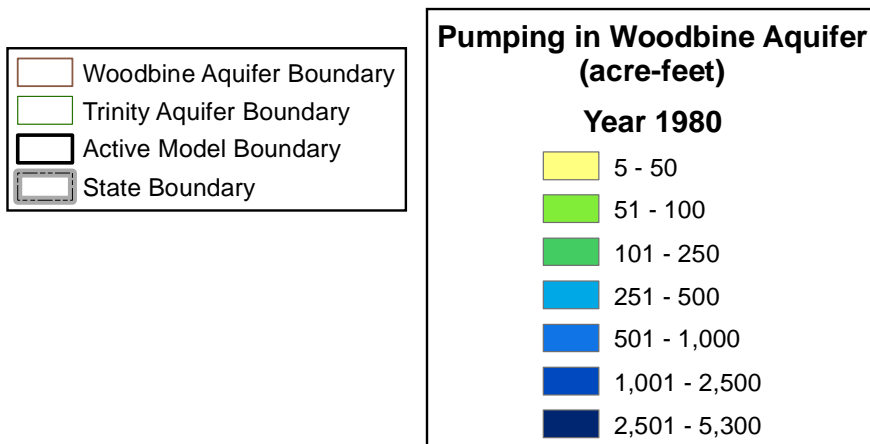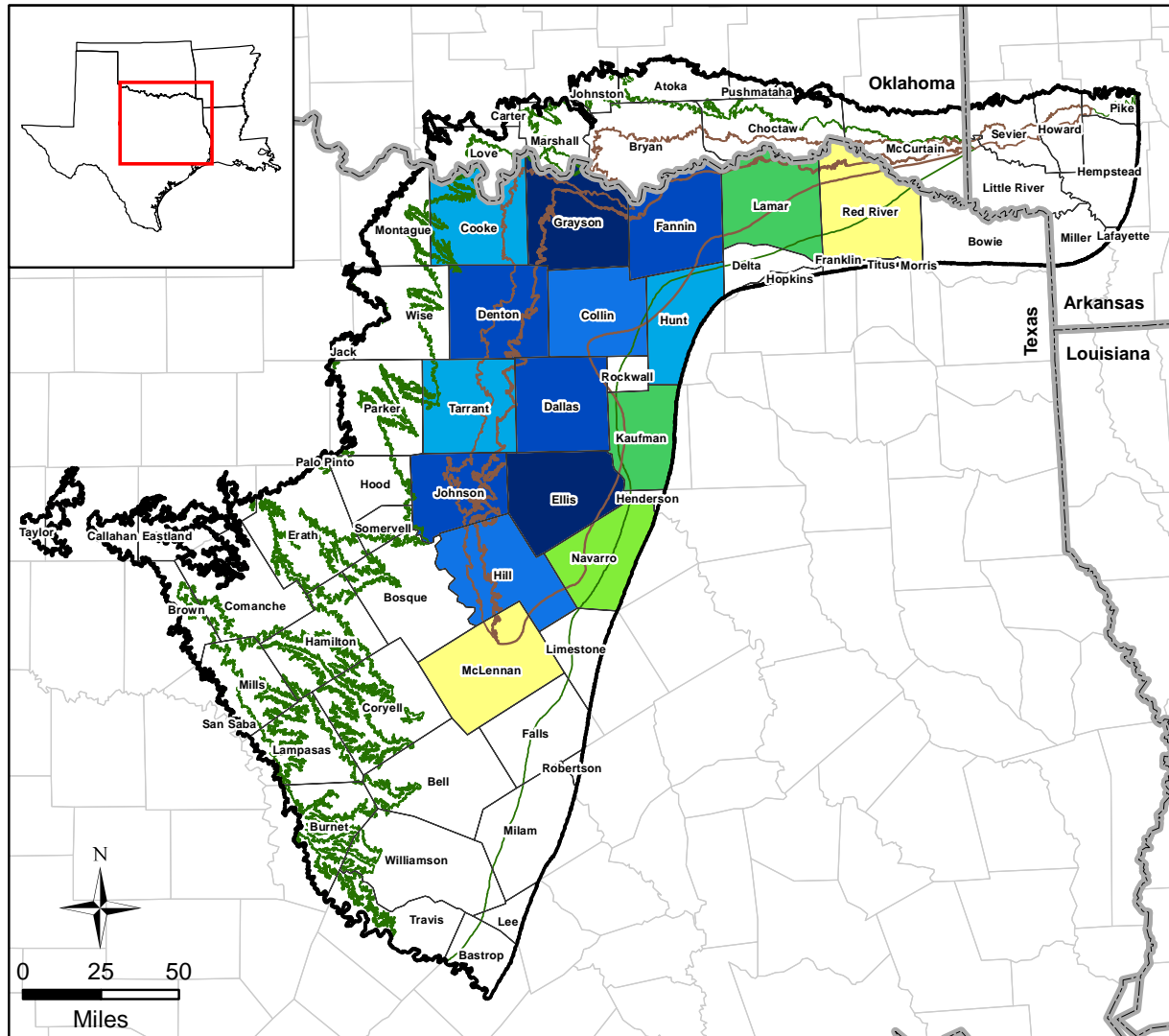
Figure 4.7.27   Estimated groundwater pumping from the Woodbine Aquifer in 1980 by county.
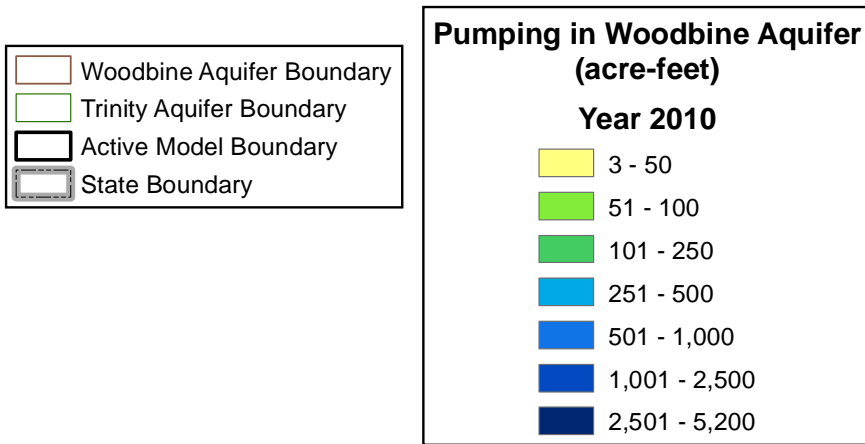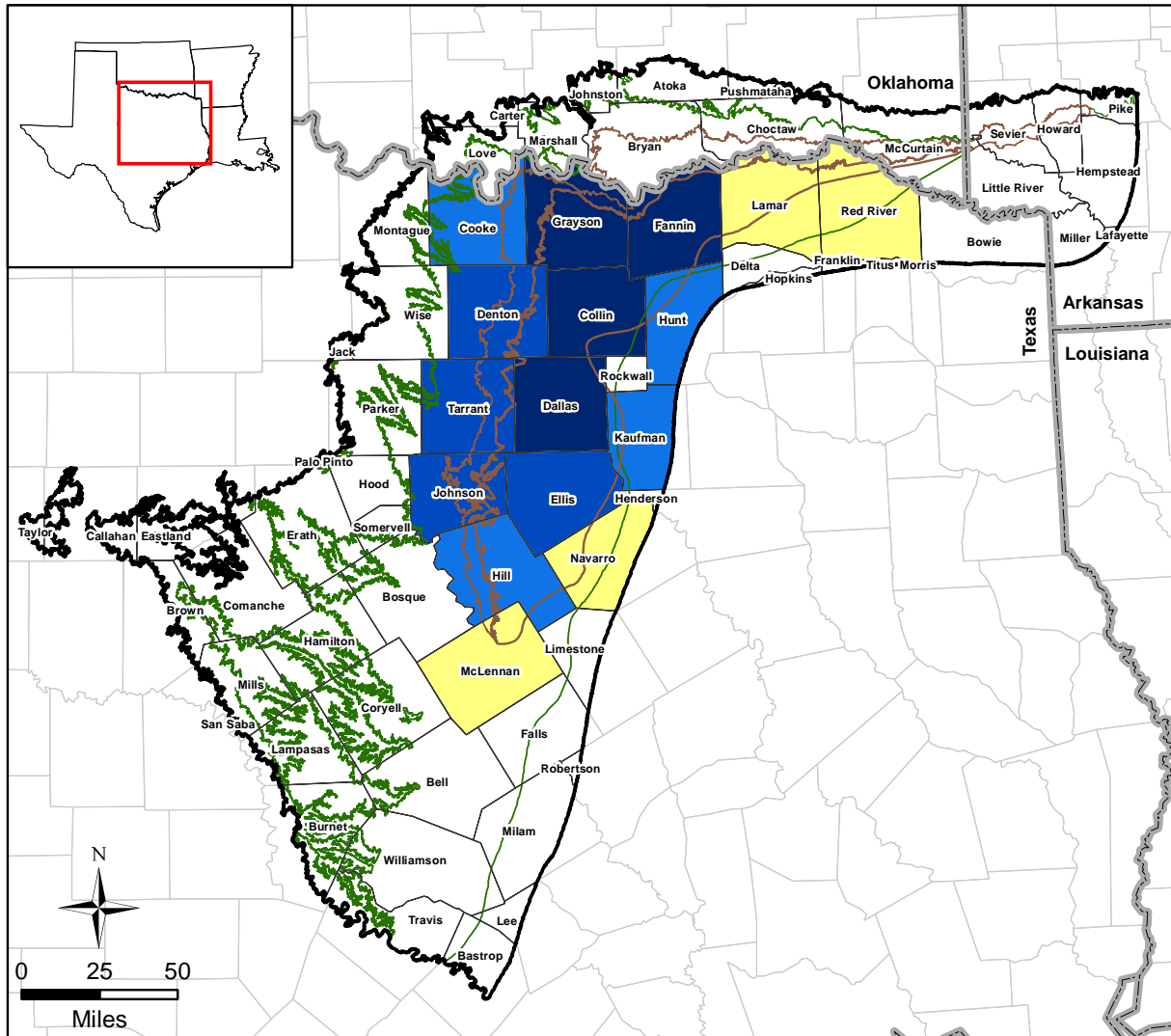
Figure 4.7.28   Estimated groundwater pumping from the Woodbine Aquifer in 2010 by county.
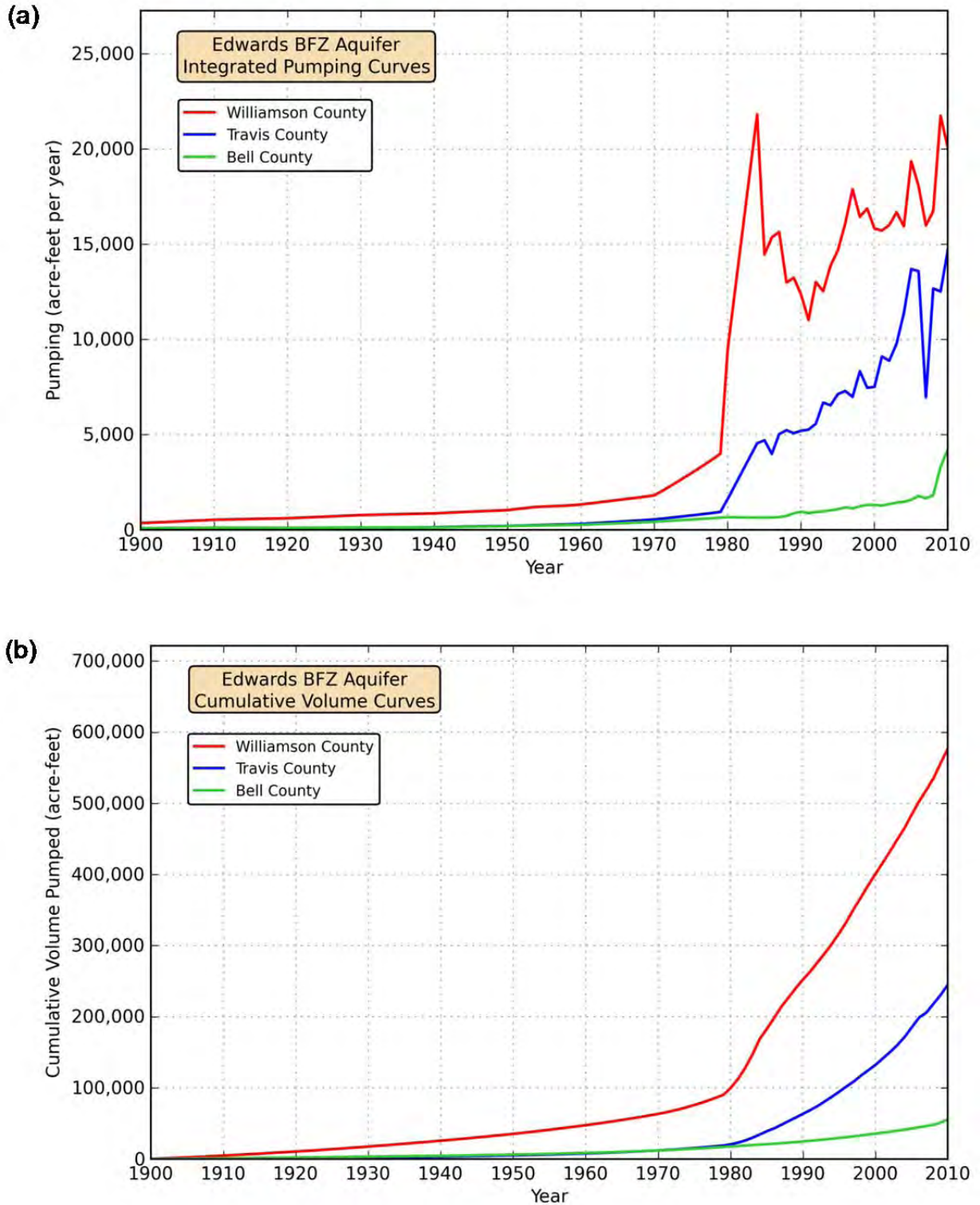
Figure 4.7.29   Times series of (a) integrated pumping curves and (b) estimated historical volumes pumped through 2010 for the Edwards BFZ Aquifer in Bell, Travis, and Williamson counties.

5.0 Conceptual Model for Groundwater Flow in the Northern Trinity and Woodbine Aquifers

The American Society for Testing and Materials (ASTM) define a groundwater conceptual model as an interpretation or working description of the characteristics and dynamics of the physical groundwater system (ASTM D5447-04) (ASTM International, 2004). The purpose of the conceptual model is to integrate site and regional hydrogeologic data into a set of assumptions and concepts that can be evaluated quantitatively using a groundwater flow model. The conceptual model for groundwater flow in the northern Trinity and Woodbine aquifers is based on the hydrogeologic setting, described in Section 4 of this report, which integrates, presents, and discusses studies and data regarding the northern Trinity and Woodbine aquifers. The conceptual model is a simplified representation of the hydrogeological features that govern groundwater flow in the aquifers. These include aquifer hydrostratigraphy, hydraulic properties, hydraulic heads, recharge, mechanisms of natural discharge, and anthropogenic discharge mechanisms including pumping and flowing wells.

Each of the elements of the conceptual model is discussed below with an attempt to summarize the key processes controlling groundwater flow in the northern Trinity and Woodbine Aquifers. This section ends with a summary of the conceptual model and a graphic showing the model layers developed based on the hydrostratigraphic layers defined in Section 4.1, the groundwater flow directions, and model inflows and outflows.

5.1 Hydrogeologic Framework

The rocks and sediments that host the northern Trinity and Woodbine aquifers formed during the geologic time period known as the Cretaceous Period, which lasted from about 145 to 65 million years ago. Cretaceous-age rocks are exposed at the surface across broad areas of Texas. The geologic units that make up the northern Trinity and Woodbine aquifers extend from the Colorado River near Austin north to southern Oklahoma and into southwestern Arkansas. Cretaceous-age stratigraphic units in central and north-central Texas lie on the northwestern margin of the Gulf of Mexico Basin. Through geologic time, the Gulf of Mexico Basin has progressively filled from the margins toward the center until achieving the shoreline configuration that exists today. Cretaceous-age strata are the oldest part of the Gulf of Mexico

Basin fill that is still exposed at the surface. The Cretaceous-age sediments were unconformably deposited on an erosional surface of Paleozoic-age geologic units of predominantly Permian- and Pennsylvanian-age. The wedge of Cretaceous-age sediments dips and thickens towards the East Texas Basin to the east, which is an ancient embayment of the Gulf of Mexico Basin that is now filled with sedimentary deposits. In many areas, especially towards the western limits of the northern Trinity Aquifer, the northern Trinity Aquifer is in direct hydraulic contact with the permeable portions of the Paleozoic-age systems (Nicot and others, 2012b).

Both the northern Trinity and Woodbine aquifers were deposited in a variety of terrestrial and marine depositional environments. This complexity in depositional environments resulted in a complex system of aquifers that can be mapped in the subsurface but have wide variation in lithology from sand and gravel dominated systems to shale and off-shore limestone dominated systems. This large degree of variability has led to a very complex geologic nomenclature.

Lithologic changes in the horizontal direction, although more gradational than vertical changes, resulted in regional differences in properties of the aquifers and formations that make up the northern Trinity and Woodbine aquifers. The northern Trinity Aquifer is composed entirely of sandstone and shale layers in the north and west, but in the rest of north-central Texas, limestones of the Glen Rose Formation separate sandstones in the lower portion of the northern Trinity Aquifer from those in the upper portion of the aquifer. The lower portion of the northern Trinity Aquifer is further subdivided in the south by limestone and shale in the Pearsall and Sligo formations. To capture geologic variation within the northern Trinity Aquifer, the study area was divided into five regions based on stratigraphic and lithologic similarities. Across these five regions, the geology was further divided into seven aquifers/formations based on significant differences in geologic properties (sandstone-dominated layers versus shale- and limestone-dominated layers). Shales have low hydraulic conductivities and include soluble mineral salts that decrease groundwater quality. Most limestones in the study area possess similar properties. Sand and sandstone, in contrast, typically have high hydraulic conductivities and are composed of relatively insoluble quartz and feldspar grains. Stratigraphic layers are physically continuous across the regions, but layer thicknesses, lithologies, and formation names change. The seven layers used in this study are, from oldest to youngest, the Hosston Aquifer, Pearsall Formation, Hensell Aquifer, Glen Rose Formation, Paluxy Aquifer, Washita/Fredericksburg groups, and Woodbine Aquifer.

The study used 1,302 geophysical logs to correlate stratigraphic boundaries and interpret lithologies. Stratigraphic unit boundaries were defined in outcrop and traced into the subsurface using modern sequence stratigraphy well log correlation techniques. Lithology was interpreted at the scale of 2 to 3 feet creating a high resolution three-dimensional lithologic data set of the aquifers. Net sand and percent sand maps were developed as well as maps of the dominant depositional environments for each aquifer/formation. This study's findings were generally consistent with the established formation definitions. A key focus of this study was establishing regional consistency for the correlation of aquifers/formations across the study area and through the many lithologic changes that occur within any given aquifer/formation.

Structural features that significantly displace aquifers/formations of the northern Trinity and Woodbine aquifers were mapped. The areas where the northern Trinity and Woodbine aquifers exist include three regions of large-scale faulting and structural deformation. The Balcones Fault Zone extends into the model area from the south through Travis, Bell, McLennan, and Hill counties. Displacements on faults in this zone range from 100 to 400 feet, which are sufficient to completely disconnect some layers (Klemt and others, 1975). The Mexia-Talco Fault Zone is a complex zone of interweaving faults that extends along the entire length of the downdip boundary of the study area. Individual faults in the Mexia-Talco Fault Zone have as much as 700 feet of displacement. Fresh groundwater in the northern Trinity and Woodbine aquifers does not extend beyond the Mexia-Talco Fault Zone. An area of faulted and folded strata occurs in Cooke and Grayson counties and extends northwest into Oklahoma. This structurally deformed area is commonly known as the Sherman Syncline and Preston Anticline.

Of the seven aquifers/formations defined in this study, the Hosston, Hensell, Paluxy, and Woodbine aquifers are considered to be aquifers because of their lithologic character (sand dominated over large portions of the study area). The Woodbine Aquifer is sand dominated in north-central Texas but loses significant sand content in the far eastern portions of Texas and Oklahoma and south of McLennan County, where the Woodbine Group is no longer considered an aquifer. The Paluxy Aquifer, also predominantly sand over most of the study area, was deposited in a coastal plain and deltaic environment in all areas except the far southern portion of the study area where it is predominantly a shale unit. The Hensell Aquifer is also predominantly a sand unit, being deposited in a coastal plain and deltaic environment over most of the study

area. The Hosston Aquifer is a sand dominated unit over most of the study area owing to it being

deposited in a coastal fluvial plain depositional environment.

5.2   Aquifer Properties

The aquifer properties that describe the hydraulic behavior of an aquifer are hydraulic conductivity and storativity. These properties are the primary control on groundwater flow rates and volumes and also are important to groundwater quality and chemical composition. Aquifer hydraulic properties are generally estimated through the analysis of aquifer pumping tests and specific capacity tests performed in wells completed in the aquifer of interest. Because storativity cannot be uniquely calculated from single well aquifer pumping tests, which are by far the vast majority of the type tests performed, these storativity data are rare. An exhaustive search for aquifer pumping test and specific capacity test data from which to estimate aquifer hydraulic properties was performed for this study.

This study collected, analyzed, and/or reviewed over 1,000 long-term (24 hours or longer) aquifer pumping tests collected from the TCEQ PWS well records and literature and over 29,000 specific capacity tests obtained from TCEQ well driller's reports. All tests were reviewed for quality of information and completion interval. Tests were rated by the isolation of the corresponding well screen in a particular aquifer/formation, with greater than 60 percent isolation to a specific aquifer/formation preferred. An assessment of the quality of the hydraulic tests resulted in 450 good aquifer pumping tests and 16,000 good specific capacity tests. Hydraulic conductivity values were estimated using multiple data sets including values available from the literature.

A GHS model was used for estimating hydraulic properties for the aquifers and formations in the northern Trinity and Woodbine aquifers. The GHS model combines depositional and lithological information interpreted in this study with aquifer pumping test data collected and analyzed to provide a framework for estimating hydraulic properties for each aquifer/formation in the model. The GHS model was used to provide an initial regional set of aquifer parameters for model calibration and to guide the adjustment of aquifer parameters during model calibration.

Development of the GHS model was performed by correlating hydraulic conductivity values determined from aquifer pumping tests to 10 litho-units and depositional environments. The litho-units are a classification system that comprises the predominant lithology and bed thickness of that lithology in the aquifers. To assist this process, detailed distributions and statistics of sand, shale, limestone, and four other mixed lithology litho-units were calculated for each

aquifer/formation and each depositional environment within that unit. In this analysis, statistics for sand bed thickness at intervals of 4 to 8 feet, 8 to 14 feet, 14 to 25 feet, and greater than 25 feet were developed. The analysis indicated that there are significant and distinguishable differences in the lithology between the aquifers/formations within the northern Trinity and Woodbine aquifers/formations. The Hosston Aquifer showed the lowest percentage of shale and the highest percentage of thick sand beds. The lithologic signatures are consistent with the depositional environments determined for the aquifers/formations. The median hydraulic conductivities for the Woodbine, Paluxy, Hensell, and Hosston aquifers are 2.2, 2.5, 3.8, and 6.8 feet per day, respectively.

Storage properties were compiled from literature for the northern Trinity and Woodbine aquifers. From the review of available aquifer pumping test data, 77 storativity values and 38 specific storage values were compiled. Initial estimates of aquifer storativity were based on literature values and a geomechanical specific storage relationship defined by Shestakov (2002), which calculates specific storage based upon depth of burial.

The aquifers and formations that comprise the northern Trinity and Woodbine aquifers are very stratified in their lithology, even within the more sand rich aquifers (see Figure 4.1.11). As a result, vertical hydraulic conductivity of the aquifers was expected to be very low and limited by the finer grained sediments (shales and limestone). As a result, significant vertical gradients are expected to exist and modeling of the northern Trinity and Woodbine aquifers requires vertical layering at least at the scale of the stratigraphic units that comprise the aquifers and formations.

5.3   Hydraulic Heads and Groundwater Flow

Water levels are generally measured as a depth to water in a well from a known measuring point, such as the top of casing. Because measuring points for wells can exist at a wide range of elevations, hydrogeologists convert depth to water to hydraulic head to understand aquifer hydraulics. Hydraulic head is equal to the height that a water column will rise in a well expressed as an elevation above mean sea level. By using elevation and the common datum of sea level, hydraulic head is a measure of potential energy that provides the information needed to estimate groundwater flow directions and, in combination with aquifer properties, provides the volume and velocity of flow within an aquifer.

Figure 5.3.1 is a schematic cross section of the northern Trinity and Woodbine aquifers showing idealized flow vectors during predevelopment. In this condition, the flow system is composed of a hierarchal set of flow systems. Very shallow, unconfined flow systems that extend from hills to valleys occur in the outcrop areas. Very deep flow systems consist of flow from recharge areas in the outcrops to the deep, confined portions of the aquifers downdip of the outcrop. This deep flow slowly discharges to shallower aquifers and aquitards (Toth, 1963). As discussed below, the shallow recharge-discharge flow systems is conceptualizes as transmitting the bulk of the aquifer flow to surficial discharge mechanisms such as streams, springs, and ET in the outcrop.

In layered aquifer systems such as the northern Trinity and Woodbine aquifers where the outcrop is at a significantly higher elevation than the deeper confined portions of the aquifers, hydraulic heads in the deeper aquifer become confined and, in some cases, can be higher than ground surface. Wells completed in areas of the aquifer where hydraulic heads were historically higher than ground surface flowed and those wells have historically been termed artesian wells. Because of the topographic slope, the availability of recharge in the outcrop, and high horizontal hydraulic conductivity relative to vertical hydraulic conductivity in these highly-stratified aquifers, artesian wells historically have been prolific in the northern Trinity and Woodbine aquifers.

Hydraulic heads have declined since the late 1800s in the northern Trinity and Woodbine aquifers starting with the drilling of wells and the practice of allowing early artesian wells to freely flow. Hill (1901) mapped the artesian zone of the northern Trinity and Woodbine aquifers

in north-central Texas. Figure 5.3.2 shows vintage post cards (Mace, 2013) of a new artesian well in Forney, Texas and an artesian well called the Sulphur Well in Glen Rose, Texas. Flowing wells were common during early development of the aquifers but many of them had diminished flows or stopped flowing by the early part of the 1900s. Once the hydraulic heads in the flowing wells declined to an elevation equal to the ground surface elevation, the wells would stop flowing. The historical presence of deep flowing wells indicates that in predevelopment vertical gradients in hydraulic heads in the confined portions of the northern Trinity and Woodbine aquifers were directed upward. This was especially true in topographically low areas of the study area.

An extensive data search was performed to collect as many aquifer water levels as possible from all available sources including the TWDB, technical reports, GCDs in the study area, and the USGS. Water-level data were used to determine hydraulic heads in the aquifers. A data set of over 98,000 water-level measurements was developed. While development of the aquifers began in the late 1800s, water-level data in the study area prior to the 1940s is uncommon. Water-level data were collected to estimate historical hydraulic head surfaces and historical hydraulic head declines, evaluate the transient behavior of hydraulic heads observed in wells, identify hydraulic head calibration targets for model calibration, and investigate vertical hydraulic head gradients.

Water-level data were filtered to retain only those data for wells that had adequate information to calculate hydraulic heads, had adequate completion information to define the completion interval, and met criteria to be a publishable value in the TWDB groundwater database. Because of the thin nature of the sands in the northern Trinity Aquifer, many wells are completed across multiple aquifers/formations, which complicated the assessment of hydraulic heads for an aquifer/formation. For multi-completed wells, the measured water level in the well does not represent a particular unit, but rather is a composite water level. The completion of wells across many aquifers/formations also enhances cross-formational flow and potentially can affect water quality within aquifers. While composite water levels may be used for model calibration, they are not useful for developing hydraulic head surfaces for individual stratigraphic units.

Assessments of regional groundwater flow direction and historical hydraulic head declines required development of regional hydraulic head surfaces. In creating those surfaces, hydraulic head data for wells completed in a single aquifer/formation were used. Hydraulic head surfaces

were created that represent predevelopment conditions. The data available for predevelopment were very sparse and almost entirely found in the confined sections of the aquifer. Predevelopment hydraulic heads in the outcrop areas were conceptualized as relatively near land surface, but their exact distribution is uncertain.

Historical hydraulic head surfaces were developed for the Woodbine, Paluxy, Hensell, and Hosston aquifers for 1950, 1970, 1990, and 2010. In addition, the estimated hydraulic head decline from predevelopment to 1950 and predevelopment to 2010 was estimated on a regional basis for these aquifers to the degree possible. Declines from predevelopment to 2010 in the confined portion of the Woodbine Aquifer range from about 200 to 400 feet. Declines in hydraulic heads in the Paluxy Aquifer from predevelopment to 2010 range from approximately 10 to 200 feet in the outcrop to as much as 700 feet in Dallas and Tarrant counties in the confined portion of the aquifer. Hydraulic head declines in the Hensell Aquifer from predevelopment to 2010 range from 25 to 400 feet in a drawdown cone centered west of McLennan County. The declines in the Hosston Aquifer between predevelopment and 2010 are regionally extensive, with drawdown centered in Tarrant, Johnson, and Ellis counties with declines of as much as 1,200 feet observed.

In addition to hydraulic head surfaces, time-series data (hydrographs) of hydraulic head data were developed and analyzed for time trends for model calibration. An analysis of vertical hydraulic gradients indicated that the upward hydraulic gradients prevalent in predevelopment times had been altered by pumping in the historical period. Using transient data from closely spaced wells completed in different aquifers, it was found that vertical hydraulic gradients were down from the Woodbine Aquifer to the Paluxy Aquifer, from the Paluxy Aquifer to the Hensell Aquifer, and from the Hensell Aquifer to the Hosston Aquifer in confined portions analyzed. This clearly demonstrates a reversal in vertical hydraulic gradients in areas of the confined system, the result of pumping and associated drawdown. Figure 5.3.3 is a schematic cross section of the northern Trinity and Woodbine aquifers showing idealized flow lines after development. A comparison of Figures 5.3.1 and 5.3.3 shows that pumping reverses vertical flow directions locally in the aquifers as a result of drawdown at depth.

Significant hydraulic head declines have also occurred in the outcrop areas of the northern Trinity and Woodbine aquifers. The declines are typically far less than those in the confined

portion because unconfined storage is several orders of magnitude greater than confined storage. Quantitative analyses of hydraulic head declines in the outcrop were difficult because of very few early water-level measurements in the outcrop areas. An analysis of hydraulic head declines in the outcrop areas of the northern Trinity and Woodbine aquifers from 1950 to after 2000 show that many areas in the Woodbine Aquifer outcrop have consistent declines in water levels, such as in Fannin, Grayson, Cooke and northern Denton counties. In the northern Trinity Aquifer, many wells indicate decreasing trends ranging from 0.1 foot per year to almost 3 feet per year in the outcrop areas, while many other wells are stable or in some cases slightly increasing.
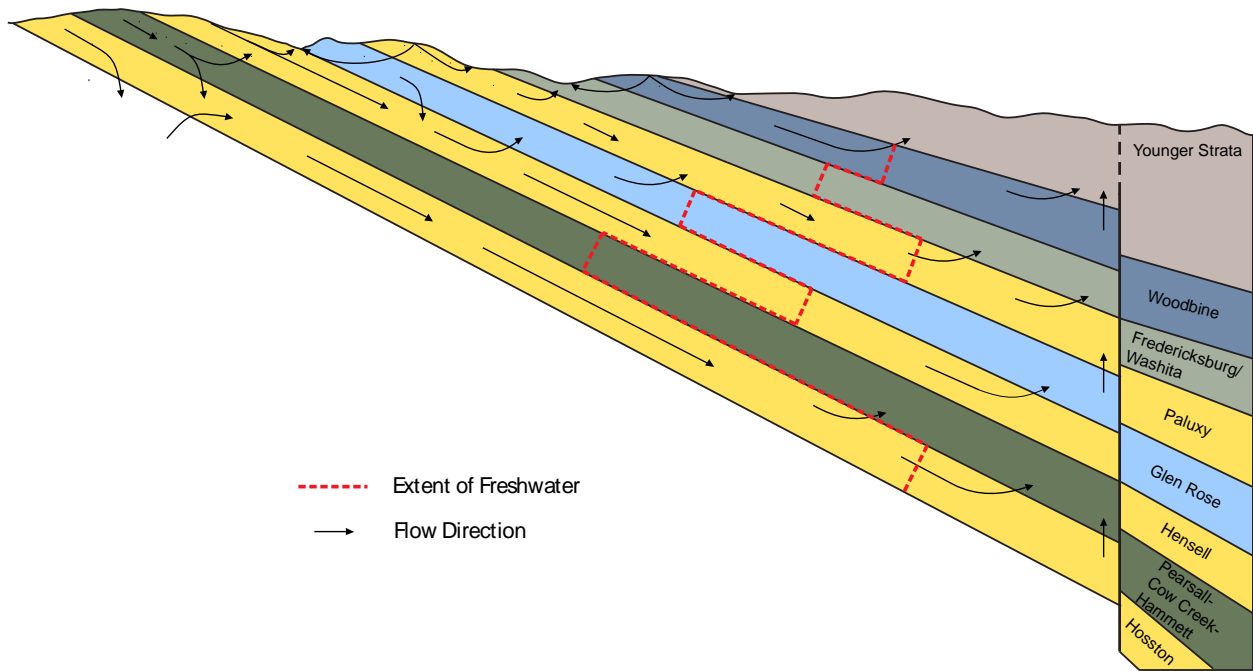
Figure 5.3.1   Schematic cross section of predevelopment conditions.

**Figure 5.3.2   Vintage post cards of flow from artesian wells in the northern Trinity Aquifer
[courtesy of Robert Mace, TWDB, Mace (2013)]**

Younger Strata

Woodbine

Fredericksburg/
Washita

Paluxy

Glen Rose

Hensell

Pearsall-
Cow Creek-
Hammett

Hosston

Flow Direction
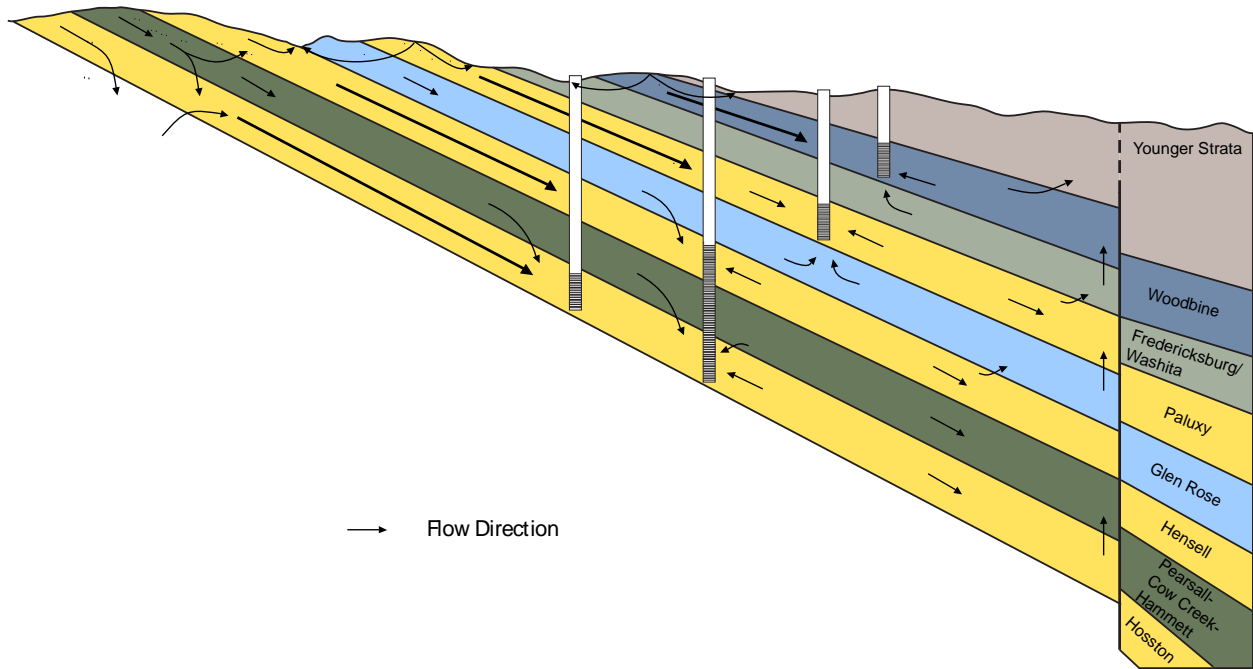
Figure 5.3.3   Schematic cross section of aquifer conditions after development.

This page intentionally left blank.

5.4   Recharge and Natural Aquifer Discharge

Recharge is defined in this study as downward flow of water reaching the water table and increasing groundwater storage (Healy, 2010). Prior to aquifer development, recharge is in equilibrium with aquifer discharge on average.

The dominant controls on recharge include precipitation, vegetation/land use, and soil characteristics (Keese and others, 2005). Potential sources of recharge to the aquifer include precipitation, irrigation return flow, and stream/reservoir leakage. Recharge can be a diffuse process if it is areally distributed, such as that derived from precipitation or irrigation return flow, or focused and occurring in localized areas, such as river or reservoir leakage. Reservoir leakage into the northern Trinity and Woodbine aquifers has been reported by several authors (Leggat, 1957; Klemt and others, 1975; Nordstrom, 1982).

Precipitation falling on the land surface partitions into evaporation from bare soil and transpiration from vegetation, runoff, and infiltration into the soil profile. Most of the infiltrated water is lost through bare soil evaporation near the surface or from transpiration through vegetation. Generally, a small fraction of the water moves below the root zone of the vegetation to recharge the aquifer and is initially stored in the unconfined portions of the aquifer closest to ground surface. The vast majority of recharge discharges locally in the outcrop area to streams and/or springs, as groundwater ET, and/or through pumping after development begins. However, some of the recharge in the unconfined aquifer moves down into the semi-confined and confined portions of the aquifer below the outcrop area before discharging locally to surficial features. A much smaller percent of recharge flows into the confined portion of the aquifer downdip of the outcrop area and discharges regionally through diffuse discharge through younger overlying sediments or through structural features such as faults. In addition to precipitation, there are many potential spatial variables that may impact recharge including soil permeability and dominant land use, such as irrigation in the west (especially Callahan, Eastland, Brown, and Comanche counties) and urbanization in the Dallas-Fort Worth Metroplex.

Several methods were used to estimate recharge including water balance methods, the CMB method, and stream hydrograph separation analyses. Stream hydrograph separation analysis (sometimes referred to as base flow analysis) was conducted on 36 stream gages and associated watersheds intersecting the outcrops of the northern Trinity Aquifer, Washita/Fredericksburg

groups, and Woodbine Aquifer. Aquifer discharge to streams, or base flow, is considered to be a lower bound estimate of aquifer recharge because some aquifer recharge discharges through the processes of groundwater ET, spring discharge, and pumping capture prior to discharging to streams. Also, some fraction of shallow recharge moves into the confined portion of the aquifer downdip of the outcrop and discharges through regional flow to younger units.

The results from the hydrograph separation analyses were used to develop a spatial and temporal model for recharge. The model was based upon regressions between annual average base flow and annual average precipitation. Because precipitation varies both spatially and temporally, the recharge model provides a method to estimate aquifer recharge across the study area for the expected range in precipitation. Average recharge ranged from a high of 5.3 inches per year in the far northeastern areas of the model outcrop to 0.6 inches per year in the far southwest. The estimated average recharge to the northern Trinity and Woodbine aquifers (including the Fredericksburg/Washita groups) based upon the hydrograph separation model totals 1,909,360 AFY, which is approximately 4.7 percent of precipitation model wide. The advantage of using hydrograph separation analyses to estimate recharge is that it provides an integrated recharge estimate over a large area of outcrop. In that sense, it averages local natural variability in recharge that is often poorly understood without local field studies and that would be averaged in a regional-scale groundwater model.

Based on hydrograph separation analyses of stream gage data, recharge is estimated to be approximately 5 percent of precipitation. While hydrograph separation analyses provide a bounding estimate of recharge, determining the amount of recharge that reaches the deeper confined portions of an aquifer downdip of the outcrop area is much harder to estimate with certainty. Often groundwater modeling or environmental tracers, such as isotopes, can provide some estimates. For conceptual purposes, it was assumed that of the 5 percent of precipitation that recharges the aquifer, more than 90 percent of that discharges within the outcrop to streams, springs, and groundwater ET. An estimated 40 percent of recharge moves into the deeper confined portions of the aquifers in the outcrop area before discharging in the outcrop. The amount of recharge that reaches the deeper confined portions of the aquifers downdip of the outcrop area is estimated to be less than 10 percent of recharge. Two things are believed to contribute to the relatively low rates of downdip recharge; the vertical confinement of the aquifer

because of the very stratified nature of the deposits and the very large outcrop area compared to

the relatively thin aquifers in the northern Trinity Aquifer.

This page intentionally left blank.

5.5 Groundwater Quality

The sediments that make up the northern Trinity and Woodbine aquifers were deposited in a mix of coastal plain, deltaic, and marine depositional environments and were likely inundated with a shallow salt-water sea as late as the late Cretaceous Period some 65 million years before present. Therefore, the water initially present in the sediments after deposition was saline. This water is initially trapped in the sediments after deposition. However, the sediments that comprise the northern Trinity and Woodbine aquifers have been subaerially exposed since the beginning of the Tertiary Period, perhaps as far back as 60 million years before present. With the aquifers above sea level, the original saline water will begin to be displaced by, and mixed with, freshwater from natural precipitation on the outcrop (Meinzer, 1923). The displacement generally occurs over a regional scale and over long time periods. This occurs when two criteria are met: (1) the permeable aquifer units are uplifted relative to sea level such that the aquifer units are at the surface to receive meteoric water and (2) the downdip portions of the aquifers have outlets through which the original connate water can be displaced (Domenico and Robbins, 1985). Both conditions appear to have been present in the northern Trinity and Woodbine aquifers for many millions of years.

Several factors have been proposed to affect the water quality in the northern Trinity and Woodbine aquifers. The dominant process is the natural dissolution of minerals and geochemical evolution that occurs as groundwater moves from recharge in the outcrop area to local and regional discharge pathways. In general, groundwater quality degrades as groundwater residence time increases. Other natural factors that affect water quality in the northern Trinity and Woodbine aquifers are deep-seated geologic structural features. The most important of these include the Mexia-Talco Fault Zone, the Balcones Fault Zone, and the Sherman Syncline and Preston Anticline. These structural features can alter water quality through the disconnection of permeable aquifers or through the vertical migration of poorer water quality along faults. Evidence for both exists in the northern Trinity and Woodbine aquifers.

This study reviewed the relevant literature discussing water quality of the northern Trinity and Woodbine aquifers and developed maps of TDS, chloride, and hydrogeochemical facies to better describe and understand the hydrodynamics of the aquifers. This study did not look at historical trends in water quality, which has been the subject of many studies in the northern Trinity and

Woodbine aquifers. The hydrogeochemical facies analysis suggests that the northern Trinity and Woodbine aquifer outcrop areas are an active recharge zone with a strong similarity in groundwater chemistry (calcium-magnesium facies) in the outcrop suggesting a well-connected shallow groundwater system. The hydrogeochemical facies provide evidence of vertical downward cross-formation flow in the southern portion of the study area where the aquifers have broad and low dipping outcrops. This conclusion is consistent with Rapp (1988).

Some anomalous hydrogeochemical facies were found in the aquifers. A sulfate hydrogeochemical facies is scattered within the outcrop of the Woodbine Aquifer and is considered to result from the presence of lignite beds. Another notable finding is the occurrence of sodium-chloride facies in the Hosston Aquifer in Denton and Collin counties and in Bell, Coryell, and northern Williamson counties. For these two areas, chloride concentrations between 100 and 500 milligrams per liter have been measured. These values are about two to three times the values of chloride measured in most other wells in the Hosston Aquifer. Based on the regional change of increases in chloride concentration with distance in the rest of the Hosston Aquifer and the other aquifers/formations, the source of the chloride is not likely mixing with groundwater from any of the units above the Hosston Aquifer. Two potential explanations for the elevated chlorides are upwelling of brines at the faults located by the high chloride concentrations or the upward migration of chlorides from the underlying Paleozoic-age sands caused by pumping the Hosston Aquifer.

TDS measurements were used to map the extent of freshwater as defined by groundwater samples with TDS concentrations less than or equal to 1,000 milligrams per liter (Figure 5.5.1). The Hosston Aquifer has the farthest downdip extent of freshwater extending, about 100 miles southeast from the northern Trinity Aquifer outcrop to Falls County with numerous freshwater wells in McLennan County. The Woodbine Aquifer has the least downdip penetration of freshwater of the aquifers in the northern Trinity and Woodbine aquifers. For most of the southern extent of the Woodbine Aquifer, the 1,000 milligrams per liter contour is about 20 miles from outcrop and is less than 5 miles in Dallas County. The short distance to brackish water is attributed primarily to the prevalence of deposits of lignite, anhydrite, and gypsum in the Woodbine Aquifer. In the northern portion of the Woodbine Aquifer (middle of Denton County) the location of the 1,000 milligrams per liter contour is considerable farther downdip than in the southern portion of the aquifer.

Domenico and Robbins (1985) found that the steady-state chemistry of an aquifer which has undergone displacement and or mixing of freshwater from recharge with initially saline aquifer water may vary widely from almost all freshwater to a mix of fresh and saline water with more saline waters being found near the discharge boundaries of the aquifer. Their research suggests that the degree at which freshwater exists within an aquifer at steady-state (predevelopment) is a function of the geometry of the recharge area as well as the heterogeneity of the aquifer materials and the natural geochemical processes between groundwater and aquifer minerals.

The freshwater extents and groundwater chemistry of the Hosston, Hensell, and Paluxy aquifers suggest that downdip flow occurred under predevelopment conditions. With the beginning of aquifer development and pumping, this downdip flow has likely increased significantly in the northern Trinity and Woodbine aquifers in the historical period as a result of pumping.

The conceptual model of the northern Trinity and Woodbine aquifers developed from this study suggests that during predevelopment conditions, higher hydraulic heads in the Hosston Aquifer than in the overlying aquifers/formations permitted enough upward vertical leakage to allow the downdip migration of low TDS waters from the outcrop area toward the southeast. After pumping in the Hosston Aquifer began and the vertical hydraulic gradients eventually reversed, groundwater with higher sulfate concentration from the overlying Glen Rose Formation and Hensell Aquifer have the potential to migrate downward through the Pearsall Formation into the Hosston Aquifer. More likely, after the onset of pumping, the mixing of waters among the aquifers and formations has likely been enhanced by wells with multiple screens and leaky casing and annulus. While vertical movement of deep groundwater through the Mexia-Talco Fault Zone likely occurs to some extent, the proposed dominant regional outlet for deep confined groundwater downdip of the outcrop is through cross-formational flow.
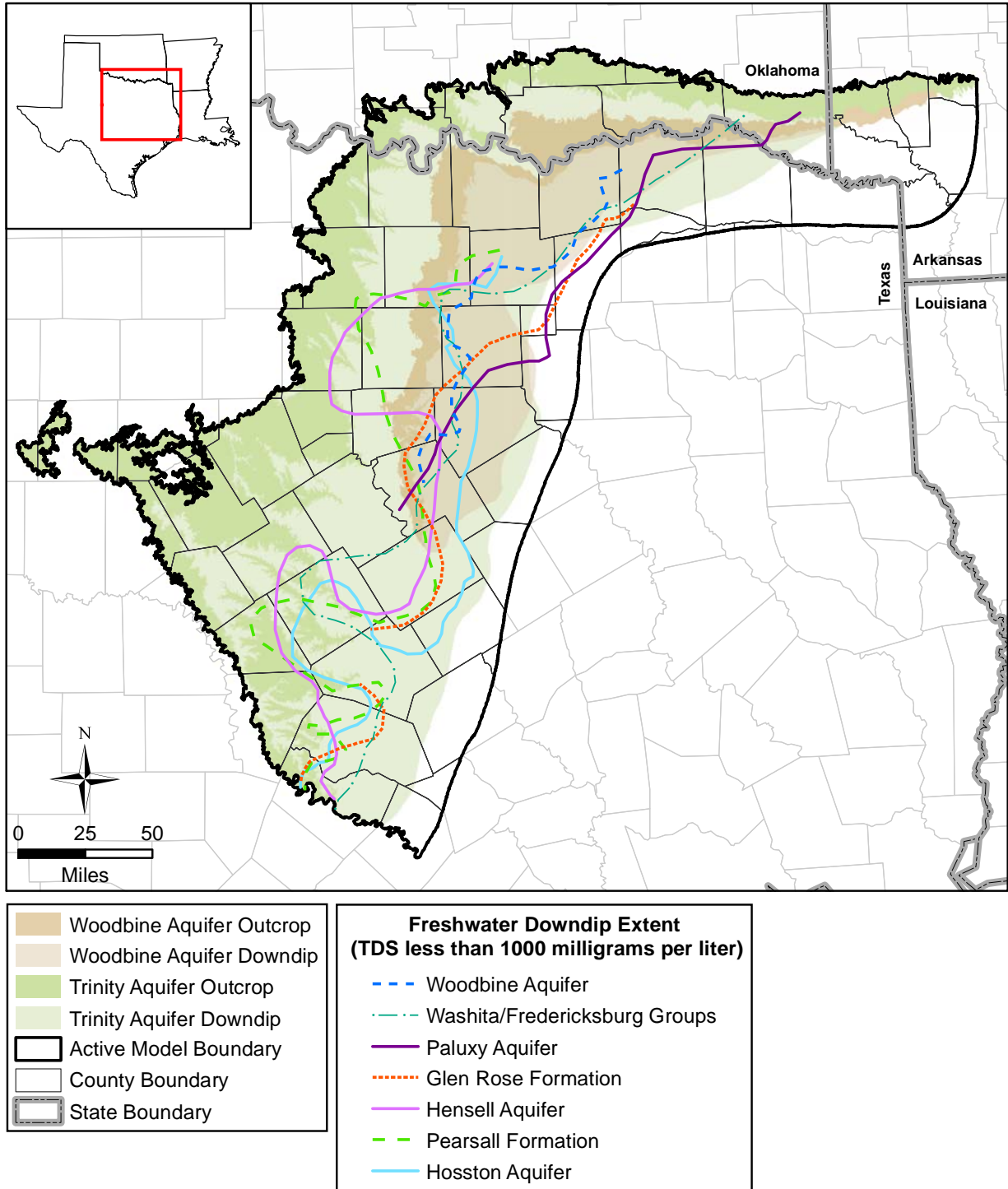
Figure 5.5.1 **Estimate of the extent of freshwater based on groundwater samples by aquifer or formation.**

5.6   Groundwater Pumping

For the northern Trinity and Woodbine aquifers in Texas, estimated historical pumping and discharge from flowing wells were obtained from the literature and calculated for the time period from 1900 to 1980. Water use survey data provided by the TWDB were used to obtain estimated historical pumping for use types municipal, manufacturing, mining (oil and gas is included in this category), power, irrigation, and livestock for the time period 1980 through 2011. Census block data were used to estimate rural domestic pumping during this same time period. Data for mining use in 2011 were obtained from Nicot and others (2011, 2012a). Additional pumping data were received from several of the GCDs in the study area. The time period for GCD data ranges from 2003 to 2012.

In Texas, the Edwards BFZ Aquifer lies within the study area and is a major aquifer as defined by the TWDB. The Edwards BFZ Aquifer has a state approved GAM (Jones, 2003) and this update to the northern Trinity and Woodbine aquifers GAM was not developed to replace or revise it. However, because pumping from that aquifer may impact hydraulic conditions in the underlying northern Trinity Aquifer, estimated pumping for the Edwards BFZ Aquifer was also developed and integrated into the pumping database for this study.

Figure 5.6.1 plots the best estimate of historical pumping in AFY from 1890 through 2010 for all aquifers and groups within the study area. A review of Figure 5.6.1 indicates that the estimated pumping in the northern Trinity Aquifer plateaus at approximately 200,000 AFY since approximately 1984, which is when the TWDB started reporting annual numbers. In 2010, pumping is estimated at 322,000 AFY for all the aquifers and groups in the study domain. The total pumping from all aquifers and groups in the study area has increased since 1980, primarily as a result of increased pumping in the Edwards BFZ Aquifer. Figure 5.6.2 plots the best estimate historical volume pumped in AFY from 1890 through 2010 for all aquifers and groups in the study area. The estimates predict that approximately 12,000,000 and 1,800,000 AFY have been pumped (or discharged through flowing wells) from the northern Trinity and Woodbine aquifers since 1890, respectively.

There are two primary types of uncertainty related to pumping estimates used in numerical models; the magnitude (and timing) of pumping and the location of pumping. The post-development history of the northern Trinity and Woodbine aquifers can be generally divided into

three time periods. The first is from approximately 1890 through 1940. During this period there are little to no pumping measurements and the work of Dutton and others (1996) was heavily relied on to estimate pumping for this period of model development. For the second period, from 1940 through 1980, pumping estimates are available from several historical sources of varying scope. Combined water use survey data available from the TWDB and pumping estimates from GCDs in GMA 8 provide pumping estimates for the third time period from 1980 through 2011.

Because of the large number of free-flowing wells between the late 1800s and about 1930, pumping during this period is uncertain and the uncertainty in the pumping estimates could be 50 percent or greater. Because most of the aquifer discharge during this time period was from flowing wells, the drawdown that could occur over this period would be limited to ground surface at the location of the flowing wells. Because the drawdown that occurred from the 1940s through present far exceeds the elevation of ground surface in the northern Trinity and Woodbine aquifers, the uncertainty in discharge volumes from flowing wells is not critical to model calibration, though it does result in uncertain hydraulic heads beginning in the 1920s. From 1940 through 1980, uncertainty in the pumping magnitude could average 20 to 25 percent and, in some counties, may reach as high as 50 percent based upon variability between published sources. Based on a single case study, the uncertainty in the pumping magnitude for the period from 1980 through 2011 could exceed 20 percent. Because many GCDs within the study area require metering of non-exempt wells, the pumping estimates are certainly improving.
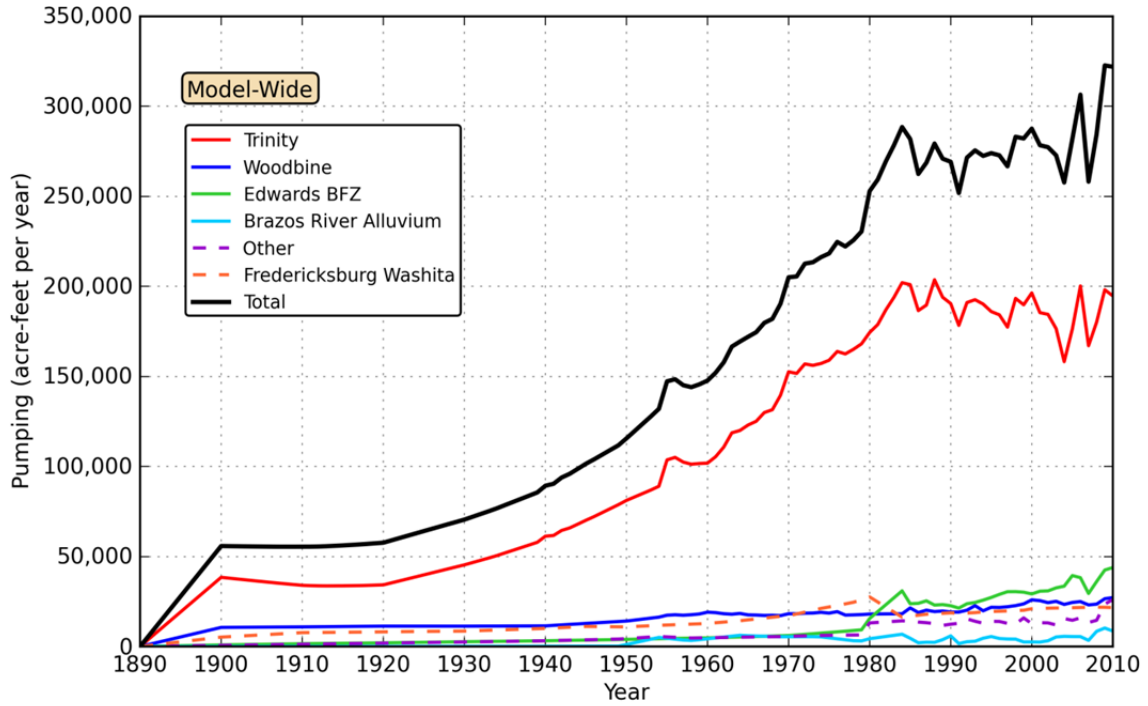
Figure 5.6.1   Estimated historical pumping for the aquifers and groups in the study area.
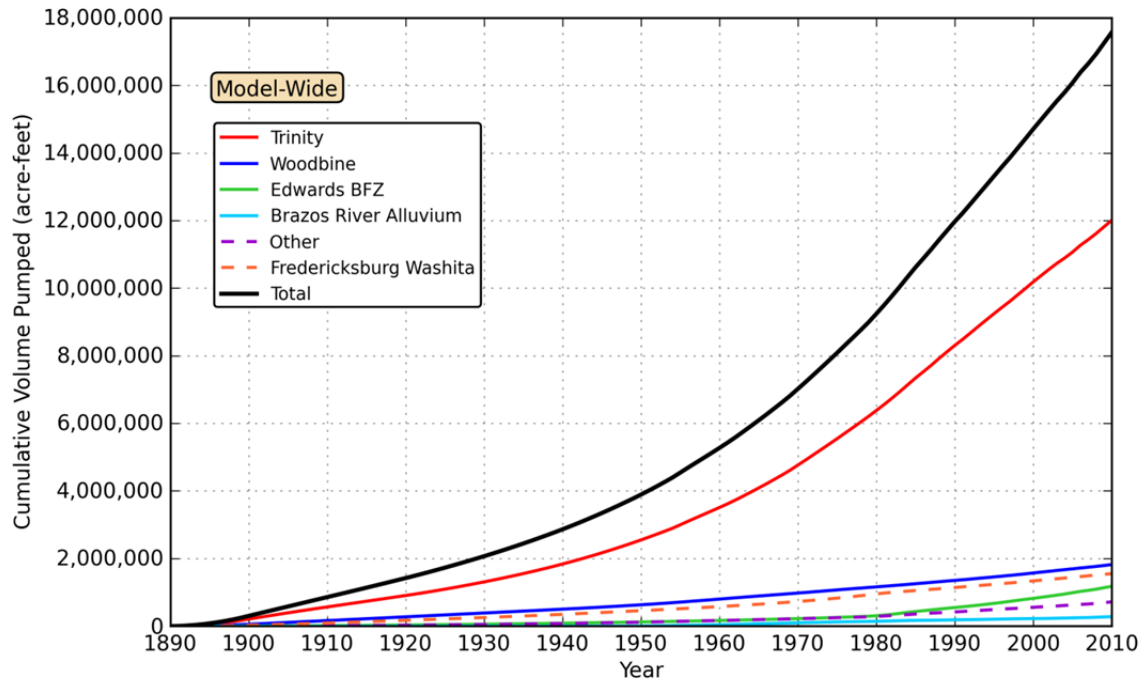
Figure 5.6.2   Estimated historical volume pumped for the aquifers and groups in the study area.

This page intentionally left blank.

5.7   Conceptual Aquifer Water Balance

The preceding discussion focused on the general hydrogeology and groundwater flow within the northern Trinity and Woodbine aquifers. In this section, the conceptual discussion of groundwater flow within these aquifers is expanded to a discussion of the aquifer's conceptual water balance in general terms.

In a natural aquifer system unaffected by anthropogenic activities, the aquifer system is in a long-term dynamic equilibrium condition generally referred to as a steady-state condition (or predevelopment). In this predevelopment state, aquifer recharge is balanced by aquifer discharge resulting in no net change in groundwater storage. Recharge may include areal recharge from precipitation, cross-formational flow from adjacent water bearing formations, and stream losses. Discharge may include stream base flow, spring flow, ET, and cross-formational flow.

Human activities alter the dynamic equilibrium of the predevelopment flow system through pumping withdrawals, changes in recharge through development and irrigation, and changes in vegetation and land use. Generally, groundwater withdrawals due to pumping have the most significant impact on aquifer hydraulics. The water removed by pumping is supplied through decreased groundwater storage, reduced groundwater discharge, and sometimes increased recharge. Generally, increased recharge as a source of water to pumping wells is negligible compared to decreased groundwater storage and decreased aquifer discharge (Alley and others, 1999). If pumping remains relatively constant, a new steady-state condition will be established. In this new case, the source of the pumped water will be drawn from some combination of reduced discharge or increased recharge. Bredehoeft (2002) terms these two volumes as capture. The sources of discharge, which are ultimately captured by pumping, include stream base flow, spring flow, groundwater ET, and cross-formational flow. In the situation of sustainable aquifer dynamics, the pumping rates are matched by the capture in discharge with a net result of water levels becoming stable (albeit at a lower level than prior to development).

The discussion above regarding pumping capture and sustainable aquifer dynamics shows that it is useful to review the conceptual flow balance of an aquifer to understand historical hydraulic heads and also as a pre-cursor to groundwater modeling. Table 5.7.1 presents an estimated average annual conceptual water balance for the northern Trinity and Woodbine aquifers and the Washita/Fredericksburg groups in regions defined as north, central, and south (Figure 5.7.1).

Table 5.7.1 provides an estimate of the recharge rate, the flow rate to the confined portions of the aquifers and formations in the outcrop area and flow to the deeply confined portions of the aquifers and formations downdip of the outcrop. Note that the values in the table are consistent with those shown in Figure 4.5.1. All flow rates are assumed to represent predevelopment conditions and the calculated average groundwater pumping from all aquifers in the study area is based on an average calculated from 1980 through 2010 for the three zones or regions shown in Figure 5.7.1. All rates are in AFY for direct comparison. Table 5.7.1 also provides the recharge flow components expressed as a percentage of average annual precipitation in each zone.

The estimate of average annual recharge is based on the recharge model developed from the results of the stream hydrograph separation analysis presented in Section 4.5. Annual average recharge varies from a high of approximately 1 million AFY (10 percent of precipitation) in the wet and humid north to approximately 350,000 AFY (1.8 percent of precipitation) in the south. Flow to the confined portions of the aquifer in the outcrop area was estimated to be approximately 2 percent of precipitation. Flow to the deep confined portion of the aquifers downdip of the outcrop area was assumed to be approximately 0.1 percent of precipitation. These percentages are within the ranges reported by other investigators.

The total annual average recharge rate for the entire study area was estimated at approximately 1.9 million AFY. However, it was estimated that only approximately 781,000 AFY of recharge actually flows to the confined aquifer in the outcrop area and ultimately discharges at the surface through streams, springs, or groundwater ET. It was estimated that only approximately 30,000 AFY of recharge actually flows to the confined aquifer downdip of the outcrop area and discharges regionally to younger sediments under predevelopment conditions. The annual average total pumping rate for all aquifers in all three zones from 1980 through 2010 is estimated to be 244,682 AFY.

A review of each water balance by region is instructive. In the northern region, pumping is very small relative to recharge. As a result, drawdown is expected to be localized in this region and for many areas to have stable hydraulic heads. Flow to the confined portions of the aquifers either discharges in the outcrop or discharges to the Little and/or Red rivers before entering Texas.

In the central region, pumping begins to be significant relative to recharge (15 percent). It was estimated that pumping in this region is approximately 24 percent of the portion of recharge that flows into the confined portion of the aquifers in the outcrop area before discharging in the outcrop.   In this case, pumping is approximately 884 percent of predevelopment flow to this downdip portion of the aquifer. As a result, drawdown is expected to be regional and extreme, especially in the confined portion of the aquifers. In the central region, a significant amount of historical pumping has occurred in the downdip confined portion of the aquifers. Water is initially taken from aquifer storage, which is lowest in the deep downdip confined portion of the aquifers. As a result, significant hydraulic head declines have occurred. Over time, the pumping volume is balanced by both a loss of storage and pumping capture, which is a decrease in aquifer discharge and an increase in recharge. The decrease in discharge results in increased cross-formational flow (and associated alteration of natural vertical gradients upward). The pumping in the downdip confined section also increases the flow from the outcrop region to the downdip confined portion of the aquifers significantly. These processes take decades to occur and, in the case of confined pumping impacts on the outcrop, could take hundreds of years.

In the southern region, pumping is even more significant relative to shallow recharge (34 percent). Similar to the central region, pumping is approximately 1,000 percent of flow to the confined downdip portion of the aquifers. This again suggests that pumping in the deeper portions of the aquifers will likely create significant hydraulic head declines regionally.

A review of the conceptual flow balance, while uncertain, provides insight into the historical declines in hydraulic heads that have occurred in the northern Trinity and Woodbine aquifers in Texas. While recharge is generally a very large volume relative to pumping, most aquifer recharge naturally discharges in the shallowest portions of the aquifers in the outcrop. As a result, water-level declines in the shallow outcrop regions exist but are generally localized. In contrast, drawdowns are both extreme and regional in extent in the downdip confined portions of the aquifers because groundwater flow to this portion of the aquifers is small relative to average aquifer pumping.

Table 5.7.1   **Conceptual water balance for the northern Trinity and Woodbine aquifers and the Washita/Fredericksburg groups defined by recharge regions.**

Region	Recharge (AFY)	Percent of Precipitation	Confined Flow in Outcrop[a] (AFY)	Downdip Confined Flow[b] (AFY)	Average Pumping[c] (AFY)
North	1,012,300	10.6%	143,298	9,553	7,996
Central	548,901	4.6%	355,048	9,468	87,778
South	348,158	1.8%	282,800	11,312	148,908
Total	**1,909,360**	**4.7%**	**781,147**	**30,333**	**244,682**

[a] estimated as 2 percent of annual average precipitation and assuming predevelopment conditions
[b] estimated as 0.1 percent of annual average precipitation and assuming predevelopment conditions
[c] average pumping rate from 1980 through 2010 based on water use survey data obtained from the TWDB
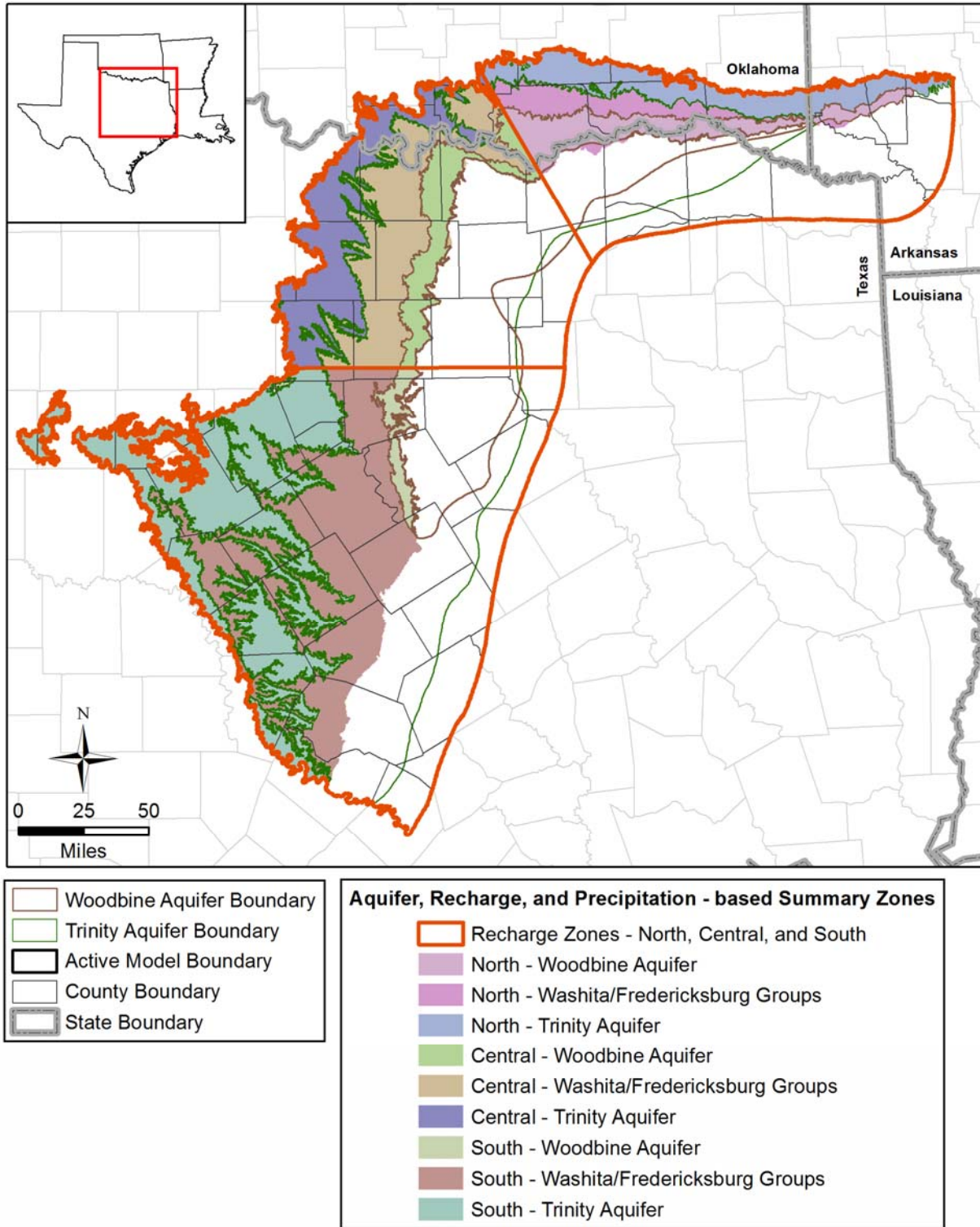
Figure 5.7.1   Map showing water balance zones referenced in Table 5.7.1.

This page intentionally left blank.

5.8   Model Implementation

Figure 5.8.1 is a simplified schematic diagram showing the conceptual implementation of the northern Trinity and Woodbine aquifers groundwater availability conceptual model under predevelopment conditions. Recharge to the aquifer system occurs in the outcrop from precipitation and through leakage from streams and reservoirs. Discharge in the outcrop occurs through ET and to surface water bodies such as springs, streams, and potentially reservoirs. Discharge in the downdip confined portion of the aquifer system occurs through cross-formational flow to overlying younger formations and potentially as upward discharge through the Mexia-Talco Fault Zone, which represents the downdip boundary. After development, pumping acts as an additional discharge mechanism. Some amount of hydraulic communication is believed to exist between the Hosston Aquifer and the sand units in the underlying Paleozoic-age formations. It is expected that this is only important locally and that the water balance of the overlying northern Trinity Aquifer far exceeds that of the Paleozoic-age strata.

The conceptual model for the northern Trinity and Woodbine aquifers is defined by seven aquifers/formations all of which have the potential to be aquifers in portions of the study area with hydraulic conductivities generally in excess of 1 foot per day. However, the dominant stratigraphic units capable of producing groundwater to a well at adequate rates and quality for use are from youngest to oldest: the Woodbine, Paluxy, Hensell, and Hosston aquifers. The conceptual model includes a shallow flow system over the entire outcrop area of all seven aquifers/formations, which is represented by part of model Layer 1 (see Figure 5.8.1).

Paleozoic-age formations, which can consist of permeable water-bearing sands and limestones as well as lower conductivity sediments, underlie the Hosston Aquifer. Many wells penetrate beneath the Hosston Aquifer into sands within the Paleozoic-age formations. In the shallow portions of the outcrop, some recharge on the Paleozoic-age formations may flow to the sands of the Hosston Aquifer and be accessed through wells completed in both the Cretaceous- and Paleozoic-age sediments. Model Layer 1 incorporates a minor amount of saturated Paleozoic-age sediments at the far updip limits of the model. However, the model does not explicitly handle the cases where wells may penetrate into sands within the Paleozoic-age formations at depth. As a result, the model may underestimate the transmissivity available to some wells dually-completed in the northern Trinity aquifer and the Paleozoic-age formations.

A wedge of younger sediments lies above the confined portion of the Woodbine Aquifer. This wedge of sediments is represented by part of model Layer 1 as it extends past the outcrop areas of the northern Trinity Aquifer, Washita/Fredericksburg groups, and Woodbine Aquifer as indicated in Figure 5.8.1. For the portion of Layer 1 representing the younger sediments, the flux-limited, general head boundaries (MODFLOW RIV package) was attached to simulate the overlying younger formations. Under predevelopment conditions, diffuse upward discharge is conceptualized to occur from the Woodbine Aquifer into these overlying younger formations.

In addition to identifying the aquifers/formations in the northern Trinity and Woodbine aquifers, the conceptual model also defines the mechanisms of recharge and natural aquifer discharge, as well as groundwater flow through the aquifer. Precipitation falling on the outcrop either runs off as surface water or evaporates at the surface, infiltrates and is lost to ET in the vadose zone, or infiltrates into the subsurface and recharges the aquifer. A large portion of the precipitation is expected to be removed via ET in or above the vadose zone, while most of the remainder runs off as surface water. On average, less than 5 percent of precipitation will become recharge. Recharge from precipitation will occur in the outcrop areas of the northern Trinity and Woodbine aquifers as well as the Washita/Fredericksburg groups. It is expected that recharge rates on average will increase from southwest to northeast, as average precipitation increases, and potential ET decreases.

Once infiltrating water becomes recharge, most will discharge through base flow, as spring or seep discharge, or as groundwater ET. Only a fraction of recharge is estimated to become recharge to the downdip portions of the confined aquifers. Once pumping begins in the historical period, the amount of flow to the downdip confined portions of the aquifers can increase significantly. Flow to the downdip confined portions ultimately discharges through pumping, vertical cross-formational flow and perhaps, to a limited extent, through structural fault zones. The Mexia-Talco Fault Zone is considered to be the downdip lateral extent of the flow system and was treated as a potential outflow zone.

It is important to note that the updated northern Trinity and Woodbine aquifers GAM is not a water quality model. However, a review of Figures 5.3.3 and 5.5.1 shows that the current model domain simulates both freshwater and brackish water as a continuous groundwater system. Any

MAG determined from this model would potentially include brackish groundwater in the water balance.
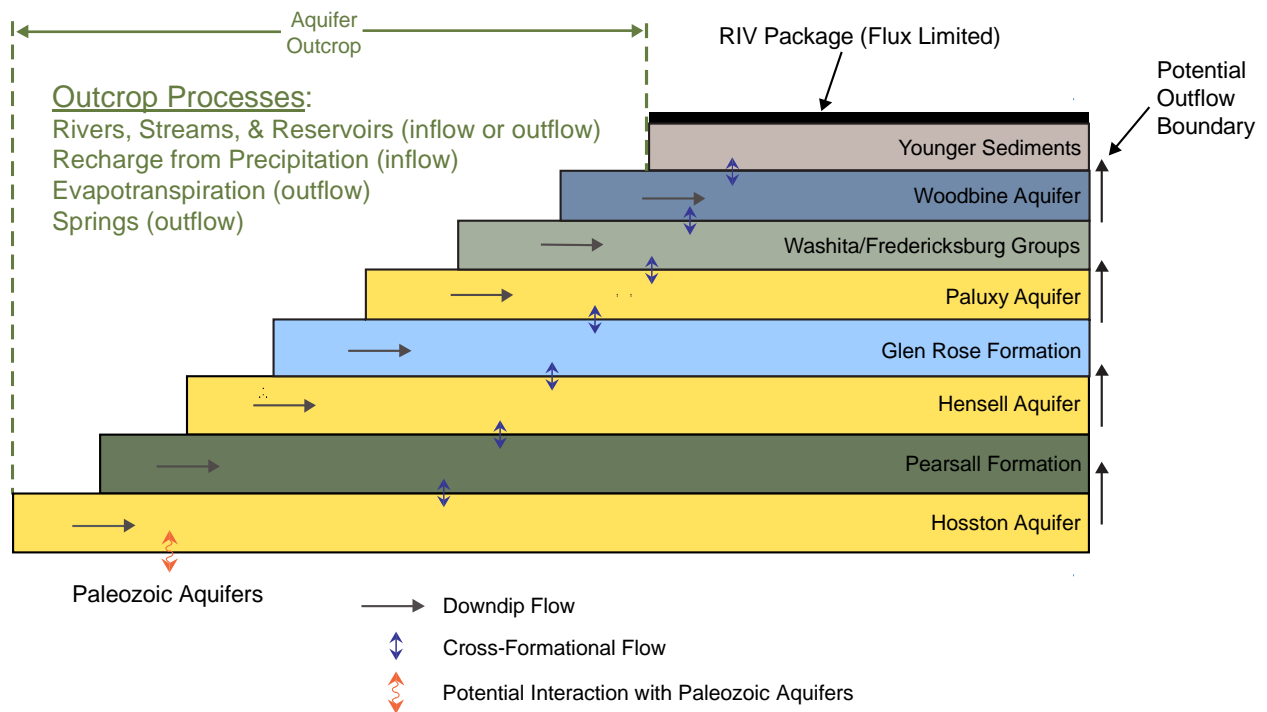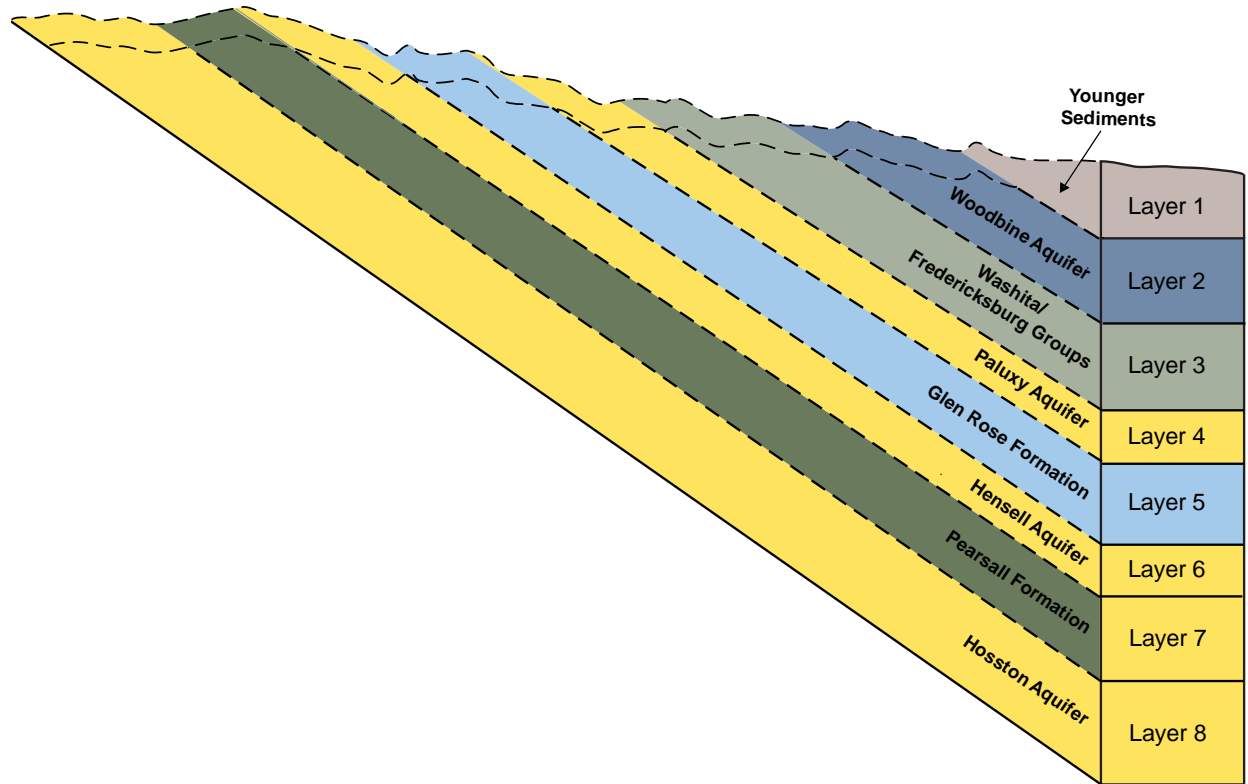
Figure 5.8.1   Conceptual groundwater model implementation strategy for the northern Trinity and Woodbine aquifers.

6.0   Model Design

Model design represents the process of translating the conceptual model for groundwater flow in the aquifer (Section 5.0) into a numerical representation, which is generally described as the model. The conceptual model for flow defines the processes that define groundwater flow and, therefore, determines the attributes for the selected simulation code. In addition to selection of the appropriate code, model design includes definition of the model grid and layer structure, the model boundary conditions, and the model hydraulic parameters. Each of these elements of the model design and their implementation are described in this section.

6.1   Code and Processor

The code selected for the updated northern Trinity and Woodbine aquifers GAM is MODFLOW-NWT (Niswonger and others, 2011). MODFLOW is a three-dimensional finite-difference groundwater flow code that is supported by enhanced boundary condition packages to handle recharge, ET, streams, springs, and reservoirs. MODFLOW-NWT provides for rigorous treatment of "dry" cells when the simulated hydraulic head goes beneath the layer bottom in convertible cells (i.e., cells that can convert between confined and unconfined conditions). In earlier versions of MODFLOW, this "dry" condition in convertible cells would result in the de-activation of those cells with the options of either allowing the cells to remain dry for the remainder of the simulation or attempting to re-wet the cells. The re-wetting of cells in the earlier versions of MODFLOW tends to lead to difficulties in model convergence as well as localized mass balance errors. In contrast, MODFLOW-NWT never de-activates "dry" cells but, rather, asymptotically reduces the transmissivity in the cells while allowing the transmissivity to increase again if and when simulated hydraulic heads go above the layer bottom without the numerically difficulties of the re-wetting process. In addition, MODFLOW-NWT allows for the automatic reduction of pumping within convertible layers when the simulated hydraulic head approaches the cell bottom. This can also be used to avoid problems with "dry" cells that occur as a result of uncertainties in pumping.

The benefits of using MODFLOW for the updated northern Trinity and Woodbine aquifers GAM include:

- MODFLOW incorporates the necessary physics represented in the conceptual model for flow described in Section 5.0 of this report.

- MODFLOW is the most widely accepted groundwater flow code in use today.

- MODFLOW was written and is supported by the USGS and is public domain.

- MODFLOW is well documented (McDonald and Harbaugh, 1988; Harbaugh and McDonald, 1996; Harbaugh and others, 2000; Harbaugh, 2005; Niswonger and others, 2011).

- MODFLOW has a large user group.

- There are numerous graphical user interface programs written for use with MODFLOW.

- The TWDB requires that GAMs be simulated in MODFLOW.

The MODFLOW data sets (input files describing the hydraulic properties and boundary conditions which constitute the numerical model) were developed to be compatible with Groundwater Vistas for Windows Version 6 (Rumbaugh and Rumbaugh, 2011). The model was executed on x86 compatible computers equipped with the Windows 7 operating system. MODFLOW is not typically a memory-intensive application in its executable form. However, given the large number of grid cells in this model, approximately 5GB of RAM is necessary. If any preprocessor (such as Groundwater Vistas) is used for a model of this size and complexity, at least 16GB of RAM is recommended.

6.2   Model Layers and Grid

MODFLOW-NWT requires a rectilinear grid. Typically, one axis of the model grid is aligned parallel to the primary direction of flow. The grid for the updated northern Trinity and Woodbine aquifers GAM is oriented with the x-axis 65 degrees counter-clockwise of east-west (Figure 6.2.1) to directly overly the grid for the 2004 northern Trinity and Woodbine aquifers GAM developed by Bené and others (2004). In this way, the grid is oriented with the primary direction of flow in Texas, which is southeast, and the 2004 GAM and this updated GAM can be compared more easily. The grid cells are quarter-mile by quarter-mile squares throughout the model domain. The model grid origin (lower left-hand corner) is located at GAM coordinates 19,067,743 feet north and 6,169,014 feet east. The model has 1,412 columns and 1,124 rows for a total of 1,587,088 grid cells per layer with a total of 12,696,704 grid cells for the eight model layers, which are described below. Not all of these grid cells are active in the model, however. The entire active model domain numbers 4,820,008 grid cells with 602,501 active grid cells per layer. Because of the small size of the model grid cells relative to the total area of the modeled region, there is no effective way to show the model grid resolution across the entire active model domain. Instead, Figure 6.2.1 shows the active model domain for the updated northern Trinity and Woodbine aquifers GAM and includes an inset with an enlargement of Rockwall County to demonstrate the model grid at the county scale.

The updated northern Trinity and Woodbine aquifers GAM is divided into seven structural layers as described in Section 4.1, with the addition of an upper surficial/younger formations layer for a total of eight model layers. Figure 6.2.2 shows an example of the vertical discretization of the model grid. Model Layer 1 represents two aspects of the model. Where the northern Trinity Aquifer, Washita/Fredericksburg groups, and Woodbine Aquifer outcrop, Layer 1 represents the shallow flow system that is dominated by inflow from recharge and outflow to surface water boundaries such as rivers, creeks, and springs along with groundwater ET. This portion of Layer 1 is referred to as the surficial outcrop area (Figure 6.2.3). In the remainder of the model area, Layer 1 represents the younger formations that overly the downdip portions of the Woodbine Aquifer and Washita/Fredericksburg groups (see Figure 6.2.3). It should be noted, however, that the inclusion of this portion of the upper layer is intended only to provide a first-order representation of the overlying younger formations as a boundary condition layer in the model.

Specifically, all recharge, pumping, and surface water interaction that occurs within the younger formations is aggregated into the river boundary condition applied to this portion of Layer 1 grid cells.

Model layers 2 through 8 represent the portions of the aquifers/formations underlying and downdip of the surficial outcrop area. The Woodbine Aquifer is represented by model Layer 2. Model Layer 3 represents the Washita/Fredericksburg groups, which includes a portion of the Edwards BFZ Aquifer at the southern extent of the model domain. The Paluxy Aquifer is represented by model Layer 4. Model Layer 5 represents the Glen Rose Formation. The Hensell Aquifer is represented by model Layer 6. Model Layer 7 represents the Pearsall Formation. The Hosston Aquifer is represented by model Layer 8. MODFLOW does not allow vertical flow through inactive cells (inactive cells must be no-flow). Therefore, where the aquifers/formations represented by model Layers 2 through 7 do not exist under the surficial outcrop area of model Layer 1, a 1-foot thickness was assigned to those layers. This provides "conduit" cells that allow vertical connection between Layer 1 and underlying Layers 3 through 8.

The upper boundary of the model is defined by ground surface as calculated by the 10-meter digital elevation model (DEM) averaged to the grid cells. In the surficial outcrop area, the base of Layer 1 denotes the base of the surficial flow system, which is set 50 feet below the 1-mile average of the estimated predevelopment water level. Where it represents the younger formations overlying the Woodbine Aquifer, the base of Layer 1 is defined by the top of the Woodbine Aquifer. The base of Layer 2 is defined as the base of the Woodbine Aquifer. A minimum layer thickness of 30 feet was enforced whereby Layer 2 basal elevations were lowered if necessary to maintain the minimum thickness. The base of the Washita/Fredericksburg groups defines the base of Layer 3. The base of Layer 4 represents the base of the Paluxy Aquifer. The base of the Glen Rose Formation is represented by the base of Layer 5. The base of Layer 6 represents the base of the Hensell Aquifer. The base of the Pearsall Formation is represented by the base of model Layer 7. The base of the Hosston Aquifer represents the base of Layer 8. In the surficial outcrop area, Layer 1, which represents the shallow water table, is simulated as convertible between confined and unconfined. All other layers are simulated as confined.
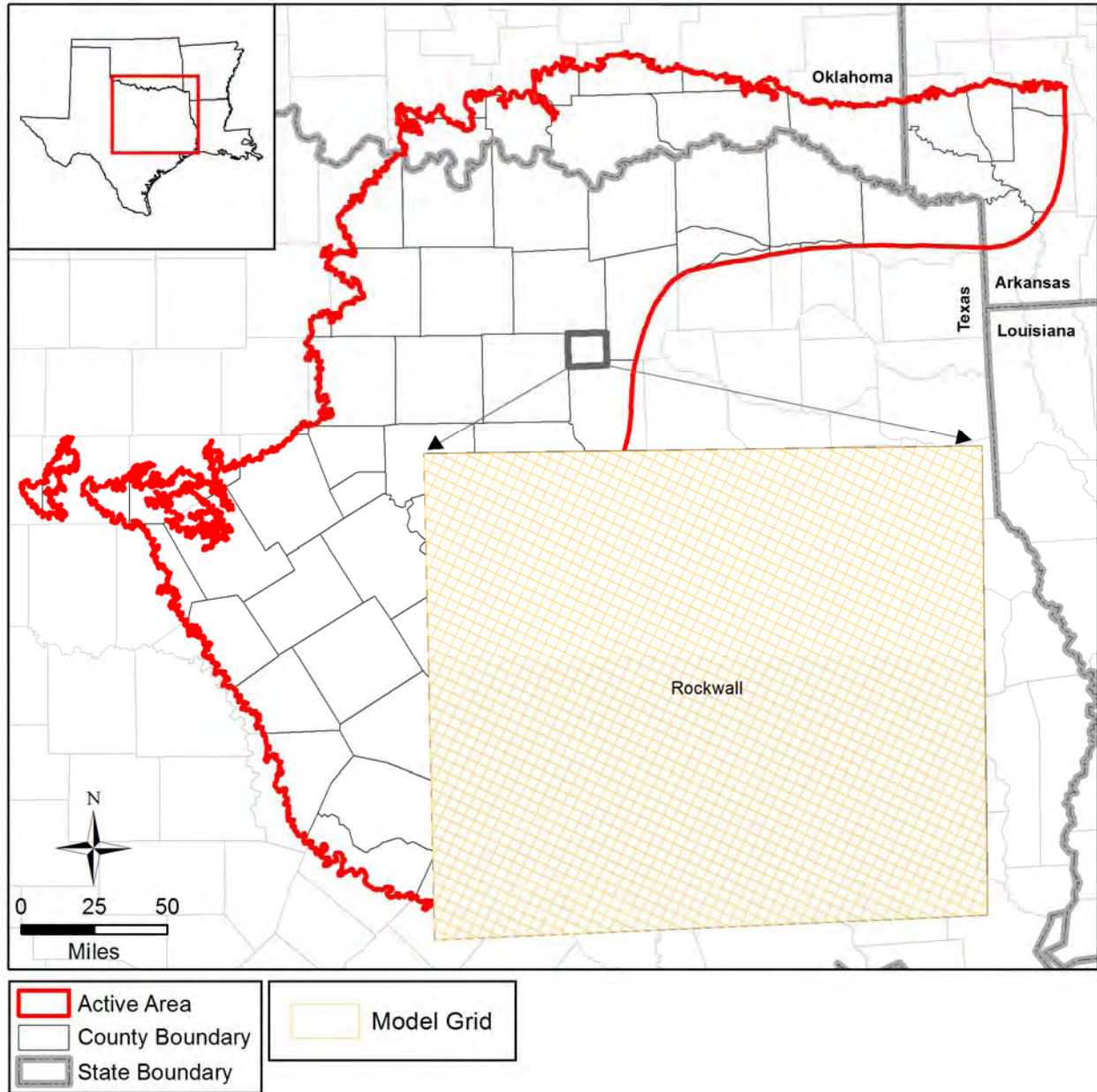
Figure 6.2.1   Active model domain and model grid at the county scale for the updated northern Trinity and Woodbine aquifers GAM.

Fred/Wash = Fredericksburg/Washita groups
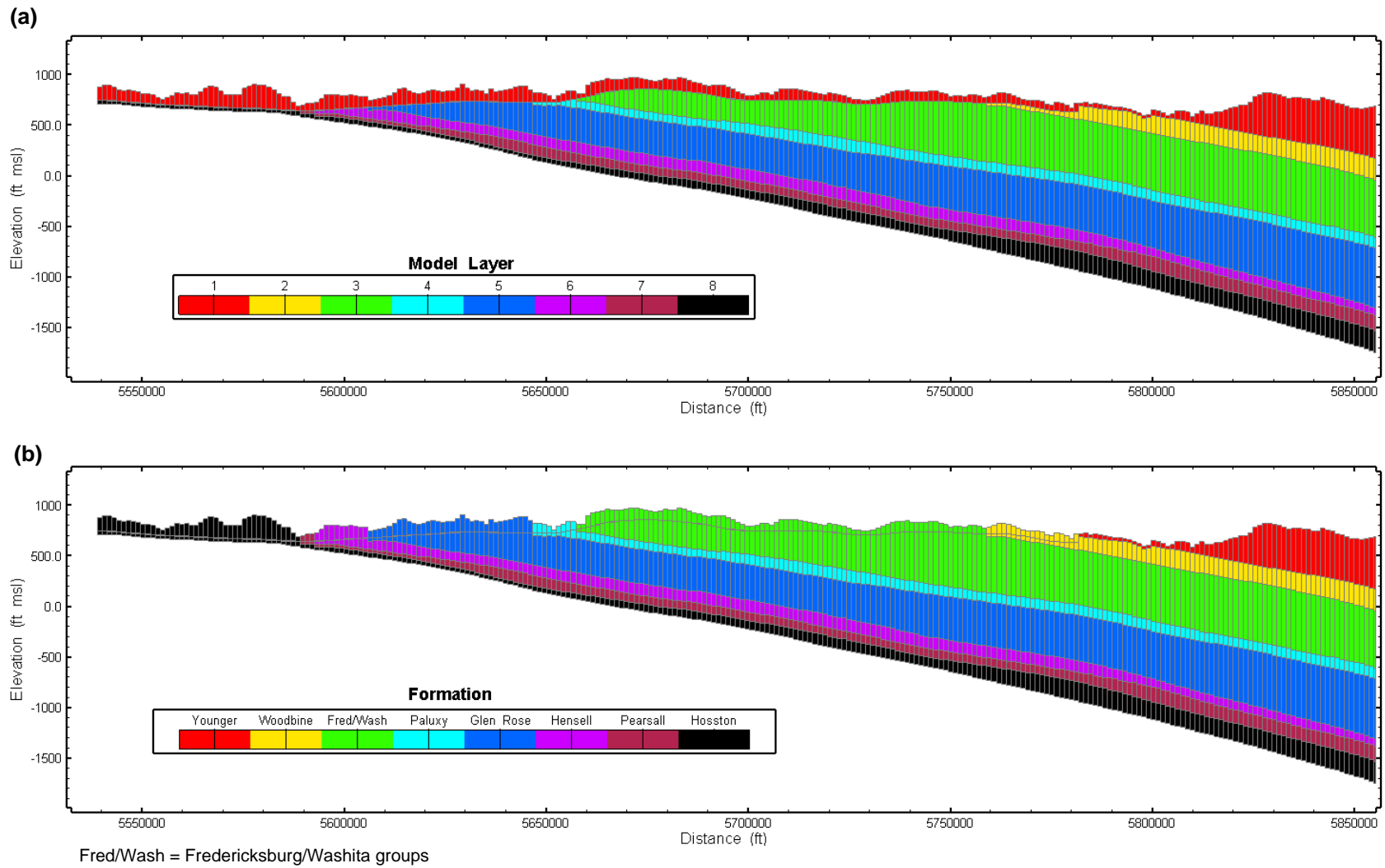
Figure 6.2.2   **Example of the vertical discretization of the model showing (a) model layers and (b) the formations corresponding to the model layering.**
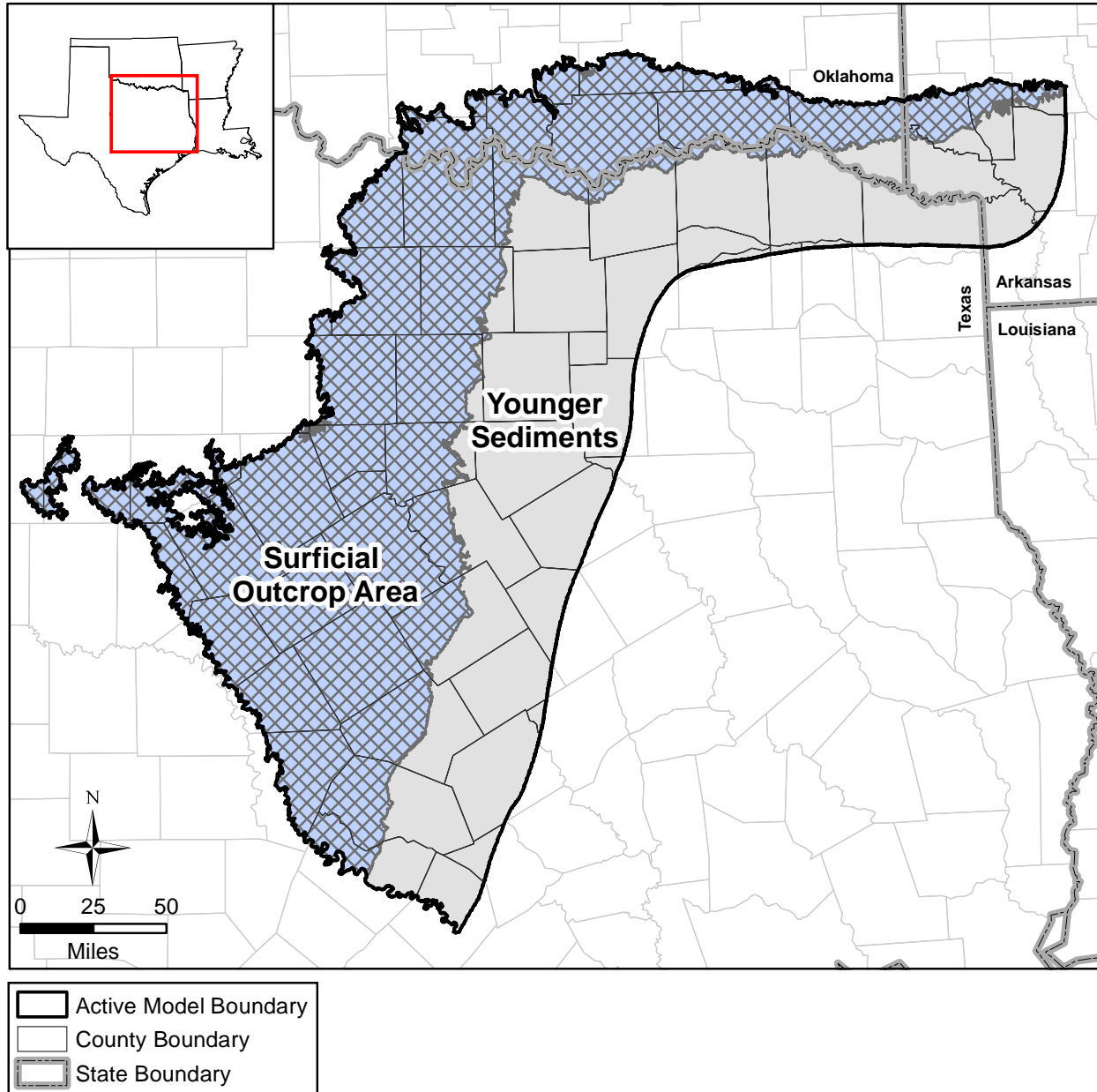
Figure 6.2.3   Surficial outcrop area and younger formations area in Layer 1.

This page intentionally left blank.

6.3   Boundary Condition Implementation

A boundary condition can be defined as a constraint put on the active model grid to characterize the interaction between the active model domain and the surrounding environment. There are generally three types of boundary conditions: specified head (First Type or Dirichlet), specified flow (Second Type or Neumann), and head-dependent flow (Third Type or Cauchy). The no-flow boundary condition is a special case of the specified flow boundary condition.

Boundaries can be either time independent or time dependent. An example of a time-dependent boundary is a pumping flow boundary (e.g., grid cell with a well) or a reservoir stage elevation. Because many boundaries require time-dependent (transient) specification, the stress periods used by MODFLOW must be specified. A stress period in MODFLOW defines the time period over which boundary and model stresses remain constant. Each stress period may have a number of computational time steps, which are some fraction of the stress period. For the transient model, yearly stress periods were used from 1890 through 2012. Therefore, transient boundaries in the model do not change over a period of less than 1 year.

Boundaries requiring specification include: lateral and vertical boundaries for each layer, surface-water boundaries, recharge boundaries, and discharge boundaries, including ET and pumping. Specified no-flow (Second Type) boundary conditions were assigned to the lateral and lower boundaries and head-dependent flow boundaries (Third Type) were assigned to specific cells within the top model layer. Surface-water boundaries, including perennial streams (river package) and ephemeral streams and riparian ET (drain package), are head-dependent flow boundaries (Third Type). Recharge is a specified flow boundary (Second Type). Pumping discharge is a specified flow boundary (Second Type).

Figures 6.3.1 through 6.3.8 show the active and inactive grid cells for model Layers 1 through 8, respectively. In these figures, "conduit cells" refer to those active cells that lie between the surficial outcrop area of Layer 1 and the confined deeper layers, as described in Section 6.2. Areas exterior to the active model boundary are colored grey to denote being inactive. Implementation of the boundary conditions for the updated northern Trinity and Woodbine aquifers GAM is described below. Unless otherwise specified below, the boundary between the active and inactive cells is a no-flow boundary.

6.3.1 Lateral Model Boundaries

The lateral model boundaries were developed to comply with structural or otherwise natural hydrologic boundaries to the best degree possible as defined by the extent of the northern Trinity and Woodbine aquifers. Beyond the extent of the northern Trinity and Woodbine aquifers, grid cells were set as inactive, creating a no-flow boundary along the intersection of the active and inactive cells.

The updip limit of the northern Trinity Aquifer outcrop defines the western and northern extents of the active model domain. This is a natural lateral no-flow boundary. The southeastern extent of the active model domain is defined by the Mexia-Talco Fault Zone, where the fault offsets are significant enough to assume to represent a lateral no-flow boundary. The southern boundary of the active model domain is defined by the Colorado River, which is a regional discharge boundary assumed to be adequately represented by a lateral no-flow boundary. The eastern extent of the northern Trinity aquifer is treated as a distance boundary to the developed portions of the aquifer and is implemented as a lateral no-flow boundary.

6.3.2 Vertical Boundaries

A no-flow boundary was used at the bottom of Layer 8 (the Hosston Aquifer). The underlying Paleozoic-age strata have some hydraulic connection to the Hosston Aquifer. It was assumed that Paleozoic-age sands that directly underlie the Hosston Aquifer primarily act as additional saturated thickness and, thereby, additional transmissivity and storativity rather than a source of hydraulic head support. Therefore, the hydraulic connection between the northern Trinity Aquifer and the Paleozoic-age strata was not explicitly included in the model.

The model has a head-dependent flow boundary (Third Type) in Layer 1 where it represents the younger formations that overly the Woodbine Aquifer. This boundary represents the diffuse regional (primarily) outflow discharge from the northern Trinity and Woodbine aquifers into the younger overlying formations. The MODFLOW river package is used to represent this boundary rather than the general-head-boundary package (Harbaugh and others, 2000) to limit the magnitude of simulated inflow from this boundary that could occur as water levels decrease due to pumping in the northern Trinity and Woodbine aquifers. It should be noted that the majority of previous GAMs and, specifically, the 2004 northern Trinity and Woodbine aquifers GAM, used the general-head-boundary package to represent cross-formational flow with overlying

formations, While the general-head-boundary package limits downward flow based on conductance, it does not limit flow based on increased downward gradients. This has led to difficulties in using such GAMs to simulate the effect of maximized pumping in the aquifers underlying such boundary conditions. In contrast to the general-head-boundary package, the river package limits the downward gradient while also limiting flow via the conductance. This approach avoids increased flow due to increased gradients when maximal pumping is applied to the underlying aquifers. In summary, the river package simulates a head-dependent flow boundary condition and requires hydraulic head and hydraulic conductance as input parameters but limits the downward gradient. The hydraulic conductance in the river package represents the composite vertical conductance of the younger formations. The difference between the hydraulic heads in the northern Trinity and Woodbine aquifers and the younger formations sets the gradient that, along with the composite vertical conductivity, governs the amount of outflow from the northern Trinity and Woodbine aquifers to the younger formations. Any flow from the younger formations to the Woodbine Aquifer is not based on the difference in hydraulic heads, but is limited by a unit gradient because the stages are set one foot above the river bottom. The composite vertical conductance was calculated based on an assumed vertical hydraulic conductivity of 0.01 feet per day and half of the thickness of the younger formations. The river boundary conditions representing the younger formations are demarcated by the word "Younger" in the river package.

To describe the elevation of the river boundary condition representing the younger formations, a subdued and lower estimate of the ground surface topography was used. Specifically, the 10-meter digital elevation model (DEM) was averaged over a moving 10-mile radius at each model grid cell and lowered by 100 feet to describe the boundary condition elevation. The water-level elevations representing the younger formations are depicted in Figure 6.3.9. This elevation was not changed with time for the transient period of the simulations, which is consistent with the far-field nature of this boundary condition.

6.3.3 Surface Water Implementation

In the surficial outcrop area of model Layer 1, surface water in perennial rivers, reservoirs, ephemeral streams, and springs in the outcrop of the northern Trinity Aquifer, Washita/Fredericksburg groups, and Woodbine Aquifer act as a head-dependent flow (Third Type) boundary condition. The MODFLOW river package was used to represent perennial

rivers and reservoirs and the MODFLOW drain package was used to represent ephemeral streams and springs. Figure 6.3.10 depicts the location of each of these boundary conditions in the surficial outcrop area of model Layer 1. Because these boundary conditions are difficult to distinguish at the scale of the entire active model domain, an insert with an enlargement for a smaller area is provided in the figure.

The river package allows for stream-related discharge during gaining conditions and for stream-related recharge during losing conditions. For perennial rivers, the river stage was set to the minimum digital elevation model (DEM) value in a given grid cell and the river bottom was set 5 feet below the river stage. If the river stage was below the base of Layer 1, the stage was set 1 foot above the layer bottom and the river bottom was reset to 5 feet below the river stage. Where reservoirs exist, the river stage was set to the time varying reservoir stage after impoundment and the areal extent of the river cells was defined by the reservoir coverage (see Table 4.6.13). Prior to reservoir impoundment, the river stage was set to an estimate of the river channel elevation and river boundary conditions were only applied to the river channel. Within the river package, rivers are demarcated by the prefix "River" followed by the river name and reservoirs are demarcated by the prefix "Reservoir" followed by the reservoir name.

The river conductance for perennial rivers was calculated based on an assumed river bed conductivity of 1 foot per day, an assumed river width of 40 feet, and the length of the river within a given model grid cell. Reservoir bed conductivities were uniformly set to 1×10^{-4} feet per day for all reservoirs in the model and the river conductance was calculated as the product of the bed conductivity and the area of the reservoir within a given model grid cell divided by an assumed bed thickness of 5 feet.

To represent ephemeral streams, the MODFLOW drain package was applied within ephemeral stream channels as described by the National Hydrography Dataset (USGS, 2012). The ephemeral streams are demarcated by the word "Ephemeral" within the drain package. The drain elevations for ephemeral streams were set 10 feet below the top of the model and the drain conductances were uniformly set to 1,000 square feet per day. Springs were also represented by the MODFLOW drain package and are demarcated by the word "Spring" in the drain package. The drain elevations for springs were set 10 feet below the top of the model and the drain conductances were uniformly set to 1,000 square feet per day.

6.3.4 Implementation of Recharge and ET

Because an evaluation of groundwater availability is largely dependent upon recharge (Freeze, 1971), aquifer recharge warrants careful examination and meaningful implementation. Ideally, recharge is constrained in magnitude through some knowledge regarding the natural discharge volumes of the aquifer. As discussed in Section 5.0, a lower bound on an estimate of total natural aquifer discharge is only available through the analysis of streamflow data through hydrograph separation analysis methods. As a result, the recharge model implemented is based upon relationships derived from hydrograph separation analyses.

In typical model applications, recharge is either homogeneously defined as a percentage of the yearly average precipitation or calibrated as an unknown parameter. Unfortunately, recharge and hydraulic conductivity can be correlated parameters preventing independent estimation when using only hydraulic head data constraints. Another compounding problem is that recharge is a complex function of precipitation rate and volume, soil type, water level and soil moisture, topography, and ET (Freeze, 1969). Precipitation, ET, water-table elevation, and soil moisture are spatially and temporally variable. Soil type, geology, and topography are spatially variable. For the updated northern Trinity and Woodbine aquifers GAM, specification of recharge for steady-state conditions and for transient conditions from 1890 through 2012 was necessary. Reliable estimates of recharge at the watershed scale, or the regional model scale (thousands of square miles for the GAMs) do not generally exist. A review of the work by Kirk and others (2012) found that their analysis of regional recharge rates could not be used because the long-term average recharge they calculated was effectively zero for most of the northern Trinity and Woodbine aquifers.

The general methodology used to define recharge is described in Section 4.5.6. In summary, three domains were defined: the southern, central, and northern domains. Separate equations were fit to describe recharge as a function of precipitation for the southern and northern domains, where sufficient data are available to perform hydrograph separation analyses to estimate base flow. In the central domain, where data for performing hydrograph separation analyses to estimate base flow are lacking, a simple linear interpolation by distance between the southern and northern equations was used. Recharge was varied temporally based on annual precipitation records at each model grid cell. To account for the dampening effect caused by the vadose zone between temporal variations in precipitation and the resulting variations in recharge to the

groundwater flow system, a dampening factor of 75 percent of the difference between the annual variation in precipitation and the 30-year average precipitation was used to describe the variation in recharge. Figure 6.3.11 shows the 30-year long term average recharge distribution for the model in inches per year.

As discussed in Section 4.5.3.3, urbanization can have an impact on recharge. Research into this subject concluded that without detailed investigation of a specific urban area, it is difficult to quantify the net change to groundwater recharge due to urbanization. In some cases, detailed studies have shown increases in recharge due to urbanization, while other studies show decreases. Because the intended use for this model is for groundwater availability assessments, it seemed most appropriate to assume that urbanization results in a net decrease in recharge. The U.S. Environmental Protection Agency (1993) general guidelines for representing changes to the water cycle imposed by urbanization were used to alter recharge in urban areas of the active model domain. The National Land Cover data set (Fry and others, 2011) was used to identify current developed areas, where impervious cover could impact recharge and runoff. The data set includes four classifications of increasing development. The model grid was intersected with the "developed" classifications to identify the model grid cells where development has occurred, along with a categorical estimate of the level of the development. A spatial density calculation was then performed on the model grid to create a coverage of development density. For temporal variation of developed land, the densest areas were assumed to have developed first. The model grid cells with developed land were sorted by density, and the population growth curve in the region, from 1900 to 2010, was used to develop decadal quintiles of population in the region. These quintiles were used to "activate" the developed model grid cells through time, again starting with the densest and moving outward.

When a model grid cell with developed land was activated for a given stress period, recharge was decreased in that cell by 16 percent, based on estimates from U.S, Environmental Protection Agency (1993). This scenario was based on an assumed 10 percent increase in runoff, 2 percent decrease in ET, and 4 percent reductions to shallow and deep infiltration (U.S. Environmental Protection Agency, 1993). Figure 6.3.12 shows the impact of urbanization on recharge for the years 1950, 1970, 1990, and 2010.

For the simulation of ET, the MODFLOW drain package was used for riparian cells neighboring perennial streams in the surficial outcrop area of model Layer 1. The locations of the ET drains are depicted in Figure 6.3.10 along with surface water boundary conditions. The drain package (Harbaugh and others, 2000) was used so that only head-dependent outflow would be simulated. The MODFLOW ET package was not used to avoid a rate-oriented boundary condition that is unbound by the physical constraints of recharge and hydraulic properties. Parameters needed in the drain package include the drain elevation, which was set to 10 feet below the top of the model, and the drain conductance, which was uniformly set to 1,000 square feet per day. ET is demarcated by the word "ET" within the drain package. In contrast to the 2004 GAM for this aquifer system, which applied ET to every model cell within the outcrop, this updated model was constrained to apply ET only to riparian areas along perennial streams and to ephemeral stream channels.

6.3.5 Implementation of Pumping Discharge

A number of wells drilled into the northern Trinity and Woodbine aquifers in the late 1800s and early 1900s were artesian and flowed when initially completed. Although they were likely not heavily pumped while they still flowed, discharge from these wells amounted to a significant volume of groundwater from the northern Trinity and Woodbine aquifers. The locations of these flowing wells, and associated inferred layer or layers in which they are completed, are shown in Figure 6.3.13. To account for discharge from these wells, drain cells were implemented in the model at their locations. These flowing wells are demarcated by the word "Flowing" in the drain package. The drain elevation for each flowing well was set to the average land surface elevation for the model grid cell in which the well is located. The drain conductance was uniformly set to the relatively large value of 1,000 square feet per day for all of the flowing wells. This results in the discharge rate from the flowing wells being governed primarily by the properties of the formation and assumes that the wells themselves play a minor role in restricting flow.

Pumping discharge is a primary stress on the transient model. Pumping discharge is a cell dependent specified flow boundary. The procedural techniques used to estimate historical pumping by aquifer and county and the temporal distribution of that pumping are provided in Section 4.7. Seven water use categories (municipal, manufacturing, power generation, mining, livestock, irrigation, and rural domestic) were investigated. Estimates of groundwater pumping in Texas from 1980 through 2011 were developed based on water use survey data provided by

the TWDB, which consists of pumping estimates by water use category and aquifer by county. Pumping estimates for 2012 were not available from the TWDB at the time the updated model was developed; therefore, pumping in 2012 was set equal to that in 2011. Pumping volumes during the period prior to 1980 were estimated by county and aquifer through calculations and a literature review. These estimates are considered more uncertain than the 1980 through 2011 estimates. The literature estimates of early 1900 pumping include estimates of discharge associated with free flowing wells. That component of the historical pumping estimates was removed since discharge from flowing wells is implemented in the model using the MODFLOW drain package as described above. To divide pumping prior to 1980 between the different water use categories, the total pumping was apportioned to each category based on the average ratio of that category to total pumping calculated from the period between 1980 and 2012. The total pumping within the model over the transient period is presented in Figure 6.3.14.

The distribution of pumping to model grid cells was completed differently depending on the area of the active model domain and the water use category. In Texas, the estimated pumping for a county was assigned to wells located in the county based on well data from the TWDB and GCDs. The vertical distribution of pumping was assigned based on the pumping estimates for each aquifer in the county and the aquifer(s)/formation(s) in which the wells in the county are completed.

Two methods were used to assign the spatial distribution of pumping in the Texas portion of the active model domain. When available, pumping data received from GCDs were specifically assigned using pumping volumes and well locations. In general, the GCD pumping data are associated with an entity, such as a municipality, but not associated with specific wells. To distribute the pumping to wells, the pumping volume for an entity was equally distributed to wells identified with that entity as given in the GCD well database. Vertically, this pumping was distributed based on the completion interval for the wells. No modification to GCD pumping data, either in volume or location, was made during model calibration.

Once GCD pumping data were assigned, the total pumping volume for a county was compared to the pumping volume for the GCD data. If the total volume was less than the GCD volume, no additional pumping was assigned to that county. If the total volume was more than the GCD volume, the difference was assigned based on the pumping estimates for each aquifer in the

county and the reported use for the water pumped from the wells in the county. For the water

use categories manufacturing, power generation, mining, livestock, irrigation, and rural

domestic, pumping was distributed uniformly between the wells identified with that water use

and with a drill date prior to the date associated with the pumping. For municipal pumping,

which constitutes the majority (55 percent) of the total pumping in the northern Trinity and

Woodbine aquifers, pumping was distributed between wells identified as municipal wells based

on observed reductions in hydraulic heads at the wells and drill dates prior to the estimated

pumping date. Because the reductions in hydraulic heads observed in the aquifers are

predominately the result of pumping for municipal purposes, the observed areas of hydraulic

head declines in the aquifers provide the most reliable guide for assigning the spatial distribution

of municipal pumping in each aquifer. Using this methodology, pumping at the individual

municipal wells was not uniform but, rather, varied spatial. The spatial distributions of total

pumping in the northern Trinity and Woodbine aquifers for the years 1950, 1980, and 2010 are

depicted in Figures 6.3.15 through 6.3.20. Outside of Texas, the pumping from the Antlers

Aquifer model by Oliver and others (2013) was applied directly.
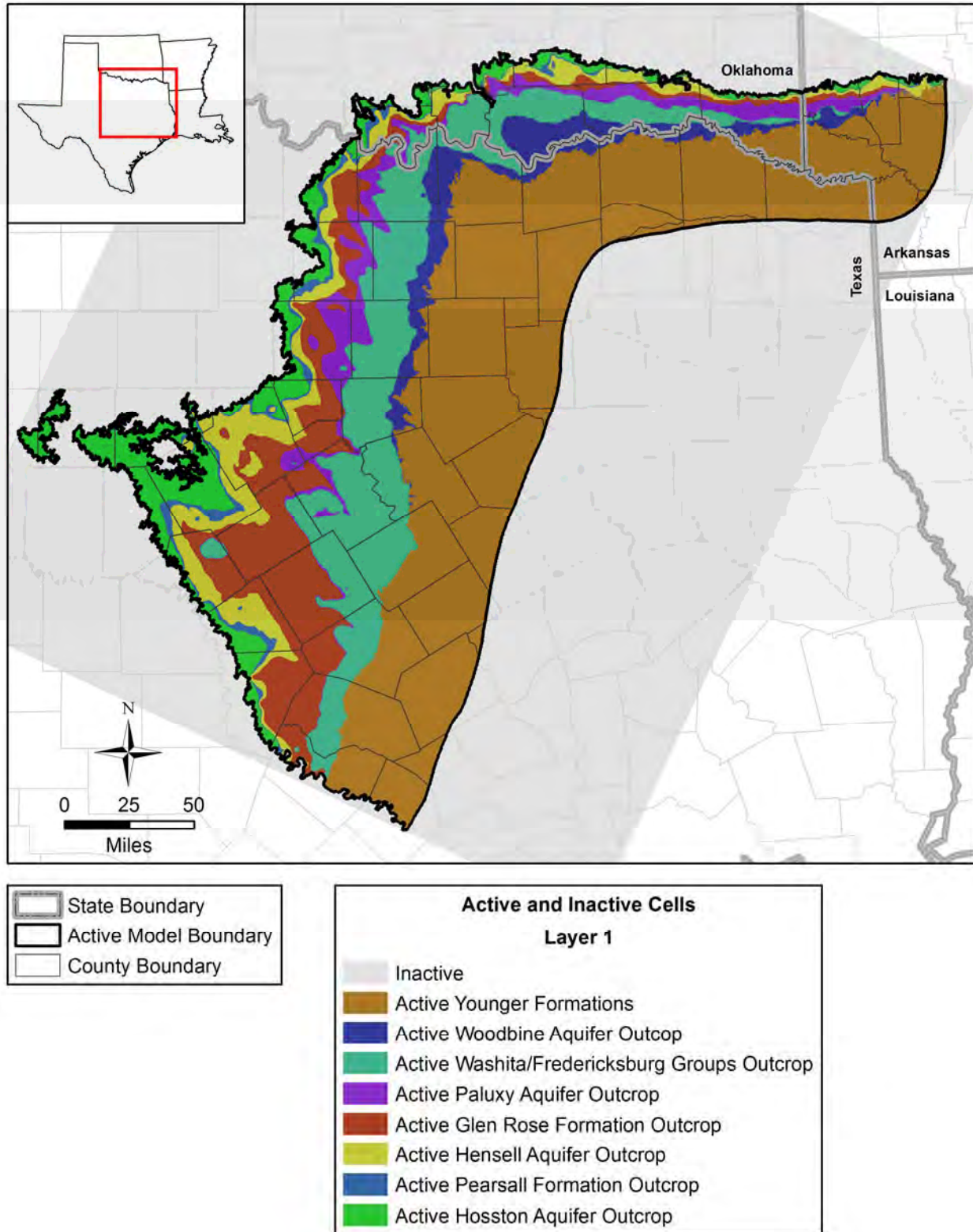
Figure 6.3.1   Layer 1 active/inactive model grid cells.
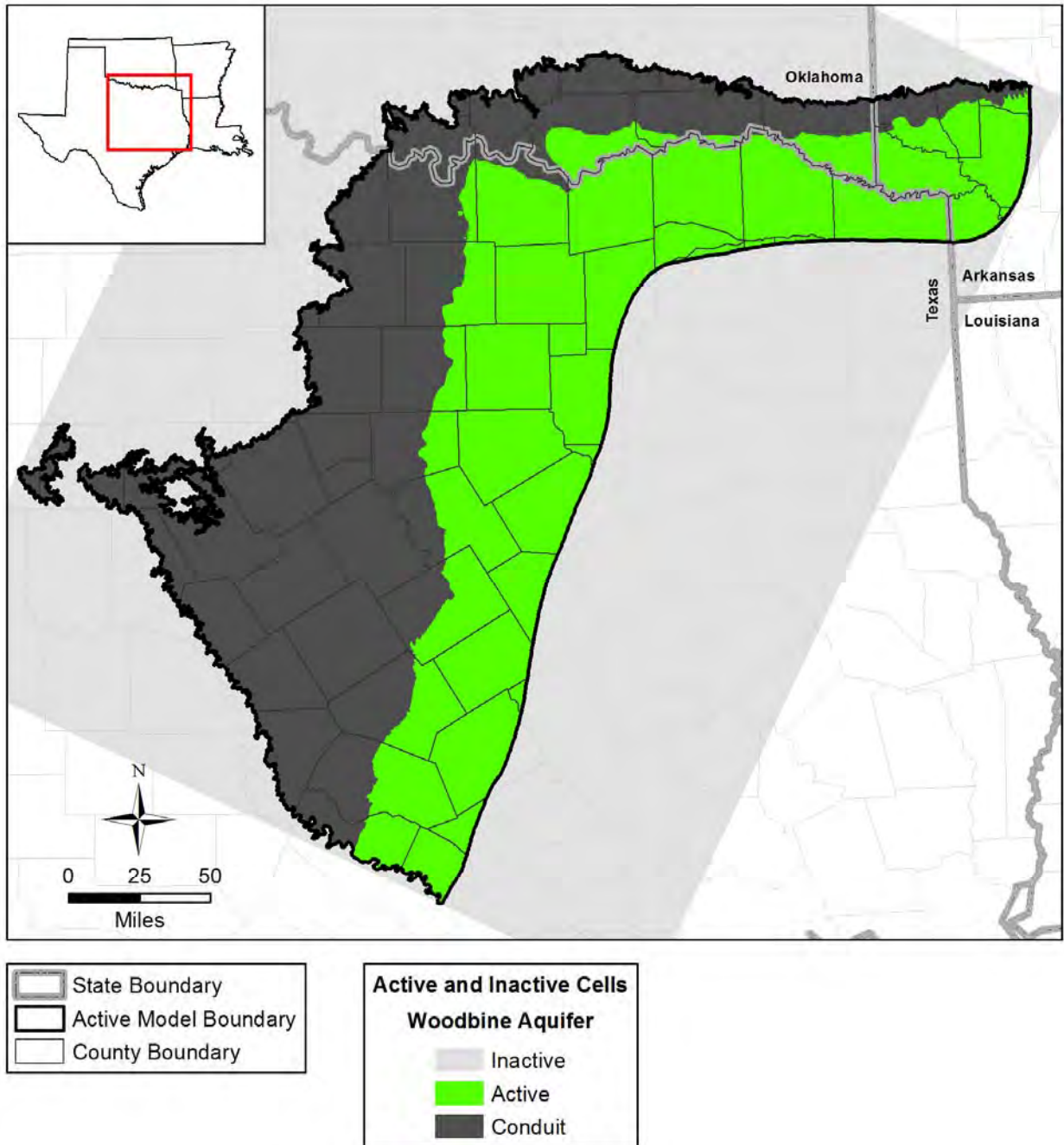
Figure 6.3.2   Layer 2 active/inactive model grid cells.
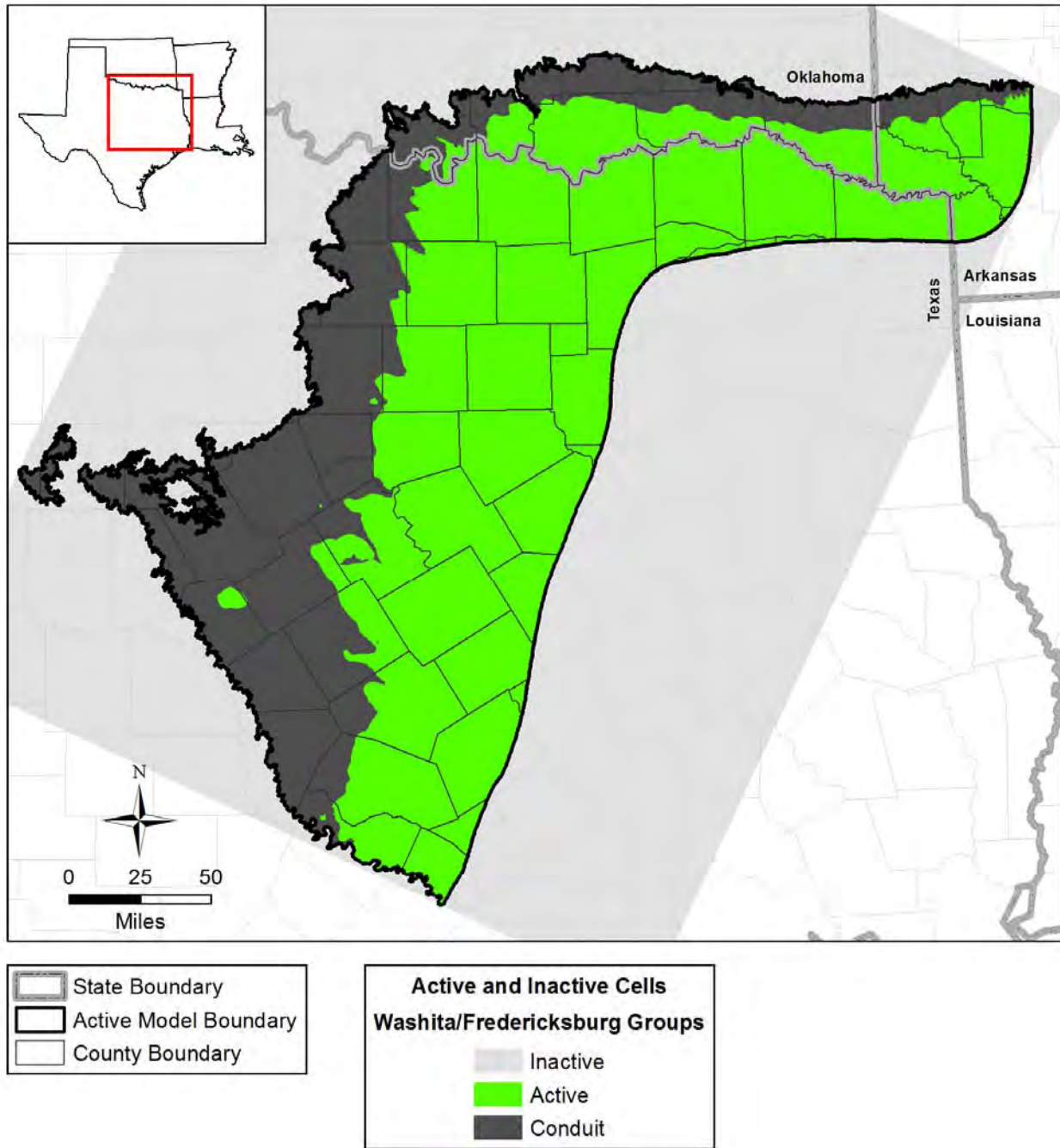
Figure 6.3.3   Layer 3 active/inactive model grid cells.
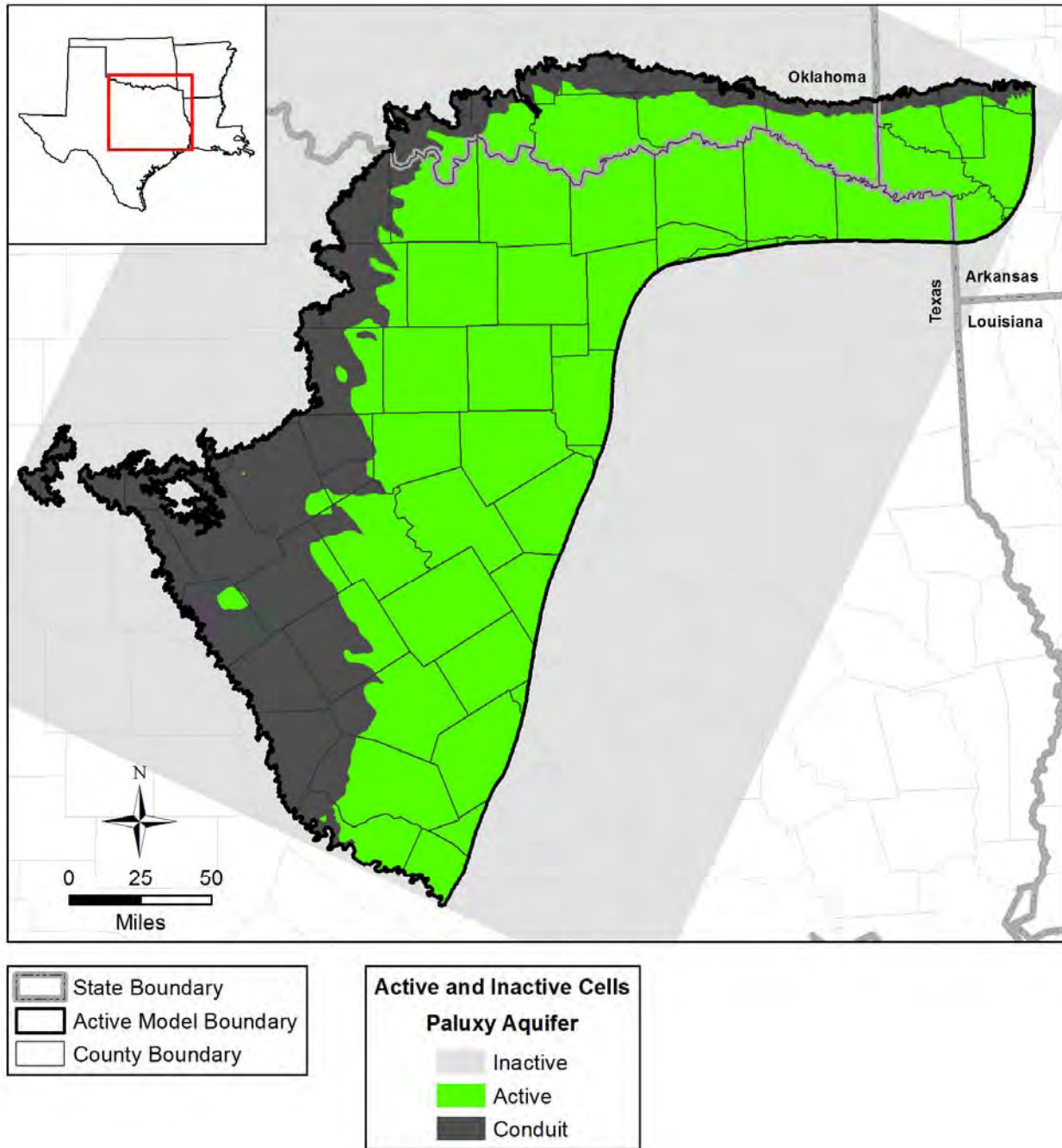
Figure 6.3.4   Layer 4 active/inactive model grid cells.
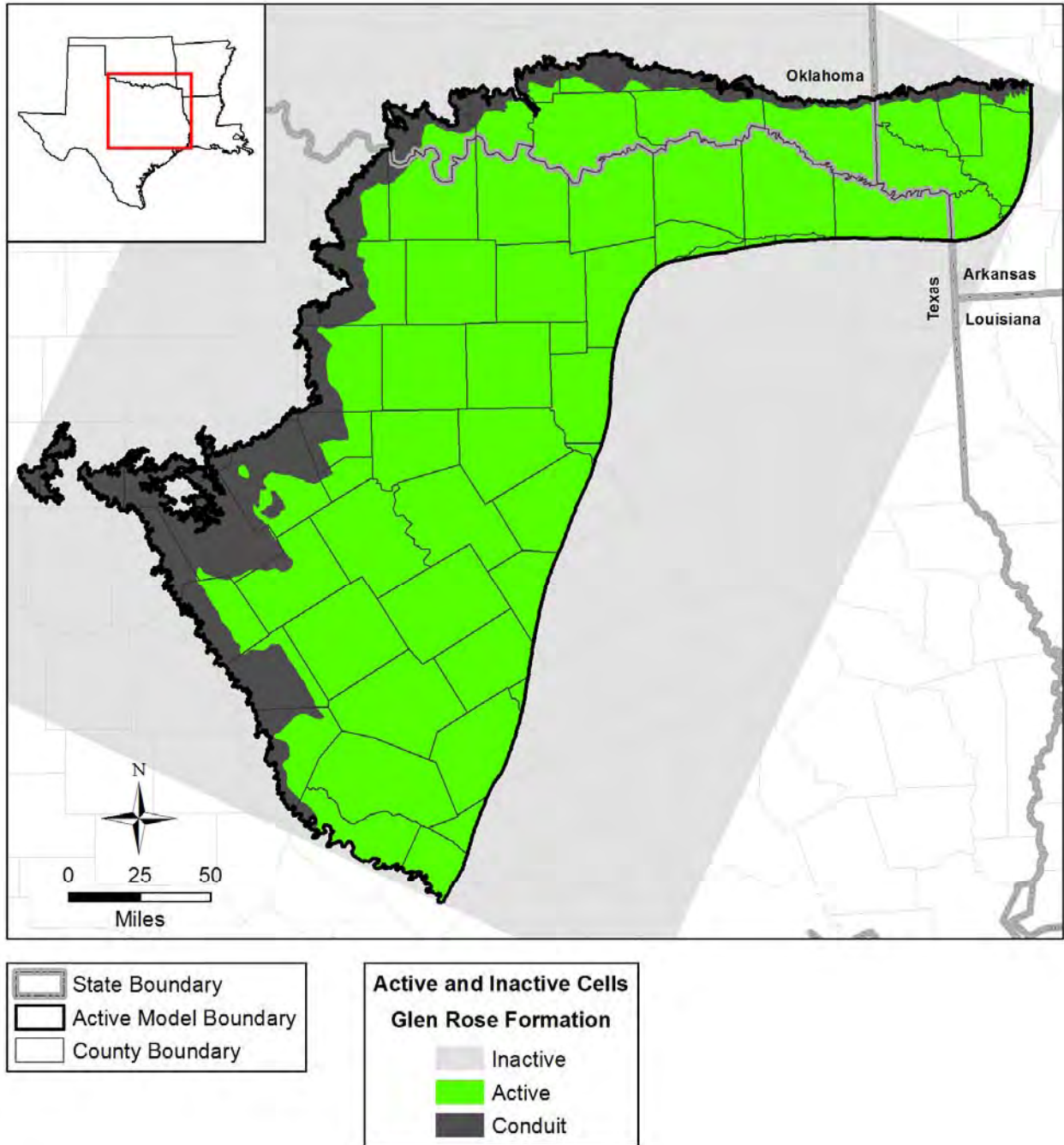
Figure 6.3.5   Layer 5 active/inactive model grid cells.
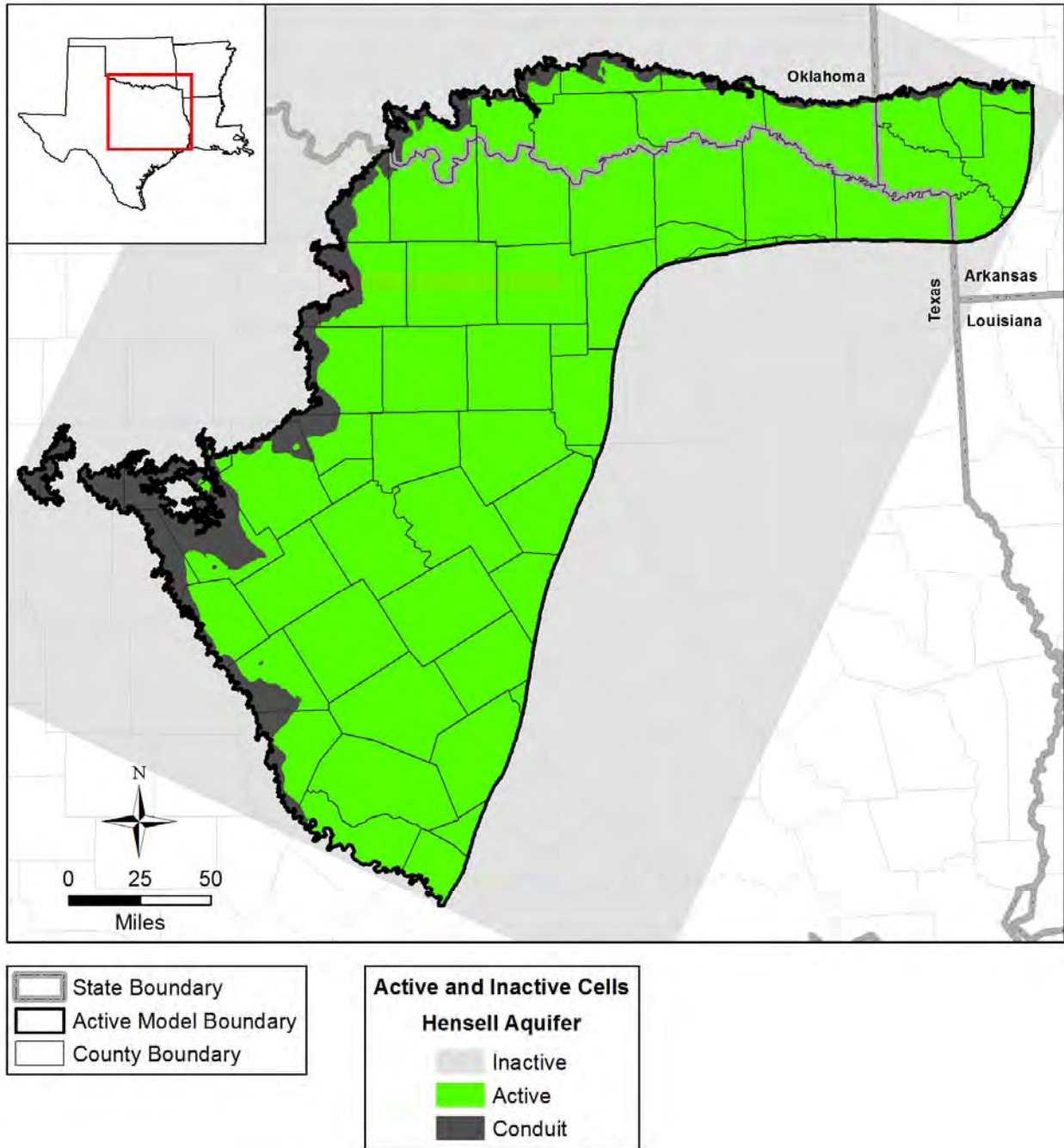
Figure 6.3.6   Layer 6 active/inactive model grid cells.
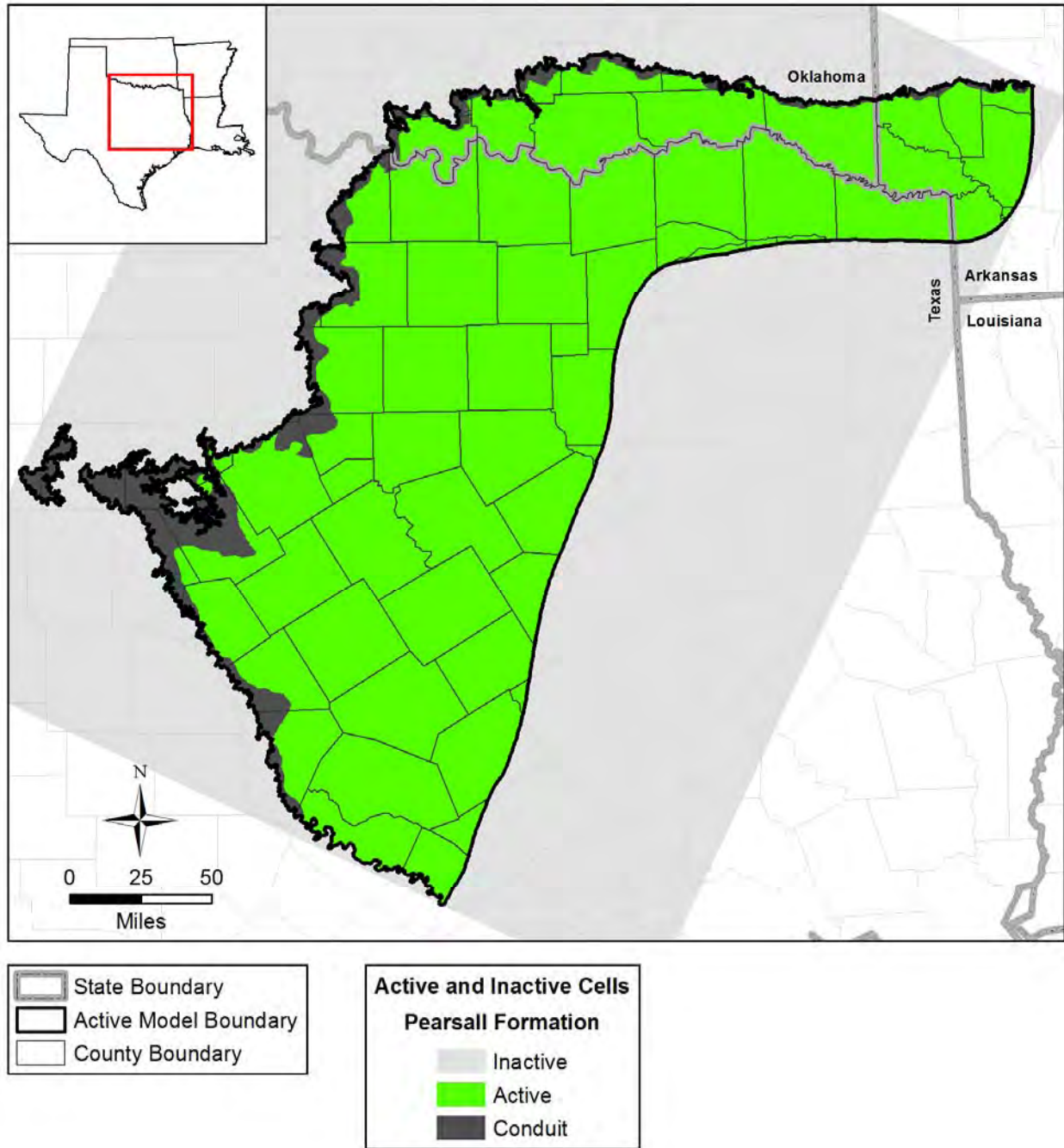
Figure 6.3.7   Layer 7 active/inactive model grid cells.
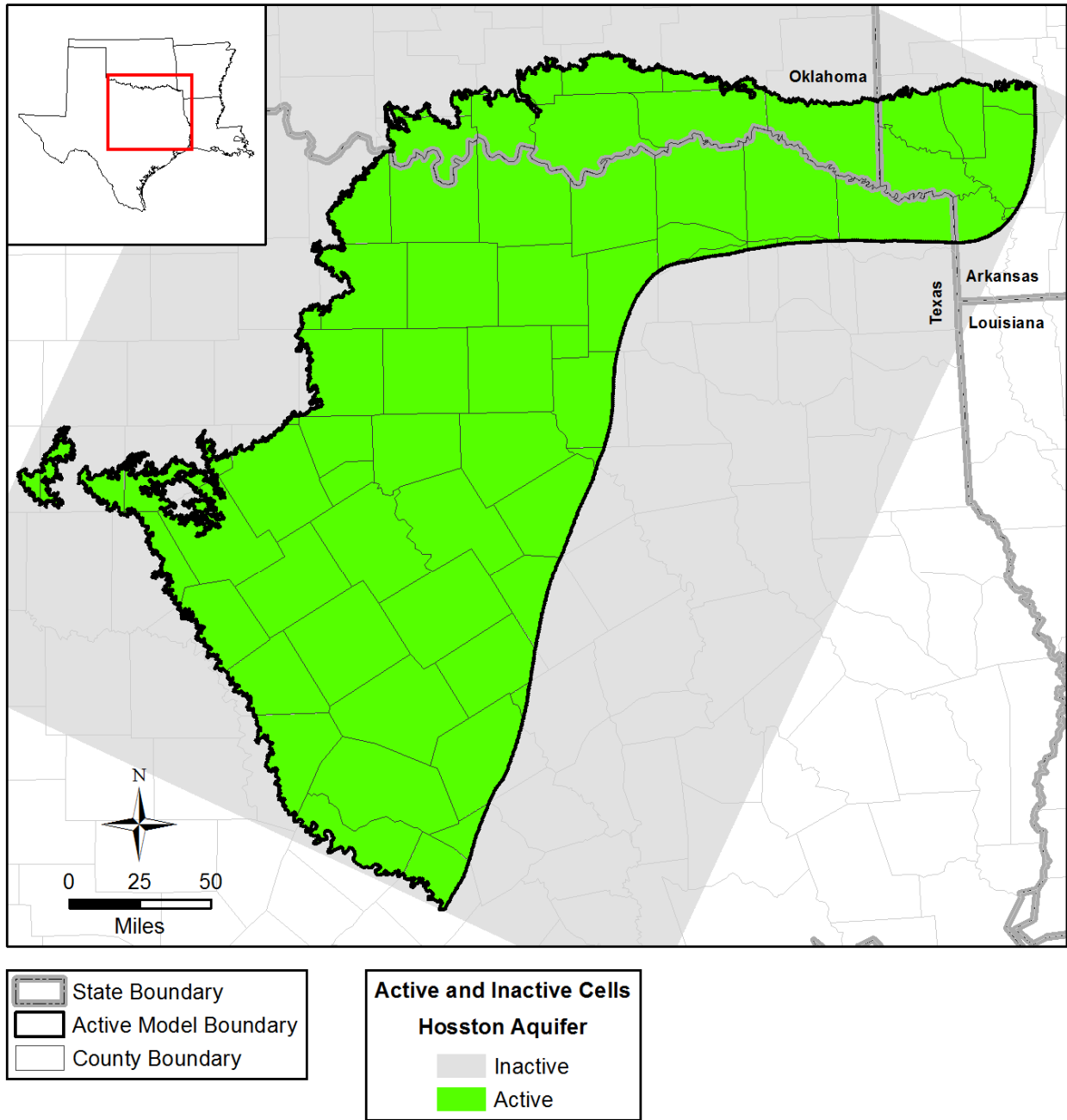
Figure 6.3.8   Layer 8 active/inactive model grid cells.
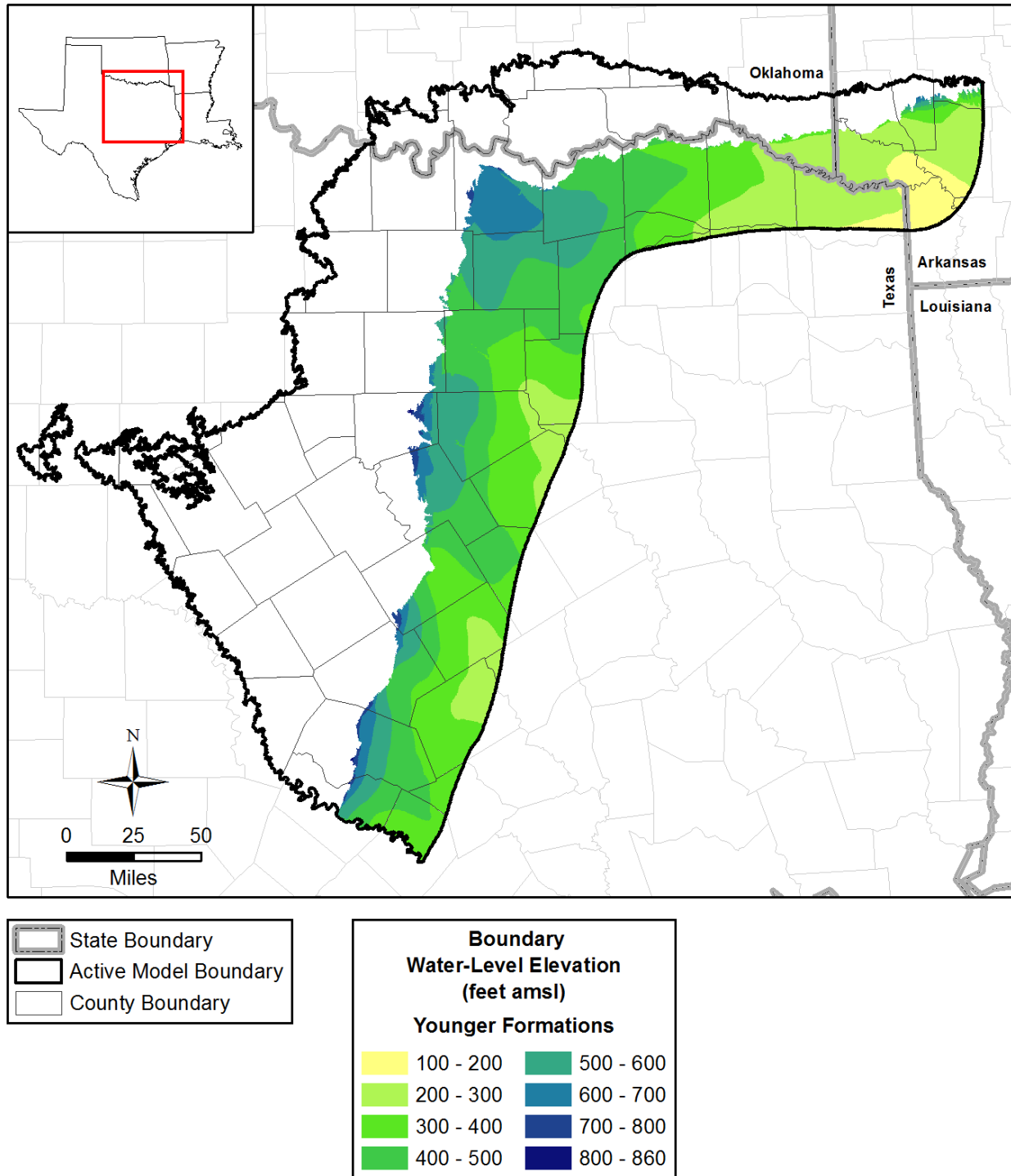
Figure 6.3.9 **Boundary water-level elevations (hydraulic heads) in feet amsl for the younger formations in Layer 1.**
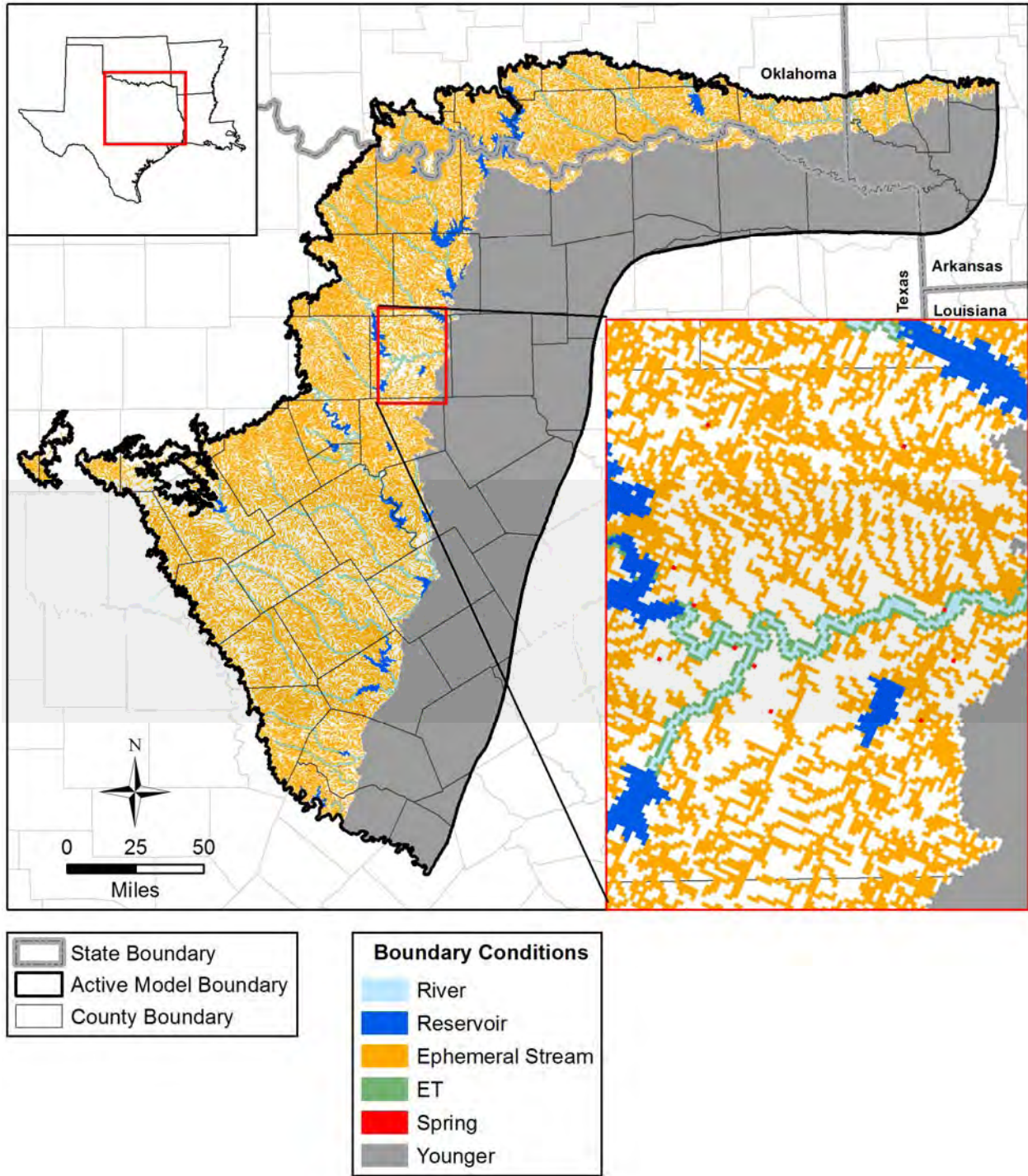
Figure 6.3.10   Layer 1 surface water boundary conditions.
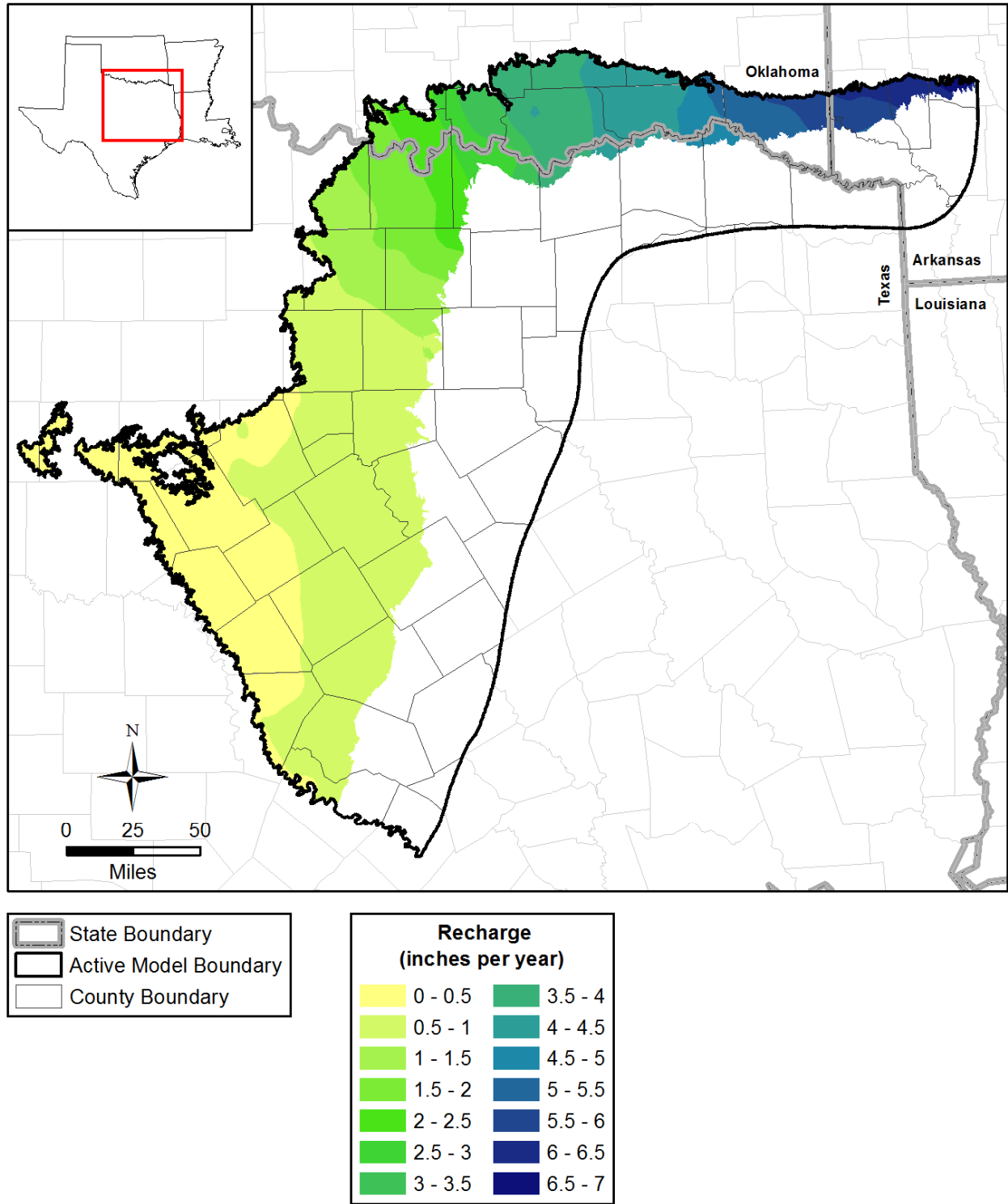
Figure 6.3.11   Average recharge distribution in inches per year.
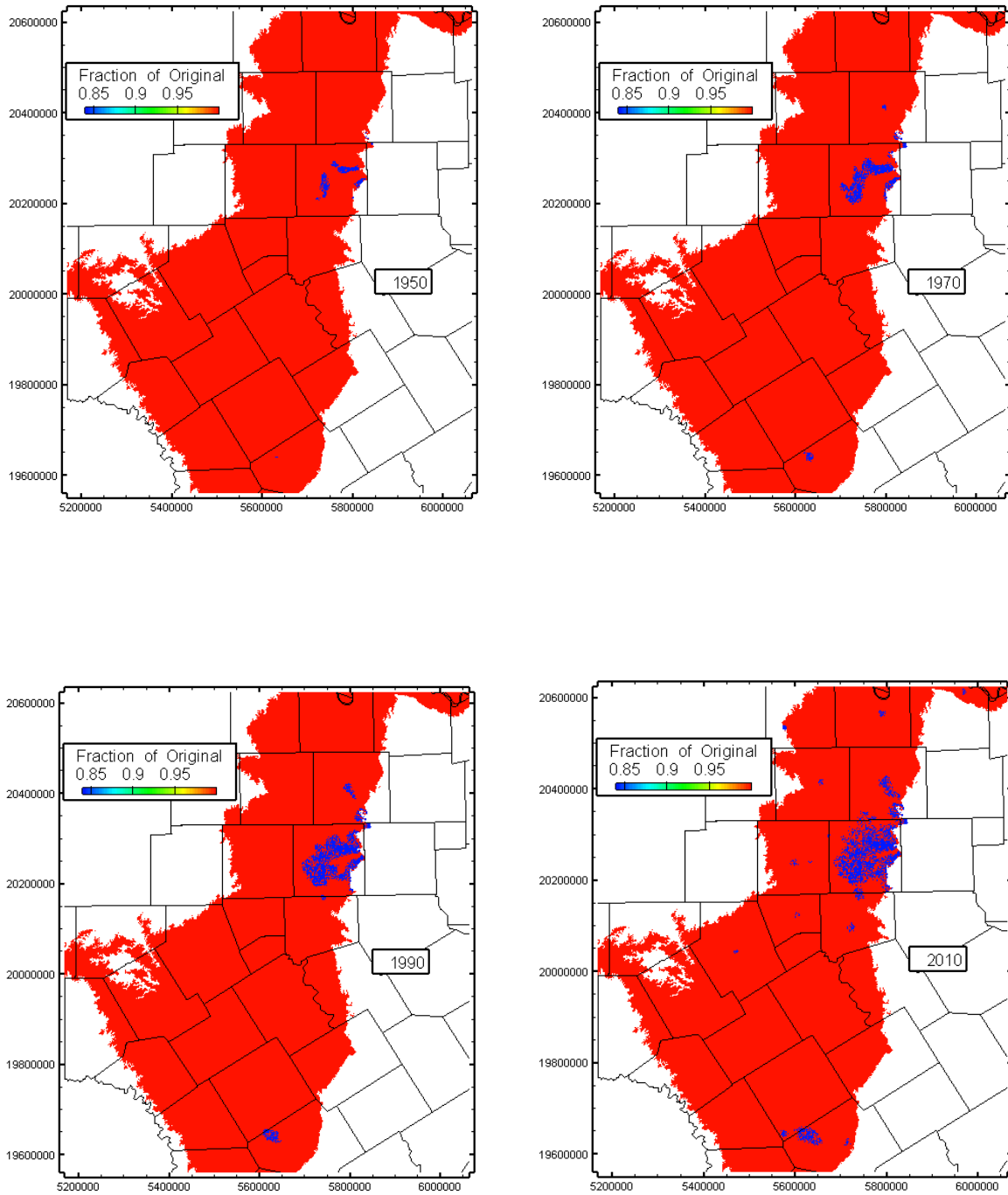
Figure 6.3.12   Impact of urbanization on recharge for 1950, 1970, 1990, and 2010.
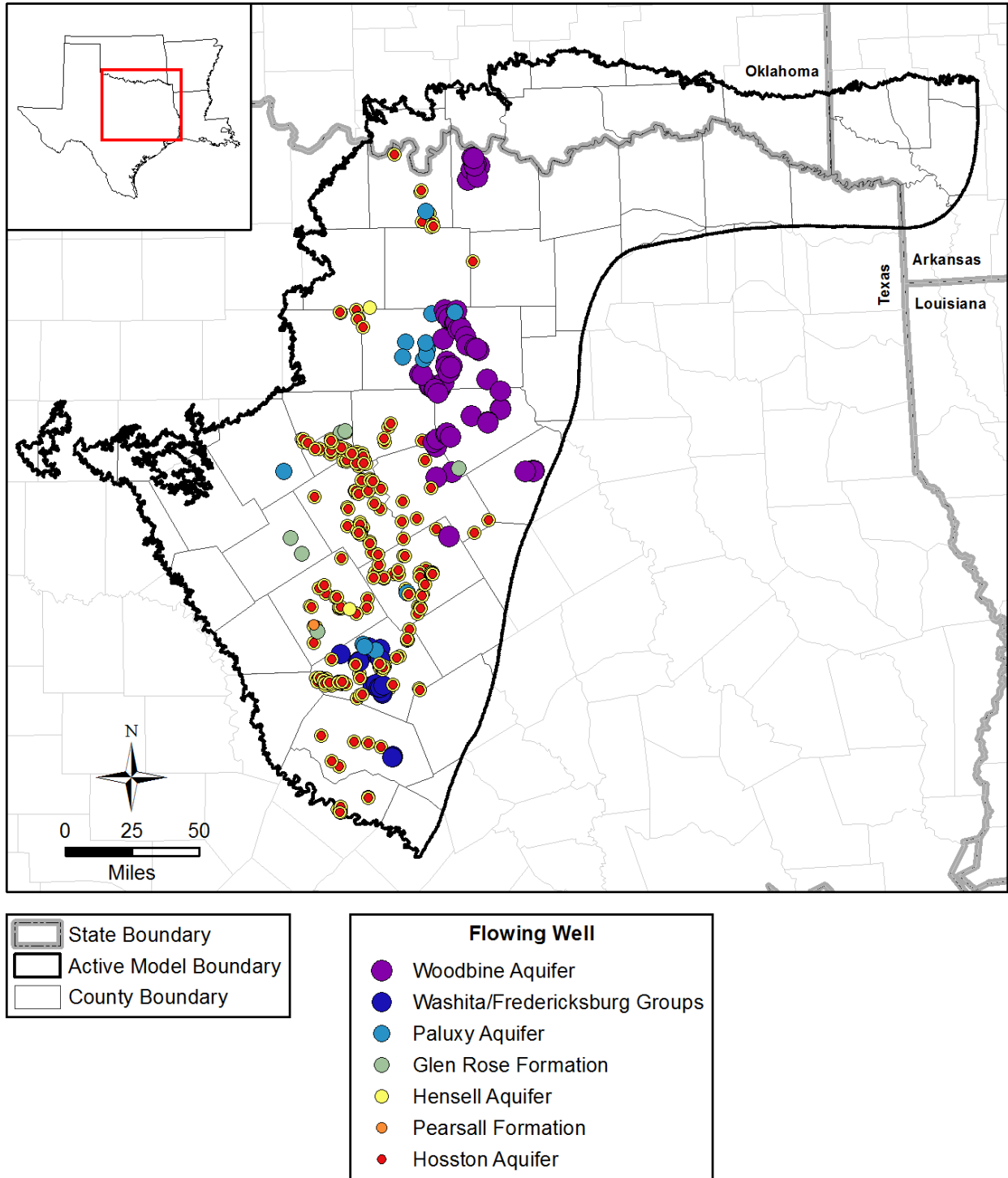
Figure 6.3.13   Flowing well locations and completion layers.
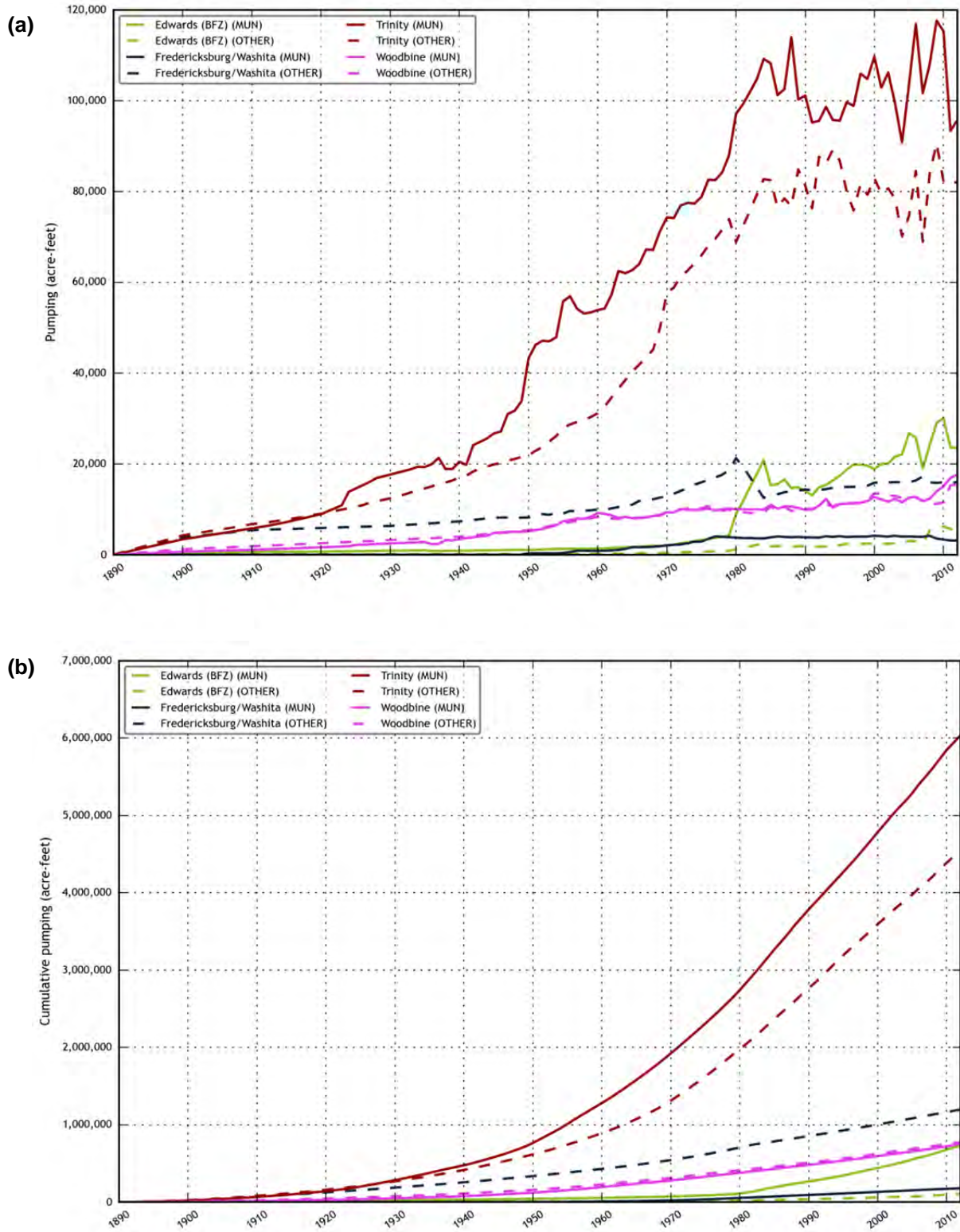
Figure 6.3.14   Plots of (a) temporal and (b) cumulative model pumping in AFY.
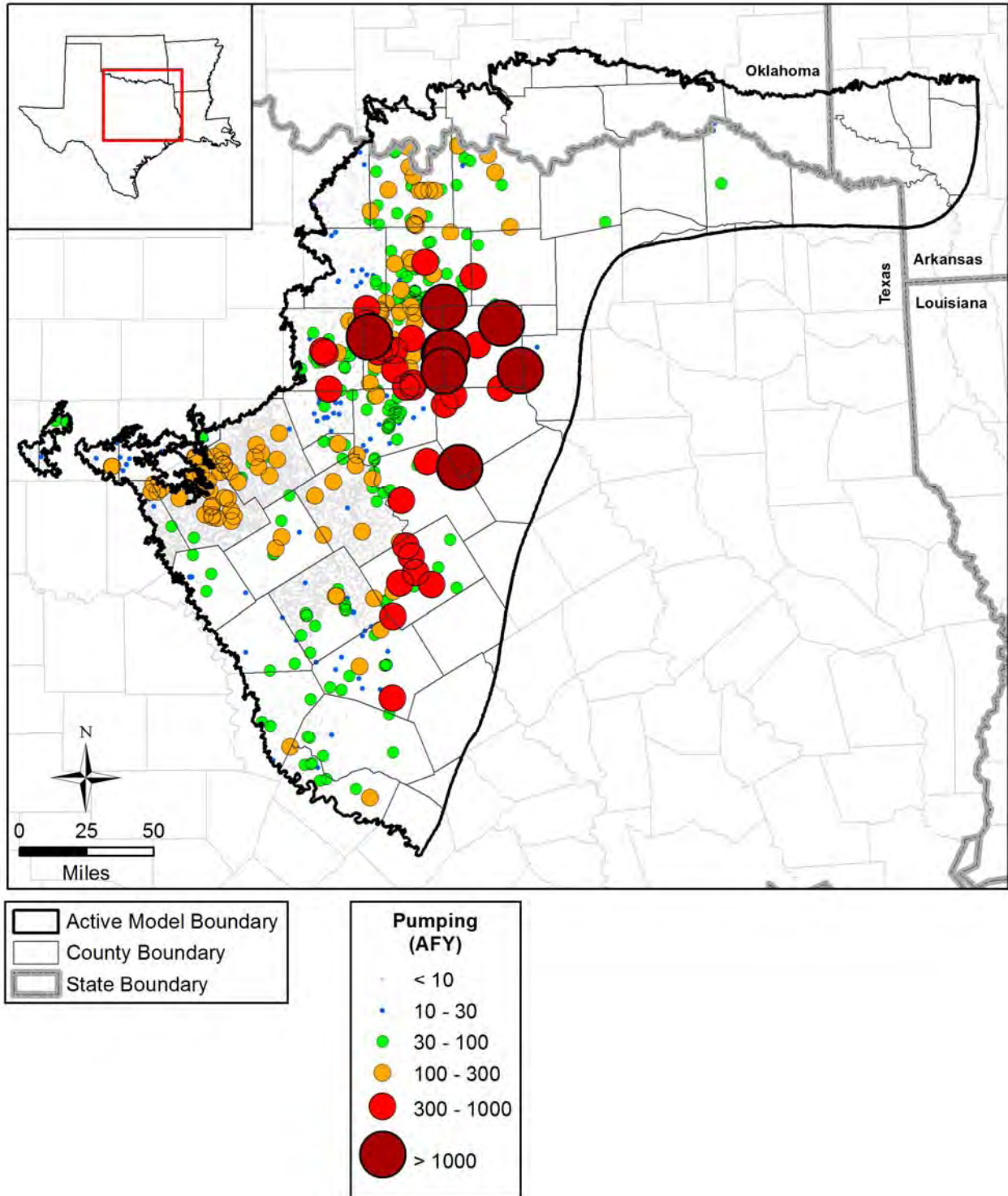
Figure 6.3.15   Model pumping distribution in AFY for the northern Trinity Aquifer in 1950.
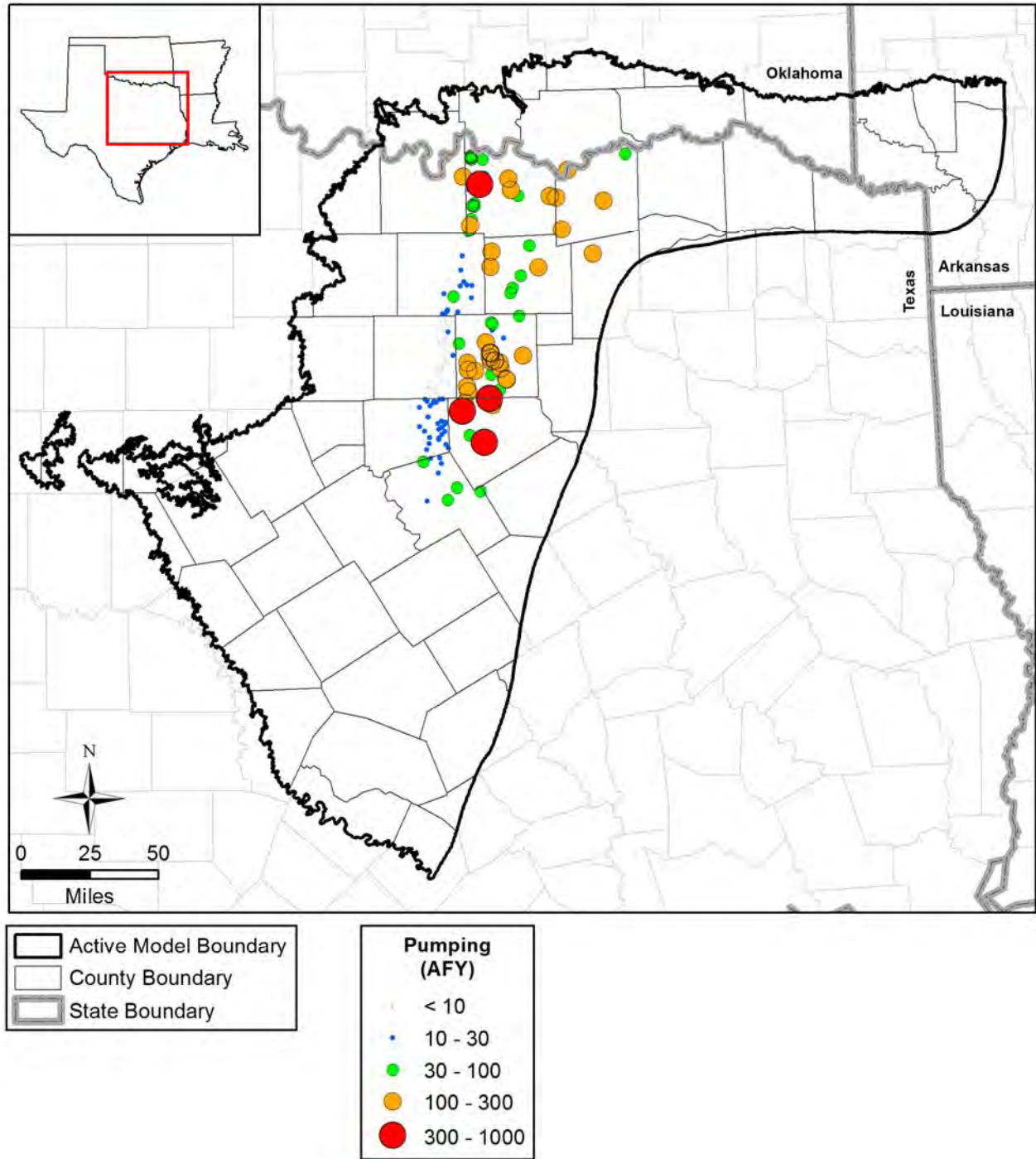
Figure 6.3.16   Model pumping distribution in AFY for the Woodbine Aquifer in 1950.
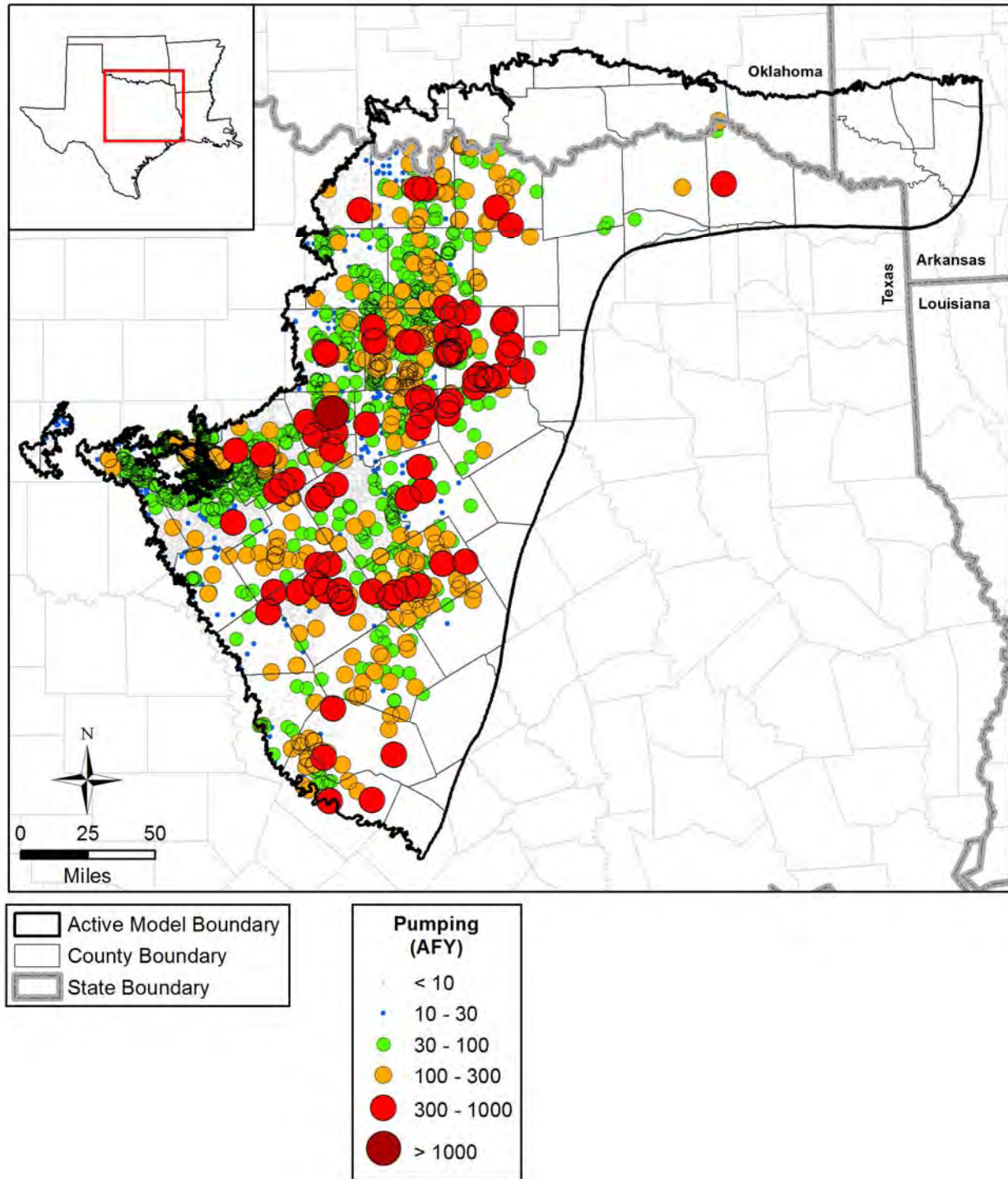
Figure 6.3.17   Model pumping distribution in AFY for the northern Trinity Aquifer in 1980.
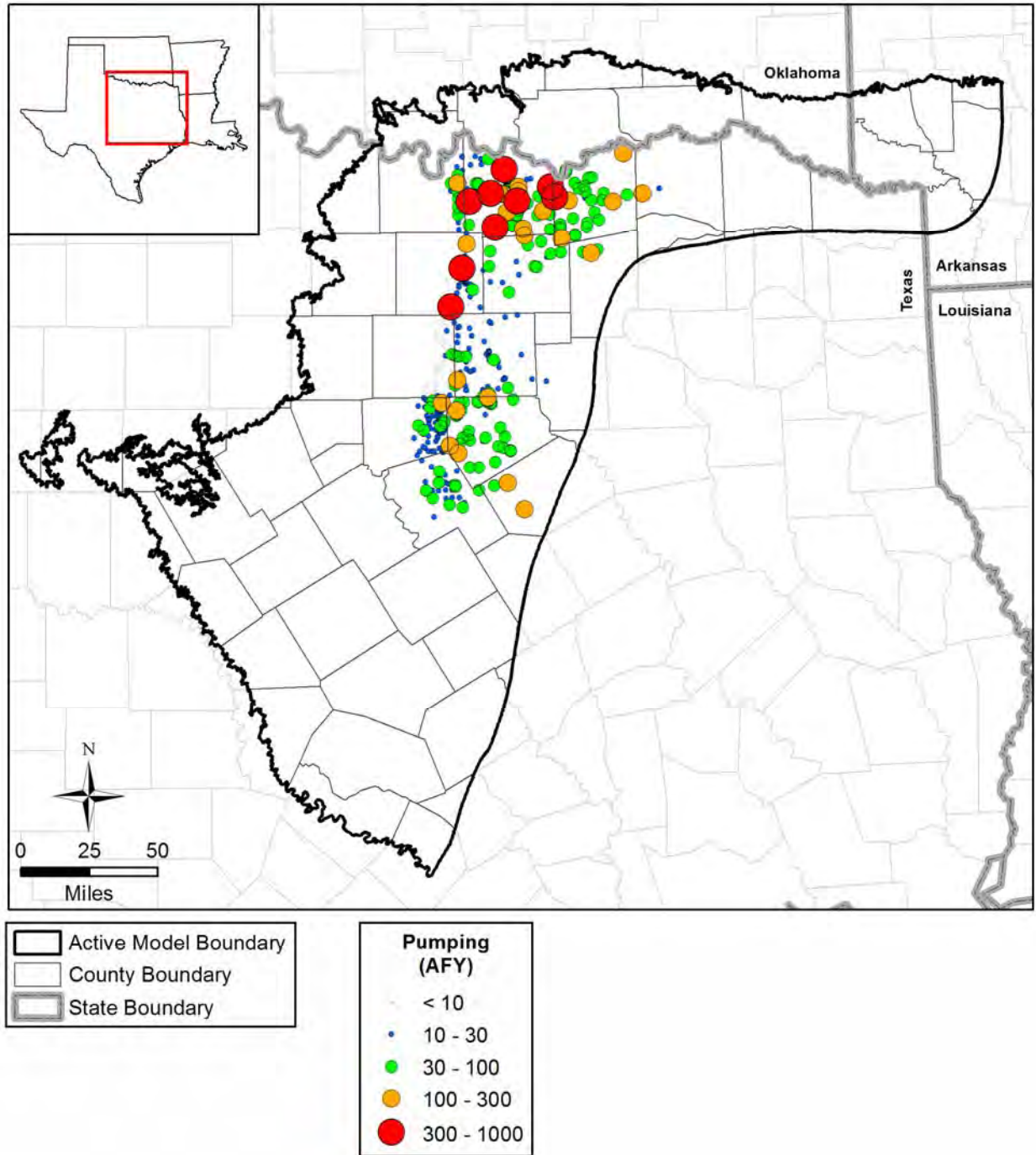
Figure 6.3.18   Model pumping distribution in AFY for the Woodbine Aquifer in 1980.
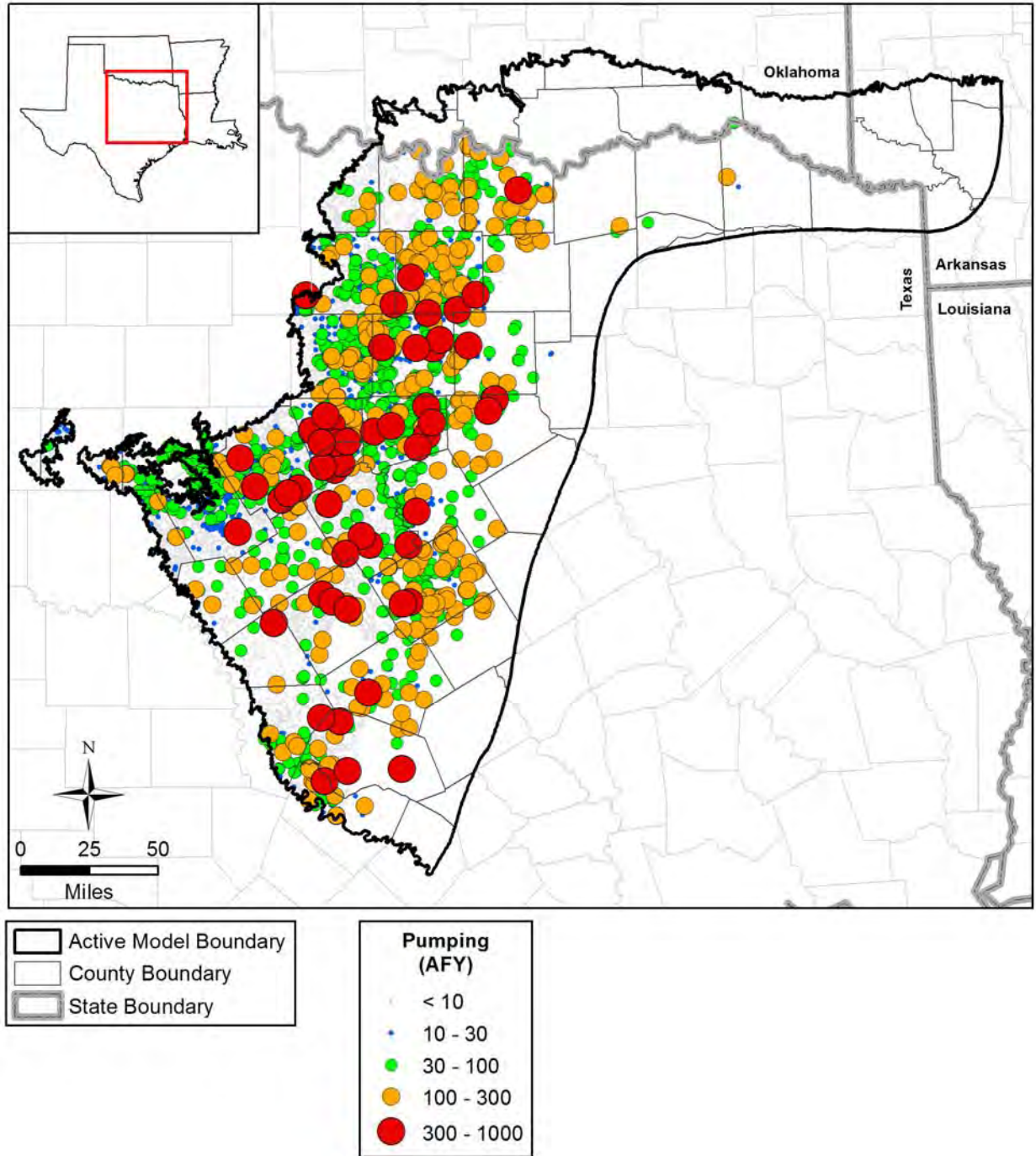
Figure 6.3.19 Model pumping distribution in AFY for the northern Trinity Aquifer in 2012.
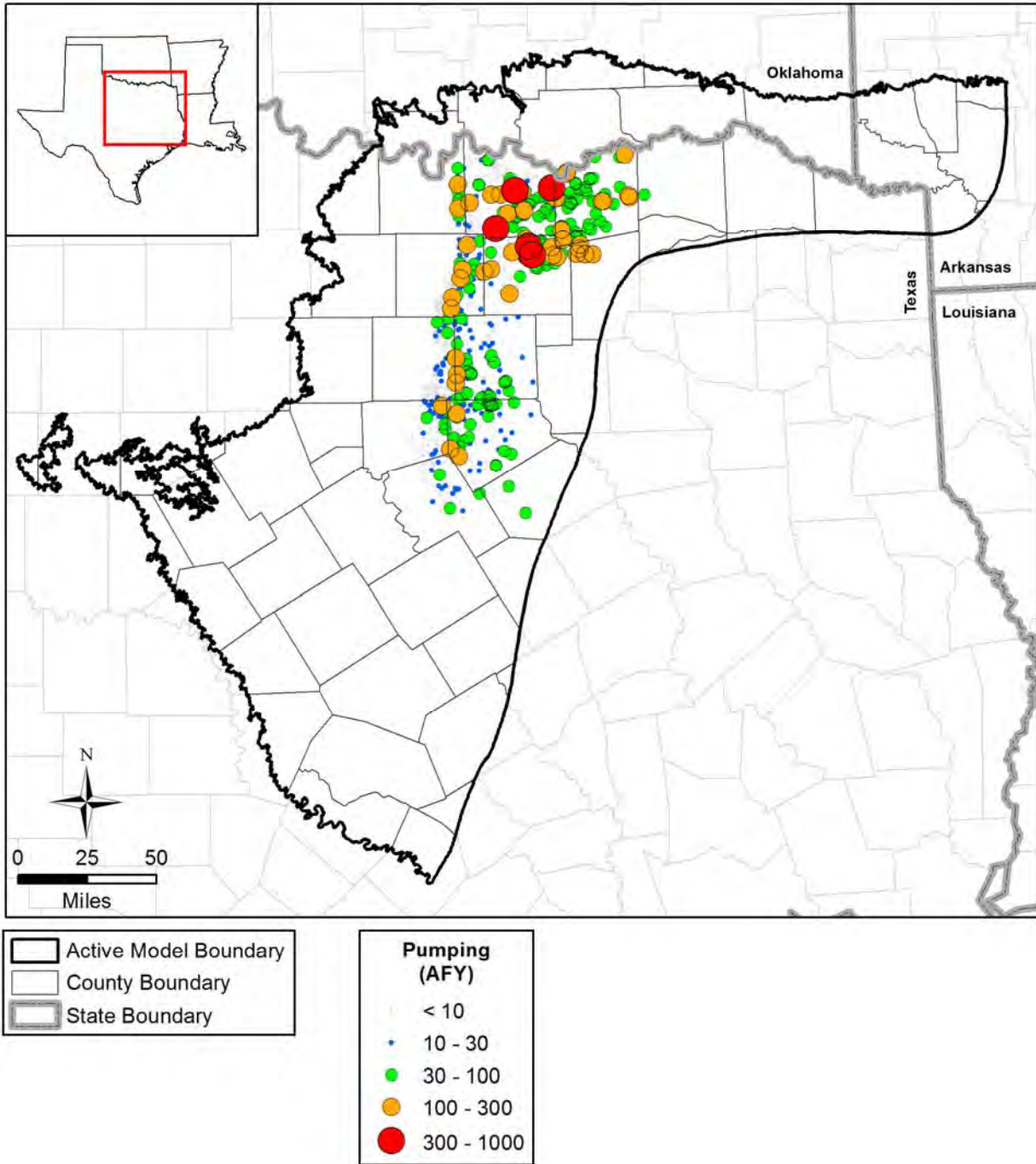
Figure 6.3.20   Model pumping distribution in AFY for the Woodbine Aquifer in 2012.

This page intentionally left blank.

6.4   Model Hydraulic Parameters

The primary hydraulic parameters for implementation in the model are hydraulic conductivity for the steady-state model and hydraulic conductivity and storage coefficient for the transient model. The following subsections describe the methods used to distribute these two parameters in the active model domain.

6.4.1 Hydraulic Conductivity

A challenge in constructing a regional model is developing "effective" hydraulic conductivity values representative of the different lithologies present in a model grid cell and across an aquifer. In many models, detailed lithologic data within the aquifer is used to develop grid-scale estimates of effective hydraulic conductivity. Estimating average effective hydraulic conductivity given assumptions for flow dimension, layer geometry, and correlation scales have been investigated by Warren and Price (1961) and Gutjahr and others (1978). For one-dimensional horizontal flow through layers of lithologies combined in parallel, the appropriate effective hydraulic conductivity is the weighted arithmetic average (Freeze and Cherry, 1979). For one-dimensional vertical flow that is perpendicular to layers of lithologies, the effective hydraulic conductivity is the harmonic average (Freeze and Cherry, 1979).

For the northern Trinity and Woodbine aquifers, the geophysical logs for 988 boreholes were analyzed and translated into a continuous lithologic profile. As discussed in Section 4.2, these lithologic profiles were translated into 10 litho-units for developing estimates of horizontal hydraulic conductivity. For estimating vertical hydraulic conductivity, the lithologic profiles were translated into nine litho-units focusing on limestone and shale lithologies, which dominate vertical hydraulic conductivity. These nine litho-units were: 4-foot shale, 10-foot shale, 4-foot limestone, 10-foot limestone, shaley limestone, clayey sand, poorly sorted sand, wells sorted sand, and sand. These two sets of litho-units were used to construct estimates of "effective" hydraulic conductivity in a model grid cell based on the theory of one-dimensional flow though layered media.

The following three-step process was used to initially implement hydraulic conductivity in the model using the lithologic information generated in Section 4.2:

1. At the 988 geophysical log locations where continuous profiles of the litho-units were developed, the litho-units that constitute the entire thickness of each model layer were determined.

2. At the 988 geophysical log locations, the effective horizontal and vertical hydraulic conductivity for each model layer was calculated based on a thickness weighted average of the hydraulic conductivities of the litho-units comprising the model layers at that location. The effective horizontal hydraulic conductivity was calculated based on a thickness weighted arithmetic average and the effective vertical hydraulic conductivity was calculated based on a thickness weighted harmonic average.

3. Kriging conducted with the algorithms in ArcGIS was used to interpolate a hydraulic conductivity (horizontal and vertical) for each grid cell in the active model domain using the calculated effective hydraulic conductivities at the geophysical log locations. The effective hydraulic conductivity values for each grid cell were then adjusted to account for decreases in hydraulic conductivity related to increased compaction and reduction in porosity that occur with increased depths of burial. The decrease in hydraulic conductivity was modeled as an exponential function of depth based on a review of previous research. Because clays are more susceptible to compaction than sands, the reduction with depth applied to the effective vertical hydraulic conductivity was greater than the reduction with depth applied to the effective horizontal hydraulic conductivity.

For model Layers 2 through 8, the initial baseline hydraulic conductivity distributions are shown in Figures 4.2.18 through 4.2.24, respectively, and the initial baseline transmissivity distributions are shown in Figures 4.2.25 through 4.2.31, respectively, in Section 4.2 of this report.

The approach used to assign effective horizontal and vertical hydraulic conductivities in model Layer 1 differed from that described above. For the portion of Layer 1 that represents the younger formations, uniform properties were applied. The horizontal hydraulic conductivity was initially set to 0.1 feet per day and the vertical hydraulic conductivity set to 1.0×10^{-4} feet per day. Because the primary purpose of this portion of Layer 1 is to act as a boundary condition, uniform effective hydraulic conductivity values were considered to be appropriate.

In the portion of Layer 1 that represents the surficial outcrop area of the northern Trinity Aquifer, Washita/Fredericksburg groups, and Woodbine Aquifer, the hydraulic conductivity of each

outcropping aquifer or formation was assigned. Because flow in the surficial outcrop area is meant to represent horizontal flow within the aquifer, the effective horizontal conductivity of the outcropping aquifer was used for both the horizontal and vertical hydraulic conductivities. Where alluvium is present in the outcrop as defined by the surface geology, a uniform and relatively high horizontal hydraulic conductivity of 100 feet per day was assigned. The alluvium was assumed to have a much higher hydraulic conductivity than the northern Trinity and Woodbine aquifer formations because it is re-worked material laid down in a high-energy fluvial depositional system without significant consolidation.

The downdip terminus of the active model domain is defined by the Mexia-Talco Fault Zone, which many investigators, including Dutton and others (1996), have conceptualized as a potential discharge area for the northern Trinity and Woodbine aquifers. To implement this potential vertical hydraulic connection at the Mexia-Talco Fault Zone, an increased vertical hydraulic conductivity of 0.01 feet per day was assigned to model grid cells in the vicinity of the fault zone in model Layers 2 through 8. By increasing the vertical hydraulic conductivity at the Mexia-Talco Fault Zone to 0.01 feet per day, model behavior was improved, however, additional increases beyond 0.01 feet per day did not further improve model behavior.

6.4.2 Fault Conductance

Numerous faults with significant vertical displacement affect the structure and hydraulic properties of the northern Trinity and Woodbine aquifers. The effect of the Balcones Fault Zone on the hydraulic properties was implemented through the MODFLOW horizontal flow barrier package. This MODFLOW package results in an added horizontal resistance to flow between groups of neighboring grid cells through a prescribed conductance term. The Balcones Fault Zone was assumed to propagate vertically through model Layers 2 through 8. An initial conductance of 0.001 square feet per day was assumed for the Balcones Fault Zone with the intent that this would be altered during the calibration process. The Mexia-Talco Fault Zone at the downdip terminus of the active model domain contains large displacements resulting in what is conceptualized to be both a termination to horizontal flow and an increase to vertical flow. An additional horizontal flow barrier was placed in Layer 1 between the portion of the layer representing the surficial outcrop area and the portion representing the younger formations. The purpose of this horizontal flow barrier was to restrict flow between the younger formations represented by boundary conditions and the surficial outcrop area. The locations for the

horizontal flow barriers are depicted in Figure 6.4.1. The conductances initially assigned to the horizontal flow barriers were adjusted during model calibration based on simulated flow behavior.

6.4.3 Storage Coefficient

Model Layer 1 represents the unconfined conditions in the active model domain and was assigned a specific yield of 0.1. Model Layers 2 through 8, which represent the deeper portions of the aquifers and formations, were modeled as confined. The storage coefficient for confined aquifers is equal to the aquifer thickness times the specific storage. Equation 6.4.1 was used to calculate specific storage for model layers 2 through 8. Equation 6.4.1 is based on the semi-empirical relationship developed by Shestakov (2002) based on an analysis of specific storage values calculated from aquifer pumping tests assuming a homogeneous medium. As part of this study, the relationship by Shestakov (2002) was modified to account for a heterogeneous medium with various percentages of shale, limestone, and sand as observed in the northern Trinity Aquifer, Washita/Fredericksburg groups, and Woodbine Aquifer. The modified equation is:

$$Ss = Ss_{min} + OM \; \frac{A1*[SF+shM*shF+LM*LF]}{A2*[DM*D^{DE}]} \qquad\qquad (6.4.1)$$

where

Ss = specific storage

Ss_{min} = minimum value for specific storage

OM = an overall multiplier

$A1$ = a numerator coefficient

SF = sand fraction

shM = a shale multiplier

shF = shale fraction

LM = a limestone multiplier

LF = limestone fraction

$A2$ = a denominator coefficient

DM = a depth multiplier

D = depth

DE = a depth exponent

A form of Equation 6.4.1 was used by Young and others (2009) to calculate specific storage for a regional model of the Lower Colorado River Basin.

The basis of the modified relationship given by Equation 6.4.1 was a reasonable fit to literature values for specific storage in the northern Trinity Aquifer. Figure 6.4.2 shows is a graph of specific storage as a function of depth on a log scale. Shown in this figure are the relationship developed by Shestakov (2002) and nine specific storage values obtained from aquifer pumping tests conducted in the northern Trinity Aquifer. These observed values were filtered from thirty specific storage values obtained as part of a literature review. All of the observed specific storage values were calculated from aquifer pumping test data where the pumping well and the observation well both had well screen lengths greater than 150 feet.

As shown in Figure 6.4.2, the literature values of specific storage plot below the semi-empirical curve of Shestakov (2002). To develop the parameters for Equation 6.4.1, a new curve was generated using the parameter values shown in Table 6.4.1. This new curve provides a reasonable fit to the observed data as shown in Figure 6.4.2. As shown in Table 6-1, several of the equation parameters are based on information specific to the model grid cell. The depth is calculated based on the midpoint of the grid cell. The sand, shale, and limestone fractions are calculated based on the composition of the litho-units that comprise the thickness of the model grid cell and sum to the value of 1.0.

Table 6.4.1   Descriptions and values for the parameters in Equation 6.4.1.

Model Parameter		Value
Ssmin	minimum specific storage value	1×10^{-8}
OM	overall multiplier	1
A1	numerator coefficient	0.0012
SF	sand fraction	grid cell specific
shM	shale multiplier	3
shF	shale fraction	grid cell specific
LM	limestone multiplier	0.33
LF	limestone fraction	grid cell specific
A2	denominator coefficient	100
DM	depth multiplier	10
D	depth (ft)	grid cell specific
DE	depth exponent	0.95
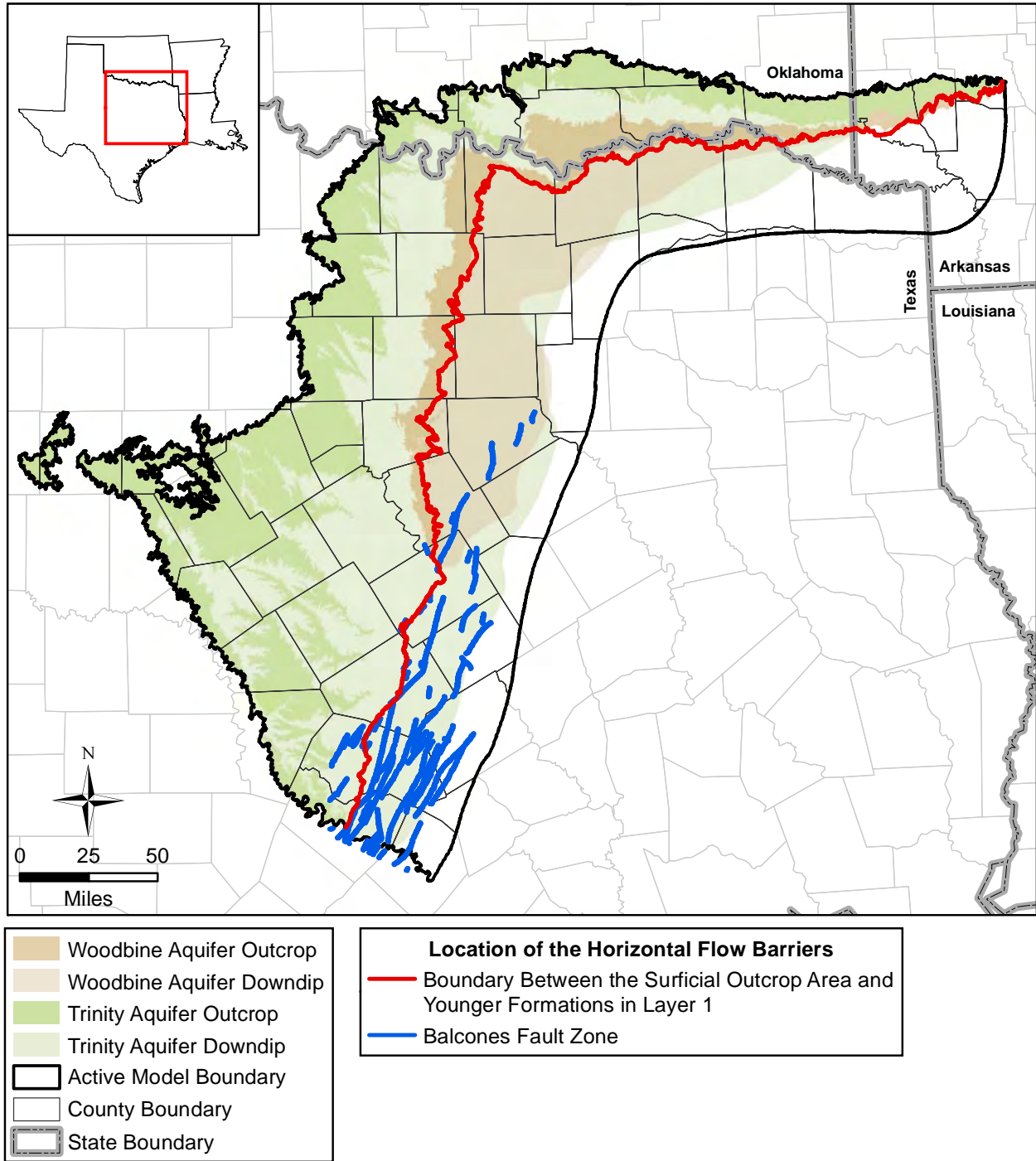
Figure 6.4.1   Location of horizontal flow barriers.
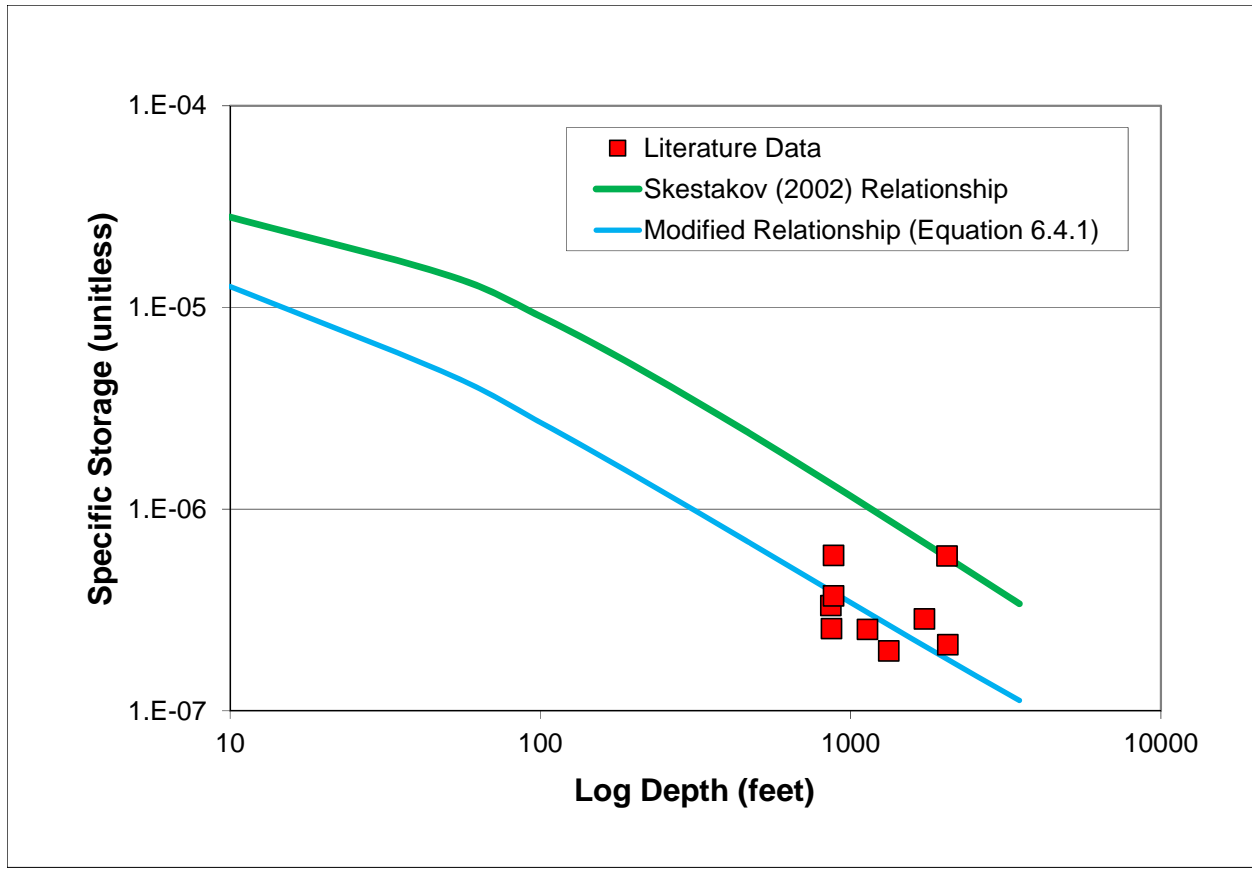
Figure 6.4.2   Specific storage versus log depth for literature data, the Skestakov (2002) relationship, and the modified relationship used for the northern Trinity and Woodbine aquifers GAM.

7.0   Modeling Approach

The updated northern Trinity and Woodbine aquifers GAM was developed using a modeling protocol that is standard to the groundwater modeling industry and has been adopted by the TWDB in their GAM Program. This protocol is based upon industry standards and American Society for Testing and Materials (ASTM) standard guides D5447-04, D5609-94, D5610-94, D5981-96, D5490-93, D5611-94 and D5718-95 (ASTM International, 2004, 2008a, 2008b, 2008c, 2008d, 2008e, 2006, respectively). The GAM protocol includes: (1) the development of a conceptual model for groundwater flow in the aquifers, including defining physical limits and properties, (2) model design, (3) model calibration, (4) sensitivity analysis, and (5) reporting.

Best practice for groundwater modeling includes both model calibration and model sensitivity analysis. In the context of groundwater modeling, model calibration can be defined as the process of producing an agreement between model simulated hydraulic heads and aquifer discharges, and field measured hydraulic heads and aquifer discharges through the adjustment of independent variables. Because the steady-state and transient models for the updated northern Trinity and Woodbine aquifers GAM are combined within a single model, changes to the model made during calibration were propagated to both the steady-state and transient models. The generally accepted practice for groundwater calibration includes performance of a sensitivity analysis. A sensitivity analysis entails the systematic variation of the calibrated parameters and stresses with re-simulation of aquifer conditions. The approach generally used in modeling and used in this study is called a "one-off" sensitivity analysis because the approach varies one model parameter or boundary condition stress at a time to see what impact each parameter or boundary condition independently has on the calibrated model performance. Those parameters that strongly change the simulated aquifer hydraulic heads and discharges are important parameters to the calibration. It is important to note that a standard "one-off" sensitivity analysis does not estimate parameter uncertainty, since limited parameter space is investigated and parameter correlation is not considered. In other words, parameters were not varied simultaneously and the combined effect of parameter variations was not investigated.

This page intentionally left blank.

7.1   Calibration

Groundwater models are inherently non-unique in that multiple combinations of hydraulic parameters and aquifer stresses can reproduce measured aquifer hydraulic heads. To reduce the impact of non-uniqueness, the calibration method described by Ritchey and Rumbaugh (1996) was employed. This method includes (1) calibrating the model using parameter values (i.e., hydraulic conductivity, storage coefficient, and recharge) that are consistent with measured values, (2) calibrating to multiple hydrologic conditions, and (3) using multiple calibration performance measures, such as hydraulic heads and discharge rates, to assess calibration. Each of these elements is discussed below.

To ensure that the model parameter values for hydraulic conductivity and specific storage are consistent with measurement values, algorithms were used to constrain model values. These algorithms use semi-empirical relationships based on properties calculated from aquifer pumping tests and principals of one-dimensional groundwater flow and one-dimensional consolidation theory.

The initial horizontal and vertical hydraulic conductivity distributions for the model layers were developed based on hydraulic conductivity values estimated for litho-units defined in Section 4.2. The analysis performed in Section 4.2 found that, for any given litho-unit, the variability of horizontal hydraulic conductivity estimated from aquifer pumping test data is usually close to a factor of five. This variability as it correlates to the litho-units for each aquifer/formation provides bounds for modification of horizontal hydraulic conductivity during calibration.

Estimates of vertical hydraulic conductivity for the litho-units were taken from the literature. During model calibration, adjustment of horizontal and vertical hydraulic conductivity was held to within plausible ranges based on available data and literature values. The initial transmissivity field estimates based upon the best-fit litho-unit hydraulic conductivities were adjusted during calibration within the range of observed variation and generally to the minimum degree possible to meet the calibration criteria. Adjustments during calibration were also made to depth decay parameters for hydraulic conductivity based upon pre-defined minimum and maximum values.

To constrain storage values used in the model, a relationship was developed based upon lithology and depth of burial and fit to the observed field data. An investigation was conducted

prior to model calibration to investigate the allowable variation in values for the parameters used to calculated storage parameters. This investigation indicated that relatively minor changes in the relationship's parameter values generated values for specific storage inconsistent with measured values. The investigation also showed that the indicated minor variations in the parameter values did not have a notable impact on the hydraulic heads predicted by the model. Consequently, only minor modification to parameter values occurred during model calibration. This ensured that the model calibration did not allow unrealistic storage values in order to improve the match to measured hydraulic heads.

Recharge was based upon regression models of groundwater yield on a surface water basin analysis of stream hydrographs. Because the recharge model is a regression fit between stream base flow and precipitation, it is, by definition, an average model that may not appropriately reproduce highs and lows in the base flow/precipitation relationship for any given basin. In addition, multiple basins were combined to define the model wide relationship. The end result for recharge was that it was reasonably constrained in a model average sense but some leeway was allowed in adjusting the recharge function during calibration.

Adjustments to aquifer parameters from initial estimates were minimized, to the extent possible, to meet the calibration criteria. As a general rule, parameters with few measurements were adjusted preferentially as compared to parameters with good supporting data.

The updated northern Trinity and Woodbine aquifers GAM was calibrated for two time periods, one representing steady-state conditions and the other representing transient conditions. The steady-state calibration considers the predevelopment time period prior to extensive aquifer development. The transient calibration period considers the time period from 1890 through 2012 to include as many hydraulic head observations as possible and to incorporate the early hydraulic head declines that resulted from initial development and the practice of allowing wells to freely flow and the historical onset of significant groundwater development in the 1950s. Section 4.3 describes the aquifer hydraulic heads and how they were derived for use in the steady-state and transient calibration periods. Pumping estimates based on historical records were applied on an annual time scale in the transient calibration period. Flowing wells were simulated as drains, which is the most appropriate boundary condition for their application to a groundwater model.

Recharge varies temporally based on annual precipitation, reservoir stages vary temporally based on measurements, and stream stage remains constant throughout the transient period.

The model was calibrated through a wide range of hydrological conditions. The steady-state model represents a period of equilibrium where aquifer recharge and aquifer discharge were in balance. The transient calibration period (1890 through 2012) represents a time of transient aquifer behavior. Calibrating to the transient period helps constrain the model parameterization because a wider range of hydrologic conditions are encountered and simulated. The sensitivity of the transient model to certain parameters differs from that of the steady-state model.

Calibration requires development of calibration targets and specification of calibration measures. The issue of non-uniqueness is best addressed by using as many types of calibration targets as possible. The primary calibration target is hydraulic head (water level). Long-term base flow estimates for streams were also used as calibration targets. In addition, the artesian conditions necessary to produce discharge to flowing wells was considered and groundwater ages consistent with observed freshwater at depth were calculated using reverse particle tracking. Simulated hydraulic heads were compared to measured hydraulic heads at specific observation points through time (hydrographs) to ensure that model water levels are consistent with hydrogeologic trends.

Springs were assumed to constitute a small portion of the total discharge from the northern Trinity and Woodbine aquifers, but were included in the model nonetheless. Flowing wells constitute a large portion of the total discharge from the aquifers between predevelopment and the onset of significant active pumping. The lack of true quantitative estimates of discharge for most flowing wells and springs precludes direct comparison of simulated discharge to hard estimates of discharge by these two mechanisms. Rather, simulated flow from flowing wells and springs were only evaluated in a qualitative manner to ensure that simulated predevelopment heads were generally above land surface and flows were not inconsistent with estimates made during the conceptual model phase.

Traditional calibration measures (Anderson and Woessner, 1992), such as the mean error, the mean absolute error, and the root mean square error, quantify the average error in the calibration process. The mean error is the mean of the differences between simulated hydraulic heads and measured hydraulic heads:

$$mean\ error = \frac{1}{n} \sum_{i=1}^{n} (h_s - h_m)_i \qquad (7.1.1)$$

where

h_s = simulated hydraulic head (feet amsl)

h_m = measured hydraulic head (feet amsl)

n = number of calibration measurements

The mean absolute error is the mean of the absolute value of the differences between simulated hydraulic heads and measured hydraulic heads:

$$mean\ absolute\ error = \frac{1}{n} \sum_{i=1}^{n} \left| (h_s - h_m)_i \right| \qquad (7.1.2)$$

The root mean square error is the average of the squared differences between simulated heads and measured heads:

$$root\ mean\ square\ error = \left[\frac{1}{n} \sum_{i=1}^{n} (h_s - h_m)_i^2 \right]^{0.5} \qquad (7.1.3)$$

The difference between a measured hydraulic head and a simulated hydraulic head is termed a residual.

The mean absolute error was used as the basic calibration metric for hydraulic heads. For TWDB GAMs, the required calibration criterion for hydraulic heads is a mean absolute error that is less than or equal to 10 percent of the observed hydraulic head range in the aquifer being simulated. To provide information on model performance with time, the mean absolute error was calculated for each year in the transient calibration period. The mean absolute error is useful for describing model error on an average basis but, as a single measure, does not provide insight into spatial trends in the distribution of residuals.

Examination of the distribution of residuals is necessary to determine if they are randomly distributed over the model grid and not spatially biased. Post plots of hydraulic head residuals for both the steady-state and transient portions of the updated model of the northern Trinity and Woodbine aquifers were used to check for spatial bias. These plots indicate the magnitude and direction of the differences between observed and simulated hydraulic heads. Finally, plots of

simulated versus observed hydraulic heads and residual versus observed hydraulic heads were used to determine if bias varies with the magnitude of the observed hydraulic heads.

This page intentionally left blank.

7.2 Calibration Target Uncertainty

Calibration targets are uncertain. In order to not "over-calibrate" a model, which is a stated desire for TWDB GAMs, the calibration criteria should be defined consistently with the uncertainty in calibration targets. Uncertainty in water-level measurements can be the result of many factors including measurement errors, scale errors, and various types of averaging errors that are both spatial and temporal. The primary calibration criteria for hydraulic head is a mean absolute error less than or equal to 10 percent of the observed hydraulic head variation within the aquifer being modeled. The range in the observed water levels across the northern Trinity and Woodbine aquifers in the study area is 2,797 feet during steady-state and 2,951 feet during transient conditions. This leads to acceptable mean absolute errors of 280 and 295 feet for the steady-state and transient models, respectively. Comparison of this mean absolute error to an estimate of the hydraulic head target errors indicates the level of calibration the underlying hydraulic head targets can support.

Water-level measurement errors are typically on the order of tenths of feet and, at a GAM scale, can be considered insignificant. However, measuring-point elevation errors can be significant. The error (standard deviation) in averaging ground surface elevations from a 10-meter digital elevation model (DEM) to quarter-mile by quarter-mile model grid cells averages 12 feet within the outcrop of the northern Trinity and Woodbine aquifers. Another error is caused by combining multiple aquifer textures (i.e., sediment types) into quarter-mile by quarter-mile grid cells represented by one simulated hydraulic head. No coincident hydraulic heads (i.e., hydraulic head data for more than one well located in a single grid cell) are available with which to assess this error mechanism, however. When these errors are added together, the average error in model hydraulic heads could easily equal 30 to 40 feet. Calibrating to mean absolute error values significantly less than 40 feet would constitute over-calibration of the model and parameter adjustments to reach that mean absolute error are not supported by the uncertainty in hydraulic head.

The predevelopment hydraulic heads are discussed in Section 4.3.2. Few, if any, true predevelopment hydraulic heads exist within the northern Trinity and Woodbine aquifers. To provide an estimate of the predevelopment hydraulic heads, the first water level observed in a given well was used. This allowed calibration of the steady-state model to different hydrologic

conditions than those of the transient model, however, it was expected that these hydraulic heads are biased low compared to true predevelopment conditions. As a result, a steady-state calibration state that is biased high rather than low in terms of simulated hydraulic heads was favored.

7.3   Conceptual Model Uncertainty

The conceptual model of nearly any hydrogeologic system has aspects that are uncertain. This is especially true the greater the complexity of the aquifer system. Section 4 details the conceptual model for the northern Trinity and Woodbine aquifers, which is very complex, especially with respect to model structure and model properties.

The overlying younger formations and underlying Paleozoic-age formations are uncertain boundaries to the model that are poorly constrained. The lower model boundary has been defined as a no-flow boundary. However, it is known, and documented in this report, that in some cases in the study area the Hosston Aquifer lies unconformably on permeable sands and gravels of Paleozoic-age formations. It is expected that hydraulic communication between the Hosston Aquifer and the Paleozoic-age formations is only important locally and that the water balance of the overlying northern Trinity Aquifer far exceeds that of the Paleozoic-age formations. This issue was discussed with the TWDB and it was determined that implementing the lower boundary as a no-flow boundary was a conservative assumption since the model will be used principally as a groundwater availability model. The Upper Trinity GCD is funding the development of a groundwater model of the Paleozoic-age formations underlying the northern Trinity Aquifer. That model will be used by the Upper Trinity GCD to estimate groundwater availability and recoverable storage in the Paleozoic-age formations and as a management tool.

This page intentionally left blank.

7.4   Sensitivity Analysis

A sensitivity analysis was performed on the steady-state and transient calibrated models to determine the impact of changes in a calibrated parameter on the predictions of the calibrated model. A standard "one-off" sensitivity analysis was performed. This means that hydraulic parameters or stresses were adjusted from their calibrated "base case" values one by one while all other hydraulic parameters remained unperturbed.

This page intentionally left blank.

8.0   Steady-State Model

The steady-state model developed for the northern Trinity and Woodbine aquifers represents a predevelopment period when hydraulic heads in the aquifer are assumed to be constant owing to an assumed long-term equilibrium between aquifer recharge and natural aquifer discharge. This section details calibration of the steady-state model and presents the steady-state model results. The sensitivity of the steady-state model to various hydrologic parameters is also described.

8.1   Calibration

This section describes the steady-state calibration targets and potential calibration parameters, including horizontal and vertical hydraulic conductivity, recharge, ET, general-head boundaries, and stream conductance.

8.1.1   Calibration Targets

Water-level measurements are typically needed as targets for steady-state calibration. Selection of water-level measurements representative of steady-state conditions is a challenge for most groundwater modeling studies and was discussed in Section 4.3.2 for this study. Steady-state targets included water-level measurements from 96 well locations in the northern Trinity and Woodbine aquifers. Compared to the more than 27,000 water-level measurements at over 17,000 well locations available for the transient period, there is a distinct lack of water-level data for the steady-state model.

Due to this lack of water-level measurements for use as calibration targets, additional metrics were used to constrain the steady-state model. The number of reported flowing wells in the northern Trinity and Woodbine aquifers during the transient model period is indicative of artesian conditions during the steady-state period. Water quality measurements also indicate significant downdip penetration of freshwater in the Hosston and Hensell aquifers. Qualitatively matching both of these conditions added constraints to the steady-state model.

8.1.2   Horizontal and Vertical Hydraulic Conductivities

Section 6.4.1 described the determination of initial horizontal and vertical hydraulic conductivities for the model. Figures 8.1.1 through 8.1.8 depict the calibrated horizontal hydraulic conductivity fields for each layer in the steady-state model. The main changes to the

horizontal hydraulic conductivity values involved layer-wise adjustments. Generally, both horizontal and vertical hydraulic conductivities were lowered from initial estimates during calibration and these changes to hydraulic properties are detailed in Section 9. Calibrated hydraulic properties were evaluated and subsequently adjusted to remain within the range of values determined from the analysis of aquifer pumping tests. The resulting hydraulic parameters are, therefore, considered consistent within the uncertainty range of initial estimates.

In the steady-state model, vertical flow of groundwater from one layer to another is controlled primarily by the vertical hydraulic conductivity of the confining units (i.e., Pearsall Formation, Glen Rose Formation, and Washita/Fredericksburg groups) and, to a lesser degree, the primary productive units (i.e., Hosston, Hensell, Paluxy, and Woodbine aquifers). As described in Section 6.4.1, the vertical hydraulic conductivity for each of the aquifers/formations was calculated based on a harmonic averaging of estimates of lithologic properties. While depth decay was applied to both the horizontal and vertical hydraulic conductivity estimates, the depth-based consolidation of clayey sediments was considered to be greater than that of sandy sediments. Because clayey sediments govern the vertical hydraulic conductivity and sandy sediments govern the horizontal hydraulic conductivity, the depth-decay in hydraulic conductivity was more pronounced in the vertical direction. Under this formulation, vertical hydraulic conductivity was based on the same lithology as that for the horizontal conductivity, but was calculated independently as described in Section 6.4.1.

The calibrated vertical hydraulic conductivities for the model layers are shown in Figures 8.1.9 through 8.1.16. In these figures, note that the vertical hydraulic conductivity was set equal to the horizontal conductivity in the updip portions of each layer where they are connected through "conduit" layers to the portion of the surficial layer representing that same formation. In this way, surficial sediments of the Hosston Aquifer are connected to confined sediments of the Hosston Aquifer through the horizontal hydraulic conductivity of the Hosston Aquifer, and likewise for the other aquifers/formations. This accounts for the high "vertical" hydraulic conductivity values apparent at the updip limits of each layer in Figures 8.1.9 through 8.1.16. Additionally, the higher degree of vertical connectivity conceptualized along the Mexia-Talco Fault Zone is evident in the higher vertical hydraulic conductivity values at the downdip limit of each layer.

8.1.3   Recharge and Groundwater ET

Recharge in the outcrop of the steady-state model was based on a function dependent on the
30-year average precipitation and location in the active model domain. Implementation if
recharge is discussed in Section 6.3.4. Altering recharge and hydraulic conductivity
concurrently leads to inherently non-unique calibrations (Castro and Goblet, 2003).
Furthermore, using data to constrain recharge has been demonstrated to be more efficient at
stabilizing the groundwater inverse problem than constraining hydraulic conductivity values
when calibrating primarily to hydraulic head data (Weiss and Smith, 1998). For these reasons,
recharge in the outcrop areas was not altered during the calibration process for the steady-state
model.

The implementation of ET is discussed in Section 6.3.4. ET occurs only in the outcrop areas of
the northern Trinity and Woodbine aquifers and the Washita/Fredericksburg groups along
riparian zones neighboring perennial stream channels, which comprises only a small portion of
the outcrop areas. Sensitivity analyses indicated that the simulated hydraulic heads in the
aquifers/formations are relatively insensitive to variations in the rate of ET compared to other
model parameters. Accordingly, the ET parameters controlling ET rates were unaltered during
the calibration process.

8.1.4   Head-Dependent Boundaries Representing Younger Formations

As mentioned in Section 6.3.2, cross-formational flow between the northern Trinity and
Woodbine aquifers and the younger overlying formations is represented by a head-dependent
boundary condition employed using the MODFLOW river package. The hydraulic heads in the
head-dependent boundaries in Layer 1 were estimated based on a moving 10-mile average of the
10-meter digital elevation model (DEM). The head-dependent boundary conductances were
based on the estimated vertical hydraulic conductivities and thicknesses of the younger
formations overlying the Woodbine Aquifer. The conductance of these head-dependent
boundaries was unchanged during the calibration process.

8.1.5   Stream Conductances

The 37 perennial streams within the footprint of the outcrop areas of the northern Trinity and
Woodbine aquifers and the Washita/Fredericksburg groups were represented using the
MODFLOW river package. No base flow estimates exist during the predevelopment period for

the perennial streams. The effect of stream parameters on model results is discussed in the

sensitivity analysis section (Section 8.3).
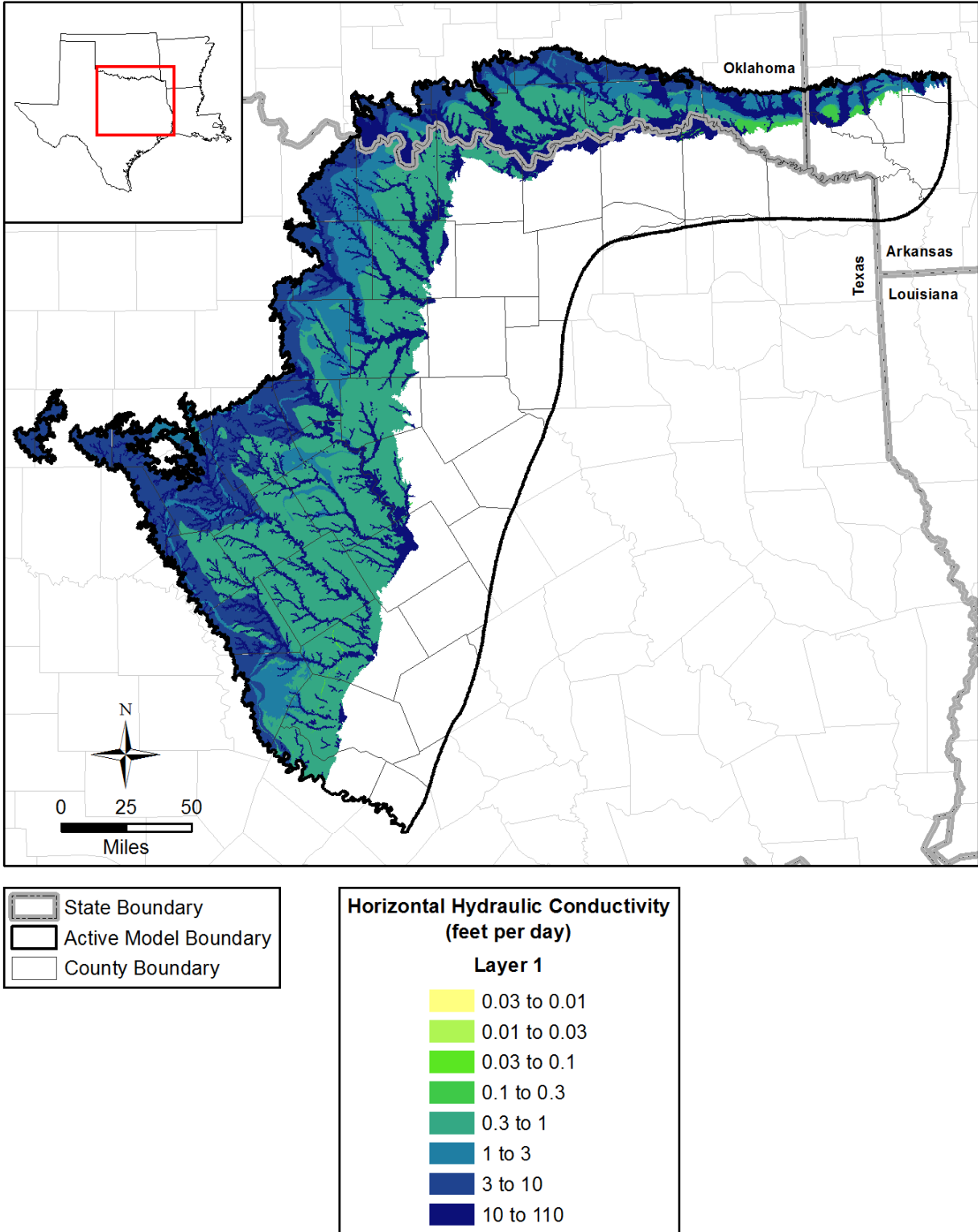
Figure 8.1.1   **Calibrated horizontal hydraulic conductivity in feet per day for the surficial outcrop area of Layer 1.**
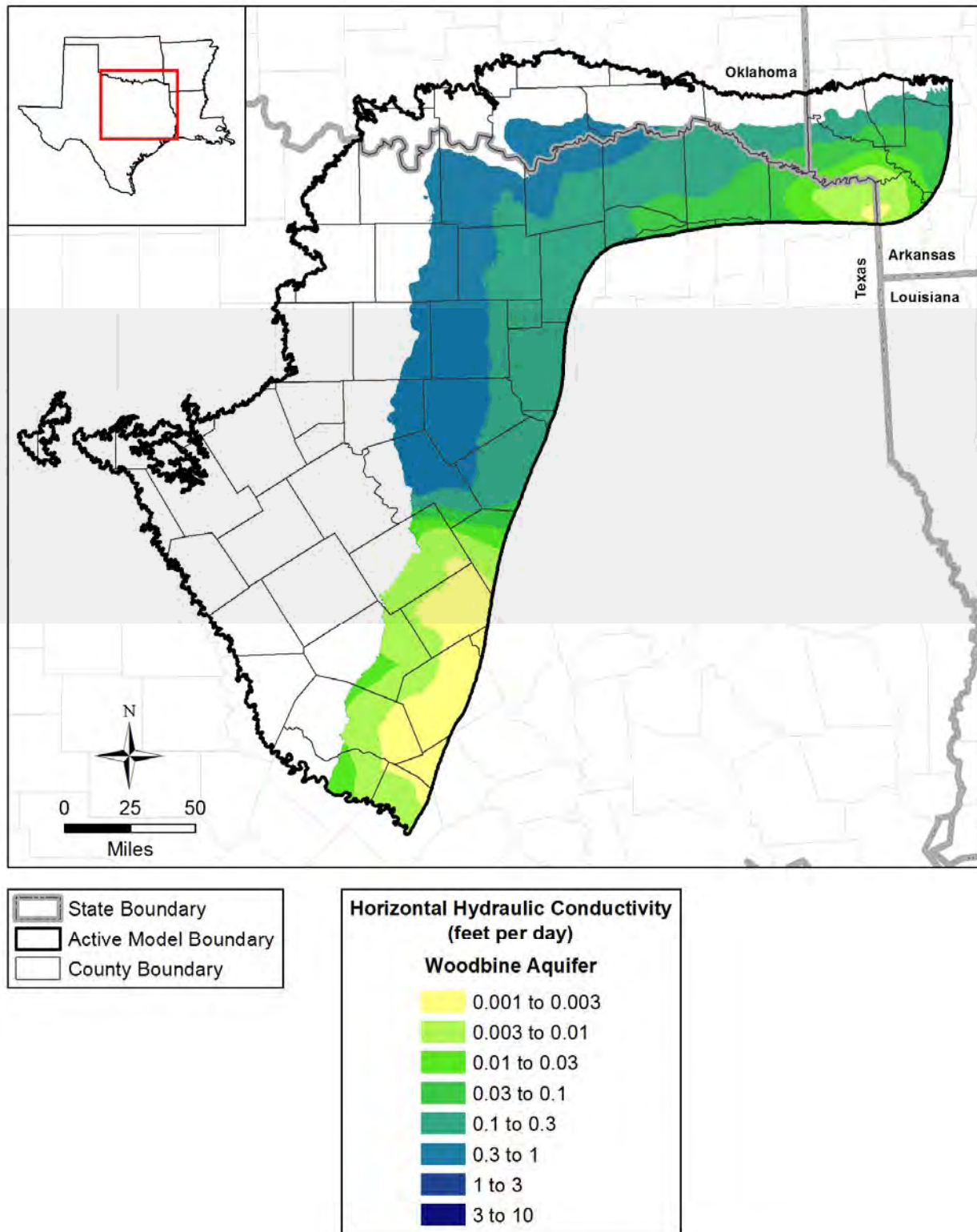
Figure 8.1.2   Calibrated horizontal hydraulic conductivity in feet per day for the Woodbine Aquifer.
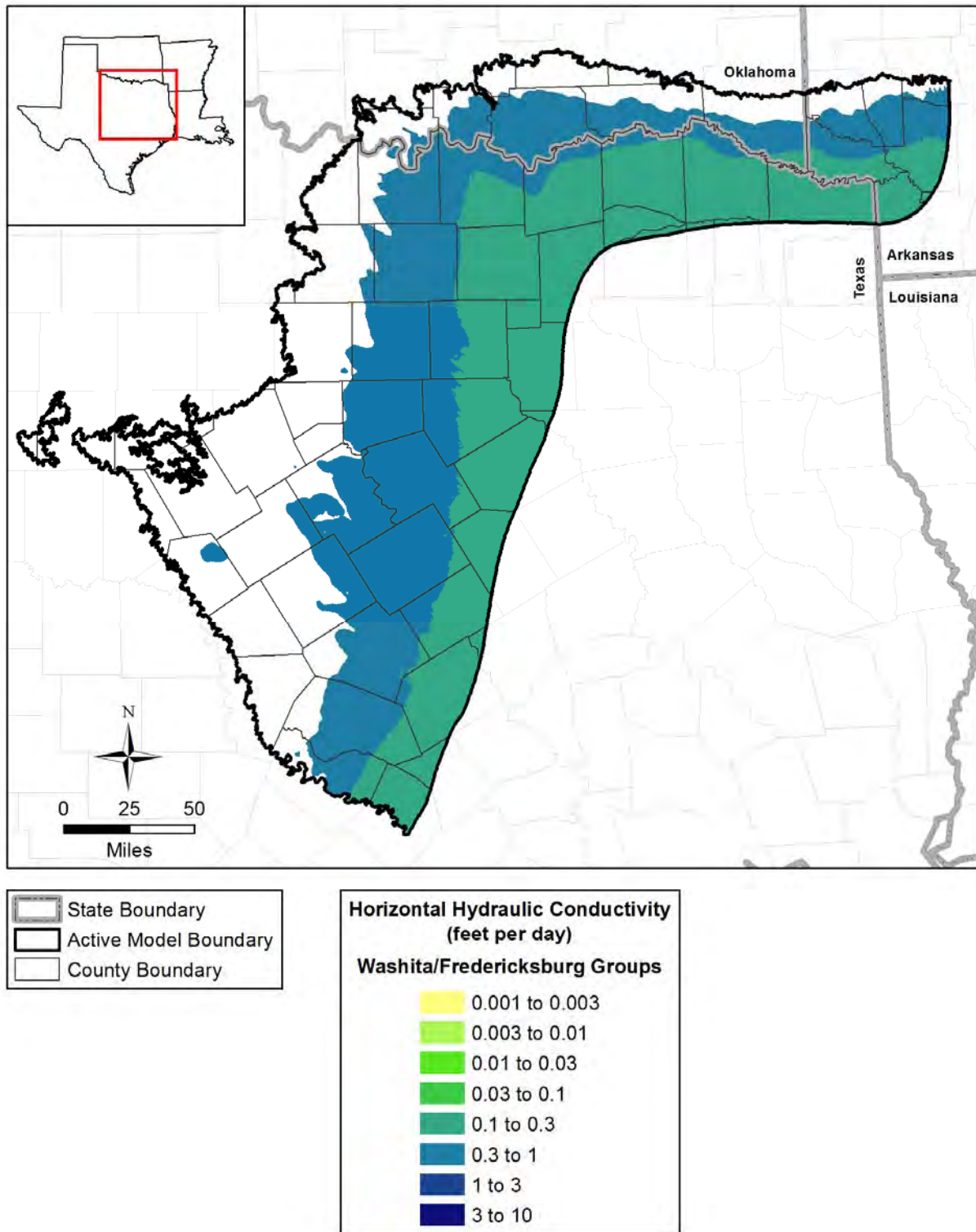
Figure 8.1.3   Calibrated horizontal hydraulic conductivity in feet per day for the Washita/Fredericksburg groups.
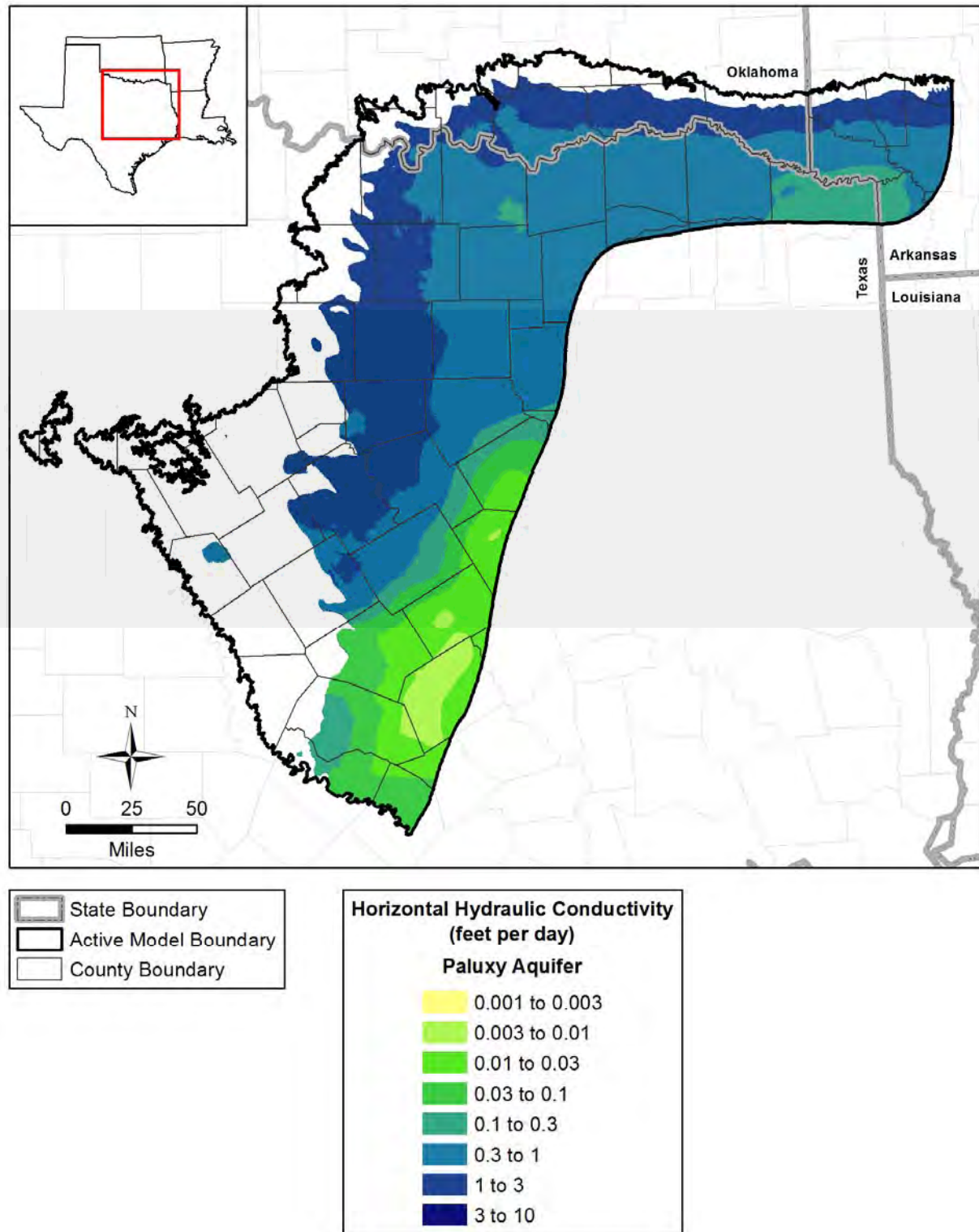
Figure 8.1.4   Calibrated horizontal hydraulic conductivity in feet per day for the Paluxy Aquifer.
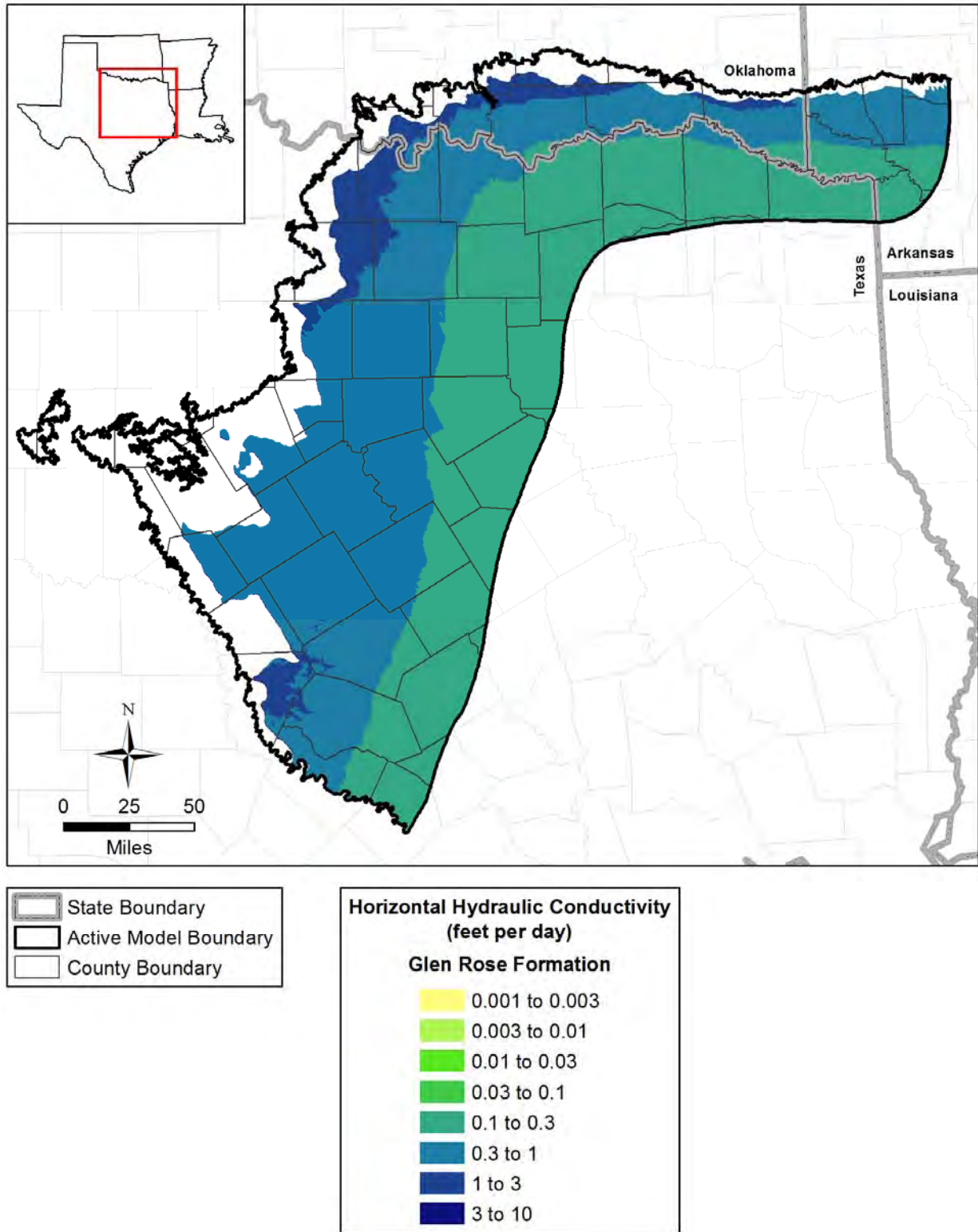
Figure 8.1.5 **Calibrated horizontal hydraulic conductivity in feet per day for the Glen Rose Formation.**
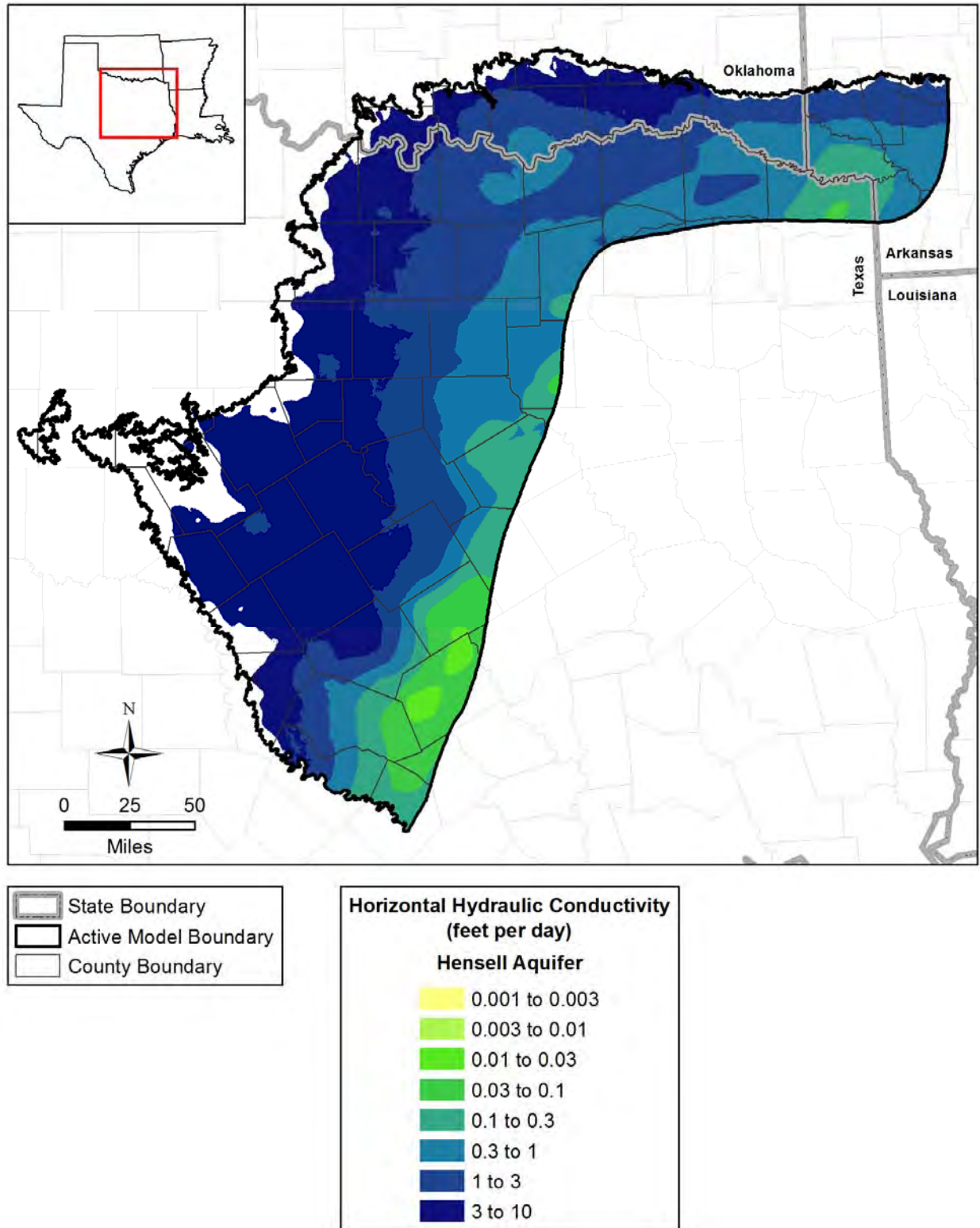
Figure 8.1.6   Calibrated horizontal hydraulic conductivity in feet per day for the Hensell Aquifer.

Legend:
- State Boundary
- Active Model Boundary
- County Boundary

Horizontal Hydraulic Conductivity (feet per day)
Pearsall Formation

- 0.001 to 0.003
- 0.003 to 0.01
- 0.01 to 0.03
- 0.03 to 0.1
- 0.1 to 0.3
- 0.3 to 1
- 1 to 3
- 3 to 10
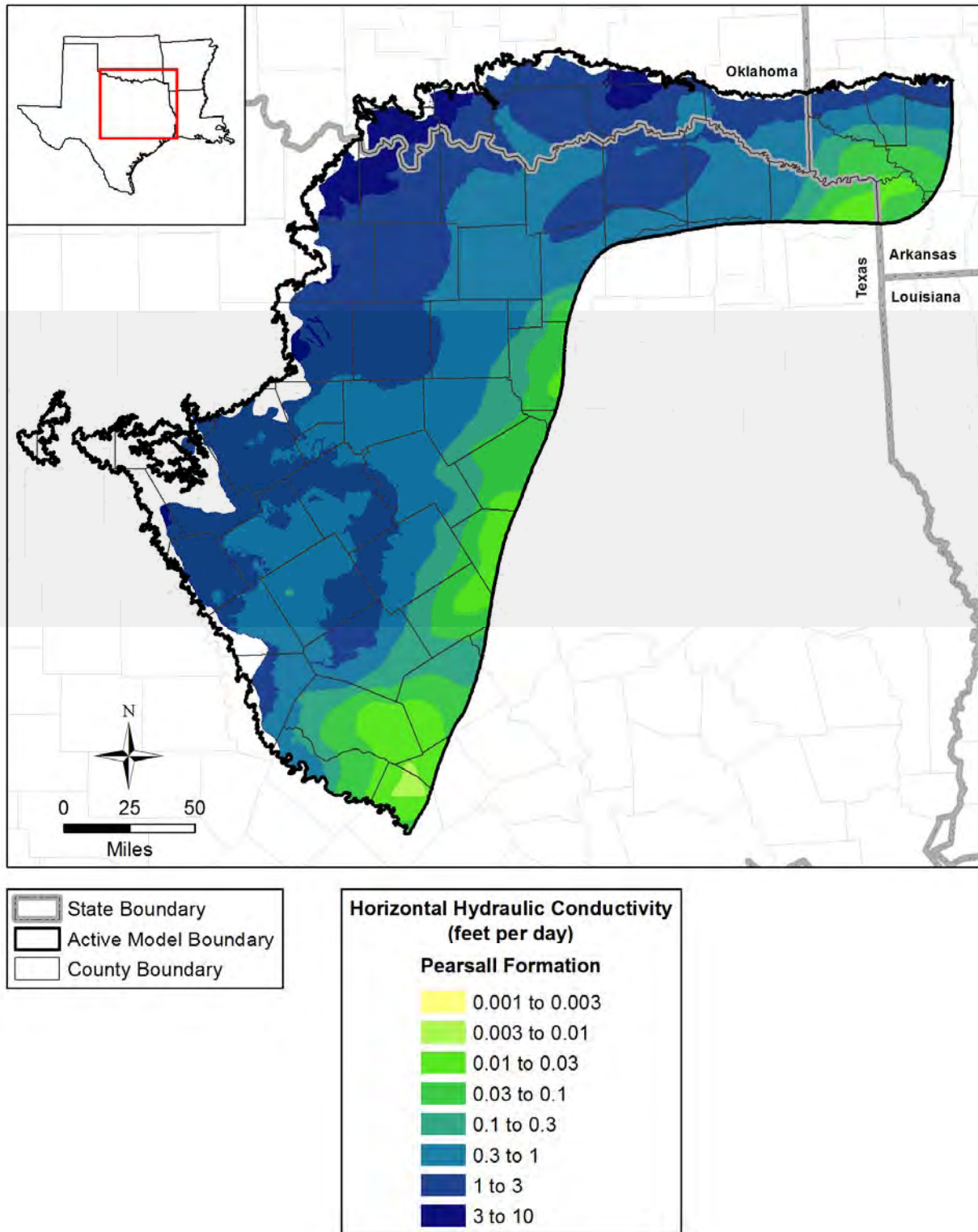
Figure 8.1.7   Calibrated horizontal hydraulic conductivity in feet per day for the Pearsall Formation.
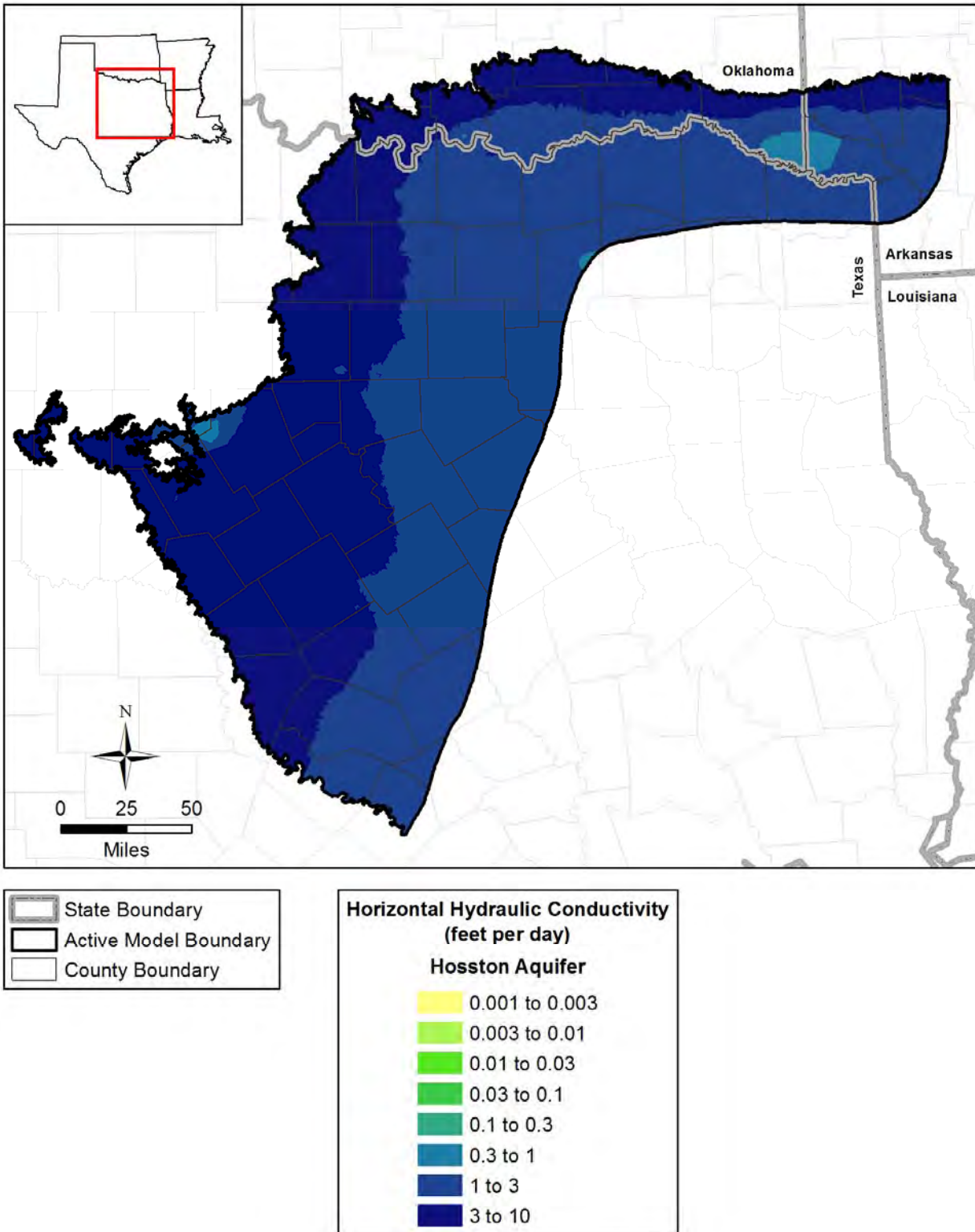
Figure 8.1.8   Calibrated horizontal hydraulic conductivity in feet per day for the Hosston Aquifer.
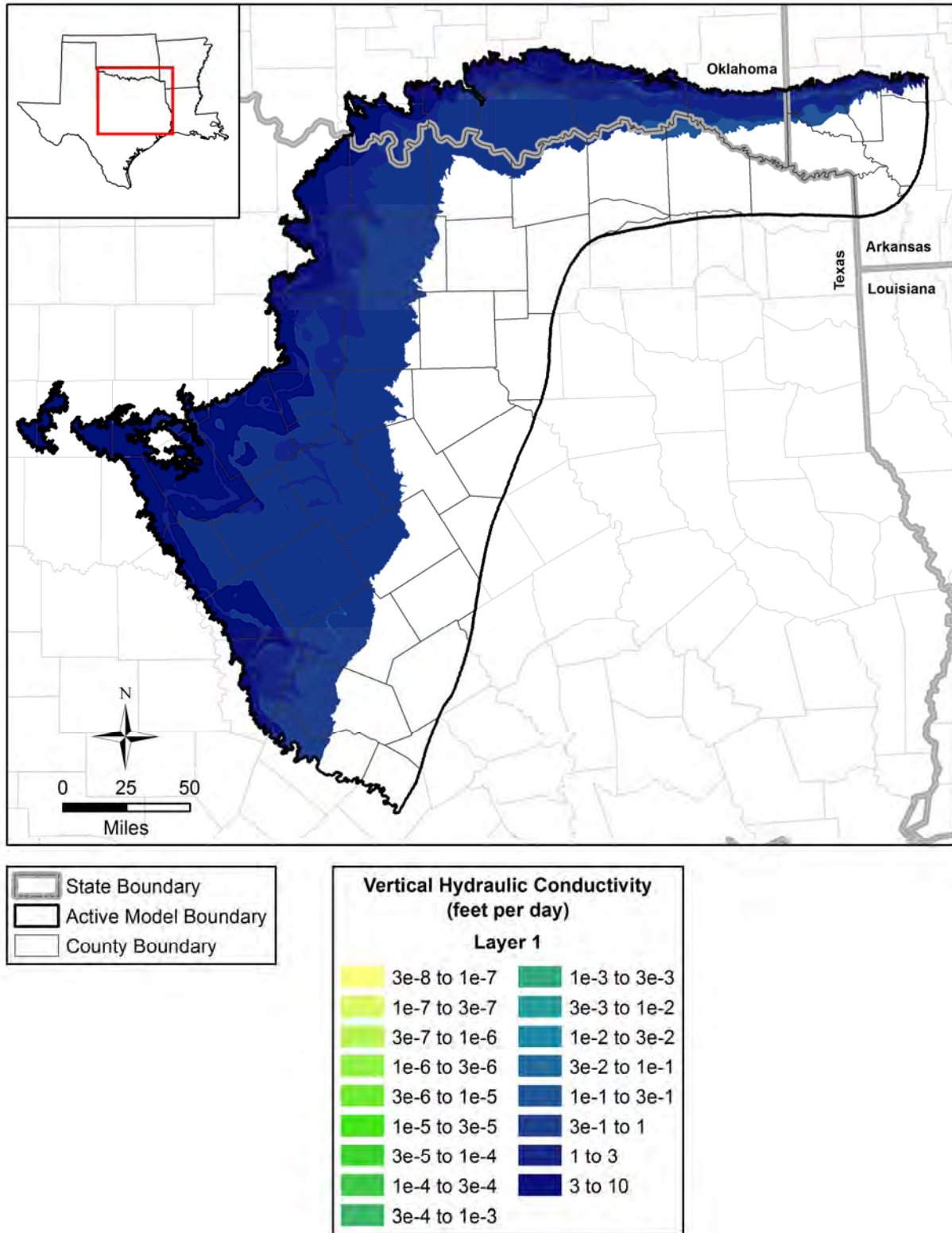
Figure 8.1.9   Calibrated vertical hydraulic conductivity in feet per day in the surficial outcrop area of Layer 1.
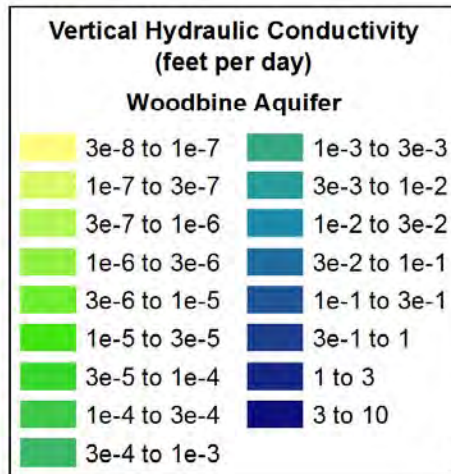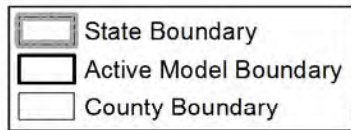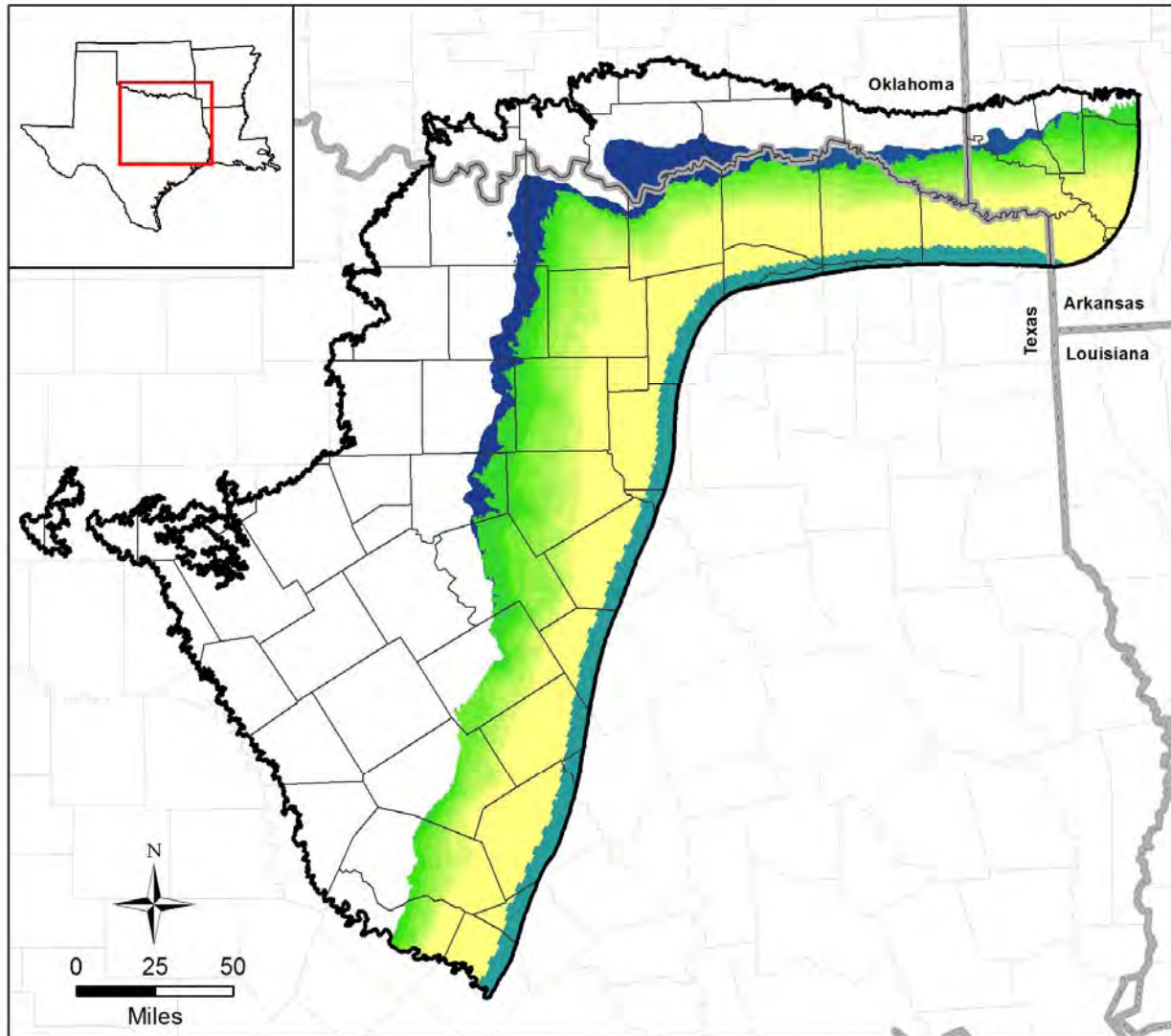
Figure 8.1.10   Calibrated vertical hydraulic conductivity in feet per day for the Woodbine Aquifer.
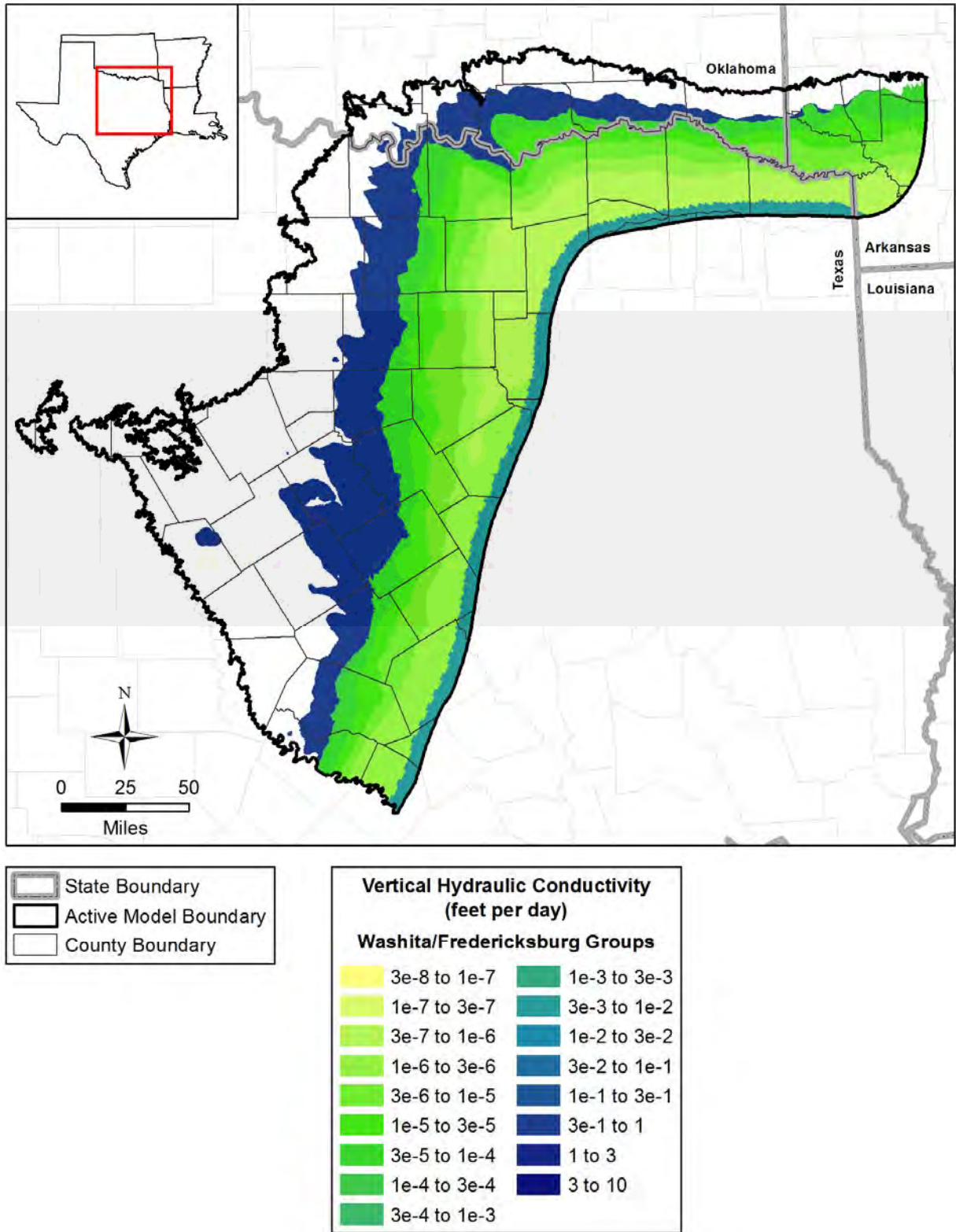
**Figure 8.1.11   Calibrated vertical hydraulic conductivity in feet per day for the
                   Washita/Fredericksburg groups.**
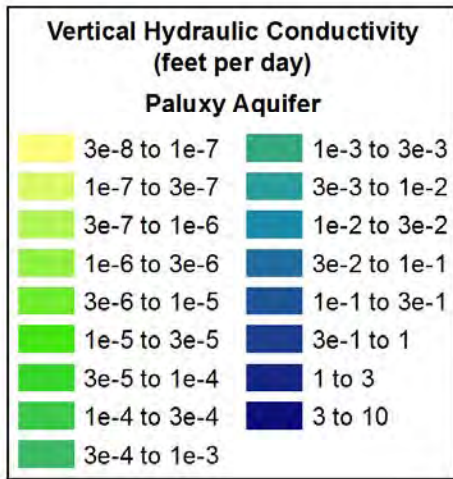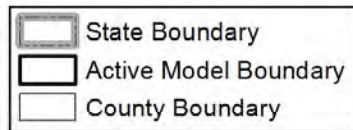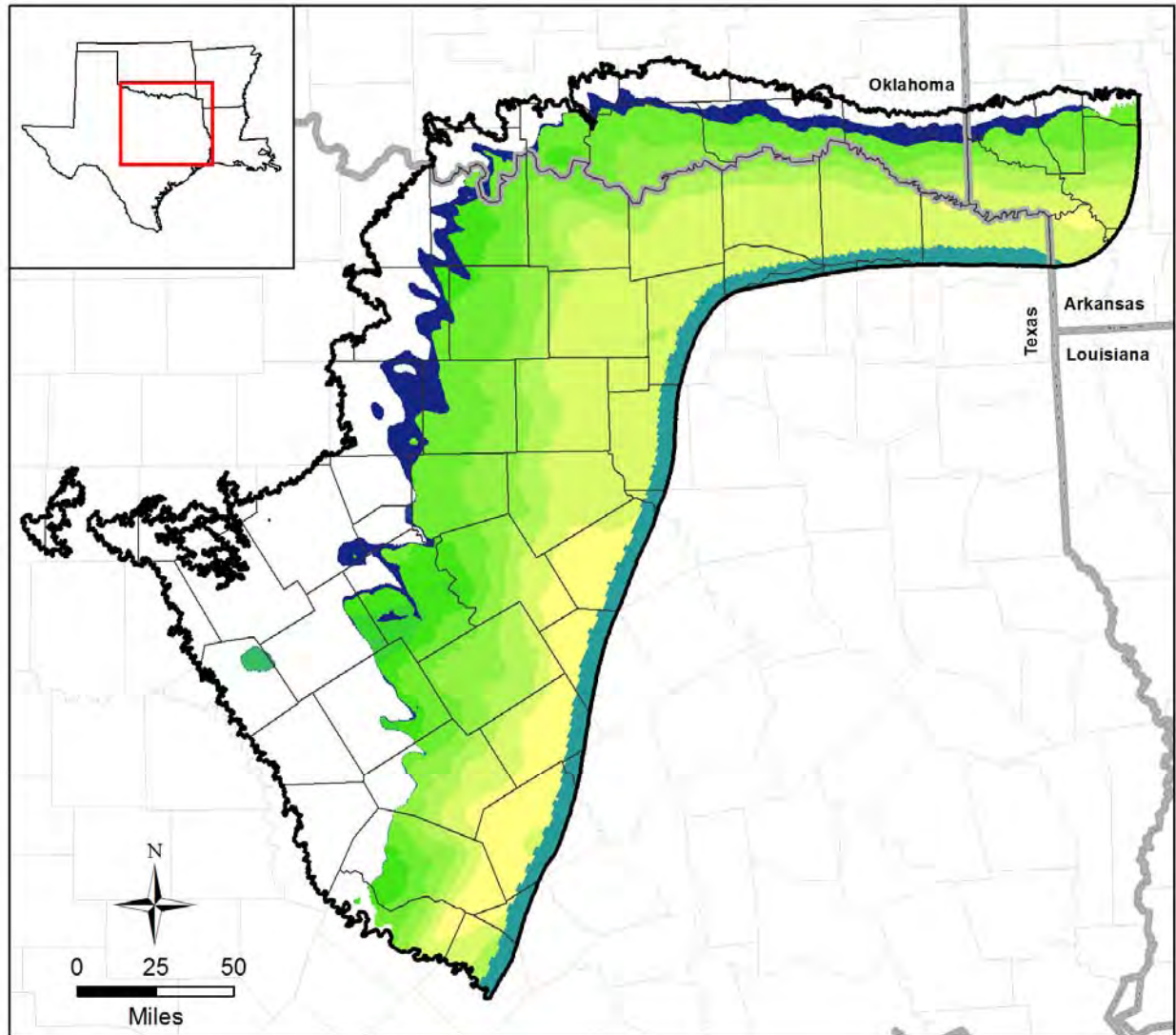
Figure 8.1.12   Calibrated vertical hydraulic conductivity in feet per day for the Paluxy Aquifer.
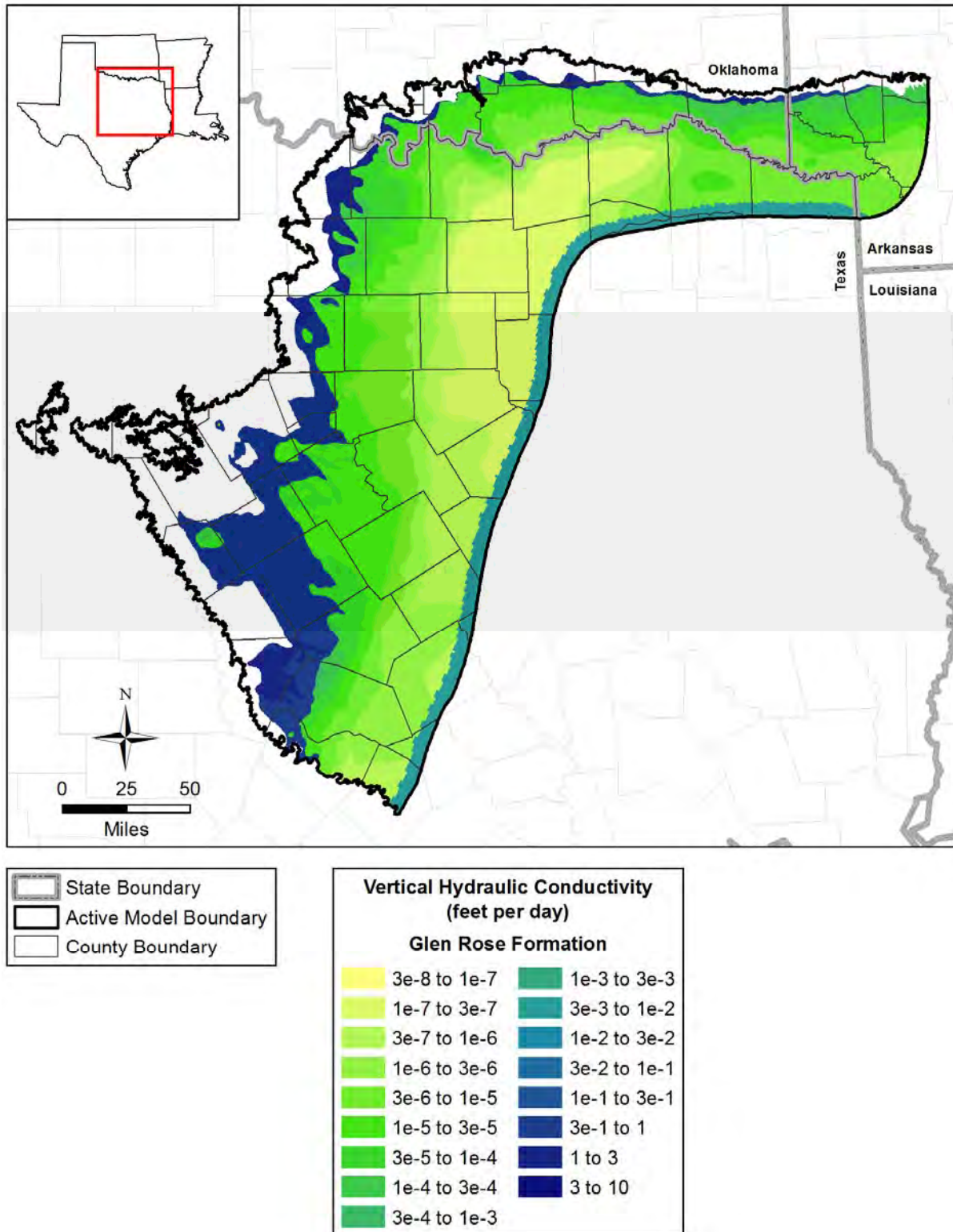
Figure 8.1.13   Calibrated vertical hydraulic conductivity in feet per day for the Glen Rose
                 Formation.
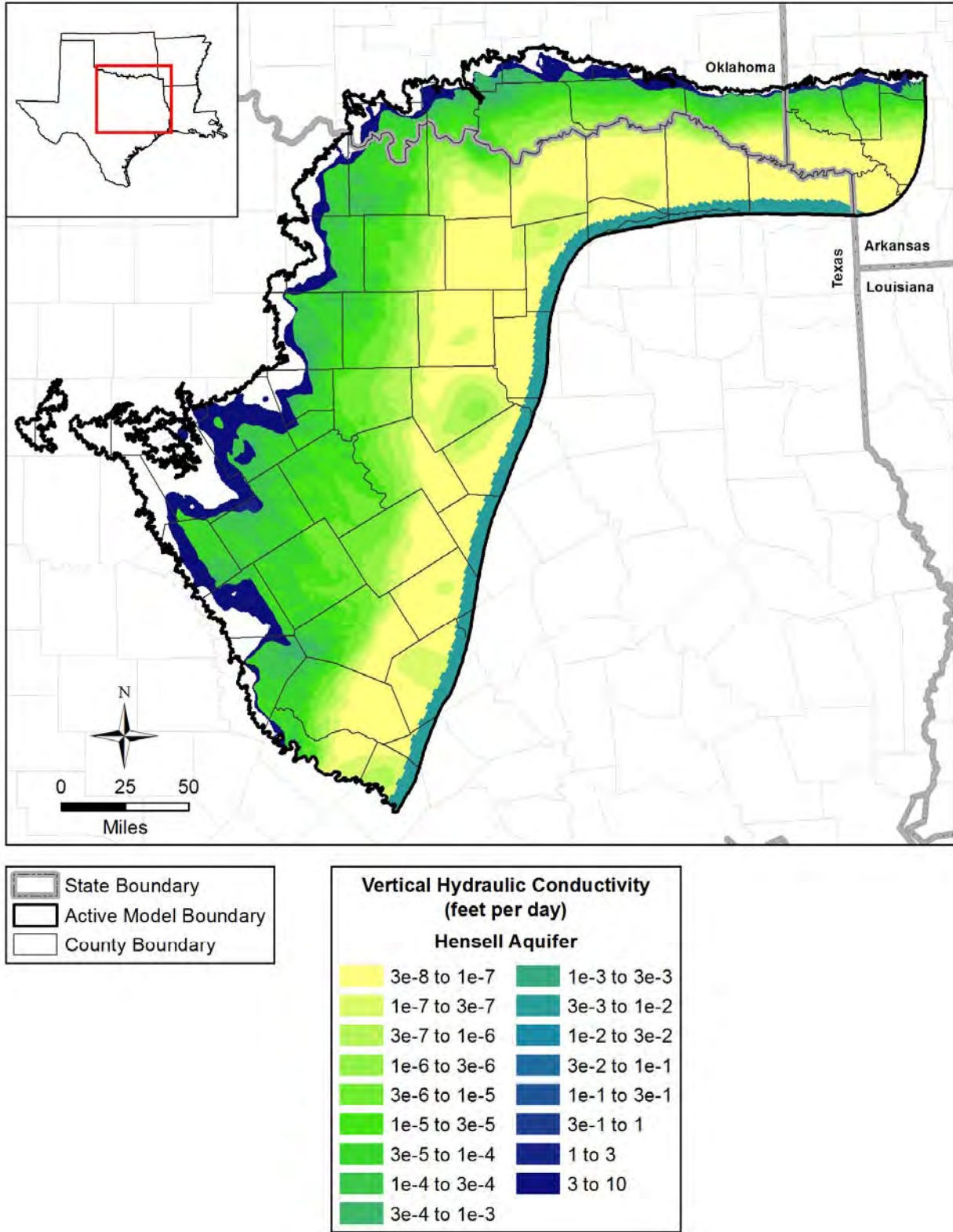
Figure 8.1.14   Calibrated vertical hydraulic conductivity in feet per day for the Hensell Aquifer.
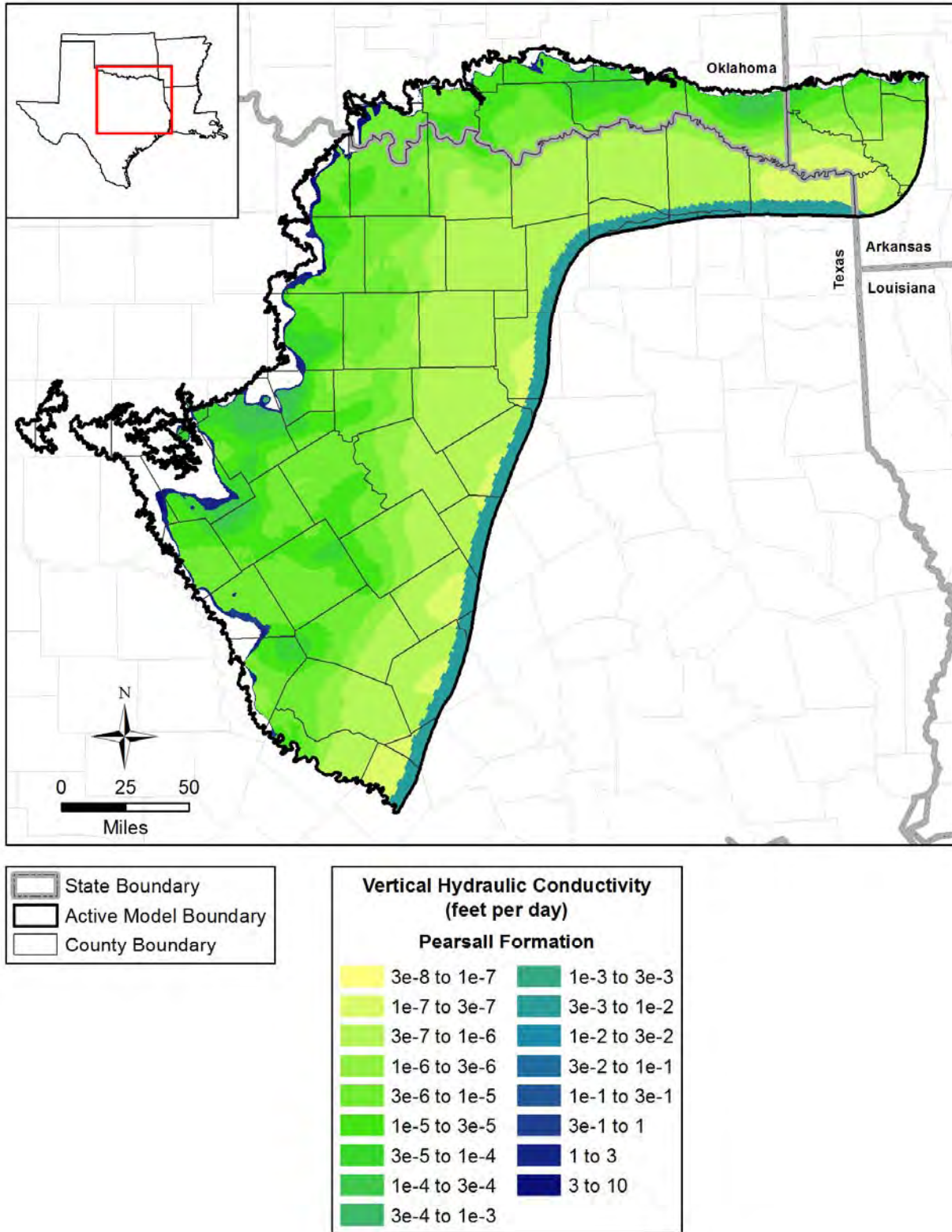
Figure 8.1.15   Calibrated vertical hydraulic conductivity in feet per day for the Pearsall Formation.
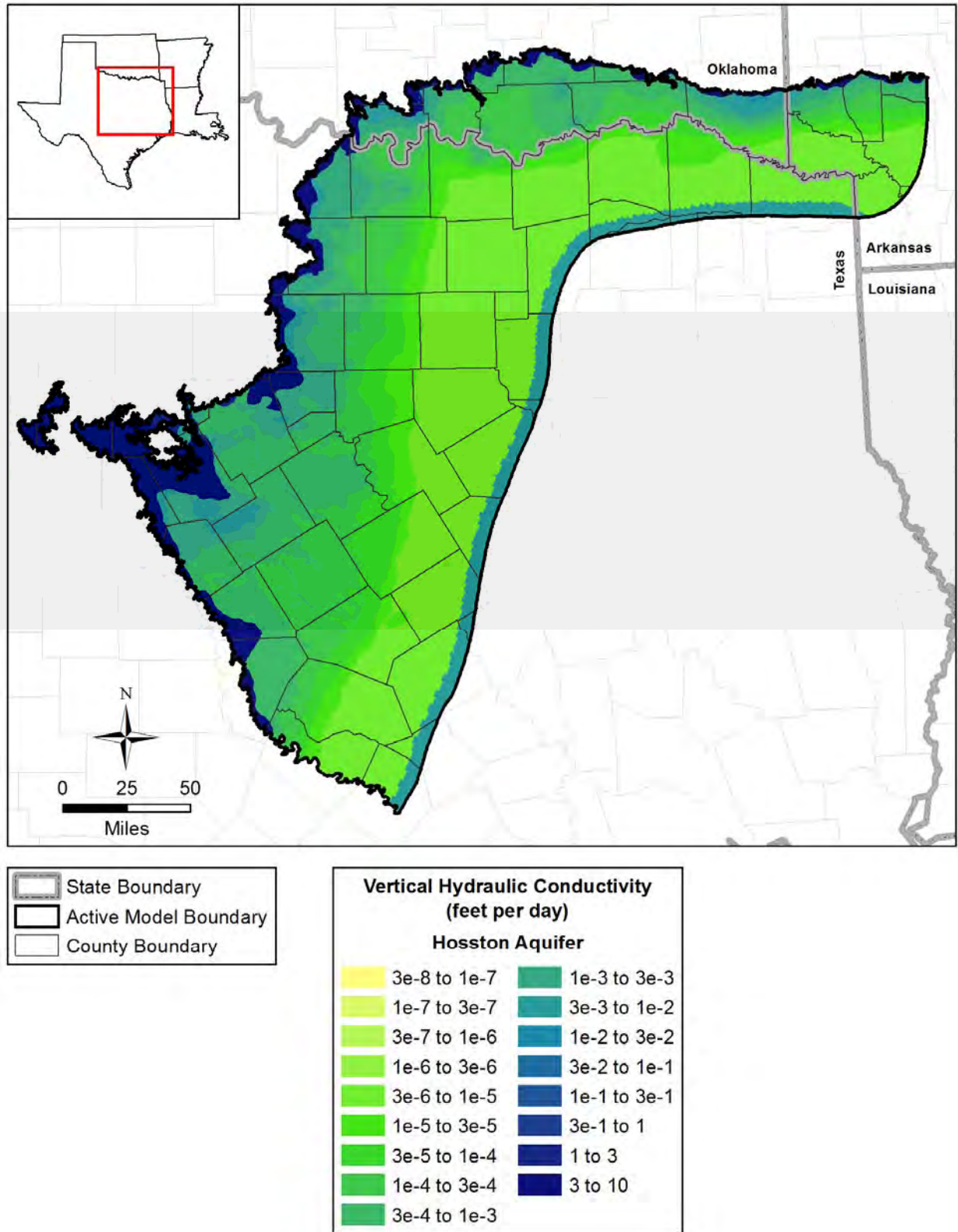
Figure 8.1.16   Calibrated vertical hydraulic conductivity in feet per day for the Hosston Aquifer.

8.2   Simulation Results

Calibration results for models are not unique and this is especially true for steady-state models. Calibrated results can be obtained by numerous combinations of recharge and vertical and horizontal hydraulic conductivities. For this reason, holding constant certain model inputs during calibration is best if good prior knowledge of that parameter input is available. Best modeling practices include looking at other performance metrics that may be less quantitative than hydraulic heads but help provide constraint to the model calibration. In this case, these metrics are artesian conditions and integrated groundwater velocities, which can be qualitatively correlated to observed water quality. Results of the steady-state model calibration are presented below.

8.2.1   Hydraulic Heads

A comparison of simulated and observed hydraulic heads by model layer is shown in Figure 8.2.1. Figure 8.2.2 shows a plot of residuals versus observed hydraulic heads, where residuals are defined as:

$$\text{residual} = \text{head}_{\text{simulated}} - \text{head}_{\text{measured}} \qquad (8.2.1)$$

A positive residual indicates that the model overpredicted the hydraulic head, while a negative residual indicates underprediction. The residuals are unequally split between underpredicting (44 percent) and overpredicting (56 percent) observed values, indicating an overall bias towards simulating higher than measured hydraulic heads, for reasons described below.

The steady-state model is assumed to represent predevelopment conditions with no effects from pumping. Since true predevelopment water-level measurements do not exist, the measurements prior to and including 1900 were used for the steady-state targets. Additionally, flowing wells as estimated from Hill (1901) were used as steady-state targets using the land surface elevation as a surrogate for hydraulic head. Land surface elevations were used because measured heights above ground surface for the flowing wells are not available. In many cases, some unknown amount of pumping or depressurization of the aquifer through flowing wells and an associated hydraulic head decline had occurred prior to the water-level measurements. All of these factors lead to a bias towards lower hydraulic heads in the measurements and a corresponding positive bias in the residuals. This positive bias is considered to be acceptable under these conditions.

Figure 8.2.3 shows a post plot of the residuals for all of the targets in the steady-state model. The small, black markers indicate an absolute residual of less than 30 feet, which is in the typical range of the mean absolute error. Most counties where targets are available show residuals in this lower range. In addition, each county with more than a few targets has residuals that are both positive (red and yellow markers) and negative (light and dark blue markers), indicating little spatial bias on a county basis.

Figures 8.2.4 through 8.2.11 show the simulated hydraulic heads for each model layer. These figures show a general west-northwest to east-southeast groundwater gradient following the structural dip in the northern Trinity and Woodbine aquifers and the Washita/Fredericksburg groups, as well as the regional trend in land surface elevation.

The calibration statistics for the steady-state model are summarized in Table 8.2.1. The adjusted mean absolute error (i.e., mean absolute error divided by the range in observed hydraulic heads) is 9.1 percent for the steady-state model. This is within the acceptable GAM standard of 10 percent for the adjusted mean absolute error. The mean error for the steady-state model is 12.0 feet, likely reflecting, at least in part, the low bias in the water-level measurements and ground surface elevations at flowing well locations used as predevelopment targets.

Because only the surficial outcrop area in Layer 1 was simulated to be convertible between confined and unconfined conditions as discussed in Section 6.2, only Layer 1 transmissivities had the capacity to vary as a function of simulated saturated thickness. A comparison of the simulated steady-state hydraulic heads with the basal elevation of all the active cells in model Layers 1 through 8 shows that less than 0.004 percent of the cells have a hydraulic head below the base of the aquifer/formation. This equates to 148 "dry" cells out of the 3,946,146 active cells that are not "conduit" cells. These "dry" cells are deemed insignificant in the context of the simulated model results.

Figure 8.2.12 shows the simulated artesian condition in the Hensell Aquifer along with known locations of early flowing wells. Simulated artesian hydraulic heads range from just above land surface to more than 300 feet amsl in McLennan and Falls counties and tend to follow topographically low regions. This compares well to measured heads in flowing wells ranging from 92 to 175 feet in McLennan County (Hill, 1901). Out of a total of 420 flowing well locations, 304 exhibit artesian conditions within the Hensell Aquifer. An additional 47 wells

exhibit flowing conditions in the Hosston Aquifer. This qualitative check indicates that the steady-state model is consistent with regard to the artesian conditions necessary to produce flowing wells

8.2.2 Streams, Springs, and ET

No appropriate stream gain/loss targets exist for the predevelopment period. The simulated stream net gain/loss for each of the streams in contact with the surficial outcrop area is shown in Figure 8.2.13. This flow amounts to a net gain of 751,185 AFY across the entire outcrop area.

The simulated discharge at springs is shown in Figure 8.2.14. For springs fed by the northern Trinity and Woodbine aquifers, the Washita/Fredericksburg groups, and the Edwards BFZ Aquifer, the localized drainage system and geometry of the springs are likely at a scale considerably smaller than that which the model can feasibly simulate. This hinders quantitative comparison between simulated and observed spring flows. Accordingly, no attempt to match spring flows was made during calibration of the steady-state model. The occurrence of flowing conditions when wells were first drilled into the aquifers is indicative of artesian conditions during predevelopment. However, qualitatively the simulated hydraulic heads should be above land surface at the spring and flowing well locations during the predevelopment period.

The simulated ET discharge for the steady-state model totals approximately 53,000 AFY. ET occurs in 1,434 of the 11,565 riparian cells with the average and maximum simulated rates equivalent to 11 and 44 inches per year, respectively. These rates are consistent with the expected range of potential actual groundwater ET rates.

8.2.3 Cross-Formational Flow

The simulated cross-formational flow between Layers 2 through 8 and both the surficial layer and the overlying younger formations in Layer 1 is depicted in Figure 8.2.15. This figure indicates a net downward flow from the surficial layer to the confined layers in the inter-stream portions of the outcrop area and a net upward flow into the portions of the outcrop area with perennial streams. The steady-state model also exhibits a net diffuse upward cross-formational flow to the overlying younger formations.

8.2.4 Groundwater Age

As discussed in Section 5.5 and depicted in Figure 5.5.1, freshwater (TDS less than 1,000 milligrams per liter) extends at depth in the northern Trinity Aquifer. This indicates

relatively young (geologically speaking) water at depth. To estimate groundwater ages in the steady-state model, reverse particle tracking was simulated using MODPATH (Pollock, 1994). Particles were placed at the center of each active model cell. The particles were then run in reverse assuming a porosity of 0.25, and the particle travel times were analyzed. The 30,000- and 100,000-year contours of groundwater age for the Hensell and Hosston aquifers are shown in Figure 8.2.16. The figure indicates simulated groundwater ages less than 100,000 years penetrating to depth in both aquifers, which is consistent with the water quality data. These contours are based on an assumed effective transport porosity of 0.25 as compared to the specific yield of Layer 1, assumed to be 0.1. If the effective transport porosity were 0.15, these contours would represent 18, 000 and 60,000 years, respectively. Downdip velocities are sufficient for this relatively young, freshwater to occur, even given the modest amount of flow to the downdip confined portions of the aquifers, prior to groundwater development in these areas.

8.2.5 Water Budget

Tables 8.2.2 and 8.2.3 summarize the water budget for the steady-state model in terms of volume and percent of total inflow, respectively. The overall mass balance error for the steady-state model is 0.00007 percent in the MODFLOW list output, well under the groundwater availability model requirement of 1 percent. The only boundary condition exhibiting net inflow to the model is recharge. The recharge inflow to the northern Trinity and Woodbine aquifers totals 1,766,567 AFY. Water discharges the northern Trinity and Woodbine aquifers through ephemeral streams (54.1 percent of net inflow), perennial streams (41.7 percent of net inflow), riparian ET (3.0 percent of net inflow), net upward cross-formational flow to the overlying younger formations (0.8 percent of net inflow), and to springs (0.1 percent of net inflow). The water budgets for the steady-state model by county and by GCD are summarized in Tables 8.2.4 and 8.2.5, respectively. Note that the "Lateral" field indicates water that is moving laterally into or out of the county or GCD.

Table 8.2.1   Calibration statistics for the steady-state model.

Count	Mean Error (feet)	MAE (feet)	Range (feet)	Adjusted MAE
96	12.0	59.8	660	0.091

MAE = mean absolute error

Table 8.2.2   Water budget for the steady-state model (all rates reported in AFY).

Pre-development	Cross-formational Flow			Recharge	ET	Ephemeral Streams	Perennial Streams	Spring	Younger
	Surficial	Top	Bottom						
Younger Formations	0	0	8,354	0	0	0	0	0	-13,711
Woodbine Aquifer	2,561	-8,354	5,901	326,201	-13,334	-197,776	-97,917	-61	0
Wash/Fred groups	5,886	-5,901	275	532,484	-6,633	-270,802	-236,638	-286	0
Paluxy Aquifer	1,859	-275	-1,565	245,673	-6,771	-113,235	-120,812	-126	0
Glen Rose Formation	16,844	1,565	-18,638	230,422	-6,503	-83,409	-131,395	-86	0
Hensell Aquifer	-11,214	18,638	-6,579	208,440	-11,756	-130,060	-67,678	-188	0
Pearsall Formation	3,374	6,579	-9,899	45,455	-3,697	-38,571	-24,689	0	0
Hosston Aquifer	-7,050	9,899	0	177,891	-4,352	-122,037	-58,080	-343	0
Total	12,259	22,151	-22,151	1,766,567	-53,046	-955,888	-737,209	-1,090	-13,711

Table 8.2.3   Water budget for the steady-state model with values expressed as a percentage of total inflow.

Pre-D Formation	Cross-formational Flow			Recharge	ET	Ephemeral	Perennial	Spring	Younger
	Surficial	Top	Bottom						
Younger	0.0%	0.0%	0.5%	0.0%	0.0%	0.0%	0.0%	0.0%	-0.8%
Woodbine	0.1%	-0.5%	0.3%	18.5%	-0.8%	-11.2%	-5.5%	0.0%	0.0%
Wash-Fred	0.3%	-0.3%	0.0%	30.1%	-0.4%	-15.3%	-13.4%	0.0%	0.0%
Paluxy	0.1%	0.0%	-0.1%	13.9%	-0.4%	-6.4%	-6.8%	0.0%	0.0%
Glenrose	1.0%	0.1%	-1.1%	13.0%	-0.4%	-4.7%	-7.4%	0.0%	0.0%
Hensell	-0.6%	1.1%	-0.4%	11.8%	-0.7%	-7.4%	-3.8%	0.0%	0.0%
Pearsall	0.2%	0.4%	-0.6%	2.6%	-0.2%	-2.2%	-1.4%	0.0%	0.0%
Hosston	-0.4%	0.6%	0.0%	10.1%	-0.2%	-6.9%	-3.3%	0.0%	0.0%
Total	0.7%	1.3%	-1.3%	100.0%	-3.0%	-54.1%	-41.7%	-0.1%	-0.8%

Table 8.2.4   Water budget in the steady-state model by county (all rates reported in AFY).

County	State	Lateral	Recharge	Perennial	Ephemeral	ET	Spring	Younger Formations
Bastrop	TX	332	0	0	0	0	0	-332
Bell	TX	3,692	21,688	-19,310	-6,079	0	-198	205
Bosque	TX	4,734	35,928	-24,600	-15,817	-245	0	0
Bowie	TX	464	0	0	0	0	0	-464
Brown	TX	-2,086	5,386	0	-3,277	0	-22	0
Burnet	TX	-7,359	16,916	-4,105	-5,314	-138	0	0
Callahan	TX	-520	4,385	0	-3,866	0	0	0
Collin	TX	-30	0	0	0	0	0	31
Comanche	TX	5,669	19,133	-11,172	-12,444	-1,154	-32	0
Cooke	TX	-4,537	88,998	-34,498	-47,356	-2,588	-21	0
Coryell	TX	671	33,304	-28,525	-5,384	-67	0	0
Dallas	TX	1,126	406	-1,155	0	0	0	-376
Delta	TX	572	0	0	0	0	0	-572
Denton	TX	4,436	62,351	-31,506	-34,113	-667	-78	-423
Eastland	TX	341	7,209	0	-7,550	0	0	0
Ellis	TX	22	0	0	0	0	0	-22
Erath	TX	-10,843	26,761	-6,060	-9,843	-14	0	0
Falls	TX	605	0	0	0	0	0	-605
Fannin	TX	2,088	30,658	-23,430	-6,589	-2,489	0	-236
Franklin	TX	115	0	0	0	0	0	-115
Grayson	TX	19,994	61,122	-41,340	-39,229	-243	0	-304
Hamilton	TX	-2,767	21,971	-17,488	-1,715	0	0	0
Henderson	TX	223	0	0	0	0	0	-223
Hill	TX	-398	14,833	-8,781	-5,454	-379	0	178
Hood	TX	1,993	12,359	-9,504	-4,680	-168	0	0
Hopkins	TX	143	0	0	0	0	0	-143
Hunt	TX	347	0	0	0	0	0	-347
Jack	TX	-535	2,429	0	-1,894	0	0	0
Johnson	TX	-6,180	23,353	444	-17,712	-16	-18	130
Kaufman	TX	712	0	0	0	0	0	-712
Lamar	TX	6,000	22,002	-22,232	-3,680	-2,005	-12	-72
Lampasas	TX	2,917	15,173	-11,727	-6,096	0	-268	0
Lee	TX	383	0	0	0	0	0	-383
Limestone	TX	237	0	0	0	0	0	-237
McLennan	TX	3,866	16,784	-18,325	-1,867	-524	0	65
Milam	TX	1,281	0	0	0	0	0	-1,281
Mills	TX	-5,582	11,932	2,274	-8,624	0	0	0
Montague	TX	-6,399	33,807	-8,579	-17,160	-1,671	0	0

Table 8.2.4, continued

County	State	Lateral	Recharge	Perennial	Ephemeral	ET	Spring	Younger Formations
Morris	TX	3	0	0	0	0	0	-3
Navarro	TX	1,233	0	0	0	0	0	-1,233
Palo Pinto	TX	-240	407	0	-167	0	0	0
Parker	TX	-5,350	30,783	-9,184	-15,968	-281	0	0
Red River	TX	4,380	25,224	-12,503	-13,596	-2,949	0	-556
Robertson	TX	232	0	0	0	0	0	-232
Rockwall	TX	-16	0	0	0	0	0	15
Somervell	TX	5,070	5,964	-10,086	-948	0	0	0
Tarrant	TX	4,041	37,867	-22,079	-19,654	-205	-106	136
Taylor	TX	-371	694	0	-323	0	0	0
Titus	TX	163	0	0	0	0	0	-163
Travis	TX	2,902	7,515	-8,309	-2,049	0	0	-59
Williamson	TX	-2,094	19,259	-13,957	-3,418	0	0	210
Wise	TX	668	48,484	-13,409	-32,665	-2,960	-118	0
Atoka	OK	2,203	81,017	-22,976	-56,969	-3,244	-31	0
Bryan	OK	-14,259	190,311	-56,588	-114,237	-5,227	0	0
Carter	OK	-359	10,367	0	-9,991	-18	0	0
Choctaw	OK	-6,279	190,518	-64,965	-115,847	-3,390	-40	1
Johnston	OK	-484	34,688	-10,250	-23,076	-879	0	0
Love	OK	6,417	50,245	-27,901	-22,495	-6,193	-71	0
Marshall	OK	-10,268	68,548	-13,063	-45,025	-193	0	0
McCurtain	OK	-4,054	164,610	-69,315	-87,715	-2,385	-49	-1,093
Pushmataha	OK	-1,994	33,154	-5,135	-25,783	-202	-40	0
Hempstead	AR	258	0	0	0	0	0	-258
Howard	AR	-2,903	48,904	-9,018	-31,736	-2,228	0	-3,019
Lafayette	AR	9	0	0	0	0	0	-9
Little River	AR	1,744	5,705	-6,673	-353	-107	0	-317
Miller	AR	126	0	0	0	0	0	-126
Pike	AR	1,068	29,290	-10,243	-17,867	-1,833	0	-414
Sevier	AR	2,426	97,837	-32,023	-59,502	-8,383	0	-357

ET = evapotranspiration   TX = Texas   OK = Oklahoma   AR = Arkansas

Table 8.2.5   Water budget in the steady-state model by GCD (all rates reported in AFY).

GCDs	Lateral	Recharge	Perennial	Ephemeral	ET	Spring	Younger
Brazos Valley GCD	211	0	0	0	0	0	-211
Central Texas GCD	-7,695	16,887	-4,081	-4,972	-138	0	0
Clearwater UWCD	3,392	21,225	-18,647	-5,975	0	-198	201
Fox Crossing Water District	-4,728	11,620	1,644	-8,536	0	0	0
Lost Pines GCD	698	0	0	0	0	0	-698
Middle Trinity GCD	356	115,491	-71,208	-43,253	-1,350	-32	0
Neches & Trinity Valleys GCD	211	0	0	0	0	0	-211
North Texas GCD	3,758	152,264	-71,580	-80,984	-2,961	-99	-398
Northern Trinity GCD	3,626	37,766	-21,341	-19,879	-205	-106	139
Post Oak Savannah GCD	1,291	0	0	0	0	0	-1,290
Prairielands GCD	-1,669	44,212	-18,540	-23,759	-525	-18	299
Red River GCD	-4,131	88,846	-34,178	-47,599	-2,397	0	-540
Saratoga UWCD	3,567	15,283	-12,144	-6,438	0	-268	0
Southern Trinity GCD	3,114	16,622	-17,297	-1,973	-524	0	58
Upper Trinity GCD	-7,532	124,024	-41,005	-70,316	-5,053	-118	0

UWCD = Underground Water Conservation District
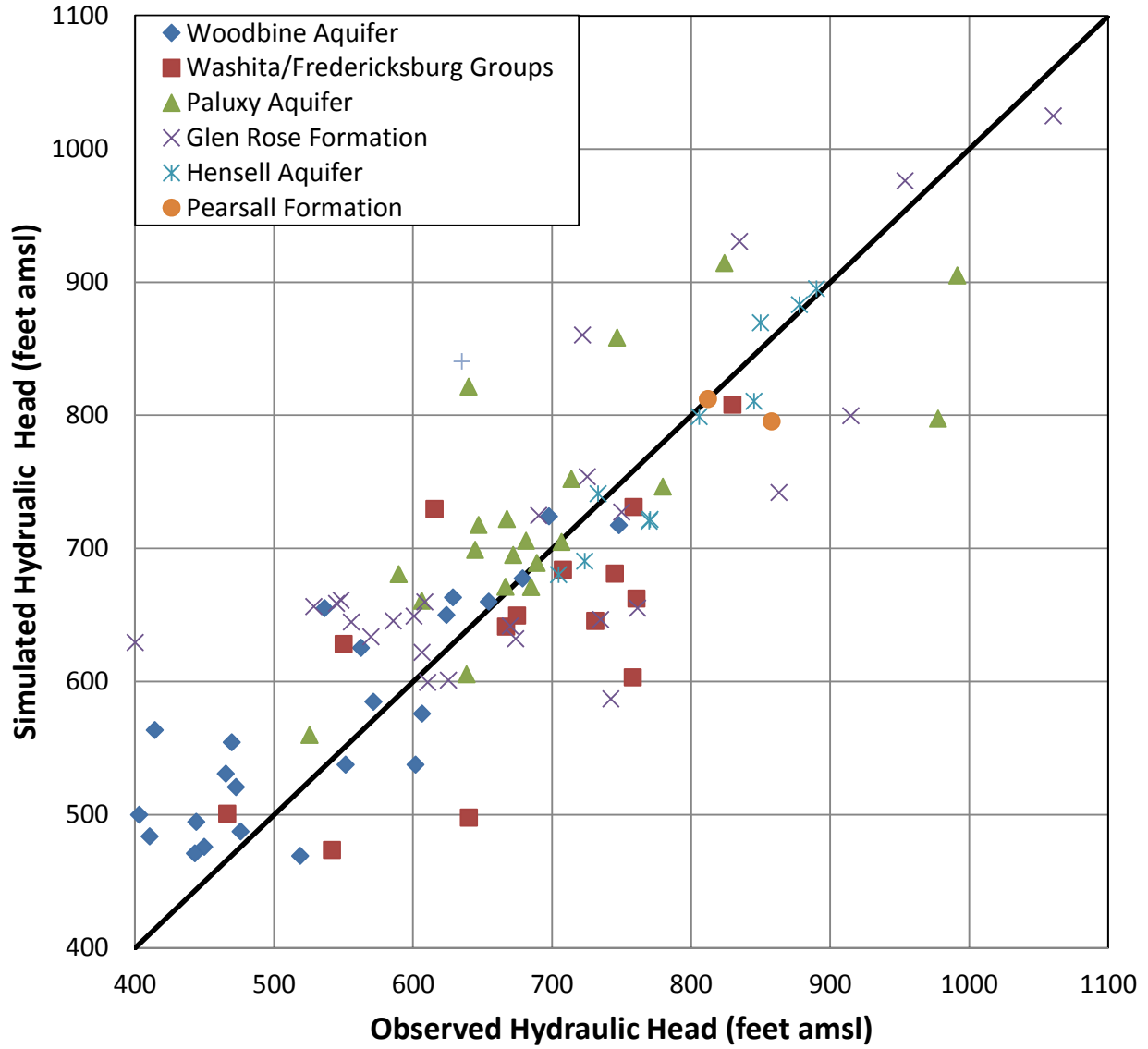
Figure 8.2.1   Plot of simulated versus observed hydraulic heads in feet amsl for the steady-state model.
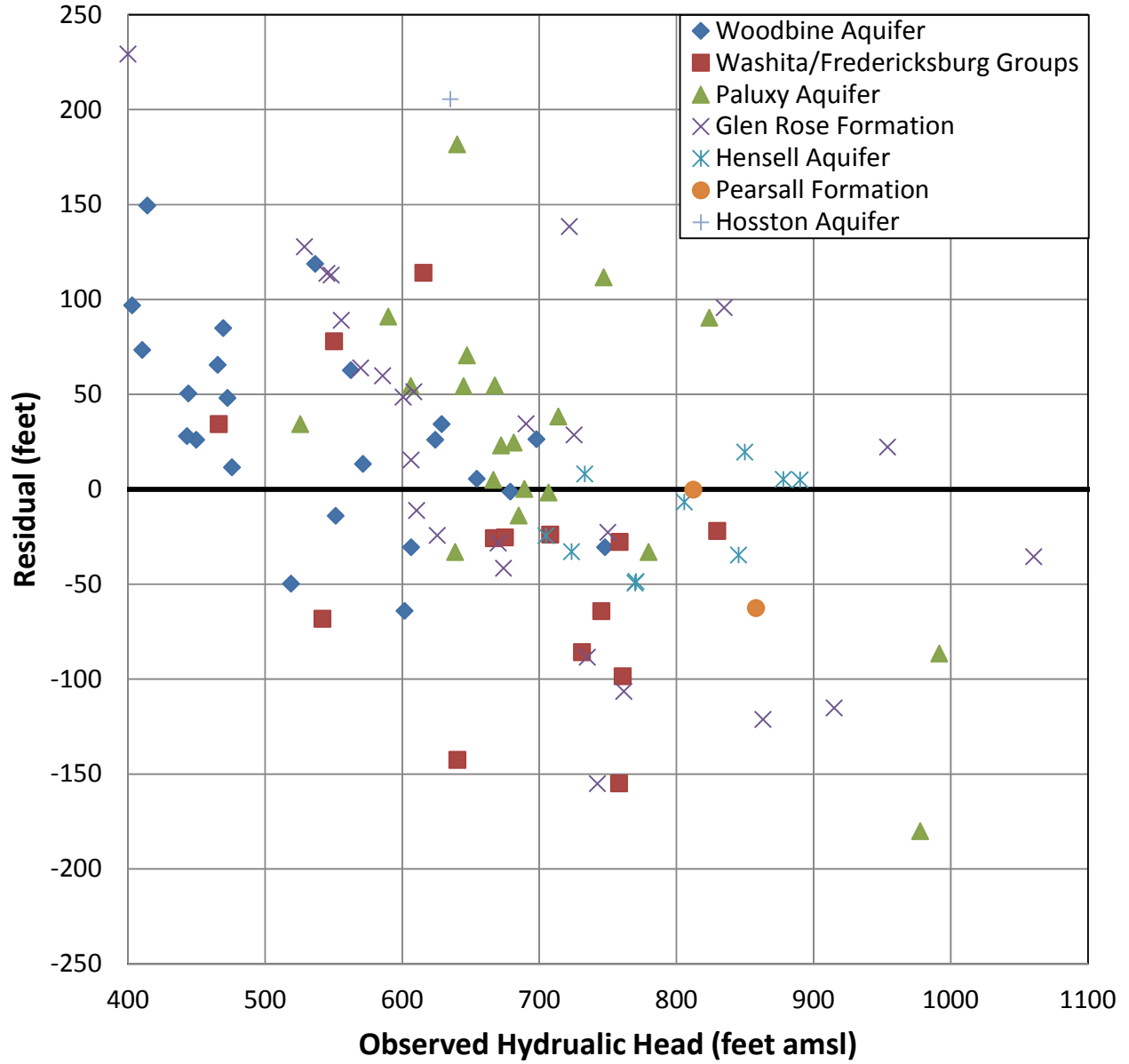
Figure 8.2.2   Plot of residual versus observed hydraulic heads in feet for the steady-state model.
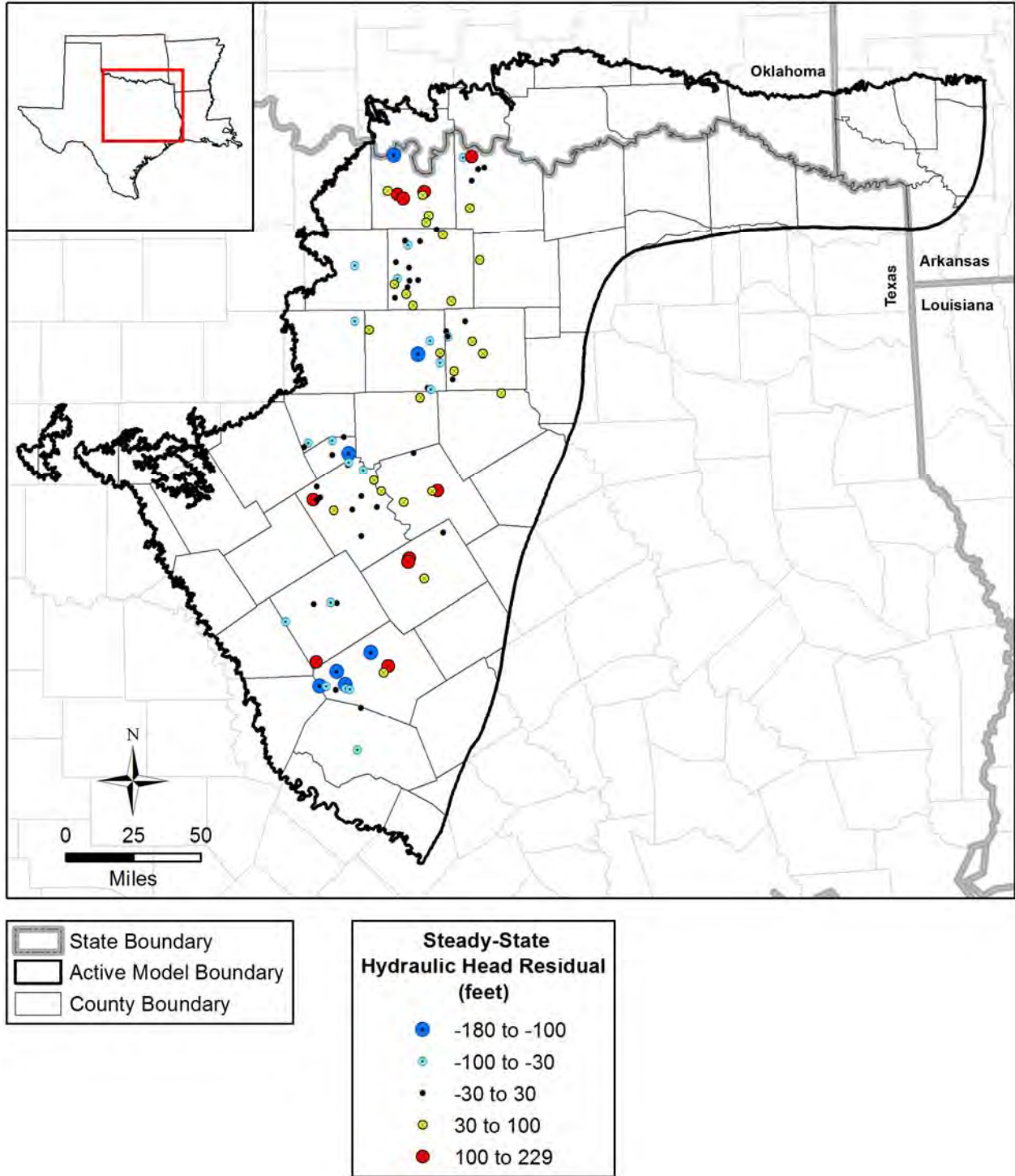
Figure 8.2.3   Post plot of simulated hydraulic head residuals in feet for the steady-state model.
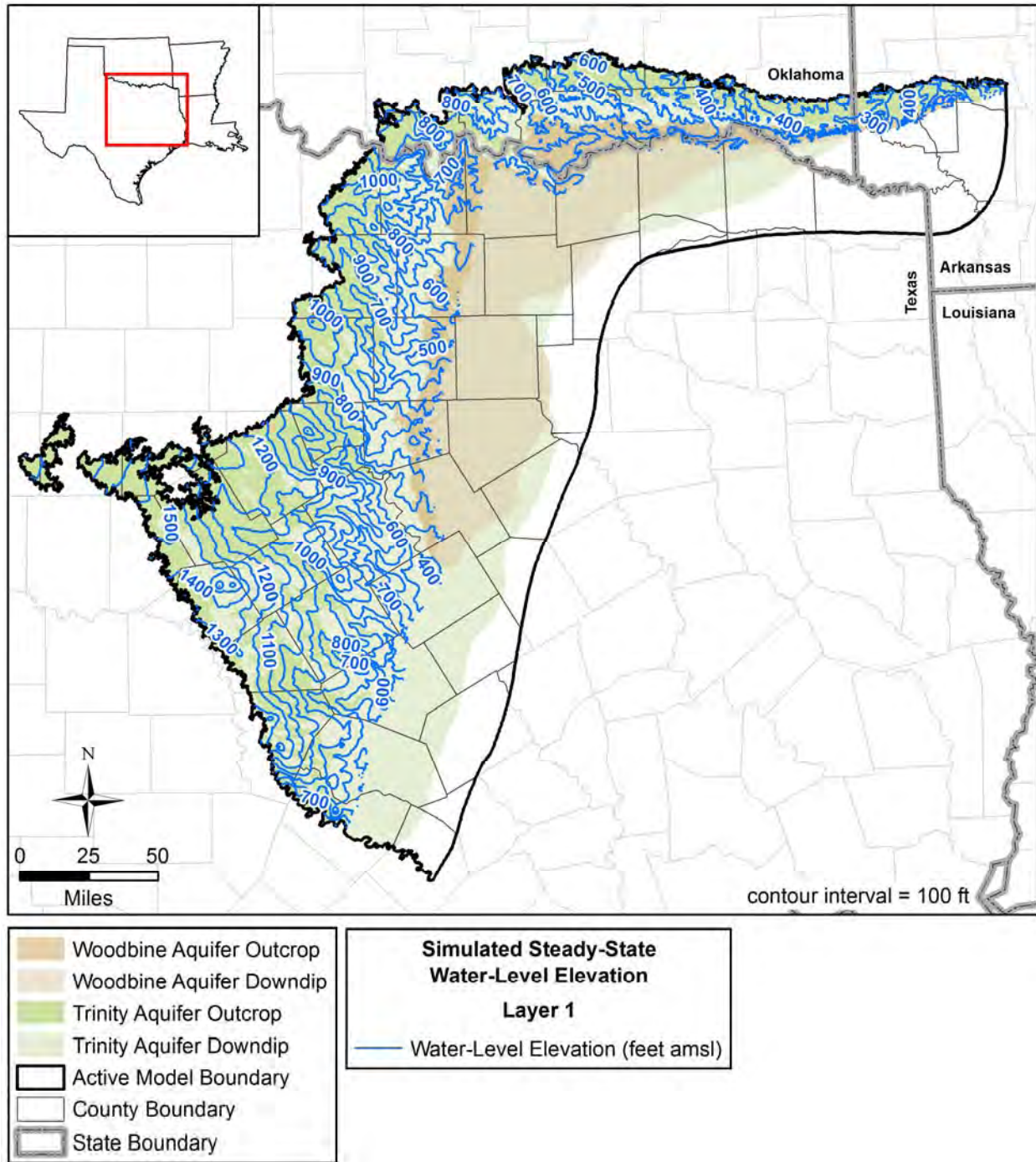
Figure 8.2.4   Simulated water-level elevations (hydraulic heads) in feet amsl for the surficial outcrop area of Layer 1.
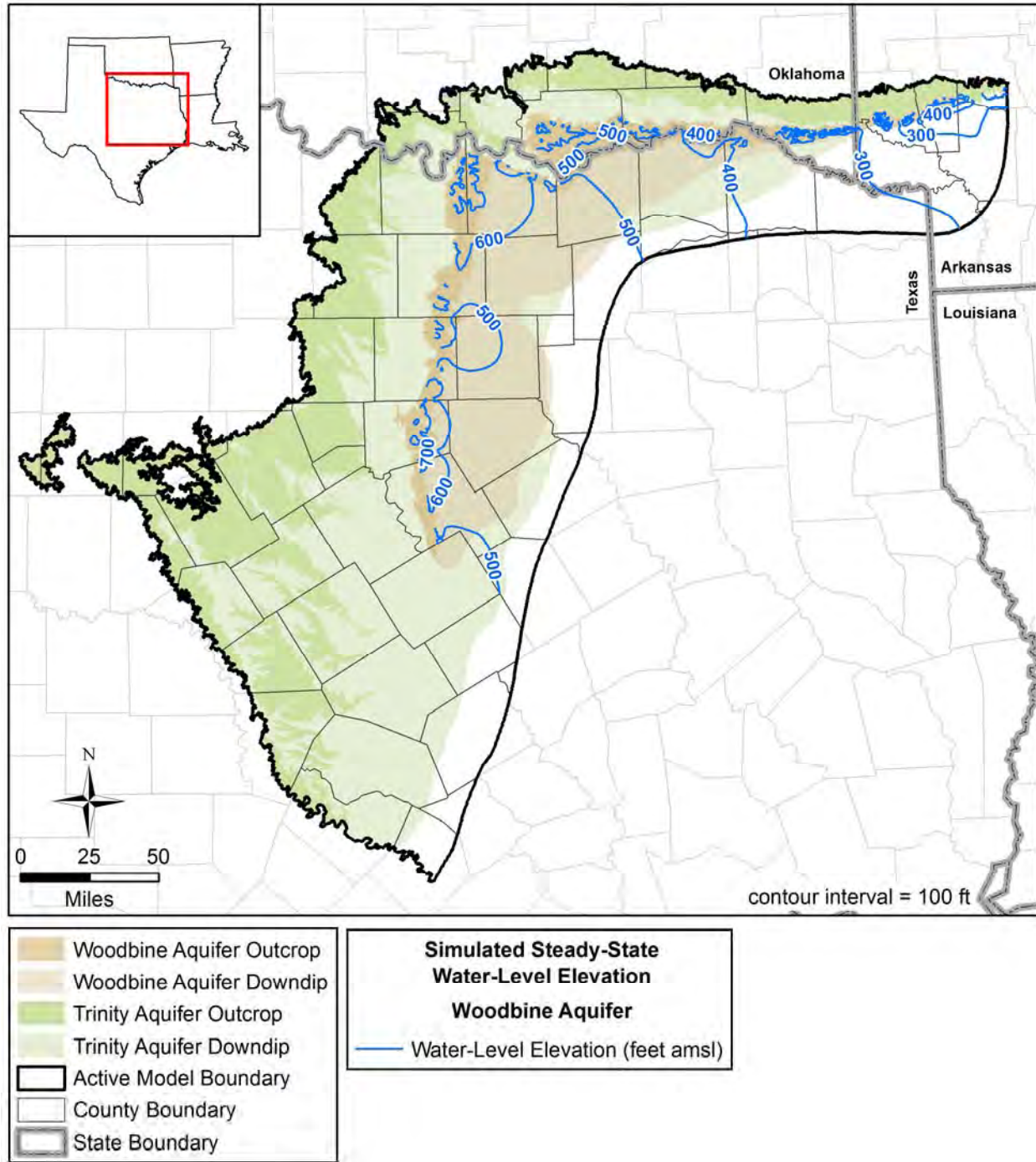
Figure 8.2.5   Simulated water-level elevations (hydraulic heads) in feet amsl for the Woodbine Aquifer.
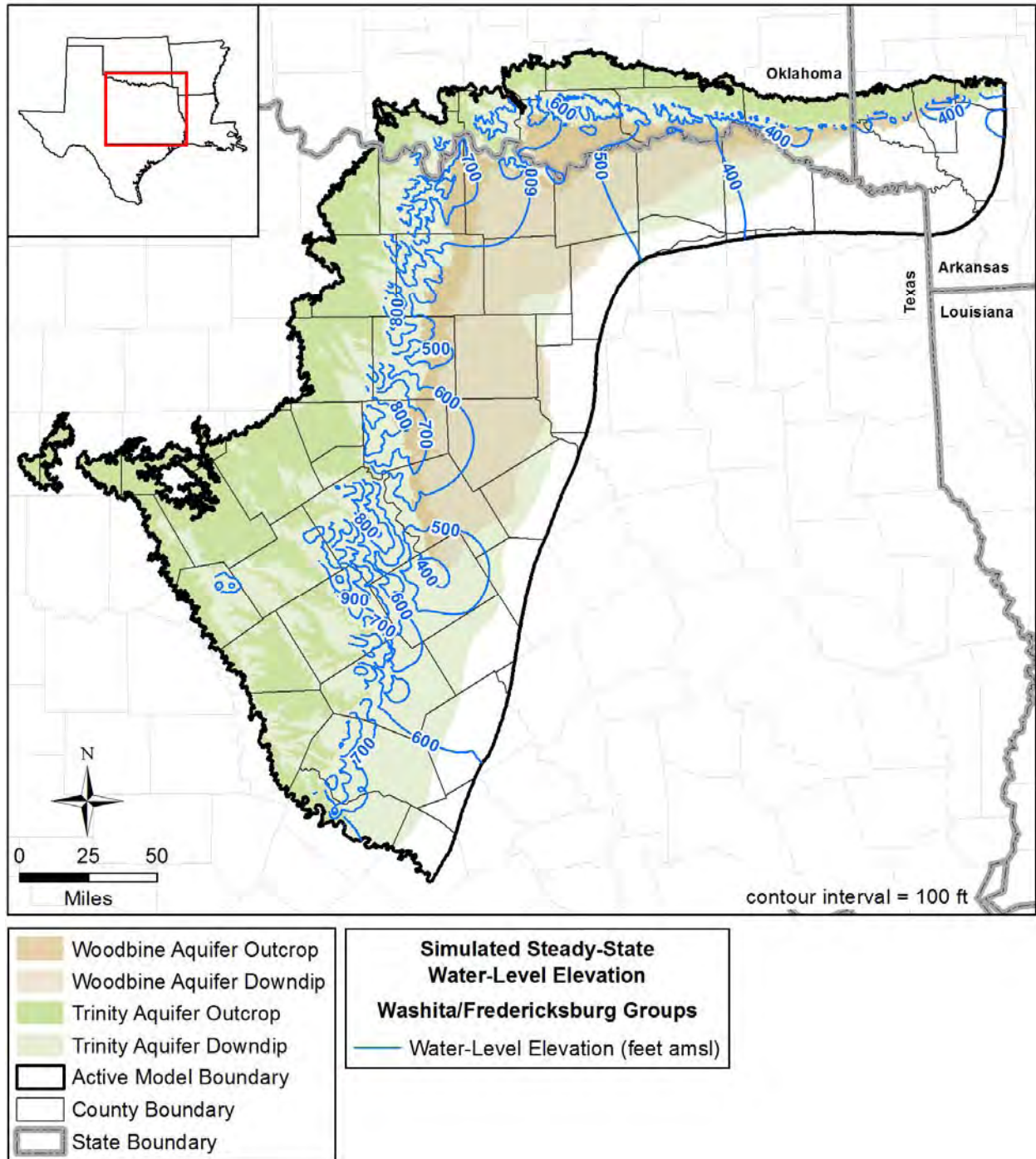
Figure 8.2.6   Simulated water-level elevations (hydraulic heads) in feet amsl for the Washita/Fredericksburg groups.
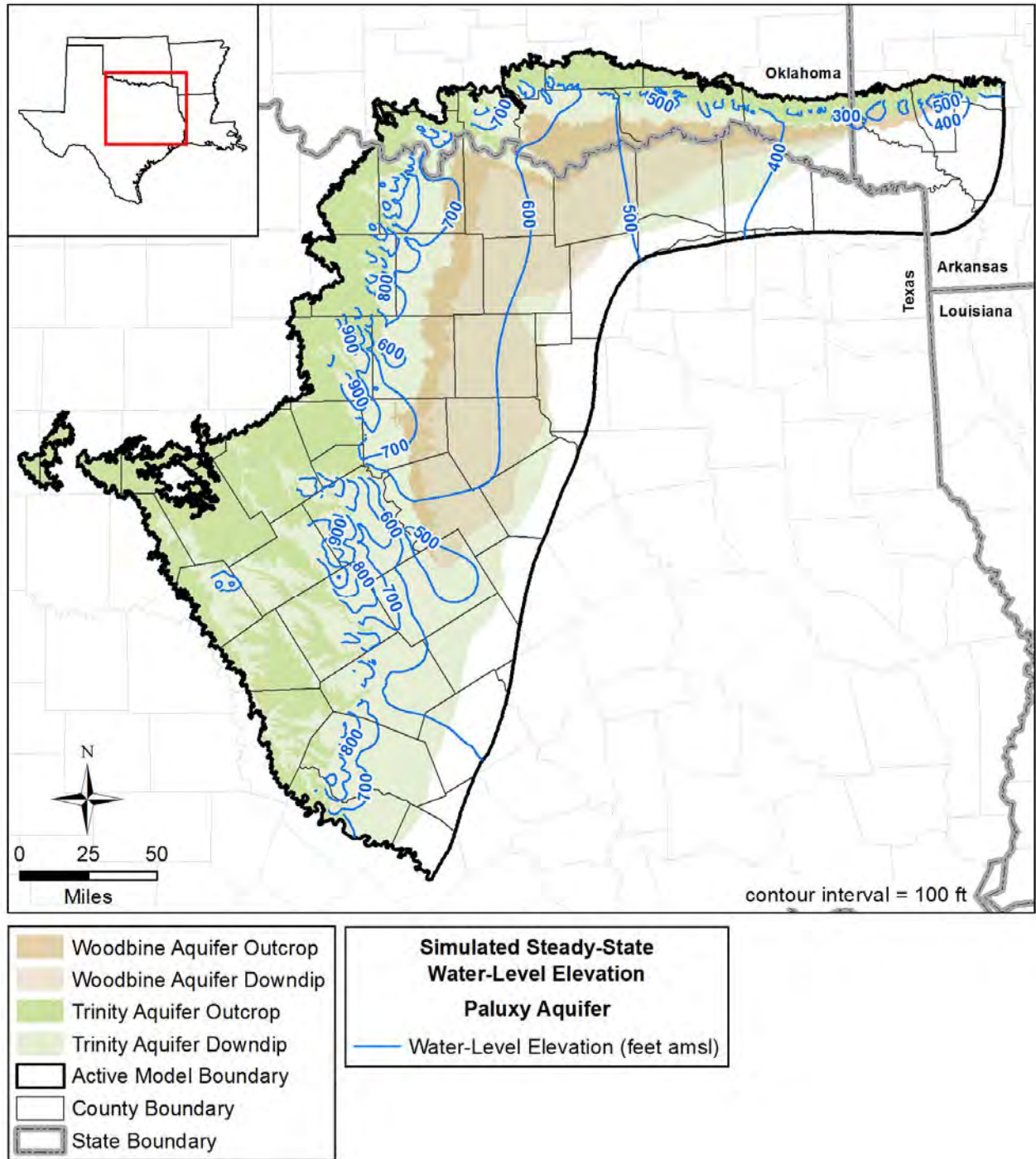
Figure 8.2.7 **Simulated water-level elevations (hydraulic heads) in feet amsl for the Paluxy Aquifer.**
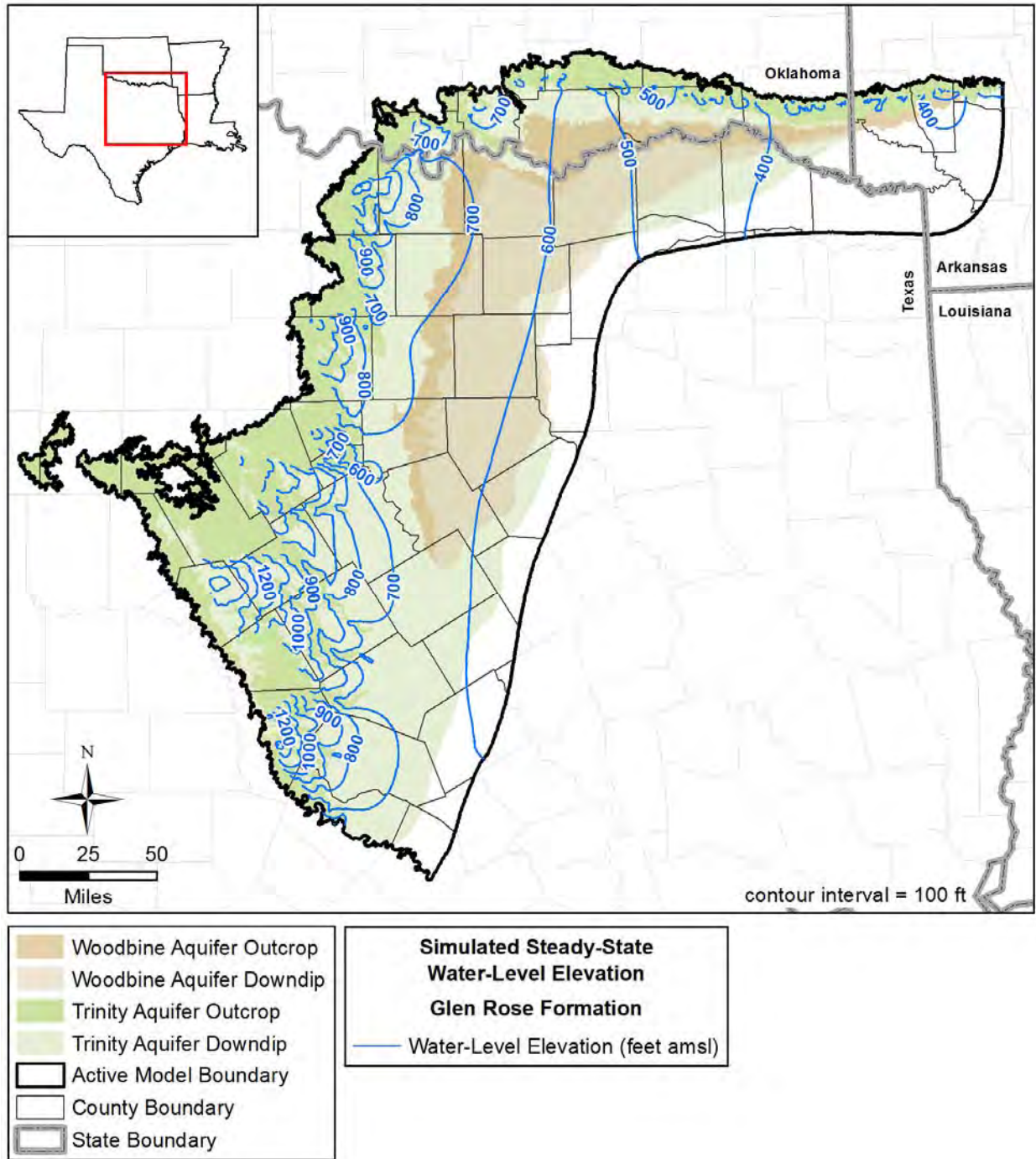
Figure 8.2.8   Simulated water-level elevations (hydraulic heads) in feet amsl for the Glen Rose Formation.
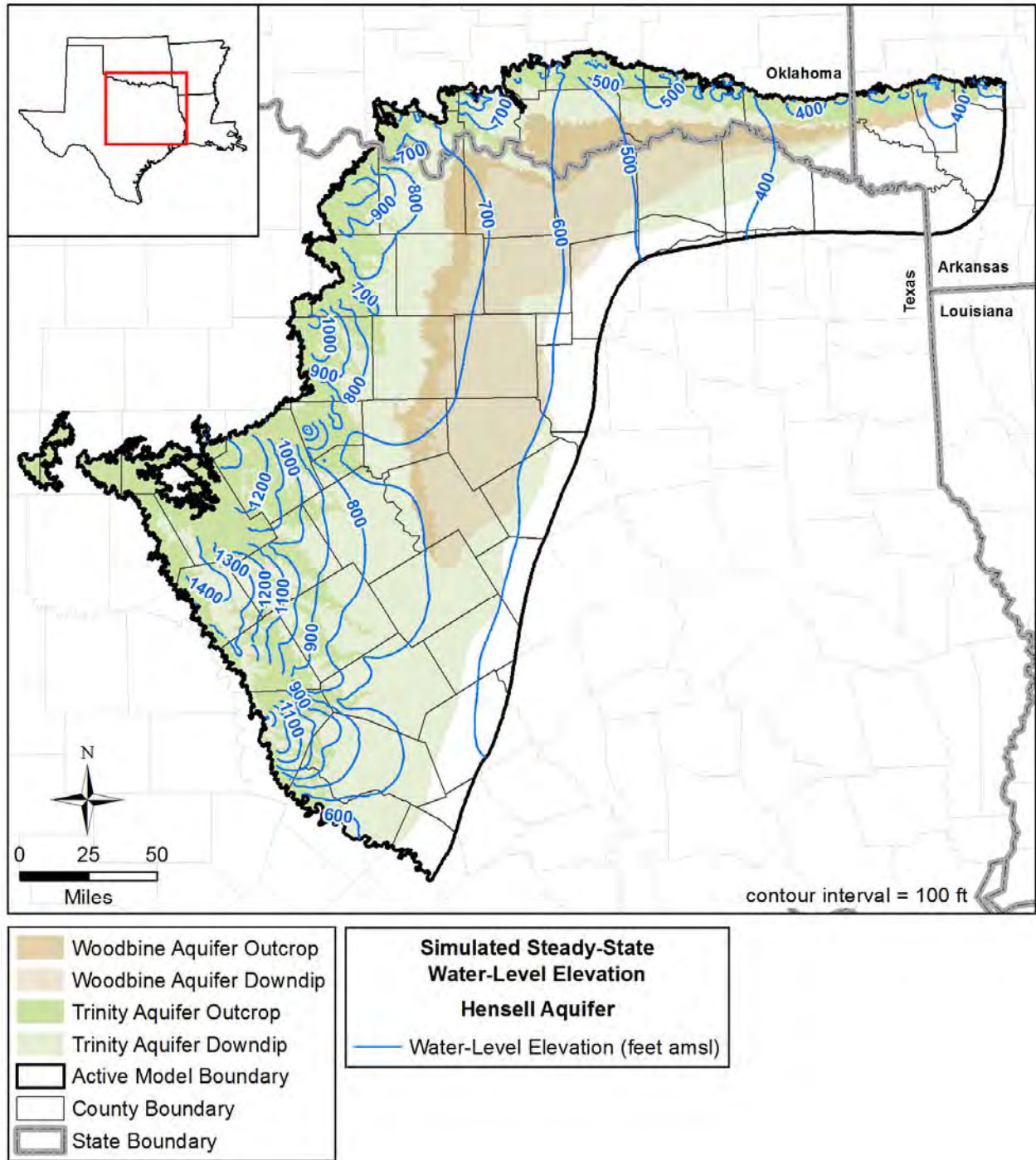
Figure 8.2.9   Simulated water-level elevations (hydraulic heads) in feet amsl for the Hensell Aquifer.
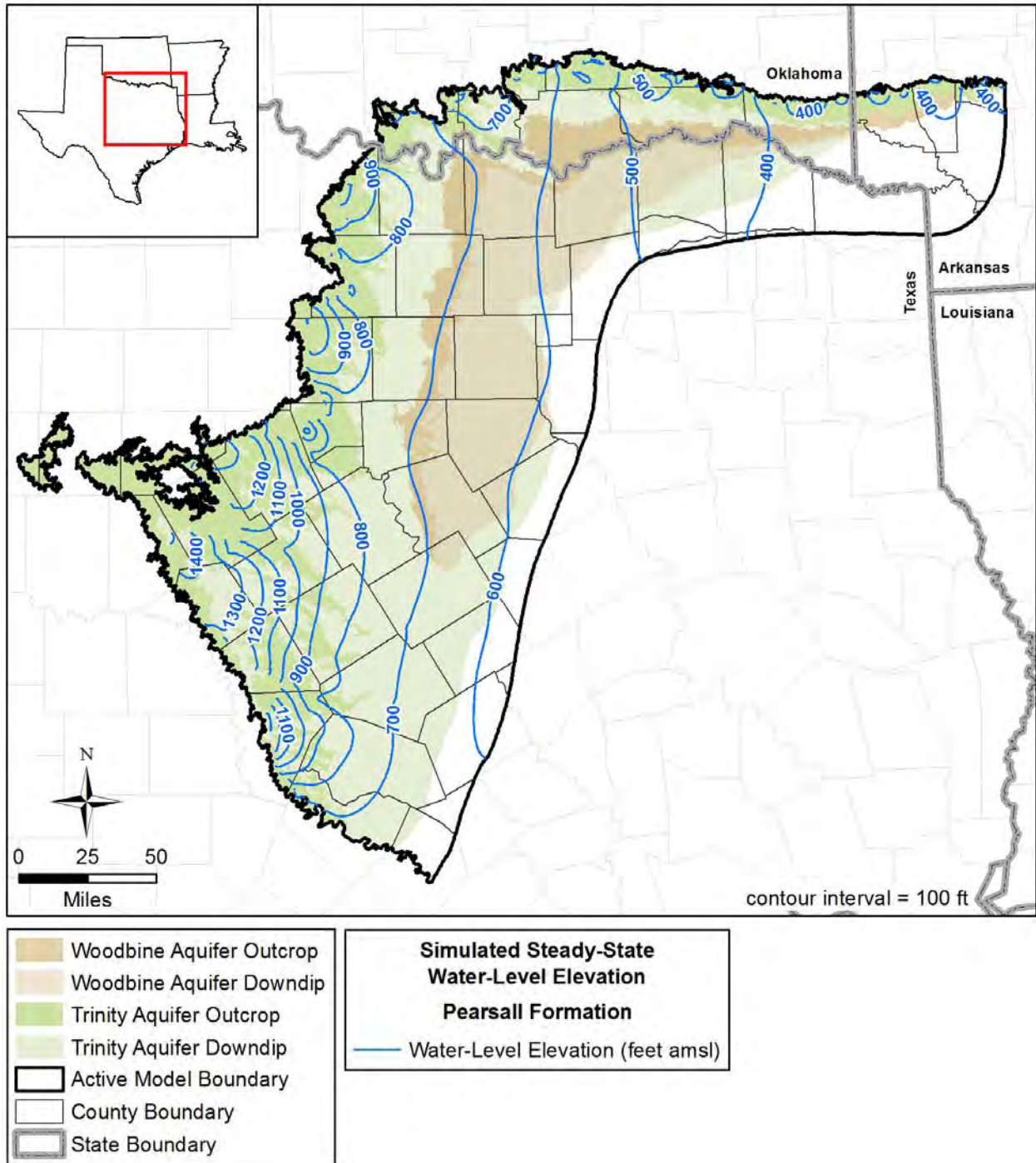
Figure 8.2.10   Simulated water-level elevations (hydraulic heads) in feet for the Pearsall Formation.
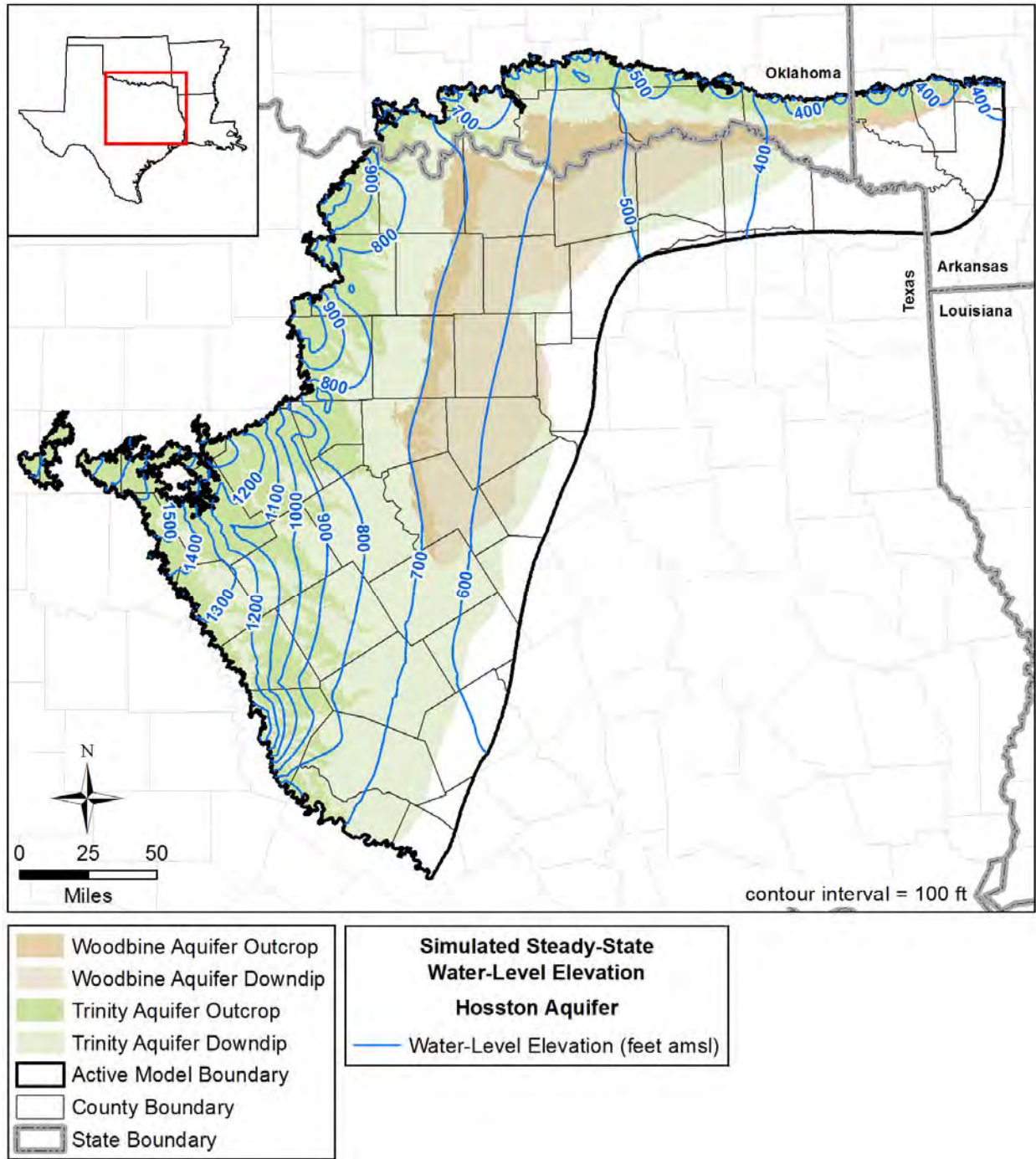
Figure 8.2.11   Simulated water-level elevations (hydraulic heads) in feet for the Hosston Aquifer.
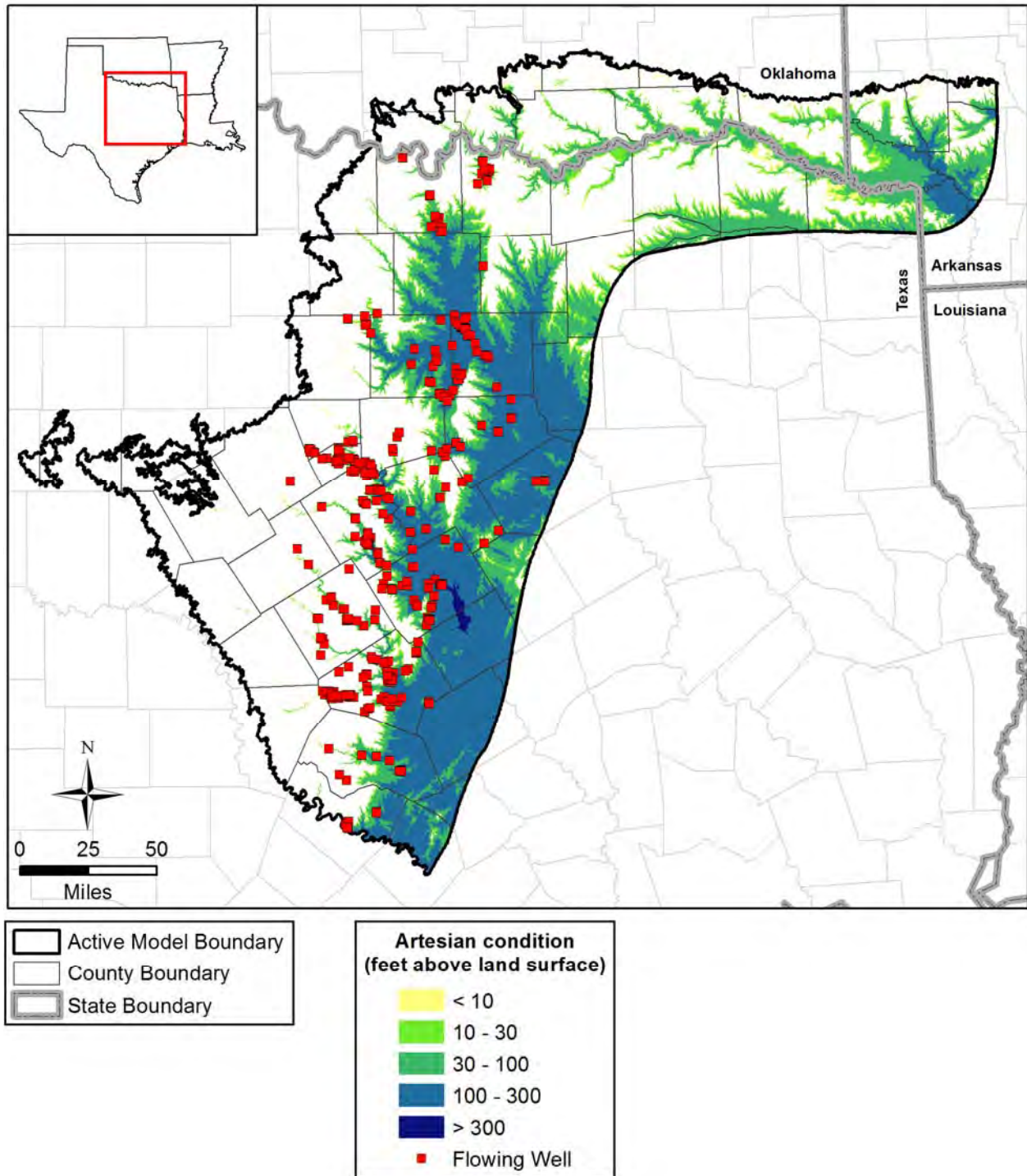
Figure 8.2.12   Simulated predevelopment artesian conditions in the Hensell Aquifer and flowing well locations.
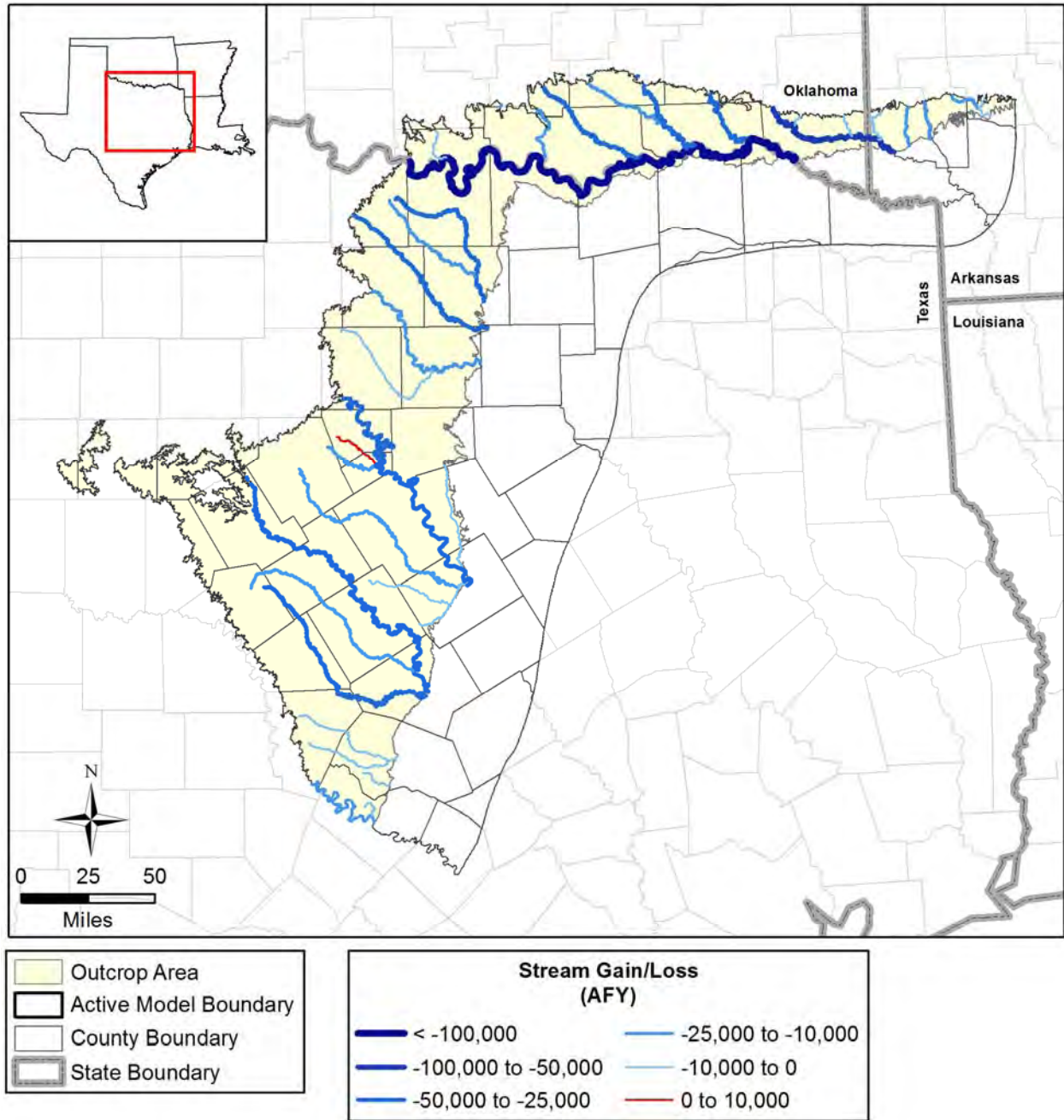
Figure 8.2.13 Steady-state model stream gain/loss in AFY (negative values denote gaining streams).
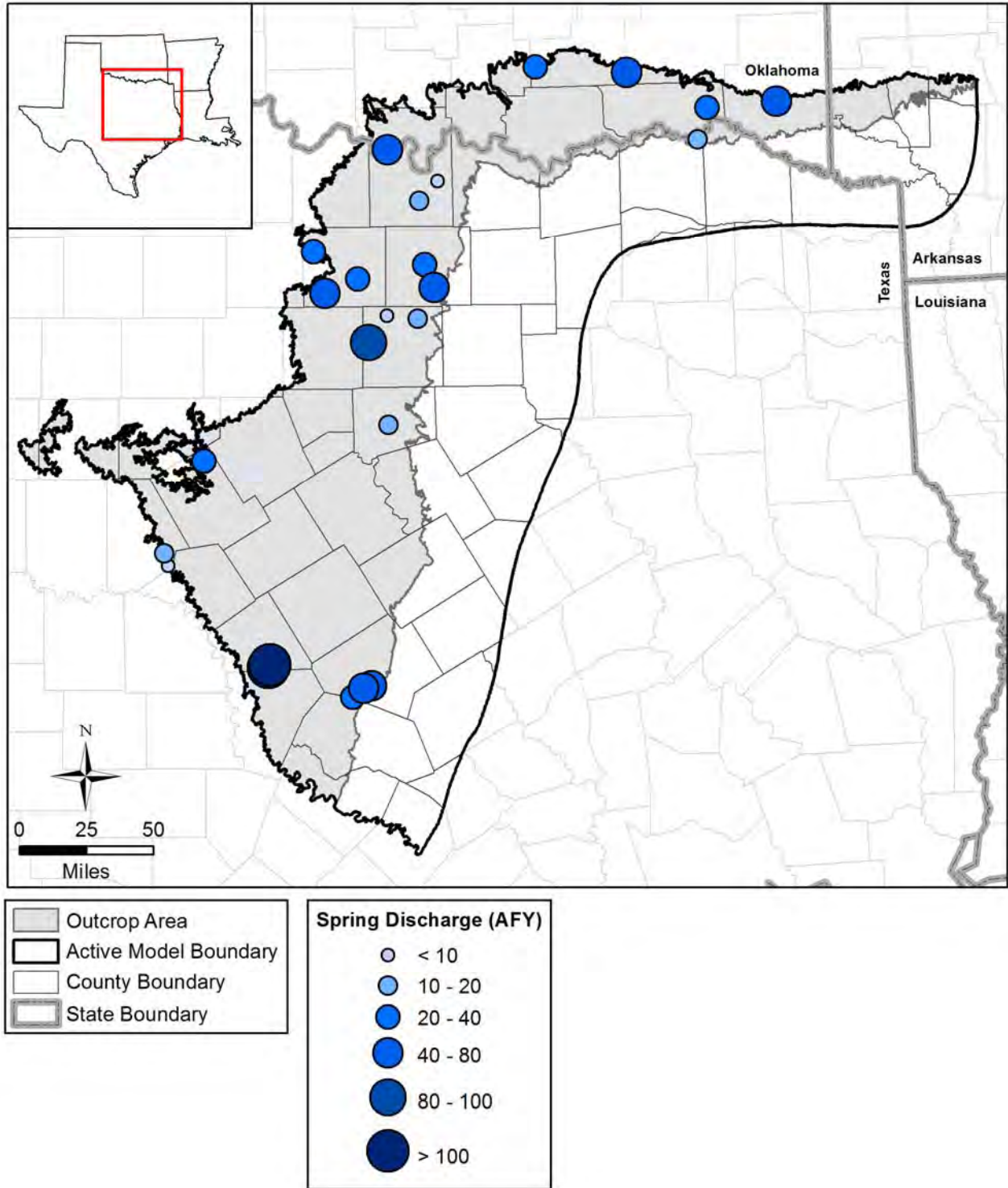
Figure 8.2.14   Simulated spring flow rates in AFY in the steady-state model.
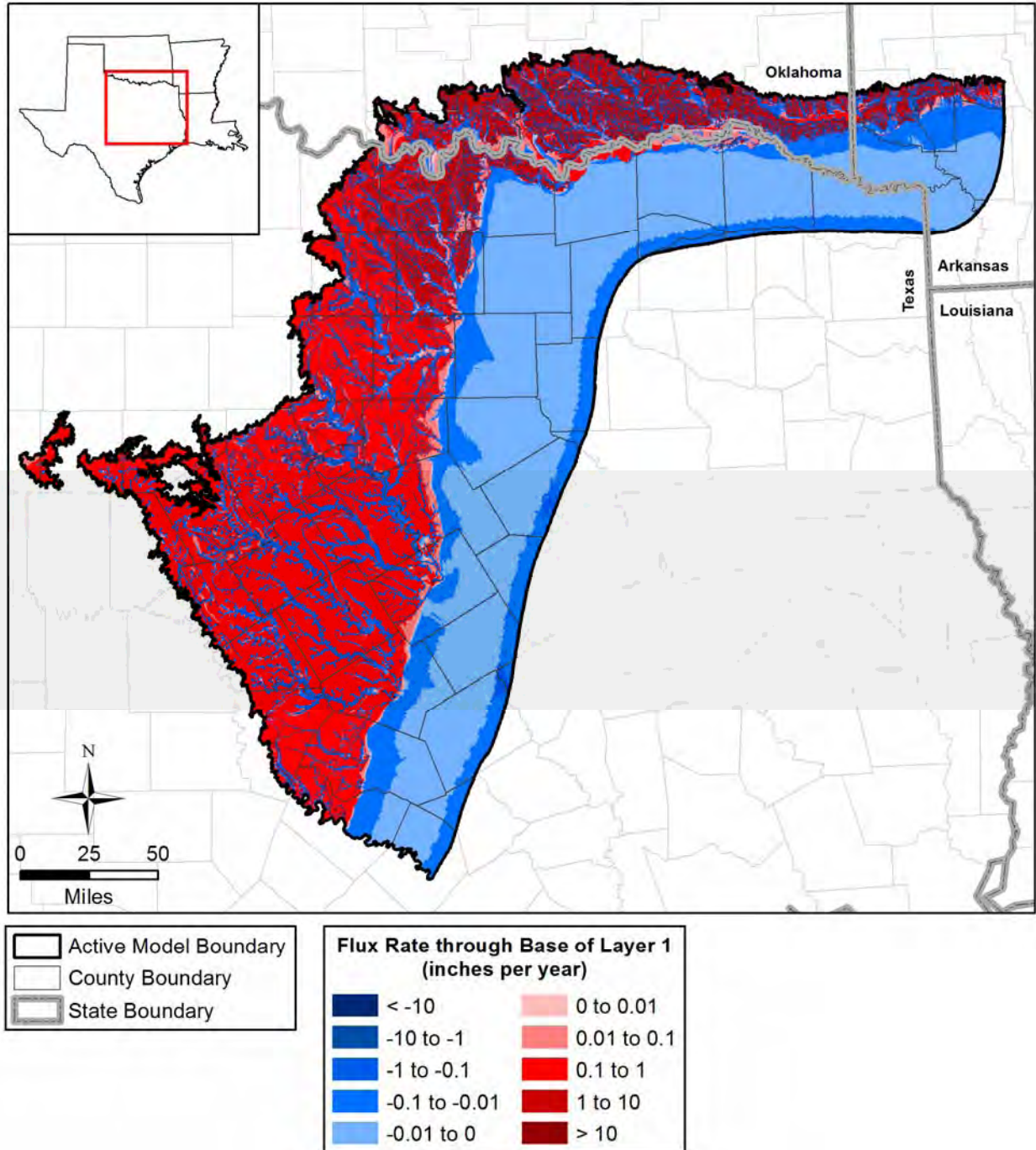
Figure 8.2.15 **Simulated downward cross-formational flow between the surficial outcrop area and younger formations in Layer 1 and Layers 2 through 8 (negative values indicate upward flow).**
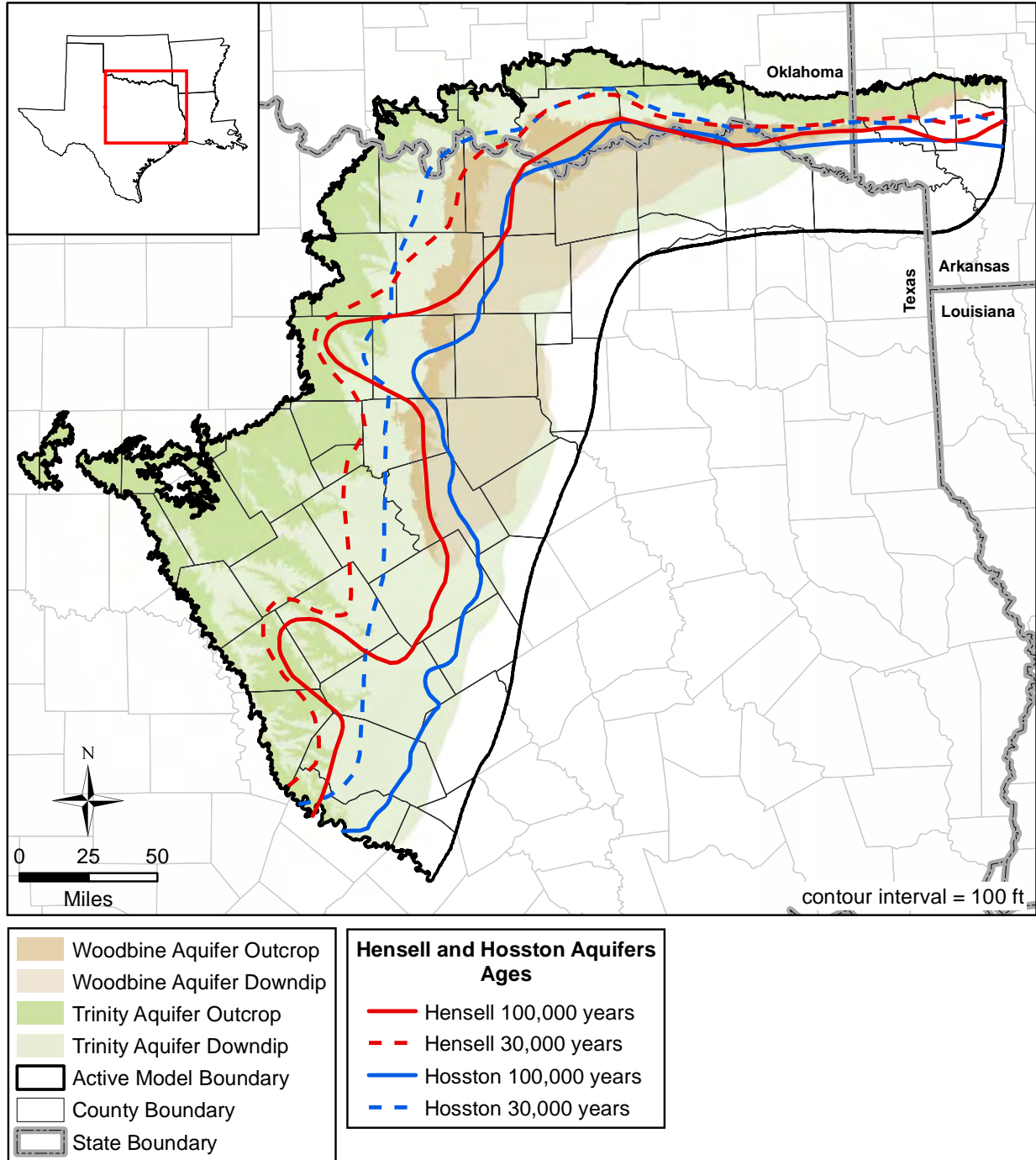
Figure 8.2.16   Simulated groundwater age contours in the Hensell and Hosston aquifers.

8.3   Sensitivity Analysis

A sensitivity analysis was performed on the calibrated steady-state model. A sensitivity analysis provides a means of formally describing the impact of varying specific parameters or groups of parameters on model outputs. In this sensitivity analysis, input parameters were systematically increased and decreased from their calibrated values while the change in hydraulic heads and outflows was recorded. Four simulations were completed for each parameter sensitivity, where the input parameters were varied either according to:

$$\text{(new parameter)} = \text{(old parameter)} * \text{factor} \tag{8.3.1}$$

or

$$\text{(new parameter)} = \text{(old parameter)} * 10^{(\text{factor - 1})} \tag{8.3.2}$$

and the factors were 0.5, 0.9, 1.1, and 1.5. Parameters such as recharge were varied linearly using Equation 8.3.1. For parameters such as hydraulic conductivity, which are typically thought of as log-varying, Equation 8.3.2 was used. For the output variable, the mean difference between the calibrated simulated hydraulic head and the sensitivity simulated hydraulic head was calculated as:

$$MD = \frac{1}{n} \sum_{i=1}^{n} \left(h_{sens,i} - h_{cal,i} \right) \tag{8.3.3}$$

where

$\quad$ MD = mean difference

$\quad$ $h_{sens,i}$ = sensitivity simulation hydraulic head at active grid cell i

$\quad$ $h_{cal,i}$ = calibrated simulation hydraulic head at active grid cell i

$\quad$ n = number of active grid cells, or the number of target locations

Equation 8.3.3 was applied separately both model-wide (i.e. in all active grid cells) and at target locations only. If the results are different between these two applications, it can be an indication that the targets are poorly distributed. However, if the results did not differ substantially, the second case will not be specifically discussed in this section.

Similarly, the mean difference in flows was calculated for flow boundaries, i.e.:

$$MD = \frac{1}{n} \sum_{i=1}^{n} \left(q_{sens,i} - q_{cal,i} \right) \tag{8.3.4}$$

where

> MD = mean difference
>
> $q_{sens,i}$ = sensitivity simulation flow at active grid cell i
>
> $q_{cal,i}$ = calibrated simulation flow at active grid cell i
>
> n = number of cells for flow boundary

For the steady-state sensitivity analysis, 28 combinations of input parameters and output metrics were investigated. For those parameters that would affect the shallow hydraulic heads, both flow and hydraulic head output metrics were considered. Whether hydraulic head, flow, or both were considered are noted in parentheses in the list below.

1. Horizontal hydraulic conductivity of the surficial outcrop area of Layer 1 (hydraulic head, flow), as well as the seven confined layers (hydraulic head).
2. Vertical hydraulic conductivity of the younger formations (hydraulic head), as well as the seven deeper formations (hydraulic head).
3. Recharge in the surficial outcrop area of Layer 1 (hydraulic head, flow).
4. Conductance for the head dependent boundary cells attached to the younger formations (hydraulic head).
5. River conductance in the surficial outcrop area of Layer 1 (hydraulic head, flow).
6. Conductance in the surficial outcrop area of Layer 1 drain boundaries representing groundwater ET (hydraulic head, flow).
7. Conductance in the surficial outcrop area of Layer 1 drain boundaries representing ephemeral streams (hydraulic head, flow).
8. Conductance in the surficial outcrop area of Layer 1 drain boundaries representing springs (hydraulic head, flow).

Equation 8.3.1 was used for sensitivity 3, while Equation 8.3.2 was used for the remaining sensitivities.

Figure 8.3.1 shows the sensitivity in hydraulic heads to variation in the horizontal hydraulic conductivity in the surficial outcrop area of Layer 1. Because the surficial outcrop area of Layer 1 sets the updip hydraulic head boundary, decreasing horizontal hydraulic conductivity increases hydraulic heads in the surficial outcrop area of Layer 1, which then propagate throughout the model. Increasing horizontal hydraulic conductivity has the reverse effect.

In the confined layers, decreasing the horizontal hydraulic conductivity has the effect of restricting downdip flow, which increases hydraulic heads in the outcrop/shallow portion of the layer, but will typically decrease hydraulic heads in the deeper portion, since hydraulic heads decrease at a faster rate as water moves downdip. So, depending on the area of the outcrop compared to the confined area, overall hydraulic heads may respond differently to changes in horizontal hydraulic conductivity. Figure 8.3.2 shows the sensitivity to changes in the Woodbine Aquifer, where the hydraulic heads in the Woodbine Aquifer are lower for lower horizontal hydraulic conductivity and other aquifers are mostly unaffected. Figure 8.3.3 shows the sensitivity to changes in the horizontal hydraulic conductivity in the Washita/Fredericksburg groups, which, with a large outcrop area, shows a positive mean hydraulic head difference for lower horizontal hydraulic conductivity. These increased hydraulic heads in the outcrop propagates throughout the rest of the layer. Figure 8.3.4 shows a mixed sensitivity to variation of horizontal hydraulic conductivity in the Paluxy Aquifer. The deeper Hosston Aquifer and Pearsall Formation show a decrease in hydraulic heads with the decreasing conductivity, the younger formations show the opposite trend, and mixed trends are observed for layers in between. The trends are similar for the remaining layers shown in Figures 8.3.5 through 8.3.8, with the deeper layers showing the most prominent decreased hydraulic heads with decreased horizontal hydraulic conductivity. The hydraulic heads in the Hensell Aquifer, Pearsall Formation, and Hosston Aquifer are most sensitive to the horizontal hydraulic conductivity in that layer, followed by over- or underlying layers.

Figure 8.3.9 shows the hydraulic head sensitivity to changes in vertical hydraulic conductivity in the younger formations. Upward flow through the younger formations is the primary discharge mechanism for deep flow paths, so decreasing the vertical hydraulic conductivity causes hydraulic heads to build up in the other layers. A similar trend in hydraulic head change is shown in Figure 8.3.10 for changes in the vertical hydraulic conductivity of the Woodbine Aquifer, since it overlies the other formations. For the Washita/Fredericksburg groups, shown in Figure 8.3.11, hydraulic heads in underlying layers increase with decreasing vertical hydraulic conductivity, but the overlying Woodbine Aquifer shows the opposite trend, since there is a larger hydraulic head drop upward across the Washita/Fredericksburg groups from those underlying layers. Sensitivity to vertical hydraulic conductivity in the Paluxy Aquifer and Glen Rose Formation continue this trend in Figures 8.3.12 and 8.3.13, with hydraulic heads in the

underlying layers increasing with decreasing vertical hydraulic conductivity, and hydraulic heads in overlying layers decreasing or staying flat. Moving to the deeper formations, Figures 8.3.14 through 8.3.16 show increasing hydraulic heads in all layers with decreasing vertical hydraulic conductivity, with the exception of the response of hydraulic heads in the Hosston Aquifer to vertical conductivity in the Pearsall Formation (Figure 8.3.15). This response suggests that updip portions of the Hosston Aquifer receive cross-formational flow downward through the Pearsall Formation.

Figure 8.3.17 shows the expected response of hydraulic heads to variation in recharge. Increasing recharge results in increasing hydraulic heads in all layers. Figure 8.3.18 shows the small increase in hydraulic heads with a decrease in the conductance of the head dependent boundary cells in the younger formations. The response is identical to the sensitivity to vertical hydraulic conductivity in the younger formations, although smaller in comparison. Figures 8.3.19 through 8.3.22 show the sensitivity of hydraulic heads to the conductances of the various boundary types in the surficial outcrop area of Layer 1. In all cases, decreasing conductance restricts flow out these boundaries and, thus, increases hydraulic heads.

Figure 8.3.23 shows the sensitivity in flows from the surficial discharge boundaries to variation in the horizontal hydraulic conductivity in the surficial outcrop area of Layer 1. Because the alluvium around the river boundaries has the highest horizontal hydraulic conductivity, the river flows dominate this sensitivity. The increasing river flows correspond to a slight decrease in the discharge to the other surface boundaries. Figure 8.3.24 shows the sensitivity of boundary flow to changes in recharge in the surficial outcrop area of Layer 1. Flow out of the river boundaries have the highest relative increase with increasing recharge. Figure 8.3.25 shows the sensitivity of flow to changing conductance in the river boundaries. Flow increases out of the rivers with increasing conductance. This decreases flow to the other surficial discharge boundaries, including ET and springs. A similar trend is shown in Figures 8.3.26 and 8.3.27, where an increasing conductance in one of the surficial boundaries increases flow out of that boundary, and decreases flow out of the remaining boundaries. Springflow is such a small portion of the water budget, that changes in springflow have virtually no effect on the flow in the other boundaries (Figure 8.3.28).
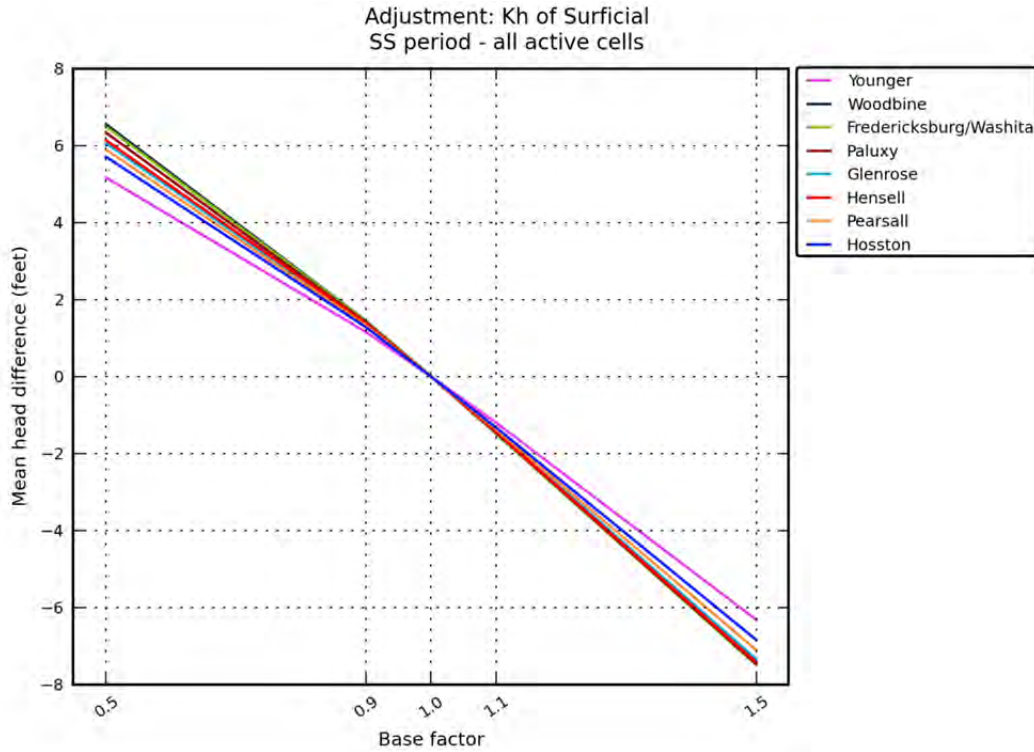
Figure 8.3.1   Hydraulic head sensitivity in feet for the steady-state model to changes in horizontal hydraulic conductivity of the surficial outcrop area of Layer 1.
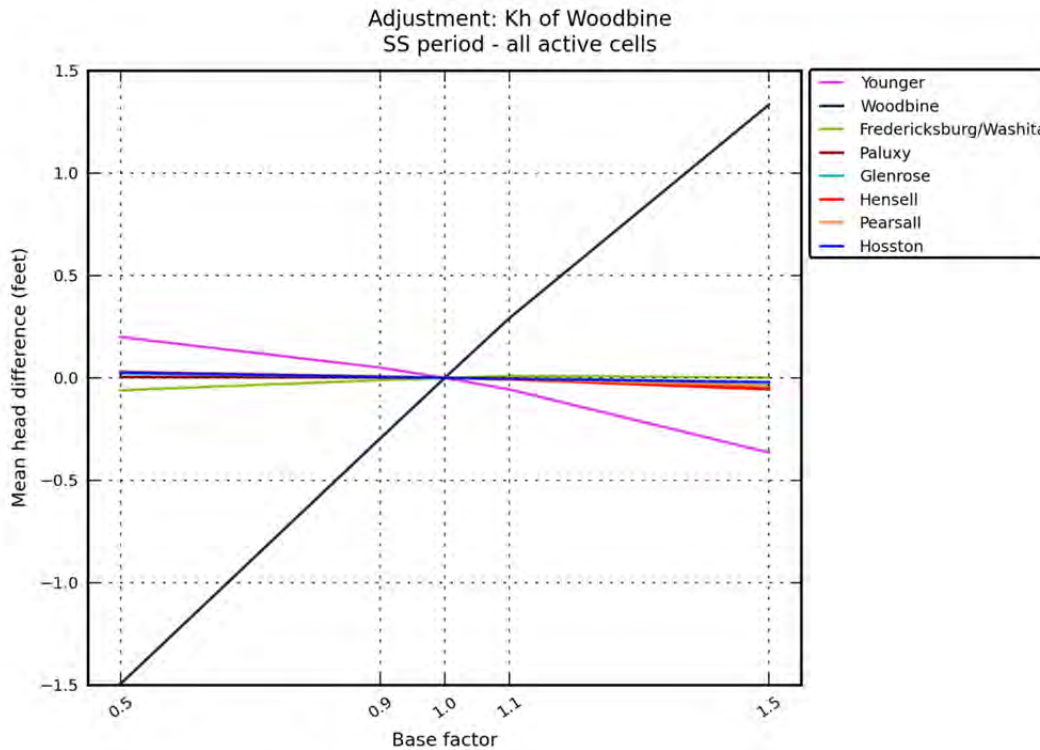
Figure 8.3.2   Hydraulic head sensitivity in feet for the steady-state model to changes in horizontal hydraulic conductivity of the Woodbine Aquifer.
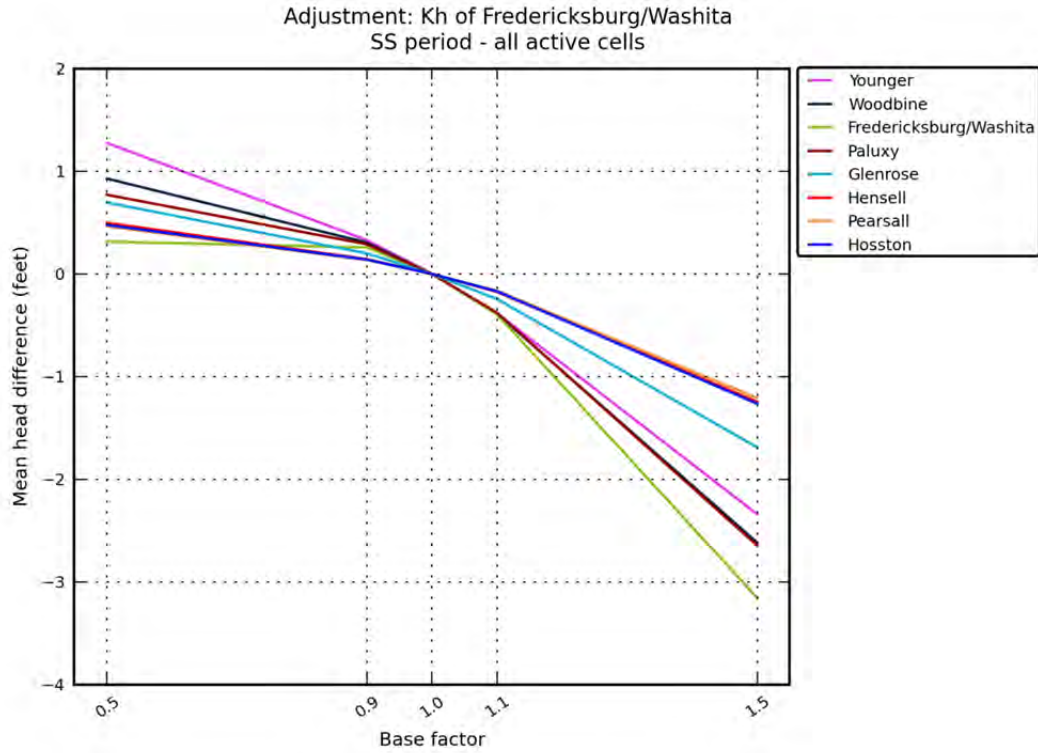
Figure 8.3.3   **Hydraulic head sensitivity in feet for the steady-state model to changes in horizontal hydraulic conductivity of the Washita/ Fredericksburg groups.**
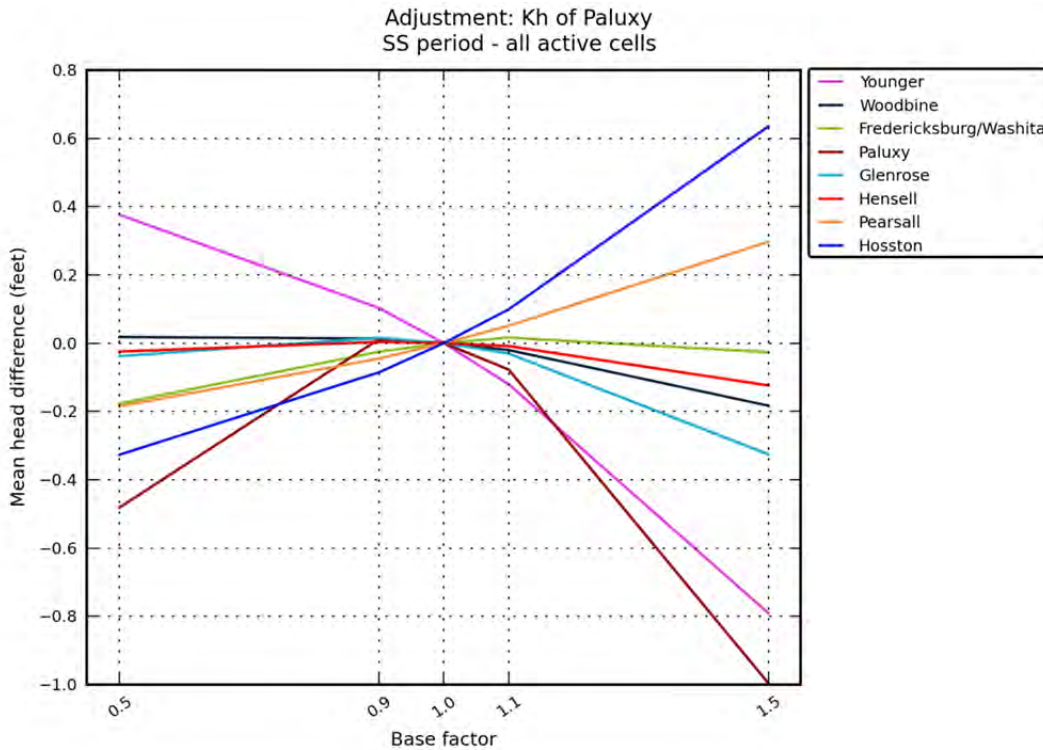
Figure 8.3.4   **Hydraulic head sensitivity in feet for the steady-state model to changes in horizontal hydraulic conductivity of the Paluxy Aquifer.**
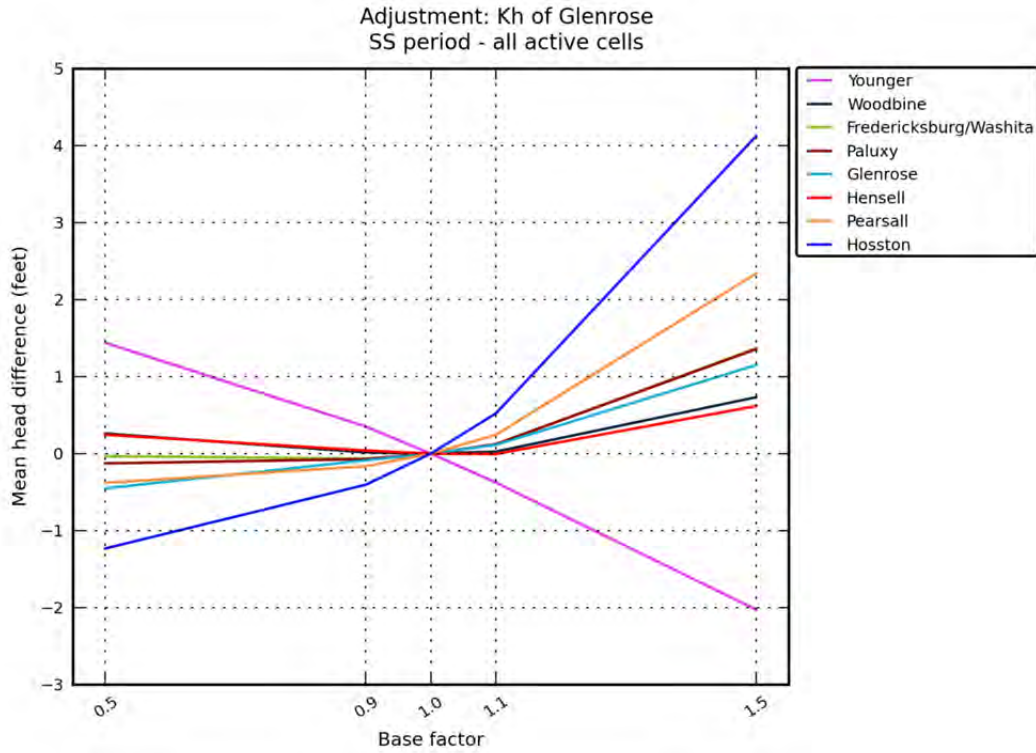
Figure 8.3.5   **Hydraulic head sensitivity in feet for the steady-state model to changes in horizontal hydraulic conductivity of the Glen Rose Formation.**
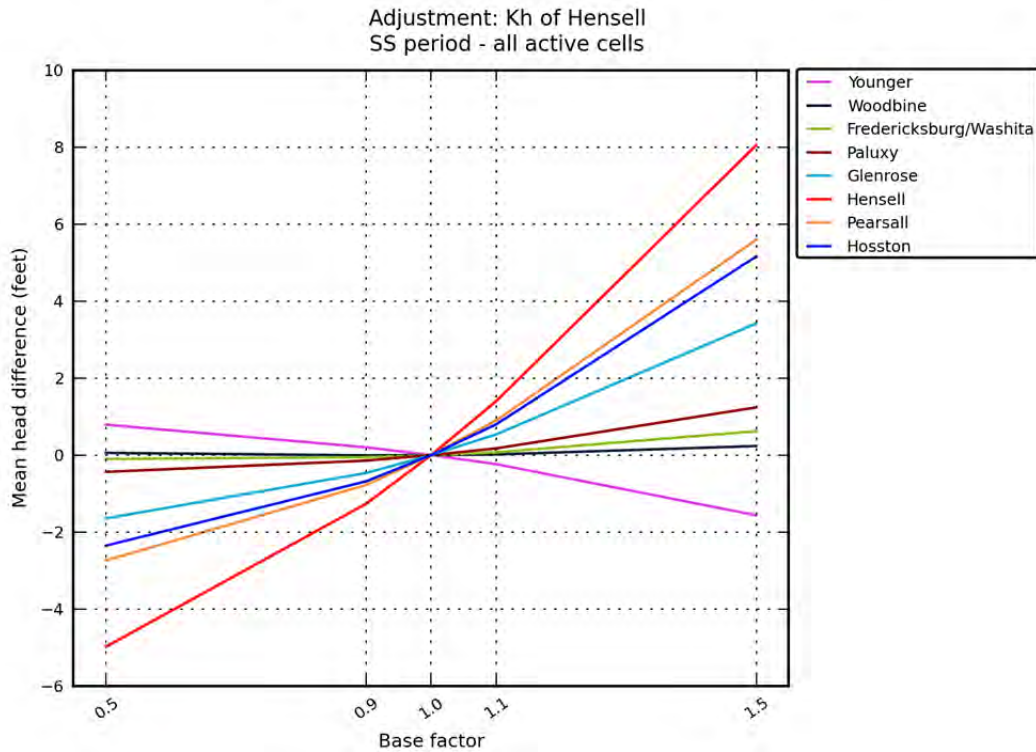
Figure 8.3.6   **Hydraulic head sensitivity in feet for the steady-state model to changes in horizontal hydraulic conductivity of the Hensell Aquifer.**
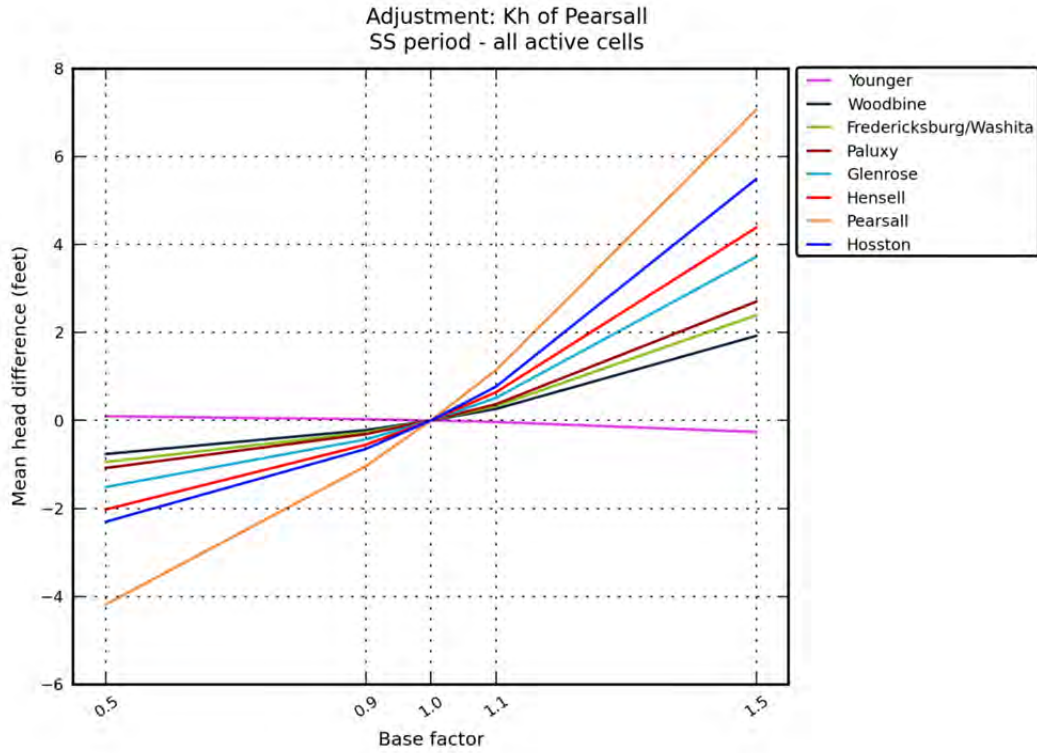
Figure 8.3.7 **Hydraulic head sensitivity in feet for the steady-state model to changes in horizontal hydraulic conductivity of the Pearsall Formation.**
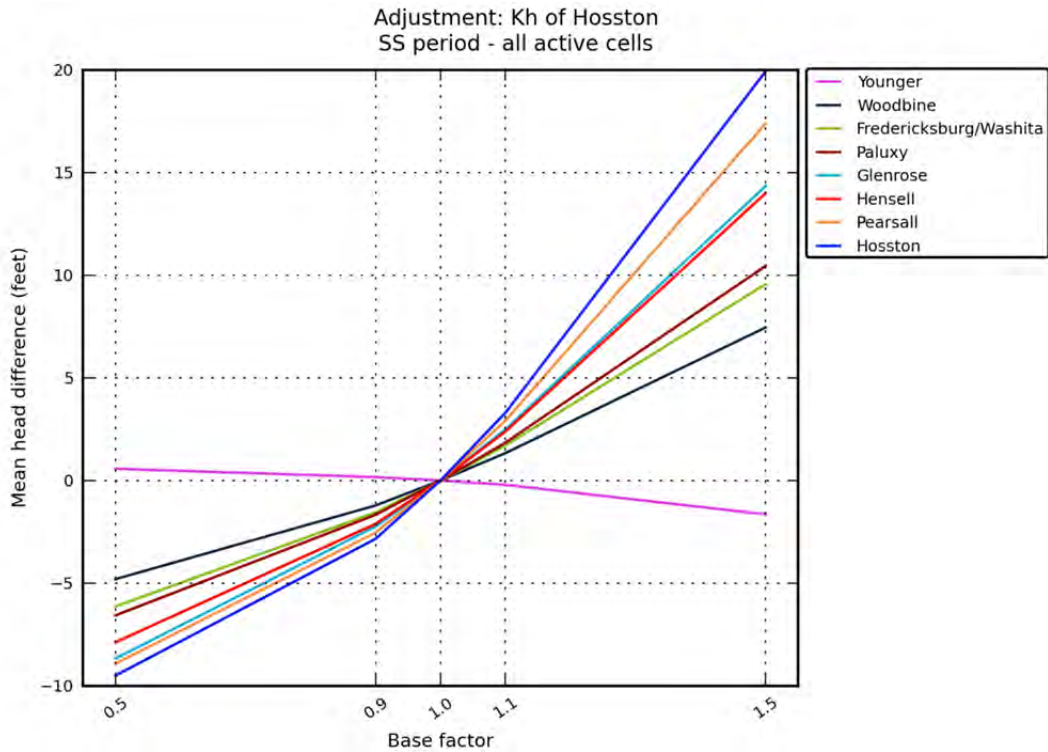
Figure 8.3.8 **Hydraulic head sensitivity in feet for the steady-state model to changes in horizontal hydraulic conductivity of the Hosston Aquifer.**
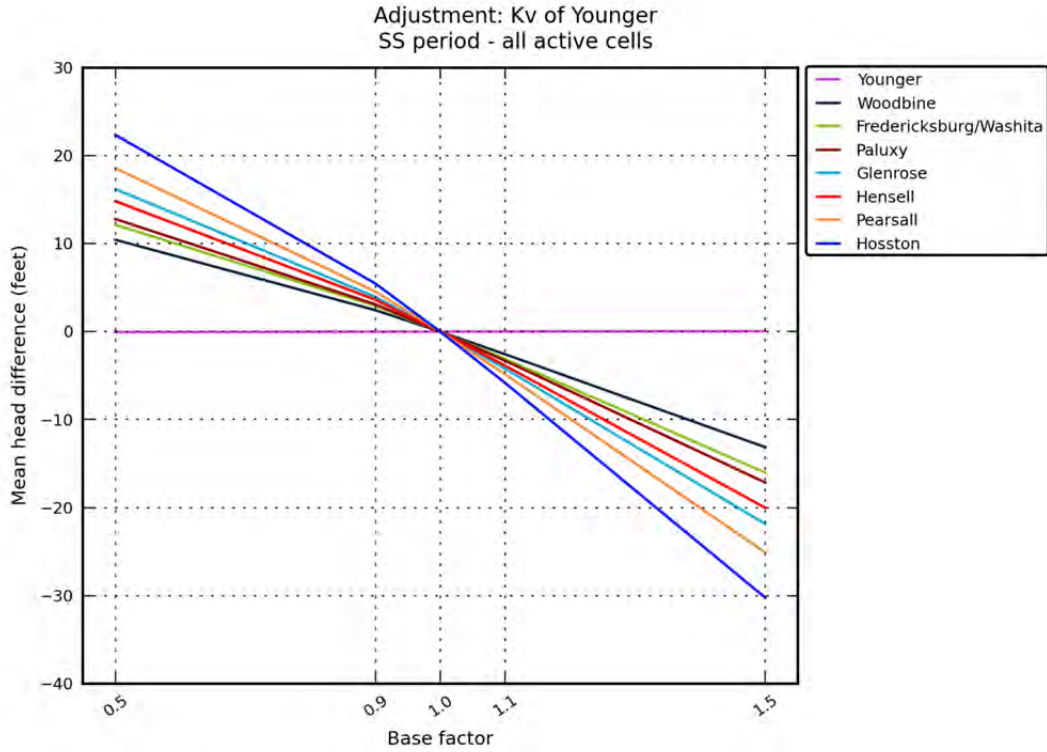
Figure 8.3.9   **Hydraulic head sensitivity in feet for the steady-state model to changes in vertical hydraulic conductivity of the younger formations.**
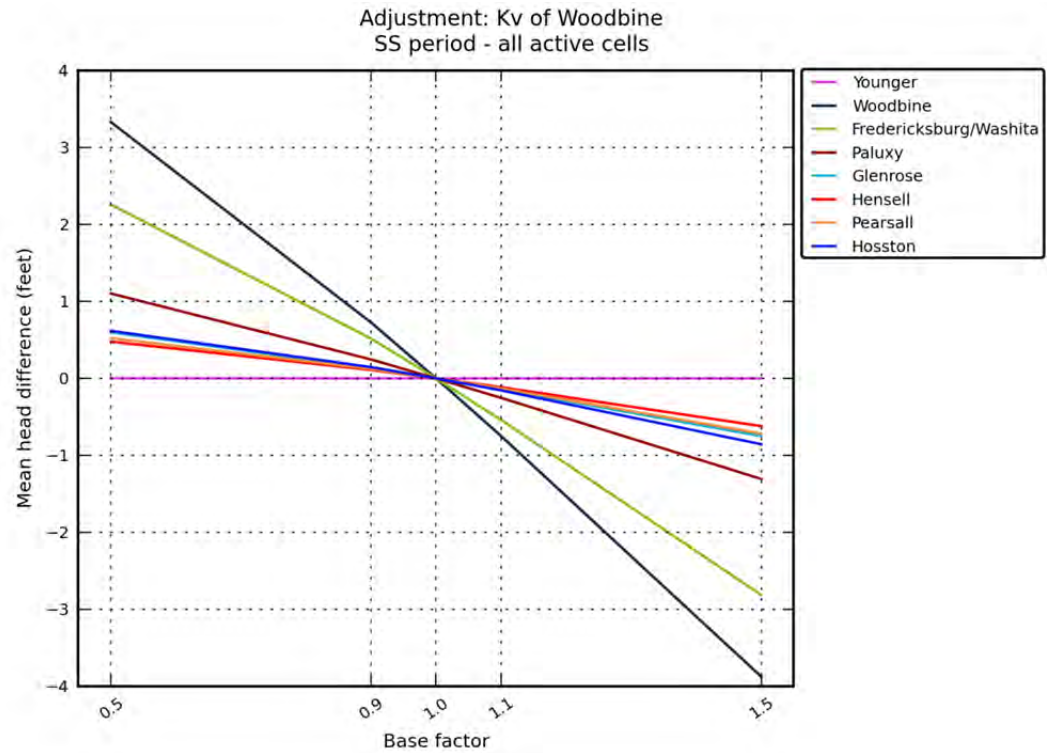
Figure 8.3.10   **Hydraulic head sensitivity in feet for the steady-state model to changes in vertical hydraulic conductivity of the Woodbine Aquifer.**
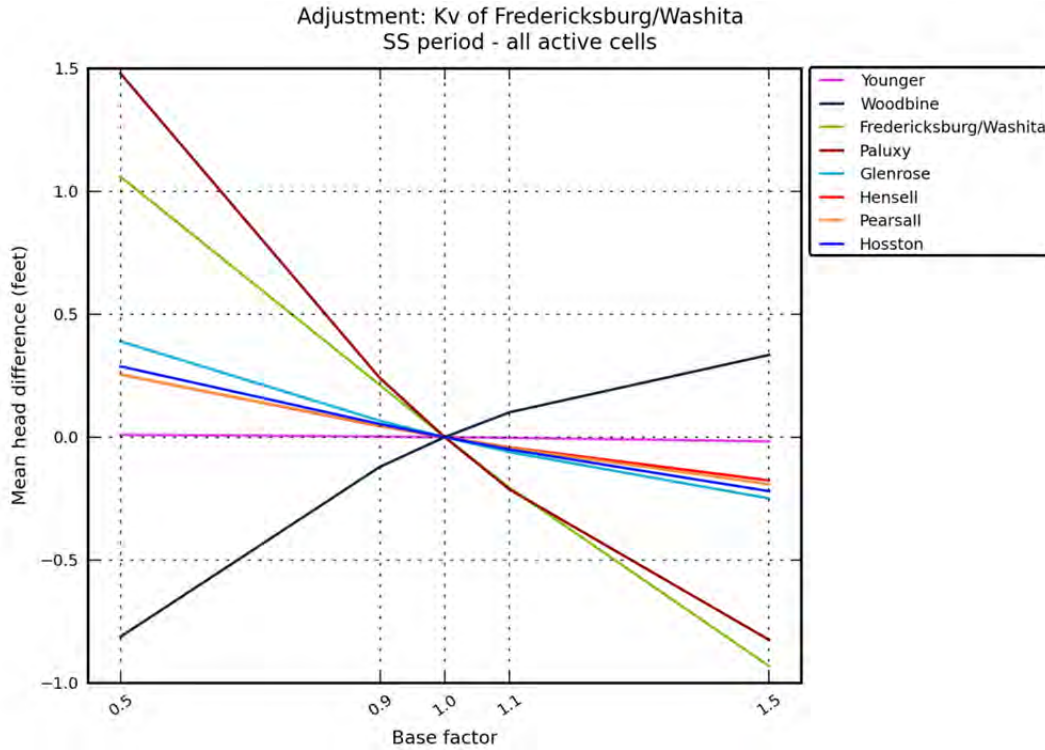
Figure 8.3.11   Hydraulic head sensitivity in feet for the steady-state model to changes in vertical hydraulic conductivity of the Washita/ Fredericksburg groups.
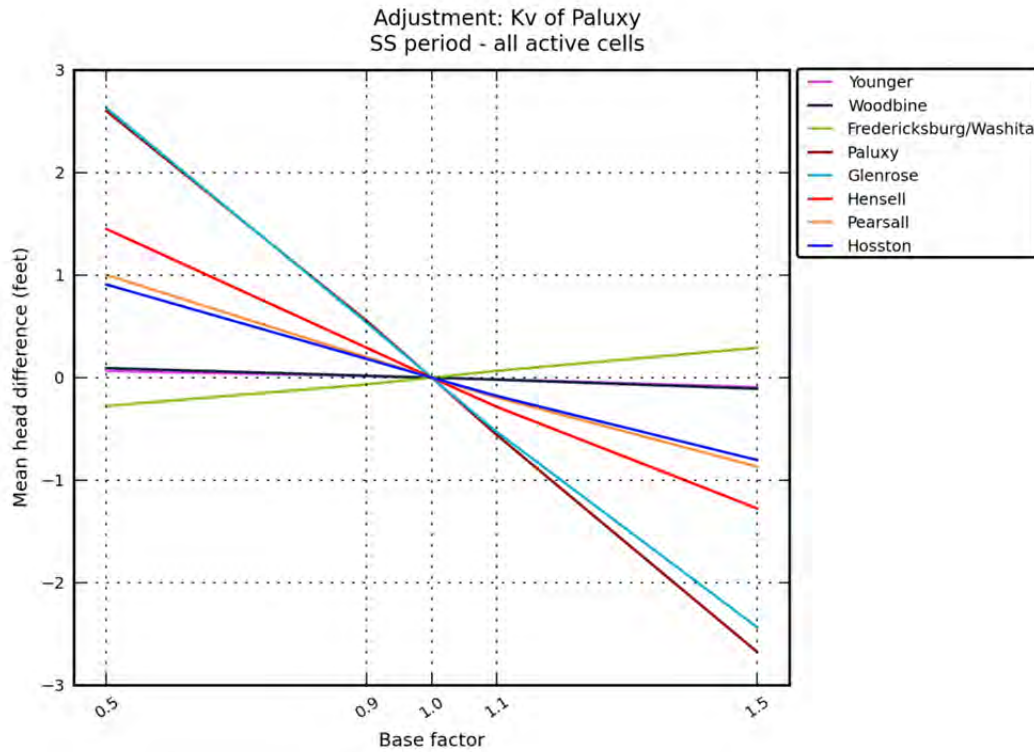
Figure 8.3.12   Hydraulic head sensitivity in feet for the steady-state model to changes in vertical hydraulic conductivity of the Paluxy Aquifer.
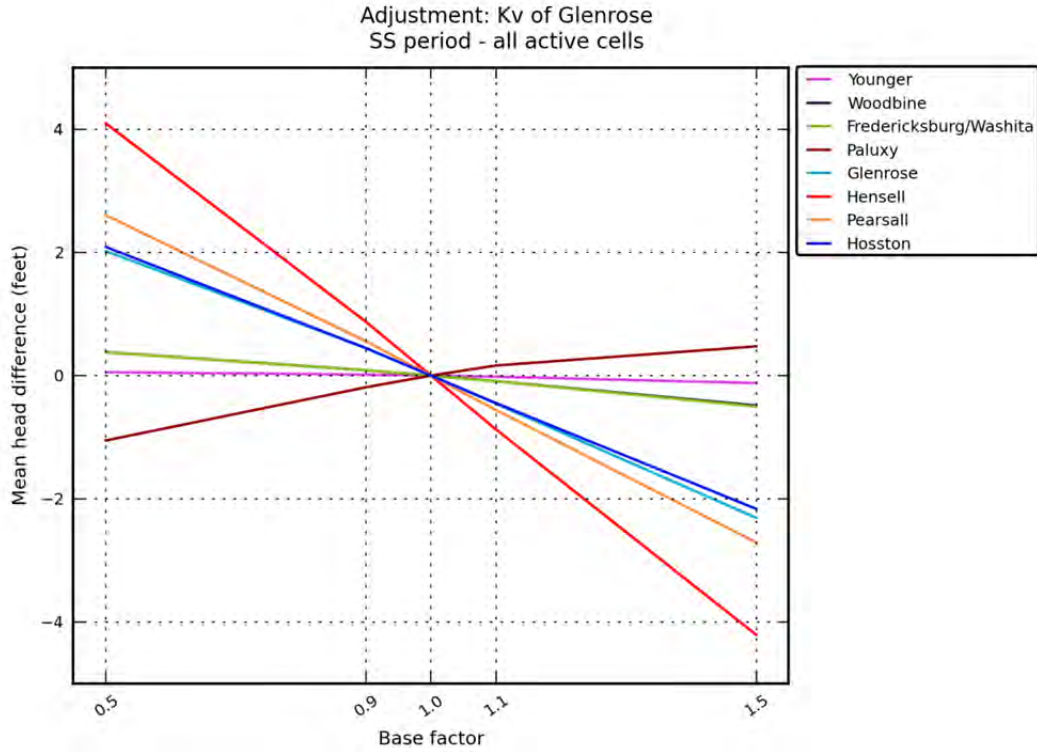
Figure 8.3.13   Hydraulic head sensitivity in feet for the steady-state model to changes in vertical hydraulic conductivity of the Glen Rose Formation.
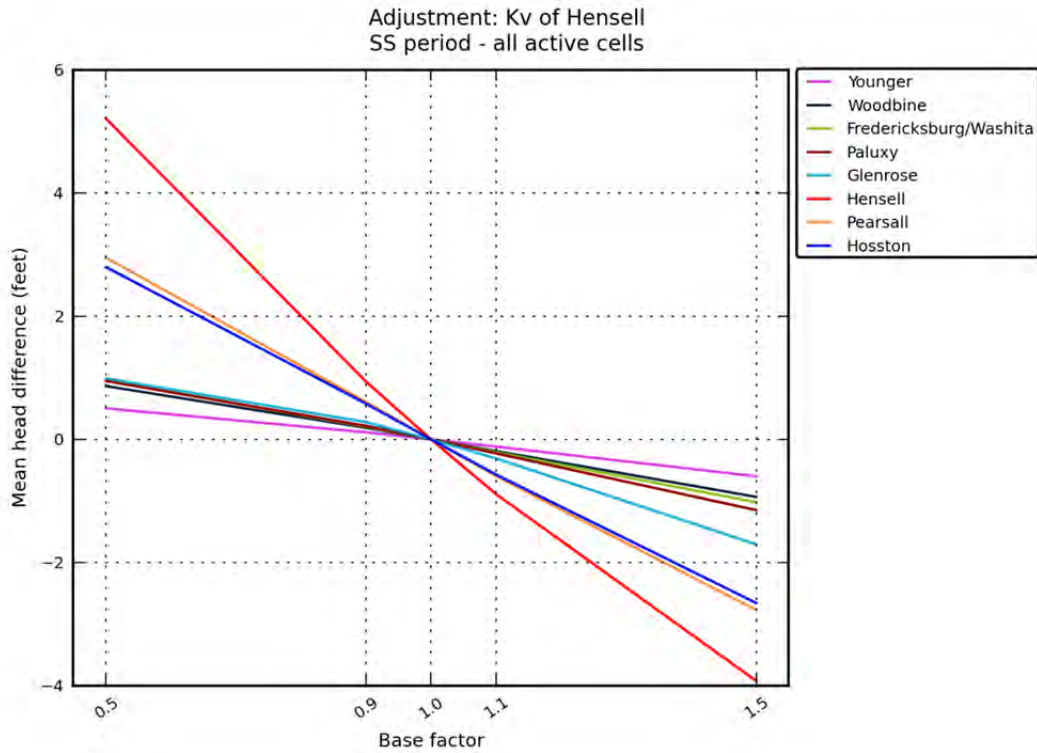
Figure 8.3.14   Hydraulic head sensitivity in feet for the steady-state model to changes in vertical hydraulic conductivity of the Hensell Aquifer.
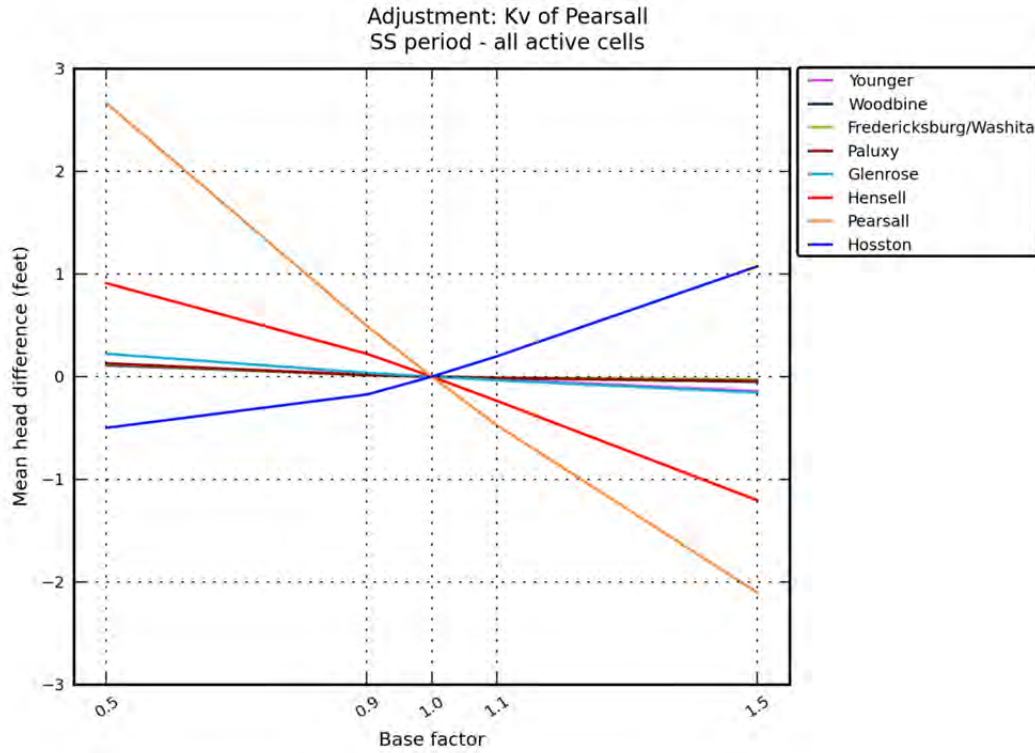
Figure 8.3.15 **Hydraulic head sensitivity in feet for the steady-state model to changes in vertical hydraulic conductivity of the Pearsall Formation.**
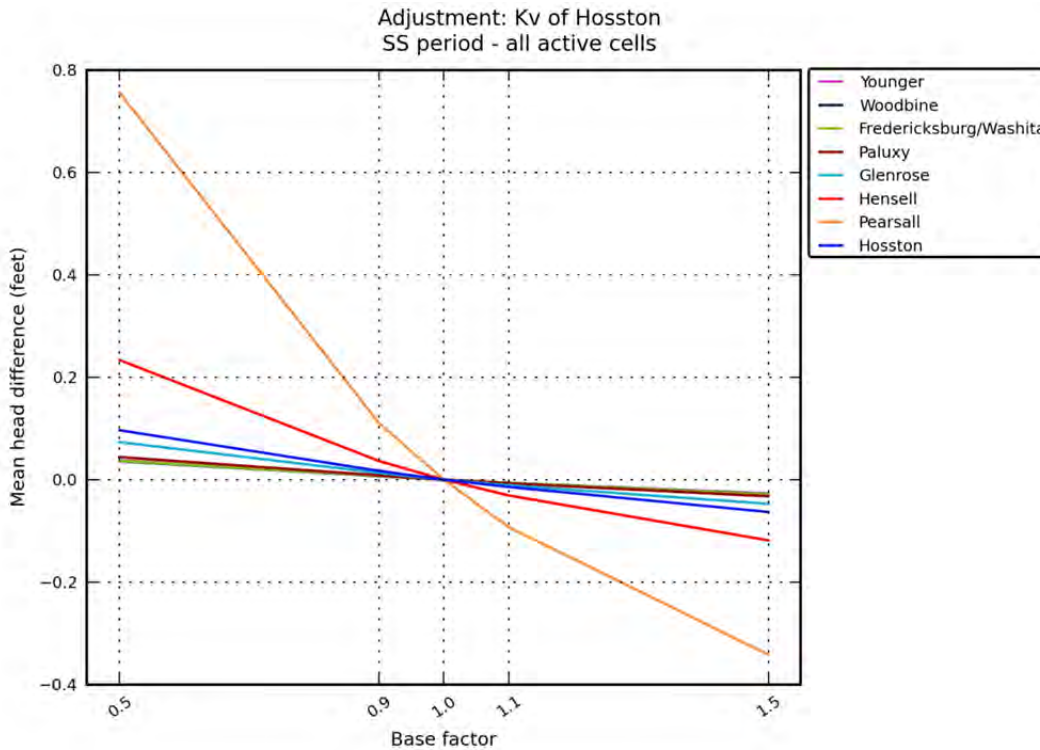
Figure 8.3.16 **Hydraulic head sensitivity in feet for the steady-state model to changes in vertical hydraulic conductivity of the Hosston Aquifer.**
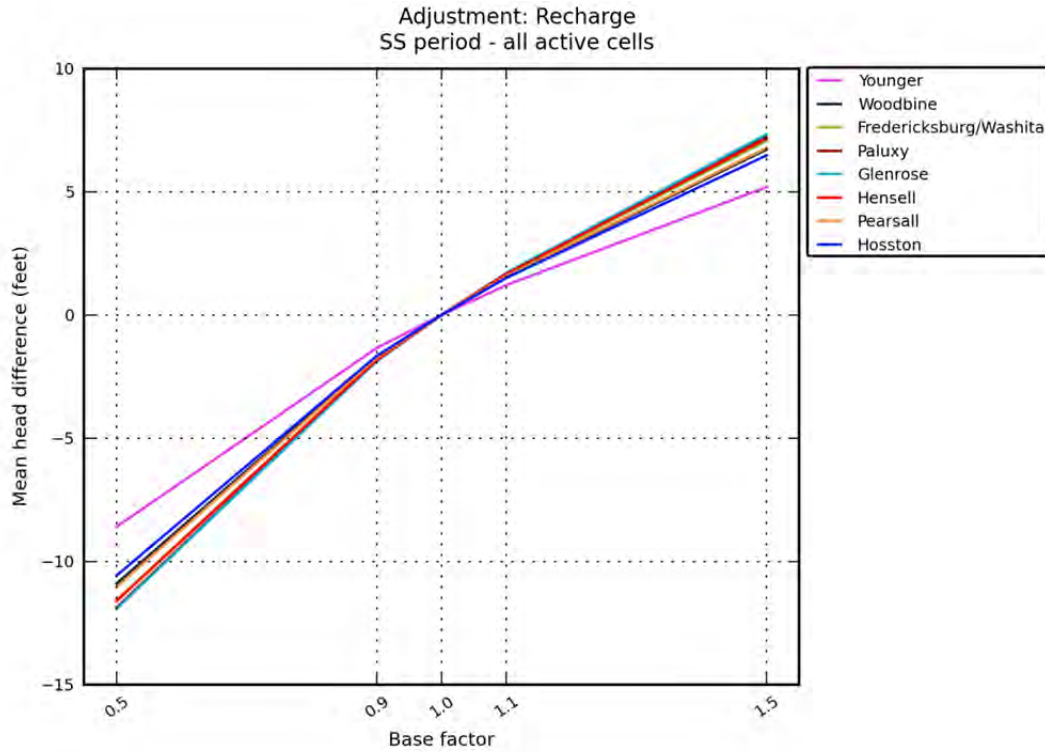
Figure 8.3.17   Hydraulic head sensitivity in feet for the steady-state model to changes in recharge in the surficial outcrop area of Layer 1.
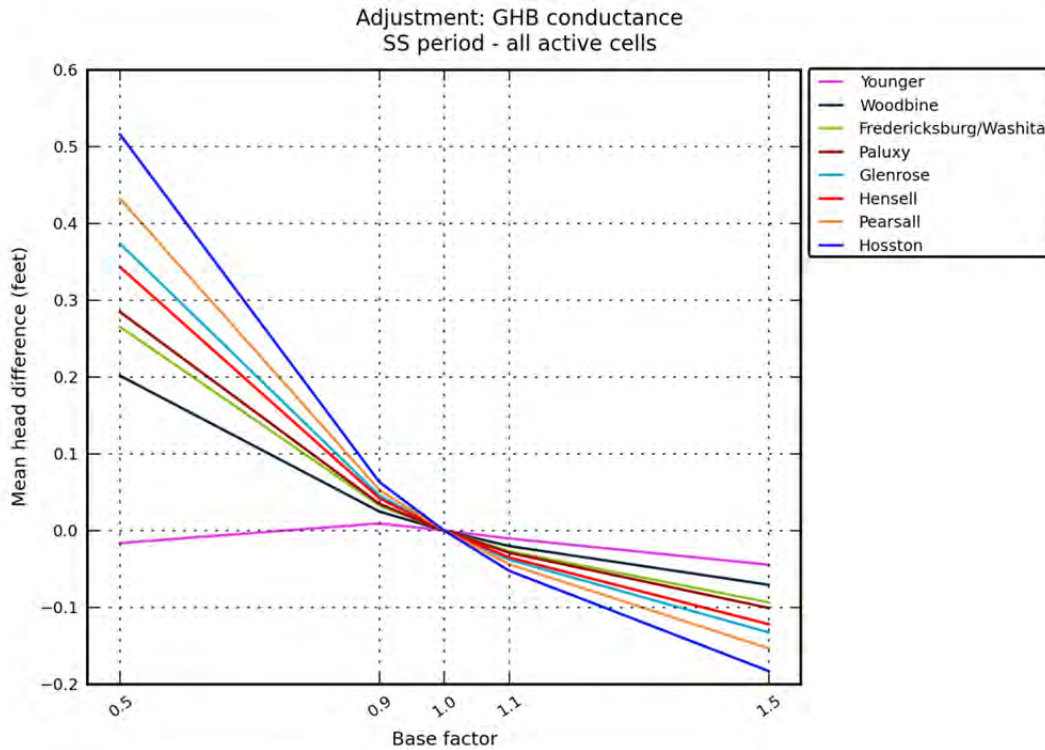
Figure 8.3.18   Hydraulic head sensitivity in feet for the steady-state model to changes in the head dependent boundary cells in the younger formations.
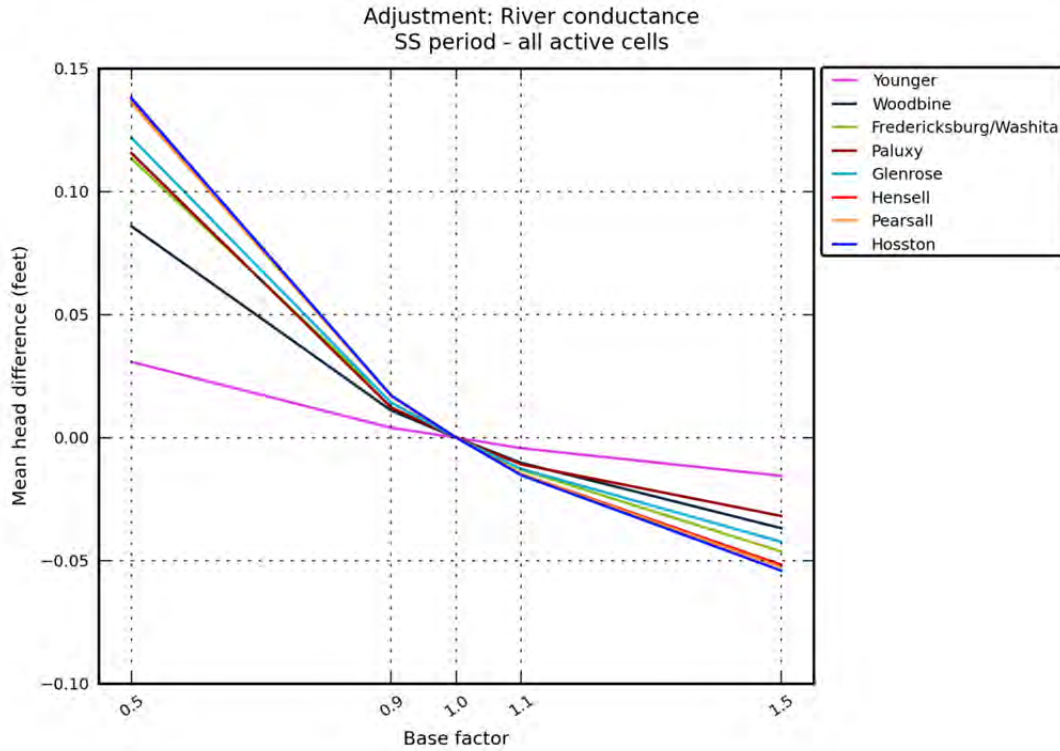
Figure 8.3.19 **Hydraulic head sensitivity in feet for the steady-state model to changes in river conductance in the surficial outcrop area of Layer 1.**
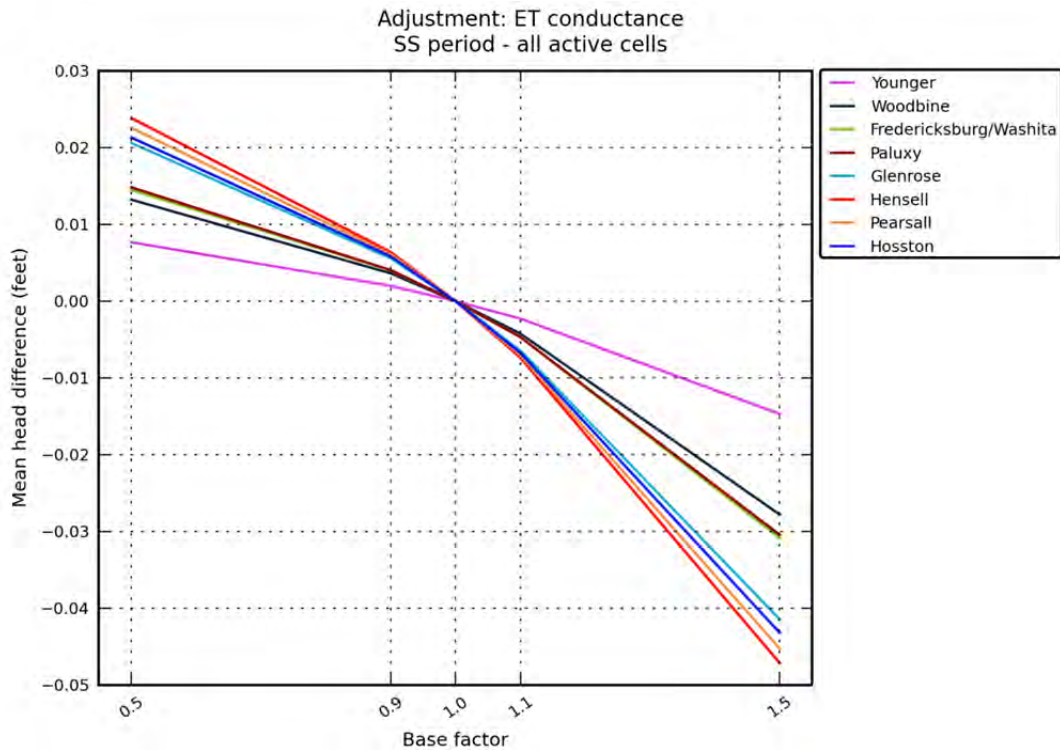
Figure 8.3.20 **Hydraulic head sensitivity in feet for the steady-state model to changes in drain boundary conductance, representing groundwater ET.**
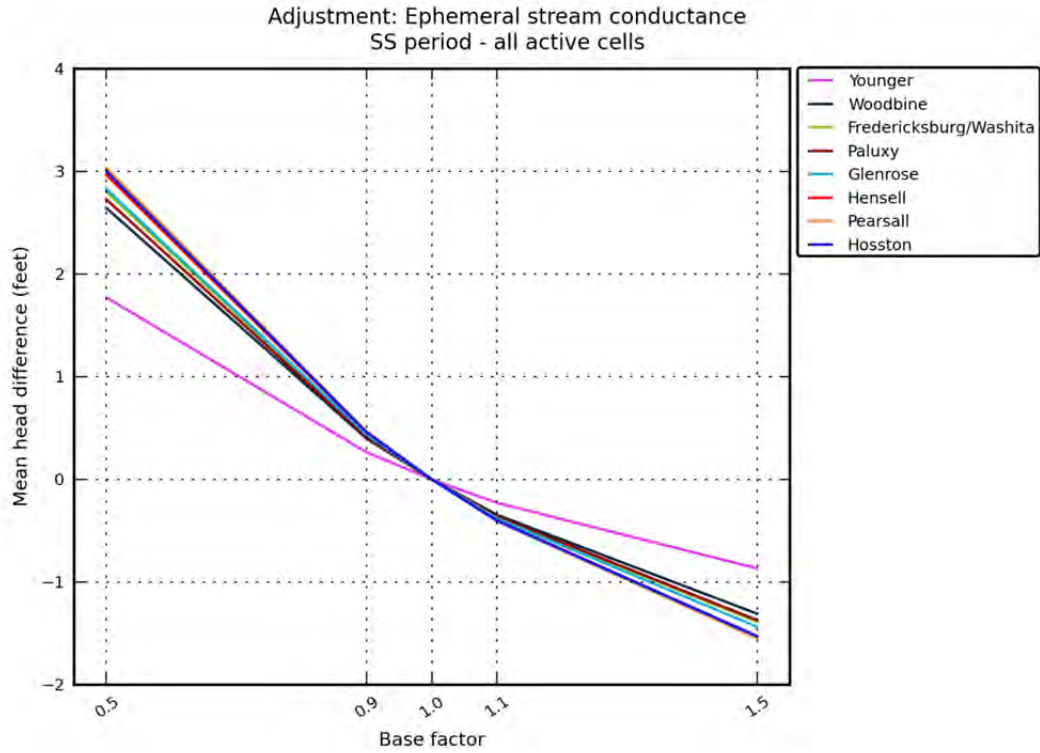
Figure 8.3.21   Hydraulic head sensitivity in feet for the steady-state model to changes in drain boundary conductance, representing ephemeral streams.
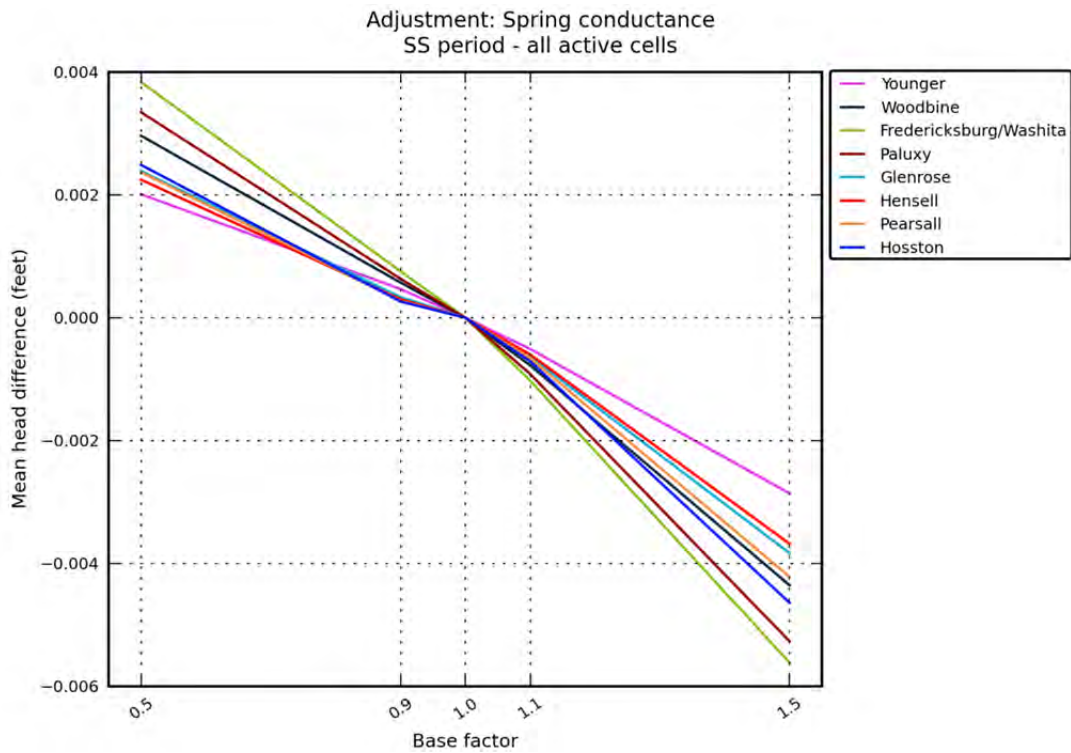
Figure 8.3.22   Hydraulic head sensitivity in feet for the steady-state model to changes in drain boundary conductance, representing springs.
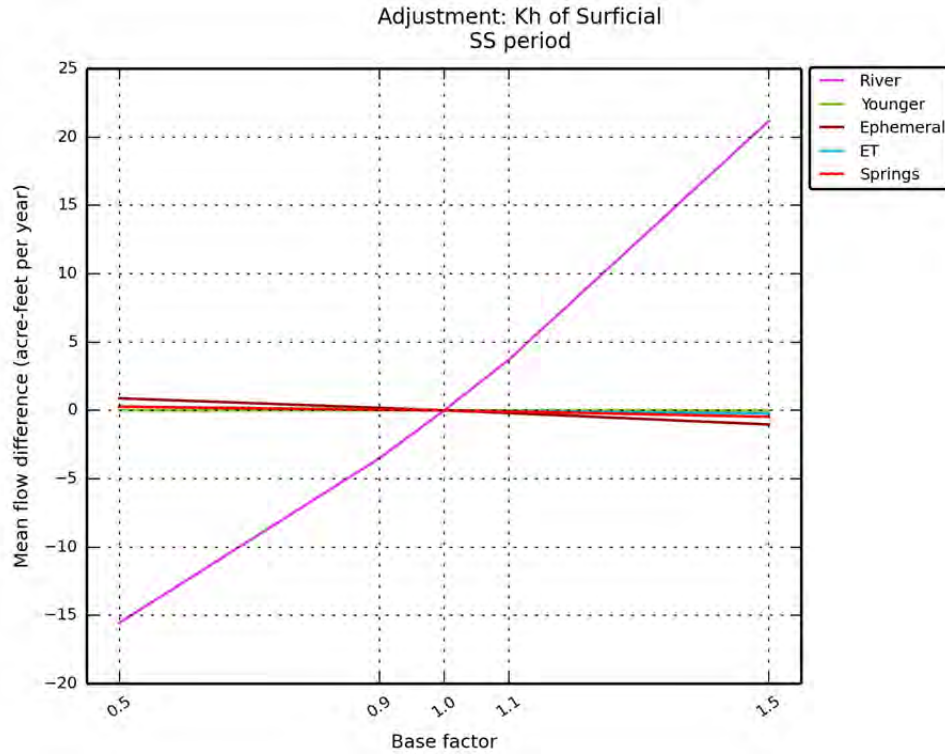
Figure 8.3.23 **Flow sensitivity in AFY for the steady-state model to changes in horizontal hydraulic conductivity of the surficial outcrop area of Layer 1.**
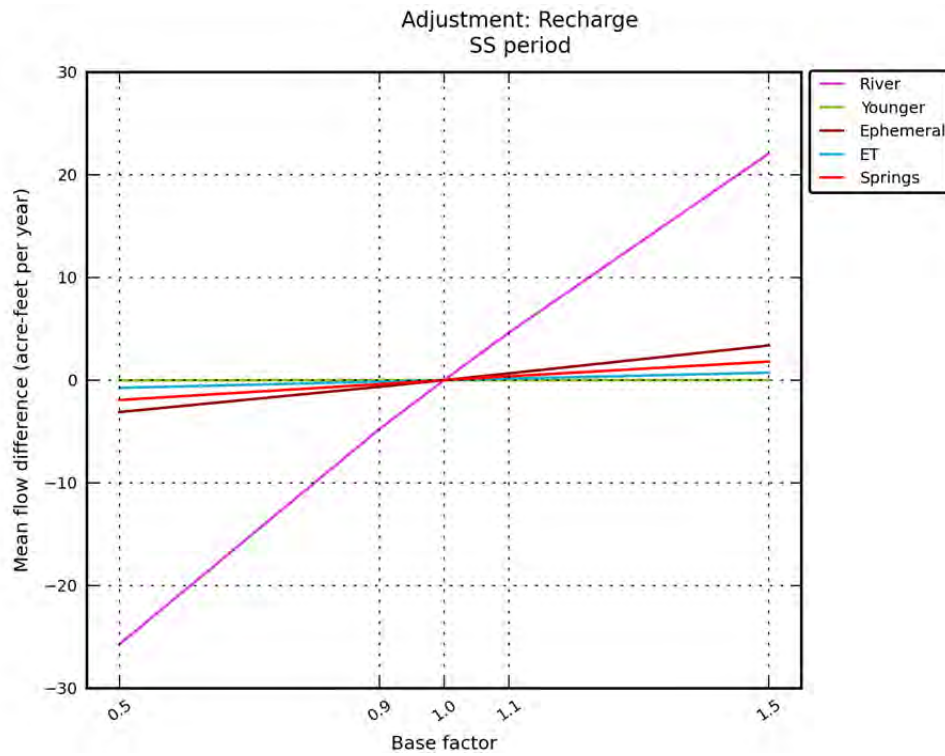
Figure 8.3.24 **Flow sensitivity in AFY for the steady-state model to changes in recharge in the surficial outcrop area of Layer 1.**
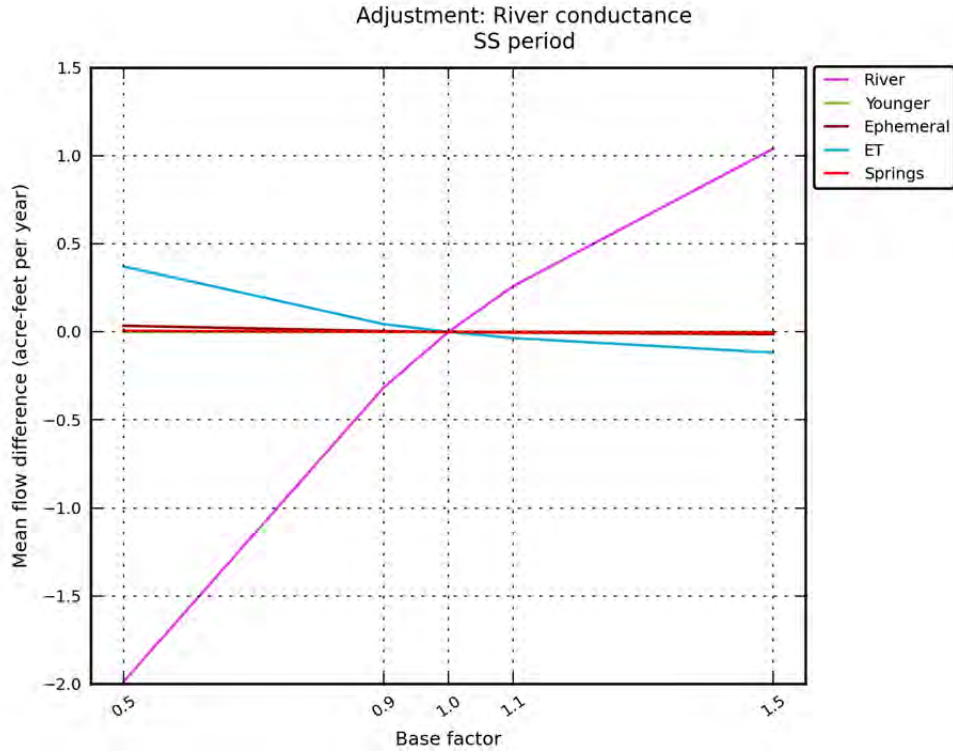
**Figure 8.3.25   Flow sensitivity in AFY for the steady-state model to changes in river conductance
in the surficial outcrop area of Layer 1.**
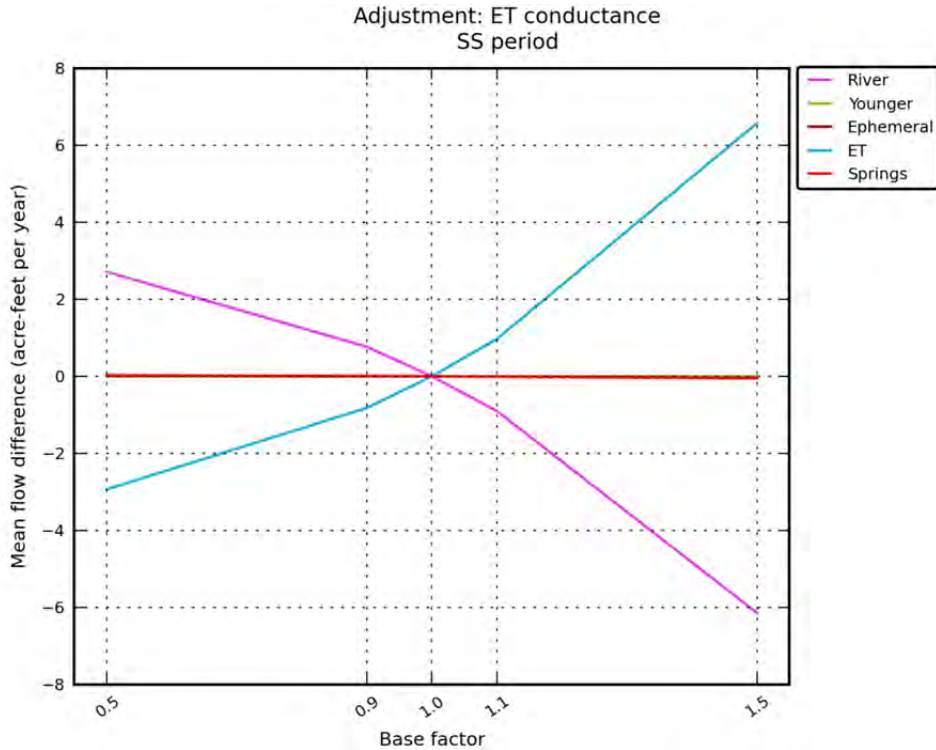
**Figure 8.3.26   Flow sensitivity in AFY for the steady-state model to changes in drain boundary
conductance, representing groundwater evapotranspiration.**
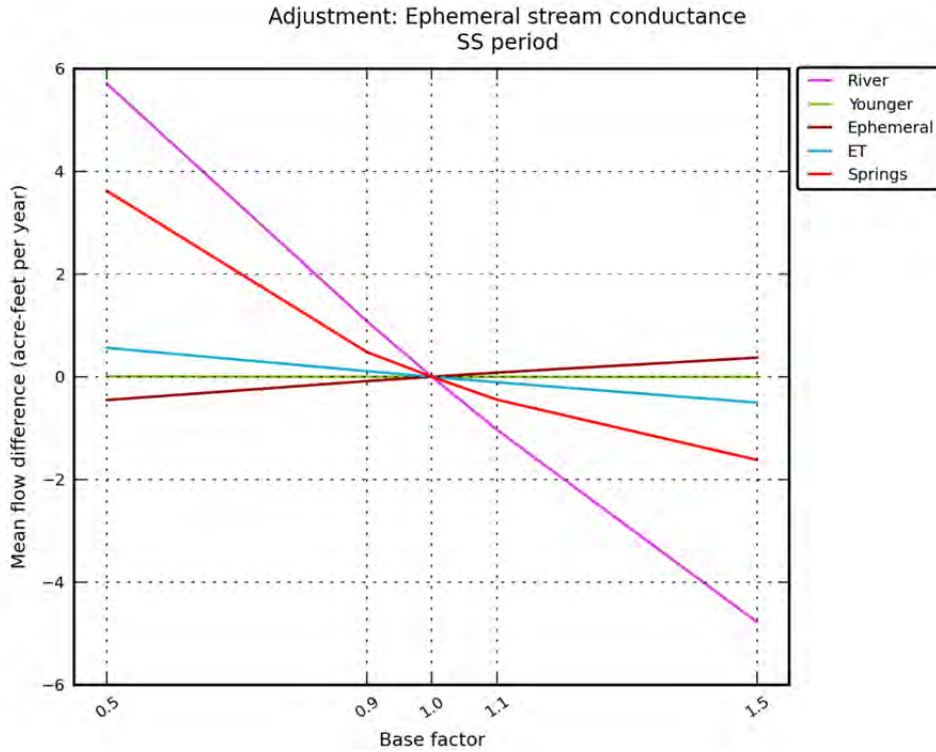
Figure 8.3.27   Flow sensitivity in AFY for the steady-state model to changes in drain boundary conductance, representing ephemeral streams.
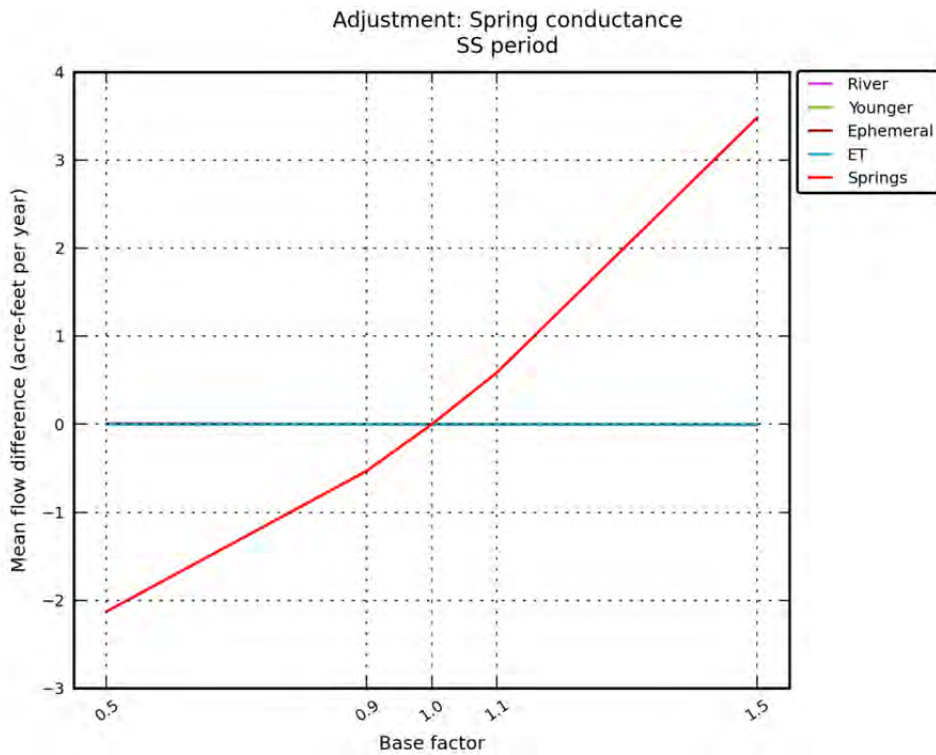
Figure 8.3.28   Flow sensitivity in AFY for the steady-state model to changes in drain boundary conductance, representing springs.

9.0   Transient Model

The transient model developed for the northern Trinity and Woodbine aquifers simulates a period from 1890 through 2012. This section details calibration of the transient model and presents the transient model results. The sensitivity of the transient model to various hydrologic parameters is also described.

9.1   Calibration

This section describes the transient calibration targets and the calibration parameters that were adjusted during transient model calibration. Model calibration was primarily carried out in an automated fashion using the parameter estimation program PEST (Doherty, 2005) on a 48-node computing cluster. The calibration parameters used in the PEST calibration involved layer-wise multipliers and depth decay coefficients for both horizontal and vertical hydraulic conductivity and an overall multiplier for storativity. Following calibration, these parameters were evaluated and altered so that the resulting hydraulic conductivity and storativity fields remained consistent with field measurements where available.

9.1.1   Calibration Targets

Wells with transient calibration targets were selected as described in Section 4.3. Many of the wells are completed across multiple model layers. For those wells without screen information, no water level target was used. As described in Section 7.1, the transient calibration period was from 1890 through 2012. Measurements in this period were examined closely to judge their historical record and their consistency with neighboring targets. A one-off cross validation analysis was performed, whereby a sample was removed, the other observations were kriged, and the difference between the missing sample and the predicted value at that location was recorded. This is a common statistical technique for identifying spatial outliers in a data set. A small percentage of the samples with hydraulic heads that differed significantly from hydraulic heads in nearby wells were then removed from the target data set to help purge the data set of outliers, and remove some of the statistical noise. This resulted in a total of 27,490 individual hydraulic head measurements from over 17,000 wells used as calibration targets for the transient model. Separating the hydraulic head targets by layer, the Woodbine Aquifer has 2,809 targets, the

Washita/Fredericksburg Group has 2,788 targets, the Paluxy Aquifer has 4,183 targets, the Glen Rose Formation has 4,372 targets, the Hensell Aquifer has 3,492 targets, the Pearsall Formation has 2,687 targets, and the Hosston Aquifer has 7,159 targets.

Wells for hydrograph comparisons were chosen from the entire historical period from 1890 to 2012. The many hydrographs that showed evidence of drawdown indicate that drawdown began occurring long before 1980, after which historical pumping estimates from the TWDB water use survey data are available. This motivated the inclusion of pre-1980 measurements in the transient calibration. Wells that had at least five water-level measurements were chose for hydrograph comparison, which resulted in 706 hydrographs.

Base flow estimates at 33 stream gages within the outcrop of the northern Trinity and Woodbine aquifers were available during the transient calibration period. The analysis that resulted in these base flow estimates are detailed in Section 4.5.4.1. Comparing simulated outflow to observed streamflows at the locations and over the time periods associated with the base flow estimates provided another constraint to the model parameters governing boundary conditions and hydraulic properties.

9.1.2 Storage Properties

Specific yield in the surficial outcrop area of Layer 1 was not changed from its initial value during transient calibration. In the confined layers, the shale multiplier and limestone multiplier, parameters ShM and LM in Equation 6.4.1 and Table 6.4.1, were changed during transient calibration to 1.5 and 0.01, respectively. Subsequently, the overall multiplier governing specific storage, parameter OM in Equation 6.4.1 and Table 6.4.1, was calibrated using PEST. This resulted in an increase from 1 to 3.7 during transient calibration. The corresponding calibrated storativity distributions for the confined layers (Layers 2 through 8) are shown in Figures 9.1.1 through 9.1.7.

9.1.3 Horizontal and Vertical Hydraulic Conductivities

The majority of the adjustments in horizontal and vertical hydraulic conductivities in the confined layers of the model occurred during transient calibration. Because of the lack of predevelopment hydraulic head calibration targets and the significant amount of drawdown observed during the transient period, the transient model provided a better opportunity for

calibrating hydraulic conductivities than the steady-state model, since the non-unique relationship between recharge and aquifer conductivities described in Section 8.1.3 is minimized under the stressed, transient conditions.

As mentioned in Section 6.3.5, pumping was applied to specific wells, weighted by observed drawdown for a given county, aquifer, and water use category combination. However, with the initial steady-state parameterization of horizontal and vertical hydraulic conductivity, simulated drawdowns in the transient model were not sufficient to match the observed drawdowns. To match these drawdowns, horizontal and vertical hydraulic conductivities were reduced from the steady-state calibration estimates, which were generally near the initial estimates. Both horizontal and vertical hydraulic conductivities had to be reduced in order to simulate drawdowns similar to the observed drawdowns. The final calibrated horizontal and vertical hydraulic conductivities are presented in Section 8.1.2.

The reductions in hydraulic conductivities improved the characteristics of the simulated drawdowns compared to observed drawdowns in most instances. Tables 9.1.1 and 9.1.2 summarize the initial and calibrated statistics, respectively, for the horizontal hydraulic conductivities used for each aquifer/formation.

Table 9.1.1   Initial horizontal hydraulic conductivity statistics by aquifer/formation.

Aquifer/Formation	Horizontal Hydraulic Conductivity (feet per day)							
	Mean	Standard Deviation	Median	Percentiles				
				5	25	50	75	95
Woodbine Aquifer	0.9	0.7	2.2	0.2	1.1	2.2	3.3	4.2
Washita/Fredericksburg Groups	1.4	0.3	2.1	0.6	1.1	2.1	3.1	4.0
Paluxy Aquifer	1.1	0.6	2.5	0.2	1.2	2.5	3.7	4.7
Glen Rose Formation	1.7	0.4	2.3	0.5	1.1	2.3	3.4	4.3
Hensell Aquifer	2.7	1.1	3.8	0.4	1.9	3.8	5.7	7.2
Pearsall Formation	2.7	1.2	5.4	0.5	2.7	5.4	8.1	10.2
Hosston Aquifer	4.9	1.1	6.8	0.7	3.5	6.8	10.2	13.0

Table 9.1.2   Calibrated horizontal hydraulic conductivity statistics by aquifer/formation.

Aquifer/Formation	Horizontal Hydraulic Conductivity (feet per day)							
	Mean	Standard Deviation	Median	Percentiles				
				5	25	50	75	95
Woodbine Aquifer	0.21	0.23	0.15	0.002	0.01	0.15	0.32	0.73
Washita/Fredericksburg Groups	0.40	0.24	0.32	0.13	0.18	0.32	0.61	0.81
Paluxy Aquifer	0.65	0.52	0.47	0.01	0.26	0.47	1.06	1.61
Glen Rose Formation	0.50	0.32	0.37	0.18	0.21	0.37	0.77	1.04
Hensell Aquifer	2.25	1.88	1.67	0.09	0.70	1.67	3.66	5.79
Pearsall Formation	0.98	0.86	0.84	0.03	0.29	0.84	1.27	2.81
Hosston Aquifer	3.23	2.07	2.27	1.17	1.46	2.27	5.13	7.02
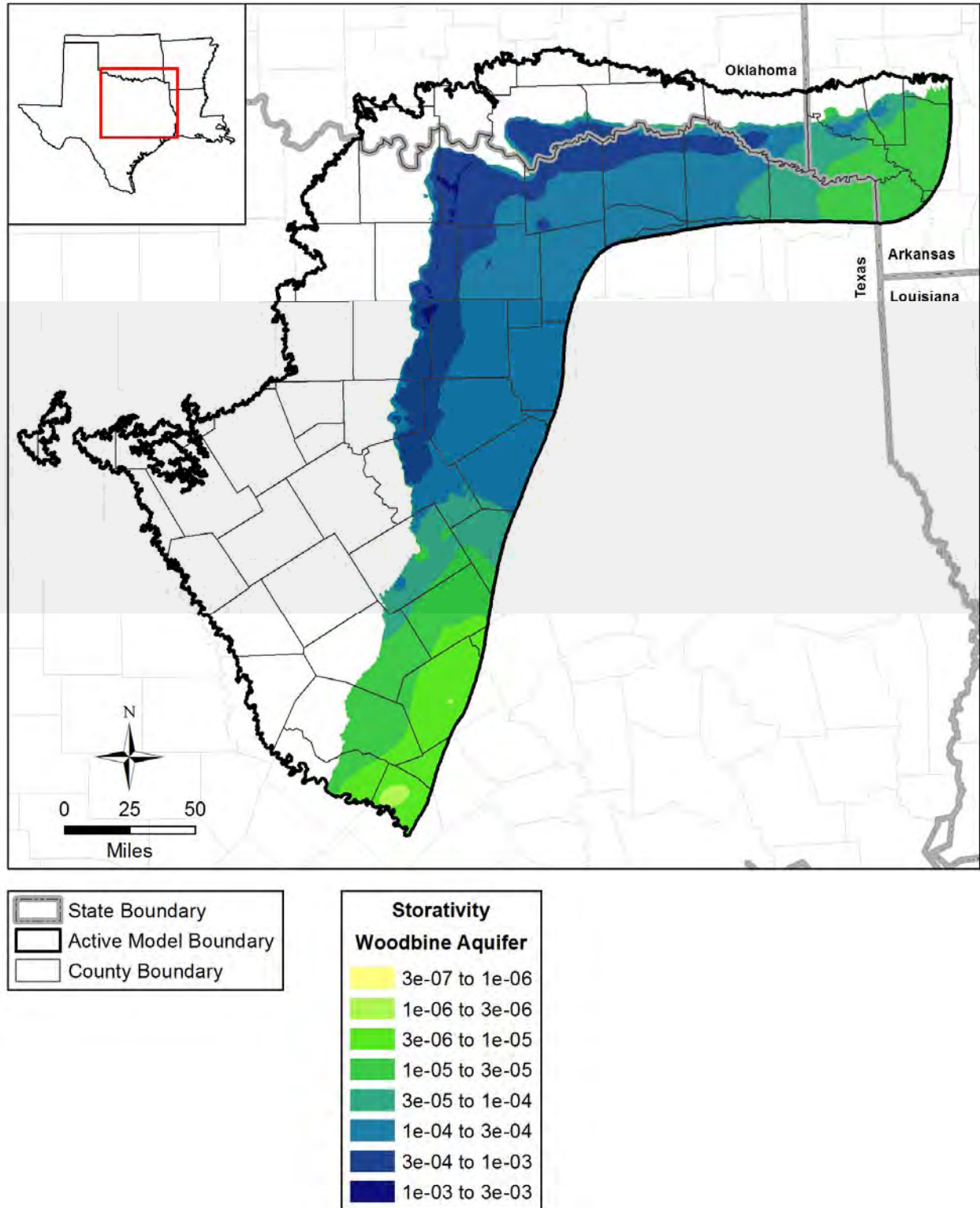
Figure 9.1.1   Calibrated storativity distribution for the Woodbine Aquifer (Layer 2).

State Boundary
Active Model Boundary
County Boundary

Storativity
Washita/Fredericksburg Groups

3e-07 to 1e-06
1e-06 to 3e-06
3e-06 to 1e-05
1e-05 to 3e-05
3e-05 to 1e-04
1e-04 to 3e-04
3e-04 to 1e-03
1e-03 to 3e-03
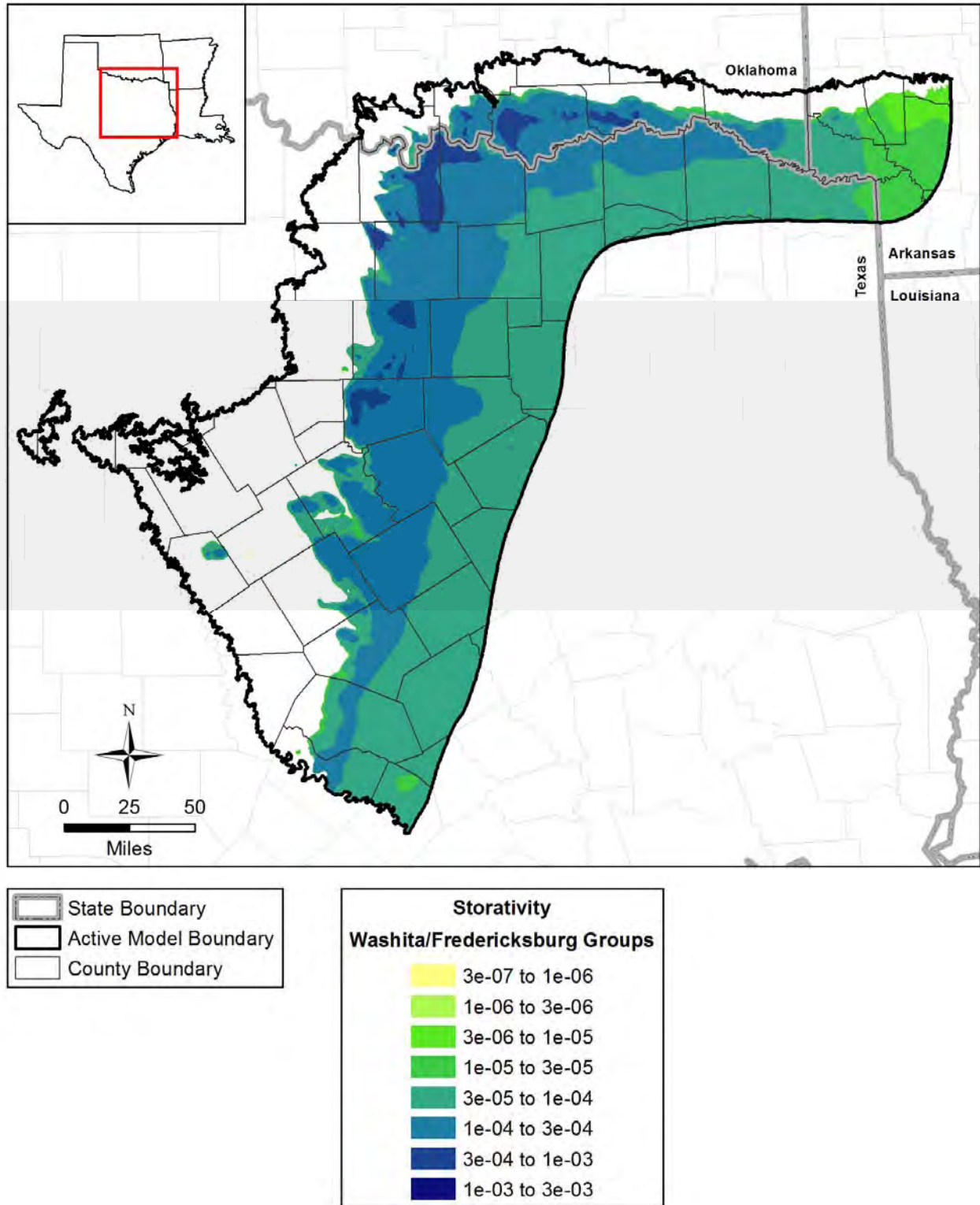
**Figure 9.1.2   Calibrated storativity distribution for the Washita/Fredericksburg groups
(Layer 3).**
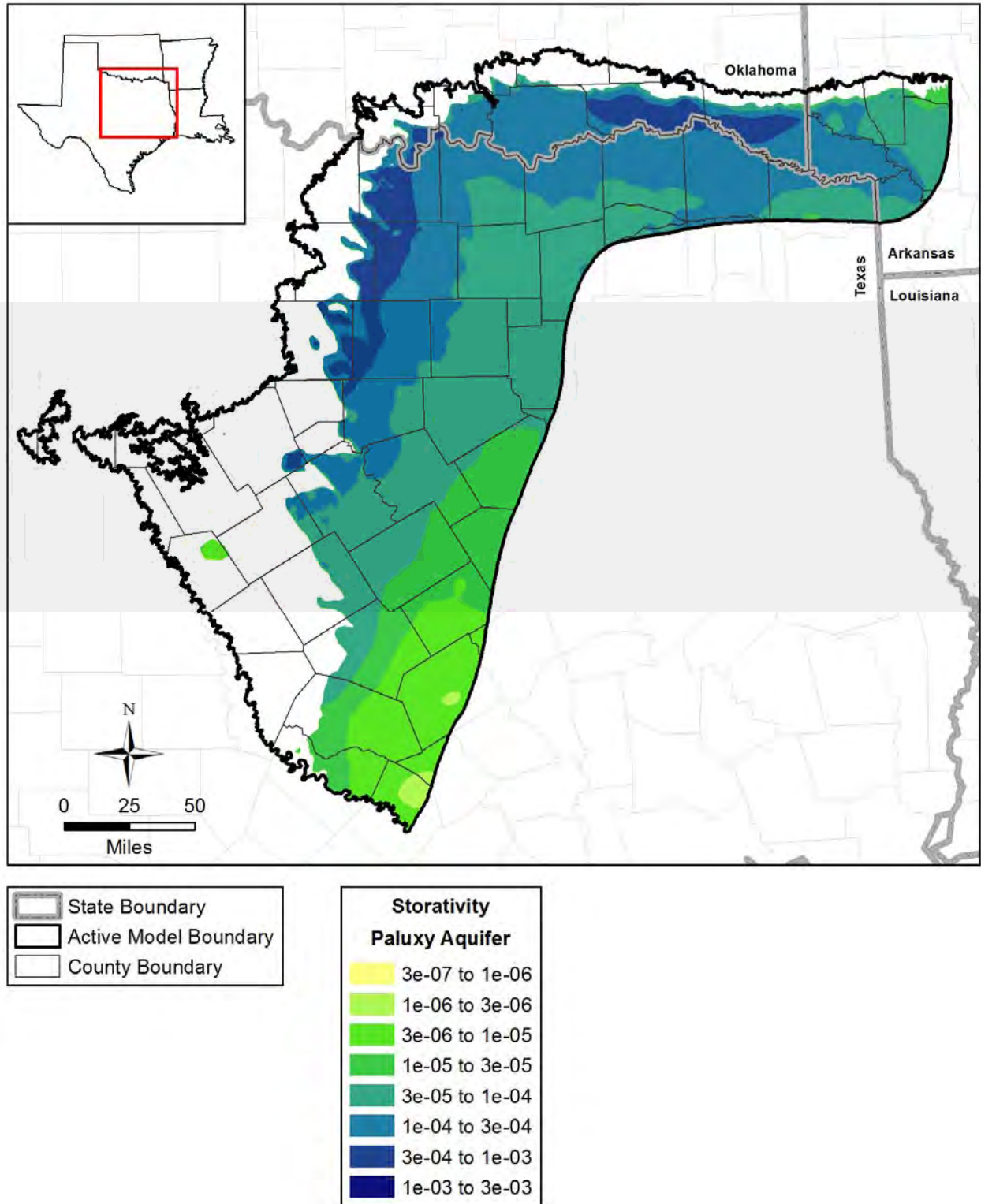
Figure 9.1.3   **Calibrated storativity distribution for the Paluxy Aquifer (Layer 4).**
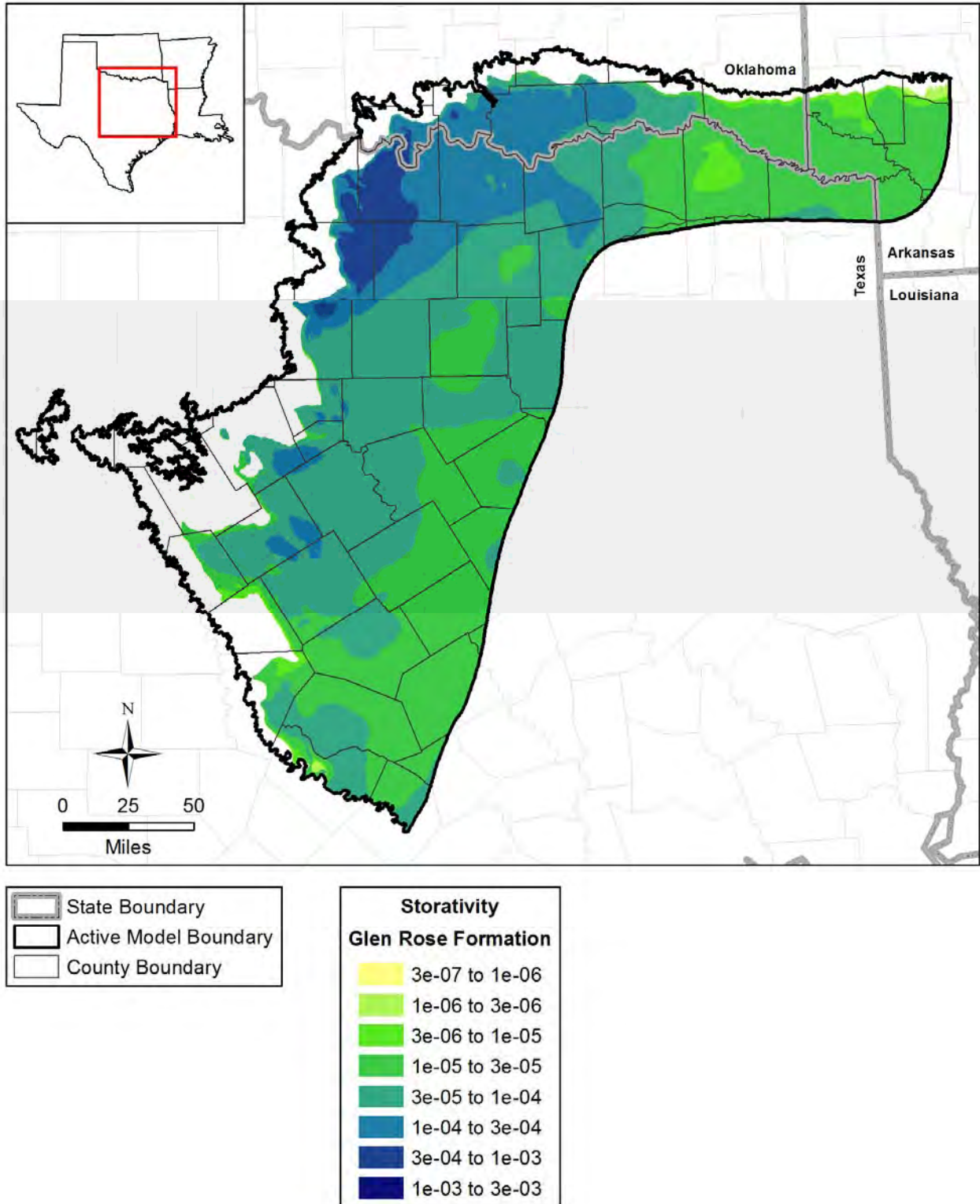
Figure 9.1.4   Calibrated storativity distribution for the Glen Rose Formation (Layer 5).
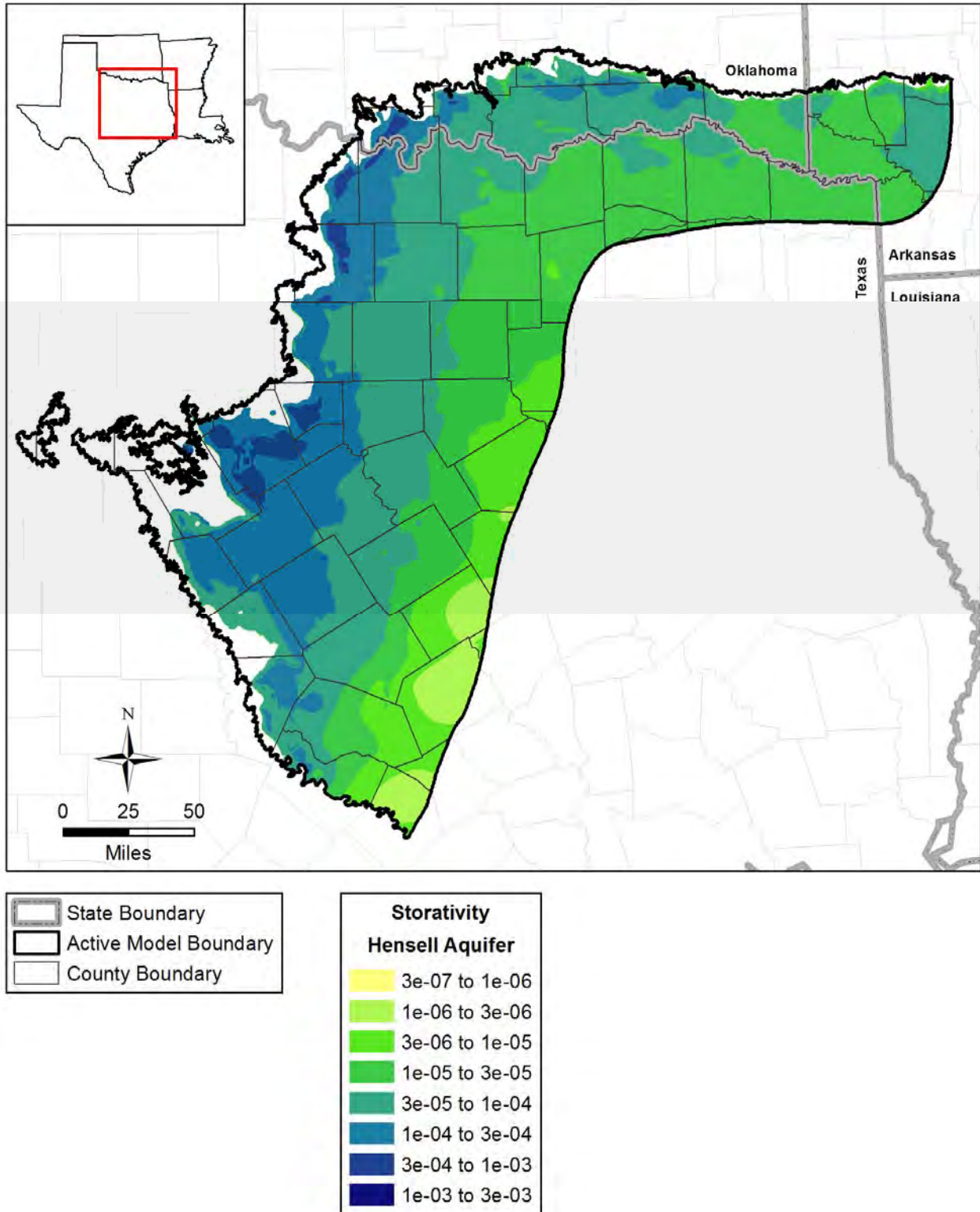
Figure 9.1.5   Calibrated storativity distribution for the Hensell Aquifer (Layer 6).
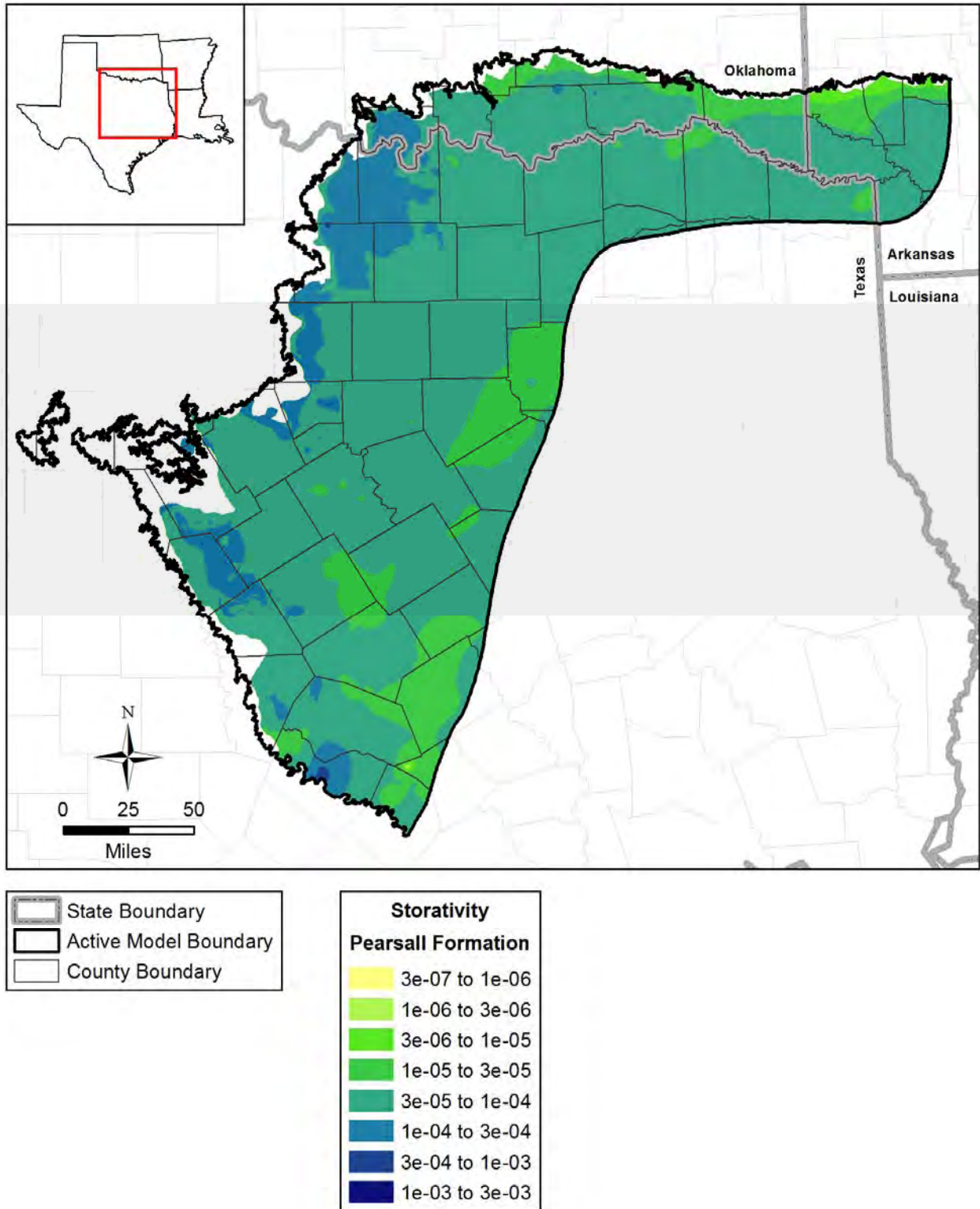
Figure 9.1.6   Calibrated storativity distribution for the Pearsall Formation (Layer 7).
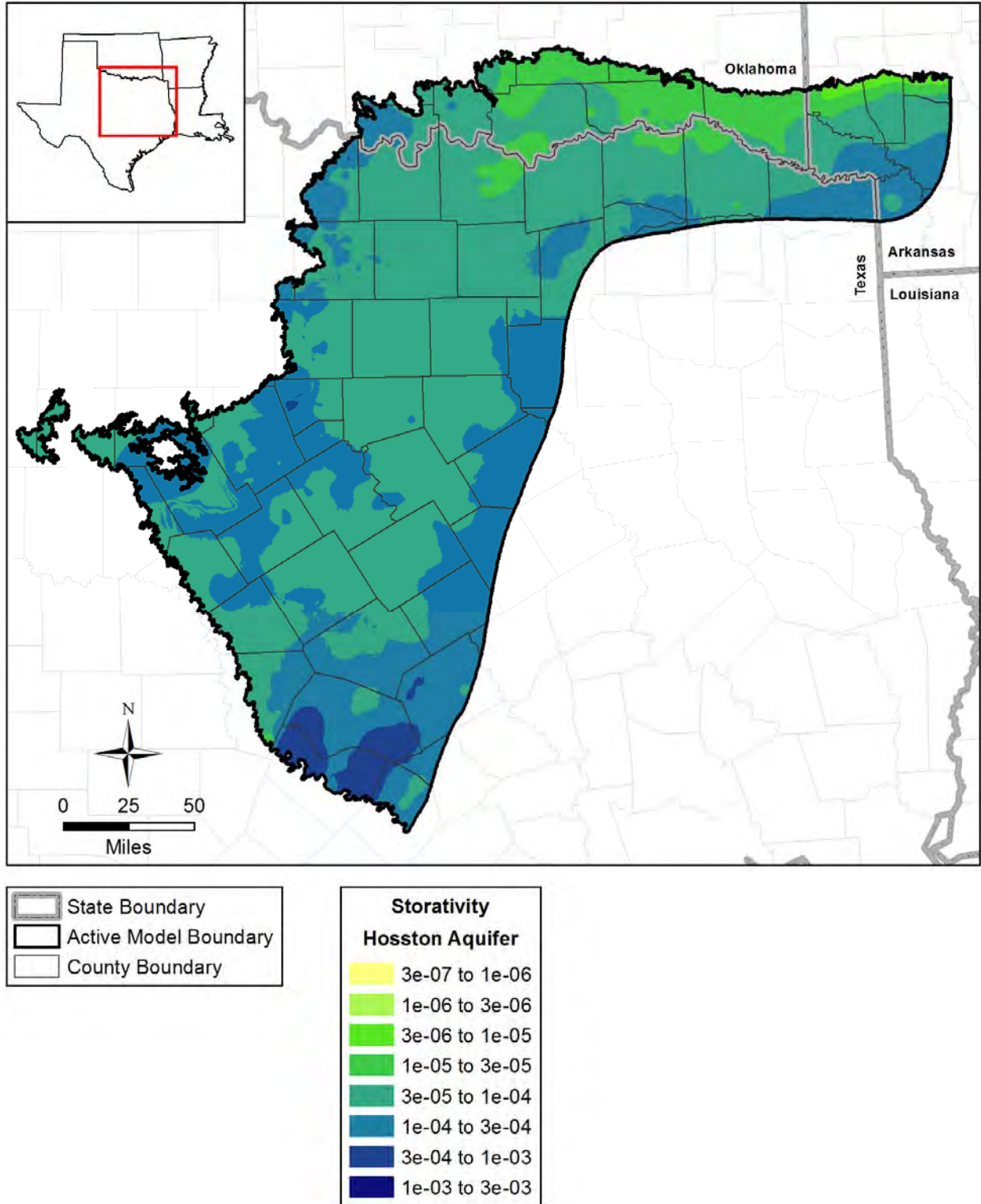
Figure 9.1.7   Calibrated storativity distribution for the Hosston Aquifer (Layer 8).

This page intentionally left blank.

9.2   Simulation Results

9.2.1 Hydraulic Heads

The transient model was calibrated to the hydraulic head targets described in Section 9.1.1. A crossplot of simulated versus observed hydraulic heads for the transient calibration period is shown in Figure 9.2.1. The crossplot shows normal scatter around the 1:1 line, with slightly more scatter for lower hydraulic heads. Figure 9.2.2 shows a plot of residuals versus observed hydraulic heads (the calculation of residuals is described in Section 8.2.1). The residuals show a relatively even distribution of positive and negative around the constant zero axis with more scatter evident for the lower observed hydraulic heads in the Hosston Aquifer. Some low bias can be seen in the residuals for the Paluxy Aquifer at the higher observed hydraulic heads.

Table 9.2.1 shows the calibration statistics for the model in the portion of the transient period from 1980 through 2012. This time period was the primary focus of the model calibration because it coincides with the pumping estimates from the TWDB water use survey data which, at the time of model development, were available for 1980 and 1984 through 2011 and considered to have the least degree of uncertainty. Because significant drawdown is observed in the northern Trinity and Woodbine aquifers prior to 1980, the entire transient record from 1890 through 2012 was considered in the transient calibration. The mean absolute error for the primary calibration period from 1980 to 2012 ranges from 38.3 to 56.2 feet for individual layers. This is higher than the range in the potential measurement errors described in Section 7.2, indicating a degree of mismatch between the simulated and observed hydraulic heads. The mean absolute error divided by the range in observed hydraulic heads ranges from 1.8 to 5.2 percent or less in all the aquifers/formations, however, indicating a reasonable fit given the large magnitudes of the observed drawdowns. The mean error for the entire model during the primary calibration period is 9.1 feet, a minimal bias given the overall range in measured hydraulic heads.

Table 9.2.2 shows the calibration statistics for the transient period from 1890 through 1949, the early period prior to the most significant development in the aquifer (and a period of few hydraulic head measurements).   Table 9.2.3 shows the calibration statistics for the transient period from 1950 through 1979, when the most significant aquifer development was occurring, and prior to estimates of pumping from the water use survey. Examining these statistics from

multiple time periods provides information about how the calibration changes through time. For the pre-1950 period, the mean absolute error ranges from 28.3 to 74.1 feet and the mean absolute error for the period between 1950 and 1980 ranges from 34.2 to 64.3. The mean absolute error divided by the range is less than 10 percent in all units with the exception of the Washita/Fredericksburg groups prior to 1950 when it is 14.5 percent. Generally speaking, the calibration statistics do not vary appreciably for the three time periods, although the overall mean absolute error does improve slightly from the very early time period prior to 1950 as more water level measurements become available.

Figures 9.2.3 through 9.2.9 show post plots of the average residuals for all of the targets in the transient calibration period by aquifer/formation. The yellow and green circle markers with a black outline indicate an absolute residual of less than 50 feet, which is in the typical range of the mean absolute error for the transient model. Each county where targets are available shows residuals in this lower range. In addition, most counties that contain multiple targets have residuals that are both positive (cool-colored markers in the blue family) and negative (warm-colored markers in the red family), indicating little spatial bias on a county basis.

There are several areas that indicate some spatial bias in the residuals, however. Figure 9.2.5 shows a cluster of negative residuals in the Paluxy Aquifer in Erath County indicating that simulated heads are biased low there. Figure 9.2.7 shows a cluster of positive residuals in the Hensell Aquifer in portions of Hamilton, Bosque, Erath, Somervell, and Hood counties indicating that some simulated hydraulic heads trend high in that region. Figures 9.2.8 and 9.2.9 also show a similar positive bias in the same region in the Pearsall Formation and Hosston Aquifer, respectively. A small cluster of negative residuals in the Hosston Aquifer in southern Dallas County is also apparent in Figure 9.2.9, indicating that the regional drawdown, which matches well in northern Ellis County, does not match quite as well in southern Dallas County.

Figures 9.2.10 through 9.2.25 show the simulated hydraulic heads and drawdown results for 1950 and 2012 in the surficial outcrop area of Layer 1 and in the confined portion of the seven aquifers/formations. The hydraulic heads in the surficial outcrop area of Layer 1 in 1950 and 2012 shown in Figure 9.2.10 include portions of the seven aquifers/formations that comprise the northern Trinity and Woodbine aquifers and the Washita/Fredericksburg groups. As with the

steady-state model, the hydraulic heads in the surficial outcrop area of Layer 1 reflect the topography, with lower hydraulic heads in the river basins and higher hydraulic heads in the interbasin areas. The change in hydraulic heads between 1950 and 2012 is unremarkable, reflecting the generally unchanging hydraulic heads in the shallow, unconfined portion of the aquifers/formations. The simulated drawdown from predevelopment in the surficial outcrop area of Layer 1 is shown for 1950 and 2012 in Figure 9.2.11. Minimal drawdown in the shallow surficial layer is evident for both years. Recall from Section 6.2 that the surficial layer represents approximately the first 50 feet of saturated sediments in the unconfined portions of the aquifers. When drawdown occurs in the outcrop, it typically occurs in deeper portions of the outcrop that are semi-confined, and are represented by the most updip portions of Layers 2 through 8.

Figure 9.2.12 shows the hydraulic heads in the Woodbine Aquifer in 1950 and 2012. Hydraulic heads in this aquifer in 1950 range from less than 100 to over 700 feet amsl, with the lowest hydraulic heads centered in southern Dallas County. In 2012, simulated hydraulic heads range from less than -100 to over 700 feet amsl, with the area of lowest hydraulic heads extending from northeastern Collin County to southwestern Fannin County. The simulated drawdown in the Woodbine Aquifer is shown for 1950 and 2012 in Figure 9.2.13. The areas of maximum drawdown exceed 400 feet in 1950 and 700 feet in 2012 and coincide with the locations of the lowest hydraulic heads apparent in Figure 9.2.12.

Figure 9.2.14 shows the hydraulic heads in the Washita/Fredericksburg groups in 1950 and 2012. Hydraulic heads in this layer in 1950 range from less than 400 feet amsl to more than 900 feet amsl, with the gradient generally sloping from west to east and from the outcrop to the subcrop. In 2012, simulated hydraulic heads range from less than 100 feet amsl to more than 900 feet amsl, with a noticeably steeper west-to-east gradient than in 1950. The simulated drawdown in the Washita/Fredericksburg groups is shown for 1950 and 2012 in Figure 9.2.15. In 1950, a maximum drawdown of little more than 100 feet is simulated along the subcrop extent of the layer in Kaufman, Henderson, and Navarro counties. The maximum drawdown increases by 2012 to more than 400 feet in Kaufman, Henderson, Navarro, and Limestone counties. Localized drawdown exceeding 600 feet is also apparent in the Edwards BFZ Aquifer portion of this layer in Williamson and Travis counties.

Figure 9.2.16 shows the hydraulic heads in the Paluxy Aquifer in 1950 and 2012. Hydraulic heads in this aquifer in 1950 range from about 300 to over 900 feet amsl, with the gradient generally sloping from west to east and from the outcrop to the subcrop. In 2012, simulated hydraulic heads range from less than -500 to over 900 feet amsl, with the lowest hydraulic heads in northern Collin County. The simulated drawdown in the Paluxy Aquifer is shown for 1950 and 2012 in Figure 9.2.17. The areas of maximum drawdown exceed 500 feet in 1950 and 800 feet in 2012 and coincide with the locations of the lowest hydraulic heads apparent in Figure 9.2.16.

Figure 9.2.18 shows the hydraulic heads in the Glen Rose Formation in 1950 and 2012. Hydraulic heads in this formation in 1950 range from less than 400 feet amsl to more than 1,400 feet amsl, with the gradient generally sloping from west to east and from the outcrop to the subcrop. In 2012, simulated hydraulic heads range from less than 100 feet amsl to more than 1,400 feet amsl, with a noticeably steeper west-to-east gradient than in 1950. The simulated drawdown in the Glen Rose Formation is shown for 1950 and 2012 in Figure 9.2.19. The areas of maximum drawdown exceed 300 feet in 1950 and 400 feet in 2012 in Dallas County.

Figure 9.2.20 shows the hydraulic heads in the Hensell Aquifer in 1950 and 2012. Hydraulic heads in this aquifer in 1950 range from less than 400 feet amsl to about 1,400 feet amsl, with the gradient generally sloping from west to east and from the outcrop to the subcrop. In 2012, simulated hydraulic heads range from less than 100 feet amsl to about 1,400 feet amsl, with the lowest hydraulic heads in northeastern Dallas County and eastern McLennan County. The simulated drawdown in the Hensell Aquifer is shown for 1950 and 2012 in Figure 9.2.21. The areas of maximum drawdown exceed 200 feet in 1950 and 800 feet in 2012, and coincide with the locations of the lowest hydraulic heads apparent in Figure 9.2.20.

Figure 9.2.22 shows the hydraulic heads in the Pearsall Formation in 1950 and 2012. Hydraulic heads in this formation in 1950 range from less than 400 feet amsl to about 1,400 feet amsl, with the gradient generally sloping from west to east and from the outcrop to the subcrop. In 2012, simulated hydraulic heads range from less than about 0 feet amsl to about 1,400 feet amsl, with the lowest hydraulic heads in eastern Johnson County. The simulated drawdown in the Pearsall Formation is shown for 1950 and 2012 in Figure 9.2.23. An area of regional, maximum

drawdown exceeds 200 feet in 1950 spreading across Denton, Tarrant, Dallas, Johnson, Ellis, and Hill counties. By 2012, a small area of maximum drawdown exceeds 800 feet in Johnson County. The 100 foot drawdown contour extends well updip into the area of the Trinity Aquifer outcrop, including Montague, Wise, Parker, Hood, and Somerville counties.

Figure 9.2.24 shows the hydraulic heads in the Hosston Aquifer in 1950 and 2012. Hydraulic heads in this aquifer in 1950 range from less than 0 feet amsl to more than 1,800 feet amsl, with the lowest hydraulic heads along the boundary between Tarrant and Dallas counties. In 2012, simulated hydraulic heads range from approximately -900 feet amsl to more than 1,800 feet amsl, with the lowest hydraulic heads in western Ellis County. The simulated drawdown in the Hosston Aquifer is shown for 1950 and 2012 in Figure 9.2.25. The areas of maximum drawdown exceed 800 feet in 1950 and 1,200 feet in 2012, and coincide with the locations of the lowest hydraulic heads apparent in Figure 9.2.24. As with the Pearsall, drawdowns of 100 to 200 feet extend updip into the outcrop portions of the Trinity Aquifer, affecting Montague, Wise, Parker, Hood, and Somerville counties.

Figures 9.2.26 through 9.2.35 show simulated and observed hydraulic heads for many of the same representative hydrographs displayed in Section 4.3.3. In this way, hydrographs shown here were not selected based on the fit between simulated and observed hydraulic heads. Instead, they were selected based on spatial coverage within each aquifer/formation and to be representative of the trends in hydraulic heads observed in a given region. The historical period from 1900 through 2012 is shown on the hydrographs. The y-axis for the hydrographs is divided into 25-, 50-, or 100-foot intervals depending on the magnitude of the measured or simulated data. Hydrographs are shown for wells specific to each aquifer/formation or completed in multiple aquifers/formations in the northern Trinity Aquifer (e.g., wells completed in both the Paluxy Aquifer and Glen Rose Formation). Appendix I contains plots for all 706 hydrograph comparisons (see Section 9.1.1) used to inform calibration of the transient model

Figure 9.2.26 shows hydrographs for wells completed in the Woodbine Aquifer. These hydrographs indicate significant simulated drawdowns ranging from approximately 75 feet to over 500 feet, with the larger drawdowns occurring in the confined section of the aquifer.

Simulated hydraulic heads are in good agreement with observed hydraulic heads but tend to underpredict the observed drawdown by a discrepancy on the order of 25 feet.

Hydrographs for wells completed in the Paluxy Aquifer are shown in Figure 9.2.27. Significant simulated drawdown ranging from 150 to 600 feet is apparent in all but one well. Simulated hydraulic heads are consistent with observed hydraulic heads for most wells.

Figure 9.2.28 shows hydrographs for wells completed in the Hensell Aquifer. Wells in the outcrop area of the Hensell Aquifer exhibit relatively small amounts of observed and simulated drawdown. Simulated hydraulic heads in the outcrop area can either underpredict or overpredict observed hydraulic heads depending on the well. In the confined portion of the Hensell Aquifer, drawdown exceeding 200 feet is observed and simulated hydraulic heads are in good agreement with observed hydraulic heads, but tend to underpredict the observed drawdown somewhat.

Hydrographs for wells completed in the Hosston Aquifer are shown in Figure 9.2.29. Significant drawdown exceeding 950 feet is simulated in the confined portion of the Hosston Aquifer. This is consistent with the hundreds of feet of drawdown observed in these wells. Less drawdown is observed for wells in the outcrop area with almost no observed or simulated drawdown for the two wells at the updip limit of the Hosston Aquifer.

Figure 9.2.30 shows hydrographs for wells completed in both the Paluxy Aquifer and Glen Rose Formation. These hydrographs document several hundred feet of observed drawdown in several wells in the confined portion of these units, which are matched by simulated drawdowns. The simulated hydraulic heads in one well in Grayson County underpredict a sharp observed decline in hydraulic heads and there is no mechanism in the model to replicate the rapid 300 feet of recovery observed in a well in Coryell County. There is very little simulated or observed drawdown in the one well in the outcrop area.

Hydrographs for wells completed in both the Hensell Aquifer and Glen Rose Formation or both the Hensell Aquifer and Pearsall Formation are shown in Figure 9.2.31. Very little drawdown is observed or simulated in wells located in the outcrop area. Significant simulated drawdown up to 600 feet is apparent in most wells in the confined portion of these units. Simulated hydraulic

heads are consistent with observed hydraulic heads for most wells, but one well in Burnet
County has observed hydraulic heads varying 100 feet and very little simulated drawdown.

Figure 9.2.32 shows hydrographs for wells completed in both the Hosston Aquifer and Pearsall
Formation. These hydrographs indicate significant simulated drawdown in the confined portion
of these units, exceeding 500 feet in most wells and over 1,000 feet in some wells. Simulated
and observed hydraulic heads remain relatively stable in the outcrop area. Simulated hydraulic
heads are in very good agreement with observed hydraulic heads in most wells.

Hydrographs for wells completed in the Glen Rose Formation are shown in Figure 9.2.33.
Significant observed and simulated drawdown is apparent in the confined portion of the
formation, with little drawdown in the outcrop area. Simulated hydraulic heads are consistent
with observed hydraulic heads for most wells, but underestimate the drawdown significantly for
one well in Hamilton County.

Figure 9.2.34 shows hydrographs for wells completed in the Pearsall Formation. These
hydrographs indicate stable water levels in the outcrop area and significant drawdowns of several
hundred feet occurring in the confined portions of the formation. Simulated hydraulic heads are
in good agreement with observed hydraulic heads at most wells.

Hydrographs for wells completed in the Edwards BFZ Aquifer are shown in Figure 9.2.35.
Although these wells are in the confined portion of the aquifer, comparatively less drawdown is
observed than in the northern Trinity and Woodbine aquifers. Simulated hydraulic heads are
consistent with observed hydraulic heads in some wells and appear to overpredict drawdown in
one well at late time, although measurements have ceased.

Because only the surficial outcrop area in Layer 1 was simulated to be convertible between
confined and unconfined conditions as discussed in Section 6.2, only Layer 1 transmissivities
had the capacity to vary as a function of saturated thickness. A comparison of the simulated
hydraulic heads at the end of the transient period in 2012 with the basal elevation of all the active
cells in the model Layers 1 through 8 shows that less than 0.05 percent of the cells had hydraulic
heads below the base of the aquifer/formation. This equates to 1,891 "dry" cells out of the

3,946,146 active cells that were not "conduit" cells. These "dry" cells are deemed insignificant in the context of the simulated model results.

9.2.2 Stream Discharge

The simulated outflow of groundwater to stream boundary conditions in watersheds associated with the stream gages were compared to the estimated base flows in each of these watersheds in Figure 9.2.36. Simulated base flows overpredict and underpredict estimated base flows in relatively even numbers and are consistent with the estimates overall. This is somewhat to be expected since recharge was based on these base flow estimates, but it also indicates that the bed conductances assumed for the perennial and ephemeral streams did not need to be adjusted during model calibration.

9.2.3 Water Budget

The transient model had an overall volumetric budget error of 0.0000002 percent, which is well under the groundwater availability model requirement of 1 percent. Table 9.2.4 shows the water budget for the transient model in terms of net flux into or out of each of the aquifers/formations in the model for the years 1980, 1990, 2000, and 2010. The conventions are similar to those used in the steady-state water budget. Negative numbers indicate flow out of the aquifers/formations, while positive numbers indicate flow into the aquifers/formations. The first three columns detail cross-formational flow in each of the units. The *surficial flow* term represents flow across units within the surficial outcrop area of Layer 1, while the *confined* cross-formational flow is marked by the "Top" and "Bottom" fields and represents flow across aquifers/formations deeper than Layer 1. "Top" indicates flow in or out of the top of aquifers/formations in the confined portion, while "Bottom" indicates flow in or out of the bottom of aquifers/formations that lie below the surficial layer. The water budgets in 2012 by county and by GCD are summarized in Tables 9.2.4 and 9.2.5, respectively. Note that the "Lateral" field indicates water that is moving laterally into or out of the county or GCD.

Overall, the water budget is dominated by recharge and stream discharge, which, depending on the year, makes up as much as 100 percent of the inflow and as much as 82 percent of the outflow, respectively. Flow into and out of storage can vary significantly depending on variations in recharge, ranging anywhere from 40 percent of inflow to the model to 28 percent of

model outflow. Pumping makes up between 11 and 13 percent of the discharge, ET makes up
between 2 and 3 percent of discharge, and reservoirs, springs and flowing wells also make up a
small fraction of the discharge. It should be noted that MODFLOW-NWT allows for the
automatic reduction of pumping in convertible cells when the simulated hydraulic head
approaches the cell bottom, which was used to stably handle uncertainties in pumping within the
surficial layer. Only the surficial layer (Layer 1) was convertible and use of this option resulted
in an average reduction in pumping of 1.0 percent with a maximum reduction of less than
1.9 percent occurring in 1909. This reduction in pumping is considered to be well within the
range of uncertainty in pumping estimates and insignificant with respect to the overall water
balance.

Figure 9.2.37 shows the running total model water budget for the historical period in terms of net
flow to or from the model. It depicts what was previously stated, that recharge dominates the
inflow and the combination of perennial and ephemeral streams dominate the outflow in the
water budget. It is also clear that variations in recharge are reflected in net changes to storage.
A gradual increase in pumping throughout the historical period is evident along with the
relatively small portion of the water budget that is associated with pumping. The reservoirs and
overlying younger formations constitute a very small portion of the water budget. Additional
analysis of the water budget, with perspective on historical and future production in the aquifer,
is provided in Section 12.

Table 9.2.1   **Calibration statistics for the primary transient model calibration period (1980 through 2012).**

Unit	Count	Mean Error (feet)	Mean Absolute Error (feet)	Range (feet)	MAE/Range
All	21234	9.1	48.7	2891	0.017
Woodbine Aquifer	2093	19.0	50.8	975.5	0.052
Wash/Fred Groups	2044	-11.8	42.4	1658	0.026
Paluxy Aquifer	3655	-11.0	46.9	1778	0.026
Glen Rose Formation	3735	-11.1	38.3	2166	0.018
Hensell Aquifer	2410	17.0	54.9	2369	0.023
Pearsall Formation	1962	27.6	48.8	2262	0.022
Hosston Aquifer	5335	30.8	56.2	2690	0.021

MAE = mean absolute error   Wash/Fred = Washita/Fredericksburg

Table 9.2.2   **Calibration statistics for the early period of the transient model (1890 through 1949).**

Unit	Count	Mean Error (feet)	Mean Absolute Error (feet)	Range (feet)	MAE/Range
All	480	4.8	57.6	1656	0.035
Woodbine Aquifer	86	-5.6	54.1	639.2	0.085
Wash/Fred Groups	98	-34.9	72.6	500.1	0.145
Paluxy Aquifer	50	50.1	74.1	873.8	0.085
Glen Rose Formation	62	-3.9	44.3	1531	0.029
Hensell Aquifer	35	-5.6	28.3	1218	0.023
Pearsall Formation	45	20.5	48.0	931.9	0.051
Hosston Aquifer	104	30.7	60.5	1206	0.050

MAE = mean absolute error   Wash/Fred = Washita/Fredericksburg

Table 9.2.3   **Calibration statistics for the middle period of the transient model (1950 through 1979).**

Unit	Count	Mean Error (feet)	Mean Absolute Error (feet)	Range (feet)	MAE/Range
All	6140	6.4	47.8	2529	0.019
Woodbine Aquifer	653	36.2	47.8	767.7	0.062
Wash/Fred Groups	716	4.6	41.9	1047	0.040
Paluxy Aquifer	561	11.5	64.3	1587	0.040
Glen Rose Formation	586	-1.8	41.3	1707	0.024
Hensell Aquifer	1093	22.3	48.8	1883	0.026
Pearsall Formation	681	6.0	34.2	1589	0.022
Hosston Aquifer	1850	-11.7	51.6	2468	0.021

MAE = mean absolute error   Wash/Fred = Washita/Fredericksburg

Table 9.2.4   Water budget for the transient model. Values reported in AFY. Negative numbers indicate flow out of the unit.

1980	Cross-formational Flow			Recharge	ET	Ephemeral	Perennial	Reservoir	Spring	Younger	Well	Flowing	Storage
Unit	Surficial	Top	Bottom										
Younger Formations	0	0	-2,313	0	0	0	0	0	0	-9,756	0	0	5,647
Woodbine Aquifer	17,993	2,313	-2,870	348,250	-13,255	-189,629	-93,459	-2,547	-56	0	-19,424	-900	-13,119
Wash/Fred Groups	49,915	2,870	-20,875	639,582	-7,998	-267,058	-186,977	-13,072	-234	0	-35,241	-18	-98,129
Paluxy Aquifer	19,540	20,875	-17,916	286,293	-6,997	-112,334	-100,153	404	-118	0	-25,252	-35	-39,594
Glen Rose Formation	56,934	17,916	-65,791	289,389	-6,470	-81,345	-120,107	14	-81	0	-13,283	-57	-30,544
Hensell Aquifer	10,481	65,791	-46,725	232,918	-11,746	-127,525	-55,024	110	-179	0	-30,690	-823	-12,780
Pearsall Formation	17,439	46,725	-62,858	48,412	-3,616	-36,388	-22,087	-295	0	0	-7,764	-12	8,776
Hosston Aquifer	15,986	62,858	0	188,659	-4,191	-118,217	-51,244	-445	-338	0	-96,295	-502	23,019
Total	188,288	219,348	-219,348	2,033,503	-54,272	-932,495	-629,052	-15,832	-1,006	-9,756	-227,948	-2,346	-156,723

1990	Cross-formational Flow			Recharge	ET	Ephemeral	Perennial	Reservoir	Spring	Younger	Well	Flowing	Storage
Unit	Surficial	Top	Bottom										
Younger	0	0	-4,235	0	0	0	0	0	0	-8,803	0	0	7,632
Woodbine Aquifer	20,299	4,235	-5,221	411,233	-13,381	-196,508	-96,624	-1,960	-59	0	-19,979	-894	-65,039
Wash/Fred Groups	51,541	5,221	-25,125	692,893	-8,291	-278,076	-184,599	-4,683	-232	0	-34,003	0	-150,231
Paluxy Aquifer	21,639	25,125	-20,988	309,630	-7,125	-115,506	-101,995	548	-115	0	-28,739	-45	-55,432
Glen Rose Formation	62,167	20,988	-72,767	278,896	-6,612	-82,828	-117,757	71	-82	0	-14,525	-22	-15,314
Hensell Aquifer	13,763	72,767	-53,784	243,027	-11,934	-129,666	-56,186	-76	-183	0	-33,424	-606	-16,953
Pearsall Formation	19,010	53,784	-68,826	54,819	-3,670	-36,764	-22,646	-267	0	0	-8,673	-7	2,349
Hosston Aquifer	25,107	68,826	0	203,414	-4,214	-119,728	-51,456	-168	-328	0	-102,338	-261	9,506
Total	213,526	250,945	-250,945	2,193,913	-55,227	-959,076	-631,265	-6,535	-998	-8,803	-241,681	-1,836	-283,482

Table 9.2.4, continued

2000	Cross-formational Flow			Recharge	ET	Ephemeral	Perennial	Reservoir	Spring	Younger	Well	Flowing	Storage
Unit	Surficial	Top	Bottom										
Younger	0	0	-5,407	0	0	0	0	0	0	-7,940	0	0	9,365
Woodbine Aquifer	24,864	5,407	-5,976	231,840	-13,556	-208,440	-96,990	-4,596	-64	0	-26,241	-904	136,163
Wash/Fred Groups	58,069	5,976	-25,510	345,628	-8,652	-298,137	-181,195	-11,257	-227	0	-41,062	0	226,979
Paluxy Aquifer	23,325	25,510	-21,510	173,587	-7,235	-124,408	-99,809	-459	-118	0	-31,035	-56	91,566
Glen Rose Formation	64,531	21,510	-73,590	142,829	-6,716	-88,150	-114,108	-540	-85	0	-16,179	-6	125,376
Hensell Aquifer	17,688	73,590	-56,062	151,900	-12,074	-137,903	-56,508	-821	-198	0	-37,487	-520	89,177
Pearsall Formation	21,485	56,062	-72,303	32,744	-3,702	-38,336	-22,424	-384	0	0	-8,821	-15	25,638
Hosston Aquifer	22,725	72,303	0	127,805	-4,270	-126,396	-50,753	-991	-318	0	-105,581	-226	91,890
Total	232,686	260,358	-260,358	1,206,333	-56,205	-1,021,770	-621,787	-19,048	-1,010	-7,940	-266,407	-1,727	796,154

2010	Cross-formational Flow			Recharge	ET	Ephemeral	Perennial	Reservoir	Spring	Younger	Well	Flowing	Storage
Unit	Surficial	Top	Bottom										
Younger	0	0	-7,420	0	0	0	0	0	0	-7,627	0	0	9,404
Woodbine Aquifer	21,636	7,420	-6,971	544,714	-13,796	-204,964	-107,655	-2,573	-63	0	-26,577	-891	-172,305
Wash/Fred Groups	67,228	6,971	-27,389	909,151	-8,914	-301,781	-202,037	-9,475	-231	0	-53,264	0	-299,655
Paluxy Aquifer	26,241	27,389	-23,316	404,045	-7,341	-123,518	-111,930	-731	-116	0	-32,936	-66	-125,378
Glen Rose Formation	73,258	23,316	-81,254	385,280	-6,772	-87,765	-128,021	-485	-84	0	-19,430	0	-94,777
Hensell Aquifer	17,848	81,254	-58,662	321,638	-12,192	-135,759	-62,043	-417	-193	0	-41,580	-290	-78,788
Pearsall Formation	21,703	58,662	-76,762	67,901	-3,725	-37,784	-23,681	-319	0	0	-7,074	-12	-9,069
Hosston Aquifer	19,051	76,762	0	255,432	-4,283	-124,772	-55,219	-531	-311	0	-104,484	-162	-38,619
Total	246,965	281,774	-281,774	2,888,161	-57,024	-1,016,342	-690,585	-14,530	-999	-7,627	-285,345	-1,421	-809,188

Wash/Fred = Washita/Fredericksburg

Table 9.2.5   Water budget by county for 2012. All values reported in AFY. Negative values indicate flow out of the county.

County	State	Lateral	Recharge	Perennial	Ephemeral	ET	Spring	Younger	Reservoir	Wells	Flowing	Storage
Bastrop	TX	43	0	0	0	0	0	-323	0	0	0	280
Bell	TX	1,939	8,470	-14,255	-6,567	-39	-137	404	-1,009	-8,162	-37	19,588
Bosque	TX	3,320	15,799	-22,180	-17,991	-529	0	0	-72	-4,193	0	25,846
Bowie	TX	388	0	0	0	0	0	-460	0	0	0	72
Brown	TX	-2,166	2,734	0	-3,454	0	-29	0	0	-1,043	0	3,959
Burnet	TX	-9,369	6,899	-2,018	-5,658	-151	0	0	-331	-3,075	0	13,702
Callahan	TX	-535	2,027	0	-3,772	0	0	0	0	-2,221	0	4,502
Collin	TX	3,268	0	0	0	0	0	93	0	-7,159	0	3,798
Comanche	TX	4,676	10,286	-8,372	-11,184	-995	-1	0	-62	-23,233	0	28,884
Cooke	TX	-5,155	50,674	-26,810	-48,490	-3,186	-22	0	-1,121	-6,106	0	40,217
Coryell	TX	-1,970	14,857	-26,881	-5,897	-72	0	0	0	-3,521	0	23,694
Dallas	TX	5,852	209	-721	0	0	0	364	0	-8,652	0	2,947
Delta	TX	202	0	0	0	0	0	-536	0	-60	0	394
Denton	TX	9,736	35,044	-23,970	-34,302	-743	-73	-30	70	-16,970	0	31,238
Eastland	TX	277	3,582	0	-7,042	0	0	0	0	-6,276	0	9,458
Ellis	TX	7,014	0	0	0	0	0	889	0	-8,979	0	1,076
Erath	TX	-11,029	13,563	-4,622	-8,899	-13	0	0	0	-16,023	0	27,023
Falls	TX	862	0	0	0	0	0	-535	0	-817	0	490
Fannin	TX	2,327	20,574	-22,431	-6,447	-2,471	0	-158	58	-4,329	0	12,876
Franklin	TX	71	0	0	0	0	0	-111	0	0	0	40
Grayson	TX	16,363	36,461	-20,692	-34,982	-151	0	194	-5,503	-15,358	0	24,547
Hamilton	TX	-5,478	10,693	-17,231	-1,943	0	0	0	0	-1,716	0	15,675
Henderson	TX	-2	0	0	0	0	0	-196	0	0	0	198
Hill	TX	-119	6,436	-6,582	-6,921	-432	0	940	-10	-3,732	0	10,421
Hood	TX	-2,121	6,071	-3,759	-4,804	-290	0	0	53	-6,351	0	11,204
Hopkins	TX	-2	0	0	0	0	0	-130	0	0	0	132
Hunt	TX	-887	0	0	0	0	0	-238	0	-441	0	1,566
Jack	TX	-550	1,361	0	-2,062	0	0	0	0	-65	0	1,315
Johnson	TX	-1,491	10,932	826	-19,986	-10	-22	897	117	-9,880	0	18,618

Table 9.2.5, continued

County	State	Lateral	Recharge	Perennial	Ephemeral	ET	Spring	Younger	Reservoir	Wells	Flowing	Storage
Kaufman	TX	-786	0	0	0	0	0	-555	0	-52	0	1,393
Lamar	TX	5,704	14,399	-21,388	-3,809	-1,992	-14	-57	0	-66	0	7,222
Lampasas	TX	2,263	6,919	-11,659	-6,406	0	-260	0	0	-537	0	9,680
Lee	TX	112	0	0	0	0	0	-362	0	0	0	249
Limestone	TX	-1,447	0	0	0	0	0	-39	0	0	0	1,486
McLennan	TX	14,436	7,440	-20,600	-2,372	-219	0	194	631	-13,271	0	13,761
Milam	TX	340	0	0	0	0	0	-1,209	0	-1	0	871
Mills	TX	-4,989	6,142	2,253	-8,991	0	0	0	0	-3,961	0	9,546
Montague	TX	-8,181	19,803	-8,227	-17,764	-1,661	0	0	0	-372	0	16,403
Morris	TX	3	0	0	0	0	0	-3	0	0	0	0
Navarro	TX	-773	0	0	0	0	0	-991	0	-123	0	1,888
Palo Pinto	TX	-248	220	0	-184	0	0	0	0	0	0	212
Parker	TX	-10,002	16,528	-7,219	-15,087	-247	0	0	81	-7,650	0	23,595
Red River	TX	4,543	17,482	-12,311	-14,327	-2,956	0	-546	0	-371	0	8,486
Robertson	TX	25	0	0	0	0	0	-211	0	0	0	185
Rockwall	TX	-108	0	0	0	0	0	15	0	0	0	93
Somervell	TX	4,384	2,769	-9,654	-944	0	0	0	347	-3,060	0	6,170
Tarrant	TX	8,471	19,369	-17,746	-21,039	-302	-87	478	1,554	-21,922	0	31,226
Taylor	TX	-383	310	0	-334	0	0	0	0	-146	0	552
Titus	TX	132	0	0	0	0	0	-160	0	0	0	28
Travis	TX	8,771	2,689	-172	-2,168	-322	0	467	-2,038	-19,295	0	12,083
Williamson	TX	-6,159	6,770	-4,918	-3,642	0	0	972	2	-20,074	-4	27,078
Wise	TX	-6,369	29,484	-10,647	-32,766	-2,891	-111	0	49	-6,761	0	30,011
Atoka	OK	1,416	50,902	-21,853	-57,857	-3,194	-30	0	0	-522	0	31,136
Bryan	OK	-13,986	118,838	-46,006	-116,660	-5,166	0	0	-2,008	-1,153	0	66,142
Carter	OK	-461	5,902	0	-9,931	-19	0	0	-32	-225	0	4,766
Choctaw	OK	-7,291	127,103	-51,189	-121,046	-3,441	-40	1	-1,264	-988	0	58,159
Johnston	OK	-164	20,271	-8,521	-22,447	-833	0	0	-665	-2,041	0	14,401
Love	OK	3,587	28,521	-20,257	-24,068	-7,739	-70	0	-926	-1,616	0	22,569
Marshall	OK	-4,196	39,323	-1,175	-47,015	-265	0	0	-7,234	-2,226	0	22,788
McCurtain	OK	-4,507	122,654	-67,175	-89,543	-2,384	-50	-1,101	-34	-285	0	42,424

Table 9.2.5, continued

County	State	Lateral	Recharge	Perennial	Ephemeral	ET	Spring	Younger	Reservoir	Wells	Flowing	Storage
Pushmataha	OK	-2,261	22,787	-5,061	-27,520	-212	-46	0	0	-187	0	12,499
Hempstead	AR	249	0	0	0	0	0	-258	0	0	0	8
Howard	AR	-2,845	38,705	-8,263	-30,541	-2,180	0	-2,824	0	-56	0	8,004
Lafayette	AR	9	0	0	0	0	0	-9	0	0	0	0
Little River	AR	1,704	4,206	-6,354	-365	-105	0	-319	0	-3	0	1,235
Miller	AR	119	0	0	0	0	0	-126	0	0	0	6
Pike	AR	1,045	25,543	-9,608	-17,776	-1,812	0	-389	0	-34	0	3,030
Sevier	AR	2,379	73,714	-29,541	-58,541	-8,238	0	-360	0	-263	0	20,850

Table 9.2.6   Water budget by GCD for 2012. All values reported in AFY. Negative numbers indicate flow out of the GCD.

GCD	Lateral	Recharge	Perennial	Ephemeral	ET	Spring	Younger	Reservoir	Wells	Flowing	Storage
Brazos Valley GCD	27	0	0	0	0	0	-191	0	0	0	164
Central Texas GCD	-9,723	6,870	-2,049	-5,304	-151	0	0	-293	-3,148	0	13,798
Clearwater UWCD	1,407	8,269	-13,376	-6,448	-39	-137	405	-1,008	-8,135	-37	19,293
Fox Crossing Water District	-4,170	5,977	1,623	-8,901	0	0	0	0	-3,843	0	9,314
Lost Pines GCD	165	0	0	0	0	0	-669	0	0	0	504
Middle Trinity GCD	-7,611	54,652	-60,379	-43,735	-1,271	-1	0	-151	-47,142	0	105,851
Neches & Trinity Valleys GCD	-12	0	0	0	0	0	-185	0	0	0	197
North Texas GCD	10,972	86,279	-55,015	-82,373	-4,015	-95	60	-1,110	-30,304	0	75,600
Northern Trinity GCD	8,818	19,264	-17,667	-21,206	-302	-87	469	1,541	-22,055	0	31,224
Post Oak Savannah GCD	321	0	0	0	0	0	-1,216	0	0	0	896
Prairielands GCD	12,274	20,147	-18,376	-27,513	-780	-22	2,711	419	-24,758	0	35,909
Red River GCD	-3,552	55,072	-18,851	-43,303	-2,381	0	38	-4,538	-19,683	0	38,079
Saratoga UWCD	2,917	6,962	-12,082	-6,759	0	-260	0	0	-540	0	9,762
Southern Trinity GCD	13,750	7,367	-19,562	-2,504	-219	0	185	631	-13,303	0	13,655
Upper Trinity GCD	-24,811	71,017	-30,022	-70,291	-5,064	-111	0	255	-21,834	0	80,863

UWCD = Underground Water Conservation District
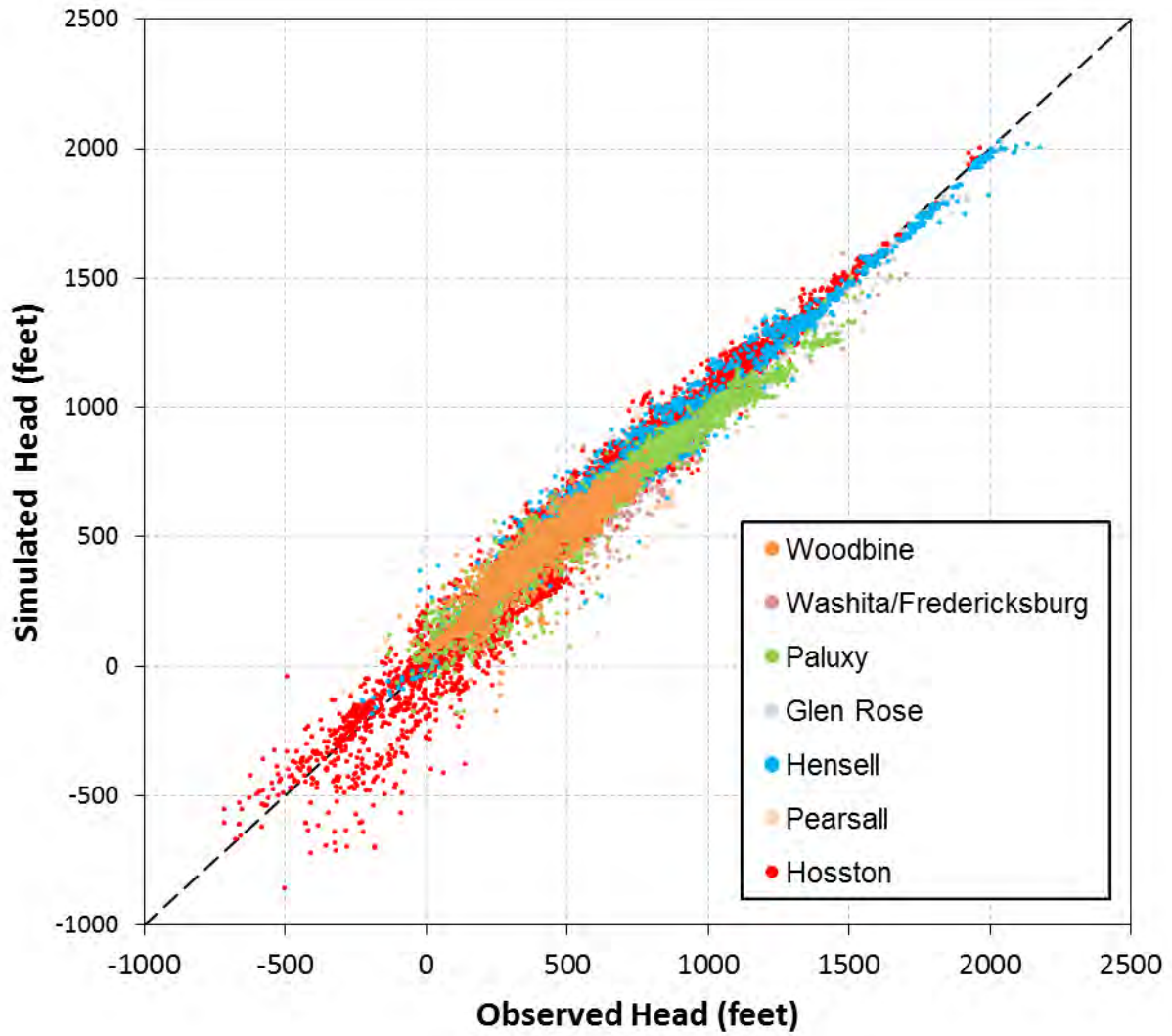
Figure 9.2.1 **Crossplot of observed versus simulated hydraulic heads in feet amsl for the
transient calibration period (1890 to 2012).**
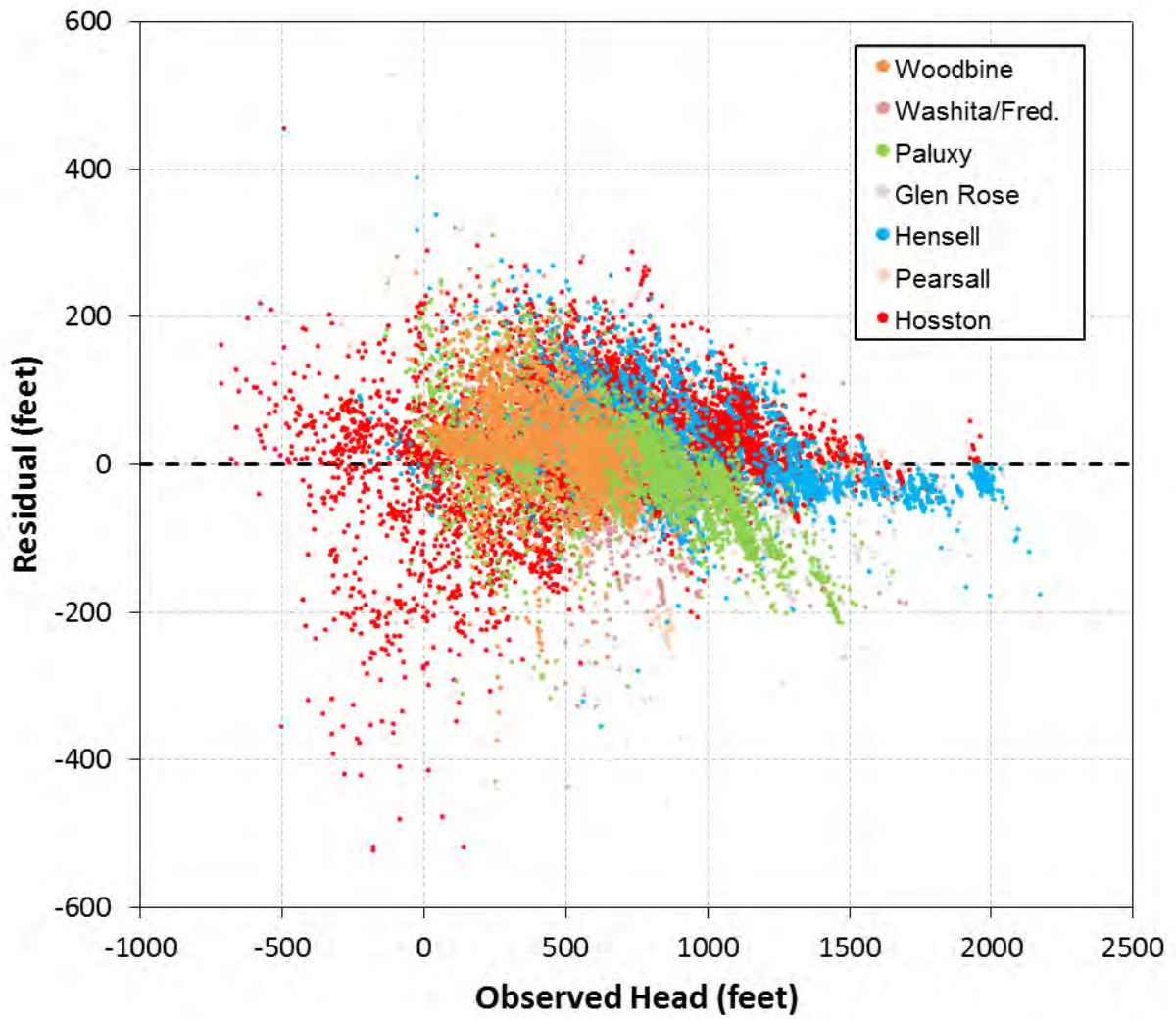
Figure 9.2.2 **Plot of observed hydraulic heads in feet amsl versus residuals in feet for the transient calibration period (1890 to 2012).**
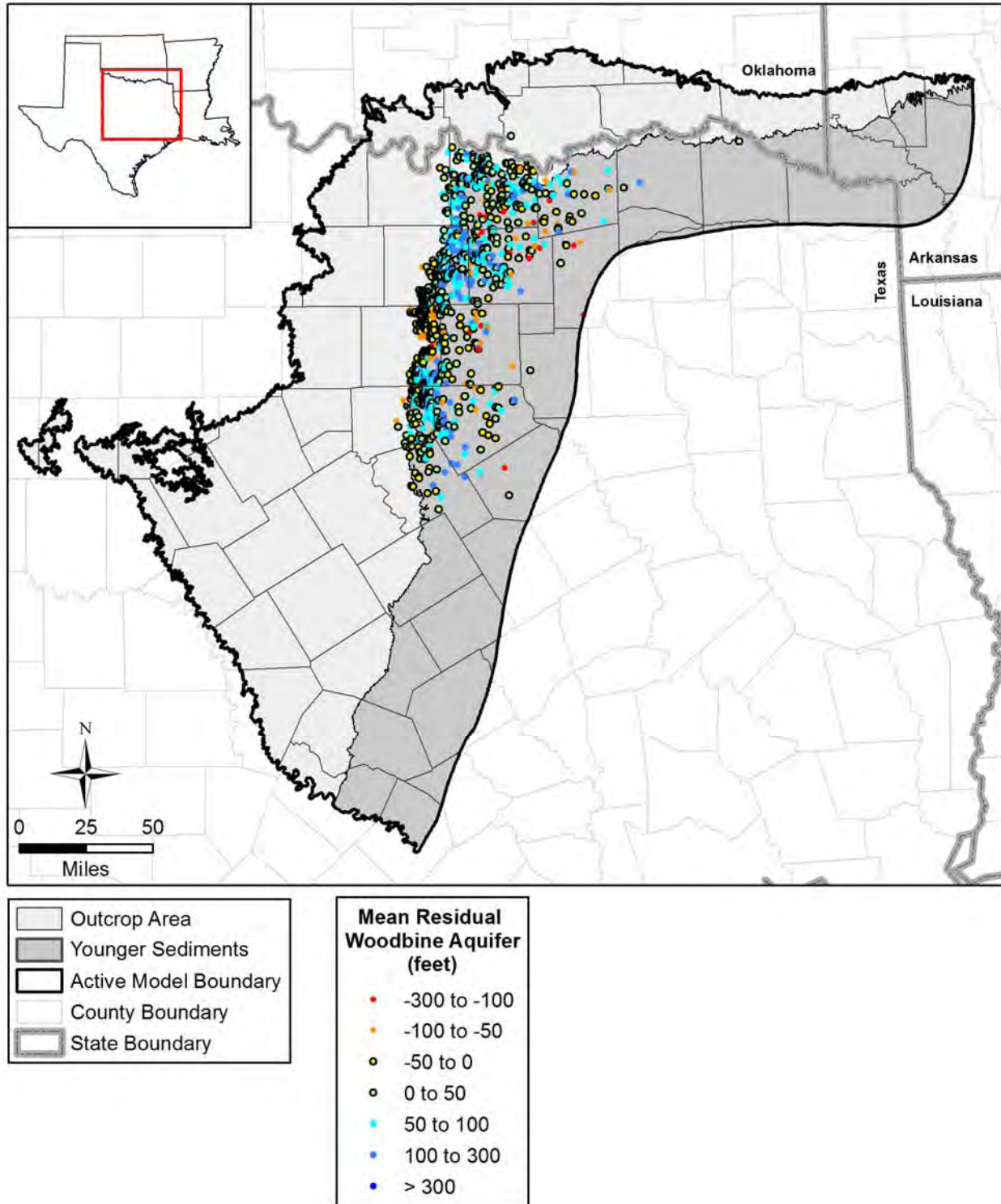
Figure 9.2.3   **Spatial distribution of hydraulic head residuals in feet in the Woodbine Aquifer for the transient calibration period (1890 to 2012).**
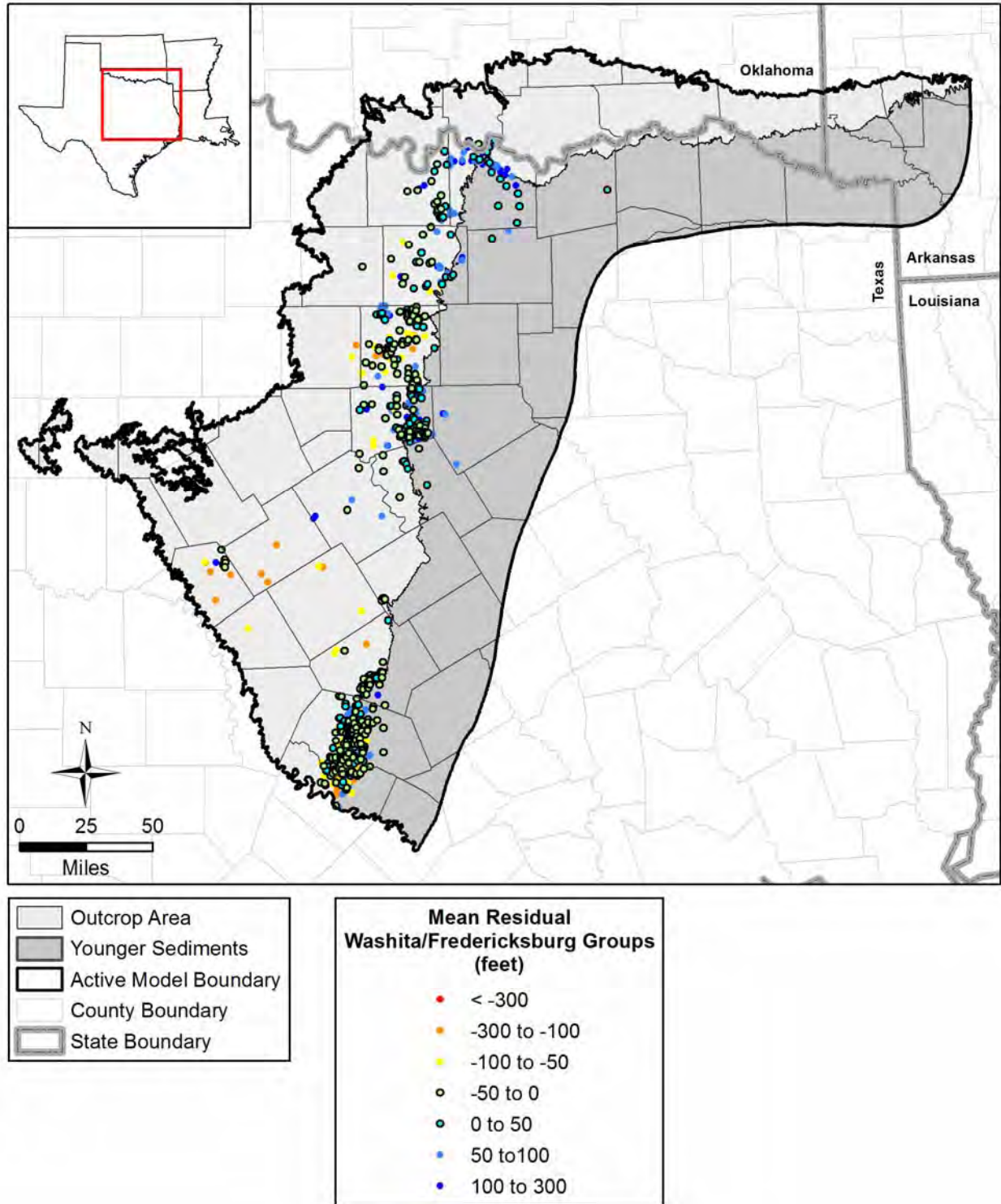
Figure 9.2.4   **Spatial distribution of hydraulic head residuals in feet in the Washita/ Fredericksburg groups for the transient calibration period (1890 to 2012).**
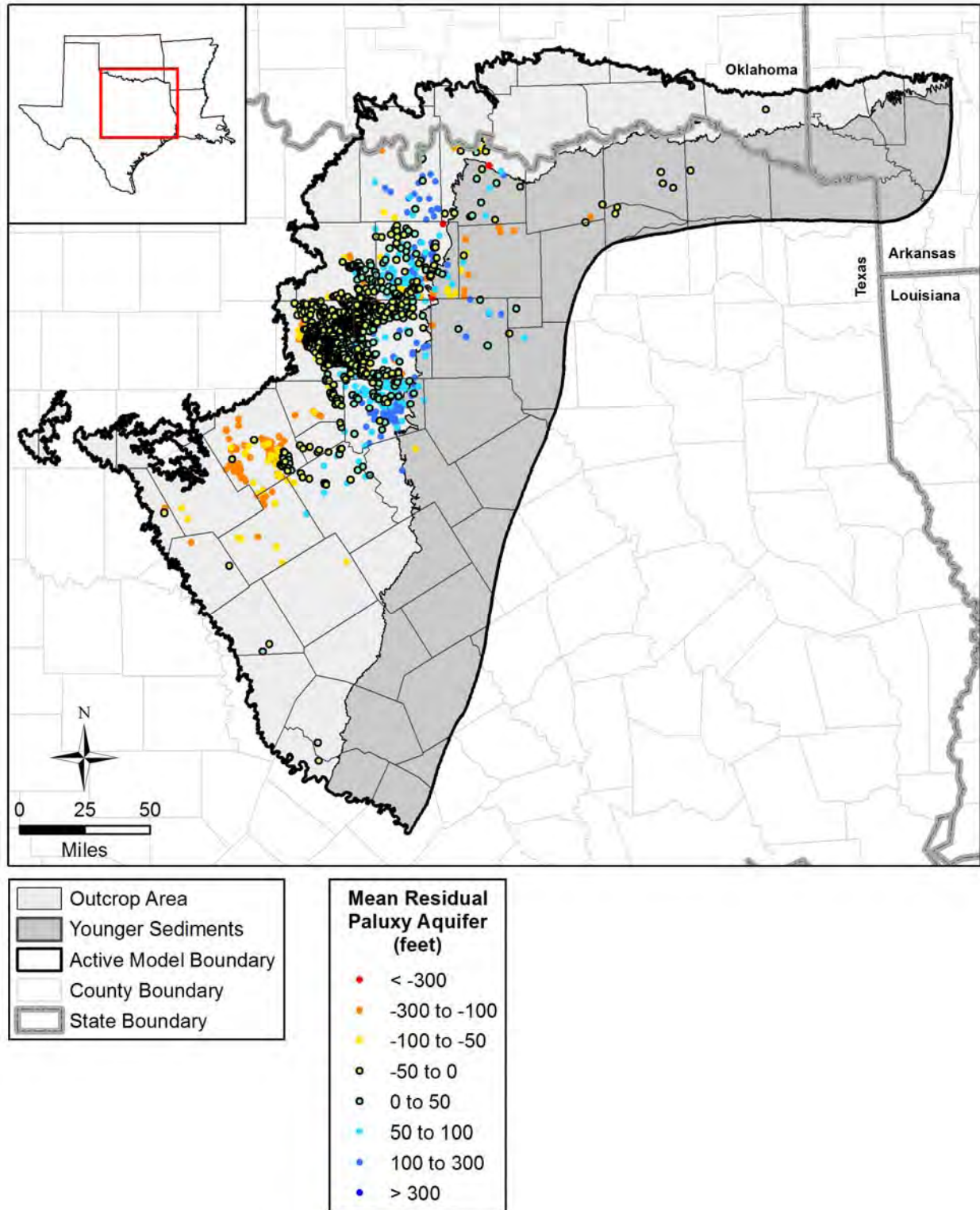
Figure 9.2.5 **Spatial distribution of hydraulic head residuals in feet in the Paluxy Aquifer for the transient calibration period (1890 to 2012).**
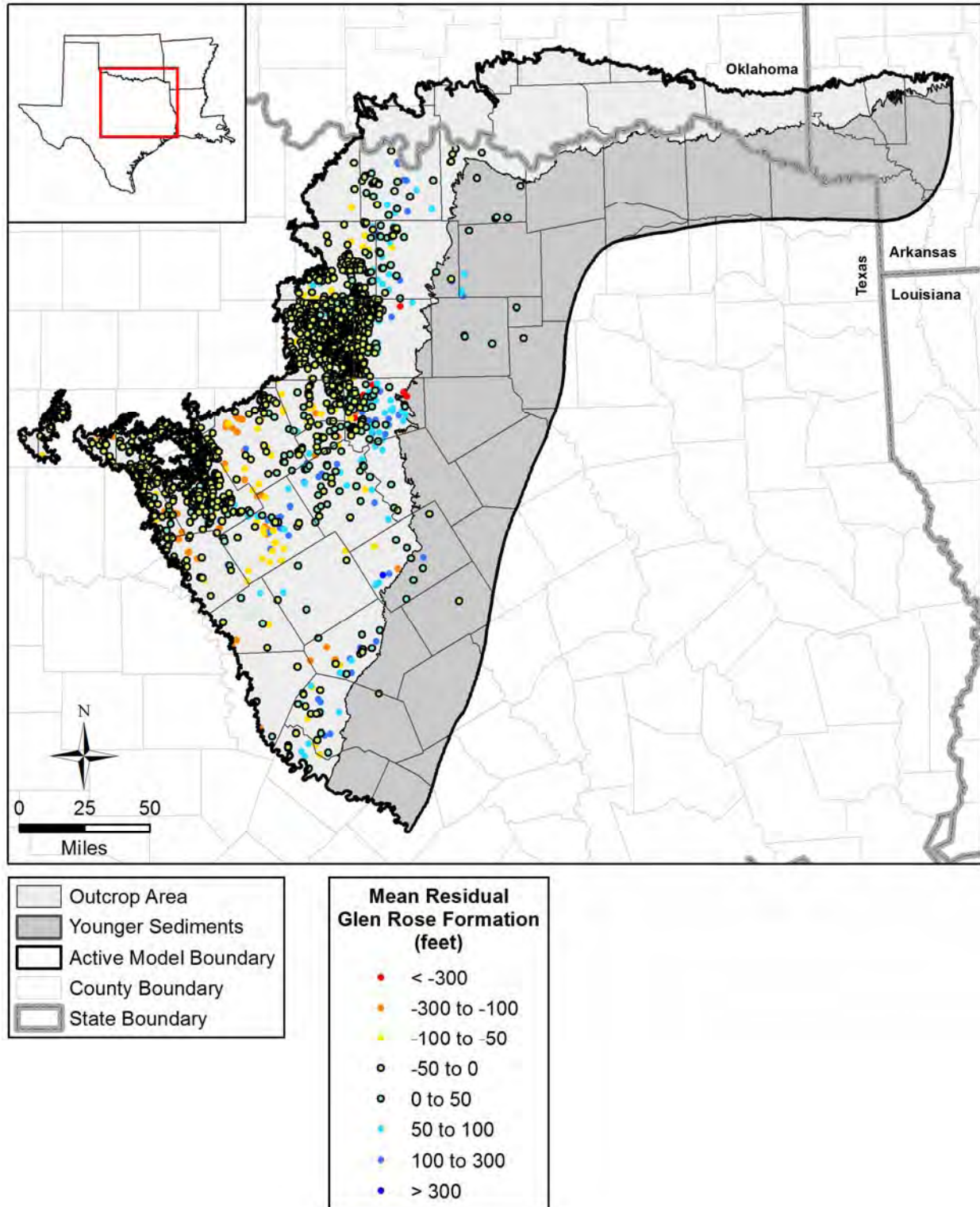
Figure 9.2.6   **Spatial distribution of hydraulic head residuals in feet in the Glen Rose Formation for the transient calibration period (1890 to 2012).**
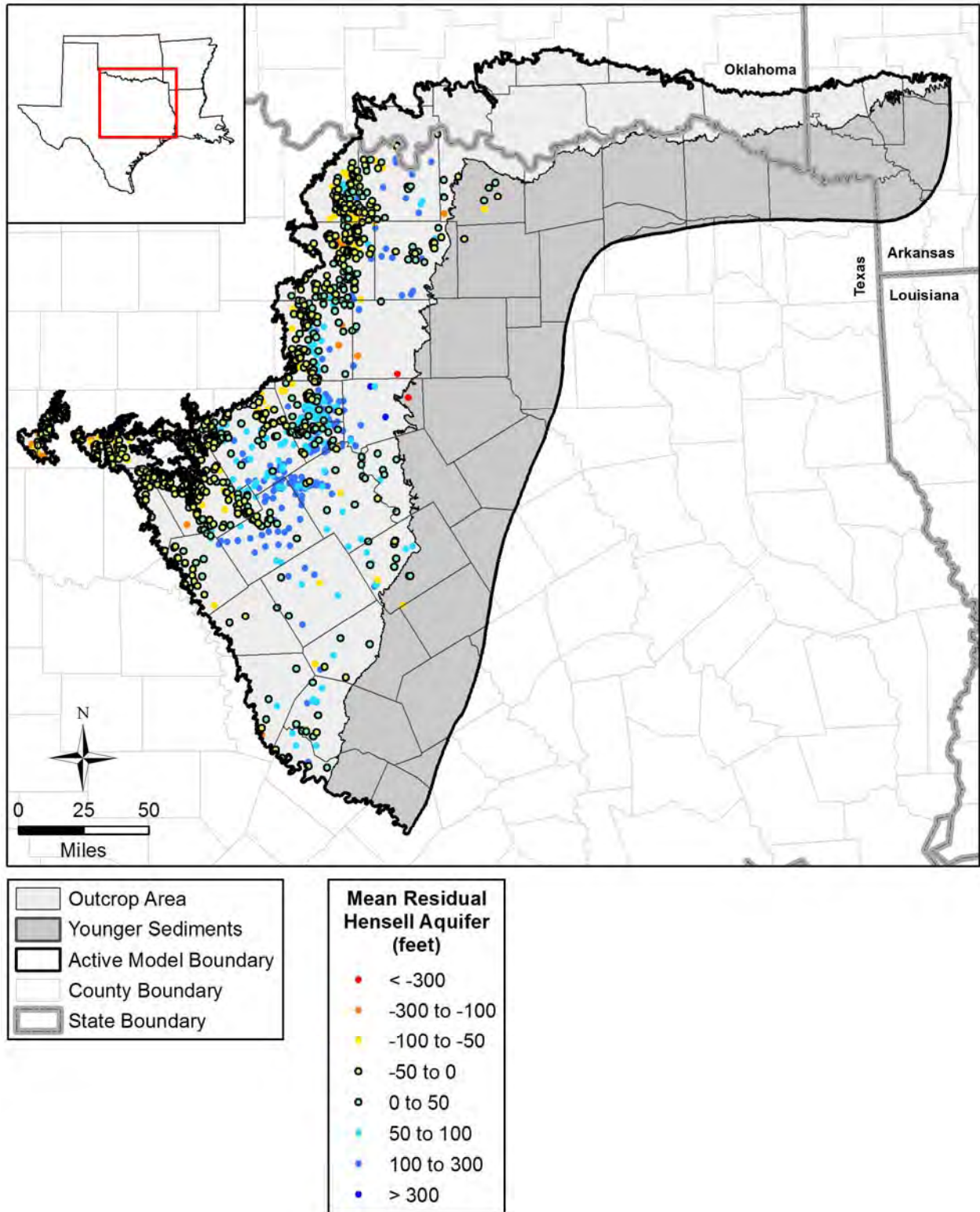
Figure 9.2.7   Spatial distribution of hydraulic head residuals in feet in the Hensell Aquifer for the transient calibration period (1890 to 2012).
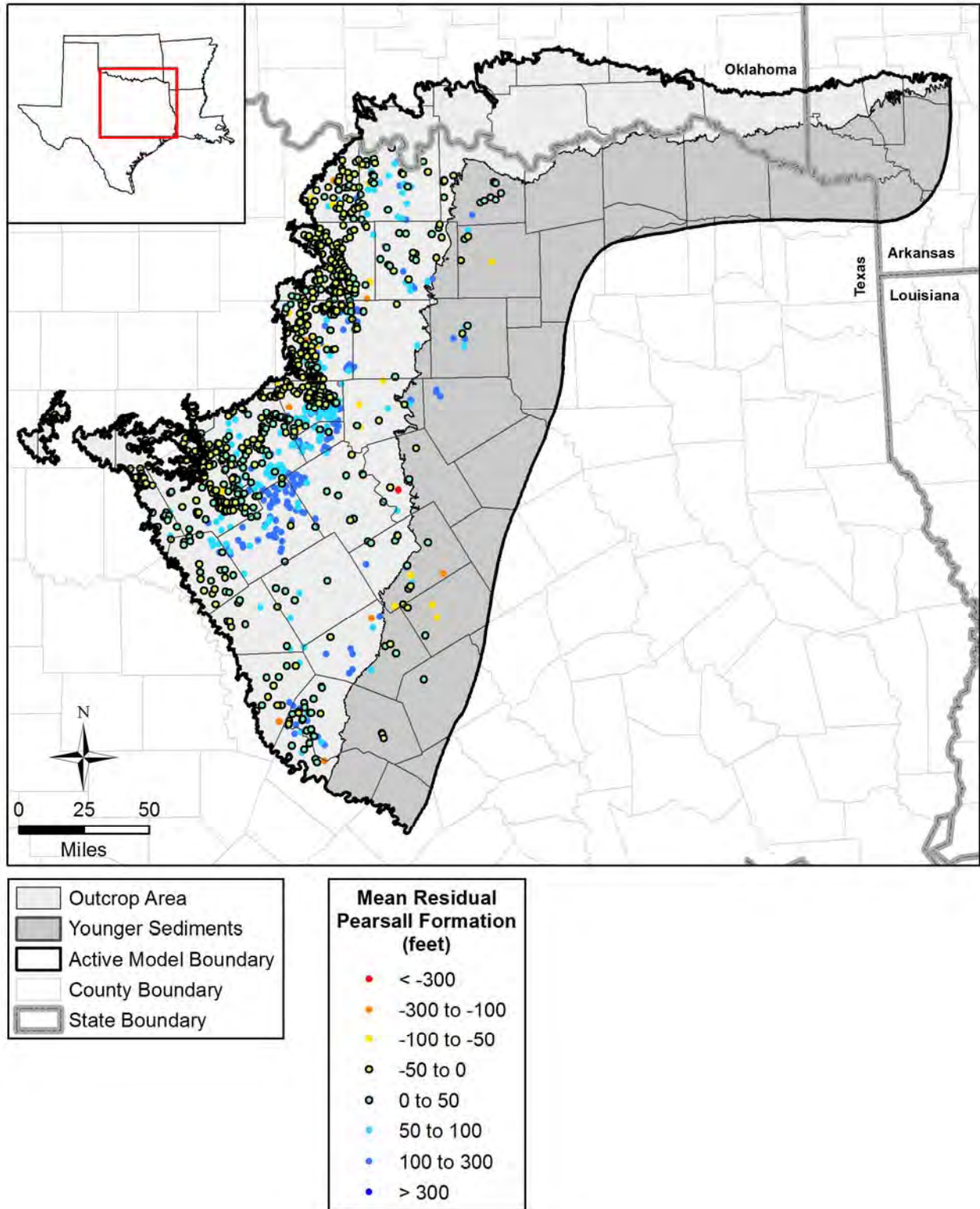
Figure 9.2.8   Spatial distribution of hydraulic head residuals in feet in the Pearsall Formation for the transient calibration period (1890 to 2012).
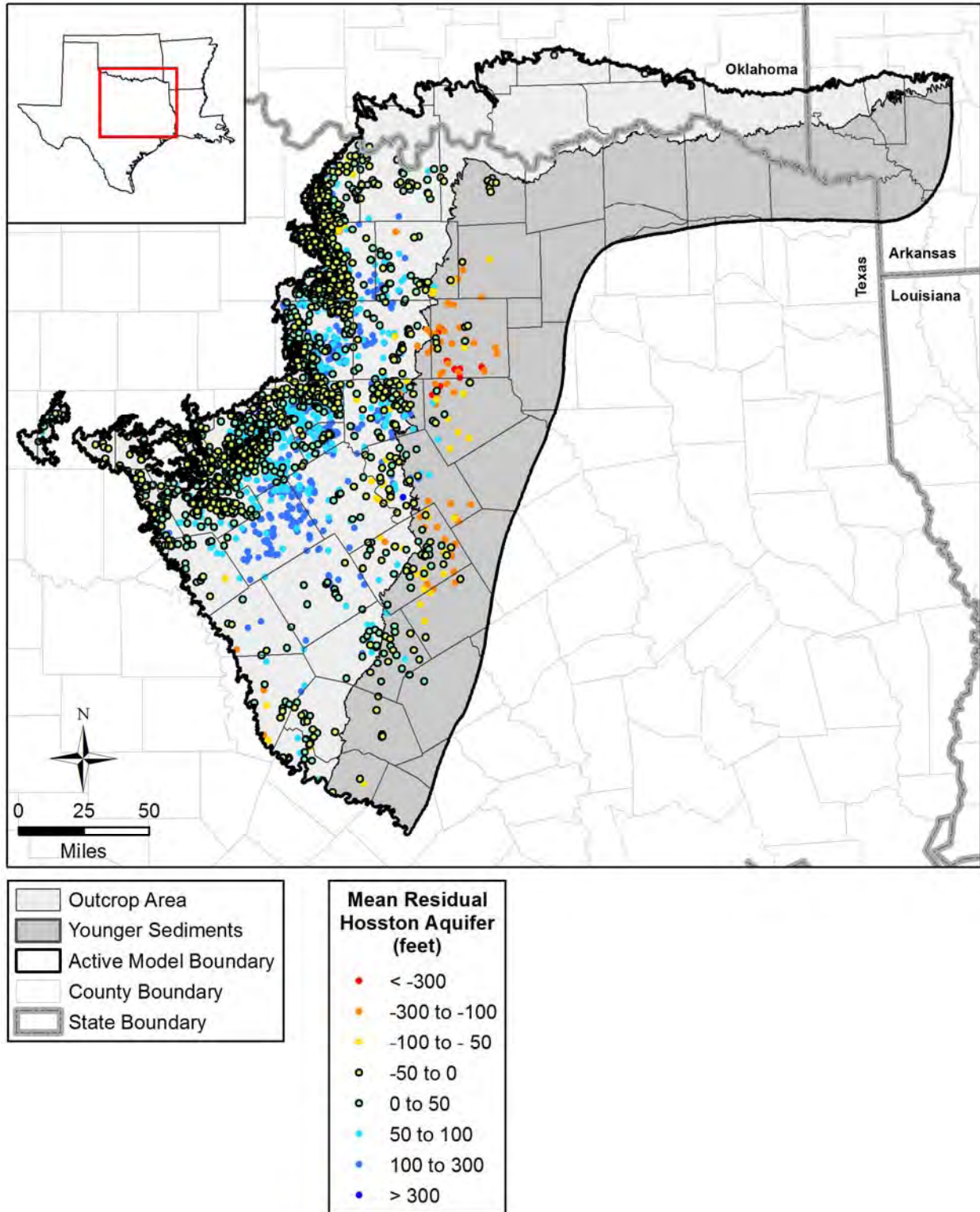
Figure 9.2.9   **Spatial distribution of hydraulic head residuals in feet in the Hosston Aquifer for the transient calibration period (1890 to 2012).**
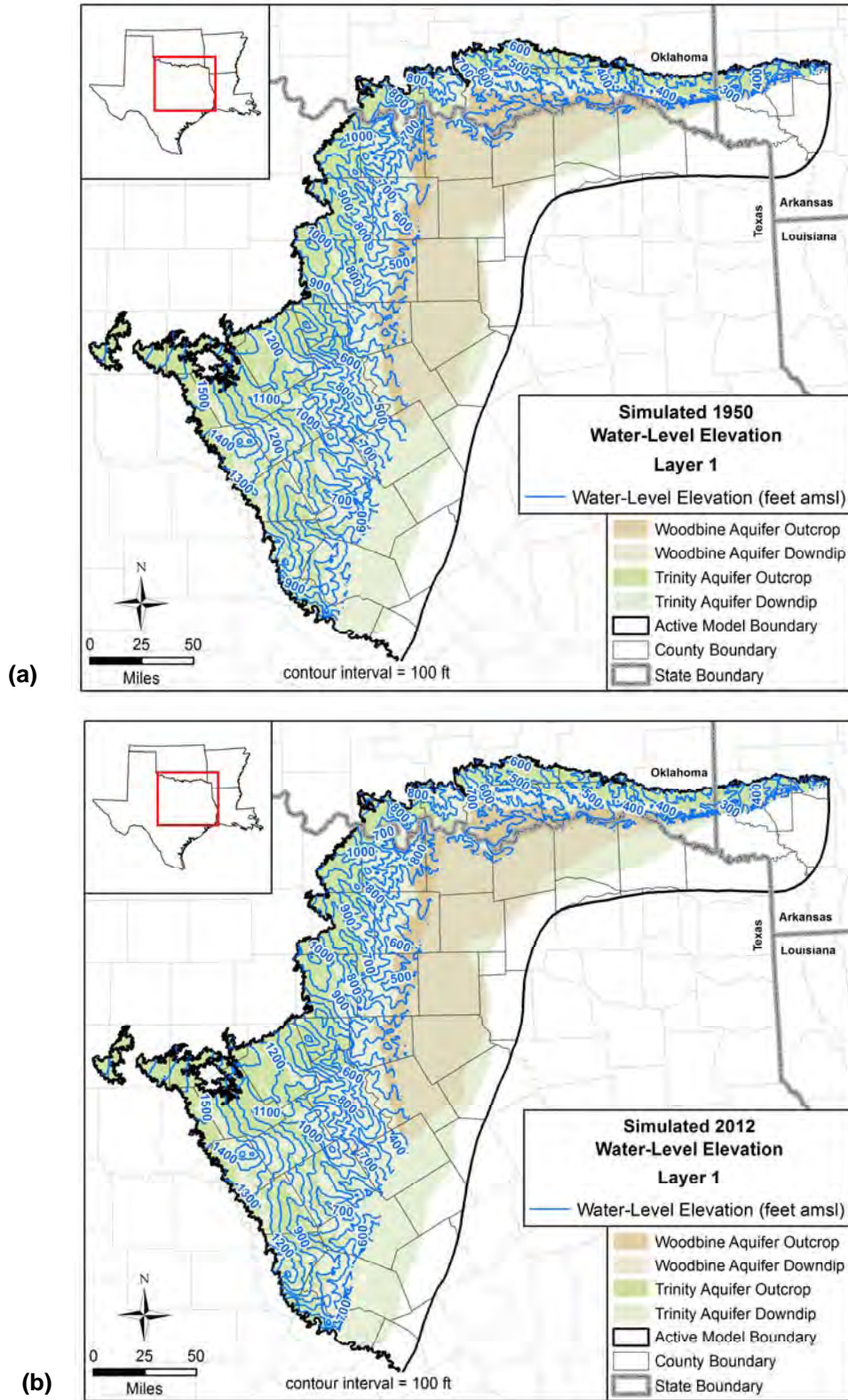
Figure 9.2.10 Simulated water-level elevations (hydraulic heads) in feet amsl in the surficial outcrop area in Layer 1 in (a) 1950 and (b) 2012.
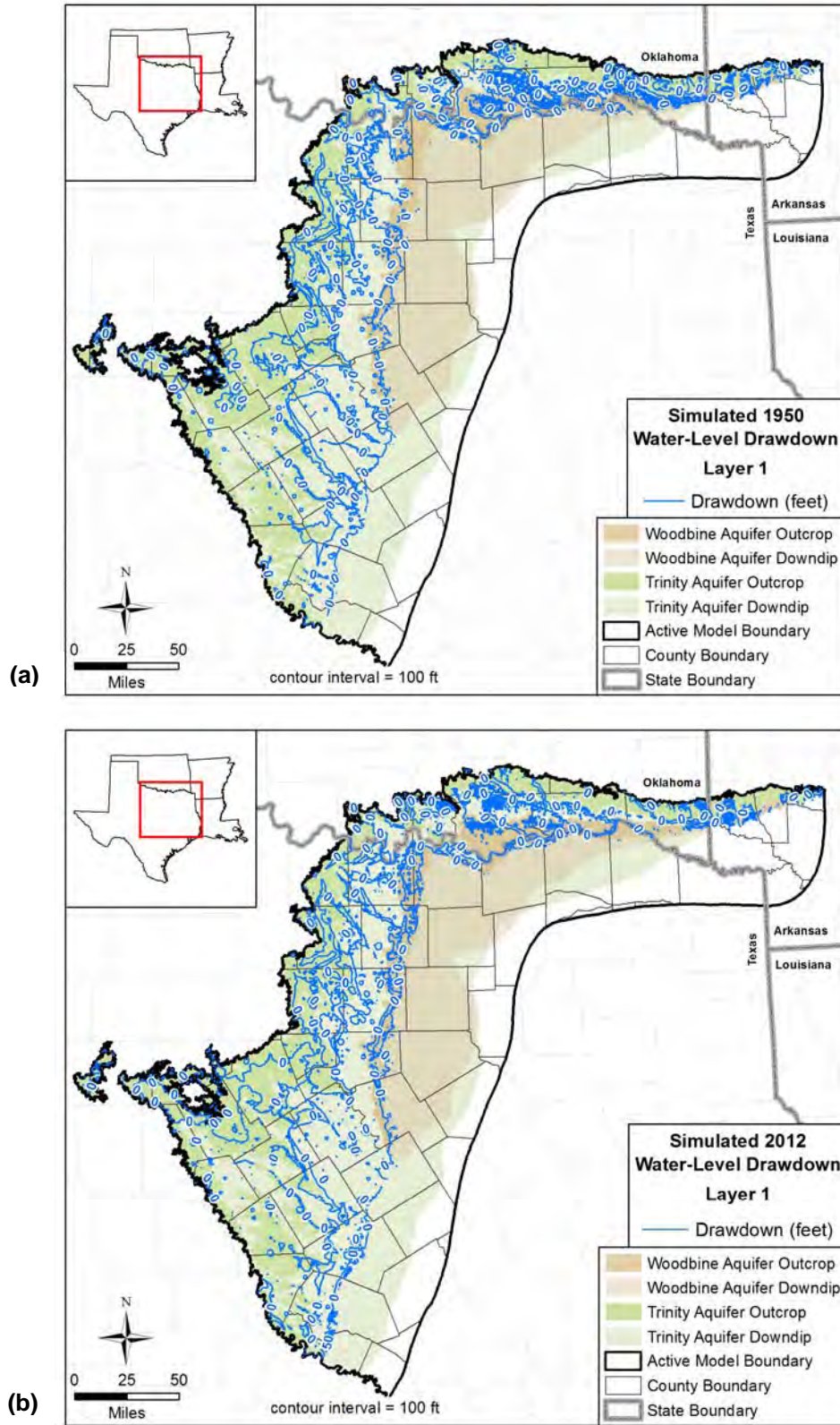
Figure 9.2.11   Simulated drawdown in feet in the surficial outcrop area of Layer 1 in (a) 1950 and (b) 2012.
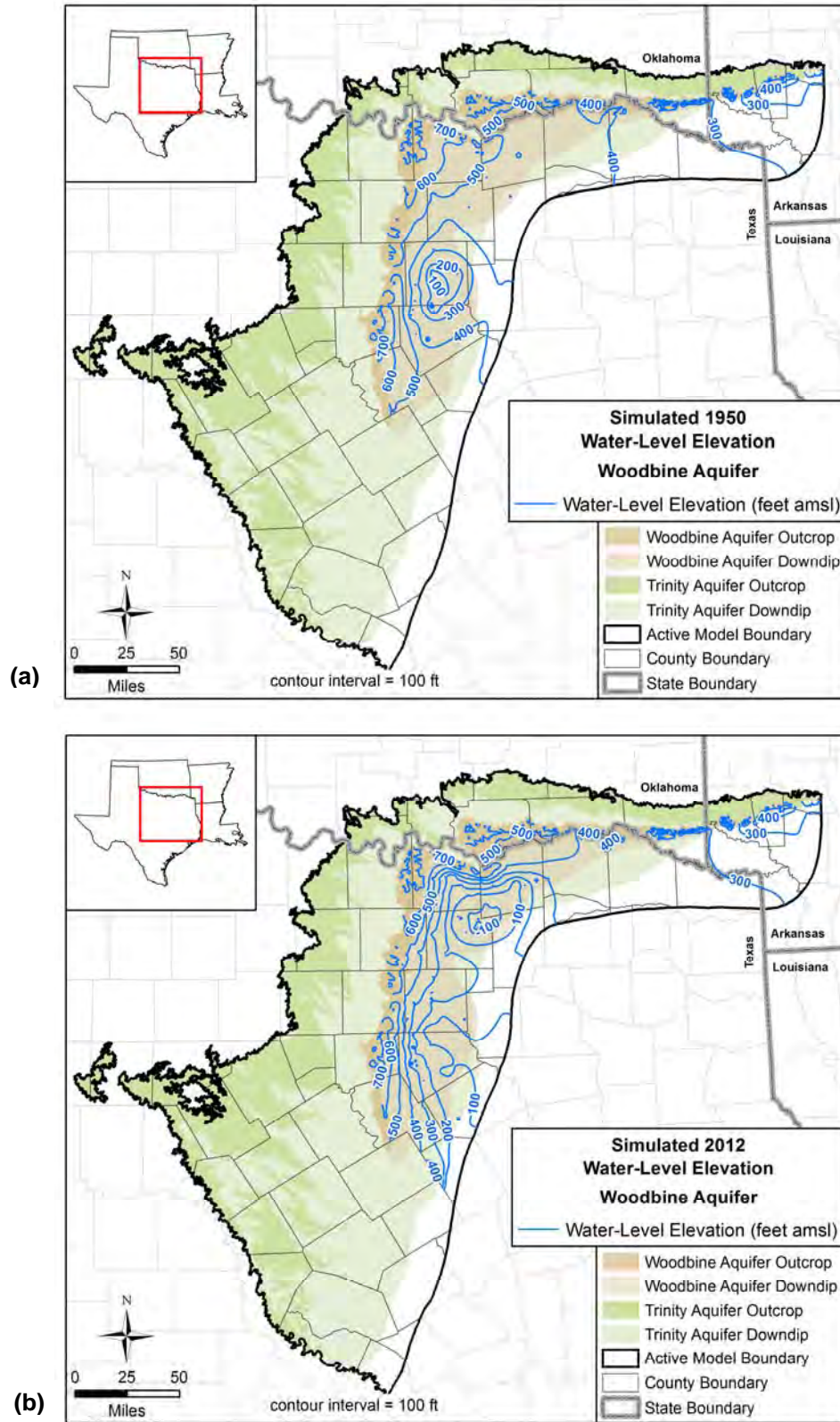
Figure 9.2.12   **Simulated water-level elevations (hydraulic heads) in feet amsl in the Woodbine Aquifer in (a) 1950 and (b) 2012.**
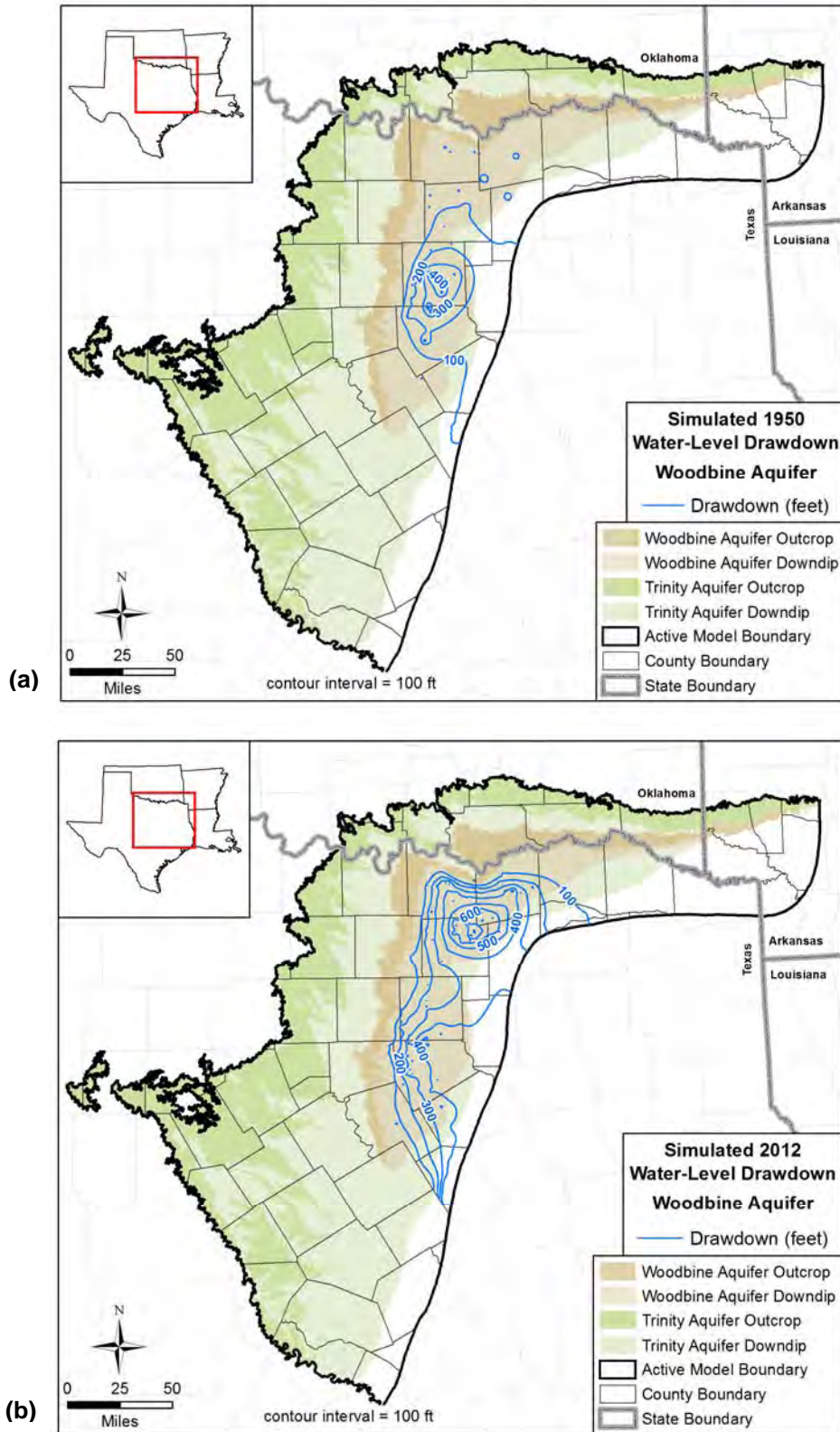
Figure 9.2.13   Simulated drawdown in feet in the Woodbine Aquifer in (a) 1950 and (b) 2012.
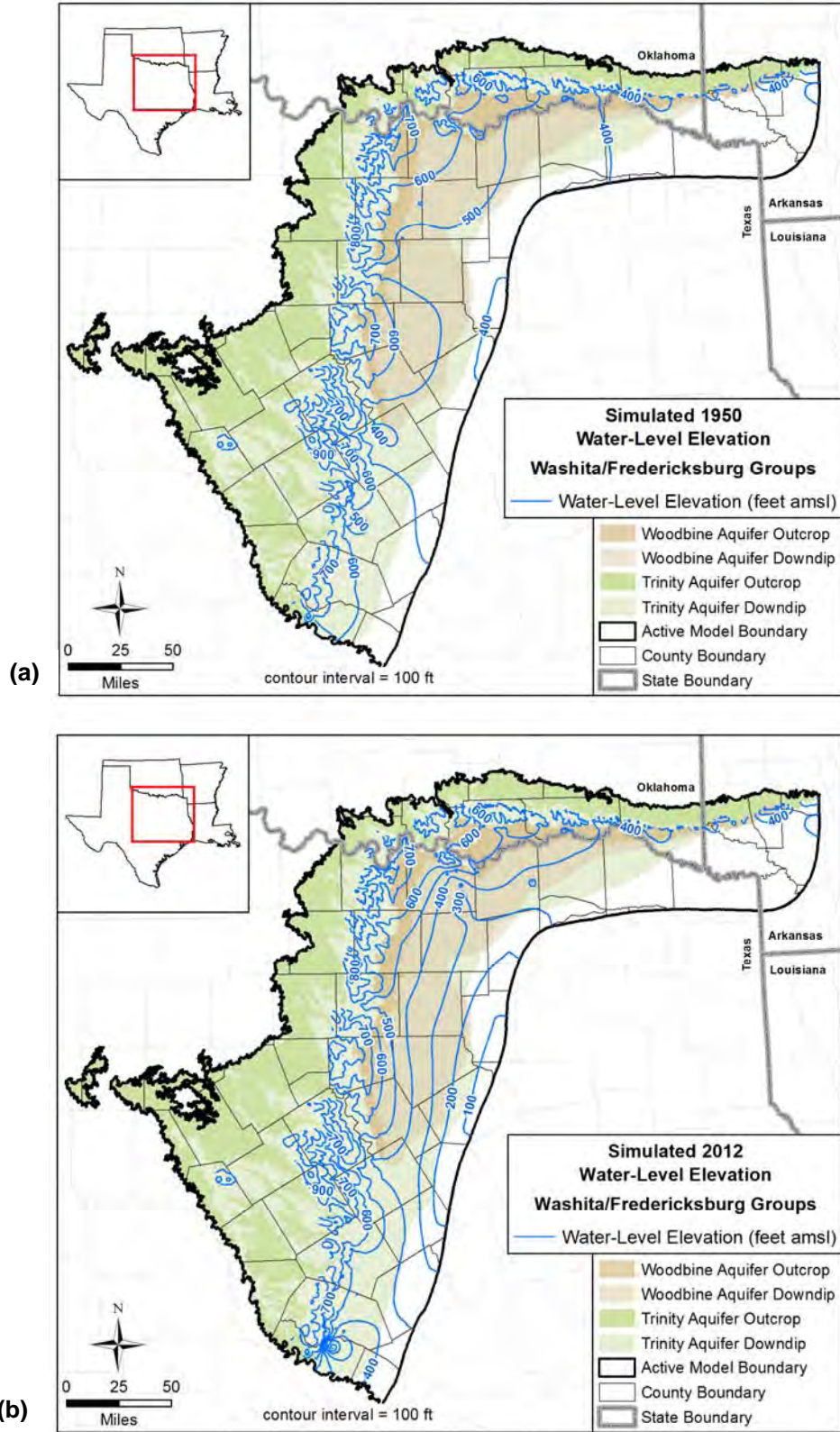
Figure 9.2.14   Simulated water-level elevations (hydraulic heads) in feet amsl in the Washita/Fredericksburg groups in (a) 1950 and (b) 2012.
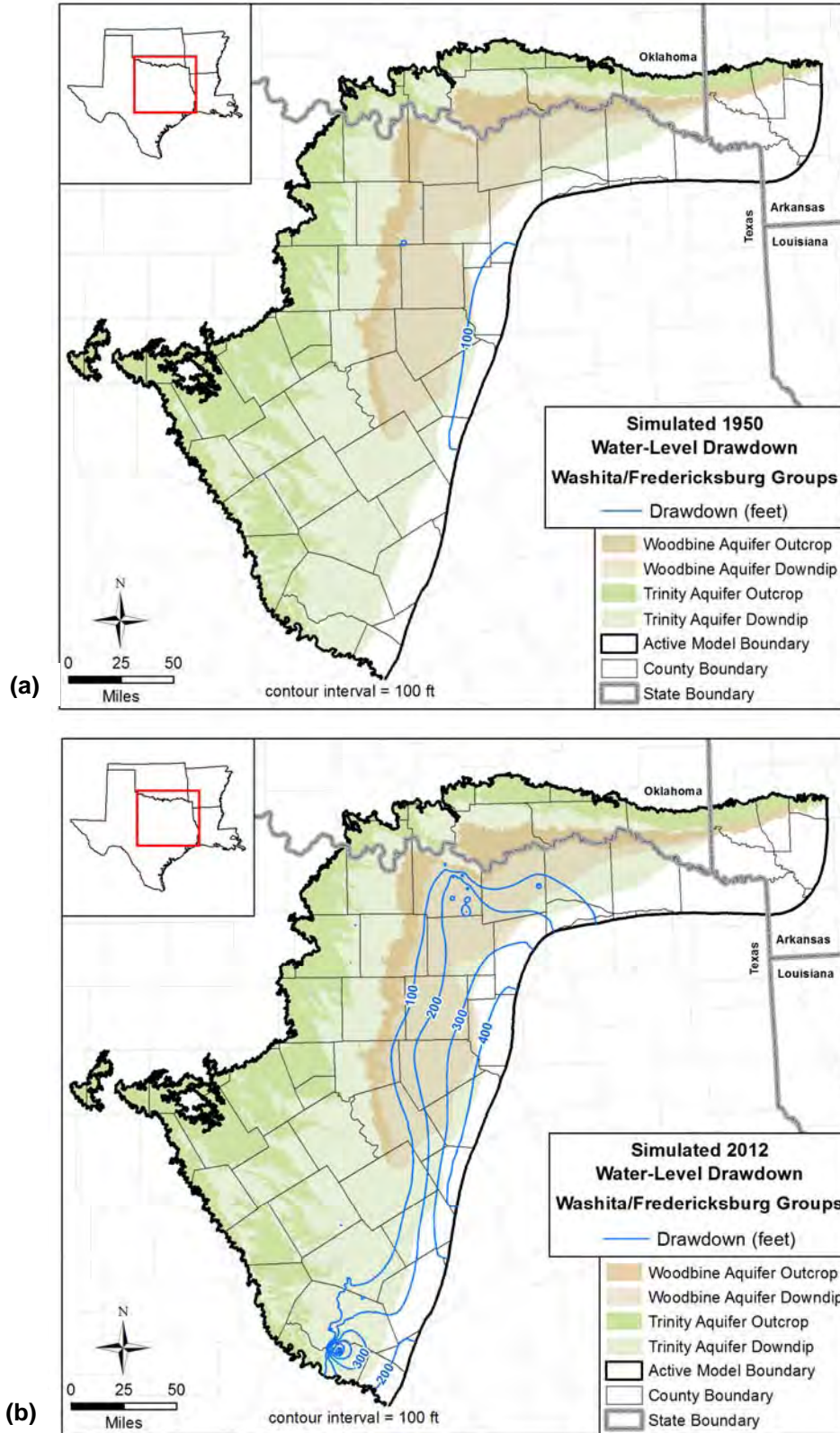
**Figure 9.2.15   Simulated drawdown in feet in the Washita/Fredericksburg groups in (a) 1950 and
(b) 2012.**
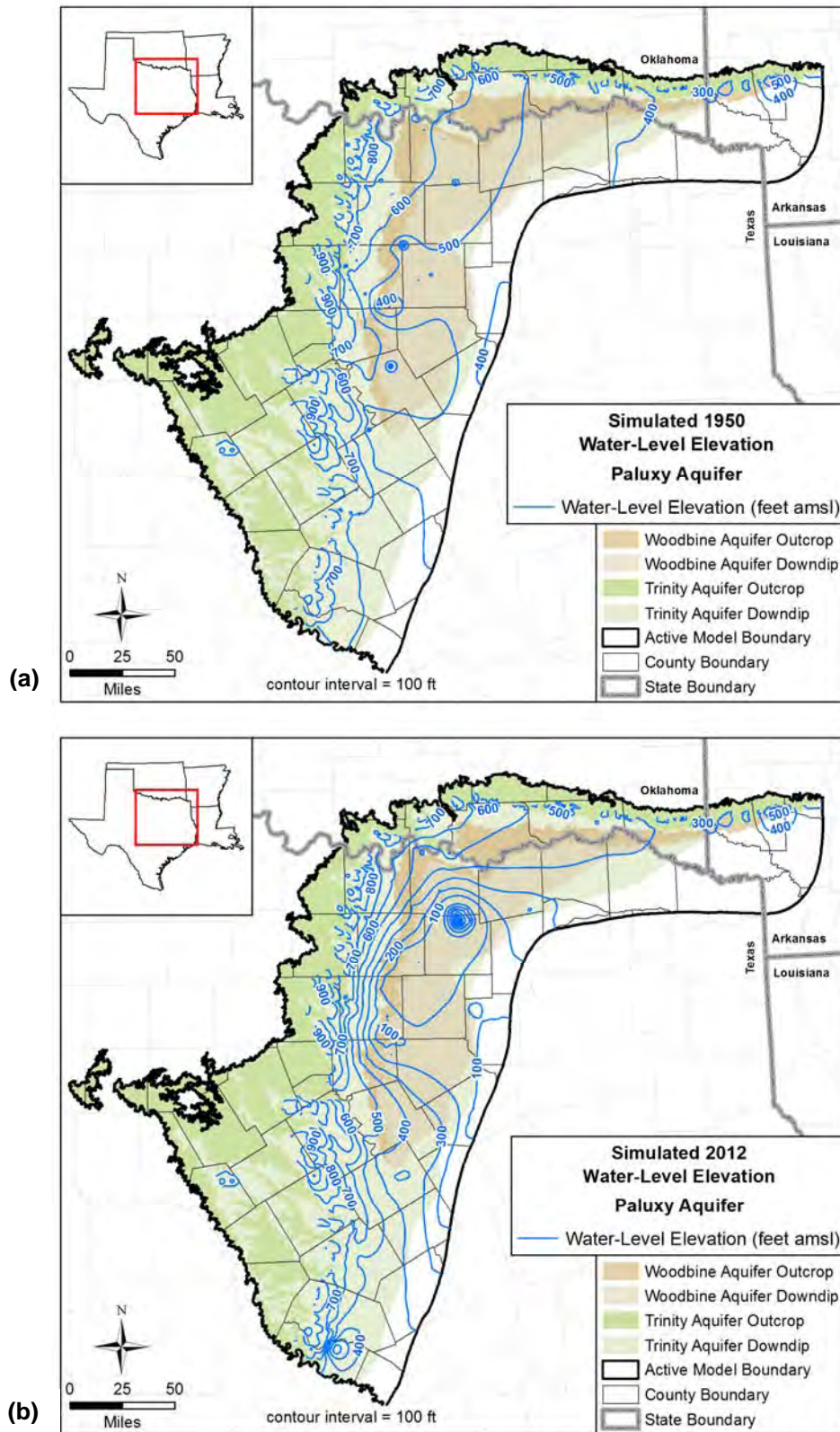
Figure 9.2.16 Simulated water-level elevations (hydraulic heads) in feet amsl in the Paluxy Aquifer in (a) 1950 and (b) 2012.
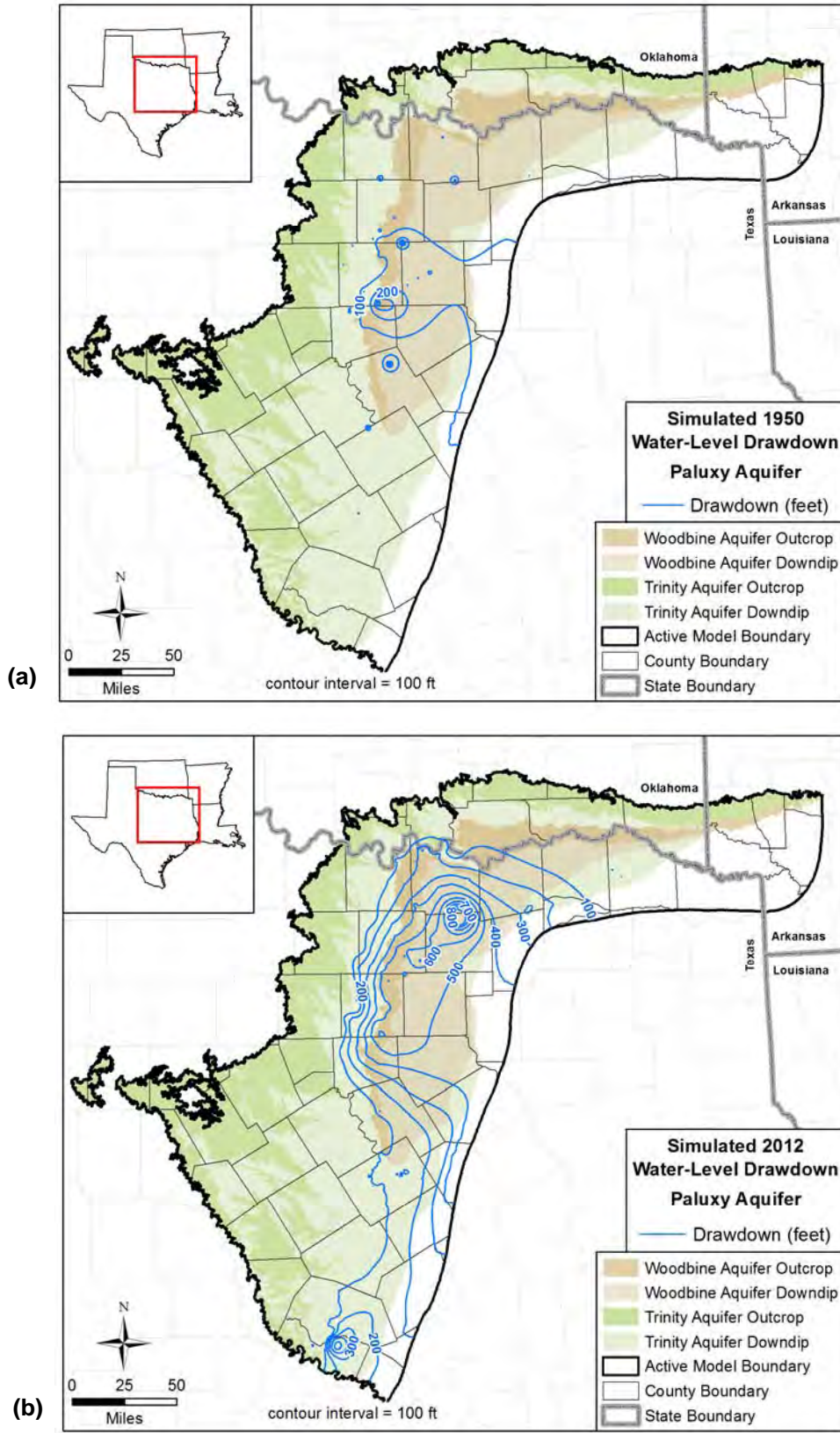
Figure 9.2.17   Simulated drawdown in feet in the Paluxy Aquifer in (a) 1950 and (b) 2012.
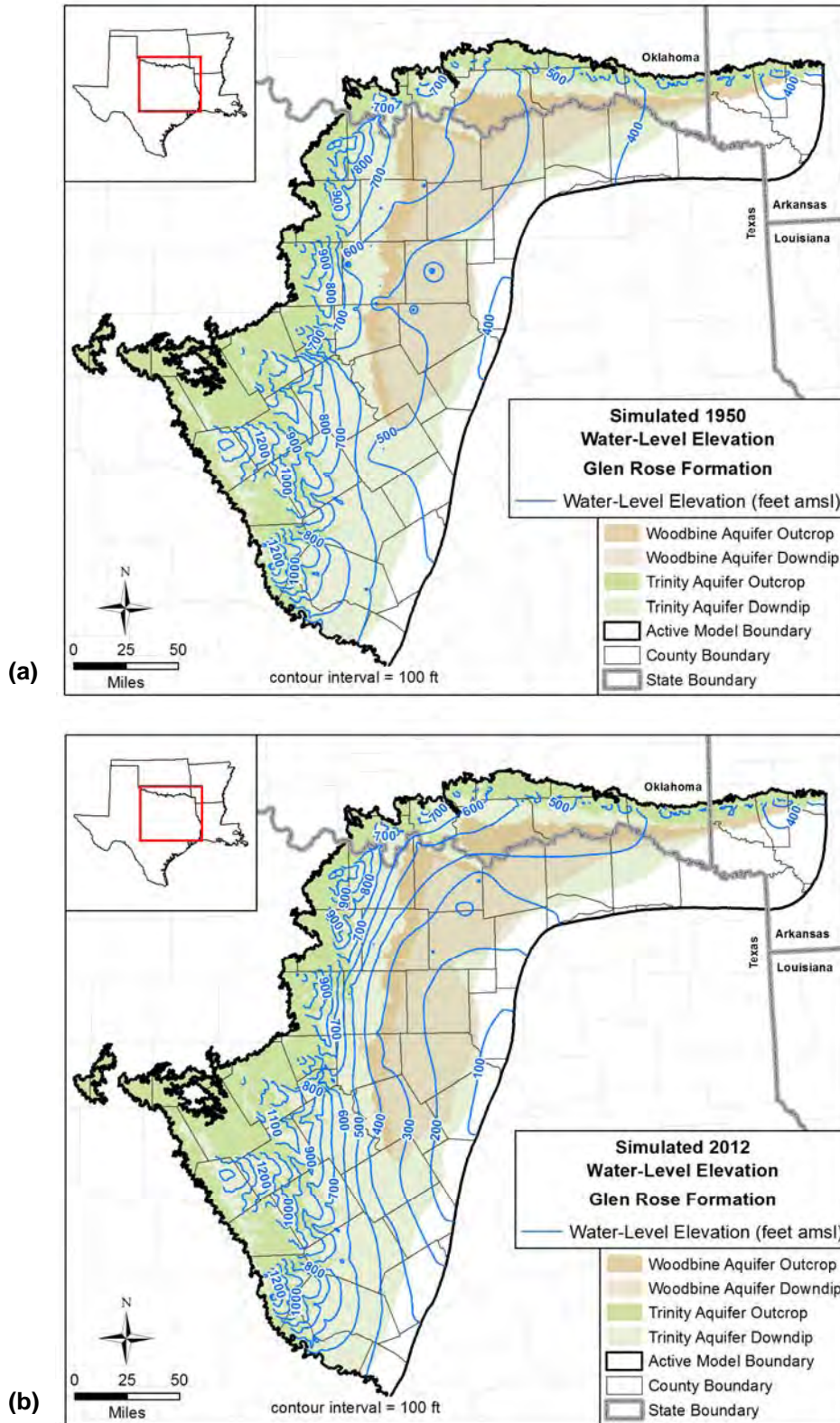
Figure 9.2.18   Simulated water-level elevations (hydraulic heads) in feet amsl in the Glen Rose Formation in (a) 1950 and (b) 2012.
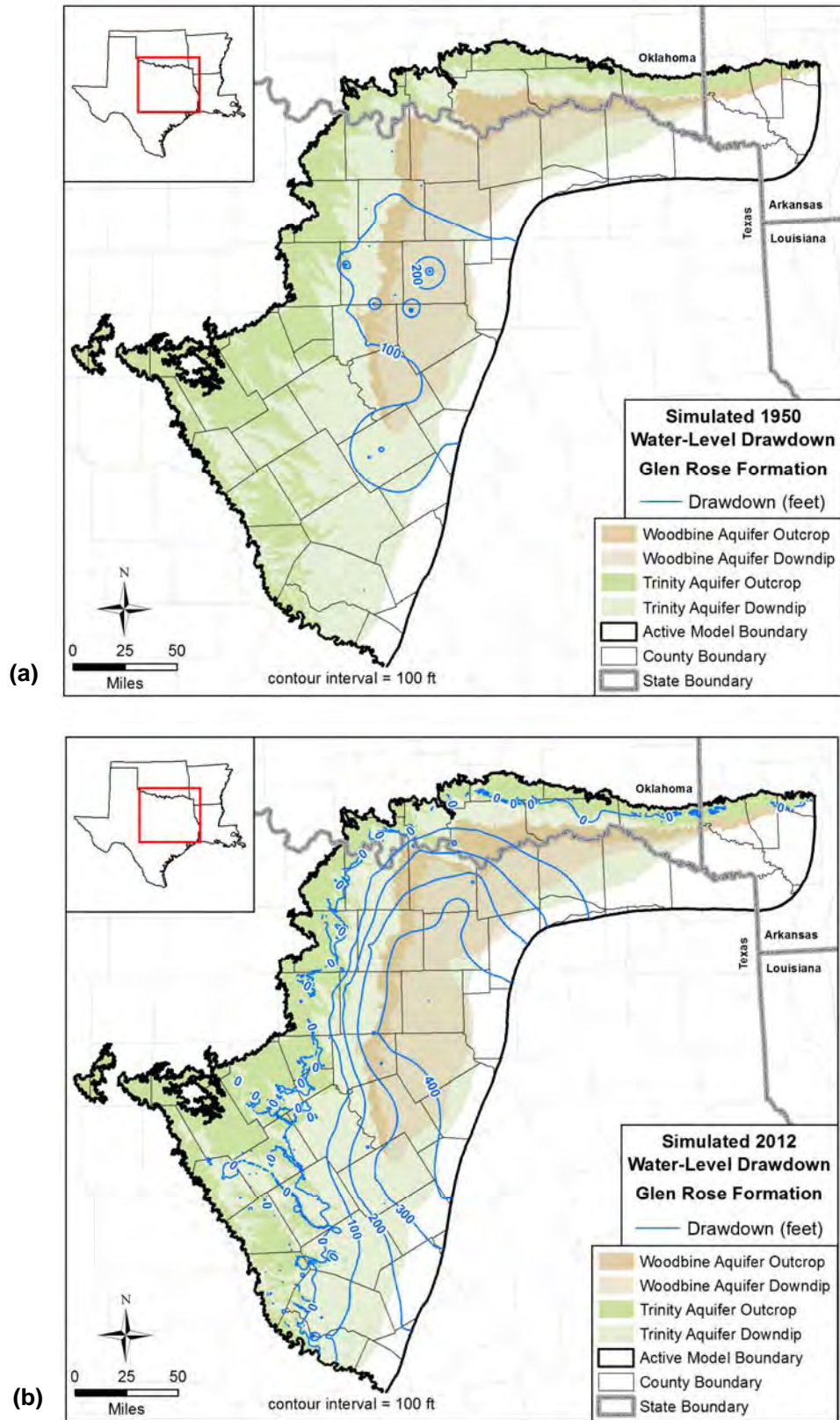
Figure 9.2.19   Simulated drawdown in feet in the Glen Rose Formation in (a) 1950 and (b) 2012.
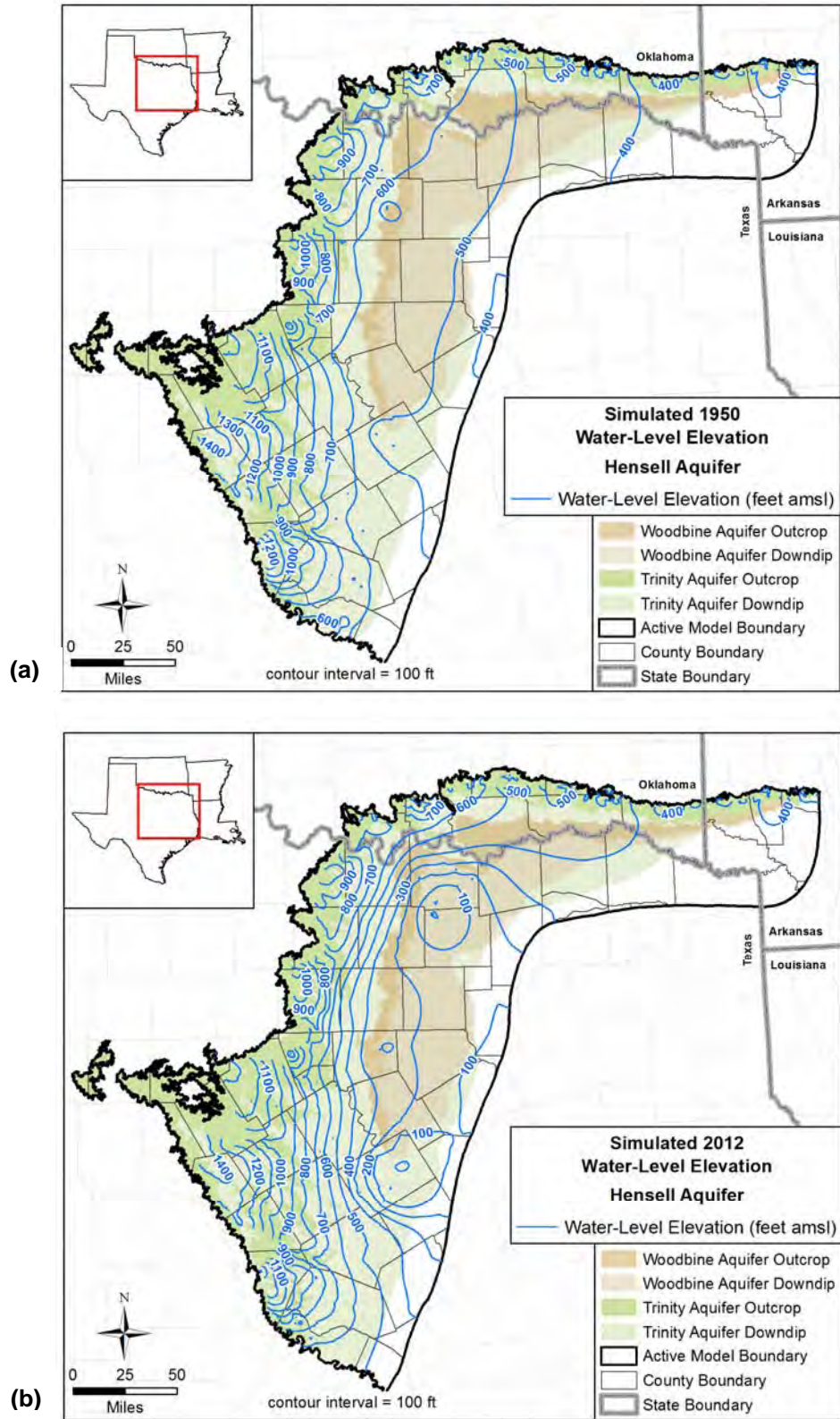
Figure 9.2.20 Simulated water-level elevations (hydraulic heads) in feet amsl in the Hensell Aquifer in (a) 1950 and (b) 2012.
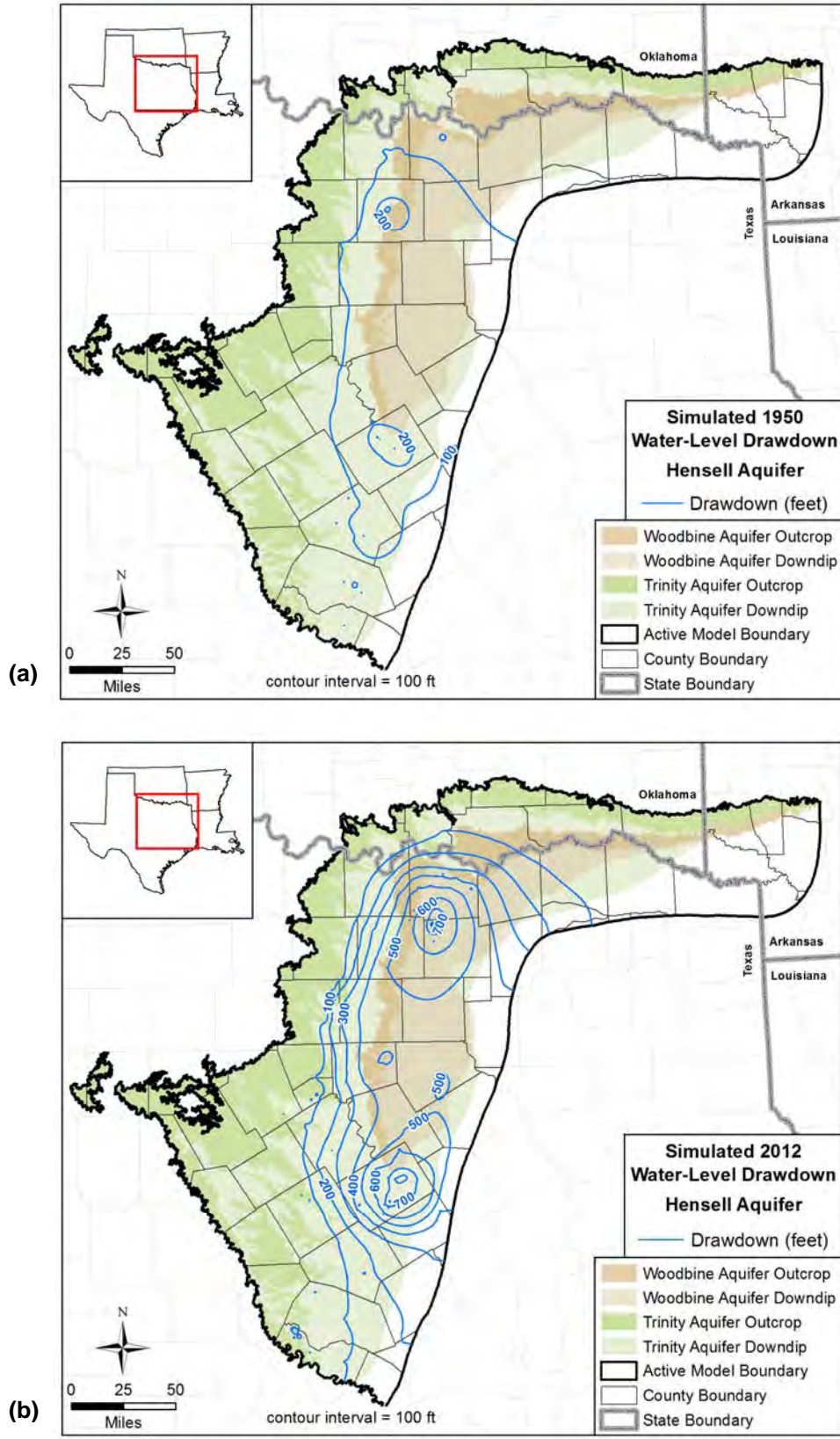
Figure 9.2.21   Simulated drawdown in feet in the Hensell Aquifer in (a) 1950 and (b) 2012.
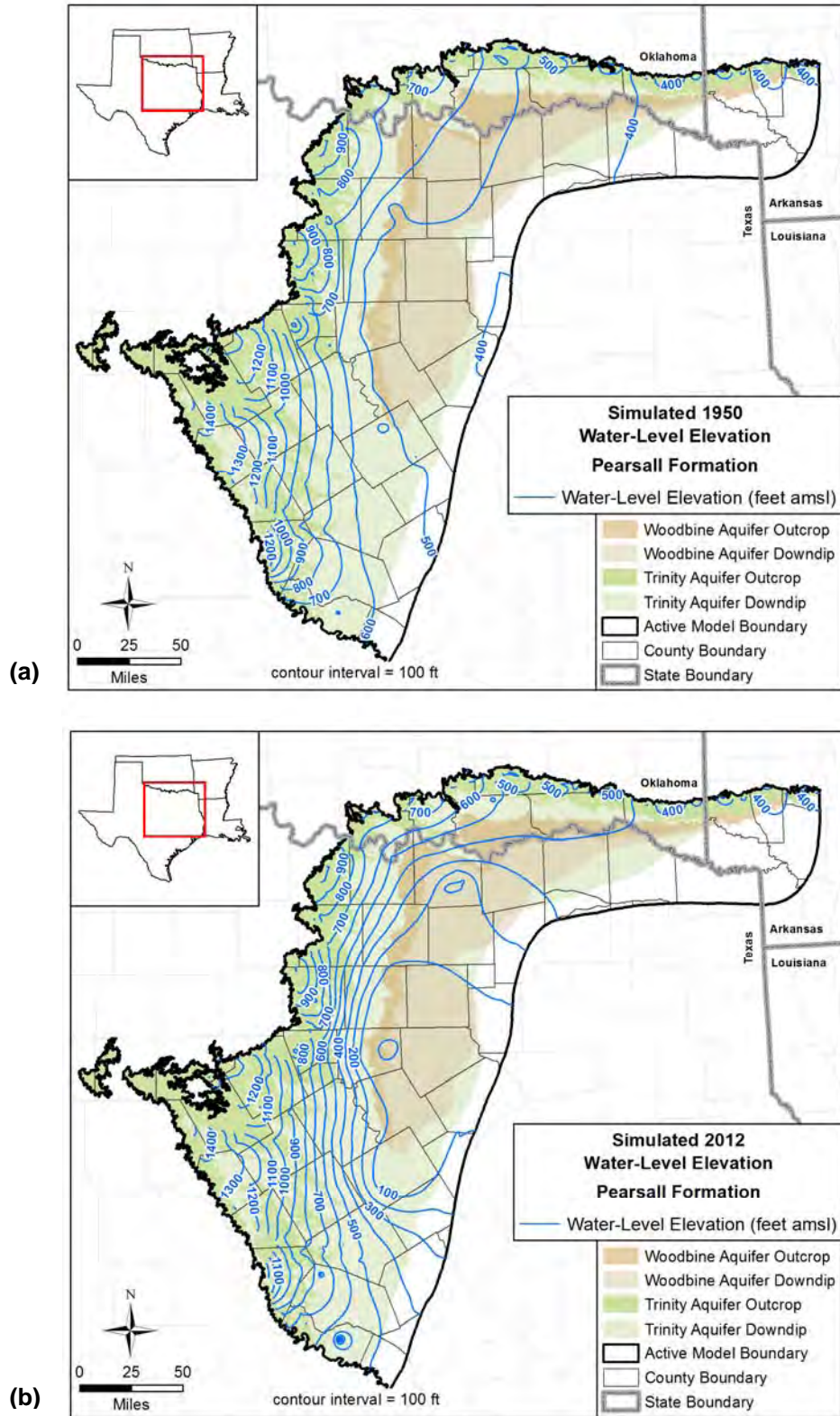
**Figure 9.2.22   Simulated water-level elevations (hydraulic heads) in feet amsl in the Pearsall
Formation in (a) 1950 and (b) 2012.**
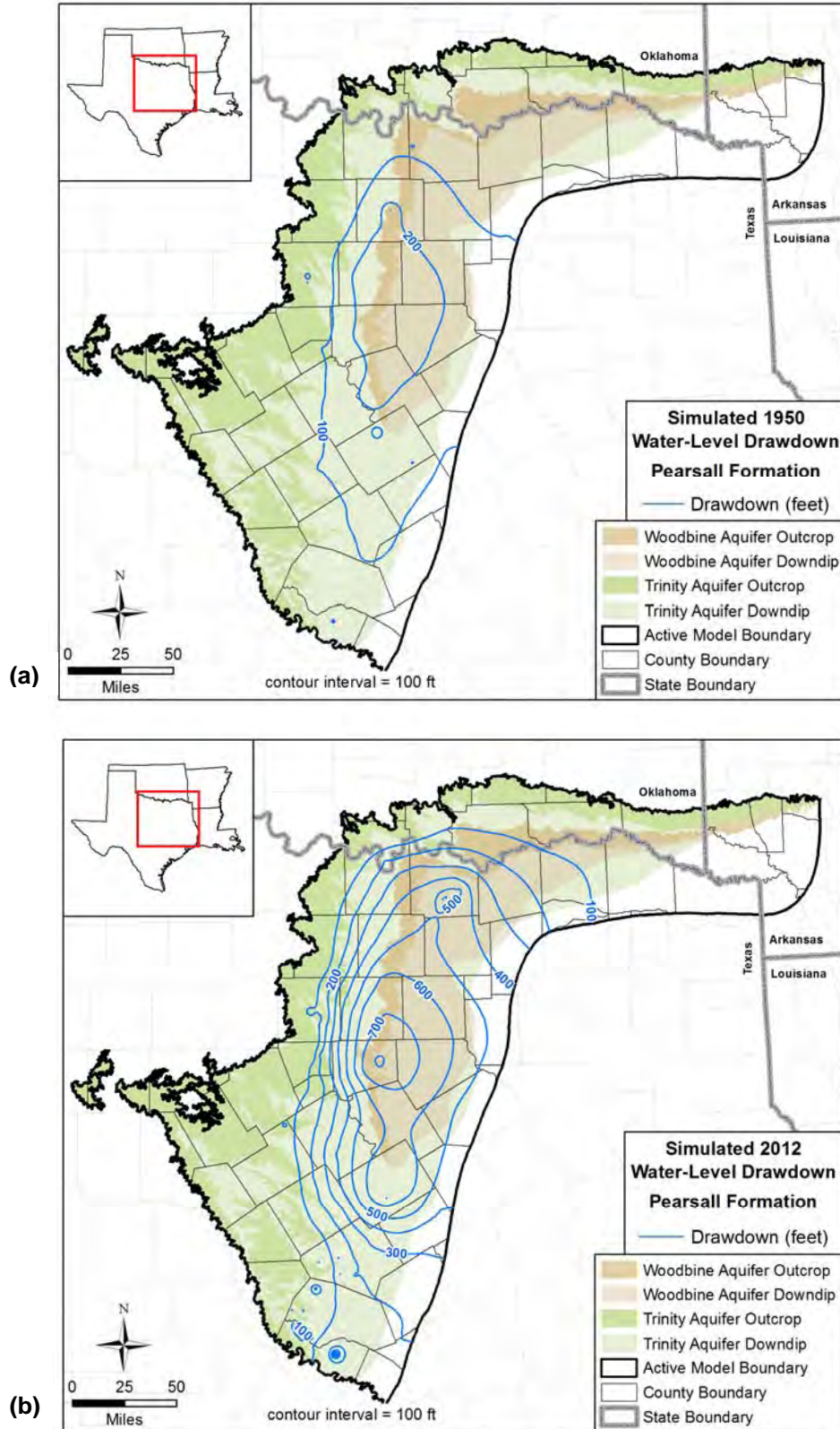
Figure 9.2.23   Simulated drawdown in feet in the Pearsall Formation in (a) 1950 and (b) 2012.
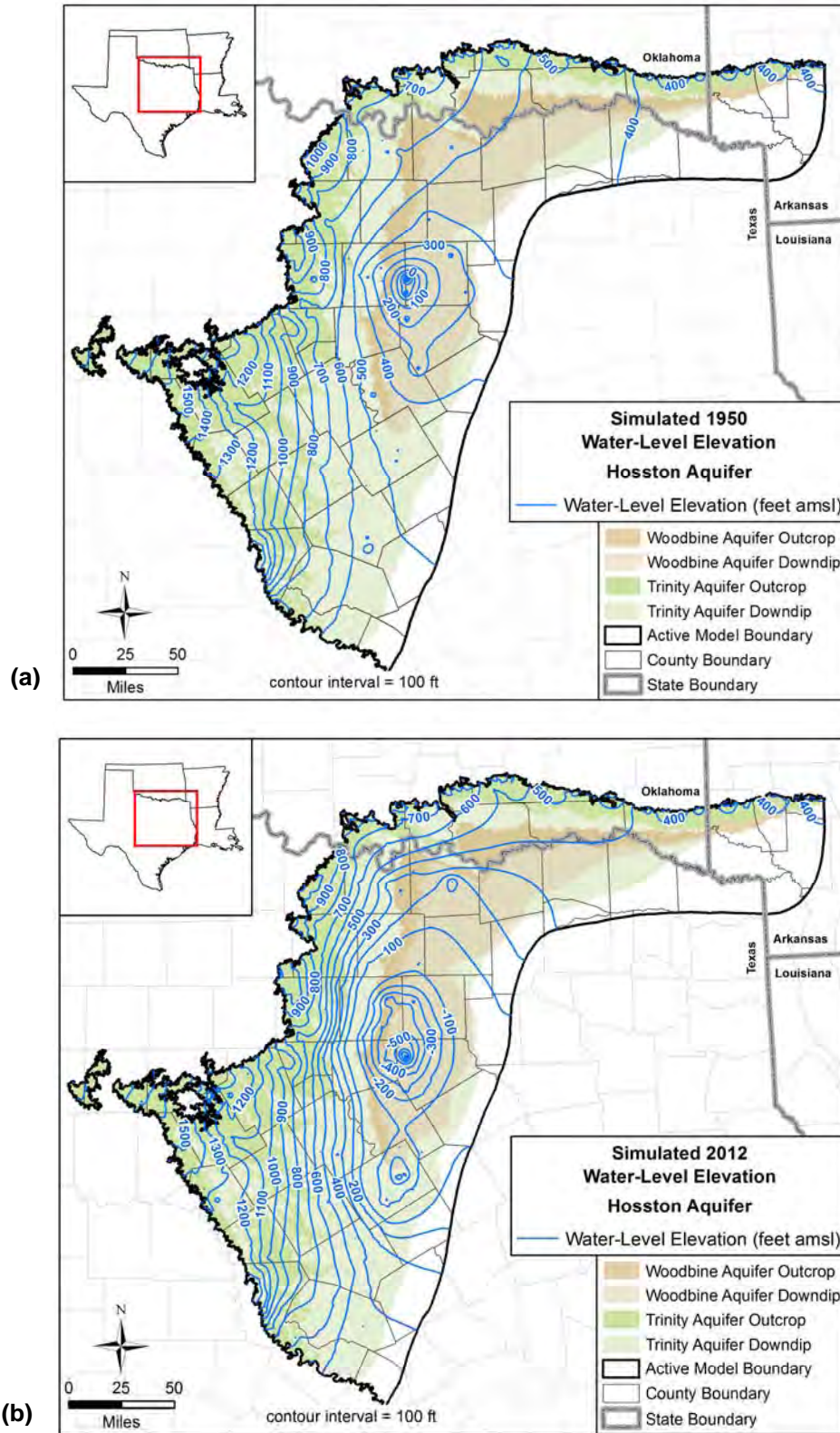
Figure 9.2.24 **Simulated water-level elevations (hydraulic heads) in feet amsl in the Hosston
Aquifer in (a) 1950 and (b) 2012.**
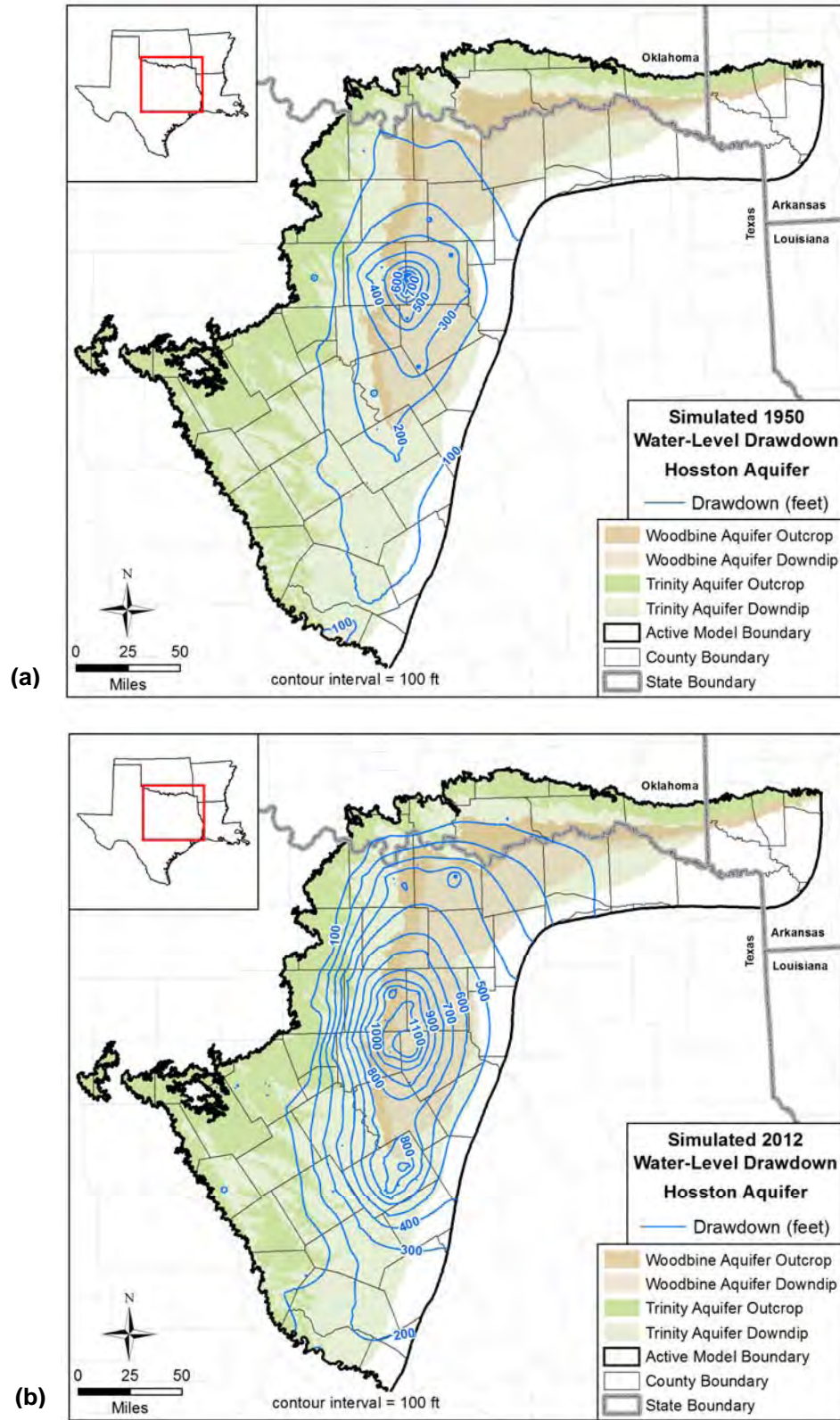
Figure 9.2.25   Simulated drawdown in feet in the Hosston Aquifer in (a) 1950 and (b) 2012.

This page intentionally left blank.
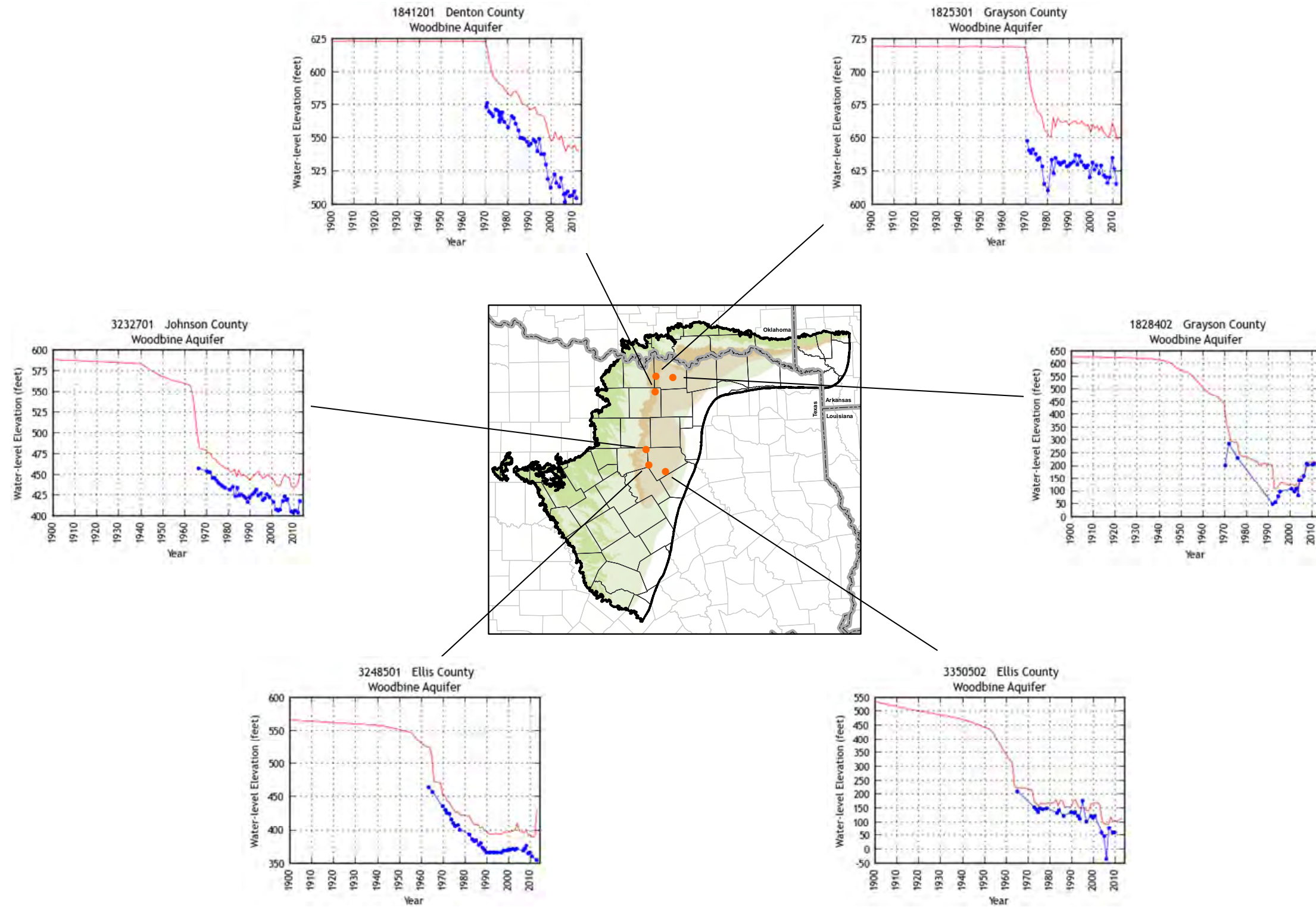
Figure 9.2.26   Selected hydrographs for wells completed in the Woodbine Aquifer showing hydraulic heads in feet amsl. (Symbols indicate observed hydraulic heads and solid lines indicate simulated hydraulic heads.)
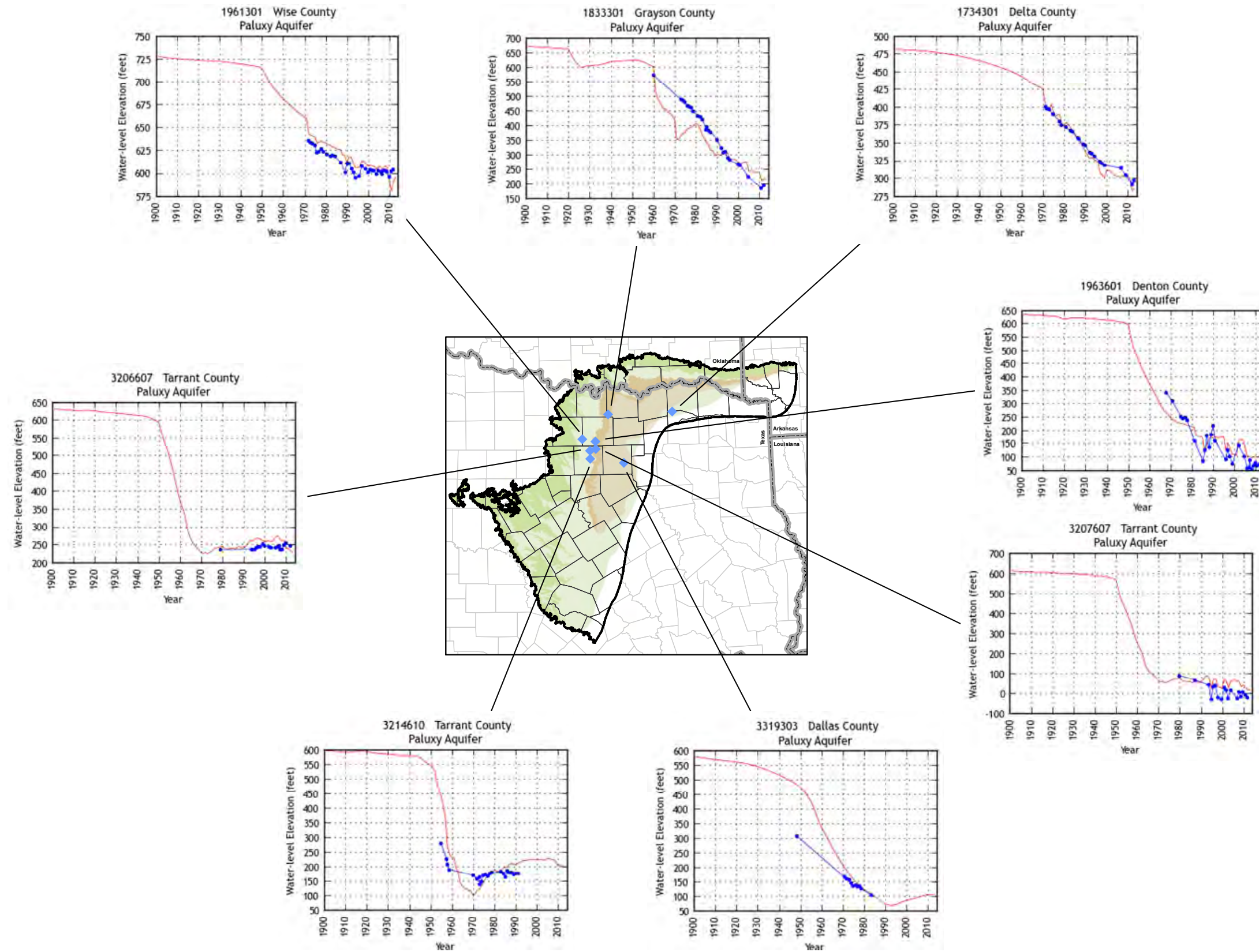
Figure 9.2.27   Selected hydrographs for wells completed in the Paluxy Aquifer showing hydraulic heads in feet amsl. (Blue lines and symbols indicate observed hydraulic heads and red lines indicate simulated hydraulic heads.)
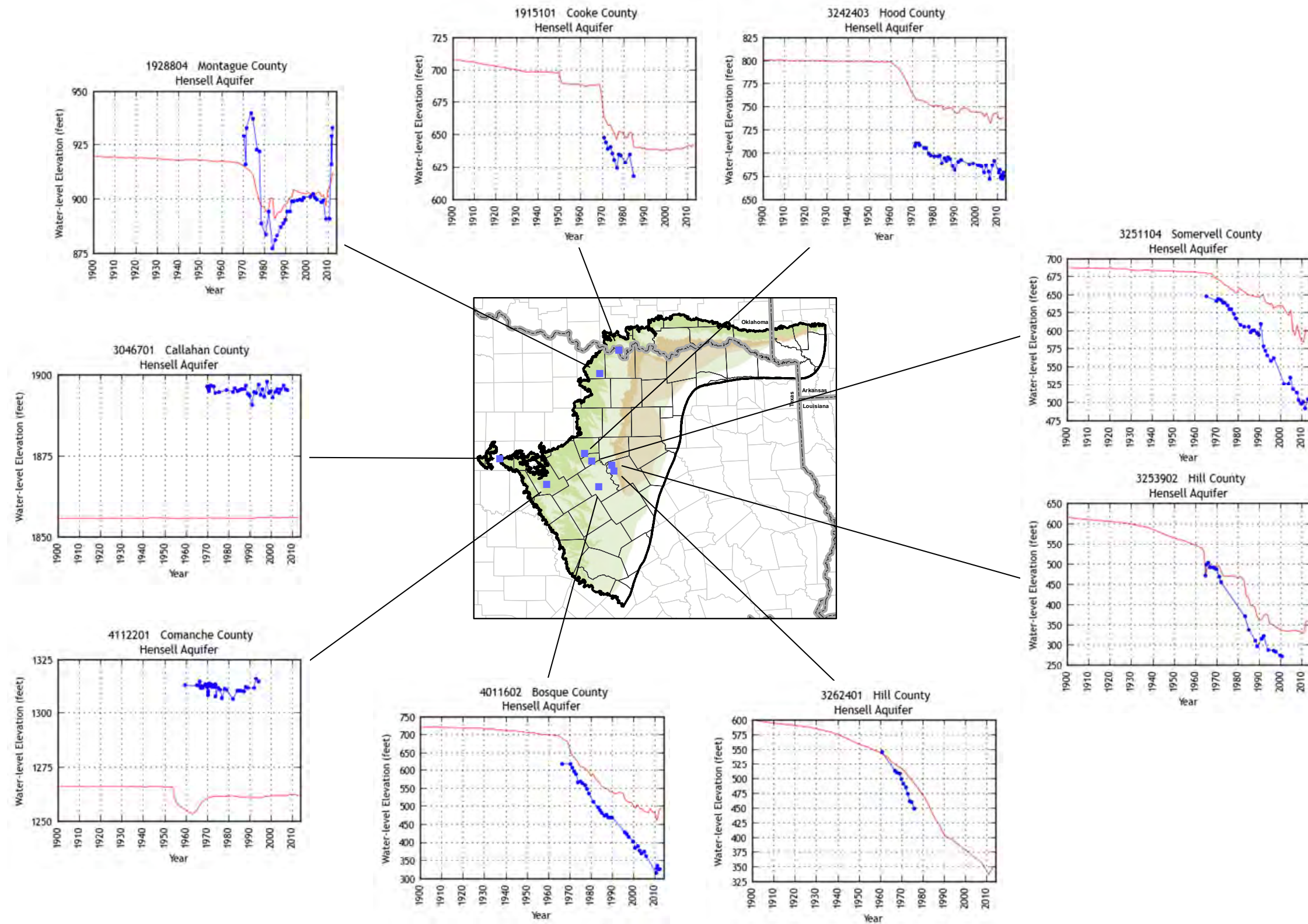
Figure 9.2.28   Selected hydrographs for wells completed in the Hensell Aquifer showing hydraulic heads in feet amsl. (Blue lines and symbols indicate observed hydraulic heads and red lines indicate simulated hydraulic heads.)
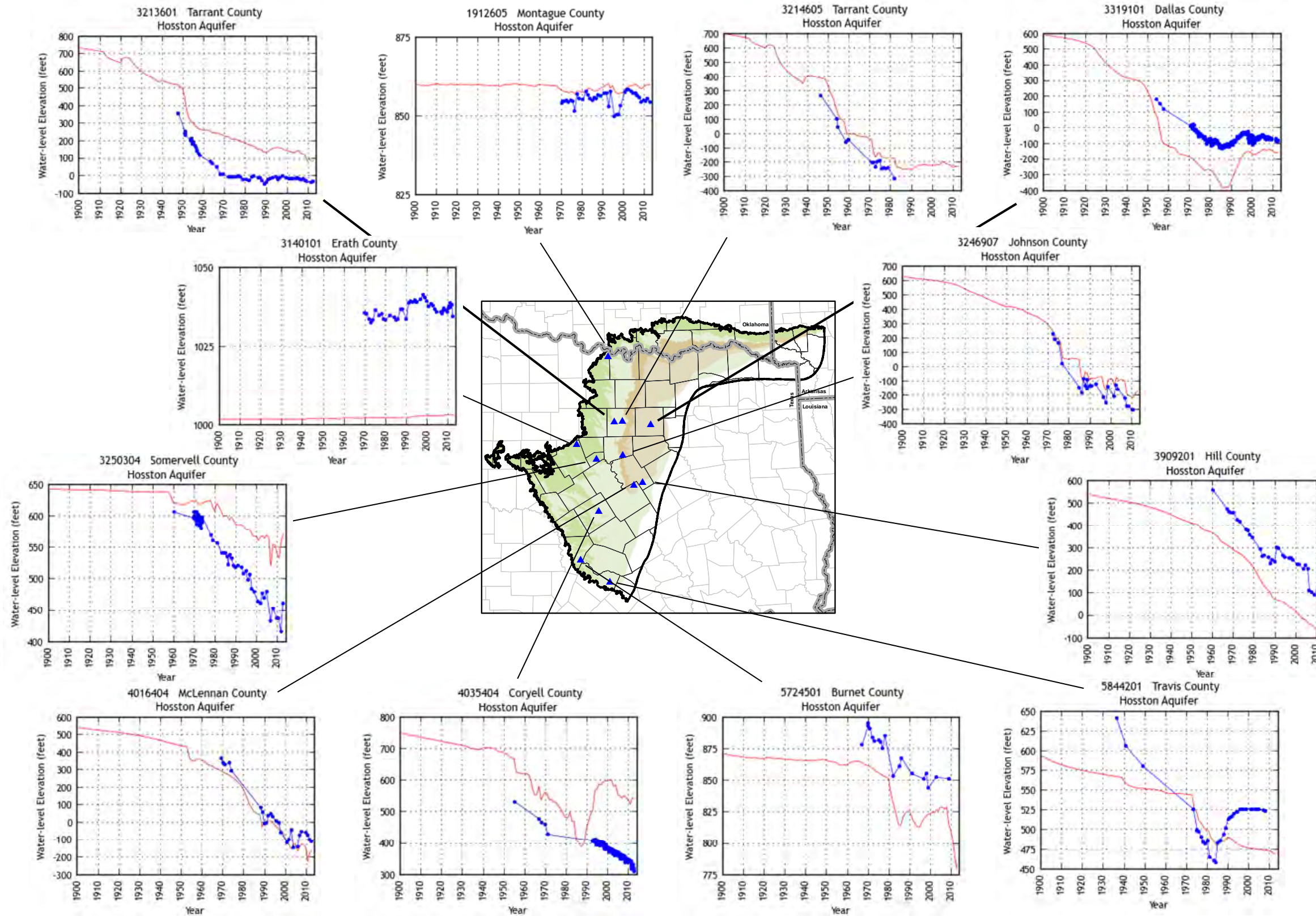
Figure 9.2.29   Selected hydrographs for wells completed in the Hosston Aquifer showing hydraulic heads in feet amsl. (Blue lines and symbols indicate observed hydraulic heads and red lines indicate simulated hydraulic heads.)
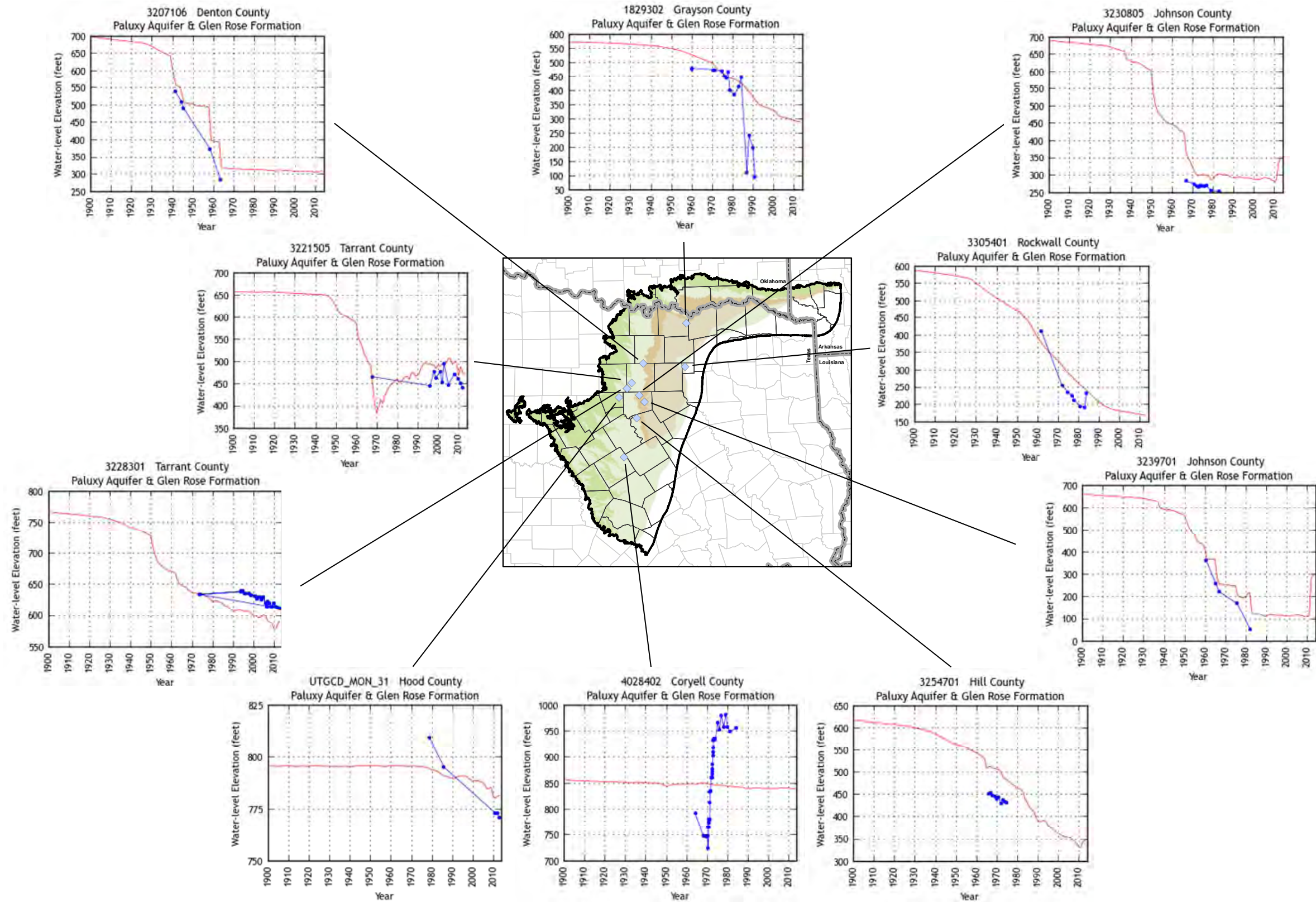
Figure 9.2.30   Selected hydrographs for wells completed in both the Paluxy Aquifer and Glen Rose Formation showing hydraulic heads in feet amsl. (Blue lines and symbols indicate observed hydraulic heads and red lines indicate simulated hydraulic heads.)
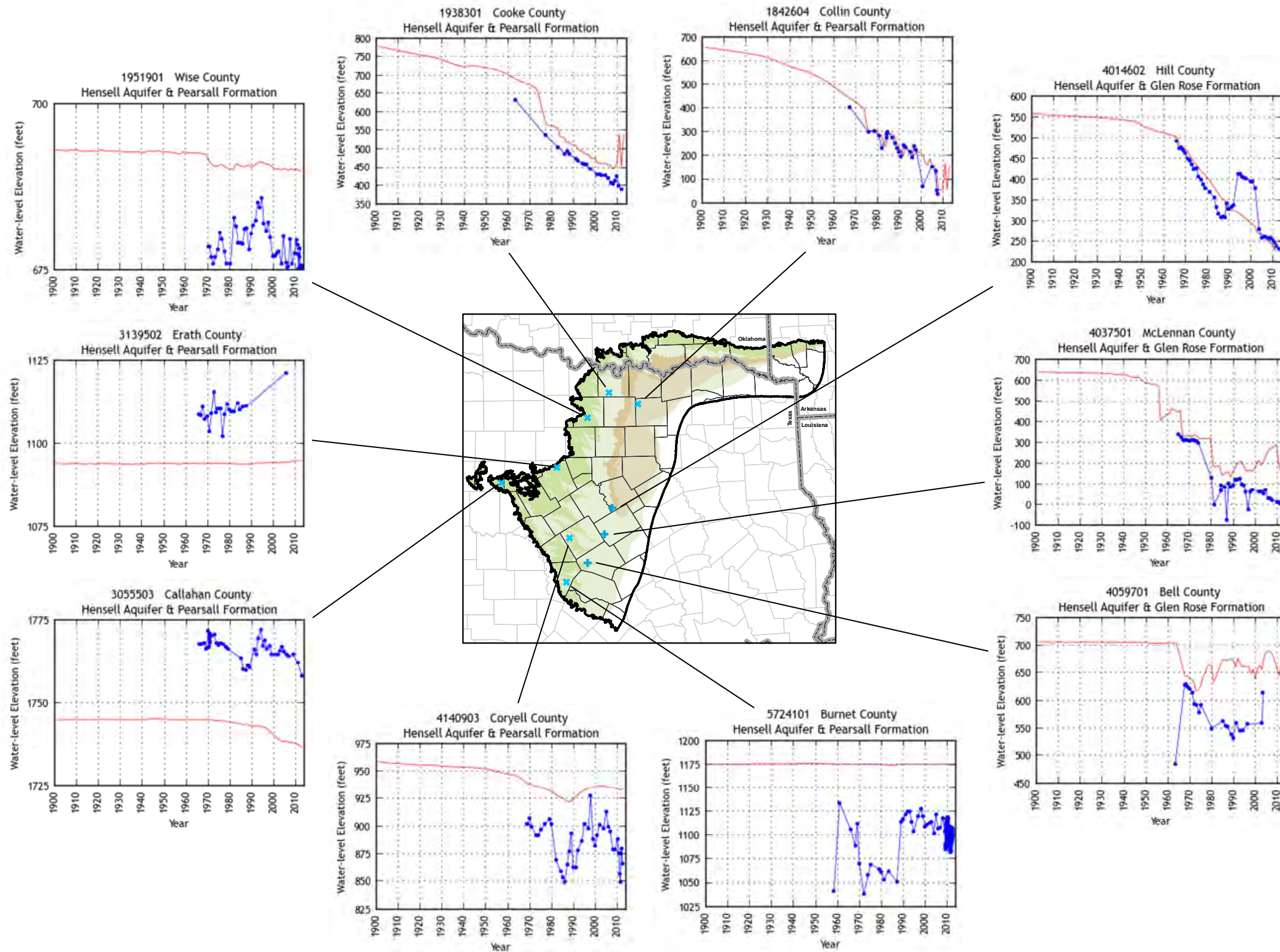
Figure 9.2.31 Selected hydrographs for wells completed in both the Hensell Aquifer and Glen Rose Formation or both the Hensell Aquifer and Pearsall Formation showing hydraulic heads in feet amsl. (Blue lines and symbols indicate observed hydraulic heads and red lines indicate simulated hydraulic heads.)
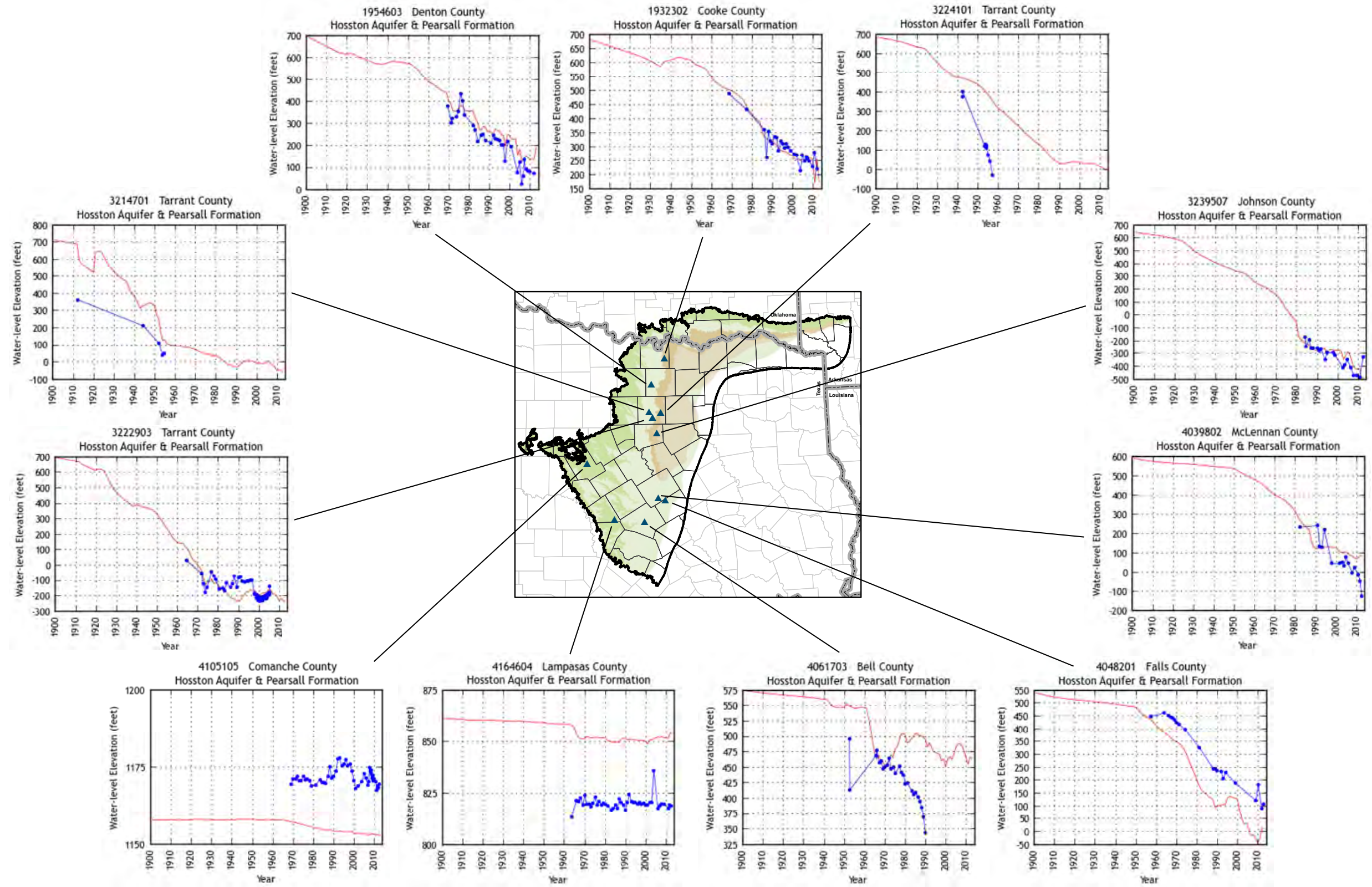
Figure 9.2.32 Selected hydrographs for wells completed in both the Hosston Aquifer and Pearsall Formation showing hydraulic heads in feet amsl. (Blue lines and symbols indicate observed hydraulic heads and red lines indicate simulated hydraulic heads.)
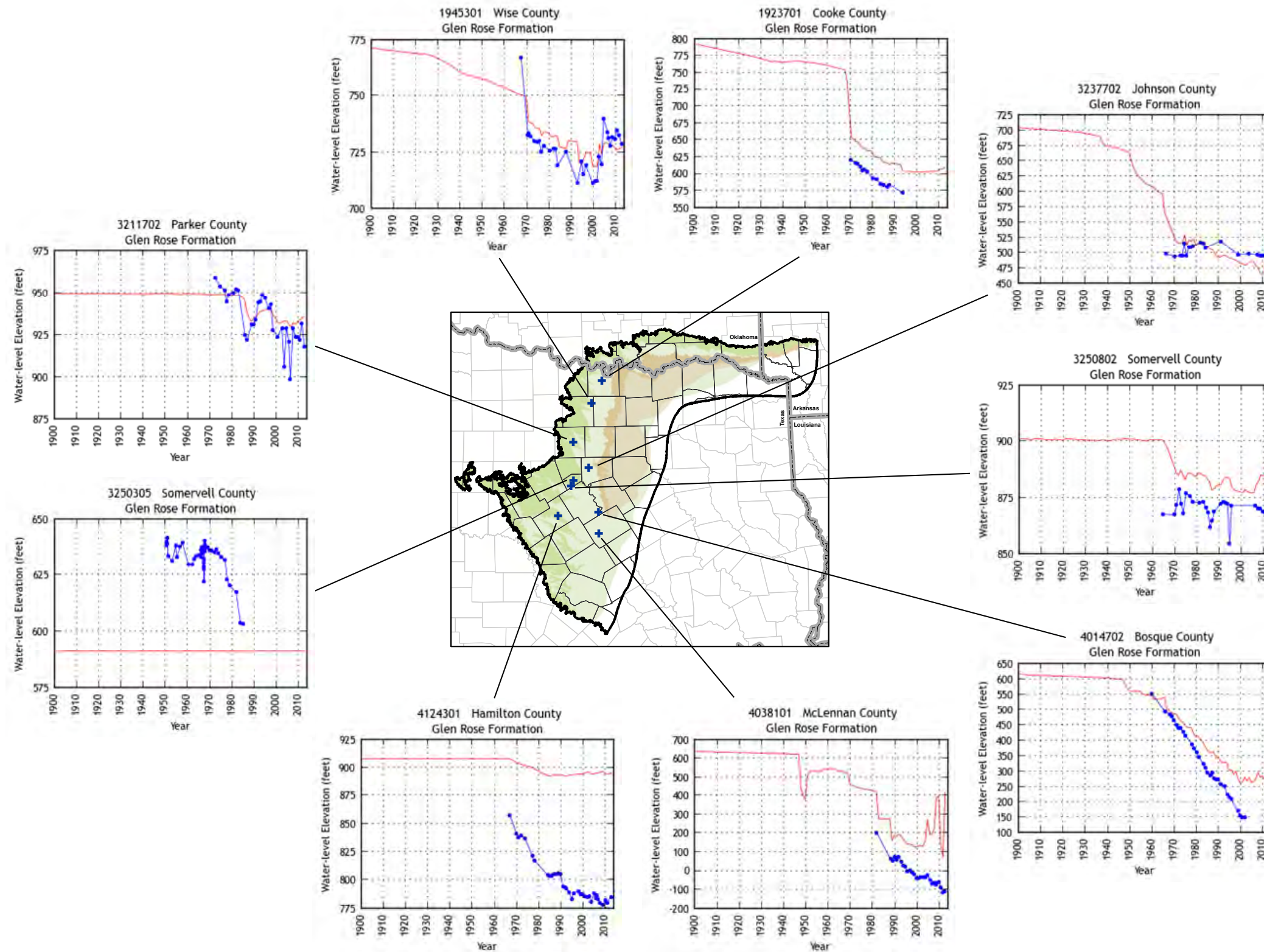
Figure 9.2.33   Selected hydrographs for wells completed in the Glen Rose Formation showing hydraulic heads in feet amsl. (Blue lines and symbols indicate observed hydraulic heads and red lines indicate simulated hydraulic heads.)
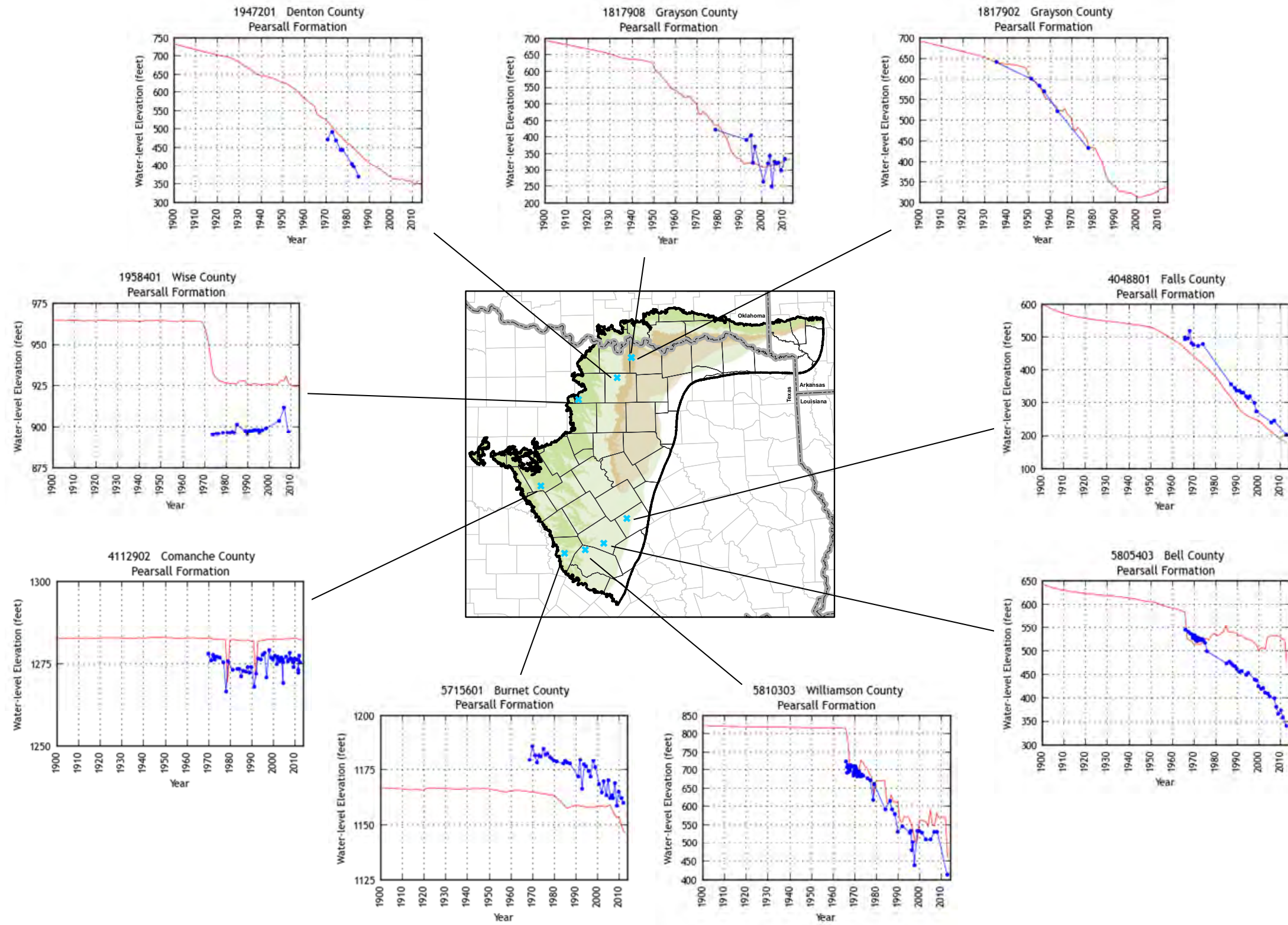
Figure 9.2.34   Selected hydrographs for wells completed in the Pearsall Formation showing hydraulic heads in feet amsl. (Blue lines and symbols indicate observed hydraulic heads and red lines indicate simulated hydraulic heads.)
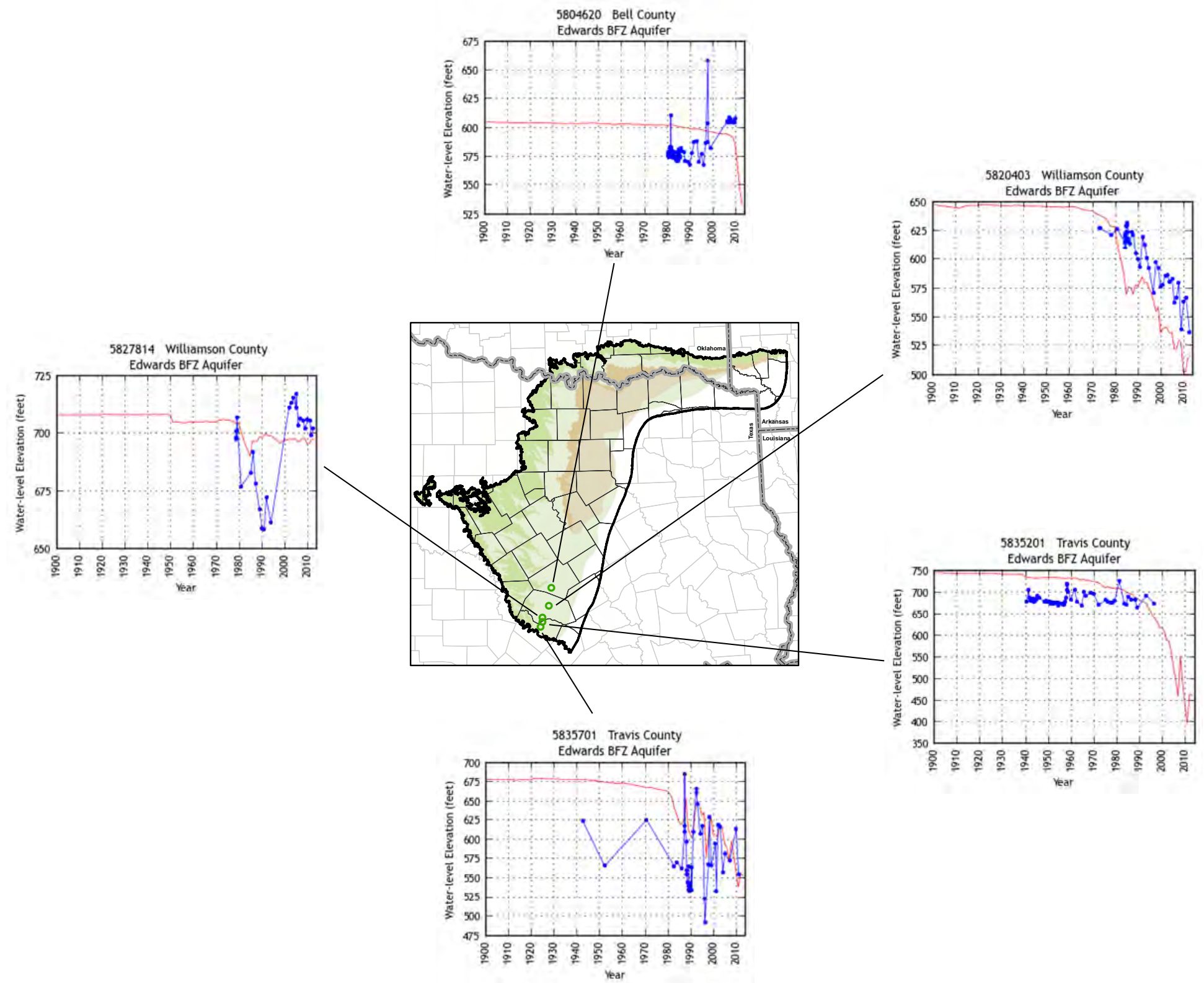
Figure 9.2.35   Selected hydrographs for wells completed in the Edwards BFZ Aquifer showing hydraulic heads in feet amsl. (Blue lines and symbols indicate observed hydraulic heads and red lines indicate simulated hydraulic heads.)
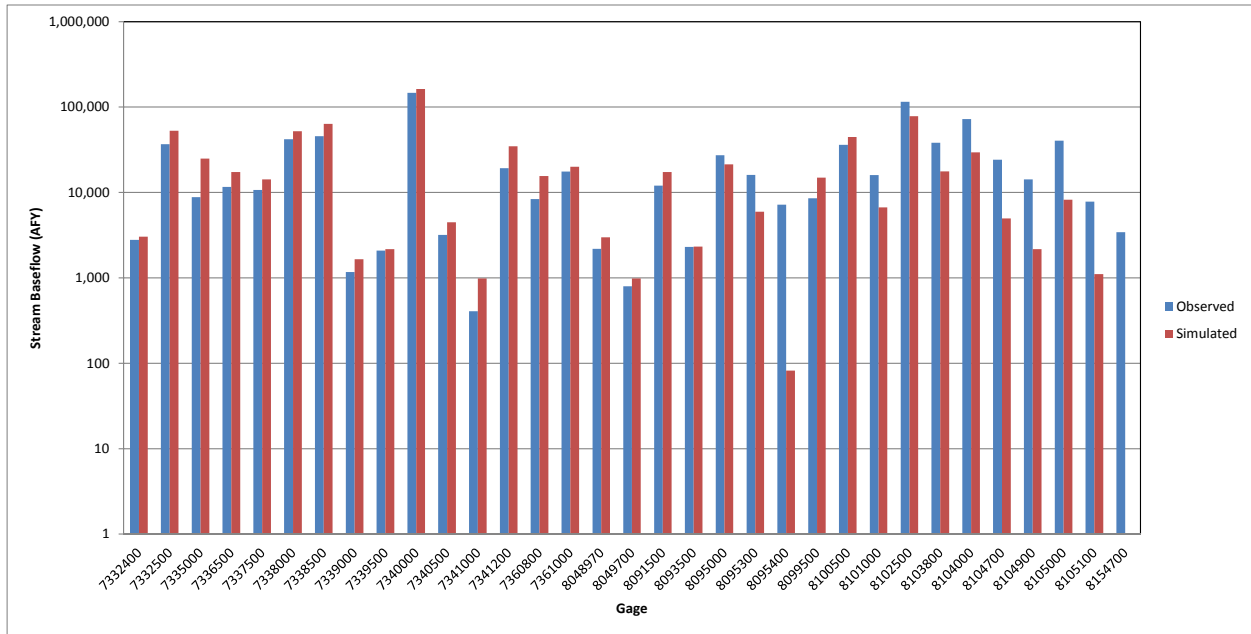
Figure 9.2.36   Observed and simulated base flow to streams.
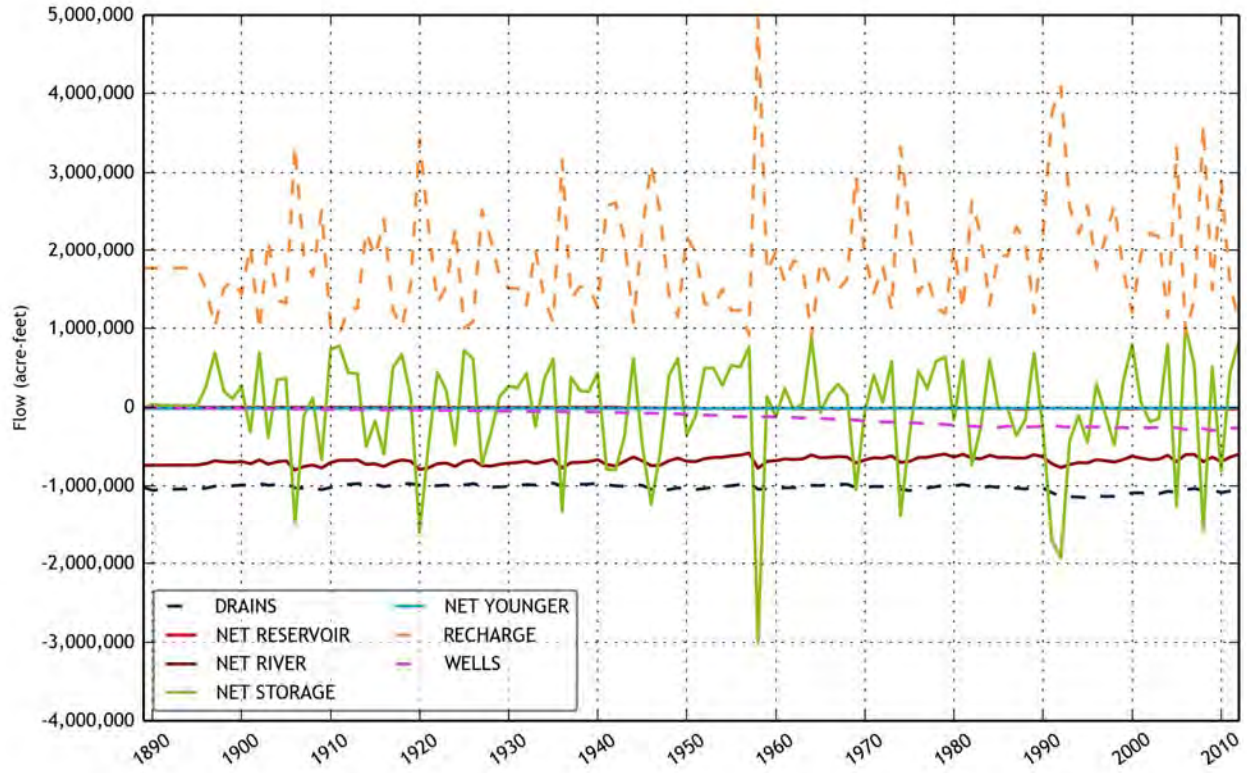
Figure 9.2.37   Total model water budget in AFY from 1890 to 2012.

9.3 Sensitivity Analysis

A sensitivity analysis was performed on the calibrated transient model. Section 8.3 discusses the approach for sensitivity analyses for the steady-state model. The analyses were similar for the transient model. In addition to the sensitivities for the steady-state model, the transient model adds storage properties, reservoirs, and pumping sensitivities, for a total of 39 combinations of input parameters and output metrics:

1. Horizontal hydraulic conductivity of the surficial outcrop area of Layer 1 (hydraulic head, flow), as well as the seven confined layers (hydraulic head).

2. Vertical hydraulic conductivity of the younger formations (hydraulic head), and the seven confined layers (hydraulic head).

3. Specific yield of the surficial outcrop area of Layer 1 (hydraulic head), and specific storage of the seven confined layers (hydraulic head).

4. Pumping (hydraulic head)

5. Recharge in the surficial outcrop area of Layer 1 (hydraulic head, flow).

6. River conductance in the surficial outcrop area of Layer 1 (hydraulic head, flow).

7. Reservoir conductance in the surficial outcrop area of Layer 1 (hydraulic head, flow).

8. Conductance for the head dependent boundary cells attached to the younger formations (hydraulic head).

9. Conductance in the surficial outcrop area of Layer 1 drain boundaries representing groundwater ET (hydraulic head, flow).

10. Conductance in the surficial outcrop area of Layer 1 drain boundaries representing ephemeral streams (hydraulic head, flow).

11. Conductance in the surficial outcrop area of Layer 1 drain boundaries representing springs (hydraulic head, flow).

Equation 8.3.1 was used for sensitivities 4 and 6, while equation 8.3.2 was used for the remaining sensitivities.

Figure 9.3.1 shows the hydraulic head sensitivity for variation in horizontal hydraulic conductivity in the surficial outcrop area of Layer 1. The response is nearly identical to that for the steady-state model, with hydraulic heads increasing with decreasing conductivity, due to

restriction in flow out to the boundaries in the surficial outcrop area of Layer 1. Similarly, the response to variation in horizontal hydraulic conductivity in the Woodbine Aquifer, shown in Figure 9.3.2, is similar to the steady-state model. Figure 9.3.3 shows the sensitivity to changing horizontal hydraulic conductivity in the Washita/Fredericksburg groups. The younger formations show increased hydraulic heads, similar to the steady-state model, because the initial hydraulic heads are higher due to higher initial outcrop/shallow hydraulic heads, while all other layers show decreased hydraulic heads. These decreased hydraulic heads are the result of increased drawdown in the Washita/Fredericksburg groups, and the propagation of this drawdown to other layers throughout the transient period. Figures 9.3.4 through 9.3.8 show similar trends, with significantly increased drawdown (decreased hydraulic heads) in the layer in which the horizontal hydraulic conductivity is reduced, and corresponding additional drawdown in other layers, depending on their vertical proximity to the affected layer. For example, Figure 9.3.8 shows that variation in the horizontal hydraulic conductivity in the Hosston Aquifer results in the largest decrease in hydraulic heads in that aquifer, followed in ascending order by the Pearsall Aquifer, Hensell Aquifer, and Glen Rose Formation.

Figure 9.3.9 shows the hydraulic head sensitivity to changes in vertical hydraulic conductivity in the younger formations. The results are similar to the steady-state model, with lower vertical conductivity increasing hydraulic heads due to restriction in upward discharge of deeper flow paths. Similarly, Figure 9.3.10 shows a transient response that is similar to the steady-state response in Figure 8.3.10 for changes in the vertical hydraulic conductivity of the Woodbine Aquifer. The response in the Woodbine Aquifer itself is more mixed since, with decreased vertical hydraulic conductivity, initial hydraulic heads are higher, but once pumping begins, hydraulic heads trend lower than for base case.

Figure 9.3.11 shows the same mixed result to changing vertical hydraulic conductivity in the Washita/Fredericksburg groups as was seen for the steady-state model, with a change in the Paluxy Aquifer response, due to the effects of pumping. Figure 9.3.12 shows a clear decrease in hydraulic heads in the Paluxy Aquifer with decreasing vertical hydraulic conductivity in the Paluxy Aquifer, with a minor effect on the other layers. Figure 9.3.13 shows a more mixed response to changing vertical hydraulic conductivity in the Glen Rose Formation. Hydraulic heads in the Glen Rose Formation are higher overall, due to the decreased impact of drawdown

in adjacent and deeper layers. Figure 9.3.14 shows a similar effect for the variation in vertical

hydraulic conductivity in the Hensell Aquifer. Figure 9.3.15 shows a clear decrease in hydraulic

heads in the Hosston Aquifer with decreasing vertical hydraulic conductivity in the Pearsall

Formation, indicating that the heavy pumping in the Hosston Aquifer has induced downward

vertical flow from and through the Pearsall Formation in the transient period. Figure 9.3.16

shows a similar decrease in hydraulic heads in the Hosston Aquifer with decreasing vertical

hydraulic conductivity in the Hosston Aquifer, with a similar increase in hydraulic heads in the

Hensell Aquifer and Pearsall Formation, because drawdown in the Hosston Aquifer has less

effect on those units due to the restriction in vertical flow.

Figure 9.3.17 shows the effects of changing specific yield in the unconfined surficial outcrop

area of Layer 1. The overall change in hydraulic head is very small (note the small y-axis range),

with a small decrease in hydraulic heads with decreasing specific yield. A decrease in specific

yield results in more drawdown response to pumping. Figure 9.3.18 shows the sensitivity of

hydraulic heads to changes in specific storage in the confined layers. Similar to specific yield,

lower specific storage results in more drawdown under pumping stress, and lower hydraulic

heads. Figure 9.3.19 shows the sensitivity of hydraulic heads to variation in pumping, with the

expected response, where increased pumping results in decreased hydraulic heads. The Hosston

Aquifer shows the greatest sensitivity to pumping change, followed in ascending order by the

rest of the layers. Similarly, hydraulic heads respond to recharge in the expected way, as shown

in Figure 9.3.20, with increasing hydraulic heads with increasing recharge. The magnitude of the

sensitivity is similar for all of the layers. Figures 9.3.21 through 9.3.26 show the response in

hydraulic heads to variation in the conductances in the various boundaries in the surficial outcrop

area of Layer 1. In all cases, decreasing conductance restricts flow out the boundaries, causing

hydraulic heads to increase in the in steady-state, which propagates to the transient period. This

effect is large enough to not be offset by pumping in the surficial outcrop area of Layer 1 during

the transient period.

Figure 9.3.27 shows the sensitivity of flow to the surficial discharge boundaries due to changes

in horizontal hydraulic conductivity in the surficial outcrop area of Layer 1. The response is

similar to that in the steady-state model, where the high conductivity of the alluvium around the

river boundaries leads to a dominating flow increase in those cells. The sensitivity of flow to

recharge, shown in Figure 9.3.28, has the expected result of increased flow in all boundaries with increased recharge. Figures 9.3.29 through 9.3.33 show similar trends, where an increasing conductance in one of the surficial boundaries increases flow out that boundary, and decreases flow out the remaining boundaries. Both reservoir flow and springflow are such a small portion of the water budget, that changes their flows have virtually no effect on the flow in the other boundaries (Figures 9.3.30 and 9.3.33).
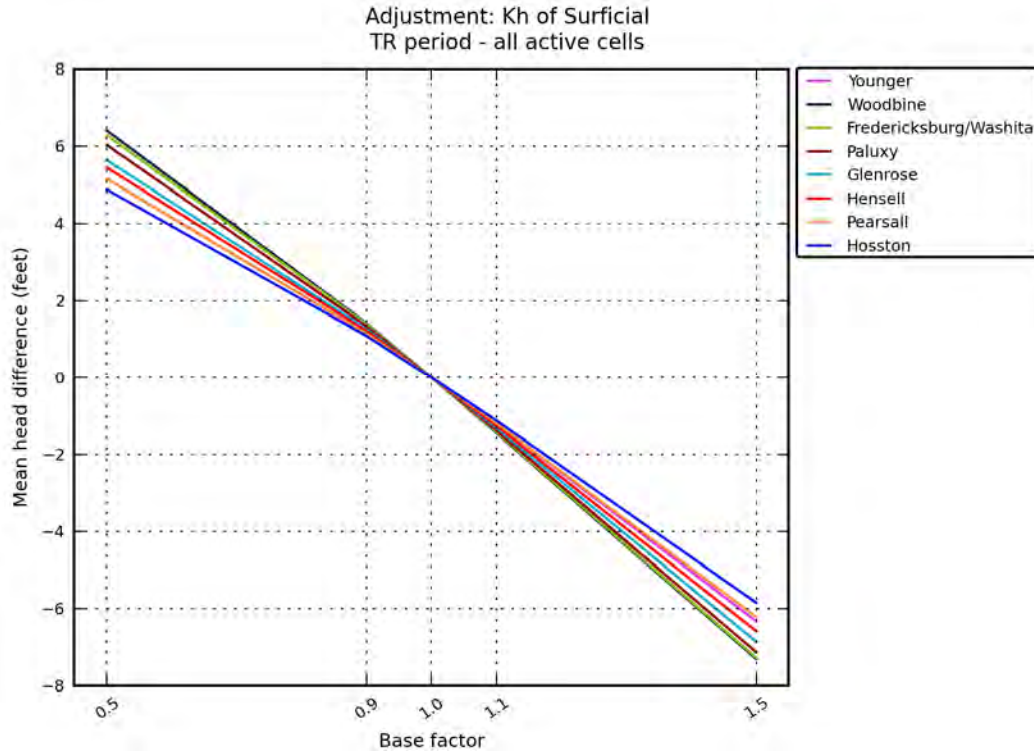
Figure 9.3.1   Hydraulic head sensitivity in feet for the transient model to changes in horizontal hydraulic conductivity of the surficial outcrop area of Layer 1.
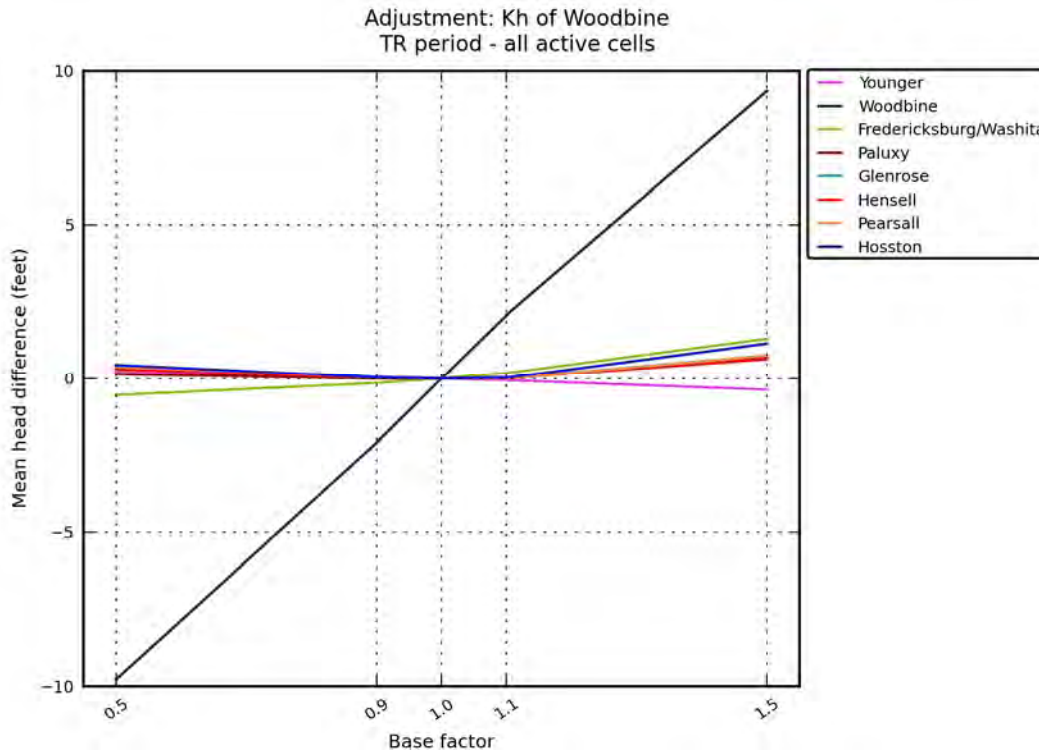
Figure 9.3.2   Hydraulic head sensitivity in feet for the transient model to changes in horizontal hydraulic conductivity of the Woodbine Aquifer.
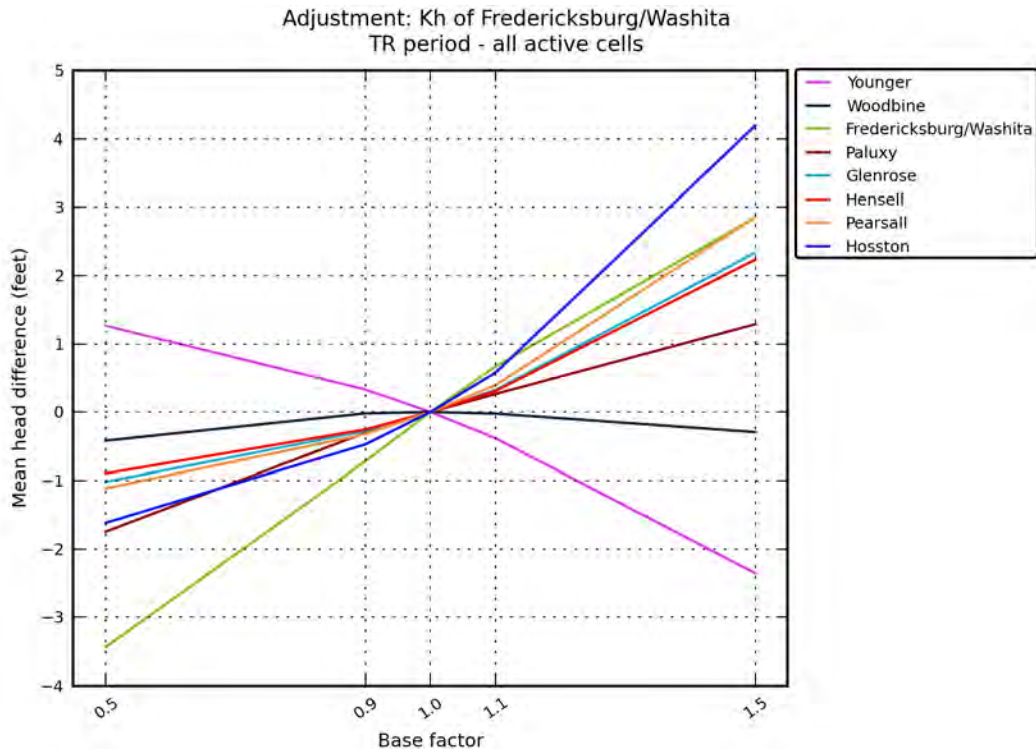
Figure 9.3.3   **Hydraulic head sensitivity in feet for the transient model to changes in horizontal hydraulic conductivity of the Washita/ Fredericksburg groups.**
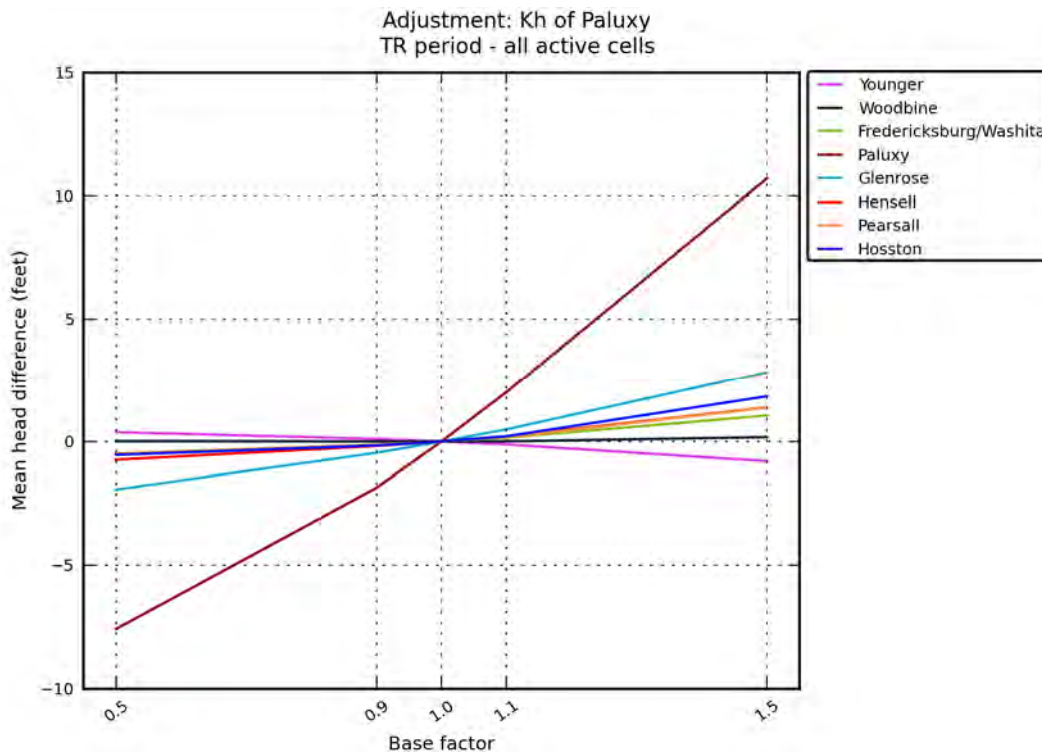
Figure 9.3.4   **Hydraulic head sensitivity in feet for the transient model to changes in horizontal hydraulic conductivity of the Paluxy Aquifer.**
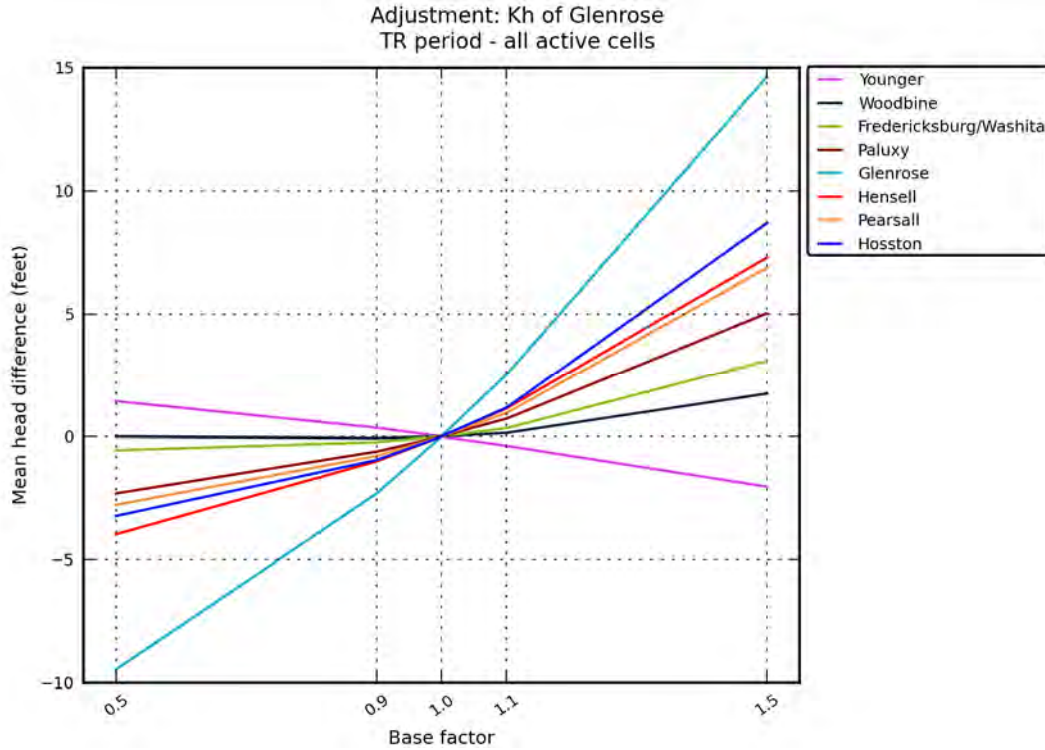
Figure 9.3.5 **Hydraulic head sensitivity in feet for the transient model to changes in horizontal hydraulic conductivity of the Glen Rose Formation.**
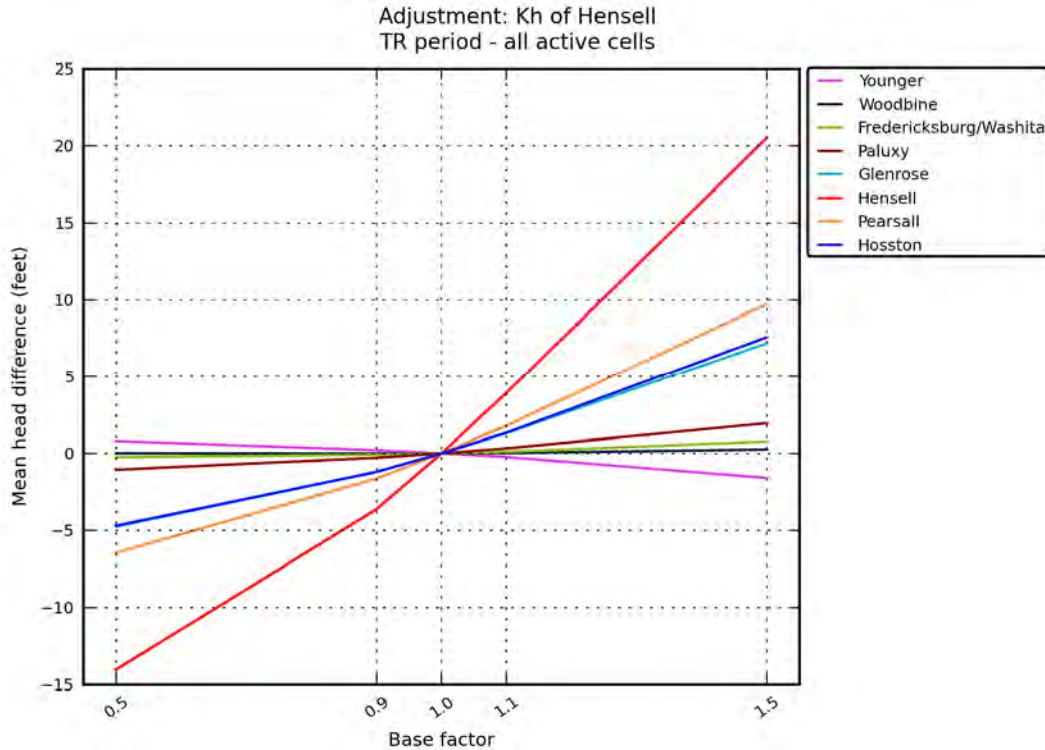
Figure 9.3.6 **Hydraulic head sensitivity in feet for the transient model to changes in horizontal hydraulic conductivity of the Hensell Aquifer.**
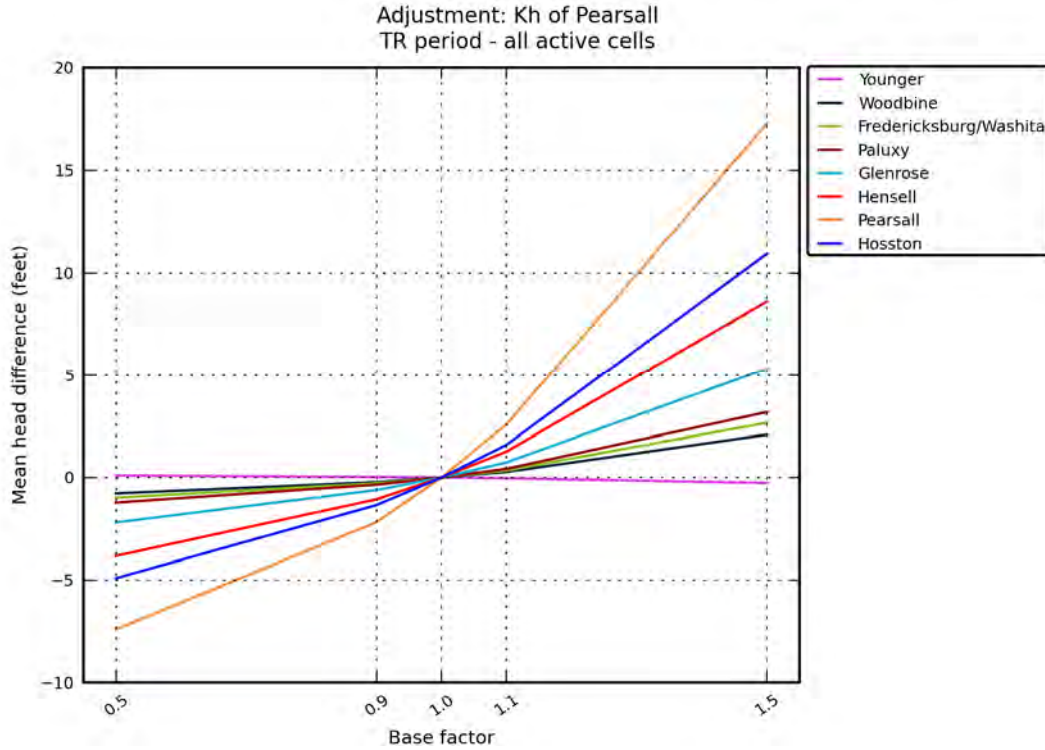
Figure 9.3.7   **Hydraulic head sensitivity in feet for the transient model to changes in horizontal
hydraulic conductivity of the Pearsall Formation.**
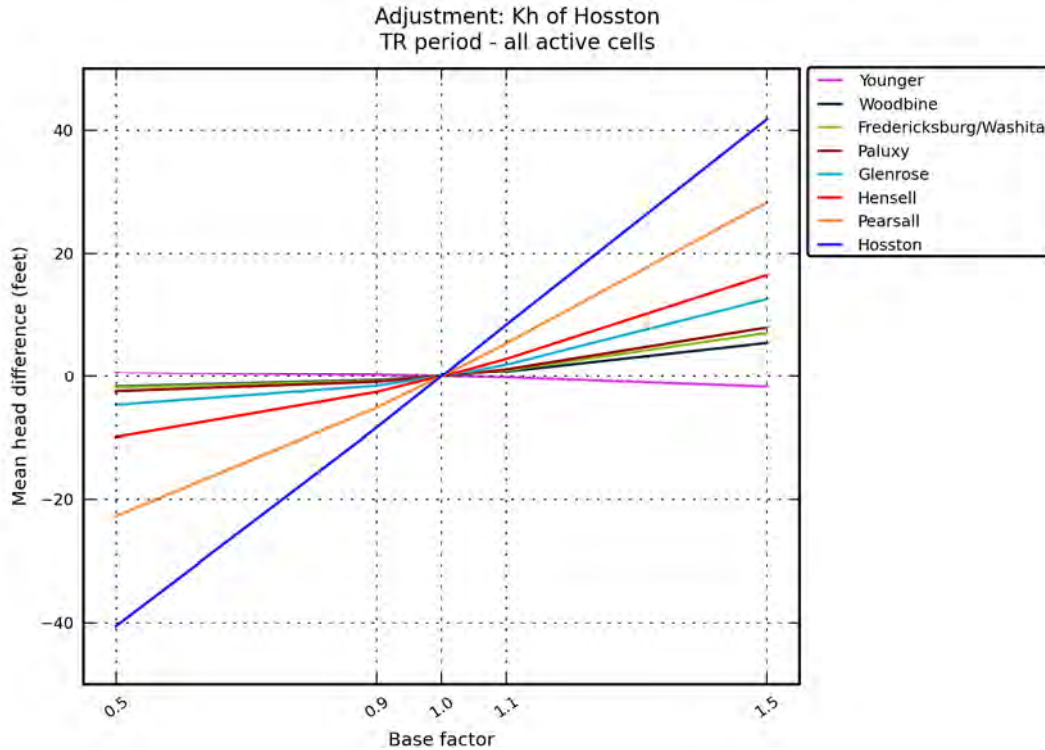
Figure 9.3.8   **Hydraulic head sensitivity in feet for the transient model to changes in horizontal
hydraulic conductivity of the Hosston Aquifer.**
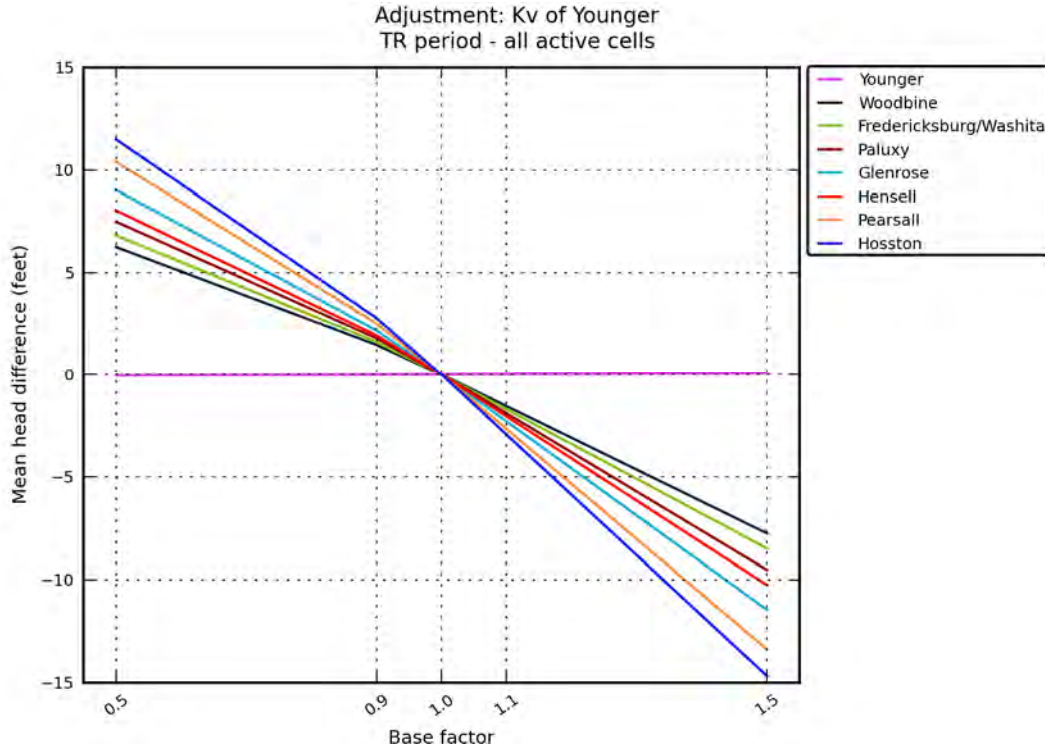
Figure 9.3.9   **Hydraulic head sensitivity in feet for the transient model to changes in vertical hydraulic conductivity of the younger formations.**
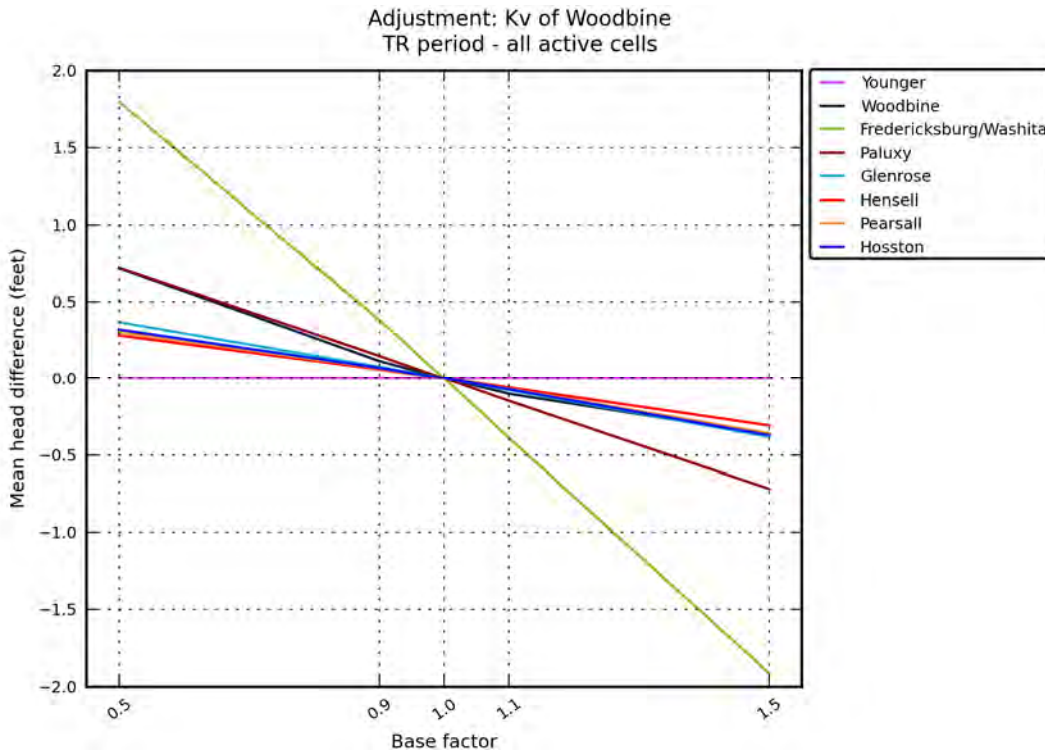
Figure 9.3.10   **Hydraulic head sensitivity in feet for the transient model to changes in vertical hydraulic conductivity of the Woodbine Aquifer.**
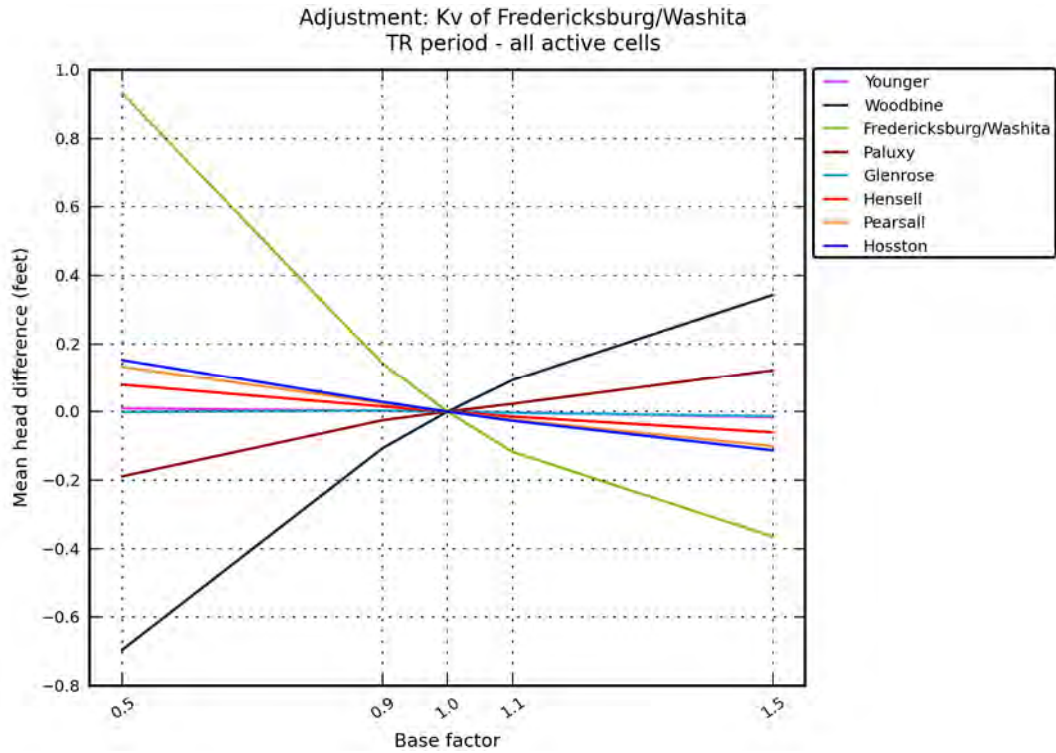
Figure 9.3.11 **Hydraulic head sensitivity in feet for the transient model to changes in vertical hydraulic conductivity of the Washita/ Fredericksburg groups.**
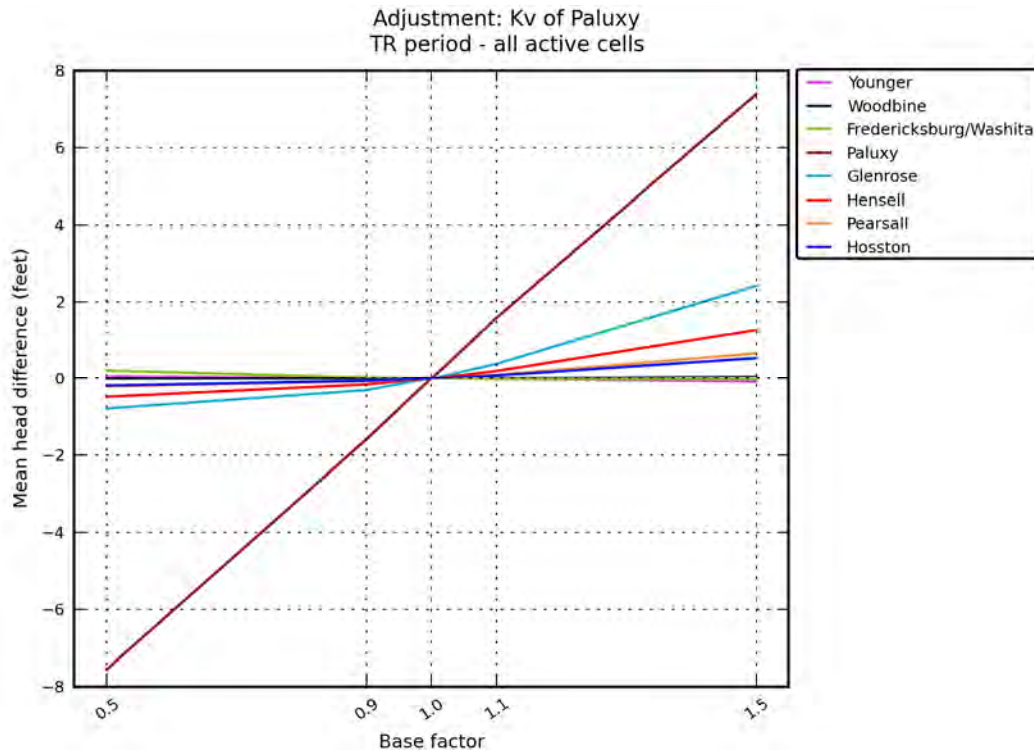
Figure 9.3.12 **Hydraulic head sensitivity in feet for the transient model to changes in vertical hydraulic conductivity of the Paluxy Aquifer.**
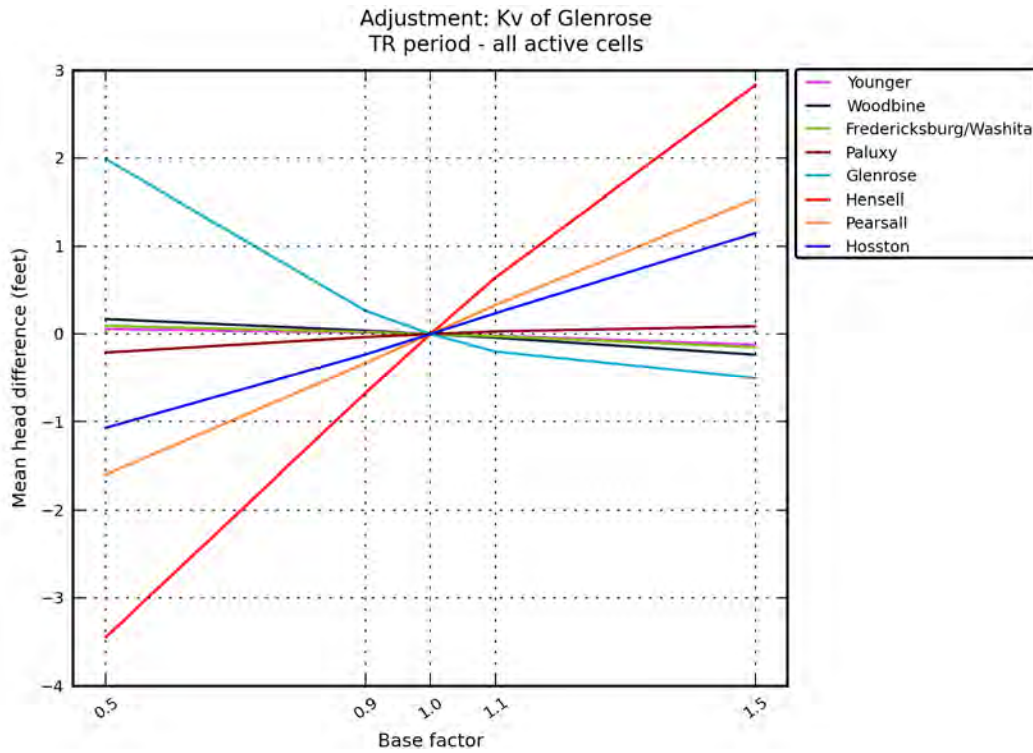
Figure 9.3.13   **Hydraulic head sensitivity in feet for the transient model to changes in vertical hydraulic conductivity of the Glen Rose Formation.**
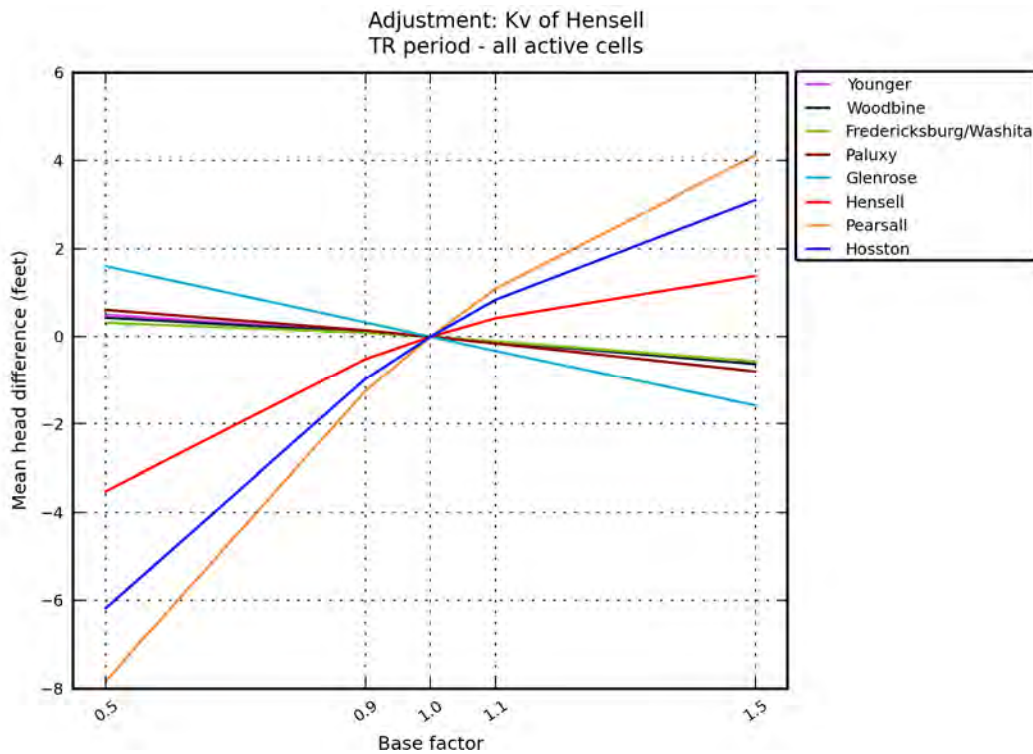
Figure 9.3.14   **Hydraulic head sensitivity in feet for the transient model to changes in vertical hydraulic conductivity of the Hensell Aquifer.**
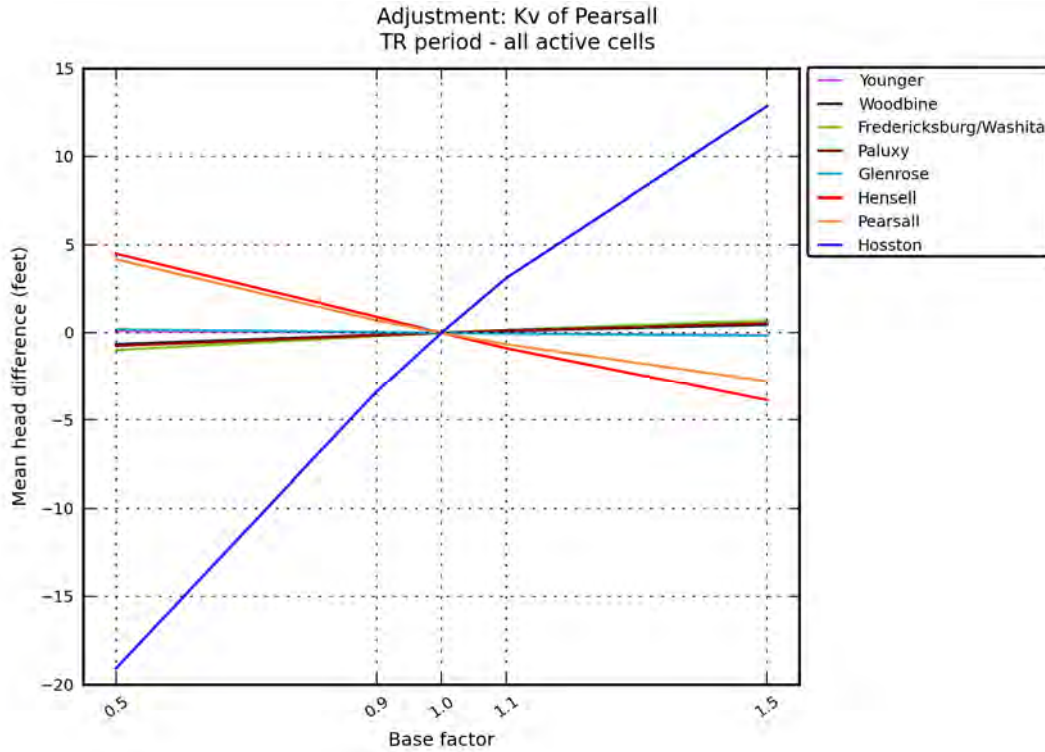
Figure 9.3.15 **Hydraulic head sensitivity in feet for the transient model to changes in vertical hydraulic conductivity of the Pearsall Formation.**
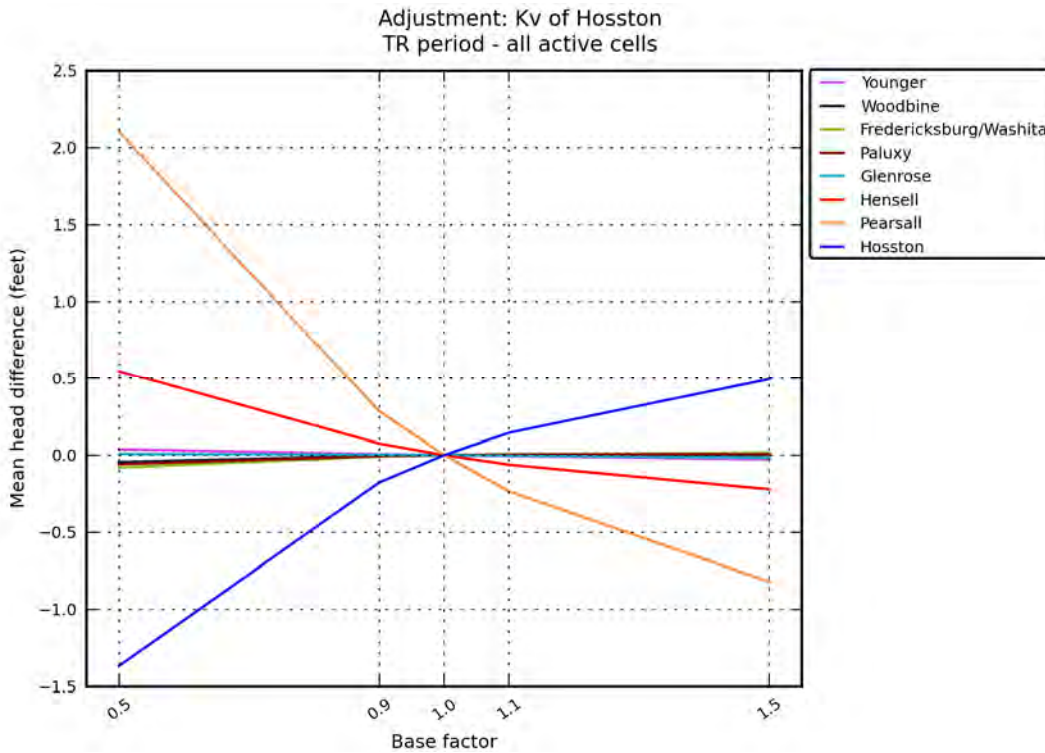
Figure 9.3.16 **Hydraulic head sensitivity in feet for the transient model to changes in vertical hydraulic conductivity of the Hosston Aquifer.**
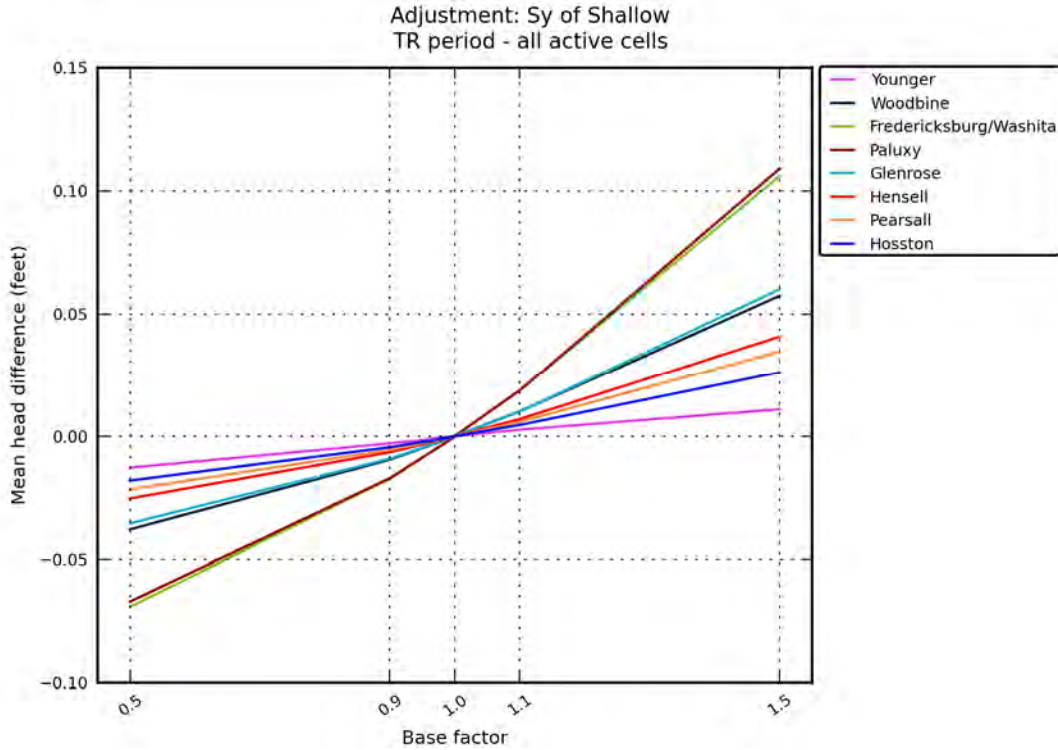
Figure 9.3.17   Hydraulic head sensitivity in feet for the transient model to changes in specific yield in the surficial outcrop area of Layer 1.
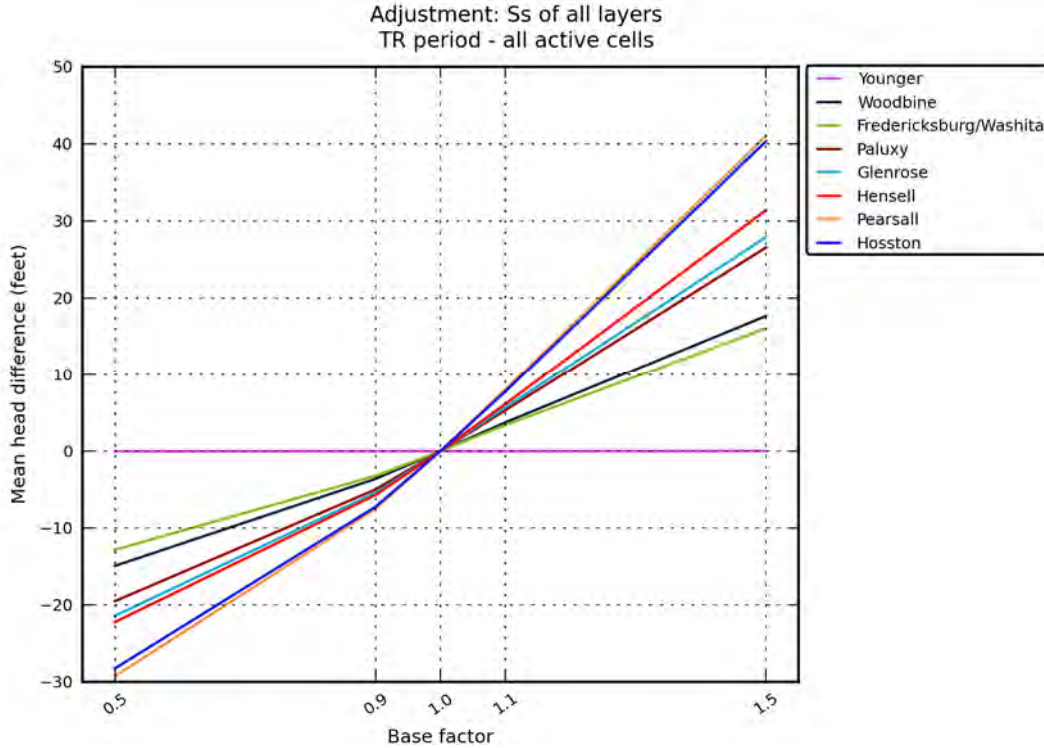
Figure 9.3.18   Hydraulic head sensitivity in feet for the transient model to changes in specific storage in the confined layers.
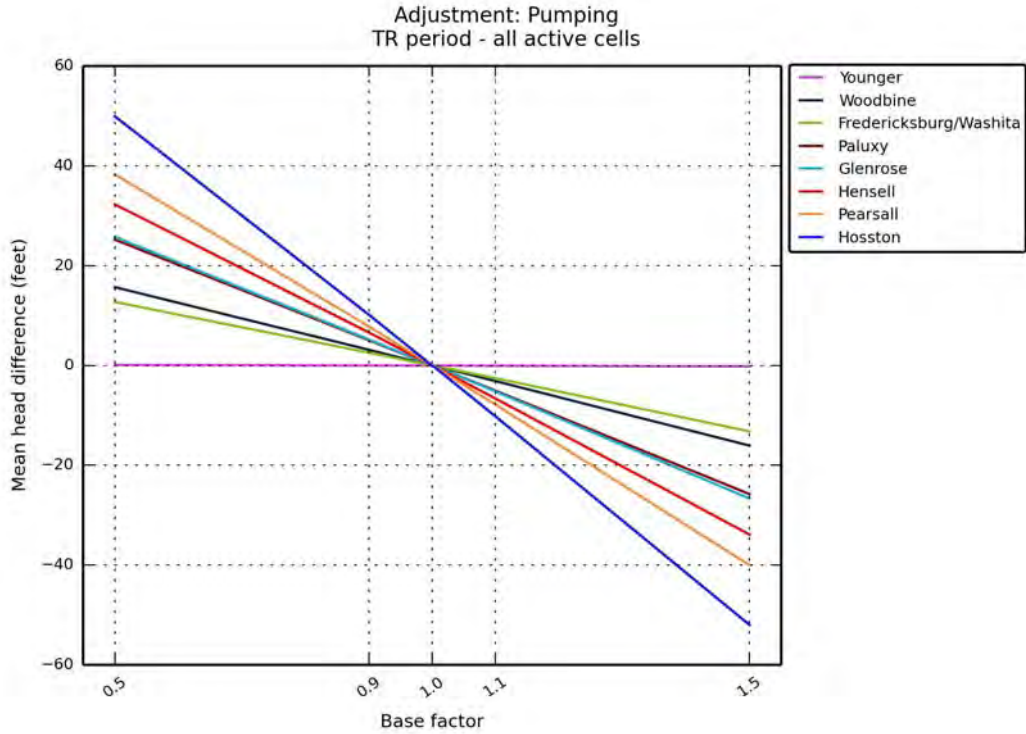
Figure 9.3.19   **Hydraulic head sensitivity in feet for the transient model to changes in pumping rate.**
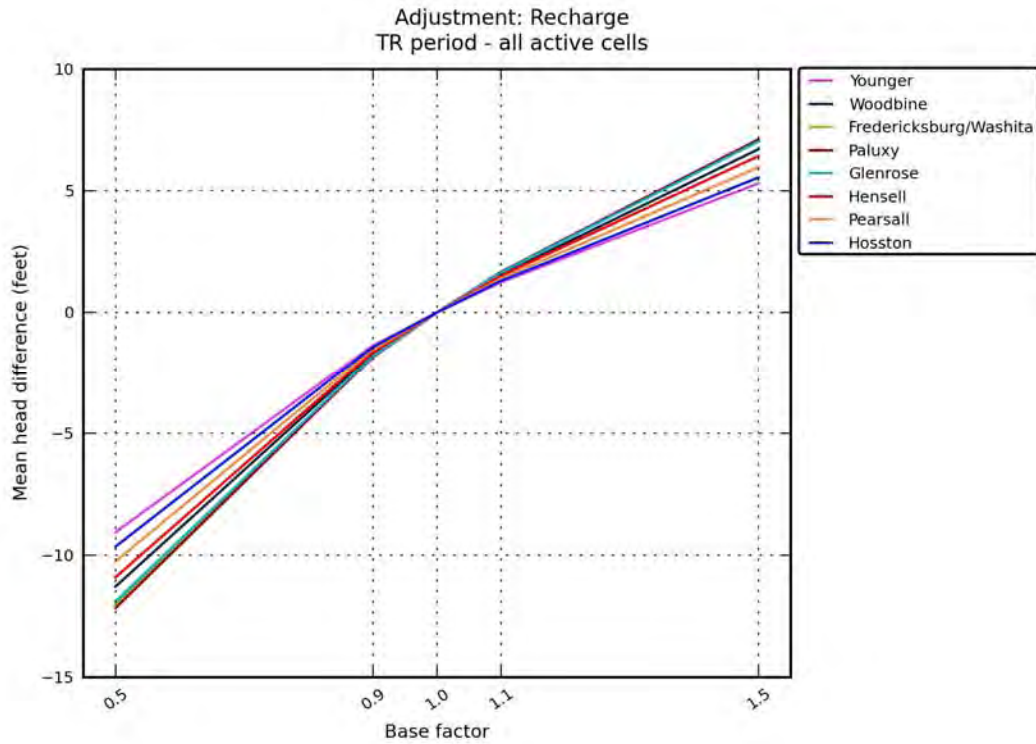
Figure 9.3.20   **Hydraulic head sensitivity in feet for the transient model to changes in recharge in the surficial outcrop area of Layer 1.**
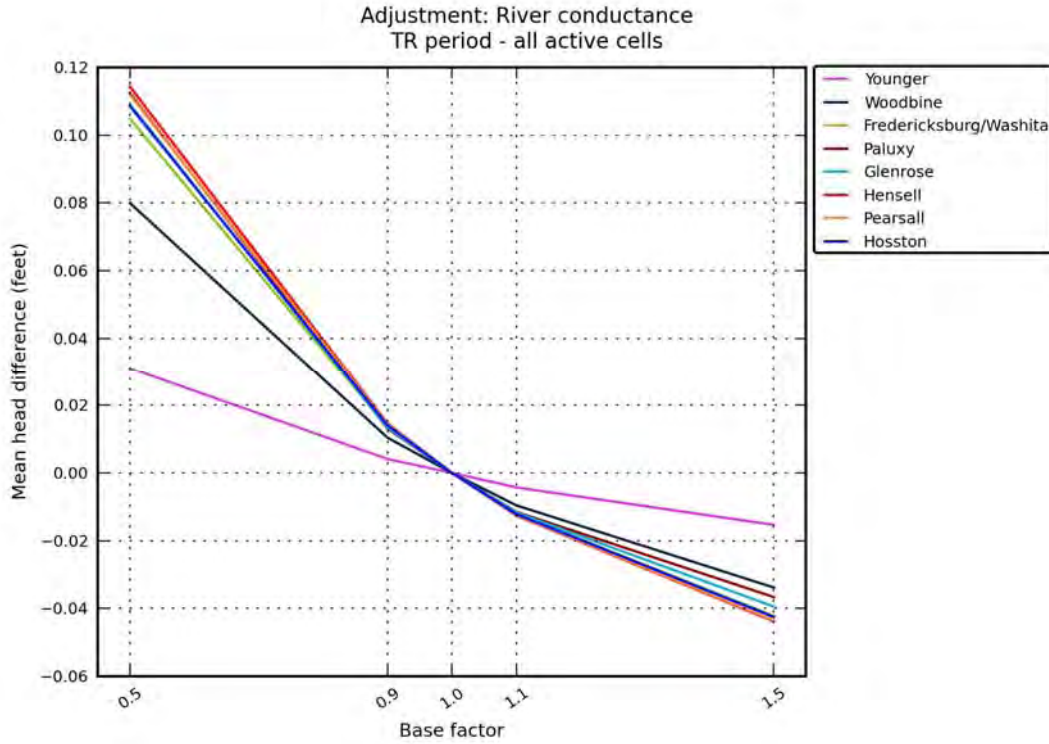
Figure 9.3.21 **Hydraulic head sensitivity in feet for the transient model to changes in river conductance in the surficial outcrop area of Layer 1.**
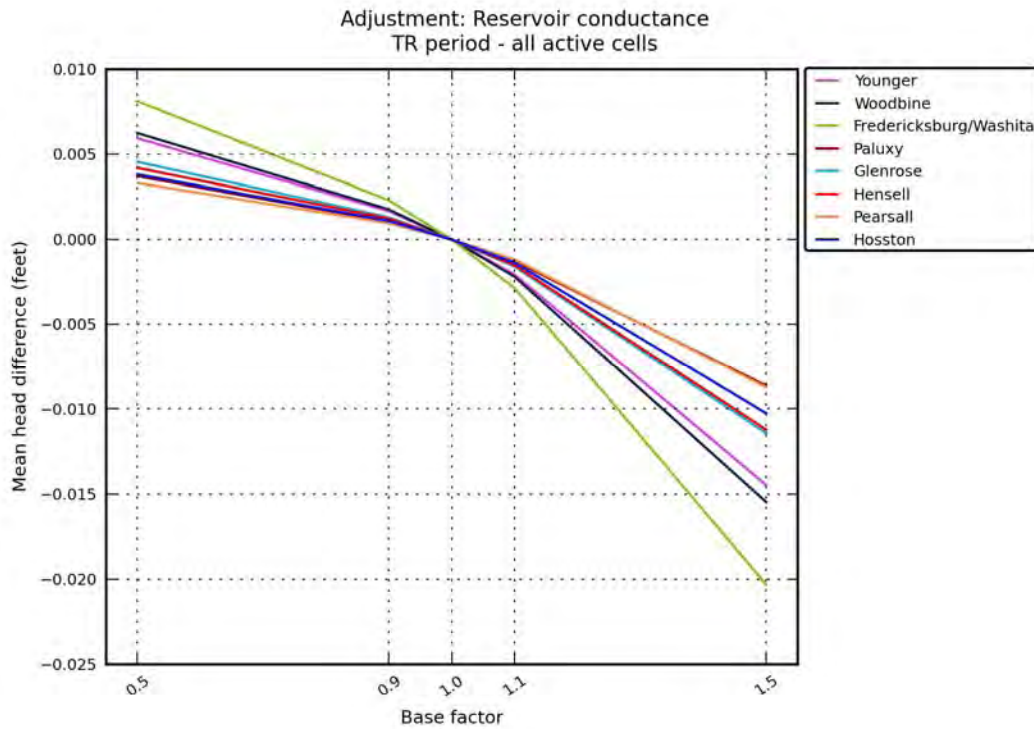
Figure 9.3.22 **Hydraulic head sensitivity in feet for the transient model to changes in reservoir conductance in the surficial outcrop area of Layer 1.**
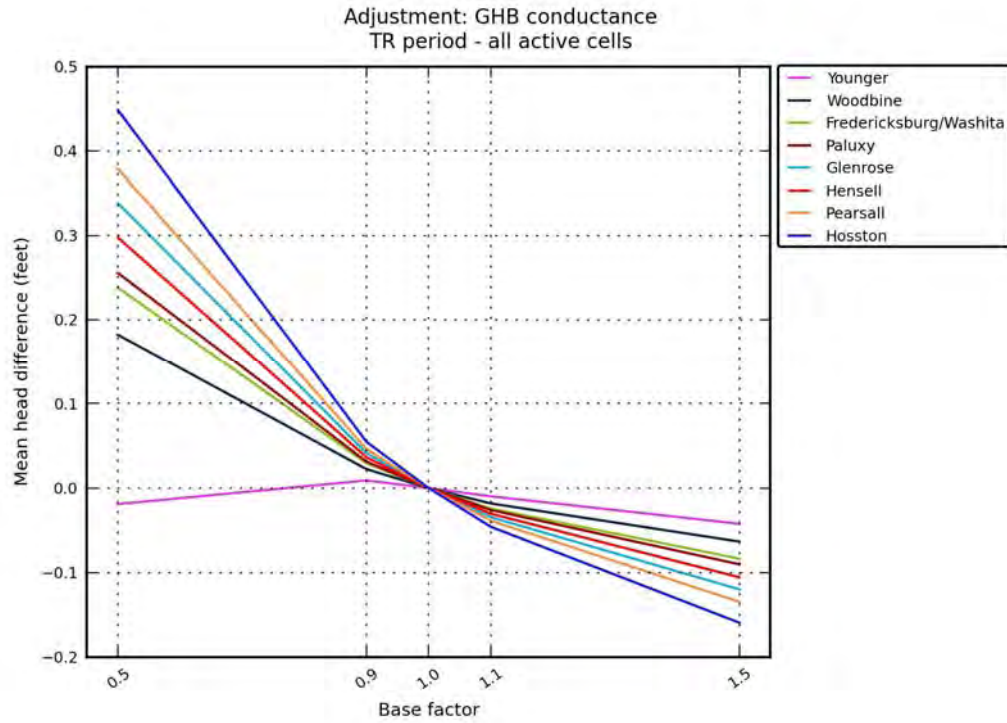
Figure 9.3.23   **Hydraulic head sensitivity in feet for the transient model to changes in the conductance of the head dependent boundary cells in the younger formations.**
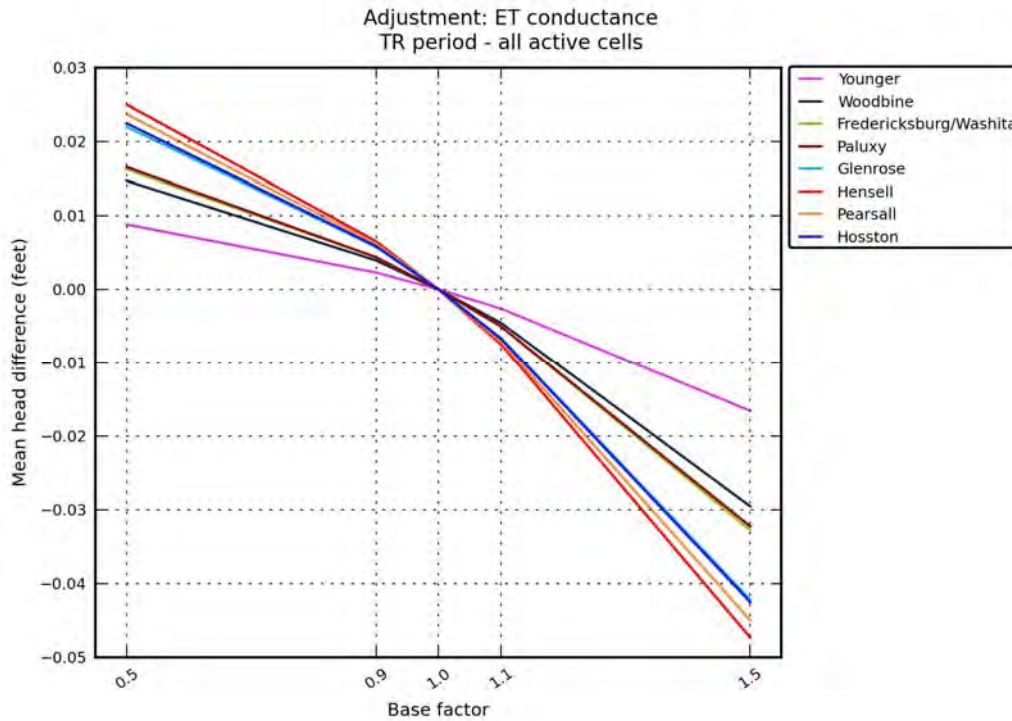
Figure 9.3.24   **Hydraulic head sensitivity in feet for the transient model to changes in drain boundary conductance, representing groundwater ET.**
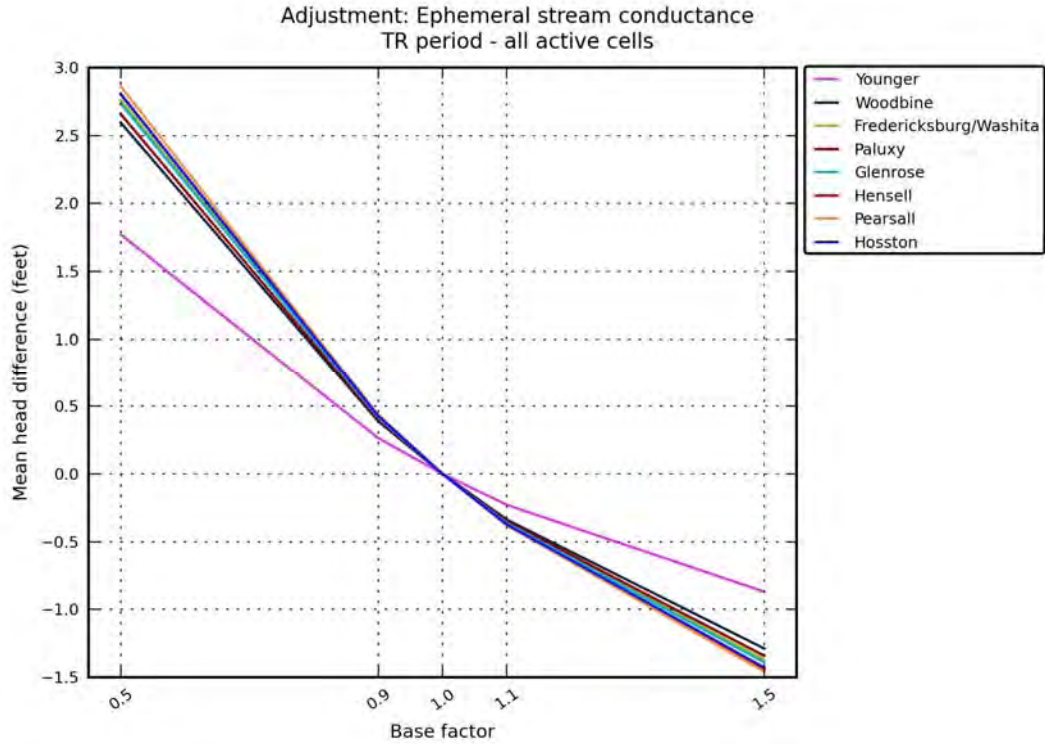
Figure 9.3.25   Hydraulic head sensitivity in feet for the transient model to changes in drain boundary conductance, representing ephemeral streams.
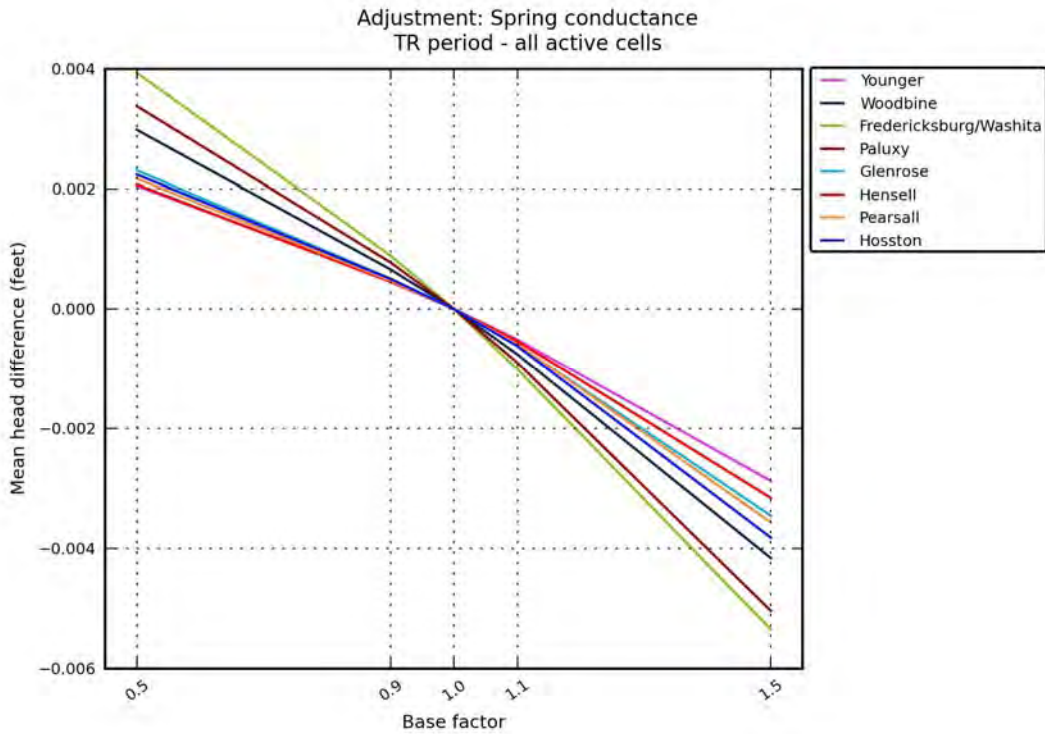
Figure 9.3.26   Hydraulic head sensitivity in feet for the transient model to changes in drain boundary conductance, representing springs.
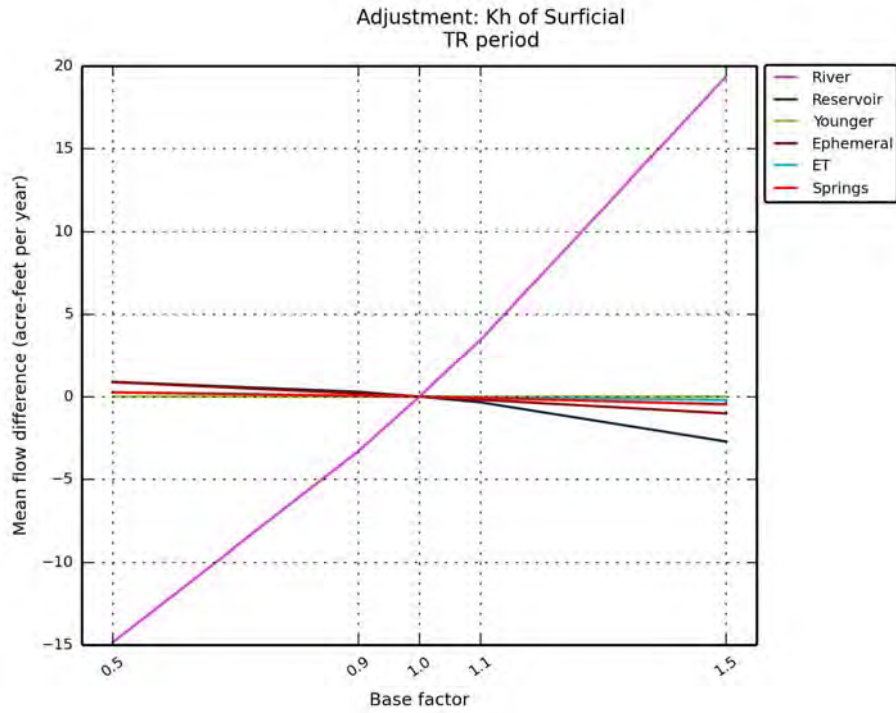
Figure 9.3.27   **Flow sensitivity in AFY for the transient model to changes in horizontal hydraulic conductivity of the surficial outcrop area of Layer 1.**
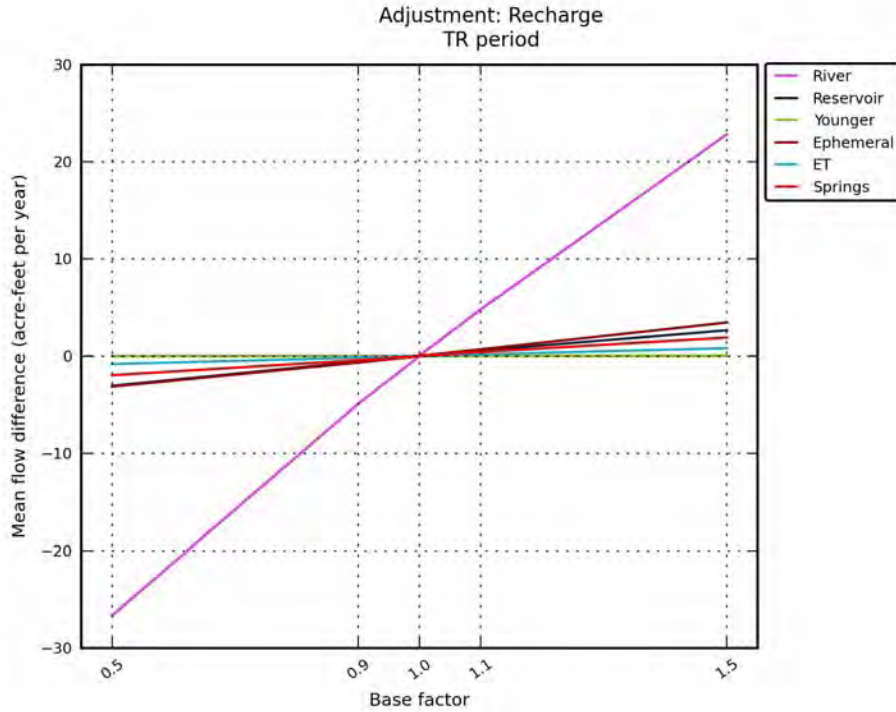
Figure 9.3.28   **Flow sensitivity in AFY for the transient model to changes in recharge in the surficial outcrop area of Layer 1.**
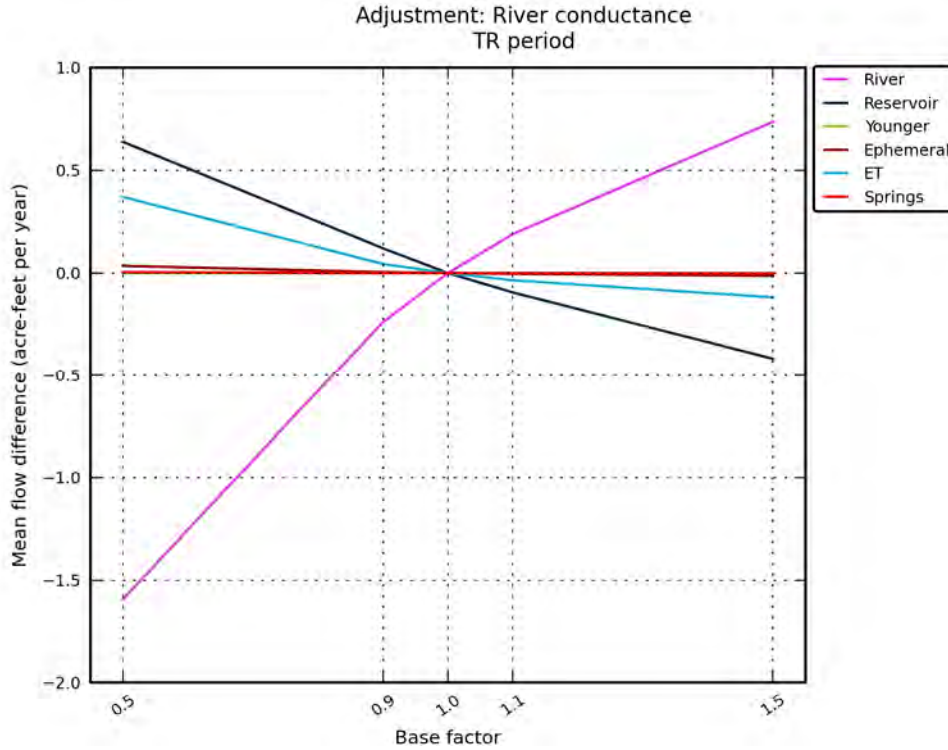
Figure 9.3.29   Flow sensitivity in AFY for the transient model to changes in river conductance in the surficial outcrop area of Layer 1.
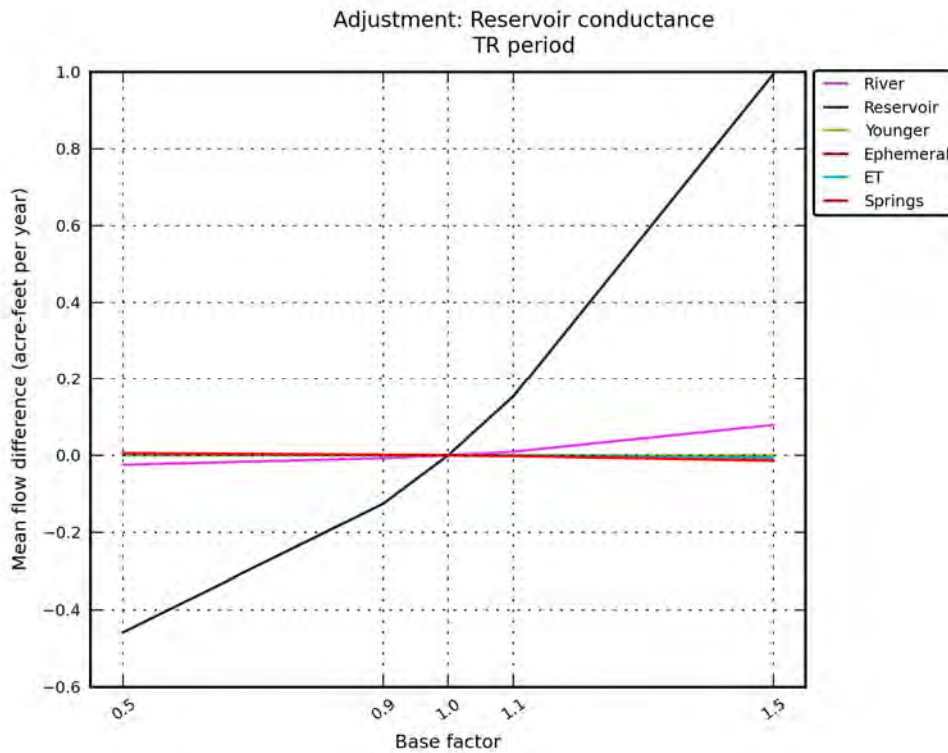
Figure 9.3.30   Flow sensitivity in AFY for the transient model to changes in reservoir conductance in the surficial outcrop area of Layer 1.
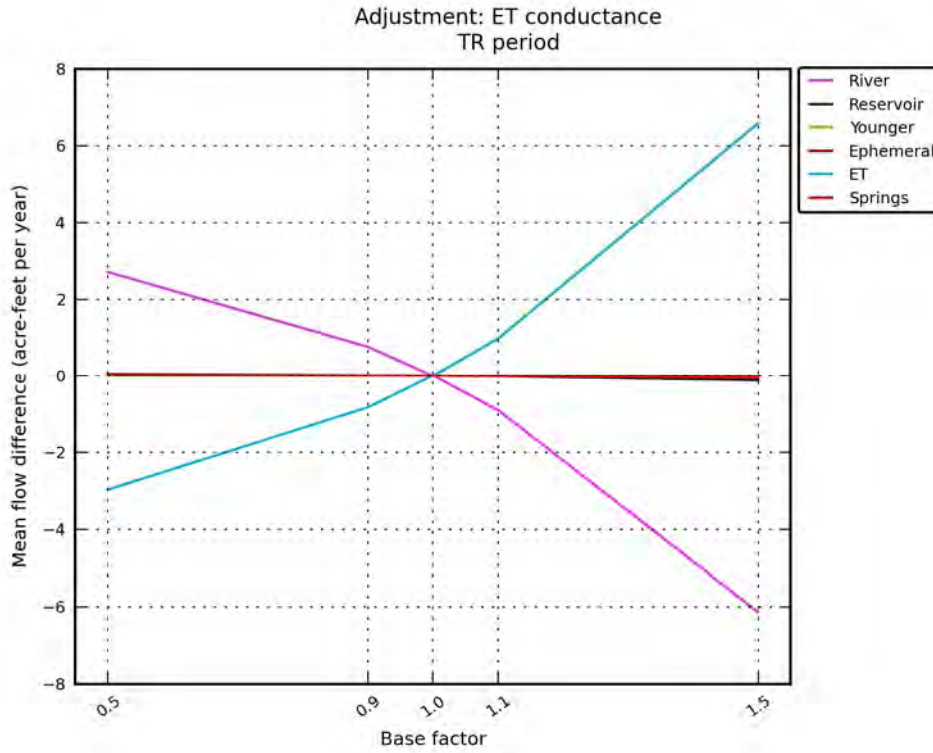
Figure 9.3.31 Flow sensitivity in AFY for the transient model to changes in drain boundary conductance, representing groundwater ET.
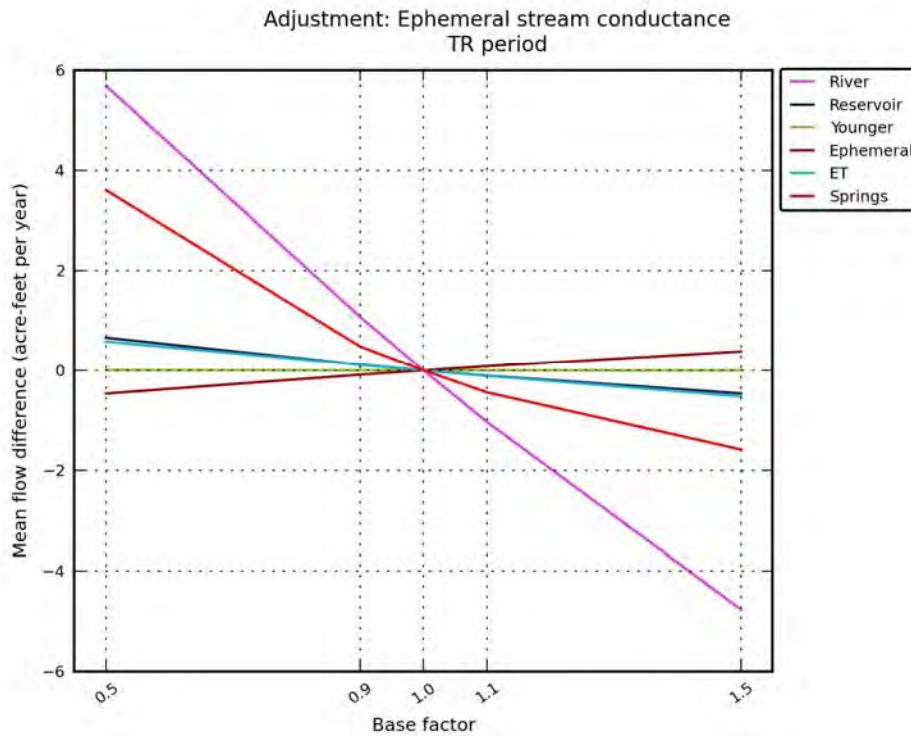
Figure 9.3.32 Flow sensitivity in AFY for the transient model to changes in drain boundary conductance, representing ephemeral streams.
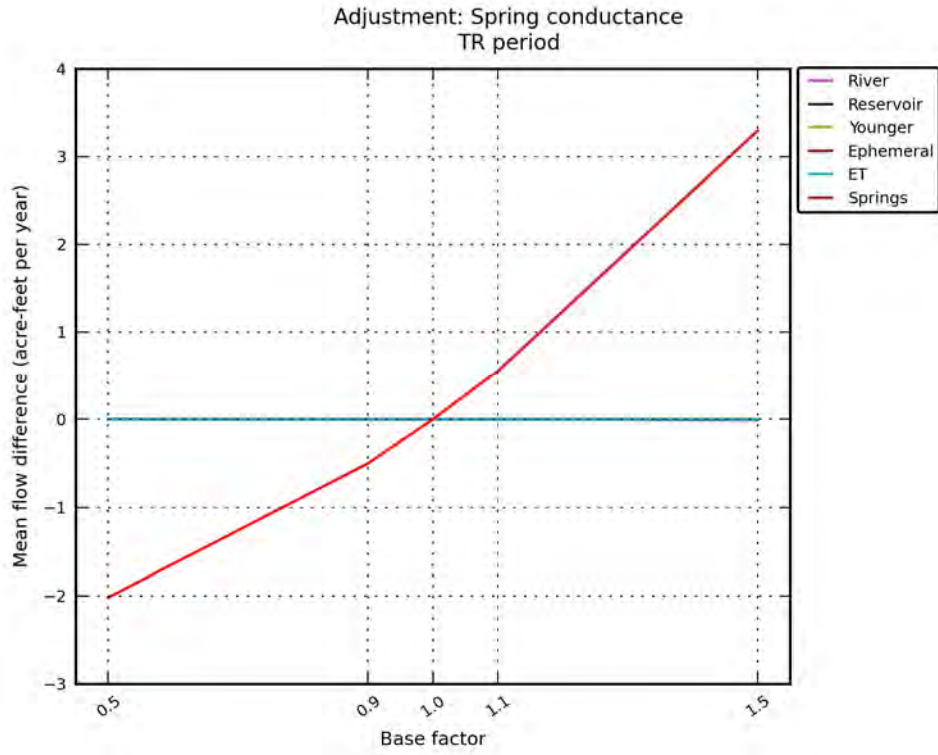
Figure 9.3.33 **Flow sensitivity in AFY for the transient model to changes in drain boundary conductance, representing springs.**

This page intentionally left blank.

10.0 Limitations of the Model

A model can be defined as a representation of reality that attempts to explain the behavior of some aspect of reality, but is always less complex than the real system it represents (Domenico, 1972). As a result, limitations are intrinsic to models. Model limitations can be grouped into several categories including: (1) key limitations in the data supporting a model, (2) key assumptions used to construct the model, and (3) limitations regarding model applicability. The limitations of this modeling study are discussed in the following paragraphs consistent with these categories.

10.1   Key Limitations of Supporting Data

Developing the supporting database for a large regional model with a large number of grid cells is a challenge because the information available does not, and never will, provide sufficient coverage to satisfy the data requirements of the model. For every type of data required by the northern Trinity and Woodbine aquifers GAM, whether it be measured hydraulic heads, aquifer properties, or river properties, there are areas in the model where additional data would help improve the model's representation of the physical system.

A key fact is that, despite the vast amount of information and data used in constructing this updated model, there is, nonetheless, a lack of specific types of data. Without a proper balance of different types of data that describe the temporal and spatial properties of the groundwater system, a modeler is required to develop assumptions to help guide the model construction and calibration.

Based on past experience with developing GAM models, the most significant data gaps and sources of uncertainty are with the temporal and spatial definition of historical pumping, interpreting data from wells with multiple screens that intersect multiple model layers or wells with no completion information, and the representations of hydraulic properties of the aquifers, confining units, and faults at the scale of the model grid cells. For the case of model faults, direct data regarding properties at any scale are lacking. Each of these issues is discussed below.

10.1.1 Historical Pumping

Pumping is the primary model input parameter that causes changes in hydraulic heads. Pumping impacts tend to be localized near a well because the effects of pumping on hydraulic heads decays exponentially as the distance from the pumping well increases. Therefore, accurately simulating the effects of pumping on hydraulic heads requires accurate placement of pumping both spatially and temporally. If the timing and placement of pumping is not accurate, the model will simulate a difference between measured and observed hydraulic heads. One measure of the accumulation of these differences is the root-mean square (RMS) error of the model (see Section 7.1). Assuming that one knows the timing and volume of pumping that should occur in each model grid cell, then changes to model parameters to better match observed and simulated hydraulic heads during calibration are well constrained because of the elimination of error in pumping allocation to the model grid. Unfortunately, this would never be the case unless all wells were metered and all wells were perfectly characterized. As a result of the reality of not having pumping exactly correct, model hydraulic properties may be adjusted to some unknown degree during calibration to reduce the model mismatch (or RMS error). Changing hydraulic properties, although good for improving the model calibration, is actually not ideal for the utility of the model because the changes in the model parameters may not be appropriate and, therefore, will introduce inaccuracies in future predictions of hydraulic heads.

Because very large historical drawdowns of greater than 1,000 feet have occurred in the aquifer, incorrect representation of historical pumping could be a significant obstacle for achieving a satisfying model calibration as well as a source of introduced error in the calibrated model parameters. Prior to 1980, the spatial distribution of pumping across the active model domain is uncertain and this uncertainty becomes larger with each preceding decade. For some counties, in addition to limited data with which to estimate total pumping for some years, data are limited as to how historical pumping was distributed spatially among grid cells and vertically among model layers. Most of the drawdown in the aquifer occurred prior to 1980, which is the period over which the least amount of information is available regarding pumping. Thus, it is possible that the assumptions and data used to develop pumping for the model prior to 1980 introduced bias into the model calibration. This possibility is most likely in areas of the model where relatively

little information was available for assigning the spatial and temporal variation in pumping and, though rarely discussed, is inherent in every Texas GAM to some degree.

10.1.2 Multi-Layer Well Completions and Unknown Completion Data

Most of the well data used to calibrate the model are from wells with screens that intersect multiple model layers or wells with no available completion data. The intersection of a well screen across multiple aquifer(s)/formation(s) means that the measured water level represents some type of composite value. For wells with no screen information, the representative aquifer(s)/formation(s) for water-level data are unknown or highly uncertain. As a result, assumptions are required for calculating aquifer properties from aquifer pumping tests, for developing a pumping file for model calibration, and for assigning hydraulic heads to specific model layers. These assumptions introduce uncertainty and an unknown amount of error into the model calibration that otherwise would not exist if the wells were screened within a single model layer and the well completions were known.

10.1.3 Aquifer and Fault Hydraulic Properties

Section 4.2.1.3 discusses the importance of accounting for the scale-dependence of aquifer properties when assigning properties to model grid cells. As stated by Bethke (1989), the "task of inferring regional hydraulic conductivity is among the most significant challenges in basin hydrology." An attempt has been made to address this problem by inferring hydraulic properties from the large database of lithologic data derived from the interpretation of geophysical logs. While this approach offers a good constraint on properties, it nevertheless cannot overcome the general lack of data and information available regarding several important aquifer parameters and modeling assumptions. Among the parameters for which there are very few field estimates for constraining and conditioning the model calibration are: the vertical hydraulic conductivity of the litho-units and how this property may change as a function of depth of burial; the impact of the faults on horizontal and vertical flow; and the effective unconfined storage properties of the different aquifers near ground surface and as a function of depth. Without good data to constrain these properties, the conceptual model assumptions regarding cross-formational flow between aquifers and upward flow as a result of the Mexia-Talco Fault Zone contain uncertainty.

10.1.4 Other Important Data Gaps

The steady-state model was calibrated using 96 water-level measurements. These 96 measurements provide minimal coverage across the active model domain for the eight model layers. Fortunately, other types of measurements are available to constrain the steady-state calibration, such as evidence of artesian hydraulic heads at the locations of the flowing wells in the early 1900s and evidence of significant downdip penetration of freshwater in the Hosston and Hensell aquifers based on water quality measurements. Despite these additional constraints, the significance of not having a comprehensive set of calibration targets for the steady-state model adds to model uncertainty. Any biased error in the hydraulic head calibration target will propagate throughout the rest of the model and have the greatest impact during early simulation years.

Besides comparing predicted and measured hydraulic heads, another useful approach for checking the reasonableness of the steady-state model calibration is to compare the predicted groundwater ages from the model with groundwater ages estimated from ^{14}C measurements. The value of this comparison is explained in detail in a TWDB study of the Gulf Coast Aquifer System (Young and others, 2014). As part of this study, the groundwater ages from the steady-state model have been calculated in Section 9 for comparison to observed freshwater extent in the Hensell and Hosston aquifers. Unfortunately, these ages could not be compared to quantified ages calculated from ^{14}C measurements due to the lack of such data in the TWDB groundwater database.

Another important input parameter, especially related to the aquifer outcrop and shallow subcrop, is recharge. Recharge is a very difficult parameter to measure because it varies both spatially and temporally. In this study, river base flow estimates, climate data, and chloride concentrations in the groundwater were used to estimate recharge. Despite extensive efforts, sufficient data to develop reliable estimates of recharge values over much of the central portion of the model were lacking. This is a key data gap, increasing uncertainty in that part of the model.

10.2   Key Assumptions Regarding the Model Construction and Calibration

There are several potentially key assumptions regarding model construction and calibration. Below each of these key assumptions will be discussed.

- *Use of river-head boundaries to simulate the hydraulic interaction between the Woodbine Aquifer and the overlying formations*. The aquifer properties and hydraulic heads in the younger formations were not characterized during for project. Interaction between the younger formations and the Woodbine Aquifer is assumed to occur throughout most of the model, and is included in the model through the use of a boundary condition. The choice of a boundary condition to represent the younger formations is based upon the assumption that interaction between the Woodbine and the younger formations is not significant enough warrant explicit consideration in the model. River-head boundaries were used instead of general head boundaries to prevent the general head boundaries from acting as a potential unlimited source of water to the Woodbine Aquifer.

- *Use of a no-flow boundary between the Hosston Aquifer and Paleozoic-age strata.* While interaction between the Hosston Aquifer and the underlying Paleozoic-age strata may be locally important, it is not considered to be regionally important and is poorly characterized. After discussions with the TWDB, it was agreed that it was conservative to maintain the lower boundary as a no-flow boundary, since the model will be used principally for groundwater availability assessment. As a result, the sands in the Paleozoic-age strata were not included in the model and a no-flow boundary was imposed at the base of the Hosston Aquifer. Because the Paleozoic-age strata were not included, pumping associated with the Paleozoic-age strata was not included in the county pumping estimates.

- *Function for Estimating Recharge*. To model recharge, the model outcrop area was divided into three sections as discussed in Section 4.5.6. For each of these sections, a single function was used to estimate recharge from precipitation. This approach was used because of the lack of recharge information for numerous watersheds, especially for those in the central portion of the model, and to promote consistency across the model. A consequence of this approach is that the spatial variability of recharge is likely smoothed relative to the natural variability.

- *Use of the Well Package*. Many of the wells in the study area are completed across multiple model layers. The MODFLOW well package used to simulate pumping does not have the sophistication to simulate pumping from multiple layers and therefore pumping estimates must be assigned by layer prior to model simulation. One potential solution, was to use the more sophisticated connected linear network package coupled with the well package that was advertised as part of the new unstructured grid version of MODFLOW (MODFLOW-USG) developed by Panday and others (2013). After building an unstructured grid and starting to use the new model and connected linear network package, a major limitation in this new package was discovered. This limitation relates to the requirement that a connected linear network be active during the entire modeling period. As a result, wells drilled in any time frame, say 1990, would have to be in the model from predevelopment. This would result in induced groundwater cross-formational flow in the wells during early times. As a result, use of the unstructured grid model was abandoned and an approach employing the well package in the standard, finite-difference version of MODFLOW was used.

- *Drains to Represent Flowing Wells.* The model does not have the capability of representing vertical flow in a borehole that connects and intersects multiple layers. Such capabilities would provide the opportunity to more accurately simulate the flow from artesian wells that occurred during the early 1900s. In order to represent these flowing wells, the MODFLOW drain package was used. Outflow through the drains was limited by the formation in which the drain was placed. A limitation of the drain package, however, is that it does not accurately simulate the near-well hydraulics that are necessary to create cones-of-depression locally around a well. A good multi-layer well package, such as that implemented in MODFLOW SURFACT (Hydrogeologic, 2010) can accomplish this. As a result, the hydraulic head value being used by the drain package for the shut-in pressure of the well is too high and the decay of flow rate over time from the well could be significantly under estimated. The benefit of using the drain package is that it will not allow heads to decline below ground surface.

10.3 Limits for Model Applicability

The northern Trinity and Woodbine aquifers GAM was developed to update the 2004 GAM
(Bené and others, 2004) with new data and information that has come available since the 2004
GAM was developed and to advance the calibration to near current conditions while making
improvements to the model. The use of this model is for regional planning within GMA 8 and
for use by GCDs within GMA 8 in their management of groundwater resources.

To help accomplish these objectives, the northern Trinity and Woodbine aquifers GAM was built
with a constant grid-block area of one-sixteenth of a square mile. This resolution provides the
capability for improved and more accurate placement of wells, rivers, and other hydraulic
boundary conditions. This finer resolution, however, should not be interpreted as meaning the
model is capable of accurate predictions at the scale of one-sixteenth of a square mile. This is
because, across much of the model domain, several key model parameters are based on
interpretations of data that represent averages over distances greater than several square miles.
This issue of scale is inherent in any regional model. The finer model grid resolution does
improve model representation of the aquifer response to pumping.

Because of model size and data constraints, the model is not appropriate for use in accurately
predicting drawdown in a single well during pumping. For single borehole drawdown during
pumping or well spacing calculations, analytic models are more appropriate. The model does,
however, provide information, such as hydraulic properties and aquifer structure, useful for
informing analytic calculations. For regional estimates of drawdown over the scale of several
square miles or greater, data support and level of calibration in the area of interest should be
considered when using the model.

The predictive capability of the model is tied not only to the availability of spatial data but also
to that of temporal data. The lack of data over short time periods for use in developing model
boundary conditions means that stress periods of less than 1 year were not warranted. Use of
annual stress periods precludes the ability of the model to predict seasonal hydraulic head or
flow variability. Temporal variability at a scale of less than 1 year is likely not important to
regional water planning and GCD groundwater management. However, if modifications to the
model would be necessary to investigate processes that vary over a time scale less than 1 year,
such as seasonal variability in base flow, the length of the model stress periods would have to be

decreased. An example application requiring refined temporal resolution is coupling the model

to a monthly surface water availability model.

11.0 Future Improvements

To use models to predict future conditions requires a commitment to improve the model as new data and modeling technologies become available or when modeling assumptions or implementation issues change. The northern Trinity and Woodbine aquifers GAM is no different. Through the modeling process, changes to the model to improve performance or data needs to better constrain model calibration are typically identified. Future improvements to the model, beyond the scope of the current groundwater availability model, are discussed below.

11.1 Additional Supporting Data

An exhaustive search of existing data was performed to develop and support calibration of the updated northern Trinity and Woodbine aquifers GAM. However, no new field measurements were collected as part of this study. Several types of additional data or new field measurements would provide useful information for confirming central components of the conceptual model (Section 5) and, in so doing, support future model calibrations. These data include measurements of ^{14}C concentrations in groundwater, additional aquifer pumping test data, and estimated recharge rates based on new recharge studies. Each of these data types are discussed below.

The collection of ^{14}C concentrations in groundwater samples from wells would provide a simple but effective approach for checking the groundwater ages calculated by the steady-state model. The most useful locations for ^{14}C concentrations would be the downdip regions of the aquifers and away from the outcrops. The ^{14}C concentrations are relatively easy to obtain, as it simply involves collecting a groundwater sample and sending it off for a chemical analysis. The cost to chemically analyze a groundwater sample for ^{14}C concentration is about $2,000. The collection of ^{14}C data could be done in phases, with the first phase focused on sampling the Hosston Aquifer. Because of the large outcrop area and strongly varying climate, aquifer structure, and aquifer lithology, ^{14}C measurements along multiple transects from north to south would provide the most useful data.

Performing aquifer pumping tests in areas where property estimates are lacking would be beneficial for validating the aquifer properties in the current model and for supporting future model recalibration. Aquifer pumping tests should be conducted for at least 8 hours and, if

possible, nearby wells should be monitored for water-level changes during the test. Properly designed and implemented multi-well aquifer pumping tests provide information from which vertical hydraulic conductivity and storage properties can be calculated at a scale useful for validating the aquifer parameters used in the model. A possible method for collecting additional aquifer pumping test data is for GCDs to require such tests to be performed and the data submitted to the GCD as an administrative requirement for a well permit. In many GCDs, there is already a permit volume over which an aquifer pumping test is required.

For a large area of the active model domain that includes the central portion of the study area updip of the highest urbanization, local recharge estimates are not available and were developed based on data available for the far southern and far northern portions of the study area. This is because most stream gages in the central, and most populated, portion of the study area are regulated and hydrograph separation analysis to estimate base flow is problematic. Although the approach used for developing recharge estimates for this portion of the model compare reasonably well with the CMB methods (see Section 4.5), there has been significant anthropogenic contamination of the shallow groundwater in the area which has the potential to bias recharge estimates made this. Additional research into recharge processes between Waco and the Texas-Oklahoma state line would be beneficial.

11.2   Future Model Implementation Improvements

Considering future model recalibration as new data are collected and/or new understanding of the northern Trinity and Woodbine aquifers is achieved is recommended. There are many new GCDs in the northern portion of the study area that are actively pursuing research into the groundwater resources of the northern Trinity and Woodbine aquifers. It is expected that better data and, consequently, a greater understanding of the aquifers will be achieved over the next several years.

The upper Trinity GCD is currently funding the development of a model of Paleozoic-age strata located west of and underlying a significant portion of the northern outcrop region of the northern Trinity Aquifer. It is known that in some areas, the Hosston Aquifer lies unconformably on permeable sands and gravels of these Paleozoic-age strata. The updated northern Trinity and Woodbine aquifers GAM assumes a no-flow boundary between the Hosston Aquifer and the Paleozoic-age strata. It is recommended that future studies take the findings from the model of the Paleozoic-age strata and this updated GAM to better define the importance of this no-flow boundary condition.

With anticipated advancements to modeling software, two future model improvements are recommended for consideration. The first is to apply the new MODFLOW unstructured grids code (MODFLOW-USG) to the northern Trinity and Woodbine aquifers. The second improvement would be the coupling of the updated GAM with Analytic Element Models to better predict responses to pumping for small radial distances. These two potential improvements are described below.

11.2.1 Use of the USGS Unstructured Grid Version of MODFLOW

As mentioned in Section 10, Version 1 of MODFLOW-USG (Panday and others, 2013) was evaluated for this study. After identifying a problem with the connected linear network package and finding the model documentation incomplete, this option was abandoned. A concern with using the early version of MODFLOW-USG was that there might be problems with the code that would not be discovered until late in the project, which led to an unacceptable risk to the project. Since the initial analysis of the code, another version of MODFLOW-USG has been released. However, this version became available late in the project and, therefore, could not be evaluated

while still meeting the contracted schedule. The MODFLOW-USG simulator offers some attractive capabilities that should be considered by GMA 8 once it is capable of handling a model of the complexity of the northern Trinity and Woodbine aquifers GAM. Once the MODFLOW-USG version has been demonstrated to be properly documented, error free, and adequately supported by commercial graphical interfaces, such as Groundwater Vistas, it is recommended that GMA 8 consider converting the MODFLOW-NWT model into a MODFLOW-USG model. However, due to the significant differences in how the two codes are formulated, development of an initial exploratory model is recommended. The Edwards Aquifer Authority is currently developing an exploratory alternative model to MODFLOW using a finite-element model to see if it offers advantages.

The biggest benefit of MODFLOW-USG is that it provides the capability of simulating pumping from wells screened across multiple model layers. This capability will reduce the number of assumptions and potential sources of bias associated with model calibration and reduce potential problems with adding new wells into the model in future simulations. MODFLOW-USG also provides the capability to pinch out model layers and grid cells. This capability will also eliminate the need for the numerous thin "conduit" grid cells that currently exist between the surficial outcrop area of Layer 1 and the underlying confined layers. This will result in reducing the number of grid cells, which reduces the size of the model and, therefore, model run times. MODFLOW-USG also provides the capability to use non-rectangular grid cells, which allows greater flexibility in defining model aquifer boundaries.

11.2.2 Coupling of the Model with an Analytical Element Model (AEM) for Near-Field Prediction

Despite having grid cells that are a quarter of a mile square, the updated model does not have the capability of accurately predicting the impacts of a pumping well on hydraulic heads within a well or in the close vicinity of a well extending out several grid cell dimensions. This limitation of most finite-difference regional models occurs because of two issues. The first issue is that wells can only be located at the center of a grid cell and well screens are assumed to extend across the full extent of the model layer. The second issue is that the finite difference solution technique used by the model is an approximate solution to the groundwater flow equation close

to a pumping well. The error associated with this approximation is greatest at the location of the well and rapidly diminishes with distance beyond the grid cell in which the well is located.

To avoid problems with approximate solutions to predicting drawdown near a pumping well, analytical solutions should be used. Current investigations are underway to couple the new Analytical Element Model code called TTIM (Bakker and Strack, 2003) with numerical codes such as MODFLOW-USG. The Analytical Element Model code provides an exact solution to the groundwater flow equation enabling simulation of drawdown in the near vicinity (1 foot) of a pumping well. Such a coupling would greatly improve the ability of the GAM to simulate pumping impacts from a single pumping well at distances less than a mile away. This type of enhancement could make the state GAMs a viable tool for assessing individual well permits and spacing rules commonly considered by GCDs.

This page intentionally left blank.

12.0 Conclusions

This report documents the development of a three-dimensional groundwater availability model for the northern Trinity and Woodbine aquifers. The model also includes the Washita/Fredericksburg groups as a confining layer separating the northern Trinity Aquifer from the overlying Woodbine Aquifer. The model was developed to be an updated northern Trinity and Woodbine aquifers GAM for the purposes of planning and groundwater management in GMA 8. This GAM development effort is unique in Texas in that the entire effort was organized and funded by four GCDs in GMA 8. Desiring to make improvements and updates to the 2004 GAM, and to enhance understanding of the northern Trinity and Woodbine aquifers, four GCDs within GMA 8 entered an inter-local agreement in 2012 to support and fund a new and updated GAM for these two aquifers in GMA 8. These four GCDs are North Texas, Northern Trinity, Prairielands, and Upper Trinity GCDs. This work has been performed in a public process similar to that used by the TWDB in their GAM Program. A Technical Advisory Committee comprised of technical representatives of the GCDs within GMA 8, the TWDB, and the USGS formed a technical review committee for this effort. The work benefited from the involvement of a wide group of stakeholders, including the GCDs within GMA 8.

The model was developed using the groundwater simulation code MODFLOW-NWT (Niswonger and others, 2011). MODFLOW is a three-dimensional finite-difference groundwater flow code that is supported by enhanced boundary condition packages to handle recharge, ET, streams, springs, and reservoirs. The updated northern Trinity and Woodbine aquifers GAM is divided into eight model layers. Model Layer 1 represents the shallow surficial flow system in the outcrop areas of the northern Trinity Aquifer, Washita/Fredericksburg groups, and Woodbine Aquifer and the younger formations overlying the Woodbine Aquifer and Washita/Fredericksburg groups east of the outcrop areas. Model Layers 2 through 8 represent the Woodbine Aquifer, Washita/Fredericksburg groups, Paluxy Aquifer, Glen Rose Formation, Hensell Aquifer, Pearsall Formation, and Hosston Aquifer, respectively.

The grid cells in the updated model are refined relative to the 2004 GAM to enable more accurate placement of wells, rivers, and other hydraulic boundary conditions within the model domain. The model has 1,412 columns and 1,124 rows for a total of 12,696,704 grid cells for the

eight model layers. The model grid origin (lower left-hand corner) is located at GAM coordinates 19,067,743 feet north and 6,169,014 feet east and the model is oriented with the x-axis 65 degrees counter-clockwise of east-west to directly overly the grid for the 2004 northern Trinity and Woodbine aquifers GAM.

This updated northern Trinity and Woodbine aquifers GAM was developed using a modeling protocol that is standard to the groundwater modeling industry and has been adopted by the TWDB in their GAM Program. This protocol is based upon industry standards and ASTM standard guides. The GAM protocol includes: (1) the development of a conceptual model for groundwater flow in the aquifers, including defining physical limits and properties, (2) model design, (3) model calibration, (4) sensitivity analysis, and (5) reporting. The model was calibrated to steady-state conditions considered representative of predevelopment and to transient conditions from 1890 through 2012.

The steady-state model was calibrated to water-level measurements from 96 well locations in the northern Trinity and Woodbine aquifers. To better constrain the steady-state model, several other qualitative metrics of calibration were used. These included a comparison to locations of flowing wells and the location and extent of the artesian zone as compared to the literature. Particle tracking was performed to qualitatively evaluate whether groundwater age dates were consistent with observed water quality data in the aquifers. The adjusted mean absolute error (i.e., mean absolute error divided by the range in observed hydraulic heads) is 9.1 percent for the steady-state model, which is within the acceptable GAM standard. The model reasonably reproduced flowing conditions from most identified flowing wells and also reproduced an artesian zone as estimated by Hill (1901). Groundwater travel time contours showed reasonable agreement with the extent of freshwater in the Hensell and Hosston aquifers.

The steady-state long-term average recharge to the northern Trinity and Woodbine aquifers totals 1,766,567 AFY, which is an average rate of approximately 1.6 inches per year. Water discharges from the northern Trinity and Woodbine aquifers through ephemeral streams (54.1 percent of net inflow), perennial streams (41.7 percent of net inflow), riparian ET (3.0 percent of net inflow), net upward cross-formational flow to the overlying younger formations (0.8 percent of net inflow), and to springs (0.1 percent of net inflow). It is important to note that only 0.8 percent of

the entire water budget (recharge) gets to the confined downdip aquifers and discharges through diffuse discharge to the overlying younger formations or through the Mexia-Talco Fault Zone.

The model was successfully calibrated to transient aquifer conditions from 1890 through 2012. The model satisfactorily reproduced observed aquifer hydraulic heads and hydraulic head declines across this time period using 27,490 individual water-level measurements during the calibration period. Wells selected for hydrograph comparisons were chosen from the entire historical period from 1890 to 2012. Because a great deal of the observed declines in hydraulic heads occurred before 1980, hydrographs that showed evidence of drawdown across the entire transient calibration period were used in calibration of the transient model, which resulted in 706 hydrographs selected for use. Simulated stream gains from groundwater were compared to available base flow targets.

The transient model performs well at reproducing transient hydraulic heads across the historical calibration period. The model hydraulic heads residuals (defined as the simulated hydraulic heads minus the observed hydraulic heads) show no systematic bias, with a relatively even distribution around zero. The calibration statistics for all layers meet the GAM requirements. The mean absolute error from 1980 to 2012 ranges from 38.3 to 56.2 feet across all model layers. The mean absolute error divided by the range in observed hydraulic heads for this time period ranges from 1.8 to 5.2 percent for all model layers.

Calibration statistics for the transient period from 1890 through 1949 and from 1950 through 1979 were also calculated. Much fewer calibration hydraulic head measurements exist for the pre-1950 time period. For the pre-1950 period, the mean absolute error ranges from 28.3 to 74.1 feet and the mean absolute error for the period between 1950 and 1980 ranges from 34.2 to 64.3 feet. The mean absolute error divided by the range is less than 10 percent in all units for both time periods, with the exception of the Washita/Fredericksburg groups prior to 1950, when it is 14.5 percent.

The northern Trinity and Woodbine aquifers are extremely complex aquifers. The variability in nature, lithology, thickness, outcrop area, and structural dip is significant within the confines of these aquifers. This makes modeling of these aquifers with a single model and gridding approach very challenging. There are areas in the study area where a significant portion of the confined portions of the aquifers is in the outcrop region. The structural dip of the aquifers is

very flat in the outcrops and becomes much steeper in the subcrop. These conditions lead to a situation where the flow system in the outcrop area of the aquifers is largely independent of the deep confined portions of the aquifers in predevelopment conditions. The connection between the outcrop and the deep downdip regions of the aquifers becomes very important with aquifer development, which is discussed below.

The aquifers and formations that comprise the northern Trinity and Woodbine aquifers are very stratified in their lithology, even within the more sand rich aquifers, such as the Paluxy or Hosston aquifers. As a result, vertical hydraulic conductivity of the aquifers is expected to be very low because it is limited by the finer grained sediments (i.e., shales and limestone). As a result of historical pumping, significant vertical gradients exist within the northern Trinity and Woodbine aquifers between the aquifers and confining formations and these gradients have existed over many decades. This vertical stratification and low vertical hydraulic conductivity of the northern Trinity and Woodbine aquifers has implications for groundwater availability in the aquifers, especially in the deeper confined portions.

The downdip portions of confined aquifers are expected to have very low aquifer storativity. This has been corroborated by this model and other models developed for these aquifers. Because the vertical hydraulic conductivity of the aquifers and formations is very low due to stratification, very low predevelopment groundwater flow to the downdip confined portions of the aquifers might be expected even though the sand aquifers are laterally extensive and have relatively high horizontal hydraulic conductivity. This condition has also been corroborated by this model and others developed for these aquifers. Under predevelopment conditions, only 0.8 percent of the average recharge in the aquifer outcrop reaches the confined aquifers downdip of the outcrop. This is a very low percent of the predevelopment water balance. However, particle tracking within the aquifers demonstrates that this low flow rate is within reason based upon a general comparison to the extent of freshwater in the aquifers. The northern Trinity and Woodbine aquifers have been sub-aerially exposed since the end of the Cretaceous Period, or approximately 65 million years before present. Under predevelopment conditions, the northern Trinity and Woodbine aquifers were full and essentially all recharge was rejected back to the surface through discharge to surface processes.

Development of the aquifers as a groundwater resource has changed that dynamic. Table 12.0.1 provides a summary of select components of the northern Trinity and Woodbine aquifers simulated water balance for predevelopment, 1940, 1950, 1960, 1980, 1990, 2000, and 2010. This table summarizes aquifer recharge, the total model simulated pumping, the net flow from the shallow unconfined water table aquifers (surficial outcrop area represented by Layer 1) to the confined aquifers and formations, the pumping rate for model cells deeper than 300 feet below the base of Layer 1 (considered the deep confined section), the net flow to the deep downdip confined aquifers and formations (again defined by 300 feet below the base of Layer 1), and the amount of groundwater coming out of storage that is a result of pumping within the downdip confined aquifers and formations.

Table 12.0.1 shows that total aquifer pumping increases steadily from the 1940s to present, with a slowing of the increase between 1960 and 1980. Net flow from the shallow unconfined water table aquifer (table column 4) to the confined aquifers and formations is effectively zero in predevelopment, but continually increases as total pumping increases. This represents a net transfer of water from the shallow unconfined aquifers to the shallow confined aquifers in response to pumping. More important is the interaction between the shallow confined system and the deep confined system. Column 5 of Table 12.0.1 tabulates pumping in the deep confined system. The rate increases through 1960 and then plateaus to a slower rate of increase past 1980. Column 6 of Table 12.0.1 summarizes the downdip flow to the deep confined aquifers over time in response to pumping in the deep aquifers. The last column of Table 12.0.1 summarizes the water that comes from deep aquifer storage in response to pumping. It is striking to note that by 1980, less than 30 percent of the groundwater pumped in the deep confined aquifers came from storage but, rather, came from pumping capture from the updip portions of the aquifers. By 2010, storage provides approximately 12 percent of the groundwater pumped in the deep confined aquifers.

This condition is the result of the very low vertical hydraulic conductivities of the northern Trinity and Woodbine aquifers and formations and the low aquifer storativity. The result is that deep pumping quickly depletes available storage with very large hydraulic head declines, which occurred by the 1980s. As a result, the groundwater must be supplied by capture of water that would normally discharge at ground surface in the outcrop. This is an inefficient process since it takes a long time for the deepest wells to benefit from the discharge capture of the shallower

groundwater. The net result is that hydraulic heads in the deep portions of the aquifers keep declining, even as rates of groundwater use remain relatively stable.

Like all models, the updated Trinity and Woodbine aquifers GAM has limitations and can be improved. Key limitations regarding data gaps are explained in detail in Section 10 and are not reproduced here. There are several key assumptions that are potentially important to the model regarding construction and calibration. Both the boundary to the younger formations overlying the northern Trinity and Woodbine aquifers and the model base boundary have uncertainty in their character and in their implementation in the model. The approach used for both boundaries is consistent with most regional models. However, the lower boundary with the Paleozoic-age strata is a potential limitation to the current model in local areas of the model domain. The underlying Paleozoic-age strata are an uncertain boundary to the model that is poorly constrained. While interaction between the Hosston Aquifer and the underlying Paleozoic-age strata may be locally important, it is not considered to be regionally important and is poorly characterized. After discussions with the TWDB, it was agreed that it was conservative to maintain the lower boundary as a no-flow boundary since the model will be used principally as a groundwater availability model. In the outcrop area or the northern Trinity aquifer, this assumed boundary condition may be a model limitation.

Scale is always an issue for any regional finite-difference model. Despite having grid cells that are only one sixteenth of a square mile, the model does not have the capability to accurately predict the impacts of a pumping well on hydraulic heads in the vicinity of the well within a distance of several grid dimensions. The finer model grid resolution does improve the representation of well locations and aquifer properties in the model, however. For calculation of drawdown at a well during pumping or well spacing calculations involving distances of several miles or less, analytic models should be used. This model provides information such as hydraulic properties, aquifer structure, and aquifer hydraulic heads that will be useful for local-scale analytic calculations. This data provides a good baseline which can always be augmented by new data sources.

The updated northern Trinity and Woodbine aquifers GAM documented in this report represents a large step forward in the understanding of the northern Trinity and Woodbine aquifers and provides a very good foundation for future planning activities as well as future research. This

model offers distinct advantages over the 2004 northern Trinity and Woodbine aquifers GAM. The data supporting this model is publicly available and will allow other investigators to build on this work or use source data in local groundwater management situations throughout the study area. Also, this model includes a true steady-state simulation that defines the hydraulic heads for the transient period in one simulation. The transient model has been transiently calibrated (1890 to 2012) to a greatly expanded calibration hydraulic head target data set and has been calibrated across the historical decline in hydraulic heads that started in the late 1800s, but accelerated in the later 1940s through the present. This calibration of the hydraulic head declines offers better constraint on aquifer storage parameters. Calibration metrics to observed hydraulic heads have been improved model wide using many more calibration targets. Finally, this model has incorporated data from many of the GCDs within GMA 8 and, because it is calibrated through 2012, offers the most up-to-date tool for regional planning calculations. This model has advanced the work that was started with the 2004 GAM and provides stakeholders the information underlying the model.

Table 12.0.1   Transient water balance for the northern Trinity and Woodbine aquifers and the Washita/Fredericksburg groups for select components of the water balance.

Year	Recharge (AFY)	Total Pumping (AFY)	Net Confined Flow[a] (AFY)	Deep Pumping[b] (AFY)	Net Downdip Confined Flow[c] (AFY)	Deep Storage[d] (AFY)
1889	1,766,549	0	503	0	2	0
1940	1,266,049	-58327.1	53,298	-31,749	23,446	8,304
1950	2,181,606	-91299.1	72,248	-48,113	30,401	17,713
1960	1,972,149	-121543	95,138	-61,981	42,364	19,617
1980	2,033,527	-227956	185,324	-104,552	75,799	28,755
1990	2,193,932	-241691	212,141	-107,284	92,347	14,937
2000	1,206,348	-266419	232,231	-117,533	100,167	17,363
2010	2,888,125	-285357	248,096	-127,078	112,140	14,937

[a] net model flow in AFY from the surficial outcrop area of Layer 1 to underlying layers
[b] model pumping that occurs approximately below a depth of 300 feet below the base of the surficial outcrop area of Layer 1
[c] net model flow in AFY that occurs to aquifers at a depth of 300 feet below the base of the surficial outcrop area of Layer 1
[d] model outflow from storage in AFY occurring within aquifers at a depth of 300 feet below the base of the surficial outcrop area of Layer 1

13.0 Acknowledgements

The authors of this study would like to thank the Directors of the North Texas, Northern Trinity, Prairielands, and Upper Trinity GCDs for their support and funding of the model developed and documented in this report. We would also like to thank Mr. Bill Mullican who has performed as Contract Manager ("owner's representative"), provided oversight of our activities, and also provided communication between the technical team and the Contract Management Committee representing the four funding districts. We appreciate the member Districts of GMA 8 for supporting our efforts directly with data and their participation in the Technical Advisory Committee, which is composed of the following representatives:

Member[a]	Affiliation
Bill Mullican	NTWO Project Contract Manager and TAC Chairman
Dirk Aaron[b]	Clearwater GCD
Bobby Bazan[b]	Post Oak Savannah GCD
Al Blair[b]	Southern Trinity GCD
Dan Caudle	Upper Trinity GCD
Hughbert Collier	North Texas GCD
Joe B. Cooper[b]	Middle Trinity GCD
Dennis Erinakes	Prairielands GCD
David Gattis	Red River GCD
Joshua Grimes	Prairielands GCD
Robert Joseph	USGS representing the Northern Trinity GCD
Robert Mace	TWDB (Larry French designated alternate)
Bob Patterson	Upper Trinity GCD
Drew Satterwhite[b]	North Texas GCD
Richard Sawey	Northern Trinity GCD
Jerry Shi	TWDB
Mitchel Sodek	Central Texas GCD

[a] in May 2014
[b] denotes new member

We would also like to thank the individuals who spent countless hours, many on personal time, reviewing the Draft Conceptual Model and/or the Draft Final Model Report. Their reviews were complete and thoughtful, and they have made this final model and report a much better product. These individuals and affiliations are: Mr. Hughbert Collier, P.G., Mr. Lou Fleischhauer, P.G, and Mr. Peter Schulmeyer, P.G. of Collier Consulting, Inc; Mr. Dennis Erinakes, P.G. of the Prairielands GCD; Mr. Mike Massey of the Upper Trinity GCD; Mr. Bill Mullican, P.G. of Mullican and Associates; Dr. Robert Mace, P.G., Mr. Larry French, P.G., Ms. Cindy Ridgeway,

14.0 References

Adkins, W.S., 1923, Geology and mineral resources of McLennan County, Texas: Bureau of Economic Geology, The University of Texas at Austin, Bulletin 2430, Austin, TX.

Adkins, W.S., 1933, The Mesozoic Systems in Texas: in Sellards, E.H., Adkins, W.S., and Plummer, F.B., The geology of Texas, Bureau of Economic Geology, The University of Texas at Austin, Bulletin 3232, Austin, TX.

Adkins, W.S., and Arick, M.B., 1930, Geology of Bell County, Texas: Bureau of Economic Geology, The University of Texas at Austin, Bulletin 3016, Austin, TX.

Adkins, W.S., and Lozo, F.E., 1951, Stratigraphy of the Woodbine and Eagle Ford, Waco area: in The Woodbine and adjacent strata of the Waco area of central Texas, Fondren Science Series 4, Southern Methodist University, Dallas, TX

Al-Sefry, S.A., and Sen, Z., 2006, Groundwater rise problem and risk evaluation in major cities of arid lands – Jedddah case in Kingdome of Saudi Arabia: Water Resources Management, vol. 20, p. 91-108.

Alger, R.P., 1966, Interpretation of electric logs in fresh water wells in unconsolidated formations: 7th Annual Symposium Transactions: Society of Professional Well Log Analysts, paper CC.

Allen, R.G., Pereira, L.S., Raes, D., and Smith, M., 1998, Crop evapotranspiration – Guidelines for computing crop water requirements: Food and Agriculture Organization of the United Nations (FAO), FAO Irrigation and drainage paper 56, Rome, Italy, http://www.fao.org/docrep/X0490E/X0490E00.htm.

Alley, W.M., Reilly, T.E., and Franke, O.L., 1999, Sustainability of ground-water resources. USGS, Circular 1186.

Alpay, O.A., 1972, A practical approach for defining reservoir heterogeneity: Journal of Petroleum Technology, vol. 24, p. 841-848.

Ambrose, M.L., 1990, Ground-water protection and management strategies for north-central Texas: A Critical Area Ground-Water Study: Texas Water Commission Critical Area File Report, March 1990.

American Society for Testing and Materials (ASTM) International, 2004, Standard guide for application of a ground-water flow model to a site-specific problem: Designation: D5447 – 04, West Conshohocken, PA.

American Society for Testing and Materials (ASTM) International, 2006, Standard guide for documenting a ground-water flow model application: Designation: D5718 – 95 (Reapproved 2006), West Conshohocken, PA.

American Society for Testing and Materials (ASTM) International, 2008a, Standard guide for defining boundary conditions in ground-water flow modeling: Designation: D5609 – 94 (Reapproved 2008), West Conshohocken, PA.

American Society for Testing and Materials (ASTM) International, 2008b, Standard guide for defining initial conditions in ground-water flow modeling: Designation: D5610 – 94 (Reapproved 2008), West Conshohocken, PA.

American Society for Testing and Materials (ASTM) International, 2008c, Standard guide for calibrating a ground-water flow model application: Designation: D5981 – 96 (Reapproved 2008), West Conshohocken, PA.

American Society for Testing and Materials (ASTM) International, 2008d, Standard guide for comparing ground-water flow model simulations to site-specific information: Designation: D5490 – 93 (Reapproved 2008), West Conshohocken, PA.

American Society for Testing and Materials (ASTM) International, 2008e, Standard guide for conducting a sensitivity analysis for a ground-water flow model application: Designation: D5611 – 94 (Reapproved 2008), West Conshohocken, PA.

Anderson, M.P., and Woessner, W.W., 1992, Applied groundwater modeling: Academic Press, San Diego, California.

Anderson, M.P., and Woessner, W.W., 2002, Applied groundwater modeling. simulation of flow and advective transport: Academic Press, San Diego, CA, p. 377.

Appleyard, S.J., Davidson, W.A., and Commander, D.P., 1999, The effects of urban development on the utilisation of groundwater resources in Perth, Western Australia: in Groundwater in the urban environment – selected city profiles, Chilton, J. (ed), AA Balkema, Rotterdam, Netherlands, p. 97–104.

Ashworth, J.B., 1983, Ground-water availability of the lower Cretaceous formations in the Hill Country of south-central Texas: Texas Department of Water Resources, Report 273, Austin, TX.

Atlee, W.A., 1962, The lower Cretaceous Paluxy Sand in central Texas: Baylor Geological Studies, Bulletin 2, Baylor University, Waco, TX.

Back, W., 1966, Hydrochemical facies and groundwater flow patterns in northern part of the Atlantic Coastal Plain: USGS, Professional Paper 498-A.

Back, W., Hanshaw, B.B., Plummer, L.N., Rahn, P.H., Rightmire, C.T., and Rubin, M., 1983, Process and rate of dedolomitization: mass transfer and ^{14}C dating in a regional carbonate aquifer: Geological Society of America, vol. 94, no. 12, p. 1415-1429.

Bain, J.S., 1973, The nature of the Cretaceous-PreCretaceous contact, north-central Texas: Baylor Geological Studies, Bulletin 25, Baylor University, Waco, TX.

Baker, E.T., Jr., 1960, Geology and ground-water resources of Grayson County, Texas: TWDB, Bulletin 6013, Austin, TX.

Baker, B.B., 1971, Occurrence and availability of ground water in the vicinity of Commerce, Texas: TWDB, unnumbered report, Austin, TX.

Baker, B.B., Dillard, J.W., Souders, V.L., and Peckham, R.C., 1963a, Reconnaissance investigation of the ground-water resources of the Sabine River basin, Texas: Texas Water Commission, Bulletin 6307, Austin, TX.

Baker, E.T., Jr., Long, A.T., Jr., Reeves, R.D., and Wood, L.A., 1963b, Reconnaissance investigation of the ground-water resources of the Red River, Sulphur River, and Cypress Creek basins, Texas: Texas Water Commission, Bulletin 6306, Austin, TX.

Baker, B., Duffin, G., Flores, R., and Lynch, T., 1990a, Evaluation of water resources in part of central Texas: TWDB, Report 319, Austin, TX.

Baker, B., Duffin, G., Flores, R., and Lynch, T., 1990b, Evaluation of water resources in part of north-central Texas: TWDB, Report 318, Austin, TX.

Bakker M, and Strack, O., 2003, Analytic elements for multiaquifer flow: Journal of Hydrology, v. 271,no. 1-4, p. 119-129.

Baldwin, E.E., 1974, Urban geology of the Interstate Highway 35 growth corridor between Belton and Hillsboro, Texas: Baylor Geological Studies, Bulletin 27, Baylor University, Waco, TX.

Baldys, S., and Schalla, F.E., 2011, Base Flow (1966-2009) and streamflow gain and loss (2010) of the Brazos River form the New Mexico – Texas state line to Waco, Texas: USGS, Scientific Investigations Report 2011-5224.

Bayha, D.C., 1967, Occurrence and quality of ground water in Montague County, Texas: TWDB, Report 58, Austin, TX.

Beach, J.A., Huang, Y, Symank, L., Ashworth, J.B., Davidson, T., Vreugdenhil, A.M., and Deeds, N.E., 2009, Nacatoch Aquifer groundwater availability model: prepared for the TWDB by LBG-Guyton Associates and INTERA, Inc, http://www.twdb.state.tx.us/groundwater/models/gam/nctc/NCTC_Model_Report.pdf.

Bené, J., Harden, B., O'Rourke, D., Donnelly, A., and Yelderman, J., 2004, Northern Trinity/Woodbine groundwater availability model: Prepared for the TWDB by R.W. Harden & Associates, Inc., with Freese and Nichols, Inc, HDR Engineering, Inc., LBG Guyton Associates, USGS, and Dr. Joe Yelderman, Jr., http://www.twdb.state.tx.us/groundwater/models/gam/trnt_n/TRNT_N_Model_Report.pdf.

Bennett, R.R., 1942, Memorandum on ground-water resources in the area about 8 miles north of
    Belton: U.S. Department of the Interior, Geological Survey, Open-File Report.

Bethke, C.M., 1989, Modelling subsurface flow in sedimentary basins: Geol. Rundsch. 78,
    p. 129-154.

Beynon, B.E., 1991, Ground-water quality monitoring of the Trinity Aquifer in the vicinity of
    Erath County: TWDB, Report 331, Austin, TX.

Blakey, R.C., 2011, Paleogeographic maps: Colorado Plateau Geosystems, Arizona USA.

Bluntzer, R.L., 1992, Evaluation of ground-water resources of the Paleozoic and Cretaceous
    aquifers in the Hill Country of central Texas: TWDB Report 339, Austin, TX.

Boone, P.A., 1968, Stratigraphy of the basal Trinity (Lower Cretaceous) sands of central Texas:
    Baylor Geological Studies, Bulletin No. 15, Baylor University.

Borrelli, J., Fedler, C.B., and Gregory, J.M., 1998, Mean crop consumptive use and free-water
    evaporation for Texas: Prepared for the TWDB by the Department of Civil Engineering,
    Texas Tech University, Lubbock, TX,
    http://www.twdb.texas.gov/publications/reports/contracted_reports/doc/95483137.pdf.

Bosch, D.J., Lohani,V.K., Dymond, R.L., Kibler, D.F., and Stephenson, K., 2003, Hydrological
    and fiscal impacts of residential development: Virginia case study: Journal of Water
    Resources Planning and Management, vol. 129, no. 2, p 107-114.

Bradbury, K.R., and Muldoon, M.A., 1900, Hydraulic conductivity determinations in unlithified
    glacial and fluvial materials. in Neilsen, D.M., and Johnson, A.I., (eds) Groundwater and
    vadose monitoring: ASTM, STP. 1053, p. 138-151.

Bradfield, H.H., 1957, The geology and geophysics of Cooke and Grayson counties, Texas: The
    Dallas Geological Society and the Dallas Geophysical Society, Dallas, TX.

Bradley, R.G., 1999, Updated evaluation of water resources within the Trinity Aquifer area,
    central Texas: TWDB, Open-File Report 99-03, Austin, TX.

Bredehoeft, J.D., 2002, The water budget myth revisited: Why hydrogeologists model:. Ground Water, vol., 40, no. 4, p. 340-345.

Broom, M.E., Alexander, W.H., Jr., and Myers, B.N., 1965, Ground-water resources of Camp, Franklin, Morris, and Titus counties, Texas: TWDB, Bulletin 6517.

Brown, Jr., L.F., Solis-Iriarte, R.F., and Johns, D.A., 1990, Regional depositional systems tracts, paleogeography, and sequence stratigraphy, upper Pennsylvanian and lower Permian strata, north- and west-Central Texas: Bureau of Economic Geology, The University of Texas at Austin, Report of Investigations 197, Austin, TX.

Brune, G., 2002, Springs of Texas, Volume 1, 2nd edition: Texas A&M University Agriculture series, No. 5, Texas A&M University Press, College Station, TX.

Brune, G., and Duffin, G.L., 1983, Occurrence, availability, and quality of ground water in Travis County, Texas: TWDB, Report 276, Austin, TX.

Bryan, F., 1951, The Grand Prairies of Texas: in The Woodbine and adjacent strata of the Waco area of central Texas, Fondren Science Series 4, Southern Methodist University, Dallas, TX.

Bullard, F.M., 1925, Geology of Love County Oklahoma: Oklahoma Geological Survey, Bulletin 33, University of Oklahoma, Norman, OK.

Bullard, F.M., 1926, Geology of Marshall County Oklahoma, Oklahoma Geological Survey, Bulletin No. 39, The University of Oklahoma, Norman, OK.

Bullard, F.M., 1931, The geology of Grayson County, Texas: Bureau of Economic Geology, The University of Texas at Austin, Bulletin 3125, Austin, TX.

Bullard, F.M., and Cuyler, R.H., 1930, A preliminary report on the geology of Montague County, Texas: Bureau of Economic Geology, The University of Texas at Austin, Bulletin 3001, Austin, TX.

Bureau of Economic Geology, 1992, Geology of Texas – page-sized color map and text: Bureau of Economic Geology, The University of Texas at Austin, Austin, TX.

Bureau of Economic Geology, 2012, Digital 15-minute GAT (Geologic Atlas of Texas) Quads for the State of Texas: website http://www.beg.utexas.edu/pubs/15minquads.php.

Bybee, H.P., and Bullard, F.M., 1927, The geology of Cooke County, Texas: Bureau of Economic Geology, The University of Texas at Austin, Bulletin 2710, Austin, TX.

Cade, C.A., Evans, J., and Bryant, S.L., 1994, Analysis of permeability controls; a new approach: Clay Mineralogy, vol. 29, p. 491-501.

Carmen, P.C, 1939, Permeability of saturated sands, soils and clays: Journal of Agricultural Science 29, pp. 262-273.

Caskey, T.L., 1961, Geology of western Coryell County, Texas: M.S. Thesis, The University of Houston, Houston, TX.

Castro, M.C., and Goblet, P., 2003, Calibration of regional groundwater flow models: Working toward a better understanding of site-specific systems: Water Resources Research, v. 39, no. 6, p. SBH 13-1 - SBH 13-25.

Caughey, C.A., 1977, Depositional systems in the Paluxy Formation (Lower Cretaceous), northeast Texas-oil, gas, and groundwater resources: Bureau of Economic Geology, The University of Texas at Austin, Geological Circular 77-8, Austin, TX.

Central Texas GCD and Partridge, T., 2011, Trinity Aquifer characterization and groundwater availability assessment Burnet County: Central Texas GCD publication.

Chaudhuri, S., and Ale, S., 2013, Characterization of groundwater resources in the Trinity and Woodbine aquifers in Texas: Science of the Total Environment, p. 452-453; 338-348.

Chebotarev, I.I., 1955, Metamorphism of natural waters in the crust of weathering:. Geochimica et Cosmochimica Acta, vol. 8, 22-48, 137-170, 198-212.

Cho, Y., 2013, County population: personal communication via email from Yun Cho at the TWDB to Toya Jones of INTERA, Inc., dated May 30, 2013.

Chow, V.T., Maidment, D.R., and Mays, L.W., 1988, Applied hydrology: McGraw-Hill, Inc.

Christian, B., and Wuerch, D., 2012, Compilation of results of aquifer tests in Texas: TWDB, Report 381, Austin, TX.

Collier, H.A., 1993, Borehole geophysical techniques for determining the water quality and reservoir parameters of fresh and saline water aquifers in Texas – volume I of II: TWDB Report 343, Austin, TX.

Cooper, H.H., and Jacob, C.E., 1946, A generalized graphical method for evaluating formation constants and summarizing well history: Transactions, American Geophysical Union, vol. 2, p. 526-534.

Cronin, J.G., Follett, C.R., Shafer, G.H., and Rettman, P.L., 1973, Reconnaissance investigation of the ground-water resources of the Brazos River Basin, Texas: Texas Water Commission, Bulletin 6310, Austin, TX.

Cumley, J.C., 1943, Records of wells and springs, drillers' logs, water analyses, and map showing locations of wells and springs, Dallas County, Texas: Texas State Board of Water Engineers, Miscellaneous Report 66, Austin, TX.

Cumley, J.C., Cromack, G.H., and Follett, C.R., 1942, Records of wells and springs, drillers' logs, water analyses, and map showing locations of wells and springs, Williamson County, Texas: Texas State Board of Water Engineers, Miscellaneous Report 298, Austin, TX.

Cutter, C., 1894, Cutter's guide to the city of Waco: publication information unknown.

Dagan, G., 1986, Statistical theory of groundwater flow and transport; pore to laboratory, laboratory to formation and formation to regional scale: Water Resources Research, vol. 22, 1205–1355.

Dane, C.H., 1929, Upper Cretaceous formations of southwestern Arkansas: Arkansas Geological Survey, Bulletin 1, Little Rock, AR.

Davis, D.A., 1938, Records of wells, drillers' logs, and water analyses, and map showing location of wells, Brown County, Texas: Texas State Board of Water Engineers, Miscellaneous Report 23, Austin, TX.

Davis, L.V., 1960, Geology and ground-water resources of southern McCurtain County, Oklahoma: Oklahoma Geological Survey, Bulletin 86, University of Oklahoma, Norman, OK.

Davis, S.N., 1969, Porosity and permeability of natural material. Flow through porous materials, ed. DeWeist, R.J.M: New York , Academic Press, p. 54-89.

Davis, K.W., 1974, Stratigraphy and depositional environments of the Glen Rose Formation, north-central Texas,: Baylor Geological Studies, Bulletin 26, Baylor University, Waco, TX.

Davis, R.E., and Hart, D.L., 1978, Hydrologic data for the Antlers Aquifer, southeastern Oklahoma: USGS, Open-File Report 78-1038.

Deeds, N., Kelley, V., Fryar, D., Jones, T., Whallon, A.J., and Dean, K., 2003, Groundwater availability model for the southern Carrizo-Wilcox Aquifer: Prepared for the TWDB by INTERA, Inc, and Parsons, http://www.twdb.state.tx.us/groundwater/models/gam/czwx_s/CZWX_S_Full_Report.pdf.

Diehl, M.L., 2011, Intra-aquifer characterization and potential management impacts: Trinity Aquifer, Central Texas: M.S. Thesis, Baylor University, Waco, TX.

Dodge, C.F., 1952, Stratigraphy of the Woodbine Formation in the Arlington Area, Tarrant County, Texas: Field & Laboratory, vol. 20, no. 2, p. 66-78.

Dodge, C.F., ed., 1968, Stratigraphy of the Woodbine Formation, Tarrant County, Texas: Geologic Society of America, South-Central Section Field Trip Guidebook, 76 p.

Dodge, C.F., 1969, Stratigraphic nomenclature of the Woodbine Formation, Tarrant County, Texas: Texas Journal of Science, vol. 21, p. 43-62.

Doherty, J., 2005, PEST, model-independent parameter estimation, user manual, 5th edition: Watermark Numerical Computing, http://www.pesthomepage.org/Downloads.php, 336 p.

Domenico, P.A., and G.A. Robbins, 1985, The dsplacement of connate water from aquifers, Geological Society of America Bulletin, vol. 96, p. 328-335.

Domenico, P.A., 1972, Concepts and models in groundwater hydrology: McGraw-Hill, New York, NY.

Domenico, P.A., and Schwartz, F.W., 1990, Physical and chemical hydrogeology: John Wiley and Sons, New York, NY.

Duffin, G.L, and Musick, S.P., 1991, Evaluation of water resources in Bell, Burnet, Travis, Williamson and parts of adjacent counties, Texas: TWDB, Report 326, Austin, TX.

Dunne, T., and Leopold, L.B., 1978, Water in environmental planning: W. H. Freeman and Company, San Francisco, CA.

Dutton, A.R., and Richter, B.C., 1990, Regional geohydrology of the Gulf Coast Aquifer in Matagorda and Wharton counties: Development of a numerical model to estimate the impact of water-management strategies: Prepared for the Lower Colorado River Authority, Austin, TX.

Dutton, A.R., Mace, R.E., Nance, H.S., and Blüm, M., 1996, Geologic hydrogeologic framework of regional aquifers in the Twin Mountains, Paluxy, and Woodbine formations near the SSC site, north-central Texas: Topical Report prepared for the Texas National Research Laboratory Commission by the Bureau of Economic Geology, The University of Texas at Austin, Austin, TX.

Dutton, A.R., 2013, Pre-development hydraulic heads in 1996 model: personal communication between Alan Dutton at the University of Texas at San Antonio and Van Kelley of INTERA Incorporated via telephone, June 19, 2013.

Evans, J., Cade, C., and Byrant, S. 1997, A geological approach to permeability predictions in clastic reservoirs: in Kupecz, J.A., Gluyas, J., and Bloch, S., eds., Reservoir quality predictions in sandstones and carbonates, AAPG Memoir 69, p. 91-101.

Ewing, T.E., 1990, Tectonic map of Texas scale 1:750,000, 4 sheets: Bureau of Economic Geology, The University of Texas at Austin, Austin, TX.

Ewing, T.E., 1991, Structural framework: in Salvador, A., ed., The geology of North America: the Gulf of Mexico basin, v. J: Boulder, Colorado, Geological Society of America, p. 31-52.

Fiedler, A.G., 1934, Artesian water in Somervell County Texas: U.S. Department of the Interior, Water-Supply Paper 660, Washington, DC.

Fisher, W.L., and Rodda, P.U., 1966, Nomenclature revision of the basal Cretaceous rocks between the Colorado and Red Rivers, Texas: Bureau of Economic Geology, The University of Texas at Austin, Report of Investigations 58, Austin, TX.

Fisher, W.L., and Rodda, P.U., 1967, Lower Cretaceous sands of Texas: Stratigraphy and resources: Bureau of Economic Geology, The University of Texas at Austin, Report of Investigations 59, Austin, TX.

Flawn, P.T., Goldstein, Jr., A., King, P.B., and Weaver, C.E., 1961, The Ouachita system: The University of Texas at Austin, Publication 6120, 401 p.

Fogg, G.E., and Kreitler, C.W., 1982, Ground-water hydraulics and hydrochemical facies in Eocene aquifers of the East Texas Basin: Bureau of Economic Geology, The University of Texas at Austin, Report of Investigations No. 127, Austin, TX.

Fogg, G.E., 1986, Stochastic analysis of aquifer interconnectedness, with a test case in the Wilcox Group, east Texas: Ph.D. Dissertation, The University of Texas at Austin.

Fogg, G.E., and Blanchard, P.E., 1986, Empirical relations between Wilcox ground-water quality and electric log resistivity, Sabine uplift area: in Geology and ground-water hydrology of deep-basin lignite in the Wilcox Group of east Texas, Kaiser, W.R., ed., Bureau of Economic Geology, The University of Texas at Austin Austin, TX.

Folk, R.L., 1980, Petrology of sedimentary rocks: Hemphill Publishing Company, Austin, TX.

Forman, R.T.T., 2014, Urban ecology: science of cities: Cambridge University Press, Cambridge, United Kingdom.

Freeze, R.A., 1969, The mechanism of natural ground-water recharge and discharge. 1. One-dimensional, vertical, unsteady, unsaturated flow above a recharging or discharging ground-water flow system: Water Resources Research, v. 5, no. 1, p. 153-171.

Freeze, R.A., 1971, Three-dimensional, transient, saturated-unsaturated flow in a groundwater basin: Water Resources Research, v. 7, no. 2, p. 347-366.

Freeze, R.A., and Cherry, J.A., 1979, Groundwater: Prentice Hall, Englewood Cliffs, N.J.

Freyberg, D., 1988, An exercise in ground-water modeling calibration and prediction: Groundwater, vol. 26, no. 3, p. 350-360.

Fry, J., Xian, G., Jin, S., Dewitz, J., Homer, C., Yang, L., Barnes, C., Herold, N., and Wickham J., 2011, Completion of the 2006 national land cover database for the conterminous United States, Photogrammetric Engineering and Remote Sensing (PE&RS), vol. 77, no. 9, p. 858-864.

Garcia-Fresca, B., and Sharp, J.M., Jr., 2005, Hydrogeologic considerations of urban development: urban-induced recharge: Reviews in Engineering Geology, vol. 16, p. 123-136.

Garcia-Fresca, B., 2006, Urban-enhanced groundwater recharge: review and case study of Austin, Texas, USA: in Urban groundwater, meeting the challenge, International Association of Hydrogeologists Selected Papers, Howard, K.W.F., ed., Taylor & Francis: London, UK, p. 3-18.

Gee, G.W., and Hillel D., 1988, Groundwater recharge in arid regions: review and critique of estimation methods: Hydrological Processes, vol. 2, p. 255-266.

George, W.O., 1940, Records of wells and springs, drillers' logs, water analyses, and map showing locations of wells and springs, Callahan County, Texas: Texas State Board of Water Engineers, Miscellaneous Report 29, Austin, TX.

George, W.O., 1942, Ground water in the vicinity of Burnet and Bertram, Burnet County, Texas: U.S. Department of the Interior, Geological Survey, Open-File Report.

George, W.O., and Barnes, B.A., 1945, Results of tests on wells at Waco, Texas: TWDB, Report M288, Austin, TX.

George, W.O., and Broadhurst, W.L., 1943, Ground water resources at Grand Prairie, Texas and vicinity: USGS Open-File Report.

George, W.O., and Rose, N.A., 1942, Ground water resources of Fort Worth and vicinity, Texas: TWDB, Report M087, Austin, TX.

George, P.G., Mace, R.E. and Petrossian, R., 2011, Aquifers of Texas: TWDB, Report 380, Austin, TX.

Griffith, G.E., Bryce, S.B., Omernik, J.M., and Rogers, A., 2007, Ecoregions of Texas: TCEQ, Austin, TX. 125p.

Gutjahr, A.L., Gelhar, L.W., Bakr, A.A., and MacMillan, J.R., 1978, Stochastic analysis of spatial variability in subsurface flows -2, Evaluation and application: Water Resources Research, v. 14, no. 5, p. 953-959.

Guyton, W.F., and George, W.O., 1943, Results of pumping test of wells at Camp Hood, Texas: U.S. Department of the Interior, Geological Survey, Open-File Report, TWDB, Report M031, Austin, TX.

Hall, W.D., 1976, Hydrogeologic significance of depositional systems and facies in lower Cretaceous sandstones, north-central Texas: Bureau of Economic Geology, The University of Texas at Austin, Geological Circular 76-1, Austin, TX.

Hall, D.W., and Turk, C.J., 1975, Aquifer evaluation using depositional systems – an example in north central Texas: Groundwater, vol. 13, no. 6, p. 472-483.

Hamlin, H.S., Smith, D.A., and Akhter, M.S., 1988, Hydrogeology of Barbers Hill salt dome, Texas coastal plain: Bureau of Economic Geology, The University of Texas at Austin, Report of Investigations 176, Austin, TX.

Hamman, R.R., 2001, High resolution sequence stratigraphy of the Cretaceous Woodbine
    Formation, Henderson and Navarro counties, Texas: M.S. Thesis, The University of Texas at
    Austin, Austin, TX.

Harbaugh, A.W., 2005, MODFLOW-2005, the U.S. Geological Survey modular ground-water
    model – the ground-water flow process: USGS, Techniques and Methods 6-A16.

Harbaugh, A.W., and McDonald, M.G., 1996, User's documentation for MODFLOW-96, An
    update to the U.S. Geological Survey modular finite-difference ground-water flow model:
    USGS, Open-File Report 96-485.

Harbaugh, A.W., Banta, E.R., Hill, M.C., and McDonald, M.G., 2000, MODFLOW-2000, The
    U.S. Geological Survey modular ground-water model - User guide to modularization
    concepts and the ground-water flow process: USGS, Open-File Report 00-92.

Harbor, J.M., 1994, A practical method for estimating the impact of land-use change on surface
    runoff, groundwater recharge and wetland hydrology: Journal of The American Planning
    Association, vol. 60, no. 1, p. 95-108.

Hart, D.L., Jr., 1974, Reconnaissance of the water resources of the Ardmore and Sherman
    quadrangles, southern Oklahoma: Oklahoma Geological Survey, Map HA-3, prepared in
    cooperation with the USGS, The University of Oklahoma, Norman, OK.

Hart, Jr., D.L., and Davis, R.E., 1981, Geohydrology of the Antlers Aquifer (Cretaceous),
    southeastern Oklahoma: Oklahoma Geological Survey, Circular 81, 33 p, The University of
    Oklahoma, Norman, OK.

Hayward, O.T., and Brown, L.F., Jr., 1967, Comanchean (Cretaceous) rocks of central Texas:
    Society of Economic Paleontologists and Mineralogists, Permian Basin Section,
    Publication 67-8.

Healy, R.W., 2010, Estimating groundwater recharge: Cambridge University Press, 256 p.

Heitmuller, F.T., and Reece, B.D., 2003, Database of historically documented springs and spring
    flow measurements in Texas: USGS, Open-File Report 03-315,
    http://pubs.usgs.gov/of/2003/ofr03-315/.

Hendricks, L., ed., 1957, Geology of Parker County, Texas: The University of Texas at Austin,
    Publication 5724.

Henningsen, E.R., 1962, Water diagenesis in lower Cretaceous Trinity aquifers of central Texas:
    Baylor Geological Studies, Bulletin 3, Baylor University, Waco, TX.

Herczeg A.L., and Edmunds, W.M., 2000, Inorganic ions as tracers: In Environmental Tracers in
    Subsurface Hydrology, eds. Cook, P., and Herczeg, A.L., Kluwer Academic, Boston, MA.

HGL, 2010, MODFLOW-SURFACT Software (Version 3.0) Overview: Installation
    Registration, and Running Procedures: Hydrogeologic, Inc., Herndon, VA.

Hill, R.T., 1891, The Comanche Series of the Texas-Arkansas region: Geological Society of
    America, Bulletin, vol. 2, p. 503-528.

Hill, R.T., 1894, Geology of parts of Texas, Indian Territory, and Arkansas adjacent to the Red
    River: Geological Society of America Bulletin, vol. 5, p. 297-338.

Hill, R.T., 1901, Geography and geology of the Black and Grand Prairies, Texas with detailed
    descriptions of the Cretaceous formations and special reference to artesian waters: USGS,
    21st Annual Report, Washington, DC, part 7.

Holland, J.M., 2011, An exploration of the ground water quality of the Trinity Aquifer using
    multivariate statistical techniques: M.S. Thesis, University of North Texas, Denton, TX.

Holland, T.W., 2007, Water use in Arkansas, 2005: USGS, Scientific Investigations
    Report 2007-5241.

Hooker, P.J., McBridge, D., Brown, M.J., Lawrence, A.R., and Gooddy, D.C., 1999, An
    integrated hydrogeological case study of a post-industrial city in the West Midlands of

England. in Groundwater in the urban environment – selected city profiles, Chilton, J. ed.,
AA Balkema, Rotterdam, Netherlands, p. 145–150.

Hopkins, J., 1996, Water quality in the Woodbine Aquifer: TWDB, Hydrologic Atlas No. 4,
Austin, TX.

Hudak, P.F., and Wachal, D.J., 2001, Effects of brine injection wells, dry holes, and plugged
oil/gas wells on chloride, bromide, and barium concentrations in the Gulf Coast Aquifer,
southeast Texas, USA: Environmental Monitoring and Assessment, vol. 17, p. 249-264.

Hudak, P.F., and Sanmanee, S., 2003, Spatial patterns of nitrate, chloride, sulfate, and fluoride
concentrations in the Woodbine Aquifer of north-central Texas: Environmental Monitoring
and Assessment, vol. 82, no. 3, p. 311-320.

Huffman, G.G., Alfonsi, P.P., Dalton, R.C., Duarte-Vivas, A., and Jeffries, E.L., 1975, Geology
and mineral resources of Choctaw County, Oklahoma: Oklahoma Geological Survey,
Bulletin 120, The University of Oklahoma, Norman, OK.

Huffman, G.G., Hart, T.A., Olson, L.J., Currier, J.D., and Ganser, R.W., 1978, Geology and
mineral resources of Bryan County, Oklahoma: Oklahoma Geological Survey, Bulletin 126,
The University of Oklahoma, Norman, OK.

Huffman, G.G., Bridges, K.F., Ganser, R.W., Holtzman, A.M., Jr., and Merritt, M.L., 1987,
Geology and mineral resources of Marshall County, Oklahoma: Oklahoma Geological
Survey, Bulletin 142, The University of Oklahoma, Norman, OK.

Information Handling Services (iHS), 2013, U.S. well data: iHS website,
http://www.ihs.com/products/oil-gas/ep-data/well/united-states.aspx, accessed 2013.

Johnston, R.H., 1997, Hydrologic budgets of regional aquifer systems of the United States for
predevelopment and development conditions: USGS, Professional Paper 1425.

Jones, I.C., 2003, Groundwater availability modeling: northern segment of the Edwards Aquifer,
Texas: TWDB, Report 358,

http://www.twdb.state.tx.us/publications/reports/numbered_reports/doc/R358/Report%20358
%20Northern%20Edwards.pdf.

Jones, P.H., and Buford, T.B., 1951, Electric logging applied to ground water exploration:
Geophysics, vol. 16, p. 115-139**.**

Keese, K.E., Scanlon, B.R., and Reedy R.C., 2005, Assessing controls on diffuse groundwater
recharge using unsaturated flow modeling: Water Resources Research, vol. 41, W06010,
doi:06010.01029/02004WR003841.

Keller, C., Van dr Kamp, G., and Cherry, J.A., 1986, Fracture permeability and groundwater
flow in clayey till near Saskatoon, Saskatchewan: Canadian Geotehnical Journal, vol. 23,
p. 229-240.

Kelley, V.K., and Ewing, J.E., 2014, Northern Trinity and Woodbine aquifers GAM overhaul
project – predictive simulations to support the GMA-8 joint-planning process: technical
memorandum to Bill Mullican, Contract Manager for the Northern Trinity and Woodbine
aquifers GAM Overhaul Project, dated August 29, 2014.

Kirk, A., Groenveld, D., Barz, D., Herring, J., and Murray S., 2012, Ground water recharge
model: Calibration and validation for remotely-sensed dual coefficient (RDC) GMA8 ET
estimation: prepared for the TWDB by HydroBio,
http://www.twdb.texas.gov/publications/reports/contracted_reports/doc/1004831114_Hydro
Bio.pdf.

Klemt, W.R., Perkins, R.D., and Alvarez, H.J., 1975, Ground-water resources of part of central
Texas with emphasis on the Antlers and Travis Peak formations, Volume 1: TWDB,
Report 195, Austin, TX.

Klemt, W.R., Perkins, R.D., and Alvarez, H.J., 1976, Ground-water resources of part of central
Texas with emphasis on the Antlers and Travis Peak Formations, Volume 2: TWDB,
Report 195, Austin, TX.

Krauskopf, K.B., 1979, Introduction to geochemistry, 2nd edition: McGraw-Hill, Inc.

Kuniansky, E.L., 1989, Precipitation, streamflow, and base flow in west-central Texas, December 1974 through March 1977: USGS, Water -Resources Investigation Report 88-4218.

Kuniansky, E.L., and Holligan, K.Q., 1994, Simulations of flow in the Edwards-Trinity aquifer system and continuous hydraulically connected units, west-central Texas: USGS, Water-Resources Investigations Report 93-4039.

Laine, L.L. and Cummings, T.R., 1963, Surface water of Kiamichi River basin in southern Oklahoma: USGS, Open-File report.

Lambe, T.W., and Whitman, R.V., 1969, Soil Mechanics: John Wiley and Sons, Inc., New York, NY.

Langley, L., 1999, Updated evaluation of water resources in part of north-central Texas, 1990-1999: TWDB, Report 349, Austin, TX.

Larkin, T.J., and Bomar, G.W., 1983, Climatic Atlas of Texas: Texas Department of Water Resources. LP-192, Austin, Texas.

LBG Guyton Associates and INTERA. 2012, Catahoula Aquifer characterization and modeling evaluation in Montgomery County: prepared for the Lone Star Groundwater Conservation District, Conroe, TX.

LBG-Guyton Associates in association with NRS Consulting Engineers, 2003, Brackish groundwater manual for Texas regional water planning groups: Prepared for the TWDB, http://www.twdb.texas.gov/publications/reports/contracted_reports/doc/2001483395.pdf.

Lee, H.L., 1958, Woodbine strata of northwest Hill County, Texas: M.S. Thesis, The University of Texas at Austin, Austin, TX.

Leggat, E.R., 1957, Geology and ground-water resources of Tarrant County, Texas: TWDB, Bulletin 5709, Austin, TX.

Leopold, L.B. 1968, Hydrology for urban land planning - a guidebook on the hydrologic effects of urban land use: USGS, Geological Survey Circular 554.

Lerner, D.N., Issar, A.S., and Simmers, I., 1990, Groundwater recharge: a guide to understanding and estimating natural recharge: International Contributions to Hydrogeology, Vol. 8, International Association of Hydrogeologists, Verlag Heinz Heise, Hannover, Germany.

Lerner, D.N., 2002, Identifying and quantifying urban recharge: a review: Hydrogeology Journal, vol. 10, p. 143 – 152.

Lewis, J.M, and Esralew, R.A., 2009, Statistical summaries of streamflow in and near Oklahoma through 2007: USGS, Scientific Investigations Report 2009–5135.

Livingston, P., 1945, Ground-water resources at Sherman, Texas: TWDB, Report M249, Austin, TX.

Livingston, P., and Bennett, R., 1942, Ground water in the vicinity of McGregor, McLennan County, Texas: U.S. Department of the Interior, Geological Survey, Open-File Report.

Livingston, P., and Hastings, W.W., 1942, Test well at proposed army camp 5 miles southeast of Gatesville, Texas: U.S. Department of the Interior, Geological Survey, Open-File Report.

Loucks, R.G., Dodge, M.M., and Galloway, W.E., 1984, Regional controls on diagenesis and reservoir quality in lower Tertiary sandstones along the Texas Gulf Coast, in Clastic Diagenesis, eds McDonald, D.A., and Surdam, R.C., American Association of Petroleum Geologists Memoir 37.

Ludwig, A.M., 1973, Water resources of Hempstead, Lafayette, Little River, Miller, and Nevada counties, Arkansas: USGS, Water Supply Paper 1998.

Mace, R. E., 1998, Ground-water flow and solute transport in a fractured chalk outcrop, north-central Texas: Ph.D. Dissertation, The University of Texas at Austin, Austin, TX, 412 p.

Mace, R.E., 2013, Personal collection of vintage post cards of flowing wells: personal communication from Robert Mace with the TWDB to Van Kelley with INTERA, Inc.

Mace, R.E., Chowdhury, A.H., Anaya, R. and Way, S.C., 2000, Groundwater availability of the
Trinity Aquifer, Hill Country Area, Texas: numerical simulations through 2050: TWDB,
Report 353, Austin, TX.
http://www.twdb.state.tx.us/publications/reports/numbered_reports/doc/R353/Report353.pdf.

Macpherson, G.L., 1983, Regional trends in transmissivity and hydraulic conductivity, lower
Cretaceous sands, north-central Texas: Ground Water, vol. 21, no. 5, p. 577-583.

Magara, K., 1978, Compaction and fluid migration – practical petroleum geology: Elsevier
Scientific Publishing Company, New York, NY.

Maidment, D.R., 1992, Handbook of hydrology: McGraw-Hill, Inc.

Makuchk, S.D., Carlson, D.A., Cherkauer, S.D., and Malik, P., 1999, Scale dependency of
hydraulic conductivity in heterogeneous media: Ground Water, vol. 37, no.6, p. 904-919.

Marcher, M.V., and Bergman, D.L., 1983, Reconnaissance of the water resources of the
McAlester and Texarkana quadrangles, southeastern Oklahoma: Oklahoma Geological
Survey, Map HA-9, prepared in cooperation with the USGS, The University of Oklahoma,
Norman, OK.

Masch, F.D., and Denny, K.J., 1966, Grain size distribution and its effects on the permeability of
unconsolidated sands: Water Resources Research, vol. 2, no. 4, p. 665-677.

McDonald, M.G., and Harbaugh, A.W., 1988, A Modular Three-Dimensional Finite-Difference
Ground-Water Flow Model: U.S. Geological Survey, Techniques of Water-Resources
Investigations, Book 6, chapter A1.

McGowen, M.K., and Harris, D.W., 1984, Cotton Valley (upper Jurassic) and Hosston (lower
Cretaceous) depositional systems and their influence on salt tectonics in the East Texas
Basin: Bureau of Economic Geology, The University of Texas at Austin, Geological
Circular 84-5, Austin, TX.

Meinzer, O.E., 1923, Outline of groundwater hydrology: USGS Water Supply Paper 494.

Miller, R.S., 1988, User's Guide for RIV 2- A Package for Routing and Accounting of River Discharge for a Modular, Three-Dimensional, Finite-Difference, Groundwater Flow Model: USGS, Open-File Report 88-345.

Morton, R.B., 1992, Simulation of ground-water flow in the Antlers Aquifer in southeastern Oklahoma and northeastern Texas: USGS, Water-Resources Investigations Report 88-4208.

Mosteller, M.A., 1970, Subsurface stratigraphy of the Comanchean series in east central Texas: Baylor Geological Studies, Bulletin 19, Baylor University, Waco, TX.

Mount, J.R., 1962, Ground-water conditions in the vicinity of Burnet, Texas: Texas Water Commission, Memorandum Report 62-01, Austin, TX.

Mount, J.R., 1963, Ground-water availability at Whitney, Hill County, Texas: Texas Water Commission, LD-0263-MR, Austin, TX.

Muller, D.A., and Price, R.D., 1979, Ground-water availability in Texas, estimates and projections through 2030: TWDB, Report 238, Austin, TX.

Myers, B.N., 1969, Compilation of results of aquifer tests in Texas: TWDB, Report 98, Austin, TX.

Nance, H.S., Laubach, S.E., and Dutton, A.R., 1994, Fault and joint measurements in Austin Chalk, superconducting super collider site, Texas: Gulf Coast Association of Geological Societies, Transactions, vol. 44, p. 521-532.

National Atmospheric Deposition Program (NADP), 2013, NADP maps and data, NTN (National Trends Network) data: website http://nadp.sws.uiuc.edu/data/, accessed 2013.

Neglia, S., 1979, Migration of fluids in sedimentary basins: American Association of Petroleum Geologists Bulletin, vol. 63, p. 573- 597.

Nicot, J-P., Hebel, A.K., Ritter, S.M., Walden, S., Baier, R., Galusky, P., Beach, J., Kyle, R., Symank, L., and Breton, C., 2011, Current and projected water use in the Texas mining and

oil and gas industry, Texas: Bureau of Economic Geology, The University of Texas at
Austin, Austin, TX.

Nicot, J-P., Reedy, R.C., Costley, R.A., and Huang, Y., 2012a, Oil and gas water use in Texas:
Update to the 2011 Mining Water Use Report, Texas: Bureau of Economic Geology, The
University of Texas at Austin, Austin, TX.

Nicot, J-P., Wolaver, B.D., Huang, Y., Howard, T., Costley, R., Breton, C., Walden, S., Baier R.,
and Strassberb, G., 2012b, Feasibility for using alternative water sources for shale gas well
completions: Prapared for the Gas Technology Institute by the Bureau of Economic Geology,
The University of Texas at Austin, Austin, TX.

Niswonger, R.G., Panday, S., and Ibaraki, M., 2011, MODFLOW-NWT, a Newton formulation
for MODFLOW-2005: USGS, Techniques and Methods 6-A37, 44 p.

Nordstrom, P.L., 1982, Occurrence, availability, and chemical quality of ground water in the
Cretaceous aquifers of north-central Texas: Texas Department of Water Resources,
Report 269, Austin, TX.

Nordstrom, P.L., 1987, Ground-water resources of the Antlers and Travis Peak Formations in the
outcrop area of north central Texas: Texas Water Commission, Report 298, Austin, TX.

Oklahoma Water Resources Board, 2013, Oklahoma surface water resources, Arkansas and Red
river drainage basins: website
http://www.owrb.ok.gov/maps/pdf_map/SW%20Arkansas%20Red%20River%20Basins.pdf

Oliver, W.B., 1971, Depositional systems in the Woodbine Formation (Upper Cretaceous),
northeast Texas: Bureau of Economic Geology, The University of Texas at Austin, Report of
Investigations 73, Austin, TX.

Oliver, W., Harding, J., and Lupton, D., 2013, Development of a groudwater model for the
Antlers Aquifer in southeastern Oklahoma: Prepared for The Chactaw and Chickasaw
Nations by INTERA Incorporated.

Ophori, D.U., and Tóth, J., 1989, Patterns of groundwater chemistry, Ross Creek Basin, Alberta, Canada: Ground Water, vol. 27, no. 1, pp. 20-26.

O'Rourke, D., Cross, B., and Symank, L., 2011, Anthropogenic groundwater contamination in Texas aquifers, Volumes I and II (plates): Prepared for the TWDB by LBG-Guyton Associates, http://www.twdb.texas.gov/publications/reports/contracted_reports/doc/1004831126_gwcontamination.pdf and http://www.twdb.texas.gov/publications/reports/contracted_reports/doc/1004831126_Vol%20IIPlates.pdf.

Owen, M.T., 1979, The Paluxy Sand in north-central Texas: Baylor Geological Studies, Bulletin 36, Baylor University, Waco, TX.

Ozdogan, M., and Gutman, G., 2008, A new methodology to map irrigated areas using multi-temporal MODIS and ancillary data: An application example in the continental US: Remote Sensing of Environment, vol. 112, no. 9, p. 3520-3537.

Panday, S, Langevin, C.D., Niswonger, R.G., Ibaraki, Motomu, and Hughes, J.D., 2013, MODFLOW–USG version 1: An unstructured grid version of MODFLOW for simulating groundwater flow and tightly coupled processes using a control volume finite-difference formulation: U.S. Geological Survey Techniques and Methods, book 6, chap. A45, 66 p., http://pubs.usgs.gov/tm/06/a45.

Papadopulos, I.S., and Cooper, H.H., 1967, Drawdown in a well of large diameter: Water Resources Research, vol. 3, no. 1, p. 241-244.

Parker, N.C., Allen, K., Arnold, K., Baker, R., Bradley, R., Cameron, G., Haskell, S., Holt, E., and Zimmerman, E., 2003, The Texas GAP analysis project: Final Report, 1135.

Peckham, R.C., Souders, V.L., Dillard, J.W., and Baker, B.B., 1963, Reconnaissance investigation of the ground-water resources of the Trinity River Basin, Texas: Texas Water Commission, Bulletin 6309, Austin, TX.

Plummer, F.B., and Sargent, E.C., 1931, Underground waters and subsurface temperatures of the Woodbine sand in northeast Texas: Bureau of Economic Geology, The University of Texas at Austin, Bulletin 3138, Austin, TX.

Pollock, D.W., 1994, User's Guide for MODPATH/MODPATH-PLOT, Version 3: A particle tracking post-processing package for MODFLOW, the U.S. Geological Survey finite-difference ground-water flow model: U.S. Geological Survey Open-File Report 94-464, 6 ch.

Price, J.C., 1951, The south Bosque oil field: in The Woodbine and adjacent strata of the Waco area of central Texas, Fondren Science Series 4, Southern Methodist University, Dallas, TX.

Price, R.D., Walker, L.E., and Sieh, T.W., 1983, Occurrence, quality, and availability of ground water in Callahan County, Texas: TWDB, Report 278, Austin, TX.

PRISM Climate Group, 2013, 50-Year Normals and 30-Year Normals: Oregon State University, website http://prism.oregonstate.edu, accessed 2013.

PRISM Climate Group, 2014, 30-Year Normals: Oregon State University, website http://prism.oregonstate.edu/normals/, accessed April, 2014.

Prudic, D.E., Konikow, L.F., and Bant, E.R., 2004, A new stream- flow routing (SFR1) package to simulate stream-aquifer interaction with MODFLOW-2000: USGS, Open-File Report 2004-1042.

Rapp, K.B., 1988, Groundwater Recharge in the Trinity Aquifer, Central Texas: Baylor Geological Studies, Bulletin 46, Baylor University, Waco, TX.

Reedy, R.C., Scanlon, B.R., Walden, S., and Strassberg, G., 2011, Naturally occuring groundwater contamination in Texas: Prepared for the TWDB by the Bureau of Economic Geology, The University of Texas at Austin, Austin, TX. http://www.twdb.texas.gov/publications/reports/contracted_reports/doc/1004831125.pdf.

Refsgaard, J.C. vqn der Sluijs, J.P., Brown. J., and van de Keur, P., 2006, A framework for dealing with uncertainty due to model structure error: Advances in Water Resources, vol. 29, no. 11, 1586-1597.

Rettman, P.L., 1987, Ground-water resources of Limestone County, Texas: TWDB, Report 299, Austin, TX.

Reutter, D.C., 1996, National water-quality assessment of the Trinity River Basin, Texas – Well and water-quality data from the outcrop of the Woodbine Aquifer in urban Tarrant County, 1993: USGS, Open-File Report 96-413.

Ridgeway, C., and Petrini, H., 1999, Changes in groundwater conditions in the Edwards and Trinity aquifers, 1987-1997, for portions of Bastrop, Bell, Burnet, Lee, Milam, Travis, and Williamson Counties, Texas: TWDB, Report 350, Austin, TX.

Ritchey, J.D., and Rumbaugh, J.O., eds., 1996, Subsurface fluid-flow (ground-water and vadose zone) modeling, ASTM STP 1288: American Society for Testing and Materials, West Conshohocken, PA., p. 61 - 80.

Rodgers, R.W., 1967, Stratigraphy of Glen Rose Limestone, central Texas: in Comanchean (lower Cretaceous) stratigraphy and paleontology of Texas, Society of Economic Paleontologists and Mineralogists, Permian Basin Section, Midland, TX.

Rose, N.A., 1943, Results of pumping test of wells at Tank Destroyer Center, north Camp Hood, near Gatesville, Texas: U.S. Department of the Interior, Geological Survey, Open-File Report.

Rose, N.A., and George, W.O., 1942, Ground-water resources in selected areas in Erath, Hood and Hamilton counties, Texas: Texas State Board of Water Engineers, duplicated report.

Rose, S. and Peters, N.E., 2001, Effects of urbanization on streamflow in the Atlanta area (Georgia, USA): a comparative hydrological approach: Hydrological Processes, vol. 15, p. 1441-1457.

Rovey, C.W., II, and Cherkauer, D.S., 1995, Scale dependency of hydraulic conductivity measurements: Ground Water, vol. 33, no. 5, p. 769-780.

Rumbaugh, J.O., and Rumbaugh, D.B., 2011, Guide to using Groundwater Vistas version 6: Environmental Simulations, Inc.

Rutledge, A.T., 1998, Computer programs for describing the recession of ground-water
      discharge and for estimating mean ground-water recharge and discharge from streamflow
      records--update: USGS, Water- Resources Investigations Report 98-4148.

Salvador, A., ed., 1991, The Gulf of Mexico Basin: The geology of North America, Volume J,
      Geological Society of America, Gounder, CO.

Salvador, A., and Muneton, J.M.Q., 1989, Stratigraphic correlation chart the Gulf of Mexico
      Basin: in Salvador, A., ed., The Gulf of Mexico Basin, The geology of North America,
      Volume J, Geological Society of America, Boulder, CO.

Scanlon, B.R., Dutton, A.R., and Sophocleous, M., 2002a, Groundwater recharge in Texas:
      Prepared for the TWDB by the Bureau of Economic Geology, The University of Texas at
      Austin and the Kansas Gelogical Survey,
      http://www.twdb.texas.gov/publications/reports/contracted_reports/doc/2000483340.pdf.

Scanlon, B.R., Healy, R.W., and Cook, P.G., 2002b, Choosing appropriate techniques for
      quantifying groundwater recharge: Hydrogeology. Journal, vol. 10, p. 18-39.

Scanlon, B., Keese, K., Bonal, N., Deeds, N., Kelley, V., and Litvak, M., 2005, Evapo-
      transpiration estimates with emphasis on groundwater evapotranspiration in Texas: Prepared
      for the TWDB by the Bureau of Economic Geology and School of Biological Sciences, The
      University of Texas at Austin and INTERA, Inc.
      https://www.twdb.texas.gov/groundwater/docs/BEG_ET.pdf.

Scanlon, B.R., Reedy, R.C., and Tachovsky, J.A., 2007, Semiarid unsaturated zone chloride
      profiles: Archives of past land use change impacts on water resources in the southern High
      Plains, United States: Water Resources Research., vol. 43, W03437,
      doi:10.1029/2006WR005769.

Scanlon, B.R., Reedy, R.C., Gates, J.B., and Gowda, P.H., 2010, Impact of agroecosystems on
      groundwater resources in the central High Plains, USA: Agriculture, Ecosystems, &
      Environment, vol. 139, no. 4, p. 700-713.

Schulze-Makuch, D., Carlson, D.A., Cherkauer, D.S., and Malik, P., 1999, Scale dependency of hydraulic conductivity in heterogeneous media: Ground Water, vol. 37, no.6, p. 904-919.

Scott, G., and Armstong, J.M., 1932, The geology of Wise County, Texas: Bureau of Economic Geology, The University of Texas at Austin, Bulletin 3224, Austin, TX.

Shestakov, V., 2002, Development of relationship between specific storage and depth of sandy and clay formations: Environmental Geology, vol., 42, nos. 2-3, p. 127-130.

Shuler, E.W., 1918, The Geology of Dallas County: Bureau of Economic Geology, The University of Texas at Austin, Bulletin 1818, Austin, TX.

Shumard, B.F., 1860, Observations upon the Cretaceous strata of Texas: St. Louis Academy of Science, Transactions, vol. 1, St. Louis, MO.

Slade, R.M, Bentley, J.T., and Michaud, D., 2002, Results of streamflow gain-loss studies in Texas, with Emphasis on gains from and losses to major and minor aquifers: USGS, Open-File Report 02–068.

Stramel, G.L., 1951, Ground-water resources of Parker County, Texas: TWDB, Bulletin 5103, Austin, TX.

Stricklin, Jr., F.L., Smith, C.I., and Lozo, F.E., 1971, Stratigraphy of lower Cretaceous Trinity deposits of central Texas: Bureau of Economic Geology, The University of Texas at Austin, Report of Investigations 71, Austin, TX.

Sundstrom, R.W., 1948, Results of pumping tests on the city wells at Waxahachie, Texas: TWDB, Report M292, Austin, TX.

Sundstrom, R.W., and Barnes, B.A., 1942, Ground-water resources in the vicinity of Gatesville, Texas: USGS, Open-File Report.

Sundstrom, R.W., Hastings, W.W., and Broadhurst, W.L., 1945, Public water supplies in eastern Texas: TWDB, Miscellaneous Report 214, Volumes I and II, Austin, TX.

Sundstrom, R.W., Broadhurst, W.L., and Dwyer, B.C., 1947, Public water supplies in central and north-central Texas: TWDB, Miscellaneous Report 213, Austin, TX.

Taff, J.A., 1892, Reports on the Cretaceous area north of the Colorado River: Third Annual Report of the Geological Survey of Texas, 1891, Austin, TX.

Taylor, H.D., 1976, Water-level and water-quality data from observations wells in northeast Texas: TWDB, Report 98, Austin, TX.

Taylor, H.D., 1978, Occurrence, quantity, and quality of ground water in Taylor County, Texas: TWDB, Report 224, Austin, TX.

Texas Board of Water Engineers, 1961, Historical ground-water uses by municipalities for the years 1955 through 1959 for selected areas in Texas: Texas Board of Water Engineers, Miscellaneous Report 293, Austin, TX.

Texas State Historical Society, 2013, Population history of selected cities, 1850 – 2010: website http://www.texasalmanac.com/topics/population, accessed February, 2013.

Texas Natural Resources Information System, 2013, Strategic mapping program (StratMap): website https://www.tnris.org/StratMap.

Theis, C.V., 1935, The relation between the lowering of the piezometer surface and the rate and duration of discharge of a well using groundwater storage: Transactions American Geophysical Union 2, p. 519-524.

Thompson, D.R., 1967a, Occurrence and quality of ground water in Brown County, Texas: TWDB, Report 46, Austin, TX.

Thompson, G.L., 1967b, Ground-water resources of Ellis County, Texas: TWDB, Report 62, Austin, TX.

Thompson, G.L., 1969, Ground-water Resources of Johnson County, Texas: TWDB, Report 94, Austin, TX.

Thompson, G.L., 1972, Ground-water resources of Navarro County, Texas: TWDB, Report 160, Austin, TX.

Thornton, T.S., 1992, Geohydrology of Pike and Howard counties, Arkansas: M.S. Thesis, Department of Geology, The University of Arkansas.

Tororelli, R.L., 2009, Water use in Oklahoma 1950-2005: USGS, Scientific Investigations Report, 2009-5212.

Toth, J., 1963, A theoretical analysis of groundwater flow in small drainage basins, Journal of Geophysical Research, vol. 68, no. 16, p. 4795-4812.

TWDB, 1999, Maps & GIS data, GIS data, River authorities and special law districts: http://www.twdb.state.tx.us/mapping/gisdata.asp.

TWDB, 2001, Surveys of irrigation in Texas, 1958, 1964, 169, 1974, 1979, 1984, 1989, 1994 and 2000. TWDB, Report 347, Austin, TX.

TWDB, 2006a, Maps & GIS data, GIS data, Major aquifers: http://www.twdb.state.tx.us/mapping/gisdata.asp.

TWDB, 2006b, Maps & GIS data, GIS data, Minor aquifers: http://www.twdb.state.tx.us/mapping/gisdata.asp.

TWDB, 2007a, Water for Texas 2007: 2007 State Water Plan, TWDB, http://www.twdb.texas.gov/waterplanning/swp/2007/.

TWDB, 2007b, Maps & GIS data, GIS data, Groundwater Management Areas: http://www.twdb.state.tx.us/mapping/gisdata.asp.

TWDB, 2008, Maps & GIS data, GIS data, Regional Water Planning Areas: http://www.twdb.state.tx.us/mapping/gisdata.asp.

TWDB, 2009, Precipitation & evaporation data: https://www.twdb.state.tx.us/surfacewater/conditions/evaporation/index.asp

TWDB, 2010a, Maps & GIS data, GIS data, Groundwater Conservation Districts:

http://www.twdb.state.tx.us/mapping/gisdata.asp.

TWDB, 2010b, Maps & GIS data, GIS data, Major river basins:

http://www.twdb.state.tx.us/mapping/gisdata.asp, accessed February 2010.

TWDB, 2012, 2012 Water for Texas: 2012 State Water Plan, TWDB,

http://www.twdb.state.tx.us/waterplanning/swp/2012/index.asp.

TWDB, 2013a, TWDB groundwater database:

http://www.twdb.state.tx.us/groundwater/data/gwdbrpt.asp, accessed February, 2013.

TWDB, 2013b, Submitted driller's reports database:

http://www.twdb.state.tx.us/groundwater/data/drillersdb.asp, accessed March, 2013.

TWDB, 2013c, Water use survey data:

http://www.twdb.state.tx.us/waterplanning/waterusesurvey/index.asp, accessed March, 2013.

TWDB, 2014, Groundwater availiablity models:

http://www.twdb.state.tx.us/groundwater/models/gam/index.asp.

Tyler, N, and Finley, R.J., 1991, Architectural controls on the recovery of hydrocarbons from

sandstone reservoirs: in The three-dimensional facies architecture of terrigenous clastic

sediments and its implications for hydrocarbon discovery and recovery, Miall, A.D., and

Tyler, N., eds., Concepts in Sedimentology and Paleontology, vol. 3, p. 1–5, Society of

Economic Paleontologists and Mineralogists.

U.S. Army Corps of Engineers, 2013a, Hugo Lake, monthly charts of reservoir data: U.S. Army

Corps of Engineers, Water Control Data System, Tulsa District, http://www.swt-

wc.usace.army.mil/HUGOcharts.html, accessed 2013.

U.S. Army Corps of Engineers, 2013b, Lake Texoma, Denison Dam, monthly charts of reservoir

data: U.S. Army Corps of Engineers, Water Control Data System, Tulsa District,

http://www.swt-wc.usace.army.mil/DENIcharts.html, accessed 2013.

U.S. Census Bureau, 2013, TIGER/line® Shapefiles and TIGER/line® Files: U.S. Census
    Bureau, http://www.census.gov/geo/maps-data/data/tiger-line.html.

U.S. Department of Agriculture, 1994, State soil geographic (STATSGO) data base: National
    Resource Conservation. Service, Miscellaneous Publications No. 1492.

U.S. Department of Agriculture, 1995, Soil survey geographic data base, SSURGO: Natural
    Resource Conservation Service, Miscellaneous. Publication 1527.

U.S. Environmental Protection Agency (EPA), 1993, Guidance specifying management
    measures for sources of nonpoint source pollution in coastal waters: U.S. Environmental
    Protection Agency, Office of Water, EPA 840-B-92-002 January 1993, Washington, DC.

U.S. Geological Survey, 2002, Physiographic divisions of the conterminous U.S.:
    http://water.usgs.gov/GIS/metadata/usgswrd/XML/physio.xml#stdorder.

U.S. Geological Survey, 2012, National Hydrography Dataset , http://nhd.usgs.gov/.

U.S. Geological Survey, 2013a, USGS Water-Quality Data for the Nation: website
    http://waterdata.usgs.gov/nwis/qw, accessed 2013.

U.S. Geological Survey, 2013b, USGS surface-water data for the nation:
    http://waterdata.usgs.gov/nwis/sw, accessed January 2013.

U.S. Department of Agriculture, 2012, Historical census publications: U.S. Department of
    Agriculture, http://www.agcensus.usda.gov/Publications/Historical_Publications/index.php.

U.S. Department of Agriculture, 2013, Natural resource conservation service, Arkansas-White-
    Red basins inter-agency committee:
    http://www.ar.nrcs.usda.gov/technical/arkansas_white_red.html.

Wahl, K.L., and Wahl, T.L., 1995, Determining the flow of Comal Springs at New Braunfels,
    Texas: Texas Water '95, American Society of Civil Engineers, San Antonio, TX:
    August 16-17, 1995.

Walker, J.D., and Geissman, J.W., compilers, 2009, Geologic time scale: Geological Society of America.

Warren, J.E., and Price, H.S., 1961, Flow in heterogeneous porous media: Society of Petroleum Engineers Journal, v. 1, p. 153-169.

Weiss, R., and Smith, L., 1998, Efficient and responsible use of prior information in inverse methods: Ground Water, v. 36, no. 1, p. 151-163.

Wermund, 1996, Physiography of Texas: Bureau of Economic Geology, The University of Texas at Austin, http://www.beg.utexas.edu/UTopia/images/pagesizemaps/physiography.pdf.

Westfall, A.O., and Cummings, T.R., 1963, Surface water of Muddy Boggy River basin in southwestern Oklahoma: USGS, Open-File report 63-148.

Whitaker, F.F., and Smart, P.L., 2000, Characterising scale-dependence of hydraulic conductivity in carbonates: evidence from the Bahamas: Journal of Geochemical Exploration, vol. 69-70, p. 133-137.

White, D.E., 1973, Ground-water resources of Rains and Van Zandt counties, Texas: TWDB, Report 169, Austin, TX.

White, J.W., 1961, Investigation of salt water contamination in a Woodbine well near Sherman, Grayson County, Texas: Texas Board of Water Engineers, Contamination Report 10, Austin, TX.

Williams, T.A., and Williamson, A.K., 1989, Estimating water-table altitudes for regional ground-water flow modeling. U.S. Gulf Coast: Groundwater, vol. 27, no. 3, p. 333-340.

Winslow, A.G., and Kister, L.R., 1956, Saline-water resources of Texas: USGS, Water-Supply Paper 1365.

Winton, W.M., 1925, The geology of Denton County: Bureau of Economic Geology, The University of Texas at Austin, Bulletin 2544, Austin, TX.

Winton, W.M., and Adkins, W.S., 1919, The geology of Tarrant County: Bureau of Economic
    Geology, The University of Texas at Austin, Bulletin 1931, Austin, TX.

Winton, W.M., and Scott, G., 1922, The geology of Johnson County, Texas: Bureau of
    Economic Geology, The University of Texas at Austiln, Bulletin 229, Austin, TX.

Wolock, D.M., 2003a, Flow characteristics at U.S. Geological Survey streamgages in the
    conterminous United States: USGS, Open-File Report 03-146,
    http://ks.water.usgs.gov/pubs/abstracts/of.03-146.htm.

Wolock, D.M., 2003b, Base-flow index grid for the conterminous United States: USGS, Open-
    File Report 03–263, http://ks.water.usgs.gov/pubs/abstracts/of.03-263.htm.

Woodruff, C.M., Jr., and McBride, M.W., 1979, Regional assessment of geothermal potential
    along the Balcones and Luling-Mexia-Talco faults zones, central Texas: Division of
    Geothermal Energy, U.S. Department of Energy, DOE/ET/28375-1, performed by the
    Bureau of Economic Geology, The University of Texas at Austin, Austin, TX.

Woodruff, C.M., Jr., Gever, C., Snyder, F.R., and Wuerch, D.R., 1983, Integration of geothermal
    data along the Balcones/Ouachita trend, central Texas: Office of Scientific and Technical
    Information, U.S. Department of Energy, DOE/ID/12057-T8, performed by the Bureau of
    Economic Geology, The University of Texas at Austin, Austin, TX.

Woodruff, C.M., Jr., Macpherson, G.L., Gever, C., Caran, S.C., and El Shazly, A.G., 1984,
    Geothermal potential along the Balcones/Ouachita trend, central Texas – ongoing assessment
    and selected case studies: Division of Geothermal Energy, U.S. Department of Energy,
    DOE/ID/12057—T6, performed by the Bureau of Economic Geology, The University of
    Texas at Austin, Austin, TX.

Young, S.C., and Tu, K., 2001, Basewide groundwater flow model for Kelly Air Force Base,
    Texas: Prepared for the Air Force Civil Engineer Center (AFCEE), Brooks Air Force Base,
    TX.

Young, S.C., and Budge, T., 2002, Development and application of a calibrated ground-water
flow and transport model for the T-25 area at Soldier System Center (SSC): prepared for
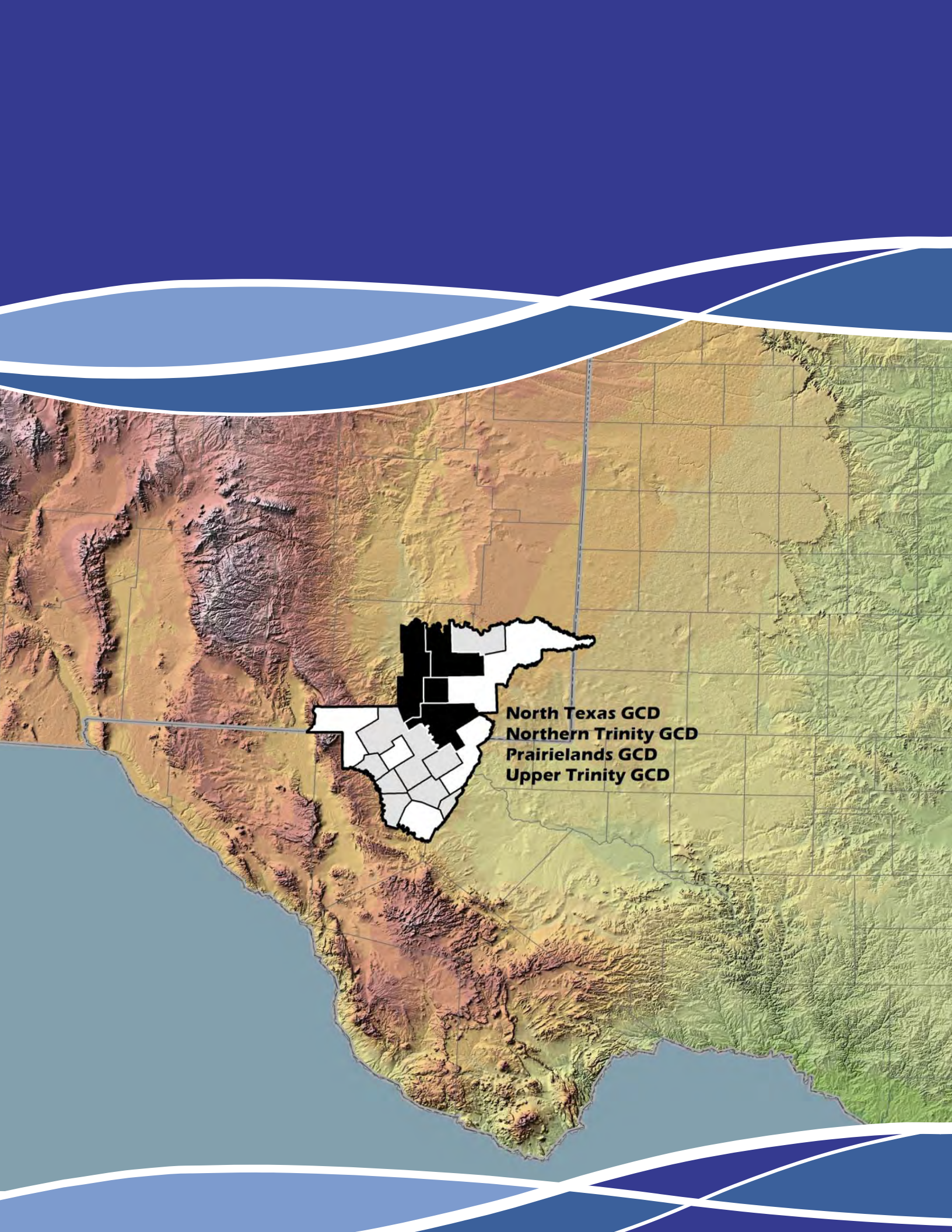Solider System Center, Natick, MA by HydroGeologic Inc., Final Report.

Young, S.C., and Kelley, V., eds., 2006, A site conceptual model to support the development of a
detailed groundwater model for Colorado, Wharton, and Matagorda counties: unpublished
report prepared for the Lower Colorado River Authority, Austin, TX.

Young. S.C., Kelley, V., Budge, T., Deeds, N., and Knox, P., 2009, Development of the LCRB
Groundwater Flow Model for the Chicot and Evangeline Aquifers in Colorado, Wharton, and
Matagorda Counties: Lower Colorado River Authority.

Young. S.C., Pinkard, J., Basset, R.L., and Chowdhury, A., 2014, Hydrochemical Evaluation of
the Texas Gulf Coast Aquifer System and Implication for Developing Groundwater
Availability Model: prepared by INTERA Incorporated, TWDB Contracted Report, TWDB,
Austin, TX.

North Texas GCD
Northern Trinity GCD
Prairielands GCD
Upper Trinity GCD